Universidad Complutense de Madrid
Facultad de CC. Físicas
Departamento de Física de la Tierra, Astronomía y Astrofísica II
(Astrofísica y CC. de la Atmósfera)

CARMENES-UCM: scientific preparation, multiplicity, chromospheric activity and kinematics

CARMENES-UCM: Preparación científica, multiplicidad, actividad cromosférica y cinemática

Dirigido por
Dr. José A. Caballero Hernández
Prof. Dr. David Montes Gutiérrez

Memoria que presenta
D^{a}. Miriam Cortés Contreras
para aspirar al grado de
Doctor en Astrofísica
Madrid, septiembre de 2016

Universidad Complutense de Madrid
Facultad de CC. Físicas
Departamento de Física de la Tierra, Astronomía y Astrofísica II
(Astrofísica y CC. de la Atmósfera)

CARMENES-UCM: scientific preparation, multiplicity, chromospheric activity and kinematics

CARMENES-UCM: Preparación científica, multiplicidad, actividad cromosférica y cinemática

Dirigido por
Dr. José A. Caballero Hernández
Prof. Dr. David Montes Gutiérrez

Memoria que presenta
D^{a}. Miriam Cortés Contreras
para aspirar al grado de
Doctor en Astrofísica
Madrid, noviembre de 2016

Some of the figures and material included in this document have already been published in *The Observatory* and *Astronomy & Astrophysics*.

A mi familia,
a Diego,
a la vida que crece dentro de mí

Agradecimientos

"Si quieres llegar rápido, camina solo; si quieres llegar lejos, camina acompañado."
— Proverbio africano

Esta tesis ha sido como una carrera de fondo en la que el esfuerzo y la constancia me han permitido llegar lejos. Cada zancada me ha proporcionado herramientas y cada tropiezo conocimiento. Ahora que llego a la meta siento la satisfacción de ver cumplidos muchos objetivos y las ganas de participar en nuevos proyectos.

Este trabajo no habría sido lo que es de no ser por el apoyo de mis directores, Dr. José Antonio Caballero y Prof. Dr. David Montes. Gracias por vuestra confianza y por todo lo que me habéis enseñado. Quiero agradecer al consorcio CARMENES la oportunidad de haber realizado mi tesis en un proyecto tan fascinante. Un agradecimiento especial para el Dr. Víctor Béjar, por participar en este proyecto conmigo. Gracias por tu paciencia y por las largas discusiones de las que tantísimo he aprendido. Gracias también al Prof. Dr. Ansgar Reiners por acogerme en su grupo durante unos meses. Gracias al Instituto de Astrofísica de Canarias y al Institut für Astrophysik Göttingen por aceptarme en mis estancias, las cuales me han hecho crecer como investigadora y como persona. Extiendo este agracimiento a las personas que he conocido en estos lugares y que han enriquecido mi experiencia, así como a las profesoras y profesores, compañeras y compañeros del departamento, en especial, a la Profa. Dra. Elisa de Castro, Profa. Dra. María José Fernández, Prof. Dr. Manuel Rego y Prof. Dr. Manuel Cornide, y cómo no, a mis compañeros de fatigas, Javi, Hugo, Víctor y Miguel, con quienes he compartido tanto.

Quiero dedicar unas palabras a todas las personas que me han acompañado en esta carrera: a las que han hecho el recorrido más difícil, porque me han hecho más fuerte, y a las que me han dado ánimos y lo han hecho más llevadero. También a quienes me enseñaron a calzarme las zapatillas y me señalaron el comienzo del camino, así como a quien, pequeña y veloz, me ha motivado en las carreras cortas que dan sentido a esta alegoría. Un sentido gracias a mi familia, que ha hecho del desorden un caos agradable. Sofía, crecer junto a ti ha sido una lección de coraje y determinación que pongo en práctica cada día. Tere y Ricardo, gracias por vuestra comprensión y cariño, por vuestros consejos y las deliciosas comidas que los han acompañado. Jorge, siempre presente y atento, gracias por tus fantásticas sorpresas. Gracias, Ana y Manolo. Me habéis enseñado que todo es posible y habéis sido para mí un ejemplo a seguir. Mi agradecimiento más especial para la persona que ha estado en los entrenamientos y se ha atrevido a correr conmigo: Diego. Gracias por creer en mí.

No querría terminar sin mencionar a las compañeras y compañeros que conocí en el punto de partida y que hoy leen estas líneas. Espero que mis palabras sirvan de avituallamiento en el camino hacia su meta.

Por último, gracias a ti, que estás leyendo estas líneas, por tu interés en este trabajo que espero disfrutes.

En Madrid, a 5 de septiembre de 2016

Acknowledgements

"If you want to go quickly, go alone. If you want to go far, go together.
— African proverb

This thesis has been like a long-distance race, in which the effort and persistence allowed me to go far. Each stride has provided me the tools, and each tumble the knowledge. Now I reach my goal, I feel the satisfaction of all the accomplished objectives, and the strong longing for participating in new projects.

This thesis would not have been what it is if it were not for the constant support of my supervisors, Dr. José Antonio Caballero y Prof. Dr. David Montes. Thank you for your trust and for everything you have taught me. I would like to start by thanking the CARMENES consortium for giving me the chance to develop my thesis in a such amazing project. I want to especially thank Dr. Víctor Béjar for participating with me in this project. Thank you for your patience and the long discussions of which I have learned so much. I also express my gratitutde to Prof. Dr. Ansgar Reiners for welcoming me in his group for a few months. Thanks to the Instituto de Astrofísica de Canarias y al Institut für Astrophysik Göttingen for accepting me during my stays, which made me grow as a researcher, as well as a person. I extend my thanks to all the people I have met in these places and that enriched my experience, as well as to the teachers and colleagues in the department, especially to Profa. Dra. Elisa de Castro, Profa. Dra. María José Fernández, Prof. Dr. Manuel Rego, y Prof. Dr. Manuel Cornide, and of course, my fellow sufferers Javi, Hugo, Víctor and Miguel, with whom I have shared so much.

I would like to say a few words to the people who have gone by my side during this race: to those that made harder the tour, because they made me stronger, and to those that cheered me up and made it easier. Also to those who taught me to put my running shoes on and pointed me the start line, as well as who, small and fast, motivated me in the short races that give sense to this allegory. A heartfelt thanks to my family, who made a nice chaos out of a mess. Sofía, growing up with you has been a lesson of courage and determination that I put in practice every day. Tere and Ricardo, thanks for your understanding and care, for your advices and the delicious meals that came with them. Jorge, always present and thoughtful, thank yoou for your fantastic surpises. Thanks, Ana and Manolo. I have learned from you that everything is possible and you have been an example to follow. My most special thank to the person who went with me during my trainings and dared to run with me: Diego. Thank you for believing in me.

I would not like to finish without mentioning the colleagues I met at the starting point and who read these lines. I hope that my words serve as provisioning in the way to your goals.

Last but not least, thank you, the reader of these lines, for you interest on this work that I hope you enjoy.

Madrid, September 5, 2016

Resumen

Contexto

Las estrellas enanas de tipo M respresentan cerca de dos tercios de las estrellas en la Galaxia, lo que las convierte en objetivos perfectos para el estudio de formación y evolución estelar al final del diagrama Hertzsprung-Russell. El máximo de emisión de energía de las estrellas M se sitúa en el infrarrojo, entre 0.9 y 1.5 μm. Las Ms de campo tienen masas entre 0.6 y 0.08 $M_\odot$, lo que las sitúa entre las estrellas que queman helio e hidrógeno y los objetos subestelares. Por esta razón, no está delimitado el proceso de formación dominante, también relacionado con la frecuencia de enanas M y estrellas poco masivas en sistemas binarios y múltiples. Por otro lado, en el régimen de enanas M, tienen lugar importantes cambios en la estructura interna, pasando de ser parcial a totalmente convectivas hacia los últimos tipos en la secuencia principal.

La poca masa de las enanas M las convierten en objetivos óptimos para la caza de exoplanetas, especialmente con el método Doppler, que saca provecho del elevado cociente entre la masa del planeta y la masa de la estrella. CARMENES es un espectrógrafo de alta resolución (R>80 000) con dos canales, visible (0.52–0.96 μm) e infrarrojo (0.96–1.71 μm), situados en el telescopio de 3.5 m en el Observatorio de Calar Alto en Almería (España), cuyo propósito principal es la detección de exo-Tierras en la zona de habitabilidad de las enanas M.

Esta tesis se ha desarrollado en el marco del proyecto CARMENES, bajo el auspicio del Consorcio homónimo, que está compuesto por 11 instituciones españolas y alemanas. El instrumento CARMENES, operativo desde enero de 2016, está observando entorno a 300 enanas M durante al menos 600 noches de tiempo garanizado. Estas observaciones durarán, al menos, tres años. El análisis llevado a cabo en esta tesis forma parte de la preparación científica necesaria para la selección de esas estrellas.

Objetivos y metodología

Para seleccionar adecuadamente las 300 enanas M que CARMENES está observando, he construido el catálogo de entrada de CARMENES, llamado Carmencita. Está compuesto por ∼2200 enanas M y contiene docenas de parámetros, incluyendo astrometría precisa, fotometría, información sobre multiplicidad e indicadores de actividad, entre otros. Estos parámetros han sido recopilados principalmente de la literatura, pero también se han derivado a partir de imágenes y espectros de baja y alta resolución por parte de miembros del Consorcio.

Para confirmar la binariedad de sistemas con al menos una enana M, hemos tomado imágenes de baja resolución en la banda R de Johnson con los instrumentos TCP y CAMELOT del telescopio IAC80 en el Observatorio del Teide (Tenerife, España) de 54 sistemas binarios o múltiples. Los resultados de este estudio se presentan en el primer artículo publicado en esta tesis.

Para descartar compañeros binarios cercanos que puedan introducir variaciones espúreas en las medidas de velocidad radial, hemos observado 490 enanas M de Carmencita supuestamente aisladas en la banda I de Johnson con el instrumento de "lucky imaging" FastCam del telescopio Carlos Sánchez en el Observatorio del Teide. El análisis y los resultados se presentan en el segundo artículo publicado en este trabajo.

Para completar la búsqueda de compañeras binarias entorno a las estrellas M de Carmencita, he llevado a cabo una búsqueda de compañeros de movimiento propio usando catálogos públicos de todo el cielo y herramientas del observatorio virtual.

Resultados y conclusiones

En esta tesis presento distancias espectro-fotométricas para casi 900 enanas M, movimientos propios derivados a partir de catálogos astrométricos para más de 500 y componentes de velocidades galactocéntricas para cerca de 1600. Además, cuatro estrellas M de Carmencita son candidatos viejos del halo Galáctico y 354 pertenecen a grupos jóvenes de movimiento, la mayoría de las cuales est entre las 446 estrellas asociadas al disco joven de la Galaxia. Presento una lista con las 50 estrellas más activas de Carmencita que presentan emisión en Hα y en rayos X, y que son además rápidas rotadoras con cinemática asociada a edades tempranas (<200 Ma). En toda la muestra, se observa un incremento en la fracción de estrellas activas hacia tipos más tardíos y límites en los niveles de actividad cromosférica y coronal, de acuerdo con trabajos anteriores.

La fracción de multiplicidad a cualquier rango de separaciones angulares es del 19.1% en Carmencita y del 26.5–28.7% en dos muestras distintas limitadas en volumen. He analizado la distribución de las separaciones físicas proyectadas de los sistemas con primarias M para Carmencita y estas dos muestras y he observado que siguen una ley de potencias de acuerdo con la ley de Öpik en el intervalo entre 1 au y 3160 au.

A partir de las imágenes de baja resolución de TCP y CAMELOT, hemos descartado dos pares no ligados debido a las diferencias entre sus movimientos propios y confirmado 52 pares físicamente ligados. La búsqueda de compañeros de movimiento propio en torno a nuestras estrellas de Carmencita ha concluido con 13 posibles compañeras con separaciones entre 33 y 430 arcsec (640 y 9600 au). Cinco compañeras tienen masas en el límite o por debajo de la quema de hidrógeno. Tres de ellas tienen además las energías de ligadura más bajas y son candidatas a los grupos de β Pictoris y Ursa Major o al disco joven de la Galaxia.

De las 80 compañeras detectadas en la bśqueda de Fastcam, 30 son nuevos descubrimientos y 17 presentan variaciones orbitales en cinco años. La fracción de multiplicidad de la muestra observada es de 16.7±2.0%, y de 19.5±2.3% en la muestra corregida de sesgo para separaciones angulares entre 0.2 y 5 arcsec (1.4–65.6 au). La contribución de binarias y sistemas múltiples de la literatura a otros rangos de separaciones angulares incrementa la fracción de multiplicidad en la muestra limitada en volumen hasta, al menos, el 36%, superior a la estimada previamente en este trabajo.

El catálogo Carmencita será un recurso público de gran potencial que servirá no sólo para la selección de la muestra de CARMENES, sino también para una mejor caracterización de estas estrellas frías y poco masivas.

Abstract

Context

M dwarfs represent near two-thirds of the stars in the Galaxy, which converts them into perfect targets for the study of stellar formation and evolution at the end of the Hertzsprung-Russell diagram. Their emission peaks in the infrared, between 0.9 and 1.5 μm. The low masses of field M dwarfs (from 0.6 to 0.08 $M_\odot$), place them between helium and hydrogen burning stars, and substellar objects. For this reason, there is no restricted their dominant formation process, also related to the frequency of M dwarfs and low mass stars in binary and multiple systems. On the other hand, in this regime, important structural changes take place, and they become fully convective towards later spectral subtypes in the main sequence.

They are excellent targets for exoplanet hunting due to their low masses, especially with the Doppler method, which takes advantage of the high mass ratio between the star and the planet. CARMENES is a high-resolution spectrograph (R>80 000) with two chanels, visible (0.52–0.96 μm) and infrared (0.96–1.71 μm), located at the 3.5 telescope at the Calar Alto Observatory in Almería (Spain). Its main purpose is to detect exoEarths in the habitability zone of M dwarfs.

This thesis has been developed in the frame of the CARMENES project, under the auspices of the CARMENES Consortium, which is composed by 11 German and Spanish institutions. The CARMENES instrument, operative since January 2016, is observing around 300 M dwarfs during at least 600 nights of guaranteed time during at least three years. The analysis carried out in this thesis is part of the science preparation needed for the target selection.

Aims and methodology

To properly select the 300 targets that CARMENES observes, I built the CARMENES input catalogue, dubbed Carmencita. It is composed by ∼2200 M dwarfs and contains dozens of parameters, including accurate astrometry, photometry, multiplicity information and activity indicators, among others. These parameters were compiled mainly from the literature, but also were derived from low- and high-resolution imaging and spectroscopy obtained by the Consortium members.

To confirm binarity with at least one M dwarf, we took low-resolution images in the *R*-band with the TCP and CAMELOT instruments at the IAC80 telescope at the Observatorio del Teide (Tenerife, Spain) of 54 binary or multiple systems. The results of this study are presented in the first published paper collected in this thesis.

In order to discard close binary companions that may induce spurious variations in the radial velocity measurements, we observed 490 single Carmencita M dwarfs in the *I*-band with the lucky imager FastCam at the Telecopio Carlos Sánchez at the Observatorio del Teide. The analysis and

results are presented in the second paper published in this thesis.

To complete the search of binary companions around the Carmencita M dwarfs, I performed a proper-motion search using all-sky public catalogues and virtual observatory tools.

Results and conclusions

In this thesis, I present spectro-photometric distance of almost 900 M dwarfs, proper motions derived from astrometric catalogues of more than 500, Galactic space velocity components of near 1600. In addition, four Carmencita M dwarfs are old halo candidates and 354 belong to young moving groups, the majority of which is among the 446 M dwarfs associated to the Galactic young disc. I also present a list with the 50 stars most active in the sample, which show Hα and X-rays emission, are rapid rotators and kinematics related to young ages (<200 Ma). In the whole sample, we observed an increment of the active fraction of stars towards later spectral subtypes and a saturation limit in the chromospheric and coronal activity levels, in agreement with previous works.

The multiplicity fraction of M dwarfs at any range of angular separations is of 19.1% in Carmencita and of 26.5–28.7% in two different volume limited samples. I analyzed the projected physical separation distribution of all the systems with M dwarf primaries in Carmencita and those two samples and I observed that they follow a power-law distribution according to the Öpik's law in the range between 1 au and 3160 au.

From the TCP and CAMELOT low-resolution images, we discarded as physically bound two pairs due to their different proper motions and confirmed physical binding of 52 pairs. The search of common proper motion companions around Carmencita M dwarfs led to 13 potential companions with separations between 33 and 430 arcsec (640 and 9600 au). Five companions have masses at or below the hydrogen burning limit. Three of them have also the lowest binding energies and are β Pictoris, Ursa Major and young disc candidate members.

Of the 80 companions detected in the FastCam survey, 30 are new discoveries and 17 show orbital variations within 5 years. The multiplicity fraction in the observed sample is of 16.7±2.0% and in the bias corrected sample is of 19.5±2.3% for angular separations from 0.2 to 5.0 arcsec (1.4–65.6 au). The contribution of binaries and multiples with angular separations shorter than 0.2 arcsec, larger than 5.0 arcsec, and of spectroscopic binaries identified from previous searches, although not complete, increases the multiplicity fraction of M dwarfs in the volume limited sample up to at least 36%, higher than the previously estimated fraction in this thesis.

The Carmencita catalogue will be a very powerful public resource that will serve not only for CARMENES targets selection, but also for a better characterization of these cool and low-mass stars.

Contents

1

Introduction

In 1995, the first exoplanet was discovered orbiting a main sequence star by Michel Mayor and Didier Queloz. The planet, 51 Peg b, orbits a solar-like star closer than the closest planet in our Solar System, and with almost half of the mass of Jupiter. After the prove that our Solar System is not the only one in the Galaxy, several questions have come up: how are the other planets, their atmospheres and configurations around their stars? What kind of stars do they orbit around? Is there also a planet where life could be sustained?

More than 2 000 planets have been discovered since then. They are found orbiting giants and main sequence stars, single or binary systems, and their masses range from less than one Earth mass ($M_\oplus$) to around 80 Jupiter masses (M_{Jup}). The wide variety of planetary systems is an indicator of the diversity that populates the Milky Way. Nevertheless, the majority of the detected exoplanets are Jupiter giants usually orbiting too close to its star due to the bias of the detection methods, although some Earth-mass planets have also been detected.

The science of planet hunting is now focused on the detection of Earth-like planets in the habitable zone (HZ) of the star, which is defined as the position not too close nor to far to the star at which the exoplanet can retain liquid water on its surface (Kasting et al. 1993). An Earth-like planet is a rocky planet expected to have between 0.8 and 5 $M_\oplus$, as well as a well-defined surface, geothermal activity, and an atmosphere and a dynamo generation of magnetic field to protect it from stellar events. (Scalo et al. 2007).

Several instruments have been developed to look for Earth-like planets in the HZ of solar-like stars, such as HARPS (Mayor et al. 2003) and its twin HARPS-N (Cosentino et al. 2012). The difficulty on finding them due to their low signal and the inaccuracy of the measurements with the current instrumentation has lead to a recent new branch of planet searches born to look around less massive stars with the Doppler technique (e.g., CARMENES, Quirrenbach et al. 2014; IRD, Kotani et al. 2014; HPF, Mahadevan et al. 2014; Spirou, Artigau et al. 2014). This method takes advantage on the high planet-star mass ratio of less massive stars such as M dwarfs. However, the viability of the habitability conditions of planets around M dwarfs is constrained, since the width of the HZ is only about one-fifth to 1/50th of the width of that of a G star (Tarter et al. 2007). In addition, these planets are likely to be synchronous rotators as a consequence of tidal damping, having a side permanently illuminated by the star, while the other side resides in the darkness (Kasting et al.

1993; Joshi et al. 1997).

In this context, the CARMENES project has been developed. CARMENES is the acronym of *Calar Alto high-Resolution search for M dwarfs with Exoearths with Near-infrared and optical Échelle Spectrographs* (Quirrenbach et al. 2014). It is the name of a project, an instrument and a consortium. Overall, this project aims to find Earth-like planets around M dwarfs with the radial velocity method in a wide spectral coverage. Different Spanish and German institutions integrate the CARMENES Consortium, and work together to build the CARMENES instrument and to perform the previous scientific preparation and the subsequent science exploitation of the data.

To optimize the chances of finding exo-Earths in the habitable zone around M dwarfs, it is essential to properly select the best targets to be observed with CARMENES. This thesis aims to help by providing a complete catalogue of M dwarfs with the most important and updated parameters, as part of the scientific preparation previous to the observations. Following subsections set the basis of this thesis and serve the introduction for the content in following chapters: Sections 1.1 and 1.2 describe the evolutive stage of M-type dwarfs and their main characteristics, as well as a review of planet searches around low mass stars, making special emphasis on M dwarfs as hosts of exoplanets and the radial velocity technique. Section 1.3 introduces binarity and multiplicity in M dwarfs and low mass stars. Section 1.4 is entirely dedicated to the CARMENES project, consortium and instrument. With this general overview, Section 1.5 summarizes the objectives of the work carried out, which will be presented in detail in following chapters.

1.1 M dwarfs

M-type stars represent about two-thirds of the stars in the Milky Way and constitute around the 40% of the total stellar mass in the Galaxy (Gould et al. 1996; Bochanski et al. 2010). They are among the coolest and smallest stars ($2300\,\mathrm{K} \lesssim T_{\mathrm{eff}} \lesssim 3800\,\mathrm{K}$, $0.1\,R_{\odot} \lesssim \mathrm{R} \lesssim 0.6\,R_{\odot}$; Reid & Hawley 2005) only followed by L, T and recently typed Y stars (Kirkpatrick et al. 1999; Burgasser et al. 2006; Cushing et al. 2011). Their abundance makes them excelent targets to broadly study the formation and evolution processes involving stellar objects at the bottom of the main-sequence in the Herzsprung-Russell diagram, which is shown in Fig. 1.1. Their evolution has an important repercussion in the evolution of the Galaxy on timescales longer than the current age of the universe (Laughlin et al. 1997).

1.1.1 Spectroscopy

Spectral typing is the way in which stars are categorized. The spectral types are determined by comparison of the relative strenght of specific spectral features within a determined wavelength range against observations of standard stars (stars with known absolute magnitudes and luminosity class). Spectral typing progressed from blue and warm to red and cool stars: from the ultraviolet emission of B stars to the infrarred of M, L, T and Y dwarfs. The current classification system was stablished in the mid 20th century by Morgan et al. (1943) in the visual and blue range (4000–6000 Å) and was later extended to redder wavelengths (6500–9000 Å) by Kirkpatrick et al. 1991. The spectra of the stars account for the variations and processes that take place at their internal and external layers and are related to some fundamental stellar parameters such as the effective temperature (T_{eff}), the mass ($\mathcal{M}$), the radius (R), the luminosity (L) or the surface gravity (g).

In the optical range, the stronger molecular bands in M dwarfs spectra are the titanum oxide (TiO), vanadium oxide (VO) and calcium hydride (CaH). The TiO bands dominate the spectra and

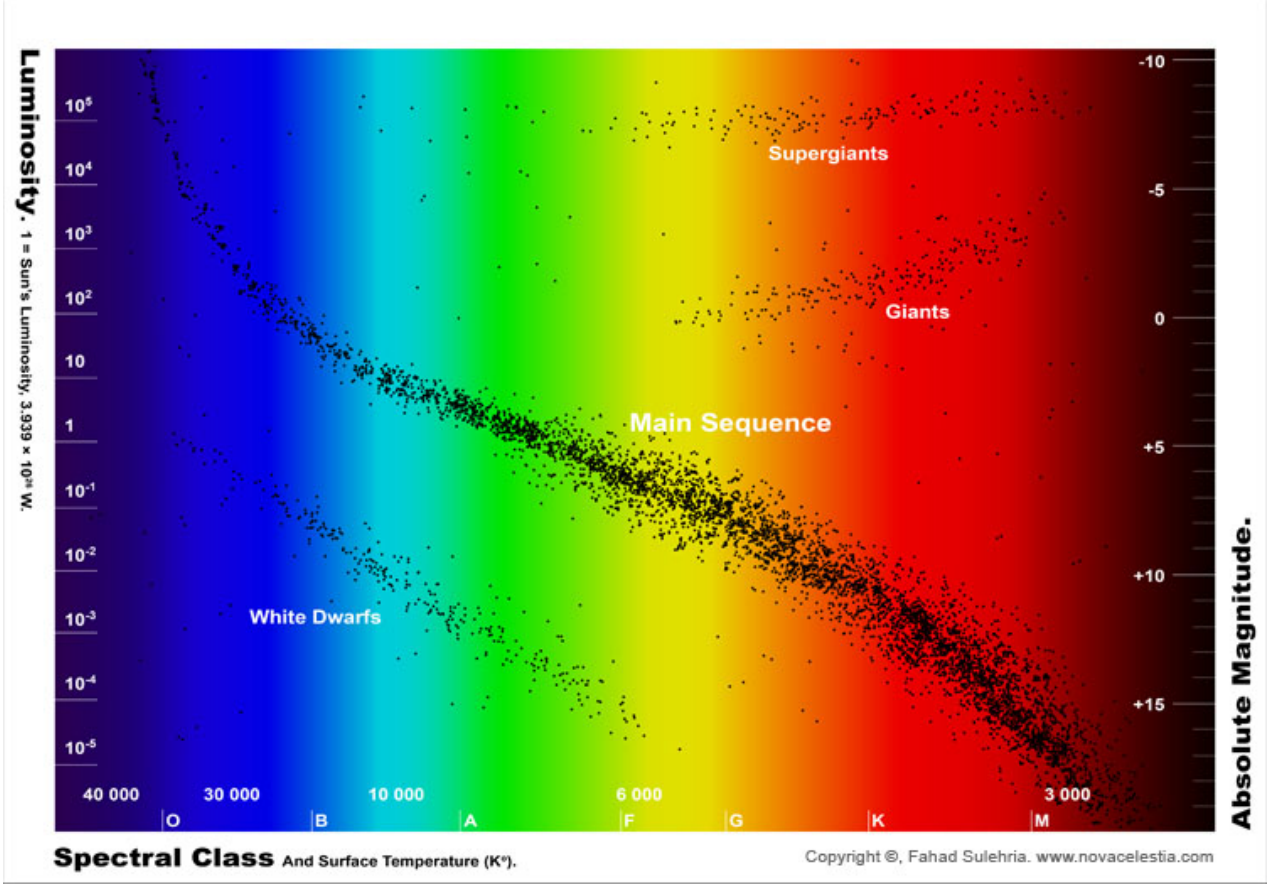

FIGURE 1.1— Hertzsprung Russell Diagram. Spectral class and temperature are shown on the x-axis, luminotisy and absolute V magnitude on the left and right y-axes, respectively. Figure courtesy from Astronomical Illustrations and Space Art, by Fahad Sulehria (http://www.novacelestia.com).

have been commonly used since the first spectral type designations. The regime where the TiO bands are measured strongly affects the spectral classification. Besides, the strenght of TiO grows from early- to late-types and becomes useless at M6, where is starts to saturate. For spectral types later than M6, metal hydrides bands (MgH, FeH and CaH) are used. They also grow towards later spectral types and do not reach saturation. On the other hand, the strongest atomic lines in the optical regime are Ca I, the Na I doublets, the K I doublet and the Ca II infrared triplet, although the Ca I and Ca II are also affected by the saturation of the TiO band at later spectral subtypes. Fig. 1.2 shows the spectra of an M4.5 and an M9.0 dwarfs with the main spectral features in the 4000–9000 Å interval, and Fig. 1.3 shows low-resolution spectra in the 4200–8300 Å range from K3.0 V to M8.0 V. It can be seen the evolution of the TiO bands towards later spectral types.

1.1.2 Photometry

The Sloan Digital Sky Survey (SDSS; York et al. 2000, Eisenstein et al. 2011) is a large-scale, CCD-based survey currently undergoing. It provides detailed three-dimensional maps of the Universe, with deep multi-colour images covering one third of the sky, and over five million astronomical spectra since its first light in 1988 (Alam et al. 2015). The camera has five filters comprising the optical window: u' (3595 Å), g' (4640 Å), r' (6122 Å), i' (7440 Å), z' (8897 Å). Because of the increasing luminosity of M dwarfs towards larger wavelengths, the *griz* filters are the most appropriate ones

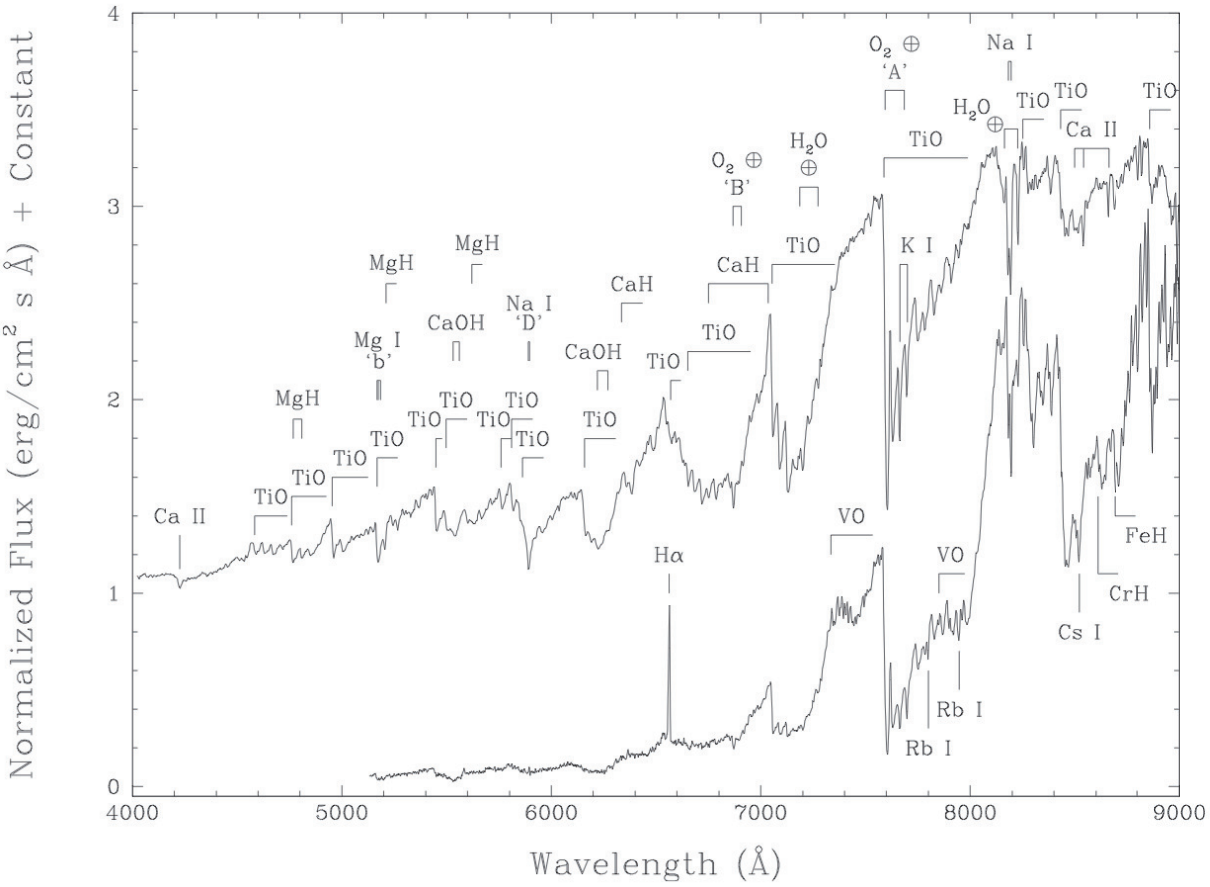

FIGURE 1.2— Optical spectra of the M4.5 dwarf υ And B (top, Lowrance et al. 2002) and the M9.0 dwarf LHS 2065 (bottom, Kirkpatrick et al. 1997). Main lines and bands are labeled on the M4.5 dwarf, and the features appearing at cooler temperatures on the M9.0 dwarf. Telluric absorption bands are not sutracted (⊕). Fluxes are normalized to unity at 7500 Å and a vertical offset of one unit in the M4.5 spectrum separates it from the M9.0 dwarf. Figure from Gray & Corbally (2009).

for characterizing M dwarfs.

At shorter wavelengths, M dwarfs present X rays flares (from 0.1 to 100 Å) or ultraviolet excess (from 100 to 3800 Å) as a consequence of their coronal and chromospheric activity, respectively. The opacity of the atmosphere of the Earth at these wavelengths makes necessary to observe the sky from balloons, sounding rockets or orbital satellites. The *ROSAT* satellite (Voges et al. 1999) and the *Chandra* (Evans et al. 2010) and *XMM-Newton* (Rosen et al. 2016) X rays observatories, have surveyed the sky to collect the high emission of the hottest stars in the Galaxy, and gathered the excess produced in cool stars due to magnetic activity. The *ROSAT* satellite surveyed 105 924 sources in soft X rays (0.1–2.4 keV; 100–5 Å) and the extreme ultraviolet (0.025–0.2 keV; 500–60 Å). The *Chandra* X rays observatory provides high resolution spectra in the 0.4–10.0 keV and 0.07–2.0 keV bands for near 94 700 sources, and the *XMM-Newton* X rays observatory, the largest and more powerful satellite ever built in Europe, provides images in the 0.15–12 keV band, and low resolution spectra in the 0.33–2.50 keV band for 396 910 sources. In the ultraviolet, M dwarfs are faint, with magnitudes around 18–23 mag in the far ultraviolet (1344–1786 Å) and the near ultraviolet (1771–2831 Å) of *GALEX*, the *Galaxy Evolution Explorer* launched in 2003 (Bianchi et al. 2011). *GALEX*

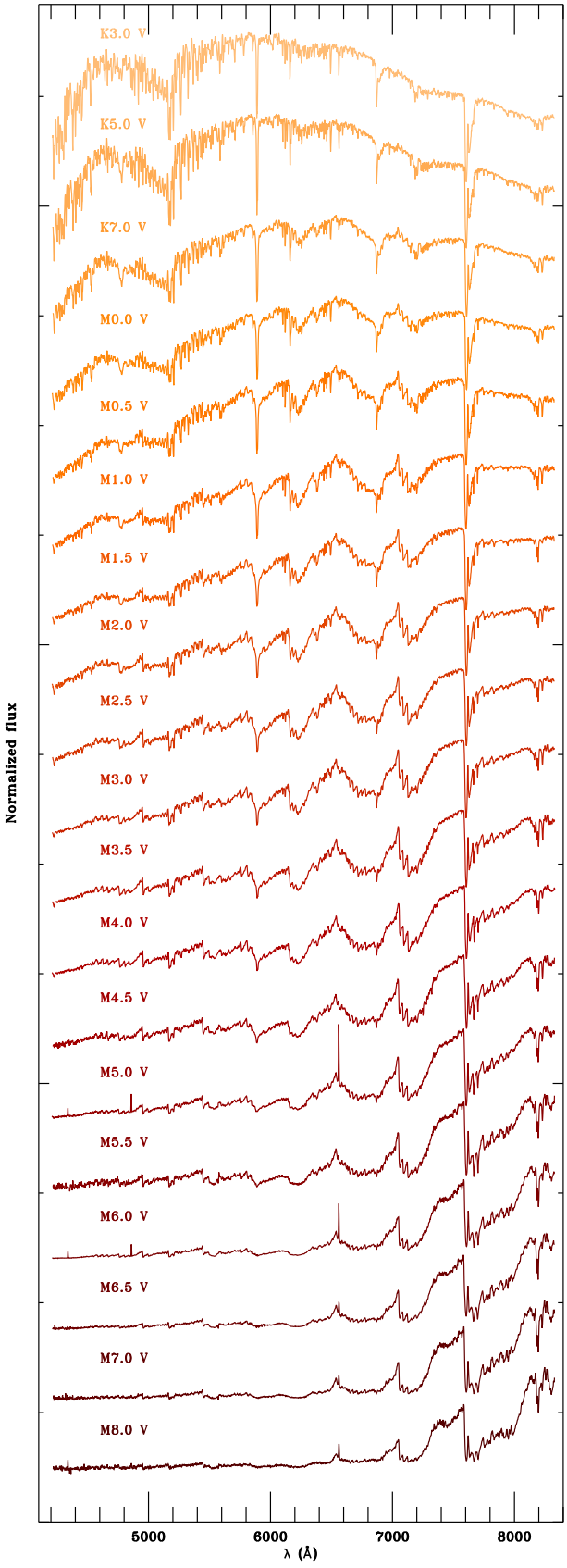

FIGURE 1.3— Low resolution CAFOS spectra of prototype dwarfs from K3.0 to M8.0 used as prototypes for spectral typing (Alonso-Floriano et al. 2015).

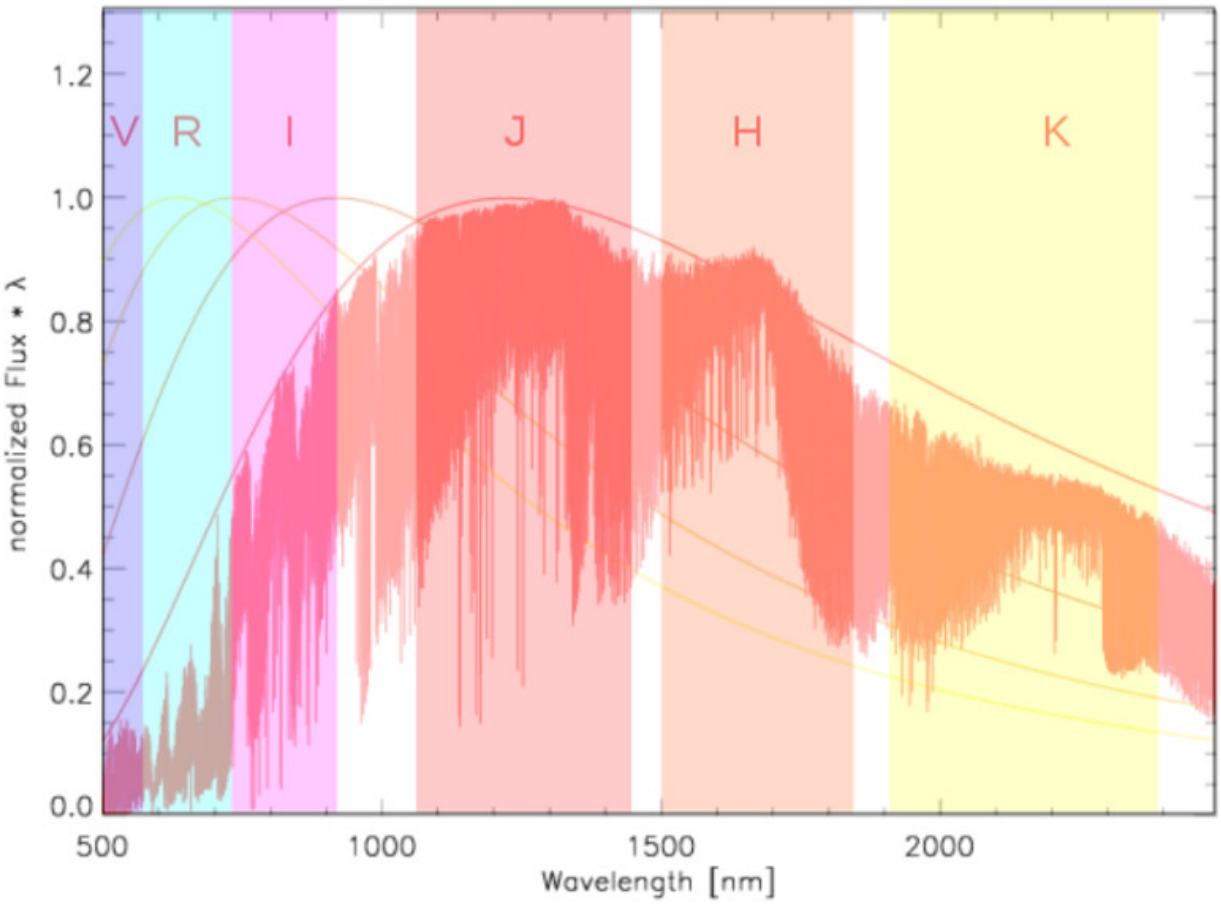

FIGURE 1.4— PHOENIX synthetic spectrum of an M dwarf. Black body spectral energy distributions for some effective temperatures are ploted in colour lines. Optical and near-infrared passbands are superposed.

was operative until 2012 and provided photometry in these two bands for more than $6.53\,10^7$ sources.

In the infrared wavelength range, the water absorption bands present in the Earth's atmosphere strongly affect the spectra of cool low mass stars, and it is in this precisly range where the energy distribution of M dwarfs peaks, between 0.9 and 1.5 μm. Because of their luminosity in the infrared, large surveys have been carried out to characterize the cooler and most numerous stars in the Galaxy in this range. In the near infrared, ground-based photometry have been succeeded. The Two Micron Sky Survey (TMSS, Newgebauer & Leighton 1969) first surveyed the sky in the $JHKL$ bands (1–4 μm). The catalogue containted around 5 600 sources, many of them M dwarfs. The TMSS catalogue was afterwards replaced by the Deep Near Infrared Survey catalogue (DENIS, Epchtein et al. 1997), which provided photometry in the I, J and K_s bands (0.85, 1.25 and 2.15 μm) for 355 220 325 point sources, and the 2-Micron All Sky Survey catalogue (2MASS, Skrutskie et al. 2006), which covered the JHK_s bands (1.25 μm, 1.65 μm, and 2.17 μm) for 470 992 970 point sources. The mid-infared photometry (from $\sim$5 to $\sim$30 μm) is strongly affected by thermal emission as well as by atmospheric absorption bands. To avoid atmospheric contribution, space-based observatories have become crucial for mid- and far- infrared observations of late-type dwarfs. The *Infrared Astronomical Satellite IRAS* extends the survey to the passbands centered in 12, 25, 60 and 100 μm

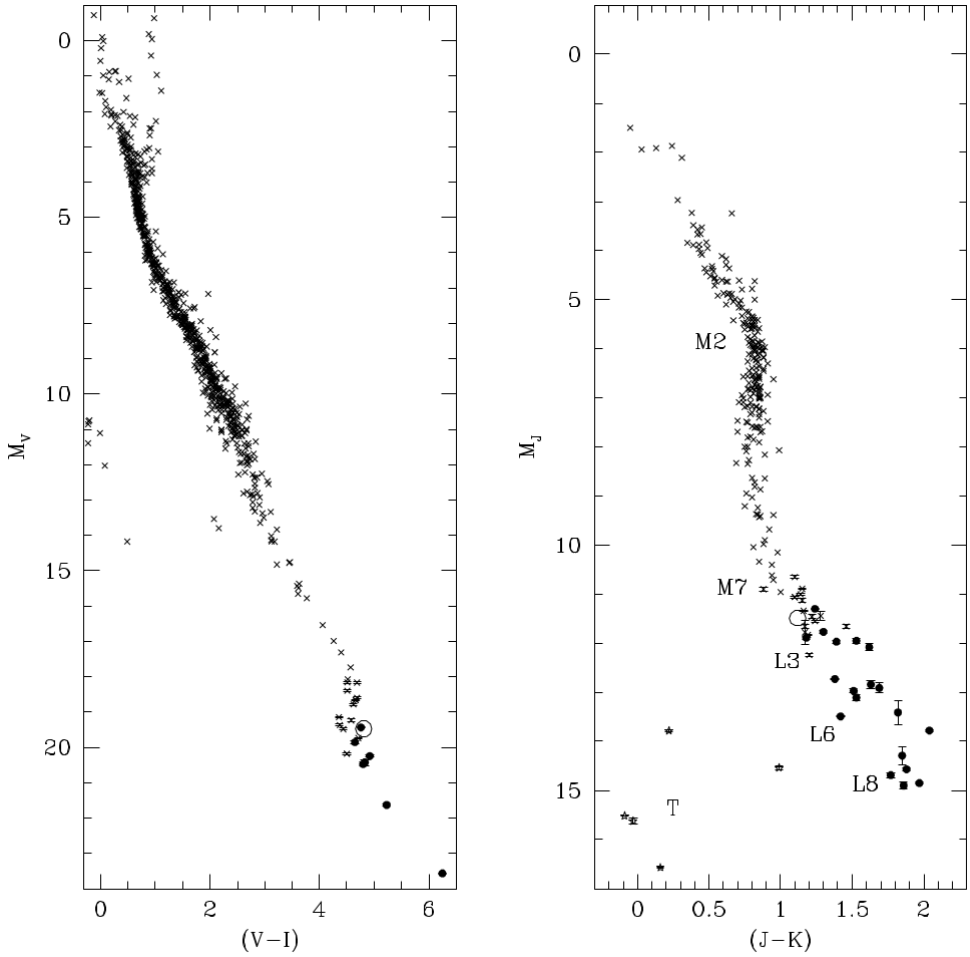

FIGURE 1.5— Colour-magnitude diagrams in the M_V-$(V-I)$ (left) and M_J-$(J-K)$ (right) planes. Crosses represent data for nearby stars, crosses with errorbars represent ultracool M dwarfs, filled circles show L dwarfs, and five-point stars mark T dwarfs. Figure from Reid et al. (2003).

and includes almost half billion faint sources.The three instruments placed at the *Space Infrared Telescope Spitzer* provide images at 3.5, 4.5, 6.3 and 8.0 μm with IRAC (InfraRed Array Camera), images and low-resolution spectra in the range from 20 to 160,μm with MIPS (Multiband Imaging Photometer Spectrometer) and low to moderate resolution in the interval between 5 and 40 μm with IRS (InfraRed Spectrograph). The *Wide-field Infrared Survey Explorer* (*WISE*; Wright et al. 2010) completed the survey in the W1, W2, W3 and W4 passbands centered in 3.4 μm, 4.6 μm, 12 μm and 22 μm, and provided astrometry and photometry for more than $3\,10^6$ sources. The WISE catalogue (Cutri et al. 2012) was extended by the ALLWISE program (Cutri et al. 2013), which enhanced the sensivity and accuracy of the former. This catalogue is highly useful for detecting and characterizing the coolest objects in the Galaxy (e.g., the Y2 dwarf WISE J085510.83071442.5 by Luhman 2014).

Fig. 1.4 shows a synthetic spectrum of an M dwarf and the coverage of different photometric passbands. These photometric bands can be used to alternatively derive some parameters of a star such as the the effective temperature, the distance or even the spectral type and the mass with the proper relations. The accuracy obtained from them does not surpass spectroscopic determinations, but they are specially usefull in this wavelength regime.

The colour of the stars is also affected by age, activity, abundance or temperature (Chamberlain & Aller 1951; Sandage & Eggen 1959), and it is therefore useful to identify subdwarfs and very cool objects or giants, due to their magnitude difference with the main sequence (see Fig. 1.1). Colour-magnitude and colour-colour diagrams are a twofold instrument built from photometry and spectroscopy. On one hand, they show the trend of stellar evolution and the general behaviour of each class. On the other hand, they can be used as a tool to determine stellar parameters (i.e., photometric distances or spectral types) from colour-magnitude relations.

For M dwarfs, colours based on optical and near-infared passbands are the best choice as they represent two opposite points of the observed slope in the spectra of cool stars. Fig. 1.5 shows two examples of colour-magnitude diagrams specific of cool low mass stars. In any case, a well determined distance is critical in the application of these diagrams for a class or spectral type determination.

1.1.3 Luminosity function

Because of their low intrinsic luminosities (from $5\,10^{-4}$ to $0.2\,L_{\odot}$), M dwarfs are not visible with the unaided eye and they have therefore been the cause and the partial solution to the "missing mass" problem in the galactic disc. This problem arised in the last century from the differences found between semi-theoretical dynamical mass density estimates and observed mass density distributions in the Galaxy (Oort 1932, 1965; Zwicky 1937; Rubin & Ford 1970). The gravitational force involved in the observed motion of stars relative to the Galactic Plane requires a local mass density to be hold of $0.15\,\mathrm{M}_{\odot}\,\mathrm{pc}^{-3}$ (Oort 1932, 1965). The sum of the contributions of the visible star components of the solar neighbourhood, gas, and dust derived from Luyten's (Luyten 1939) and Kuiper's (Kuiper 1942) luminosity functions from high proper motion catalogues, gave a lower mass density than predicted.

The observed mass density is derived from the initial mass funtion (IMF) (i.e., the total number density of stars created in a particular environment per unit mass; Miller & Scalo 1979), which depends on the luminosity function. This missing mass problem is, thus, also understood as a luminosity problem. The main contributors to the luminosity function in the Galaxy are massive stars, while low mass stars could significatively contribute to the mass due to their large number but less to the luminosity. Sanduleak (1965) and Weistrop (1972) accounted for the large number of low luminosity stars and derived a mass density about five times higher than that of Luyten, apparently solving the "missing mass" issue. These low luminosity stars were thought to be low velocity dispersion objects that were not included in the high proper motion catalogues used by Luyten (Gliese 1972). But their presence implied gravitational instability that was not sustained by kinetic energy, and that would induce gravitational collapse (Schmidt 1974). Moreover, the derived luminosity function implied a much higher number density of low mass stars than observed. This had a simple explanation: the spectophotometric parallaxes used were higher (i.e., lower distances) than photometric ones, which implied that the stars were actually more distant and brighter. Then, the derived velocity dispersions increased over a factor of two (Jones 1973, Faber et al. 1976, Weistrop 1976), and the space density decreased to values closer to those obtained from Luyten's luminosity function.

Despite the efforts, this "problem" was not really understood until the end of the last century, when more recent analysis concluded that the observed local dynamical mass barely changed but the local mass density did from $0.15\,\mathrm{M}_{\odot}\,\mathrm{pc}^{-3}$ to $0.076\,\mathrm{M}_{\odot}\,\mathrm{pc}^{-3}$ (Crézé et al. 1998).

1.1.4 Formation

The study of M dwarfs is also important because they stage the transition between helium and hydrogen burning stars (O, B, A, F, G and K) and substellar objects. Masses of field M dwarfs range between 0.6 and 0.075 $M_\odot$ (Reid & Hawley 1995). For objects with masses lower than 0.07 $M_\odot$ ($\sim$72 M_{Jup}), the temperature in the core is not enough to sustain hydrogen fusion and they become brown dwarfs. The transition between them strongly depends on the age and it could be at M or even L spectral types (Burrows et al. 1997; Baraffe et al. 1998; Chabrier et al. 2000; Zapatero Osorio et al. 2006; Kirkpatrick et al. 2011).

The formation process involving low mass stars is not certain. Star-like formation occurs from turbulent self-gravitating clouds that form bound high density clusters. When the kinetic energy of the gas pressure in the clusters does not support the potential energy of the gravitational force, they go through gravitational collapse and fragment the cloud into star forming cores. It is accepted that low mass stars and brown dwarfs form from core fragmentation in giant molecular clouds in the same way as more massive stars do (Nordlund & Padoan 2003; Elmegreen 2011), although there are other theories under discussion:

- Reipurth & Clarke (2001), Goodwin et al. (2004), Bate (2012) modeled that low mass stars and brown dwarfs form by core fragmentation from the same molecular cloud but stop accreting material due to dynamical interactions with fragments or protostars that could eject them from the core.

- Also instabilities in massive circumstellar discs may induce gravitational fragmentation that produces low mass companions to massive stars. Dynamical interactions with other companions or nearby stars play an important role in the ejection of the pre-stellar cores, leading to single low mass stars and brown dwarfs (Goodwin & Whitworth 2007; Stamatellos & Whitworth 2009).

- Whitworth & Zinnecker (2004) consider photo-erosion of the low-mass protostars in massive star forming regions, as the responsible of the arrest of accretion and consequent formation of very low mass, brown dwarfs and planetary mass objects.

1.1.5 Internal structure and activity

It is in the M dwarf regime where significant structural internal changes take place during the evolution towards cooler subtypes. Main sequence early and mid M dwarfs have convective envelopes and radiative cores, in which resides the 70%–90% of the mass of the star. At mid- M dwarfs ($\sim$ M3.5-M4.0 V), convection starts to dominate and the star finally becomes fully convective for the later subtypes (Chabrier & Baraffe 1997; Reiners 2008; Reiners & Basri 2009; Stassun et al. 2011; Shulyak et al. 2014). Fig. 1.6 represents the regions of partial and full convection during pre-main sequence evolution and on the main sequence in the HR diagram.

The presence of a convection zone allows dynamo generation of magnetic flux. This magnetic activity is observed in the emission of the Hα atomic line at 6563 Å, or through higher rotational velocities. Hα emission is used to study stellar chromospheric activity (Hawley et al. 1996; West et al. 2004; Reiners et al. 2013), while rotational velocities are conected to an $\alpha-\Omega$ dynamo situated at the radiative-convective boundary (Durney et al. 1993; Mohanty & Basri 2003; Reiners et al. 2014). M dwarfs exhibit these increasing related activity features with decreasing mass, i.e. with

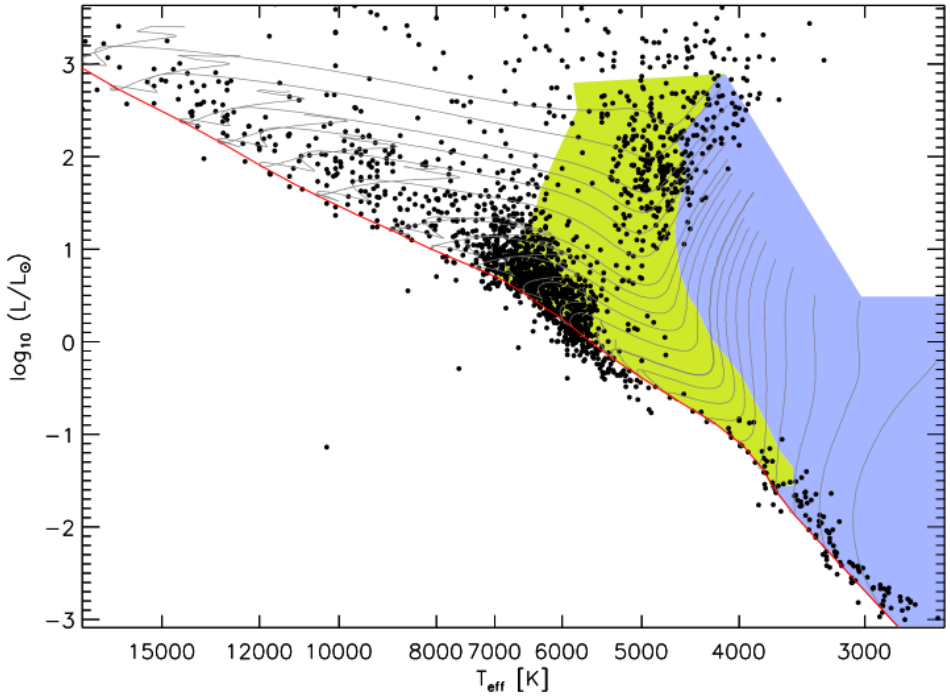

FIGURE 1.6— HR diagram showing the regions where stars have outer convective envelopes (green) and fully convective stars (blue). In gray are represented the evolutionary tracks from Siess et al. (2000), and the red line indicates the ZAMS. Figure from Reiners (2008).

decreasing temperatures towards later spectral subtypes.

Coronal activity is closely connected to chromospherical activity. The emission of X rays in M dwarfs is associated to high coronal temperatures, at which the kinetic energy is high enough not to permit gravitational binding of the plasma, requiring a magetic confinment. The X rays luminosity in M dwarfs increases as well towards $\sim$M5.0 V, i.e. towards the transitional range between partial and full convective interiors (Delfosse et al. 1998).

In the ultraviolet, most of the flux contribution comes from the chromosphere, and only part (20–30 %) from the photosphere. Walkowicz & Hawley (2009) showed that there is a positive correlation between chromospherically active stars and UV emission, and also between chromosperic and coronal activity.

In addition, young stars display more magnetic activity, either from X ray emission, Hα emission or rotation, than older ones, suggesting an age-activity connection (Soderblom et al. 1991; Mamajek & Hillenbrabd 2008). In M dwarfs, it has also been observed that activity decays with age (Silvestri et al. 2005; West et al. 2015)

1.2 Planet hunting around low mass stars

Up to date, around 3 500 exoplanets (confirmed and pending of confirmation) have been detected and registered in the Exoplanet Encyclopedia[1]. Of them, almost 90% has been discovered within

[1] `http://exoplanet.eu/`

the last six years (2010). After the transit method (the one that detects the presence of a planet by measuring the variation on the incoming light from the star as the body crosses it through its orbit), the Doppler technique (consisting of measuring variations in the radial velocity of the star caused by the gravitational effect of another body) is the most efficient method in number of discoveries: 2691 and 685 detected planets respectively, which together make more than 95% of the detections.

To confirm a planet by primary transits, it must be big enough to produce a measurable variation in the incoming flux of the star, and must have short enough periods to be able to repeatedly measure these variations. To confirm a planet by measuring radial velocity variations, it must be massive and close enough to affect the rotation of its host star. Although both methods are capable of detecting Earth-mass planets, the transit one is strongly biased toward short separations to the host star, while the Doppler technique detects planets in a wider range of projected physical separations for the same planetary masses. Fig. 1.7 compares the semi-major axis versus the mass of the detected exoplanets with both methods. The semi-major axes and masses of most of the exoplanets detected by transits range from approximately 0.01 to 0.5 au and from $2.1\,10^{-4}$ to $2.5\,M_{Jup}$ (0.07–$795\,M_{\oplus}$) respectively, while the intervals of the bulk of radial velocity detections vary from 0.02 to 6 au and from $3.2\,10^{-3}$ to $10\,M_{Jup}$ (1–$3200\,M_{\oplus}$).

Apart from the two techniques for planet hunting described before, there are also other methods used for exoplanetary detections, such as microlensing and direct imaging. Both methods work well for "face on" planets. The former is based on the gravitational effect of the planet on the passing light on a distant background star. It is well-suited for low mass planets but is highly chance-dependent and requires a big amount of telescope time. The latter is simply based on the direct seeing of the star in an image. It is also chance-dependent and it mainly detects bright planets orbiting at great distances from a nearby star. They require high human and telescope time resources and the result ends in the detection of only 50 and 72 planets with these two methods up to date.

Of the 3530 detected planets, only one third have spectral type classification of their host stars according to the Exoplanet Encyclopedia, turning out that 930 are solar-like stars (F, G and K) and 117 are M dwarfs. In terms of masses, from the 3530 planets, 1404 have mass determinations: over 300 of them have masses under $0.1\,M_{Jup}$ ($32\,M_{\oplus}$) and less than one hundred have terrestial masses (up to $5\,M_{\oplus}$). This reveals the still poor characterization of the exoplanets and their host stars.

Of the 2107 detected planets, only one half have spectral type classification of their host stars according to the Exoplanet Encyclopedia, turning out that 708 are solar-like stars (F, G and K) and 103 are M dwarfs. In terms of masses, from the 2107 planets, 1302 have mass determinations: over three hundred of them have masses under $0.1\,M_{Jup}$ ($32\,M_{\oplus}$) and less than 100 have terrestial masses (up to $5\,M_{\oplus}$). This reveals the still poor characterization of the exoplanets and their host stars.

The wide variety of planets and planetary systems found outside our frontiers (the "planetary zoo"), stands out the apparent uniqueness of the composition and position of the Earth in the Solar System. Some planets are orbiting so close to its star that their surfaces reach temperatures as high as 4200 K, or so far that their surfaces are as cool as Neptune with around 50 K. What is true, is that the high luminosity planet-star contrast, and low radius- and mass-ratios prevent us from detecting Earth-like planets orbiting solar-like stars with the current instrumenation. For this reason, planet searches are now focusing in surveying low mass stars, where the star-planet contrast is relatively large. As M dwarfs are cooler than solar-like stars, the separation of the HZ is also shorter, which makes them prime targets for search and monitorization of planets.

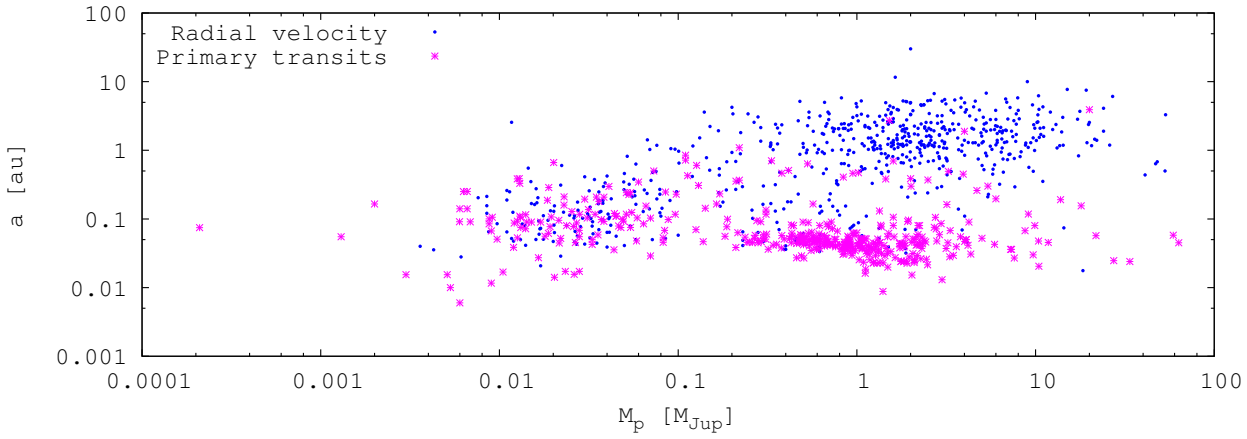

FIGURE 1.7— Masses and semi-major axes in logarithmic scale measured for the exoplanets detected with the transit (magenta asterisks) and Doppler methods (blue dots).

1.2.1 Radial velocity technique

This technique consists of measuring the wavelength shift ($\Delta\lambda$) of a spectral line that appears at λ_0 produced by the motion of the star towards or away from the observer (blue-shift or red-shift respectively):

$$\frac{\Delta\lambda}{\lambda_0} = \frac{V_r}{c}, \tag{1.1}$$

where c is the speed of light and V_r the radial component of the velocity or radial velocity.

A planet that orbits a star slightly modifies the center of mass of the system and produces the wavelength shift aimed to be measured with a certain periodicity. The semi-amplitude of the radial velocity variation has the form:

$$K_* = \left(\frac{2\pi G}{P}\right)^{1/3} \frac{\mathrm{M}_p \sin i}{(\mathrm{M}_p + \mathrm{M}_*)^{2/3}} \frac{1}{\sqrt{(1-e^2)}}, \tag{1.2}$$

where G is Newton's constant, P the orbital period, i the inclination angle between the orbital plane and the plane perpendicular to the sightline, e the eccentricity of the orbit, M_p the mass of the planet, and M_* the mass of the star (Cumming et al. 1999). This equation could be approximated as:

$$K_* \propto a^{-1/2} \frac{\mathrm{M}_p \sin i}{(\mathrm{M}_p + \mathrm{M}_*)^{1/2}} \approx (a\mathrm{M}_*)^{-1/2}, \tag{1.3}$$

for circular orbits with semi-major axis a and $\mathrm{M}_* >> M_p$. From this equation, we see that the lower the mass of the star, the higher the radial velocity semi-amplitude induced by the planet. In addition, the lower luminosity of low mass stars with respect to solar-like stars, locates the HZ closer to the star (at $\sim$0.1 au rather than $\sim$1 au), which results on an even higher induced semi-amplitude. For example, the semi-major amplitude caused by a planet like the Earth around a star like the Sun is of $K \approx 0.09\,\mathrm{m\,s^{-1}}$ for a system observed edge-on ($i = 90°$). This is below the detection limits of current instruments. On the contrary, an Earth-mass planet around an M dwarf would produce an amplitude ten times larger ($K \approx 1\,\mathrm{m\,s^{-1}}$). For this reason, low mass stars are excelent targets for

potentially habitable planet hunting with the Doppler technique.

TABLE 1.1— High-resolution near-infrared spectrographs.

Instrument name	Telescope (diameter)	$\Delta\lambda$ (λ coverage) [μm]	R ($\Delta\lambda/\lambda$)	Remark	First light
CSHELL	IRTF (3.0 m)	1.00–5.00 (0.0025)	40,000	Decommissioned	1993
Phoenix	KPNO (2.1/4.0 m)	1.00–5.00 (0.005)	70,000	Operating	1996
IRCS	Subaru (8.2 m)	0.90–5.60 ($\sim$0.2)	20,000	Polarimetry, AO	1999
NIRSPEC	Keck (10 m)	0.95–5.50 ($\sim$0.1)	25,000	AO	1999
CRIRES	VLT UT1 (8.2 m)	0.95–5.20	100,000	AO	2006
ARIES	MMT (6.5 m)	1.00–2.5	50,000	Operating	2007
GIANO[a]	TNG (3.6 m)	0.95–2.45	50,000	Operating	2012
NAHUAL	GTC (10.4 m)	0.90–2.40	70,000	Cancelled	...
IRET	ARC (3.5 m)	0.80–1.35	22,000	Cancelled	...
PRVS	Gemini (8.1 m)	0.95–1.80	70,000	Cancelled	...
MINERVA-Red	Mt. Hopkins (2$\times$0.7 m)	0.84–0.89	50,000	Cheap	2015
CARMENES	CAHA (3.5 m)	0.50–1.70	>80,000	VIS & NIR channels	2015
iSHELL	IRTF (3.0 m)	1.00-5.00 (0.25)	70,000	Gas cell, upgrade	2016
IRD	Subaru (8.2 m)	0.97–1.75	70,000	Laser comb, ceramics, AO	2016
HPF	HET (10 m)	0.84–1.30	50,000	Laser comb	2017
CRIRES+	VLT UT (8.2 m)	1.00–5.00 (0.40)	100,000	Polarimetry, upgrade	2018
SPIRou	CFHT (3.6 m)	0.98–2.35	75,000	Polarimetry	2018
TARdYS	TAO (6.5 m)	0.84–1.11	54,000	Cheap	2018
NIRPS	La Silla (3.6 m)		85,000-100,000	Being built	2018
NIRES	TMT (30 m)	1.00–2.50	100,000	Design review	>2020
GMTNIRS	GMT (25 m)	1.00–5.00	$\geq$60,000	Design review	>2020
HIRES	E-ELT (39 m)	0.31–2.50	100,000	Notional, 2–4 channels	2024

Notes. [a]GIARPS (Carleo et al. 2015) is the new common feeding for HARPS-N and GIANO.

Originally, radial velocity surveys for planet hunting mostly focused on solar-type stars (from F7 to K types), but the increasing interest on low mass stars as exoplanet hosts, focuses the surveys around them: ESO CES, UVES and HARPS (Zechmeister et al. 2009, 2013), CRIRES (Bean et al. 2010), and HARPS (Bonfils et al. 2013a). These instruments can achieve high radial velocity precisions, of $\sim$1 m s^{-1} in the best case of HARPS, but they were built to survey solar-like stars and, thus, operate in the visible part of the spectrum. Only CRIRES operates in the infrared but its accuracy downs to 5–10 m s^{-1}. Table 1.1 summarizes the most representative instruments, together with their wavelength coverage and resolution (see also Crossfield 2014; Caballero et al. 2015). Three of them have already been cancelled (IRET, Zhao et al. 2010; NAHUAL, Martín et al. 2010; PRVS, Jones et al. 2008), and CRIRES and CSHELL are being renewed to CRIRES+ and iSHELL, respectively. CARMENES (Quirrenbach et al. 2014) is operating since January 1^{th} 2016 at the 3.5 m telescope at the Calar Alto Observatory (Almería, Spain) and will be followed in short by IRD (Kotani et al. 2014), HPF (Mahadevan et al. 2014), and SPIRou (Artigau et al. 2014). The spectrographs HIRES (Maiolino et al. 2013), NIRES (Skidmore et al. 2015), and GMTNIRS (Jaffe et al. 2006; Lee et al. 2010) are expected to be operative by the end of the next decade at 30–40 m class telescopes.

Other intermediate-high resolution spectrographs that have been used to perform Doppler spectroscopy are: UCLES (Diego et al. 1990), ELODIE (Baranne et al. 1996) and afterwads CORALIE (Queloz et al. 2000) and SOPHIE (Bouchy et al. 2007), FINDS Exo-Earths (Spronck et al. 2010) or

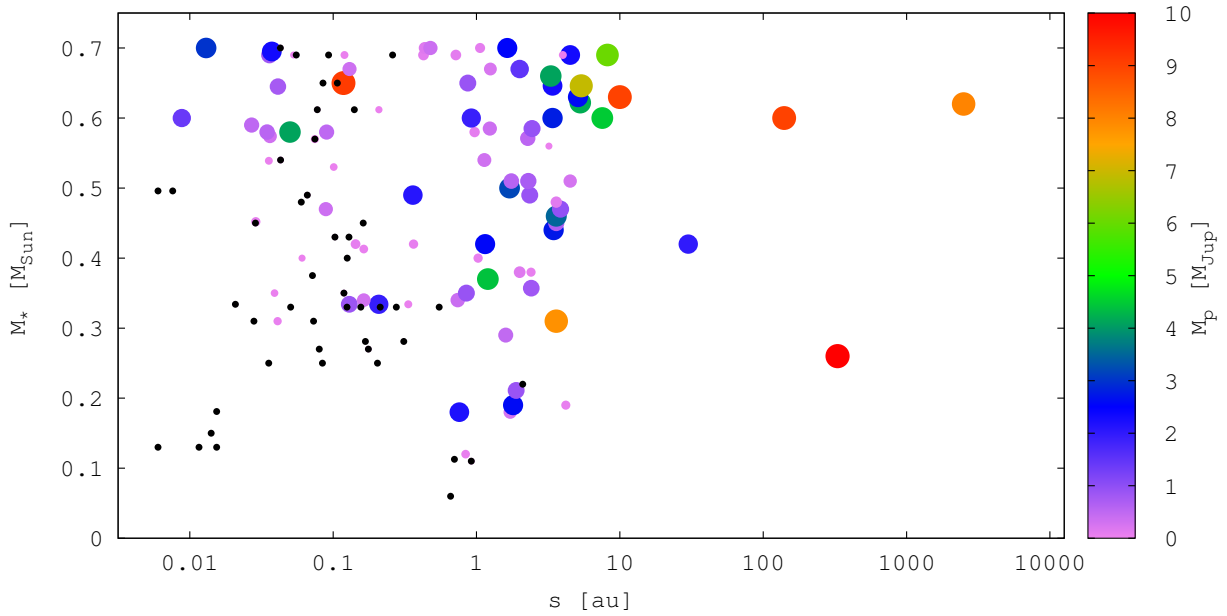

FIGURE 1.8— Semi-major axis of planets as a function of the parent star mass in the M dwarf mass regime. Black circles represent planets with masses lower than $10\,M_{\oplus}$. Colourbar indicates the mass of the planet. The size of the circles is related to the mass of the planet in logarithmic scale but the black ones.

APF (Vogt et al. 2014). They have achieved the detection of hot Jupiters or even super-Earths and brown dwarfs around solar-like stars (Bouchy et al. 2016; O'Toole et al. 2009; Wittenmyer et al. 2016). Several projects have been born since the early 1990s aiming to surpass the current accuracy limits and build a new generation of high-resolution spectrographs. Not all of them have succeed, but have anyway served for improvement. As an example in the optical, ESPRESSO aims to attain a precision of less than $10\,cm\,s^{-1}$ for solar-like stars (Pepe et al. 2010).

Although most of the detected exoplanet candidates come from primary transits, this method also presents a high number of false positive detections (Santerne et al. 2012), and many of the planet candidates requiere radial velocity follow-up to be confirmed. Besides, the full potential of the transit method is achieved from space telescopes such as *COROT* and *Kepler*, and the following *TESS* or *PLATO* (due for lunch in 2018 and 2024, respectively), to avoid photometric perturbations produced by the atmosphere, while the radial velocity techique can be exploited from ground telescopes.

Apart from exo-Earths detection, confirmation, follow-up and characterization, these instruments will also provide an efficient tool for studying stellar activity on M dwarfs, protoplanets and evolved planetary systems, supergiants, as well as the interstellar and circumstellar medium. The future of high-precision radial velocity surveys will expand in the near-infrared around low mass stars, where they emit the bulk of their energy (see Fig. 1.4 for M dwarfs). In this range, their spectra are less influenced by stellar activity than in the optical range (e.g., Martín et al. 2006; Reiners et al. 2010; Figueira et al. 2010), and a radial velocity accuracy of the $m\,s^{-1}$ level is enough to detect Earth-like planets in the HZ. Nevertheless, operating in the infrared implies challenging technological issues, such as the behaviour of hybrid CMOS sensors, the telluric absorption of the Earth's atmosphere or the cooling system of the instrument to minimize thermal noise.

1.2.2 M dwarfs hosting exoplanets

M dwarfs have not been targeted for planet searches as extensively as late-F,G and K stars, but in the last decade, a high number of exoplanets orbiting M dwarfs have been reported. M dwarfs host some of the least massive exoplanets found: Kepler–138 b, c and d, with masses $\leq 1\,M_\oplus$ orbiting an M1 V (Kipping et al. 2014), GJ676 A d and e orbiting an M0 V (Anglada-Escudé & Tuomi 2012) or GJ 876 d around an M4 (Pasinetti-Frascani et al. 2001). It has been observed that the lower the $T_{\rm eff}$ of the star, the higher the occurence of small planets (2–4 $R_\oplus$) around stars in the M0–F2 dwarf range (Howard et al. 2012). The majority of the exoplanets found around these cool dwarfs have been detected with radial velocities (Mayor et al. 2009), followed by far by imaging (e.g., Luhman et al. 2006; Deacon et al. 2016), transits (e.g., Marcy 2009; Charbonneau et al. 2009) and microlensing (e.g., Bennett et al. 2008; Han et al. 2016). Fig. 1.8 shows the semi-major axis of the planets as a function of the mass of the star host in the M dwarf regime of the planets registered up to date. It is limited to planetary masses lower than $10\,M_{\rm Jup}$ and represents separately Earth- and superEarth-mass planets (up to $10\,M_\oplus$). These low mass planets orbit at ~ 1 au or less from their stars (some of them actually lie in the HZ at around 0.1 au), and their periods range from 0.18 to 3500 d (Beaulieu et al. 2013; Rappaport et al. 2013).

The low number of planets detected around M dwarfs compared to those around solar-like stars prevents us from deriving confident statistics, and the frequency of Earth-type planets in the HZ of M dwarfs (η) is still poorly contrained. The η parameter measures the abundance of planets as a function of mass and orbital distance. From microlensing observations, Cassan et al. (2012) claimed that every star host planets in the Milky Way. They derived ratios of $0.17^{+0.60}_{-0.9}$, $0.52^{+0.22}_{-0.29}$ and $0.62^{+0.35}_{-0.37}$ for Jupiters (0.3–10 M_{Jup}), Neptunes (10–30 $M_\oplus$) and super-Earths (5–10 $M_\oplus$) at 0.5–10 au from the parent star, respectively. More specifically, the number of Earth-size planets per M dwarf has been estimated in 0.41^{+51}_{-13} from HARPS radial velocities (Bonfils et al. 2013c) and $0.51^{+0.10}_{0.20}$ from *Kepler* data (Kopparapu 2013). However, this frequence could depend on the constraints of the HZ (Kopparapu 2013). Table 1.2 lists the exact number of confirmed planets orbiting around M dwarfs up to date. CARMENES webpage[2] will host an updated version of this table.

1.3 M dwarfs in binary and multiple systems

The production of binary stars is intrinsically correlated to the star formation process, and M dwarfs in binary systems play an important roll in the determination of the dominant formation scenarios. It is not clear whether the presence of a companion enhances or prevents planet formation, and there is a limited number of exoplanet hosts in binary systems (even less in triple systems, of which there are only 17 that harbour exoplanets; Ginski et al. 2015) to answer to this question (Mugrauer et al. 2007; Mugrauer & Neuhäuser 2009).

The binary fraction quantifies the number of pairs in a given sample, and allows us to compare the population of binaries at different mass ranges and scenarios (e.g., field stars or stars in clusters). From these frequencies we can investigate the star forming conditions and the evolutionary histories of both, star multiple systems and their associated discs and planets.

[2] `http://carmenes.caha.es`

Table 1.2: M dwarfs with confirmed exoplanets discovered by transit or radial velocity methods.

Host star & Planet		Sp. type	P [d]	a [au]	$\mathcal{M}$ [$M_\oplus$]	Reference[a]	Method[b]
GX And	b	M2V	11.4433 ± 0.0016	0.0717 ± 0.003	5.40 ± 0.64	How14	RV
CD–44 170	b	M0.5V	$15.82^{+0.05}_{-0.03}$	$0.101^{+0.009}_{-0.013}$	$13.0^{+4.1}_{-6.4}$	Tuo14	RV
CD–23 1056	b	M0V	57.44 ± 0.04	0.13	127.12	Bry09; For11	RV
BD–21 784	b	M0V	$5.235^{+0.003}_{-0.006}$	$0.053^{+0.004}_{-0.007}$	$10.17^{+6.36}_{-6.04}$	Tuo14	RV
L 229–091	b	M3.5	8.6330 ± 0.0016	0.0607 ± 0.0001	10.6 ± 0.6	Bon13b	RV
	c		25.64 ± 0.02	0.1254 ± 0.0001	7.31 ± 0.95	Bon13b	RV
	d		601 ± 7	1.027 ± 0.009	21.9 ± 2.9	Bon13b	RV
EPIC 210490365	b	M4.5	3.484552 ± 0.000031	...	...	Mann16	PT
L 591–006	b	M2.5	30.60 ± 0.02	0.14	25.7 ± 1.6	AD15	RV
	d		124.0 ± 0.4	0.364	22.2 ± 1.6	AD15	RV
V830 Tau	b	M0	$4.93 \pm$	0.057 ± 0.001	244.7 ± 47.7	Don16	RV
BD+18 683	b	M2.5V	8.784 ± 0.005	0.066	9.534	End08; For09	RV
Wolf 1539	b	M3.5	2290 ± 60	2.41 ± 0.04	260.6 ± 22.2	How10	RV
L 736–030	b	M2V	$17.380^{+0.018}_{-0.020}$	$0.103^{+0.006}_{-0.014}$	$8.3^{+3.5}_{-5.4}$	Tuo14	RV
	c		$24.33^{+0.05}_{-0.07}$	$0.129^{+0.007}_{-0.017}$	$6.4^{+3.8}_{-4.1}$	Tuo14	RV
L 521–002	b	M2.5	14.207 ± 0.007	0.089	111.4 ± 1.6	AD15	RV
CVSO 30	b	M3	0.448413 ± 0.00004	0.00838 ± 0.00072	1970^{+604}_{-540}	VE12	PT
HATS-6	b	M1V	3.3252725 ± 0.0000021	$0.03623^{+4.2E-4}_{-5.7E-4}$	101.4 ± 22.2	Hart15	PT
HD 41004 B	b	M2	1.32363 ± 0.000089	0.0177	5847 ± 70	Zucke04	RV
BD–21 1377	b	M1/M2V	471^{+20}_{-12}	$0.97^{+0.12}_{-0.09}$	31.8 ± 15.9	Tuo14	RV
K2-26	b	M1	$14.5665^{+0.0016}_{-0.002}$	...	...	Bei16	PT
LP 424–004	b	M1.5	3.33671 ± 0.00005	0.0356 ± 0.0010	14.0 ± 1.6	Bon12; LP14	PT
GJ 317	b	M3.5	692 ± 5	1.15 ± 0.05	572 ± 16	John07; AT12	RV
	c		10000	30 ± 10	635.6	John07; AT12	RV
L 320–124	b	M3.5	1.62893 ± 0.000031	0.0154 ± 0.0015	1.62 ± 0.54	BT15	PT
LP 905–036	b	M2.5	2.6456 ± 0.0007	0.0287 ± 0.0011	6.99 ± 1.27	Bon11	RV
HD 304043	b	M3.5V	$26.16^{+0.08}_{-0.10}$	$0.119^{+0.014}_{-0.011}$	$9.85^{+5.72}_{-3.81}$	Tuo14	RV
K2-22	b	M0V	0.381071 ± 0.000001	0.0088 ± 0.0008	$445^{+0.0}_{-445}$	SO15	PT
K2-3	b	M0.0V	10.05449 ± 0.00026	0.0775 ± 0.0039	8.3 ± 2.1	Sin15	PT
	c		24.64354 ± 0.00117	0.1405 ± 0.0067	$2.1^{+2.1}_{-1.3}$	Sin15	PT
	d		44.5598 ± 0.0059	0.2086 ± 0.01	11.1 ± 3.5	Mont15	PT
CD–31 9113	b	M1.5	$7.370^{+0.003}_{-0.004}$	$0.060^{+0.004}_{-0.008}$	5.4 ± 1.9	Don10; Tuo14	RV
	c		3700 ± 200	3.6	44.5	Del13	RV
Ross 1003	b	M4V	41.397 ± 0.016	0.163506 ± 0.00004	95.3 ± 6.4	Hag10	RV
Ross 905	b	M2.5	2.64394 ± 0.0001	0.0289 ± 0.0010	22.2 ± 1.6	But04; Sou10	PT
Proxima Centauri	b	M5.5V	11.186 ± 0.001	0.0485 ± 0.041	1.27 ± 0.19	AE16	RV
HO Lib	b	M2.5V	5.36865 ± 0.00009	0.04	15.89	Bon05b; For11	RV
	c		12.918 ± 0.002	0.07	5.40	Udr07; For11	RV
	e		3.14945 ± 0.00017	0.03	1.91	May09; For11	RV
NLTT 41135	b	M5.1	2.889475 ± 0.000025	0.024 ± 0.001	10710 ± 900	Irw10	PT
K2-33	b	M3.3	5.42513 ± 0.00029	0.0409 ± 0.0023	$1144^{+0.00}_{-1144}$	Dav16	PT
LP 804–27	b	M3V	111.7 ± 0.7	636	2	Apps10	RV
Wolf 1061	b	M3V	4.8876 ± 0.0014	0.035509 ± 0.0000007	1.36 ± 0.23	Wri15	RV
	c		17.867 ± 0.011	0.08427 ± 0.00004	4.26 ± 0.38	Wri15	RV
	d		67.27 ± 0.12	0.2039 ± 0.0002	5.21 ± 0.67	Wri15	RV
BD+25 3173	b	M1.5	598.3 ± 4.2	1.135 ± 0.035	104 ± 10	John09	RV
	c		4.4762 ± 0.0004	0.0430 ± 0.0010	9.5 ± 2.5	Witt13	RV
GJ 1214	b	M4.5V	$1.58040482 \pm 0.00000018$	0.0141 ± 0.0003	3.36 ± 0.95	Cha09	PT
BD+11 3149	b	M1.0V	13.74 ± 0.02	0.089	1990^{+250}_{-240}	Aff16	RV
	c		2.6498 ± 0.0008	0.029	785 ± 86	Aff16	RV
CD–34 11626C	b	M1.5V	7.2004 ± 0.0017	$0.0505^{+0.004}_{-0.005}$	5.72 ± 1.27	Bry09; AE13	RV
	c		28.14 ± 0.03	$0.125^{+0.012}_{-0.013}$	$3.18^{+15.89}_{-19.07}$	Bon11; AE13	RV
	d		$91.6^{+0.8}_{-0.9}$	$0.276^{+0.02}_{-0.03}$	$5.08^{+1.91}_{-1.59}$	AE12; AE13	RV
	e		62.2 ± 0.6	0.213 ± 0.02	$2.54^{+1.59}_{-1.27}$	AE13	RV
	f		$39.03^{+0.19}_{-0.20}$	$0.156^{+0.014}_{-0.017}$	2.54 ± 1.27	AE13	RV
	g		256^{+14}_{-8}	$0.549^{+0.052}_{-0.058}$	$4.45^{+2.54}_{-2.22}$	AE13	RV
CD–46 11540	b	M2.5	4.6944 ± 0.0018	0.04	12.71	Bon07; WF11	RV
CD–51 10924A	b	M0V	1050.3 ± 1.2	1.80 ± 0.07	1590 ± 95	For11; AE12	RV

Table 1.2: M dwarfs with confirmed exoplanets discovered by transit or radial velocity methods (cont.).

Host star & Planet		Sp. type	P [d]	a [au]	$\mathcal{M}$ [$M_\oplus$]	Reference[a]	Method[b]
	c		4400.0	5	953	AT12	RV
	d		3.6000 ± 0.0008	0.0413 ± 0.0014	4.45 ± 0.64	AT12	RV
	e		35.37 ± 0.07	0.187 ± 0.007	11.44 ± 1.59	AT12	RV
BD+68 946	b	M3.5V	38.14 ± 0.015	0.16353 ± 0.00004	18.43 ± 2.22	Burt14	RV
CD–44 11909	b	M3.5V	$17.48^{+0.06}_{-0.04}$	$0.08^{+0.014}_{-0.004}$	$4.45^{+3.81}_{-2.54}$	Tuo14	RV
	c		$57.3^{+0.4}_{-0.5}$	$0.176^{+0.030}_{-0.009}$	$8.58^{+5.72}_{-4.45}$	Tuo14	RV
Kepler-138	b	M1V	$10.31320643 \pm 0.0000265$	0.0746	$0.0667^{+0.0002}_{-0.0001}$	Row14	PT
	c	M1V	$13.78164^{+1.9E-4}_{-1.4E-4}$	...	$1.01^{+0.41}_{-0.35}$	Row14	PT
	d	M1V	23.08933 ± 0.00071	...	$1.01^{+0.42}_{-0.34}$	Row14	RV
Kepler-45	b	M	2.455239 ± 0.000005	0.027 ± 0.003	160 ± 3	Sza12	PT
BD–05 5715	b	M3.5V	1914 ± 26	2.35	286 ± 16	But06; Mont14	RV
	c		7000^{+2000}_{-6000}	...	264	Mont14	RV
LP 700–006	b	M4	2.260455 ± 0.000041	0.0214 ± 0.0013	...	Hir16	PT
EPIC 206011691	b	M0	$9.32414^{+5.9E-4}_{-6.3E-4}$	$0.0731^{+0.0057}_{-0.0067}$	...	Pet15	PT
	c		$15.5012^{+9.3E-4}_{-9.9E-4}$	$0.1026^{+0.0079}_{-0.0094}$	...	Pet15	PT
IL Aqr	b	M4 V	61 ± 4	0.20832 ± 0.00002	612 ± 1	Mar98; Riv10	RV
	c		30.23 ± 0.19	0.12959 ± 0.00002	202.4 ± 0.6	Mar01; Riv10	RV
	d		1.94 ± 0.01	0.0208066 ± 0.0000002	5.4 ± 0.3	Riv05; Riv10	RV
	e		124.69 ± 90	0.3343 ± 0.0013	12.4 ± 0.3	Riv10	RV
2MUCD 12171	b	M8	1.510848 ± 0.000019	0.01111 ± 0.0004	...	deW16	PT
	c		2.421848 ± 0.000028	0.01522 ± 0.00055	...	deW16	PT
	d		$18.202^{+54.0}_{-14.0}$	0.08 ± 0.06	...	deW16	PT

Notes. [a]References of the discovery and, if not the same, planet properties. AD15: Astudillo-Defru et al. (2015); AE12: Anglada-Escudé et al. (2012); AE13: Anglada-Escudé et al. (2013); AE16: Anglada-Escudé et al. (2016); Aff16: Affer et al. (2016); Apps10: Apps et al. (2010); AT12: Anglada-Escudé & Tuomi (2012); Bei16: Beichman et al. (2016); Bon05b: Bonfils et al. (2005b); Bon07: Bonfils et al. (2007); Bon11: Bonfils et al. (2011); Bon12: Bonfils et al. (2012); Bon13b: Bonfils et al. (2013b); Bry09: Bryden et al. (2009); BT15: Berta-Thomson et al. (2015); Burt14: Burt et al. (2014); But04: Butler et al. (2004); But06: Butler e al. (2006); Cha09: Charbonneau et al. (2009); Dav16: David et al. (2016); Del13: Delfosse et al. (2013); deW16: de Wit et al. (2016); Don10: Donnison (2010); Don16: Donati et al. (2016); End08: Endl et al. (2008); For09: Forveille et al. (2009); For10: Forveille et al. (2010); For11: Forveille et al. (2011); John07: Johnson et al. (2007); John09: Johnson et al. (2009); Hag10: Haghighipour et al. (2010); Hart15: Hartman et al. (2015); Hir16: Hirano et al. (2016); How10: Howard et al. (2010); How14: Howard et al. (2014); Irw10: Irwin et al. (2010); Lee12: Lee et al. (2012); LP14: López & Fortney (2014); Mann16: Mann et al. (2016); Mar98: Marcy et al. (1998); Mar01: Marcy et al. (2001); May09: Mayor et al. (2009); Mont14: Montet et al. (2014); Mont15: Montet et al. (2015); Pet15: Petigura et al. (2015); Riv05: Rivera et al. (2005); Riv10: Rivera et al. (2010); Row14: Rowe et al. (2014); Sin15: Sinukoff et al. (2015); SO15: Sanchis-Ojeda et al. (2015); Sou10: Southworth (2010); Sza12: Szabo et al. (2012); Tuo14: Tuomi et al. (2014); Udr07: Udry et al. (2007); VE12: Van Eyken et al. (2012); WF11: Wang & Ford (2011); Witt13: Wittenmyer et al. (2013); Wri15: Wright et al. (2015); Zucke04: Zucker et al. (2004). [b] Primary Transits (PT); Radial Velocity (RV).

The most recent and complete study of the influence of stellar multiplicity on planet formation was carried out in the series of papers iniciated by Wang et al. (2014). For multiple systems with separations lower than 20 au, the multiplicity rate of planet host stars is significantly lower than for a field control sample in the solar neighbourhood. In the specific case of giant planets these rates are 0^{+5}_{-0}% and 18 ± 2% respectively. At separations between 100 and 2000 au, the stellar multiplicity rate of multiple transiting planet systems and single transiting planet systems are very similar (8.0 ± 4.0% and 6.4 ± 5.8% respectively), and are lower but compatible with the multiplicity rate derived for field stars (12.5 ± 2.8%). Hence, the abundance of planets in multiple systems with separations smaller than 2000 au appears to be smaller than for single stars, due to the dynamical influence of the companions. This suggests that the presence of a close companion suppresses planet formation and evolution. Nonetheless, more studies of exoplanets in known multiple systems or companion searches around planet host stars need to be performed for a significant statistical analysis. In the low mass regime, with the scarce number of M dwarfs with known exoplanets detected with radial-

velocity and transit methods (Rivera et al. 2005; Charbonneau et al. 2009; Bonfils et al. 2013a) is not possible yet to analyze how stellar multiplicity at such low masses affects planet formation.

From multiplicity surveys in young clusters (∼1–2 Ma) we can obtain information relative to the multiplicity distribution as a function of the star density and infer the intial conditions of binary formation. On one hand, the observed multiplicitiy distribution in young clusters for G5–M5.5 stars (0.1–30 $M_\odot$) appears to be similar to the distribution of field stars for separations greater than ∼100 au and up to 620 au, despite higher density regions are expected to favour dynamical interactions (Kroupa 1995a, b, c; Parker et al. 2009). At lower separations, at which dynamical disruption processes do not significantly interfere, there is an overabundance of binaries in low-density regions (King et al. 2012a, 2012b) and an excess of low mass binaries compared to field binaries (see also Biller et al. 2011; Kraus et al. 2011). These results lead to the assumption that all low mass stars form in binary or multiple systems (Goodwin & Whitworth 2007; King et al. 2012a). For stellar densities high enough, simulations on dynamical evolution over time would led to the observed frequency of field stars (Kroupa 1995a, b, c; Parker et al. 2009). On the other hand, the discrepancies between binary distributions in different density scenarios, imply a not universal star formation rate and, hence, a not universal star formation process (King et al. 2012b; Duchêne et al. 2004; Goodwin 2010).

Regarding the multiplicity frequency of M dwarfs, the first complete study was carried out by Fischer & Marcy (1992). From a radial velocity and wide-field imaging compilation, the infered multiplicity fraction was 42 %, close to the 44–65 % fraction of solar-like stars (Duquennoy & Mayor 1991; Raghavan et al. 2010). It is the highest fraction given for these stars and has not been reproduced by the numerous studies of field M dwarfs performed during the last decade (e.g., Bergfors et al. 2010; Ward-Duong et al. 2015). In comparison with solar-like and lower mass primaries, there is an observed decreasing trend of the multiplicity frequency towards lower masses, also supported by hydrodynamical simulations (Bate 2009, 2012): from the ∼ 65 % of solar-like stars (Duquennoy & Mayor 1991), through the 21–32 % of M dwarfs (Bergfros et al. 2010; Jódar et al. 2013; Janson et al. 2012, 2014), to the ∼ 12 % and ∼ 9 % of L and T dwarfs (Reid et al. 2008 and Burgasser et al. 2003, respectively).

1.3.1 Close binaries

The detection of close binaries is subject to the projected separation of the components and their masses. The most common finding methods used are radial velocity, speckle interferometry, adaptive optics and lucky imaging. Due to the spacial overlap with low-resolution images and other procedures to find physical companions, I will refer to close separations when angular separations are shorter than 5 arcsec.

The radial velocity method, as explained in Section 1.2.1, is highly efficient at very short separations. The effect of a stellar companion around an M dwarf would induce a variation in the radial velocity a thousand times larger than an exoplanet (i.e., in the $km\,s^{-1}$ scale rather than $m\,s^{-1}$). For larger separations, high-resolution imaging is required, although their detection is limited to bright enough companions.

The light coming from a star passes through the atmosphere and becomes diffracted and affected by atmospheric turbulences. To avoid such distortions, high angular resolution cameras have been improved since the early 1980s (Mccarthy & Cobb 1986; Beckers 1993; Graves et al. 1994) with the

aim of giving diffraction-limited images. In spite of the decrease of the angular resolution towards longer wavelengths, at these wavelengths the atmosphere stability permits longer integration times and a higher signal. Speckle interferometry, adaptive optics and lucky imaging take advantages of it. These techniques are based on very short exposure time images (from 10 to 100 ms), in order to avoid the effects associated to the variation of the atmosphere and to obtain images close to the diffraction limit.

- The speckle interferometry was developed in 1970 (Labeyrie 1970) and further improved under the same statement: the application of Fourier techniques to reconstruct the source structure from the speckle pattern obtained with short integrated images. Each image has short enough exposure times to "freeze" the atmosphere but has low number of photons and, hence, low signal. For these reason, hundreds of images are required.

- The adaptive optics technique is based on the removal of the wavefront distortions introduced by the atmosphere, typically with a deformable mirror whose surface is designed to be adjusted to match the wavefront distortion (Roddier 1988). The guiding system has evolved from the natural one (NGS), which follows a field star, to the laser guide system (LGS), which guides the telescope through a laser beam. The diffraction limit of this technique ranges from 0.022 mas at 0.85 μm to 0.06 mas at 0.9 μm, and the field of view varies from 10×10 to 56×50 depending on the camera (AOB/KIR at CFHT, Thomas et al. 1998; Keck AO at Keck II, Wizinowich et al. 2000; NACO at VLT UT, Lenzen et al. 2003, Rousset et al. 2003).

- The lucky imaging technique (Tubbs et al. 2002) consists of taking frames of thousands of images each with high speed and low noise cameras. This method has two possible ouputs: a combination of all the obtained images or a combination of the selected percentage (typically 1, 10 or 50%) of the best images, useful to obtain a better quality outcome. The resolution limits of this technique range from 0.06 to 0.15 mas in the I-band. The typical field of view of these imagers is around $24 \times 24\,\mathrm{arcsec}^2$ or less and they operate in the infrared I, i' and z' bands (LuckyCam at NOT, Law et al. 2006; FastCam at TCS, NOT or WHT, Oscoz et al. 2008; AstraLux Norte at CAHA, Hormuth et al. 2008; AstraLux Sur at NTT, Hippler et al. 2009). A combination of the adaptive optics and lucky imaging techniques (AOLI) has been deployed (Mackay et al. 2012), getting the best of each.

It has been studied whether low mass binaries have some impact in the inferred mass function, since photometric parallax studies have systematically neglected them because of their faintness. Low mass binaries might actually have some influence in the mass function, specially at masses lower than $0.5\,\mathrm{M}_\odot$ (Kroupa et al. 1991; Kroupa 2001), at which stars slightly contribute to the luminosity function.

Apart from the implication of low mass binaries in star-formation scenarios, they are also essential in the determination of physical properties of stars, specially masses, which is possible when the pairs complete at least one orbit during a human lifetime and heliocentric distances are well known. The described methods allow us to determine high precision dynamical masses. Using them for well-characterized M dwarfs, we can estimate photometric masses for isolated stars and stars in systems with long periods by relating luminosities (absolute magnitudes) and masses (Delfosse et al. 2000; Xia et al. 2008). When the star comprises an eclipsing binary, a combined analysis of astrometric, spectroscopic and photometric data allows to determine the radius, distance and even effective temperatures through light and radial velocity curves (Torres et al. 2010). The study of the

long-time behaviour of the period of eclipsing binaries permits to determine the orbit of the system, and also serves to identify the presence of a distant companion orbiting around the common centre of mass with the eclipsing binary (see Irwin 1959; Mayor, 1990).

Chapter 4 goes more into detail of the behaviour of close M dwarf binarity, as a result of a lucky imaging search of companions around M dwarfs performed in this thesis.

1.3.2 Wide and very wide binaries

The existence of cool dwarfs in wide multiple systems helps in the investigation of their formation and evolution, as well as to understand star formation processes and the sub-structure in star forming regions. They are of special interest if the other component is a Sun–like star (useful for metallicity studies; Bonfils et al. 2005a, Rojas-Ayala et al. 2012, Mann et al. 2014, Newton et al. 2014), a white dwarf (useful for nuclear-age determination; Garcés et al. 2011) or even an identical M dwarf with different rotation period or X–ray emission (useful for comparative magnetic breaking models; Caballero et al. 2010).

Companions to M dwarfs separated by more than 5 arcsec (the lower limit considered here to name them wide) can be more easily identified with photographic plate digitisations, low-resolution CCD images, and astrometric catalogues. By-eye comparison of images over different epochs as in Luyten (1979), it is simple to associate companionship for maximum separations of dozens of arcminutes but less than 1 deg, depending on the magnitudes of the stars and the field density. Astrometric catalogues allow us to measure proper motions by using the position of the star at different epochs, and to look for common proper motion stars in the field. This method is commonly used for common-proper motion searches in a wide range of separations (of the order of degrees), and it is specially useful for faint companions (using the most suitable bands), which may not have proper motion measurements in the literature. These search methods will be described in more detail in Chapters 3 and 5.

In general terms, there is not consensus about the maximum projected separation at which a wide pair is still physically bound and orbits around its centre of mass. Moreover, the limit between very wide bound pairs with very low binding energies and common proper motion pairs (pairs sharing proper motion without any discernible relative orbital motion; Batten 1973) is not defined, and the discussion whether wide binaries shall also include common proper motion pairs remains open (Caballero et al. 2009 and references therein). Besides, members of stellar kinematic groups travel together and might share common proper motion and Galactic spatial velocities (UVW) in addition to their common origin (the disolution of an open cluster or the result of global dynamical mechanisms in the Galaxy), and their ages are constraint at $\tau \leqslant 600$ Ma or less (Soderblom & Mayor 1993; Montes et al. 2001; Zuckerman & Song 2004). Depending on the total mass of the system, the separation of very wide pairs could reach $\sim 2\,10^5$ au (~ 1 pc) or more (Caballero 2009, 2010; Shaya & Olling 2011), although the limit is commonly considered to be at $\sim 2\,10^4$ au (~ 0.1 pc), which is the typical size of protostellar cores (Weinberg et al. 1987; Close et al. 1990; Tokovinin & Lépine 2012). Systems with such separations could either be weakly bound binaries or unbound members of the same stellar kinematic group. However, few pairs have been found at this regime in the Galactic disc, probably due to their lower chances of survival through dynamical encounters over time.

The most recent catalog of very wide low mass pairs, SLoWPoKeS (Dhital et al. 2010) evidences

the existence of common proper motion low mass pairs with projected separations larger than 500 au in the range from K5 to M7 stars. In this regime, the separation distribution of the pairs shows a break at $\sim 2\,10^4$ au (~ 0.1 pc), suggesting different formation mechanisms or significatively different dynamical history. Pairs with separations closer than that value are expected to survive 10 Ga or longer, while ultra-wide pairs are not expected to last more than a few Ga (Dhital et al. 2012). Also binarity fraction is affected at these ranges and strongly depends on the separation of the components. For projected separations up to 1000 au, the binarity fraction is in agreement with the frequency found at closer separations ($\leqslant$ 300 au), being around 20%. High order multiplicity fraction appears to increase with increasing the separation between components. Wide pairs with separations up to 2000 au show a multiplicity fraction of 21%, while components separated by more than 4000 au can harbor simultaneusly closer components and increase the fraction up to 77% (Law et al. 2010; Dhital et al. 2012). These results indicate the influence of dynamics in the formation and stability of binary and higher-order multiples. Besides, the decreasing higher-order multiplicity with Galactic height, i.e., with age, proves the dynamical disruption of the systems over time (Dhital et al. 2012).

1.4 CARMENES

After an overview of the actual status of the knowledge of low mass objects, stands out their relevance in modern astrophysics. The abundance of M dwarfs makes them an atractive sample for statistics of low mass stars formation and evolution processes, as well as planet occurrence. It is crucial to study these stellar objects to understand the physics of planet formation and evolution and its dependence on stellar host mass.

This section will describe CARMENES as the three fundamental vertices of a triangle: a project, led by a consortium in charge of the construction of an instrument.

1.4.1 The project

In 2008, the announcement of an open call for ideas for new instrumentations for the CAHA observatory put several proposals on the table, among which were some designs for high-resolution single-object and multi-object spectrographs in the visible wavelength range with similar science cases as CARMENES, coming from spanish and german institutions. In prediction of what could and would be, both, spanish and german projects merged into a prime project with increasing probabilities of obtaining funds and thus, more viability and visibility.

In early 2009 the instrument CARMENES became the first instrument proposed, accepted and co-led by a spanish institution that would be built for and in operation at CAHA. At the end of the year, the CAHA Executive Committee selected CARMENES as the next-generation instrument for the CAHA 3.5 m telescope. Initially and according to the defined schedule, the CARMENES instrument was supposed to have its first light in 2014 but, due to a delay in its construction and set-up among other reasons, it had its first light at the end of 2015 and fully operates since January 2016.

The main scientific objective of the project is detecting by Doppler effect Earth-size planets around M dwarfs in their habitable zones by achieving a radial velocity precision of $1\,\mathrm{m\,s^{-1}}$, enough to detect a $2\,M_\oplus$ planet in the habitable zone of an M5 V star or super-Earths ($5\,M_\oplus$) around stars later than M4 V. Fig. 1.9 shows the position of the habitable zone as a function of the mass of the host star (i.e., the spectral type) and the expected masses and precision of planet detections. Fig. 1.10 shows the radial velocity curve obtained from CARMENES VIS (optical) channel produced

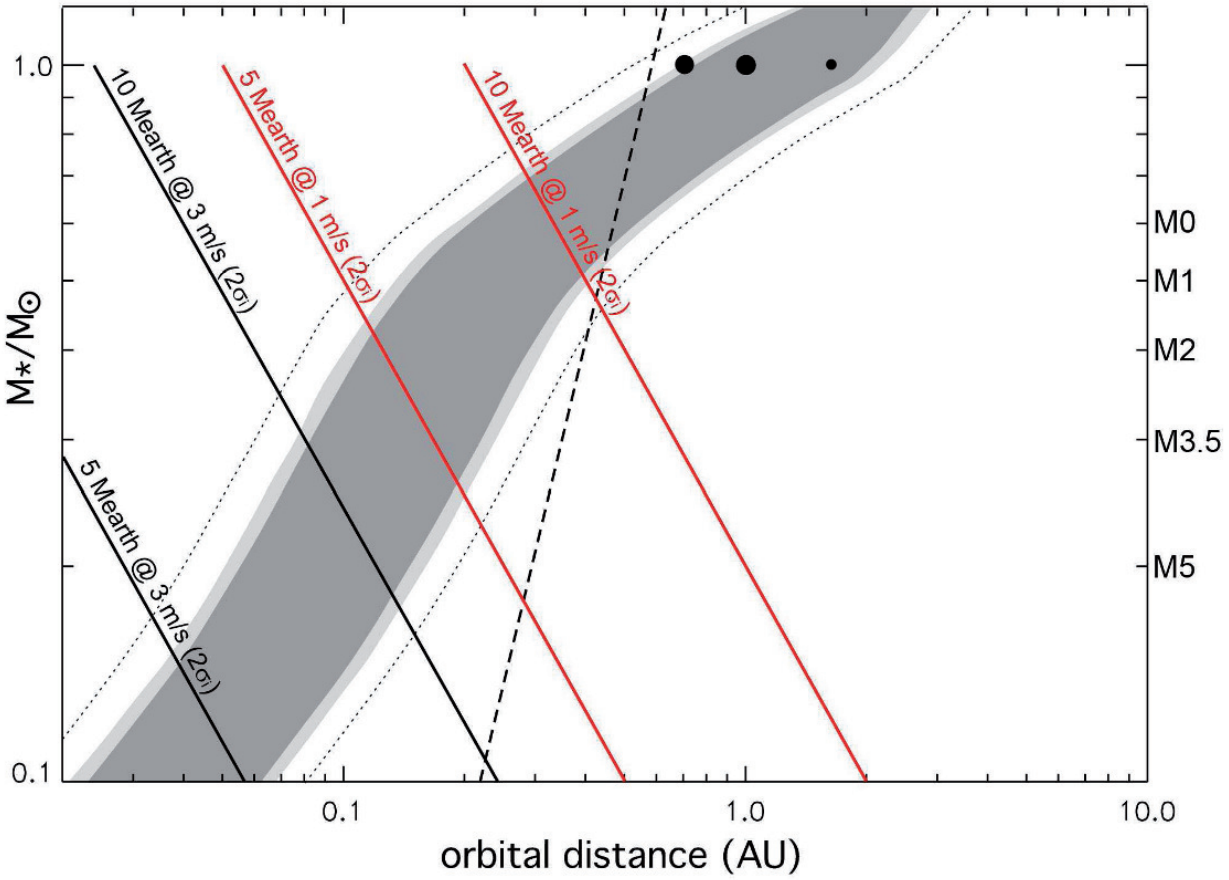

FIGURE 1.9— Dependence of the habitable zone (shaded area) on the stellar mass and orbital separation. An estimation of spectral types is indicated in the right y-axis. Dashed line ilustrates tidal locking separation. Solid lines represent the detection limits at the significance of twice the individual measurement error (σ_i) of super-Earth planets (5–10 $M_\oplus$) at different radial velocity precisions (1 m s^{-1} – red– and 3 m s^{-1} – black–). To the left of the lines lie the accesible region. Figure from Quirrenbach et al. (2010).

by a 2.6 d period planet orbiting around Ross 905 (GJ 436). The orbital parameters of the system are also displayed.

During Guaranteed Time Observations (600 nights with a possible buffer of another 150 nights) until at least 2018, CARMENES will target around 300 well-characterized late-type main sequence M dwarfs. Assuming that about 40% of the M dwarfs have low mass planets according to recently published planet distribution statistics and in the absence of noise sources other than instrumental noise, near 130 exoplanets would induce radial velocity semi-amplitudes greater than 1 m s^{-1}. Of them, more than 80% would be detected with CARMENES. Accounting for stellar activity on one third of the CARMENES survey, the number of planets with signal above the detection threshold would reduce to 30, some of them expected to be in their habitable zones (Quirrenbach et al. 2014, García-Piquer et al. 2016). However, this project will constrain the properties of planets around low mass stars and will provide statistical information concerning their orbital distribution, frequencies and masses, as well as a unique data set for studies of rotation, activity and stellar atmospheres due to the wavelenght coverage of the spectra in the visible and the near-infrared.

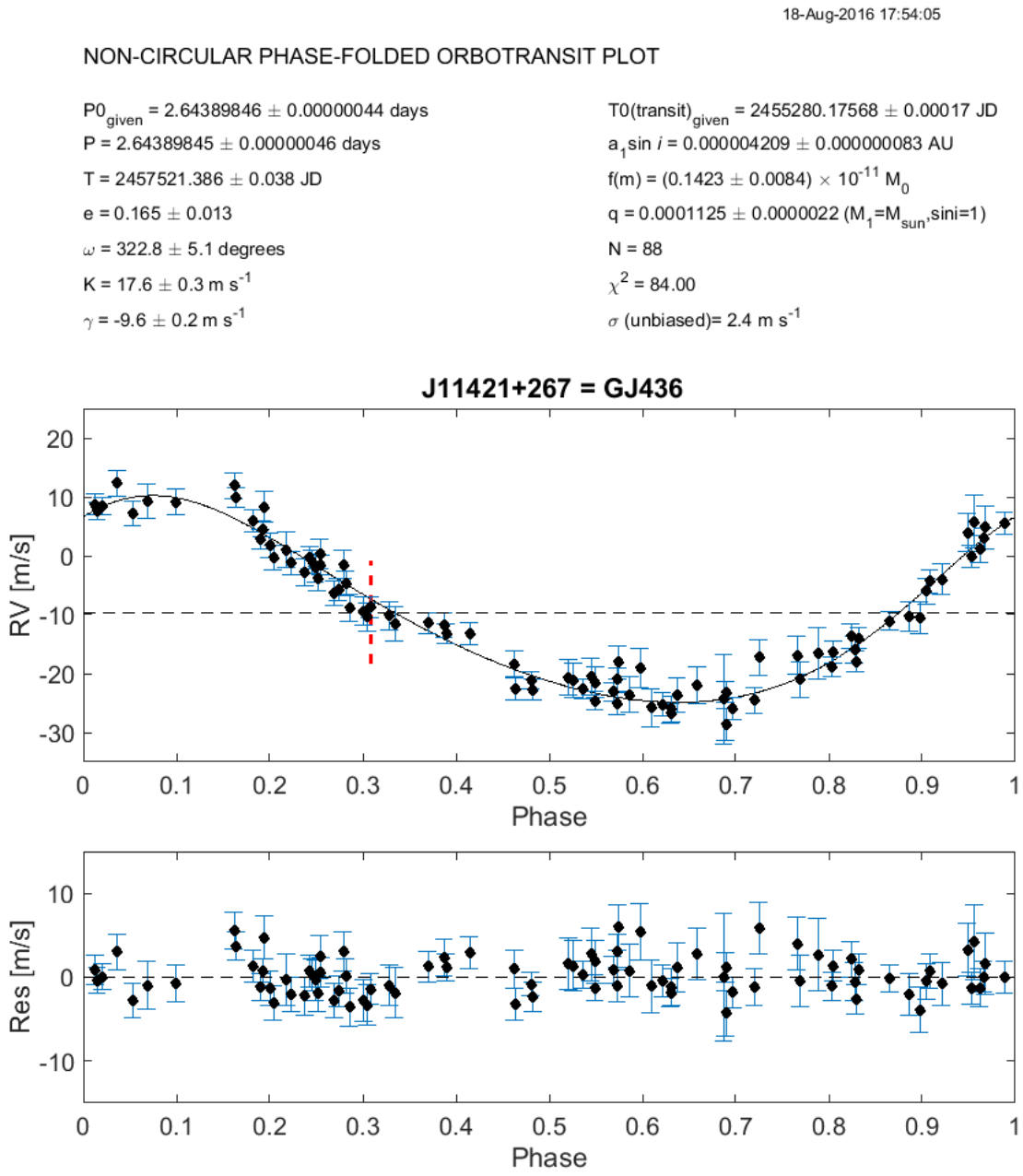

FIGURE 1.10— Radial velocity curve and residuals of Ross 905 (GJ 436) b obtained from CARMENES VIS spectra.

CARMENES can also be used for other scientific cases needing high precision radial velocity measurements, high-resolution and large spectral coverage or simultaneus observations in the visible and the near-infrared range. Some of these possible cases could be (see Amado et al. 2015):

- Asteroseismology: it is a very recent field of research on M dwarfs. The detection and study of oscillations in pulsating M dwarfs provide a tool for accurately determine global physical properties of hosting M dwarfs and help to discern stellar intrinsic radial velocity jitter from variations produced by an orbiting body. The discovery of pulsations in M dwarfs would constrain the exact position in the HR diagram of the line separating stars with fully convective

and partially convective interiors, for which only theoretical studies exist. The understanding of the internal structure and evolution of these M dwarfs has a direct connection with the understanding of planet formation and evolution around low mass stars. Also the study of solar-like oscillations in red giants and the attempt to perform mode identification in the complicated frequency spectrum of classical pulsators, with or without planets, will benefit from high resolution, simultaneous VIS+NIR observations with large spectral coverage.

- Stellar magnetic activity: The generation of magnetic activity in the Sun and cooler stars is not yet well understood and niether is how magnetic fields originate the wide variety of activity phenomena observed at different atmospheric levels. Stellar magnetic activity is observed for cool, young and evolved stars but its behaviour in extremely cool stars has never been deeply studied. The visual and near-infrared spectra from CARMENES will "feed" fundamental studies of activity, which could discriminate bewteen activity induced radial velocity signals or motion around the barycentre of the system.

- Stellar fundamental parameters: Bright massive stars present very few lines in their optical spectrum. CARMENES will extend the high-resolution spectral coverage to help in the determination of effective temperatures, surface gravity, rotation velocity and abundances of these stars.

- Exoplanetary atmospheres: high-resolution near-infrared observations allow to resolve molecular bands of giant planet atmospheres in individual lines as well as to measure their Doppler shift and detect specific molecules in the atmosphere of exoplanets.

- Follow-up for space missions: Time series obtained with CARMENES will serve space missions (*Gaia*, *TESS*, *PLATO*) to confirm planet candidates, analyse asteroseismic or magnetic activity, or characterize targets from snapshots.

- Others: Chemical abundance determinations of planet hosts for comparing stars with and without planets; proto-planetary and proto-stellar discs; proper motion moving groups and cluster member kinematics; chemical tagging; high precision radial velocity measurements for eclipsing binaries (Rossiter-McLaughlin effect); near-infrared spectra for embedded objects; planetary nebulae; Solar System; gamma ray bursts; interstellar and circumstellar medium; etc.

1.4.2 The consortium

The CARMENES Consortium has increased its members since the begining of the project. Today, there are eleven institutions involved in the design and construction of the instrument, the scientific preparation and the managmenet of the project divided into five spanish, five german and the Calar Alto Observatory. It counts with more than 100 members of the eleven institutions and 45 industrial collaborators and manufacturers from all around the world that provide system engineering services, detectors or cameras.

CARMENES has been funded by the Max Planck Gesellschaft, the Consejo Superior de Investigaciones Científicas, the European Union through ERDF (FEDER) funds, and the members of the CARMENES Consortium, with additional contributions by the Spanish Ministerio de Innovación y Ciencia/Ministerio de Economía y Competitividad (MICINN/MINECO), the state of Baden-Württemberg, the Deutsche Forschungsgemeinschaft, the Klaus Tschira Stiftung, and the

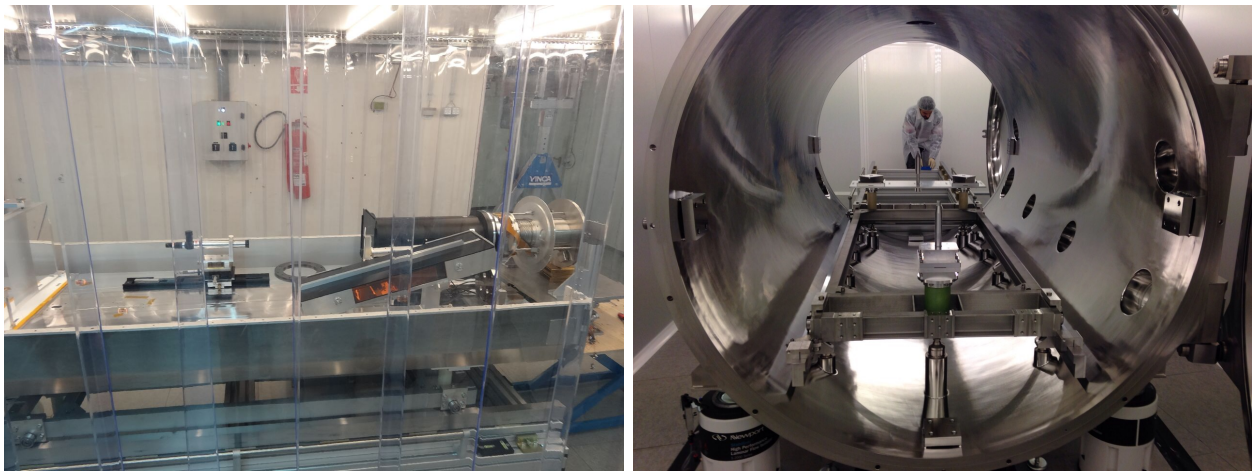

FIGURE 1.11— VIS optical bench with échelle grating and camera plus detection unit in the coudé room clean on the left, and the interior of the NIR vacuum tank on the right.

Junta de Andalucía.

Each institution has a main task, although they do not work independently but as the different pieces of a clock. Here is a brief description of all of them at first light:

- Max-Planck-Institut für Astronomie (Heidelberg): near-infrared detector system (including CMOS mosaic, cryostat, electronics and readout software).
- Instituto de Astrofísica de Andalucía (Granada): near-infrared spectrograph (opto-mechanics, electronics, control, final assembly). This is also the institution of the deputy principal investigator.
- Landessternwarte Königstuhl (Heidelberg): visible spectrograph (opto-mechanics, CCD detector system, final assembly) and front-end (opto-mechanics). The principal investigator and the deputy system engineer belongs to this institution.
- Institut de Ciències de l'Espai (Barcelona): instrument control system and scheduler, and project scientist.
- Insitut für Astrophysik Göttingen (Göttingen): visible and near-infrared vacuum systems, Fabry-Pérot etalons, pipeline, high-resolution spectroscopy science preparation and deputy project scientist.
- Universidad Complutense de Madrid (Madrid): construction and maintenance of the input catalogue (Carmencita, see below), sample characterisation using low-resolution spectroscopy and high-resolution imaging, and numerous science preparation tasks.
- Thüringer Landessternwarte Tautenburg (Tautenburg): near-infrared and visible calibration units.
- Instituto de Astrofísica de Canarias (Tenerife): construction of key mechanical components of visible and near-infrared channels.

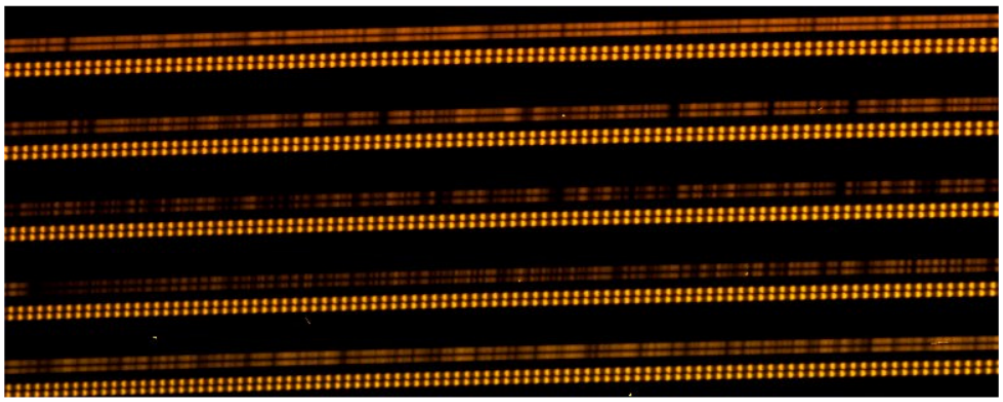

FIGURE 1.12— Detail on a CARMENES spectrum with the Fabry-Pérot for simultaneus calibration.

- Hamburger Sternwarte (Hamburg): electronics of the visible spectrograph and front-end, and responsible for the acquisition and guiding system.
- Centro de Astrobiología (Madrid): coordination of management, science preparation, data server, and website. The deputy project manager belongs to this institution.
- Centro Astronómico Hispano-Alemán (Calar Alto): interlocks, coudé room refurbishing, operation and maintenance of the instrument.

1.4.3 The instrument

The next generation instrument CARMENES, has been built for the 3.5 m telescope at the Calar Alto Observatory. It consists of two separated échelle spectrographs placed in the interior of a vacuum tank to guarantee the temperature-stabilized environment required to achive the desired precision in the radial velocity measurements of $1\,\mathrm{m\,s^{-1}}$. The vacuum tanks are instead located in climatic chambers inside the coudé laboratory of the 3.5 m dome. The purpose of the double channel is to maximize the radial velocity precision and to allow at the same time to separate Keplerian motion of a planet from activity effects, and thus, to directly discriminate false-positive radial velocity signals. The two channels (spectrographs) cover the visible $VRIZ$ bands (0.52 to 0.96 μm) and near-infrared YJH bands (0.96 to 1.71 μm), and the working temperatures in the tanks are 285 K for the visible channel (VIS) and 140 K for the near-infrared channel (NIR). Both channels are cooled with liquid nitrogen and have a mostly constant temperature within ± 0.01 K over 24 h. This is especially important for the NIR, due to the high sensitivity to thermal noise. Fig. 1.11 shows an image of an optical bench (left) and a vacuum tank (right).

The VIS spectrograph is equipped with a 4112×4096 pixel CCD and achives a spectral resolution of 94 600, while the NIR spectrograph is equipped with a mosaic of two 2048×2048 pixel HgCdTe detectors and achives a spectral resolution of 80 400. Each spectrograph is coupled to the telescope with two optical fibres, which operate simultaneously, one for the target and one for the calibration light. Each channel has, in total, seven optical fibres. The front end receives the starlight and calibration light through circular fibers with a low concentration of hydroxyl groups, in order to obtain high internal throughput within the whole spectral range. These fibers are connected to octogonal cross-sections fibers before entering the vakuum tank of each spectrograph to ensure good stability of the output and to minimize the effect of the possible change in the illumination in the

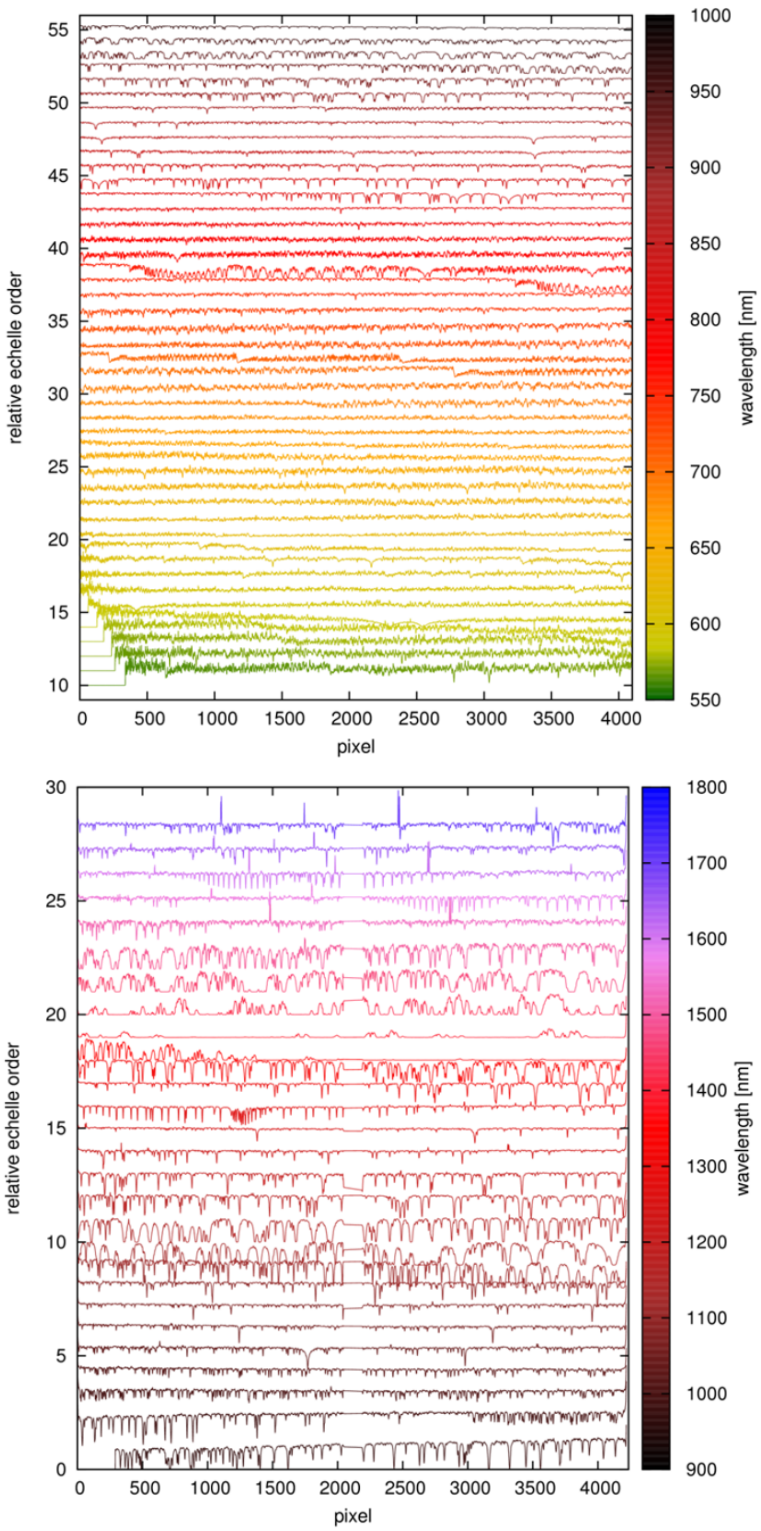

FIGURE 1.13— CARMENES extracted spectra of the Luyten star with the VIS (top) and NIR (bottom) channels. Stellar lines and telluric lines, as well as the gap between the two NIR detectors, are seen.

near field. The calibration light consists of emission-line lamps (U-Ne, U-Ar and Th-Ne for the VIS and the NIR) and Fabry-Pérot etalons.

The simultaneous extraction of the light from the science and the calibration fibres, requires a series of calibration exposures at the beginning, during and at the end of the night, used to trace the differential drift of the spectrograph from night to night. The wavelenght solution used for science observations is determined from the "master" lamps. These lamps are also used for calibration of the "daily" calibration lamps. Fig. 1.12 shows a section of a CARMENES spectrum. The spectrum lines and the Fabry-Pérot are clearly differenciated. Fig. 1.13 shows the extracted spectrum in both channels.

The CARMENES front-end is attached to the Cassegrain focus of the telescope and provides mechanical interface to handle it. It allows the use of other instruments, such as PMAS (Roth et al. 2005), with a flat 45° mirror that can be retracted to let the light pass through to the instrument. The front-end contains a dichroic beam splitter to conduct the light into the fibres, and an atmospheric dispersion corrector. A separated camera controls the guiding of the target.

The instrument control system (ICS) provides a coordination and management tool to operate the instrument (Guàrdia et al. 2012; García-Piquer et al. 2014). It interacts with every subsystem that connects with the instrument, from the detectors and calibration units to the interfaces of the telescope and the dome. It also manages the operational scheduler, which takes into account the weather conditions, target visibility, or the position and phase of the Moon to select the observable targets in the most efficient way (García-Piquer et al. 2016). Fig. 1.14 shows a scheme of the control architecture of the instrument.

Only a few high-stabilized high-resolution spectrographs can provide the high precision required on the radial velocity measurements for Earth-like planet detection and CARMENES is willing to be one of them.

1.4.4 The sample

For a more apropriate selection of the targets and make a profitable use of CARMENES observing time, an extensive compilation of information of M dwarfs has been carried out and put together in the CARMENES input Catalogue, dubbed Carmencita (*CARMENES Cool dwarf Information and daTa Archive*; Caballero et al. 2013, 2016, in prep.). It contains dozens of parameters of more than 2 000 M dwarfs of the solar neighbourhood, compiled from the literature or measured by the different consortium members from our own data. This database includes names and reliable spectral types, astrometric and kinematic parameters (accurate coordinates, proper motions, parallaxes and spectro-photometric distances, radial and Galactocentic space velocities), 19 photometric bands covering from the ultraviolet to the mid-infrared, multiplicity data (angular separations, names and spectral types of the companions), activity and age indicators (Hα pseudo-equivalent width, X-ray count rates and hardness ratios, rotational velocities and periods, flare flag), atmospheric parameters, ($T_{\rm eff}$, $\log g$, [Fe/H]), and full references, as well as some information related to the observations carried out by the Consortium for the characterization of the stars.

The CARMENES Consortium is particularly interested on the brightest stars of the latest types (later than M4.0 V) and moderately active. Stars included in this catalogue satisfy two criteria:

- They must be observable from Calar Alto. This is, their declinations must be greater than

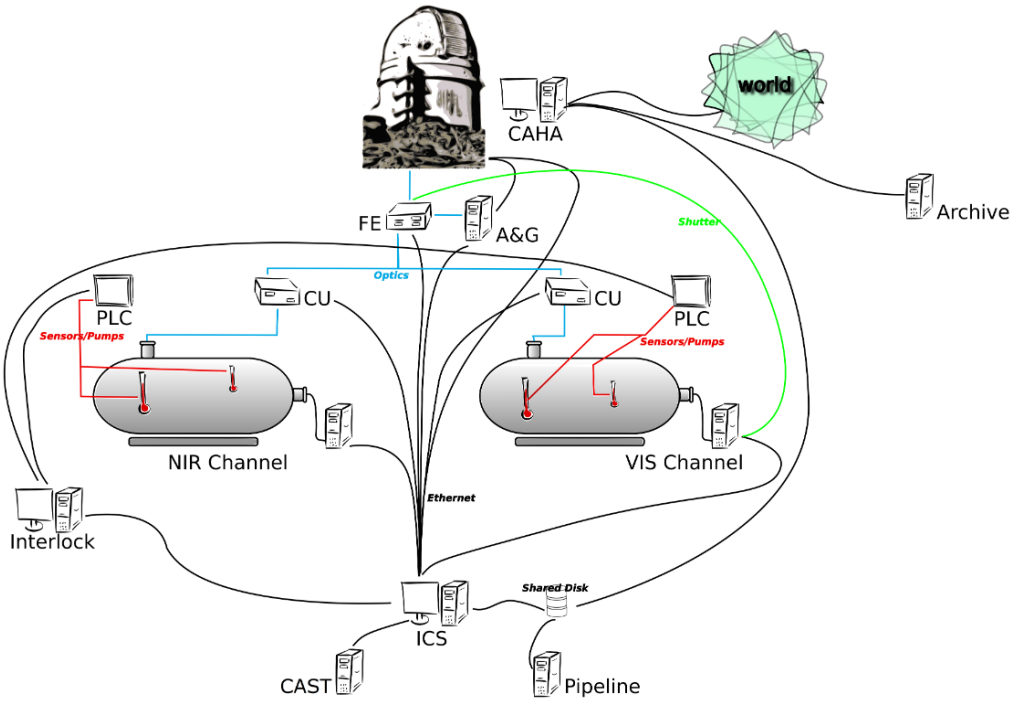

FIGURE 1.14— CARMENES system architecture. Calibration unit (CU), A&G (acquisition and guiding), FE (front-end electronics) and PLC (programmable logic controllers, one set for each cannel). Image from García-Piquer et al. (2014).

-23 deg for having distances to the zenith < 60 deg and air masses at culmination < 2.0.

- They should be among the latest and brightest M dwarfs from the solar neighbourhood according to a 2MASS J magnitude–spectral type relation defined according to the magnitude limits of the instrument. Only stars with reliable spectroscopic spectral type determination between M0.0 V and M9.5 V and brighter than 11.5 mag in the J-band are included. Apart from the Carmencita sample, the consortium would include some non-Carmencita late and single M dwarfs of interest during GTO observations.

To avoid variations in the radial velocity induced by a binary companion of an M dwarf, binaries separated by less than 5 arcsec will not be considered for the CARMENES selection, although many of them are included in Carmencita.

For the characterization of the sample, big efforts have being done by the consortium members in the determination of spectral types with low-resolution spectra (Alonso-Floriano et al. 2015), the measure of fundamental parameters ($T_{\rm eff}$, $\log g$, [Fe/H]; Vera et al. in prep.), the determination of rotational velocities and identification of spectroscopic binaries (Jeffers et al. 2016), or the search of bound companions with low- and high-resolution images, and astrometric catalogues (see Chapters 3, 4 and 5). Chapter 2 will go deep into Carmencita and the general properties of our M dwarfs.

1.5 Objectives and description of the work

This thesis has been developed in the frame of an international proyect in close colaboration with Spanish and German researchers, mainly from Madrid, where a dozen of MSc theses and several

PhD theses have been elaborated.

The main objective of this work is to provide a complete and revised collection of M dwarfs with an extensive selection of parameters, from which the best candidates to host exoplanets will be selected for CARMENES observations. To this purpose, I performed a comprehensive search in the literature of several parameters for more than 2 000 M dwarfs in the solar neighbourhood and built the CARMENES input Catalogue (Carmencita) described in Chapter 2. Some parameters, such as proper motions and distances were computed with my own elaborated scripts. From these data compilation, I analyzed several properties of our M dwarfs, such as multiplicity, kinematics or activity.

While fulfilling Carmencita and after gathering together this information I focused my work on multiplicity of M dwarfs. I compiled binarity information from the literature, mainly from the Washington Double Star catalogue (WDS, Mason et al. 2001-2015), and performed an astrometric analysis of 54 pairs with an M dwarf component with low-resolution images from the TCP and CAMELOT instruments at the IAC80 Telescope in the Observatorio del Teide (Tenerife, Spain). This analysis was published in a refereed journal, which is presented in Chapter 3.

The need of discarding for the final selection stars in Carmencita with companions closer than 5 arcsec required a thoroughgoing search, first in the literature and then with our own methods (i.e., performing high-resolution imaging observations) of close companions to our stars. This task resulted in a three-months stay and several short visits to the Instituto de Astrofísica de Canarias (Tenerife, Spain). This work was developed by analysing thousands of high-resolution images for almost 500 M dwarfs of Carmencita from the lucky imager FastCam at the Carlos Sánchez Telescope in the Observatorio del Teide (Tenerife, Spain). The multiplicity study of M dwarfs with companions at close separations was accepted for publication in A&A and is presented in Chapter 4.

After the multiplicity survey of M dwarfs at close separations and to complete the analysis, I carried through a search of common-proper-motion companions to all the Carmencita M dwarfs. To do this, I matched the proper motions of our stars, coming mainly from the PPMXL and *Hipparcos* catalogues, but also measured by us, with the same proper motion catalogues in a 10^4 au radius search using Aladin and STILTS Virtual Observatory tools. A description of this search is detailed Chapter 5.

A broader multiplicity study claims to be carried out from the results obtained in this work to better constrain M dwarf multiplicity, also linked to planetary formation around low mass stars. In first instance, components in binary systems can be characterized by measuring separations and estimating masses and periods for the shortest ones. For the closest tight systems it is also possible to derive dynamical masses, and from the more separated and weakly bound pairs we can help establishing the limits between multiple bound systems and stellar kinematic groups, together with the previous kinematic analysis performed. By identifing new companions and classifying them, we can also infer the actual conditions of these type of stars in the solar neighbourhood to compare them with multiplicity frequency in young clusters and help in the understanding of low mass binary formation. The forthcoming CARMENES results would address this research topic towards the presence of low mass planets around binary or multiple systems involving an M dwarf.

References

[1] Affer, L., Micela, F., Damasso, M. et al. 2016, arXiv:1607.03632

[2] Alam, S., Albareti, F. D., Allende Prieto, C. et al. 2015, ApJS, 219, 12

[3] Alonso-Floriano, F. J., Morales, J. C., Caballero, J. A. et al. 2015, A&A, 577, A12

[4] Amado, P. J., & CARMENES Consortium 2015, Highlights of Spanish Astrophysics VIII, 701

[5] Anglada-Escudé, G. & Tuomi M. 2012, A&A, 548, A58

[6] Anglada-Escudé, G., Arriagada, P., Vogt, S. S. et al. 2012, ApJ, 751, L16

[7] Anglada-Escudé, G., Tuomi M., Gerlach, E. et al. 2013 A&A, 556, A126

[8] Anglada-Escudé, G. Amado, P. J., Barnes, J. et al. 2016, Nature, 536, 437

[9] Apps, K., Clubb, K. I., Fischer, D. A. et al. 2010, PASP, 122, 156

[10] Artigau, É., Kouach, D., Donati, J.-F. et al. 2014, Proc. SPIE, 9147, E15

[11] Astudillo-Defru, N., Bonfils, X., Delfosse, X. et al. 2015, A&A, 575, A119

[12] Bailey, J., Butler, R. P., Tinney C. G. et al. 2009, ApJ, 690, 743B

[13] Baraffe, I., Chabrier, G., Allard, F., & Hauschildt, P. H. 1998, A&A, 337, 403

[14] Baranne, A., Queloz, D., Mayor, M., Adrianzyk, G. et al. 1996, A&AS, 119, 373

[15] Bate, M. R. 2009, MNRAS, 392, 590

[16] Bate, M. R. 2012, MNRAS, 419, 3115

[17] Batten, A. H. 1973, Binary and multiple systems of stars, Oxford (New York: Pergamon Press, International series of monographs in natural philosophy, 51)

[18] Bean, J. L., Seifahrt, A., Hartman, H. et al. 2010, ApJ, 713, 410

[19] Beaulieu J.-Ph., Bennett D., Fouqué., W. A. et al. 2013 Nature, 439, 437

[20] Beckers, J. M. 1993, ARA&A, 31, 13

[21] Beichman, Ch., Livingstn, J., Werner, M. et al. 2016, ApJ, 822, 39

[22] Bennett, D., Bond, I. Udalski, A. et al. 2008, ApJ, 684, 663

[23] Bergfors, C., Brandner, W., Janson, M. et al. 2010, A&A, 520, A54

[24] Berta-Thomson, Z., Irwin, J., Charbonneau, D. et al. 2015, Nature, 527, 204

[25] Bianchi L., Herald J., Efremova B. et al. 2011, Ap&SS, 335, 161

[26] Biller, B., Allers, K., Liu, M. et al. 2011, ApJ, 730, 39

[27] Bochanski, J. J., Hawley, S. L., Covey, K. R. et al. 2010, AJ, 139, 2679

[28] Bonfils, X., Delfosse, X., Udry, S. et al. 2005a, A&A, 442, 635

[29] Bonfils, X., Forveille, Th., Delfosse, X. et al. 2005b A&A, 443, L15

[30] Bonfils, X., Mayor, M., Delfosse, X. et al. 2007 A&A, 474, 293

[31] Bonfils, X., Gillon, M., Forveille, T. et al. 2011, A&A, 528, A111

[32] Bonfils, X., Gillon, M., Udry, S. et al. 2012, A&A, 546, A24

[33] Bonfils, X., Delfosse, X., Udry, S. et al. 2013a, A&A, 549, A109

[34] Bonfils, X., Lo Curto, G., Correia, A. C. M. et al. 2013b, A&A, 556, A110

[35] Bonfils, X., Bouchy, F., Delfosse, X. et al. 2013c, European Physical Journal Web of Conferences, 4705004

[36] Bouchy, F., Udry, S., Moutou, C., Delfosse, X. et al. 2007, sf2a, conf, 377

[37] Bouchy, F., Ségransan, D., Díaz, R. F., Forveille et al. 2016, A&A, 585, A46

[38] Bryden, G., Beichman, C., Carpenter, J. et al. 2009, ApJ, 705, 1226

[39] Burgasser, A. J., Kirkpatrick, J. D., Reid, I. N. et al. 2003, ApJ, 586, 512

[40] Burgasser, A. J., Geballe, T. R., Leggett, S. K., Kirkpatrick, J. D., & Golimowski, D. A. 2006, ApJ, 637, 1067

[41] Burrows, A., Hubbard, W. B., Lunine, J. I. et al. 1997, Planets Beyond the Solar System and the Next Generation of Space Missions, 119, 9

[42] Burt, J., Vogt, S. S., Butler, R. P. et al. 2014, ApJ, 789, 114

[43] Butler, P., Vogt, S., Marcy, G. et al. 2004, ApJ, 617, L580

[44] Butler, R. P., Johnson, J. A., Marcy, G. W. et al. 2006, PASP, 118, 1685

[45] Caballero, J. A. 2009, A&A, 507, 251

[47] Caballero, J. A. 2010, A&A, 514, A98

[47] Caballero, J. A., Montes, D., Klutsch, A. et al. 2010, A&A, 520, A91

[48] Caballero, J. A., Cortés-Contreras, M., Alonso-Floriano, F. J. et al. 2013, Protostars and Planets VI Posters, 20

[49] Caballero, J. A., Suvrath, M., Kopparapu, R. 2015, SatMeet4–Habitable planets, M dwarfs and NIR spectrographs, Pathways towards habitable planets II, published on-line

[50] Carleo, I. & Gratton, R. 2015, Mem. S.A.It., 86, 478

[51] Cassan, A., Kubas, D., Beaulieu, J.-P. et al. 2012, Nature, 481, 167

[52] Chabrier, G. & Baraffe, I. 1997, A&A, 327, 1039

[53] Chabrier, G., Baraffe, I., Allard, F., & Hauschildt, P. 2000, ApJ, 542, 464

[54] Chamberlain, J. N. & Aller, L. H. 1951, ApJ, 114, 52

[55] Charbonneau, D., Berta, Z. K., Irwin, J. et al. 2009, Nature, 462, 891

[56] Close, L. M., Richer, H. B., Crabtree, D. R. 1990, AJ, 100, 1968

[57] Cosentino, R., Lovis, C., Pepe, F. et al. 2012, Proc. SPIE, 8446, E1V

[58] Crossfield, I. J. M. 2014, A&A, 566, A130

[59] Cumming, A., Marcy, G. W. & Butler, R. P. 1999, ApJ, 526, 890

[60] Cutri, R. M., Wright, E. L., Conrow, T. et al. 2012, yCat, 2311, 0

[61] Cutri, R. M., Wright, E. L., Conrow, T. et al. 2013, yCat, 2328, 0

[62] Cushing, M. C., Kirkpatrick, J. D., Gelino, C. R. et al. 2011, ApJ, 743, 50

[63] Crézé M., Chereul, E., Bienayme, O. & Pichon, C. 1998, A&A, 329, 920

[64] Dahn, C. C., Liebert, J. & Harrington, R. S 1986, AJ, 91, 621

[65] David, T., Hillenbrand, L., Petigura, E. et al. 2016, Nature, 534, 658

[66] Deacon, N., Schlieder, J. & Murphy S. 2016 MNRAS, 457, 3191

[67] Delfosse, X., Forveille, T., Perrier, C. & Mayor, M. 1998, A&A, 331, 581

[68] Delfosse, X., Forveille, T., Ségransan, D. et al. 2000, A&A, 364, 217

[69] Delfosse, X., Bonfils, X., Forveille, Th. et al. 2013, A&A, 553, A8

[70] de Wit, J., Wakeford, H., Gillon, M. et al. 2016, arxiv:160601103

[71] Dhital, S., West, A. A., Stassun, K. G. & Bochanski, J.J. 2010 AJ, 139, 2566

[72] Dhital, S., Stassun, K. G. & West, A. A. 2012, AAS, 21913205

[73] Diego, F., Charalambous, A., Fish, A. & Walker, D. D. 1990, Proc. SPIE, 1235, 562

[74] Donati, J.-F., Moutou, C., Malo, L. et al. 2016, Nature, 534, 662

[75] Donnison, J. 2010, MNRAS, 406, 1918

[76] Duchêne G., Bouvier J., Bontemps S. et al. 2004, A&A, 427,651

[77] Duquennoy, A. & Mayor, M. 1991, A&A, 248, 485

[78] Durney, B. R., De Young, D. S., & Roxburgh, I. W. 1993, Sol. Phys, 145, 207

[79] Eisenstein, D. J., Weinberg, D. H., Agol, E. et al. 2011, AJ, 142, 72

[80] Elmegreen B., G. 2011, AJ, 731, 61

[81] Endl, M., Cochran, W. D., Wittenmyer, R. A., & Boss, A. P. 2008, ApJ, 673, 1165

[82] Epchtein, N., de Batz, B., Capoani, L. et al. 1997, The Messenger, 87, 27

[83] Evans, I. N., Primini, F. A., Glotfelty, K. J. et al. 2010, ApJS, 189, 37

[84] Faber, S. M., Burstein, D., Tinsley, B. M. & King, I. R. 1976, AJ, 81, 45

[85] Figueira, P., Pepe, F., Melo, C. H. F. et al. 2010, A&A, 511, A55

[86] Fischer, D. A. & Marcy, G. W. 1992, ApJ, 396, 178

[87] Forveille, T., Bonfils, X., Delfosse, X. et al. 2009, A&A, 493, 645

[88] Forveille, T., Bonfils, X., Lo Curto, G. et al. 2010, A&A, 526, A141

[89] Forveille, T., Bonfils, X., Delfosse, X. et al. 2011, A&A, 562, A141

[91] García-Piquer, A., Guàrdia, J., Colomé e, J. et al. 2014, Proc. SPIE 9152, 21

[91] García-Piquer, A., Morales, J. C., Ribas, I. et al. 2016, A&A, submitted

[92] Ginski, C., Mugrauer, M., Seeliger, M. et al. 2015, MNRAS, 457, 2173

[93] Gliese, W. 1972, QJRAS, 13, 138

[94] Goodwin, S. P., Whitworth, A. P. & Ward-Thopmson, D. 2004, A&A, 419, 543

[95] Goodwin, S. P., & Whitworth, A. P. 2007, A&A, 466, 943

[96] Goodwin S. P., 2010, Phil. Trans. R. Soc. A, 368, 851

[97] Gould, A., Bahcall, J. N., & Flynn, C. 1996, ApJ, 465, 759

[98] Garcés, A., Catalán, S. & Ribas, I, 2011, A&A, 531, A7

[99] Graves, J. E., Roddier, F., Northcott, M. et al. 1994, Proc. SPIE, 2201, 502

[100] Gray, R. O., & Corbally, C., J. 2009, Stellar Spectral Classification by Richard O. Gray and Christopher J. Corbally. Princeton University Press

[101] Guàrdia, J., Colomé, J., Ribas, I. et al. 2012, Proc. SPIE, 8451, E2S

[102] Haghighipour, N., Vogt, S. S., Butler, R. P. et al. 2010, ApJ, 715, 271

[103] Han, C., Jung, Y., Udalski, A. et al. 2016, ApJ, 822, 75

[104] Hartman, J., Bayliss, D. Brahm, R. et al. 2015, AJ, 149, 166

[105] Hawley, S. L., Gizis, J. E., & Reid, I. N. 1996, AJ, 112, 2799

[106] Hippler, S., Bergfors, C., Brandner, W. et al., 2009, The Messenger, 137, 14

[107] Hirano, T., Fukui, A., Mann, A. et al. 2016, ApJ, 820, 41

[108] Hormuth, F., Hippler, S., Brandner, W. et al. 2008, Proc. SPIE, 7014, 48

[109] Howard, A. W., Johnson, J. A., Marcy, G. W. et al. 2010, ApJ, 721, 1467

[110] Howard, A. W., Marcy, G. W., Bryson, S. T. et al. 2012, ApJS, 201, 15

[111] Howard, A. W., Marcy, G. W., Fischer, D. et al. 2014, ApJ, 794, 51

[112] Irwin, J. B. 1959, AJ, 64, 159

[113] Irwin, J. B., Buchhave, L., Berta, Z. et al. 2010, ApJ, 718, 1553

[114] Jaffe, D. T., Mar, D. J., Warren, D., & Segura, P. R. 2006, Proc. SPIE, 6269, 4

[115] Janson, M., Hormuth, F., Bergfors, C. et al. 2012, ApJ, 754, 44

[116] Janson, M., Bergfors, C., Brandner, W. et al. 2014, ApJ, 789, 102

[117] Jeffers, S. V., Schöfer, P., Lamert, A. et al. 2016, A&A, submitted

[118] Jódar, E., Pérez-Garrido, A., Díaz-Sánchez, A. et al. 2013, MNRAS, 429, 859

[119] Johnson, A., Butler, R. P., Marcy, G. W. et al. 2007, ApJ, 670, 833

[120] Johnson, A., Howard, A., Marcy, G. W. et al. 2009, PASP, 122, 149

[121] Jones, D. H. P. 1973, MNRAS 161, 19

[122] Jones, H. R. A., Rayner, J., Ramsey, L. et al. 2008, Proc. SPIE, 7014, E0Y

[123] Joshi, M. M., Haberle, R. M., & Reynolds, R. T. 1997, Icarus, 129, 450

[124] Kasting, J. F., Whitmire, D. P., & Reynolds, R. T. 1993, Icarus, 101, 108

[125] King, R. R., Parker, R. J., Patience, J. & Goodwin, S. P. 2012a, MNRAS, 421, 2025

[126] King, R. R., Goodwin, S. P., Parker, R. J. & Patience, J. 2012b, MNRAS, 427, 2636

[127] Kipping, D., Nesvorny, D., Buchhave, L. et al. 2014, ApJ, 784, 28

[128] Kirkpatrick, J. D., Henry, T. J. & McCarthy, D. W. Jr. 1991, ApJS, 77, 417

[129] Kirkpatrick, J. D., Beichman, C. A. & Skrutskie, M. F. 1997, ApJ, 476, 311

[130] Kirkpatrick, J. D., Reid, I. N., Liebert, J. et al. 1999, ApJ1, 519, 802

[131] Kirkpatrick, J. D., Cushing, M. C., Gelino, C. R. et al. 2011, ApJS, 197, 19

[132] Kopparapu, R. K. 2013, ApJ, 767, L8

[133] Kotani, T., Tamura, M., Suto, H. et al. 2014, Proc. SPIE, 9147, 14

[134] Kraus, A. L., Ireland, M. J., Martinache, F. & Hillenbrand, L. A. 2011, ApJ, 731, 8

[135] Kroupa, P., Gilmore, G., & Tout, C. A. 1991, MNRAS, 251, 293

[136] Kroupa P., 1995a, MNRAS, 277, 1507

[137] Kroupa P., 1995b, MNRAS, 277, 1491

[138] Kroupa P., 1995c, MNRAS, 277, 1522

[139] Kroupa, P. 2001, MNRAS, 322, 231

[140] Kuiper, G.P., 1942, ApJ, 95, 201

[141] Labeyrie, A. 1970, A&A, 6, 86

[142] Laughlin, G., Bodenheimer, P. & Adams, F. C. 1997, 482, 420

[143] Law, N. M., Hodgkin, S. T. & Mackay, C. D. 2006, MNRAS, 368, 1917

[144] Law, N. M., Dhital, S., Kraus, A. et al. 2010, ApJ, 720 ,1727

[145] Lee, S., Yuk, I.-S., Lee, H. et al. 2010, Proc. SPIE, 7735, 2K

[146] Lee, B.-C., Han, I. & Park, M.-G. 2012, A&A, 549, A2

[147] Lenzen, R., Hartung, M., Brandner, W. et al. 2003, Proc. SPIE 4841, 944

[148] López, E. D. & Fortney, J. J. 2014, ApJ, 792, 1

[149] Lowrance, P. J., Kirkpatrick, J. D. & Beichman, C. A. 2002, ApJ, 572, L79

[150] Luhman, K. L., Wilson, J. Brandner, W. et al. 2006, ApJ, 649, 894

[151] Luhman, K. L. 2014, ApJ, 786, L18

[152] Luyten, W.J. 1939, Publications of the Astronomical Observatory, University of Minnesota, 2, 121

[153] Luyten, W. J. 1979, New Luyten catalogue of stars with proper motions larger than two tenths of an arcsecond and first supplement (Minneapolis)

[154] Mackay, C., Rebolo, R. , Femenia, B. et al. 2012, Proc. SPIE 8446, 47

[155] Mahadevan, S., Ramsey, L. W., Terrien, R. et al. 2014, Proc. SPIE, 9147, 1G

[156] Maiolino, R., Haehnelt, M., Murphy, M. T. et al. 2013, arXiv:1310.3163

[157] Mamajek, E. E. & Hillenbrand, L. A. 2008, ApJ, 687, 1264

[158] Mann, A. W., Deacon, N. R., Gaidos, E. et al. 2014, AJ, 147, 160

[159] Mann, A. Gaidos, E. Mace, G. et al. 2016, ApJ, 818, 46

[160] Marcy G., Butler, P., Vogt, S. et al. 1998, ApJ, 505, L147

[161] Marcy, G. W., Butler, R. P., Fischer, D. et al. 2001, ApJ, 556, 296

[162] Marcy G. 2009, Nature, 462, 853

[163] Martín, E. L., Guenther, E. W., Barrado y Navascués, D. et al. 2005, AN, 326, 1015

[164] Martín, E. L., Guenther, E. W., Zapatero Osorio, M. R. et al. R. 2006, ApJ, 644, L75

[165] Martín, E. L., Guenther, E. W., Del Burgo, C. et al. 2010, ASPC, 430, 181

[166] Mason, B. D., Wycoff, G. L., Hartkopf, W. I. et al. 2001, AJ, 122, 3466

[167] Mason, B. D., Wycoff, G. L., Hartkopf, W. I., Douglass, G. G. & Worley, C. E. 2015, VizieR on-line catalogue, B/WDS

[168] Mayer, P. 1990, Bulletin of Astronomical Institutes of Czechoslovakia, 41, 231

[169] Mayor, M., & Queloz, D. 1995, Nature, 378, 355

[170] Mayor, M., Pepe, F., Queloz, D. et al. 2003, The Messenger, 114, 20.

[171] Mayor, M., Bonfils, X., Forveille, T. et al. 2009, A&A, 507, 487

[172] McCarthy, D. W., Jr. & Cobb, M. L. 1986, Proc. SPIE 0627, 797

[173] Miller, G. E., & Scalo, J. M. 1979, ApJS, 41, 513

[174] Mohanty, S., & Basri, G. 2003, ApJ, 583, 451

[175] Montes, D., López-Santiago, J., Gálvez, M. C. et al. 2001, MNRAS, 328, 45

[176] Montet, B. T., Crepp, J. R., Johnson et al. 2014, ApJ, 781, 28

[177] Montet, B., Morton, T., Foreman-Mackey, D. et al. 2015, ApJ, 809, 25

[178] Morgan, W. W., Keenan, P. C. & Kellman, E. 1943, An Atlas of Representative Stellar Spectra, Chicago: Univerersity Chicago Press

[179] Morgan, D. P., West, A., Garcés, A. et al. 2012, AJ, 144, 93

[180] Mugrauer, M., Neuhäuser, R., & Mazeh, T. 2007, A&A 469, 755

[181] Mugrauer, M. & Neuhäuser, R. 2009, A&A 494, 373

[182] Murray, S. D. & Lin D. C. 1996, ApJ, 467, 728

[183] Newgebauer, G. & Leighton, R.B. 1969, The Two Micron Sky Survey, NASA SP-3047

[184] Newton, E. R., Charbonneau, D., Irwin, J. et al. 2014, AJ, 147, 20

[185] Nordlund, A. & Padoan P. 2003, *Lecture Notes in Physics*, 614, 271

[186] Oort, J. J. 1932, Bulletin of the Astronomical Institutes of the Netherlands, 6, 249

[187] Oort, J. J. 1965, Galactic Structurem University of Chicago Press

[188] Oscoz, A., Rebolo, R., López, R. et al. 2008, Proc. SPIE, 7014, E47

[189] O'Toole, S., Tinney, C. G., Butler, R. P. et al. 2009, ApJ, 697, 1263

[190] Parker R. J., Goodwin, S. P., Kroupa, P. & Kouwenhoven, M. B. N. 2009, MNRAS, 397, 1577

[191] Pasinetti-Frascani, L., Pastori, L., Covino, S. & Pozzi, A. 2001, A&A, 367, 521

[192] Pepe, F. A., Cristiani, S., Rebolo, R. et al. 2010, Proc. SPIE, 7735, E0

[193] Petigura, A. Schlieder, J., Crossfield, I. et al. 2015 ApJ, 811, 102

[194] Queloz, D., Mayor, M., Weber, L., Blécha, A. et al. 2000, A&A, 354, 99

[195] Quirrenbach, A., Amado, P. J., Mandel, H. et al. 2010, Proc. SPIE, 7735, 37Q

[196] Quirrenbach, A., Amado, P. J., Caballero, J. A. et al. 2014, Proc. SPIE, 9147, E1F

[197] Raghavan, D., McAlister, H. A., Henry, T. J. et al. 2010, ApJS, 190, 1

[198] Rappaport, S., Sanchís-Ojeda R., Rogers, L. et al. 2013, ApJL, 773 , L15

[199] Reid, I. N., Hawley, S. L., & Gizis, J. E. 1995, AJ, 110, 1838

[200] Reid, I. N., Cruz, K. L., Allen, P. et al 2003, AJ, 125, 354

[201] Reid, I. N., & Hawley, S. L. 2005, New Light on Dark Stars Red Dwarfs, Low-Mass Stars, Brown Dwarfs, Praxis Publishing Ltd

[202] Reid I. N., Cruz, K. L., Burgasser, A. J. & Liu. M. C. 2008, AJ, 135, 580

[203] Reipurth, B., & Clarke, C. 2001, AJ, 122, 432

[204] Reiners, A. 2008, Reviews in Modern Astronomy, 20, 40

[205] Reiners, A., & Basri, G. 2009, ApJ, 705, 1416

[206] Reiners, A., Bean, J. L., Huber, K. F. et al. 2010, ApJ, 710, 432

[207] Reiners, A., Shulyak, D., Anglada-Escudé, G. et al. 2013, A&A, 552, A103

[208] Reiners, A., Schüssler, M., & Passegger, V. M. 2014, ApJ, 794, 144

[209] Roddier, F. 1988, Applied Optics, 27, 1223

[210] Rigaut, F., Salmon, D., Arsenault, R. et al. 1998, PASP, 110, 152

[211] Rivera, E. J., Lissauer, J. J., Butler, R. P. et al. G. W. 2005, ApJ, 634, 625

[212] Rivera, E. J., Laughlin, G., Butler, R. P. et al. 2010, ApJ, 719, 890

[213] Roeser S., Demleitner M. & Schilbach E. 2010, AJ, 139, 2440

[214] Rojas-Ayala, B., Covey, K. R., Muirhead, P. S., & Lloyd, J. P. 2012, ApJ, 748, 93

[215] Rosen S. R., Webb N. A., Watson, M. G. et al., 2016, A&A, 590, A1

[216] Roth, M. M., Kelz, A., Fechner, T. et al. 2005, PASP, 117, 620

[217] Rousset, G. Lacombe, F., Puget, P. et al. 2003, Proc. SPIE 4839, 140

[218] Rowe, J., Bryson, T., Marcy, G. et al. 2014, ApJ, 784, 45

[219] Rubin, V. C. & Ford, W. K., Jr. 1970, IAUS, 38, 61

[220] Salpeter, E. E. 1955, ApJ, 121, 161

[221] Sanchís-Ojeda, R., Rappaport, S., Pallé, E. et al. 2015, ApJ, 812, 112

[222] Sandage, A. & Eggen, O.J. 1959, MNRAS, 119, 278

[223] Sanduleak, N. 1965, PhD thesis, Case Institute Technology

[224] Santerne, A., Díaz, R. F., Moutou, C. et al. 2012, A&A, 545, A76

[225] Scalo, J., Kaltenegger, L., Segura, A. G. et al. 2007, Astrobiology, 7, 85

[226] Schmidt, M. 1974, *Highlights in Astronomy*, 3, 450

[227] Shaya, E. J., & Olling, R. P. 2011, ApJS, 192, 2

[228] Shulyak, D., Reiners, A., Seemann, U., Kochukhov, O., & Piskunov, N. 2014, A&A, 563, A35

[229] Siess, L., Dofour, E. & Forestini, M. 2000, A&A, 358, 593

[230] Silvestri, N. M., Hawley, S. L. & Oswalt, T. D. 2005, AJ, 129, 2428

[231] Sinukoff, E., Howard, A. Petigura, E. et al. 2015, arxiv:v151109213

[232] Skidmore, W., TMT International Science Development Teams, Science Advisory Committee, TMT 2015, RAA, 15, 1945

[233] Skrutskie, M. F., Cutri, R. M., Stiening, R. et al. 2006, AJ, 131, 1163

[234] Soderblom, D. R. Duncan, D. K. & Johnson, D. R. H. 1991, ApJ, 375, 722

[235] Soderblom, D. R. & Mayor, M. 1993, AJ, 105, 226

[236] Southworth, J. 2010, MNRAS, 408, 1689

[237] Spronck, J. F. P., Schwab, C., Fischer, D. A. et al. 2010, Proc. SPIE, 7735, E0W

[238] Stamatellos, D., & Whitworth, A. P. 2009, MNRAS, 392, 413

[239] Stassun, K. G., Hebb, L., Covey, K. et al. 2011, 16th Cambridge Workshop on Cool Stars, Stellar Systems, and the Sun, 448, 505

[240] Szabo, R., Szabo, G., Dalya, G. et al. 2012, A&A, 553, A17

[241] Tarter, J. C., Backus, P. R., Mancinelli, R. L. et al. 2007, Astrobiology, 7, 30

[242] Thomas, J., Barrick, G. & Beuzit J.-L. 1998, Proc. SPIE 3353, 94

[243] Tokovinin, A., & Lépine, S. 2012, AJ, 144, 102

[244] Torres, G., Andersen, J. & Giménez, A. 2010, A&ARv, 18, 67

[245] Tubbs, R. N., Baldwin, J. E., Mackay, C. D. & Cox, G. C. 2002, A&A, 387, L21

[246] Tuomi, M., Jones, H., Barnes, J. et al. 2014, MNRAS, 441, 1545

[247] Udry, S., Bonfils, X., Delfosse, X. et al. 2007, A&A, 469, L43

[248] Van Eyken, J., Ciardi, D. von Braun, K. et al. 2012, ApJ, 755, 42

[249] Voges, W., Aschenbach, B., Boller, T. et al. 1999, A&A, 349, 389

[250] Vogt, S. S., Radovan, M., Kibrick, R. et al. 2014, PASP, 126, 359

[251] Walkowicz, L. M. & Hawley, S. L. 2009, AJ, 137, 3297

[252] Wang, Ji., & Ford, E. B. 2011, MNRAS, 418, 1822

[253] Wang, Ji., Xie, J.-W., Barclay, T. & Fischer, D. A. 2014, ApJ, 783, 4

[254] Ward-Duong, K., Patience, J., De Rosa, R. J. et al. 2015, MNRAS, 449, 2618

[255] Weinberg, M. D., Shapiro, S. L., Wasserman, I. 1987, ApJ, 312, 367

[256] Weistrop, D. W. 1972, AJ, 77, 849

[257] Weistrop, D. W. 1976, ApJ, 204, 113

[258] West, A. A., Hawley, S. L., Walkowicz, L. M. et al. 2004, AJ, 128, 426

[259] West, A. A., Weisenburger, K. L., Irwin, J. et al. 2015, ApJ, 812, 3

[260] Whitworth, A. P., & Zinnecker, H. 2004, A&A, 427, 299

[261] Wittenmyer, R. A., Wang, S., Horner, J. et al. 2013, ApJS, 208, 1

[262] Wittenmyer, R. A., Butler, R. P., Tinney, C. G. et al. 2016, ApJ, 819, 28

[263] Wizinowich, P., Acton, D. S., Shelton, C. et al. 2000, PASP, 112, 315

[264] Wright, E. L., Eisenhardt, P. R. M., Mainzer, A. K. et al. 2010, AJ, 140, 1868

[265] Wright, D., Wittenmeyer, R., Tinney, C. et al. 2015, ApJ, 817, L20

[266] Xia, F., Ren, S. & Fu, Y. 2008, Ap&SS, 314, 51

[267] York, D. G., Adelman, J., Anderson, J. E. Jr. et al. 2000, AJ, 120, 1579

[268] Zapatero Osorio, M. R., Martín, E. L., Bouy, H. et al. 2006, ApJ, 647, 1405

[269] Zechmeister, M., Kürster, M. & Endl, M. 2009, A&A, 505, 859

[270] Zechmeister, M., Kürster, M., Endl, M. et al. 2013, A&A, 552, A78

[271] Zhao, B., Ge, J., Nguyen, D. C., Wang, J., & Groot, J. 2010, Proc. SPIE, 7735, 54

[272] Zucker, S., Mazeh, T., Santos, N. et al. 2004, A&A, 426, 695

[273] Zuckerman, B. & Song, I. 2004, ARA&A, 42, 685

[274] Zwicky, F. 1937, ApJ, 86, 217

2

Carmencita

2.1 Description and classification

Carmencita is the *CARMENES Cool dwarf Information and daTa Archive* (Caballero et al. 2013, 2016). It is an M dwarf database created to provide a selection of M dwarfs in the solar neighbourhood, from which chosing the best targets that CARMENES will observe during Guaranteed Time Observations.

Carmencita contains exactly 2176 M dwarfs with spectral types from M0.0 V to M9.5 V, from which near 300 will be monitored with CARMENES over at least three years in order to detect the signal of exoplanets. In particular, in order to detect exoEarths in the habitable zone with the Doppler effect technique (see Section 1.2.1 in Chapter 1). All these stars were selected according to the following two criteria:

- The stars must be observable from Calar Alto (i.e., $\delta \geq -23\,\mathrm{deg}$).
- The stars satisfy a magnitude-spectral type relation based on the 2MASS J-band magnitude and defined to select the brightest stars of each spectral subtype. Moreover, none of them is fainter than 11.5 mag in the 2MASS J-band.

The high number of stars in the catalogue required a classification to assign priorities and to address the characterization of the potential targets of CARMENES. In a first step, the stars were divided into:

- *Alpha*: From the initial selection, these are the brightest single stars of each spectral subtype and the best targets to be observed. They have the maximum priority for CARMENES.
- *Beta*: After the *Alpha* stars, they are single and relatively bright and are the backup for the observations.
- *Gamma*: These are the faintest among the brightest single M dwarfs of the original selection. They constitute the bulk of the catalogue.
- *Delta*: As explained in Section 1.2.1, the radial velocity method is highly sensitive to the presence of another companion close to the star. If this companion is a star-mass body and

TABLE 2.1— Limiting J-band magnitudes and number of stars per spectral subtype and category.

Spectral type	SS	*Alpha* J [mag]	#	*Beta* J [mag]	#	*Gamma* J [mag]	#	*Delta* J [mag]	#
M0		<7.0	27	7.0 – 7.3	17	7.3 – 8.5	152	...	55
M1	S3	<7.5	43	7.5 – 7.8	14	7.8 – 9.0	226	...	44
M2		<8.0	47	8.0 – 8.3	33	8.3 – 9.5	219	...	81
M3	S2	<8.5	84	8.5 – 8.8	56	8.8 – 10.0	302	...	140
M4		<9.0	80	9.0 – 9.3	43	9.3 – 10.5	221	...	119
M5		<9.5	22	9.5 – 9.8	14	9.8 – 11.0	57	...	33
M6	S1	<10.0	4	10.0 – 10.3	2	10.3 – 11.5	20	...	1
M7		<10.5	2	10.5 – 10.8	1	10.8 – 11.5	6	...	1
M8		<11.0	2	11.0 – 11.3	3	11.3 – 11.5	2	...	2
M9		<11.5	1	...	0	...	0	...	0
#			312		183		1205		476

it is close enough, it could affect the radial velocity measurments and induce variations in the amplitude that prevent us from measuring the effect o a planet-mass body. For this reason, any M dwarf with a binary component closer than an arbitrary angular separation (ρ) of 5 arcsec has been excluded regardless of its magnitude or spectral subtype. This separation was established to ensure a clean measure of the radial velocity and to avoid the gravitational influence of the companion. This criterion was strictly applied and also includes visual stars (i.e., not bound or background) that could contaminate the spectra and photometry, as well as spectroscopic and eclipsing binaries. In addition, the photometry of a star with a very bright companion could also be affected by it, even if they are separated by more than 5 arcsec. These stars were also excluded and added together to the *Delta* category.

Approximately the 300 M dwarfs that CARMENES will survey should also be equally distributed into early-, mid- and late- type dwarfs. To this purpose, a secondary classification was defined to account for the number of *Alpha* and *Beta* stars in each range of spectral subtype, namely the SS classification. It is is divided into $S1$, that contains all the stars with spectral types later than M4.0 V, $S2$, that includes only M3.0 V, and $S3$, that contains all M0.0–M2.0 dwarfs. The SS subsampling is used as a reference. Except for some additions, all the $\sim$ 300 *Alpha* stars are the 300 M dwarfs that CARMENES monitors. Table 2.1 shows the magnitude limits for each spectral subtype of the previous classification, together with the number of stars belonging to each category and spectral subtype. The magnitude limit of the *Alpha* class defines the completeness magnitude at which every virtually known M dwarf brighter than that limit is included in the database. The distribution of stars within each spectral type and class is shown in the right panel of Fig. 2.1.

One of the first columns in the Carmencita database refers to a three charatcer flag defined to easily handle the most important information contained in the catalogue and related to the classification. From these flags it is possible to know to which class the star belongs and why. Table 2.2 describes these flags. The first character is related to binarity and refers to companions (visual or physical) at less than 5 arcsec, with the only exeption of bright companions that photometrically contaminate our M dwarfs at any angular separation. The second character indicates whether the declination of the star is too low or too close to the zenit, and the third character is directly related to the class definitions given in Table 2.1. From the combination of the three characters the stars

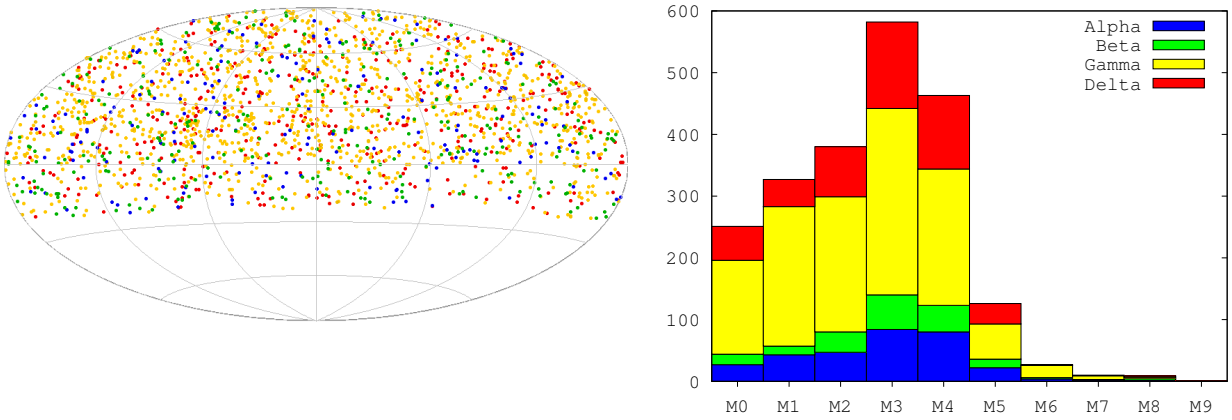

FIGURE 2.1— Sky (left) and spectral type (right) distributions of Carmencita stars. Blue stands for *Alpha*, green for *Beta*, yellow for *Gamma* and red for *Delta* classes in both figures.

will be classified into the less priority class achieved. This is, if the star is single with a "." but is faint for its spectral type with an "F", it will be *Gamma*. Another example, if it has an "F" but is not single and has a companion closer than 5 arcseconds, it will automatically turn into *Delta*. Only "." in the first and third characters will give an *Alpha* star as a result.

As explained in Chapter 2.1, the 2-Micron All Sky Survey (2MASS) scanned the sky with the near-infrared JHK filters and provided precise coordinates for almost half million stars up to a 3σ limiting sensitivity of 17.1 mag in the J-band. We therefore used this catalogue to obtain equatorial coordinates and J-band photometry of the M dwarfs to which we applied the selection criteria described in Table 2.1. As can be seen in the left panel of Fig. 2.1, our M dwarfs are homogeneusly ditributed on the sky. To prepare the observations with CARMENES and elaborate the finding charts, the J2000.0 coordinates were converted to J2016.0 by using the proper motion of the stars (Kim 2015). These new coordinates were also included in Carmencita.

TABLE 2.2— Description of the flags defined in Carmencita.

Flag	Character	Meaning	Class
Binarity indicator	.	Single	*Alpha*
	B	Resolved physical	
	V	Resolved visual	
	v	Possible resolved visual	
	S	Spectroscopic double or triple	*Delta*
	E	Eclipsing binary	
	X	No 2MASS JHK_s	
	J	Contamination by a bright companion at any separation	
Declination indicator	.	$\delta > 13\,\mathrm{deg}$	*Alpha*
	m	$-23\,\mathrm{deg} < \delta$ or $\delta > +87\,\mathrm{deg}$	
Magnitude–spectral type	.		*Alpha*
	f		*Beta*
	F		*Gamma*

The M dwarf stars of the catalogue were taken from different sources. They were initially selected from the Research Consortium on Nearby Stars catalogue (RECONS; Henry et al. 1994; Kirkpatrick et al. 1995; Riedel et al. 2014; Winters et al. 2015 and references therein) and the Palomar/Michigan State University survey catalogue of nearby stars (PMSU; Reid et al. 1995, 2002; Hawley et al. 1996; Gizis et al. 2002), which list M dwarfs up to 10 and 25 pc respectively. Afterwards, we revised several sources, such as the high proper–motion catalogues of Lépine et al. (2003, 2009, 2011, 2013) or the series of papers "Meeting the Cool Neighbors" (Cruz & Reid 2002; Cruz et al. 2003, 2007; Reid et al. 2003, 2004, 2008a). Table 2.3 provides the sources from which our M dwarfs were taken.

Table 2.3— Main sources of the CARMENES database.

Source	Reference	Number of stars
The Palomar/MSU nearby star spectroscopic survey	PMSU[a]	687
A spectroscopic catalog of the brightest ($J < 9$) M dwarfs in the northern sky	Lépine et al. (2013)	430
G. P. Kuipers spectral classifications of proper-motion stars	Bidelman (1985)	285
An all-sky catalog of bright M dwarfs	Lépine & Gaidos (2011)	254
Spectral types of M dwarf stars	Joy & Abt (1974)	222
Spectral classification of high-proper-motion stars	Lee (1984)	118
Meeting the Cool Neighbors	PMSU+[b]	23
Research Consortium on Nearby Stars catalog	RECONS[c]	22
...	Other[d]	135

Notes. [a] PMSU: Reid et al. (1995, 2002); Hawley et al. (1996); Gizis et al. (2002).
[b] PMSU+:Cruz & Reid (2002); Cruz et al. (2003, 2007); Reid et al. (2003, 2004, 2007, 2008a).
[c] RECONS: Henry et al. (1994, 2006); Kirkpatrick et al. (1995); Jao et al. (2011); Riedel et al. (2014); Winters et al. (2015) and references therein.
[d] Other: Bochanski et al. (2005); Caballero (2007, 2009, 2012); Deacon et al. (2012); Fleming et al. (1988); Frith et al (2013); Giclas et al. (1959); Gigoyan et al. 2010; ; Gizis & Reid (1997); Gizis et al. (2000); Gray et al. (2003); Kirkpatrick et al. (1991); Law et al. (2008); Lépine et al. (2003, 2009); Lodieu et al. (2005); Metodieva et al. (2015); Mochnacki et al. (2002); Newton et al. (2014); Phan-Bao & Bessell (2006); Reiners & Basri (2007); Riaz et al. (2006); Scholz et al. (2005); Shkolnik et al. (2009); Yi et al. (2014).

Every star in Carmencita has been named with our own identifier, dubbed Karmn name ("Karmn" is the classic Arabic name for poem, and is one of the sources of the Spanish name "Carmen"). It takes the form "Karmn JHHMMm+DDd", where "J" stands for the standard equinox of J2000.0 and HHMMm+DDd for truncated equatorial coordinates. The right-most digit of the fields HHMMm and DDd should be computed as the truncated low integer of m = (SS/6) and d = (MM/6), respectively. For binary pairs with similar HHMMm+DDd, we added North/South or East/West to distinguish them.

To ensure that the CARMENES guaranteed time is invested in the most promising targets, it is critical to characterize them. To this purpose, dozens of parameters were compiled, from astrometry to photometry, multiplicity and activity indicators. These parameters were taken from many different sources, but also measured from new observations carried out by the Consortium (see Fig. 2.2). For example, we (i.e., the Consortium) derived spectral types from low resolution spectra to confirm the literature spectral types (Alonso-Floriano et al. 2015a), looked with high resolution imaging for close companions (see Chapter 4), measured the pseudoequivalent width of Hα in low and high resolution spectra (Alonso-Floriano et al 2015a; Schöfer 2015), computed radial and rotational velocities (Schöfer 2015 and Jeffers et al. 2016, respectively), and derived fundamental parameters such as the metallicity, effective termperature or gravity (Passegger et al. 2016).

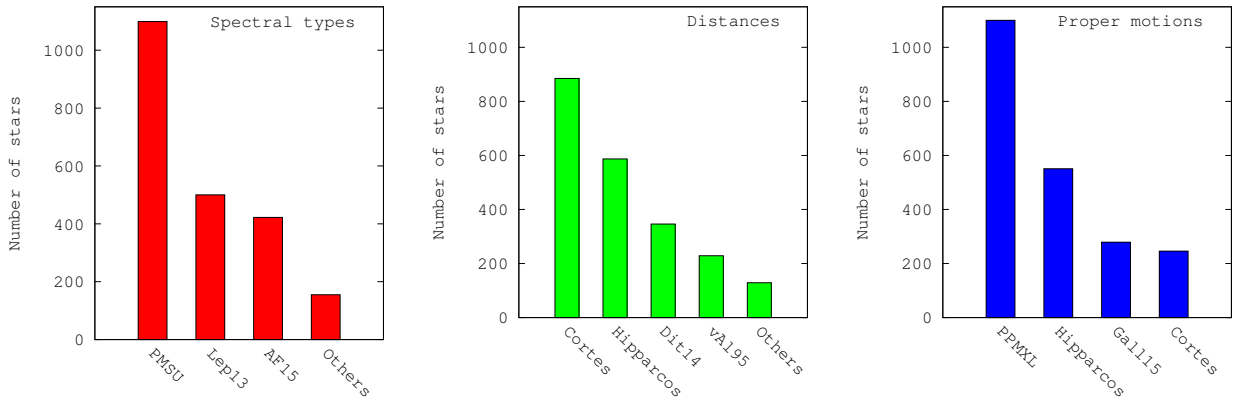

FIGURE 2.2— Histograms of references. From left to right: spectral types (red), distances (green) and proper motions (blue). *Left panel:* AF15: Alonso-Floriano et al. (2015a); Lep13: Lépine et al. (2013); Others: see Table B.1 in Appendix B; PMSU: Reid et al. (1995, 2002); Hawley et al. (1996); Gizis et al. (2002). *Middle panel:* Cortés: This work; Dit14: Dittmann et al. (2014); *Hipparcos*: Perryman et al. (1997), van Leeuwen (2007)); Others: see Table B.1 in Appendix B. *Right panel:* Cortés: This work; Gall15: Gallardo (2015); *Hipparcos*: van Leeuwen (2007); PPMXL: Roeser et al. (2010).

The primary compilation of the data took almost three years, taking into account the implementation of new parameters like more photometric bands and the addition of more stars in rare cases. Hence, it has being continously updated with more recent measurements obtained by us or published in the literature. Table B.1 in Appendix B provides the list of parameters and references included in the database that are recorded in more than 150 columns. A further description and analysis of some of them will be related in following sections.

2.2 Spectral types and methodology

Among all the compiled parameters, spectral types are one of the most decisive for CARMENES monitoring because they determine the class to which the star belongs together with J-band photometry and, thus, assign priorities to CARMENES potential targets.

The Consortium has therefore made additional observational efforts to achieve new low resolution optical spectroscopy in order to increase the number of bright, late M dwarfs and to confirm that the spectral types used for the Carmencita selection are correct. In particular, low resolution spectroscopy with CAFOS at the 2.2 m Calar Alto telescope was performed for 753 stars. Spectral types, surface gravity, metallicity and Hα chromospheric emission were derived and published by Alonso-Floriano et al. (2015a). Observations included high-proper motion M dwarf candidates from Lépine & Shara (2005) and Lépine & Gaidos (2011), M dwarf candidates in nearby young moving groups, in multiple systems containing FGK-type primaries targeted for metallicity studies, in weakly bound binary systems at the point of disruption by the Galactic gravitational field, M dwarfs resulting from new massive Virtual Observatory searches, M dwarfs in Carmencita with uncertain spectral types and with well-determined spectral types for comparison (Alonso-Floriano et al. 2015a and references therein). The oberved sample contained 679 M dwarfs, of which 422 are Carmencita stars.

Carmencita spectral types were mainly taken from Alonso-Floriano et al. (2015a), Lépine et al.

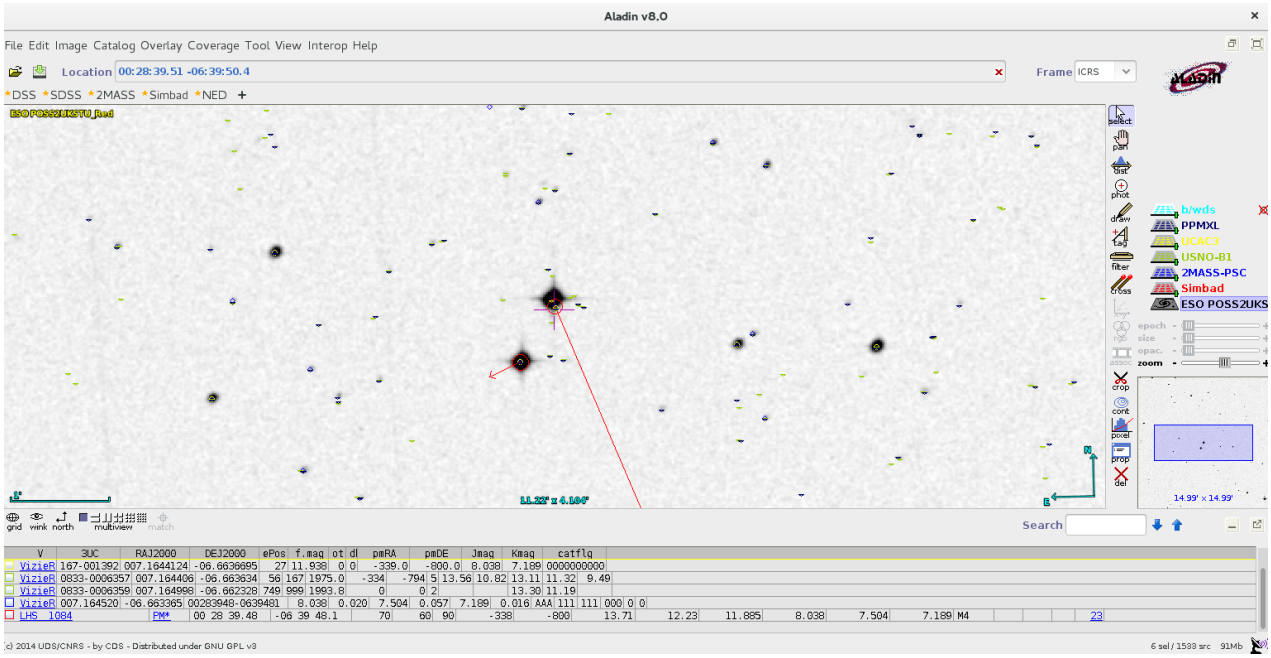

FIGURE 2.3— Snapshot of a single star of the catalogues search method with Aladin.

(2013), PMSU in that order of priority, although near 150 of them came from many other sources. All of them were taken in the first place from spectroscopic surveys. In the case of close M binaries, the photometric derivations of the spectral types of the components were adopted. Left panel in Fig. 2.2 shows the histogram of the main references from which the spectral types in our database were adopted. The complete list of references can be found in Table B.1 in Appendix B.

The distribution of Carmencita stars with the spectral type and class is shown in the right panel of Fig. 2.1. The most abundant stars in our input catalogue are M3 V followed by M4 V, and only 175 are dwarfs with spectral types later than M5 V. Regarding the *Alpha* stars, they are more uniformely distributed up to M5 V, although there are still more M3 V and M4 V. For this reason the *SS* subsampling was defined (see Section 2.1). Spectral types for all the Carmencita stars are given in Table B.2 in Appendix B.

The compilation of the Carmencita stars was initiated by other Carmenes team members, and revised and continued by myself afterwards. Here I will describe the method carried out.

For each dwarf in each source from Table 2.3, we checked whether the two selection criteria were fulfilled: the declination must be $\delta > -23\,\mathrm{deg}$ and it must satisfy the spectral type-J magnitude relation described in Table 2.1. Unfortunately, some of these sources had not on-line published tables and this task needed to be performed one by one directly from the tables in the refereed article. For those stars that passed the cut, an extensive procedure was performed using the Virtual Observatory tools Aladin Sky Atlas (Bonnarel et al. 2000), Simbad astronomical database (Wenger et al. 2000), VizieR service (Ochsenbein et al. 2000), and the Tool for OPerations on Catalogues And Tables Topcat (Taylor 2005). This method was executed in the following order for all of the 2176 M dwarfs of the database:

1. Visual inspection with the Aladin Sky Atlas:

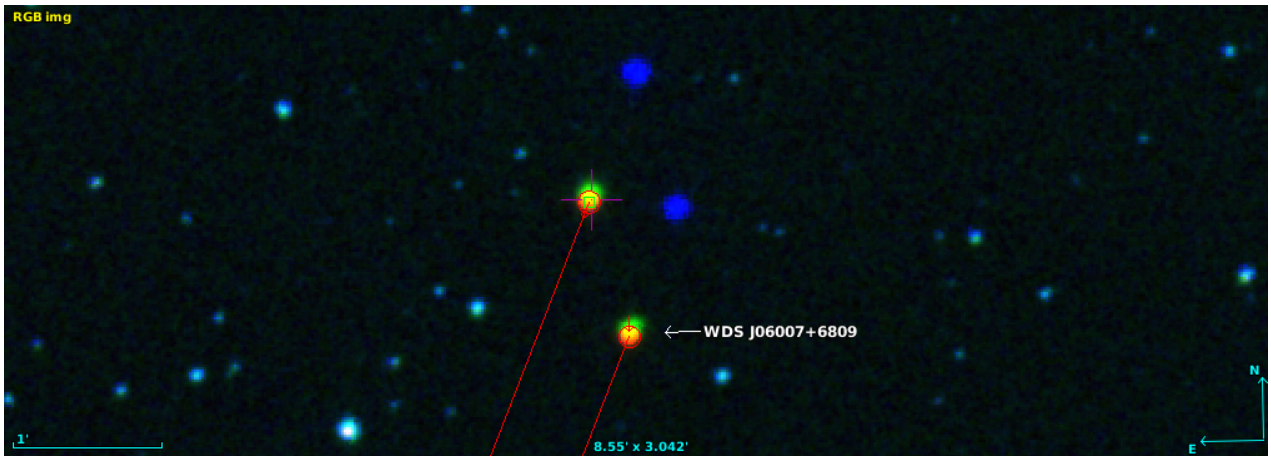

FIGURE 2.4— False-colour composed image of the high proper-motion pair WDS J06007+6809 composed by the two Carmencita M dwarfs LP 057–040 abd LP 057–041 (blue: POSS-I ∼1950, green: POSS-II ∼1990, red: 2MASS ∼1999).

I displayed the Palomar Observatory Sky Survey (POSS) I and II images with a radius of 1 arcmin around the coordinates given in the catalogue/article, and queried the 2MASS (Skrutskie et al. 2006), USNO-B1 (Monet et al. 2003), UCAC3 (Zacharias et al. 2010) , PPMXL (Roeser et al. 2010), *ROSAT* (Voges et al. 1999) and Washington Double Star (WDS, Mason et al. 2001-2015) catalogues to obtain the 2MASS coordinates, RI_NJHK_s photometric bands and proper motion of the star, while checking if it has X ray emission or a known physically bound companion. The UCAC3 catalogue was later supplied by the UCAC4 (Zacharias et al. 2013) and, when it was not available, by the CMC14 and the more recent CMC15 catalogues (Evans et al. 2002).

In some cases, to confirm that the star had or not an associated common proper motion companion, I also visually checked a false-colour or a blinked composition of two or more images at different epochs, such as POSS-I (mid 1950s) and 2MASS (late 1990s). In this way, it was possible to see if another star in the field comoved with our target. This exercise was also done when our target had a close companion in recent images (POSS-II or 2MASS), in order to verify the motion of both stars and to see if the photometry of our target was compromised, or if our star was only passing through or close to the background source in that epoch, and the proper motion of it and/or of our star was high enough not to interfer with our target by the time of CARMENES observations (2016). Fig. 2.3 shows a snapshot of this procedure, and Fig. 2.4 shows an example of the resulting false-colour composed image. A clear common proper motion pair was chosen for this example.

Displaying the images and the catalogs together served also to assign the source catalogue to the correct star when our target had high proper motion or the epoch of the catalogue was old and, thus, the coordinates of the target did not correspond to those of the catalogue. It was also useful for highly populated fields, where the measures could belong to a nearby source and not to our target.

2. Literature search in the Simbad astronomical database:

   After a first and quick compilation with Aladin, I made use of Simbad. It displays on the top of the technical datasheet the coordinates of the star together with the most relevant information: spectral type, proper motion, parallax (if any) and some photometric bands. On the bottom

of the webpage it also shows a list of parameters, of which all the available measurments can be displayed. Among them, the spectral type, distances or radial velocity measurements can be found.

In the first place, I compared the spectral types given in those frames with the spectral type of our M dwarf source, as well as tried to confirm similar proper motions in different sources, typically in *Hipparcos* (van Leeuwen 2007), the Lépine & Shara Proper Motions catalogue (Lépine & Shara 2005) and the PPMXL catalogue. Distances (parallactic of preference) were also taken from the information available in Simbad, and came mainly from *Hipparcos* (van Leeuwen 2007), Dittmann et al. (2014), and the General Catalogue of Trigonometric Stellar Parallaxes (van Altena et al. 1995). Photometric distances were taken otherwise (PMSU or Lépine et al. 2013 among others).

Simbad also displays the published articles that include our source. The number of them could range between a couple and hundreds. Among them, I looked specifically for planet information, multiplicity reports not recordered in the WDS or youth and activity indicators such as flares.

3. Compilation from the VizieR library service:

   During the initial compilation of the data of each star, this service was mainly used to obtain parameters from the PMSU catalogue, from which we selected the spectral type, the distance (if there was no parallax determination), radial and galactocentric space velocities, the Hα pseudoequivalent width, TiO5 and CaH_2 indices and M_V absolute magnitude.

   Sometimes and for specific targets, VizieR served to display all the catalogues available to easily compare parameters among different literature sources.

   Once all or almost all the Carmencita stars were put together, VizieR was used in a more practical way, by introducing as input all the coordinates of our stars and selecting one unique catalogue to look, for example, for radial or rotational velocities.

The described process refers to the initial stage of the database. Once it was complete, a more efficient way to compile data was carried out with VizieR and Topcat for all our Carmencita database.

2.3 Distances

Almost 60% of our distances come from parallax determinations. Of them, 90% were adopted from the General Catalogue of Trigonometric Stellar Parallaxes (van Altena et al. 1995), the new *Hipparcos* astrometric catalogue (van Leeuwen 2007) and the MEarth survey (Dittmann et al. 2014).

For those stars without parallaxes, we initially took photometric distances available in the literature (e.g., PMSU; Lépine et al. 2013). Photometric distances are not reliable as parallactic ones, since they need precise photometry and do not account for the contribution of close binary companions. In some cases, photometric distance determinations significantly varied from source to source for the same star or even for the two stars of a binary system. In other cases, the error bars associated were large to make us mistrust the distances. Sometimes, the reason for this was the presence of a close or very bright binary companion that affected the photometry. These differences, the diversity of the sources and methods used to derive them, and the lack of distances for around 7% of the database lead us to the need of homogeneising and computing our own spectro-photometric distances. To this purpose we derived an absolute J magnitude-spectral type relation based on single stars with good quality 2MASS J magnitude, confident spectral types and parallactic distances. The fit answers to a parabolic function and takes the form:

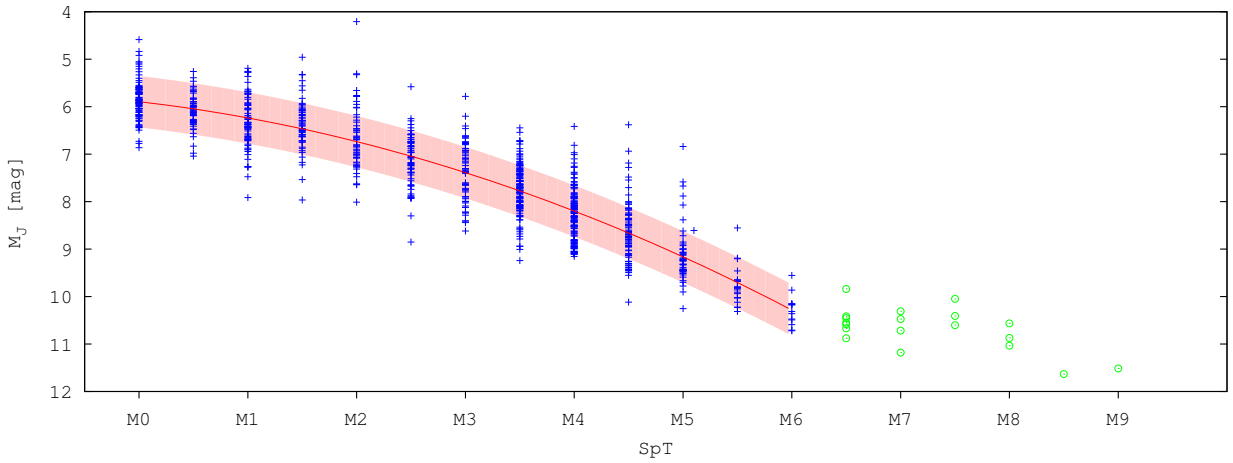

FIGURE 2.5— M_J absolute magnitude vs. spectral type of all the stars with parallactic distances in Carmencita. Dark blue crosses stand for the M0–M6 dwarfs used for the fit, while green open circles stand for M6.5-M9.0 dwarfs only plotted for completeness. The red solid line and shadowed region going from M0 V to M6 V represent our fit $\pm 1\sigma$.

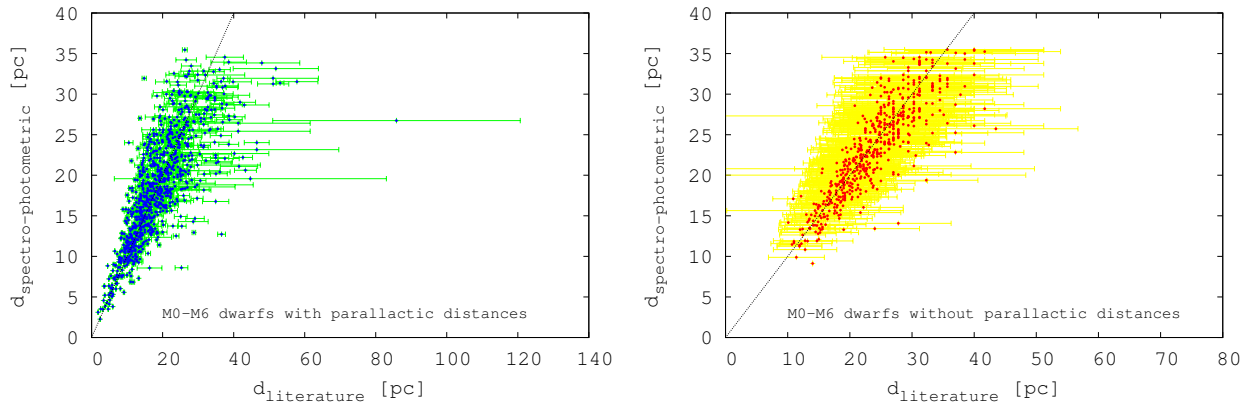

FIGURE 2.6— Comparison of the previous distances with the computed distances from our fit. Black dashed lines represent the relation 1:1. *Left panel*: our parallactic distances with blue dots and green error bars. *Right panel*: photometric distances with red dots and yellow error bars).

$$M_J = a\ \mathrm{SpT}^2 + \mathrm{b}\ \mathrm{SpT} + \mathrm{c}, \tag{2.1}$$

where $a = 0.078 \pm 0.007$ mag, $b = 0.265 \pm 0.038$ mag and $c = 5.895 \pm 0.044$ mag, and SpT indicates the numerical spectral subtype within the M range. Due to the low number of stars later than M6, this relation is only valid for earlier spectral subtypes (from M0 to M6 included). Very close binaries can not be used for the fit and the spectro-photometric distances derived for them should be carefully considered, since the 2MASS photometry and the spectral type determination provide the joint contribution of the two components. This means that the pair looks brighter and, thus, closer to the Sun than it actually is. Real distances of very close binaries are greater than the spectro-photometric distances as explained before (by a factor of 1.4 for equal mass binaries). Only by separating the photometry and spectral type for each component it is possible to derive the real distance of the system.

The number of stars used for the fit is 920, all of them belonging to the *Alpha*, *Beta* and *Gamma*

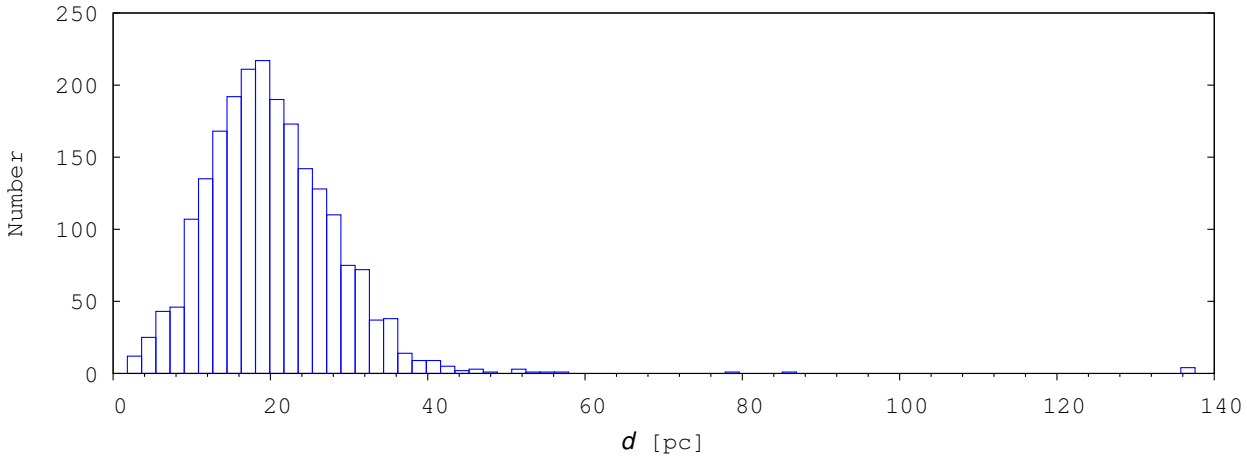

FIGURE 2.7— Distance distribution of the Carmencita sample. This and all the histograms here represented follow the definition given by Freedman & Diaconis (1981) to determine the size of the bins.

classes indistinctly. We computed spectro-photometric distances for 884 *Alpha*, *Beta*, *Gamma* and *Delta* M0–M6 dwarfs, acounting for the 730 stars with previous photometric distances and the 154 stars without any previous distance estimation to our knowledge. Still five stars in the M6.5 V–M9 V interval remained with literature photometric distances. The remaining 367 stars correspond to the *Delta* class M dwarfs with parallactic ditances, which I did not use for the fit.

The relation here applied has been revised over time with the implementations of newly published parallaxes, such as those of Dittman et al. (2014) and Weinberger et al. (2016). Nonetheless, the relation M_J-spectral type has barely varied (Cortés-Contreras et al. 2013, 2014, 2016). Fig. 2.5 shows the data used for the fit, and Fig. 2.6 shows in the left and right panels, the comparison with previous parallactic and photometric distances, respectively. The scatter between the new computed distances and parallactic distances is as low as could be expected from the data used for the fit shown in the left panel. There are only a few outliers with high errors associated to the parallactic distance. There also appears to be dispersion with previous photometric distances, but their errors were significatively high. Hence, we provide improved distances for more than 800 M dwarfs.

Table 2.4 lists the 14 Carmencita M dwarfs at less than 11 pc according to our spectro-photometric determinations. A parallax determination will be needed to confirm their proximity to the Sun. Among them, there is one spectroscopic binary and seven have companions at less than 1 arcsec. This means that they look brighter due to the presence of the companion and may appear to be closer to us than they actually are. Stars with companions at separations greater than 5 arcsec are considered as single stars.

Fig. 2.7 presents the histogram of distances in Carmencita. In spite of the wide interval of distances (from 1.8 to 137.0 au), the mean distance in the sample is around 20 pc, and 90% of Carmencita stars lie within 30 pc from the Sun. The closest star in our sample is the M3.5 V Barnard's star at 1.8 pc and the farthest stars are the four Taurus components discussed in Section 2.4.2. HIP 20122 is also an apparently far star at 85.8 pc, although its parallactic distance error is of 41%. From our M_J-spectral type relation, we locate it at 26.8 pc, which is also not correct due to the very

TABLE 2.4— Stars with the shortest spectro-photometric distances.

Karmn	Name	d [pc]	Multiplicity
J01221+221	G 034–023	10.2	Resolved Physical[a,b]
J02026+105	RX J0202.4+1034	8.8	Single
J04429+214	2MASS J04425522+0935544	10.9	Single
J05243–160	1RXS J052419.1-160117	10.0	Resolved Physical
J06354–040	2MASS J06352986-0403185	8.2	Resolved Physical
J07001–190	2MASS J07000682-1901235	9.4	Single
J07349+147	TYC 777–141–1	9.1	Resolved Physical[a,b]
J09156–105	G 161–007	7.7	Resolved Physical
J10125+570	LP 092–048	9.9	Single
J10367+153	RX J1036.7+1521	10.4	Resolved Physical
J14321+081	LP 560–035	9.2	Single
J19354+377	RX J1935.4+3746	9.2	SB1[b]
J21376+016	GSC 00543–00620	10.7	Resolved Physical
J22114+409	1RXS J221124.3+410000	10.1	Single

Notes. [a] They need confirmation of physical binding (see Chapter 4). [b] Distance corrected from binarity (see Chapter 4).

poor quality of 2MASS photometry. In any case, it is certaintly closer than 85 pc. Distances to our Carmencita stars are included in Table B.2 in Appendix B.

2.4 Kinematics

2.4.1 Proper motions

Astrometric and proper motion catalogues such as LSPM-North (Lépine & Shara 2005), PPMXL (Roeser et al. 2010) or *Hipparcos* (van Leeuwen 2007) supplied us 96% of the proper motions gathered in Carmencita. The main references of the adpoted proper motions and the number of sources are shown in the right panel of Fig. 2.2. Nonetheless, the LSPM catalogue does not provide proper motion errors, and PPMXL, the most extense proper motion catalogue, gives relatively high errors (from $4\,\mathrm{mas\,a^{-1}}$ and up to $10\,\mathrm{mas\,a^{-1}}$) compared to the $2.2\,\mathrm{mas\,a^{-1}}$ mean errors of *Hipparcos*. For this reason, I computed proper motions for 250 Carmencita dwarfs from astrometric catalogues running a macro in Aladin Sky Atlas and a self-built python script to handle the data of the catalogues. These stars were selected because the uncertainties on their total proper motion were $\delta\mu \geq 8\,\mathrm{mas\,a^{-1}}$, their total proper motions were $\mu \leq 50\,\mathrm{mas\,a^{-1}}$ or they did not have proper motion error estimations, which was the case of Luyten (1976), PMSU and LSPM catalogues. This task was completed by Gallardo (2015), who computed proper motions for another 279 Carmencita stars following the same procedure, originally presented by Caballero (2010).

After computing the proper motions, I compared our own determinations with previously tabulated proper motions. For those stars with differences between values $\Delta\mu$, $\Delta\mu_\alpha$ or $\Delta\mu_\delta$ (with μ the total proper motion, and μ_α and μ_δ the right ascention and declination components of the proper motion) greater than $50\,\mathrm{mas\,a^{-1}}$, I iterated for a second time in order to identify the source of discrepancy and to reach more accurate proper motions.

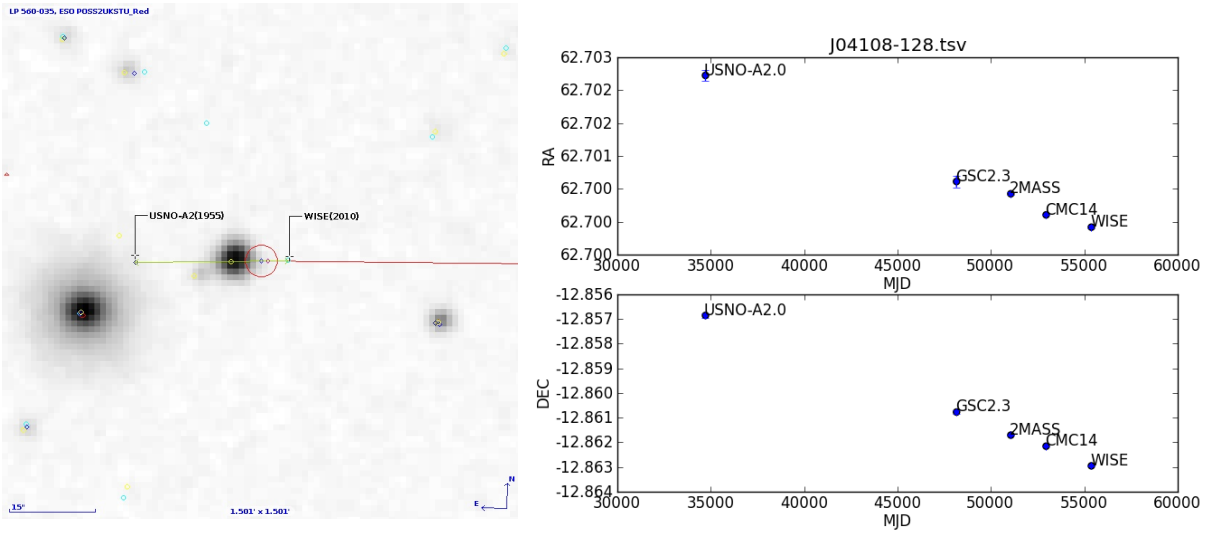

FIGURE 2.8— Ilustration of the tasks 1 (left) and 2 (right) followed for computing proper motion calculations. The two examples used show the M6.0 V J14321+081 (LP 560–035) on the left and the M5.5 V J04108-128 (LP 714–037) on the right, with total proper motions of 0.5 and 0.4 arcsec a^{-1}, respectively.

The method followed consisted of:

1. Loading images and catalagues in Aladin Sky Atlas:

   Typically the POSS-II image was loaded, together with the astrometric catalogues USNO-A2.0 (Monet et al. 1998), GSC2.3 (Morrison et al. 2001), 2MASS (Skrutskie et al. 2006), CMC14/15 (Evans et al. 2002), SDSS III (Ahn et al. 2012) and ALLWISE (Cutri et al. 2012, 2014), to cover from early 1950s to 2011, this is, 60 a in the best cases. The more epochs and the wider temporal interval, the better determination of the proper motion. In some cases, the AC2000.0 catalogue (Urban et al. 1998) was also included. Its mean epoch of observation is 1907, which gave us over a century coverage.

   Due to the presence of high proper motion stars and stars in very populated fields, this task could not have been totally automated, since the selection of the right point source of each catalogue is crucial. The example shown on the left panel in Fig. 2.8 ilustrates the problem: the faint source close to our target would have contaminated our data for calculations if all the catalogue entries around our object within a certain radius would have been chosen.

2. Computing proper motions from the catalogues information:

   The information needed from each catalogue was the J2000.0 right ascension and declination and their position errors, epoch of measurement transformed to Modified Julian Day (MJD) and name of the catalogue. Once I had a ".tsv" file for each dwarf, I ran my python scripts to select the corresponding cells and computed the proper motions from the definitions of the μ_α and μ_δ proper motion components:

$$\mu_\alpha = \mu \sin\phi \sec\delta, \tag{2.2}$$

$$\mu_\delta = \mu \cos\phi, \tag{2.3}$$

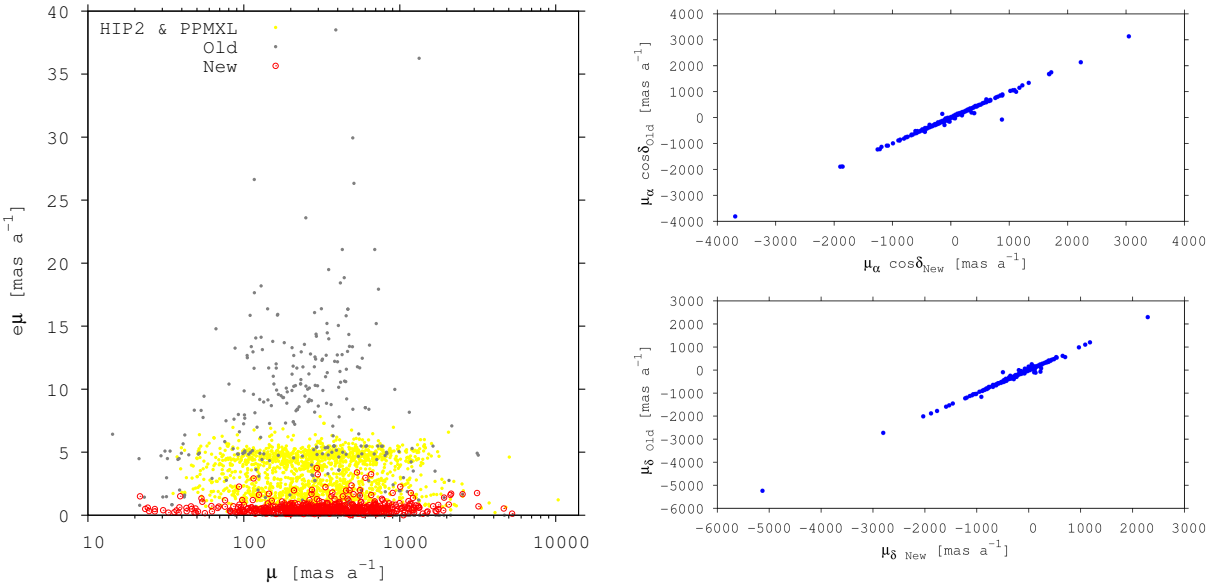

FIGURE 2.9— *Left panel:* Error of the total proper motion vs. proper motion comparison of previous tabulated values (gray filled circles) with our new determinations (red open circles). Yellow represent the literature non modified proper motion. *Right panels:* Comparison of previous and newly determined proper motion components.

where μ is the proper motion, ϕ the position angle and δ the declination. Hence, the total proper motion of the star is:

$$\mu^2 = \mu_\alpha^2 \cos\delta^2 + \mu_\delta^2. \tag{2.4}$$

This task was carried out in different steps in order to detect and clean spurious data (e.g., when the position loaded did not correspond to our target or one catalogue had several position determinations for the same epoch). We then obtained the most clean data used for computing proper motions. The right panel in Fig. 2.8 shows the right ascention and declination coordinates of the star in degrees versus the MJD. The example was chosen to see the clear motion of the star in both directions.

The typical temporal coverage was between 20 a and 60 a in most of our determinations, although with the inclusion of the AC2000.0 catalogue, it reached more than 100 a in some cases. The resulting proper motions here derived have smaller errors than the literature ones, and do not exceed 4 mas a^{-1}. Error bars of the total proper motions in our database are therefore limited to less than 8 mas a^{-1}. The improvement achieved can be seen in the left panel of Fig. 2.9, which also represents the *Hipparcos* and PPMXL proper motions.

The right panel of Fig. 2.9 shows the comparison between the right ascension and the declination components of the new proper motions with those previously tabulated in the literature. In general, we found our values to be in good agreement with previous ones. For dicrepant values, a detailed analysis revealed wrong literature determinations, probably due to mistaken catalogue point sources associated to stars in the field. We consider that our proper motion determinations are a correction to previous ones due to the manual treatment, specially in crowded fields or binary systems separated by less than 10–15 arcsec, where the scatter presented between previous and new proper

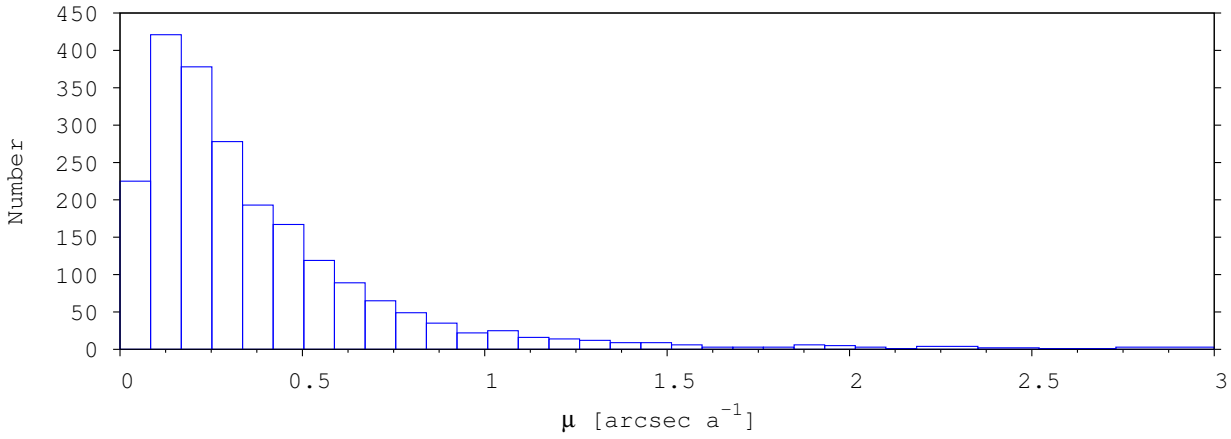

FIGURE 2.10— Proper motion distribution of the Carmencita sample. For a more detailed histogram, there are not represented the eleven Carmencita stars with proper motions larger than 3000 mas a^{-1}.

motions tends to be higher.

The proper motion distribution of Carmencita is shown in Fig. 2.10. There are ten dwarfs with proper motions larger than 3 arcsec a^{-1} that are not displayed in the histogram. Among them, it is the closest and fastest M dwarf near to the Sun: Barnard's star, with 10.4 arcsec a^{-1}. Table B.3 in Appendix B includes the proper motions and references of all the Carmencita stars.

2.4.2 Galactic space velocity components

As described in Chapter 2.1, stellar kinematic groups (SKG) or moving groups are composed by stars that share the same space motions and probably the same origin. There are several young moving groups characterized in the solar vicinity, such as Taurus-Auriga, Argus, IC 2391, the Local Association (LA) or Pleiades Supercluster, Hercules-Lyra (Her-Lyr), Ursa Major (UMa), Castor, and Hyades. The Local Association group includes the young groups TW Hydrae (TW Hya), η Chamaleontis (η Cha), β Pictoris (β Pic), Columba (Col), Carina (Car), AB Doradus (AB Dor) and Tucana-Horologium (Tuc-Hor). Their ages range from $\sim$10 Ma to $\sim$600 Ma and are listed together with their mean Galactocentric velocities and ages in Table 2.5.

Despite the high number of young candidate searches in the literature, among the revised surveys (Zuckermann et al. 2004; Torres et al. 2006; Shkolnik et al. 2009, 2012; Schlieder et al. 2012a, 2012b; Elliott et al. 2014; Alonso-Floriano et al. 2015b; the BANYAN series: Malo et al. 2013, 2014a, 2014b and Gagné et al. 2014, 2015a, 2015b) only 87 Carmencita dwarfs had been associated to young SKG.

To kinematically associate our Carmencita targets to an SKG, we derived the UVW galactic space velocities accounting for the parameters compiled in Carmencita. The Galactocentric velocity components can be computed from the distance, the radial velocity (V_r) and the (μ_α, μ_δ) proper motion components using:

$$\begin{bmatrix} U \\ V \\ W \end{bmatrix} = B \begin{bmatrix} V_r \\ k\frac{\mu_\alpha}{\pi} \\ k\frac{\mu_\delta}{\pi} \end{bmatrix}, \tag{2.5}$$

TABLE 2.5— Stellar kinematic groups.

Name	Age [Ma]	Reference[a]	U, V, W [km s^{-1}]
Taurus-Auriga	1–10	KH95, Luh04	–16.4, –13.2, –11.0
Argus	~ 40	Torr08	–22.2, –14.4, –5.0
IC 2391	~ 50	Barr04	–20.6, –15.7, –9.1
Local Association	$10 - 150$		–11.6, –21.0, –11.4
TW Hya	~ 10	Bell15	
η Cha	$10 - 15$	Mam99, Bell15	
β Pic	~ 25	Mess16	
Col	~ 40	Bell15	
Car	~ 40	Bell15	
AB Dor	~ 150	Bell15	
Tuc-Hor	~ 50	Bell15	
Her-Lyr	$200 - 300$	Eis13	–12.4, –26.0, –8.1
UMa	≥ 300	Gia79, SM93	14.9, 1.0, –10.7
Castor	≥ 300	Barr98, Mam13	–10.7, –8.0, –9.7
Hyades	~ 600	Perr98	–39.7, –17.7, –2.4

Notes. [a] Barr98: Barrado y Navascués (1998); Barr04: Barrado y Navascués et al. (2004); Bell15: Bell et al. (2015); Eis13: Eisenbeiss et al. (2013); Gia79: Giannuzzi (1979); KH95: Kenyon & Hartmann (1995); Luh04: Luhman (2004); Mam99: Mamajek et al. (1999); Mam13: Mamajek et al. (2013); Mess16: Messina et al. (2016); Perr98: Perryman et al. (1998); SM93: Soderblom & Mayor (1993); Torr08: Torres et al. (2008).

where $k = 4.74057\,\mathrm{km\,s^{-1}}$ and B is a 3×3 coordinates matrix of the form:

$$B = \begin{bmatrix} -0.06699 & -0.87276 & -0.48354 \\ +0.49273 & -0.45035 & +0.74458 \\ -0.86760 & -0.18837 & +0.46020 \end{bmatrix} \cdot \begin{bmatrix} +\cos\alpha\cos\delta & -\sin\alpha & -\cos\alpha\sin\delta \\ +\sin\alpha\cos\delta & +\cos\alpha & -\sin\alpha\sin\delta \\ +\sin\delta & 0 & +\cos\delta \end{bmatrix}, \qquad (2.6)$$

where α and δ are the equatorial coordinates (Johnson & Soderblom 1987).

Eggen (1984, 1989) defined the kinematic boundaries of the young disc population as: $-50 < \mathrm{U} < +20$, $-30 < \mathrm{V} < 0$ and $-25 < \mathrm{W} < +10$ in km s^{-1}. This criteria, together with the knowledge of the Galactocentric velocities associated to each moving group plus a dispersion of 10 km s^{-1}, allowed us to identify young disc population and stellar kinematic group members as in Montes et al. (2001).

It is also possible to kinematically identify disc and halo populations as in Bensby et al. (2003, 2005). These populations are actually subdivided into thin disc, thick disc, transition between the thin and thick discs, and halo. The thin and thick disc are two different populations with contrasted velocity dispersions. In fact, glactocentric velocities increase from the thin disc to the halo populations. Separating different populations delimits the ages of the stars: stars populating the thick disc reach ages greater than ~ 8 Ga, while in the thin disc stars are younger and in the halo they are as old as the Galaxy ($\sim$13 Ga).

Carmencita contains 1592 radial velocities, either from the literature or measured from high-resolution spectra taken by the Consortium with CAFE, FEROS and HRS (Schöfer 2015). The

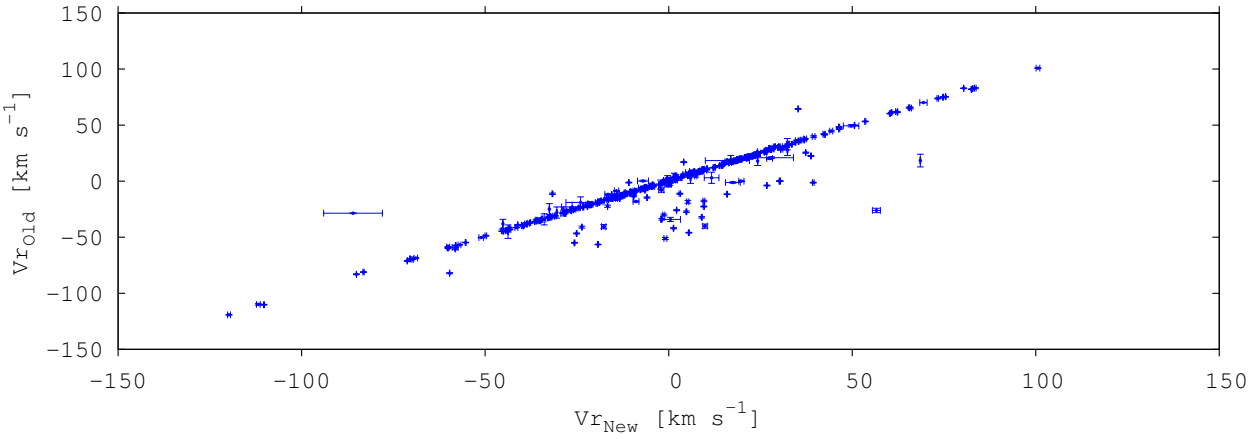

FIGURE 2.11— Comparison of the measured values of radial velocity from high-resolution spectra (new) and literature values (old).

radial velocities, together with the compiled and measured distances and proper motions, allowed us to compute the UVW components by applying Eq. 2.5. The comparison of our determined velocities with the 1261 velocities compiled from the literature (mainly from PMSU) is in good accordance (see Fig. 2.11). In addition, 353 stars in Carmencita with no radial velocities have UV, UW, or VW estimations from Lépine et al. (2013). The three components are needed for a kinematic analysis and thus, these stars were not considered. Table B.3 in Appendix B lists the UVW space velocities in the Carmencita sample.

Böttlinger diagrams in Fig. 2.12 ilustrate the Eggen's boundaries in the (U,V) plane, and the location of young stellar kinematic groups in the (U,V) and (V,W) planes. The number of stars that satisfy Eggen's criteria and thus, are young disc candidates, and the number of stars that could be associated to SKGs are summarized in Table 2.6. The youngest stars, i.e. those belonging to Taurus, Argus and TW Hydra, are listed in Table 2.7, and the complete list of Carmencita associations is given in Table B.4 in Appendix B.

The Toomre diagram in Fig. 2.13 represents $(U^2 + W^2)^{1/2}$ vs. V. It shows the candidates here suggested for the thin and thick disc and halo populations. The dashed constant space velocities drawn following the local standard of rest (LSR; $v = (U^2_{LSR} + V^2_{LSR} + W^2_{LSR})^{1/2}$) indicate the variance of velocities outwards the Galaxy and, thus, towards older populations. The number of thin, thick disc, transition between them and halo candidates are in Table 2.8, in which also young and old candidate members found in the literature are included.

Regarding the 446 Galactic young disc population stars, we provided radial velocity measurements from high-resolution spectra for 155 of them (Schöfer 2015). Of the 446, 55 were previously associated in the literature to the SKGs Argus, IC 2391, Local Association (β Pictoris, Columba, Carina, AB Doradus, Tucana-Horologium), Hercules-Lyra or Castor. We identified another 212 stars, which kinematics was associated to young SKGs. The remaining 179 stars did not have galactocentric space velocities that fit into the SKGs studied here (see Table 2.5). Besides, of the 87 M dwarfs found as SKGs members in the literature, we associated 55 to the young disc, 11 to the thin disc, and one to the transitional thin-thick disc populations. The remaining 20 have no radial

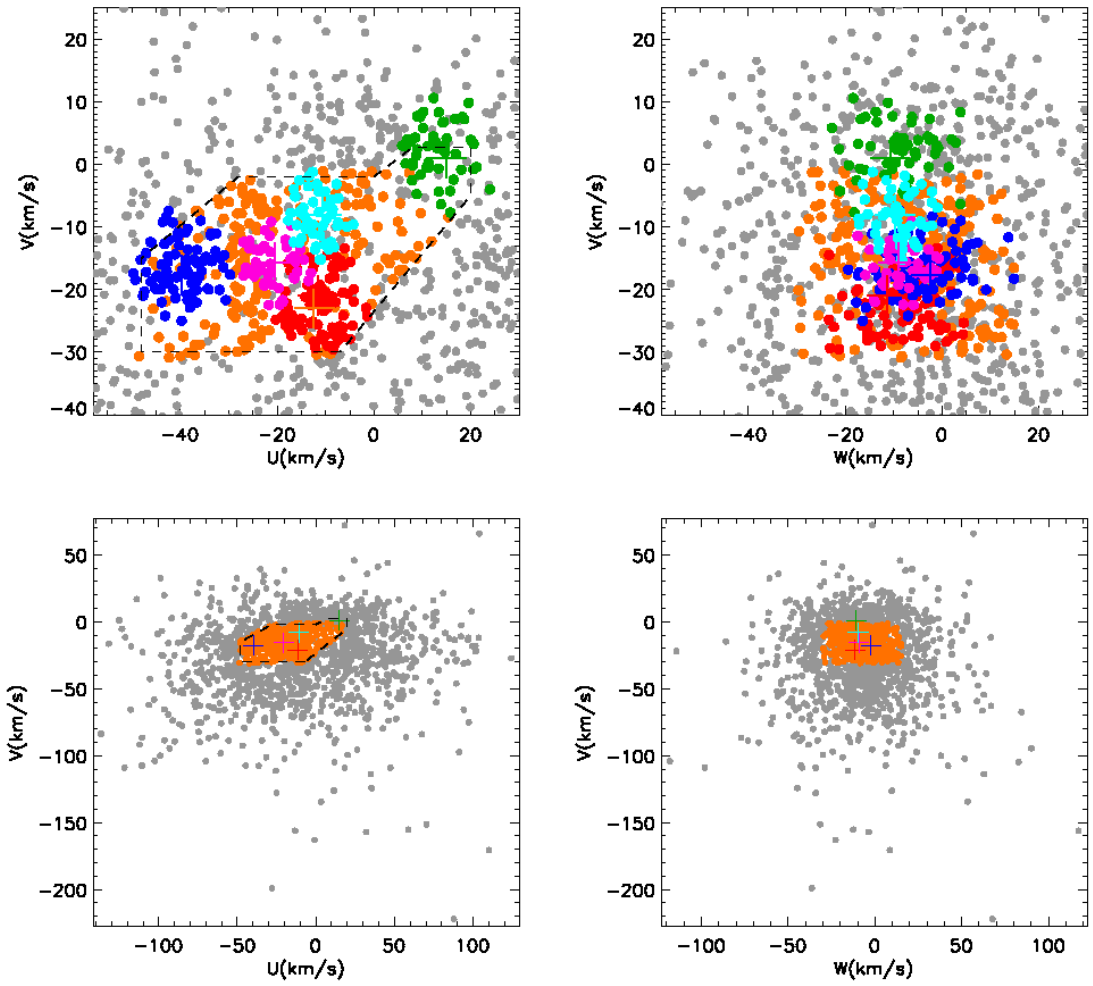

FIGURE 2.12— Böttlinger diagrams representing the (U,V) and (V,W) Galactocentric velocity planes. Dashed line limits Eggen's young disc population criteria. Orange dots represent stars within that boundaries and gray dots represent the rest of the sample. Top diagrams display the zoom of the bottom ones. Stellar kinematic group members are displayed in different colours: UMa (green), Castor (light blue), Local Association (red), IC 2391 (magenta), Hyades (dark blue).

velocity measurements in Carmencita. The star associated by us to the transitional thin-thick disc population is o^{02} Eri C, which wide companions are o^{02} Eri A and o^{02} Eri B. The system belongs to the young β Pictoris moving group (Alonso-Floriano et al. 2015b). The radial velocity of the C component is probably affected by the relative orbital motion around the B component and, hence, disrupts its kinematics. Among the 11 thin disc population stars, there are four spectroscopic binaries that were associated in the literature to the Local Association (J09193+620 (LP 091–014) and J16554-083S (V1054 Oph) by Tetzlaff et al. 2011) and Castor (J23318+199E and J23318+199W (EQ Peg Aab and EQ Peg Bab)). Their identification as thin disc population stars in our analysis could be explained by the radial velocity variations caused by the presence of the companion.

In Carmencita, there are four halo population stars, which are listed in Table 2.9: J02462–049 (LP 651–007) and J02575+107 (Ross 791), which are two single M dwarfs; J14575+313 (Ross 53 AB), which is a close binary separated by 0.80 arcsec; J20050+544 (V1513 Cyg Aab), which is a

TABLE 2.6— Number of stellar kinematic group members and candidates.

SKG	Num.
Taurus-Auriga	4
Argus	4
IC 2391	25
Local Association	
TW Hya	1
β Pic	33
Col	1
Car	1
AB Dor	23
Tuc-Hor	1
Other LA[a]	86
Her-Lyr	1
UMa	55
Castor	35
Hyades	82

Notes. [a] Stars kinematically restricted to the Local Association without specific membership.

TABLE 2.7— The youngest stars in Carmencita.

Karmn	Name	SKG	Ref.[a]
J00505+248	FT Psc AB	Argus	Malo14a
J04206+272	XEST 16–045	Taurus	Re10
J04294+262	FW Tau ABC	Taurus	Re10
J04313+241	V927 Tau AB	Taurus	Re10
J04433+296	Haro 6–36	Taurus	BG06
J09449–123	G 161–071	Argus	Malo13
J11477+008	FI Vir	TW Hya	Rei02
J15555+352	G 180–011	Argus	Malo14a

Notes. [a] BG06: Bertout & Genova (2006); Malo13: Malo et al. (2013); Malo14a: Malo et al. (2014a); Re10: Rebull et al. (2010); Rei02: Reid et al. (2002).

spectroscopic binary composed by an M subdwarf and a white dwarf with a T8 wide component at 188.5 arcsec.

It is not restricted to our Galaxy the formation process that leads to the presence of two different disc populations. Hence, the identification and further characterization of stars belonging to each of them, will also contribute to give shape to the overall scenario.

2.5 Multiplicity

An important aspect of M dwarfs is their membership in binary and multiple systems, which is helpful in the investigation of cool dwarf formation processes, and the precise determinations of the masses and radius of the components allows to constrain the input parameters of evolutionary models.

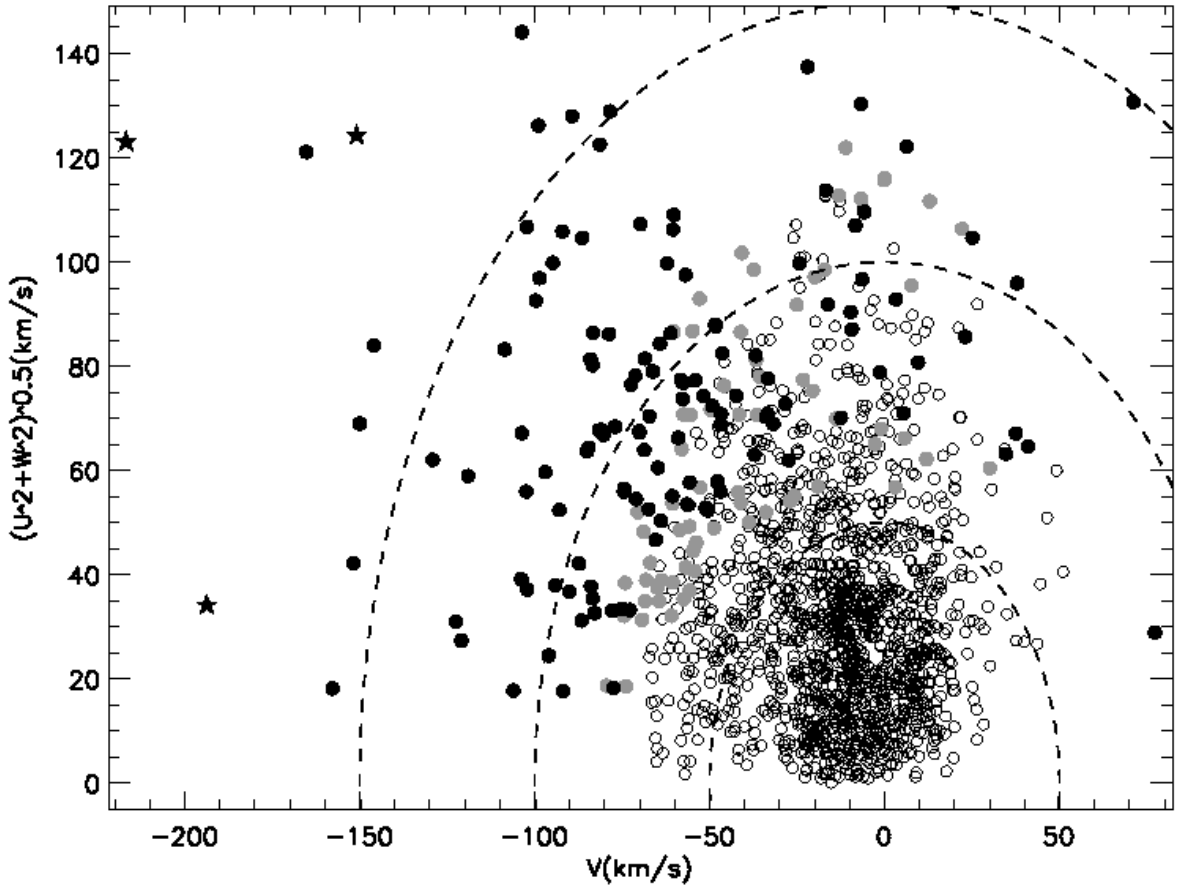

FIGURE 2.13— Toomre diagram representing $(U^2 + W^2)^{1/2}$ vs. V. Open circles stand for thin disc population, gray filled circles for thin-thick disc transition population, filled black circles for thick disc population and stars for halo population. Dashed lines indicate constant singular space velocities following the local standard of rest ($v = (U^2_{LSR} + V^2_{LSR} + W^2_{LSR})^{1/2}$) in steps of 50 km s^{-1}.

We compiled angular separations for all the known binaries in Carmencita, as well as the spectral types of the companions and difference of magnitudes in most cases. These data were mostly taken from the WDS. The search of close binary systems (i.e., angular separations (ρ) <5 arcsec) was also completed with the results of high resolution surveys of speckle (e.g., Balega et al. 2004, 2006, 2007), adaptive optics (e.g., Beuzit et al. 2004; Ward-Duong et al. 2015), lucky imaging (e.g., Bergfors et al. 2010; Janson et al. 2012, 2014a; Jódar et al. 2013), and radial velocity (e.g., Shkolnik et al. 2009).

In addition, we performed our own lucky imaging survey to ensure that the CARMENES GTO targets are single M dwarfs (see Chapter 4), and the CARMENES Consortium took high-resolution spectra with FEROS at the 2.2 m of the European Southern Observatory (La Silla, Chile), CAFE at the 2.2 m telescope in Calar Alto (Almería, Spain), and HRS at the 9.2 m HET (Texas), which permited us to identify near 35 new spectroscopic binaries in Carmencita through radial velocity semiamplitude variations (Schöfer 2015; Jeffer et al. in prep).

Almost 70 % of Carmencita is composed by single M dwarfs, which means that the remaining

TABLE 2.8— Stellar population classification.

Population	Num.
Young disc	446
Thin disc	937
Thin/thick transition	69
Thick disc	136
Halo	4

TABLE 2.9— Halo stars in Carmencita.

Karmn	Name	SpT	Ref.[a]
J02462–049	LP 651–007	M6.0 V	This work
J02575+107	Ross 791	M3.0 V	This work
J14575+313	Ross 53 AB	M2.0 V+	This work
J20050+544	V1513 Cyg Aab	sdM1.0 + WD	Mace13

Notes. [a] Reference of halo membership: Mace13: Mace et al. (2013).

30 % is completed with binaries and multiples at any range of physical separations. I will continue with the division at 5 arcsec defined for the *Delta* class stars. In Carmencita, 322 stars have one or more close binary companions (separated by less than 5 arcsec), 267 have one or more wide companions (by definition, separated by more than 5 arcsec) and 88 have both, close and wide companions. In addition, 32 stars have doubtful membership in binary or multiple systems at any separation, which could be resolved with another (high-resolution) imaging survey in most cases.

M dwarfs components of the same binary or multiple system were included individually in Carmencita if they were separated enough to be characterized photometrically and spectroscopically. Accounting for it and regardless of the angular separation between components, the number of binary and multiple systems are 439 and 118, respectively. Moreover, additional 23 and 13 binary and multitple candidate systems, respectively, need binding confirmation of one or more components.

Binary and multiple systems can be formed by all the possible compositions, including a spectroscopic binary, a close resolved physical companion (ρ <5 arcsec) and/or a wide physical companion (ρ > 5 arcsec). In addition, it is also possible that the primary, when it is not a Carmencita star (e.g., FGK star), is instead a spectroscopic binary or has other companions that could have not been gathered here by unawareness. Thus, the number of binaries may decrease with increasing the number of multiples.

Eclipsing binaries (EB) are of special interest since they can be used for calibration of stellar properties. In Carmencita, there are four *Delta* eclipsing binaries, all of them belonging to triples or high-order multiple systems: J03372+691 (LP 054–019) is a very close quadruple system kinematically young (Montes priv. comm.); J07346+318 (YY Gem CD) is an EB and the C component of a multiple system in which the A and B components are the Castor A and Castor B spectroscopic binaries at 70.5″composed by an A1 V+ and an M1.0 V+, respectively; J08316+193S (CU Cnc) has an M4.0 V wide companion (CV Cnc), which is a close binary pair at 10.10 arcsec, and candidate to the Galactic young disc population (Montes priv. comm.); J16343+571 (CM Dra) has a white

TABLE 2.10— Eclipsing binaries in Carmencita.

Karmn	Name	Spectral type	Multiplicity[a]	Ref.[b]	P [d]	Ref.[c]
J03372+691	LP 054–019	M3.5 V+	EB + SB2	Irw09; Shk10	0.771	Irw09
J07346+318	YY Gem CD	M1.0 V+	Wide + EB	Zas09	0.814	TR02
J08316+193S	CU Cnc	M3.5 V+	Wide + EB + RP	Luy97; Del99a; Beu04	2.77	Del99a
J16343+571	CM Dra	M4.5 V+	Wide + EB	Luy97; Irw09	1.268	Mor09

Notes. [a] EB: eclipsing binary; SB2: double-lined spectroscopic binary; RP: resolved physical companion at less than 5 arcsec; Wide: companion at a separation larger than 5 arcsec. [b] Beu04: Beuzit et al. (2004); Del99a: Delfosse et al. (1999a); Irw09: Irwin et al. (2009); Luy97: Luyten (1997); Shk10: Shkolnik et al. (2010); Zas09: Zasche et al. (2009). [c] Del99a: Delfosse et al. (1999a); Irw09: Irwin et al. (2009); Mor09: Morales et al. (2009); TR02: Torres & Ribas (2002).

dwarf companion at 26.3 arcsec, which age is limited at 100–200 Ma (Terrien et al. 2012). The main properties of the four systems are listed in Table 2.10.

2.5.1 Spectral types

First, we summarize the spectral type of the components in our Carmencita sample. Table 2.11 shows the number of companions to our Carmencita stars for each spectral type, and Fig. 2.14 represents the distribution of the companions spectral types as a function of the M spectral subtype in Carmencita for close (bottom right) and wide (top and left) systems. Multiple systems with close and wide companions simultaneously are counted twice, since the spectral types of the wide and close components are given separately. In the specific cases of M+M systems in which both components belong to Carmencita, as only one component is the primary, we counted them once. This means that, if 185 Carmencita stars also have Carmencita stars as companions, their contribution will be 93 in the table (in this case, there is one triple system with three M Carmencita components), and the rest (42) are M secondaries not belonging to Carmencita. By lack of awareness, spectral typing on a primary that is instead a binary system could be missing.

There are 24 Carmencita stars with a white dwarf companion, either at close or wide separation and in a binary or multiple systems. One of them belongs to the halo of the Galaxy, five are thick disc population, and 16 belong to the thin disc. Two of them have not been associated to any population to our knowledge, and J04153–076 (o^{02} Eri C) is a multiple system that has been associated to the transitional thin-thick disc population as well as to the β Pictoris moving group. This system was discused in Section 2.4.2.

The separation applied here into close and wide binaries is related to the initial classification of *Delta* stars, for simplicity. This separation cut is also used in Chapter 4 for completeness reasons, for deriving the multiplicity fraction of M dwarfs at low separations and, thus, will be maintained here. Details and discussion can be found in the corresponding chapter. Here, I will focus on the multiplicity in Carmencita in more general terms.

2.5.2 Multiplicity fraction

In our Carmencita sample, 359 dwarfs are distributed into 259 wide binary and multiple systems, which translates into 16% of the sample. Regarding the close pairs, 412 Carmencita stars are in 405 close binary and multiple systems, which represents 19% of the sample. Near one fourth of these

TABLE 2.11— Spectral types of the Carmencita confirmed companions.

Spectral type	Wide ($\rho > 5$ arcsec)	Close ($\rho < 5$ arcsec)
WD	20	3
WD+K	1	0
A, A+A	2	0
F, F+F	6	0
F+G	2	0
F+K	1	0
F+M	1	0
G, G+G	13	0
G+K	1	0
K, K+K	39	1
K+M	3	0
K+T	1	0
M[a]	134	68
L	4	3
T	6	0
Unknown[b]	25	331

Notes. [a] M companions belonging to Carmencita were counted once. [b] With no spectral type to our knowledge.

412 M dwarfs spectroscopic binaries, have a resolved physical component separated by less than 5 arcsec plus a spectroscopic companion, or are eclipsing binaries. Since the close and wide subsets are treated separately, the percentage of M dwarfs in binary and multiple systems in Carmencita is not the sum of the individual percentages. Accounting together for the close and wide pairs, 28% of Carmencita stars are physically bound to another hotter or cooler star.

To derive the multiplicity fraction of M dwarfs, it is necessary to account for all the systems with an M-type primary. In our Carmencita sample, we derived the multiplicity fraction for two intervals of angular separations: less and greater than 5 arcseconds. Due to the overlap between the wide and close subsets (close systems may have also a wide component and vice versa), these fractions shall not be summed together, since these systems would be counted more than once. Taking this into consideration, it is possible to derive a general multiplicity frequency for M dwarfs in Carmencita at all ranges of angular separations.

Since Carmencita is a selection biased sample, it is more convenient to build a volume limited sample to properly determine the multiplicity fraction of M dwarfs. Therefore, I built two different volume limited samples. The first one (VLS1 hereafter) is complete up to 87% within 12 pc and is composed by 317 M0–M9 dwarfs. The second one (VLS2 hereafter) is limited to M0–M5 dwarfs, is complete up to 86% within 17 pc and contains 774 dwarfs. These volume limited samples were built assuming that all M dwarfs are known within 7 pc and that their density in the solar vicinity is constant. This is a generous assumption for the VLS1, since the number of known late M dwarfs in Carmencita is low due to their faintness, and we are probably missing a non negligible amount of them.

I derived the multiplicity fractions for M dwarfs in the close and wide regimes separately, and at any range of angular separations for the Carmencita sample and the VLS1 and VLS2 subsamples.

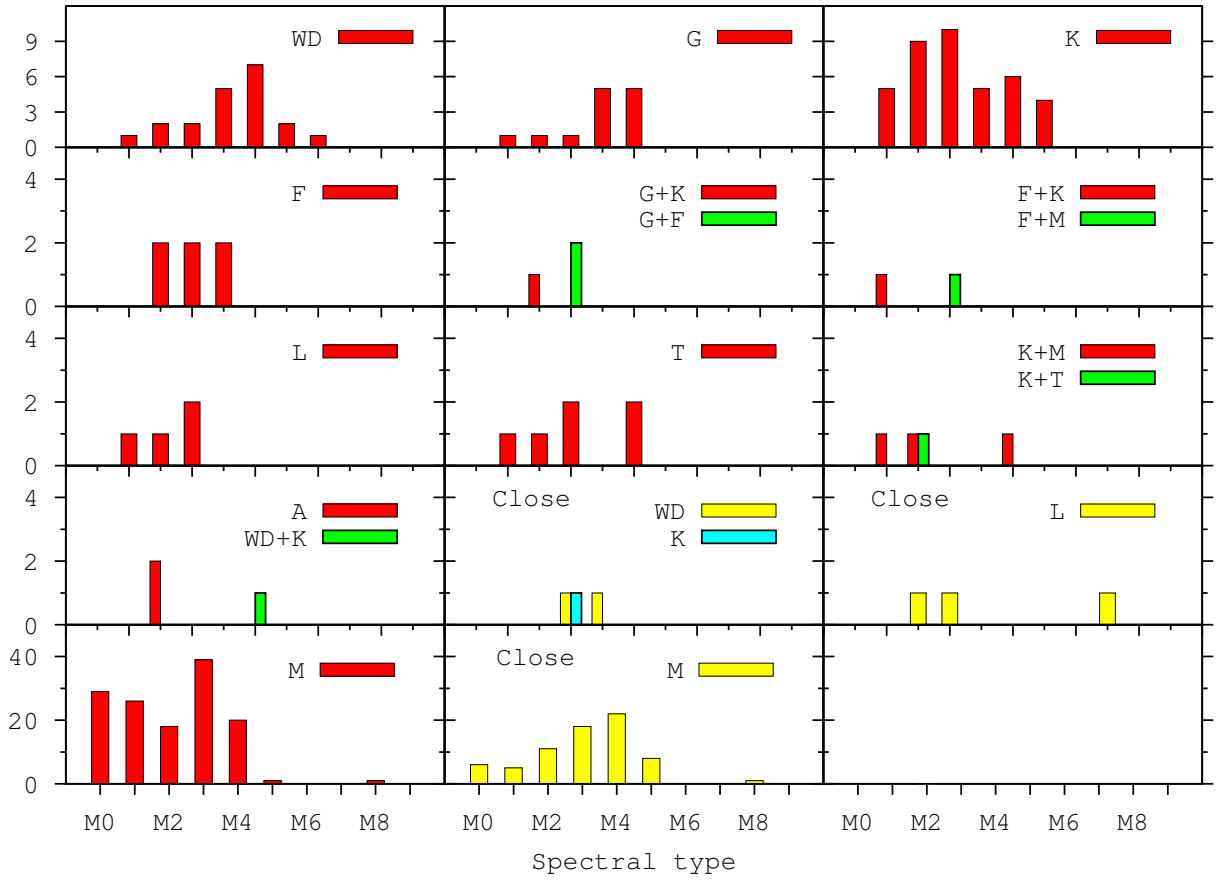

FIGURE 2.14— Spectral type distribution of the companions as a function of the spectral subtype of Carmencita stars. Red and green bars stand always for the wide systems, and yellow and blue for the close ones (indicated also in the corresponding diagrams).

Table 2.12 summarizes the multiplicity fractions obtained here for each sample and in each interval of angular separations.

The M multiplicity fraction of systems separated by more than 5 arcsec is the same in the three subsets within Poissonian errors. The main differences appear in the close regime. While for the VLS1 and VLS2 subsets the frequency is the same within errorbars, for the whole Carmencita sample there are about 8% less systems. This result extends to the multiplicity frequency that accounts for systems at any angular separation. This difference is related to the contribution of the more distant dwarfs, for which companions are faint and distant to be detected regardless of the separation to its primary. On the contrary, the contribution of late M dwarfs in the VLS1 with respect to the VLS2 does not appear to be relavant. This is due to the contribution of the spectroscopic binaries, which detection, as explained in Section 1.2.1 in Chapter 1, depends on the masses of the components and not on their brightness.

The multiplicity fraction in the close regime is conspicuously higher compared to the wide regime in all the subsets. On one hand, M dwarfs have been deeply studied with high resolution imaging and radial velocitiy surveys (Leinert et al. 1997, Daemgen et al. 2007, Bowler et al. 2015 among others). On the other hand and despite the possible failure in the detection of the faintest compan-

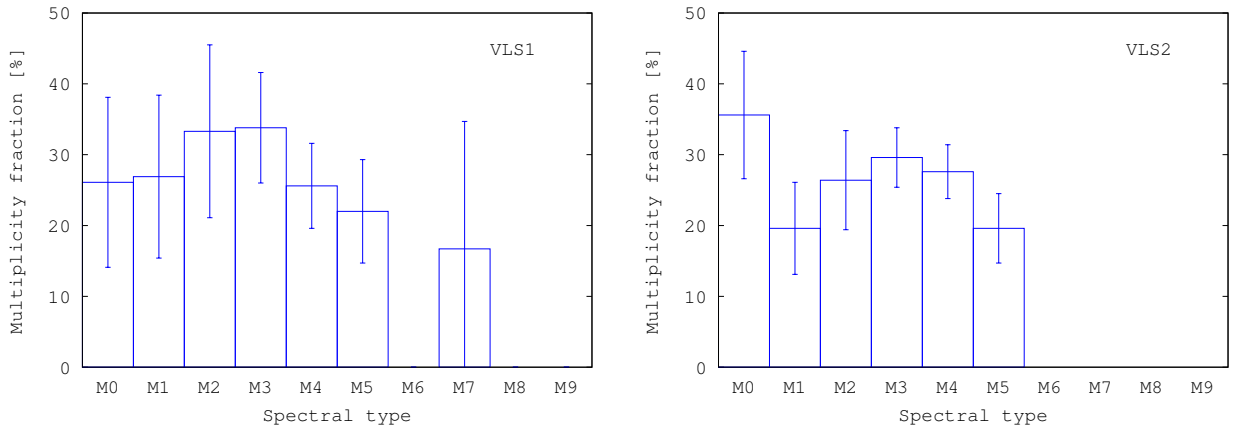

FIGURE 2.15— Multiplicity fraction dependence with the primary spectral type. *Left panel:* VLS1. *Right panel:* VLS2.

ions, it is more feasible the detection of equally or less bright companions at wide separations, even with low resolution imaging. The reason of this is the high dependence on astrometric catalogues of the methods followed in wide binary surveys (and thus, on photometry), which may not detect the faintest sources. In addition, and in spite of the extensive search in the literature that has been done, a complete search of wide companions around the Carmencita M dwarfs has not been carried out yet, and the volume limited samples defined here are not complete in angular separations.

TABLE 2.12— Multiplicity fractions in Carmencita (in %).

	Wide	Close	Wide & Close
Carmencita	6.5 ± 0.6	17.0 ± 1.0	19.1 ± 1.0
VLS1	7.6 ± 1.6	25.2 ± 3.2	26.5 ± 3.2
VLS2	8.0 ± 1.0	24.8 ± 2.0	28.7 ± 2.2

We want to compare our derived multiplicity fractions of M dwarfs with those given in the literature. The two surveys of reference in this case are those of Fischer & Marcy (1992) and Ward-Duong et al. (2015), who analyzed M dwarfs multiplicity at separations up to 10 000 au and distances of 20 pc and 25 pc respectively. The ranges of projected physical separations achieved in our samples are 0.5–2900 au and 0.5–3000 au in VLS1 and VLS2 respectively, far from the 10 000 au coverage of the referenced surveys. However, it does not seem to affect to our results, in light of the obtained M multiplicity fractions in Carmencita. Both fractions lie just between the $23.5 \pm 3.5\%$ given by Ward-Duong et al. (2015) and the $42 \pm 9\%$ given by Fischer & Marcy (1992), consistent within the error bars with both of them.

The M dwarf multiplicity fraction at all angular separations obtained here, has also intermediate values between those derived for solar-like stars (44–65% – Duquennoy & Mayor 1991; Raghavan et al. 2010), and very low mass stars and brown dwarfs ($15 \pm 7\%$ for M8.0–L0.5 dwarfs, Close et al. 2003; 10–15% for M7–L8 dwarfs, Reid et al. 2008b; $9^{+15}_{-4}\%$ for T dwarfs, Burgasser et al. 2003). The literature fraction of the lowest mass systems are derived only from high resolution imaging and, thus, only take into account close companions.

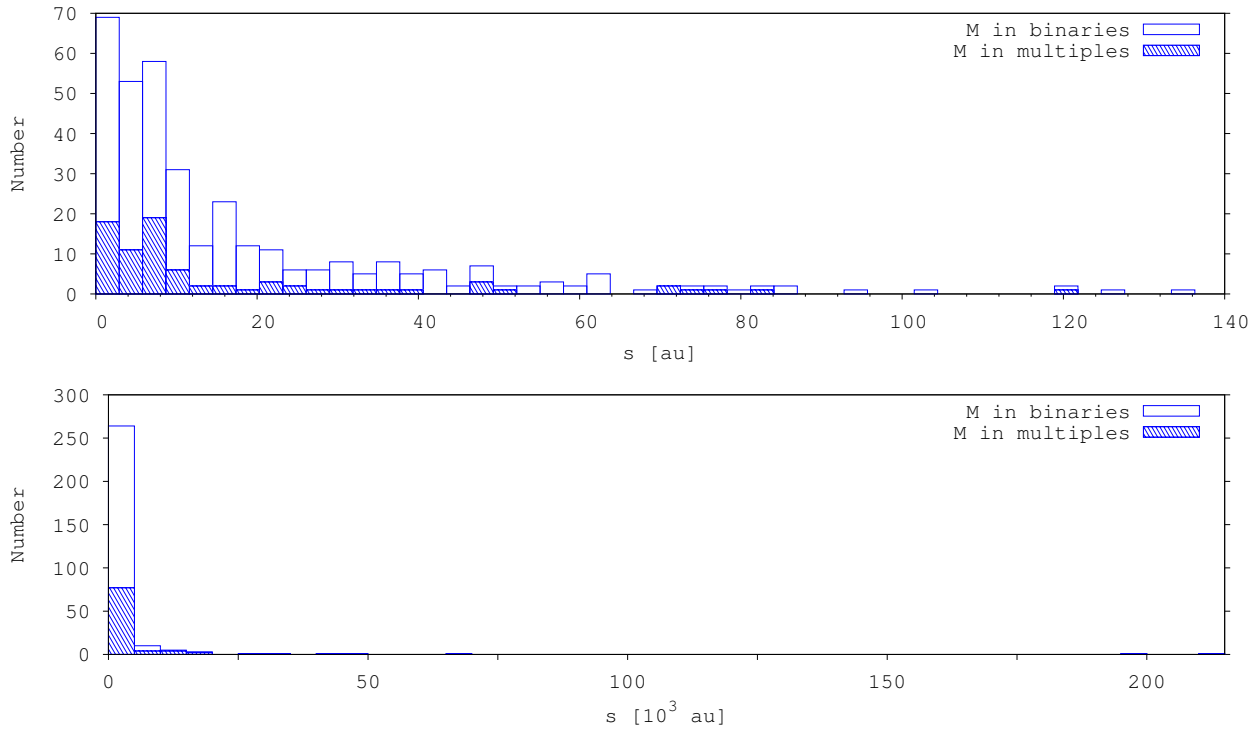

FIGURE 2.16— Projected physical separation distribution of close (top) and wide (bottom) systems in Carmencita. Empty bars represent all binaries, while dashed bars stand for triple and multiple systems.

Fig. 2.15 shows the multiplicity fraction as a function of the spectral type of the primary considering both close and wide companions. The left panel stands for the VLS1, which includes all M0–9 V in 12 pc. Within Poissonian error bars, the multiplicity fractions look constant. The distribution of the VLS2 on the right panel, which includes all M0–5 V in 17 pc, is also consistent with a flat distribution. We can not make a strong statement about these distributions, because the defined samples are complete in a certain volume of space but not in the search of companions at the separations considered. The VLS2 distribution can be compared with the distribution on Figure 5 from Chapter 4, which also represents the multiplicity fraction of M dwarfs in a volume limited sample containing all M0–5 V in 14 pc. Differently to the analysis presented here, it analyzes the presence of companions at angular separations between 0.2 and 0.5 arcsec. From the comparison of both figures we see that, again, the fraction of M1 binaries and multiples looks lower compared to other spectral types but not significatively. Furthermore, the general trend would also appear to be decreasing towards later spectral types (noticed as well in the VLS1 distribution), although there is not a clear slope and the errors associated match with a flat occurrence.

The multiplicity fraction of M dwarfs would also be age dependent, as seen in Section 1.3. From the association of the 1592 Carmencita stars to the different stellar populations in the Galaxy, I analized the frequency of M dwarf primaries in the young disc population and in the sample defined by the populations of the thin disc, the thick disc and of the halo. Of the 446 M dwarfs belonging to the young disc population, $35.0 \pm 3.2\%$ are M dwarf primaries in binary or multiple systems. On the contrary, of the 1146 M dwarfs that belong to the thin and thick discs, and halo populations,

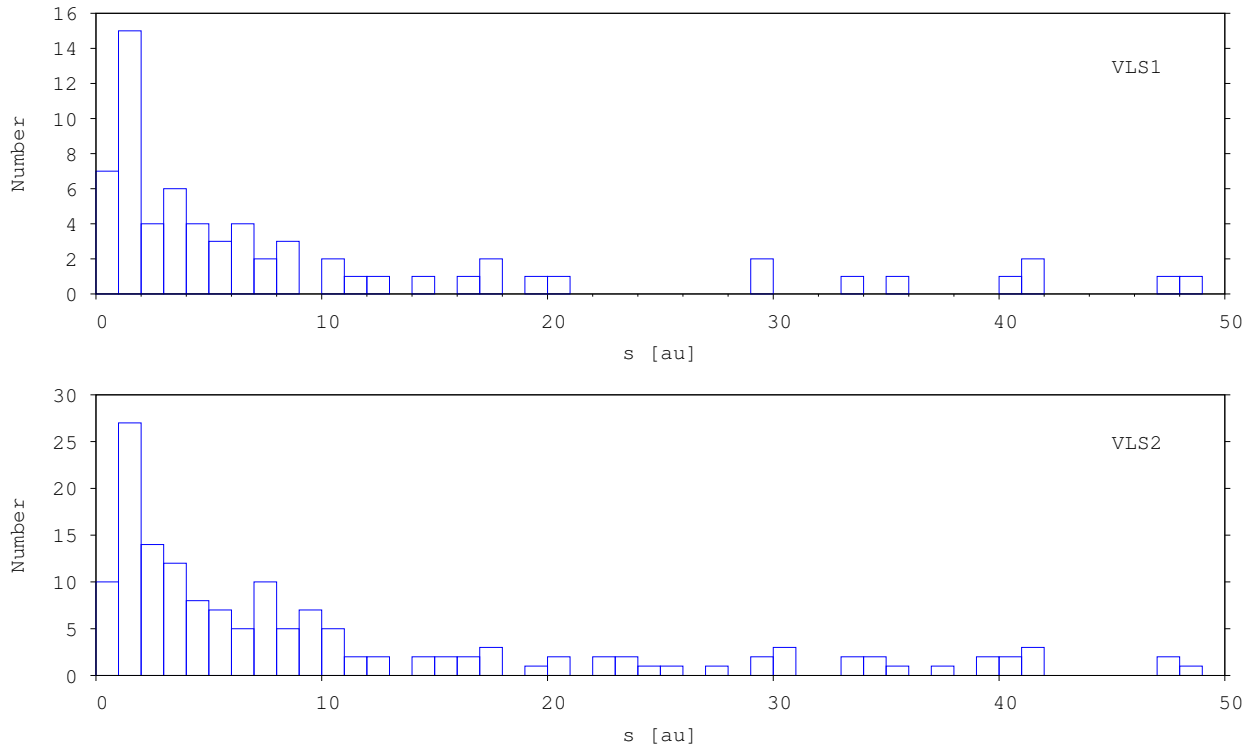

FIGURE 2.17— Projected physical separation distribution of the VLS1 (top) and the VLS2 (bottom) samples. Both histograms are truncated at 50 au.

the fraction is $25.0 \pm 1.6\%$. In an analog way as before, I built a volume limited sample for each subsample in order to derive an unbiased multiplicity fraction. Both volume limited samples are complete up to 85–86% at 12 pc. The one of the young disc population contains 100 M0–9 dwarfs, while the one of the older populations contains 200 M0–9 dwarfs. The frequencies derived are $35.0 \pm 7.0\%$ and $29.0 \pm 4.3\%$, respectively. Within Poissonian errorbars, the fraction of M dwarf primaries in binary or multiple systems is the same in both age regimes, although a higher fraction in the young sample would be expected according to Goodwin & Whitworth (2007) and King et al. (2012). The unbiased samples derived in this analysis are, however, not complete in the search of M dwarf companions. In addition, the age of the young disc population is not properly delimited and could have components as old as 1 Ga. At this age, binary systems formed in early stages could have been dynamically disrupted. The dependence on the age of young M dwarfs multiplicity should be analized within a few dozens of Ma, when formation process are still undergoing.

2.5.3 Angular and physical separation distributions

In this Section I analyze the distribution in angular (ρ) and projected physical (s) separations of the pairs. To convert angular into physical separations, I used the small angle approximation $\tan\rho \approx \rho$. Hence:

$$s = \rho d, \tag{2.7}$$

where d is the distance to the system. Used distances are those compiled from the literature or estimated spectro-photometrically by us, as explained in Section 2.3.

Fig. 2.16 shows the projected physical separation distributions of close and wide systems in Carmencita on the top and bottom panels, respectively. Dashed bars represent separations in triple and multiple systems in both panels. Projected physical separations in the close subset range from 0.3 to 135.2 au, and in the wide subset from 28 to $2.1\,10^5$. The superposition in physical separations of these subsets is limited to 25 systems from 28 au and greater separations. Close systems with projected physical separations under 50 au represent 90% of the subset, while 90% of wide systems have separations lower than 2900 au. This distribution has its maximum between 0.3 and 3.0 au. However, it considers the separations of the Carmencita M dwarf to any companion, hotter or cooler. The two widest pairs correspond, in fact, to two M dwarfs in a hierarchical quintuple system composed of a K6.0 V primary (HD 221503), an M2.0 V+ close binary (HD 221503 BC) separated by 9 au and by 5150 au to its primary, and an M3.0 V+ wide spectroscopiv binary (GJ 1284 Dab) at $2.1\,10^5$ au from its primary. The given separations correspond to the A-Dab and B-Dab triples. It is among the widest pairs known involving low mass stars components (Caballero 2010). Moreover, the separation of ~ 1 pc is near the boundary between physically bound pairs and proper motion companions.

To properly analyze this distribution in M systems, I consider the separation of the companions to M primaries in the VLS1 and the VLS2 samples. These distributions are shown in Fig. 2.17. Both of them peak between 2 and 3 au. This is in agreement with what is observed in M binaries from high resolution imaging surveys (see Chapter 4 and references therein). Furthermore, from the comparison between these distributions and the previous one (the one on top in Fig. 2.16), we infer that the contribution of hotter components is restricted to larger separations. Actually, for solar-like primaries, the distribution peaks around 30 au according to Duquennoy & Mayor (1991) and Raghavan et al. (2010), which means that the hotter the primary, the larger the separation to binary companions.

These distributions also serve us to analyze the probability distribution of close and wide pairs in the solar neighbourhood. Hereafter, "close" and "wide" will not refer to the 5 arcsec restriction defined before, but to a more general concept. In particular, the Öpik's law (Öpik 1924) reproduces the probability or, more precisely, the density of pairs at some determined physical separations by a power of law of the form:

$$\begin{aligned} f(a) &\propto a^{-1}, \\ N(a) &\propto \log a, \end{aligned} \tag{2.8}$$

where a is the semimajor axis, *f(a)* is the frequency distribution of separations, and *N(a)* is the cumulative distribution. A more general enunciation of the Öpik's law would be:

$$\begin{aligned} f(a) &\propto a^{-\lambda}, \\ N(a) &\propto a^{-\lambda+1}, \end{aligned} \tag{2.9}$$

where λ is a coefficient to be determined (Weinberg et al. 1987; Close et al. 1990), and $\lambda = 1$ gives the original Öpik's law.

In the following discussion, I consider $a \approx s$, since the difference between the expectation values of $\log a$ and $\log s$ ($E(\log a)$ and $E(\log s)$, respectively) has been estimated in 0.11–0.15 (1.3–1.4 au) according to Couteau (1960) and Kuiper (1942).

Fig. 2.18 displays the $\log s$ cumulative distribution. For comparison, there are represented all the systems with an M primary in Carmencita, the VLS1, and the VLS2 samples. The power of law in

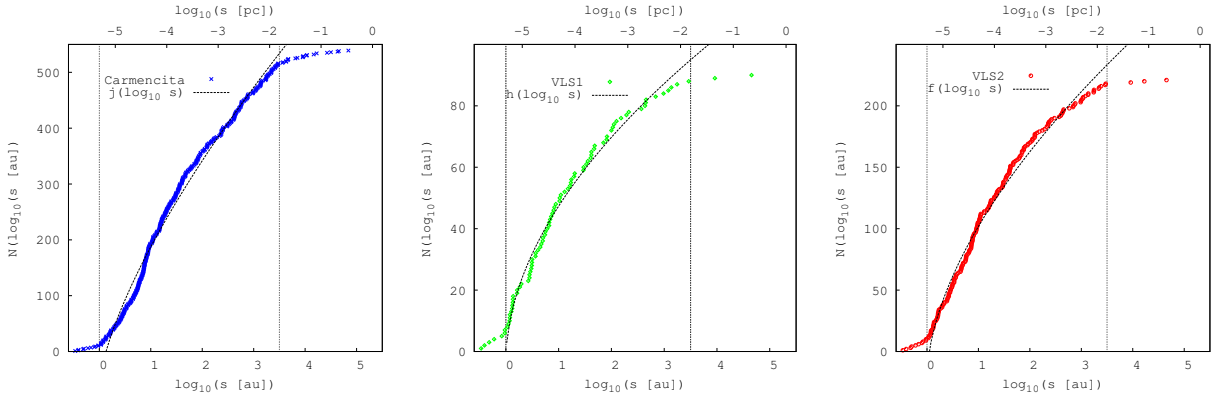

FIGURE 2.18— Cumulative distribution of the logarithm of the projected physical separations of all the primaries in Carmencita (blue crosses, left panel), the VLS1 (green diamonds, middle panel), and VLS2 (red open circles, right panel). The fitting functions $j(\log s)$, $h(\log s)$, and $f(\log s)$ are overplotted in black dashed lines. Its range of application es delimited with vertical black dotted lines.

Eq. 2.9 can only be fitted in pieces, in an intermediate interval of separations between the closest and widest pairs. This statement was proved by Poveda & Allen (2004). At very close separations, the contribution of binary and multiple systems is affected by the non-detected companions, either due to faintness or to closeness (spectroscopic binaries). At wide separations, the systems are affected by gravitational encounters and their number tend to decrease with time. The different slopes may also be associated to different formation scenarios: disc fragmentation for the closest pairs, and cloud contraction for the widest (see Section 1.1.4). In our distribution, a first approximation of the interval of application of the Öpik's law in its general formulation lies approximately between 0 and 3.5 in $\log s$ (between ~ 1 au and ~ 3160 au). The best fit of Eq. 2.9 was then determined within the 0–3.5 $\log s$ interval for each subset as:

$$N(log\ s) = a + b\ log\ s^{-\lambda+1}, \tag{2.10}$$

where a, b and λ are free parameters.

The solution obtained for each subset is given in Table 2.13, together with the standard deviation of the fit (σ) and the confident level (CL) of the Kolmogorov-Smirnov (KS) test performed to quantify the goodness of the fit. For the systems in the Carmencita sample, a power-law function does not provides a good fit to the data. On the contrary, it fits better for the VLS1 and VLS2 subsets. In addition, the values obtained for λ are very similar in the volume limited samples, and slightly differ from the value infered for Carmencita. The confidence level of the fits are 96–97% for the volume limited samples and downs to 30% for Carmencita.

TABLE 2.13— Fit parameters to the general formulation of the Öpik's law.

Subset	a	b	λ	σ	CL [%]
Carmencita	–58.8 ± 4.9	246.3 ± 5.2	0.30 ± 0.01	15.8	0.30
VLS1	–2.7 ± 1.9	50.1 ± 2.2	0.47 ± 0.02	2.5	0.97
VLS2	19.5 ± 3.1	121.3 ± 3.4	0.41 ± 0.02	6.4	0.96

Dorda (2011) carried out a statistical analysis of the Öpik's law in its alternative enunciation for the first Carmencita table ever built. He included every system containing also more massive primaries and defined several intervals of separations to run the KS test. With a CL of 95% or higher and within –0.09 and 3.45 $\log s$ ($\sim$0.8–2800 au), the derived λ derived were between $\lambda = 0.8$ and $\lambda = 0.9$. The difference between the values of Dorda (2011) and those obtained in this work resides in the consideration of more massive components and, in light of our results, in the distance completeness of the sample. The incompleteness in angular separations affects overall to the closest systems, which are excluded of the analysis, and the widest, which maximum angular separation needs to be defined. Thus, not a relevant contribution could be expected. Despite this circumstance and the lack of delimitation in the range of physical separations to apply the power-law, both volume limited samples, VLS1 and VLS2, consistently satisfy the general hipothesis of the Öpik's law between 1 and 3160 au.

Another statistical analysis of the cumulative s distribution was performed by Close et al. (1990) in a volume limited sample complete at projected physical separations greater than $6.6\,10^7$ au ($\sim$3 arcsec at 20 pc), $M_V < 9.0$ mag, $\pi > 0.04$ arcsec and $\delta > -12\,^\circ$. In this case, they derived $\lambda \sim 1.3$–1.4 with a CL greater than 80% for a mass-unbiased sample. The interval of separations in the analysis covered from $\sim$65 au to $\sim$20500 au, while in this work we span from 1 au to 3160 au. Systems in our samples in the $\sim$3160–70 000 au interval were excluded due to the pronounced change of tilt in the cumulative distribution. This noticeable difference stands out the effect of the mass in the range of separations in binary and multiple systems: the higher the mass of the primary, the larger the separation at which the companions are found. Besides, the sample of multiples in Close et al. (1990) is limited to 45, which compared to the 79 (VLS1), 205 (VLS2) and 485 (Carmencita) of our subsets, enriches the quality of the statistics presented here.

The population and age of the systems would also influence the $\log s$ cumulative distribution (Poveda et al. 2007). For the moment, it is not possible to separate young and old pairs in our samples, since a deep age analysis needs to be done.

2.6 Photometry

Up to 19 photometric bands were revised and included in Carmencita, covering from the ultraviolet to the infrared. They are listed in Table 2.14, together with the effective wavelength ($\lambda_{\rm eff}$), the cero point flux (F^0_λ), and the filter and magnitude systems. The bands R_a from UCAC3 and UCAC4 (Zacharias et al. 2009; 2013), I_N from USNO-B1.0 (Monet et al. 1998), and JHK_s from 2MASS (Skrutskie et al. 2006) were compiled for all the stars in the database, when available. The rest of the bands were compiled by Abellán (2013) and Holgado (2014) for near 450 stars, because their analysis focused on the brightest stars (i.e., *Alpha* and *Beta* class stars). The main photometric analysis was carried out by Abellán (2013) and Holgado (2014), which will be described and complemented here.

Reviewed surveys were *GALEX* (Bianchi et al. 2011), SDSS (Gunn et al. 2006), Tycho-2 (Høg et al. 2000), UCAC3 and UCAC4 (Zacharias et al. 2010, 2013), CMC14 (Evans et al. 2002), USNO-B1.0 (Monet et al. 2003), 2MASS (Skrutskie et al. 2006), and *WISE* (Cutri et al. 2012, 2014).

The spectral energy distributions (SED) of our stars can be displayed with the compiled photometry, by transforming apparent magnitudes into fluxes from the following relation:

TABLE 2.14— Compiled photometric filters.

Filter	Filter system	$\lambda_{\rm eff}$ [Å]	F^0_λ [erg/cm^2/s/Å]	Magnitude system
FUV	*GALEX*	1542.26	4.576×10^{-8}	AB
NUV	*GALEX*	2274.37	2.104×10^{-8}	AB
u'	Sloan	3594.93	8.423×10^{-9}	AB
B_T	Tycho-2	4280.00	6.598×10^{-9}	Vega
B	Johnson	4378.12	6.293×10^{-9}	Vega
g'	Sloan	4640.42	5.055×10^{-9}	AB
V_T [a]	Tycho-2	5340.00	3.984×10^{-9}	Vega
V	Johnson	5466.11	3.575×10^{-9}	Vega
r'	Sloan	6122.33	2.904×10^{-9}	AB
R_a	Johnson	6695.58	1.882×10^{-9}	Vega
i'	Sloan	7439.49	1.967×10^{-9}	AB
J	2MASS	12350	3.129×10^{-10}	Vega
H	2MASS	16620	1.133×10^{-10}	Vega
K_s	2MASS	21590	4.283×10^{-11}	Vega
W1	*WISE*	33526	8.1787×10^{-12}	Vega
W2	*WISE*	46028	2.415×10^{-12}	Vega
W3	*WISE*	115608	6.5151×10^{-14}	Vega
W4	*WISE*	220883	5.0901×10^{-15}	Vega

Notes. [a] M_V absolute magnitude from PMSU was also included in Carmencita.

$$m_\lambda = -2.5 \log_{10}\left(\frac{F_\lambda}{F^0_\lambda}\right) \rightarrow F_\lambda = F^0_\lambda \; 10^{-m_\lambda/2.5}, \tag{2.11}$$

where F^0_λ is the cero point flux at the λ wavelength. The SED represents λF_λ vs. λ, and allows us to identify infrared excess typical of young stars that show a remnant of the molecular cloud in which they form in the shape of a circumstellar disc. No such excess was found in the near 160 M dwarfs for which enough photometric bands were available.

The high number of well characterized M dwarfs permited us to determine stellar prototypes for each spectral subtype, i.e., stars with a spectral energy distribution of reference. These prototypes can be used to compare the SED of stars with the same spectral suptype. It was specially helpful for stars with several spectral types in the literature, which deviate by more than ± 0.5 spectral subtypes. In addition, the stellar prototypes also served to discard spurious photometric data or to easily detect any excess. These stellar prototypes were selected from stars with the largest number of photometric bands, and required no overlap between different spectral subtypes. Moreover, earlier spectral subtypes must have high emission in the more energetic bands compared to later spectral subtypes. The filters used were *u*, *B*, *g*, *V*, *r*, *i*, *J*, *H*, *K*, and *W*1-*W*4. The Tycho-2 B_T and V_T filters were not considered due to their large associated errors and the absence of photometry in many stars. The SED of the stellar prototypes are shown in Fig. 2.19, and the list of the used stars in Table 2.15. The M3.0 V and M4.0 V stars turned out to be a triple and a binary system identified afterwards: J09011+019 (Ross 625) is an M3.0 V double lined spectroscopic binary (Bonfils et al.

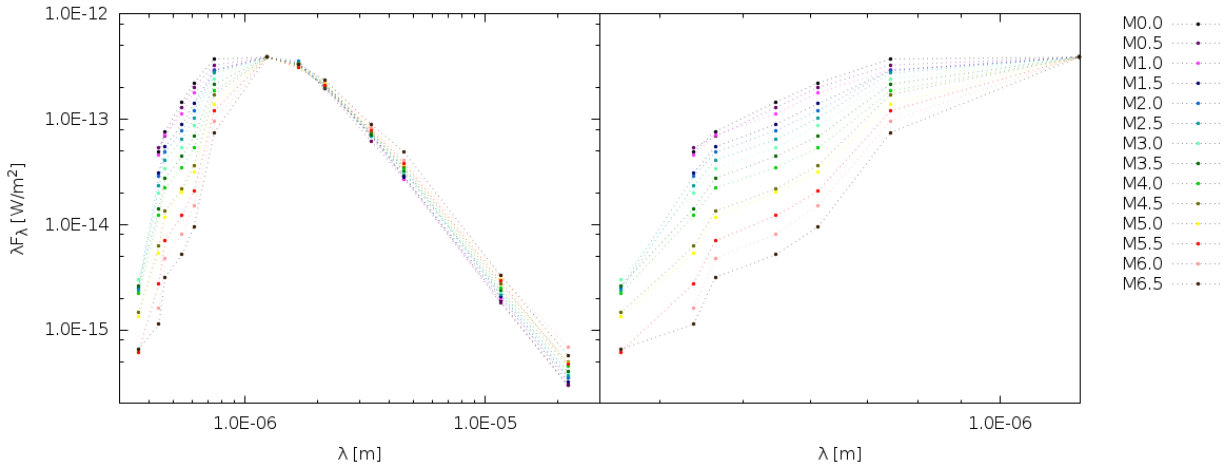

FIGURE 2.19— Spectral energy distribution of the stellar prototypes of each spectral subtype. On the left are displayed all the photometric bands and on the right only bands bluewards of J-band. All the SEDs are normalized to J=10 mag. Figure from Holgado (2014).

2013) with a faint companion at ∼3 arcsec, and J15191-127 (LP 742–061) is an M4.0 V with a faint companion at ∼0.2 arcsec (see Chapter 4). However, the presence of another faint source in the system does not signifficantly affect to the SED and, hence, they remain as SED stellar prototypes.

TABLE 2.15— Spectral energy distribution stellar prototypes.

Karmn	Name	J [mag]	SpT	Ref[a]
J12123+544S	HD 238090	6.875	M0.0 V	PMSU
J18353+457	BD+45 2743	6.881	M0.5 V	AF15a
J02565+554w	Ross 364	7.425	M1.0 V	PMSU
J00136+806	G 242–048	7.756	M1.5 V	AF15a
J22115+184	Ross271	6.725	M2.0 V	PMSU
J21019-063	Wolf 906	7.563	M2.5 V	AF15a
J09011+019	Ross 625	7.932	M3.0 V	PMSU
J09423+559	GJ 363	8.374	M3.5 V	PMSU
J15191-127	LP 742–061	8.507	M4.0 V	PMSU
J13005+056	FN Vir	8.553	M4.5 V	PMSU
J20260+585	Wolf 1069	9.029	M5.0 V	PMSU
J00067-075	GJ 1002	8.323	M5.5 V	PMSU
J02142-039	LP 649–072	10.481	M6.0 V	PMSU
J10564+070	CN Leo	7.085	M6.5 V	PMSU

Notes. [a] AF15a: Alonso-Floriano et al. (2015a); PMSU: Reid et al. (1995, 2002); Hawley et al. (1996); Gizis et al. (2002).

In addition, Holgado (2014) determined empirically the limits of angular separations and difference J magnitudes at which a bright companion contaminates the J-band magnitude of the M dwarf in Carmencita, shown in Fig. 2.20. Stars above the gray dashed line are thus *Delta* stars.

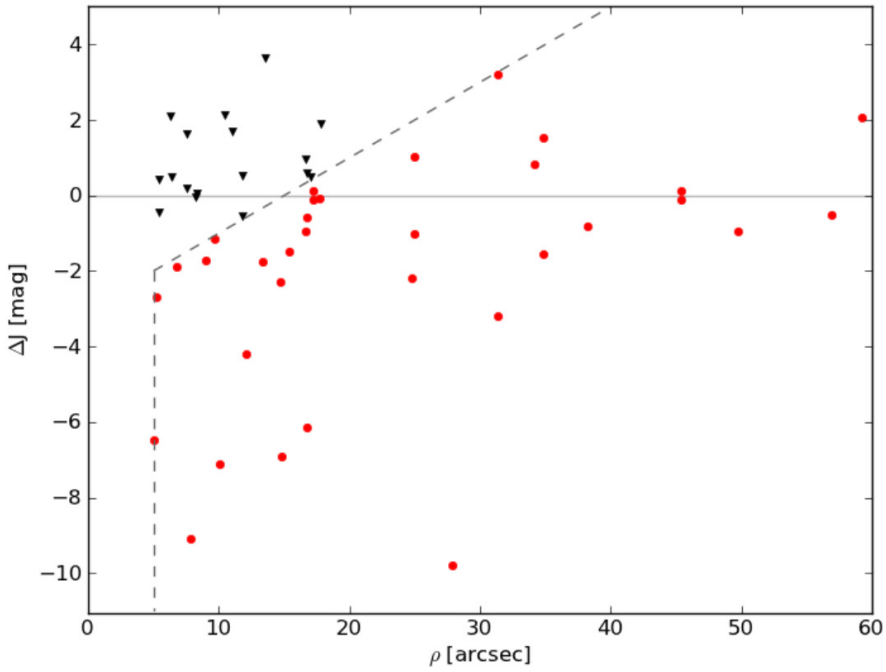

FIGURE 2.20— Difference of J magnitudes vs. angular separation (ρ) for binaries separated by 60 arcsec or less. ΔJ is defined as $J_{\mathrm{M\,V}} - J_{\mathrm{comp}}$. Black triangles represent stars which photometry is affected by the companion. Red circes represent the rest. Gray solid line separates equally bright components, and gray dashed line delimits the separation at which the photometry of our star is contaminated. Figure from Holgado (2014).

In addition, after the CARMENES survey started, we discarded J16578+476 (V1090 Her B) as an *Alpha* star due to the contamination of the primary at 5.05 arcsec.

2.6.1 Colour-spectral type and colour-colour diagrams

With the compiled photometric bands we built colour-spectral type and colour-colour diagrams, with which it is possible to determine colour indices for each spectral subtype and colour-colour relations. These diagrams also permited us to identify wrong photometrc data, and the indices allowed us to infer photometric spectral subtypes for any object without spectroscopic determination, within the M0.0–M6.5 dwarf regime.

The combination of optical and infrared filters were more convinient for an index determination, such as the $r' - J$ and the $r' - K_s$ colours. On the contrary, infrared colours involving 2MASS and *WISE* displayed high colour dispersion, preventing us from an accurate photometric spectral type assignation. Colours with *GALEX* filters also showed a high dispersion, while those with Sloan's were probed to display less scatter. Regarding the B_T and V_T filters from Tycho, the differences with the corresponding Johnson's filters were noticeable as expected. Besides, no Tycho-2 photometry was available for stars later than M4.5,V and thus, they were not used to estimate indices. Colour indices in Table B.5 in Appendix B were obtained from the mean value of the colours per spectral subtype, and the errors from the standard deviation. As an example, Fig. 2.21 shows the $r' - J$ colour versus the spectral subtype.

Ultraviolet and infrared colours can be used as activity indicators, since activity in M dwarfs

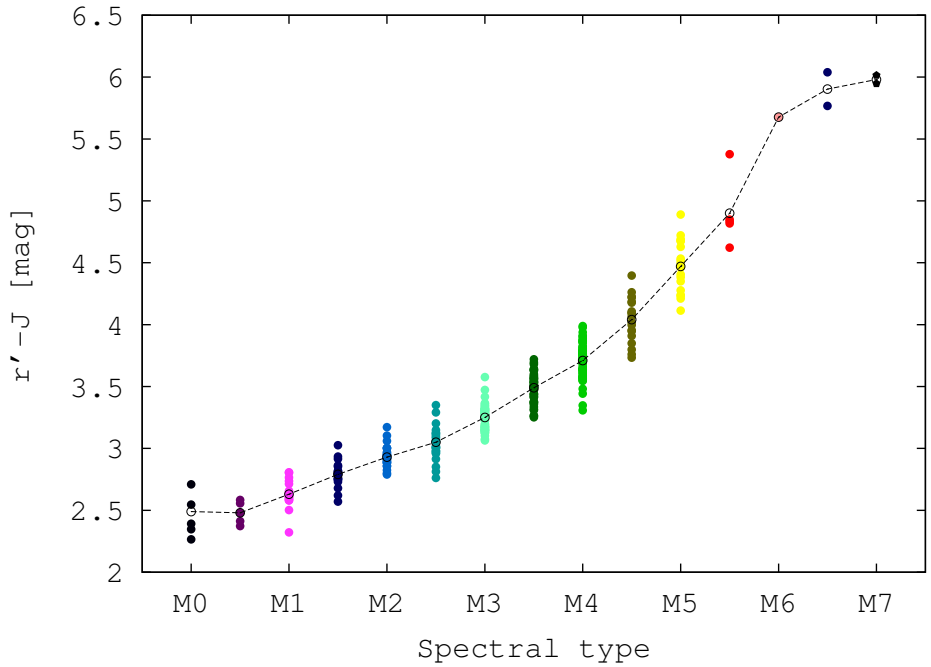

FIGURE 2.21— $r' - J$ vs. spectral type. Filled circles represent data used for index estimation, open circles indicate the position of the mean value, connected with dashed lines. Colours are the same as in Fig. 2.19. Figure from Holgado (2014).

produces excesses at these wavelengths from the chromosphere and the corona. These excesses are related to the high rotation of the star, which generates strong dynamos that produce these activity emissions. In the ultraviolet, filters in the optical or the infrared must be chosen to represent the continuum of the star. In this case, I chose V and the $r' - J$ colour due to its low dispersion. In Fig. 2.22, are represented on the left the dependence of the $NUV - V$ with the spectral subtype, and on the right the $NUV - V$ versus $r' - J$ diagram. There are represented the $\sim$150 Carmencita stars with NUV, V, and r' photometry, and rapid rotators (those with $v \sin i > 4\,\mathrm{km\,s^{-1}}$) and chromospherically active stars (those with $pEW(\mathrm{H}\alpha) \leq -0.75\,\text{Å}$) are differenciated. We used the limit at $pEW(\mathrm{H}\alpha) = -0.75\,\text{Å}$ for comparison with West et al. (2011), although the emission is temperature dependent (i.e., depends on the spectral type). Despite the scarce number of stars, the relation is clear: dwarfs with strong Hα emission have all $NUV - V < 7.6\,\mathrm{mag}$, many of them being also rapid rotators. On the contrary, stars rotating fast ($v \sin i > 4\,\mathrm{km\,s^{-1}}$) do not necessarily show magnetic activiy, as exampled by the six stars with $NUV - V > 7.6\,\mathrm{mag}$. Three stars show $NUV - V > 7.6$ colours consistent with magnetic activity, but have no $pEW(\mathrm{H}\alpha)$ measurement or values slightly higher than the activity limit imposed. The three stars are J01437–060 (BPS CS 22962–0011), J12063–132 (StM 164), J18174+483 (TYC 3529-1437-1).

In the infrared, I used 2MASS and *WISE* bands to detect infared excesses associated to the presence of a circumstelar disc (i.e., young stars). In this case, I represented $W1 - W3$ versus $W1 - W4$ and $NUV - W1$ versus $J - W2$ in the bottom panel of Fig. 2.22. Together with the Carmencita stars involving these bands, there are overplotted stars with X rays emission and with active chromospheres ($pEW(\mathrm{H}\alpha) \leq -0.75\,\text{Å}$). The $W1 - W3$ versus $W1 - W4$ diagram on the left shows $W1 - W4$ colours of chromospherically active stars greater than $\sim$0.17 mag. On the $NUV - W1$ versus $J - W2$ diagram, these stars mostly lie below the dashed line ploted to visually

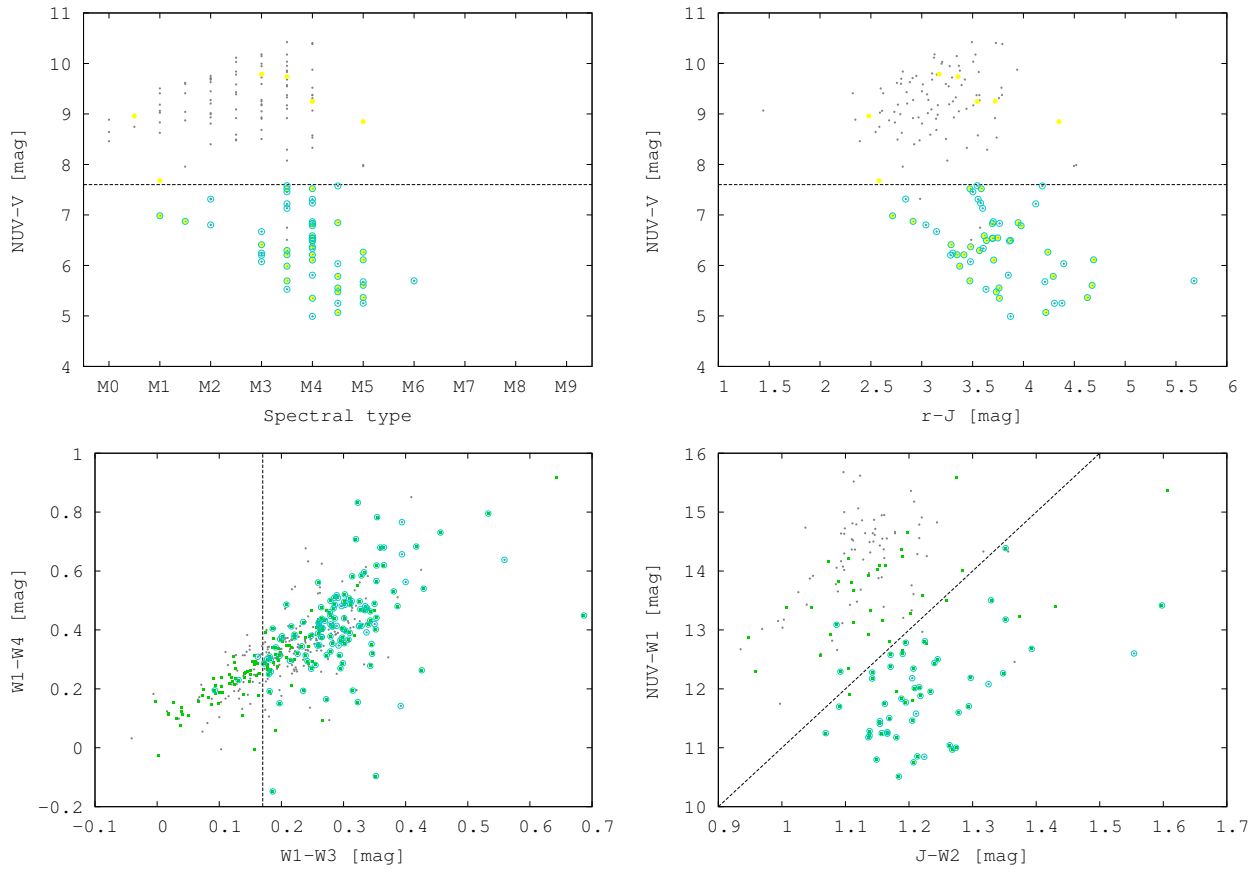

FIGURE 2.22— *Top panels:* $NUV - V$ vs. spectral subtype on the left and $NUV - V$ vs. $r' - J$ on the right. Gray circles represent Carmencita stars, yellow circles represent rapid rotators ($v \sin i > 4\,\mathrm{km\,s^{-1}}$), and light blue open circles represent the chromospherically active stars ($pEW(\mathrm{H}\alpha) \leq -0.75$ Å). Horizontal dashed line separates approximately, the active and the non active stars. *Bottom panels:* $W1 - W3$ vs. $W1 - W4$ and $NUV - W1$ vs. $J - W2$ diagrams on the left and right panel, respectively. Gray circles represent Carmencita stars, green squares represent X-ray emitters and blue open circles represent the chromospherically active stars ($pEW(\mathrm{H}\alpha) \leq -0.75$ Å). The vertical dashed line on the left panel limits the presence of chromospherically active stars to $W1 - W4 > 0.17$ mag, and the dashed line on the right panel shows the region where most of the chromospherically active stars lie.

delimit them.

2.7 Activity

CARMENES is interested in relatively quiet stars for the exoplanet search, since very active stars could mimic the presence of planets. Several activity indicators have been compiled in Carmencita, such as the Hα pseudoequivalent width ($pEW(\mathrm{H}\alpha)$), the rotational period (P_{rot}) and rotational velocity ($v \sin i$), and X ray count rates. In this section, I will not go into particular objects but into the general behaviour of our M dwarfs, and will not define a complete sample, since it is unbiased to magnetic activity detections.

The compilation work has been completed by González-Álvarez (2014), who compiled X ray count rates and hartness ratios from *ROSAT*, *Chandra* and *XMM-Newton*, Hidalgo (2014), who compiled rotational periods from the literature, and Martínez-Rodríguez (2014) and Schöfer (2015), who obtained Hα and $v \sin i$ from high-resolution spectroscopy. In particular, a correlation of Carmencita

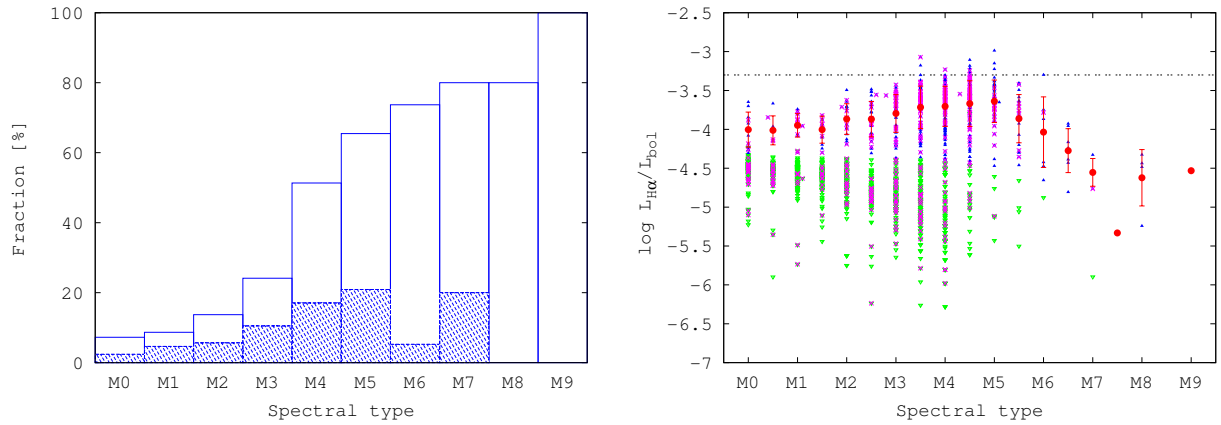

FIGURE 2.23— *Left panel:* Distribution of active M dwarfs as a function of the spectral subtype. Dashed bars represent the *Delta* binary class stars. *Right panel:* Normalized Hα luminosity vs. spectral type. Blue filled triangles represent active stars with $pEW(\mathrm{H}\alpha) \leq -0.75$ Å, green open triangles represent stars with $pEW(\mathrm{H}\alpha) > -0.75$ Å, and magenta crosses indicate the *Delta* stars. Red filled circles indicate the mean values of the active stars and the standard deviation for each spectral subtype. The black dashed line indicates the saturation limit for young open clusters by Barrado y Navascués & Martín (2003).

stars with ESO public catalogues[1] permited us to obtain public high-resolution UVES spectra for 61 stars, and HARPS high-resolution spectra for 236 stars. Together with the FEROS, CAFE and HRS high-resolution spectra obtained by the CARMENES Consortium for 480 Carmencita stars, a total of 620 M stars aknowledge for high-resolution spectroscopy. These instruments cover the spectral wavelength interval between 300 nm and 1100 nm. In this range, several activity indicator lines are formed, like the Balmer series Hα, H_β, H_γ and H_δ, and Ca II H & K lines, among others, and could be directly measured by us. Directly from the spectra and from the literature, we obtained several parameters activity related, such as Hα pseudo-equivalent width, $v \sin i$ or P_{rot}. The sources from which these values were taken are listed in Table B.1 in Appendix B.

2.7.1 Hα

Magnetically active stars were defined as stars with $pEW(\mathrm{H}\alpha) \leq -0.75$ Å by West et al. (2011). In Carmencita, 2101 stars have Hα measurements, of which 26% satisfy this activity criterion. Fig. 2.23 shows on the left the fraction of chromospherically active stars according to this criterion as a function of the spectral subtype. This fraction increases from the 7–14% of M0–M2 dwarfs, to the 24% of M3 dwarfs and steeply increases to the 51% of M4 dwarfs and reaches 80-100% for M7–M9 dwarfs. A similar trend was found by Hawley et al. (1996), West et al. (2008), and Reiners et al. (2012). The increase of magnetic ativity at mid M dwarfs is directly correlated to the internal structural change into fully convective cores, which occurs in this regime. The reason of the higher number of active M dwarfs at later spectral types could be due to the longer period of time that late M dwarfs are able to show emission with respect to earlier types (Hawley et al. 1996).

Besides, we identificated the close binary systems (i.e., systems separated by less than 5 arcsec) among the active dwarfs, which constitute 37% of the subsample. This fraction increases towards later spectral subtypes slower than the fraction of active dwarfs does. This result is supported by Morgan et al. (2012), who associated the decrease of activity related to close systems to the decrease

[1] `http://archive.eso.org/eso/eso_archive_adp.html`

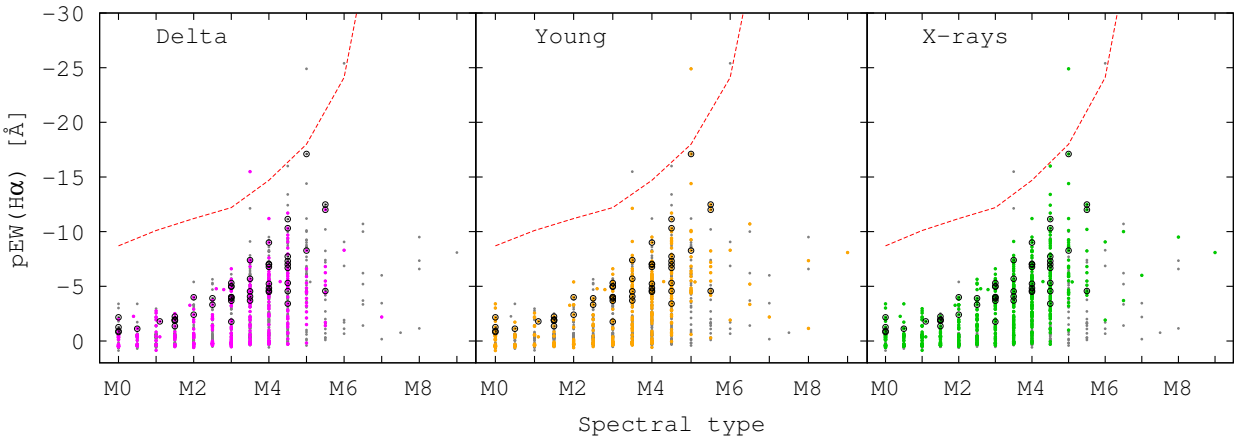

FIGURE 2.24— Hα pseudoequivalent with vs. the spectral type. Gray dots represent the Carmencita sample, the red dashed curve stands for the empirical chromospheric activity limit at $\log L_{\mathrm{H}\alpha}/L_{bol} = -3.3$ by Barrado y Navascués & Martín (2003). On the left panel, magenta filled circles represent the *Delta* class stars; in the middle panel, orange filled circles represent the young stars and candidates from Section 2.4.2; and in the right panel green filled circles represent the X-ray emitters. Black open circles represent the most active stars in the sample.

in sensivity in the detections of close binary companions.

The strength of the magnetic activity can be measured with the normalized Hα luminosity, computed for active stars from the equation given by Walkowicz et al. (2004):

$$\frac{L_{\mathrm{H}\alpha}}{L_{bol}} = \chi \ |pEW(\mathrm{H}\alpha)|, \tag{2.12}$$

where $|pEW(\mathrm{H}\alpha)|$ is the absolute value of the pseudoequivalent width of the Hα emission line and χ is a function of the effective temperature (T_{eff}). By taking the logatithm in this equation:

$$\log\left(\frac{L_{\mathrm{H}\alpha}}{L_{bol}}\right) = \log\chi + \log|pEW(\mathrm{H}\alpha)|, \tag{2.13}$$

where $\log\chi$ is:

$$\log\chi = a + bT_{\mathrm{eff}} + cT_{\mathrm{eff}}^2 + dT_{\mathrm{eff}}^3 + eT_{\mathrm{eff}}^4 + fT_{\mathrm{eff}}^5, \tag{2.14}$$

and $a = -67.3424$, $b = 0.111938$, $c = -8.26212\ 10^{-5}$, $d = 3.04492\ 10^{-8}$, $e = -5.51137\ 10^{-12}$, $f = 3.90255\ 10^{-16}$, and T_{eff} is the effective temperature in K (Reiners & Basri 2008). Of the M dwarfs with $pEW(\mathrm{H}\alpha)$ measurements, almost 370 have T_{eff} measured from our own high-resolution spectra (Passegger et al., in prep.). For consistency, I estimated effective temperatures for all of them from the results of Kenyon & Hartmann (1995) and Golimowski et al. (2004).

The representation of the chromospheric activity level from Eq. 2.13 versus the spectral type is shown on the right panel in Fig. 2.23. I differenciated active and non-active dwarfs according to the previous definition, and overplotted the *Delta* class stars. I also indicated the mean value of active stars for each spectral subtype. As noted before, 37% of M active dwarfs are found in close binary or multiple systems. Among the "non-active" dwarfs, this fraction downs to 16%, almost half. We found a saturation limit of the chromospheric activity level in agreement with the saturation limit of $\log L_{\mathrm{H}\alpha}/L_{bol} = -3.3$ observed by Barrado y Navascués & Martín (2003) in young open clusters

TABLE 2.16— Stars with strong Hα emission.

Karmn	Name	SpT	X Rays	Youth	Ref[a]
J01567+305	NLTT 6496	M4.5 V	Y	?	AF15a
J05084–210	2MASS J05082729–2101444	M5.0 V	Y	β Pic	Malo14a
J07523+162	LP 423–031	M6.0 V	N	$\sim$100 Ma	Shk09
J09449–123	G 161–071	M5.0 V	Y	Argus	Malo13
J09593+438W[b]	G 116–072 A	M3.5 V	N	25–300 Ma	Shk09

Notes. [a] AF15a: Alonso-Floriano et al. (2015a); Malo13: Malo et al. (2013); Malo14a: Malo et al. (2014a); Shk09: Shkolnik et al. (2009). [b] It has an unconfirmed close companion (Bowler et al. 2015). [c] It is a wide component, which primary (MV Vir) has been associated to the β Pic moving group by Malo et al. (2013).

and in late field dwarfs by Mohanty & Basri (2003). For spectral subtypes from M0 to M5, the mean magnetic activity strength looks constant within the errorbars and then drops towards later spectral subtypes. Although not enough data validate the statistics, since there are less than 25 M6–M9 dwarfs, this decrease is in accordance with previous data (Stauffer et al. 1994; Hawley et al. 1996).

The Hα pseudoquivalent width is an activity indicator and, hence, youth indicator. The relation between this parameter and the spectral type is well studied, and it is helpful to distinguish between young stars and brown dwarfs that show accretion from those that show chromospheric emission. In Fig. 2.24 the Hα pseudoquivalent width is represented versus the spectral type. The red dashed line indicates the empirical saturation limit of $\log L_{\mathrm{H}\alpha}/L_{bol} = -3.3$ per each spectral subtype found by (Barrado y Navascués & Martín (2003). In the three panels of this figure, are represented separately for comparison the *Delta* class stars (left panel), the young stars and candidates from Section 2.4.2 (middle panel), and the X-ray emitters (right panel). The most intetersting targets are the 50 stars with X ray emission and young kinematics (related to Argus and IC 2391 moving groups, and the Local Association), which together with the Hα emission converts them into vey likely late young star candidates. These objects are marked with open black circles in the figures and are bold-faced in Table B.4 in Appendix B. Moreover, around 23 of them have also companios at separations shorter than 5 arcsec, which makes them prime targets for orbital follow up in order to determine dynamical masses of young stars. In these figures, we observe that the cooler the star, the greater the Hα emission of our stars, as noticed by Basri & Marcy (1995). Three stars lie over the boundary between chromospheric and accretion emission, and another two lie at or just below it (J01567+305 and J09449–123). All of them are listed in Table 2.16 and are old enough to be accreting M dwarfs.

2.7.2 Rotational periods

Young active stars, apart from the high Hα emission, also display short rotational periods P_{rot} (West et al. 2015). We compiled rotational periods from the literature for 269 Carmencita stars. References can be found in Table B.1 in Appendix B.

The relation between the Hα pseudoequivalent and the rotational period is showed on top in Fig. 2.25, where there are represented the same subsets as in Fig. 2.24. In this case, binarity is not relevant, since wide enough pairs will not interfere in the measurements of the rotational period, and pairs close enough to have orbital periods (P_{orb}) compared to their rotational periods would be tidaly locked, and the periods would equal ($P_{\mathrm{orb}} = P_{\mathrm{rot}}$). In the middle and right panels, most of the young stars and candidates, as well as most of the X-ray emitters, have $P_{\mathrm{rot}} < 30$ d.

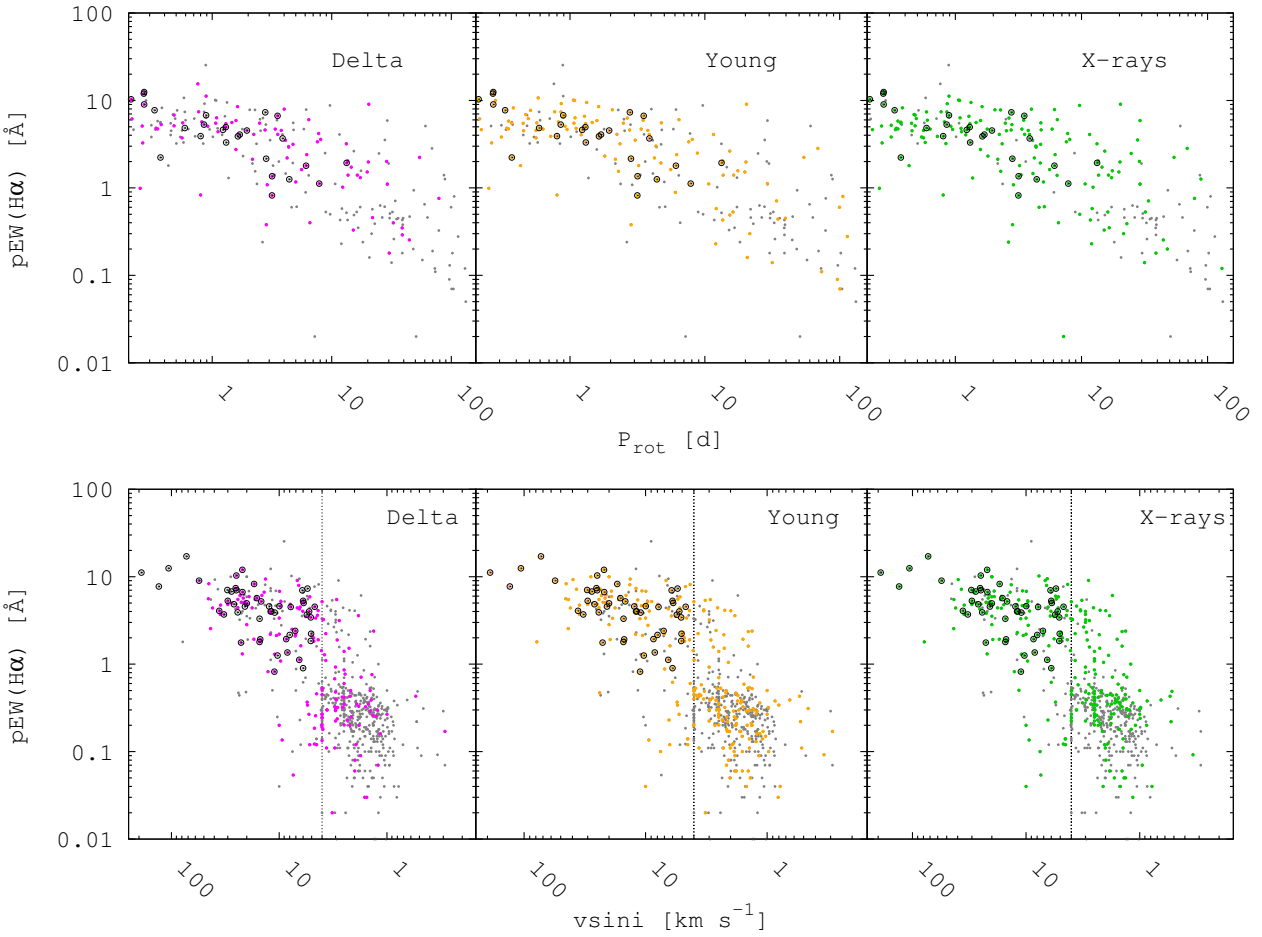

FIGURE 2.25— Hα pseudoequivalent width vs. rotational period (top panel) and vs. rotational period (bottom panel) in logarithmic scale. Vertical dotted lines indicate the rapid rotators limit at $v \sin i = 4\,\mathrm{km\,s^{-1}}$. Colour and symbol code is the same as used in Fig 2.24.

Stands out J17198+265 (V639 Her), a young M4.5 V star with X ray emission and a companion separated by more than 5 arcseconds but bright enough to compromise its photometry. Its Hα emission ($pEW(\mathrm{H}\alpha) = -9.07$ Å) is larger than expected for a 20 d rotational period. The star presents flares, and therefore the emission could have been measured during an activity transitory process. On the other side, J10238+438 (LP 212–062) is the only star with high Hα emission ($pEW(\mathrm{H}\alpha) = -5.1$ Å) for its measured period of near 60 d that has no other activity or youth indicator. The 50 X-ray emitters with young kinematics and Hα emission represented with open black circles display periods shorter than 14 d.

2.7.3 Rotational velocities

Rotational velocities ($v \sin i$) were also compiled for more than 700 Carmencita stars, half of which were measured directly from our high-resolution spectra (Jeffers et al.2016). Typical values for M dwarfs range from $3\,\mathrm{km\,s^{-1}}$ to $30\,\mathrm{km\,s^{-1}}$, approximately, although fast rotators can reach dozens of $\mathrm{km\,s^{-1}}$.

Active stars have short periods, and hence, rotate fast, since:

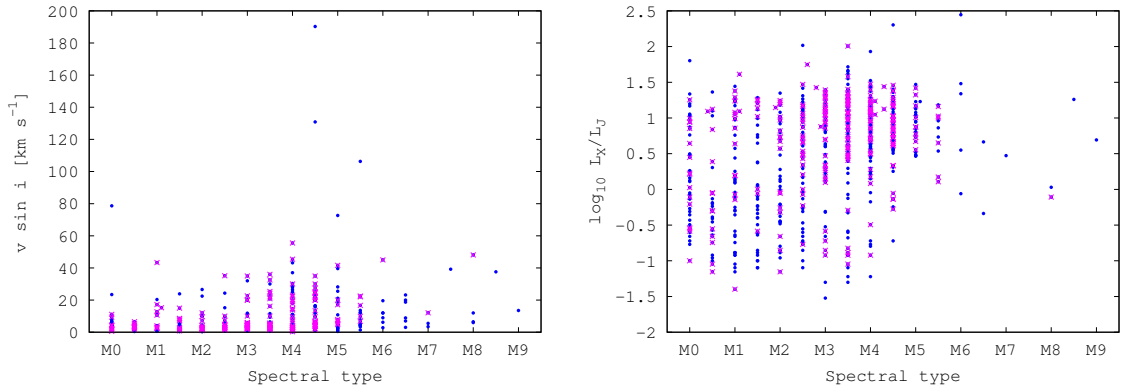

FIGURE 2.26— $v \sin i$ vs. spectral type (left panel) and $\log L_X/L_J$ vs. spectral type (right panel). Blue circles represent the entire sample, and magenta crosses the *Delta* stars.

$$P_{\rm rot} = \frac{2\pi R \sin i}{v \sin i}, \tag{2.15}$$

where R is the star radius. We considered rapid rotators to be stars with $v \sin i \geq 4\,{\rm km\,s^{-1}}$. Half of the dwarfs with velocity measurements rotate within this limit.

In Fig. 2.26 we can see the dependence of $v \sin i$ with the spectral type on the left. Mid M dwarfs tend to rotate faster than earlier dwarfs in our sample, as seen before in the right panel on Fig. 2.23. Binarity appears also to play an important role in the rotation of the star, since disc truncation mechanisms or tidal effects may induce higher rotation rates (Morgan et al. 2012). We relate the presence of 40% binary or multiple systems among the rapid rotators. The star with the highest velocity ($190.3\,{\rm km\,s^{-1}}$) is J04173+088 (LTT 11392), an active ($pEW({\rm H}\alpha) = 11.15$ Å), X-ray emitter, kinematically young candidate with a 0.2 d period.

Fig. 2.27 shows the relation between Hα via its normalized luminosity and the rotational period on the panel on top and the rotational velocity on the panel on bottom.In light of this figures, the activity-rotation connection is observed, since chromospherically active stars ($\log L_{{\rm H}\alpha}/L_{bol} \geqslant -4$) tend also to rotate fast (Mohanty & Basri 2003). Besides, among the fastest rotators ($v \sin i > 30\,{\rm km\,s^{-1}}$) is also observed X rays emission and young kinematics. Nearly 90% of the magnetically active stars that have $\log L_{{\rm H}\alpha}/L_{bol} \geqslant -4$), have periods shorter than 10 d.

2.7.4 X rays

The emission in X rays of cool stars is associated to high coronal temperatures, and is related to magnetic activity. X rays luminosity is age and rotation dependent. As we saw in previous sections, rotation, X rays emission and youth are connected.

In Carmencita, 33% of the stars are X-ray emitters. The collection of the count rates, fluxes or luminosities was compiled from the *ROSAT* satellite, the *Chandra* and *XMM-Newton* X rays observatories mostly by González-Álvarez (2014).

The dependence of M dwarfs displaying X rays emission with the spectral type is shown on the right panel in Fig. 2.26. Since we can not derive L_{bol}, we represented the relation of luminosities

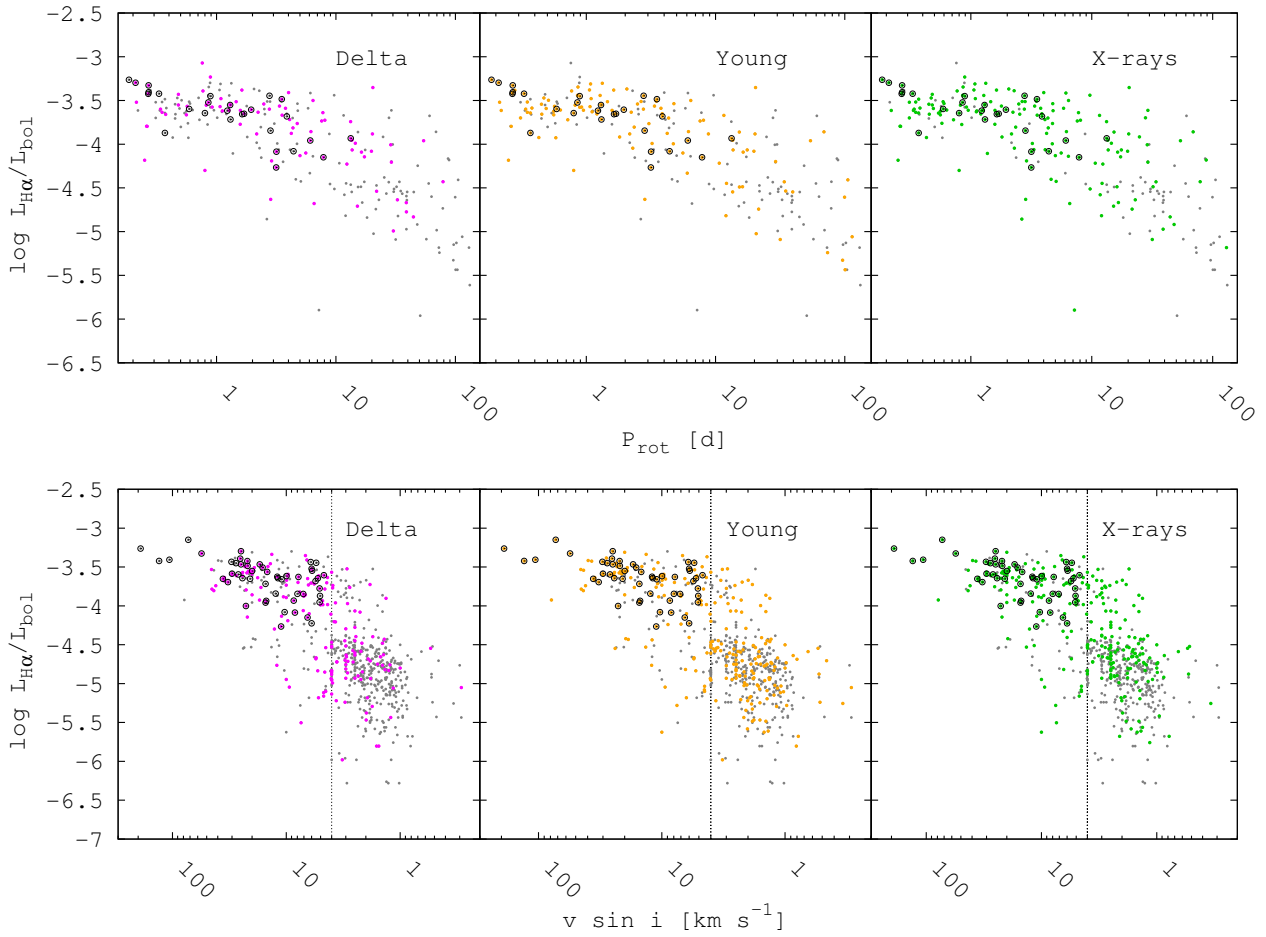

FIGURE 2.27— Normalized Hα luminosity vs. rotational period (top panel) and vs. rotational velocity (bottom panel) in logarithmic scale. Vertical dotted lines indicate the rapid rotators limit at $v \sin i = 4\,\mathrm{km\,s^{-1}}$. Colour and symbol code is the same as used in Fig 2.24.

L_X/L_J, due to the peak of the energy emission of M dwarfs near the J-band. The trend of increasing X rays emission towards mid M dwarfs is also observed here, and it decreases from mid M dwarfs towards later spectral subtypes due to the physical internal changes occurring in the star. We also see the saturation of the emission at $\log L_X/L_J \approx 1.5$, which translates into $\log L_X = 31$ (in cgs), as observed by Pizzolato et al. (2003). It is also noticeable the presence of close binaries and multiples, which account for between one third and half of the emitting stars from M0 to M5 and in M8 subtypes.

The relation between X rays activity and rotation is shown in the top and bottom panels of Fig. 2.28. We used the L_X/L_J ratio and the rotational velocities instead of the rotational periods, since they are equivalent. As in previous plots, different panels show the close binaries, young candidates and chromospherically active stars defined as stars with $\log pEW(\mathrm{H}\alpha) \leq -0.75$ Å. Black open circles represent the most active stars, as in previous figures. There is also indicated the rapid rotation limit established at $v \sin i = 4\,\mathrm{km\,s^{-1}}$. The intensity of the emission in X rays slowly increases with the increasing velocity of rotation (i.e., with decreasing periods) up to $4\,\mathrm{km\,s^{-1}}$. At faster rotations, coronal emission reaches saturation. In some cases, saturation becomes at lower

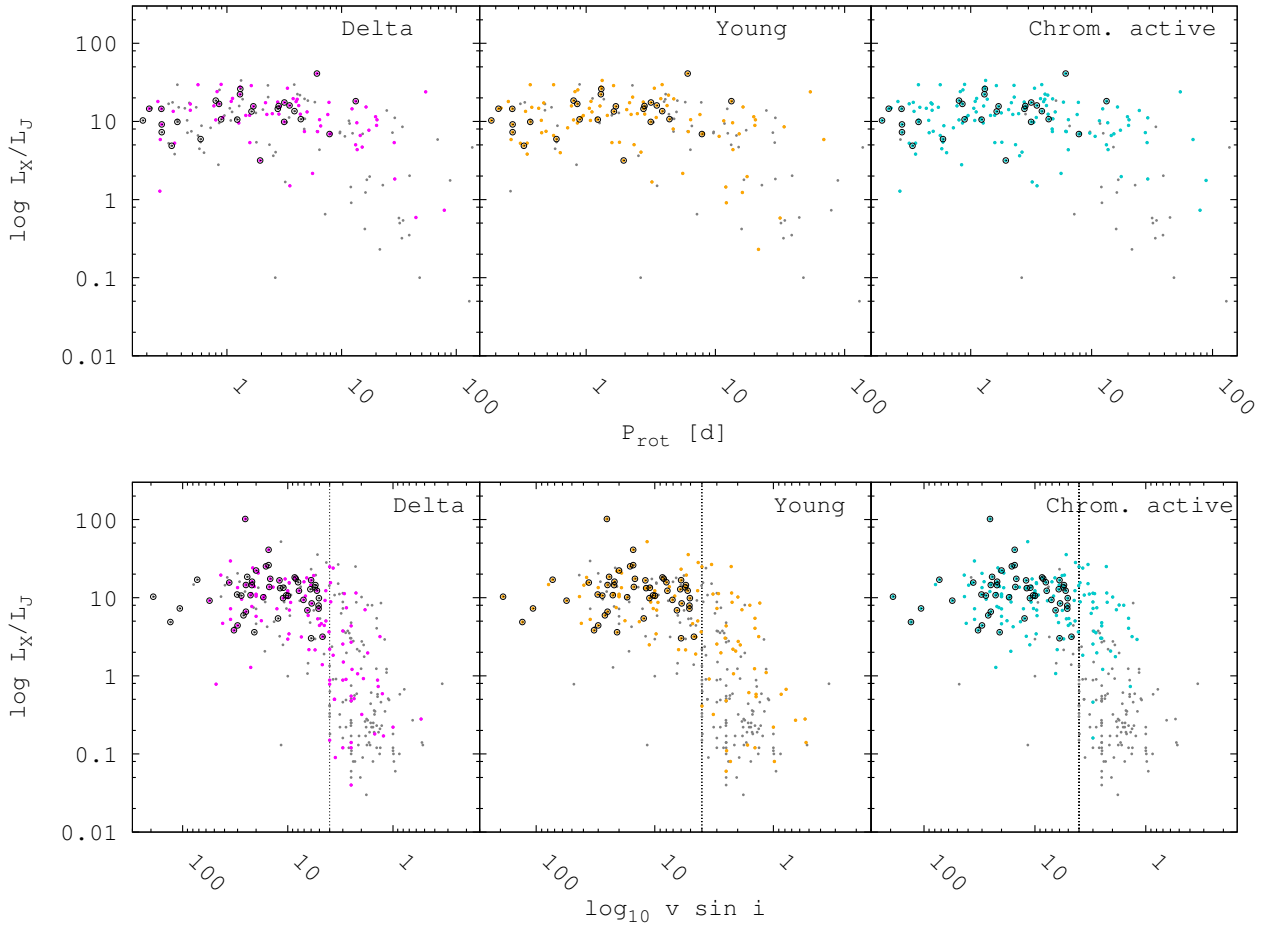

FIGURE 2.28— L_X/L_J vs. rotational velocity in logaritmic scale (top panel) and vs. rotational period (bottom panel). As in similar figures, gray dots represent the Carmencita sample and black open circles represent the most active stars. On the left panel, magenta filled circles represent the *Delta* class stars; in the middle panel, orange filled circles represent the young stars and candidates from Section 2.4.2. And in the right panel blue filled circles represent the magnetically active stars with $pEW(\mathrm{H}\alpha) \leq -0.75$ Å. Vertical dotted lines indicate the rapid rotators limit at $v \sin i = 4\,\mathrm{km\,s^{-1}}$.

values than the canonical limit, down to even three orders of magnitude ($\log L_X = 28$). This behaviour is known as "supersaturation phenomenon" and seems to be age dependent (Prosser et al. 1996). In all the panels of Fig. 2.28, the majority of the *Delta*, young and magnetically active stars are rapid rotators (short rotational periods) and with high X rays emission.

2.7.5 The most active and young stars

In Carmencita, there are 50 M dwarfs that satisfy the activity criteria mentioned before: they have Hα in emission with $pEW(\mathrm{H}\alpha) \leq -0.75$ Å, $v \sin i \geq 4\,\mathrm{km\,s^{-1}}$, and X rays emission. In addition, they show kinematics belonging to the youngest groups (< 200 Ma): Argus, IC 2391, and Local Association. These stars are marked with black open circles in Fig. 2.24, 2.25, 2.27, and 2.28.

The pseudoequivalent widths of their Hα emission range from –0.82 to –17.1 Å, they rotate with velocities from 3.32 to 190.28 $\mathrm{km\,s^{-1}}$, and their normalized X rays luminosities are limited to the 3.02–101.61 interval (0.5–2 in logarithmic scale). Half of them have of them also rotational periods,

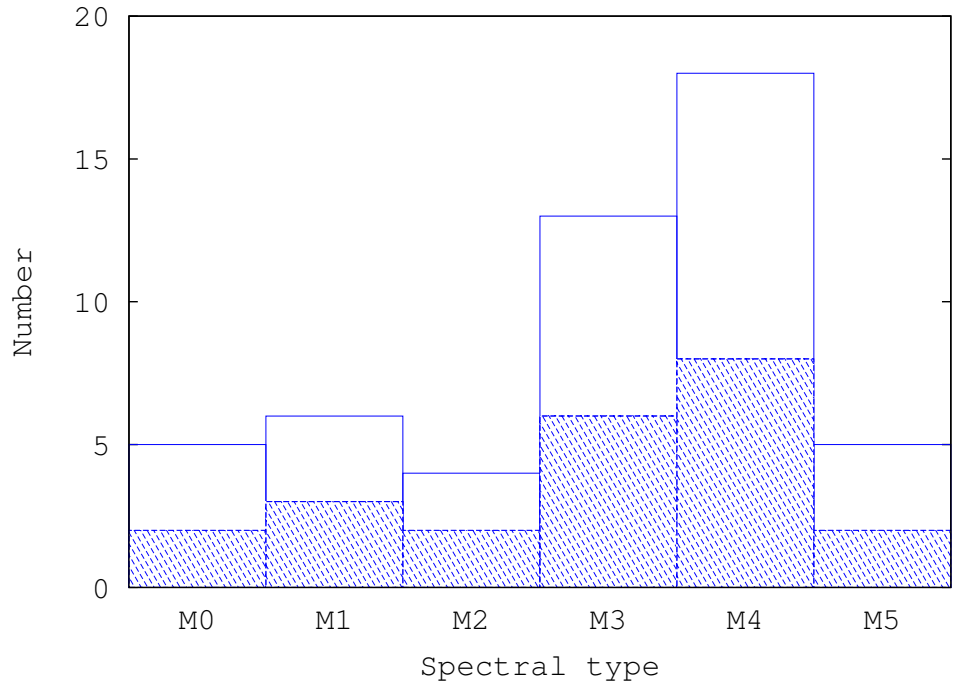

FIGURE 2.29— Spectral type distribution of the stars displaying Hα emission ($pEW(\mathrm{H}\alpha) < -0.75$ Å), high rotation velocity ($v \sin i \geq 4\,\mathrm{km\,s^{-1}}$), X rays emission and very young kinematics. Dashed bars represent the *Delta* class stars.

which range from 0.2 to 13.3 d. From Fig. 2.24, we see an increasing $pEW(\mathrm{H}\alpha)$ towards later spectral subtypes. Fig. 2.25 shows the narrow interval of rotational periods that they have, with probably one exception: J05068-215E (BD–21 1074 A) with a 13.3 d period. Five of the six fastest rotators are included in this subset of 50 dwarfs. The sixth is the M0.0 V star J23083-154 (HK Aqr). It is a star with high rotational velocity ($v \sin i \geq 78.63\,\mathrm{km\,s^{-1}}$) that does not belong to this sample due to its kinematics related to Castor (age > 300 Ma).

Their spectral type distribution is shown in Fig. 2.29, as well as the number of stars with companions closer than 5 arcsec (*Delta* class) with dashed bars. Most of the 50 stars are M3 and M4 dwarfs, and near half have a close companion. The *Delta* class stars are almost equally distributed per spectral subtype.

Among these active stars, stands out the M5.0 V J09449-123 (G 161–071). It is a single star that belongs to the Argus moving group with near 40 Ma, rotates at $72.64\,\mathrm{km\,s^{-1}}$ and it is among the strongest X-ray emitters. Since accretion ends after 10 Ma, the star was probably observed during a flare.

2.7.6 The most active stars observed by CARMENES

Since January 2016, when CARMENES started to operate, 294 Carmencita M dwarfs have been observed with the instrument. Of them, 107 stars with more than five observations done by mid-July have been investigated for chromospheric activity by analyzing the Ca II infrared triplet, since activity introduces variations in the equivalent width of these lines over time. This analysis led to 12 M dwarfs with strong activity (Brinkmöller 2016). Table 2.17 lists them together with flags that indicate if they have Hα in emission with $pEW(\mathrm{H}\alpha) \leq -0.75$ Å, $v \sin i \geq 4\,\mathrm{km\,s^{-1}}$, X rays emission,

TABLE 2.17— Active stars observed with CARMENES.

Karmn	Name	$pEW(\mathrm{H}\alpha)$	X Rays	vsini	Ca II	std(RV)
J07319+362N	BL Lyn	×	×		×	
J07361–031	BD–02 2198		×		×	
J07446+035	YZ CMi	×	×	×		×
J09425+700	GJ 360		×	×	×	
J10564+070	CN Leo	×	×		×	
J11026+219	DS Leo		×	×	×	
J11055+435	WX UMa	×	×	×	×	
J12156+526	StKM 2–809	×	×	×	×	×
J12189+111	GL Vir	×	×	×		×
J12428+418	G 123–055	×	×		×	
J15218+209	OT Ser	×	×	×	×	
J16313+408	G 180–060	×		×	×	×
J16570–043	LP 686–027	×	×	×		×
J17338+168	1RXS J173353.5+165515	×	×	×	×	×
J18174+483	TYC 3529–1437–1		×		×	
J19511+464	G 208–042	×	×	×		×
J22012+283	V374 Peg	×	×	×		×

or strong Ca II absorption. All of them are single stars, (i.e., have no known companion at less than 5 arcsec). In this case, I am not considering the age of the stars.

One of those stars and another five[2], listed as well in Table 2.17, show standard deviations in the radial velocity measurements obtained with CARMENES spectra that vary from near $150\,\mathrm{m\,s^{-1}}$ to $900\,\mathrm{m\,s^{-1}}$ over five to six measurements. All of them are fast rotators, Hα and X-rays emitters and display rotational periods of less than one day or are members to young stellar kinematic groups. An extra flag has been added to the table to indicate whether the stars display high radial velocity variations within the CARMENES observations.

Specially active M dwarfs in the table with $pEW(\mathrm{H}\alpha) \leq -2$ Å and $v \sin i \geq 20\,\mathrm{km\,s^{-1}}$ are marked in boldface. Their rotational periods range from 0.27 to 0.59 d and are kinematically young candidates: J12156+526 (StKM 2–809) is an Ursa Major candidate that shows strong X-rays emission, J12189+111 (GL Vir) is a Hyades candidate that displays the highest radial velocity standard deviation and a 0.5 d rotational period, J17338+169 (1RXS J173353.5+165515) is a candidate of the Local Association with a 0.27 d rotational period, J19511+464 (G 208–042) is a candidate of IC 2391 that has a rotational period of 0.59 d, and J22012+283 (V374 Peg) is a Castor candidate with a rotational period of 0.45 d.

These 17 stars will not be observed with CARMENES, since high activity levels prevent us from detecting any signals of exoplanets orbiting around.

[2]Included in a new category (*Epsilon*)

2.8 Summary

Carmencita, the CARMENES database for exoEarths search, is the most comprehensive compilation of parameters of M dwarfs in the solar neighbourhood. Stars in Carmencita satisfy a J magnitude-spectral type relation, which selects the most bright dwarfs per spectral subtype. The compiled information includes:

- Spectral types from low resolution spectra taken by the CARMENES Consortium, and from a number of literature sources.
- Precise astrometry:
  - Coordinates in J2000.0, which were translated into J2016.0.
  - Parallaxes and distances. For over 880 M0–6 V stars without parallax, I computed photometric distances from our own M_J-spectral type relation.
  - Radial velocities derived from high resolution spectral by the Consortium and also compiled from the literarture.
  - Proper motions. For more than 500 dwarfs, we computed proper motions from astrometric catalogues with a time coverage between 60 a and 100 a. These motions improve or correct previous determinations from the literature.
  - Galactic space velocities computed by us from the coordinates, proper motions and parallaxes.
- Photometric bands covering from the ultraviolet with *GALEX* to the infrared with *WISE*. Up to 19 filters were included.
- Multiplicity information. For physical resolved pairs, we included discoverer code, angular separation and reference, name and spectral type of the companion, and difference of magnitude between components. Unresolved pairs (eclipsing and spectroscopic binaries) were indicated and properly referenced.
- Activity indicators:
  - Hα pseudoequivalent width derived from low and high resolution spectra by the Consortium, and taken from the literature as well.
  - X rays emission. We computed fluxes and relative luminosities L_X/L_J from *ROSAT* count rates and compiled fluxes from *Chandra* and *XMM-Newton*.
  - Rotational velocities $v \sin i$ and periods $P_{\rm rot}$. Rotational velocities were mostly derived by the Consortium from high resolution spectra.
  - Flag for flare stars.
- Membership to stellar kinematic groups and stellar population, infered from the UVW space velocities computed in this work. Also literature associations were included.
- Stellar parameters ($T_{\rm eff}$, $\log g$, [Fe/H]) derived from high resolution spectra by the Consortium.

Low- and high-resolution spectra and images were taken to guarantee the best single and well characterized dwarfs to observe with CARMENES.

In this work, special interest was put in close binarity, since a companion at less than an arbitrary angular separation of 5 arcsec may induce spurious variations on the radial velocity measured and give false positive planet detections. A high resolution imaging survey has been carried out and will be described in Chapter 4.

Regardig multiplicity at all separation ranges, I derived the M dwarf multiplicity fraction for the Carmencita sample and for two volume limited samples differenciated by the included spectral types: VLS1 includes all M0–M9 dwarfs upt 12 pc, while VLS2 includes all M0–M5 dwarfs up to 17 pc. The derived fractions were similar in the volume limited samples (26.5% and 28.7% for VLS1 and VLS2, respectively), and were higher in these samples than in Carmencita (19.1%). This difference is explained by the lack of close companion detections of the more distant stars that do not belong to the volume limited samples. Although our samples are not complete in the range of considered angular separations (from the close spectroscopic binaries to more than 1 000 au), these fractions are in agreement with the multiple frequency of M dwarfs observed in other works ($42 \pm 9\%$, Fischer & Marcy 1992; $23.5 \pm 3.5\%$, Ward-Duong et al. 2015), and has intermediate values of the frequencies of solar-like (44–65% – Duquennoy & Mayor 1991; Raghavan et al. (2010) and ver low mass stars (from $15 \pm 7\%$ of M8.0-L0.5 dwarfs – Close et al. 2003 – to $9^{+15}_{-4}\%$ of T dwarfs – Burgasser et al. 2003 –).

On the other side, the multiplicity fractions derived in the young disc population and the sample defined by the thin and thick discs, and the halo are $35.0 \pm 7.0\%$ and $29.0 \pm 4.3\%$, in their respective volume limited samples. This result reveals no dependece on the age of the M dwarf multiple frequency, although the age of the young sample population should be better restricted and the young sample delimited to less than a few hundred Ma.

I performed an analysis of the distribution of physical separations in M binary and multiple systems, and tested the general ennunciation of the Öpik's law. The cumulative distribution of physical separations follows a power-law with a confidence level of more than 96% for the volume limited samples. This law could only be applied in a restricted interval of physical separations, which in our case comprises from 1 au to 3160 au. This cut off may be related to different formation processes of M dwarf multiple systems. M dwarf multiple systems with larger separations are scarce and do not follow a power-law. This is also observed in systems with more massive primaries. The main difference between massive systems and low massive ones is the interval of physical separations in which the power-law could be applied (for solar-like stars it could range from 65 to 20 500 au; Close et al. 1990). To our knowledge, this is the first analysis of a power-law distribution in this spectral type regime ever carried out.

The large amount of activity indicators compiled here allowed us to analyze the relation between the spectral type and age with activity. We found that activity increases towards mid M dwarfs, and confirmed the dependence of the pseudoequivalent width of Hα, X rays luminosity and rotational velocity with spectral subtype. Mod- to late-M dwarfs present strongest Hα emission, are generally X-ray emitters and rotate fast. We also found evidence that supports the connection between activity and age, and observed that young stars rotate faster and show stronger magnetic activity than evolved ones. The increase of activity (either through a faster rotation or a stronger Hα emission) towards mid M subtypes, appears to be connected to the internal restructuring from partially to fully convective cores, as suggested by Reiners & Basri (2008). We found the $NUV - V$ colour to be also a good indicator of chromospherically active stars, which show colours below ~ 7.6 mag.

Infrared colours have not proved to be good indicators of coronal activity.

In this work, we found near 100 kinematically young M dwarfs, 50 of which are candidate members to the Argus, IC 2391, and Local Association groups with ages lower than 200 Ma. These stars also show strong Hα emission, are rapid rotators and X-ray emitters. The activity relations studied here, demonstrate that many of the remaining stars are also rotational and magnetically active. An individual treatment would led to more definitive results.

At the moment of writing these lines, the analysis of the first semester of CARMENES data starts to feed back Carmencita. Between early January and late July 2016, 294 Carmencita stars had been observed with both VIS and NIR channels. For 107 of them, an analysis of the equivalent width of the Ca II triplet has been performed by other Consortium members and revealed strong activity levels for 12 of the 107 M dwarfs. The six most active stars, which also display the largest standard deviation of radial velocity, have been recently discarded for observing with CARMENES, due to the influence of magnetic activity in the spectra.

As can be seen from this short analysis, the potential of Carmencita is huge. It is not only a very powerful tool for its main purpose in CARMENES (i.e., identifying the 300 best GTO targets), but also for the optimization of the observational resources: the better characterized a target, the better profit for the observations and following analysis. Besides, it permits a statistical treatment of M dwarfs, from kinematics to activity and multiplicity, helpful in the study of the evolution from the early stages of M dwarf formation.

References

[1] Andersen, B. N. & Pettersen, B. R. 1975, A&A, 41, 459

[2] Abellán, F. J. 2013, MSc thesis, Universidad Complutense de Madrid, Spain

[3] Adelman-McCarthy, J. K. et al. 2011, *The SDSS Photometric Catalog, Release8*2011, yCat, 2306, 0

[4] Agrawal, P. C., Rao, A. R. & Sreekantan, B. V. 1986, MNRAS, 219, 225

[5] Ahn, C. P., Alexandroff, R., Allende-Prieto, C. et al. 2012, ApJS, 203, 21

[6] Al-Shukri, A. M., McAlister, H. A., Hartkopf, W. I. et al. 1996, AJ, 111, 393

[7] Alonso-Floriano, F. J., Morales, J. C., Caballero, J. A. et al. 2015a, A&A, 577, A128

[8] Alonso-Floriano, F. J., Caballero, J. A., Cortés-Contreras, M. et al. 2015b, A&A, 583, A85

[9] Alonso-Santiago, J. 2011, MSc thesis, Universidad Complutense de Madrid, Spain

[10] Ambartsumyan, V. A., Mirzoyan, L. V., Parsamyan, E. S. et al. 1973, Afz, 9, 461

[11] Anderson, E., Francis, C. 2012, AstL, 38, 331

[12] Ansdell, Me., Gaidos, E., Mann, A. W. et al. 2015, ApJ, 798, 41

[13] Antonova, A., Hallinan, G., Doyle, J. G. et al. 2013, A&A, 549, A131

[14] Astudillo-Defru, N., Bonfils, X., Delfosse, X. et al. 2015, A&A, 575, A119

[15] Balega, I. I., Balega, Y. Y., Hofmann, K.-H., Maksimov, A. F. et al. 2002, A&A, 385, 87

[16] Balega, I. I., Balega, Y. Y., Maksimov, A. F. et al. 2004, A&A, 422, 627

[17] Balega, I. I., Balega, A. F., Maksimov, E. V. et al. 2006, BSAO, 59, 20

[18] Balega, I. I., Balega, Yu. Yu., Maksimov, A. F. et al. 2007, AstBu, 62, 339

[19] Balega, I. I., Balega, Yu. Yu., Gasanova, L. T. et al. 2013, AstBu, 68, 53

[20] Barnes, J. R., Jenkins, J. S., Jones, H. R. A. et al. 2014, MNRAS, 439, 3094

[21] Barrado y Navascués, D. 1998, A&A, 339, 831

[22] Barrado y Navascués, D. & Martín, E. L. 2003, AJ, 126, 2997

[23] Barrado y Navascués, D., Stauffer, J. R. & Jayawardhana, R. 2004, ApJ, 614, 38

[24] Basri, G. & Marcy, G. W. 1995, AJ, 109, 762

[25] Bell, C. P., Mamajek, E. E. & Naylor, T. 2015, MNRAS, 454, 593

[26] Bensby, T., Feltzing, S., Lundström, I. & Ilyin, I. 2005, A&A, 433, 185

[27] Bensby, T., Feltzing, S. & Lundström, I. 2003, A&A, 410, 527

[28] Bergfors, C., Brandner, W., Janson, M. et al. 2010, A&A, 520, A54

[29] Bernat, D., Martinache, F., Ireland, M. et al. 2012, ApJ, 756, 8

[30] Bertout, C. & Genova, F. 2006, A&A, 1, 1

[31] Beuzit, J.-L., Ségransan, D., Forveille, T. et al. 2004, A&A, 425, 997

[32] Bianchi, L., Herald, J., Efremova, B. et al., 2011, Ap&SS, 335, 161

[33] Bidelman, W. P. 1985, ApJS, 59, 197

[34] Bidelman, W. P. 1988, Bulletin d'Information du Centre de Donnees Stellaires, 34, 35

[35] Biller, B. A., Liu, M. C., Wahhaj, Z. et al. 2013, ApJ, 777, 160

[36] Binks, A. S & Jeffries, R. D. 2014, MNRAS, 438, L11

[37] Bochanski, J. J., Hawley, S. L., Reid, I. N. et al. 2005, AJ, 130, 1871

[38] Bonfils, X., Gillon, M., Udry, S. & Armstrong, D. 2012, A&A, 546, A27

[39] Bonfils, X., Delfosse, X., Udry, S. et al. 2013, A&A, 549, A109

[40] Bonnarel, F., Fernique, P., Bienaymé, O. et al. 2000, A&AS, 143, 33

[41] Bopp, B. W. & Fekel F. C. Jr., 1977, PASP, 89, 65

[42] Bowler, B. P., Liu, M. C., Shkolnik, E. L. & Tamura, M. 2015, ApJS, 216, 7

[43] Briceño, C., Calvet, N., Kenyon, S. & Hartmann, L. 1999, AJ, 118, 1354

[44] Briceño, C., Hartmann, L., Stauffer, J. & Martín, E. 1998, AJ, 115, 2074

[45] Brinkmöller, M. 2016, BSc thesis, Ruprecht-Karls-Universität Heidelberg, Germany

[46] Browning, M. K., Basri, G., Marcy, G. W. et al. 2010, AJ, 139, 504

[47] Burgasser, A. J., Kirkpatrick, J. D., Reid, I. N. et al. 2003, ApJ, 586, 512

[48] Burgasser, A. J., Logsdon, S. E., Gagné, J. et al. 2015, ApJS, 220, 18

[49] Burgasser, A.J., Simcoe, R. A., Bochanski, J. J. et al. 2010, ApJ, 725, 1405

[50] Burningham, B., Pinfield, D. J., Leggett, S. K. et al. 2009, MNRAS, 395, 1237

[51] Burt, J., Vogt, S. S., Butler, R. P. et al. 2014, ApJ, 789, 114

[52] Buscombe, W. 1998, *MK spectral classifications: general catalogue*

[53] Butters, O. W., West, R. G., Anderson, D. R. et al. 2010, A&A, 520, L10

[54] Caballero, J. A. 2007, ApJ, 667, 520

[55] Caballero, J. A. 2009, A&A, 507, 251

[56] Caballero, J. A. 2010, A&A, 514, A98

[57] Caballero, J. A., Montes, D., Klutsch, A. et al. 2010, A&A, 520, A91

[58] Caballero, J. A. 2012, The Observatory, 132, 1

[59] Caballero, J. A., Cortés-Contreras, M., Alonso-Floriano, F. J. et al. 2013, Protostars and Planets VI Posters, 20

[60] Caballero, J. A., Cortés-Contreras, M., Alonso-Floriano, F. J. et al. 2016, 19th Cambridge Workshop on Cool Stars, Stellar Systems, and the Sun, DOI: 10.5281/zenodo.60060

[61] Charbonneau, D., Berta, Z. K., Irwin, J. et al. 2009, Nature, 462, 891

[62] Christy, J. M. 1978, AJ, 83, 1225

[63] Chugainov, P. F. 1974, IzKry, 52, 3

[64] Close, L. M., Siegler, N., Freed, M. & Biller, B. 2003, ApJ, 587, 407

[65] Close, L. M., Richer, H. B., Crabtree, D. R. 1990, AJ, 100, 1968

[66] Cortés-Contreras, M., Caballero, J, A., Alonso-Floriano, F. J., et al. 2013, Highlights of Spanish Astrophysics VII, 646, Proceedings of the X Scientific Meeting of the Spanish Astronomical Society

[67] Cortés-Contreras, M., Caballero, J. A. & Montes, D. 2014, The Observatory, 134, 348

[68] Cortés-Contreras, M., Béjar, V. J. S., Caballero, J. A. et al. 2016 A&A, in press, arXiv:1608.08145

[69] Couteau, P. 1960, Journal des Observateurs, 43, 41.

[70] Crifo, F., Phan-Bao, N., Delfosse, X. et al. 2005, A&A, 441, 653

[71] Cruz, K. L. & Reid, I. N. 2002, AJ, 123, 2828

[72] Cruz, K. L., Reid, I. N., Liebert, J., Kirkpatrick, J. D. & Lowrance, P. J. 2003, AJ, 126, 2421

[73] Cruz, K. L., Reid, I. N., Kirkpatrick, J. D. et al. 2007, AJ, 133, 439

[74] Cutri, R. M., Wright, E. L., Conrow, T. et al. 2012, yCat, 2311, 0

[75] Cutri, R. M., Wright, E. L., Conrow, T. et al. 2014, yCat, 2328, 0

[76] Cvetković, Z., Pavlović, R., Ninković, S. & Stojanović, M. 2012, AJ, 144, 80

[77] Daemgen, S., Siegler, N., Reid, I. N. & Close, L. M. 2007, ApJ, 654, 558

[78] Davison, C. L., White, R. J., Henry, T. J. et al. 2015, AJ, 149, 106

[79] Davison, C. L., White, R. J., Jao, W.-C. et al. 2014, AJ, 147, 26

[80] Dawson, P. C. & De Robertis, M. M. 2005, PASP, 117, 1

[81] Deacon, N. R., Hambly, N. C. & Cooke, J. A. 2005, A&A, 435, 363

[82] Deacon, N. R., Liu, M. C., Magnier, E. A. et al. 2012, ApJ, 757, 100

[83] de Bruijne, J. H. J. & Eilers, A.-C. 2012, A&A, 546, 61

[84] Delfosse, X., Forveille, T., Perrier, C. & Mayor, M. 1998, A&A, 331, 581

[85] Delfosse, X., Forveille, T., Mayor, M. et al. 1999a, A&A, 341, L63

[86] Delfosse, X., Forveille, T., Beuzit, J.-L. et al. 1999b, A&A, 344, 897

[87] Deshpande, R., Martín, E. L., Montgomery, M. M. et al. 2012, AJ, 144, 99

[88] Devor, J., Charbonneau, D., O'Donovan, F. T. et al. 2008, AJ, 135, 850

[89] Dieterich, S. B., Henry, T. J., Jao, W.-C. et al. 2014, AJ, 147, 94

[90] Dittmann, J. A., Irwin, J. M., Charbonneau, D. & Berta-Thompson, Z. K. 2014, ApJ, 784, 156

[91] Docobo, J. A., Tamazian, V. S., Balega, Y. Y. & Melikian, N. D. 2006, AJ, 132, 994

[92] Dorda, R. 2011, MSc thesis, Universidad Complutense de Madrid, Spain

[93] Drake, S., Osten, R., Page, K. L., Kennea, J. A. et al. 2014, ATel, 6121, 1

[94] Dupuy, T. J. & Liu, M. C. 2012, ApJS, 201, 19

[95] Duquennoy, A. & Mayor, M. 1988, A&A, 200, 135

[96] Duquennoy, A. & Mayor, M. 1991, A&A, 248, 485

[97] Dyer, E. R. Jr. 1954, AJ, 59, 218

[98] Eggen, O. J. 1984, AJ, 89, 1350

[99] Eggen, O. J. 1989, PASP, 101, 54

[100] Eisenbeiss, T., Ammler-vonEiff, M., Roell, T. et al. 2013, A&A, 556, A53

[101] Elliott, P., Bayo, A., Melo, C. H. F. et al. 2014, A&A, 568A, 26

[102] Elliott, P., Huélamo, N., Bouy, H., Bayo, A. et al. 2015, A&A, 580A, 88

[103] Endl, M., Cochran, W.D., Kürster, M. et al. 2006, ApJ, 649, 436

[104] Endl, M., Cochran, W.D., Tull, R. G. & MacQueen, P. J. 2003, AJ, 126, 3099

[105] Endl, M., Cochran, W.D., Wittenmyer, R. A. & Boss, A. P. 2008, ApJ, 673, 1165

[106] Evans, D. S. 1975, MNSSA, 34, 51

[107] Evans, D. S. 1979, IAUS, 30, 57

[108] Evans, D. W., Irwin, M. J. & Helmer, L. 2002, A&A, 395, 347

[109] Evans, I. N., Primini, F. A., Glotfelty, K. J. et al. 2010, ApJS, 189, 37

[110] "Fabricius, C., Hø g, E., Makarov, V. V. et al. 2002, A&A, 384, 180"

[111] Fischer, D. A. & Marcy, G. W. 1992, ApJ, 396, 178

[112] Fleming, T. A., Liebert, J., Gioia, I. M. & Maccacaro, T. 1988, ApJ, 331, 958

[113] Freedman, D & Diaconis, P. 1981, *Probability Theory and Related Field*, 57, 4, 453

[114] Frith, J., Pinfield, D. J., Jones, H. R. A. et al. 2013, MNRAS, 435, 2161

[115] Gliese, W. & Jahreiβ, H. 1979, A&AS, 38, 423

[116] Gagné, J., Lafrenière, D., Doyon, R. et al. 2014, ApJ, 783, 121

[117] Gagné, J., Lafrenière, D., Doyon, R. et al. 2015a, ApJ, 798, 73

[118] Gagné, J., Faherty, J. K., Cruz, K. L. et al. 2015b, ApJS, 219, 33

[119] Gallardo, I. 2015, MSc thesis, Universidad Complutense de Madrid, Spain

[120] Gatewood, G. 1996, A&AS, 188, 4011

[121] Gatewood, G. & Coban, L. 2009, AJ, 137, 402

[122] Gershberg, R. E., Katsova, M. M., Lovkaya, M. N. et al. 1999, A&AS, 139, 555

[123] Giacobbe, P., Damasso, M., Sozzetti, A. et al. 2012, MNRAS,424, 3101

[124] Giannuzzi, M. A. 1979, A&A, 77, 214

[125] Giclas, H. L., Slaughter, C. D. & Burnham, R. 1959, Lowell Observatory Bulletin, 4, 136

[126] Gigoyan, K. S., Hambaryan, V. V. & Azzopardi, M. 1998, Astrophysics, 41, 356

[127] Gigoyan, K. S., Sinamyan, P. K., Engels, D. & Mickaelian, A. M. 2010, Ap, 53, 123

[128] Gillon, M., Jehin, E., Lederer, S. M. et al. 2016, Nature, 533, 221

[129] Gizis, J. E. 1997, AJ, 113, 806

[130] Gizis, J. E. & Reid, I. N., 1997, PASP, 109, 1233

[131] Gizis, J. E., Monet, D. G., Reid, I. N. et al. 2000, AJ, 120, 1085

[132] Gizis, J. E., Reid, I. N. & Hawley, S. L. 2002, AJ, 123, 3356

[133] Glebocki, R., Gnacinski, P. & Stawikowski, A. 2000, AcA, 50, 509

[134] Glebocki, R. & Gnacinski, P. 2005, yCat, 3244, 0

[135] Gliese, W. & Jahreiss, H. 1991, *Preliminary Version of the Third Catalogue of Nearby Stars*, NASA/AstronomicalDataCenter, Greenbelt

[136] Golimowski, D. A., Leggett, S. K., Marley, M. S., et al. 2004, AJ, 127, 3516

[137] González-Álvarez, E. 2014, MSc thesis, Universidad Complutense de Madrid, Spain

[138] Goodwin, S. P., & Whitworth, A. P. 2007, A&A, 466, 943

[139] Gray, R. O., Corbally, C. J., Garrison, R. F., McFadden, M. T. & Robinson, P. E. 2003, AJ, 126, 2048

[140] Gray, R. O., Corbally, C. J., Garrison, R. F. et al. 2006, AJ, 132, 161

[141] Gunn, J. E., Siegmund, W. A., Mannery, E. J. et al., 2006, ApJ, 131, 2332

[142] Hambaryan, V., Neuhäuser, R. & Stelzer, B. 1999, A&A, 345, 121

[143] Harlow, J. J. B. 1996, AJ, 112, 2222

[144] Haro, G., Chavira, E. & González, G. 1975, IBVS, 1031, 1

[145] Harrington, R. S., Christy, J. W. & Strand, K. A. 1981, AJ, 86, 909

[146] Harrington, R. S. & Dahn, C. C. 1980, AJ, 85, 454

[147] Hartman, J. D., Bakos, G. Á., Stanek, K. Z. & Noyes, R. W. 2004, AJ, 128, 1761

[148] Hartman, J. D., Bakos, G. Á., Kovács, G. & Noyes, R. W. 2010, MNRAS, 408, 475

[149] Hartman, J. D., Bakos, G. Á., Noyes, R. W. et al. 2011, AJ, 141, 166

[150] Hawley, S. L., Gizis, J. E. & Reid, I. N. 1996, AJ, 112, 2799

[151] Henry, T. J., Kirkpatrick, J. D. & Simons, D. A. 1994, AJ, 108, 1437

[152] Henry, T. J., Jao, W.-C., Subasavage, J. P. et al. 2006, AJ, 132, 2360

[153] Herbig, G. H. & Moorhead, J. M. 1965, ApJ, 141, 649

[154] Herrero, E., Ribas, I., Jordi, C. et al. 2012, A&A, 537, A147

[155] Hidalgo, D. 2014, MSc thesis, Universidad Complutense de Madrid, Spain

[156] Høg, E., Fabricius C., Makarov V.V. et al. 2000, A&A, 355, L27

[157] Hojaev. A. S. 1986, Afz, 24, 65

[158] Holgado, G. 2014, MSc thesis, Universidad Complutense de Madrid, Spain

[159] Horch, E. P., Bahi, L. A. P., Gaulin, J. R. et al. 2012, AJ, 143, 10

[160] Horch, E. P., Falta, D., Anderson, L. M. et al. 2010, AJ, 139, 205

[161] Horch, E. P., Gómez, S. C., Sherry, W.H. et al. 2011, AJ, 141, 45

[162] Houdebine, E. R. 2010, MNRAS, 407, 1657

[163] Houdebine, E. R. & Mullan, D. J. 2015, ApJ, 801, 106

[164] Howard, A. W., Johnson, J. A., Marcy, G. W. et al. 2010, ApJ, 721, 1467

[165] Hunt-Walker, N. M., Hilton, E. J. et al. 2012, PASP, 124, 545

[166] Ireland, M. J., Kraus, A., Martinache, F. et al. 2008, ApJ, 678, 463

[167] Irwin, J, Zachory, B. K., Burke, C. J. et al. 2010, ApJ, 747, 56

[168] Irwin, J.,Zachory, B. K., Burke, C. J. et al. 2011 ApJ, 727, 56

[169] Irwin, J., Charbonneau, D., Zachory, B. K. et al. 2009, ApJ, 701, 1436

[170] Jackson, P. D., Kundu, M. R. & White, S. M. 1987, LNP, 291, 103

[171] Jahreiβ, H., Meusinger, H., Scholz, R.-D. & Stecklum, B. 2008, A&A, 484, 575

[172] Janson, M., Hormuth, F., Bergfors, C. et al. 2012, ApJ, 754, 44

[173] Janson, M., Bergfors, C., Brandner, W. et al. 2014a, ApJ, 789, 102

[174] Janson, M., Bergfors, C., Brandner, W. et al. 2014b, ApJS, 214, 17

[175] Jao, W.-C., Henry, T. J., Subasavage, J. P. et al. 2005, AJ, 129, 1954

[176] Jao, W.-C., Henry, T. J., Subasavage, J. P. et al. 2011, AJ, 141, 117

[177] Jeffers, S. V., Schöfer, P., Lamert, A. et al. 2016, A&A, submitted

[178] Jenkins, L. F. 1952, *General catalogue of trigonometric stellar parallaxes*, Yale University Observatory, USA

[179] Jenkins, L. F. 1963, *General catalogue of trigonometric stellar parallaxes*, Yale University Observatory, USA

[180] Jenkins, J. S., Ramsey, L. W., Jones, H. R. A. et al. 2009, ApJ, 704, 975

[181] Johnson, D. R. H. & Soderblom, D.R. 1987, AJ, 93, 864

[182] Johnson, J. A. & Apps, K. 2009, ApJ, 699, 933

[183] Johnson, J. A., Howard, A. W., Marcy, G. W. et al. 2010, PASP, 122, 149

[184] Joy, A. H. & Abt, H. A. 1974, ApJS, 28, 1

[185] Jódar, E., Pérez-Garrido, A., Díaz-Sánchez, A. et al. 2013, MNRAS, 429, 859

[186] Kenyon, S. J. & Hartmann, L. 1995, ApJS, 101, 117

[187] Kim, M. 2015, MSc thesis, Ruprecht-Karls-Universität Heidelberg, Germany

[188] King, R. R., Parker, R. J., Patience, J. & Goodwin, S. P. 2012, MNRAS, 421, 2025

[189] Kiraga, M. & Stepien, K. 2007, AcA, 57, 149

[190] Kiraga, M. 2012, AcA, 62, 67

[191] Kirkpatrick, J. D., Henry, T. J. & McCarthy, D. W., Jr. 1991, ApJS, 77, 417

[192] Kirkpatrick, J. D., Henry, T. J. & Simons, D. A. 1995, AJ, 109, 797

[193] Koen, C. & Eyer, L. 2002, MNRAS, 331, 45

[194] Koen, C., Kilkenny, D., van Wyk, F. & Marang, F. 2010, MNRAS, 403, 1949

[195] Konopacky, Q. M., Ghez, A. M., Barman, T. S. et al. 2010, ApJ, 711, 1087

[196] Korhonen, H., Vida, K., Husarik, M. et al. 2010, AN, 331, 772

[197] Kuiper, G. P. 1942, ApJ, 95, 201

[198] Lafrenière, D., Doyon, R., Marois, C. et al. 2007, ApJ, 670, 1367

[199] Lampens, P., Strigachev, A. & Duval, D. 2007, A&A, 464, 641

[200] Latham, D.W., Stefanik, R. P., Torres, G. et al. 2002, AJ, 124, 1144

[201] Law, N. M., Hodgkin, S. T. & Mackay, C. D. 2006, MNRAS, 368, 1917

[202] Law, N. M., Hodgkin, S. T. & Mackay, C. D. 2008, MNRAS, 384, 150

[203] Lee, S.-G. 1984, AJ, 89, 702

[204] Leggett, S. K., Saumon, D., Burningham, B. et al. 2010, ApJ, 720, 252

[205] Leinert, C., Zinnecker, H., Weitzel, N., Christou, J. et al. 1993, A&A, 278, 129

[206] Leinert, C., Henry, T., Glindemann, A. & McCarthy, D. W., Jr. 1997, A&A, 325, 159

[207] Lépine, S., Rich, R. M. & Shara, M. M. 2003, AJ, 125, 1598

[208] Lépine, S. & Shara, M. M. 2005, AJ, 129, 1483

[209] Lépine, S. & Bongiorno, B. 2007, AJ, 133, 889

[210] Lépine, S., Thorstensen, J. R., Shara, M. M. & Rich, R. M. 2009, AJ, 137, 4109

[211] Lépine, S. & Gaidos, E. 2011, AJ, 142, 138

[212] Lépine, S., Hilton, E. J., Mann, A. W. et al. 2013, AJ, 145, 102

[213] Lippincott, S. L. 1952, ApJ, 115, 582

[214] Llamas, M. 2014, MSc thesis, Universidad Complutense de Madrid, Spain

[215] Lodieu, N., Scholz, R.-D., McCaughrean, M. J. et al. 2005, A&A, 440, 1061

[216] López-Santiago, J., Montes, D., Crespo-Chacón, I. & Fernández-Figueroa, M. J. 2006, ApJ, 643, 1160

[217] Luhman, K. L. 2004, ApJ, 617, 1216

[218] Luyten, W. J. 1997, VizieR Online Data Catalog I/130, *LDS Catalogue: Doubles with Common Proper Motion (Luyten 1940-87)*, Originally published in: Publ. Astr. Obs. Univ. Minnesota III, part 3, 35, and Proper motion survey with the 48-inch Schmidt Telescope XXI, XXV, XIX, XL, L, LXIV, LV, LXXI, Univ. Minnes. (1940-1987)

[219] Mace, G. N., Kirkpatrick, J. D., Cushing, M.C. et al. 2013, ApJ, 777, 36

[220] Maldonado, J., Martínez-Arnáiz, R. M., Eiroa, C. et al. 2010, A&A, 521, A12

[221] Malkov, O. Y., Tamazian, V. S., Docobo, J. A. & Chulkov, D. A. 2012, A&A, 546, A69

[222] Malo, L., Doyon, R., Lafrenière, D. et al. 2013, ApJ, 762, 88

[223] Malo, L., Artigau, É., Doyon, R. et al. 2014a, ApJ, 788, 81

[224] Malo, L., Doyon, R., Feiden, G. A. et al. 2014b, ApJ, 792, 37

[225] Malogolovets, E. V., Balega, Y. Y., Rastegaev, D. A. et al. 2007, AstBu, 62, 117

[226] Mamajek, E. E., Lawson, W. A. & Feigelson, E. D. 1999, ApJ, 516L, 77

[227] Mamajek, E. E., Bartlett, J. L., Seifahrt, A. et al. 2013, AJ, 146, 154

[228] Marcy, G. W., Lindsay, V. & Wilson, K. 1987, PASP, 99, 490

[229] Marcy, G. W. & Chen, H. 1992, ApJ, 390, 550

[230] Marcy, G. W., Butler, R. P., Vogt, S. S. et al. 1998, ApJ, 505, L147

[231] Mariotti, J.-M., Perrier, C., Duquennoy, A. & Duhoux, P. 1990, A&A, 230, 77

[232] Martínez-Rodríguez, H. 2014, MSc thesis, Universidad Complutense de Madrid, Spain

[233] Martinache, F., Lloyd, J. P., Ireland, M.J. et al. 2007, ApJ, 661, 496

[234] Martínez-Arnáiz, R., Maldonado, J., Montes, D. et al. 2010, A&A, 520, A79

[235] Mason, B. D., Wycoff, G. L., Hartkopf, W. I., Douglass, G. G. & Worley, C. E. 2001, AJ, 122, 3466

[236] Mason, B. D., Wycoff, G. L., Hartkopf, W. I., Douglass, G. G. & Worley, C. E. 2015, VizieR on-line catalogue, B/WDS

[237] McCarthy, C., Zuckerman, B. & Becklin, E. E. 2001, AJ, 121, 3259

[238] McQuillan, A., Aigrain, S. & Mazeh, T. 2013, MNRAS, 432, 1203

[239] Melikyan, N. D., Tamazian, V. S., Natsvlishvili, R. S. & Karapetian, A. A. 2013, Ap, 56, 8

[240] Messina, S., Desidera, S., Turatto, M. et al. 2010, A&A, 520, A15

[241] Messina, S. Lanzafame, A. C., Feiden, G. A. et al. 2016, arXiv:1607.06634

[242] Metodieva, Y., Antonova, A., Golev, V. et al. 2015, MNRAS, 446, 3878

[243] Mochnacki, S. W., Gladders, M. D., Thomson, J. R. et al. 2002, AJ, 124, 2868

[244] Mohanty, S. & Basri, G. 2003, ApJ, 583, 451

[245] Monet, D. G. 1998, AAS, 19312003M

[246] Monet, D. G., Levine, S. E., Canzian, B. et al. 2003, AJ, 125, 984

[247] Montagnier, G., Ségransan, D., Beuzit, J.-L. et al. 2006, A&A, 460, L19

[248] Montes, D., López-Santiago, J., Gálvez, M. C. et al. 2001, MNRAS, 328, 45

[249] Morales, J. C., Ribas, I., Jordi, C. et al. 2009, ApJ, 691, 1400

[250] Morgan, D. P., West, A. A., Garcés, A. et al. 2012, AJ, 144, 93

[251] Morrison, J. E., McLean, B. & GSC-Catalog II Construction Team, 2001, American Astronomical Society, Division on Dinamical Astronomy Meeting, 32, 0603

[252] Moór, A., Szabó, G. M., Kiss, L. L. et al. 2013, MNRAS, 435, 1376

[253] Mullan, D. J. 1974, ApJ, 192, 149

[254] Mullan, D. J., Stencel, R. E. & Backman, D. E. 1989, ApJ, 343, 400

[255] Newton, E. R., Charbonneau, D., Irwin, J. et al. 2014, AJ, 147, 20

[256] Nidever, D.L., Marcy, G. W., Butler, R. P. et al. 2002 ApJS, 141, 503

[257] Norton, A. J., Wheatley, P. J., West, R. G. et al. 2007, A&A, 467, 785

[258] Ochsenbein, F., Bauer, P. & Marcout, J. 2000, A&AS, 143, 23

[259] Öpik, E. 1924, Publications de L'Observatoire Astronomique de l'Universite de Tartu, 25, 6

[260] Passegger, V. M., Reiners, A., Jeffers, S. V. et al. 2016, arXiv:1607.08738

[261] Pecaut, M. J. & Mamajek, E. E. 2013, ApJS, 208, 9

[262] Perryman, M. A. C., Lindegren, L., Kovalevsky, J. et al. 1997, A&A, 323, L49

[263] Perryman, M. A. C., Brown, A. G. A., Lebreton, Y. et al. 1998, A&A, 331, 81

[264] Pesch, P. & Bidelman, W. 1997, PASP, 109, 643

[265] Pettersen, B. R. 1975, A&A, 41, 87

[266] Pettersen, B. R. 1991, MmSAI, 62, 217

[267] Pettersen, B. R. 2006, Obs, 126, 397

[268] Pettersen, B. R. & Griffin, R. F. 1980, Obs, 100, 198

[269] Phan-Bao, N. & Bessell, M. S. 2006, A&A, 446, 515

[270] Pickles, A. & Depagne, É. 2010, PASP, 122, 1437

[271] Pizzolato, N., Maggio, A., Micela, G., Sciortino, S. & Ventura, P. 2003, A&A, 397, 147

[272] Pojmański, G. 2002, AcA, 52, 397

[273] Pourbaix, D., Tokovinin, A. A., Batten, A. H. et al. 2004, A&A, 424, 727

[274] Poveda, A. & Allen, C. 2004, RMxAC, 21, 49

[275] Poveda, A., Allen, C. & Hernández-Alcántara, A. 2007, IAUS, 240, 417

[276] Pravdo, S. H., Shaklan, S. B., Henry, T. J. & Benedict, G. F. 2004, ApJ, 617, 1323

[277] Pravdo, S. H., Shaklan, S. B., Wiktorowicz, S. J. et al. 2006, ApJ, 649, 389

[278] Prosser, C. F., Randich, S., Stauffer, J. R. et al. 1996, AJ, 112, 1570

[279] Raghavan, D., McAlister, H. A., Henry, T. J. et al. 2010, ApJS, 190, 1

[280] Rajpurohit, A. S., Reylé, C., Allard, F. et al 2013, A&A, 556, A15

[281] Rebull, L. M., Padgett, D. L., McCabe, C. E. et al. 2010, ApJS, 186, 259

[282] Reid, I. N., Hawley, S. L. & Gizis, J. E. 1995, AJ, 110, 1838

[283] Reid, I. N., Gizis, J. E. & Hawley, S. L. 2002, AJ, 124, 2721

[284] Reid, I. N., Cruz, K. L., Allen, P. et al. 2003, AJ, 126, 3007

[285] Reid, I. N., Cruz, K. L., Allen, P. et al. 2004, AJ, 128, 463

[286] Reid, I. N., Cruz, K. L. & Allen, P. 2007, AJ, 133, 2825

[287] Reid, I. N., Cruz, K. L., Kirkpatrick, J. D. et al. 2008a, AJ, 136, 1290

[288] Reid, I. N., Cruz, K. L., Burgasser, A. J. & Liu. M. C. 2008b, AJ, 135, 580

[289] Reiners, A. 2007, A&A, 467, 259

[290] Reiners, A. & Basri, G. 2007, ApJ, 656, 1121

[291] Reiners, A. & Basri, G. 2008, ApJ, 684, 1390

[292] Reiners, A. & Basri, G. 2009, ApJ, 705, 1416

[293] Reiners, A., Joshi, N. & Goldman, B. 2012, AJ, 143, 93

[294] Reyes-Sánchez, K. P. 2014, MSc thesis, Valencian International University, Spain

[295] Reylé, C., Scholz, R.-D., Schultheis, M., Robin, A. C. & Irwin, M. 2006, MNRAS, 373, 705

[296] Riaz, B., Gizis, J. E. & Harvin, J. 2006, AJ, 132, 866

[297] Riddle, R. L., Tokovinin, A., Mason, B. D., 2015, ApJ, 799, 4

[298] Riedel, A. R., Murphy, S. J., Henry, T. J. et al. 2011, AJ, 142, 104

[299] Riedel, A. R., Subasavage, J. P., Finch, C. T. et al. 2010, AJ, 140, 897

[300] Riedel, A. R., Finch, C. T., Henry, T. J. et al. 2014, AJ, 147, 85

[301] Roeser, S., Demleitner, M. & Schilbach, E. 2010, AJ, 139, 2440

[302] Rosen S. R., Webb N. A., Watson, M. G. et al., 2016, A&A, 590, A1

[303] Schlieder, J. E., Lépine, S. & Simon, M. 2010, AJ, 140, 119

[304] Schlieder, J. E., Lépine, S., Rice, E. et al. 2012a, AJ, 144, 109

[305] Schlieder, J. E., Lépine, S. & Simon, M. 2012b, AJ, 143, 80

[306] Schmidt, S. J., Cruz, K. L., Bongiorno, B. J. et al 2007, AJ, 133, 2258

[307] Schöfer, P. 2015, MSc thesis, Georg-August-Universität Göttingen, Germany

[308] Scholz, R.-D., Meusinger, H. & Jahreiβ, H. 2005, A&A, 442, 211

[309] Shkolnik, E., Liu, M. C. & Reid, I. N. 2009, ApJ, 699, 649

[310] Shkolnik, E. L., Hebb, L., Liu, M. C. et al. 2010, ApJ, 716, 1522

[311] Shkolnik, E. L., Anglada-Escudé, G., Liu, M. C. et al. 2012, ApJ, 758, 56

[312] Siebert, A., Williams, M. E. K., Siviero, A. et al. 2011, AJ, 141, 187

[313] Skiff, B. A. 2014, *General Catalogue of Stellar Spectral Classifications*, yCat, 1, 2023

[314] Skrutskie, M. F., Cutri, R. M., Stiening, R. et al. 2006, AJ, 131, 1163

[315] Soderblom, D. R. & Mayor, M. 1993, AJ, 105, 226

[316] Stauffer, J. B. & Hartmann, L. W. 1986, PASP, 98, 1233

[317] Stauffer, J. R., Liebert, J., Giampapa, M. et al. 1994, AJ, 108, 160

[318] Stauffer, J. R., Balachandran, S. C., Krishnamurthi, A. et al. 1997, ApJ, 475, 604

[319] Stern, R. A., Schmitt, J. H. M. M. & Kahabka, P. T. 1995, ApJ, 448, 683

[320] Strand, K. Aa. 1977, AJ, 82, 745

[321] Strassmeier, K. G. 2009 A&ARv, 17, 251

[322] Subasavage, J. P., Jao, W.-C., Henry, T. J. et al. 2009, AJ, 137. 4547

[323] Svestka, Zd. 1954, BAICz, 5, 4

[324] Tanner, A. M., Gelino, C. R. & Law, N. M. 2010, PASP, 122, 1195

[325] Taylor, M. B. 2005, ASPC, 347, 29

[326] Terrien, R. C., Fleming, S. W., Mahadevan, S. et al. 2012, ApJ, 760, L9

[327] Terrien, R. C., Mahadevan, S., Bender, C.F. et al. 2015, ApJ, 802, L10

[328] Tetzlaff, N., Neuhäuser, R. & Hohle, M. M. 2011, MNRAS, 410, 190

[329] TokovininA. A. 1992, A&A, 256, 121

[330] Tokovinin, A. A. & Smekhov, M. G. 2002, A&A, 382, 118

[331] Tokovinin, A., Thomas, S., Sterzik, M. & Udry, S. 2006, A&A, 450, 681

[332] Tokovinin, A., Mason, B. D. & Hartkopf, W.I. 2010, AJ, 139, 743

[333] Tokovinin, A., Mason, B. D., Hartkopf, W. I. et al. 2015, AJ, 150, 50

[334] Tomkin, J. & Pettersen, B. R. 1986, AJ, 92. 1424

[335] Torres, G. & Ribas, I. 2002; ApJ, 567, 1140

[336] Torres, C. A. O., Quast, G. R., da Silva, L. et al. 2006, A&A, 460, 695

[337] Torres, C. A. O., Quast, G. R., Melo, C. H. F. & Sterzik, M. F. 2008, *Young Nearby Loose Associations*, ed. Reipurth, B. p.757

[338] Upgren, A. R. & Harlow, J. J. B. 1996, PASP, 108, 64

[339] Urban, S. E., Corbin, T. E., Wycoff, G. L. et al. 1998, AJ, 115. 1212

[340] van Altena, W. F., Lee, J. T. & Hoffleit, E. D. 1995, *The general catalogue of trigonometric [stellar] parallaxes*, New Haven, Yale University Observatory, 4th ed.

[341] van Leeuwen, F. 2007, A&A, 474, 653

[342] Voges, W., Aschenbach, B., Boller, T. et al. 1999, A&A, 349, 389

[343] Walkowicz, L. M., Hawley, S. L. & West, A. A. 2004, PASP, 116, 1105

[344] Wang, J. & Ford, E. B. 2011, MNRAS, 418, 1822

[345] Ward-Duong, K., Patience, J., De Rosa, R. J. et al. 2015, MNRAS, 449, 2618

[346] Weinberg, M. D., Shapiro, S. L., & Wasserman, I. 1987, ApJ. 312, 367

[347] Weinberger, A. J., Boss, A. P., Keiser, S. A. et al. 2016, AJ, 152, 24

[348] Weis, E. W. 1987, AJ, 93, 451

[349] Wenger, M., Ochsenbein, F., Egret, D. et al. 2000, A&AS, 143, 9

[350] West, A. A., Hawley, S. L., Bochanski, J. J. et al. 2008, AJ, 135, 785

[351] West, A. A., Morgan, D. P., Bochanski, J. J. et al. 2011, AJ, 141, 97

[352] West, A. A., Weisenburger, K. L., Irwin, J. et al. 2015, ApJ, 812, 3

[353] White, R. J. & Ghez, A. M. 2001 ApJ, 556, 265

[354] White, R. J., Gabor, J. M., & Hillenbrand, L. A. 2007, AJ, 133, 2524

[355] White, S. M., Jackson, P. D. & Kundu, M. R. 1989, ApJS, 71, 895

[356] Wilson, R. E. 1953, *General catalogue of stellar radial velocities*, GCRV, C, 0

[357] Winters, J. G., Henry, T. J., Lurie, J. C. et al. 2015, AJ, 149, 5

[358] Woitas, J., Leinert, C., Jahreiβ, H. et al. 2000, A&A, 353, 253

[359] Wright, D. J., Wittenmyer, R. A., Tinney, C. G., Bentley, J. S. & Zhao, J. 2016, ApJ, 817, L20

[360] Yi, Z., Luo, A., Song, Y. et al. 2014, AJ, 147, 33

[361] Zacharias, N., Finch, C., Girard, T. et al. 2010, AJ, 139, 2184

[362] Zacharias, N., Finch, C. T., Girard, T. M. et al. 2013, AJ, 145, 44

[363] Zasche, P., Wolf, M., Hartkopf, W. I., Svoboda, P. et al. 2009, AJ, 138, 664

[364] Zechmeister, M., Kürster, M. & Endl, M. 2009, A&A, 505, 859

[365] Zuckerman, B., Song, I. & Bessell, M. S. 2004, ApJ, 613, L65

[366] Zuckerman, B., Rhee, J. H., Song, I. & Bessell, M. S. 2011 ApJ, 732, 61

3

Cool dwarfs in wide multiple systems

This chapter corresponds to the published paper *Cool dwarfs in wide multiple systems. Paper 5: New astrometry of 54 wide pairs with M dwarfs* (Cortés–Contreras et al. 2014, Obs, 134, 348).

Investigating cool dwarfs in wide pairs is a crucial step in our approach to the understanding of their formation and evolution. In the Carmencita catalogue, as we saw in Chapter 2, there are several M dwarfs belonging to known binary or multiple systems. All their relative information, such as orbital parameters, angular separation, difference of magnitudes between components and the spectral type of the companion or companions, if existent, has been compiled mainly from the Washington Double Star Catalogue (WDS) but also from the literature and then integrated in Carmencita in a specific section named "Multiplicity". Before introducing this information in our database we checked by eye if angular separations (ρ) and position angles (θ) at different epochs (typically those provided by the WDS but also with the inspection of separations in SDSS images), were consistent with the common proper motion of the components. This is not, however, a confident way to test binarity, but the easiest one and sometimes, as we can see in the next published study, a deep analysis disentangles binarity. It should be noted that not always the lack of information difficults the study but the excess of it could also be confusing.

In the following paper we performed an astrometric analysis for 54 tabulated pairs with an M dwarf being one of the components. We provided new angular separations and position angles measurements from low–resolution images taken during 2012 with the TCP and CAMELOT instruments at the 0.82 m IAC80 telescope at the Observatorio del Teide. Nine pairs showed noticeable ρ and θ differences compared to the values of the first epochs, or very different catalogued proper–motions. For them, we compiled all the tabulated measurements, measured ρ and θ on photographic plate digitizations and from the astrometry provided by all-sky catalogues and compare them to verify if they were actually comoving (see two examples in Fig. 3.1). We computed proper motions of each component of the most controversial pairs. Two of them had components with different proper motions, which proves that they are not physically bound. For the 52 physically bound pairs we compiled the spectral type of the components, their distances and masess, and computed projected physical separations, reduced orbital periods and reduced binding energies ($-U_g^*$). We found a threshold at $-U_g^* \approx 10^{34}$ J, and five weakly bound systems with binding energies below 10^{35} J, which could survive in the Galactic disc as much as the age of the Galaxy. Another ten systems show appreciable orbital variation (up to 50% in the position angle), and have orbital periods shorter than 1000 a.

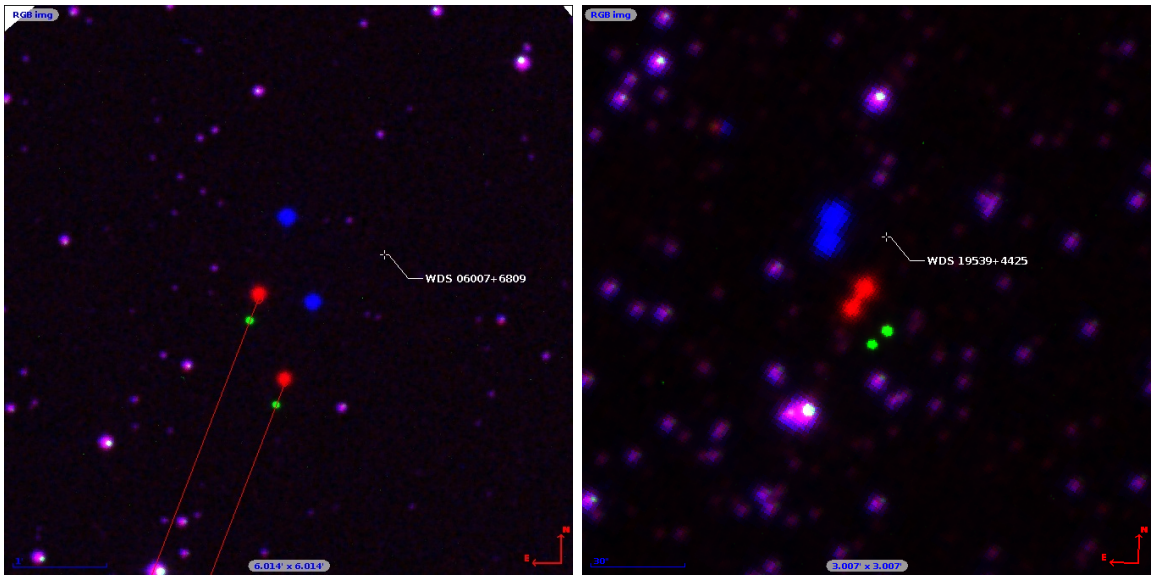

FIGURE 3.1— False-colour composite images of two of our high common proper-motion pairs (blue: POSS-I ∼1950, red: POSS-II ∼1990, green: IAC80 ∼2012).

Of them, three are binaries, two are triples, one is quadruple and one is quintuple (see Fig. 3.2). We propose them for a more detailed study of their orbits, with the aim of determining dynamical masses of the M components. Some of these results were included in the Carmencita catalogue.

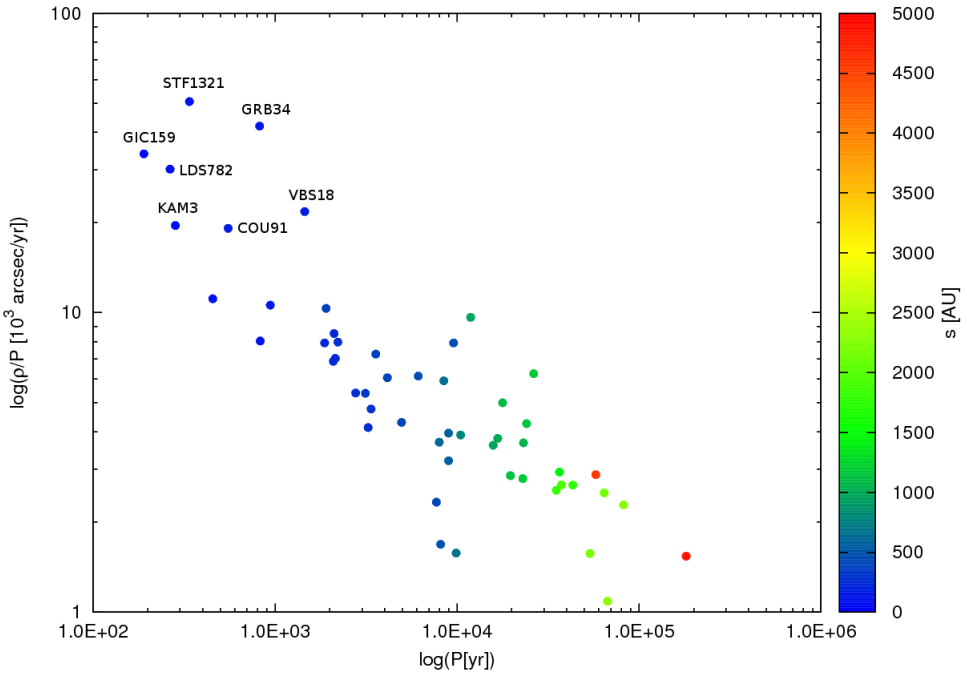

FIGURE 3.2— Angular variation vs. periods in logarithmic scale. Colour-bar represent the projected physical separation of the systems. The seven labeled systems present large orbital variations and short periods.

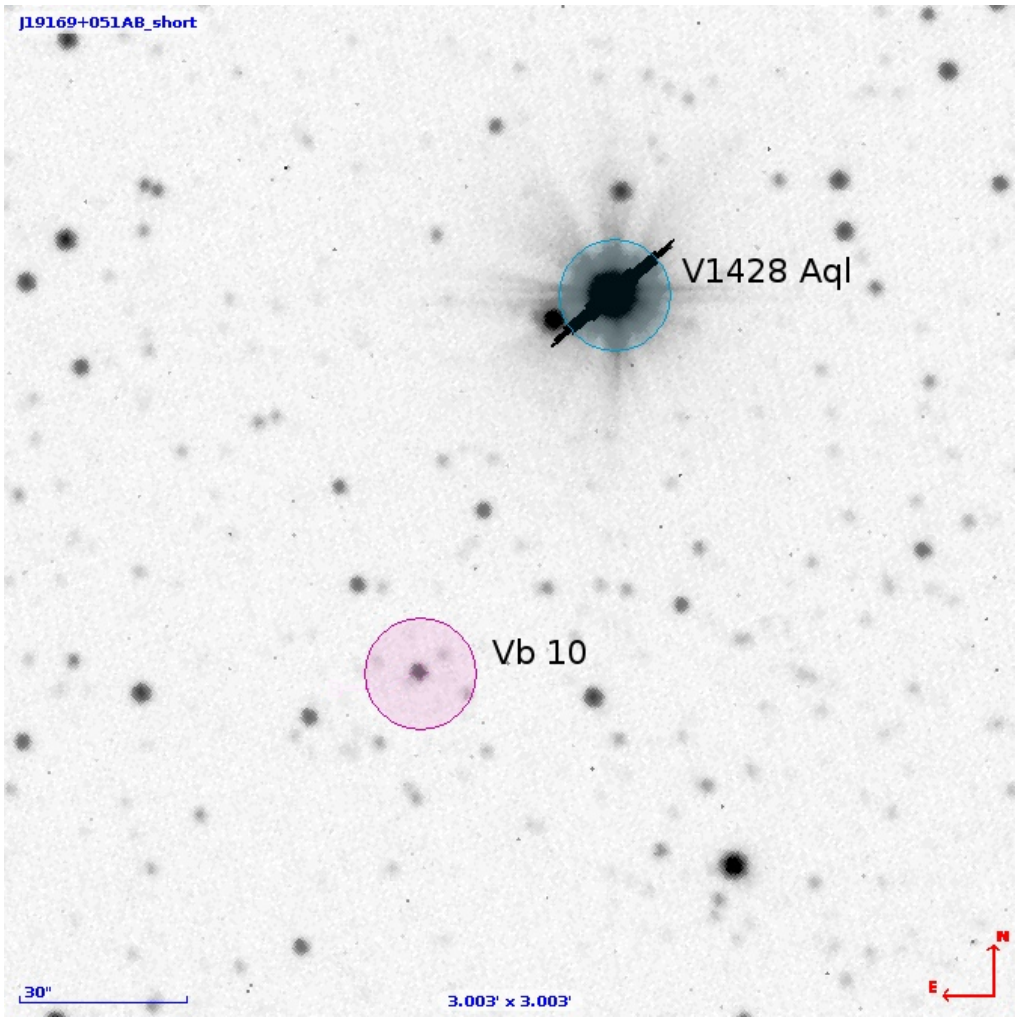

FIGURE 3.3— Finding chart of J19169+051 (vB 10) from a TCP image with exposure time of 60 s in October 2012. The saturated star is the primary V1428 Aql.

The observation of our M dwarfs with low-resolution imagers also provided a new epoch useful for identifying high proper motion stars in a more recent epoch. It is the case of J19169+051S (vB 10), which is an M8.0 V that moves at 1.4 arcsec a^{-1} in a populated field. A finding chart of this object, physical companion of the M2.5 V V1428 Aql, is shown in Fig. 3.3.

COOL DWARFS IN WIDE MULTIPLE SYSTEMS PAPER 5: NEW ASTROMETRY OF 54 WIDE PAIRS WITH M DWARFS

By Miriam Cortés-Contreras,
Departamento de Astrofisica, Universidad Complutense de Madrid

José A. Caballero
Centro de Astrobiología (CSIC–INTA), Madrid, Spain

and David Montes
Departamento de Astrofisica, Universidad Complutense de Madrid

We investigate the membership in double, triple, or higher-order-multiplicity systems of 54 pairs, with at least one bright M dwarf, in the solar neighbourhood. These M dwarfs are potential targets of radial-velocity surveys for exoplanets. We measure angular separations and position angles from optical images taken with *TCP* and *CAMELOT* at the *IAC80* telescope at the Observatorio del Teide, and complement them with our measurements on photographic-plate digitizations. We also use data in the *Washington Double Star Catalogue* and other bibliographic sources. We confirm the physical binding of 52 multiple systems, for which we comprehensively compile, derive, and provide basic astrophysical parameters in a homogeneous way (spectral types, heliocentric distances, projected physical separations, individual masses, estimated orbital periods, binding energies). Of the 52 systems, 38 are double, 11 are triple, and three are quadruple with a variety of architectures. Four systems contain white dwarfs, six systems display variations of position angle larger than 12° (1/30 orbit) on a scale of decades, and seven systems are located at less than 10 pc. We provide new information, or correct published data, for the most remarkable multiple systems and identify some of them for high-resolution imaging and spectroscopic follow-up.

Introduction

There are thousands of cool main-sequence stars in known pairs, many of which have projected physical separations of hundreds or thousands of astronomical units (Paper 1 of this series and references therein[1]). The existence of cool dwarfs in wide multiple systems helps in the investigation of their formation and evolution, especially if the other component is a Sun-like star (useful for, *e.g.*, metallicity studies), a white dwarf (useful for, *e.g.*, nuclear-age determination), or even an identical M dwarf with different rotation period or X-ray emission (useful for, *e.g.*, comparative magnetic-braking models). Besides, the nearest systems have correspondingly very wide angular separations and, therefore, can easily be resolved from the ground with standard imagers and telescopes of moderate size. In some cases, and with long enough astrometric

monitoring, one can study the relative movement of the two stars in the pair without the aid of high-resolution-imaging devices (speckle, adaptive optics, lucky imaging), which is of great help for determining dynamical masses.

In this work, we investigate in detail several dozen wide pairs with M dwarfs with a threefold objective: confirming their true common proper-motion (and, thus, membership in a physical system), homogenously characterizing a large set of pairs, many of which have never been investigated astrometrically in detail, and searching for remarkable, multiple, wide systems (*i.e.*, pair candidates for which an astrometric orbit can be calculated, systems with secondaries without proper spectral-type determinations, the most fragile pairs at the boundary of disruption by the Galactic gravitational field, or triple — and quadruple — systems).

Observations

Originally, the observational programme that led to the results presented here was aimed at imaging stars selected as potential targets for upcoming near-infrared radial-velocity exoplanet surveys (such as *HPF*[2], *SPIRou*[3] or, especially, *CARMENES*[4]). Such stars must be the least-active, brightest, latest-type M dwarfs[5] with no companions at less than 5 arcsec (a separation at which the flux of any visual or physical companion could affect the radial-velocity measurement of the main target[6]). We used the 0·82-m *IAC80* telescope at the Observatorio del Teide for imaging 103 fields with at least one such M dwarf. The targets were selected from a large list of potential targets because of poor UCAC3[7] optical photometry (at the time of preparing the observations, UCAC4[8] had not yet been published), presence of nearby sources in virtual-observatory images that may prevent accurate spectroscopic follow-up, or even membership in hypothetical common-proper-motion pairs or multiple systems of unknown status. The observations were performed in service mode from mid-2012 to the beginning of 2013.

Owing to a problem in one of the instruments at the *IAC80*, we observed 99 fields with the *Tromsø CCD Photometer* (*TCP*[9]) and four fields only with the *Cámara Mejorada Ligera del Observatorio del Teide* (*CAMELOT*[10]). *TCP* and *CAMELOT* provide fields of view and pixel scales of 9·2 × 9·2 arcmin^2 and 0·537 arcsec/pixel, and 10·37 × 10·37 arcmin^2 and 0·304 arcsec/pixel, respectively (Fig. 1). In both cases, we used the Johnson *R* filter in short (~60 s) and long (~300 s) exposures, which increased our dynamic range in the innermost arcseconds close to the targets. We also tuned the exposure times to *try* to avoid saturation.

Of the 103 fields, 56 had at least one known candidate companion to the M dwarf, either brighter or fainter than our nominal target. The reader must not deduce that the binary frequency of M dwarfs is higher than 50% because our sample was biassed towards stars in binaries and triple systems (multiplicity, either in the form of very close binaries of equal brightness or systems with very bright primaries, tends to affect photometric measurements).

Unfortunately, the images for three systems were not useful because of intense saturation of the primaries. In particular, we also observed but discarded from the analysis: WDS 03575–0110 (BU 543: BD–01 565 AB), WDS 04153–0739 (STF 518: o Eri AB-C), and WDS 20408+1956 (LDS 1045: GJ 797 AB). As a result, our final sample consisted of 53 double or triple systems with at least one M dwarf. Of them, 52 were observed with *TCP* and one (WDS 13484+2337) with *CAMELOT*.

Astrometric analysis

After applying bias and flat-field corrections, we measured angular separations ρ and position angles θ on the best processed images of each pair (in general, the long-duration images for systems with all their components faint, the short-duration images for the rest). Both ρ and θ were measured taking into account the pixel size and the detector orientation of *TCP* and *CAMELOT* (Fig. 1). We used the *imexam* task within the IRAF environment or the *distance* task within the *Aladin* sky atlas[11] for measuring on-CCD separations between stellar photocentroids, depending on the quality of the match of their point-spread functions to a Gaussian profile (the brightest stars had guyot-like PSFs). Uncertainties were calculated by error propagation. The *Aladin* measurement errors were higher than IRAF's due to the uncertainty in the by-eye estimation of the stellar photocentroids (about 0·4 arcsec; *i.e.*, a bit less than one *TCP* pixel), but still acceptable for our purposes.

Table I summarizes our results. Since WDS 02457+4456 was supposed to be triple, we tabulate 54 pairs in 53 systems. We provide their *Washington Double Star Catalogue* (*WDS*[12]) identifications, discoverer codes, recommended names of both primary and secondary (note our restricted use of the letters A, B, C, a, and b), and *IAC80* angular separations, position angles, and observation epochs in Julian years. Measured angular separations range from 5·05 arcsec to 4·65 arcmin. The ρ and θ values tabulated for WDS 07397+3328, marked in parenthesis, must *not* be used for astrometric purposes (see below).

We studied a further nine pairs for which we had controversial information on common proper motion, such as very different catalogued values of proper motion, or of ρ or θ at the first and last epochs as tabulated by *WDS* or with respect to our own measurements. We applied the same virtual-observatory astrometric methodology as by Caballero[13] and the rest of papers in this series. In particular, we used our own astrometry on *SuperCOSMOS* digitizations of digital sky survey POSS-I and II (first and second Palomar Observatory Sky Survey) and *UKST* (*United Kingdom Schmidt Telescope*) photographic plates[14], the astrometry provided by the wide-field and all-sky catalogues 2MASS[15],

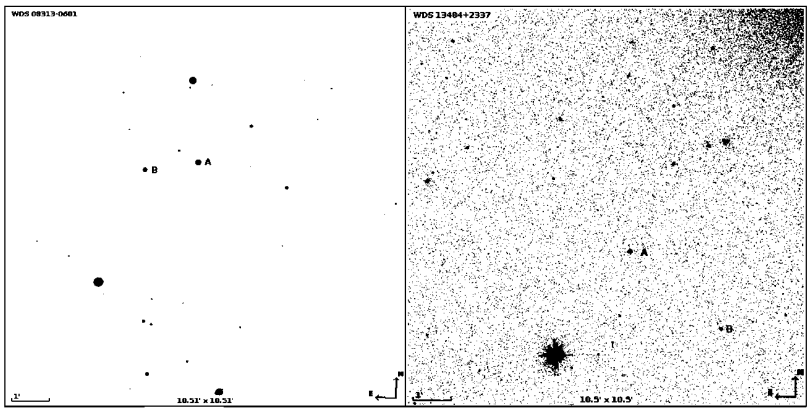

FIG. 1

Representative images taken with *TCP* (*left*, WDS 08313–0601) and *CAMELOT* (*right*, WDS 13484+2337). A and B components are tagged in both images. Exposure times were 60 s each. The 50·85-degree tilt of the *TCP* field of view is obvious.

TABLE I

Astrometry of 54 star pairs investigated with IAC80

WDS	*Disc.*	*Name 1*	*Name 2*	ρ [*arcsec*]	θ [*deg*]	*Epoch*
00137+8038	LDS 1503	G 242-048	LP 012-304	13·41±0·02	125·68±0·02	2012·683
00164+1950	LDS 863	EZ Psc	LP 404-062	25·07±0·03	58·2±0·2	2012·683
00184+4401	GRB 34	GX And	GQ And	34·5±0·4	65·1±0·4	2012·683
01119+0455	GIC 20	LHS 1212	LHS 1213	63·60±0·02	145·69±0·02	2012·703
02361+0653	PLQ 32	HD 16160 AB	BX Cet	164·6±0·4	109·1±0·4	2012·716
02457+4456	LDS 5393	G 078-004	LP 197-048	17·90±0·10	65·9±0·3	2012·716
	GIC 34		G 078-003	89·11±0·10	267·6±0·3	2012·716
02565+5526	LDS 5401	Ross 364	Ross 365	16·9±0·4	20·5±0·4	2012·719
03242+2347	LDS 884	GJ 140 AB	GJ 140 C	99·62±0·10	118·2±0·3	2012·714
03398+3328	ES 327	HD 278874 A	HD 278874 B	15·56±0·40	293·6±0·4	2012·719
03510+1414	JLM 1	PM I03510+1413 A	PM I03510+1413 B	28·74±0·02	319·01±0·02	2012·719
05033+2125	LDS 6160	HD 285190 A	HD 285190 BC	166·30±0·10	240·9±0·3	2012·719
05342+1019	LDS 6189	Ross 45 A	Ross 45 B	5·05±0·02	188·17±0·02	2012·809
05599+5834	GIC 61	EG Cam	G 192-012	161·04±0·10	119·4±0·3	2012·809
06007+6809	LDS 1201	LP 057-041	LP 057-040	56·07±0·02	196·53±0·02	2012·812
06423+0334	GIC 65	G 108-021	G 108-022	49·99±0·02	39·79±0·02	2012·812
07307+4813	GIC 75	GJ 275·2 A	EGGR 52 AB	102·70±0·02	153·67±0·02	2012·812
07319+3613	LDS 6206	VV Lyn AB	BL Lyn	37·57±0·10	352·2±0·3	2012·812
07397+3328	LDS 3755	G 090-016	LP 256-044	(13·66±0·02)	(48·84±0·02)	2012·812
08082+2106	COU 91	BD+21 1764 A	BD+21 1764 Bab	10·6±0·4	144·0±0·4	2012·866
08313-0601	LDS 221	LP 665-021	LP 665-022	84·35±0·02	97·06±0·02	2012·867
08427+0935	LUY 6218	BD+10 1857 AabB	BD+10 1857 C	114·7±0·4	96·2±0·4	2012·927
08526+2820	LDS 6219	ρ Cnc A	ρ Cnc B	85·1±0·4	127·6±0·4	2012·927
09008+0516	OSV 2	Ross 686	Ross 687	29·45±0·02	115·52±0·02	2012·927
09144+5241	STF 1321	HD 79210	HD 79211	17·2±0·4	96·4±0·4	2012·954
09288-0722	GIC 87	Ross 439 A	Ross 439 B	35·59±0·03	83·4±0·2	2012·954
09427+7004	OSV 3	GJ 360	GJ 362	89·0±0·4	76·6±0·4	2012·954
10261+5029	LDS 1241	LP 127-371	LP 127-372	14·37±0·02	25·36±0·02	2012·954
10585-1046	LDS 4041	BD-10 3166	LP 731-076	21·6±0·4	212·7±0·4	2012·957
11055+4332	VBS 18	BD+44 2051A	WX UMa	31·6±0·4	124·5±0·4	2012·957
11080-0509	LDS 852	GJ 1142 A	EGGR 76	278·80±0·02	339·0±0·2	2012·957
12123+5429	VYS 5	BD+55 1519A	BD+55 1519B	14·8±0·4	11·8±0·4	2012·957
12576+3514	LDS 5764	BF CVn	BD+36 2322Bab	16·1±0·4	226·0±0·4	2012·957
13196+3507	HJ 529	BD+35 2436Aab	BD+35 2436B	17·9±0·4	132·2±0·4	2012·957
13484+2337	LDS 4410	GJ 1179 A	EGGR 438	187·49±0·02	229·61±0·02	2013·026
18180+3846	GIC 151	LHS 462	LHS 461	9·97±0·03	277·2±0·2	2012·768
19072+2053	LDS 1017	HD 349726	Ross 731	114·5±0·4	289·9±0·4	2012·755
19147+1918	LDS 1020	Ross 733	Ross 734	40·80±0·02	178·71±0·02	2012·755
19169+0510	LDS 6334	V1428 Aql	V1298 Aql (vB 10)	75·8±0·4	152·1±0·4	2012·755
19464+3201	KAM 3	BD+31 3767A	BD+31 3767B	5·5±0·4	134·7±0·4	2012·755
19510+1025	J 124	o Aql A	o Aql B	21·3±0·4	218·2±0·4	2012·755
19539+4425	GIC 159	V1581 Cyg AB	GJ 1245 C	6·45±0·02	70·42±0·02	2012·755
19566+5910	GIC 161	BD+58 2015A	BD+58 2015B	72·89±0·10	253·2±0·3	2012·757
20446+0854	LDS 1046	LP 576-040	LP 576-039 'AB'	15·08±0·03	344·1±0·2	2012·757
20555-1400	LDS 6418	GJ 810 A	GJ 810 B	107·19±0·02	184·61±0·02	2012·757
20568-0449	LDS 6420	FR Aqr	EGGR 202 (vB 11)	14·94±0·03	309·8±0·2	2012·757
21011+3315	LDS 1049	LP 340-547	LP 340-548	56·86±0·10	94·4±0·3	2012·741
21148+3803	AGC 13 AF	τ Cyg AB	τ Cyg Cab	89·5±0·4	184·2±0·4	2012·741
21161+2951	LDS 1053	Ross 776	Ross 826	26·02±0·02	258·84±0·02	2012·741
21440+1705	LDS 6358	G 126-031	G 126-030	64·09±0·02	346·01±0·02	2012·749
22058+6539	NI 44	G 264-018 A	G 264-018 B	6·66±0·03	136·5±0·2	2012·749
22173-0847	LDS 782	FG Aqr A	Wolf 1561 BC	7·98±0·02	214·40±0·02	2012·757
23294+4128	GIC 193	G 190-028	G 190-027 AB	17·65±0·02	213·70±0·02	2012·757
23573-1259	LDS 830	LP 704-015	LP 704-014 AB	19·69±0·02	294·44±0·02	2012·757

CMC14[16], GSC 1·3 and 2·2[17], SDSS-DR9[18], and *WISE*[19], and our observations with *IAC80*. The epochs of observation, ρ and θ values, and origin of every measurement (76 in total, most of which are new) are provided in Table II.

TABLE II

Virtual-observatory astrometric follow-up of nine pairs

WDS	*Epoch*	*ρ* [*arcsec*]	*θ* [*deg*]	*Origin*
02457+4456	1951·971	80·74	269·50	POSS-I Red
	1983·021	84·79	268·66	GSC 1·3
	1989·748	86·15	268·54	POSS-II Red
	1998·868	87·14	268·27	2MASS
	2003·084	87·74	268·03	SDSS-DR9
	2004·010	86·57	268·20	POSS-II Blue
	2004·067	87·74	268·12	CMC14
	2005·535	86·69	268·26	POSS-II InfraRed
	2010·096	88·71	267·95	*WISE*
	2012·716	89·11	267·60	This work [*TCP*]
	Average	…	…	
03398+3328	1955·807	15·20	293·47	POSS-I Red
	1988·716	15·75	293·87	POSS-II Red
	1989·669	15·91	295·82	POSS-II Blue
	1990·882	15·14	293·58	POSS-II InfraRed
	1998·758	15·43	294·46	2MASS
	2010·118	15·41	294·28	*WISE*
	2012·719	15·56	293·57	This work [*TCP*]
	Average	15·48±0·28	294·15±0·83	This work
07397+3328	1955·117	13·03	56·30	POSS-I Red
	1990·079	12·67	59·11	POSS-II Red
	1998·170	12·78	57·42	2MASS
	1998·988	12·64	56·49	POSS-II InfraRed
	2007·139	13·07	58·88	SDSS-DR9
	2012·812	(13·66)	(48·84)	This work [*TCP*]
	Average	12·84±0·20	57·6±1·3	This work
09288−0722	1953·929	36·04	84·54	POSS-I Red
	1984·177	35·79	83·76	GSC 2·2
	1986·000	35·78	83·68	UKST InfraRed
	1991·268	35·51	83·44	UKST Red
	1999·046	35·83	83·96	2MASS
	1999·771	35·60	83·94	UKST Blue
	2004·067	35·69	83·62	CMC14
	2010·355	35·62	83·59	*WISE*
	2012·957	35·59	83·35	This work [*TCP*]
	Average	35·73±0·17	83·8±0·3	This work
10585−1046	1954·246	18·01	219·67	POSS-I Red
	1986·285	19·66	216·15	GSC 1·3
	1992·037	20·44	215·43	UKST Red
	1995·218	20·63	215·16	UKST InfraRed
	1993·124	20·75	214·47	2MASS
	2004·059	20·99	213·87	CMC14
	2010·423	21·46	213·67	*WISE*
	2012·957	21·61	212·74	This work [*TCP*]
	Average	…	…	
12123+5429	1955·284	14·32	9·92	POSS-I Red
	1984·163	14·40	8·94	GSC 1·3
	1991·347	14·57	10·00	POSS-II Red
	1995·309	14·19	8·05	POSS-II Blue
	1998·167	14·61	10·47	POSS-II InfraRed
	1999·339	14·66	9·50	2MASS
	2001·962	14·62	9·58	SDSS-DR9
	2010·371	14·63	9·69	*WISE*
	2012·957	14·81	11·79	This work [*TCP*]
	Average	14·53±0·19	9·77±1·03	This work

TABLE II (*concluded*)

WDS	*Epoch*	ρ [*arcsec*]	θ [*deg*]	*Origin*
20446+0854	1953·751	14·90	343·92	POSS-I Red
	1984·511	14·78	343·21	GSC 1·3
	1987·492	14·88	345·04	POSS-II Red
	1990·624	14·91	343·79	POSS-II Blue
	1994·441	15·00	345·16	POSS-II InfraRed
	2000·349	15·13	344·06	2MASS
	2000·738	15·07	344·02	SDSS-DR9
	2002·364	15·10	344·21	CMC14
	2010·337	15·00	344·51	*WISE*
	2012·784	15·08	344·11	This work [*TCP*]
	Average	14·98±0·11	344·21±0·58	This work
22058+6539	1954·594	6·97	135·55	POSS-I Red
	1991·697	6·48	134·43	POSS-II Red
	1993·554	6·59	133·88	POSS-II Blue
	1994·586	~6·7	~135	POSS-II InfraRed
	1999·744	6·76	135·70	2MASS
	2010·025	6·65	137·11	*WISE*
	2012·749	6·66	136·51	This work [*TCP*]
	Average	6·69±0·17	135·53±1·22	This work
23294+4128	1952·631	17·69	211·02	POSS-I Red
	1984·645	17·52	211·09	GSC 1·3
	1987·793	17·69	214·98	POSS-II Blue
	1989·751	17·60	213·59	POSS-II Red
	1995·624	17·72	213·97	POSS-II InfraRed
	1999·755	17·67	213·89	2MASS
	2002·597	17·68	213·84	CMC14
	2010·497	17·65	213·96	*WISE*
	2012·757	17·65	213·70	This work [*TCP*]
	Average	17·65±0·06	213·7±1·1	This work

Two of our pairs, shown in italics in Table I, turned out to be optical systems (*i.e.*, not physical binaries). As a result, we do not compute average ρ and θ values for them in Table II. One of the visual binaries is WDS 02457+4456 AB (GIC 34), which is formed by the red dwarfs G 78–4 (M0·5 V) and G 78–3 (M5·0 V). In spite of being 4·5 subtypes cooler, the hypothetical secondary is only about $0^m{\cdot}5$ fainter than the primary. Neither unresolved high-order multiplicity, metallicity, nor inflation[20], could explain such an overbrightness. Furthermore, in his Masters thesis, Dorda[21] had already reported a significant difference in proper motion between the two stars (from *Hipparcos*[22] and PPMXL[23]). Our astrometric follow-up showed a clear linear variation of both ρ and θ between 1951 December and 2012 September, with an amplitude of 8·4 arcsec in angular separation. Indeed, their proper motions, measured by us, were found to be quite different (G 78–4: +411·8±4·5, −124·6±1·2 mas yr^{-1}; G 78–3: +276·4±3·6, −167·8±2·7 mas yr^{-1}). The simplest explanation for these observables is that G 78–3 is in the foreground at an estimated distance of 13·6±1·1 pc, while G 78–4 is located further at 23·1±1·2 pc. However, the latter forms the true common-proper-motion pair WDS 02457+4456 AC (LDS 5393) together with the ultracool dwarf LP 197–48 (see below). To sum up, WDS 02457+4456 is not a triple system, but only a double one. However, and quite interestingly, G 78–4 and G 78–3 are, with angular separation only about 1·5 arcmin, the closest unrelated M dwarfs in the *CARMENES* input catalogue[6].

The other visual binary is WDS 10585–1046 (LDS 4041), which is formed by BD−10 3166, a super-metal-rich K0 V star at 64–80 pc that hosts an exoplanet candidate[24,25,26], and LP 731–076, an M4 V star at about only 11 pc[25,27]. In

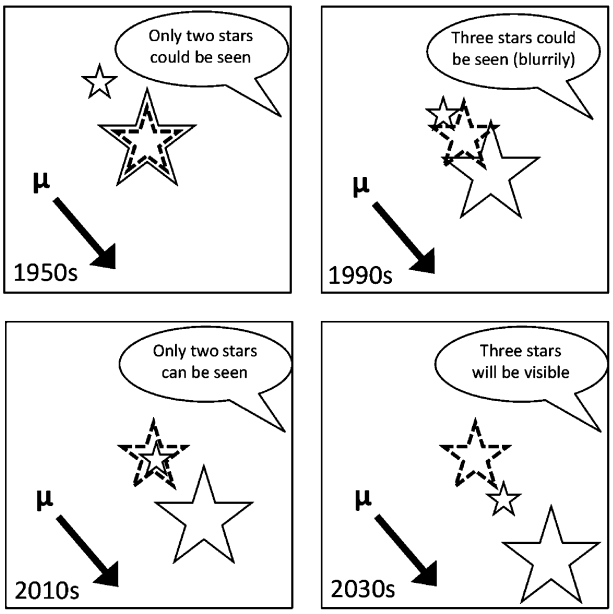

FIG. 2

Sketch explaining the apparent "triple" system WDS 07397+3328, formed by a physical binary of bright and faint stars (solid lines) moving to the southwest and a (fixed) background star of intermediate brightness (dashed lines). In the 1950s the bright primary overpowered the background star, while in the 2010s it is the background star that overpowers the faint secondary.

this case, our astrometric study showed deviations of 3·6 arcsec in ρ and 6·9 deg in θ in almost six decades, with different proper motions (especially in declination: BD–10 3166: –181·1±3.0, –5·2±1·8 mas yr^{-1}; LP 731–076: –187·7±3·9, –77·2±0·9 mas yr^{-1}).

The case of the system WDS 07397+3328 (LDS 3755) is so pure chance that it deserves a comic strip (Fig. 2). The primary is G 090–016 (M2·0 V), which at the POSS-I epoch (1955 February) was aligned with a background star, and the secondary is LP 256–44, which *today* is now aligned with the same background star. We had to take special care to disentangle the secondary from the interloper, of intermediate brightness between the primary and the secondary, in the photographic plates obtained in the 1990s. Actually, our *IAC80* astrometric measurement is strongly affected by the background star (ρ and θ values in Tables I and II — in parenthesis — correspond instead to the angular separation and position angle of the background star with respect to the primary). Probably because of this unfortunate alignment, it has never been possible to take a spectrum of the secondary.

WDS tabulates an angular separation of 38·0 arcsec for the first astrometric epoch of WDS 09288–0722 (GIC 87), in 1964. This value contrasted with the most recent measures, by 2MASS and by ourselves, which lie at about 35·7 arcsec. From Table II, the constancy of the ten astrometric epochs between 1953 December and 2012 December led us to conclude that Ross 439 A and

TABLE III

Catalogued and measured proper motions of physical pairs VYS 5 and GIC 193

WDS	*A*		*B*		*Ref.*
	$\mu_\alpha cos\delta$ [*mas yr*$^{-1}$]	μ_δ [*mas yr*$^{-1}$]	$\mu_\alpha cos\delta$ [*mas yr*$^{-1}$]	μ_δ [*mas yr*$^{-1}$]	
12123+5429	+250	+100	+250	+100	Giclas[29]
(VYS 5)	+232	+90	...	...	USNO-B1[31]
	+233	+91	+182	+37	LSPM[30]
	+231·5±1·3	+89·9±1·3	...	...	HIP[22]
	+245·3±3·9	+85·9±2·1	+245·6±4·2	+92·0±2·1	This work
23294+4128	+460	−50	+460	−50	Giclas[29]
(GIC 193)	...	...	+220	−82	USNO-B1[31]
	...	...	+224·8	−83·5	PPMXL[23]
	+415	−41	+415	−41	LSPM[30]
	+412·8±3·3	−53·5±5·1	+400·0±4·2	−45·3±2·4	This work

B do form a common-proper-motion pair separated by 35·73±0·16 arcsec (the Giclas' measure in 1964[28] is only listed in the *WDS* as being to the nearest degree and nearest arcsecond, so it is just an estimated value).

Two more pairs have components with discordant tabulated proper motions for primaries and secondaries. In one, WDS 12123+5429 (VYS 5) is a pair of two bright early-type red dwarfs: BD +55 1519A (M0·0 V) and BD +55 1519B (M3·0 V). In the other, WDS 23294+4128 (GIC 193) is composed of G 190–28 (M3·5 V) and G 190–27 AB (M4·0 V+m5: V). As shown in Table III, some tabulated proper motions were incorrect (LSPM's for VYS 5, USNO-B1 and PPMXL's for GIC 193), while the two pairs actually move together through space.

The remaining dubious pairs for which we confirmed the constancy of their angular separations and position angles and, therefore, their common proper motions with an astrometric study were WDS 03398+3328, WDS 20446+0854, and WDS 22058+6539. They will be discussed next.

Results

For the 52 physical pairs (after discarding WDS 02457+4456 AB and WDS 10585–1046 in the previous section), we list their basic astrophysical parameters in Table IV. In particular, we provide:

(*i*) *Spectral types of primaries and secondaries*. When available, they were taken from the most reliable sources, which were the *Palomar/Michigan State University Catalogue* (*PMSU*)[32] and the preliminary results of the *CARMENES* science preparation[33–36]. Only in five cases were primaries earlier than K7 (*i.e.*, from F0 to K3), for which we took spectral types from the *Simbad* database[37–41]. There were also four systems containing white dwarfs, which are described below. Spectral typing was not available for four wide faint secondaries: LP 197–48 (WDS 02457+4456 B), PM I03510+1413 B (WDS 03510+1414 B), LP 256–44 (WDS 07397+3328 B), and G 264–18 B (WDS 22058+6539 B). For these, we estimated spectral types in the intervals m5: V to m7: V based on magnitude differences with respect to the primaries and a J-band absolute magnitude–spectral-type relationship for M dwarfs[42] (we write 'm' instead of 'M' for spectral types derived from photometry). Of these, only PM I03510+1413 B had another photometric spectral-type estimation (m5 V[43], identical to ours). As described below, we also estimated photometric spectral types of 13 M dwarfs

TABLE IV

Basic astrophysical data of 52 physical pairs

WDS	*Sp. Type 1*	*Sp. Type 2*	*d* [*pc*]	*s* [*AU*]	M_1 [$M_\odot$]	M_2 [$M_\odot$]	$P^\star$ [10^3 *yr*]	$-U^\star_g$ [10^{33} *J*]
00137+8038	M1·5V	M5·0V	19·6 ± 0·7	263 ± 9	0·46 ± 0·05	0·18 ± 0·04	3·2 ± 0·2	560 ± 140
00164+1950	M4·0V	M4·0V	16 ± 4	410 ± 90	0·25 ± 0·03	0·25 ± 0·03	4·1 ± 1·3	270 ± 70
00184+4401	M1·0V	M3·5V	3·587 ± 0·010	123·8 ± 1·5	0·50 ± 0·04	0·27 ± 0·05	0·82 ± 0·04	1900 ± 400
01119+0455	M3·0V	M3·5V	15·9 ± 0·5	1010 ± 30	0·32 ± 0·05	0·27 ± 0·05	16·7 ± 1·3	150 ± 40
02361+0653	K3V+M7·0V	M4·0V	7·18 ± 0·02	1182 ± 4	0·85 ± 0·03	0·25 ± 0·03	26·3 ± 0·6	320 ± 40
02457+4456	M0·5V	m6:V	23·1 ± 1·2	410 ± 20	0·52 ± 0·02	~0·13 ± 0·03	~7·5 ± 0·6	~290 ± 70
02565+5526	M1·0V	M3·0V	19·5 ± 1·8	330 ± 30	0·50 ± 0·04	0·32 ± 0·05	3·1 ± 0·5	860 ± 170
03242+2347	M0·0V+m1:V	M2·0V	19·5 ± 1·0	1940 ± 100	1·04 ± 0·06	0·41 ± 0·05	43 ± 4	390 ± 60
03398+3328	K5V	M3·0V	43 ± 3	670 ± 50	1·30 ± 0·10	0·32 ± 0·05	9·9 ± 1·2	1100 ± 200
03510+1414	M4·5V	m5:V	(14·4 ± 1·0)	410 ± 30	0·22 ± 0·04	~0·18 ± 0·04	~5·4 ± 0·7	~170 ± 50
05033+2125	M1·5V	M5·0V+m6:V	27 ± 6	4600 ± 1000	0·46 ± 0·05	~0·31 ± 0·07	~160 ± 60	~55 ± 19
05342+1019	M3·0V	M4·5V	(17·5 ± 0·7)	89 ± 3	0·32 ± 0·05	0·22 ± 0·04	0·52 ± 0·04	1400 ± 300
05599+5834	M0·5V	M4·0V	13·5 ± 0·3	2180 ± 50	0·52 ± 0·02	0·25 ± 0·03	64 ± 3	105 ± 13
06007+6809	M3·5V	M4·0V	20·1 ± 0·7	1130 ± 40	0·27 ± 0·05	0·25 ± 0·03	19·6 ± 1·5	110 ± 20
06423+0334	M3·5V	M4·0V	12·8 ± 0·5	640 ± 20	0·27 ± 0·05	0·25 ± 0·03	8·4 ± 0·6	190 ± 40
07307+4813	M4·0V	DA10+da10	11·10 ± 0·10	1140 ± 10	0·25 ± 0·03	~0·90 ± 0·04	~24·9 ± 0·6	~450 ± 40
07319+3613	M2·5V+m5:V	M3·5V	11·9 ± 0·5	446 ± 18	~0·55 ± 0·09	0·27 ± 0·05	~5·7 ± 0·5	~590 ± 150
07397+3328	M2·0V	m6:V	36 ± 4	490 ± 50	0·41 ± 0·05	~0·13 ± 0·03	~9·7 ± 1·7	~190 ± 50
08082+2106	K7V	M3·0V+m3:V	16·6 ± 0·5	176 ± 9	0·60 ± 0·10	~0·64 ± 0·10	~0·70 ± 0·07	~3900 ± 900
08313–0601	M1·5V	M3·0V	26·4 ± 1·9	2220 ± 160	0·46 ± 0·05	0·32 ± 0·05	54 ± 6	120 ± 20
08427+0935	K7V+k7:V+M0·0V	M2·5V	15·4 ± 0·6	1770 ± 60	1·74 ± 0·22	0·37 ± 0·05	38 ± 3	640 ± 120
08526+2820	G8V	M4·5V	12·34 ± 0·11	1051 ± 11	0·90 ± 0·10	0·22 ± 0·04	23·2 ± 1·2	330 ± 70
09008+0516	M3·0V	M3·5V	21 ± 3	620 ± 100	0·32 ± 0·05	0·27 ± 0·05	8 ± 2	250 ± 70
09144+5241	M0·0V	M0·0V	5·8 ± 0·2	100 ± 4	0·54 ± 0·02	0·54 ± 0·02	0·34 ± 0·02	5200 ± 400
09288–0722	M2·5V	M4·5V	16·2 ± 1·0	580 ± 40	0·37 ± 0·05	0·22 ± 0·04	9·0 ± 1·0	250 ± 60
09427+7004	M2·0V	M3·0V	12·3 ± 0·3	1090 ± 20	0·41 ± 0·05	0·32 ± 0·05	17·8 ± 1·0	210 ± 40
10261+5029	M4·0V	M4·0V	(16·6 ± 1·0)	239 ± 14	0·25 ± 0·03	0·25 ± 0·03	1·85 ± 0·18	460 ± 80
11055+4332	M1·0V	M5·0V	4·85 ± 0·02	154 ± 2	0·50 ± 0·04	0·18 ± 0·04	1·45 ± 0·07	1000 ± 200
11080–0509	M3·0V	DA3·1	17 ± 4	4800 ± 1000	0·32 ± 0·05	0·56 ± 0·03	180 ± 60	66 ± 18
12123+5429	M0·0V	M3·0V	15·5 ± 0·3	230 ± 8	0·54 ± 0·02	0·32 ± 0·05	1·87 ± 0·11	1300 ± 200
12576+3514	M1·5V	M4·0V+m4:V	19·3 ± 1·1	310 ± 19	0·46 ± 0·05	~0·50 ± 0·04	~1·84 ± 0·18	~1300 ± 200
13196+3507	M0·5V+m0·5:V	M3·0V	13·3 ± 0·3	237 ± 7	~1·04 ± 0·04	0·32 ± 0·05	~2·10 ± 0·11	~2500 ± 400
13484+2337	M5·5V	DA10	12·1 ± 0·3	2270 ± 60	0·16 ± 0·03	0·45 ± 0·02	88 ± 4	58 ± 11

TABLE IV (*concluded*)

WDS	Sp. Type 1	Sp. Type 2	d [pc]	s [AU]	M_1 [$M_\odot$]	M_2 [$M_\odot$]	P^* [10^3 yr]	$-U^*_g$ [10^{33} J]
18180+3846	M3·0V	M4·0V	10·7 ± 0·4	107 ± 4	0·32 ± 0·05	0·25 ± 0·03	0·61 ± 0·05	1300 ± 300
19072+2053	M2·0V	M2·0V	8·51 ± 0·16	974 ± 19	0·41 ± 0·05	0·41 ± 0·05	11·9 ± 0·6	300 ± 50
19147+1918	M3·5V	M3·5V	19·1 ± 1·1	780 ± 40	0·27 ± 0·05	0·27 ± 0·05	10·4 ± 1·1	170 ± 40
19169+0510	M2·5V	M8·0V	5·87 ± 0·03	445 ± 3	0·37 ± 0·05	0·10 ± 0·01	9·6 ± 0·5	150 ± 20
19464+3201	M0·5V	M2·0V	13·6 ± 0·3	75 ± 6	0·52 ± 0·02	0·41 ± 0·05	0·28 ± 0·03	5000 ± 700
19510+1025	F8V	M3·5V	19·19 ± 0·11	408 ± 8	1·32 ± 0·15	0·27 ± 0·05	5·0 ± 0·3	1500 ± 300
19539+4425	M5·5V+m7:V	M5·5V	4·56 ± 0·03	29·4 ± 0·2	~0·27 ± 0·04	0·16 ± 0·03	~0·121 ± 0·007	~2600 ± 600
19566+5910	K7V	M3·5V	31·7 ± 1·8	2310 ± 130	0·60 ± 0·10	0·27 ± 0·05	68 ± 7	120 ± 30
20446+0854	M1·5V	M3·5V+m3·5:V	(21·8 ± 0·4)	330 ± 6	0·46 ± 0·05	0·54 ± 0·10	1·86 ± 0·12	1300 ± 300
20555-1400	M4·0V	M5·0V	13 ± 3	1400 ± 300	0·25 ± 0·03	0·18 ± 0·04	37 ± 13	56 ± 19
20568-0449	M4·0V	DC10	17·7 ± 1·2	264 ± 18	0·25 ± 0·03	0·37 ± 0·06	2·5 ± 0·3	620 ± 130
21011+3315	M3·0V	M3·5V	(16·6 ± 0·7)	940 ± 40	0·32 ± 0·05	0·27 ± 0·05	15·0 ± 1·3	160 ± 40
21148+3803	FoIV+G1V	M2·5V+m4:V	20·34 ± 0·16	1820 ± 16	2·5 ± 0·2	~0·62 ± 0·06	~31·5 ± 1·4	~1500 ± 200
21161+2951	M3·5V	m4·5:V	(13·9 ± 0·7)	362 ± 18	0·27 ± 0·05	0·22 ± 0·04	4·0 ± 0·4	290 ± 80
21440+1705	M4·0V	M4·5V	15·3 ± 0·6	980 ± 40	0·25 ± 0·03	0·22 ± 0·04	17·4 ± 1·4	100 ± 20
22058+6539	M3·5V	m6:V	(13·7 ± 0·7)	92 ± 4	0·27 ± 0·05	~0·13 ± 0·03	~0·77 ± 0·08	~700 ± 300
22173-0847	M4·0V	M5·0V+m7:V	10·0 ± 0·3	80 ± 2	0·25 ± 0·03	~0·29 ± 0·05	~0·31 ± 0·02	~1600 ± 300
23294+4128	M3·5V	M4·0V+m5:V	14·9 ± 0·5	263 ± 9	0·27 ± 0·05	0·43 ± 0·07	1·22 ± 0·10	780 ± 190
23573-1259	M3·0V	M4·0V+m5:V	(18·1 ± 0·7)	357 ± 15	0·32 ± 0·05	~0·43 ± 0·07	~2·17 ± 0·18	~680 ± 160

in very close pairs (not resolved in our images) from published magnitude differences and improved previous determinations of two resolved secondaries based on available data. Except for a few cases (*e.g.*, τ Cyg Ca and Cb), all our spectral-type estimations are new.

(*ii*) *Heliocentric distances, d.* For 45 cases, the distances to the primaries were parallactic and compiled from the literature[22,44–46]. For the other seven cases, tabulated in parenthesis, we calculated spectro-photometric distances from a custom-made quadratic M_J–spectral-type relation. For deriving it, we compiled a ~1000-star sample of M dwarfs with J-band apparent magnitudes and parallactic distances, to be used for another programme (Cortés-Contreras, in prep.). As shown in Table V, calculated values reasonably match, and perhaps improve, previous spectro-photometric distance estimations[32,43]. All systems except six are located at less than 20 pc; seven systems are located at less than 10 pc.

TABLE V

Spectrophotometric distances comparison

WDS	*d* [*pc*] (*Other authors*)		*d* [*pc*] (*This work*)	
	A	*B*	*A*	*B*
03510+1414	16·3[43]	14·1[43]	14·4 ± 1·0	...
05342+1019	10·9 ± 3·3[32]	28·0 ± 8·4[32]	17·5 ± 0·7	12·9 ± 0·7
10261+5029	18·0 ± 5·4[32]	19·2 ± 5·8[32]	16·6 ± 1·0	17·7 ± 1·0
20446+0854	17·9 ± 5·4[32]	12·0 ± 3·6[32]	21·8 ± 0·4	15·0 ± 0·7 (single) 21·2 ± 1·0 (double)
21011+3315	15·8 ± 4·7[32]	19·4 ± 5·8[32]	16·6 ± 0·7	17·4 ± 0·8
21161+2951	12·6 ± 3·8[32]	18·6 ± 5·4[32]	13·9 ± 0·7	13·5 ± 0·9
22058+6539	24·0 ± 7·2[32]	...	13·7 ± 0·7	...
23573−1259	20·0 ± 5·8[32]	12·9 ± 3·9[32]	18·1 ± 0·7	15·6 ± 0·9 (single) 22·0 ± 1·3 (double)

(*iii*) *Projected physical separations, s.* They are just the product $s = \rho d$, ρ being the angular separation listed in Table I (in epoch interval 2012·6–2013·1).

(*iv*) *Individual masses for both primary and secondary, M_1 and M_2.* Masses of M dwarfs were calculated with a spectral-type–mass relationship used internally by the *CARMENES* Consortium[4] and checked with previous estimations, when available[47]. Masses of primaries with earlier spectral types and of white dwarfs were obtained from the literature[41,48–51].

(*v*) *Reduced orbital periods, $P^\star$.* They were computed from the relationship $(M_1 + M_2)\ P^2 = a_2{}^3$ (in convenient units), where $a = a_1 + a_2$, $M_1 a_1 = M_2 a_2$ and the semi-major axis a was replaced by the projected physical separation s. Calculated reduced periods range from slightly over one century to several millennia. Reduced periods match actual ones to within a factor of three, depending on actual eccentricity[52].

(*vi*) *Reduced binding energies*[13], $-U_g{}^\star$. We used $U_g{}^\star = -GM_1M_2s^{-1}$, where again the actual physical separation r, which can be approximated by a at low eccentricities, was replaced by s. In the case of wide multiple systems with very long orbital periods, of over one thousand years, for which it is very hard (if not impossible) to determine orbits and semi-major axes, $-U_g{}^\star$ allows easy comparison of binding energies of systems published by different authors[53,54].

M dwarf–white dwarf binaries

Four of our pairs contain degenerate remants: WDS 07307+4813 (with EGGR 52 AB; $5{\cdot}9^{+2{\cdot}7}_{-1{\cdot}4}$ Gyr[50]), WDS 11080–0509 (with EGGR 76; $3{\cdot}9^{+1{\cdot}4}_{-1{\cdot}3}$ Gyr[50]), WDS 13484+2337 (with EGGR 438; 4·72 Gyr[51]) and WDS 20568–0449 (with

EGGR 202; 4·27 Gyr[51]). Interestingly, the system including EGGR 52 AB may be triple (see below). Although the white dwarfs are listed in Table I (and in *WDS*) as secondaries because they are fainter in the optical and near-infrared than the M dwarfs, they are more massive[41,50,51,55,56]. Furthermore, masses of the main-sequence stars that evolved into the white dwarfs were in all cases above one solar mass.

Actual ages of the four systems are longer than the cooling times of the remnants, which lie in the narrow interval between 3·9 and 5·9 Gyr[50,51]; once the stellar progenitor's main-sequence lifetime is added, actual system ages are considerably older (> 6–7 Gyr).

Given the relatively large projected physical separations of the four pairs, from 260 to 4800 AU, we can assume that the components have evolved as single stars (but see Morgan *et al.*[57]) and that there may exist a dynamical evolution associated with the remnant progenitor evolution (*i.e.*, an increase of the physical separation when the star quits the main sequence and loses mass).

Hierarchical triple and quadruple systems

As shown in Table VI, there are 16 stars in 14 systems that are close binaries unresolved in our *IAC80* images. Three of them are double-lined spectroscopic binaries: WDS 08082+2106 Ba,Bb (BD +21 1764 Ba,Bb[58]), WDS 08427+0935 Aa,Ab (BD +10 1857 Aa,Ab[59]), and WDS 23573–1259 Ba,Bb (LP 704–014 AB[60]). The other 13 stars have been resolved with high-resolution imagers (*i.e.*, *Hubble Space Telescope*, adaptive optics, lucky imaging, speckle). Fig. 3 illustrates the following discussion.

The WDS 21148+3803 system, composed of τ Cyg AB and τ Cyg Cab, is one of the only three quadruples in our sample. It was thought to be a quintuple because of a low-metallicity, low-mass, esdK-type star companion candidate at about 534 arcsec to the primary and out of the *IAC80* field of view, namely LSR J2115+3804 (LEP 100 I[61]). A simple astrometric analysis discards it as a physical quintuple system because of the different proper motions (Cortés-Contreras, in

TABLE VI

Unresolved binaries in hierarchical triple (and quadruple) systems

WDS	*Disc.*	*Binary*	ρ_{close} [*arcsec*]	ρ_{wide}/ρ_{close}	$\Delta mag\,(band)$ [*mag*]
02361+0653	GKI 1	HD 16160 AB	3·394[66]	62·6–48·5	10·84(*V*)[66]
			2·63[67]		5·29(K_s)[67]
03242+2347	WOR 4	GJ 140 AB	2·247[22]	44·4	1·27(*Hp*)[68]
05033+2125	LAW 13	HD 285190 BC	0·310[69]	536	1·3(i')[69]
					0·8(z')[69]
07307+4813	WNO 49	EGGR 52 AB	0·656[70]	184	0·0(*V*)[70]
07319+3613	BEU 11	VV Lyn	0·684[71]	54·9	2·02(*K*)[71]
08082+2106	...	BD+21 1764 Bab[58]	<0·66[58]	>16	...
08427+0935	ST 8	BD+10 1857 AabB	1·236[72]	92·8	3·9(800 nm)[72]
	...	BD+10 1857 Aa,Ab[59]	...	...	...
12576+3514	...	BD+36 2322 Bab	...	...	0·061(Ks)[63]
13196+3507	BAG 11	BD+35 2436 Aab	0·065[73]	275	0·0: (600 nm)[73]
19539+4425	MCY 3	V1581 Cyg AB	0·594[74]	10·9	1·29(F180M)[74]
					1·18(F207M)[74]
					1·08(F222M)[74]
20446+0854	...	LP 576–039 'AB'	...	...	...
21148+3803	AGC 13 AB	τ Cyg AB	0·637[22]	140	2·89(*Hp*)[68]
	JOD 20	τ Cyg Cab	0·40[75]	224	1·55(*I*)[75]
22173-0847	BEU 22	Wolf 1561 AB	0·978[71]	8·16	3·15(z')[76]
					1·18(*K*)[71]
23294+4128	...	G 190–027 AB	...	...	0·27(*H*)[63]
23573–1259	...	LP 704-014 AB[60]	...	...	...

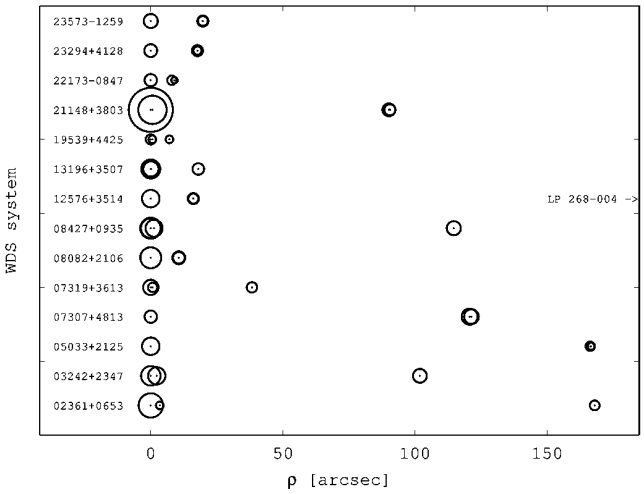

FIG. 3

Architecture of triple and quadruple star systems in our sample. Sizes of circles are approximately proportional to star mass. Primaries are located at $\rho = 0$ arcsec. The quaternary of WDS 12576+3514 (LP 268–4) is out of the diagram at $\rho = 760{\cdot}2$ arcsec.

prep.). Besides, Daley's companion candidate to τ Cyg AB, DAL 38 G[62], is also a background star according to PPMXL data.

The quadruple system WDS 08427+0935 is composed of a 21-d spectroscopic binary[59] which is the brightest component of a 62-yr astrometric double, which in turn has a wide, proper-motion, M-dwarf companion of lower mass imaged with *TCP*. As a result, this system has an interesting architecture of consecutive 'pairs' of stars separated by ~0·16, 18·9, and 1770 AU. Perhaps not by chance, both the WDS 21148+3803 and WDS 08427+0935 quadruples are, with over 2 $M_{\odot}$, the most massive of our systems.

The other quadruple system in our sample, of slightly over 1 $M_{\odot}$, is WDS 12576+3514. It consists of the variable star BF CVn (M1·5 V), a double companion at about 4 arcmin (M4·0 V+m4: V, for which ΔKs has only been provided[63]), and a wide proper-motion companion of only about 0·08 $M_{\odot}$ located at 12·7 arcmin (approximately 14 700 AU) to the primary and outside the *TCP* field of view, namely LP 268–4 (LEP 60[64,65]).

As previously noticed, since our initial sample of 106 observing fields was biassed towards multiple systems, it would be incorrect to derive here a frequency of binaries. However, we can get some reliable statistics on the minimum frequency of higher-order multiples since there was no *a-priori* bias towards them in our sample. There are at least 11 triples and three quadruples among our list of 52 physical systems studied (there can be still unknown close binaries or very wide proper-motion companions awaiting discovery), which results in minimum frequencies of triples and quadruples among multiple systems with M dwarf components of $21^{-8\%}_{+11\%}$ and $6^{-4\%}_{+5\%}$ (*i.e.*, roughly one out of five 'binaries' is actually a triple, and roughly one out of 17 'binaries' is actually a quadruple). The non-detection of quintuples (or higher order) points to a frequency of them among multiple systems with M-dwarf components of less than 1·9%. For comparison, see Tokovinin[48] for frequency and statistics of triple

and quadruple systems among multiple systems at all stellar masses.

From the variety of system architectures in Table VI and Fig. 3, we do not see any relation between ρ_{wide}/ρ_{close} ratios (from about eight to over 500) and mass ratios, probably because of the small sample size if compared with previous comprehensive, dedicated works[48]. However, although tertiary companions tend to have masses comparable to the components of the inner binary, we find that the fraction of triple systems where the outer companion has the smallest mass is significantly larger than previously measured (about two thirds, in comparison with 46% measured by Tokovinin[48]). Besides, systems with large ρ_{wide}/ρ_{close} ratios are expected to be in stable configurations; however, the compact systems with low ρ_{wide}/ρ_{close} ratios, such as WDS 19539+4425 (GIC 159 + MCY 3) and WDS 22173–0847 (LDS 182 + BEU 22), may deserve further study of long-term dynamical stability, spin alignment, or possible orbital evolution. These studies may be also extended to the hierarchical quadruple system WDS 08427+0935 (LUY 6218 + ST 8).

The most fragile systems

We have identified five systems with reduced binding energies $-U_g^\star$ equal to or below 10^{35} J. Two of them are the M-dwarf–white-dwarf pairs WDS 11080–0509 and WDS 13484+2337, whose actual binding energies depend closely on a better estimation of the white-dwarf masses. The other three fragile systems are composed of M dwarfs only: WDS 05033+2125 (which is actually a triple system), WDS 20555–1400, and WDS 21440+1705. The five of them have parallactic distance measurements and projected physical separations between 1000 and 4600 AU, approximately; there are other systems in our sample with similar projected physical separations but larger binding energies because of their larger (product of) mass. WDS 21440+1705 could be even more fragile than tabulated if the secondary were later than M4·5 V (see below). According to the Weinberg *et al.*[77] relationships, and with the parameters given by Close *et al.*[53] and Dhital *et al.*[54], the five systems can survive in the Galactic disc for amounts of time comparable to the age of the Universe.

Binaries with periods shorter than one millenium

We looked for extra publicly-available data on the pairs with the shortest orbital periods. Our typical astrometry baseline coverage was of 60 yr (*e.g.*, since the USNO-A2 epoch of the first Palomar Observatory Sky Survey in the early 1950s to our recent epoch of *IAC80* data). In some cases, when the *Astrographic Catalogue* AC2000·2[78] or very old *WDS* data were available, coverage was longer than one century. Within that time span, some systems, especially those with the shortest periods, displayed appreciable variations of position angle. In Table VII we list ten systems with the shortest reduced periods, of less than 1000 yr in all cases but one, and the largest θ variations ($\Delta\theta/360$), of up to over 50% of their orbits. Because of non-zero eccentricity, these fractions of orbit in position angle do not translate linearly into fractions of orbit in reduced period ($\Delta t/P^\star$). In general, systems with larger/shorter fraction of orbit in θ than in $P^\star$ were observed close to their periapses/apoapses. Only one 'pair', the triple system WDS 08082+2106 A–Bab (BD+21 1764), is close to its periapsis.

Very few of our systems have been the subject of orbital studies. For example, WDS 09144+5241 (STF 1321) shows a smooth change of position angle of 52°·4 and of angular separation of 3·9 arcsec since the first astrometric epoch in 1821[79,80]. WDS 19464+3201 (KAM 3) also displays a large change of angular

TABLE VII

Physical systems with measured variations of position angle

WDS	*Disc.*	$\Delta\theta$ [*deg*]	$\Delta\theta/360$	Δt [*yr*]	$\Delta t/P^{\star}$	*Apsis*
00184+4401	GRB 34	25	0·07	150	0·19	Apo.
05342+1014	LDS 6189	2·8	0·008	53	0·06	…
08082+2106 A-Bab	COU 91	180	0·5	120	0·2	Peri.
09144+5241	STF 1321	52	0·15	200	0·6	Apo.
11055+4332	VBS 18	25	0·07	60	0·06	…
18180+1846	GIC 151	13	0·04	52	0·06	…
19464+3201	KAM 3	7·4	0·03	76	0·3	Apo.
19539+4425 AB-C	GIC 159	36	0·10	60	0·3	Apo.
22058+6539	NI 44	0·76	0·002	13	0·02	Apo.
22173−0847 A-BC	LDS 782	1·9	0·005	63	0·2	Apo.

separation of 3·25 arcsec[81,82], which led some authors incorrectly to classify it as an unbound pair[83,84] (Cortés-Contreras *et al.*, in prep.). Of the ten systems in Table VII, six displayed changes of the position angle larger than 12°, which is about 1⁄30 of a full orbit. In forthcoming papers we will investigate further all these systems which are interesting for the determination of dynamical masses of M dwarfs without the aid of high-resolution imagers.

Final remarks

In Table VIII, we summarize key comments on each star system investigated. This last table and the previous content is in the follow-on to the spirit of our series of papers in these pages, which is to shed light on how wide multiple systems with M-dwarf components could form and evolve, by way of a simple but detailed examination of some selected systems.

TABLE VIII

Summary of remarks on the 52 physical systems

WDS	*Remarks*
00137+8038	(LDS 1503) ...
00164+1950	(LDS 863) During the late 1990s and early 2000s, the primary of the binary system passed, from the observer's point of view, at only about 5 arcsec, by a Sun-like background star of null proper motion and similar brightness. This fact led *Simbad* and some authors to mix up the coordinates of the two stars. In 2014 and onwards, the primary of the true binary system is the southern star of the visual trio.
00184+4401	(GRB 34) Pair with period shorter than one millenium and appreciable orbital variation.
01119+0455	(GIC 20) ...
02361+0653	(PLQ 32 + GKI 1) Triple system (primary is a close double).
02457+4456	(LDS 5393) False triple, actual double system with astrometric follow-up; true secondary with estimated spectral type at m6:V.
02565+5526	(LDS 5401) …
03242+2347	(LDS 884 + WOR 4) Triple system (primary is an active, close double).
03398+3328	(ES 327) Pair made of two *HD* stars of relatively low proper motion with astrometric follow-up. Several different spectral types have been proposed for the primary in the interval from K2IV to K5V[37,85,86]; its *Hipparcos* distance (43±3 pc) is significantly larger than the spectro-photometric distance to the secondary provided by Riaz *et al.*[87] (29 pc) or estimated by us with our custom-made SpT–M_J relation (21 pc). We may need the ESA *Gaia* space mission and/or a detailed spectroscopic analysis to understand what is wrong with this system (age, metallicity, incorrect *Hipparcos* parallax of the primary, wrong PMSU and Riaz *et al.* spectral types, or unresolved multiplicity of the secondary).
03510+1414	(JLM 1) Poorly-known pair with spectro-photometric distance only[43,88]; secondary with estimated spectral type at m5:V. We propose for the first time that the primary, the secondary, or both are associated with the X-ray source 1RXS J035101·5+141404.
05033+2125	(LDS 6160 + LAW 13) Fragile, triple system (secondary is a close double).

TABLE VIII (*continued*)

WDS	*Remarks*
05342+1019	(LDS 6189) Pair with period shorter than one millenium, spectro-photometric distance, and appreciable orbital variation.
05599+5834	(GIC 61) …
06007+6809	(LDS 1201) …
06423+0334	(GIC 65) …
07307+4813	(GIC 75 + WNO 49) Triple system with a double white dwarf (EGGR 52 AB). The primary might in turn be a very close binary separated by 0·054 arcsec, which would make the system quadruple[70].
07319+3613	(LDS 6206 + BEU 11) Triple system (primary is a close double).
07397+3328	(LDS 3755) Pair with astrometric follow-up; sketched in Fig. 2, showing background star; true secondary with estimated spectral type at m6:V.
08082+2106	(COU 91) Triple system with period shorter than one millenium and appreciable orbital variation. Secondary is a spectroscopic binary of unknown parameters[58].
08313-0601	(LDS 221) TCP image in Fig. 1, left panel.
08427+0935	(LUY 6218 + ST 8) Quadruple system in a hierarchical arrangement with three orbital periods of about 0·057, 62, and 23 200 yr containing a spectroscopic binary, and a close 'pair' and a wide companion.
08526+2820	(LDS 6219) Pair with very bright primary of Bayer designation (ρ Cnc) that is also a bright multiplanet system host.
09008+0516	(OSV 2) …
09144+5241	(STF 1321) Pair with period shorter than one millenium and appreciable orbital variation.
09288-0722	(GUC 87) Pair with astrometric follow-up.
09427+7004	(OSV 3) …
10261+5029	(LDS 1241) Pair with spectro-photometric distance only.
11055+4332	(VBS 18) Pair with reduced period shorter than 1500 yr and appreciable orbital variation.
11080-0509	(LDS 852) Fragile system with a white dwarf (EGGR 76).
12123+5429	(VYS 5) Pair with discordant catalogued proper motions with astrometric follow-up.
12576+3514	(LDS 5764) Quadruple system made of an early M dwarf (BF CVn), a close-binary intermediate M dwarf and a wide companion at the substellar boundary out of *TCP* field of view. The close pair has no *WDS* designation yet.
13196+3507	(HJ 529 + BAG 11) Triple system (primary is a close double) of relatively small proper motion. Although first measured in 1827[89], the first reliable astrometric measurement of the wide pair was 69 years later[90].
13484+2337	(LDS 4410) Fragile system with a white dwarf (EGGR 438); *CAMELOT* image in Fig. 1, right panel.
18180+3846	(GIC 151) Pair with appreciable orbital variation.
19072+2053	(LDS 1017) …
19147+1918	(LDS 1020) Pair of two supposed M3·5V stars (PMSU) with a faint background visual companion at $\rho \sim 3{\cdot}5$ arcsec to the primary (2MASS J19143845+1919123). The primary is 1·5 mag brighter in J than the secondary and has *Hipparcos* parallactic distance. Oddly, Shkolnik *et al.*[91] classified the primary as a single M4·5V. The scenario that best matches the observables is that the primary is actually an M1V (more massive than listed in Table IV). Low-resolution spectroscopy is needed to confirm this hypothesis.
19169+0510	(LDS 6334) Pair at low Galactic latitude made up of two well-known stars, V1428 Aql and vB 10, that have received together almost 600 citations. *WDS* tabulates only three epochs from 1942 and 1999, and the last one (2MASS) is wrong. We performed a simple astrometric follow-up with public and *IAC80* data covering numerous epochs over 70 years and found no orbital variation (Cortés-Contreras *et al.*, in prep.).
19464+3201	(KAM 3) Pair with period shorter than one millenium and appreciable orbital variation. The position angle of the two first astrometric measurements in 1935·77 and 1936·71 by van de Kamp[92] had uncertainties larger than 2 deg.
19510+1025	(J 124) Pair with a very bright F8V-spectral-type primary of Bayer designation (o Aql). "AC" in *WDS*; all extra *WDS* pair candidates are visual, unbound pairs. All astrometric measurements of the pair[93,94,95] have been affected by the brightness of the primary.
19539+4425	(GIC 159 + MCY 3) Triple system at less than 5 pc with the shortest reduced period in our sample and appreciable orbital variation (primary is a close double).
19566+5910	(GIC 161) …
20446+0854	(LDS 1046) Pair of supposed M1·5V and M3·5V stars (PMSU) with spectro-photometric distance only and with astrometric follow-up. The primary is brighter by $0^{m}{\cdot}47$ in J than the secondary. We have assumed that the secondary is in turn an equal-brightness, close binary, which makes the system a triple. High-resolution imaging and/or spectroscopy are needed to confirm this hypothesis.

TABLE VIII (*concluded*)

WDS	*Remarks*
20555-1400	(LDS 6418) …
20568-0449	(LDS 6420) Pair with a white dwarf (EGGR 202).
21011+3315	(LDS 1049) Pair with spectro-photometric distance only.
21148+3803	(AGC 13 AB, AF + JOD 20) Bright quadruple system of Bayer designation (τ Cyg) made of two close binary systems of 0·2–0·6 arcsec separated by 1·5 arcmin.
21161+2951	(LDS 1053) Pair of two supposed M3·5V stars (PMSU) with spectro-photometric distance only. The primary is brighter by 0·85 mag in J than the secondary. We have assumed an m4·5V spectral type for the secondary (in italics in Tables IV and V). Low-resolution spectroscopy is needed to confirm this hypothesis.
21440+1705	(LDS 6358) Fragile pair of supposed M4·0V and M4·5V stars (PMSU). The primary is brighter by 0·77 mag in J than the secondary and has parallactic distance. The scenario that best matches the observables is that the secondary is actually an M5·0V or even M5·5V (less massive than listed in Table IV). Low-resolution spectroscopy is needed to confirm this hypothesis.
22058+6539	(NI 44) Poorly-known pair with astrometric follow-up, spectro-photometric distance only, period shorter than one millenium, and no spectral characterization of secondary.
22173-0847	(LDS 782 + BEU 22) Triple system (secondary is a close double). The angular separation and position angle of the first astrometric measurement of the wide 'pair', by Luyten[96] in 1920 (ρ = 7 arcsec, θ = 225 deg), had large uncertainties.
23294+4128	(GIC 93) Triple system with astrometric follow-up and discordant catalogued proper motions. Secondary is a close double with no *WDS* designation yet.
23573-1259	(LDS 830) Triple system with spectro-photometric distance only. Secondary is a spectroscopic binary of unknown parameters[60]. From Table V and simple spectral-type–absolute-magnitude relations, the secondary cannot be an equal brightness binary.

Acknowledgements

We thank Bill Hartkopf for his enthusiastic referee report, Laura Toribio san Cipriano for her service-mode observations at *IAC80*, F. Javier Alonso-Floriano and Alexis Klutsch for their spectral-typing advice, and Brian Mason for his prompt responses to our numerous *WDS* data requests. This article is based on observations with the *IAC80* telescope operated by the Instituto de Astrofísica de Canarias in the Spanish Observatorio del Teide. Financial support was provided by the Spanish MICINN under grants AYA2011-30147-C03-02 (UCM) and AYA2011-30147-C03-03 (CAB).

References

(1) J. A. Caballero, *The Observatory*, **132**, 1, 2012.
(2) S. Mahadevan *et al.*, *SPIE*, **8446**, E1S, 2012.
(3) S. Thibault *et al.*, *SPIE*, **8446**, E30, 2012.
(4) A. Quirrenbach *et al.*, *SPIE*, **8446**, E0R, 2012.
(5) A. Reiners *et al.*, *ApJ*, **710**, 432, 2010.
(6) J. A. Caballero *et al.*, *Protostars and Planets VI* (prpl Conf.), 2K020, 2013.
(7) N. Zacharias *et al.*, *AJ*, **139**, 2184, 2010.
(8) N. Zacharias *et al.*, *AJ*, **145**, 44, 2013.
(9) R. Østensen & J. E. Solheim, *Baltic Astronomy*, **9**, 411, 2000.
(10) http://www.iac.es/telescopes/pages/en/home/instruments/camelot.php
(11) F. Bonnarel *et al.*, *A&AS*, **143**, 33, 2000.
(12) B. D. Mason *et al.*, *AJ*, **122**, 3466, 2001.
(13) J. A. Caballero, *A&A*, **507**, 251, 2009.
(14) N. C. Hambly *et al.*, *MNRAS*, **326**, 1279, 2001.
(15) M. F. Skrutskie *et al.*, *AJ*, **131**, 1163, 2006.
(16) *Carlsberg Meridian Catalogue*, number 14, VizieR on-line catalogue I/304.
(17) B. M. Lasker *et al.*, *AJ*, **136**, 735, 2008.
(18) C. P. Ahn *et al.*, *ApJS*, **203**, 21, 2012.
(19) R. M. Cutri *et al.*, *WISE All-Sky Data Release*, VizieR on-line catalogue II/311.
(20) J. A. Caballero *et al.*, *A&A*, **520**, A91, 2010.
(21) R. Dorda, MSc thesis, Universidad Complutense de Madrid, Spain, 2011.

(22) F. van Leeuwen, *A&A*, **474**, 653, 2007.
(23) S. Roeser *et al.*, *AJ*, **139**, 2440, 2010.
(24) R. P. Butler *et al.*, *ApJ*, **545**, 504, 2000.
(25) R.-D. Scholz *et al.*, *A&A*, **442**, 211, 2005.
(26) R. P. Butler *et al.*, *ApJ*, **646**, 505, 2006.
(27) B. Rojas-Ayala *et al.*, *ApJ*, **748**, 93, 2012.
(28) H. L. Giclas, R. Burnham, Jr. & N. G. Thomas, *Lowell Observatory Bulletin*, **8**, 89, 1978.
(29) H. L. Giclas, R. Burnham, Jr. & N. G. Thomas, *Lowell Observatory Bulletin*, **6**, 271, 1966.
(30) S. Lépine & M. M. Shara, *AJ*, **129**, 1483, 2005.
(31) D. G. Monet *et al.*, *AJ*, **125**, 984, 2003.
(32) I. N. Reid *et al.*, *AJ*, **110**, 1838, 1995.
(33) A. Klutsch *et al.*, *Proceedings of the 2012 Annual Meeting of the French Society of Astronomy and Astrophysics* (SF2A Conf.), 357, 2012.
(34) F. J. Alonso-Floriano *et al.*, *Proceedings of the X Scientific Meeting of the Spanish Astronomical Society* (HSA7 Conf.), 431, 2013.
(35) R. Mundt *et al.*, *Protostars and Planets VI* (prpl Conf.), 2K055, 2013.
(36) F. J. Alonso-Floriano *et al.*, *Protostars and Planets VI* (prpl Conf.), 2K021, 2013.
(37) A. N. Vyssotsky, *AJ*, **61**, 201, 1956.
(38) T. W. Edwards, *AJ*, **81**, 245, 1976.
(39) D. Montes *et al.*, *MNRAS*, **328**, 45, 2001.
(40) A. J. Cenarro *et al.*, *MNRAS*, **396**, 1895, 2009.
(41) T. S. Boyajian *et al.*, *ApJ*, **757**, 112, 2012.
(42) J. A. Caballero, A. J. Burgasser & R. Klement, *A&A*, **488**, 181, 2008.
(43) J. Lendínez & F. M. Rica, *El observador de estrellas dobles*, **10**, 84, 2013.
(44) R. S. Harrington & C. C. Dahn, *AJ*, **85**, 454, 1980.
(45) W. F. van Altena *et al.*, *General Catalogue of Trigonometric Stellar Parallaxes* (Yale University Observatory, New Haven), 1995.
(46) J. A. Dittmann *et al.*, *ApJ*, **784**, 156, 2014.
(47) T. J. Henry *et al.*, *ApJ*, **512**, 864, 1999.
(48) A. Tokovinin, *MNRAS*, **389**, 925, 2008.
(49) M. W. Muterspaugh *et al.*, *AJ*, **140**, 1657, 2010.
(50) A. Garcés, S. Catalán & I. Ribas, *A&A*, **531**, A7, 2011.
(51) N. Giammichele *et al.*, *ApJS*, **199**, 29, 2012.
(52) A. Tokovinin, *AJ*, **147**, 86, 2014.
(53) L. M. Close *et al.*, *ApJ*, **660**, 1492, 2007.
(54) S. Dhital *et al.*, *AJ*, **139**, 2566, 2010.
(55) J. B. Holberg *et al.*, *ApJ*, **571**, 512, 2002.
(56) J. B. Holberg *et al.*, *AJ*, **135**, 1225, 2008.
(57) D. P. Morgan *et al.*, *AJ*, **144**, 93, 2012.
(58) E. L. Shkolnik *et al.*, *ApJ*, **716**, 1522, 2010.
(59) A. Duquennoy & M. Mayor, *A&A*, **200**, 135, 1988.
(60) J. E. Gizis, I. N. Reid & S. L. Hawley, *AJ*, **123**, 3356, 2002.
(61) S. Lépine, M. R. Rich & M. M. Shara, *AJ*, **125**, 1598, 2003.
(62) J. Daley, *Journal of Double Star Observations*, **4**, 34, 2008.
(63) E. L. Shkolnik *et al.*, *ApJ*, **758**, 56, 2012.
(64) S. Lépine & B. Bongiorno, *AJ*, **133**, 889, 2007.
(65) M. Cortés-Contreras *et al.*, *Proceedings of the X Scientific Meeting of the Spanish Astronomical Society* (HSA7 Conf.), 646, 2013.
(66) D. A. Golimowski *et al.*, *AJ*, **120**, 2082, 2000.
(67) A. M. Tanner, C. R. Gelino & N. M. Law, *PASP*, **122**, 1195, 2010.
(68) M. A. C. Perryman *et al.*, *A&A*, **323**, L49, 1997.
(69) N. Law *et al.*, *MNRAS*, **384**, 150, 2008.
(70) O. Yu. Malkov *et al.*, *A&A*, **546**, A69, 2012.
(71) J.-L. Beuzit *et al.*, *A&A*, **425**, 997, 2004.
(72) J. A. Docobo *et al.*, *AJ*, **132**, 994, 2006.
(73) I. I. Balega *et al.*, *A&AS*, **140**, 287, 1999.
(74) S. B. Dieterich *et al.*, *AJ*, **144**, 64, 2012.
(75) E. Jódar *et al.*, *MNRAS*, **429**, 859, 2013.
(76) C. Bergfors *et al.*, *A&A*, **520**, A54, 2010.
(77) M. D. Weinberg *et al.*, *ApJ*, **312**, 367, 1987.
(78) S. E. Urban *et al.*, *AJ*, **115**, 1212, 1998.
(79) F. G. W. Struve, *AN*, **14**, 249, 1837.
(80) N. A. Shakht *et al.*, *Astrophysics*, **53**, 227, 2010.
(81) W. S. Mesrobian, T. D. Griess & J. C. Titter, *AJ*, **77**, 392, 1972.
(82) I. S. Izmailov *et al.*, *Astronomy Letters*, **36**, 349, 2010.
(83) P. Lampens & A. Strigachev, *A&A*, **367**, 521, 2001.

(84) A. Strigachev & P. Lampens, *A&A*, **422**, 1023, 2004.
(85) F. Ochsenbein, *Bulletin d'Information du Centre de Donnees Stellaires*, **19**, 74, 1980.
(86) E. Anderson & C. Francis, *Astronomy Letters*, **38**, 331, 2012.
(87) B. Riaz, J. E. Gizis & J. Harvin, *AJ*, **132**, 866, 2006.
(88) J. Lendínez, *El observador de estrellas dobles*, **8**, 112, 2012.
(89) J. F.W. Herschel, *MemRAS*, **3**, 47, 1829.
(90) R. G. Aitken, *AN*, **142**, 77, 1896.
(91) E. L. Shkolnik *et al.*, *ApJ*, **699**, 649, 2009.
(92) P. van de Kamp, *PASP*, **48**, 313, 1936.
(93) R. Jonckhèere, *Journal Astronomique de l'Observatoire d'Hem*, **7**, 1910.
(94) S.W. Burnham, *Journal Astronomique de l'Observatoire d'Hem*, **11**, 1910.
(95) J. S. Schlimmer, *Journal of Double Star Observations*, **9**, 230, 2013.
(96) W. J. Luyten, *Publications of the Astronomical Observatory of the University of Minnesota*, **3**, 1, 1941.

CORRESPONDENCE

To the Editors of 'The Observatory'

Comment on a Test for Lutz–Kelker Bias in Pulsar Parallax Measurements

In a recent letter[1] I argued that the alleged Lutz–Kelker (hereinafter LK[2]) bias was derived with faulty assumptions and analysis, and that the Lutz–Kelker (L–K) correction should be not be applied when stars are selected either by a lower bound on parallax or by a bound on magnitude. Since publication of that note, it has been drawn to my attention that Verbiest *et al.*[3] compared results of older and more recent parallax measurements for a population of pulsars, finding a trend which they attributed to L–K bias. The purpose of this letter is to re-examine their data and analysis to establish whether such a trend exists and, if a trend does exist, to assess whether it can be attributed to the L–K bias or to some other cause.

The L–K bias supposedly arises because LK used the stellar distribution as a factor in the probability distribution for true parallax given the observed parallax. They considered stars on a shell of a particular observed parallax, and argued that, because there are more stars outside the shell than inside, it is likely that a given star will be outside the shell. Since this is true for all shells, they concluded that this causes a bias which "exists at all values of parallax". I pointed out[1] that we do not select stars on a particular shell and that the integrals used by LK do not include stars at all parallaxes (the behaviour of those integrals is pathological) but impose a lower bound depending on true parallax, which cannot be known in practice. The apparent L–K bias is created by selection using that bound. Measurements can be assumed unbiassed and there is no realistic stellar selection to which the L–K bias applies.

Verbiest *et al.* based their test on Binney & Merrifield[4], who used a luminosity function to moderate the L–K bias. The rationale for that is even less clear than that of the strictly volumetric adjustment suggested by LK, since there is no direct dependency of parallax measurements on stellar luminosity and any Malmquist bias[5] towards selection of bright stars is better considered separately. In fact, the Binney & Merrifield correction is strictly not a correction for bias but an adjustment taking luminosity distance into account. However, if we wish to find a best estimate combining parallax distance and luminosity distance, this would be better done by taking the mean of the two measurements, not in a treatment of bias.

4

High–resolution imaging with FastCam

This chapter corresponds to the second paper of CARMENES related to the science preparation. The paper was accepted to publication in August 2016 in the Astronomy & Astrophysics journal under the title *CARMENES input catalogue of M dwarfs II. High-resolution imaging with FastCam* (Cortés-Contreras et al. 2016, A&A, in press, arXiv:1608.08145, DOI:10.1051/0004-6361/201629056).

As noticed in Chapter 1, CARMENES will observe near 300 M dwarfs in the solar neighbourhood looking for Earth-like planets in their habitable zones. To avoid the variations induced by a close star companion in the radial velocity measurements, any M dwarf with a close companion at an arbitrary separation of less than 5 arcsec will be discarded. For this reason, we performed an extensive search of low mass companions to our Carmencita stars.

We took thousands of high resolution images in the I-band with the lucky imager FastCam at the 1.5 m Telescopio Carlos Sánchez of 490 Carmencita M dwarfs, selected among the potential CARMENES targets. We detected 80 bound companions in 76 systems, 30 of which are new discoveries. We measured angular separations and position angles of all of them, as well as the magnitude differences between components. We determined the individual magnitudes of each component, and the spectral types and masses of the M dwarf components. For stars older than 300 Ma, we derived masses from our own mass-magnitude relation, while for younger stars, we used the evolutionary models of the Lyon group (Baraffe et al. 2015). We computed a lower limit to the orbital period. Of our detected systems, 26 have periods shorter than 50 a, and 17 show variations in their orbital parameters within five years.

We built a volume limited sample using the Carmencita database. Within the completeness range of angular separations between 0.2 and 5 arcsec, we derived a multiplicity fraction of $19.5 \pm 2.3\%$. The contribution of binaries at separations greater and lower than 5 arcsec, as well as spectroscopic binaries, may increase the multiplicity fraction to at least 36%. This result is consistent with the obtained fractions in similar M dwarf multiplicity surveys (e.g., Leinert et al. 1997; Bergfors et al. 2010; Janson et al. 2012), and has intermediate values between solar-like stars and very low mass stars (see Table 1 in the article).

The companions in binary systems are found closer to their primaries for lower masses, with increasing separations for increasing masses. We found a peak in the distribution of projected physical

separations in our volume limited sample at 2.5–7.5 au, in agreement with the distributions of Jódar et al. (2013), Janson et al. (2012, 2014), and Ward-Duong et al. (2015). This peak is found near 30 au for solar-like primaries (Raghavan et al. 2010).

Several multiplicity surveys have been carried out centered in M dwarfs. This work provides a statistical unbiased multiplicity fraction built from a complete volume limited sample, which is composed by 425 M dwarfs. We also provide a list of young close binaries, and propose the pairs with the shortest periods for a follow-up in order to determine dynamical masses.

Astronomy & Astrophysics manuscript no. .FC23.tex
September 7, 2016

CARMENES input catalogue of M dwarfs

II. High-resolution imaging with FastCam

M. Cortés-Contreras[1], V. J. S. Béjar[2], J. A. Caballero[3,4], B. Gauza[2], D. Montes[1], F. J. Alonso-Floriano[1], S. V. Jeffers[5], J. C. Morales[6], A. Reiners[5], I. Ribas[6], P. Schöfer[5], A. Quirrenbach[4], P. J. Amado[7], R. Mundt[8], and W. Seifert[4]

[1] Departamento de Astrofísica y Ciencias de la Atmósfera, Facultad de Ciencias Físicas, Universidad Complutense de Madrid, 28040 Madrid, Spain, e-mail: micortes@ucm.es
[2] Instituto de Astrofísica de Canarias, Vía Láctea s/n, 38205 La Laguna, Tenerife, Spain, and Departamento de Astrofísica, Universidad de La Laguna, 38206 La Laguna, Tenerife, Spain
[3] Centro de Astrobiología (CSIC-INTA), PO Box 78, 28691 Villanueva de la Cañada, Madrid, Spain
[4] Landessternwarte, Zentrum für Astronomie der Universität Heidelberg, Königstuhl 12, 69117 Heidelberg, Germany
[5] Institut für Astrophysik, Friedrich-Hund-Platz 1, 37077 Göttingen, Germany
[6] Institut de Ciències de l'Espai (CSIC-IEEC), Campus UAB, c/ de Can Magrans s/n, 08193 Bellaterra, Spain
[7] Instituto de Astrofísica de Andalucía (CSIC), Glorieta de la Astronomía s/n, 18008 Granada, Spain
[8] Max-Planck-Institut für Astronomie, Königstuhl 17, 69117 Heidelberg, Germany

Received 06 Jul 2016; Accepted 23 Aug 2016

ABSTRACT

Aims. We search for low-mass companions of M dwarfs and characterize their multiplicity fraction with the purpose of helping in the selection of the most appropriate targets for the CARMENES exoplanet survey.
Methods. We obtained high-resolution images in the *I* band with the lucky imaging instrument FastCam at the 1.5 m Telescopio Carlos Sánchez for 490 mid- to late-M dwarfs. For all the detected binaries, we measured angular separations, position angles, and magnitude differences in the *I* band. We also calculated the masses of each individual component and estimated orbital periods, using the available magnitude and colour relations for M dwarfs and our own M_J-spectral type and mass-M_I relations. To avoid biases in our sample selection, we built a volume-limited sample of M0.0-M5.0 dwarfs that is complete up to 86 % within 14 pc.
Results. From the 490 observed stars, we detected 80 companions in 76 systems, of which 30 are new discoveries. Another six companion candidates require additional astrometry to confirm physical binding. The multiplicity fraction in our observed sample is 16.7 ± 2.0 %. The bias-corrected multiplicity fraction in our volume-limited sample is 19.5 ± 2.3 % for angular separations of 0.2 to 5.0 arcsec (1.4–65.6 au), with a peak in the distribution of the projected physical separations at 2.5–7.5 au. For M0.0-M3.5 V primaries, our search is sensitive to mass ratios higher than 0.3 and there is a higher density of pairs with mass ratios over 0.8 compared to those at lower mass ratios. Binaries with projected physical separations shorter than 50 au also tend to be of equal mass. For 26 of our systems, we estimated orbital periods shorter than 50 a, 10 of which are presented here for the first time. We measured variations in angular separation and position angle that are due to orbital motions in 17 of these systems. The contribution of binaries and multiples with angular separations shorter than 0.2 arcsec, longer than 5.0 arcsec, and of spectroscopic binaries identified from previous searches, although not complete, may increase the multiplicity fraction of M dwarfs in our volume-limited sample to at least 36%.

Key words. stars: binaries: close – stars: late-type – stars: low mass

1. Introduction

The multiplicity of low-mass stars provides constraints to models of stellar and planet formation and evolution (Goodwin et al. 2007; Burgasser et al. 2007; Duchêne & Kraus 2013). M dwarfs, which have approximate masses of between 0.1 and 0.6 $M_\odot$, account for two thirds of the stars in the solar neighbourhood and probably the Galaxy. However, in spite of their abundance and the increasing number of M-dwarf high-resolution imaging surveys in the past decade (Beuzit et al. 2004; Law et al. 2008; Bergfors et al. 2010; Janson et al. 2012, 2014a; Jódar et al. 2013; Bowler et al. 2015; Ward-Duong et al. 2015), the multiplicity of M dwarfs is not yet well constrained, at least by comparison with the better determination for Sun-like stars (Duquennoy & Mayor 1991; Raghavan et al. 2010; Tokovinin 2011). Published values range between 13.6 % and 42 %. Thus, the binary fraction of M dwarfs seems intermediate between the one of Sun-like stars and very low mass binaries. In Table 1 we summarise the multiplicity fractions and semi-major axis coverage of some of the main multiplicity surveys carried out from F6 to T dwarfs.

The typical separation of low-mass stars in a binary system tends to decrease with the mass of the primary, which makes the detection of faint companions at resolvable separations more difficult (Jeffries & Maxted 2005; Burgasser et al. 2007; Caballero 2007; Bate 2012; Luhman 2012). In addition, the presence of a stellar companion influences planet formation (Wang et al. 2014a, 2014b, 2015a, 2015b). The limited number of exoplanet hosts in binary and multiple systems (Mugrauer et al. 2007; Mugrauer & Neuhäuser 2009; Ginski et al. 2015) and the relatively small number of M dwarfs with known exoplanets detected with radial-velocity and transit methods (Rivera et al. 2005; Charbonneau et al. 2009; Bonfils et al. 2013) prevents a significant sta-

Table 1. Stellar multiplicity fractions.

Reference	Investigated spectral type	$d_{\rm lim}$ [pc]	Multiplicity fraction [%]	Projected physical separation, s [au]	Survey method[a]
Duquennoy & Mayor 1991	F7–G9	22	~ 65	~ 0.01–225	RV, WI
Raghavan et al. 2010	~ F6–K3	25	44 ± 3	~ 0.005–100 000	RV, AO, S, WI
Reid & Gizis 1997	K2–M6	8	32	~ 0.1–1800	RV, S, WI
Leinert et al. 1997	M0–M6	5	26 ± 9	~ 1–100	S
Fischer & Marcy 1992	M	20	42 ± 9	0–10 000	RV, WI
Jódar et al. 2013	K5-M4	25	$20.3^{+6.9}_{-5.2}$	~ 0–80	LI
Ward-Duong et al. 2015	K7–M6	15	23.5 ± 3.2	~ 3–10 000	AO, WI
Bergfors et al. 2010	M0.0–M6.0	52	32 ± 6	3–180	LI
Janson et al. 2012	M0.0–M5.0	52	27 ± 3	3–227	LI
Law et al. 2008	M4.5–M6.0	<15.4>	$13.6^{+6.5}_{-4.0}$	~ 0–80	LI
Siegler et al. 2005	M6.0–M7.5	30	9^{+4}_{-3}	$\geqslant 3$	AO
Janson et al. 2014a	M5.0–M8.0	36	21–27	~ 0.5–100	LI
Close et al. 2003	M8.0–L0.5	33	15 ± 7	<15	AO
Bouy et al. 2003	M7.0–L8.0	20	10–15	1–8	HST
Reid et al. 2008	L	20	$12.5^{+5.3}_{-3.0}$	<3	HST
Burgasser et al. 2003	T	<10>	9^{+15}_{-4}	1–5	HST

Notes. [(a)] AO: Adaptive optics; HST: *Hubble Space Telescope*; LI: Lucky imaging; RV: Radial velocity; S: Speckle; WI: Wide-field imaging.

tistical analysis of how stellar multiplicity at such low masses affects planet formation.

Because of their low effective temperatures, M dwarfs emit the bulk of their energy in the near-infrared. It makes them difficult to observe with the required radial-velocity precision with the current spectrographs for exoplanet hunting (e.g. HARPS at the 3.6 m ESO La Silla Telescope, HARPS-N at the 3.6 m TNG, and UVES at the 8.2 m ESO VLT), which operate in the optical. The prompt development of stable near-infrared spectrographs with wide wavelength coverage and high spectral resolution for radial-velocity surveys of M dwarfs has therefore been identified as critical by numerous decadal panels, funding agencies, and international consortia. Some noteworthy high-resolution near-infrared spectrographs currently under developement are IRD at 8.2 m Subaru (Tamura et al. 2012), HPF at 9.2 m HET (Mahadevan et al. 2014), and SPIRou at 3.6 m CFHT (Donati et al. 2014). The high-resolution spectrograph CARMENES (Amado et al. 2013; Quirrenbach et al. 2014[1]) at 3.5 m Calar Alto covers from 520 nm to 1710 nm and has started its science survey in January 2016.

CARMENES is the name of the double-channel spectrograph (near-infrared and optical) of the Spanish-German consortium that built it, and of the science project that is being carried out during guaranteed-time observations (GTO). For at least 600 GTO clear nights in the time frame between 2016 and 2018, CARMENES will spectroscopically monitor about 300 carefully selected M dwarfs with the goal of detecting low-mass planets in their habitable zones. With a long-term 1 m s^{-1} radial-velocity precision, the consortium aims at being able to detect 2 $M_\oplus$ planets orbiting in the habitable zone of M5 V stars and super-Earths around earlier stars (García-Piquer et al. 2016). In addition to the detection of the individual planets themselves, the ensemble of objects will provide sufficient statistics to assess the overall distribution of planets around M dwarfs: frequency, masses, and orbital parameters.

To optimise the observational strategy of the instrument and its scientific return, the consortium has built Carmencita, the CARMENES input catalogue (Caballero et al. 2013; Quirrenbach et al. 2015; Alonso-Floriano et al. 2015a). It consists of almost 2200 of the brightest M dwarfs of each spectral subtype observable from Calar Alto, from which we will select the approximately 300 single GTO stars. By single we mean stars without close visual (physically bound) or optical (unbound) stellar or substellar companions that may induce real or artificial radial-velocity variations and, therefore, contaminate the precise CARMENES measurements (Guenther & Wuchterl 2003; Ehrenreich et al. 2010; Guenther & Tal-Or 2010; Bonfils et al. 2013).

As part of our efforts to determine the multiplicity of M dwarfs and to select the best targets for radial-velocity surveys for exoplanets, we performed a high-resolution imaging search of close companions with the lucky imaging instrument FastCam at the Telescopio Carlos Sánchez, as described in this paper. Preliminary results of this work were presented as conference proceedings by Béjar et al. (2012) and Cortés-Contreras et al. (2015a, 2015b). This paper is the second item of the series called the CARMENES input catalogue of M dwarfs. In the first paper, Alonso-Floriano et al. (2015a) carried out a low-resolution optical spectroscopic analysis of a number of poorly known dwarfs to constrain their spectral types. Furthermore, this work will soon be complemented with on-going searches of unresolved spectroscopic binaries and triples identified in a large collection of high-resolution optical spectra (Montes et al. 2015; Jeffers et al. in prep.) and of wide companions to M dwarfs supported by virtual observatory tools (cf., Cortés-Contreras et al. 2013, 2014; Alonso-Floriano et al. 2015b).

[1] http://carmenes.caha.es

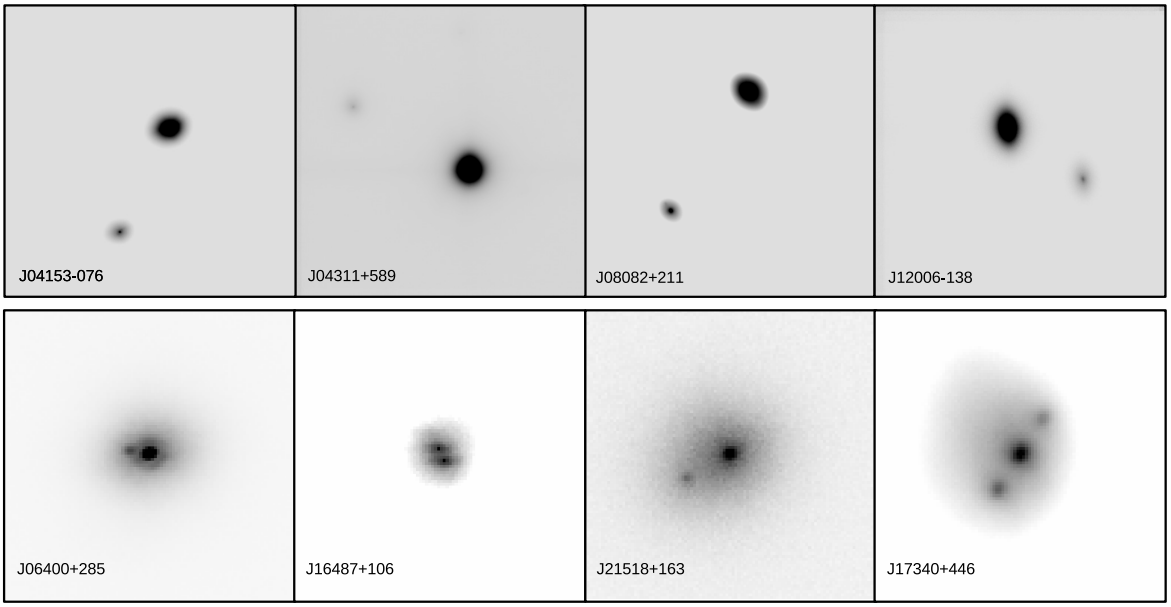

Fig. 1. Selection of images of multiple systems identified by us with FastCam. North is up and east is left. The upper row scale is 20×20 arcsec^2, that of the lower row 4×4 arcsec^2. Images at the top were obtained with the shift & add mode, while the bottom images were obtained with the "lucky image" mode.

The bottom right image (J17340+446) is an examlpe of the so-called false triple effect.

2. Observations

Of the almost 2200 M dwarfs currently in Carmencita, we selected 490 Carmencita targets for being observed with the FastCam lucky imager (Oscoz et al. 2008) at the 1.5 m Telescopio Carlos Sánchez at the Observatorio del Teide (Tenerife, Spain). The high-resolution imager FastCam is equipped with an L3CCD Andor 512×512 detector with very low electron noise and high readout speed. It has a field of view of 21.2×21.2 arcsec^2 and an approximate pixel size and orientation of the detector of 0.0425 arcsec and 91.9 deg, respectively. FastCam delivers nearly diffraction-limited images, which at the Telescopio Carlos Sánchez and in the *I* band have full-width at half maxima of approximately 0.15 arcsec.

We carried out the observations during 26 nights in 15 runs from October 2011 to January 2016. For each target, we obtained typically ten blocks of 1000 frames each in the Johnson-Cousins *I* band using the electron multiplication mode. Typical frame exposure times were in the 35–50 ms range. On average, each star was imaged during 500 s in total. The typical Strehl ratio in our observations varies with the percentage of the best-quality frames chosen in the reduction process: from 0.2 for the 100% to 0.4 for the 1%. For astrometric calibration purposes, we also observed the globular cluster M3 and 18 astrometric standard binary stars from the Aitken Double Star catalogue (ADS – Aitken 1932; Scardia et al. 1995) with the same method and on several occasions.

Each frame was bias subtracted and then processed with the FastCam dedicated software developed at the Universidad Politécnica de Cartagena (see Labadie et al. 2010; Jódar et al. 2013). We ran the lucky image (on five blocks) and shift & add processing modes separately. The first allows selecting the fraction of the best-quality frames (we chose 1 %, 10 %, and 50 %), aligns the selected frames using the brightest speckle, and combines them, producing six final lucky images per target. The second mode aligns all the block frames and then combines them, resulting in one unique image per target. Shift & add produces deeper images than the lucky image mode, but with slightly poorer resolution. The M3 standard field was reduced only with the shift & add mode. In Fig. 1 we show a selection of the processed images at two different spatial scales.

In Table A.1, we provide the list of 490 observed M-dwarf targets with the following column information: identification number, our Carmencita identifier (Quirrenbach et al. 2015; Alonso-Floriano et al. 2015a), J2000 coordinates and *J*-band magnitude from the Two-Micron All-Sky Survey (Skrutskie et al. 2006), spectral type and its reference, distance and its reference, and the FastCam observation date and exposure time. Figure 2 shows the histograms of spectral types, *J*-band magnitudes, heliocentric distances, and total proper motions of the observed sample. Spectral types range from M0.0 V to M7.0 V, *J* from 4.2 mag to 10.4 mag, distances from 1.8 pc to 39.1 pc, and proper motions from 0.03 arcsec a^{-1} to 10.6 arcsec a^{-1}. Because of their closeness, 97 % of our targets have total proper motions larger than 100 mas a^{-1}.

Our sample of 490 observed Carmencita targets consisted mainly of the brightest stars in the *J* band for each spectral subtype (see Sect. 2 in Alonso-Floriano et al. 2015a) that were (*i*) not known spectroscopic binaries, (*ii*) not resolved systems with visual or optical companions at angular separations smaller than 5 arcsec, and (*iii*) not studied with high-resolution imaging devices before the start of our observations by speckle, adaptive optics, or lucky imaging (Beuzit et al. 2004; Law et al. 2008; Bergfors et al. 2010; Jódar et al. 2013; Janson et al. 2012). Some high-resolution imaging (Janson et al. 2014a; Ansdell et al. 2015; Bowler et al. 2015; Ward-Duong et al. 2015) and

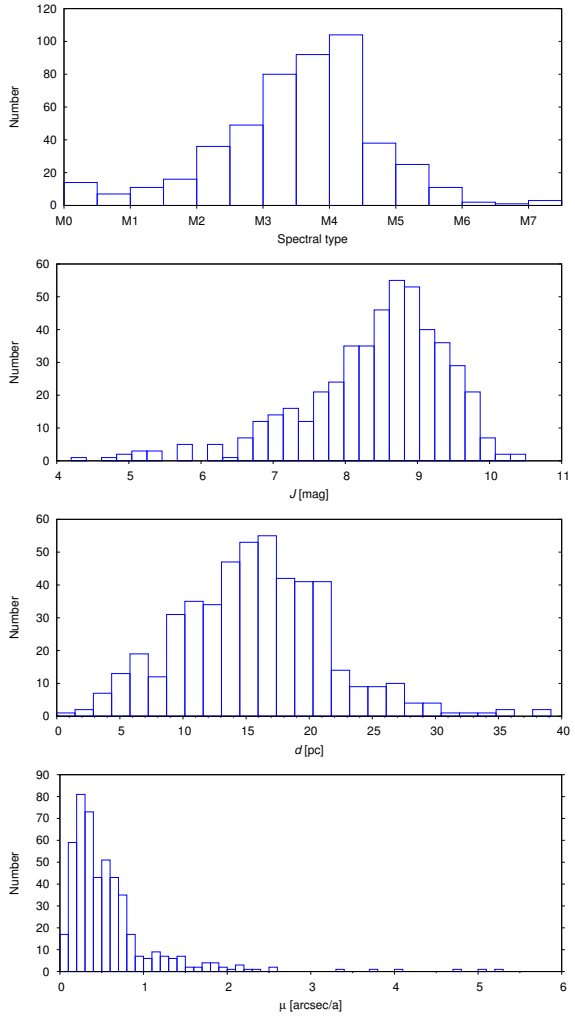

Fig. 2. Distributions of spectral type, J-band magnitude, distance, and proper motion of the 490 observed M-dwarf targets. The sizes of the bins follow the definitions given by Freedman & Diaconis (1981). The lowest panel does not display Barnard's star, with $\mu = 10.4$ arcsec a^{-1}.

spectroscopic (Bonfils et al. 2013; Llamas 2014; Schöfer 2015) surveys have been performed afterwards and have tabulated several objects in common with our target list. In addition, we also observed (*a*) some dubious or poorly investigated close multiple systems (including spectroscopic binary candidates), (*b*) a few stars with possible visual companions at angular separations smaller than 5 arcsec that needed confirmation or better characterisation, and (*c*) four known binaries with estimated orbital periods shorter than five years that were previously proposed for follow-up by Cortés-Contreras et al. (2013): J05085–181 (GJ 190), J13317+292 (DG CVn), J23174+196 (G 067–053), and J23455–161 (LP 823–004).

To confirm the physical binding of pairs (i.e. that the components share a common proper motion), we observed 54 targets more than once, and up to eight times. Accounting for the 490 M dwarfs, 18 ADS pairs and M3 calibration field, and the different epochs, we acquired 7670 images in total with FastCam.

Table 2. FastCam adopted plate scale and orientation for each run night.

Observation date[a]	Pixel scale [mas/pix]		Orientation [deg]	
	x	y	x	y
23 Oct 2011*	42.25	42.56	92.08	91.60
24 Oct 2011	42.25	42.56	92.08	91.60
25 Oct 2011	42.25	42.56	92.08	91.60
30 Jan 2012	42.25	42.56	92.08	91.60
31 Jan 2012	42.25	42.56	92.08	91.60
25 Mar 2012*	42.31	42.61	91.79	91.64
26 Mar 2012*	42.30	42.62	91.82	91.65
27 Mar 2012	42.30	42.62	91.82	91.65
10 Jul 2012*	42.48	42.61	92.11	91.91
11 Jul 2012*	42.49	42.64	92.03	91.77
12 Jul 2012*	42.32	42.54	91.96	91.99
16 Sep 2012	42.32	42.54	91.96	91.99
17 Sep 2012	42.32	42.54	91.96	91.99
13 Jan 2013*	42.26	42.69	91.94	91.63
14 Jan 2013*	42.21	42.59	91.85	91.63
28 Feb 2014*	42.26	42.69	91.99	91.70
01 Mar 2014	42.26	42.69	91.99	91.70
02 Mar 2014	42.26	42.69	91.99	91.70
22 May 2014	42.26	42.69	91.99	91.70
09 Dec 2014*	42.26	42.99	91.97	91.96
14 Apr 2015*	42.28	42.37	92.18	91.65
15 Apr 2015	42.28	42.37	92.18	91.65
09 Jun 2015	42.28	42.37	92.18	91.65
29 Jul 2015	42.28	42.37	92.18	91.65
17 Nov 2015	42.28	42.37	92.18	91.65
07 Jan 2016	42.28	42.37	92.18	91.65

[a] M3 calibration field was observed on nights marked with an asterisk.

3. Analysis

3.1. Astrometry

The first step of the analysis was computing the pixel size and detector orientation with common IRAF tasks (Tody 1986). To do this, we determined the centroids of the brightest stars in the M3 standard field with `imcentroid`. Using the celestial coordinates in the ACS Survey of Galactic Globular Clusters (Sarajedini et al. 2007) and the pixel coordinates in our images, we then determined the transformation equations with `ccmap` by fitting to a general transformation of order two. Table 2 lists the pixel scales and orientations of the detector for each night. For nights without M3 images, we used the calibration of the closest night with computed plate solution. Pixel scale and rotation angle in the centre of the detector in the x and y axes are similar within the different campaigns with almost negligible variations from night to night. Their mean values are 42.31 ± 0.09 mas/pixel and 42.63 ± 0.15 mas/pixel in pixel scale and 91.98 ± 0.12 deg and 91.74 ± 0.15 deg in orientations of the detector in the x and y axes, respectively. The uncertainties are the standard deviations of the measurements.

To double-check that our astrometric solutions were correct, we calculated angular separations (ρ) and position angles (θ) for each ADS binary. To do that, we measured the x and y positions of each star with `imcentroid`, and transformed them into

equatorial coordinates using the astrometric solution of the corresponding night with `cctran`. Table A.2 shows the previously published values of ρ, θ, the epochs of observation and references, and our measured values in different epochs. Our errors in ρ and θ were derived from the standard deviation of the measurements in all images within the same night and the determined astrometric solutions on different nights. In general, the measured values of ρ and θ of the same pair on different nights were consistent within 3σ between them and with tabulated values from recent works. In some cases, the quality of our measurements surpassed previous publications.

We carried out a visual inspection for companions to our 490 Carmencita targets and found 137 additional sources in 116 systems, for which we measured the relative positions and position angles following the same procedure as described above for the ADS binaries. In some epochs of nine stars with companions very close to the resolution limit of our images, we were unable to measure the photocentroid of both components with `imcentroid` and, hence, we used the brightest pixel to measure their positions. In these cases, the uncertainties in the determination of ρ and θ were larger and we adopted a typical error bar of one pixel.

We classified the 137 sources into three groups: (*i*) 51 optical companions (i.e. unbound, Table A.3), (*ii*) 80 physical companions (i.e. bound, Table A.4), and (*iii*) six unconfirmed companions (bottom of Table A.4). For the classification, we used old photographic plate digitisations and all-sky surveys provided by the Aladin sky atlas (Bonnarel et al. 2000), previous astrometry tabulated by the Washington Double Star Catalogue (WDS, Mason et al. 2001) and/or our own multi-epoch astrometric measurements together with the target proper motions (mostly from van Leeuwen 2007 and Roeser et al. 2010).

Most of the 51 optical companions are null-proper-motion point-like sources in photographic plates of the first National Geographic Society – Palomar Observatory Sky Survey in the mid-1950s. For the rest of the companions, we performed a multi-epoch analysis of their relative positions. We considered as optical (unbound) companions those that show ρ and θ values in different epochs consistent within 3σ with null proper motion and inconsistent by more than 3σ with the proper motion of the M dwarfs. Otherwise, we considered them as physically bound. For five of the six unconfirmed binaries, we only had one epoch, and for the other (J07349+147), the ρ and θ values at different epochs did not allow us to distinguish between null or common proper motion.

Figure 3 displays the measured ρ and θ values of all the detected pairs. It shows a homogeneous distribution of the position angle of the companions, which discards possible false detections associated with, for example, optical ghosts.

3.2. Photometry

In Table A.4 we list magnitude differences in the I band for the 80 physical and six likely physical pairs. To measure the magnitude difference of the binaries, we performed aperture and point spread function (PSF) photometry using the `phot`, `psf`, and `allstar` routines in the `daophot` package of IRAF.

For wide enough pairs, we used the primary star PSF as a reference for the secondary. In these cases, magnitude differences from aperture photometry and PSF fitting did not differ significantly. Since the PSF varies depending on the focus and sky position, for close pairs we chose the most appropriate single star observed during the same night as a reference to compute the PSF. For five pairs, we were unable to measure the ΔI between components using PSF photometry, and we estimated it from the peak flux ratio of the PSF subtracted image, and for J23455–161, we perceived the companion and could not measure the magnitude difference.

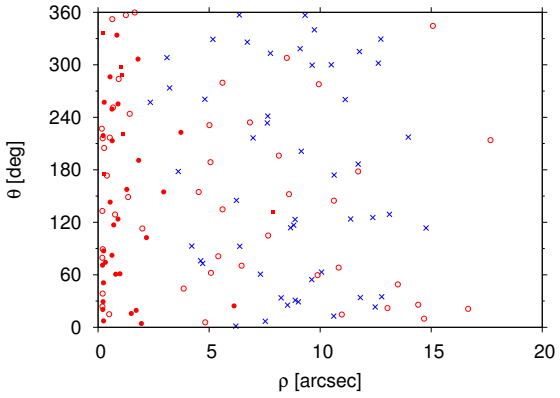

Fig. 3. Diagram of θ vs. ρ for all the 137 measured pairs. Filled red circles are new physically bound pairs, small filled red squares are unconfirmed related pairs, open red circles are known physically bound pairs, and blue crosses are optically unrelated pairs.

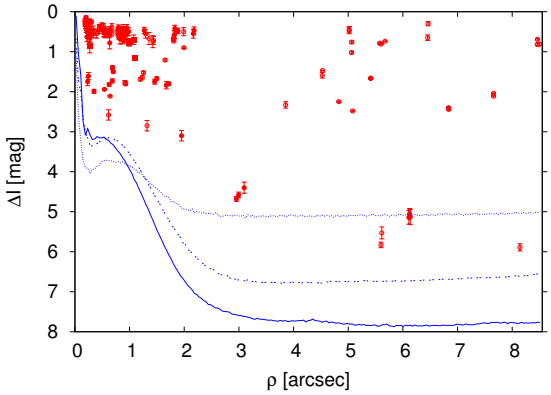

Fig. 4. Diagram of ΔI vs. ρ up to 8.5 arcsec for the physical pairs. Colour and symbol code is as in Fig. 3. Solid, dashed, and dotted lines indicate the 3σ detection limits for primaries in the magnitude ranges $I < 10$ mag, 10 mag $\leq I < 11$ mag, and $I \geq 11$ mag, respectively.

A few close pairs showed a so-called false triple effect associated with the reduction process by the FastCam software, based on the selection of the brightest pixel. When both components are of similar brightness, this software may not distinguish between the primary and secondary and, in the process of aligning, selects the brightest pixel in one or another star, resulting in an apparent triple system. For equal brightness binaries, this may lead to a degeneracy in the determination of the position angle of 180 deg. The option `2stars` in the FastCam reduction software, which takes this ambiguity into account, solved this effect in most cases. For the rest, we determined the real flux ratio of the pair by following the procedure described by Law (2006):

$$F_R = \frac{2I_{13}}{I_{12}I_{13} + \sqrt{I_{12}^2 I_{13}^2 - 4I_{12}I_{13}}}, \quad (1)$$

where $I_{12} = F_1/F_2$ and $I_{13} = F_1/F_3$, and F_1, F_2 and F_3 are the fluxes of the images in the positions of the true primary, true secondary, and spurious tertiary, respectively.

In Fig. 4 we plot the measured magnitude differences in the I band and angular separations of the companions. Most of them are of similar brightness ($\Delta I \approx 0.0$–1.0 mag) and are located at angular separations smaller than 2.5 arcsec. Figure 4 also shows the contrast curves of our survey as a function of angular separation. The maximum magnitude difference in each stacked image depends on the brightness of the primary star. For this reason, we considered three different groups in our sample according to their I magnitude, from which we selected four single stars covering different spectral types to obtain a representative mean contrast curve. For each star, we estimated the detection limit as a function of the angular separation as three times the standard deviation of the number of counts in ten-pixel-wide annuli centred on the target. This detection limit was converted into ΔI using the peak flux value of the star. The maximum magnitude difference in the detection of possible companions at angular separations between 0.2 and 1.0 arcsec varies from 3 to 4 mag and from 5 to 7 mag at separations larger than 2 arcsec, depending on the brightness of the primary star. The limiting magnitude of our survey is about $I \approx 17$ mag, and we were able to detect all sources brighter than this limit at angular separations greater than 3 arcsec. This implies that at separations larger than 3 arcsec, the detection of companions earlier than M8 dwarfs is complete up to 40 pc, which corresponds to the entire sample, and the detection of companions earlier than M9 dwarfs is complete up to 25 pc, which is in most of our sample.

4. Results and discussion

4.1. Detected binaries

Of the 490 observed stars, we confirmed with our data 80 companions in 76 systems, of which 30 are presented here for the first time. In addition, there are also six unconfirmed binaries that need additional epochs to confirm the physical binding. The majority of the optical components of the survey were easily identified using previous available data, and most of the remaining ones were confirmed as physically bound companions using our own measurements at different epochs. Therefore, we considered the six unconfirmed binaries as very probably physically bound rather than unbound pairs. We took into account the six binaries for the determination of the multiplicity fraction.

The 86 pairs are listed in Table A.4. In the last column of the table, we include the multiplicity flag from version 1.2 of the Guide Star Catalog (Morrison et al. 2001), which is "False" for 18 of the 30 new confirmed binaries,"True" for 10 of them and has no entry for the close companions of J08082+211 and J15191–127. For the 30 new binaries, and to our knowledge, there are no other references to binarity.

Of the 80 physical companions, 48 are tabulated by WDS (second column in Table A.4), of which two were previously suggested by Behall & Harrington (1976; J05333+448) and Bowler et al. (2015; J15496+348) and confirmed here. Another two were recently presented by Ward-Duong et al. (2015; J05034+531) and Ansdell et al. (2015; J06212+442), and one of the new companions resolved here is most likely associated with a spectroscopic binary identified by Bonfils et al. (2013; J15191–127). The remaining 29 are pairs with no previous binarity references to our knowledge.

Some of the measured companions were not detected in all epochs because of the relative motion of the components and the crossing of the companion behind or in front of the primary star (J05078+179 and J05333+448), presence of the companion near the diffraction limit (J13317+292, J15496+348, J16487+106, and J21012+332), and a focus problem (J06400+285).

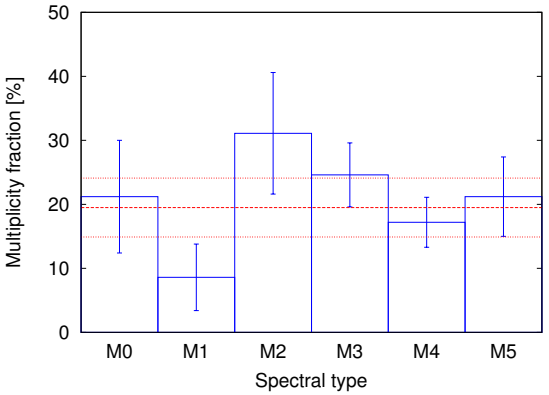

Fig. 5. Multiplicity fraction as a function of spectral type from M0.0 V to M5.0 V in the volume-limited sample with separations from 0.2 to 5.0 arcsec. Error bars are Poissonian. Horizontal dashed and dotted lines are the global multiplicity fraction and the $\pm 2\,\sigma$ values.

4.2. Multiplicity fraction

Of the 490 observed M dwarfs, 408 are single and 82 (76+6) are in binary or multiple systems within the FastCam field of view. This gives a close multiplicity fraction of 16.7 ± 2.0 %, by assuming a Poissonian distribution of the errors. Nevertheless, it must not be taken as a real M-dwarf multiplicity fraction because of the selection bias of the observed sample: we did not include many stars that were previously observed in similar studies or that had known visual companions at less than 5 arcsec.

For statistical purposes, we grouped all our Carmencita (Sect. 1) and FastCam targets in a combined sample. Of the 2176 Carmencita stars, 1141 M dwarfs have been surveyed with FastCam or with high-resolution imagers with similar capabilities (Beuzit et al. 2004; Lafrenière et al. 2007; Law et al. 2008; Bergfors et al. 2010; Janson et al. 2012, 2014a; Jódar et al. 2013; Bowler et al. 2015; Ward-Duong et al. 2015). For completeness, we considered a range of angular separations from 0.2 to 5 arcsec to our targets. The lower limit was given by the FastCam spatial resolution and the upper limit by the maximum separation at which we could detect companions to at least 90 % of the observed stars. Of the 1141 surveyed M dwarfs, 219 have physical companions in this interval of angular separations (55 from this work and 164 from other publications), which gives a close multiplicity fraction of 19.2 ± 1.4 %.

To avoid any selection bias and give a more reliable multiplicity fraction, we proceeded by building a volume-limited sample with a maximum distance of 14 pc and a completeness of 86 %. This completeness was estimated by assuming that all M0–M5 dwarfs are known within 7 pc and that their density in the solar vicinity is constant. This third sample is composed of 425 dwarfs with spectral types between M0.0 V and M5.0 V, of which 83 have companions (either from FastCam and other works) in the range from 0.2 to 5.0 arcsec. This translates into a close multiplicity fraction of 19.5 ± 2.3 %, which is consistent within error bars with the 13.6 %–27 % fractions obtained

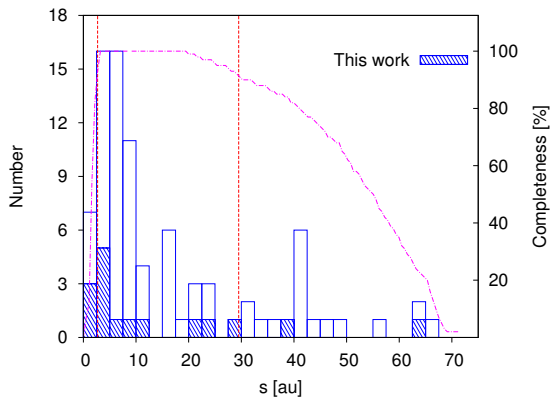

Fig. 6. Projected physical separation distribution of the binaries in the volume-limited sample. Dashed bars represent our binaries. Vertical dashed lines mark the 90 % completeness limits, and the dash-dotted curve represents the completeness as a function of the projected physical separation.

for M dwarfs in most surveys (Table 1), although some authors provided higher multiplicity fractions (Fischer & Marcy 1992; Bergfors et al. 2010). In Sects. 4.8 and 4.9 we estimate the contribution to the multiplicity fraction of pairs separated by less than 0.2 arcsec and more than 5 arcsec.

4.3. Dependence of multiplicity on spectral type

To estimate the spectral types of the individual components of the binaries, we used the $I - J$ colours and M_I absolute magnitudes as a function of spectral type for M dwarfs from Table 3 in Kirkpatrick et al. (1994), together with the 2MASS photometry and spectral type of the pair.

For pairs resolved by 2MASS, we used these relations and values to obtain the I magnitude of the primary, and obtained the I magnitude of the secondary from our measured ΔI. We derived the absolute M_I magnitudes through the distance modulus and inferred the spectral types of the secondaries with the M_I-spectral type relation of Kirkpatrick et al. (1994).

For pairs not resolved by 2MASS, the J-band magnitude involves the contribution of all the components in the system. In these cases, we obtained the I magnitude of the system from the $I - J$ colours and the global spectral types of the pairs from the literature. Using the I magnitude and our measured ΔI, we computed the individual I magnitudes. We calculated the individual M_I absolute magnitudes by applying the distance modulus, and estimated individual spectral types from the M_I-spectral type relation.

The distances in our sample come mostly from literature parallax determinations (see references in Table A.1). For stars without parallactic distance, we calculated spectro-photometric distances from our own M_J-spectral type relation. This relation was obtained from a polynomial fit using single stars with well-determined spectral types between M0 V and M6 V, parallactic distances, and 2MASS J-band photometry from the Carmencita sample, and has the form:

$$M_J = a\ \mathrm{SpT}^2 + \mathrm{b\ SpT} + \mathrm{c}, \quad (2)$$

where $a = 0.078 \pm 0.007$ mag, $b = 0.265 \pm 0.038$ mag and $c = 5.895 \pm 0.044$ mag, and SpT indicates the numerical spectral subtype within the M range.

For very close binaries, spectro-photometric distances are not reliable since the 2MASS photometry and the spectral type determination do not provide the contribution of the two components separately. In these cases, in an iterative way, we estimated new individual spectro-photometric distances for the two components in the system from spectral type estimations based on the global spectral type, the M_I-spectral type relation, the individual I magnitudes, and the distance modulus. These updated distances are given in Table A.1. Given the low number of close binaries not resolved in our survey (~ 10 %, see Sect. 4.8), we do not expect many additional unresolved components.

The individual spectral types are listed in Table A.5. SpT column indicates the combined spectral type of the system from which individual spectral types were derived. In the SpT_1 and SpT_2 columns, the spectral types indicated with capital "M" come from the literature, and with lower case "m" refer to our estimated spectral types.

In Fig. 5 we show the dependence of the multiplicity fraction of M dwarfs on the spectral type in our volume-limited sample. The multiplicity fractions for different spectral subtypes are consistent within the error bars among them, except for M1 stars, for which it is lower. We compared this distribution with the global multiplicity fraction obtained in the previous section and performed a χ^2 test. Without the M1 contribution, the distribution is consistent with a flat distribution with a confident level of 96 %.

In addition, our determined multiplicity fraction has intermediate values between Sun-like (44 %–65 %) and very low mass stars and brown dwarfs (9 %–15 %). This agrees with the generally accepted decreasing trend of the multiplicity fraction with decreasing mass of the primaries (Table 1).

4.4. Projected physical separation distribution

To study the distribution of the binaries in the volume-limited sample, we converted angular separations (ρ) into projected physical separations (s) by using the small-angle approximation $\tan\rho \approx \rho$. Hence, $s \approx \rho d$. The distances d come from parallax or photometry as in Sect. 4.3.

In Fig. 6 we show the projected physical separation distribution of the binaries in the volume-limited sample. We also represent the completeness of the volume-limited sample as a function of projected physical separation, and draw the completeness limits with a confidence level of 90 %, which correspond to the s interval between 2.6 and 29.5 au. We estimated these values as those separations at which we are able to detect companions in 90 % of the sample.

The projected physical separations of the observed pairs in the volume-limited sample range from 1.4 to 65.6 au and their distribution peaks at 2.5–7.5 au. This is consistent with the values of 5–10 au found by Jódar et al. (2013) for M0–M4 dwarfs, and of ~6 au found by Janson et al. (2014) for M3–M8 dwarfs and Ward-Duong et al. (2015) for M0–M6 dwarfs. However, these values are lower than those found for Sun-like stars (Duquennoy & Mayor 1991; Raghavan et al. 2010) and more similar to those found for ultracool dwarfs (4–6 au for M8.0–L0.5, Close et al. 2003; 2–4 au for M7.0–L8.0, Bouy et al. 2003; <3 au for L dwarfs, Reid et al. 2008).

Within the physical separation completeness range from 2.6 to 29.5 au, there are 61 M dwarfs with low-mass companions in our volume-limited sample. This translates into a multiplicity fraction of 14.4 ± 2.0%, which is lower than the fraction derived

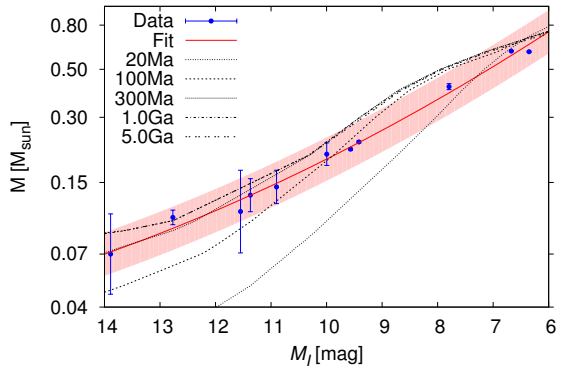

Fig. 7. Mass $\mathcal{M}$ vs. Absolute magnitude M_I. Blue points represent the dynamical masses and absolute magnitudes taken from the literature. The red solid line and shadowed area represent the best-fit $\pm 3\,\sigma$. Different dashed lines display the BT-Settl evolutionary models at 20 Ma, 100 Ma, 300 Ma, 1 Ga, and 5 Ga.

in Sect. 4.2 as a result of the missing systems at larger separations (see Fig. 6).

4.5. Masses

We derived masses from our own mass-luminosity relation in the Johnson-Cousins I band. To our knowledge, there is no published mass-luminosity relation employing this band. We collected dynamical masses and I -band magnitudes of eleven low-mass stars from different works (Delfosse et al. 2000; Henry 2004; Reid et al. 2004; Tokovinin 2008) and obtained an M_I-$\mathcal{M}$ relation using a parabolic fit of the form:

$$\log \mathcal{M} = a\, M_I^2 + b\, M_I + c, \tag{3}$$

where $\mathcal{M}$ is the mass, M_I is the absolute I -band magnitude, $a = 0.005 \pm 0.002\,\mathrm{mag}^{-2}$, $b = -0.222 \pm 0.037\,\mathrm{mag}^{-1}$, and $c = 1.035 \pm 0.180$. This relation is valid for main-sequence stars in the M_I interval between 6 and 14 mag, which corresponds to $\sim$ M0–M8 spectral types. Figure 7 shows the data taken from the literature, the corresponding best fit, and the comparison with BT-Settl evolutionary models from the Lyon group (Baraffe et al. 2015).

In some of our detected pairs, one or both components are also spectroscopic binaries (see Table 6). For these we estimated individual masses assuming equally bright components.

For main-sequence stars, the luminosity and effective temperatures are unambiguosly related to the mass, and thus, the relation in Eq. 3 is only valid for stars older than ~ 300 Ma, as inferred from Fig. 7. For stars younger than 300 Ma, the mass-luminosity relation strongly depends on the age. We searched for young stars in our sample by collecting radial velocities from the literature (Caballero et al. in prep.) and computing UVW Galactocentric space velocities as in Montes et al. (2001) for 452 of the 490 observed stars (there are 38 stars without radial velocities). Of these, 155 have U and V velocity components inside or near the boundaries that delineate the young-disc population (Montes et al. 2016). In total, 42 stars of our 82 multiple systems are candidate members in young stellar kinematic groups. We checked the literature and found that 26 of the 42 are relatively old interloper stars that do not show any youth feature or have been poorly investigated. The remaining 16 stars are confirmed members of stellar kinematic groups or the young-disc population. Their associations and ages are listed in Table 3.

Since $I - J$ colours of young stars and field stars do not show significant differences (see Bihain et al. 2010; Peña-Ramírez et al. 2016), we applied the colour-spectral-type relation from Kirkpatrick et al. (1994) to derive the individual I magnitudes of these stars as explained in Sect. 4.3. We considered Castor, Ursa Majoris, and young-disc members old enough to be main-sequence stars, and thus, to apply our mass-M_I relation with confidence. For these calculations, we assumed the ages given in Table 3. These stars appear in italics in Table A.5. The candidate pair to IC 2391 does not have a parallactic distance. Hence, we estimated its mass from the $I - J$ colours and the BT-Settl evolutionary models from the Lyon group (Baraffe et al. 2015). We also applied these models to derive masses from the individual I magnitudes and parallactic distances for β Pic, Columba/Carina and Local Association members.

Table A.5 lists the inferred I magnitudes (Sect. 4.3) and mass values of the components of 76 of our systems. All of the detected companions have absolute magnitudes brighter than 14 mag, the lowest limit of our empirical mass-magnitude relation, which corresponds to masses close to the hydrogen-burning limit ($\sim 0.07\,\mathrm{M}_\odot$). The only exception is the unconfirmed companion of J04352–161, which has an absolute magnitude fainter than 14 mag, and we were unable to determine its mass with the method explained before.

4.6. Mass ratios

The upper panel in Fig. 8 shows the mass ratio ($\mathcal{M}_2/\mathcal{M}_1$) histogram of our binaries in Table A.5. This global distribution slightly increases towards higher mass ratios and has its maximum above 0.8. The slightly lower number of equal-mass pairs with mass ratios near unity is not significant and could be related to the effect of the reduction process using the brightest pixel, which artificially sharpens the PSF of the primary with respect to the PSF of the secondary, and may produce a lower flux ratio than expected. This distribution is also affected by our sensitivity limit. While in spectral types earlier than M3.5 (i.e. more massive stars) our search of companions is complete for mass ratios greater than 0.3, in later spectral types (i.e. less massive stars) the search is complete for mass ratios greater than 0.35–0.60.

Empty and dashed bars represent the mass ratio distributions of M0.0-M3.5 and M4.0-M5.5 primaries, respectively. The distribution of the former shows the same trend as the global distribution, with a peak around 0.8–0.9. For the latter, the distribution increases towards higher ratios. As explained before, this might be due to our observational bias.

The high occurrence of binaries with mass ratios above 0.8 can also be seen in the lower panel in Fig. 8, which represents the spectral type of the primary versus the mass ratio. For later spectral types, our detected binaries also tend to have similar masses. This may be due to the lack of sensitivity to lower mass ratios at later spectral types. The distribution differs with the more homogeneous mass ratio distributions observed by Janson et al. (2012, 2014). The number of binaries with mass ratios closer to unity (i.e. similar masses) for M0.0-M3.5 contrasts with the relatively low numbers presented in Bergfors et al. (2010) in this range, but is more similar to their distribution for later M4.0-M5.5 spectral types.

Figure 9 displays the occurrence of mass ratios with physical separations. Pairs with separations shorter than 50 au tend

Table 3. Target members of stellar kinematic groups.

Karmn	Name	Moving group	Ref.[a]	Assumed age [Ma]	Ref.[b]
J01221+221	G 034–023	Young disc	Abe14	≥ 300	This work
J04153–076	o^{02} Eri C	β Pic	AF15	~ 20	Bell15
J05019+099	LP 476–207	β Pic	AF15	~ 20	Bell15
J05068–215E	BD–21 1074 A	β Pic	AF15	~ 20	Bell15
J05068–215W	BD–21 1074 BC	β Pic	AF15	~ 20	Bell15
J05103+488	G 096–021 AB	IC 2391?	This work	~ 50	Barr04
J10028+484	G 195–055	Local Association?	This work	~ 100	Bas96
J10196+198	BD+20 2465	Castor	Cab10	≥ 300	Barr98, Mam13
J12123+544S	BD+55 1519 A	UMa	Mon01	≥ 300	Gia79,SM93
J12123+544N	BD+55 1519 B	UMa	Mon01	≥ 300	Gia79, SM93
J13317+292	DG CVn AB	Columba/Carina	Ried14	~ 40	Bell15
J18548+109	V 1436 Aql B	Castor	Cab10	≥ 300	Barr98, Mam13
J23293+414S	G 190–027	Local Association	Klu14	~ 100	Bas96
J23293+414N	G 190–028	Local Association	Klu14	~ 100	Bas96
J23318+199 E	EQ Peg Aab	Castor	Cab10	≥ 300	Barr98, Mam13
J23318+199 W	EQ Peg Bab	Castor	Cab10	≥ 300	Barr98, Mam13

Notes. [(a)] Abe14: Aberasturi et al. 2014; AF15: Alonso-Floriano et al. 2015b; Cab10: Caballero 2010; Klu14: Klutsch et al. 2014; Mon01: Montes et al. 2001; Ried14: Riedel et al. 2014. [(b)] Barr04: Barrado y Navascués et al. 2004; Barr98: Barrado y Navascués 1998; Bas96: Basri et al. 1996; Bell15: Bell et al. 2015; Gia79: Giannuzzi 1979; Mam13: Mamajek et al. 2013; SM93: Soderblom & Mayor 1993.

to have mass ratios over 0.8, while pairs at larger separations present a more homogeneous distribution.

Similar studies also show this observed trend in the relation between separation of the components and mass ratio: near equal-mass pairs (mass ratios ≥ 0.8) are found at smaller separations. Moverover, the lower the mass of the primary, the higher the mass ratio and the closer the semi-major axis at which companions are found (Jódar et al. 2013: Janson et al. 2012, 2014). The closer distance to the Sun of our sample compared to the samples of Bergfors et al. (2010) and Janson et al. (2014), who investigated the mass ratio at larger separations, may explain the difference with our results in the mass ratio distribution. However, Monte Carlo simulations of Sun-like stars and M-dwarf surveys from Duquennoy & Mayor (1991) and Raghavan et al. (2010), and Fischer & Marcy (1992) and Janson et al. (2012), respectively, suggest that the mass ratio distributions could be independent of the separation and dynamical evolution (Reggiani & Meyer 2011, 2013).

4.7. Periods and orbital motion

We derived periods for 70 systems with Kepler's third law, the masses of the components, and the maximum projected physical separations (Sect. 4.4). Since these measures are a lower limit estimate to the semi-major axis, the periods given in Table A.5 should be also considered as a lower limit.

In total, 26 systems have periods shorter than 50 a, of which 13 are known bound systems, 10 are newly discovered binaries, and three are the unconfirmed pairs J01221+221, J07349+147, and J10028+484.

Of the 26 systems, we consider four triple systems here: J05078+179, J08082+211, and J16554–083S, which are formed by a spectroscopic binary plus a third resolved component, and J23293+414S, for which we resolved the three components of the system. In addition, the "triples" J08082+211 and J16654–083S belong to a hierarchical quadruple and quintuple system, respectively, with the fourth and fifth components outside the field of view of FastCam (Sect. 4.9).

Several systems were observed repeatedly during the programme, which allowed us to perform a multi-epoch analysis. Some of them showed appreciable variation of angular separation and position angle in different epochs of our data. When these variations were larger than $3\,\sigma$ with respect to constant values of ρ and θ and were consistent with an orbital trajectory, we considered that the orbital motion of the pair was detected. Because of the large uncertainties, the variations of ρ and θ of the pairs J05333+448, J08066+558, and J20407+199 lie within $3\,\sigma$ and therefore they do not fulfil our criterion, but they show appreciable variations that are probably related to the orbital motion. However, the time baseline is not long enough to provide a precise estimate of the orbital parameters of the systems.

Table 4 lists these 16 systems, of which 13 are new. We tabulate the WDS discoverer code of the previously known pairs, the number of used epochs, the time interval between the first and last measured epoch, and the estimated periods. We show an example of one of these binaries (J12332+090) in Fig. 10.

4.8. Known close and spectroscopic binaries (not detected in our search)

In the observed sample there were also previously known pairs that we were unable to resolve because of the small separation of the components ($\rho \lesssim 0.2$ arcsec) and/or the faintness of the companion. These pairs are listed in Table 5. In addition, there were

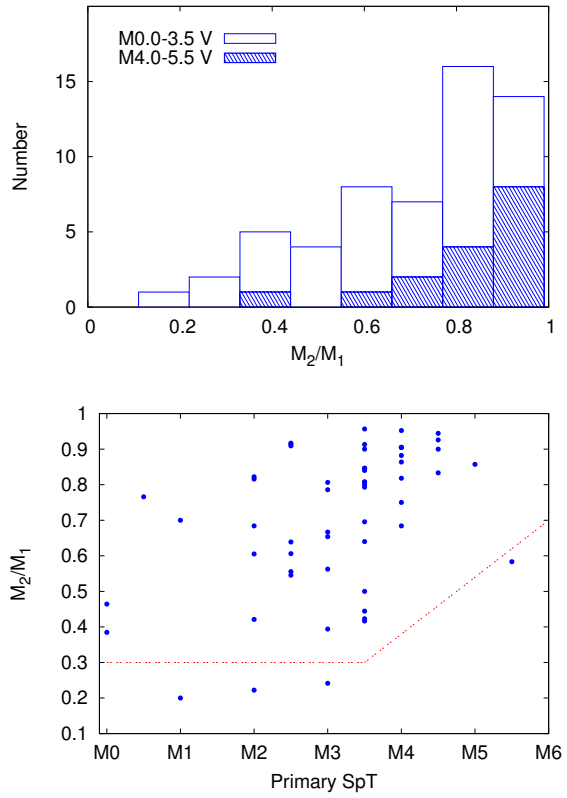

Fig. 8. *Top panel*: mass ratio distribution of our binaries. Empty and dashed bars separate the mass ratio distribution of M0.0–M3.5 and M4.0–M5.5 dwarfs. *Bottom panel*: mass ratio of the pairs vs. spectral type of the primary. The red dashed line represents the mass ratio completeness limits. The standard error of the mean mass ratio is 0.03 and the error bar is ± 0.5 in spectral type.

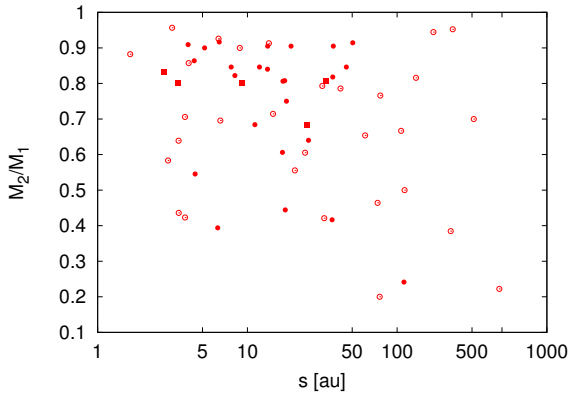

Fig. 9. Mass ratio vs. projected physical separation. Colour and symbol code is as in Fig. 3.

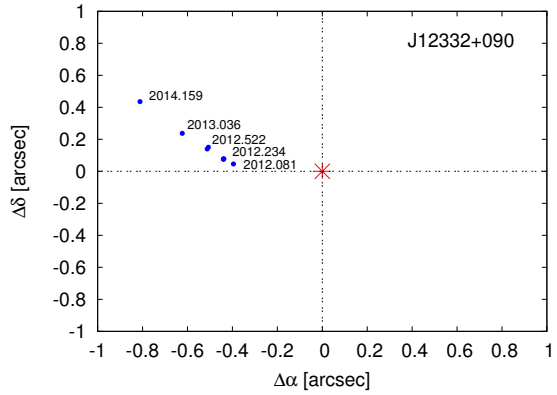

Fig. 10. Orbital variation of the pair J12332+090 from our FastCam data. The asterisk marks the position of the primary. Five of the eight epochs are labelled.

also previously known spectroscopic binaries, taken into account for the period estimation of our detected binaries in Table A.5. They are listed in Table 6.

The close multiplicity fraction of 19.5 ± 2.3 % given in Sect. 4.2 is a lower limit of the total multiplicity fraction of M dwarfs, since it only includes physical companions in the interval of angular separations between 0.2 and 5.0 arcsec. Although studies of spectroscopic binaries and very close binaries (ρ < 0.2 arcsec) are not complete, we know from the literature that we are missing 47 very close additional binaries in this range in our volume-limited sample (e.g. Delfosse et al. 2013; Schöfer et al. 2015; Tokovinin et al. 2015). This number is consistent with the fractional incidence of eclipsing binaries obtained from surveys like *Kepler* (Shan et al. 2015), and increases the given binary fraction by 11 %. Hence the multiplicity fraction at separations smaller than 5 arcsec would be at least ∼ 30 %.

4.9. Known companions at separations larger than 5 arcsec

Many of our FastCam stars have stellar or substellar companions outside the field of view of the instrument or at angular separations larger than the 5.0 arcsec cut-off defined for statistical purposes. We compiled the multiplicity information of all

Table 4. Systems with measurable orbital motion.

Karmn	WDS	Epochs	Δ*t* [a]	*P* [a]
J02518+294	...	3	4.2	130
J05068–215W	DON 93	3	1.2	62
J05078+179	...	2	1.1	50
J05333+448	BH 76	6	2.3	8.3
J06400+285	...	3	1.0	20
J08066+558	...	4	3.2	26
J08082+211	...	2	3.8	33
J08595+537	...	2	1.1	19
J11355+389	...	5	3.0	31
J11521+039	...	2	1.1	15
J12332+090	REU 1	8	2.1	16
J13180+022	...	4	3.1	73
J14210+275	...	2	3.0	97
J16487+106	...	3	1.1	10
J17530+169	...	5	3.0	110
J20407+199	RAO 23	2	2.8	8.4
J21518+136	...	3	3.0	66

Table 5. Astrometric properties of previously known imaging companions at $\rho < 5$ arcsec not resolved or detected in our data.

Karmn	WDS	Discoverer code	ρ [arcsec]	θ [deg]	Epoch [a]	Ref.[a]	Δmag (band) [mag]
J00088+208	00089+2050	BEU 1	0.133	271.9	2012.02	Jan14a	1.59 (i')
J05085–181	05086–1810	WSI 72	0.07	44.4	2011.04	WD15	0.1 (K_s)
J04311+589	...	...	0.07		1965.702	Str77	0.5 (V)
J06523–051	06523–0510	WSI 125	0.18	149.6	2010.068	Mas01	0.5 (o)
J07307+481	...	...	0.054	...	1960.60	Harr81	...
J09177+462	09177+4612	JNN 68	0.204	37.5	2011.073	Bow15	0.102 (K_s)
J10513+361	10513+3607	BWL 26	0.206	119.60	2012.357	Bow15	3.3 (H)
J12290+417	12290+4144	BWL 31	0.0503	255.5	2011.469	Bow15	0.647 (H)
J16241+483	16240+4822	HEN 1	0.1387	295.4	2006.62	Mar07	2.781 ($H_{\rm cont}$)
J16354+350[b]	16355+3501	BWL 44	0.092	25.62	2011.469	Bow15	0.406 (H)
J17177+116[c]	...	...	...	...	1977	Chr78	...
J18387–144	18387–1429	HDS 2641	0.107	358	1991	DN00	0.04 (Hp)
J19122+028	19121+0254	AST 1	0.16	319.7	2007.36	WD15	0.80 (H)
J20298+096[d]	20298+0941	AST 2	0.160	89.1	2012.66	Jan14a	2.72 (z')
J20433+553	20433+5521	LLO 1	0.854	20.2	2007.66	Ire08	5.06 (H)
J21013+332	21013+3314	JNN 288	0.142	34.0	2012.01	Jan14a	1.07 (i')
J21160+298E	21161+2951	BWL 56	0.0543	354.6	2011.47	Bow15	0.37 (H)
J21313–097	21313–0947	BLA 9	0.16	128.2	2005.33	WD15	1.12 (H)
J23174+196	23175+1937	BEU 23	0.145	220.2	2012.65	Jan14b	1.17 (J)

Notes. [a] Bow15: Bowler et al. 2015; Chr78: Christy 1978; DN00: Dommanget & Nys 2000; Harr81: Harrington et al. 1981; Ire08: Ireland et al. 2008; Jan14a: Janson et al. 2014a; Jan14b: Janson et al. 2014b; Mar07: Martinache et al. 2007; Mas01: Mason et al. 2001; Str77: Strand 1977; Tok15: Tokovinin et al. 2015; WD15: Ward-Duong et al. 2015 [b] The BWL 44 companion at 2.2 arcsec is optical. [c] Astrometric perturbation with a 10 a period estimation in Chr78. [d] Spectroscopic binary identified by Benedict et al. 2000 and resolved by Janson et al. 2014a for the first time.

of them using our observations and the WDS catalogue. Of the wide binaries present in the WDS catalogue, nearly 60 % come from the Luyten Double Star Catalogue (Luyten 1997) and the Lowell Proper Motion Survey (Giclas et al. 1971). In Table A.6, we list for each wide system the WDS discoverer code, names, spectral types, and angular separation.

As a summary, of the 490 observed stars, 50 are M-dwarf primaries with M-type wide companions, four with white dwarf companions, one with an L-dwarf, and three with a T-dwarf secondary. In addition, 11 M secondaries have F (2), G (3), K (4) or white dwarf (3) primaries. Five tertiary M dwarfs are in triple systems involving K+M (1), G+K (1), K+DA (1) or K+K (2) primaries.

In our volume-limited sample are 25 M dwarf primaries with wide M, L, or T dwarf secondaries at separations larger than 5 arcsec. Although our search at wide separations is not complete, since we carried out a compilation from different studies in the literature, we estimated an increment in the multiplicity fraction of 6 % (25 systems out of 425 M dwarfs in our volume-limited sample), which added to the percentage estimated for pairs at separations closer than 0.2 arcsec, and spectroscopic binaries would translate into a minimum multiplicity fraction at all separations of ~ 36 %.

5. Summary

We obtained high-resolution images in the I band of 490 M dwarfs of the CARMENES input catalogue (Carmencita) with the lucky imaging instrument FastCam at the 1.5 m Telescopio Carlos Sánchez.

Among the 490 observed M dwarfs, we identified 80 physically bound companions in 76 systems, of which 30 are presented here for the first time, plus six unconfirmed companions. For all of them, we measured angular separations, position angles, and I-band magnitude differences. From the ΔI differences, together with 2MASS photometry, spectral type, and colour-magnitude relations for field M dwarfs, we estimated individual I-band magnitudes and spectral types of each component. We also derived individual masses $\mathcal{M}$ and estimated orbital periods for these pairs from our own $\mathcal{M}$-M_I relation. For these calculations, we used parallactic distances. When not available, we derived spectro-photometric distances from our determined M_J-spectral type relation.

For our observed sample, we determined a multiplicity fraction of 16.7 ± 2.0 %. However, our sample has a strong selection bias because we discarded M stars with previously known companions at separations smaller than 5 arcsec. To obtain an unbiased multiplicity fraction, we built a volume-limited sample of Carmencita stars observed with FastCam and similar high-resolution imagers. It contains 425 M0–5 dwarfs and is complete up to 86 % within 14 pc. For this sample, we derived a multiplicity fraction of 19.5 ± 2.3 % in the completeness range of angular separations between 0.2 and 5.0 arcsec, which agrees with previously reported values (Leinert et al. 1997; Janson et al. 2012, 2014; Jódar et al. 2013; Ward-Duong et al. 2015). The multiplicity fraction is consistent with a flat distribution from M0 V to M5 V within Poissonian error bars, and has intermediate values between solar-type stars and very low mass stars and brown dwarfs in accordance with the decreasing tendency observed towards lower masses.

The distribution of the number of pairs as a function of projected physical separation has a maximum between 2.5 and 7.5 au and decreases at wider separations. The pairs with projected physical separations smaller than 50 au tend to have mass ratios higher than 0.8, while for larger separations this distribution is more uniform.

Table 6. Known spectroscopic binaries in the observed sample.

Karmn	Spectroscopic binarity	Ref.[a]
J03346–048	SB3	Llam14
J03526+170	SB2	Bon13
J04252+080S	SB2	Llam14
J04352–161	SB2	RB09
J04488+100	SB2	Jeff16
J05019+099	SB2	Del99
J05032+213	SB2	Jeff16
J05078+179	SB1	Jeff16
J05342+103S[b]	SB	Rein12
J05466+441	SB2	Jeff16
J07418+050	SB2	Llam14
J08082+211	SB2	Shk10
J09011+019	SB2	Jeff16
J09120+279	SB2	Jeff16
J09143+526	SB1	Jeff16
J11036+136	SB1	Jeff16
J12142+006	SB2	Bon13
J12191+318	SB2	Jeff16
J12290+417	SB2	Jeff16
J14171+088	SB2	Jeff16
J14368+583	SB2	Jeff16
J15191–127	SB	Bon13
J16255+260	SB2	Jeff16
J16487+106	SB2	Jeff16
J16554-083S	SB	Pett84
J18411+247S	SB2	GR96
J19354+377	SB1	Jeff16
J20433+553	SB2	Ire08
J20445+089N[c]	SB1	Jeff16
J23096–019	SB2	Jeff16
J23174+382	SB2	Jeff16
J23318+199E	SB1	Del99
J23318+199W	SB1	Del99
J23573–129W	SB2	Jeff16

Notes. [(a)] Bon13: Bonfils et al. 2013; Del99: Delfosse et al. 1999; GR96: Gizis & Reid 1996; Ire08: Ireland et al. 2008; Jeff16: Jeffers et al. in prep; Llam14: Llamas 2014; Pett84: Pettersen et al. 1984; RB09: Reiners & Basri 2009; Rein12: Reiners et al. 2012; Shk10: Shkolnik et al. 2010 [(b)] From the spectral types and magnitude differences of the components, we infer that the spectroscopic binary is the B companion. [(c)] Equal-brightness close binary previously suggested by Cortés-Contreras et al. 2014.

We estimated that 26 of our systems have orbital periods shorter than 50 a, of which 10 are newly discovered systems. In 17 of them, we were able to detect orbital variations within our own multi-epoch measurements. These systems are especially interesting for future astrometric follow-up for determining their orbital solutions and measuring dynamical masses.

For our volume-limited sample, we also collected from the literature the physically bound companions at separations closer than 0.2 arcsec and larger than 5 arcsec, and unresolved spectroscopic binaries. The addition of these systems may increase the multiplicity fraction derived in this work to at least 36 %, a value consistent with the 42 ± 9 % obtained by Fischer & Marcy (1992). Nevertheless, the sample is not complete at separations beyond the completeness limit of our survey (0.2–5.0 arcsec) and, hence, this value must only be considered as a rough estimation.

Finally, we provided a complete sample of multiple M dwarfs useful for studying the effect of low-mass stellar multiplicity on planet formation with the help of CARMENES and other near-infrared high-resolution spectrographs.

Acknowledgements. We thank A. Pérez-Garrido for the provision and support of the FastCam reduction software and X. Bonfils for the supply of radial velocity measurements from the ESO HARPS GTO Program ID 072.C-0488. MCC thanks L. Peralta de Arriba, V. Pereira and H. M. Tabernero for their assistance and valuable conversations. This article is based on observations made with the Telescopio Carlos Sánchez operated on the island of Tenerife jointly by the Instituto de Astrofísica de Canarias and the Universidad de La Laguna in the Spanish Observatorio del Teide. This research made use of SIMBAD, operated at Centre de Données astronomiques de Strasbourg (France), the NASA's Astrophysics Data System, the Washington Double Star catalogue (WDS) maintained at the U.S. Naval Observatory, and the Image Reduction and Analysis Facility (IRAF), distributed by the National Optical Astronomy Observatory and operated by the Association of Universities for Research in Astronomy (AURA) under a cooperative agreement with the National Science Foundation. CARMENES is funded by the German Max-Planck-Gesellshaft (MPG), the Spanish Consejo Superior de Investigaciones Científicas (CSIC), the European Union through FEDER/ERF funds, and the members of the CARMENES Consortium (Max-Planck Institut für Astronomie, Instituto de Astrofísica de Andalucía, Landessternwarte Königstuhl, Institut de Ciènces de l'Espai, Institut für Astrophysik Göttingen, Universidad Complutense de Madrid, Thüringer Landessternwarte Tautenburg, Instituto de Astrofísica de Canarias, Hamburger Sternwarte, Centro de Astrobiología, and the Centro Astronómico Hispano-Alemán), with additional contributions by the Spanish Ministry of Economy, the state of Niedersachsen, the German Science Foundation (DFG), and by the Junta de Andalucía. Financial support was also provided by the Junta de Andalucía, and the Spanish Ministries of Science and Innovation and of Economy and Competitiveness, under grants 2011-FQM-7363, AP2009-0187, AYA2014-54348-C3-01/02/03-R, AYA2015-69350-C3-2-P, ESP2013-48391-C4-1-R, and ESP2014-57495-C2-2-R.

References

Aberasturi, M., Caballero J. A., Montesinos B. et al. 2014, AJ, 148, 36
Aitken, R. G. & Doolittle, E. 1932, *New general catalogue of double stars within 120° of the north pole*, Carnegie Institution of Washington, USA
Alonso-Floriano, F. J., Morales, J. C., Caballero, J. A. et al. 2015, A&A, 577, A128
Alonso-Floriano, F. J., Caballero, J. A., Cortés-Contreras, M., Solano, E. & Montes, D. 2015, A&A, 583, A85
Amado, P. J. Quirrenbach, A., Caballero, J. A. et al. 2013, Highlights of Spanish Astrophysics VII, 842
Ansdell, M., Gaidos, E., Mann, An. W. et al. 2015, ApJ, 798, 41
Artigau, E., Kouach, D., Donati, J.-F. et al. 2014, Proc. SPIE, 9147, E15
Baraffe, I., Homeier, D., Allard, F. & Chabrier, G. 2015 A&A, 577, A42
Barrado y Navascués, D. 1998, A&A, 339, 831
Barrado y Navascués, D., Stauffer, J. R. & Jayawardhana, R. 2004,ApJ, 614, 38
Basri, G., Marcy, G. W. & Graham, J. R. 1996, ApJ, 458, 600
Basri, G. & Reiners, A. 2006, AJ, 132, 663
Bate, M. R. 2012, MNRAS, 419, 3115
Behall, A.L. & Harrington, R.S. 1976, PASP 88, 204
Béjar, V. J. S., Gauza, B., Caballero, J. A. et al. 2012, 17th Cambridge Workshop on Cool Stars, Stellar Systems, and the Sun, published on-line
Bell, C. P., Mamajek, E. E. & Naylor, T. 2015, MNRAS, 454, 593
Benavides, R. 2014, *El Observador de Estrellas Dobles*, 12, 21
Benedict, G. F., McArthur, B. E., Franz, O. G. et al. 2000, AJ, 120, 1106
Bergfors, C., Brandner, W., Janson, M. et al. 2010, A&A, 520, A54
Beuzit, J.-L., Ségransan, D., Forveille, T. et al. 2004, A&A, 425, 997
Bihain, G., Rebolo, R., Zapatero Osorio, M. R. et al. 2010, A&A, 519, A93
Bonfils, X., Delfosse, X., Udry, S. et al. 2013, A&A, 549, A109
Bonnarel, F., Fernique, P., Bienaymé, O. et al. 2000, A&AS, 143, 33
Bouy, H., Brandnder, W., Martín, E. L. et al. 2003, AJ, 126, 1526
Bowler, B. P., Liu, M. C., Shkolnik, E. L. & Tamura, M. 2015, ApJS, 216, 7
Burgasser, A. J., Kirkpatrick, J. D., Reid, I. N. et al. 2003, ApJ, 586, 512
Burgasser, A. J., Reid, I. N., Siegler, N. et al. 2007, Protostars and Planets V, 427
Caballero, J. A. 2007, ApJ, 667, 520
Caballero, J. A. 2010, A&A, 514, A98
Caballero, J. A., Cortés-Contreras, M., López-Santiago, J. et al. 2013, Highlights of Spanish Astrophysics VII, 645
Charbonneau, D., Berta, Z. K., Irwin, J. et al. 2009, Nature, 462, 891
Christy, J. M. 1978, AJ, 83, 10

Cortés-Contreras, M., Caballero, J. A., Alonso-Floriano, F. J. et al. 2013, Highlights of Spanish Astrophysics VII, 646
Cortés-Contreras, M., Caballero, J. A. & Montes, D. 2014, The Observatory, 134, 348
Cortés-Contreras, M., Béjar, V. J. S., Caballero, J. A. et al. 2015, Highlights of Spanish Astrophysics VIII, 597
Cortés-Contreras, M., Caballero, J. A., Béjar, V. J. S. et al. 2015, 18th Cambridge Workshop on Cool Stars, Stellar Systems, and the Sun, 805
Close, L. M., Siegler, N., Freed, M. & Biller, B. 2003, ApJ, 587, 407
Cruz, K. L., Reid, I. N., Liebert, J. et al. 2003, AJ, 126, 2421
Dawson, P. C. & De Robertis, M. M. 2005, PASP 117, 1
Deacon, N. R., Liu, M. C., Magnier, E. A. et al. 2012, ApJ, 757, 100
Delfosse, X., Forveille, T., Beuzit, J.-L. et al. 1999, A&A, 344, 897
Desidera, S., Carolo, E., Gratton, R. et al. 2011 A&A, 533, A90
Dieterich, S. B., Henry, T. J., Golimowski, D. A. et al. 2012, AJ, 144, 64
Dittmann, J. A., Irwin, J. M., Charbonneau, D. & Berta-Thompson, Z. K. 2014, ApJ 784, 156
Dommanget, J. & Nys, O. 2000, A&A, 363, 991
Duchêne, G. & Kraus, A. 2013, ARA&A, 51, 269
Duquennoy, A. & Mayor, M. 1991, A&A, 248, 485
Fischer, D. A. & Marcy, G. W. 1992, ApJ, 396, 178
Freedman, D & Diaconis, P. 1981, *Probability Theory and Related Field*, 57, 4, 453
García-Piquer, A., Morales, J. C., Ribas, I. et al. 2016, A&A, submitted
Gatewood, G. & Coban, L. 2009, AJ, 137, 402
Giannuzzi, M. A. 1979, A&A, 77, 214
Giclas H. L., Burnham Jr. R. & Thomas N.G. 1971, *Lowell proper motion survey Northern Hemisphere*, Lowell Observatory, Flagstaff, Arizona
Gigoyan, K. S., Sinamyan, P. K., Engels, D. & Mickaelian, A. M. 2010, Astrophysics, 53, 123
Ginski, C., Mugrauer, M., Seeliger, M. et al. 2015, MNRAS, 457, 2173
Gizis J. E. & Reid I. N. 1996 AJ, 111, 365
Gizis, J. E., Reid, I. N. & Hawley, S. L. et al. 2002, AJ, 123, 3356
Goldman, B., Bouy, H., Zapatero Osorio, M. R. et al. 2008, A&A, 490, 763
Goodwin, S. P., Kroupa, P., Goodman, A. & Burkert, A. 2007, Protostars and Planets V, 133
Gray, R. O., Corbally, C. J., Garrison, R. F. et al. 2003, AJ, 126, 2048
Gray, R. O., Corbally, C. J., Garrison, R. F. et al. 2006, AJ, 132, 161
Guenther, E. W. & Wuchterl, G. 2003, A&A, 401, 677
Guenther, E. W. & Tal-Or, L. 2010, A&A, 521, A83
Hartkopf, W. I. & Mason, B.D. 2011, AJ, 142, 56
Harrington, R. S. & Dahn C. C. 1980, AJ, 85, 454
Harrington, R. S., Christy, J. W. & Strand, K. A. 1981, AJ, 86,909
Hawley, S. L., Gizis, J. E. & Reid, I. N. 1996, AJ, 112, 2799
Henry, T. J. 2004, ASPC, 318, 159
Henry, T. J., Jao, W.-C, Subasavage, J. P. et al. 2006, AJ, 132, 2360
Hershey, J. L. & Taff, L. G. 1998, AJ, 116, 1440
Ireland, M. J., Kraus, A., Martinache, F. et al. 2008 ApJ, 678, 463
Jeffries, R. D. & Maxted, P. F. L. 2005, AN, 326, 944
Janson, M., Hormuth, F., Bergfors, C. et al. 2012, ApJ, 754, 44
Janson, M., Lafrenière, D., Jayawardhana, R. et al. 2013, ApJ, 773, 170
Janson, M., Bergfors, C., Brandner, W. et al. 2014, ApJ, 789, 102
Janson, M., Bergfors, C., Brandner, W. et al. 2014, ApJS, 214, 17
Jenkins, L. F. 1952, *General catalogue of trigonometric stellar parallaxes*, Yale University Observatory, USA
Jenkins, L. F. 1963, *General catalogue of trigonometric stellar parallaxes*, Yale University Observatory, USA
Jenkins, J. S., Ramsey, L. W., Jones, H. R. A. et al. 2009 ApJ, 704, 975
Joergens, V. 2008, A&A, 492, 545
Jódar, E., Pérez-Garrido, A., Díaz-Sánchez, A. et al. 2013, MNRAS, 429, 859
Kirkpatrick, J. D. & McCarthy, D. W. Jr 1994, AJ, 107, 333
Klutsch, A., Freire Ferrero, R., Guillout, P. et al. 2014, A&A, 567, A52
Koen, C., Kilkenny, D., van Wyk, F. & Marang, F. 2010, MNRAS, 403, 1949
Labadie, L., Rebolo, R., Femenía, B. et al. 2010, Proc. SPIE, 7735, E0X
Lafrenière, D., Doyon, R., Marois, C. et al. 2007, ApJ, 670, 1367
Law, N. M. 2006, PhD thesis, Institute of Astronomy & Selwyn College, Cambridge University, UK
Law, N. M., Hodgkin, S.T. & Mackay, C. D. 2008, MNRAS, 384, 150
Leinert, C., Henry, T., Glindemann, A. & McCarthy, D. W. Jr. 1997, A&A, 325, 159
Lépine, S., Hilton, E. J., Mann, A. W. et al. 2013 AJ, 145, 102
Llamas, M. 2014, MSc thesis, Universidad Complutense de Madrid, Spain
Losse, F. 2010, Observations & Travaux, 75, 17
Luhman, K. L. 2012, ARA&A, 50, 65
Luyten, W. J. 1997, VizieR Online Data Catalog I/130, *LDS Catalogue: Doubles with Common Proper Motion (Luyten 1940-87)*, Originally published in: Publ. Astr. Obs. Univ. Minnesota III, part 3, 35, and Proper motion survey with the 48-inch Schmidt Telescope XXI, XXV, XIX, XL, L, LXIV, LV, LXXI, Univ. Minnes. (1940-1987)
Mahadevan, S., Ramsey, L. W., Terrien, R. et al. 2014, Proc. SPIE, 9147, E1G
Mamajek, E. E., Bartlett, J. L., Seifahrt, A. et al. 2013, AJ, 146, 154
Martinache, F., Lloyd, J. P., Ireland, M. J. et al. 2007, ApJ, 661, 496
Mason, B. D., Wycoff, G. L., Hartkopf, W. I., Douglass G. G. & Worley C.E. 2001, AJ, 122, 3466
Mason, B. D., Hartkopf, W. I. & Friedman, E. A. 2012, AJ, 143,124
Mason, B. D., Hartkopf, W. I. & Hurowitz, H. M. 2013, AJ, 146, 56
Montagnier, G., Ségransan, D., Beuzit, J.-L., et al. 2006 A&A, 460, L19
Montes, D., López-Santiago, J., Gálvez, M. C. et al. 2001, MNRAS, 328, 45
Montes, D., Caballero, J. A., Jeffers, S. et al. 2015, Highlights of Spanish Astrophysics VIII, 605
Montes, D., Caballero, J. A., Gallardo, I. et al. 2016, IAUS, 314, 71
Morrison, J. E., Röser, S., McLean, B. et al. 2001, AJ, 121, 1752
Newton, E. R., Charbonneau, D., Irwin, J., et al. 2014, AJ, 147, 20
Oscoz, A., Rebolo, R., López, R. et al. 2008, Proc. SPIE, 7014, E47
Peña-Ramírez, K., Béjar, V. J. S. & Zapatero Osorio, M. R. 2016, A&A, 586, A157
Pettersen, B.R, Evans, D.S. & Coleman, L.A. 1984, ApJ, 282, 214
Quirrenbach, A., Amado, P. J., Caballero, J. A., et al. 2014, Proc. SPIE, 9147, E1F
Quirrenbach, A., Caballero, J. A., Amado, P. J. et al. 2015, 18th Cambridge Workshop on Cool Stars, Stellar Systems, and the Sun, 18, 897
Raghavan, D., McAlister, H. A., Henry, T. J. et al. 2010, ApJS, 190, 1
Reggiani, M. & Meyer, M. R. 2011, ApJ, 738, 60
Reggiani, M. & Meyer, M. R. 2013, A&A, 553, A124
Reiners, A. & Basri, G. 2009, ApJ, 705, 1416
Reiners, A., Joshi, N. & Goldman, B. 2012, AJ, 143, 93
Reid, I. N., Hawley, S. L. & Gizis, J. E. 1995, AJ, 110, 1838
Reid, I. N. & Gizis, J. E. 1997, AJ, 113, 2246
Reid, I. N. & Cruz, K. L. 2002, AJ, 123, 2806
Reid, I. N., Cruz, K. L., Burgasser, A. J. et al. 2004, AJ, 128, 463
Reid I. N., Cruz, K. L., Burgasser, A. J. & Liu. M. C. 2008, AJ, 135, 580
Riedel, A. R., Subasavage, J. P., Finch, C. T. et al. 2010, AJ, 140, 897
Riedel, A. R., Finch, C. T., Henry, T. J. et al. 2014, AJ, 147,85
Riaz, B., Gizis, J. E. & Harvin, J. 2006, AJ, 132, 866
Röser, S., Demleitner, M. & Schilbach, E. 2010, AJ, 139, 2440
Rivera, E. J., Lissauer, J. J., Butler, R. P. et al. 2005, ApJ, 634, 625
Sarajedini, A., Bedin, L. R., Chaboyer, B. et al. 2007, AJ, 133, 1658
Scardia, M., Ghiringhelli, D. & Debehogne, H. 1995, AN, 316, 125
Scardia, M., Prieur, J. L., Pansecchi, L., Argyle, R.W. & Sala, M. 2011, AN, 332, 508
Scardia, M., Prieur, J. L., Pansecchi, L. et al. 2013, MNRAS, 434, 2803
Schlimmer, J. S. 2013, Journal of Double Star Observations, 9, 230
Schöfer, P. 2015, MSc thesis, Institut für Astrophysick Göttingen, Germany
Scholz, R.-D., Meusinger, H. & Jahrei*β*, H. 2005, A&A, 442, 211
Shan, Y., Johnson, J. A. & Morton, T. D. 2015, ApJ, 813, 75
Shkolnik, E. L., Hebb, L., Liu, M. C. et al. 2010, ApJ, 716, 1522
Siegler, N., Close, L. M., Cruz, K. L. et al. 2005, ApJ, 621, 1023
Silvestri, N. M., Hawley, S. L., Oswalt, T. D. 2005, AJ, 129, 2428
Simon-Díaz, S., Caballero, J. A., Lorenzo, J. et al. 2015, ApJ, 799, 169
Soderblom, D. R., & Mayor, M. 1993, AJ, 105, 226
Strand K. Aa. 1977, AJ, 82, 9
Subasavage, J. P., Jao, W.-C., Henry, T. J. et al. 2009, AJ, 137, 4547
Tamura, M., Suto, H., Nishikawa, J. et al. 2012, Proc, SPIE, 8446, E1T
Thorel, J. C., Thorel, Y. & Verhas, P. 2011, Observations & Travaux 78, 20
Tody, D. 1986, Proc. SPIE, 627, 733
Tokovinin, A. 2008, MNRAS, 389, 925
Tokovinin, A. 2011. AJ, 141, 52
Tokovinin, A., Mason, B. D., Hartkopf, W. I. et al. 2015, AJ, 150, 50
van Altena, W. F., Lee, J. T. & Hoffleit, D. 1995, *General catalogue of trigonometric stellar parallaxes*, Yale University Observatory, USA
van Leeuwen, F. 2007, A&A, 474, 653
Wang, J., Xie, J.-W., Barclay, T. & Fischer, D. A. 2014a, ApJ, 783, 4
Wang, J., Fischer, D. A., Xie, J.-W. & Ciardi, D. R. 2014b ApJ 791, 111
Wang, J., Fischer, D. A., Horch, E. P. & Xie, J.-W 2015a, ApJ, 806, 248
Wang, J., Fischer, D. A., Xie, J.-W & Ciardi, D. R. 2015b, ApJ, 813, 130
Weinberger, A. J., Boss, A. P., Keiser, S. A. et al. 2016, AJ, 152, 24
Ward-Duong, K., Patience, J., De Rosa, R. J. et al. 2015, MNRAS, 449, 2618
Zuckerman B. & Song I. 2014, ARA&A, 42, 685

5

Search for wide companions in Carmencita

In previous chapters, M dwarfs have been the subject of multiplicity studies at wide separations (up to ~ 300 arcsec) in Chapter 3, and at short separations (down to 0.2 arcsec) in Chapter 4. This chapter addresses the search of companions at much wider separations to our Carmencita stars.

5.1 Introduction

The presence of low mass stars in binary and multiple systems at any range of physical separations is widely under study (see Chapter 4 for short separations, and Latham et al. 1984, Caballero 2007 or Alonso-Floriano et al. 2015 for lager separations). Binaries at wide separations are of high interest, specially in the low mass regime, since their properties are related to their formation scenarios, which could be different for different binary constraints.

The maximum separation of a system depends on the total mass capable of sustaing gravitational binding. This separation is set at around $2\,10^4$ au, which translates into ~ 0.1 pc (Weinberg et al. 1987; Close et al. 1990; Tokovinin & Lépine 2012), although it could reach $\sim 2\,10^5$ au (near 1 pc) or more (Caballero 2009; Shaya & Olling 2011). It is not easy to disentangle whether a very wide pair is physically bound or not, since observing orbital motion would take thousands of years. In these cases, parameters such as the distance, the radial velocity or activity/youth indicators could help. Besides, there is not a clear separation between wide pairs with low binding energies and common proper motion pairs. As an example, Carmencita contains one of the widest systems involving low mass stars. It was discovered by Shaya & Olling (2011), and the maximum separation between components reaches 1.02 pc. It is composed by a K6 primary (HD 221503), an M2.0 close binary (J23327-167 AB) and an M3.0 double lined spectrscopic binary (J23302-206 AB). A sketch of the system is shown in Fig. 5.1. Only a few substellar companions to M dwarfs have been found at separations larger than 40 au (e.g. TWA 5 b, c, Lowrance et al. 1999; G196-3B, Rebolo et al. 1998; GJ 1001B, Goldman et al. 1999; G1 229B, Nakajima et al. 1995; LP 261-75B, Burgasser et al. 2005, Reid & Walkowicz 2006; GJ 618.1B, Wilson et al. 2001; G203-050B, Radigan et al. 2008), despite the searches that have been carried out (Oppenheimer et al. 2001; Hinz et al. 2002; McCarthy & Zuckerman 2004; Allen & Reid 2008; Daemgen et al. 2007). Also the searches around very low mass stars ($\mathcal{M} \leq 0.1\,\mathrm{M}_\odot$) have provided sparse results (Burgasser et al. 2007; Caballero 2007; Radigan et al. 2009).

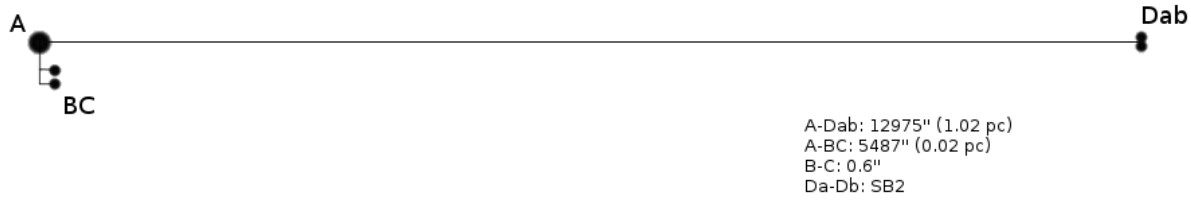

FIGURE 5.1— Sketch of the widest system in Carmencita HD 221503 ⊕ J23327-167 BC ⊕ J23302-206 Dab.

In this chapter, I describe a common proper motion search carried out for the Carmencita stars with the Virtual Observatory tools STILTS and Topcat, and a self-built python code. The employed method is detailed in Section 5.2.1. It goes from the initial search around our M dwarfs to the cleaning of the sample. The astrometric and photometric analyses are described in Section 5.2.4, and the results and discussion are presented in Section 5.3.

5.2 Analysis

5.2.1 Search of companion candidates

I looked for common proper motion companions to our Carmencita stars at a maximum separation (s) of 10^4 au. To this purpose, I used the compiled and measured proper motions and distances from Carmencita (see Tables B.2 and B.3 in Appendix B for values and references). With the script provided by Enrique Solano, which makes use of the Virtual Observatory tool *Starlink Tables Infrastructure Library Tool Set* (STILTS; Taylor 2006), I looked for stars with similar proper motions in the PPMXL (Roeser et al. 2010), APOP (Qi et al. 2015), and UrHip (Frouard et al. 2015) proper motion catalogues. I defined a radius of 10^4 au centered in our star and converted it to angular separations (ρ) from $\rho = s/d$. The reason of comparing the three catalogues was to include possible corrections to the PPMXL catalogue, since UrHip and APOP have been recently published, as well as provide higher precision in the proper motion determinations. The accuracy of PPMXL ranges from 4 to more than 10 mas a^{-1}, of UrHip is around 0.35 mas a^{-1}, and of APOP ranges from less than 4 to 9 mas a^{-1}. The three of them have a limiting magnitude of $R \sim 18$ mag ($V \sim 20$ mag).

I applied the following selection criteria to the search:

- The proper motion of the Carmencita star must be $\mu \geq 30$ mas a^{-1}. In this way, I avoided the high number of spurious potential candidates that would result for the slowest targets. This criterium discarded six stars with lower proper motions in the Carmencita sample, and defined the sample of the search in 2170 M dwarfs.

- The relative difference between the total proper motion of our target (μ_1)and of the potencial candidate (μ_2), defined as:

$$\Delta\mu = \left|\frac{\mu_1 - \mu_2}{\mu_1}\right|, \tag{5.1}$$

must be less than 0.2 (20%). The same condition was applied in the position angle, defined as:

$$\phi = \mathrm{atan2}(\mu_\alpha \cos\delta, \mu_\delta), \tag{5.2}$$

where μ_α and μ_δ are the right ascension and declination components of the proper motion.

- I considered only companions brighter than $J = 15.5$ mag, since faint infrared sources are also faint in the optical, and are close to the magnitude limits of the proper motion catalogues used here. Besides, the fainter the target, the larger the astrometric errors in proper motions. On the contrary, this selection prevents us from detecting "ultra-low mass" companions.

At the given distances, the search radii covered from 2 to $\sim$90 arcmin, and the mean search radius was 10 arcmin.

5.2.2 Candidates clean-up

In a first instance, the common proper motion candidates obtained from each of the three catalogues were independent. Thus, I obtained 674 PPMXL companion candidates to 470 Carmencita stars, 109 APOP companion candidates to 95 Carmencita stars, and 266 UrHip companion candidates to 213 Carmencita stars. They summed 1049 candidates in total. For each independent table, I checked the Washington Double Star catalogue (WDS; Mason et al. 2001, 2015) and found that:

– From the PPMXL companion candidates list, 228 sources belonged to 172 known systems tabulated in the WDS, and 23 were spurious data. There remained 423 companion candidates to 266 Carmencita stars.

– From the APOP companion candidates list, 49 stars belonged to 36 known systems tabulated in the WDS, and two were spurious sources. There remained 58 companion candidates to 52 Carmencita stars.

– From the UrHip companion candidates list, 113 sources were known companions in 75 systems in the WDS, 42 were spurious data, and 111 were companion candidates to 105 stars.

After the identification of spurious candidates (i.e., background sources or with several entries for the same catalogue) in a first glance and of the known WDS systems, the number of companion candidates for further anaysis was 592 ($423 + 58 + 111$). For the proper analysis, all the candidates were put together. I eliminated duplicities among catalogues. It was the case of 51 companion candidates. However, in the remaining 543 candidates to 343 dwarfs, there still are spurious sources, mostly from PPMXL (this catalogue shows in many cases several entries for the same source). They were identified and removed in the next step.

5.2.3 Selection of common proper motion candidates

The total proper motion of a star has the form of the quadratic sum of the components in right ascension and declination. Hence, I applied a selection criterium over these components separately:

- For stars with $\mu < 100$ mas a^{-1}:

$$\begin{aligned} \Delta\mu_\alpha &= \left|\frac{\mu_{\alpha_1} - \mu_{\alpha_2}}{\mu_{\alpha_1}}\right| \leq 0.50 \\ \Delta\mu_\delta &= \left|\frac{\mu_{\delta_1} - \mu_{\delta_2}}{\mu_{\delta_1}}\right| \leq 0.50 \end{aligned} \tag{5.3}$$

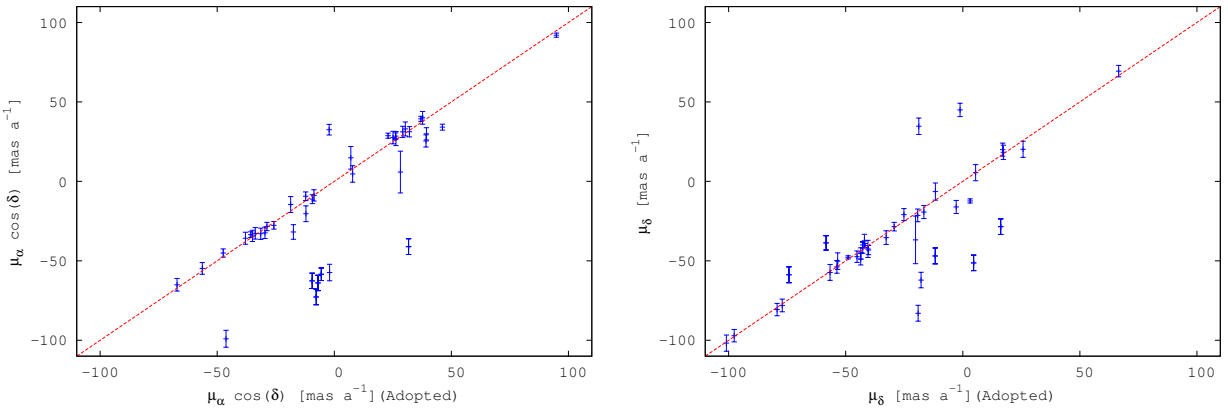

FIGURE 5.2— Comparative diagrams of the right ascension and declination components of the proper motion between PPMXL and the computed values in this work.

- For stars with $\mu \geq 100\,\mathrm{mas\,a^{-1}}$:

$$\begin{aligned} \Delta\mu_\alpha &= \left|\frac{\mu_{\alpha_1} - \mu_{\alpha_2}}{\mu_{\alpha_1}}\right| \leq 0.30 \\ \Delta\mu_\delta &= \left|\frac{\mu_{\delta_1} - \mu_{\delta_2}}{\mu_{\delta_1}}\right| \leq 0.30 \end{aligned} \tag{5.4}$$

where μ_α and μ_δ are the right ascension and declination components of the proper motion of the Carmencita star (1) and the companion candidate (2).

The number of companion candidates was reduced from 543 to 213: 45 stars with $\mu < 100\,\mathrm{mas\,a^{-1}}$ and 167 stars with $\mu \geq 100\,\mathrm{mas\,a^{-1}}$. For the slowest 45 candidate systems, I computed the proper motions of the potential companions as in Chapter 2. In some cases, they differed from the tabulated PPMXL values due to the slow motion and the possible mixing with another close star in populated fields. Fig. 5.2 compares the literature values of the proper motions with my computed values for these stars. Again, I applied the criteria in Eq. 5.3 with the new proper motions and discarded 19 candidates. Thus, there were 26 potential candidates to 23 Carmencita stars for further study with $\mu < 100\,\mathrm{mas\,a^{-1}}$.

Regarding the candidate systems with $\mu \geq 100\,\mathrm{mas\,a^{-1}}$ and their associated errors, I cut at $\delta\mu = 4\,\mathrm{mas\,a^{-1}}$ and computed the proper motions of the stars with higher $\delta\mu$. PPMXL fails in dense fields and points to background objects with fake high proper motions. Of the 40 companion candidates with $\delta\mu \geq 4\,\mathrm{mas\,a^{-1}}$, 35 were spurious points. The high number of invalid canditates made me mistrust the rest of the data. I therefore downed the cut to $1 < \delta\mu < 4\,\mathrm{mas\,a^{-1}}$. Of the 20 candidates with errors in this interval, five were associated to known bound systems not recognized before, four were associated to the Carmencita target of search whose coordinates differed from the 2MASS J2000.0 reference coordinates, and five were spurious candidates. The remaining six stars were potencial common proper motion candidates to our Carmencita stars. Of the 108 remaining sources with $\mu \geq 100\,\mathrm{mas\,a^{-1}}$ and $\delta\mu \leq 1\,\mathrm{mas\,a^{-1}}$, nine were spurious sources. Then, the six targets with $1 < \delta\mu < 4\,\mathrm{mas\,a^{-1}}$, together with the previously five sources with $\delta\mu \geq 4\,\mathrm{mas\,a^{-1}}$, and the valid sources with $\mu \geq 100\,\mathrm{mas\,a^{-1}}$ and $\delta\mu \leq 1\,\mathrm{mas\,a^{-1}}$, make 110 high proper motion companion candidates. In addition, accounting for the 26 candidates with $\mu < 100\,\mathrm{mas\,a^{-1}}$, we finally have 136

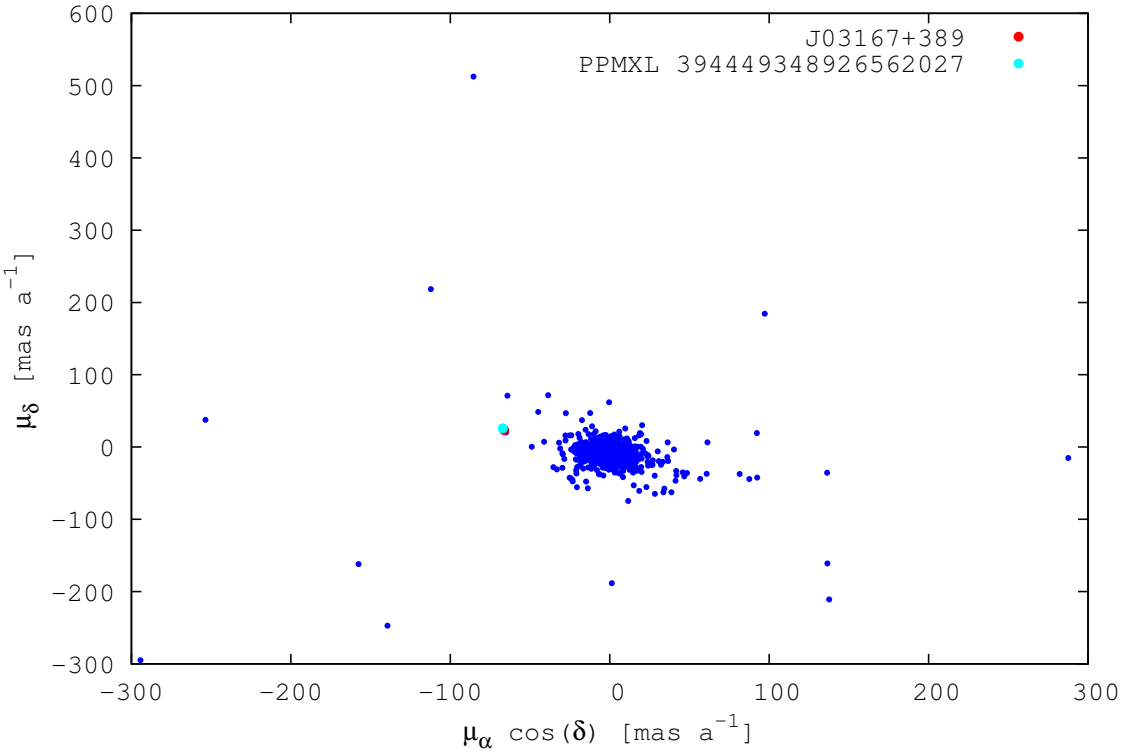

FIGURE 5.3— Proper motion diagram of all PPMXL sources in a 30 arcmin-radius circular area centered on J03167+389 (HAT 168–01565; dark blue filled circles). The red filled circle is the Carmencita dwarf and the light blue filled circle is the companion candidate.

potential common proper motion companions to 132 dwarfs.

Of the 136 potential candidates, 28 stars had a WDS entry with a measured angular separation to the companion not consistent with the tabulated value in the catalogue. A detailed inspection revealed that 11 of the 28 candidates were actually the Carmencita targets themselves with coordinates at a more recent epoch, 16 were associated to known binary systems and one was a real common proper motion candidate. Hence, the 136 potential companions reduced to 109 sources. The non identification of some WDS companions in previous steps was due to the difference of angular separations between the tabulated value and the separation measured from the 2MASS coordinates of our target and the coordinates of the companion candidate of the proper-motion catalogue. This happend more often in high proper motion stars or in fields with very bright and relatively close sources.

I cross-matched the coordinates of the PPMXL, UrHip, and APOP candidates with the 2MASS catalogue and found that 67 UrHip and four PPXML high proper motion candidates refered in fact to the Carmencita target itself. This was not noticed previously due to the non-zero separation of the position of the star in the proper motion catalogue and our target centered on the 2MASS coordinates, as explained before. This is mainly observed among the UrHip candidates, which have a more recent astrometry (2012.3-2014.6 from URAT1). It translates into a mean angular separation of 15 arcsec for proper motions of 1000 mas a^{-1}. Any companion at that angular separation was difficult to have been previously mis-identified, but I preferred to check them individually to ensure that I did not discard any potential candidate by mistake. This left 38 common proper motion

candidates to 34 Carmencita M dwarfs.

5.2.4 Proper motion and photometric analysis

To see the positions of the Carmencita stars and their candidates in a proper motion diagram, I plotted for each pair all the stars in the field at a 30 arcmin-radius from the Carmencita star. Fig. 5.3 shows the proper motion diagram of J03167+389 (HAT 168–01565) and its potential companion as an example. Diagrams corresponding to the rest of the candidates are displayed in Fig. D.1–D.14 and D.15–D.33 in Appendix D.

I took advantage of the kinematics and age information compiled in Carmencita, i.e., the association of M dwarfs to stellar kinematic groups or to the young Galactic disc (see Section 2.7 in Chapter 2). Among the 34 Carmencita dwarfs, there are confirmed or likely members to young stellar kinematics groups. Table 5.1 summarizes these groups and the number of stars belonging to them. In Appendix D, Table D.1 lists the 34 Carmencita stars, their distances, proper motions, kinematic associations and references, and Table D.2 contains the 38 candidate companions with their coordinates and proper motions.

To determine whether the candidate companions are true companions to our M dwarfs, I made use of the M_J vs. $J - K_s$ diagram and the BT-Settl evolutionary models from the Lyon group (Baraffe et al. 2015) at different ages. The J and K_s magnitudes were obtained from 2MASS, and the M_J absolute magnitude was computed using the distances from Carmencita. For the candidate companions, I used the same distance as the Carmencita star. If they are true companions, they are at the same distance, and hence, lie over the same isochrone. Fig. 5.4 shows this diagram for J03167+389 (HAT 168–01565)and its candidate companion. For the comparison of the potential companions, I ploted the isochrones at 20, 100, 300, and 500 Ma, together with those at 1 and 2 Ga. Diagrams associated to the 34 Carmencita M dwarfs and their corresponding candidate companions are displayed in Fig. D.1–D.14 and D.15–D.33 in Appendix D.

5.3 Results and discussion

5.3.1 Known and new common proper motion pairs

I analysed the companion candidates to our Carmencita M dwarfs from the proper motion and colour-magnitude diagrams. Names, spectral types, J-band magnitudes, angular separations and position angles, and young kinematics information are listed in Table 5.2 for the most likely companions. The slowest pairs have more uncertainty in their proper motion determinations, and hence, were more difficult to confirm. Some companions were not clearly confirmed and remained dubious. They were also included in the table. Comments on most likely companions and the dubious pairs are noted here. When clear, the rejected companions are not mentioned.

Likely companions:

- J03167+389 (HAT 168-01565): At a spectrophotometric distance of 18.9 pc and with a relatively low proper motion of 66.7 mas a^{-1}, this M3.5 V has a candidate companion 1.05 mag fainter in the J-band.

- J05320–030 (V1311 Ori): This M2.0 V is a β Pictoris close binary separated by 0.2 arcsec with estimated spectral types M2.0 V + M3.5 V (Janson et al. 2012). It has a common proper

TABLE 5.1— Age association of the analyzed M dwarfs.

Association	Age [Ma]	Reference[a]	Number of stars
Stellar kinematic groups			
β Pictoris	5	Mess16	5
Local Association	$10 - 150$		2
Ursa Major	≥ 300	Gia79, SM93	3
Castor	≥ 300	Barr98, Mam13	1
Galactic young disc			
YD			4
Old or wihout age association			
Old?			20

Notes. [a] Barr98: Barrado y Navascués 1998; Gia79: Giannuzzi 1979; Mam13: Mamajek et al. 2013; Mess16: Messina et al. 2016; SM93: Soderblom & Mayor 1993.

motion companion candidate almost three magnitudes fainter in the J-band. The confirmation of the companionship would convert the system into a low mass triple one.

- J05456+729 (2MASS J05453880+7255127) and J05458+729 (2MASS J05454973+7254072): These Carmencita stars have proper motions of 140.4 and 138.8 mas a^{-1}, respectively. They were analyzed independently, and their common motion was confirmed in this work. The pair is composed by an M2.5 V (J05458+729) and an M3.0 V (J05456+729) at 27 pc separated by 80.6 arcsec. There is no information related to their ages.

- J07497–033 (2MASS J07494215-0320338): It is a kinematically young M3.5 V with spectrophotometric distance that has a candidate companion 0.85 mag fainter in the J-band.

- J09040–159 (2MASS J09040555-1555184): It is an M2.5 V at a spectrophotometric distance of 26.5 pc. Its candidate companion is V405 Hya, a relatively young K2 V star (Najakima & Morino 2012) at a parallactic distance of 28.3 pc. The common distance is thus confirmed independently.

- J18174+483 (TYC 3529-1437-1): It is a relatively slow M2.5 V with a candidate companion 2.7 mag fainter in the J-band that appears to be at the same spectrophotometric distance. Errors associated prevent us from confirming or rejecting the system.

Doubtful companionship:

- J03303+3446 (2MASS J03302331+3440325): It is an M4.0 V at a spectrophotometric distance of 22.9 pc. Its total proper motion is 54.8 mas a^{-1} and its kinematics indicates that it could be a young star in the Galactic thin disc. It has two proper motion companion candidates: PPMXL 3071421786149345561 and PPMXL 3071422664308970376. The colour-magnitude diagram indicates that the former does not lie at the same distance, and the later, although it does not match within the errorbars, lies close enough to be a possible companion.

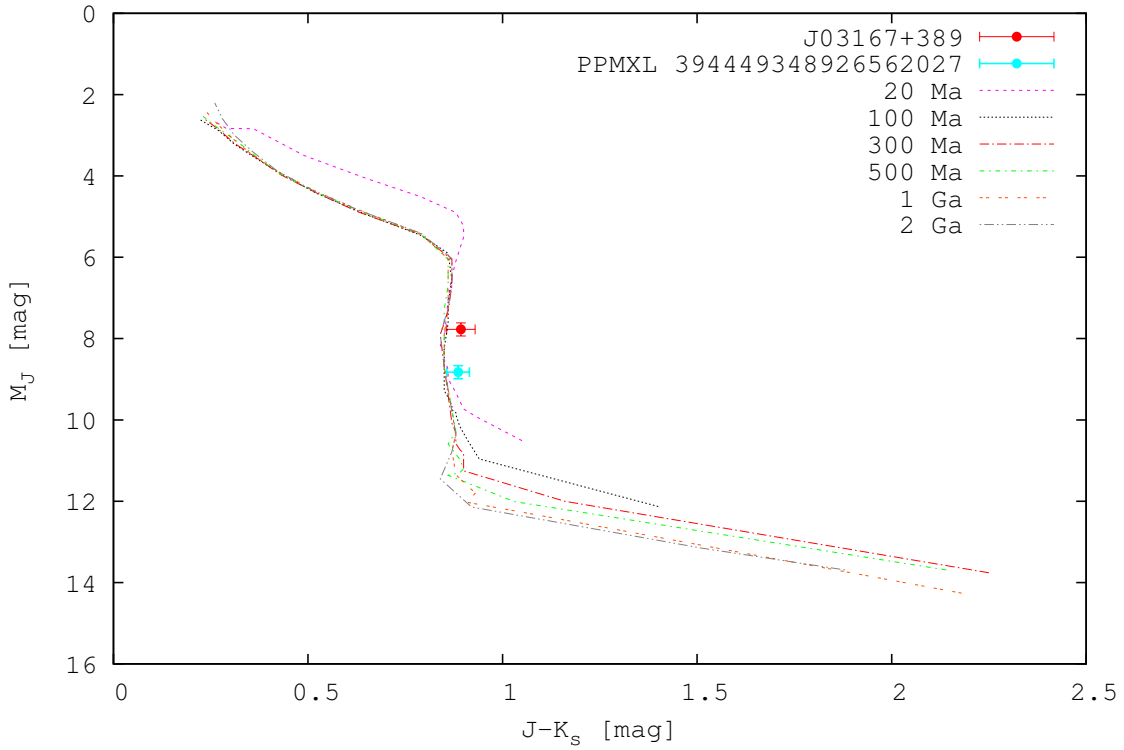

FIGURE 5.4— Colour-magnitude diagram showing the position of J03167+389 (HAT 168–01565; red filled circle) and its companion candidate (light blue filled square). Different colour lines represent the isochrones from 20 Ma to 2 Ga from Baraffe et al. (2015).

- J07310+460 (1RXS J073101.9+460030): It is an M4.0 V at a spectrophotometric distance of 22.4 pc and is a likely member of the young Galactic thin disc that moves at 99.8 mas a^{-1}. It has three companion candidates: PPMXL 99836854202795669 (candidate 1), PPMXL 1004326060565163279 (candidate 2), and PPMXL 1004373792460974930 (candidate 3). Candidate 2 is discarded by the colour-magnitude diagram. Candidate 1 shares proper motion, but its position in the colour-magnitude diagram would be compatible with a true companion only if the star is older than 100 or 200 Ma. For younger ages and according to the isocrhones, it would be a background star with similar proper motion. Candidate 3 lies at the same distance and has a slightly different proper motion, and has found to be an M3.0+M4.0 close binary separated by 0.2 arcsec (Janson et al. 2012). The wide separations between the three stars make them unlikely to be a physically bound multiple system, and the available information prevents us from determining which of them could be actually bound to J07310+460.

- J11307+549 (StKM 1–950): This M1.0 V has a faint candidate companion with similar proper motion. The spectrophotometric distance of 33.2 pc is compatible for our M dwarf and the candidate in the case of young ages (near 20 Ma; see Fig. D.9). We lack any age or activity information relative to these objects, with the exception of the low Hα emission in our M primary. More activity indicators, such as high rotation or X rays emission would be of help. Since we can not infer the age of the star, this pair remains unconfirmed.

- J13417+582 (StM 187): This is a close binary M3.0 + M4.0 V separated by 0.7 arcsec (Janson et al. 2012). There is a 30% difference on the proper motions of this M3.5 V+ and its candidate

TABLE 5.2— Common proper motion companions properties.

Name	SpT	J [mag]	ρ arcsec	θ deg	Youth[a]	Ref.[b]
Likely companions						
J03167+389 PPMXL 394449348926562027	M3.5 V	9.157 10.209	183.04 ± 0.12	38.62 ± 0.01		
J05320–030 PPMXL 2591858631666979215	M2.0 V+	7.879 10.580	254.59 ± 0.68	5.06 ± 0.01	β Pic	Malo13
J05458+729 J05456+729	M2.5 V M3.0 V	9.338 9.395	80.57 ± 0.13	323.53 ± 0.01		
PPMXL 2856105300336770891 J07497–033	M3.5 V	8.039 8.891	233.35 ± 0.13	214.02 ± 0.01	Cas	Mon16
V405 Hya J09040–159	K2 V M2.5 V	7.005 9.156	219.46 ± 0.47	262.67 ± 0.01		
J18174+483 PPMXL 191371594233401412	M2.5 V	9.058 11.724	84.04 ± 0.22	163.06 ± 0.04		
Doubtful companions						
J03303+346 PPMXL 3071422664308970376	M4.0 V	9.995 10.549	90.83 ± 0.15	62.32 ± 0.03	YD	Mon16
J07310+460 PPMXL 99836854202795669	M4.0 V	9.948 11.898	225.47 ± 0.18	158.79 ± 0.01	YD	Mon16
PPMXL 1004373792460974930 J07310+460	M3.0 V+ M4.0 V	9.776 9.948	430.01 ± 0.80	296.00 ± 0.04	YD	Mon16
J11307+549 PPMXL 1021315941850983881	M1.0 V	8.846 12.952	33.0 ± 0.2	198.9 ± 0.1		
J13417+582 PPMXL 799317777967965521	M3.5 V+	8.733 13.365	350.35 ± 0.47	187.44 ± 0.04	UMa	Mon16
J15480+043 PPMXL 5210004709267384143	M2.5 V	9.058 10.262	245.51 ± 0.14	208.53 ± 0.01		
J16120+033 APOP 53884+0000138	M2.0 V	8.127 9.957	33.71 ± 0.35	10.0 ± 0.1	UMa	Mon16
Known companions						
ι Leo J11238+106	F3+ M0.5 V	3.082 7.787	331.3[c]	346		
LP 569-015 J18135+055	M1.5 V M4.0 V	8.432 9.702	322.2[d]	13	D	Mon16

Notes. [a] βPic: β Pictoris; Cas: Castor; D: Thin Disc; UMa: Ursa Major; YD: Young Disc [b] Malo13: Malo et al. 2013; Mon16: Montes priv. comm. [c] WDS 11239+1032 (STF 536). [d] WDS 18136+0527 (LDS 1007).

companion. However, the total motion of the star ($94.6\,\mathrm{mas\,a^{-1}}$) and the almost compatible distance for both stars, prevent us from discarding nor confirming companionship.

- J15480+043 (RX J1548.0+0421): This M dwarf has a common proper motion candidate but according to the colour-magnitude diagram, it may not be at the same distance, although it can not be ruled out completely.

- J16120+033 (TYC 371-1053-1): This star and its companion candidate apparently lie at the same distance. Their proper motions differ in the declination component. The apparent large difference may be associated to the relatively low proper motion of our M dwarf (67.2 mas a^{-1}).

Rejected pairs after the analysis:

- J23317–027: This star had already been included in a proper motion search by Alonso-Floriano et al. (2015). In this work, a more detailed analysis on the proper motion of the candidate companion here proposed, revealed different proper motions for them and, thus, no companionship.
- J03288+264: This M3.0 V has a common proper motion companion candidate that would lie at the same distance, but its proper motion components differ from those of our M dwarf, which discards them as true companions.
- J11008+120: The PPMXL proper motion of this pair differs from the proper motion tabulated in the Lépine & Shara Proper Motions catalogue (LSPM; Lépine & Shara 2005). I therefore computed the proper motion of the star from astrometric catalogues and confirmed the proper motion of PPMXL. This computed proper motion has been updated in Table D.1, and the name of the star is marked in italics. The companionship of the HIP 53859 candidate is discarded.

While performing this analysis, a wrong PPMXL proper motion came out for J10155-164. The tabulated total proper motion was 210.2 mas a^{-1}, and the computed value from astrometric catalogues is 460.1 mas a^{-1}. The proper motion was corrected in Table D.1 and the star was marked in italics too. Its candidate companion was also marked in italics in Table D.2. With the new proper motion, there are no common proper motion companion candidates in the field.

In addition, two candidate companions to our Carmencita stars were found to be their known primaries in the WDS catalogue. The candidate companion to J11238+106 is ι Leo, an F3 V spectroscopic binary at 331.3 arcsec, tabulated in WDS under STF1536 (AB,C). Also J18135+055 has a candidate companion that corresponds to a known companion at 372.0 arcsec, under LDS1007 in the WDS. The WDS names were associated to the primary and hence, they did not appear in our WDS search around our M dwarfs. These stars were included at the end of Table 5.2.

5.3.2 Projected separations and binding energies

Angular separations (ρ) of our likely and dubious companions range from 33.0 arcsec to 7.2 arcmin. With the distances (d) from Table D.1, I computed the projected physical separations (s) of the likely and doubtful pairs from Table 5.2 by using the small angle approximation $\tan\rho \approx \rho$:

$$s = \rho d \tag{5.5}$$

From the J magnitudes, the distances and the evolutionary models from the Lyon group, I obtained the absolute M_J magnitudes and inferred the masses of the stars, in order to derive the binding energies of the systems from:

$$-U_g^* = \frac{G\mathcal{M}_1\mathcal{M}_2}{s} \tag{5.6}$$

where G is the graviational constant, $\mathcal{M}_1$ and $\mathcal{M}_2$ are the masses of the primary and the secondary respetively, and s is the projected physical separation (Caballero 2009). The stars

TABLE 5.3— Masses and binding energies of the common proper motion systems.

Name	M_J [mag]	$\mathcal{M}$ [$M_\odot$]	s [10^3 au]	$-U_g^*$ [10^{33} J]	Youth
Likely companions					
J03167+389	7.77	0.32	3.5 ± 0.1	1.9	
PPMXL 394449348926562027	8.83	0.19			
J05320–030	6.74[a]	0.28[b]	4.3 ± 0.8	0.05	β Pic
PPMXL 2591858631666979215	9.44	0.04			
J05458+729	7.04	0.44	2.3 ± 0.1	23	
J05456+729	7.39	0.39			
PPMXL 2856105300336770891	6.92	0.46	3.9 ± 0.1	9.8	Cas
J07497–033	7.78	0.32			
V405 Hya	4.89	0.80	5.8 ± 0.1	38	
J09040–159	7.04	0.44			
J18174+483	6.74	0.49	1.35 ± 0.02	2.0	
PPMXL 191371594233401412	10.69	0.08			
Doubtful companions					
J03303+346	8.20	0.26	2.1 ± 0.8	2.0	YD
PPMXL 3071422664308970376	8.75	0.19			
J07310+460	8.20	0.26	5.0 ± 0.2	0.24	YD
PPMXL 99836854202795669	10.15	0.10			
PPMXL 1004373792460974930	8.02[a]	0.38[b]	9.6 ± 0.4	1.8	YD
J07310+460	8.20	0.26			
J11307+549	6.24	0.57	1.09 ± 0.02	4.3	
PPMXL 1021315941850983881	10.35	0.09			
J13417+582	7.78[a]	0.44[b]	5.4 ± 0.2	0.16	UMa
PPMXL 799317777967965521	12.41	0.05			
J15480+043	7.04	0.44	6.2 ± 0.2	3.7	
PPMXL 5210004709267384143	8.25	0.26			
J16120+033	6.73	0.49	0.64 ± 0.02	29	UMa
APOP 53884+0000138	8.56	0.21			

Notes. [a] This is the total absolute magnitude of the pair. [b] This is the sum of the masses of the components.

J05320-030 AB (V1311 Ori) and PPMXL 1004373792460974930 (companion of J07310+460 – 1RXS J073101.9+460030 –) are instead close binaries identified by Janson et al. (2012). Their masses estimations follow a spectral type-mass relation for mid-age stars ($\sim$ 500 Ma). These masses could significantly differ from the masses derived from evolutionary models for the youngest stars. For this reason, I used the magnitude differences and spectral types given in Janson et al. (2012) to derive the masses of the components from evolutionary models. In the case of J05320-030, the absolute magnitudes derived were $M_{J1} = 7.03$ mag and $M_{J2} = 8.33$ mag for the primary and the secondary, respectively. For PPMXL 1004373792460974930, the numbers were $M_{J1} = 8.26$ mag and $M_{J2} = 9.76$ mag for the primary and the secondary respectively. For calculating the masses of the stars belonging to the young disc population, I assumed an intermediate age of 300 Ma. Table 5.3 contains the physical separations, masses and binding energies of the pairs.

Projected physical separations range from 640 to 9600 au, which translates into the interval of 0.003–0.05 pc. One likely and two doubtful companions have masses close the hydrogen burning limit ($\sim 0.075\,M_\odot$): PPMXL 191371594233401412, PPMXL 99836854202795669, and PPMXL 1021315941850983881. The companion to the β Pictoris M dwarf binary J05320-030 (V1311 Ori), PPMXL 2591858631666979215, and the companion to the UMa binary J13417+582 (StM 187), PPMXL 799317777967965521, have masses below that limit (0.04-0.05 $M_\odot$), and despite they are the tertiary companion of the systems, their binding energies are very low (0.05 and $0.16\,10^{33}$ J, respectively). Together with J07310+460 $\oplus$ PPMXL 99836854202795669 pair, their binding energies are the lowest ones derived here, and since the three of them are also young, their survival over time is unlikely (Dhital et al. 2012). In general, the binding energies of the systems here derived are low (of the order of 10^{34} J or less) compared to the binding energies involved in more massive young systems (see Alonso-Floriano et al. 2015).

5.4 Summary and conclusions

I performed a proper motion search around the Carmencita stars with a radius of 10^4 au using the Virtual Observatory tools STILTS and Topcat. For completeness and comparison, I looked into the PPMXL, APOP and UrHip proper motion catalogues. The 2170 Carmencita stars with total proper motion $\mu \geq 30\,\mathrm{mas\,a^{-1}}$ were subject of this study, and only companion candidates brighter than $J \leq 15.5$ mag were considered. I found 674 companion candidates to 470 Carmencita stars from PPMXL, 109 companion candidates to 95 Carmencita stars from APOP and 266 companion candidates to 213 Carmencita stars from UrHip. In total, there were 1049 common proper motion companion candidates, of which 390 are known WDS systems and 67 were spurious data (accounting for the repetitions between catalogues). Putting together the candidates of the three catalogues and discarding any repeated candidate, there remained 543 candidate companions to 343 M dwarfs.

Due to the high number of potential candidates, I applied a second cut in the relative differences between the proper motions of our M dwarfs and the companion candidates according to Eq. 5.3 and 5.4. This cut reduced the companion candidates to 213. I computed the proper motions of 56 companion candidates from astrometric catalogues and discarded another 19 companion candidates. Of the (213-19) companion candidates, 21 were associated to known and proper motion confirmed WDS systems, 49 were spurious sources, 86 were related to the Carmencita stars themselves, and 38 remained as potential proper motion companions to 34 Carmencita stars.

I investigated the 38 potential companions and carried out a detalied astrometric and photometric analysis. It revealed two known WDS systems, for which I confirmed common proper motion. The colour-magnitude diagrams discarded 18 candidate companions, and the astrometric analysis discarded another 4 candidate companions. Thus, seven candidates are likely common proper motion companions. Of them, two candidates referred to two Carmencita stars that form a binary system. Hence, I proposed six likely common proper motion companions and seven potential doubtful pairs. Age (activity) indicators and distance determinations would be necessary to confirm or discard them.

For the 13 pairs, I measured ρ and θ, derived the masses of the components from evolutionary models and computed projected physical separations and binding energies. Separations range from 33 to 430 arcsec and from 640 to 9600 au. The widest pair is separated by 0.05 pc. Five companions have masses at or below the hydrogen burning limit. Three of them have also the lowest binding energies and are β Pic, UMa and young disc candidate members. Another four pairs are relatively

young candidate members to Castor, UMa and the young disc population.

References

[1] Allen, P. R. & Reid, I. N. 2008, AJ, 135, 2024

[2] Alonso-Floriano, F. J., Caballero, J. A., Cortés-Contreras, M. et al. 2015, A&A, 583, A85

[3] Baraffe, I., Homeier, D., Allard, F. & Chabrier, G. 2015 A&A, 577, A42

[4] Barrado y Navascués, D. 1998, A&A, 339, 831

[5] Burgasser, A. J., Kirkpatrick, J. D., & Lowrance, P. J. 2005, AJ, 129, 2849

[6] Burgasser, A. J., Reid, I. N., Siegler, N. et al. 2007, in Protostars and Planets V, 427

[7] Caballero, J. A. 2009, A&A, 507, 251

[8] Close, L. M., Richer, H. B., Crabtree, D. R. 1990, AJ, 100, 1968

[9] Daemgen, S., Siegler, N., Reid, I. N., & Close, L. M. 2007, ApJ, 654, 558

[10] Dhital, S., Stassun, K. G. & West, A. A. 2012, AAS, 21913205

[11] Dittmann, J. A., Irwin, J. M., Charbonneau, D. & Berta-Thompson, Z. K. 2014, ApJ, 784, 156

[12] Frouard J., Dorland B.N., Makarov V.V. et al. 2015, AJ, 150, 141F

[13] Gallardo, I. 2015, MSc thesis, Universidad Complutense de Madrid, Spain

[14] Giannuzzi, M. A. 1979, A&A, 77, 214

[15] Goldman, B., Delfosse, X., Forveille, T. et al. 1999, A&A, 351, L5

[16] Hinz, J. L., McCarthy, D. W., Jr., Simons, D. A. et al. 2002, AJ, 123, 2027

[17] Janson, M., Hormuth, F., Bergfors, C. et al. 2012, ApJ, 754, 44

[18] Latham, D. W., Tonry, J., Bahcall, J. N. et al. 1984, ApJ, 281, L41

[19] Lowrance, P. J., McCarthy, C. Becklin, E. E. et al. 1999, ApJ, 512, L69

[20] Malo, L., Doyon, R., Lafrenière, D. et al. 2013, ApJ, 762, 88

[21] Malo, L., Artigau, É., Doyon, R. et al. 2014a, ApJ, 788, 81

[22] Mamajek, E. E., Bartlett, J. L., Seifahrt, A. et al. 2013, AJ, 146, 154

[23] Mason, B. D., Wycoff, G. L., Hartkopf, W. I., Douglass, G. G. & Worley, C. E. 2001, AJ, 122, 3466

[24] Mason, B. D., Wycoff, G. L., Hartkopf, W. I., Douglass, G. G. & Worley, C. E. 2015, VizieR on-line catalogue, B/WDS

[25] McCarthy, C., & Zuckerman, B. 2004, AJ, 127, 2871

[26] Messina, S. Lanzafame, A. C., Feiden, G. A. et al. 2016, arXiv:1607.06634

[27] Nakajima, T., Oppenheimer, B. R., Kulkarni, S. R. et al. 1995, Nature, 378, 463

[28] Nakajima, T. & Morino, J.-I. 2012, AJ, 143, 2

[29] Oppenheimer, B. R., Golimowski, D. A., Kulkarni, S. R. et al. 2001, AJ, 121, 2189

[30] Qi Z.X., Yu Y., Bucciasrelli B., Lattanzi M.G. et al. 2015, AJ, 150, 137

[31] Radigan, J., Lafrenière, D., Jayawardhana, R. & Doyon, R. 2008, ApJ, 689, 471

[32] Radigan, J., Lafrenière, D., Jayawardhana, R. & Doyon, R. 2009, ApJ, 698, 405

[33] Rebolo, R., Zapatero Osorio, M. R., Madruga, S. et al. 1998, Science, 282, 1309

[34] Reid, I. N. & Walkowicz, L. M. 2006, PASP, 118, 671

[35] Roeser, S., Demleitner, M. & Schilbach, E. 2010, AJ, 139, 2440

[36] Schlieder, J. E., Lépine, S. & Simon, M. 2012b, AJ, 143, 80

[37] Shaya, E. J. & Olling, R. P. 2011, ApJS, 192, 2

[38] Soderblom, D. R. & Mayor, M. 1993, AJ, 105, 226

[39] Taylor, M. B. 2006, Astronomical Data Analysis Software and Systems XV, 351, 666

[40] Tokovinin, A., & Lépine, S. 2012, AJ, 144, 102

[41] van Altena, W. F., Lee, J. T. & Hoffleit, E. D. 1995, *The general catalogue of trigonometric [stellar] parallaxes*, New Haven, Yale University Observatory, 4th ed.

[42] van Leeuwen, F. 2007, A&A, 474, 653

[43] Weinberg, M. D., Shapiro, S. L., Wasserman, I. 1987, ApJ, 312, 367

[44] Wilson, J. C., Kirkpatrick, J. D., Gizis, J. E. et al. 2001, AJ, 122, 1989

6

Conclusions and future work

6.1 Conclusions

This dissertation is based on the compilation of astrometric, spectroscopic and photometric information, including multiplicity and age parameters, in order to build the most comprehensive database of M dwarfs: Carmencita. The aim of Carmencita is to provide a list of potential target candidates to observe with CARMENES. To help with the target selection, I performed an extensive search of binary companions to the Carmencita stars, either from the literature, from low- and high-resolution images obtained for this purpose, or from all-sky proper-motion catalogues. This work presents a general analysis of the Carmencita M dwarfs, and three multiplicity surveys, two of which were published in refereed journals.

The conclusions derived from this PhD thesis can be summarised as follow for the different analyses carried out:

- The Carmencita database:
  - The search of M dwarfs and data compilation is based on a spectral type-J magnitude relation defined to select the brightest stars of each spectral subtype. To date (September 2016), Carmencita contains 2176 M0–9 dwarfs with reliable spectral subtypes.
  - In Carmencita, 1286 M dwarfs have parallactic distances. Of them, I used 920 single stars to estimate spectro-photometric distances for 884 M0–6 dwarfs without parallaxes from our own M_J–spectral type relation. The mean distance of the Carmencita sample is 20.2 pc.
  - Using the astrometric catalogues USNO-A2.0, GSC2.3, 2MASS, CMC14/15, SDSS III and ALLWISE, I computed proper motions for 529 M dwarfs that had high associated errors, no error determination or with total proper motions lower than $50\,\mathrm{mas\,a^{-1}}$. Final error bars of the total proper motions in the database are limited to less than $8\,\mathrm{mas\,a^{-1}}$. The proper motion distribution in the database peaks at $100\,\mathrm{mas\,a^{-1}}$, and ten dwarfs have proper motions larger than $3000\,\mathrm{mas\,a^{-1}}$.
  - For the 1592 Carmencita dwarfs with radial velocities, either from the literature or measured by the Consortium members, I presented Galactic space velocities and classified them into halo (4), thick disc (136), transition between thin and thick disc (69), thin disc

(937), and young disc (446) population. In addition, I associated their kinematics to the Taurus-Auriga (4), Argus (4), IC 2391 (25), Local Association (146), Hercules-Lyra (1), Ursa Major (55), Castor (35) and Hyades (82) moving groups.

- I analyzed the multiplicity frequency in the Carmencita sample at any range of angular separations and in two different ranges: less than 5 arcsec (close) and greater than 5 arcsec (wide). The total multiplicity fraction is 19.1±1.0%, and the fractions at close and wide separations are 17.0±1.0% and 6.5±0.6%, respectively. I built two volume limited samples complete up to 86% that include 317 M0-M9 dwarfs within 12 pc (VLS1) and 774 M0-M5 dwarfs within 17 pc (VLS2). The multiplicity fraction derived for them barely change: 25.2±3.2% and 24.8±2.0% for VLS1 and VLS2 respectively in the close interval, 7.6±1.6% and 8.0±1.0% for VLS1 and VLS2 respectively in the wide interval, and 26.5±3.2% and 28.7±2.2% for VLS1 and VLS2 respectively at any range of angular separations. I also considered unbiased samples for the young Galactic disc population and the thin, thick and halo populations and derived an M dwarf multipicity frequency of 35.0 ± 7.0% and 29.0 ± 4.3%, respectively. The unexpected similar frequencies may be due to the wide interval of ages of the young disc population.
- The distribution of projected physical separations of all the systems in Carmencita peaks between 0.3 and 3 au, including the separations to hotter components. Considering only M dwarf primaries, the distribution of projected physical separations in the volume limited samples peaks between 2 and 3 au.
- The cumulative distribution of the projected physical separations of the systems with an M dwarf primary in Carmencita, the VLS1 and the VLS2 follow a power law of the form $N(a) \propto a^{-\lambda+1}$, which is the general ennunciation of the Öpik's law. The application of this law is restricted to the interval of ∼1–3160 au and takes the value of the λ parameter of 0.41–0.47 in the VLS1 and VLS2 and of 0.30 in the Carmencita sample with confident levels of 96–97% and 30%, respectively.
- The compilation of 19 photometric bands allowed us to obtain the spectral energy distributions of our M dwarfs, and to define stellar prototypes, as well as colour indices for each spectral subtype.
- We identified magnetically active dwarfs as stars with $pEW(\mathrm{H}\alpha) < -0.75$ Å, $P_{\rm rot} < 50$ d, $v \sin i > 4\,\mathrm{km\,s^{-1}}$ and X-ray emission. Also stars with strong Hα emission show $NUV - V$ colours lower than 7.6 mag.
- The fraction of stars with Hα emission increases towards later spectral subtypes: 7–14% of M0-M2 dwarfs, 24% of M3 dwarfs, 51–74% of M4-M6 dwarfs and 80-100% of M7-M9 dwarfs. We found a saturation limit of the chromospheric activity level around $\log L_{H\alpha}/L_{bol} = -3.3$ and listed six stars with the strongest Hα emission. We observed the activity-rotation conncection, since chromospherically active stars tend also to rotate faster.
- We found a saturation limit of coronal emission at $\log L_X/L_J = 1.5$ ($\log L_X = 31$) and observed that X-ray emitters are also fast rotators.
- We presented a list of the 50 most active stars in the Carmencita sample that show Hα emission between –0.82 and –17.1 Å, normalized X-ray emission between 3.02 and 101.61, and rotate at velocities in the range of 3.3–190.3 $\mathrm{km\,s^{-1}}$. Half of them have measured rotational periods and range from 0.2 to 13.3 d. All of them also show young kinematics (<200 Ma).

- Low-resolution images and astrometric analysis of 54 pairs with an M dwarf:
  - We performed an astrometric analysis with photographic plate digitizations, astrometric catalogues and low-resolution images taken with TCP and CAMELOT at the IAC80 telescope at the Observatorio del Teide. We discarded two pairs tabulated in the Washington Double Star catalogue and confirmed 52 physically bound pairs, for which we measured angular separation and position angles, estimated masses, periods and binding energies.
  - We found a threshold in the binding energies of the 52 pairs at 10^{34} J, and five weakly bound systems with binding energies below 10^{35} J.
  - We purpose ten systems that showed appreciable orbital variation and had orbital periods shorter than 1000 a for a more detailed study.

- High-resolution images with FastCam:
  - We carried out a high-resolution imaging survey and observed 490 M dwarfs (thought to be single) with the lucky imager FastCam at the Telescopio Carlos Sánchez at the Observatorio del Teide. We detected 80 companion in 76 systems, 30 of which are new discoveries. For all of them, we measured angular separations and position angles, computed projected physical separations, estimated masses from evolutionary models and derived periods.
  - We derived a multiplicity fraction in the observed sample with FastCam of 16.7±2.0%. We built a volume limited sample complete up to 86% within 14 pc that contains 425 M0-M5 dwarfs. The multiplicity fraction in this unbiased sample is of 19.5±2.3% for angular separations from 0.2 to 5 arcsec. The distribution of the projected physical separations of the volume limited sample peaks at 2.5–7.5 au. The contribution of binaries and multiples with angular separatins shorter than 0.2 arcsec, larger than 5.0 arcsec and spectroscopic binaries identified in previous searches in the volume limited sample, although not complete, increase the multiplicity fraction of M dwarfs up to at least 36%.
  - Among the detected systems, we observed a higher density of pairs with mass ratios over 0.8 compared to those at lower mass ratios. Binaries with projected physical separations shorter than 50 au tend to be of equal mass.
  - We estimated orbital periods shorter than 50 au for 26 of our systems, 10 of which are presented here for the first time. Of these sytems, 17 show variations in the measured angular separations and position angles due to orbital motions.

- Common proper motion search around Carmencita M dwarfs:
  - I performed a common proper motion search around all the Carmencita M dwarfs with a maximum radius of 10^4 au, using the PPMXL, UrHip and APOP all-sky proper-motion catalogues and the proper motions of the Carmencita stars as reference. I investigated 38 candidate companions, 13 of which were proposed as likely common proper motion companions.
  - For the 13 pairs, I measured angular separations and position angles, derived the masses of the components from evolutionary models, and computed projected physical separations and binding energies. Separations ranged from 33 to 430 arcsec (from 640 to 9600 au).

- Five companions of the 13 have masses at or below the hydrogen burning limit. Three of them are very weakly bound and are β Pictoris, Ursa Major and young disc candidate members.
- Another four pairs are relatively young candidate members to Castor, Ursa Major and the young disc population.

As a summary, I performed a search of companions to a representative number of M dwarfs in Carmencita at any range of angular separations with high- and low-resolution images, as well as with astrometric an proper motion catalogues. In the close regime (up to 5 arcsec), the fraction of M dwarfs in binary and multiple systems is in accordance with similar surveys. In the wide regime, the number of companions found was the expected and more observations are needed to disentangle companionship. I identified young systems and very close and very wide angular separations, targets for further analysis.

6.2 Future work

The work presented here is part of the science preparation for CARMENES. The data compilation for Carmencita has been updated with the latest measurements provided by the CARMENES Consortium or published in the literature until the publication of this thesis, and it is therefore in constant development. For this reason, the Carmencita analysis carried out in this work, specially regarding the age and magnetic activity of the stars, will need to be revised with new data that will complete the information available at the moment. For example, Gaia will provide more and precise parameters that will complete and improve our database. Carmencita has an enormous potential. It is a very powerful tool, since it allows to statistically treat M dwarfs, and also helps in the optimization of the observational resources: the better characterised a target, the better profit for the observations and following analysis.

Young M dwarfs are of special interest in the study of star and planet formation and evolution in the low mass regime. The presence of stellar or substellar components around young low-mass stars provides information of stellar and planet formation and evolution, as well as hints on the potential habitability of exoplanets around them. Therefore, the study of the kinematics of our M dwarfs will be prepared for its publication in a refereed paper. Many of the kinematically young candidates proposed in this work lack other age indicators, such as Hα emission, rotational periods or rotational velocities. For completeness in our database and in order to perform a more detailed study, I propose to make a search of young (and active) M dwarfs among the Carmencita stars by obtaning radial velocities and by measuring the Hα line from the CARMENES spectra in a short-term program, and/or by deriving rotational periods in a long-term program (perhaps in collaboration with the MEarth and APACHE teams).

Regarding the M dwarfs multiplicity, it would be interesting to differenciate those young binary stars from the older ones to independently study their occurence and parameters (angular separations, and masses and periods if possible). The analysis of the dependence of the multiplicity fraction with age should be restricted to a few dozens Ma, when formation process are still undergoing. On one hand, I propose a follow-up of the closest binaries, for which orbital motion can be measured within a few years, in order to determine dynamical masses. On the other hand, six M dwarfs with common proper motion companion candidates are kinematically young stars. Three of their candidate companions are of special interest due to their low masses. I propose them for

spectroscopic observations in order to look for age indicators and thus, to confirm or reject them as common proper motion companions to our Carmencita M dwarfs.

A

List of publications

A.1 Published in refereed journals

A.1.1 In this thesis

1. *CARMENES input catalogue of M dwarfs. II. High-resolution imaging with FastCam.*
Cortés-Contreras, M., Béjar, V. J. S., Caballero, J. A., B. Gauza, D. Montes, Alonso-Floriano, F. J., Jeffers, S. V., Morales, J. C., Reiners, A., Ribas, I., Schöfer, P., Quirrenbach, A. Amado, P. J., Mundt, R. & Seifert, W. A&A, in press, arXiv:1608.08145, DOI:10.1051/0004-6361/201629056

2. *Cool dwarfs in wide multiple systems Paper 5: New astrometry of 54 wide pairs with M dwarfs.*
Cortés-Contreras, M., Caballero, J. A. & Montes, D. 2014, The Observatory, 134, 348.

A.1.2 Additional publications

1. *CARMENES input catalogue of M dwarfs III. Rotation and activity from high-resolution spectroscopic observations*
Jeffers, S. V., Schöfer, P., Lamert, A. et al. (including **Cortés-Contreras**) 2016, A&A, submitted.

2. *Reaching the boundary between stellar kinematic groups and very wide binaries III. Sixteen new stars and eight new wide systems in the β Pictoris moving group.*
Alonso-Floriano, F. J., Caballero, J. A., **Cortés-Contreras, M.**, et al. 2015, A&A, 583, A85

3. *CARMENES input catalogue of M dwarfs. I. Low-resolution spectroscopy with CAFOS.*
Alonso-Floriano, F. J., Morales, J. C., Caballero, J. A., Montes, D., Klutsch, A., Mundt, R., **Cortés-Contreras, M.** et al. 2015, A&A, 577, A128.

A.2 Conference proceedings

1. *CARMENES: data flow*
Caballero, J. A., Guàrdia, J., López del Fresno, M. et al. (including **Cortés-Contreras**) 2016, Proc. SPIE, 9910, E0E

2. *CARMENES: an overview six months after the first light*
   Quirrenbach, A., Amado, P. J., Caballero, J. A. et al. (including **Cortés-Contreras**) 2016, Proc. SPIE, 9908, in press.

3. *CARMENES input catalogue of M dwarfs: Looking for close and wide companions.*
   Cortés-Contreras, M., Béjar, V. J. S., Caballero, J. A., et al. 2016, Highlights of Spanish Astrophysics VIII, in press, Proceedings of the X Scientific Meeting of the Spanish Astronomical Society (July 2016, Bilbao, Spain).

4. *Carmencita, the CARMENES Cool dwarf Information and daTa Archive.*
   Caballero, J. A., **Cortés-Contreras, M.**, Alonso-Floriano, F. J., et al. 2016, Highlights of Spanish Astrophysics VIII, in press, Proceedings of the X Scientific Meeting of the Spanish Astronomical Society (July 2016, Bilbao, Spain).

5. *Characterizing the CARMENES input catalogue of M dwarfs with low-resolution spectroscopu: spectral types, chromospheric activity and metallicity.*
   Alonso-Floriano, F. J., Montes, D., Caballero, J. A. et al. (including **Cortés-Contreras**) 2016, Highlights of Spanish Astrophysics VIII, in press, Proceedings of the X Scientific Meeting of the Spanish Astronomical Society (July 2016, Bilbao, Spain).

6. *Carmencita, the CARMENES input catalogue of bright, nearby M dwarfs*
   Caballero, J. A., **Cortés-Contreras, M.**, Alonso-Floriano, F. J. et al. 2016, 19th Cambridge Workshop on Cool Stars, Stellar Systems, and the Sun, DOI: 10.5281/zenodo.60060 (June 2016, Uppsala, Sweden).

7. *Kinematics of M dwarfs in the CARMENES input catalogue: membership in young moving groups.*
   D. Montes, J. A. Caballero, I. Gallardo, **Cortés-Contreras, M.** & Alonso-Floriano, F. J. 2015, Proceedings IAU Symposium No. 314, 72, Young Stars & Planets Near the Sun, 2015, J. H. Kastner, B. Stelzer, & S. A. Metchev, eds (May 2015, Atlanta, US).

8. *CARMENES. Multiplicity of M dwarfs from tenths of arcseconds to hundreds of arcminutes.*
   Cortés-Contreras, M., Béjar, V. J. S., Caballero, J. A., et al. 2015, Highlights of Spanish Astrophysics VIII, 597. Proceedings of the XI Scientific Meeting of the Spanish Astronomical Society (September 2014, Teruel, Spain).

9. *Mining public archives for stellar parameters and spectra of M dwarfs with master thesis students.*
   Caballero, J. A., Montes, D., Alonso-Floriano, F. J., **Cortés-Contreras, M.** et al. 2015, Highlights of Spanish Astrophysics VIII, 595, Proceedings of the XI Scientific Meeting of the Spanish Astronomical Society (September 2014, Teruel, Spain).

10. *CARMENES science preparation: low–resolution spectroscopy of M dwarfs.*
    Alonso-Floriano, F. J., Montes, D., Caballero, J. A., et al. (including **Cortés-Contreras**) 2015, Highlights of Spanish Astrophysics VIII, 441, Proceedings of the XI Scientific Meeting of the Spanish Astronomical Society (September 2014, Teruel, Spain).

11. *Preparation of the CARMENES Input Catalogue: Multiplicity of M dwarfs from Tenths of Arcseconds to Hundreds of Arcminutes.*
    Cortés-Contreras, M., Caballero, J. A., Béjar, V. J. S., et al. 2015, 18th Cambridge Workshop on Cool Stars, Stellar Systems, and the Sun, 18, 805 (June 2014, Flagstaff, US).

12. *Preparation of the CARMENES Input Catalogue: Mining Public Archives for Stellar Parameters and Spectra of M Dwarfs with Master Thesis Students.*
Montes, D., Caballero, J. A., Alonso-Floriano, F. J., et al. (including **Cortés-Contreras**) 2015, 18th Cambridge Workshop on Cool Stars, Stellar Systems, and the Sun, 18, 651 (June 2014, Flagstaff, US).

13. *Preparation of the CARMENES Input Catalogue: Low- and High-resolution Spectroscopy of M dwarfs.*
Alonso-Floriano, F. J., Montes, D., Caballero, J. A., et al. (including **Cortés-Contreras**) 2015, 18th Cambridge Workshop on Cool Stars, Stellar Systems, and the Sun, 18, 796 (June 2014, Flagstaff, US).

14. *CARMENES instrument overview.*
A. Quirrenbach, P. J. Amado, J. A. Caballero et al. (including **Cortés-Contreras**) 2014, SPIE, 9147, E1F.

15. *CARMENES at RIA-AstroMadrid 5. Multiplicity of M dwarfs with IAC80.*
Cortés-Contreras, M., Caballero, J. A., Montes, D. et al. 2013, A RIA-AstroMadrid Meeting, (September 2013, Madrid, Spain).

16. *CARMENES at PPVI. CARMENCITA Herbs and Spices to Help you Prepare a Genuine Target Sample.*
Caballero, J. A., **Cortés-Contreras, M.**, Alonso-Floriano, F. J., et al. 2013, Protostars and Planets VI Posters, 20 (July 2013, Heidelberg, Germany).

17. *CARMENES at PPVI. High-Resolution Spectroscopy of M Dwarfs with FEROS, CAFE and HRS.*
Alonso-Floriano, F. J., Montes, D., Jeffers, S., et al. (including **Cortés-Contreras**) 2013, Protostars and Planets VI Posters, 21 (July 2013, Heidelberg, Germany).

18. *CARMENES at PPVI. Calibrating the Metallicity of M-Dwarfs with Wide Visual Binaries.*
Montes, D., Alonso-Floriano, F. J., Tabernero, H. M., et al. (including **Cortés-Contreras**) 2013, Protostars and Planets VI Posters, 22 (July 2013, Heidelberg, Germany).

19. *CARMENES at PPVI. Low-Resolution Spectroscopy of M Dwarfs with CAFOS at Calar Alto.*
Mundt, R., Alonso-Floriano, F. J., Caballero, J. A., et al. (including **Cortés-Contreras**) 2013, Protostars and Planets VI Posters, 55 (July 2013, Heidelberg, Germany).

20. *CARMENES. II. Science case and M-dwarf sample.*
Morales, J. C., Ribas, I., Caballero, J. A., et al. (including **Cortés-Contreras**) 2013, Highlights of Spanish Astrophysics VII, 664, Proceedings of the X Scientific Meeting of the Spanish Astronomical Society (July 2012, Valencia, Spain).

21. *CARMENES. V. M dwarfs in multiple systems.*
Cortés-Contreras, M., Caballero, J, A., Alonso-Floriano, F. J., et al. 2013, Highlights of Spanish Astrophysics VII, 646, Proceedings of the X Scientific Meeting of the Spanish Astronomical Society (July 2012, Valencia, Spain).

22. *CARMENES. III. CARMENCITA, the input catalogue.*
Caballero, J. A., **Cortés-Contreras, M.**, López-Santiago, J., et al. 2013, Highlights of Spanish Astrophysics VII, 645, Proceedings of the X Scientific Meeting of the Spanish Astronomical Society (July 2012, Valencia, Spain).

23. *CARMENES. II. CARMENCITA, the input catalogue archive.*
Caballero, J. A., **Cortés-Contreras, M.**, López-Santiago, J., et al. 2012, The 17th Cool Stars, Stellar Systems and the Sun workshop (June 2012, Barcelona, Spain).

24. *Spectral characterisation of the CARMENES input catalogue.*
Klutsch, A., Alonso-Floriano, F. J., Caballero, J. A., Montes, D., **Cortés-Contreras, M.** et al. 2012, SF2A-2012: Proceedings of the Annual meeting of the French Society of Astronomy and Astrophysics, 357 (June 2012, Nice, France).

25. *CARMENES. I: instrument and survey overview.*
A. Quirrenbach, P. J. Amado, W. Seifert, et al. (including **Cortés-Contreras**) 2012, SPIE, 8446, E0R.

B

Long tables of Chapter 2

This appendix includes the tables referenced Chapter 2.

- Table B.1 contains the list of the parameters catalogued in Carmencita, together with their units and references from which they were adopted.
- Table B.2 contains the 2176 Carmencita stars with their Karmn identifier, flag, common name, spectral type, α and δ J2000.0 coordinates, and distance.

  The *Flag* description is given in Table 2.2.

  Distances derived from this work are referenced as "Cor16", and proper motions as "Cortes" and "Gal15".
- Table B.3 contains the proper motions, radial velocities and UVW galactic space velocity components for the 2176 Carmencita stars.

  "Cortes" and "Gal15" refer to the proper motions derived in this work, and "Mon16" refers to the galactocentric components derived in this work from the distances and radial velocities compiled in Carmencita.
- Table B.5 contains the 16 colour indices for spectral types from M0.0,V to M6.5 V from Holgado (2014).
- Table B.4 contains the 2176 Carmencita stars with their Karmn identifier, a marker of activity, the stelar kinematic group to which they belong or are candidates and the stellar population.

  The activity marker is defined as $pEW(H_\alpha < -0.75\,\text{Å}$, $v \sin i > 3\,\mathrm{km\,s^{-1}}$, $P_{rot} < 50\,\mathrm{d}$ and X-rays emission and rotation (satisfying the $v \sin i > 3\,\mathrm{km\,s^{-1}}$) activity.

  The kinematic groups included are AB Doradus, Argus, Carina, Castor, Columba, Hyades, Hyades cluster, Hercules-Lyra, IC 2391, Tucana-Horologium, Ursa Major, β Pictoris, Taurus, TW Hydrae and the Local Association, which includes TW Hydrae, Chamaleontis, β Pictoris, Columba, Carina, AB Doradus and Tucana-Horologium.

  Stellar populations are classified into young disc (YD), thin disc (D), transition between thin and thick disc (TD-D), thick disc (TD), and halo (H).

  Kinematically young candidates associated to stellar kinematic groups or young disc population from this work are referenced as "Mon16" (Montes priv. comm.)

Table B.1: List of the paramaters contained in Carmencita.

Parameter	Units	Col.	Description	References[a]
Karmn	JHHMMm+DDd	1	Karmen name[1]	...
Comp	...	2	Component in multiple system[2]	...
Flags	...	3	Characterization flags[3]	...
SS	...	4	Subsampling[4]	...
Name	...	5	Addopted name[5]	...
GJ	...	6	Gliese & Jahreiss designation	*a*
SpT	...	7	Spectral type	...
Ref.01	...	8	Reference of the spectral type	*b*
α_{J2016}	hms	9	Right ascention in J2016	...
δ_{J2016}	dms	10	Declination J2016.0	...
l_{J2016}	deg	11	Declination J2016 .0	...
b_{J2016}	deg	12	Galactic longitude J2016.0	...
Ref.02	...	13	Coordinates reference	*c*
$\mu_\alpha \cos\delta$, $\delta\mu_\alpha \cos\delta$	mas a^{-1}	14-15	Proper motion in right ascension and error	...
μ_δ, $\delta\mu_\delta$	mas a^{-1}	16-17	Proper motion in declination and error	...
Ref.03	...	18	Reference of the proper motion	*d*
V_r, δV_r	km s^{-1}	19-20	Radial velocity and error	...
Ref.04	...	21	Reference of the radial velocity	*e*
π, $\delta\pi$	mas	22-23	Trigonometric parallax and error	...
Ref.05	...	24	Reference of the parallax	*f*
d, δd	pc	25-26	Distance and error	...
Ref.06	...	27	Reference of the distance	*g*
U, δU	km s^{-1}	28-29	Galactic U space velocity and error	...
V, δV	km s^{-1}	30-31	Galactic V space velocity and error	...
W, δW	km s^{-1}	32-33	Galactic W space velocity and error	...
Ref.07	...	34	Reference of the galactic velocity components	*h*
FUV, δFUV	mag	35-36	*GALEX* Far-UV magnitude and error	...
NUV, δNUV	mag	37-38	*GALEX* Near-UV magnitude and error	...
Ref.08	...	39	Reference of the Far-UV and Near-UV magnitudes	*i*
u', $\delta u'$	mag	40-41	Sloan u' magnitude and error	...
Ref.09	...	42	Reference of the u' magnitude	*j*
B_T, δB_T	mag	43-44	Tycho B_T magnitude	...
Ref.10	...	45	Reference of the B_T magnitude	*k*
B, δB	mag	46-47	Johnson B magnitude and error	...
Ref.11	...	48	Reference of the B magnitude	*l*
g', $\delta g'$	mag	49-50	Sloan g' magnitude and error	...
Ref.12	...	51	Reference of the g' magnitude	*m*
V_T, δV_T	mag	52-53	Tycho V_T magnitude and error	...
Ref.13	...	54	Reference of the V_T magnitude	*k*
V, δV	mag	55-56	Johnson V magnitude and error	...
Ref.14	...	57	Reference of the V magnitude	*n*
R_a	mag	58	UCAC R aperture magnitude	...
Ref.15	...	59	Reference of the R_a magnitude	*o*
r', $\delta r'$	mag	60-61	Sloan r' magnitude and error	...
Ref.16	...	62	Reference of the r' magnitude	*p*
i', $\delta i'$	mag	63-64	Sloan i' magnitude and error	...

Table B.1: List of the paramaters contained in Carmencita (continued).

Parameter	Units	Col.	Description	References[a]
Ref.17	...	65	Reference of the i' magnitude	l
I	mag	66	I magnitude[6]	...
Ref.18	...	67	Reference of the I magnitude	q
J, δJ	mag	68-69	2MASS J magnitude and error	...
H, δH	mag	70-71	2MASS H magnitude and error	...
K_s, δK_s	mag	72-73	2MASS K_s magnitude and error	...
Q flag	...	74	JHK photometric quality flag	...
Ref.19	...	75	Reference of the JHK magnitudes	r
$W1$, $\delta W1$	mag	76-77	WISE $W1$ magnitude and error	...
$W2$, $\delta W2$	mag	78-79	WISE $W2$ magnitude and error	...
$W3$, $\delta W3$	mag	80-81	WISE $W3$ magnitude and error	...
$W4$, $\delta W4$	mag	82-83	WISE $W4$ magnitude and error	...
Ref.20	...	84	Reference of $W1W2W3W4$ magnitudes	s
Multiplicity	...	85	Flag for multiplicity [7]	...
Wide WDS	...	86	Washington Double Star reference code for wide systems	t
Wide ρ, $\delta\rho$	arcsec	87-88	Angular separation and error between components in wide systems	...
Ref.21	...	89	Reference of wide angular separation	u
Wide companion name	...	90	Common name of the wide companion(s)[8]	...
Wide companion SpT	...	91	Spectral type of the wide companion(s)	...
Wide companion Δ mag	mag	92	Difference of magnitude between components[9]	...
Wide companion Band	...	93	Photometric band of the magnitude difference	...
Ref.22	...	94	Reference of the magnitude difference	v
Close WDS	...	95	Washington Double Star reference code for close systems	t
Close ρ, $\delta\rho$	arcsec	96-97	Angular separation and error between components in close systems	...
Ref.23	...	98	Reference of close angular separation	w
Close companion name	...	99	Common name of the close companion(s)[8]	...
Close companion SpT	...	100	Spectral type of the close companion(s)	...
Close companion Δ mag	mag	101	Difference of magnitude between components[9]	...
Close companion Band	...	102	Photometric band of the magnitude difference	...
Ref.24	...	103	Reference of the magnitude difference	x
$pEW(H\alpha)$, $\delta pEW(H\alpha)$	Å	104-105	H_α equivalent width	...
Ref.25	...	106	Reference of the H_α equivalent width	y
1RXS	...	107	ROSAT All-Sky Survey Catalogue source identifier	...
CRT, δCRT	$\mathrm{cts/s^{-1}}$	108-109	Source count rate and error	...
HR1, δHR1	...	110-111	Hardness ratio 1 and error	...
HR2, δHR2	...	112-113	Hardness ratio 2 and error	...
F_X, δF_X	$\mathrm{erg\,cm^{-2}\,s^{-1}}$	114-115	X rays flux and error	...
L_X/L_J, $\delta(L_X/L_J)$	...	116-117	X rays luminosity size corrected and error	...
Ref.26	...	118	Reference of the X ray emission[1]0	z
$v \sin i$, $\delta v \sin i$	$\mathrm{km\,s^{-1}}$	119-120	Rotational velocity and error	...
Ref.27	...	121	Reference of the rotational velocity	aa
P_{rot}, δP_{rot}	d	122-123	Rotational period and error	...
Ref.28	...	124	Reference of the rotational period	ab
TiO_5	...	125	TiO_5 index	...
CaH_2	...	126	CaH_2 index	...

Table B.1: List of the paramaters contained in Carmencita (continued).

Parameter	Units	Col.	Description	References[a]
Ref.29	...	127	Reference of the TiO5 and CaH_2 indices	^{ac}
Flare	...	128	Indicates if the star presents flares[11]	...
Ref.30	...	129	Reference for flare stars	^{ad}
SKG	...	130	Stellar kinematic group membership[12]	...
Ref.31	...	131	Reference to the stellar kinematic group membership	^{ae}
Population	...	132	Galactic stellar population[13]	...
Ref.32	...	133	Reference to stellar population	^{af}
M_V	mag	134	Absolute V magnitude	...
Ref.33	...	135	Reference of the absolute V magnitude	^{ag}
$T_{\rm seff}$, $\delta T_{\rm eff}$	K	136-137	Effective temperature	...
$\log g$, $\delta \log g$	...	138-139	Surface gravity and error	...
[Fe/H], δ[Fe/H]	...	140-141	Metallicity and error	...
Ref.34	...	142	Reference of the effective temperature, surface gravity and metallicity	^{ah}
RV	...	143	Flag on target of radial velocity searching planets survey[14]	...
Planet	...	144	Flag of planets[15]	...
Ref.35	...	145	Reference of planet discovery	^{ai}
LoRes spectrum	...	146	Instrument of low resolution spectrum[16]	...
HiRes spectrum	...	147	Instrument of high resolution spectrum[16]	...
LoRes imaging	...	148	Instrument of low resolution image[16]	...
HiRes imaging	...	149	Instrument or reference of high resolution image	^{aj}
α_{J2000}	hms	150	Right ascention in J2000.0	...
δ_{J2000}	dms	151	Declination J2000.0	...
l_{J2000}	deg	152	Declination J2000.0	...
b_{J2000}	deg	153	Galactic longitude J2000.0	...
Ref.36	...	154	Coordinates reference	^{r}
Origin	...	155	Source of origin	^{ak}
Class	...	156	Carmencita class[17]	...
$\rm Spt_{num.}$	...	157	Numerical spectral subtype	...
Notes	...	158	Additional notes	...

References. [a] Gliese & Jahreiss 1979. SpT: [b] Alonso-Floriano et al. (2015a); Bidelman (1985); Bochanski et al. (2005); Briceño et al. (1998, 1999); Buscombe et al. (1998); Close et al. (2003); Cruz & Reid (2002); Cruz et al. (2003); Cvetkovic et al. (2012); Daemgen et al. (2007); Deacon et al. (2012); Fleming et al. (1988); Frith et al. (2013); Gizis & Reid (1997); Gigoyan et al. (2010); Gray et al. (2003, 2006); Joy & Abt (1974); Jahreiss et al. (2008); Janson et al. (2012); Jenkins et al. (2009); Kirkpatrick et al. (1991); Klutsch et al. priv. comm.; Koen et al. (2010); Konopacky et al. (2010); Law et al. (2008); Lépine et al. (2003, 2009, 2013); Lodieu et al. 2005); Metodieva et al.(2015); Montes et al. (2001); Newton et al. (2014); Pesch & Bidelman (1997); PMSU: (Palomar/Michigan State University survey catalogue of nearby stars) Reid et al. (1995), Hawley et al. (1996), Gizis et al. (2002); Phan-Bao & Bessell (2006); Pravdo et al. (2006); Rajpurohit et al. (2013); Reid et al. (2003, 2004, 2007); Riaz et al. (2006); Riedel et al. (2014); Scholz et al. (2005); Schmidt et al. (2007); Shkolnik et al. (2009), 2010; Skiff (2014); Strassmeier (2009); Yi et al. (2014). [c] Kim (2015. [d] Cortés-Contreras (this work); Gallardo (2015); van Leeuwen (2007); Roeser et al. (2010). [e] Binks & Jeffries (2014); Bochanski et al. (2005); de Bruijne & Eilers (2012); Burgasser et al. (2015); Caballero et al. (2010); Dawson et al. (2005); Delfosse et al. (1998); Delfosse et al. (1999a); Deshpande et al. (2012); Dyer (1954); Elliott et al. (2014); Evans (1979); Latham et al. (2002); Maldonado et al. (2010); Malo et al. (2014a); Mochnacki et al. (2002); Montes et al. (2001); Moor et al. (2013); Newton et al. (2014); PMSU: (Palomar/Michigan State University survey catalogue of nearby stars) Reid et al. (1995), Hawley et al. (1996), Gizis et al. (2002); Reiners & Basri (2009); Riedel et al. (2011); Siebert et al. (2011); Schöfer (2015); Schlieder et al. (2010); Shkolnik et al. (2010, 2012); Terrien et al. (2015); Tokovinin et al. (2002), 2015); Torres et al. (2006); Upgren & Harlow (1996); West et al. (2015); White et al. (2007); Wilson (1953); Zuckerman et al. (2011).

References (cont.) [f] Dawson et al. (2005); Dittmann et al. (2014); Dupuy & Liu (2012); Gatewood & Coban (2009); Gliese & Jahreiss (1991); Harrington & Dahn (1980); Henry et al. (2006); Ireland et al. (2008); Jao et al. (2005); Jenkins (1952); Jenkins et al. (2009); Lṕine et al. (2009); Perryman et al. (1997); Pravdo et al. (2006); Reid et al. (2002); Reidel et al. (2010); Riedel et al. (2014); Shkolnik et al. (2012); Subasavage et al. (2009); van Leeuwen (2007); Weinberger et al. (2016); Weis (1987). [g] Cortés-Contreras (this work); Cruz et al. (2003); Dawson et al. (2005); Dittmann et al. (2014); Dupuy & Liu (2012); Gatewood & Coban (2009); Gliese & Jahreiss (1991); Harrington & Dahn (1980); Henry et al. (2006); Ireland et al. (2008); Jao et al. (2005); Jenkins (1952); Jenkins (1963); Jenkins et al. (2009); Lépine et al. (2009, 2013); Lodieu et al. (2005); Newton et al. (2014); Perryman et al. (1997); Phan-Bao & Bessell (2006); Pravdo et al. (2006); Reiners & Basri (2009); Reid et al. (2002); Riedel et al. (2010); Riedel et al. (2014); Shkolnik et al. (2012); Subasavage et al. (2009); van Altena et al. (1995); van Leeuwen (2007); Weinberger et al. (2016); Weis (1987). [h] Lépine et al. (2013); Montes priv. comm. [i] Bianchi et al. (2011). [j] Adelman-McCarthy et al. (2011); Pickles et al. (2010). [k] Hog et al. (2000). [l] Adelman-McCarthy et al. (2011); Pickles et al. (2010); Zacharias et al. (2013). [m] Adelman-McCarthy et al. (2011); Zacharias et al. (2013). [n] Perryman et al. (1997); Zacharias et al. (2013). [o] Zacharias et al. (2009); (2013). [p] Evans et al. (2002); Pickles et al. (2010); Adelman-McCarthy et al. (2011); Zacharias et al. (2013). [q] Koen et al. (2010); Monet et al. (2003); Reid et al. (2004). [r] Skrutskie et al. (2006). [s] Cutri et al. (2012, 2014). [t] Mason et al. (2001-2015). [u] Alonso-Floriano et al. (2015b); Alonso-Santiago (2011); Buningham et al. (2009); Caballero (2007); Caballero et al. (2010); Cortés-Contreras priv. comm; Cortés-Conteras et al. (2016); Deacon et al. (2012); Dorda (2011); Janson et al. (2012); Tanner et al. (2010); Mason et al. (2001-2015); Tokovinin et al. (2006). [v] Cutri et al. (2012, 2014); Fabricius et al. (2002); Luyten (1997); Leggett et al. (2010); Lépine & Bongiorno (2007); Monet et al. (2003); Skrutskie et al. (2006). [w] Alonso-Santiago (2011); Al-Shukri et al. (1996); Ansdell et al. (2015); Balega et al. (2007, 2013); Bergfors et al. (2010); Bernat et al. (2012); Beuzit et al. (2004); Biller et al. (2013); Bonfils et al. (2013); Bopp & Fekel (1977); Bowler et al. (2015); Caballero priv.comm; Christy (1978); Cortés-Contreras priv. comm; Cortés-Contreras et al. (2016); Davison et al. (2014); Delfosse et al. (1999b); Docobo et al. (2006); Dorda (2011); Duquennoy & Mayor (1988); Elliott et al. (2015); Gizis et al. (2002); Harlow (1996); Harrington et al. (1981); Herbig & Moorhead (1965); Horch et al. (2010, 2011, 2012); Ireland et al. (2008); Irwin et al. (2009); Janson et al. (2012, 2014a, 2014b); Jenkins et al. (2009); Jódar et al. (2013); Joy & Abt (1974); Lampens et al. (2007); Law et al. (2008); Llamas (2014); Malkov et al. (2012); Malo et al. (2014a); Malogolovets et al. (2007); Marcy et al. (1987); Mariotti et al. (1990); Martinache et al. (2007); Mason et al. (2001-2015); Mochnacki et al. (2002); Montagnier et al. (2006); Nidever et al. (2002); Perryman et al. (1997); Pourbaix et al. (2004); Pravdo et al. (2006); Reid & Gizis (1997); Reiners & Basri (2009); Reiners et al. (2012); Schöfer (2015); Shkolnik et al. (2010); Skrutskie et al. (2006); Stauffer et al. (1997); Strand (1977); Tokovinin et al. (2010, 2015); Tomkin & Pettersen (1986); Ward-Duong et al. (2015); Woitas et al. (2000); Zasche et al. (2009). [x] Balega et al. (2007); Bergfors et al. (2010); Beuzit et al. (2004); Bowler et al. (2015); Close et al. (2003); Daemgen et al. (2007); Docobo et al. (2006); Elliott et al. (2015); Horch et al. (2010, 2011, 2012); Janson et al. (2012, 2014a); Jódar et al. (2013); Law et al. (2006, 2008); Mason et al. (2001-2015); Montagnier et al. (2006); Pravdo et al. (2004); Shkolnik et al. (2012); Skrutskie et al. (2006); Ward-Duong et al. (2015); White & Ghez 2001). [y] Alonso-Floriano et al. (2015a); Bochanski et al. (2005); Davison et al. (2015); Lépine et al. (2013); Martínez-Rodrǵuez (2014); Metodieva et al. (2015); PMSU: (Palomar/Michigan State University survey catalogue of nearby stars) Reid et al. (1995), Hawley et al. (1996), Gizis et al. (2002); Phan-Bao & Bessell (2006; Riaz et al. (2006); Riedel et al. (2014); Schöfer (2015); Shkolnik et al. (2009, 2010); West et al. (2015). [z] Voges et al. (1999); Evans et al. (2010); Rosen et al. (2016). [aa] Antonova et al. (2013); Barnes et al. (2014); ;Browning et al. (2010); Davison et al. (2015); Delfosse et al. (1998); Deshpande et al. (2012); Gizis et al. (2002); Glebocki et al. (2000, 2005); Martínez-Rodrǵuez (2014); Herrero et al. (2012); Houdebine (2010); Jeffers et al. (2016, submitted; Jenkins et al. (2009); Marcy & Chen (1992); Malo et al. (2014a); Martínez-Arnáiz et al. (2010); Mochnacki et al. (2002); Mohanty & Basri (2003); Reid et al. (2004); Reiners & Basri (2007); Reiners (2007); Reiners et al. (2012); Stauffer & Hartmann (1986); Schlieder et al. (2010, 2012b); Tokovinin (1992); Torres et al. (2006); White et al. (2007). [ab] Bergfors et al. (2010); Bidelman (1988); Chugainov (1974); Delfosse et al. (1999a); Devor et al. (2008); Giacobbe et al. (2012); Houdebine & Mullan (2015); Hartman et al. (2004, 2010, 2011); Hunt-Walker et al. (2012); Irwin et al. (2009, 2011); Kiraga (2012); Kiraga & Stepien (2007); Koen & Eyer (2002); Korhonen et al. (2010); McQuillan et al. (2013); Messina et al. (2010); Norton et al. (2007); Pojmanski (2002); Shkolnik et al. (2010); Wang & Ford (2011); West et al. (2015). [ac] Bochasnki et al. (2005); Cruz & Reid (2002); Crifo et al. (2005); Lépine et al. (2003, 2013); Phan-Bao & Bessell (2006); PMSU: (Palomar/Michigan State University survey catalogue of nearby stars) Reid et al. (1995), Hawley et al. (1996), Gizis et al. (2002); Riaz et al. (2006); West et al. (2015). [ad] Agrawal et al. (1986); Ambartsumian et al. (1973); Andersen & Pettersen (1975); Butters et al. (2010); Drake et al. (2014); Evans (1975); Gershberg et al. (1999); Martínez-Rodrǵuez (2014); Hambaryan et al. (1999); Haro et al. (1975); Hartman et al. (2011); Hojaev (1986); Jackson et al. (1987); Lippincott (1952); Melikan et al. (2013); Mullan (1974); Mullan et al. (1989); Norton et al. (2007); Pettersen (1975, 1991, 2006); Pettersen et al. (1980); Schmidt et al. (2007); Svestka (1954); White et al. (1989).

References (cont.)
[ae] Alonso-Floriano et al. (2015b); Bertout & Genova (2006); Caballero et al. (2010); Elliott et al. (2014); López-Santiago et al. (2006); Malo et al. (2013; 2014a); Montes prov. comm.; Rebull et al. (2010); Reid et al. (2002); Riedel et al. (2014); Schlieder et al. (2010, 2012a, 2012b); Shkolnik et al. (2012); Stern et al. (1995); Tetzlaff et al. (2011); Torres et al. (2006, 2008); van Altena et al. (1995); van Leeuwen (2007; Zuckerman et al. (2004, 2011). [af] Mace et al. (2013); Montes priv. comm. [ag] Anderson & Francis (2012); Deacon et al. (2005); Gizis & Reid (1997); PMSU: (Palomar/Michigan State University survey catalogue of nearby stars) Reid et al. (1995), Hawley et al. (1996), Gizis et al. (2002). [ah] Passegger et al. in prep. [ai] Astudillo-Defru et al. (2015); Bonfils et al. (2012); Burgasser et al. (2010); Burt et al. (2014); Charbonneau et al. (2009); Endl et al. (2003, 2006, 2008); Gatewood (1996); Gillon et al. (2016); Howart et al. (2010); Johnson & Apps (2009); Johnson et al. (2010); Marcy et al. (1998); Wright et al. (2016); Zechmeister et al. (2009). [aj] Ansdell et al. (2015; Balega et al. (2002, 2004, 2006, 2007, 2013); Bergfors et al. (2010); Beuzit et al. (2004); Biller et al. (2013); Bowler et al. (2015); Cortés-Contreras et al. (2016); Daemgen et al. (2007); Janson et al. (2012, 2014a); Jódar et al. (2013); Horch et al. (2011); Lafrenière et al. (2007); Law et al. (2008); Leinert et al. (1993); McCarthy et al. (2001); Riddle et al. (2015); Tokovinin et al. (2015); Ward-Duong et al. (2015). [ak] Bidelman (1985); Bochanski et al. (2005); Cruz & Reid (2002); Cruz et al. (2003); Deacon et al. (2012); Fleming et al. (1988); Frith et al. (2013); Giclas et al. (1959); Gigoyan et al. (2010); Gizis & Reid (1997); Gizis et al. (2000); Gray et al. (2003); Henry et al. (1994); Joy & Abt(1974); Kirkpatrick et al. (1991); Law et al. (2008); Lee (1984); Lépine et al. (2003, 2009, 2013); Lépine & Gaidos (2011); Lodieu et al. (2005); Metodieva et al. (2015); Mochnacki et al. (2002); Newton et al. (2014); Phan-Bao & Bessell (2006); PMSU: (Palomar/Michigan State University survey catalogue of nearby stars) Reid et al. (1995), Hawley et al. (1996), Gizis et al. (2002); Reiners & Basri (2009); RECONS: Henry et al. 1994); Kirkpatrick et al. (1995); Henry et al. (2006); Jao et al. (2011); Riedel et al. (2014); Winters et al. (2015) and references therein; Reid et al. (2003, 2004, 2007); Reyes-Sánchez (2014); Riaz et al. (2006); Scholz et al. (2005); Shkolnik et al. (2009); Yi et al. (2014).
Notes. [1] "J" stands for the standard equinox of J2000.0 and HHMMm+DDd for truncated equatorial coordinates. The right-most digit of the fields HHMMm and DDd should be computed as $m = floor(SS/6)$ and $d = floor(MM/6)$, respectively. For binary pairs with similar HHMMm+DDd, we added N/S or E/W to distinguish them. [2] A for primary, B for secondary, C for tertiary... AB, BC, Aab, ... for very close -spectroscopic or resolved- pairs. [3] See Table 2.2. [4] See Table 2.1. [5] The discovery name was used with the following priority: proper, variable in constellation, Henry Draper HD, Gliese-Jahreiss GJ < 3000, Luyten LP, Giclas G if unique, Luyten LHS, etc. For M dwarfs with variable names and those that have bright physical companions, the variable name or the name of the primary was used by adding "B" or the corresponding letter. [6] USNO-B1.0 infrared I_N magnitude, Johnson I magnitude otherwise. [7] Indicates whether the star belongs to a binary or multiple system. Wide: companions at angular separations greater than 5 arcsec; Resolved Physical: companions at angular separations lower than 5 arcsec; EB: eclipsing binaries; SB, (SB1, SB2, SB3): spectroscopic binaries (single, double or triple lined); Single: no physical companion known. [8] Or Karmen identifier if it is a Carmencita star. [9] Defined with respect to the Carmencita star as: $magnitude_{Karmn} - magnitude_{companion}$. [10] Yes: flare star; Yes?: possibly a flare star; ...: unkown. [11] X-rays emission from HRI&PSPC/ROSAT, EPIC/XMM-Newton, and ACIS/Chandra. [12] Stellar kinematic group followed by "?", and stars referenced by Mon16 indicate candidancy. AB Dor: AB Doradus; Arg: Argus; Car: Carina; Cas: Castor; Col: Columba; HS: Hyades; HSc: Hyades cluster; Her-Lyr: Hercules-Lyra; IC: IC 2391; LA: Local Association; TucHor: Tucana-Horologium; UMa: Ursa Major; bPic: β Pictoris; Tau: Taurus; TW Hya: TW hydrae. [13] YD: Young disc; D: Thin disc; TD-D: Transition Thin/Thick disc; TD: Thick disc; H: Halo. [14] Yes: confirmed target; ?: unkown. [15] Yes: confirmed planet; Yes?: unconfirmed planet; No: no planet detected. [16] Spectra and images taken by the CARMENES Consortium. [17] *Alpha*, *Beta*, *Delta*, *Gamma*.

Table B.2: Names, spectral types, distances and astrometric parameters of Carmencita stars.

Karmn	Flags[a]	Name	SpT	Ref.[b]	α (J2000)	δ (J2000)	Ref.[c]	d [pc]	ed [pc]	Ref.[d e]
J00012+139N	B.F	BD+13 5195	M0.5 V+	JA74	00:01:13.19	+13:58:30.3	2MASS	35.15	6.13	HIP2
J00012+139S	..F	BD+13 5195B	M0.0 V	Lep13	00:01:12.86	+13:58:19.7	2MASS	35.15	6.13	aHIP2
J00026+383	..F	2MASS J00024011+3821453	M4.0 V	Fri13	00:02:40.12	+38:21:45.3	2MASS	20.0	0.8	Cor16
J00033+046	..F	HIP 263	M1.5 V	Lep13	00:03:19.00	+04:41:12.9	2MASS	29.21	2.74	HIP2
J00051+457		GJ 2	M1.0 V	PMSU	00:05:10.78	+45:47:11.6	2MASS	11.25	0.18	HIP2
J00056+458	J..	HD 38B	M0.0 V	Cve12	00:05:40.90	+45:48:37.5	2MASS	11.75	0.35	aHIP1
J00067-075		GJ 1002	M5.5 V	PMSU	00:06:43.26	-07:32:14.7	2MASS	4.82	0.03	Wein16
J00077+603	B..	G 217-032	M4.0 V+	AF15	00:07:42.64	+60:22:54.3	2MASS	14.6	0.4	Dit14
J00078+676	..F	2MASS J00075079+6736255	M2.0 V	Lep13	00:07:50.80	+67:36:25.6	2MASS	21.1	0.4	Cor16
J00079+080	..F	LP 524-065	M3.0 V	PMSU	00:07:59.09	+08:00:19.1	2MASS	22.73	3.25	vAl95
J00081+479	S..	1RXS J000806.3+475659	M4.0 V+	Lep13	00:08:06.43	+47:57:02.5	2MASS	11.6	0.5	Cor16
J00084+174	..F	MCC 351	M0.0 V	PMSU	00:08:27.30	+17:25:27.5	2MASS	21.75	0.91	HIP2
J00088+208	B..	LP 404-033	M4.5 V+	PMSU	00:08:53.92	+20:50:25.2	2MASS	14.8	0.6	Dit14
J00110+052	..F	G 031-029	M1.0 V	Lep13	00:11:04.63	+05:12:32.0	2MASS	42.99	6.97	HIP2
J00115+591	..F	LSR J0011+5908	M5.5 V	AF15	00:11:31.82	+59:08:40.0	2MASS	9.23	0.04	GC09
J00118+229	..F	LP 348-040	M3.5 V	AF15	00:11:53.03	+22:59:04.7	2MASS	16.6	0.5	Dit14
J00119+330	..F	G 130-053	M3.5 V	AF15	00:11:56.54	+33:03:17.8	2MASS	18.1	0.6	Cor16
J00122+304	..F	2MASS J00121341+3028443	M4.5 V	AF15	00:12:13.41	+30:28:44.3	2MASS	20.7	0.9	Cor16
J00131+703	..f	TYC 4298-613-1	M2.0 V	Lep13	00:13:11.55	+70:23:52.8	2MASS	20.2	0.4	Cor16
J00132+693	B..	GJ 11 AB	M3.0 V+	PMSU	00:13:15.79	+69:19:37.2	2MASS	19.0	1.0	Dit14
J00133+275	..F	2MASS J00131951+2733310	M4.5 V	AF15	00:13:19.52	+27:33:31.1	2MASS	22.6	1.0	Cor16
J00136+806	..f	G 242-048	M1.5 V	AF15	00:13:38.81	+80:39:56.9	2MASS	19.59	0.67	HIP2
J00137+806	V.F	LP 012-304	M5.0 V	PMSU	00:13:43.06	+80:39:49.4	2MASS	19.59	0.67	aHIP2
J00154-161	Bm.	GJ 1005 AB	M4.0 V+	PMSU	00:15:27.99	-16:08:00.9	2MASS	5.0	0.23	HIP2
J00156+722	..F	G 242-049	M2.0 V	Lep13	00:15:36.52	+72:17:00.9	2MASS	26.3	0.5	Cor16
J00158+135	..f	GJ 12	M3.0 V	PMSU	00:15:49.20	+13:33:21.9	2MASS	10.0	0.4	Dit14
J00159-166	B..	BPS CS 31060-0015	M4.1 V+	Shk09	00:15:58.08	-16:36:57.9	2MASS	18.0	0.4	Shk12
J00162+198E		LP 404-062	M4.0 V	AF15	00:16:16.08	+19:51:51.5	2MASS	16.31	3.49	aHIP2
J00162+198W		EZ Psc	M4.0 V	AF15	00:16:14.63	+19:51:37.6	2MASS	16.31	3.49	HIP2
J00169+051	..F	GJ 1007	M4.5 V	PMSU	00:16:56.29	+05:07:26.1	2MASS	17.57	1.14	vAl95
J00169+200	B.F	G 131-047	M3.5 V+	PMSU	00:16:56.78	+20:03:55.1	2MASS	24.1	0.8	Cor16
J00173+291	..f	Ross 680	M2.0 V	PMSU	00:17:20.21	+29:10:57.8	2MASS	23.2	1.3	HIP2

Table B.2: Names, spectral types, distances and astrometric parameters of Carmencita stars (continued).

Karmn	Flags[a]	Name	SpT	Ref.[b]	α (J2000)	δ (J2000)	Ref.[c]	d [pc]	ed [pc]	Ref.[d e]
J00176-086	..F	BD-09 40	M0.0 V	PMSU	00:17:40.89	-08:40:55.9	2MASS	34.57	2.28	HIP2
J00179+209	..F	LP 404-081	M1.0 V	Lep13	00:17:59.19	+20:57:24.9	2MASS	25.3	0.3	Cor16
J00182+102	..f	GJ 16	M1.5 V	PMSU	00:18:16.59	+10:12:10.1	2MASS	16.34	0.57	HIP2
J00183+440		GX And	M1.0 V	AF15	00:18:22.57	+44:01:22.2	2MASS	3.59	0.01	HIP2
J00184+440		GQ And	M3.5 V	PMSU	00:18:25.50	+44:01:37.6	2MASS	3.6	0.1	Dit14
J00188+278	..F	LP 292-066	M4.0 V	PMSU	00:18:53.53	+27:48:50.0	2MASS	14.5	1.1	Dit14
J00201-170	.mF	LP 764-108	M1.0 V(k)+	Gra06	00:20:08.38	-17:03:40.9	2MASS	23.2	2.02	HIP2
J00204+330	..F	LP 292-067	M5.5 V	PMSU	00:20:29.22	+33:05:08.2	2MASS	12.5	0.6	vAl95
J00207+596	..F	[I81] M 134	M2.5 V	Lep13	00:20:47.73	+59:36:17.3	2MASS	23.9	0.6	Cor16
J00209+176	..F	StKM 1-25	M0.0 V	Lep13	00:20:57.19	+17:38:16.1	2MASS	31.2	0.3	Cor16
J00210+557	..F	G 217-043	M2.0 V	Ski14	00:21:04.33	+55:43:59.1	2MASS	31.0	0.6	Cor16
J00218+382	..F	G 171-051	M3.0 V	Lep13	00:21:53.93	+38:16:29.5	2MASS	20.5	0.6	Cor16
J00219+492	B.F	LP 149-056	M2.5 V+	PMSU	00:21:57.81	+49:12:38.0	2MASS	26.3	0.6	Cor16
J00234+243	V.f	GJ 1011	M4.0 V	PMSU	00:23:28.03	+24:18:24.4	2MASS	16.39	1.102	vAl95
J00234+771	..F	GJ 1010 A	M1.5 V	PMSU	00:23:28.65	+77:11:21.7	2MASS	19.2	0.7	HIP2
J00235+771	..F	GJ 1010 B	M4.0 V	PMSU	00:23:31.66	+77:11:26.8	2MASS	19.23	0.75	aHIP2
J00240+264	..F	LSPM J0024+2626	M4.0 V	AF15	00:24:03.77	+26:26:29.9	2MASS	22.1	1.4	Dit14
J00244+360	..F	G 130-067	M1.0 V	Lep13	00:24:25.88	+36:03:53.7	2MASS	33.9	0.4	Cor16
J00245+300	..F	G 130-068	M4.5 V	PMSU	00:24:34.78	+30:02:29.5	2MASS	18.94	1.58	vAl95
J00253+228	..F	LP 349-018	M4.0 V	PMSU	00:25:20.64	+22:53:12.1	2MASS	14.2	0.7	Dit14
J00268+701	..F	GJ 21	M0.5 V	PMSU	00:26:52.69	+70:08:32.6	2MASS	16.48	0.38	HIP2
J00271+496	..F	G 217-051	M4.5 V	PMSU	00:27:06.74	+49:41:53.1	2MASS	20.9	0.9	Dit14
J00279+223	B.f	LP 349-025 AB	M8.0 V+	Kon10	00:27:55.93	+22:19:32.8	2MASS	15.3	0.9	Dit14
J00286-066		GJ 1012	M4.0 V	PMSU	00:28:39.48	-06:39:48.1	2MASS	13.26	0.897	Rei02
J00288+503	B..	G 172-001 AB	M4.0 V+	Dae07	00:28:53.92	+50:22:33.0	2MASS	17.5	0.7	Dit14
J00315-058	..f	GJ 1013	M3.5 V	PMSU	00:31:35.39	-05:52:11.6	2MASS	16.1	1.2	vAl95
J00322+544	..F	G 217-056	M4.5 V	AF15	00:32:15.74	+54:29:02.7	2MASS	20.2	0.6	Dit14
J00324+672N	B..	V547 Cas Aab	M2.0 V+	PMSU	00:32:29.71	+67:14:08.0	2MASS	10.1	0.2	HIP2
J00324+672S	B..	V547 Cas B	M3.0 V	PMSU	00:32:29.80	+67:14:04.4	2MASS	10.1	0.2	aHIP2
J00325+074	B..	LP 525-039 AB	M4.0 V+	PMSU	00:32:34.81	+07:29:27.1	2MASS	11.0	0.4	Cor16
J00328-045	B.f	GR* 50 AB	M4.5 V+	AF15	00:32:53.14	-04:34:06.8	2MASS	13.3	0.6	Cor16
J00333+368	..f	G 132-004	M3.0 V	Lep13	00:33:20.48	+36:50:26.2	2MASS	18.9	0.5	Cor16
J00341+253	B.F	V493 And	M0.0 V+	Lep13	00:34:08.43	+25:23:49.8	2MASS	32.9	0.3	Cor16

Table B.2: Names, spectral types, distances and astrometric parameters of Carmencita stars (continued).

Karmn	Flags[a]	Name	SpT	Ref.[b]	α (J2000)	δ (J2000)	Ref.[c]	d [pc]	ed [pc]	Ref.[d e]
J00346+711	..F	LP 028-158	M3.5 V	PMSU	00:34:37.74	+71:11:41.9	2MASS	20.4	0.9	Dit14
J00357+025	B.F	NLTT 1930	M5.0 V+	Law08	00:35:43.13	+02:33:13.8	2MASS	18.6	1.0	Cor16
J00358+526	V.F	NLTT 1920	M2.5 V	AF15	00:35:53.22	+52:41:12.4	2MASS	16.1	2.4	vAl95
J00359+104	..F	GJ 1014	M5.0 V	PMSU	00:35:55.57	+10:28:35.2	2MASS	15.72	1.11	vAl95
J00361+455	..f	G 172-013	M2.5 V	PMSU	00:36:08.48	+45:30:57.6	2MASS	22.8	5.1	vAl95
J00374+515	..F	G 172-014	M0.5 V	Lep13	00:37:25.99	+51:33:07.3	2MASS	33.2	11.3	vAl95
J00380+169	..F	2MASS J00380386+1656028	M3.0 V	AF15	00:38:03.86	+16:56:02.9	2MASS	25.0	0.7	Cor16
J00382+523	..F	G 218-005	M0.0 V	Lep13	00:38:15.29	+52:19:55.8	2MASS	23.7	1.08	HIP2
J00385+514	..F	G 172-015	M2.5 V	PMSU	00:38:33.88	+51:27:58.0	2MASS	15.6	2.6	vAl95
J00389+306		Wolf 1056	M2.5 V	AF15	00:38:58.79	+30:36:58.4	2MASS	12.5	0.6	vAl95
J00395+149N	B.F	LP 465-062	M4.5 V+	AF15	00:39:33.74	+14:54:34.8	2MASS	26.7	2.6	Dit14
J00395+149S	..F	LP 465-061	M4.0 V	AF15	00:39:33.49	+14:54:18.9	2MASS	28.3	1.4	vAl95
J00395+605	..F	G 217-061	M2.5 V	PMSU	00:39:33.80	+60:33:15.4	2MASS	27.1	0.6	Cor16
J00409+313	..F	G 069-011	M4.0 V	PMSU	00:40:56.23	+31:22:56.5	2MASS	17.7	0.7	Dit14
J00413+558	..F	GJ 1015 A	M4.0 V	PMSU	00:41:20.78	+55:50:04.5	2MASS	23.04	1.06	vAl95
J00427+438	..F	2MASS J00424780+4349248	M2.5 V	Lep13	00:42:47.81	+43:49:24.9	2MASS	19.4	0.5	Cor16
J00428+355	S..	FF And	M1.0 V+	PMSU	00:42:48.21	+35:32:55.4	2MASS	23.3	1.55	HIP2
J00435+284	..F	GJ 1019	M4.0 V	PMSU	00:43:35.59	+28:26:41.4	2MASS	19.3	1.49	vAl95
J00443+091	..F	NLTT 2413	M4.5 V	PMSU	00:44:20.70	+09:07:34.6	2MASS	14.7	0.7	Cor16
J00443+126	..F	G 032-044	M3.5 V	PMSU	00:44:19.34	+12:37:02.7	2MASS	16.5	0.5	Cor16
J00449-152	..F	NLTT 2465	M4.5 V	PMSU	00:44:59.31	-15:16:16.7	2MASS	15.5	0.7	Cor16
J00459+337	B.f	G 132-025 AB	M4.5 V+	Law08	00:45:56.63	+33:47:10.9	2MASS	17.36	1.27	Dit14
J00463+353	..F	HAT 163-01012	M1.5 V	Lep13	00:46:21.85	+35:22:12.5	2MASS	31.1	0.5	Cor16
J00464+506	..F	G 172-022	M4.0 V	AF15	00:46:29.90	+50:38:38.9	2MASS	22.5	0.9	Cor16
J00468+160	..F	2MASS J00465328+1603028	M2.0 V	Lep13	00:46:53.29	+16:03:02.8	2MASS	21.2	0.4	Cor16
J00484+753	..F	LSPM J0048+7518	M3.0 V	AF15	00:48:29.71	+75:18:48.0	2MASS	26.6	1.2	Dit14
J00487+270	..F	G 069-024	M2.5 V	PMSU	00:48:45.56	+27:01:09.7	2MASS	22.2	0.5	Cor16
J00489+445	B.f	LP 193-584 AB	M3.0 V+	PMSU	00:48:58.22	+44:35:09.1	2MASS	22.2	0.6	Cor16
J00490+657	..F	2MASS J00490477+6544377	M2.5 V	AF15	00:49:04.77	+65:44:37.8	2MASS	28.3	0.7	Cor16
J00502+086	S.F	RX J0050.2+0837 2	M4.5 V+	AF15	00:50:17.53	+08:37:34.1	2MASS	16.5	0.7	Cor16
J00505+248	B..	FT Psc AB	M3.5 V+	PMSU	00:50:33.19	+24:49:01.0	2MASS	13.3	1.2	Dit14
J00511+225	..F	BPM 84579	M1.5 V	Lep13	00:51:10.67	+22:34:45.8	2MASS	22.9	0.3	Cor16
J00514+583	..F	Wolf 33	M0.0 V	Lep13	00:51:29.64	+58:18:07.1	2MASS	18.51	0.89	HIP2

Table B.2: Names, spectral types, distances and astrometric parameters of Carmencita stars (continued).

Karmn	Flags[a]	Name	SpT	Ref.[b]	α (J2000)	δ (J2000)	Ref.[c]	d [pc]	ed [pc]	Ref.[d e]
J00515-229	.mF	HD 4967 B	M5.5 V	PMSU	00:51:35.16	-22:54:30.8	2MASS	15.6	0.3	aHIP2
J00520+205	..F	StKM 2-77	M1.0 V	Lep13	00:52:00.03	+20:34:58.6	2MASS	31.9	3.1	HIP2
J00532+190	..F	LSPM J0053+1903	M2.5 V	Lep13	00:53:12.98	+19:03:27.1	2MASS	22.4	0.5	Cor16
J00538+459	..F	G 172-028	M0.0 V	Lep13	00:53:53.22	+45:56:40.5	2MASS	26.81	1.67	HIP2
J00540+691	..F	Ross 317	M2.0 V	AF15	00:54:00.49	+69:11:01.3	2MASS	35.1	0.7	Cor16
J00548+275	..F	G 069-032	M4.5 V	AF15	00:54:48.03	+27:31:03.6	2MASS	23.5	1.3	Dit14
J00566+174	..f	GJ 1024	M4.0 V	PMSU	00:56:38.42	+17:27:34.7	2MASS	17.73	1.29	vAl95
J00570+450		G 172-030	M3.0 V	Lep13	00:57:02.61	+45:05:09.9	2MASS	13.9	0.4	Cor16
J00577+058	..F	BD+05 127	M0.0 V	Lep13	00:57:44.56	+05:51:20.6	2MASS	20.7	0.2	Cor16
J00580+393	..F	1RXS J005802.4+391912	M4.5 V	AF15	00:58:01.16	+39:19:11.2	2MASS	15.1	0.7	Cor16
J01008+669	..F	LP 051-017	M3.5 V	PMSU	01:00:49.49	+66:56:54.7	2MASS	21.2	0.7	Cor16
J01009-044	..f	GJ 1025	M4.0 V	AF15	01:00:56.44	-04:26:56.1	2MASS	14.7	0.6	Cor16
J01013+613		GJ 47	M2.0 V	PMSU	01:01:20.06	+61:21:56.0	2MASS	11.0	0.5	vAl95
J01019+541	..f	G 218-020	M5.0 V	PMSU	01:01:59.53	+54:10:57.8	2MASS	10.9	0.3	Dit14
J01025+716		BD+70 68	M3.0 V	PMSU	01:02:32.13	+71:40:47.6	2MASS	8.1	0.1	HIP2
J01026+623		BD+61 195	M1.5 V	AF15	01:02:38.96	+62:20:42.2	2MASS	9.96	0.15	HIP2
J01032+200	B..	GJ 1026 AB	M2.0 V+	PMSU	01:03:14.09	+20:05:52.4	2MASS	16.2	0.9	HIP2
J01032+316	..F	LP 294-040	M3.5 V	PMSU	01:03:13.95	+31:40:59.9	2MASS	40.2	9.7	Dit14
J01032+712	B.F	G 242-077	M4.0 V+	AF15	01:03:14.43	+71:13:12.7	2MASS	18.34	0.88	Dit14
J01033+623		V388 Cas	M5.0 V	AF15	01:03:19.72	+62:21:55.7	2MASS	9.96	0.15	aHIP2
J01036+408	B.F	G 132-050	M0.0 V+	Lep13	01:03:40.12	+40:51:28.9	2MASS	29.89	2.08	aHIP2
J01037+408	B.F	G 132-051	M2.6 V+	Shk09	01:03:42.11	+40:51:15.8	2MASS	29.89	2.08	HIP2
J01041+108	..F	StKM 1-112	M1.0 V	Lep13	01:04:11.04	+10:51:36.4	2MASS	34.4	0.5	Cor16
J01048-181	.m.	GJ 1028	M5.0 V	PMSU	01:04:53.69	-18:07:29.3	2MASS	9.78	0.08	Wein16
J01056+284		GJ 1029	M5.0 V	PMSU	01:05:37.32	+28:29:34.0	2MASS	11.3	0.4	Dit14
J01066+152	..f	GJ 1030	M2.0 V	PMSU	01:06:41.52	+15:16:22.9	2MASS	22.1	1.1	HIP2
J01069+804	..F	NLTT 3583	M4.5 V	AF15	01:06:54.74	+80:27:34.4	2MASS	15.3	1.0	Dit14
J01078+128	..F	G 002-021	M1.5 V	Lep13	01:07:52.18	+12:52:51.9	2MASS	29.1	0.4	Cor16
J01102-118	..f	LP 707-016	M3.0 V	Sch05	01:10:17.52	-11:51:17.6	2MASS	17.7	0.5	Cor16
J01114+154	B..	LP 467-016 AB	M5.0 V+	PMSU	01:11:25.42	+15:26:21.5	2MASS	17.2	2.2	Dit14
J01116+120	..F	LP 467-015	M2.0 V	Lep13	01:11:36.66	+12:05:07.4	2MASS	27.3	0.5	Cor16
J01119+049N	..F	G 070-043	M3.0 V	PMSU	01:11:55.63	+04:55:04.9	2MASS	15.9	0.5	vAl95
J01119+049S	..F	G 070-044	M3.5 V	PMSU	01:11:57.99	+04:54:12.0	2MASS	13.0	0.9	Dit14

Table B.2: Names, spectral types, distances and astrometric parameters of Carmencita stars (continued).

Karmn	Flags[a]	Name	SpT	Ref.[b]	α (J2000)	δ (J2000)	Ref.[c]	d [pc]	ed [pc]	Ref.[d e]
J01125-169	.m.	YZ Cet	M4.5 V	PMSU	01:12:30.53	-16:59:57.0	2MASS	3.7	0.1	HIP2
J01133+589	B.F	Wolf 58	M1.5 V	Lep13	01:13:19.77	+58:55:22.4	2MASS	24.5	0.4	Cor16
J01134-229	.mF	GJ 1033	M4.0 V	PMSU	01:13:24.02	-22:54:07.8	2MASS	21.8	0.9	Cor16
J01141+790	..F	2MASS J01140633+7904007	M3.0 V	Fri13	01:14:06.34	+79:04:00.8	2MASS	28.5	0.8	Cor16
J01147+253	..F	LP 351-006	M1.5 V	Lep13	01:14:49.38	+25:19:01.2	2MASS	29.7	0.5	Cor16
J01158+470	B.F	1RXS J011549.5+470159	M4.5 V+	Law08	01:15:50.17	+47:02:02.3	2MASS	20.4	0.9	Cor16
J01161+601	..F	Wolf 59	M0.5 V	Lep13	01:16:10.06	+60:09:13.0	2MASS	28.7	0.3	Cor16
J01178+054	..F	NLTT 4318	M0.5 V	PMSU	01:17:53.26	+05:28:25.7	2MASS	20.48	4.51	HIP2
J01178+286	..F	Ross 324	M0.5 V	PMSU	01:17:50.67	+28:40:14.3	2MASS	26.7	7.6	Rei02
J01182-128	..F	GJ 56.1	M2.0 V	PMSU	01:18:15.99	-12:53:58.1	2MASS	22.1	1.7	HIP2
J01198+841	..F	GJ 1035	M5.0 V	PMSU	01:19:52.28	+84:09:32.8	2MASS	13.97	0.53	vAl95
J01214+243	..F	Ross 788	M0.0 V	Lep13	01:21:29.33	+24:19:50.1	2MASS	25.95	1.79	HIP2
J01221+221	B...	G 034-023	M4.5 V+	Lep13	01:22:10.28	+22:09:03.2	2MASS	8.9	0.4	Cor16
J01227+005	B..	NLTT 4582	M4.5 V+	PMSU	01:22:45.00	+00:32:04.2	2MASS	12.8	0.8	Dit14
J01256+097	B..	Wolf 66	M4.0 V+	PMSU	01:25:36.66	+09:45:24.4	2MASS	15.4	0.8	Dit14
J01317+209	..F	G 034-035	M2.0 V	Lep13	01:32:44.28	+20:59:16.0	2MASS	26.2	0.5	Cor16
J01324-219	.mF	CD-22 526	M1.5 Vk:	Gra06	01:32:26.26	-21:54:17.3	2MASS	17.83	0.61	HIP2
J01339-176		LP 768-113	M4.0 V	Sch05	01:33:58.00	-17:38:23.5	2MASS	13.4	0.5	Cor16
J01352-072		Barta 161 12	M4.0 V	Ria06	01:35:13.93	-07:12:51.8	2MASS	14.2	0.6	Cor16
J01369-067	B.F	LP 648-020	M3.5 V+	Rei07	01:36:55.17	-06:47:37.9	2MASS	23.95	0.42	aHIP2
J01373+610	..F	TYC 4031-2527-1	M1.5 V	Lep13	01:37:21.46	+61:05:28.6	2MASS	27.5	0.4	Cor16
J01383+572	..f	Ross 10	M2.5 V	PMSU	01:38:21.62	+57:13:57.1	2MASS	11.6	1.5	vAl95
J01384+006	..f	G 071-024	M2.0 V	PMSU	01:38:29.98	+00:39:05.9	2MASS	20.2	1.2	HIP2
J01390-179	Bm.	BL Cet + UV Cet	M5.0 V+	AF15	01:39:01.20	-17:57:02.7	2MASS	2.62	0.04	HD80
J01395+050	B.F	[R78b] 72	M3.0 V+	PMSU	01:39:31.19	+05:03:18.1	2MASS	22.4	0.6	Cor16
J01402+317	..F	G 072-023	M4.0 V	PMSU	01:40:16.49	+31:47:30.7	2MASS	18.7	0.7	Dit14
J01431+210	B.f	RX J0143.1+2101	M4.0 V+	AF15	01:43:11.87	+21:01:10.6	2MASS	16.2	0.6	Cor16
J01432+278	..F	BD+27 273	M0.0 V	PMSU	01:43:15.92	+27:50:31.6	2MASS	21.16	0.85	HIP2
J01433+043		GJ 70	M2.0 V	PMSU	01:43:20.15	+04:19:17.2	2MASS	11.4	0.3	HIP2
J01437-060	..f	BPS CS 22962-0011	M3.5 V	Ria06	01:43:45.13	-06:02:40.1	2MASS	15.8	0.5	Cor16
J01449+163	..F	Wolf 1530	M4.0 V	PMSU	01:44:58.52	+16:20:39.7	2MASS	16.39	0.994	vAl95
J01453+465	..f	G 173-018	M2.0 V	Lep13	01:45:18.20	+46:32:07.8	2MASS	25.63	1.74	HIP2
J01466-086	B..	LP 708-416	M4.0 V+	PMSU	01:46:36.81	-08:38:57.9	2MASS	14.26	2.89	vAl95

Table B.2: Names, spectral types, distances and astrometric parameters of Carmencita stars (continued).

Karmn	Flags[a]	Name	SpT	Ref.[b]	α (J2000)	δ (J2000)	Ref.[c]	d [pc]	ed [pc]	Ref.[d e]
J01480+212	..F	G 034-051	M2.5 V	PMSU	01:48:03.97	+21:12:24.4	2MASS	20.4	1.4	HIP2
J01510-061	..F	NLTT 6192	M4.5 V	PMSU	01:51:04.05	-06:07:04.8	2MASS	9.92	0.19	Hen06
J01514+213	..F	Wolf 90	M4.0 V	PMSU	01:51:24.17	+21:23:39.9	2MASS	17.8	1.2	Dit14
J01518+644		G 244-037	M2.5 V	PMSU	01:51:51.08	+64:26:06.1	2MASS	14.4	0.3	Cor16
J01518-108	..F	Ross 555	M2.0 V	PMSU	01:51:48.65	-10:48:12.0	2MASS	16.6	0.8	HIP2
J01531-210	Smf	BD-21 332 AB	M1.1 V+	Dae07	01:53:11.33	-21:05:43.3	2MASS	22.8	0.3	Cor16
J01538-149	Bm.	RBS 253	M3.0 V+	Ria06	01:53:50.77	-14:59:50.3	2MASS	12.9	0.4	Cor16
J01544+576	..f	LSPM J0154+5741S	M3.5 V	Lep13	01:54:28.07	+57:41:31.0	2MASS	14.1	0.5	Cor16
J01550+379	..F	LSR J0155+3758	M5.0 V	Lep03	01:55:02.30	+37:58:02.8	2MASS	15.8	0.7	Dit14
J01556+028	..F	LHS 6038	M1.5 V	Lep13	01:55:37.31	+02:52:58.2	2MASS	39.84	5.14	HIP2
J01567+305	..F	NLTT 6496	M4.5 V	AF15	01:56:45.71	+30:33:28.8	2MASS	21.6	1.6	Dit14
J01592+035E	B..	BD+02 305	M2.5 V	PMSU	01:59:12.39	+03:31:09.2	2MASS	31.14	3.22	HIP2
J01592+035W	S..	GJ 1041 B	M2.5 V+	PMSU	01:59:12.61	+03:31:11.4	2MASS	31.14	3.22	aHIP2
J01593+585	V..	V596 Cas	M4.0 V	PMSU	01:59:23.50	+58:31:16.2	2MASS	12.25	0.61	HIP2
J02000+437	..F	G 133-060	M2.5 V	PMSU	02:00:02.80	+43:45:28.6	2MASS	27.7	0.6	Cor16
J02001+366	..F	G 133-061	M3.5 V	PMSU	02:00:07.42	+36:39:48.1	2MASS	22.1	0.6	Dit14
J02002+130		TZ Ari	M3.5 V:	AF15	02:00:12.79	+13:03:11.2	2MASS	4.51	0.01	Wein16
J02007-103	..F	LP 709-016	M3.5 V	PMSU	02:00:47.26	-10:21:21.0	2MASS	26.5	0.9	Cor16
J02015+637		G 244-047	M3.0 V	PMSU	02:01:35.33	+63:46:11.9	2MASS	12.76	1.72	vAl95
J02019+735	B.f	LP 030-055	M4.5 V+	PMSU	02:01:54.00	+73:32:32.0	2MASS	11.43	0.07	GC09
J02020+039	..F	Wolf 109 B	M2.0 V	PMSU	02:02:03.47	+03:56:42.2	2MASS	38.6	5.0	aHIP2
J02022+103	..F	LP 469-067	M5.5 V	AF15	02:02:16.21	+10:20:13.7	2MASS	9.19	0.05	Wein16
J02026+105	V..	RX J0202.4+1034	M4.5 V	Lep13	02:02:28.24	+10:34:53.4	2MASS	8.8	0.4	Cor16
J02027+135	S.f	LP 469-073AB	M4.5 V+	PMSU	02:02:44.28	+13:34:33.6	2MASS	24.2	3.6	Dit14
J02028+047	..F	RX J0202.8+0446 2	M3.5 V	Lep13	02:02:52.09	+04:47:02.4	2MASS	17.4	0.6	Cor16
J02033-212	Sm.	G 272-145	M2.5 V+	PMSU	02:03:20.77	-21:13:42.7	2MASS	29.5	19.7	vAl95
J02044-018	..F	G 159-034	M4.0 V	PMSU	02:04:27.55	-01:52:56.1	2MASS	18.9	0.7	Cor16
J02050-176	Bmf	BD-18 359 AB	M2.5 V+	PMSU	02:05:04.93	-17:36:52.9	2MASS	9.1	0.2	HIP2
J02055+056	..F	Wolf 116	M1.0 V	Lep13	02:05:30.24	+05:41:47.5	2MASS	37.49	5.25	HIP2
J02069+451	..F	V374 And	M0.0 V	Lep13	02:06:57.18	+45:11:04.5	2MASS	18.7	1.8	vAl95
J02070+496		G 173-037	M3.5 V	Lep13	02:07:03.83	+49:38:44.1	2MASS	17.4	0.8	Dit14
J02071+642	..F	G 244-049	M4.0 V	PMSU	02:07:10.33	+64:17:11.5	2MASS	17.6	0.5	Dit14
J02082+802	..F	G 242-081	M0.0 V	Lep13	02:08:15.69	+80:13:15.7	2MASS	32.0	11.1	vAl95

Table B.2: Names, spectral types, distances and astrometric parameters of Carmencita stars (continued).

Karmn	Flags[a]	Name	SpT	Ref.[b]	α (J2000)	δ (J2000)	Ref.[c]	d [pc]	ed [pc]	Ref.[d e]
J02088+494		G 173-039	M3.5 V	PMSU	02:08:53.60	+49:26:56.6	2MASS	13.5	0.4	Cor16
J02096-143	.mf	LP 709-040	M2.5 V	PMSU	02:09:36.09	-14:21:32.1	2MASS	19.7	1.0	HIP2
J02116+185	..f	G 035-032	M3.0 V	Lep13	02:11:40.94	+18:33:37.5	2MASS	18.1	0.5	Cor16
J02123+035		BD+02 348	M1.5 V	PMSU	02:12:20.91	+03:34:31.1	2MASS	10.41	0.18	HIP2
J02129+000	..f	G 159-046	M4.0 V	PMSU	02:12:54.58	+00:00:16.8	2MASS	10.0	0.5	Dit14
J02133+368	B.F	2MASS J02132062+3648506	M4.5 V+	AF15	02:13:20.62	+36:48:50.7	2MASS	13.8	0.6	Cor16
J02142-039	..F	LP 649-072	M5.5 V	AF15	02:14:12.51	-03:57:43.4	2MASS	14.3	0.9	Cor16
J02149+174	..F	GJ 1045	M4.0 V	PMSU	02:14:59.79	+17:25:09.0	2MASS	20.41	1.25	vAl95
J02153+074	..F	Wolf 127	M1.5 V	Lep13	02:15:21.98	+07:29:38.9	2MASS	30.79	3.18	HIP2
J02155+339	..F	G 074-011	M3.5 V	PMSU	02:15:34.38	+33:57:41.8	2MASS	20.4	0.7	Cor16
J02158-126	..F	LP 709-062	M3.5 V	PMSU	02:15:48.83	-12:40:27.7	2MASS	18.0	0.6	Cor16
J02164+135	..F	LP 469-206	M5.5 V	PMSU	02:16:29.78	+13:35:13.7	2MASS	8.496	0.289	vAl95
J02171+354	..F	LP 245-010	M5.0 V	PMSU	02:17:09.93	+35:26:33.0	2MASS	10.37	0.12	vAl95
J02185+207	..F	G 035-039	M2.5 V	Lep13	02:18:35.95	+20:47:50.1	2MASS	22.9	0.5	Cor16
J02186+123	..F	RX J0218.6+1219 2	M2.5 V	Lep13	02:18:36.55	+12:18:58.0	2MASS	22.4	0.5	Cor16
J02190+238	..F	LTT 10787	M4.0 V	PMSU	02:19:02.29	+23:52:55.1	2MASS	20.6	0.8	Dit14
J02190+353	..f	Ross 19	M3.5 V	PMSU	02:19:03.06	+35:21:18.2	2MASS	17.7	2.5	vAl95
J02204+377	B.f	LP 245-017 AB	M2.5 V+	PMSU	02:20:25.24	+37:47:30.7	2MASS	24.1	0.6	Cor16
J02207+029	..F	LTT 17354	M4.5 V	PMSU	02:20:46.26	+02:58:37.5	2MASS	18.3	0.5	Dit14
J02210+368	B.f	GJ 1047 AB	M3.0 V+	PMSU	02:21:03.97	+36:53:05.4	2MASS	18.7	0.8	Dit14
J02222+478		BD+47 612	M0.5 V	PMSU	02:22:14.63	+47:52:48.1	2MASS	11.94	0.16	HIP2
J02230+181	..F	StKM 1-261	M0.5 V	Lep13	02:23:05.94	+18:10:34.8	2MASS	30.9	0.3	Cor16
J02234+227	..F	LP 353-051	M0.5 V	Lep13	02:23:26.64	+22:44:06.9	2MASS	28.69	2.34	HIP2
J02247+259	..F	LP 353-074	M0.5 V	PMSU	02:24:46.12	+25:58:34.7	2MASS	30.3	0.3	Cor16
J02254+246	..F	StKM 1-265	M2.0 V	Lep13	02:25:28.11	+24:40:36.8	2MASS	26.8	0.5	Cor16
J02256+375	..F	G 074-025	M4.0 V	PMSU	02:25:38.42	+37:32:34.0	2MASS	21.6	1.4	Dit14
J02272+545	B.F	2MASS J02271705+5432479	M4.5 V+	Law08	02:27:17.06	+54:32:47.9	2MASS	23.3	1.1	Dit14
J02274+031	..F	2MASS J02272756+0310548	M4.0 V	AF15	02:27:27.56	+03:10:54.8	2MASS	22.7	0.9	Cor16
J02277+044	B..	BD+03 339	M1.0 V+	Gra03	02:27:45.91	+04:25:55.7	2MASS	17.14	0.32	HIP2
J02282+014	..F	G 075-016	M3.0 V	PMSU	02:28:17.12	+01:26:31.0	2MASS	23.9	0.7	Cor16
J02283+219	..F	TYC 1221-1171-1	M0.5 V	Lep13	02:28:22.10	+21:59:45.7	2MASS	30.3	0.3	Cor16
J02285-200	.mF	GJ 100C	M2.5 V	AF15	02:28:31.89	-20:02:26.5	2MASS	19.4	0.5	aHIP2
J02287+156	..F	BPM 85139	M2.0 V	Lep13	02:28:46.95	+15:38:53.5	2MASS	25.8	0.5	Cor16

Table B.2: Names, spectral types, distances and astrometric parameters of Carmencita stars (continued).

Karmn	Flags[a]	Name	SpT	Ref.[b]	α (J2000)	δ (J2000)	Ref.[c]	d [pc]	ed [pc]	Ref.[d e]
J02289+120	S.F	[R78b] 140	M2.0 V+	PMSU	02:28:54.66	+12:05:20.9	2MASS	26.0	2.1	HIP2
J02289+226	B.F	BPM 85140	M2.0 V	Lep13	02:28:58.23	+22:36:24.9	2MASS	25.8	0.5	Cor16
J02292+195	..F	LP 410-033	M2.5 V	Lep13	02:29:14.12	+19:32:36.1	2MASS	24.2	0.6	Cor16
J02293+884	.mF	LP 001-052	M3.5 V	PMSU	02:29:19.11	+88:24:13.0	2MASS	18.1	0.6	Cor16
J02314+573	..F	Ross 21	M3.5 V	PMSU	02:31:27.66	+57:22:43.3	2MASS	19.0	0.8	vAl95
J02330+078	..F	LP 530-026	M2.0 V	Lep13	02:33:04.55	+07:49:42.3	2MASS	34.63	4.09	HIP2
J02336+249		GJ 102	M4.0 V	PMSU	02:33:37.17	+24:55:39.2	2MASS	9.77	0.26	vAl95
J02337+150	..F	LP 470-030	M3.0 V	PMSU	02:33:47.41	+15:00:17.3	2MASS	22.9	1.1	Dit14
J02340+417	..F	G 074-029	M3.0 V	PMSU	02:34:00.02	+41:46:49.0	2MASS	20.1	1.2	Dit14
J02345+566	..F	G 174-004	M2.0 V	Lep13	02:34:34.65	+56:36:46.1	2MASS	27.0	0.5	Cor16
J02353+235	..F	2E 591	M3.5 V	PMSU	02:35:22.61	+23:34:30.8	2MASS	22.5	0.7	Cor16
J02358+202		BD+19 381	M2.0 V	PMSU	02:35:53.28	+20:13:11.9	2MASS	13.6	0.3	HIP2
J02362+068		BX Cet	M4.0 V	AF15	02:36:15.36	+06:52:19.1	2MASS	7.18	0.02	aHIP2
J02364+554	..F	G 173-061	M3.0 V	PMSU	02:36:27.16	+55:28:34.9	2MASS	16.6	2.2	vAl95
J02367+226	..F	G 036-026	M5.0 V	AF15	02:36:44.13	+22:40:26.5	2MASS	14.1	0.8	Dit14
J02367+320	B..	G 074-034 AB	M3.5 V+	PMSU	02:36:47.81	+32:04:20.5	2MASS	15.3	3.5	vAl95
J02392+074	..F	G 076-019	M4.0 V	PMSU	02:39:17.35	+07:28:17.0	2MASS	20.3	1.2	Dit14
J02412-045	..f	G 075-035	M4.5 V	AF15	02:41:15.11	-04:32:17.7	2MASS	36.6	1.1	HIP1
J02419+435	..F	StKM 1-291	M1.0 V	Lep13	02:41:59.01	+43:34:19.5	2MASS	25.2	0.3	Cor16
J02424+182	..F	LP 410-081	M1.5 V	Lep13	02:42:25.56	+18:14:42.3	2MASS	32.73	4.42	HIP2
J02438-088	..F	Wolf 1132	M1.5 V	PMSU	02:43:53.17	-08:49:44.9	2MASS	27.46	3.4	HIP2
J02441+492	J..	θ Per B	M1.5 V	AF15	02:44:10.25	+49:13:54.1	2MASS	11.13	0.03	aHIP2
J02442+255		VX Ari	M3.0 V	PMSU	02:44:15.38	+25:31:25.0	2MASS	7.51	0.127	HIP2
J02443+109E	..F	2MASS J02442272+1057349	M5.0 V	Fle88	02:44:22.73	+10:57:34.9	2MASS	34.93	3.7	aHIP2
J02443+109W	..F	MCC 401	M1.0 V	Lep13	02:44:21.38	+10:57:41.2	2MASS	34.93	3.7	HIP2
J02455+449	..F	G 078-003	M5.0 V	PMSU	02:45:31.43	+44:56:53.1	2MASS	13.6	0.7	Cor16
J02456+449	..F	G 078-004	M0.5 V	AF15	02:45:39.63	+44:56:55.7	2MASS	23.08	1.24	HIP2
J02462-049	..F	LP 651-007	M6.0 V	PMSU	02:46:14.78	-04:59:18.2	2MASS	16.64	0.25	Wein16
J02465+164	..F	LP 411-006	M6.0 V	PMSU	02:46:34.86	+16:25:11.6	2MASS	14.6	0.7	vAl95
J02502+628	..F	G 246-012	M2.5 V	AF15	02:50:16.44	+62:51:19.8	2MASS	29.2	0.7	Cor16
J02518+062	..F	NLTT 9155	M3.0 V	PMSU	02:51:50.65	+06:13:41.4	2MASS	25.4	0.7	Cor16
J02518+294	B.F	LP 298-042	M4.0 V+	PMSU	02:51:49.73	+29:29:13.2	2MASS	22.7	1.8	Dit14
J02519+224		RBS 365	M4.0 V	Ria06	02:51:54.09	+22:27:30.0	2MASS	13.9	0.5	Cor16

Table B.2: Names, spectral types, distances and astrometric parameters of Carmencita stars (continued).

Karmn	Flags[a]	Name	SpT	Ref.[b]	α (J2000)	δ (J2000)	Ref.[c]	d [pc]	ed [pc]	Ref.[d e]
J02524+269	..F	LP 354-423	M1.0 V	PMSU	02:52:25.02	+26:58:30.5	2MASS	27.65	1.86	HIP2
J02530+168		Teegardens Star	M7.0 V	AF15	02:53:00.85	+16:52:53.3	2MASS	3.84	0.01	Wein16
J02534+174	..f	NLTT 9223	M3.5 V	Lep13	02:53:26.11	+17:24:32.5	2MASS	17.7	0.7	Dit14
J02555+268	..F	HD 18143 C	M4.0 V	AF15	02:55:35.73	+26:52:20.9	2MASS	15.9	0.8	Dit14
J02560-006	..F	LP 591-156	M5.0 V	Boc05	02:56:03.88	-00:36:33.2	2MASS	17.8	0.9	Cor16
J02562+239	B.F	LSPM J0256+2359	M5.0 V+	AF15	02:56:13.96	+23:59:10.5	2MASS	15.7	0.9	Dit14
J02565+554E	J..	Ross 365	M3.0 V	PMSU	02:56:35.07	+55:26:30.2	2MASS	22.22	1.83	avAl95
J02565+554W		Ross 364	M1.0 V	PMSU	02:56:34.35	+55:26:14.5	2MASS	22.22	1.83	vAl95
J02575+107	..F	Ross 791	M3.0 V	PMSU	02:57:31.04	+10:47:24.6	2MASS	20.0	2.3	vAl95
J02581-128	..F	LP 711-032	M2.5 V	PMSU	02:58:10.21	-12:53:06.7	2MASS	10.47	1.2	vAl95
J02591+366	B.F	Ross 331	M3.5 V+	PMSU	02:59:10.60	+36:36:40.3	2MASS	18.87	4.98	Daw05
J02592+317	..F	LP 298-052	M3.5 V	PMSU	02:59:16.70	+31:46:24.6	2MASS	22.4	0.7	Cor16
J02597+389	B.F	G 134-063	M4.5 V+	Law08	02:59:46.33	+38:55:36.3	2MASS	27.8	3.3	Dit14
J03018-165N	Bm.	BD-17 588 AC	M3.0 V+	PMSU	03:01:51.08	-16:35:30.7	2MASS	9.4	1.5	bHIP2
J03018-165S	Jm.	BD-17 588 B	M3.5 V	PMSU	03:01:51.43	-16:35:35.7	2MASS	9.4	1.5	HIP2
J03026-181	.mf	GJ 121.1	M2.5 V	AF15	03:02:38.01	-18:09:58.7	2MASS	19.58	1.53	HIP2
J03033-080	..F	StM 20	M3.0 V	AF15	03:03:21.32	-08:05:15.4	2MASS	22.2	0.6	Cor16
J03036-128	..F	LP 711-043	M3.0 V	PMSU	03:03:40.71	-12:50:31.7	2MASS	25.4	0.7	Cor16
J03037-128	..F	LP 711-044	M3.0 V	PMSU	03:03:47.83	-12:51:19.1	2MASS	23.9	0.7	Cor16
J03040-203	.mf	LP 771-077	M3.5 V	PMSU	03:04:04.52	-20:22:43.4	2MASS	17.47	0.4	Wein16
J03047+617	..F	G 246-022	M3.0 V	AF15	03:04:43.35	+61:44:09.7	2MASS	24.2	0.3	aHIP2
J03075-039	B.f	LP 652-005 AB	M0.0 V+	PMSU	03:07:33.83	-03:58:16.7	2MASS	54.67	12.73	HIP2
J03077+249	..F	LP 355-027	M4.5 V	Rei04	03:07:46.82	+24:57:55.6	2MASS	21.4	1.2	Dit14
J03090+100	..F	GJ 1055	M5.0 V	PMSU	03:09:00.16	+10:01:25.8	2MASS	11.92	0.57	vAl95
J03095+457	B..	GJ 125 AB	M2.0 V+	PMSU	03:09:30.85	+45:43:58.6	2MASS	15.8	0.5	HIP2
J03102+059	..F	EK Cet	M2.0 V	PMSU	03:10:15.47	+05:54:31.1	2MASS	16.9	1.3	HIP2
J03104+584	..F	G 246-026	M1.0 V	PMSU	03:10:26.49	+58:26:08.7	2MASS	26.2	0.3	Cor16
J03109+737	..F	GJ 1053	M5.0 V	PMSU	03:10:58.62	+73:46:18.9	2MASS	12.01	0.49	vAl95
J03110-046	..F	LP 652-062	M3.0 V	AF15	03:11:04.89	-04:36:35.8	2MASS	25.3	0.7	Cor16
J03112+011	..F	1RXS J031114.2+010655	M5.5 V	Boc05	03:11:15.48	+01:06:30.7	2MASS	15.7	0.9	Cor16
J03118+196	..F	Wolf 132	M0.5 V	Lep13	03:11:48.01	+19:40:15.4	2MASS	25.1	0.3	Cor16
J03119+615	B.f	BD+60 637	M0.0 V+	Lep13	03:11:56.85	+61:31:12.8	2MASS	40.61	3.77	HIP2
J03133+047		CD Cet	M5.0 V	PMSU	03:13:22.99	+04:46:29.4	2MASS	8.62	0.06	Wein16

Table B.2: Names, spectral types, distances and astrometric parameters of Carmencita stars (continued).

Karmn	Flags[a]	Name	SpT	Ref.[b]	α (J2000)	δ (J2000)	Ref.[c]	d [pc]	ed [pc]	Ref.[d e]
J03136+653	..F	TYC 4057-285-1	M1.5 V	Lep13	03:13:38.08	+65:21:16.8	2MASS	28.3	0.4	Cor16
J03142+286	..F	LP 299-036	M6.0 V	PMSU	03:14:12.42	+28:40:41.2	2MASS	12.7	0.3	Dit14
J03145+594	..F	Ross 369	M2.5 V	Lep13	03:14:32.73	+59:26:16.0	2MASS	19.1	0.4	Cor16
J03147+114	..F	RX J0314.7+1127	M2.0 V	AF15	03:14:47.20	+11:27:27.2	2MASS	33.4	0.6	Cor16
J03147+485	..F	Ross 346	M1.0 V	PMSU	03:14:44.89	+48:31:11.4	2MASS	19.9	3.7	vAl95
J03162+581N	B..	Ross 370 B	M2.0 V	AF15	03:16:13.90	+58:10:07.3	2MASS	14.4	0.7	aHIP2
J03162+581S	B..	Ross 370 A	M2.0 V	AF15	03:16:13.82	+58:10:02.4	2MASS	14.4	0.7	HIP2
J03167+389	..F	HAT 168-01565	M3.5 V	AF15	03:16:46.13	+38:55:27.4	2MASS	18.9	0.6	Cor16
J03172+453	B..	G 078-028 AB	M2.5 V+	Pra06	03:17:12.20	+45:22:22.1	2MASS	18.4	0.3	Pra06
J03177+252	..F	LP 355-051	M2.5 V	Gra03	03:17:45.13	+25:15:07.0	2MASS	21.6	1.39	HIP2
J03181+382		HD 275122	M1.5 V	PMSU	03:18:07.42	+38:15:08.2	2MASS	16.53	0.6	HIP2
J03181+426	..F	Wolf 140	M3.5 V	AF15	03:18:07.01	+42:40:09.1	2MASS	21.7	0.7	Dit14
J03185+103	..F	StKM 1-354	M1.5 V	Lep13	03:18:35.20	+10:18:44.6	2MASS	51.1	12.77	HIP2
J03186+326	..F	LP 299-053	M0.0 V	PMSU	03:18:38.31	+32:39:57.1	2MASS	26.35	2.29	HIP2
J03187+606	..F	Ross 371	M3.0 V	PMSU	03:18:42.61	+60:36:27.5	2MASS	25.8	0.7	Cor16
J03194+619	B.F	G 246-033	M4.0 V+	AF15	03:19:28.73	+61:56:04.6	2MASS	27.9	2.3	Dit14
J03207+397	..F	LP 198-637	M1.5 V	Lep13	03:20:45.19	+39:43:01.6	2MASS	21.1	0.3	Cor16
J03213+799		GJ 133	M2.0 V	PMSU	03:21:21.76	+79:58:02.2	2MASS	14.0	0.3	HIP2
J03217-066		G 077-046	M2.0 V	PMSU	03:21:46.89	-06:40:24.2	2MASS	16.8	0.3	Cor16
J03220+029	..F	GJ 1058	M4.5 V	PMSU	03:22:04.10	+02:56:34.7	2MASS	14.2	0.5	Dit14
J03224+271	..F	LP 355-064	M0.0 V	Lep13	03:22:28.12	+27:09:21.9	2MASS	32.31	2.86	HIP2
J03230+420	..F	GJ 1059	M5.0 V	PMSU	03:23:01.76	+42:00:27.0	2MASS	15.36	0.8	vAl95
J03233+116	..F	G 005-032	M2.5 V	PMSU	03:23:22.41	+11:41:13.4	2MASS	18.3	0.8	vAl95
J03236+056	..F	1RXS J032338.7+054117	M4.5 V	AF15	03:23:39.16	+05:41:15.3	2MASS	17.4	0.8	Cor16
J03241+237	B..	GJ 140 AB	M0.0 V+	Jen09	03:24:06.43	+23:47:07.4	2MASS	19.49	1.03	HIP2
J03242+237	..f	GJ 140C	M2.0 V	PMSU	03:24:12.81	+23:46:19.3	2MASS	19.49	1.03	aHIP2
J03247+447	..F	2MASS J03244244+4447417	M1.5 V	Lep13	03:24:42.44	+44:47:41.7	2MASS	26.3	0.4	Cor16
J03257+058	B.F	LP 532-081	M4.5 V+	PMSU	03:25:42.25	+05:51:51.9	2MASS	20.6	1.8	Dit14
J03263+171	B.F	TYC 1237-889.1	M4.0 V+	AF15	03:26:23.62	+17:09:30.9	2MASS	20.7	0.8	Cor16
J03267+192	..F	G 006-007	M4.5 V	PMSU	03:26:44.96	+19:14:40.3	2MASS	19.2	1.5	Dit14
J03272+273	..F	CK Ari	M1.0 V	Lep13	03:27:14.33	+27:23:08.8	2MASS	30.08	3.52	HIP2
J03275+222	..F	J0327+2212	M4.5 V	AF15	03:27:30.84	+22:12:38.3	2MASS	18.9	0.9	Cor16
J03284+352	..F	LSPM J0328+3515	M2.0 V	Lep13	03:28:29.22	+35:15:19.9	2MASS	28.0	0.5	Cor16

Table B.2: Names, spectral types, distances and astrometric parameters of Carmencita stars (continued).

Karmn	Flags[a]	Name	SpT	Ref.[b]	α (J2000)	δ (J2000)	Ref.[c]	d [pc]	ed [pc]	Ref.[d e]
J03286-156	.mF	LP 772-072 A	M3.5 V	PMSU	03:28:38.93	-15:37:17.1	2MASS	26.1	0.9	Cor16
J03288+264	..F	LP 356-106	M3.0 V	PMSU	03:28:49.58	+26:29:12.2	2MASS	15.0	0.6	Dit14
J03303+346	..F	2MASS J03302331+3440325	M4.0 V	AF15	03:30:23.32	+34:40:32.6	2MASS	22.9	0.9	Cor16
J03308+542	..F	LSPM J0330+5413	M5.0 V	Law08	03:30:48.90	+54:13:55.1	2MASS	9.63	0.13	Lep09
J03309+706	B.F	LP 031-368	M3.5 V+	AF15	03:30:54.74	+70:41:14.6	2MASS	22.4	0.9	Dit14
J03317+143	..F	GJ 143.3	M2.0 V	PMSU	03:31:47.12	+14:19:19.4	2MASS	22.9	3.4	HIP2
J03325+287	B.F	RX J0332.6+2843	M4.5 V+	AF15	03:32:35.79	+28:43:55.5	2MASS	13.8	0.6	Cor16
J03332+462	..F	BD+45 784B	M0.0 V	AF15	03:33:14.03	+46:15:19.4	2MASS	34.39	1.21	aHIP2
J03340+585	..F	Ross 563	M0.5 V	Lep13	03:34:00.49	+58:35:55.1	2MASS	28.1	0.3	Cor16
J03346-048	S.F	LP 653-008	M3.5 V+	PMSU	03:34:39.59	-04:50:32.9	2MASS	29.2	1.4	Ried10
J03361+313	..f	[GBM90] Per 49	M4.5 V	AF15	03:36:08.68	+31:18:39.8	2MASS	12.56	0.39	Lep09
J03366+034	..f	[R78b] 233	M4.5 V	PMSU	03:36:40.84	+03:29:19.5	2MASS	13.4	0.6	Cor16
J03372+691	E.F	LP 054-019AB	M3.5 V+	PMSU	03:37:14.08	+69:10:49.8	2MASS	36.1	1.7	Dit14
J03375+178N	S.F	LP 413-018 Aab	M2.5 V+	AF15	03:37:33.32	+17:51:14.6	2MASS	25.8	0.6	Cor16
J03375+178S	S.F	LP 413-019 Bab	M3.5 V+	AF15	03:37:33.87	+17:51:00.5	2MASS	19.2	0.6	Cor16
J03394+249	..F	KP Tau	M3.0 V	PMSU	03:39:29.72	+24:58:02.9	2MASS	19.2	1.6	Dit14
J03396+254E	..f	Wolf 204	M3.0 V	PMSU	03:39:36.21	+25:28:20.3	2MASS	21.3	9.0	bvAl95
J03396+254W	..F	Wolf 205	M3.5 V	PMSU	03:39:40.51	+25:28:47.7	2MASS	21.3	9.0	vAl95
J03397+334	..F	HD 278874 B	M3.0 V	PMSU	03:39:47.84	+33:28:30.7	2MASS	43.31	3.09	aHIP2
J03416+552	..F	TYC 3720-426-1	M0.0 V	Lep13	03:41:37.25	+55:13:06.9	2MASS	35.21	2.7	HIP2
J03430+459	B.F	NLTT 11633	M4.0 V+	AF15	03:43:02.07	+45:54:18.2	2MASS	24.6	1.1	Dit14
J03433-095	B.F	G 160-019	M4.5 V+	PMSU	03:43:22.05	-09:33:51.3	2MASS	21.7	0.8	Ried10
J03437+166	..f	BD+16 502B	M1.0 V	PMSU	03:43:45.22	+16:40:02.7	2MASS	16.69	0.67	HIP2
J03438+166	..f	BD+16 502A	M0.0 V	Lep13	03:43:52.53	+16:40:19.9	2MASS	17.71	0.6	HIP2
J03445+349	..F	HD 278968	M0.0 V	Lep13	03:44:30.94	+34:58:23.7	2MASS	25.32	1.4	HIP2
J03454+729	..F	NLTT 11646	M1.5 V	Lep13	03:45:27.94	+72:59:32.4	2MASS	46.5	23.1	vAl95
J03455+703	..F	2MASS J03453188+7018002	M1.0 V	Lep13	03:45:31.88	+70:18:00.3	2MASS	34.6	0.5	Cor16
J03459+147	..F	NLTT 11771	M1.5 V	Lep13	03:45:54.83	+14:42:52.1	2MASS	28.9	0.4	Cor16
J03463+262		HD 23453	M0.0 V	PMSU	03:46:20.12	+26:12:56.0	2MASS	14.75	0.45	HIP2
J03467+821	..F	TYC 4521-1342-1	M1.0 V	Lep13	03:46:42.00	+82:07:51.2	2MASS	35.5	0.5	Cor16
J03467-112	..F	LP 713-028	M2.5 V	PMSU	03:46:45.38	-11:17:42.3	2MASS	24.6	0.6	Cor16
J03473+086	..F	LTT 11262	M4.5 V	PMSU	03:47:20.91	+08:41:46.4	2MASS	12.58	0.55	vAl95
J03473-019		G 080-021	M3.0 V	AF15	03:47:23.33	-01:58:19.5	2MASS	16.13	0.75	HIP2

Table B.2: Names, spectral types, distances and astrometric parameters of Carmencita stars (continued).

Karmn	Flags[a]	Name	SpT	Ref.[b]	α (J2000)	δ (J2000)	Ref.[c]	d [pc]	ed [pc]	Ref.[d e]
J03479+027	..F	Ross 588	M0.5 V	PMSU	03:47:58.09	+02:47:16.2	2MASS	16.85	0.69	HIP2
J03480+686	B..	BD+68 278B	M1.5 V+	PMSU	03:48:01.74	+68:40:38.9	2MASS	17.34	0.92	aHIP2
J03486+735	..F	LP 031-218	M1.0 V	PMSU	03:48:38.22	+73:32:35.2	2MASS	16.5	0.5	vAl95
J03505+634	..F	G 246-050	M1.5 V	PMSU	03:50:33.68	+63:27:18.7	2MASS	37.51	4.05	HIP2
J03507-060	..f	GJ 1065	M3.5 V	PMSU	03:50:44.32	-06:05:40.0	2MASS	9.5	0.3	vAl95
J03510+142	..F	2MASS J03510078+1413398	M4.5 V	AF15	03:51:00.79	+14:13:39.9	2MASS	14.3	0.6	Cor16
J03510-008	..F	LP 593-068	M6.0 V	PMSU	03:51:00.05	-00:52:45.3	2MASS	13.87	0.49	Wein16
J03519+397	..F	TYC 2868-639-1	M0.0 V	AF15	03:51:58.15	+39:46:56.8	2MASS	33.58	1.47	aHIP2
J03526+170	S..	Wolf 227	M4.5 V+	PMSU	03:52:41.69	+17:01:05.7	2MASS	9.8	0.5	Dit14
J03531+625		Ross 567	M3.0 V	Lep13	03:53:10.42	+62:34:08.2	2MASS	12.0	0.3	Cor16
J03543-146	.mF	2MASS J03542008-1437388	M6.5 V	Cru03	03:54:20.09	-14:37:38.8	2MASS	15.2	2.1	Cru03
J03544-091	..F	StKM 1-430	M1.0 V	PMSU	03:54:25.62	-09:09:31.6	2MASS	20.7	0.3	Cor16
J03548+163	..F	LP 413-108	M4.0 V	AF15	03:54:53.20	+16:18:56.4	2MASS	22.5	0.9	Cor16
J03565+319	..F	HAT 214-02089	M3.5 V	AF15	03:56:33.08	+31:57:24.8	2MASS	25.4	0.8	Cor16
J03567+039	..F	Ross 23	M1.5 V	PMSU	03:56:47.39	+53:33:36.9	2MASS	26.98	2.39	HIP2
J03574-011	J..	BD-01 565B	M2.5 V	AF15	03:57:28.92	-01:09:23.4	2MASS	15.5	0.3	aHIP2
J03586+520	..F	Ross 24	M1.0 V	Lep13	03:58:36.27	+52:01:25.2	2MASS	34.4	0.5	Cor16
J03588+125	..F	G 007-014	M4.0 V	AF15	03:58:49.06	+12:30:24.2	2MASS	27.7	2.22	Dit14
J03598+260	..f	Ross 873	M3.0 V	PMSU	03:59:53.55	+26:05:24.1	2MASS	22.8	2.7	vAl95
J04011+513	..F	Ross 25	M3.5 V	PMSU	04:01:07.55	+51:23:19.6	2MASS	22.3	0.8	Dit14
J04056+057	B..	[R78b] 256 AB	M3.5 V+	PMSU	04:05:38.89	+05:44:40.8	2MASS	16.1	0.5	Cor16
J04059+712E	..F	LP 031-301	M4.0 V	CR02	04:05:57.47	+71:16:41.2	2MASS	17.51	0.37	Lep09
J04059+712W	B.f	LP 031-302 BC	M5.0 V+	CR02	04:05:56.52	+71:16:38.6	2MASS	17.51	0.37	Lep09
J04061-055	..F	2MASS J04060688-0534444	M3.5 V	AF15	04:06:06.88	-05:34:44.4	2MASS	18.6	0.6	Cor16
J04077+142	..F	LP 474-123	M0.0 V	Lep13	04:07:43.94	+14:13:24.6	2MASS	26.9	0.3	Cor16
J04079+142	..F	NLTT 12593	M2.5 V	AF15	04:07:54.80	+14:13:00.7	2MASS	27.2	0.6	Cor16
J04081+743	..F	LP 032-016	M3.5 V	AF15	04:08:11.01	+74:23:01.8	2MASS	19.7	0.7	Cor16
J04083+691	..F	LP 031-433	M4.5 V	AF15	04:08:23.72	+69:10:59.3	2MASS	22.6	2.0	Dit14
J04086+336	..f	HD 281621	M0.5 V	PMSU	04:08:37.43	+33:38:13.4	2MASS	13.45	0.49	HIP2
J04093+057	B.F	NLTT 12648	M4.5 V+	Law08	04:09:22.26	+05:46:26.9	2MASS	20.9	1.3	Dit14
J04108-128	B.F	LP 714-037 ABC	M5.5 V+	PBB06	04:10:48.10	-12:51:42.1	2MASS	18.9	2.6	PBB06
J04112+495	..F	Ross 27	M3.5 V	PMSU	04:11:13.11	+49:31:52.5	2MASS	22.7	0.7	Dit14
J04122+647	..f	G 247-015	M4.0 V	PMSU	04:12:16.93	+64:43:56.1	2MASS	11.79	0.4	vAl95

Table B.2: Names, spectral types, distances and astrometric parameters of Carmencita stars (continued).

Karmn	Flags[a]	Name	SpT	Ref.[b]	α (J2000)	δ (J2000)	Ref.[c]	d [pc]	ed [pc]	Ref.[d e]
J04123+162	..F	HG 7-124	M4.0 V	AF15	04:12:21.73	+16:15:03.3	2MASS	22.3	1.6	Dit14
J04129+526	B..	Ross 28 AB	M4.5 V+	PMSU	04:12:58.80	+52:36:42.1	2MASS	14.7	0.8	Dit14
J04131+505	B..	Ross 29	M4.0 V+	PMSU	04:13:10.16	+50:31:41.4	2MASS	18.4	0.8	Dit14
J04137+476	..F	LSPM J0413+4737E	M2.5 V	Lep13	04:13:47.86	+47:37:44.4	2MASS	24.1	0.6	Cor16
J04139+829	..F	G 222-001	M0.0 V	Lep13	04:13:55.90	+82:55:06.9	2MASS	35.51	1.61	HIP2
J04148+277	..f	HG 8-1	M3.5 V	Lep13	04:14:53.49	+27:45:28.4	2MASS	15.8	0.5	Cor16
J04153-076		o^{02} Eri C	M4.5 V	AF15	04:15:21.73	-07:39:17.4	2MASS	4.98	0.006	aHIP2
J04166-125	B.f	LP 714-058 AB	M1.5 V+	Gra06	04:16:41.73	-12:33:23.3	2MASS	21.36	1.97	HIP2
J04173+088	..f	LTT 11392	M4.5 V	PMSU	04:17:18.52	+08:49:22.1	2MASS	14.8	1.0	Dit14
J04177+410	..F	LSPM J0417+4103	M3.5 V	AF15	04:17:44.31	+41:03:13.8	2MASS	27.7	1.8	Dit14
J04188+013	..F	HIP 20122	M2.0 V	Lep13	04:18:51.45	+01:23:36.0	2MASS	85.84	34.85	HIP2
J04191+097	..F	2MASS J04190809+0944481	M3.0 V	AF15	04:19:08.09	+09:44:48.2	2MASS	33.1	0.9	Cor16
J04191-074	..F	LP 654-039	M3.5 V	AF15	04:19:06.60	-07:27:44.8	2MASS	27.5	0.9	Cor16
J04198+425	..f	LSR J0419+4233	M8.5 V	Lep03	04:19:52.13	+42:33:30.5	2MASS	10.5	0.5	Dit14
J04199+364	..F	Ross 592	M1.5 V	Lep13	04:19:59.69	+36:29:11.4	2MASS	22.27	2.03	HIP2
J04205+815	..F	2MASS J04203505+8131556	M3.0 V	AF15	04:20:35.05	+81:31:55.6	2MASS	26.2	0.7	Cor16
J04206+272	..F	XEST 16-045	M4.5 V	AF15	04:20:39.18	+27:17:31.7	2MASS	23.3	1.1	Cor16
J04207+152	B.F	HG 7-172	M4.0 V+	AF15	04:20:47.96	+15:14:09.2	2MASS	33.7	2.5	Dit14
J04218+213	..F	G 008-029	M3.5 V	PMSU	04:21:50.06	+21:19:43.4	2MASS	18.2	0.6	Cor16
J04219+751	..F	G 248-019	M2.5 V	PMSU	04:21:57.50	+75:08:28.5	2MASS	20.0	0.5	Cor16
J04221+192	..F	LP 415-636	M3.0 V	PMSU	04:22:08.27	+19:15:21.8	2MASS	23.1	0.6	Cor16
J04224+036	..F	RX J0422.4+0337	M3.5 V	AF15	04:22:25.04	+03:37:08.2	2MASS	26.1	0.9	Cor16
J04224+740	..F	LP 031-339	M1.5 V	Lep13	04:22:28.32	+74:01:27.0	2MASS	30.0	0.5	Cor16
J04225+105		LSPM J0422+1031	M3.5 V	Lep13	04:22:31.99	+10:31:18.8	2MASS	25.4	1.2	Dit14
J04225+390	..F	GJ 1070	M5.0 V	PMSU	04:22:33.49	+39:00:43.7	2MASS	18.73	1.65	vAl95
J04227+205	..F	LP 415-030	M4.0 V	AF15	04:22:42.84	+20:34:12.5	2MASS	28.3	1.1	Cor16
J04229+259	..F	G 008-031	M4.5 V	AF15	04:22:59.26	+25:59:14.8	2MASS	15.7	0.7	Cor16
J04234+495	..F	TYC 3337-1716-1	M2.5 V	Lep13	04:23:26.89	+49:34:19.0	2MASS	18.1	0.4	Cor16
J04234+809	..F	1RXS J042323.2+805511	M4.0 V	AF15	04:23:29.05	+80:55:10.2	2MASS	17.5	0.7	Cor16
J04238+092	..F	LP 535-073	M3.0 V	AF15	04:23:50.70	+09:12:19.4	2MASS	22.2	0.6	Cor16
J04238+149	..F	IN Tau	M3.5 V	AF15	04:23:50.33	+14:55:17.4	2MASS	20.1	0.7	Cor16
J04247-067	S.F	2MASS J04244260-0647313	M4.0 V+	AF15	04:24:42.61	-06:47:31.4	2MASS	18.8	0.7	Cor16
J04248+324	..F	G 039-011	M2.0 V	PMSU	04:24:49.19	+32:26:58.4	2MASS	26.1	0.5	Cor16

Table B.2: Names, spectral types, distances and astrometric parameters of Carmencita stars (continued).

Karmn	Flags[a]	Name	SpT	Ref.[b]	α (J2000)	δ (J2000)	Ref.[c]	d [pc]	ed [pc]	Ref.[d e]
J04251+515	..F	2MASS J04250968+5131578	M2.0 V	Lep13	04:25:09.68	+51:31:57.9	2MASS	25.9	0.5	Cor16
J04252+080N	..F	HG 7-207	M4.0 V	PMSU	04:25:16.92	+08:04:04.0	2MASS	27.8	1.1	Cor16
J04252+080S	S.F	HG 7-206	M2.5 V+	PMSU	04:25:15.07	+08:02:55.9	2MASS	27.7	1.1	aCortes
J04252+172	..F	V805 Tau	M3.5 V	AF15	04:25:13.53	+17:16:05.6	2MASS	18.8	0.6	Cor16
J04274+203	..F	TYC 1273-9-1	M1.5 V	Lep13	04:27:25.07	+20:22:44.4	2MASS	28.9	0.5	Cor16
J04276+595	B.F	G 175-032	M4.0 V+	PMSU	04:27:41.30	+59:35:16.7	2MASS	22.5	1.2	Dit14
J04278+117	..F	NLTT 13316	M4.0 V	PMSU	04:27:53.52	+11:46:54.8	2MASS	25.1	1.2	Dit14
J04284+176	B.f	V1102 Tau AB	M2.0 V+	Lep13	04:28:28.78	+17:41:45.4	2MASS	23.5	0.4	Cor16
J04290+219		BD+21 652	M0.5 V	Gra06	04:29:00.14	+21:55:21.5	2MASS	11.39	0.13	HIP2
J04293+142	..F	LTT 11438	M4.0 V	PMSU	04:29:18.47	+14:13:59.5	2MASS	17.0	0.7	Cor16
J04294+262	B.f	FW Tau ABC	M5.5 V+	Bri98	04:29:29.71	+26:16:53.2	2MASS	13.4	0.8	Cor16
J04302+708	..F	2MASS J04301210+7049138	M1.5 V	Lep13	04:30:12.10	+70:49:13.8	2MASS	28.7	0.4	Cor16
J04304+398	..f	V546 Per	M4.5 V	PMSU	04:30:25.27	+39:51:00.1	2MASS	10.43	0.3	vAl95
J04308-088	..F	Koenigstuhl 2A	M4.0 V	AF15	04:30:52.03	-08:49:19.3	2MASS	21.4	0.8	Cor16
J04310+367	B.F	1RXS J043100.0+364800	M3.0 V	AF15	04:31:00.01	+36:47:54.8	2MASS	25.8	0.7	Cor16
J04311+589	B..	STN 2051A	M4.0 V+	PMSU	04:31:11.48	+58:58:37.6	2MASS	5.62	0.06	HD80
J04312+422	..F	2MASS J04311499+4217111	M2.5 V	Lep13	04:31:14.99	+42:17:11.1	2MASS	18.2	0.4	Cor16
J04313+241	B.f	V927 Tau AB	M4.5 V:+	AF15	04:31:23.82	+24:10:52.9	2MASS	16.3	0.7	Cor16
J04326+098	..F	LP 475-1095	M1.5 V	Lep13	04:32:37.84	+09:51:06.5	2MASS	24.2	0.4	Cor16
J04329+001E	..F	LP 595-023	M0.5 V	AF15	04:32:56.24	+00:06:15.9	2MASS	26.2	2.6	Dit14
J04329+001N	..F	LP 595-021	M4.0 V	Rei04	04:32:55.50	+00:06:34.6	2MASS	24.0	2.5	Dit14
J04329+001S	..F	G 082-028	M3.0 V	Rei04	04:32:55.55	+00:06:29.5	2MASS	24.4	2.3	Dit14
J04333+239	B.F	V697 Tau	M3.0 V	Lep13	04:33:23.77	+23:59:27.1	2MASS	20.2	0.6	Cor16
J04335+207	..F	G 008-041	M4.0 V	PMSU	04:33:33.93	+20:44:46.2	2MASS	13.6	0.4	Dit14
J04347-004	..F	G 082-033	M4.0 V	AF15	04:34:45.32	-00:26:46.4	2MASS	16.7	0.6	Cor16
J04350+086	..F	StKM 1-495	M1.0 V	Lep13	04:35:02.56	+08:39:30.5	2MASS	33.0	0.4	Cor16
J04352-161	Sm.	LP 775-031	M7.0 V	Cru03	04:35:16.13	-16:06:57.5	2MASS	10.46	0.19	Wein16
J04366+112	..F	G 083-022	M4.0 V	PMSU	04:36:39.35	+11:13:17.4	2MASS	24.81	3.32	vAl95
J04369+593	..F	LP 084-034	M2.0 V	Lep13	04:36:58.43	+59:21:59.9	2MASS	27.34	3.72	HIP2
J04369-162	.mF	2MASS J04365738-1613065	M3.5 V	Klu13	04:36:57.38	-16:13:06.6	2MASS	18.6	0.6	Cor16
J04373+193	..F	LP 416-1644	M4.0 V	AF15	04:37:21.89	+19:21:17.5	2MASS	24.9	1.0	Cor16
J04376+528		BD+52 857	M0.0 V	Gra03	04:37:40.92	+52:53:37.2	2MASS	10.11	0.1	HIP2
J04376-024	B..	StKM 1-497 Cab	M1.1 V+	Shk09	04:37:37.46	-02:29:28.2	2MASS	29.43	0.29	aHIP2

Table B.2: Names, spectral types, distances and astrometric parameters of Carmencita stars (continued).

Karmn	Flags[a]	Name	SpT	Ref.[b]	α (J2000)	δ (J2000)	Ref.[c]	d [pc]	ed [pc]	Ref.[d e]
J04376-110		BD-11 916	M1.5 V	PMSU	04:37:41.88	-11:02:19.8	2MASS	11.1	0.21	HIP2
J04382+282	B..	G 039-029 AB	M4.0 V+	PMSU	04:38:12.56	+28:13:00.1	2MASS	12.1	0.5	Dit14
J04386-115	..f	LP 715-039	M3.5 V	AF15	04:38:37.18	-11:30:14.5	2MASS	15.1	0.5	Cor16
J04388+217	B.F	G 008-048	M3.5 V+	AF15	04:38:53.53	+21:47:54.9	2MASS	22.7	0.8	Cor16
J04393+335	B.F	RX J0439.4+3332B	M4.0 V+	AF15	04:39:23.20	+33:31:49.4	2MASS	22.1	0.9	Cor16
J04395+162	..F	LP 415-302	M5.5 V	Lep09	04:39:31.64	+16:15:44.7	2MASS	11.55	0.33	Lep09
J04398+251	..F	2MASS J04394898+2509262	M3.5 V	AF15	04:39:48.98	+25:09:26.2	2MASS	23.6	0.8	Cor16
J04403-055	..F	LP 655-048	M6.0 V	Shk09	04:40:23.25	-05:30:08.3	2MASS	9.78	0.1	Wein16
J04404-091	B.f	BD-09 956 AB	M0.0 V+	PMSU	04:40:29.28	-09:11:45.8	2MASS	19.68	1.45	HIP2
J04407+022	..F	StKM 1-502	M1.5 V	PMSU	04:40:42.49	+02:13:52.2	2MASS	19.3	0.3	Cor16
J04413+327	B.F	NLTT 13733	M4.0 V+	AF15	04:41:23.88	+32:42:22.8	2MASS	39.8	2.4	Dit14
J04414+132	..F	TYC 694-1183-1	M0.5 V	Lep13	04:41:29.67	+13:13:16.4	2MASS	29.0	0.3	Cor16
J04422+577	..F	LP 084-059	M0.0 V	Lep13	04:42:16.04	+57:42:27.5	2MASS	29.85	2.82	HIP2
J04423+207	..F	LP 415-1896	M2.0 V	Lep13	04:42:23.40	+20:46:34.3	2MASS	23.2	0.4	Cor16
J04425+204	S.F	LP 415-345	M3.0 V+	AF15	04:42:30.30	+20:27:11.4	2MASS	25.2	0.7	Cor16
J04429+095	..F	2MASS J04425522+0935544	M1.0 V	Lep13	04:42:55.22	+09:35:54.4	2MASS	33.8	0.4	Cor16
J04429+189		HD 285968	M2.0 V	PMSU	04:42:55.81	+18:57:28.5	2MASS	9.3	0.2	HIP2
J04429+214		2MASS J04425586+2128230	M3.5 V	Lep13	04:42:55.86	+21:28:23.0	2MASS	10.9	0.4	Cor16
J04433+296	..F	Haro 6-36	M5.0 V	Bri99	04:43:20.23	+29:40:06.0	2MASS	17.7	0.9	Cor16
J04444+278	..F	HD 283779	M1.5 V	PMSU	04:44:26.04	+27:51:44.6	2MASS	19.4	0.3	Cor16
J04458-144	..f	2MASS J04455273-1426259	M4.0 V	AF15	04:45:52.73	-14:26:26.0	2MASS	15.1	0.6	Cor16
J04468-112	B..	RBS 584	M3.0 V+	AF15	04:46:51.76	-11:16:47.6	2MASS	18.7	1.7	Shk12
J04471+021	..F	G 082-048	M0.0 V	PMSU	04:47:11.75	+02:09:39.7	2MASS	30.4	0.3	Cor16
J04472+206		RX J0447.2+2038	M5.0 V	AF15	04:47:12.25	+20:38:10.9	2MASS	11.0	0.6	Cor16
J04480+170	S.F	LP 416-043	M0.5 V+	Lep13	04:48:00.87	+17:03:21.6	2MASS	27.1	0.3	Cor16
J04488+100	S..	1RXS J044847.6+100302	M3.0 V+	Lep13	04:48:47.39	+10:03:02.6	2MASS	14.0	0.4	Cor16
J04494+484	B.f	G 081-034	M4.0 V+	AF15	04:49:29.47	+48:28:45.9	2MASS	21.2	0.9	Dit14
J04499+236	B.F	EM* LkCa 18	M1.0 V	Lep13	04:49:56.35	+23:41:02.9	2MASS	25.2	0.3	Cor16
J04499+711	..F	NLTT 13933	M3.5 V	AF15	04:49:55.70	+71:09:47.0	2MASS	24.3	1.2	Dit14
J04502+459	..F	LP 157-032	M1.0 V	PMSU	04:50:15.27	+45:58:50.2	2MASS	28.7	0.4	Cor16
J04504+199	..F	BPM 85800	M1.5 V	Lep13	04:50:25.45	+19:59:11.8	2MASS	28.4	0.4	Cor16
J04508+221	..F	GJ 1072	M5.0 V	PMSU	04:50:50.83	+22:07:22.5	2MASS	12.3	0.6	Dit14
J04508+261	..F	NLTT 14030	M2.5 V	PMSU	04:50:50.44	+26:07:26.8	2MASS	26.4	0.6	Cor16

Table B.2: Names, spectral types, distances and astrometric parameters of Carmencita stars (continued).

Karmn	Flags[a]	Name	SpT	Ref.[b]	α (J2000)	δ (J2000)	Ref.[c]	d [pc]	ed [pc]	Ref.[d e]
J04520+064		Wolf 1539	M3.5 V	PMSU	04:52:05.73	+06:28:35.6	2MASS	12.29	0.61	HIP2
J04524-168	Vm.	NLTT 14116	M3.0 V	Sch05	04:52:24.41	-16:49:21.9	2MASS	16.3	0.4	Shk12
J04525+407	..f	GJ 1073	M4.0 V	PMSU	04:52:34.48	+40:42:25.5	2MASS	12.7	0.3	Dit14
J04536+623	..F	G 247-039	M3.5 V	AF15	04:53:40.12	+62:19:03.9	2MASS	19.5	0.6	Cor16
J04538+158	..F	LSPM J0453+1549	M2.5 V	AF15	04:53:50.05	+15:49:15.6	2MASS	22.6	0.7	Dit14
J04538-177	.m.	GJ 180	M2.0 V	PMSU	04:53:49.95	-17:46:23.5	2MASS	12.1	0.3	HIP2
J04544+650	..F	1RXS J045430.9+650451	M4.0 V	AF15	04:54:29.82	+65:04:41.1	2MASS	44.7	38.3	HIP1
J04559+046	..F	HD 31412B	M2.0 V	AF15	04:55:54.46	+04:40:16.4	2MASS	34.92	0.69	aHIP2
J04560+432	..F	G 096-010	M4.0 V	AF15	04:56:03.54	+43:13:55.6	2MASS	14.1	0.5	Dit14
J04587+509	..F	LP 157-045	M0.5 V	PMSU	04:58:45.99	+50:56:37.9	2MASS	19.3	0.87	HIP2
J04588+498		BD+49 1280	M0.0 V	PMSU	04:58:50.58	+49:50:57.3	2MASS	16.31	0.36	HIP2
J04595+017	..f	V1005 Ori	M0.0 V	PMSU	04:59:34.83	+01:47:00.7	2MASS	25.88	1.7	HIP2
J05012+248	..f	Ross 794	M2.0 V	PMSU	05:01:15.51	+24:52:24.5	2MASS	29.1	11.3	vAl95
J05013+226	..F	LSPM J0501+2237	M4.5 V	Law08	05:01:18.03	+22:37:01.6	2MASS	13.6	0.6	Dit14
J05018+037	..F	StKM 1-539	M1.0 V	PMSU	05:01:50.57	+03:45:55.1	2MASS	23.4	0.3	Cor16
J05019+011		1RXS J050156.7+010845	M4.0 V	AF15	05:01:56.66	+01:08:42.9	2MASS	11.6	0.5	Cor16
J05019+099	B..	LP 476-207 AB	M4.0 V+	PMSU	05:01:58.81	+09:58:58.8	2MASS	24.89	1.28	Ried14
J05019-069		LP 656-038	M4.0 V	PMSU	05:01:57.47	-06:56:45.9	2MASS	5.44	0.03	Wein16
J05024-212	B..	HD 32450	M2.0 V+	Rei04	05:02:28.45	-21:15:23.6	2MASS	8.58	0.11	HIP2
J05030+213	B.f	HD 285190 BC	M5.0 V+	AF15	05:03:05.63	+21:22:36.2	2MASS	27.4	6.3	vAl95
J05032+213	S..	HD 285190 A	M1.5 V+	AF15	05:03:16.08	+21:23:56.4	2MASS	27.4	6.3	vAl95
J05033-173	.m.	LP 776-049	M3.0 V	PMSU	05:03:20.10	-17:22:24.5	2MASS	9.2	0.2	HIP2
J05034+531	..f	BD+52 911	M0.5 V	PMSU	05:03:24.02	+53:07:41.2	2MASS	13.62	0.36	HIP2
J05042+110	..f	G 097-015	M4.0 V	PMSU	05:04:14.76	+11:03:23.8	2MASS	10.3	0.2	Dit14
J05050+442	..F	2MASS J05050591+4414037	M5.0 V	AF15	05:05:05.92	+44:14:03.8	2MASS	13.6	0.7	Cor16
J05051-120	..F	LP 716-035	M3.0 V	PMSU	05:05:11.81	-12:00:28.6	2MASS	22.0	0.6	Cor16
J05060+043	..F	G 084-036	M1.0 V	PMSU	05:06:04.02	+04:20:14.3	2MASS	25.9	0.3	Cor16
J05062+046		RX J0506.2+0439	M4.0 V	AF15	05:06:12.93	+04:39:27.2	2MASS	13.9	0.5	Cor16
J05068-215E	Jm.	BD-21 1074 A	M1.5 V	PMSU	05:06:49.92	-21:35:09.2	2MASS	19.79	0.63	Ried14
J05068-215W	Bm.	BD-21 1074 BC	M3.5 V+	PMSU	05:06:49.47	-21:35:03.8	2MASS	18.33	0.73	Ried14
J05072+375	..F	1RXS J050714.8+373103	M5.0 V	AF15	05:07:14.49	+37:30:42.1	2MASS	16.7	0.9	Cor16
J05076+275	..F	TYC 1853-1649-1	M0.5 V	Lep13	05:07:36.66	+27:30:05.4	2MASS	28.5	0.3	Cor16
J05078+179	B..	Wolf 230	M3.0 V+	PMSU	05:07:49.24	+17:58:58.4	2MASS	13.4	0.4	Cor16

Table B.2: Names, spectral types, distances and astrometric parameters of Carmencita stars (continued).

Karmn	Flags[a]	Name	SpT	Ref.[b]	α (J2000)	δ (J2000)	Ref.[c]	d [pc]	ed [pc]	Ref.[d e]
J05083+756	B.F	LP 015-315	M4.5 V+	AF15	05:08:18.41	+75:38:15.5	2MASS	15.1	0.5	Dit14
J05084-210	.mf	2MASS J05082729-2101444	M5.0 V	Ria06	05:08:27.30	-21:01:44.4	2MASS	12.9	0.7	Cor16
J05085-181	Bm.	GJ 190 AB	M3.5 V+	PMSU	05:08:35.01	-18:10:17.9	2MASS	9.3	0.1	HIP2
J05091+154	..f	Ross 388	M3.0 V	PMSU	05:09:09.97	+15:27:32.5	2MASS	29.7	15.8	vAl95
J05103+095	..F	G 097-023	M2.0 V	Lep13	05:10:18.06	+09:30:07.3	2MASS	27.13	2.87	HIP2
J05103+272	..F	LSR J0510+2713	M6.0 V	Rei04	05:10:20.12	+27:14:03.2	2MASS	9.9	0.2	Lep09
J05103+488	B..	G 096-021 AB	M2.5 V+	PMSU	05:10:22.08	+48:50:32.7	2MASS	20.5	3.9	vAl95
J05106+297	V.f	G 086-028	M3.0 V	Lep13	05:10:39.56	+29:46:47.9	2MASS	17.5	0.5	Cor16
J05109+186	..F	G 085-048	M3.5 V	PMSU	05:10:57.47	+18:37:36.0	2MASS	17.4	0.3	Dit14
J05111+158	..F	StKM 1-549	M1.0 V	Lep13	05:11:09.71	+15:48:57.4	2MASS	35.3	0.4	Cor16
J05114+101	..F	LP 477-036	M1.0 V	Lep13	05:11:29.74	+10:07:15.7	2MASS	51.87	12.0	HIP2
J05127+196		GJ 192	M2.0 V	PMSU	05:12:42.23	+19:39:56.6	2MASS	12.3	0.6	HIP2
J05151-073	..F	NLTT 14750	M1.0 V	AF15	05:15:08.05	-07:20:48.6	2MASS	22.45	2.05	HIP2
J05152+236	..F	2MASS J05151753+2336260	M5.0 V	AF15	05:15:17.54	+23:36:26.1	2MASS	16.0	0.8	Cor16
J05155+591	..F	LSPM J0515+5911	M7.5 V	Lep09	05:15:30.94	+59:11:18.5	2MASS	15.22	0.3	Lep09
J05173+321	..F	G 086-037	M3.5 V	AF15	05:17:19.96	+32:07:35.0	2MASS	19.6	0.6	Cor16
J05173+458	B..	Capella Bab	M1.0 V+	PMSU	05:17:23.86	+45:50:22.9	2MASS	13.12	0.08	aHIP2
J05173+721	..F	TYC 4351-466-1	M1.0 V	Lep13	05:17:21.27	+72:10:51.5	2MASS	30.9	0.4	Cor16
J05187+464	..F	2MASS J05184455+4629597	M4.5 V	AF15	05:18:44.56	+46:29:59.5	2MASS	18.2	0.8	Cor16
J05195+649	..F	1RXS J051929.3+645435	M3.5 V	AF15	05:19:31.18	+64:54:33.6	2MASS	17.2	0.6	Cor16
J05206+587N	..F	G 191-030 A	M3.5 V	PMSU	05:20:41.38	+58:47:33.1	2MASS	24.2	0.5	Dit14
J05206+587S	..F	G 191-029 B	M3.5 V	PMSU	05:20:40.73	+58:47:19.9	2MASS	23.2	0.5	Dit14
J05211+557	..F	G 191-032	M3.0 V	PMSU	05:21:10.23	+55:45:51.4	2MASS	23.3	0.7	Cor16
J05223+305	..F	2MASS J05222053+3031097	M3.0 V	AF15	05:22:20.53	+30:31:09.7	2MASS	25.3	0.7	Cor16
J05226+795	..F	TYC 4532-731-1	M0.5 V	Lep13	05:22:39.32	+79:34:31.1	2MASS	27.0	0.3	Cor16
J05228+202	B.F	2MASS J05225013+2016360	M2.5 V+	Lep13	05:22:50.13	+20:16:36.1	2MASS	20.8	0.5	Cor16
J05243-160	Bm.	1RXS J052419.1-160117	M4.5 V+	Ria06	05:24:19.14	-16:01:15.3	2MASS	10.0	0.5	Cor16
J05256-091	B..	LP 717-036	M3.5 V+	AF15	05:25:41.67	-09:09:12.3	2MASS	13.7	0.5	Cor16
J05280+096		Ross 41	M3.5 V	PMSU	05:28:00.15	+09:38:38.3	2MASS	10.8	0.3	Dit14
J05282+029	B..	GJ 1080 A	M3.0 V+	PMSU	05:28:14.60	+02:58:14.3	2MASS	19.1	0.8	bvAl95
J05289+125	..F	HD 35956 B	M4.0 V	AF15	05:28:56.50	+12:31:53.9	2MASS	28.17	0.75	aHIP2
J05294+155E	..F	GJ 2043 A	M0.0 V:	AF15	05:29:27.04	+15:34:38.4	2MASS	17.26	0.77	HIP2
J05294+155W	..F	GJ 2043 B	M4.0 V	PMSU	05:29:26.13	+15:34:45.3	2MASS	17.4	0.8	Dit14

Table B.2: Names, spectral types, distances and astrometric parameters of Carmencita stars (continued).

Karmn	Flags[a]	Name	SpT	Ref.[b]	α (J2000)	δ (J2000)	Ref.[c]	d [pc]	ed [pc]	Ref.[d e]
J05298+320	..f	Ross 406	M3.0 V	PMSU	05:29:52.69	+32:04:52.5	2MASS	20.6	0.9	Dit14
J05298-034	..f	Wolf 1450	M2.5 V	PMSU	05:29:52.05	-03:26:29.6	2MASS	17.6	2.0	vAl95
J05306+152	..F	LSPM J0530+1514	M3.0 V	Lep13	05:30:37.23	+15:14:28.7	2MASS	20.9	0.6	Cor16
J05314-036		HD 36395	M1.5 V	AF15	05:31:27.35	-03:40:35.7	2MASS	5.66	0.04	HIP2
J05320-030	B..	V1311 Ori	M2.0 V+	AF15	05:32:04.50	-03:05:29.2	2MASS	16.9	0.3	Cor16
J05322+098	S..	V998 Ori	M3.5 V+	PMSU	05:32:14.67	+09:49:15.0	2MASS	12.8	0.6	HIP2
J05328+338	..F	NLTT 15237	M3.5 V	AF15	05:32:51.95	+33:49:47.5	2MASS	13.2	0.2	Dit14
J05333+448	B..	GJ 1081	M3.5 V+	PMSU	05:33:19.13	+44:48:58.8	2MASS	15.34	0.42	vAl95
J05337+019		V371 Ori	M2.5 V	PMSU	05:33:44.81	+01:56:43.4	2MASS	15.94	1.02	HIP2
J05339-023	..f	RX J0534.0-0221	M3.0 V	Ria06	05:33:59.81	-02:21:32.5	2MASS	17.2	0.5	Cor16
J05341+475	B.F	1RXS J053410.8+473207	M2.5 V	Lep13	05:34:10.64	+47:32:03.3	2MASS	22.0	0.5	Cor16
J05341+512	..F	G 191-004	M0.5 V	PMSU	05:34:08.70	+51:12:56.6	2MASS	25.53	1.68	HIP2
J05342+103N	..f	Ross 45 A	M3.0 V	AF15	05:34:15.14	+10:19:14.2	2MASS	17.2	0.5	Cor16
J05342+103S	S.f	Ross 45 B	M4.5 V+	AF15	05:34:15.08	+10:19:09.2	2MASS	12.7	0.6	Cor16
J05348+138		Ross 46	M3.5 V	PMSU	05:34:52.12	+13:52:47.2	2MASS	12.4	1.5	vAl95
J05360-076		Wolf 1457	M4.0 V	PMSU	05:36:00.08	-07:38:58.1	2MASS	11.3	0.4	Cor16
J05365+113		V2689 Ori	M0.0 V	Lep13	05:36:30.99	+11:19:40.2	2MASS	11.24	0.13	HIP2
J05366+112		2MASS J05363846+1117487	M4.0 V	Lep13	05:36:38.47	+11:17:48.8	2MASS	11.24	0.13	aHIP2
J05394+406	..f	LSR J0539+4038	M8.0 V	Lep03	05:39:24.74	+40:38:43.8	2MASS	10.4	0.4	Dit14
J05394+747	..F	NLTT 15320	M3.5 V	AF15	05:39:25.41	+74:46:04.9	2MASS	20.5	0.7	Cor16
J05402+126	S.f	V1402 Ori AB	M1.0 V+	PSMU	05:40:16.09	+12:39:00.8	2MASS	23.3	0.3	Cor16
J05404+248	B..	V780 Tau A	M5.5 V+	PMSU	05:40:25.70	+24:48:09.0	2MASS	10.4	0.3	vAl95
J05415+534		HD 233153	M1.0 V	AF15	05:41:30.73	+53:29:23.9	2MASS	12.28	0.08	aHIP2
J05419+153	..F	MCC 467	M0.0 V	Lep13	05:41:58.86	+15:20:14.1	2MASS	21.35	1.03	HIP2
J05421+124		V1352 Ori	M4.0 V	AF15	05:42:08.98	+12:29:25.3	2MASS	5.83	0.03	Wein16
J05422-054	..F	GJ 2045	M5.5 V	PMSU	05:42:12.72	-05:27:56.7	2MASS	12.79	0.44	vAl95
J05425+154	..F	1RXS J054232.1+152459	M3.5 V	AF15	05:42:31.78	+15:25:01.6	2MASS	21.6	0.7	Cor16
J05455-119	..F	2MASS J05453198-1158034	M4.5 V	AF15	05:45:31.98	-11:58:03.5	2MASS	15.3	0.7	Cor16
J05456+729	..F	2MASS J05453880+7255127	M3.0 V	AF15	05:45:38.80	+72:55:12.7	2MASS	25.2	0.7	Cor16
J05458+729	..F	2MASS J05454973+7254072	M2.5 V	AF15	05:45:49.74	+72:54:07.2	2MASS	28.8	0.7	Cor16
J05466+441	S..	Wolf 237	M4.0 V+	PMSU	05:46:38.45	+44:07:19.8	2MASS	21.0	0.7	Dit14
J05468+665	..F	TYC 4106-420-1	M0.5 V	Lep13	05:46:48.73	+66:30:11.6	2MASS	29.8	0.3	Cor16
J05471-052	..F	LP 658-033	M4.5 V	PMSU	05:47:09.07	-05:12:10.7	2MASS	17.0	0.6	vAl95

Table B.2: Names, spectral types, distances and astrometric parameters of Carmencita stars (continued).

Karmn	Flags[a]	Name	SpT	Ref.[b]	α (J2000)	δ (J2000)	Ref.[c]	d [pc]	ed [pc]	Ref.[d e]
J05472-000	..F	StKM 1-578	M0.0 V	PMSU	05:47:17.97	-00:00:48.7	2MASS	26.2	0.3	Cor16
J05484+077	V.F	LTT 17868	M4.0 V	PMSU	05:48:24.08	+07:45:38.8	2MASS	20.7	0.8	Cor16
J05511+122	..F	2MASS J05511039+1216101	M4.0 V	AF15	05:51:10.40	+12:16:10.2	2MASS	17.8	0.7	Cor16
J05530+047	..F	G 106-007	M1.5 V	Lep13	05:53:04.46	+04:43:07.3	2MASS	31.4	0.5	Cor16
J05530+251	..f	LSPM J0553+2507	M3.0 V	Lep13	05:53:01.80	+25:07:44.0	2MASS	17.1	0.5	Cor16
J05532+242		Ross 59	M1.5 V	PMSU	05:53:14.04	+24:15:32.9	2MASS	19.4	1.7	vAl95
J05547+109	B.F	RX J0554.7+1055	M3.0 V	Lep13	05:54:45.74	+10:55:57.1	2MASS	19.4	0.5	Cor16
J05558+406	..F	2MASS J05554841+4036498	M1.0 V	Lep13	05:55:48.41	+40:36:49.8	2MASS	32.2	0.4	Cor16
J05566-103	..F	1RXS J055641.0-101837	M3.5 V	AF15	05:56:40.66	-10:18:37.9	2MASS	18.1	0.6	Cor16
J05587+259	..F	2MASS J05584754+2557395	M1.0 V	Lep13	05:58:47.55	+25:57:39.5	2MASS	32.2	0.4	Cor16
J05588+213	B.F	NLTT 15870	M5.0 V+	AF15	05:58:53.33	+21:21:01.1	2MASS	17.9	1.1	Dit14
J05596+585	..f	EG Cam	M0.5 V	AF15	05:59:37.75	+58:35:35.1	2MASS	13.53	0.3	HIP2
J05599+585	..f	G 192-012	M4.0 V	PMSU	05:59:55.69	+58:34:15.6	2MASS	13.53	0.3	aHIP2
J06000+027		G 099-049	M4.0 V	PMSU	06:00:03.51	+02:42:23.6	2MASS	5.22	0.03	Wein16
J06007+681	..f	LP 057-040	M4.0 V	PMSU	06:00:46.50	+68:08:30.0	2MASS	20.1	0.6	avAl95
J06008+681	..F	LP 057-041	M3.5 V	PMSU	06:00:49.42	+68:09:23.8	2MASS	20.1	0.6	vAl95
J06011+595		G 192-013	M3.5 V	PMSU	06:01:11.07	+59:35:50.8	2MASS	7.5	0.1	Dit14
J06017+130	..F	LSPM J0601+1305	M2.5 V	Lep13	06:01:45.71	+13:05:01.6	2MASS	19.1	0.4	Cor16
J06023-203	.mF	LP 779-010	M3.5 V	PMSU	06:02:22.62	-20:19:44.7	2MASS	19.4	0.6	Cor16
J06024+498		G 192-015	M5.0 V	AF15	06:02:29.18	+49:51:56.2	2MASS	9.3	0.2	Jen09
J06024+663	..F	G 249-032	M4.5 V	AF15	06:02:25.54	+66:20:40.4	2MASS	17.2	0.7	Dit14
J06025+371	..F	2MASS J06023526+3707372	M1.0 V	Lep13	06:02:35.26	+37:07:37.2	2MASS	27.5	0.3	Cor16
J06034+478	..F	Wolf 261	M4.0 V	PMSU	06:03:29.58	+47:48:15.6	2MASS	23.2	0.6	Dit14
J06035+155	..F	TYC 1313-1482-1	M0.0 V	AF15	06:03:34.81	+15:31:31.0	2MASS	29.0	0.3	Cor16
J06035+168	..F	2MASS J06033461+1651457	M4.0 V	AF15	06:03:34.62	+16:51:45.7	2MASS	17.3	0.7	Cor16
J06039+261	..F	Ross 60	M3.0 V	PMSU	06:03:54.09	+26:08:55.8	2MASS	30.9	0.9	Cor16
J06054+608	..f	LP 086-173	M4.5 V	AF15	06:05:29.36	+60:49:23.2	2MASS	14.0	0.4	Dit14
J06066+465	..F	2MASS J06063789+4633463	M3.0 V	AF15	06:06:37.89	+46:33:46.3	2MASS	23.4	0.7	Cor16
J06071+335	..F	Ross 70	M2.5 V	PMSU	06:07:11.79	+33:32:37.3	2MASS	24.5	0.6	Cor16
J06075+472	..F	LSPM J0607+4712	M4.5 V	AF15	06:07:31.85	+47:12:26.6	2MASS	22.1	1.3	Dit14
J06097+001	..F	HD 291290	M0.0 V	Lep13	06:09:46.14	+00:09:32.7	2MASS	27.9	0.3	Cor16
J06102+225	V.F	2MASS J06101775+2234199	M4.0 V	AF15	06:10:17.76	+22:34:19.9	2MASS	21.6	0.8	Cor16
J06103+225	B.F	NLTT 16144	M5.0 V+	Law08	06:10:22.46	+22:34:20.8	2MASS	22.8	1.9	Dit14

Table B.2: Names, spectral types, distances and astrometric parameters of Carmencita stars (continued).

Karmn	Flags[a]	Name	SpT	Ref.[b]	α (J2000)	δ (J2000)	Ref.[c]	d [pc]	ed [pc]	Ref.[d e]
J06103+722	..F	LSPM J0610+7212	M2.5 V	AF15	06:10:18.26	+72:12:00.6	2MASS	25.5	0.7	Dit14
J06103+821		GJ 226	M2.0 V	PMSU	06:10:19.78	+82:06:25.7	2MASS	9.4	0.1	HIP2
J06105+024	..F	TYC 135-239-1	M0.0 V	Lep13	06:10:31.46	+02:25:31.1	2MASS	30.9	0.3	Cor16
J06105-218	.m.	HD 42581 A	M0.5 V	PMSU	06:10:34.62	-21:51:52.2	2MASS	5.75	0.03	HIP2
J06107+259	..F	Wolf 1058	M1.5 V	PMSU	06:10:46.31	+25:56:03.5	2MASS	30.5	8.9	vAl95
J06109+103	B..	BD+10 1032 AB	M2.5 V+	PMSU	06:10:54.81	+10:19:05.6	2MASS	10.9	0.4	HIP2
J06140+516	..F	G 192-022	M3.5 V	PMSU	06:14:02.40	+51:40:08.1	2MASS	14.9	0.4	Dit14
J06145+025	..F	G 106-035	M3.0 V	AF15	06:14:34.91	+02:30:27.4	2MASS	26.4	2.3	vAl95
J06151-164	.mf	LP 779-034	M4.0 V	AF15	06:15:11.99	-16:26:15.2	2MASS	16.5	0.6	Cor16
J06171+051	B.F	HD 43587 BC	M3.5 V+	AF15	06:17:10.65	+05:07:02.4	2MASS	19.4	0.9	Dit14
J06171+751	..f	TYC 4525-194-1	M2.0 V	Lep13	06:18:07.30	+75:06:03.3	2MASS	18.2	0.3	Cor16
J06171+838	..F	LSPM J0617+8353	M3.5 V	Lep13	06:17:05.32	+83:53:35.4	2MASS	13.9	0.9	Dit14
J06185+250	..F	G 103-029	M4.0 V	AF15	06:18:34.80	+25:03:06.4	2MASS	26.4	0.7	Dit14
J06193-066	..F	Ross 417	M3.0 V	PMSU	06:19:20.79	-06:39:21.5	2MASS	14.7	1.9	vAl95
J06194+139	..F	TYC 743-1836-1	M0.5 V	Lep13	06:19:29.48	+13:57:03.1	2MASS	22.9	0.2	Cor16
J06212+442	B.F	G 101-035	M2.0 V+	PMSU	06:21:13.00	+44:14:30.7	2MASS	25.0	0.5	Cor16
J06216+163	V.f	LP 420-005	M1.0 V	Lep13	06:21:36.58	+16:18:36.2	2MASS	23.5	1.1	Dit14
J06217+163	..F	LP 420-006	M2.5 V	Rei04	06:21:43.89	+16:19:22.3	2MASS	22.6	1.1	Dit14
J06218-227	.mF	BD-22 3005	M1.0 Vk	Gra06	06:21:53.85	-22:43:24.2	2MASS	25.0	1.97	HIP2
J06223+334	..F	TYC 2425-1286-1	M1.0 V	Lep13	06:22:20.70	+33:26:56.4	2MASS	31.9	0.4	Cor16
J06236-096	B.F	LP 720-010	M3.5 V+	AF15	06:23:38.47	-09:38:51.7	2MASS	25.6	0.9	Cor16
J06237+020	..F	TYC 141-24-1	M1.5 V	Lep13	06:23:46.45	+05:02:41.1	2MASS	20.6	0.3	Cor16
J06238+456	..F	LP 160-022	M5.0 V	AF15	06:23:51.24	+45:40:05.1	2MASS	18.6	1.1	Dit14
J06246+234		Ross 64	M4.0 V	AF15	06:24:41.32	+23:25:58.6	2MASS	8.38	0.16	vAl95
J06258+561	..F	G 192-026	M4.0 V	PMSU	06:25:53.00	+56:10:25.0	2MASS	22.32	2.34	vAl95
J06262+238	..F	1RXS J062614.2+234942	M1.5 V	Lep13	06:26:14.54	+23:49:38.4	2MASS	27.2	0.5	Cor16
J06277+093	B.f	Ross 603	M2.0 V	Lep13	06:27:43.97	+09:23:54.1	2MASS	20.3	0.4	Cor16
J06293-028	B..	V577 Mon AB	M4.5 V+	PMSU	06:29:23.39	-02:48:50.0	2MASS	4.13	0.05	HIP2
J06298-027	S.F	G 108-004	M4.0 V+	AF15	06:29:50.28	-02:47:45.5	2MASS	17.9	0.7	Cor16
J06306+456	..F	2MASS J06303755+4539215	M1.0 V	Lep13	06:30:37.56	+45:39:21.5	2MASS	34.0	0.4	Cor16
J06307+397	..F	2MASS J06304724+3947370	M2.0 V	AF15	06:30:47.24	+39:47:37.1	2MASS	34.2	0.6	Cor16
J06310+500	..F	StKM 1-598	M0.5 V	PMSU	06:31:01.16	+50:02:48.6	2MASS	23.2	0.2	Cor16
J06318+414	..f	LP 205-044	M5.0 V	PMSU	06:31:50.74	+41:29:45.9	2MASS	11.1	1.8	Jen09

Table B.2: Names, spectral types, distances and astrometric parameters of Carmencita stars (continued).

Karmn	Flags[a]	Name	SpT	Ref.[b]	α (J2000)	δ (J2000)	Ref.[c]	d [pc]	ed [pc]	Ref.[d e]
J06322+378	..F	TYC 2928-1568-1	M1.5 V	Lep13	06:32:15.06	+37:48:12.8	2MASS	22.4	0.3	Cor16
J06323-097	..F	2MASS J06322029-0943290	M4.5 V	AF15	06:32:20.29	-09:43:29.0	2MASS	17.3	0.8	Cor16
J06325+641	..F	LP 057-192	M4.0 V	AF15	06:32:30.61	+64:06:20.7	2MASS	21.4	0.9	Dit14
J06345+315	..f	G 103-041	M3.5 V	Lep13	06:34:33.44	+31:30:08.4	2MASS	15.3	0.5	Cor16
J06354-040	B..	2MASS J06352986-0403185	M5.5 V+	AF15	06:35:29.87	-04:03:18.5	2MASS	8.2	0.5	Cor16
J06361+116	..F	NLTT 16724	M4.5 V	PMSU	06:36:06.39	+11:37:03.2	2MASS	18.28	0.8	Jen09
J06361+201	..F	LP 420-004	M2.5 V	AF15	06:36:11.93	+20:08:14.2	2MASS	30.1	0.7	Cor16
J06371+175		HD 260655	M0.0 V	Lep13	06:37:10.92	+17:33:52.7	2MASS	9.75	0.16	HIP2
J06396-210		LP 780-032	M4.0 V	Sch05	06:39:37.42	-21:01:33.3	2MASS	11.5	0.5	Cor16
J06400+285	B.f	LP 307-008	M2.0 V+	PMSU	06:40:05.50	+28:35:14.3	2MASS	20.3	0.4	Cor16
J06401-164	.mF	LP 780-023	M2.5 V	AF15	06:40:08.61	-16:27:26.9	2MASS	26.0	0.6	Cor16
J06414+157	..F	Wolf 289	M4.0 V	PMSU	06:41:28.18	+15:45:48.2	2MASS	18.8	0.7	Cor16
J06421+035		G 108-021	M3.5 V	PMSU	06:42:11.18	+03:34:52.7	2MASS	15.39	0.15	Wein16
J06422+035	..f	G 108-022	M4.0 V	PMSU	06:42:13.34	+03:35:31.1	2MASS	15.04	0.39	Wein16
J06435+166	..F	G 110-014	M4.5 V	AF15	06:43:34.77	+16:41:34.9	2MASS	22.1	1.2	Dit14
J06438+511	B..	LP 121-041 AB	M2.5 V+	PMSU	06:43:49.70	+51:08:21.0	2MASS	19.2	1.5	vAl95
J06447+718	B..	G 251-016 AB	M0.5 V+	PMSU	06:44:45.76	+71:53:15.7	2MASS	21.86	1.07	HIP2
J06461+325	..F	HD 263175B	M1.0 V	AF15	06:46:07.50	+32:33:14.9	2MASS	26.24	0.69	aHIP2
J06467+159	..F	TYC 1330-879-1	M1.0 V	Lep13	06:46:45.73	+15:57:42.2	2MASS	21.7	0.3	Cor16
J06474+054	..F	G 108-027	M4.0 V	AF15	06:47:27.51	+05:24:28.2	2MASS	22.4	0.5	Dit14
J06486+532	..F	G 192-046	M1.5 V	Lep13	06:48:38.45	+53:17:29.5	2MASS	31.4	0.5	Cor16
J06489+211	..F	2MASS J06485522+2108039	M2.5 V	AF15	06:48:55.22	+21:08:03.9	2MASS	29.2	0.7	Cor16
J06490+371	..F	GJ 1092	M4.0 V	PMSU	06:49:05.42	+37:06:53.4	2MASS	13.3	0.4	vAl95
J06509-091	..F	LP 661-002	M3.5 V	AF15	06:50:59.48	-09:10:50.6	2MASS	21.1	0.7	Cor16
J06523-051	B..	BD-05 1844Bab	M2.0 V+	AF15	06:52:18.04	-05:11:24.1	2MASS	8.71	0.03	aHIP2
J06524+182	..f	LP 421-007	M4.0 V	PMSU	06:52:24.30	+18:17:04.7	2MASS	14.8	0.6	Cor16
J06540+608	B..	LP 087-237 AB	M3.0 V+	PMSU	06:54:04.20	+60:52:19.1	2MASS	10.5	0.3	HIP2
J06548+332		Wolf 294	M3.0 V	AF15	06:54:49.03	+33:16:05.9	2MASS	5.59	0.05	HIP2
J06564+121	..F	TYC 756-1685-1	M1.0 V	Lep13	06:56:25.79	+12:07:32.9	2MASS	22.5	0.3	Cor16
J06564+400	..F	BD+40 1758B	M0.5 V	PMSU	06:56:28.48	+40:05:05.6	2MASS	24.6	0.81	aHIP2
J06564+759	..F	LP 034-110	M1.0 V	Lep13	06:53:24.06	+72:55:15.0	2MASS	34.4	0.4	Cor16
J06565+440	..F	G 107-036	M4.5 V	AF15	06:56:30.94	+44:01:56.8	2MASS	21.4	1.6	Dit14
J06574+740		2MASS J06572616+7405265	M4.0 V	Lep13	06:57:26.16	+74:05:26.5	2MASS	14.0	0.5	Cor16

Table B.2: Names, spectral types, distances and astrometric parameters of Carmencita stars (continued).

Karmn	Flags[a]	Name	SpT	Ref.[b]	α (J2000)	δ (J2000)	Ref.[c]	d [pc]	ed [pc]	Ref.[d e]
J06579+623	B..	G 250-031 AB	M4.5 V+	PMSU	06:57:57.04	+62:19:19.7	2MASS	11.4	0.3	vAl95
J06582+511	..F	G 192-059	M2.0 V	Lep13	06:58:12.41	+51:08:37.9	2MASS	28.1	0.5	Cor16
J06594+193		GJ 1093	M5.0 V	PMSU	06:59:28.69	+19:20:57.7	2MASS	7.8	0.2	vAl95
J06594+195	..F	G 088-002	M3.0 V	Lep13	06:59:28.90	+19:30:34.1	2MASS	20.4	0.6	Cor16
J06596+057	..F	2MASS J06594156+0545400	M2.5 V	Lep13	06:59:41.57	+05:45:40.1	2MASS	24.0	0.6	Cor16
J07001-190	.m.	2MASS J07000682-1901235	M5.0 V	AF15	07:00:06.83	-19:01:23.6	2MASS	9.4	0.5	Cor16
J07009-023	..F	2MASS J07005978-0221330	M3.0 V	AF15	07:00:59.78	-02:21:33.0	2MASS	24.1	0.7	Cor16
J07012+008	..F	2MASS J07011554+0052419	M2.5 V	Lep13	07:01:15.54	+00:52:41.9	2MASS	22.4	0.5	Cor16
J07033+346		LP 255-011	M4.0 V	PMSU	07:03:23.17	+34:41:51.0	2MASS	13.7	0.3	Dit14
J07034+767	..F	LP 016-379	M3.5 V	Lep13	07:03:29.89	+76:46:26.1	2MASS	16.3	0.5	Cor16
J07039+527	B..	LP 122-059 AB	M5.0 V+	PMSU	07:03:55.65	+52:42:07.6	2MASS	9.2	0.2	vAl95
J07042-105	B..	Ross 54	M3.5 V+	PMSU	07:04:17.71	-10:30:30.7	2MASS	16.0	0.8	HIP2
J07044+682		GJ 258	M3.0 V	PMSU	07:04:25.94	+68:17:19.6	2MASS	14.9	0.6	HIP2
J07047+249	..F	Ross 874	M1.5 V	PMSU	07:04:49.67	+24:59:55.6	2MASS	23.0	0.4	Cor16
J07051-101	..F	2MASS J07051194-1007528	M5.0 V	AF15	07:05:11.95	-10:07:52.8	2MASS	16.1	0.8	Cor16
J07052+084	..F	G 108-052	M2.0 V	Lep13	07:05:12.31	+08:25:52.4	2MASS	26.2	0.5	Cor16
J07076+486	..F	G 107-048	M3.5 V	PMSU	07:07:37.76	+48:41:13.8	2MASS	10.8	0.4	Dit14
J07078+672	..F	G 250-034	M1.0 V	PMSU	07:07:50.44	+67:12:04.6	2MASS	17.6	0.64	HIP2
J07081-228	..f	LP 840-016	M2.0 V	Sch05	07:08:07.03	-22:48:47.2	2MASS	18.7	0.4	Cor16
J07086+307	..F	StKM 1-626	M0.0 V	PMSU	07:08:39.50	+30:42:49.9	2MASS	30.7	0.5	Cor16
J07095+698	..F	G 251-027	M2.5 V	PMSU	07:09:32.43	+69:50:57.6	2MASS	23.1	0.5	Cor16
J07100+385	S..	QY Aur AB	M4.5 V+	PMSU	07:10:01.80	+38:31:45.8	2MASS	6.3	0.1	HIP2
J07102+376	..F	LTT 17942 A	M4.0 V	PMSU	07:10:13.60	+37:40:10.5	2MASS	23.9	0.9	Dit14
J07105-087	..F	2MASS J07103147-0842485	M3.5 V	AF15	07:10:31.47	-08:42:48.5	2MASS	18.0	0.6	Cor16
J07111+434	B.F	LP 206-011 AB	M5.5 V+	AF15	07:11:11.38	+43:29:59.0	2MASS	12.85	0.5	Lep09
J07119+773	S.f	TYC 4530-1414-1	M1.5 V+	Lep13	07:11:57.05	+77:21:59.1	2MASS	17.8	0.3	Cor16
J07121+522	..F	G 193-037	M1.0 V	PMSU	07:12:11.39	+52:16:24.8	2MASS	26.85	1.77	HIP2
J07129+357	..F	2MASS J07125952+3547032	M2.5 V	Lep13	07:12:59.53	+35:47:03.2	2MASS	22.8	0.5	Cor16
J07140+507	..F	G 193-039	M0.5 V	Lep13	07:14:04.50	+50:43:33.5	2MASS	30.2	0.3	Cor16
J07163+271	B..	BD+27 1348 AB	M2.5 V+	PMSU	07:16:19.77	+27:08:33.1	2MASS	12.0	0.4	HIP2
J07163+331	..F	GJ 1096	M4.0 V	PMSU	07:16:18.02	+33:09:10.4	2MASS	14.9	0.9	vAl95
J07172-050	..F	2MASS J07171706-0501031	M3.5 V	AF15	07:17:17.06	-05:01:03.1	2MASS	16.6	0.6	Cor16
J07174+195	..F	G 088-019	M2.5 V	PMSU	07:17:29.97	+19:34:17.0	2MASS	21.2	1.0	vAl95

Table B.2: Names, spectral types, distances and astrometric parameters of Carmencita stars (continued).

Karmn	Flags[a]	Name	SpT	Ref.[b]	α (J2000)	δ (J2000)	Ref.[c]	d [pc]	ed [pc]	Ref.[d e]
J07181+392	..f	Ross 987	M0.0 V	PMSU	07:18:08.19	+39:16:29.5	2MASS	14.49	0.43	HIP2
J07182+137	..F	2MASS J07181290+1342167	M3.5 V	AF15	07:18:12.91	+13:42:16.7	2MASS	20.8	0.7	Cor16
J07195+328	..f	BD+33 1505	M0.0 V	AF15	07:19:31.27	+32:49:48.3	2MASS	19.39	0.79	HIP2
J07199+840	..F	TYC 4618-116-1	M2.5 V	Lep13	07:19:57.98	+84:04:38.2	2MASS	17.9	0.4	Cor16
J07212+005	..F	TYC 178-2187-1	M0.5 V	Lep13	07:31:12.86	+00:33:14.2	2MASS	28.3	0.3	Cor16
J07227+306	..F	G 087-036	M3.5 V	PMSU	07:22:42.03	+30:40:12.0	2MASS	23.7	1.8	vAl95
J07232+460	..F	G 107-065	M0.5 V	PMSU	07:23:14.89	+46:05:14.6	2MASS	16.41	0.5	HIP2
J07274+052		Luytens Star	M3.5 V	AF15	07:27:24.50	+05:13:32.9	2MASS	3.8	0.02	HIP2
J07274+220	..F	Ross 878	M1.5 V	PMSU	07:27:28.65	+22:02:38.4	2MASS	19.35	1.13	HIP2
J07282-187	.mf	LP 782-002	M4.5 V	PMSU	07:28:13.09	-18:47:36.0	2MASS	12.0	0.5	Cor16
J07287-032		GJ 1097	M3.0 V	PMSU	07:28:45.41	-03:17:52.4	2MASS	12.3	0.4	HIP2
J07295+359	B.F	1RXS J072931.4+355607	M1.5 V+	Lep13	07:29:31.09	+35:56:00.4	2MASS	27.3	0.4	Cor16
J07307+481	B.f	GJ 275.2 A	M4.0 V+	PMSU	07:30:42.80	+48:11:59.9	2MASS	11.1	0.1	vAl95
J07310+460	..F	1RXS J073101.9+460030	M4.0 V	AF15	07:31:01.29	+46:00:26.6	2MASS	22.4	0.9	Cor16
J07319+362N		BL Lyn	M3.5 V	AF15	07:31:57.35	+36:13:47.8	2MASS	11.87	0.49	aHIP2
J07319+362S	B..	VV Lyn AB	M2.5 V+	AF15	07:31:57.74	+36:13:10.2	2MASS	11.87	0.49	HIP2
J07319+392	..F	G 111-009	M3.0 V	PMSU	07:31:56.52	+39:13:38.5	2MASS	22.6	0.6	Cor16
J07320+173E	..F	G 088-035	M3.0 V	PMSU	07:32:02.16	+17:19:12.5	2MASS	32.71	3.98	aHIP2
J07320+173W	..F	G 088-036	M0.0 V	Lep13	07:32:02.92	+17:19:10.3	2MASS	32.71	3.98	HIP2
J07320+686	..f	G 250-049	M1.0 V	PMSU	07:32:02.04	+68:37:15.7	2MASS	25.16	1.44	HIP2
J07325+248	..F	G 088-037	M3.0 V	Lep13	07:32:30.99	+24:53:40.9	2MASS	20.9	0.6	Cor16
J07342+009	..f	GJ 1099	M2.5 V	PMSU	07:34:17.58	+00:59:09.3	2MASS	14.6	0.6	vAl95
J07344+629	..F	G 234-005	M0.5 V	PMSU	07:34:27.49	+62:56:29.6	2MASS	11.47	0.3	HIP2
J07346+223	..F	LP 365-024	M1.0 V	PMSU	07:34:39.09	+22:20:15.6	2MASS	26.74	2.51	HIP2
J07346+318	B..	YY Gem CD	M1.0 V+	Stra09	07:34:37.46	+31:52:10.2	2MASS	15.6	0.9	aHIP2
J07349+147	B..	TYC 777-141-1	M3.0 V+	Lep13	07:34:56.33	+14:45:54.5	2MASS	9.5	0.3	Cor16
J07353+548		GJ 3452	M2.0 V	PMSU	07:35:21.88	+54:50:59.0	2MASS	12.8	0.4	HIP2
J07354+482	..F	NLTT 18099	M1.0 V	Lep13	07:35:26.80	+48:14:36.0	2MASS	30.0	0.4	Cor16
J07359+785	..F	LP 017-066	M3.0 V	AF15	07:35:58.15	+78:32:52.9	2MASS	23.2	0.6	Cor16
J07361-031		BD-02 2198	M1.0 V	AF15	07:36:07.08	-03:06:38.5	2MASS	14.2	0.1	aHIP2
J07364+070	B..	G 089-032 AB	M5.0 V+	PMSU	07:36:25.13	+07:04:43.2	2MASS	8.64	0.07	Hen06
J07365-006	..F	2MASS J07363027-0039351	M3.5 V	AF15	07:36:30.27	-00:39:35.2	2MASS	21.4	0.7	Cor16
J07366+440	..F	G 111-020	M3.5 V	AF15	07:36:39.28	+44:04:48.9	2MASS	27.4	0.9	Cor16

Table B.2: Names, spectral types, distances and astrometric parameters of Carmencita stars (continued).

Karmn	Flags[a]	Name	SpT	Ref.[b]	α (J2000)	δ (J2000)	Ref.[c]	d [pc]	ed [pc]	Ref.[d e]
J07383+344	..F	TYC 2461-826-1	M0.0 V	Lep13	07:38:19.93	+34:26:58.7	2MASS	31.58	3.29	HIP2
J07384+240	..F	LSPM J0738+2400	M3.5 V	Lep13	07:38:29.52	+24:00:08.8	2MASS	16.7	0.8	Dit14
J07386-212	.m.	LP 763-001	M3.0 V	PMSU	07:38:40.89	-21:13:27.6	2MASS	10.6	0.4	HIP2
J07393+021		BD+02 1729	M0.0 V	PMSU	07:39:23.04	+02:11:01.2	2MASS	14.68	0.31	HIP2
J07395+334	..F	G 090-016	M2.0 V	PMSU	07:39:35.81	+33:27:45.8	2MASS	35.66	3.96	HIP2
J07403-174	.mf	LP 783-002	M6.0 V	PMSU	07:40:19.22	-17:24:44.9	2MASS	9.1	0.1	aSub09
J07418+050	S.F	G 050-001	M2.5 V+	PMSU	07:41:52.82	+05:02:24.3	2MASS	23.6	0.5	Cor16
J07421+500	..F	NLTT 18279	M2.5 V	Lep13	07:42:09.68	+50:04:27.6	2MASS	19.2	0.4	Cor16
J07431+181	..F	BD+18 1719	M1.0 V	PMSU	07:43:11.75	+18:10:43.4	2MASS	30.82	2.63	HIP2
J07446+035		YZ CMi	M4.5 V	PMSU	07:44:40.18	+03:33:09.0	2MASS	5.96	0.08	HIP2
J07467+574	..F	G 193-065	M4.5 V	AF15	07:46:42.03	+57:26:53.4	2MASS	20.5	0.8	Dit14
J07470+760	..F	LP 017-075	M4.0 V	AF15	07:47:05.83	+76:03:19.6	2MASS	19.5	1.0	Dit14
J07472+503		2MASS J07471385+5020386	M4.0 V	Lep13	07:47:13.85	+50:20:38.5	2MASS	13.5	0.5	Cor16
J07482+203	..F	Wolf 1421	M1.0 V	PMSU	07:48:16.17	+20:22:07.4	2MASS	14.77	0.58	HIP2
J07493+849	..F	LP 004-258	M3.0 V	PMSU	07:49:19.64	+84:58:38.4	2MASS	20.9	0.6	Cor16
J07497-033	..F	2MASS J07494215-0320338	M3.5 V	AF15	07:49:42.16	-03:20:33.8	2MASS	16.7	0.6	Cor16
J07518+055	..F	G 050-006	M4.5 V	PMSU	07:51:51.38	+05:32:57.3	2MASS	15.9	0.8	vAl95
J07519-000	B..	GJ 1103 A	M4.5 V+	PMSU	07:51:54.65	-00:00:11.7	2MASS	8.8	0.2	vAl95
J07523+162	..F	LP 423-031	M6.0 V	AF15	07:52:23.90	+16:12:15.7	2MASS	18.4	0.3	GC09
J07525+063	..F	G 050-007	M3.0 V	PMSU	07:52:33.61	+06:18:25.5	2MASS	27.8	0.8	Cor16
J07545+085	S.F	LSPM J0754+0832	M2.5 V+	AF15	07:54:34.12	+08:32:25.3	2MASS	19.9	0.5	Cor16
J07545-096	..F	2MASS J07543272-0941478	M3.5 V	AF15	07:54:32.73	-09:41:47.8	2MASS	24.2	0.8	Cor16
J07558+833		GJ 1101	M4.5 V:	AF15	07:55:53.97	+83:23:05.0	2MASS	12.4	0.5	vAl95
J07581+072	..f	G 050-012	M4.0 V	PMSU	07:58:09.10	+07:17:01.5	2MASS	12.1	0.3	Dit14
J07582+413		GJ 1105	M3.5 V	PMSU	07:58:12.70	+41:18:13.5	2MASS	8.3	0.2	Dit14
J07583+496	..f	LP 163-047	M3.5 V	Lep13	07:58:22.73	+49:39:53.4	2MASS	13.8	0.5	Dit14
J07585+155N	..F	[RHG95] 1251	M3.5 V	PMSU	07:58:30.99	+15:30:14.7	2MASS	27.5	0.9	Cor16
J07585+155S	..F	[RHG95] 1252	M4.5 V	PMSU	07:58:30.46	+15:30:00.5	2MASS	22.6	1.0	Cor16
J07590+153	..F	LP 424-004	M1.5 V	PMSU	07:59:05.87	+15:23:29.5	2MASS	29.28	0.57	Wein16
J07591+173	..F	2MASS J07590718+1719474	M4.0 V	AF15	07:59:07.19	+17:19:47.4	2MASS	17.9	0.7	Cor16
J08005+258	..f	TYC 1930-667-1	M2.0 V	Lep13	08:00:34.71	+25:53:33.5	2MASS	19.7	0.4	Cor16
J08017+237	..f	TYC 1926-794-1	M1.5 V	Lep13	08:01:43.57	+23:42:27.1	2MASS	17.4	0.3	Cor16
J08023+033	..F	G 050-016 A	M4.0 V	PMSU	08:02:22.88	+03:20:19.6	2MASS	26.6	1.8	Dit14

Table B.2: Names, spectral types, distances and astrometric parameters of Carmencita stars (continued).

Karmn	Flags[a]	Name	SpT	Ref.[b]	α (J2000)	δ (J2000)	Ref.[c]	d [pc]	ed [pc]	Ref.[d e]
J08025-130	.mF	LP 724-016	M2.5 V	AF15	08:02:32.91	-13:05:29.1	2MASS	29.9	0.7	Cor16
J08031+203	B.F	2MASS J08031018+2022154AB	M3.5 V+	AF15	08:03:10.18	+20:22:15.5	2MASS	19.7	0.6	Cor16
J08033+528	B.f	G 194-007	M1.5 V+	Lep13	08:03:19.49	+52:50:38.7	2MASS	31.38	3.34	HIP2
J08066+558	B.f	LP 123-075	M2.0 V+	PMSU	08:06:36.46	+55:53:38.4	2MASS	30.1	2.5	HIP2
J08068+367	..F	G 090-044	M3.0 V	PMSU	08:06:48.42	+36:45:39.0	2MASS	20.8	0.6	Cor16
J08069+422	..F	G 111-056	M4.0 V	AF15	08:06:55.32	+42:17:33.4	2MASS	19.2	0.4	Dit14
J08082+211	S..	BD+21 1764B	M3.0 V+	AF15	08:08:13.59	+21:06:09.4	2MASS	16.64	0.54	aHIP2
J08083+585	..F	LP 089-101	M3.0 V	PMSU	08:08:18.19	+58:31:09.6	2MASS	19.2	0.5	Cor16
J08089+328	S..	GJ 1108 BC	M2.8 V+	Shk10	08:08:55.44	+32:49:05.1	2MASS	20.7	1.3	HIP1
J08095+219	..F	LP 366-045	M1.5 V	PMSU	08:09:30.99	+21:54:17.3	2MASS	22.29	1.67	HIP2
J08103+095	..F	2MASS J08102073+0935160	M2.5 V	Lep13	08:10:20.73	+09:35:16.0	2MASS	18.5	0.4	Cor16
J08105-138	Bm.	18 Pup B	M2.5 V+	AF15	08:10:34.29	-13:48:51.4	2MASS	22.4	0.2	aHIP2
J08108+039	..F	G 050-021	M3.5 V	PMSU	08:10:53.63	+03:58:33.6	2MASS	20.8	0.5	Dit14
J08117+531	..F	G 194-014	M2.5 V	AF15	08:11:47.60	+53:11:51.3	2MASS	34.7	1.7	Dit14
J08119+087		Ross 619	M4.5 V	PMSU	08:11:57.58	+08:46:22.1	2MASS	6.8	0.02	Wein16
J08126-215	.m.	GJ 300 AB	M4.0 V+	PMSU	08:12:40.88	-21:33:05.7	2MASS	5.9	0.5	vAl95
J08158+346	..F	LP 311-008	M1.0 V	Lep13	08:15:53.93	+31:36:39.2	2MASS	34.6	0.4	Cor16
J08161+013		GJ 2066	M2.0 V	AF15	08:16:07.98	+01:18:09.2	2MASS	9.1	0.1	HIP2
J08175+209	..F	LP 367-067	M2.5 V	Lep13	08:17:31.80	+20:59:52.4	2MASS	24.5	0.6	Cor16
J08178+311	..F	G 090-052	M1.0 V	PMSU	08:17:51.30	+31:07:45.6	2MASS	21.9	0.3	Cor16
J08202+055	..F	2MASS J08201336+0532082	M2.0 V	Lep13	08:20:13.37	+05:32:08.2	2MASS	22.8	0.4	Cor16
J08258+690	..F	LP 035-347	M5.5 V	PMSU	08:25:52.85	+69:02:01.6	2MASS	11.3	0.4	Dit14
J08282+201	..F	GJ 1110	M2.5 V	PMSU	08:28:12.69	+20:08:22.8	2MASS	22.1	1.6	vAl95
J08283+350	B.f	GJ 308	M0.0 V+	PMSU	08:28:22.13	+35:00:59.1	2MASS	19.68	2.43	HIP2
J08283+553	..F	2MASS J08281881+5522424	M2.5 V	AF15	08:28:18.81	+55:22:42.4	2MASS	27.4	0.6	Cor16
J08286+660	B.f	2MASS J08284121+6602239	M4.0 V+	AF15	08:28:41.22	+66:02:23.9	2MASS	15.8	0.6	Cor16
J08293+039		2MASS J08292191+0355092	M2.5 V	Lep13	08:29:21.92	+03:55:09.3	2MASS	15.1	0.3	Cor16
J08298+267		DX Cnc	M6.5 V	AF15	08:29:49.50	+26:46:34.8	2MASS	3.6	0.04	vAl95
J08313-060	B.F	LP 665-021	M1.5 V+	PMSU	08:31:21.63	-06:02:01.7	2MASS	26.35	1.87	HIP2
J08313-104	..F	LP 725-015	M4.0 V	PMSU	08:31:23.49	-10:29:53.5	2MASS	23.7	0.9	Cor16
J08314-060	..f	LP 665-022	M3.0 V	PMSU	08:31:27.23	-06:02:12.5	2MASS	26.35	1.87	aHIP2
J08315+730		LP 035-219	M4.0 V	Lep13	08:31:30.11	+73:03:45.9	2MASS	12.2	1.6	vAl95
J08316+193N	B..	CV Cnc	M4.0 V+	PMSU	08:31:37.44	+19:23:49.5	2MASS	11.1	1.0	aHIP2

Table B.2: Names, spectral types, distances and astrometric parameters of Carmencita stars (continued).

Karmn	Flags[a]	Name	SpT	Ref.[b]	α (J2000)	δ (J2000)	Ref.[c]	d [pc]	ed [pc]	Ref.[d e]
J08316+193S	E..	CU Cnc	M3.5 V+	PMSU	08:31:37.60	+19:23:39.6	2MASS	11.1	1.0	HIP2
J08317+057	..F	2MASS J08314794+0545186	M1.0 V	Lep13	08:31:47.94	+05:45:18.6	2MASS	34.3	0.4	Cor16
J08321+844	..F	LP 005-110	M3.5 V	PMSU	08:32:10.11	+84:24:31.0	2MASS	21.5	0.7	Cor16
J08325+451	..F	2MASS J08323599+4510175	M2.5 V	Lep13	08:32:35.99	+45:10:17.5	2MASS	23.3	0.5	Cor16
J08334+185	..F	NLTT 19754	M4.5 V	PMSU	08:33:25.13	+18:31:46.0	2MASS	19.7	0.9	Dit14
J08344-011	..F	LP 605-037	M3.5 V	PMSU	08:34:25.87	-01:08:39.2	2MASS	13.6	1.8	vAl95
J08353+141	..f	LSPM J0835+1408	M4.5 V	AF15	08:35:19.93	+14:08:33.4	2MASS	23.8	0.8	Dit14
J08358+680		G 234-037	M2.5 V	PMSU	08:35:49.16	+68:04:09.7	2MASS	12.9	0.7	vAl95
J08364+264	..F	LP 311-037	M2.0 V	Lep13	08:36:26.71	+26:28:19.5	2MASS	27.9	0.5	Cor16
J08364+672	B..	BD+67 552	M0.5 V+	Lep13	08:36:25.61	+67:17:41.9	2MASS	13.78	0.24	HIP2
J08371+151	..f	NLTT 19893	M2.5 V	PMSU	08:37:07.99	+15:07:47.6	2MASS	18.96	1.33	HIP2
J08375+035	..F	LSPM J0837+0333	M4.0 V	AF15	08:37:30.21	+03:33:45.8	2MASS	18.1	0.6	Dit14
J08387+516	..F	StKM 1-711	M1.5 V	Lep13	08:38:42.22	+51:41:33.9	2MASS	27.9	0.4	Cor16
J08398+089	..F	G 052-023	M2.0 V	PMSU	08:39:48.03	+08:56:18.0	2MASS	35.2	0.7	Cor16
J08402+314		LSPM J0840+3127	M3.5 V	Lep13	08:40:15.97	+31:27:06.8	2MASS	11.1	0.2	Dit14
J08404+184	..F	AZ Cnc	M6.0 V	PMSU	08:40:29.75	+18:24:09.2	2MASS	14.06	0.2	vAl95
J08410+676	..F	LP 060-100	M4.0 V	PMSU	08:41:03.86	+67:39:38.9	2MASS	23.4	1.2	Dit14
J08413+594	..f	LP 090-018	M5.5 V	PMSU	08:41:20.13	+59:29:50.6	2MASS	9.2	0.2	Dit14
J08427+095	B..	BD+10 1857 AB	M0.0 V+	Lep13	08:42:44.55	+09:33:24.1	2MASS	15.43	0.56	HIP2
J08428+095	..f	BD+10 1857 C	M2.5 V	PMSU	08:42:52.23	+09:33:11.2	2MASS	15.43	0.56	aHIP2
J08443-104	..F	LP 726-006	M3.5 V	PMSU	08:44:22.36	-10:24:11.1	2MASS	25.4	0.8	Cor16
J08447+182	..F	NLTT 20157	M3.5 V	Lep13	08:44:45.36	+18:13:07.2	2MASS	24.0	2.0	Dit14
J08449-066	B.F	2MASS J08445566-0637259AB	M3.5 V+	AF15	08:44:55.67	-06:37:25.9	2MASS	20.4	0.7	Cor16
J08517+181	..F	Ross 622	M1.5 V	PMSU	08:51:43.87	+18:07:29.9	2MASS	18.34	1.21	HIP2
J08526+283		ρ Cnc B	M4.5 V	AF15	08:52:40.85	+28:18:58.9	2MASS	11.4	0.3	Dit14
J08531-202	.mF	2MASS J08531090-2017172	M3.0 V	AF15	08:53:10.91	-20:17:17.3	2MASS	24.4	0.7	Cor16
J08536-034		LP 666-009	M9.0 V	Jen09	08:53:36.20	-03:29:32.1	2MASS	8.7	0.08	Wein16
J08537+149	..F	StKM 1-730	M0.0 V	Lep13	08:53:43.71	+14:58:11.2	2MASS	28.4	0.3	Cor16
J08540-131	Bm.	GJ 326 AB	M2.5 V+	PMSU	08:54:05.24	-13:07:30.1	2MASS	13.0	1.9	Jen52
J08551+015	..f	BD+02 2098	M0.0 V	Lep13	08:55:07.62	+01:32:47.3	2MASS	19.79	0.36	HIP2
J08555+664	..F	2MASS J08553135+6628078	M3.0 V	Lep13	08:55:31.36	+66:28:07.8	2MASS	19.4	0.5	Cor16
J08563+126	B.F	G 041-008	M4.5 V+	Sch05	08:56:19.56	+12:39:50.1	2MASS	15.3	0.7	Cor16
J08570+116	B..	BD+12 1944 AB	M1.0 V+	PMSU	08:57:04.68	+11:38:49.1	2MASS	17.01	0.79	HIP2

Table B.2: Names, spectral types, distances and astrometric parameters of Carmencita stars (continued).

Karmn	Flags[a]	Name	SpT	Ref.[b]	α (J2000)	δ (J2000)	Ref.[c]	d [pc]	ed [pc]	Ref.[d e]
J08572+194	..F	LP 426-035	M3.5 V	AF15	08:57:15.41	+19:24:17.8	2MASS	35.1	4.2	Dit14
J08582+197	B..	EI Cnc AB	M5.5 V+	PMSU	08:58:15.19	+19:45:47.1	2MASS	5.7	0.1	Dit14
J08589+084	B..	NLTT 20670	M3.5 V+	PMSU	08:58:56.33	+08:28:25.9	2MASS	6.8	0.1	Hen06
J08595+537	B.F	G 194-047	M3.5 V+	AF15	08:59:35.93	+53:43:50.5	2MASS	17.2	0.6	Dit14
J08599+729	..F	LP 036-098	M4.0 V	PMSU	08:59:56.05	+72:57:36.5	2MASS	13.6	0.5	Dit14
J09003+218		LP 368-128	M6.5 V	AF15	09:00:23.59	+21:50:05.4	2MASS	6.37	0.11	DL12
J09005+465		GJ 1119	M4.5 V	PMSU	09:00:32.54	+46:35:11.8	2MASS	9.9	0.2	Dit14
J09008+052E	..F	Ross 687	M3.5 V	PMSU	09:00:50.33	+05:14:29.4	2MASS	20.96	3.49	bHIP2
J09008+052W	..f	Ross 686	M3.0 V	PMSU	09:00:48.53	+05:14:41.3	2MASS	20.96	3.49	bHIP2
J09011+019	S..	Ross 625	M3.0 V+	PMSU	09:01:10.49	+01:56:35.0	2MASS	12.8	0.4	Cor16
J09023+084	..f	NLTT 20817	M2.5 V	PMSU	09:02:19.88	+08:28:06.4	2MASS	19.5	1.4	HIP2
J09023+177	..F	2MASS J09022307+1746326	M4.0 V	AF15	09:02:23.08	+17:46:32.6	2MASS	19.5	0.8	Cor16
J09028+680		LP 060-179	M4.0 V	PMSU	09:02:52.85	+68:03:46.4	2MASS	11.5	0.5	Dit14
J09033+056	..f	NLTT 20861	M7.0 V	New14	09:03:20.96	+05:40:14.5	2MASS	16.0	0.0	New14
J09037+520	..F	G 194-052	M3.5 V	Lep13	09:03:42.95	+52:02:52.7	2MASS	17.0	0.5	Dit14
J09038+129	..F	LP 486-043	M2.0 V	Lep13	09:03:53.39	+12:59:28.2	2MASS	27.3	0.5	Cor16
J09040-159	.mF	2MASS J09040555-1555184	M2.5 V	AF15	09:04:05.55	-15:55:18.4	2MASS	26.5	0.6	Cor16
J09050+028	..F	LP 546-48	M1.5 V	PMSU	09:05:04.43	+02:50:03.1	2MASS	22.0	0.3	Cor16
J09057+186	..F	LP 426-056	M2.5 V	Lep13	09:05:42.96	+18:36:34.0	2MASS	24.1	0.6	Cor16
J09062+128	..F	LP 486-049	M3.5 V	PMSU	09:06:14.08	+12:51:34.8	2MASS	19.7	0.7	Cor16
J09070-221	.mF	LP 845-023	M4.5 V	PMSU	09:07:02.78	-22:08:49.4	2MASS	14.9	0.7	Cor16
J09087+665	..F	G 234-056	M2.5 V	PMSU	09:08:46.06	+66:35:38.4	2MASS	26.6	0.6	Cor16
J09091+227	..F	J0909+2247	M4.5 V	AF15	09:09:07.99	+22:47:41.3	2MASS	23.0	1.0	Cor16
J09093+401	..F	GJ 1121	M4.0 V	PMSU	09:09:23.91	+40:06:05.9	2MASS	21.9	1.6	vAl95
J09095+328	B.f	BD+33 1814 AB	M0.5 V+	Lep13	09:09:30.61	+32:49:09.2	2MASS	20.43	0.82	HIP2
J09096+067	..F	2E 2104	M3.0 V	PMSU	09:09:39.17	+06:42:10.9	2MASS	24.0	0.7	Cor16
J09099+004	..F	G 046-024	M1.0 V	Lep13	09:09:59.06	+00:23:45.2	2MASS	34.0	0.4	Cor16
J09115+126	..F	LP 487-010	M2.5 V	AF15	09:11:31.95	+12:37:23.7	2MASS	29.7	0.7	Cor16
J09115+466	..F	MCC 265	M0.5 V	PMSU	09:11:30.85	+46:37:01.4	2MASS	24.73	1.48	HIP2
J09120+279	S..	G 047-028	M3.0 V+	PMSU	09:12:02.72	+27:54:24.2	2MASS	27.8	7.5	vAl95
J09133+688		G 234-057	M2.5 V	Lep13	09:13:23.83	+68:52:30.5	2MASS	14.0	0.3	Cor16
J09140+196		LP 427-016	M3.0 V	Lep13	09:14:03.21	+19:40:06.0	2MASS	16.1	0.4	Cor16
J09143+526	S..	HD 79210	M0.0 V+	AF15	09:14:22.98	+52:41:12.5	2MASS	5.81	0.21	HIP2

Table B.2: Names, spectral types, distances and astrometric parameters of Carmencita stars (continued).

Karmn	Flags[a]	Name	SpT	Ref.[b]	α (J2000)	δ (J2000)	Ref.[c]	d [pc]	ed [pc]	Ref.[d e]
J09144+526		HD 79211	M0.0 V	AF15	09:14:24.86	+52:41:11.8	2MASS	5.81	0.21	aHIP2
J09156-105	B..	G 161-007	M5.0 V+	AF15	09:15:36.43	-10:35:47.0	2MASS	7.7	0.4	Cor16
J09160+293	..F	G 047-031	M2.0 V	Lep13	09:16:05.21	+29:19:45.2	2MASS	40.3	2.9	Dit14
J09161+018		RX J0916.1+0153	M4.0 V	Lep13	09:16:10.19	+01:53:08.8	2MASS	13.0	0.5	Cor16
J09163-186	.m.	LP 787-052	M1.5 V	PMSU	09:16:20.66	-18:37:32.9	2MASS	15.0	0.2	Cor16
J09165+841	..F	G 253-021	M1.5 V	PMSU	09:16:30.12	+84:10:59.9	2MASS	25.97	6.21	vAl95
J09168+248	..F	2MASS J09165078+2448559	M4.5 V	Rei07	09:16:50.78	+24:48:55.9	2MASS	23.0	1.0	Cor16
J09177+462	B.f	RX J0917.7+4612	M2.5 V+	Lep13	09:17:44.73	+46:12:24.7	2MASS	16.5	0.4	Cor16
J09177+584	..F	LP 090-134	M4.5 V	PMSU	09:17:46.00	+58:25:22.4	2MASS	15.53	0.96	vAl95
J09187+267	..F	G 047-033 A	M1.5 V	PMSU	09:18:46.24	+26:45:11.4	2MASS	23.2	0.4	Cor16
J09193+385N	..F	GJ 1122 B	M4.0 V	PMSU	09:19:19.04	+38:31:23.3	2MASS	16.7	0.7	Dit14
J09193+385S	..F	GJ 1122 A	M4.0 V	PMSU	09:19:18.95	+38:31:15.9	2MASS	16.7	0.8	Dit14
J09193+620	S.F	LP 091-014 AB	M0.0 V+	Shk10	09:19:22.92	+62:03:17.1	2MASS	34.76	2.72	HIP2
J09200+308	..F	RX J0920.0+3052	M1.5 V	Lep13	09:20:00.49	+30:52:39.7	2MASS	23.4	0.4	Cor16
J09201+037	..F	1RXS J092010.8+034731	M3.5 V	AF15	09:20:10.87	+03:47:25.8	2MASS	20.3	0.7	Cor16
J09209+033	..F	NLTT 21531	M3.5 V	PMSU	09:20:57.94	+03:22:06.4	2MASS	18.6	0.7	Dit14
J09213+731	..F	LP 036-181	M4.5 V	PMSU	09:21:19.55	+73:06:38.7	2MASS	11.2	0.4	Dit14
J09218+435	B..	G 115-071 AB	M4.5 V+	Law08	09:21:49.11	+43:30:28.5	2MASS	21.6	0.8	Dit14
J09218-023	..F	RAVE J092148.1-021943	M2.5 V	AF15	09:21:48.13	-02:19:43.4	2MASS	19.0	0.4	Cor16
J09228+467	..F	G 115-072	M1.0 V	Lep13	09:22:51.66	+46:47:00.8	2MASS	28.8	0.4	Cor16
J09231+223	..F	BD+22 2086B	M0.0 V	Lep13	09:23:06.16	+22:18:28.3	2MASS	36.04	3.02	aHIP2
J09238+001	..F	LP 607-039	M1.0 V	Lep13	09:23:52.56	+00:08:17.8	2MASS	27.17	1.84	HIP2
J09248+306	..F	LSPM J0924+3041	M3.5 V	AF15	09:24:50.83	+30:41:37.3	2MASS	28.3	1.0	Dit14
J09256+634	B.F	G 235-025	M4.5 V+	AF15	09:25:40.33	+63:29:19.7	2MASS	18.8	0.9	Dit14
J09275+506	..F	G 195-027	M1.5 V	PMSU	09:27:30.58	+50:39:12.8	2MASS	31.91	3.14	HIP2
J09288-073	..F	Ross 439	M2.5 V	PMSU	09:28:53.34	-07:22:14.8	2MASS	16.24	1.05	HIP2
J09289-073	..F	GJ 347 B	M4.5 V	PMSU	09:28:55.72	-07:22:11.1	2MASS	16.24	1.05	aHIP2
J09291+259	..F	NLTT 21866	M5.0 V	Law08	09:29:11.14	+25:58:09.6	2MASS	17.7	0.3	GC09
J09300+396	..F	LP 211-012	M2.5 V	PMSU	09:30:01.67	+39:37:24.0	2MASS	19.3	0.4	Cor16
J09302+265	..F	RX J0930.2+2630 1	M3.5 V	Lep13	09:30:14.45	+26:30:25.0	2MASS	23.5	0.6	Dit14
J09307+003		GJ 1125	M3.5 V	PMSU	09:30:44.58	+00:19:21.4	2MASS	9.7	0.4	HIP2
J09308+024	..F	1RXS J093051.2+0222741	M4.0 V	AF15	09:30:50.85	+02:27:20.2	2MASS	17.5	0.7	Cor16
J09313-134	Bm.	Ross 440	M3.0 V+	PMSU	09:31:19.37	-13:29:19.3	2MASS	10.0	0.4	HIP2

Table B.2: Names, spectral types, distances and astrometric parameters of Carmencita stars (continued).

Karmn	Flags[a]	Name	SpT	Ref.[b]	α (J2000)	δ (J2000)	Ref.[c]	d [pc]	ed [pc]	Ref.[d e]
J09315+202	..F	Ross 84	M2.0 V	PMSU	09:31:33.01	+20:16:58.1	2MASS	20.2	6.1	vAl95
J09319+363	..f	BD+36 1970	M0.0 V	PMSU	09:31:56.33	+36:19:12.9	2MASS	13.91	0.35	HIP2
J09328+269	..F	DX Leo B	M5.5 V	AF15	09:32:48.27	+26:59:44.3	2MASS	17.1	0.7	Dit14
J09352+612	..F	StKM 1-785	M2.0 V	PMSU	09:35:13.19	+61:14:37.0	2MASS	22.2	0.4	Cor16
J09360-061	..F	G 161-051	M3.5 V	PMSU	09:36:04.87	-06:06:55.8	2MASS	26.1	0.9	Cor16
J09360-216	.m.	GJ 357	M2.5 V	PMSU	09:36:01.61	-21:39:37.1	2MASS	9.02	0.16	HIP2
J09362+375	..F	TYC 2992-428-1	M0.0 V	AF15	09:36:15.93	+37:31:45.7	2MASS	38.65	1.45	aHIP2
J09370+405	..F	LP 211-022	M4.0 V	PMSU	09:37:03.55	+40:34:38.9	2MASS	19.3	0.4	Dit14
J09394+146	..F	NLTT 22280	M3.5 V	AF15	09:39:29.94	+14:38:49.8	2MASS	21.1	0.7	Cor16
J09394+317	..F	G 117-034	M1.5 V	Lep13	09:39:24.31	+31:45:17.3	2MASS	24.01	2.18	HIP2
J09410+220	..F	Ross 92	M4.5 V	PMSU	09:41:01.99	+22:01:29.2	2MASS	12.7	0.6	Jen09
J09411+132		Ross 85	M1.5 V	PMSU	09:41:10.33	+13:12:34.4	2MASS	11.26	0.21	HIP2
J09423+559		GJ 363	M3.5 V	PMSU	09:42:23.28	+55:59:01.6	2MASS	17.1	0.9	Dit14
J09425+700		GJ 360	M2.0 V	PMSU	09:42:34.94	+70:02:02.4	2MASS	12.28	0.27	HIP2
J09425-192	.mf	LP 788-024	M2.5 V	PMSU	09:42:35.73	-19:14:04.6	2MASS	15.7	0.9	HIP2
J09428+700		GJ 362	M3.0 V	PMSU	09:42:51.82	+70:02:22.2	2MASS	12.28	0.27	aHIP2
J09430+237	..F	LP 370-035	M1.0 V	Lep13	09:43:01.33	+23:49:22.2	2MASS	35.6	0.5	Cor16
J09439+269		Ross 93	M3.5 V	PMSU	09:43:55.63	+26:58:08.6	2MASS	14.02	0.88	HIP2
J09447-182	.m.	GJ 1129	M4.0 V	PMSU	09:44:47.31	-18:12:48.9	2MASS	10.97	0.08	Wein16
J09449-123		G 161-071	M5.0 V	AF15	09:44:54.22	-12:20:54.4	2MASS	13.26	0.15	Wein16
J09461-044	B.F	G 161-074	M4.0 V+	PMSU	09:46:09.29	-04:25:43.0	2MASS	19.9	0.8	Cor16
J09468+760		BD+76 3952	M1.5 V	PMSU	09:46:48.45	+76:02:38.8	2MASS	16.21	0.37	HIP2
J09473+263	..F	BD+26 2004	M0.0 V	Lep13	09:47:22.42	+26:18:12.8	2MASS	32.31	2.64	HIP2
J09475+129	..f	LP 488-037	M4.0 V	PMSU	09:47:34.81	+12:56:39.1	2MASS	20.3	1.2	Dit14
J09488+156	..F	G 043-002	M3.0 V	AF15	09:48:50.20	+15:38:44.9	2MASS	24.1	0.7	Cor16
J09506-138		LP 728-070	M4.0 V	Sch05	09:50:40.54	-13:48:38.6	2MASS	11.9	0.5	Cor16
J09511-123		BD-11 2741	M0.5 V	PMSU	09:51:09.64	-12:19:47.8	2MASS	13.71	0.34	HIP2
J09526-156	.mF	LP 728-071	M3.5 V	AF15	09:52:41.77	-15:36:13.8	2MASS	20.4	0.7	Cor16
J09527+554	..F	G 195-043	M1.5 V	Lep13	09:52:44.68	+55:28:19.4	2MASS	31.9	0.6	Cor16
J09531-036	S..	GJ 372	M2.0 V+	PMSU	09:53:11.78	-03:41:24.0	2MASS	16.01	0.54	HIP2
J09535+507	..F	LP 126-073	M1.5 V	Lep13	09:53:33.53	+50:45:03.8	2MASS	26.3	2.53	HIP2
J09539+209	..f	NLTT 22870	M4.5 V	PMSU	09:53:55.23	+20:56:46.0	2MASS	9.6	0.2	Dit14
J09557+353	..F	G 116-065	M3.0 V	PMSU	09:55:43.61	+35:21:42.2	2MASS	19.6	0.6	Cor16

Table B.2: Names, spectral types, distances and astrometric parameters of Carmencita stars (continued).

Karmn	Flags[a]	Name	SpT	Ref.[b]	α (J2000)	δ (J2000)	Ref.[c]	d [pc]	ed [pc]	Ref.[d e]
J09561+627		BD+63 869	M0.0 V	PMSU	09:56:08.69	+62:47:18.6	2MASS	10.56	0.14	HIP2
J09564+226	..F	NLTT 22978	M4.0 V	PMSU	09:56:27.00	+22:39:01.5	2MASS	19.2	0.8	Cor16
J09579+118	..F	NLTT 23051	M4.0 V	PMSU	09:57:57.99	+11:48:28.8	2MASS	23.9	0.9	Cor16
J09587+555	..F	G 196-001	M1.0 V	Lep13	09:58:46.69	+55:33:02.6	2MASS	34.1	0.4	Cor16
J09589+059	..F	NLTT 23096	M4.5 V	AF15	09:58:56.51	+05:58:00.1	2MASS	14.7	0.5	Dit14
J09593+438E	V.F	G 116-073 B	M4.0 V	PMSU	09:59:20.94	+43:50:25.9	2MASS	24.9	1.1	aDit14
J09593+438W	V.F	G 116-072 A	M3.5 V	PMSU	09:59:18.80	+43:50:25.6	2MASS	24.9	1.1	Dit14
J09597+472	..F	G 146-005	M4.0 V	PMSU	09:59:45.96	+47:12:11.5	2MASS	21.4	0.8	Dit14
J09597+721	..F	Pul -3 620285	M3.5 V	AF15	09:59:45.35	+72:11:59.8	2MASS	18.1	0.6	Cor16
J10004+272	..F	GJ 375.2	M0.5 V	Lep13	10:00:26.71	+27:16:01.4	2MASS	34.67	2.45	HIP2
J10007+323	..F	Wolf 335	M1.0 V	Lep13	10:00:44.42	+32:18:35.0	2MASS	26.77	2.21	HIP2
J10020+697	..F	LP 037-057	M4.0 V	AF15	10:02:05.81	+69:45:29.4	2MASS	14.4	0.4	Dit14
J10023+480		BD+48 1829	M1.0 V	PMSU	10:02:21.84	+48:05:20.9	2MASS	15.1	0.37	HIP2
J10027+149	..F	G 043-023	M4.0 V	PMSU	10:02:42.47	+14:59:12.8	2MASS	12.9	0.6	Dit14
J10028+484	B.F	G 195-055	M5.5 V+	AF15	10:02:49.36	+48:27:33.4	2MASS	16.6	0.6	Dit14
J10035+059	..F	NLTT 23292	M3.5 V	PMSU	10:03:33.37	+05:57:48.1	2MASS	20.1	0.7	Cor16
J10040+187	..F	TYC 1415-1123-1	M0.5 V	Lep13	10:04:05.99	+18:47:45.5	2MASS	41.79	4.37	HIP2
J10043+503	..f	G 196-003A	M2.5 V	Lep13	10:04:21.49	+50:23:13.6	2MASS	16.1	0.4	Cor16
J10067+417	..F	G 116-077	M0.5 V	PMSU	10:06:43.86	+41:42:53.4	2MASS	20.66	1.17	HIP2
J10068-127	..F	2MASS J10065210-1246543	M4.5 V	AF15	10:06:52.11	-12:46:54.3	2MASS	16.5	0.8	Cor16
J10069+126	..F	LP 489-035	M1.5 V	Lep13	10:06:57.83	+12:40:52.3	2MASS	29.0	0.5	Cor16
J10079+692	..F	LP 037-075	M4.0 V	PMSU	10:07:59.50	+69:14:45.8	2MASS	17.79	1.27	vAl95
J10087+027	..f	LP 549-023	M3.0 V	Lep13	10:08:44.61	+02:43:56.8	2MASS	17.4	0.5	Cor16
J10094+512	..f	LP 127-132	M4.0 V	PMSU	10:09:29.97	+51:17:19.8	2MASS	13.3	0.6	vAl95
J10094+544	..F	2MASS J10092678+5424247	M2.0 V	Lep13	10:09:26.78	+54:24:24.7	2MASS	24.1	0.5	Cor16
J10117+353	..F	G 118-037	M4.0 V	PMSU	10:11:43.93	+35:18:44.7	2MASS	17.6	0.6	Dit14
J10120-026	B..	GJ 381 AB	M2.5 V+	AF15	10:12:04.66	-02:41:04.5	2MASS	12.3	0.4	HIP2
J10122-037		AN Sex	M1.5 V	PMSU	10:12:17.69	-03:44:44.1	2MASS	7.87	0.12	HIP2
J10125+570		LP 092-048	M3.5 V	Lep13	10:12:34.81	+57:03:49.6	2MASS	9.9	0.3	Cor16
J10130+233	..F	G 054-018	M3.5 V	AF15	10:13:00.26	+23:20:50.5	2MASS	19.2	0.6	Cor16
J10133+467	..F	LP 167-017	M5.5 V	PMSU	10:13:20.98	+46:47:26.0	2MASS	17.6	0.9	Dit14
J10143+210	B.f	DK Leo	M0.5 V+	Lep13	10:14:19.19	+21:04:29.8	2MASS	23.08	0.96	HIP2
J10148+213	..F	G 054-019	M4.5 V	AF15	10:14:53.15	+21:23:46.4	2MASS	18.6	0.7	Dit14

Table B.2: Names, spectral types, distances and astrometric parameters of Carmencita stars (continued).

Karmn	Flags[a]	Name	SpT	Ref.[b]	α (J2000)	δ (J2000)	Ref.[c]	d [pc]	ed [pc]	Ref.[d e]
J10151+314	B.F	G 118-043	M4.0 V+	PMSU	10:15:06.91	+31:25:11.0	2MASS	16.8	0.7	Cor16
J10155-164	.mF	WT 1774	M4.0 V	AF15	10:15:35.40	-16:28:23.6	2MASS	17.1	0.7	Cor16
J10158+174	..f	LSPM J1015+1729	M3.5 V	Lep13	10:15:53.90	+17:29:27.2	2MASS	15.3	0.5	Cor16
J10167-119		GJ 386	M3.0 V	PMSU	10:16:46.00	-11:57:41.3	2MASS	13.6	0.5	HIP2
J10182-204	.m.	NLTT 23956	M4.5 V	Ria06	10:18:13.88	-20:28:41.4	2MASS	11.7	0.5	Cor16
J10185-117	..f	LP 729-054	M4.0 V	Sch05	10:18:35.17	-11:42:59.9	2MASS	14.5	0.6	Cor16
J10196+198	B..	BD+20 2465	M3.0 V+	AF15	10:19:36.35	+19:52:12.2	2MASS	4.89	0.07	vAl95
J10200+289	..F	G 118-051	M3.0 V	AF15	10:20:00.88	+28:57:13.1	2MASS	22.6	0.6	Cor16
J10206+492	..F	G 196-019	M2.5 V	PMSU	10:20:37.79	+49:17:45.4	2MASS	29.6	0.7	Cor16
J10238+438	..F	LP 212-062	M5.0 V	AF15	10:23:51.85	+43:53:33.2	2MASS	15.6	0.8	Dit14
J10240+366	..F	HAT 182-00646	M3.5 V	AF15	10:24:05.07	+36:39:32.6	2MASS	21.4	0.7	Cor16
J10243+119	..F	StKM 1-852	M2.0 V	PMSU	10:24:20.17	+11:57:20.7	2MASS	26.4	0.5	Cor16
J10251-102		BD-09 3070	M1.0 V	PMSU	10:25:10.88	-10:13:43.4	2MASS	12.35	0.29	HIP2
J10255+263	..F	G 054-026	M3.5 V	PMSU	10:25:30.35	+26:23:18.5	2MASS	17.8	0.6	Cor16
J10260+504E	..F	LP 127-372	M4.0 V	PMSU	10:26:03.32	+50:27:22.0	2MASS	17.4	0.7	Cor16
J10260+504W	..f	LP 127-371	M4.0 V	PMSU	10:26:02.66	+50:27:09.1	2MASS	16.4	0.6	Cor16
J10273+799	..F	2MASS J10272334+7959511	M2.0 V	Lep13	10:27:23.34	+79:59:51.1	2MASS	24.4	0.5	Cor16
J10278+028	..F	G 055-021	M3.5 V	AF15	10:27:49.67	+02:51:36.9	2MASS	21.5	0.7	Cor16
J10284+482	..F	G 146-035	M3.5 V	PMSU	10:28:27.81	+48:14:20.0	2MASS	20.96	0.97	vAl95
J10286+322	..F	G 118-061	M2.5 V	PMSU	10:28:41.37	+32:14:19.2	2MASS	25.1	0.6	Cor16
J10289+008		BD+01 2447	M2.0 V	PMSU	10:28:55.55	+00:50:27.5	2MASS	7.1	0.1	HIP2
J10303+328	..F	G 118-066	M3.5 V	PMSU	10:30:23.70	+32:50:13.5	2MASS	16.5	0.6	Cor16
J10315+570	..F	BD+57 1274 B	M4.5 V	PMSU	10:31:30.76	+57:05:18.0	2MASS	17.9	0.4	aHIP2
J10320+033	..F	2MASS J10320226+0318547	M2.0 V	Lep13	10:32:02.27	+03:18:54.8	2MASS	21.2	0.4	Cor16
J10345+463	..F	LP 167-064	M3.0 V	PMSU	10:34:30.21	+46:18:09.0	2MASS	20.4	0.7	Dit14
J10350-094		LP 670-017	M3.0 V	Sch05	10:35:01.11	-09:24:38.5	2MASS	15.0	0.4	Cor16
J10354+694		LP 037-179	M3.5 V	PMSU	10:35:27.26	+69:26:59.5	2MASS	13.2	0.7	vAl95
J10359+288	..F	RX J1035.9+2853	M3.0 V	AF15	10:35:57.25	+28:53:31.7	2MASS	23.5	0.7	Cor16
J10360+051		RY Sex	M3.5 V	PMSU	10:36:01.21	+05:07:12.8	2MASS	14.5	1.3	vAl95
J10364+415	..F	G 146-048	M2.5 V	Lep13	10:36:26.83	+41:30:06.5	2MASS	20.9	0.5	Cor16
J10367+153	B..	RX J1036.7+1521	M3.5 V+	Dae07	10:36:44.84	+15:21:39.5	2MASS	10.4	0.5	Cor16
J10368+509	..F	LP 127-502	M4.5 V	AF15	10:36:48.12	+50:55:04.1	2MASS	20.0	0.5	Dit14
J10379+127	B.f	LP 490-042	M3.0 V+	Lep13	10:37:55.28	+12:46:36.9	2MASS	18.5	0.5	Cor16

Table B.2: Names, spectral types, distances and astrometric parameters of Carmencita stars (continued).

Karmn	Flags[a]	Name	SpT	Ref.[b]	α (J2000)	δ (J2000)	Ref.[c]	d [pc]	ed [pc]	Ref.[d e]
J10384+485	..F	LP 167-071	M3.0 V	PMSU	10:38:29.81	+48:31:44.9	2MASS	26.4	0.7	Cor16
J10385+354	..F	LP 262-400	M2.5 V	Lep13	10:38:33.23	+35:29:49.2	2MASS	21.2	0.5	Cor16
J10389+250	..F	StKM 1-873	M2.0 V	Lep13	10:38:56.86	+25:05:40.3	2MASS	28.1	0.5	Cor16
J10396-069		GJ 399	M2.5 V	PMSU	10:39:40.61	-06:55:25.6	2MASS	16.4	0.8	HIP2
J10403+015	..F	TYC 254-88-1	M1.0 V	Lep13	10:40:21.47	+01:34:37.3	2MASS	32.4	0.4	Cor16
J10416+376		GJ 1134	M4.5 V	PMSU	10:41:38.10	+37:36:39.8	2MASS	10.3	0.2	vAl95
J10430-092	B.f	WT 1827 AB	M5.5 V+	AF15	10:43:02.93	-09:12:41.1	2MASS	12.3	0.4	Jao05
J10443+124	..F	LP 490-063	M3.5 V	AF15	10:44:18.82	+12:25:11.7	2MASS	26.9	1.4	Dit14
J10448+324	B.F	LP 316-604 A	M3.0 V+	PMSU	10:44:52.70	+32:24:41.2	2MASS	39.1	5.6	Dit14
J10453+385	B..	BD+39 2376	M0.5 V+	Lep13	10:45:21.48	+38:30:42.2	2MASS	13.91	0.32	HIP2
J10456-191	.mF	BD-18 3019	M0.5 V	PMSU	10:45:39.31	-19:06:50.9	2MASS	20.02	0.91	aHIP2
J10460+096	..F	G 044-035	M3.5 V	PMSU	10:46:03.92	+09:41:51.4	2MASS	21.5	0.7	Cor16
J10472+404	B.F	LP 213-067	M8.0 V+	Clo03	10:47:12.65	+40:26:43.7	2MASS	16.3	3.0	bRei02
J10474+025	B.f	Ross 895	M2.0 V+	Lep13	10:47:24.30	+02:35:32.1	2MASS	41.96	13.68	HIP2
J10482-113		LP 731-058	M6.5 V	AF15	10:48:12.58	-11:20:08.2	2MASS	4.58	0.01	Wein16
J10485+191	..F	LP 431-069	M3.0 V	PMSU	10:48:32.56	+19:09:02.3	2MASS	26.3	0.7	Cor16
J10497+355	B..	GJ 1138 AB	M4.5 V+	PMSU	10:49:45.61	+35:32:51.5	2MASS	9.7	0.3	vAl95
J10504+331		G 119-037	M4.0 V	PMSU	10:50:26.00	+33:06:05.2	2MASS	22.9	1.5	vAl95
J10506+517	..F	LP 128-032	M3.5 V	PMSU	10:50:38.25	+51:45:01.6	2MASS	20.6	0.6	Dit14
J10508+068		EE Leo	M4.0 V	AF15	10:50:52.01	+06:48:29.3	2MASS	6.94	0.04	Wein16
J10513+361	B.F	LP 263-035	M3.0 V+	PMSU	10:51:20.60	+36:07:25.6	2MASS	32.3	2.4	Dit14
J10520+005	S..	G 045-011 ABC	M4.3 V+	Shk10	10:52:03.27	+00:32:38.3	2MASS	15.5	0.7	Cor16
J10520+139	..f	GJ 403	M3.5 V	PMSU	10:52:04.41	+13:59:51.0	2MASS	13.7	0.5	Dit14
J10522+059	..F	NLTT 25568	M5.0 V	PMSU	10:52:14.23	+05:55:09.9	2MASS	11.6	0.3	Dit14
J10546-073	B..	LP 671-008	M4.0 V+	AF15	10:54:41.98	-07:18:32.7	2MASS	13.7	0.5	Cor16
J10555-093	..F	LP 671-010	M3.5 V	PMSU	10:55:34.49	-09:21:26.3	2MASS	18.6	0.5	Ried10
J10563+042	..F	2MASS J10562225+0415459	M2.5 V	AF15	10:56:22.25	+04:15:45.9	2MASS	26.7	0.6	Cor16
J10564+070		CN Leo	M6.0 V	AF15	10:56:28.86	+07:00:52.8	2MASS	2.42	0.01	Wein16
J10576+695	..F	BD+70 639	M0.0 V	Lep13	10:57:38.19	+69:35:47.9	2MASS	22.82	0.82	HIP2
J10584-107	..f	LP 731-076	M5.0 V	AF15	10:58:28.00	-10:46:30.5	2MASS	11.7	0.6	Cor16
J11000+228		Ross 104	M2.5 V	PMSU	11:00:04.32	+22:49:59.3	2MASS	6.66	0.08	HIP2
J11003+728	..F	LP 037-257	M2.0 V	Lep13	11:00:23.81	+72:52:24.5	2MASS	27.5	0.5	Cor16
J11008+120	..F	2E 2371	M5.0 V	PMSU	11:00:50.43	+12:04:10.8	2MASS	19.6	1.3	Dit14

Table B.2: Names, spectral types, distances and astrometric parameters of Carmencita stars (continued).

Karmn	Flags[a]	Name	SpT	Ref.[b]	α (J2000)	δ (J2000)	Ref.[c]	d [pc]	ed [pc]	Ref.[d e]
J11013+030	..F	G 045-027	M4.0 V	PMSU	11:01:19.66	+03:00:17.2	2MASS	13.9	0.6	vAl95
J11014+568	..F	StKM 1-902	M1.0 V	Lep13	11:01:27.11	+56:52:04.3	2MASS	35.6	0.5	Cor16
J11023+165E	..F	LP 431-071	M1.0 V	PMSU	11:02:19.31	+16:30:29.6	2MASS	41.29	20.25	HIP2
J11023+165W	..F	LP 431-070	M1.0 V	PMSU	11:02:18.04	+16:30:33.4	2MASS	41.29	20.25	aHIP2
J11026+219		DS Leo	M2.0 V	Mon01	11:02:38.33	+21:58:01.7	2MASS	11.77	0.15	HIP2
J11030+037	..F	Wolf 360	M2.5 V	AF15	11:03:04.27	+03:44:22.6	2MASS	28.4	0.7	Cor16
J11031+152	..F	LP 431-050	M3.5 V	Lep13	11:03:08.46	+15:17:51.8	2MASS	16.7	0.6	Cor16
J11031+366	..F	LP 263-064	M3.5 V	PMSU	11:03:10.00	+36:39:08.5	2MASS	24.0	0.9	Dit14
J11033+359		Lalande 21185	M1.5 V	AF15	11:03:20.24	+35:58:11.8	2MASS	2.547	0.004	HIP2
J11036+136	S..	LP 491-051	M4.0 V+	Lep13	11:03:21.25	+13:37:57.1	2MASS	16.8	1.1	Dit14
J11042+400	..F	LP 214-026	M0.0 V	Lep13	11:04:15.91	+40:00:16.6	2MASS	28.92	1.78	HIP2
J11054+435		BD+44 2051A	M1.0 V	AF15	11:05:29.03	+43:31:35.7	2MASS	4.85	0.02	HIP2
J11055+435		WX UMa	M5.5 V	AF15	11:05:31.33	+43:31:17.1	2MASS	4.85	0.02	aHIP2
J11055+450	..F	G 176-008	M0.0 V	PMSU	11:05:33.68	+45:00:31.7	2MASS	31.74	2.31	HIP2
J11057+102	..F	LP 491-060	M2.5 V	PMSU	11:05:43.16	+10:14:09.3	2MASS	19.6	1.8	HIP2
J11075+437	..F	HAT 141-00828	M3.0 V	AF15	11:07:32.08	+43:45:56.4	2MASS	32.4	0.9	Cor16
J11081-052	..f	GJ 1142 A	M3.0 V	PMSU	11:08:06.55	-05:13:46.9	2MASS	17.3	3.7	vAl95
J11108+479	..F	G 176-015	M4.0 V	PMSU	11:10:51.49	+47:57:02.1	2MASS	23.8	0.9	Cor16
J11110+304		HD 97101 B	M2.0 V	Lep13	11:11:02.46	+30:26:41.6	2MASS	11.87	0.12	aHIP2
J11113+434	B..	GJ 414.1 AB	M2.5 V+	PMSU	11:11:19.73	+43:25:03.2	2MASS	16.9	0.7	HIP2
J11118+335	B..	CW UMa	M3.5 V	PMSU	11:11:51.76	+33:32:11.2	2MASS	13.6	0.4	Dit14
J11126+189		StKM 1-928	M1.5 V	PMSU	11:12:38.99	+18:56:05.4	2MASS	15.7	0.2	Cor16
J11131+002	..F	BD+01 2535	M0.0 V	Lep13	11:13:10.06	+00:14:19.8	2MASS	25.37	1.31	HIP2
J11151+734	J..	HD 97584B	M2.5 V	AF15	11:15:11.06	+73:28:36.0	2MASS	14.7	0.3	Rei02
J11152+194	..F	G 056-026	M3.5 V	PMSU	11:15:12.40	+19:27:12.4	2MASS	16.9	0.6	Cor16
J11152-181	.mF	LP 792-009	M3.0 V	PMSU	11:15:15.50	-18:07:34.8	2MASS	28.2	0.8	Cor16
J11154+410	..F	G 122-008	M3.5 V	Lep13	11:15:26.59	+41:05:16.3	2MASS	17.4	0.6	Cor16
J11159+553	..F	StKM 1-932	M0.5 V	PMSU	11:15:54.04	+55:19:50.6	2MASS	27.5	7.5	vAl95
J11195+466	..F	LP 169-022	M5.5 V	GR97	11:19:30.59	+46:41:43.7	2MASS	10.31	0.28	Lep09
J11200+658	B..	SZ UMa AB	M0.0 V+	PMSU	11:20:05.27	+65:50:47.1	2MASS	8.92	0.08	HIP2
J11201-104		LP 733-099	M2.0 V	Ria06	11:20:06.10	-10:29:46.8	2MASS	16.4	0.3	Cor16
J11214-204	Bm.	BD-19 3242B	M2.5 V+	AF15	11:21:26.56	-20:27:09.5	2MASS	13.16	0.22	aHIP2
J11216+061	..F	GJ 1146	M3.0 V	PMSU	11:21:38.47	+06:08:25.7	2MASS	18.4	1.4	vAl95

Table B.2: Names, spectral types, distances and astrometric parameters of Carmencita stars (continued).

Karmn	Flags[a]	Name	SpT	Ref.[b]	α (J2000)	δ (J2000)	Ref.[c]	d [pc]	ed [pc]	Ref.[d e]
J11231+258	..F	LP 374-039	M5.0 V	PMSU	11:23:08.00	+25:53:37.0	2MASS	14.9	0.7	Dit14
J11233+448	..F	G 122-020	M2.5 V	PMSU	11:23:20.59	+44:48:38.8	2MASS	26.3	0.6	Cor16
J11237+085	..F	Wolf 386	M0.5 V	PMSU	11:23:44.56	+08:33:48.4	2MASS	21.36	1.09	HIP2
J11238+106	..F	BPM 87356	M0.5 V	Lep13	11:23:49.96	+10:37:07.9	2MASS	22.3	0.2	Cor16
J11239-183	.mF	LP 792-020	M3.0 V	PMSU	11:23:57.38	-18:21:48.6	2MASS	22.7	0.6	Cor16
J11240+381	..F	1RXS J112405.0+380809	M4.5 V	AF15	11:24:04.35	+38:08:10.9	2MASS	17.9	0.8	Cor16
J11247+675	..F	Ross 448	M1.0 V	Lep13	11:24:45.60	+67:33:12.6	2MASS	30.5	0.4	Cor16
J11249+024	..F	StKM 1-941	M1.0 V	Lep13	11:24:58.76	+02:28:24.5	2MASS	30.5	0.4	Cor16
J11254+782	..F	G 253-050	M2.0 V	PMSU	11:25:29.61	+78:15:56.3	2MASS	18.4	4.0	vAl95
J11266+379	..F	HAT 183-00276	M2.0 V	Lep13	11:26:37.57	+37:56:23.8	2MASS	23.3	0.4	Cor16
J11276+039	..F	BD+04 2470	M0.0 V	Lep13	11:27:38.56	+03:58:35.9	2MASS	27.29	1.45	HIP2
J11289+101		Wolf 398	M3.5 V	PMSU	11:28:56.24	+10:10:39.5	2MASS	15.7	2.7	vAl95
J11306-080		LP 672-042	M3.5 V	AF15	11:30:41.80	-08:05:42.6	2MASS	13.2	0.6	HIP2
J11307+549	..F	StKM 1-950	M1.0 V	Lep13	11:30:43.72	+54:57:27.6	2MASS	33.2	0.5	Cor16
J11311-149	.mF	LP 732-035	M4.5 V	PMSU	11:31:08.36	-14:57:20.2	2MASS	11.61	0.07	Wein16
J11315+022	..F	LP 552-068	M2.5 V	Lep13	11:31:32.85	+02:13:42.9	2MASS	24.6	0.6	Cor16
J11317+226	..f	BD+23 2359	M0.5 V	PMSU	11:31:43.39	+22:40:01.6	2MASS	15.89	0.37	HIP2
J11351-056	..F	LP 673-013	M4.5 V	PMSU	11:35:07.32	-05:39:21.9	2MASS	21.0	1.0	Cor16
J11355+389	B.F	G 122-034	M3.5 V+	PMSU	11:35:31.98	+38:55:37.3	2MASS	17.9	0.6	Cor16
J11376+587	..F	Ross 112	M2.5 V	PMSU	11:37:38.99	+58:42:42.8	2MASS	24.4	0.6	Cor16
J11404+770	..F	G 254-027	M2.0 V	Lep13	11:40:29.67	+77:04:18.9	2MASS	21.3	0.4	Cor16
J11417+427		Ross 1003	M4.0 V	PMSU	11:41:44.72	+42:45:07.3	2MASS	11.1	0.3	HIP2
J11420+147	..F	Ross 115	M3.0 V	PMSU	11:42:01.77	+14:46:35.7	2MASS	19.7	0.5	Cor16
J11421+267		Ross 905	M2.5 V	AF15	11:42:10.96	+26:42:25.1	2MASS	10.1	0.2	HIP2
J11433+253	..F	LTT 13220	M4.0 V	PMSU	11:43:23.60	+25:18:13.8	2MASS	31.6	2.0	Dit14
J11451+183	..f	LP 433-047	M4.0 V	AF15	11:45:11.92	+18:20:58.7	2MASS	15.6	0.6	Cor16
J11467-140	.m.	GJ 443	M3.0 V	PMSU	11:46:42.82	-14:00:50.5	2MASS	19.99	1.24	HIP2
J11470+700	..F	G 236-081	M4.0 V	PMSU	11:47:05.43	+70:01:58.8	2MASS	16.7	0.7	Cor16
J11474+667	..f	1RXS J114728.8+664405	M5.0 V	AF15	11:47:28.57	+66:44:02.6	2MASS	12.7	0.7	Cor16
J11476+002		LP 613-049 A	M4.0 V	PMSU	11:47:40.74	+00:15:20.2	2MASS	19.9	1.1	Dit14
J11476+786		GJ 445	M3.5 V	PMSU	11:47:41.44	+78:41:28.3	2MASS	5.36	0.05	HIP2
J11477+008		FI Vir	M4.0 V	PMSU	11:47:44.40	+00:48:16.4	2MASS	3.36	0.03	HIP2
J11483-112	..F	LP 733-024	M3.0 V	PMSU	11:48:19.43	-11:17:14.4	2MASS	21.3	0.6	Cor16

Table B.2: Names, spectral types, distances and astrometric parameters of Carmencita stars (continued).

Karmn	Flags[a]	Name	SpT	Ref.[b]	α (J2000)	δ (J2000)	Ref.[c]	d [pc]	ed [pc]	Ref.[d e]
J11485+076	..F	G 010-052	M3.5 V	AF15	11:48:35.49	+07:41:40.4	2MASS	25.9	1.4	Dit14
J11496+220	..F	BPM 87650	M0.0 V	Lep13	11:49:40.49	+22:03:53.3	2MASS	31.7	0.3	Cor16
J11509+483		GJ 1151	M4.5 V	PMSU	11:50:57.88	+48:22:39.6	2MASS	8.2	0.2	vAl95
J11511+352		BD+36 2219	M1.5 V	AF15	11:51:07.37	+35:16:18.9	2MASS	8.58	0.09	HIP2
J11519+075	..F	RX J1151.9+0731	M2.5 V	Lep13	11:51:56.81	+07:31:26.2	2MASS	22.6	0.5	Cor16
J11521+039	B..	StM 162	M4.0 V+	Lep13	11:52:09.82	+03:57:23.3	2MASS	10.9	0.4	Cor16
J11529+244	..F	G 121-028	M4.5 V	PMSU	11:52:57.91	+24:28:45.4	2MASS	18.5	2.7	Jen09
J11532-073	..F	GJ 452	M2.5 V	PMSU	11:53:16.09	-07:22:27.3	2MASS	19.6	1.4	HIP2
J11533+430	..F	TYC 3016-577-1	M1.0 V	Lep13	11:53:22.98	+43:02:57.2	2MASS	27.3	0.3	Cor16
J11538+069	..F	LP 553-059	M6.0 V	PMSU	11:53:52.67	+06:59:56.1	2MASS	14.22	0.5	vAl95
J11541+098	..f	Ross 119	M3.5 V	PMSU	11:54:07.88	+09:48:22.7	2MASS	11.55	0.12	Wein16
J11549-021	..F	2MASS J11545693-0206091	M3.0 V	AF15	11:54:56.93	-02:06:09.2	2MASS	27.0	0.8	Cor16
J11551+009	..F	Ross 129	M1.5 V	PMSU	11:55:07.21	+00:58:25.7	2MASS	26.28	1.97	HIP2
J11557-189	.mF	LP 793-044	M3.5 V	PMSU	11:55:44.26	-18:54:31.6	2MASS	27.4	0.9	Cor16
J11557-227	..F	LP 851-346	M7.5 V	Raj13	11:55:44.26	-18:54:31.6	2MASS	9.7		RB09
J11575+118	..F	Ross 122	M2.0 V	PMSU	11:57:32.78	+11:49:39.8	2MASS	24.2	1.6	HIP2
J11582+425	..F	G 122-058	M4.0 V	PMSU	11:58:17.60	+42:34:29.3	2MASS	19.0	0.7	Cor16
J11585+595	B.F	G 197-038	M0.0 V+	Lep13	11:58:35.13	+59:33:22.1	2MASS	40.02	5.67	HIP2
J11589+426	..F	G 122-060	M1.5 V	PMSU	11:58:59.48	+42:39:39.6	2MASS	27.2	0.4	Cor16
J12006-138	.mF	LP 734-011 A	M3.5 V	PMSU	12:00:36.91	-13:49:36.4	2MASS	16.4	0.5	Cor16
J12016-122	..f	LTT 4484	M3.0 V	PMSU	12:01:40.80	-12:13:53.7	2MASS	18.2	0.5	Cor16
J12023+285	S.F	GJ 455	M2.5 V+	PMSU	12:02:18.19	+28:35:14.3	2MASS	20.2	1.6	vAl95
J12054+695		Ross 689	M4.0 V	PMSU	12:05:29.75	+69:32:22.7	2MASS	14.5	0.8	Dit14
J12057+784	..F	LSPM J1205+7825	M2.5 V	Lep13	12:05:47.16	+78:25:51.5	2MASS	20.2	0.5	Cor16
J12063-132	Bmf	StM 164	M3.5 V+	Ria06	12:06:22.14	-13:14:56.0	2MASS	15.3	0.5	Cor16
J12088+303	..F	1RXS J120847.7+302120	M2.5 V	Yi14	12:08:49.52	+30:21:01.1	2MASS	24.5	0.6	Cor16
J12093+210	..F	StM 165	M2.5 V	AF15	12:09:21.81	+21:03:07.7	2MASS	30.6	0.7	Cor16
J12100-150	.m.	LP 734-032	M3.5 V	PMSU	12:10:05.60	-15:04:15.7	2MASS	12.8	0.4	Ried10
J12104-131	.mf	LP 734-034	M4.5 V	AF15	12:10:28.34	-13:10:23.5	2MASS	13.4	0.6	Cor16
J12109+410	..F	G 123-008	M0.0 V	Lep13	12:10:56.89	+41:03:27.6	2MASS	21.6	0.82	HIP2
J12111-199	.m.	LTT 4562	M3.0 V	PMSU	12:11:11.80	-19:57:37.7	2MASS	12.6	0.4	HIP2
J12112-199	.mf	LP 794-031	M3.5 V	PMSU	12:11:16.98	-19:58:21.4	2MASS	12.6	0.4	aHIP2
J12121+488	B.F	G 122-074	M2.5 V+	PMSU	12:12:11.36	+48:49:03.2	2MASS	27.7	0.7	Cor16

Table B.2: Names, spectral types, distances and astrometric parameters of Carmencita stars (continued).

Karmn	Flags[a]	Name	SpT	Ref.[b]	α (J2000)	δ (J2000)	Ref.[c]	d [pc]	ed [pc]	Ref.[d e]
J12122+714	..F	LP 039-066	M3.0 V	Lep13	12:12:15.23	+71:25:23.4	2MASS	19.3	0.5	Cor16
J12123+544N	..F	BD+55 1519 B	M3.0 V	PMSU	12:12:21.12	+54:29:23.2	2MASS	15.52	0.34	aHIP2
J12123+544S		HD 238090	M0.0 V	PMSU	12:12:20.85	+54:29:08.7	2MASS	15.52	0.34	HIP2
J12124+121	..F	2MASS J12122605+1211381	M2.0 V	AF15	12:12:26.06	+12:11:38.1	2MASS	34.0	0.6	Cor16
J12124+396	B.f	G 123-013 AB	M1.0 V+	PMSU	12:12:29.40	+39:40:28.2	2MASS	30.5	3.3	HIP2
J12133+166	..F	IV Com	M1.0 V	PMSU	12:13:20.45	+16:41:39.6	2MASS	28.04	2.74	HIP2
J12142+006	S..	GJ 1154 A	M5.0 V+	PMSU	12:14:16.54	+00:37:26.3	2MASS	7.16	0.12	Wein16
J12144+245	..F	G 059-007	M2.0 V	PMSU	12:14:26.04	+24:35:26.4	2MASS	25.3	0.5	Cor16
J12151+487	..F	BD+49 2126	M0.5 V	Lep13	12:15:08.86	+48:43:57.4	2MASS	24.88	1.21	HIP2
J12154+391	..F	G 123-016	M1.5 V	PMSU	12:15:28.38	+39:11:14.5	2MASS	26.8	0.4	Cor16
J12156+526		StKM 2-809	M4.0 V	Lep13	12:15:39.37	+52:39:08.9	2MASS	12.0	0.5	Cor16
J12162+508	B.f	RX J1216.2+5053	M4.0 V+	AF15	12:16:15.06	+50:53:37.7	2MASS	16.5	0.6	Cor16
J12168+029	B.f	GJ 1155 AB	M3.0 V+	PMSU	12:16:51.91	+02:58:04.7	2MASS	22.7	1.5	HD80
J12168+248	..F	2MASS J12165262+2451052	M1.5 V	Lep13	12:16:52.63	+24:51:05.2	2MASS	32.0	0.5	Cor16
J12169+311	..F	Sand 39	M3.5 V	PMSU	12:16:58.45	+31:09:23.4	2MASS	26.7	0.9	Cor16
J12189+111		GL Vir	M5.0 V	PMSU	12:18:59.40	+11:07:33.9	2MASS	6.44	0.04	Wein16
J12191+318	S..	LP 320-626	M4.0 V+	Lep13	12:19:06.00	+31:50:43.3	2MASS	10.4	0.4	Cor16
J12194+283	..F	Wolf 408	M0.0 V	PMSU	12:19:24.07	+28:22:56.6	2MASS	25.38	1.2	HIP2
J12198+527	..F	StKM 1-1007	M0.0 V	Lep13	12:19:48.09	+52:46:45.0	2MASS	27.96	1.73	HIP2
J12199+364	..F	G 123-036	M1.0 V	Lep13	12:29:55.03	+36:26:42.1	2MASS	26.35	2.87	HIP2
J12204+005	B..	BD+01 2684 AB	M0.0 V+	PMSU	12:20:25.51	+00:35:01.4	2MASS	15.6	0.2	Cor16
J12214+306E	B.f	Sand 57 B	M5.0 V	Jahr08	12:21:26.73	+30:38:37.6	2MASS	15.1	0.8	Cor16
J12214+306W	B.F	Sand 58 A	M4.5 V	Jahr08	12:21:27.05	+30:38:35.7	2MASS	18.4	0.9	Cor16
J12217+682	..F	G 237-061	M3.0 V	Lep13	12:21:47.62	+68:16:03.9	2MASS	19.4	0.5	Cor16
J12223+251	..F	Wolf 409	M0.0 V	PMSU	12:22:21.26	+25:10:11.9	2MASS	29.91	2.23	HIP2
J12225+123	..F	BD+28 2110	M0.0 V	Lep13	12:22:34.07	+27:36:17.0	2MASS	31.71	1.94	HIP2
J12228-040	B.F	G 013-033	M4.5 V+	AF15	12:22:50.62	-04:04:46.2	2MASS	15.8	0.7	Cor16
J12230+640		Ross 690	M3.0 V	PMSU	12:23:00.25	+64:01:50.6	2MASS	18.3	0.7	HIP2
J12235+279	..F	Wolf 411	M0.0 V	Lep13	12:23:34.72	+27:54:47.5	2MASS	34.32	3.04	HIP2
J12235+671	B..	G 237-064 AB	M2.5 V+	PMSU	12:23:33.17	+67:11:18.5	2MASS	12.9	0.5	HIP2
J12238+125	..F	HD 107888	M0.0 V	Lep13	12:23:53.54	+12:34:49.2	2MASS	21.0	1.08	HIP2
J12248-182	.m.	Ross 695	M2.0 V	PMSU	12:24:52.43	-18:14:30.3	2MASS	8.8	0.2	HIP2
J12269+270	..F	CX Com	M4.5 V	Rei04	12:26:57.37	+27:00:53.7	2MASS	24.2	0.9	Dit14

Table B.2: Names, spectral types, distances and astrometric parameters of Carmencita stars (continued).

Karmn	Flags[a]	Name	SpT	Ref.[b]	α (J2000)	δ (J2000)	Ref.[c]	d [pc]	ed [pc]	Ref.[d e]
J12274+374	..F	G 148-061	M1.5 V	Lep13	12:27:29.45	+37:26:33.2	2MASS	25.37	2.56	HIP2
J12277-032	B.f	LP 615-149	M3.5 V+	Sch05	12:27:44.72	-03:15:00.6	2MASS	15.8	0.5	Cor16
J12288-106N	B..	Ross 948 A	M2.0 V	PMSU	12:28:52.98	-10:39:50.8	2MASS	15.3	0.3	Cor16
J12288-106S	B..	Ross 948 B	M2.0 V	PMSU	12:28:53.16	-10:39:48.8	2MASS	15.5	0.3	Cor16
J12289+084	B..	Wolf 414 AB	M3.5 V+	PMSU	12:28:57.60	+08:25:31.6	2MASS	13.2	0.7	HIP2
J12290+417	B.f	G 123-035	M3.5 V+	PMSU	12:29:02.90	+41:43:49.7	2MASS	15.9	0.5	Cor16
J12292+535	..F	GJ 1159 A	M3.5 V	PMSU	12:29:14.53	+53:32:44.8	2MASS	25.1	0.6	vAl95
J12294+229	..F	LP 377-100	M4.0 V	PMSU	12:29:27.13	+22:59:46.7	2MASS	24.3	1.5	Dit14
J12299-054E	..F	LP 675-077	M4.0 V	PMSU	12:29:54.69	-05:27:20.3	2MASS	20.8	0.8	Cor16
J12299-054W	S.F	LP 675-076	M3.5 V+	PMSU	12:29:54.22	-05:27:24.1	2MASS	21.0	0.6	Ried10
J12312+086		BD+09 2636	M0.5 V	Lep13	12:31:15.79	+08:48:38.1	2MASS	13.64	0.24	HIP2
J12323+315	..F	LP 321-035	M3.0 V	PMSU	12:32:20.37	+31:35:59.4	2MASS	29.4	1.7	Dit14
J12324+203	..F	StKM 1-1021	M2.5 V	PMSU	12:32:26.32	+20:23:27.5	2MASS	25.7	0.6	Cor16
J12327+682	..F	LP 039-249	M0.0 V	Lep13	12:32:44.99	+68:15:45.4	2MASS	31.0	0.3	Cor16
J12332+090	B..	FL Vir AB	M5.0 V+	PMSU	12:33:17.38	+09:01:15.8	2MASS	4.4	0.1	Jen52
J12349+322	..F	2MASS J12345401+3214279	M3.5 V	AF15	12:34:54.01	+32:14:27.9	2MASS	21.7	0.7	Cor16
J12350+098		GJ 476	M2.5 V	PMSU	12:35:00.70	+09:49:42.5	2MASS	18.3	1.0	HIP2
J12363-043	..F	LP 675-019	M3.0 V	PMSU	12:36:22.88	-04:22:39.3	2MASS	25.7	6.9	vAl95
J12364+352	..f	G 123-045	M4.5 V	AF15	12:36:28.70	+35:12:00.8	2MASS	11.3	0.2	Dit14
J12368-019	..F	2MASS J12365214-0159007	M3.5 V	AF15	12:36:52.15	-01:59:00.7	2MASS	21.5	0.7	Cor16
J12373-208		LP 795-038	M4.0 V	Sch05	12:37:21.57	-20:52:34.9	2MASS	14.3	0.6	Cor16
J12387-043	..F	GJ 1162	M3.5 V	PMSU	12:38:47.32	-04:19:16.9	2MASS	19.7	1.2	vAl95
J12388+116		Wolf 433	M3.0 V	PMSU	12:38:52.42	+11:41:46.2	2MASS	14.4	0.6	HIP2
J12390+470	..F	G 123-049	M2.0 V	PMSU	12:39:04.61	+47:02:23.5	2MASS	21.8	2.1	HIP2
J12397+255	..F	LP 377-036	M4.5 V	Bus98	12:39:43.54	+25:30:45.7	2MASS	27.4	2.8	Dit14
J12416+482	..F	G 198-071A	M1.0 V	PMSU	12:41:37.89	+48:14:24.7	2MASS	26.8	0.4	Cor16
J12417+567	..F	RX J1241.7+5645	M3.5 V	AF15	12:41:47.37	+56:45:13.8	2MASS	22.0	0.7	Cor16
J12428+418		G 123-055	M4.0 V	Lep13	12:42:49.96	+41:53:46.9	2MASS	10.6	1.2	vAl95
J12436+251	..F	Sand 128	M3.0 V	PMSU	12:43:36.08	+25:06:21.9	2MASS	23.2	1.4	Dit14
J12440-111	..F	LP 735-029	M4.5 V	AF15	12:44:00.76	-11:10:30.2	2MASS	14.8	0.7	Cor16
J12470+466	..f	Ross 991	M2.5 V	AF15	12:47:01.02	+46:37:33.4	2MASS	20.9	1.0	HIP2
J12471-035	..f	LP 616-013	M3.0 V	PMSU	12:47:09.77	-03:34:17.7	2MASS	18.9	0.5	Cor16
J12479+097		Wolf 437	M3.5 V	PMSU	12:47:56.64	+09:45:05.0	2MASS	8.4	0.2	HIP2

Table B.2: Names, spectral types, distances and astrometric parameters of Carmencita stars (continued).

Karmn	Flags[a]	Name	SpT	Ref.[b]	α (J2000)	δ (J2000)	Ref.[c]	d [pc]	ed [pc]	Ref.[d e]
J12481+472	..F	G 123-061	M3.5 V	PMSU	12:48:09.77	+47:13:31.7	2MASS	23.3	0.8	Cor16
J12485+495	..f	RX J1248.5+4933	M3.5 V	Lep13	12:48:34.49	+49:33:54.1	2MASS	15.2	0.5	Cor16
J12490+661	S..	DP Dra AabB	M3.0 V+	PMSU	12:49:02.73	+66:06:36.6	2MASS	10.2	0.2	HIP2
J12495+094	..F	Wolf 439	M3.5 V	PMSU	12:49:34.19	+09:28:30.9	2MASS	25.2	7.9	vAl95
J12505+269	..F	LTT 13677	M3.5 V	PMSU	12:50:34.57	+26:55:23.1	2MASS	27.2	0.9	Cor16
J12508-213	..F	DENIS J125052.6-212113	M7.5 V	Lod05	12:50:52.66	-21:21:13.7	2MASS	5.1	0.6	Lod05
J12513+221	..F	GJ 1166A	M3.0 V	PMSU	12:51:23.94	+22:06:14.9	2MASS	22.3	0.6	Cor16
J12576+352E	B..	BF CVn	M1.5 V+	JA74	12:57:40.30	+35:13:30.6	2MASS	19.26	1.11	HIP2
J12576+352W	B..	BD+36 2322B	M4.0 V+	PMSU	12:57:39.35	+35:13:19.5	2MASS	19.26	1.11	aHIP2
J12583+405	B.F	LP 041-165	M1.5 V+	Lep13	12:58:21.66	+40:33:23.0	2MASS	43.84	8.17	HIP2
J12594+077	..F	LP 556-064	M5.0 V	PMSU	12:59:24.03	+07:43:55.1	2MASS	20.7	1.1	Cor16
J13000-056	..f	Ross 972	M3.0 V	PMSU	13:00:03.98	-05:37:47.7	2MASS	17.9	0.5	Cor16
J13005+056		FN Vir	M4.5 V	PMSU	13:00:33.51	+05:41:08.1	2MASS	8.35	0.17	Wein16
J13007+123	B..	DT Vir AB	M2.0 V+	Mon01	13:00:46.66	+12:22:32.6	2MASS	11.69	0.21	HIP2
J13019+335	..F	G 164-038	M1.0 V	Lep13	13:01:56.55	+33:35:25.7	2MASS	35.2	0.4	Cor16
J13027+415	..F	G 123-084	M3.5 V	AF15	13:02:47.52	+41:31:09.9	2MASS	17.9	0.6	Cor16
J13047+559	B.f	GJ 497	M0.5 V+	Lep13	13:04:46.63	+55:54:09.3	2MASS	32.65	2.45	HIP2
J13054+371	B..	G 164-042	M2.5 V+	PMSU	13:05:29.85	+37:08:10.7	2MASS	24.7	3.2	HIP2
J13068+308	..F	Sand 214	M5.0 V	PMSU	13:06:50.25	+30:50:54.9	2MASS	18.2	1.5	Dit14
J13084+169	..F	MCC 686	M1.0 V	PMSU	13:08:24.74	+16:58:18.7	2MASS	25.3	2.02	HIP2
J13088+163	..F	LP 437-012	M2.5 V	PMSU	13:08:50.59	+16:22:03.9	2MASS	27.8	0.6	Cor16
J13089+490	..F	StKM 1-1049	M0.5 V	PMSU	13:08:55.63	+49:04:49.5	2MASS	23.4	0.2	Cor16
J13095+289	..F	GJ 1167A	M4.0 V	PMSU	13:09:34.95	+28:59:06.6	2MASS	12.5	0.2	Dit14
J13102+477	..f	G 177-025	M5.0 V	AF15	13:10:12.69	+47:45:19.0	2MASS	13.1	0.5	Dit14
J13113+285	..F	LP 322-936	M5.0 V	PMSU	13:11:21.64	+28:32:41.9	2MASS	21.6	1.1	Cor16
J13118+253	..F	LP 378-688	M5.0 V	PMSU	13:11:51.79	+25:20:50.7	2MASS	20.6	1.1	Cor16
J13130+201	..F	GJ 1168	M3.5 V	PMSU	13:13:04.79	+20:11:26.5	2MASS	16.5	0.5	Cor16
J13140+038	..F	G 062-018	M3.0 V	PMSU	13:14:05.83	+03:53:58.7	2MASS	19.6	0.7	Dit14
J13142+792	..F	LP 021-095	M1.0 V	Lep13	13:14:15.50	+79:14:49.0	2MASS	29.7	0.4	Cor16
J13143+133	B..	NLTT 33370 AB	M6.0 V+	AF15	13:14:20.39	+13:20:01.2	2MASS	16.39	0.75	Lep09
J13165+278	..F	GJ 1169	M3.5 V	PMSU	13:16:32.84	+27:52:29.8	2MASS	15.6	0.5	Dit14
J13167-123	..F	LP 737-014	M3.5 V	AF15	13:16:45.46	-12:20:20.4	2MASS	22.0	0.7	Cor16
J13168+170	J..	HD 115404B	M0.5 V	AF15	13:16:51.56	+17:01:00.1	2MASS	11.1	0.1	aHIP2

Table B.2: Names, spectral types, distances and astrometric parameters of Carmencita stars (continued).

Karmn	Flags[a]	Name	SpT	Ref.[b]	α (J2000)	δ (J2000)	Ref.[c]	d [pc]	ed [pc]	Ref.[d e]
J13168+231	..F	LP 378-924	M1.5 V	PMSU	13:16:53.06	+23:10:06.9	2MASS	24.6	0.4	Cor16
J13179+362	..F	G 164-062	M1.0 V	AF15	13:17:58.39	+36:17:57.4	2MASS	21.56	0.96	HIP2
J13180+022	B.f	G 062-028	M3.5 V+	PMSU	13:18:01.81	+02:14:01.1	2MASS	21.1	1.1	Dit14
J13182+733	..F	2MASS J13181352+7322073	M3.5 V	AF15	13:18:13.52	+73:22:07.4	2MASS	22.6	0.7	Cor16
J13195+351E	S..	BD+35 2436B	M3.0 V+	PMSU	13:19:34.67	+35:06:25.9	2MASS	13.27	0.27	aHIP2
J13195+351W	B..	BD+35 2436Aab	M0.5 V+	PMSU	13:19:33.56	+35:06:37.3	2MASS	13.27	0.27	HIP2
J13196+333		Ross 1007	M1.5 V	PMSU	13:19:40.15	+33:20:47.8	2MASS	16.99	0.43	HIP2
J13197+477	B..	BD+48 2108Aab	M0.5 V+	PMSU	13:19:45.69	+47:46:40.9	2MASS	10.71	0.25	HIP2
J13209+342		BD+35 2439	M1.0 V	PMSU	13:20:57.97	+34:16:44.7	2MASS	16.04	0.47	HIP2
J13215+035	..F	LSPM J1321+0332	M1.0 V	Lep13	13:21:30.06	+03:32:59.4	2MASS	33.7	0.4	Cor16
J13215+037	..F	LP 557-059	M1.0 V	PMSU	13:21:35.24	+03:45:55.2	2MASS	28.8	0.4	Cor16
J13229+244		Ross 1020	M4.0 V	PMSU	13:22:56.74	+24:28:03.4	2MASS	13.7	0.5	vAl95
J13235+292	B..	BD+29 2405	M0.0 V+	Gra03	13:23:32.81	+29:14:14.5	2MASS	18.82	0.35	HIP2
J13239+694	..F	LP 040-109	M0.0 V	Lep13	13:23:56.02	+69:27:06.2	2MASS	32.1	0.3	Cor16
J13247-050	..F	G 014-052	M4.0 V	AF15	13:24:46.48	-05:04:19.4	2MASS	17.9	0.7	Cor16
J13251-114	..F	2MASS J13251172-1126368	M3.0 V	AF15	13:25:11.72	-11:26:36.8	2MASS	22.6	0.6	Cor16
J13254+377	B.F	BD+38 2445	M0.0 V+	Lep13	13:25:28.36	+37:43:09.8	2MASS	32.29	2.31	HIP2
J13260+275	..F	GUVVJ132602.6+273502.3	M3.0 V	AF15	13:26:02.68	+27:35:02.1	2MASS	23.5	0.7	Cor16
J13282+300	..F	BD+30 2400	M0.0 V	Lep13	13:28:17.76	+30:02:46.2	2MASS	51.12	4.39	HIP2
J13283-023E	..f	Ross 486B	M4.0 V	PMSU	13:28:21.51	-02:21:31.3	2MASS	13.89	0.55	aHIP2
J13283-023W		Ross 486A	M3.0 V	PMSU	13:28:21.06	-02:21:36.5	2MASS	13.89	0.55	HIP2
J13293+114		GJ 513	M3.5 V	PMSU	13:29:21.31	+11:26:26.5	2MASS	15.9	1.7	vAl95
J13294-143	.mF	1RXS J132923.9-142206	M3.5 V	AF15	13:29:24.08	-14:22:12.3	2MASS	18.1	0.6	Cor16
J13299+102		BD+11 2576	M0.5 V	PMSU	13:29:59.79	+10:22:37.6	2MASS	7.65	0.06	HIP2
J13300-087	..F	Wolf 485B	M4.0 V	PMSU	13:30:02.85	-08:42:25.2	2MASS	17.4	1.2	aHIP2
J13305+191	..F	GJ 1171	M4.5 V	PMSU	13:30:31.06	+19:09:34.0	2MASS	14.5	0.9	vAl95
J13317+292	B..	DG CVn AB	M4.0 V+	PMSU	13:31:46.67	+29:16:36.9	2MASS	18.02	0.77	Ried14
J13318+233	..F	G 150-007	M2.0 V	PMSU	13:31:50.57	+23:23:20.3	2MASS	23.7	0.5	Cor16
J13319+311	B.f	BD+31 2500	M0.0 V+	Lep13	13:31:58.25	+31:08:04.9	2MASS	32.01	2.68	HIP2
J13326+309	B.F	LP 323-169	M4.5 V+	AF15	13:32:39.08	+30:59:06.5	2MASS	20.5	1.1	Dit14
J13327+168	B..	VW Com AB	M2.5 V+	PMSU	13:32:44.61	+16:48:39.7	2MASS	12.8	3.2	HIP2
J13335+704	..F	2MASS J13333371+7029412	M3.5 V	AF15	13:33:33.72	+70:29:41.3	2MASS	19.5	0.6	Cor16
J13343+046	..f	BD+05 2767	M0.0 V	Lep13	13:34:21.50	+04:40:02.6	2MASS	21.32	0.7	HIP2

Table B.2: Names, spectral types, distances and astrometric parameters of Carmencita stars (continued).

Karmn	Flags[a]	Name	SpT	Ref.[b]	α (J2000)	δ (J2000)	Ref.[c]	d [pc]	ed [pc]	Ref.[d e]
J13348+201	..F	LP 379-062	M3.5 V	PMSU	13:34:49.35	+20:11:38.8	2MASS	23.9	0.8	Cor16
J13348+745	..F	LP 021-568	M3.5 V	PMSU	13:34:51.56	+74:30:13.1	2MASS	23.6	6.7	avAl95
J13358+146	..F	G 150-017	M2.5 V	Lep13	13:35:50.75	+14:41:12.4	2MASS	20.8	0.5	Cor16
J13369+229	..F	Ross 1021	M2.5 V	PMSU	13:36:55.22	+22:58:01.1	2MASS	24.4	0.6	Cor16
J13376+481	..F	BD+48 2138C	M4.0 V	PMSU	13:37:40.44	+48:07:54.2	2MASS	20.0	0.4	Dit14
J13378+481	B.f	BD+48 2138	M0.0 V+	Lep13	13:37:51.20	+48:08:17.4	2MASS	22.14	0.9	HIP2
J13386+258	..f	Ross 1022	M3.0 V	PMSU	13:38:37.05	+25:49:49.6	2MASS	18.7	0.5	Cor16
J13386-115	..F	2MASS J13384087-1132077	M4.5 V	AF15	13:38:40.87	-11:32:07.8	2MASS	16.2	0.7	Cor16
J13388-022	..F	Ross 488	M2.0 V	PMSU	13:38:53.45	-02:15:47.1	2MASS	23.5	0.5	Cor16
J13394+461	B..	BD+46 1889	M1.5 V+	AF15	13:39:24.10	+46:11:11.5	2MASS	13.01	0.27	HIP2
J13401+437	..f	Ross 1026	M3.5 V	PMSU	13:40:08.98	+43:46:37.8	2MASS	16.7	1.1	HD80
J13413-091	..F	2MASS J13412122-0907171	M2.5 V	AF15	13:41:21.22	-09:07:17.1	2MASS	30.2	0.7	Cor16
J13414+489	..F	StM 186	M3.5 V	AF15	13:41:27.66	+48:54:45.8	2MASS	17.6	0.6	Cor16
J13415+148	..F	LTT 18344	M1.0 V	PMSU	13:41:31.89	+14:49:26.7	2MASS	33.4	0.5	Cor16
J13417+582	B.f	StM 187	M3.5 V+	Lep13	13:41:46.31	+58:15:19.8	2MASS	15.5	0.5	Cor16
J13421-160	Bm.	LP 798-025	M4.0 V+	PMSU	13:42:09.91	-16:00:23.3	2MASS	14.3	0.6	Cor16
J13427+332		Ross1015	M3.5 V	PMSU	13:42:43.29	+33:17:25.5	2MASS	9.3	0.3	HIP2
J13430+090	..F	G 063-050	M3.0 V	PMSU	13:43:01.27	+09:04:23.6	2MASS	21.9	0.6	Cor16
J13434+111	..F	TYC 896-760-1	M0.5 V	Lep13	13:43:24.95	+11:06:43.9	2MASS	29.9	0.3	Cor16
J13444+516	B.f	Ross 492 AB	M2.0 V+	PMSU	13:44:28.29	+51:41:08.7	2MASS	24.3	3.7	vAl95
J13445+249	..F	LP 379-098	M1.0 V	Lep13	13:44:33.67	+24:57:05.6	2MASS	31.1	0.4	Cor16
J13450+176		BD+18 2776	M1.0 V	Koe10	13:45:05.03	+17:47:10.5	2MASS	13.6	0.18	HIP2
J13455+609	..F	MCC 699	M0.5 V	Lep13	13:45:31.38	+60:58:57.8	2MASS	31.53	1.29	HIP2
J13457+148		HD 119850	M1.5 V	PMSU	13:45:43.54	+14:53:31.8	2MASS	5.39	0.03	HIP2
J13458-179	.m.	LP 798-034	M3.5 V	PMSU	13:45:50.75	-17:58:04.8	2MASS	10.2	0.5	HIP2
J13477+214	B.F	BD+22 2632	M0.0 V+	Lep13	13:47:42.41	+21:27:37.4	2MASS	28.03	2.06	HIP2
J13481-137	.mF	LP 738-014	M4.5 V	Dea12	13:48:07.22	-13:44:32.1	2MASS	22.4	1.0	Cor16
J13482+236	..F	GJ 1179 A	M5.5 V	PMSU	13:48:13.41	+23:36:48.7	2MASS	12.1	0.3	vAl95
J13485+563	..F	Ross 493	M1.5 V	Lep13	13:48:35.02	+56:20:08.1	2MASS	26.9	0.4	Cor16
J13488+041	..F	Wolf 1494	M4.0 V	PMSU	13:48:48.62	+04:06:02.3	2MASS	14.6	0.5	Dit14
J13490+026	..F	Wolf 1495	M1.5 V	PMSU	13:49:01.04	+02:47:28.2	2MASS	18.8	0.4	Cor16
J13503-216	.mF	LP 798-041	M3.5 V	AF15	13:50:23.77	-21:37:19.3	2MASS	21.7	0.7	Cor16
J13507-216	.mF	LP 798-044	M3.0 V	PMSU	13:50:44.00	-21:41:26.4	2MASS	19.8	0.6	Cor16

Table B.2: Names, spectral types, distances and astrometric parameters of Carmencita stars (continued).

Karmn	Flags[a]	Name	SpT	Ref.[b]	α (J2000)	δ (J2000)	Ref.[c]	d [pc]	ed [pc]	Ref.[d e]
J13508+367	..F	Ross 1019	M3.5 V	PMSU	13:50:51.82	+36:44:16.9	2MASS	15.8	0.8	Dit14
J13518+127	..F	RX J1351.8+1247	M2.0 V	Lep13	13:51:52.91	+12:47:07.3	2MASS	25.7	0.5	Cor16
J13526+144	B.f	G 150-046	M2.0 V+	PMSU	13:52:36.20	+14:25:20.9	2MASS	18.0	0.3	Cor16
J13528+656	..F	LP 066-278	M1.0 V	PMSU	13:52:50.05	+65:37:19.8	2MASS	26.77	1.41	HIP2
J13528+668	..F	LP 066-274	M5.0 V	PMSU	13:52:50.60	+66:49:06.5	2MASS	14.2	0.3	Dit14
J13529+536	..F	LP 097-259	M1.0 V	Lep13	13:52:55.59	+56:36:20.2	2MASS	30.3	0.4	Cor16
J13534+129	B..	BD+13 2721	M0.0 V+	Lep13	13:53:27.58	+12:56:34.5	2MASS	20.95	0.73	HIP2
J13536+776		RX J1353.6+7737	M4.0 V	Lep13	13:53:38.77	+77:37:08.3	2MASS	12.0	0.4	Dit14
J13537+521	B.F	2MASS J13534589+5210298AB	M3.5 V+	AF15	13:53:45.89	+52:10:29.9	2MASS	18.6	0.6	Cor16
J13537+788	..F	LTT 18361	M0.0 V	PMSU	13:53:47.17	+78:51:06.9	2MASS	24.15	0.7	HIP2
J13582+125		Ross 837	M3.0 V	PMSU	13:58:13.93	+12:34:43.8	2MASS	11.32	1.5	vAl95
J13582-120	..F	LP 739-002	M4.5 V	AF15	13:58:16.22	-12:02:59.2	2MASS	16.3	0.7	Cor16
J13583-132	.mF	LP 739-003	M4.0 V	AF15	13:58:19.56	-13:16:24.8	2MASS	18.1	0.7	Cor16
J13587-000	..F	LP 619-009	M3.5 V	PMSU	13:58:43.61	-00:04:47.4	2MASS	27.4	0.9	Cor16
J13591-198	.m.	LP 799-007	M4.0 V	PMSU	13:59:10.46	-19:50:03.5	2MASS	10.77	0.1	Ried14
J14010-026		HD 122303	M1.0 V	PMSU	14:01:03.25	-02:39:18.1	2MASS	10.03	0.16	HIP2
J14019+154	B.f	GJ 536.1	M0.0 V+	Lep13	14:01:58.73	+15:29:40.5	2MASS	27.72	3.13	HIP2
J14019+432	..F	2MASS J14015879+4316427	M2.5 V	AF15	14:01:58.79	+43:16:42.7	2MASS	28.0	0.7	Cor16
J14023+136	..F	MCC 150	M0.5 V	PMSU	14:02:19.61	+13:41:22.9	2MASS	19.86	0.8	HIP2
J14024-210	.mF	LP 799-014	M3.5 V	PMSU	14:02:28.89	-21:00:36.9	2MASS	19.0	0.6	Cor16
J14025+463N	B..	BD+47 2112A	M0.5 V	PMSU	14:02:33.24	+46:20:26.6	2MASS	11.3	0.5	vAl95
J14025+463S	B..	BD+47 2112B	M0.5 V	PMSU	14:02:33.13	+46:20:23.9	2MASS	11.3	0.5	avAl95
J14039+242	..F	LSPM J1403+2440	M2.5 V	Lep13	14:03:54.82	+24:40:41.5	2MASS	23.9	0.6	Cor16
J14041+207	B.F	BD+21 2602C	M1.0 V+	Lep13	14:04:09.22	+20:44:31.4	2MASS	36.72	2.16	aHIP2
J14062+693	..f	NLTT 36313	M3.0 V	Lep13	14:06:14.87	+69:18:41.9	2MASS	18.5	0.5	Cor16
J14082+805		BD+81 465	M1.0 V	PMSU	14:08:12.98	+80:35:50.0	2MASS	16.92	0.34	HIP2
J14083+758	..F	G 255-049	M0.5 V	PMSU	14:08:22.74	+75:51:07.1	2MASS	24.9	4.5	vAl95
J14121-005	B.F	LP 619-049	M2.5 V+	PMSU	14:12:11.02	-00:35:04.5	2MASS	24.9	2.1	vAl95
J14130-120	S.f	GQ Vir	M4.5 V+	PMSU	14:13:04.92	-12:01:26.3	2MASS	11.9	0.5	Cor16
J14142-153	.mF	LTT 5581	M3.5 V	PMSU	14:14:17.01	-15:21:12.5	2MASS	30.2	4.5	aHIP2
J14144+234	..F	LP 381-017	M3.5 V	PMSU	14:14:26.56	+23:27:34.0	2MASS	22.3	0.7	Cor16
J14152+450		Ross 992	M3.0 V	PMSU	14:15:17.07	+45:00:53.6	2MASS	16.3	1.6	vAl95
J14153+153	..F	TYC 1469-782	M2.0 V	Lep13	14:15:20.48	+15:23:03.6	2MASS	24.2	0.5	Cor16

Table B.2: Names, spectral types, distances and astrometric parameters of Carmencita stars (continued).

Karmn	Flags[a]	Name	SpT	Ref.[b]	α (J2000)	δ (J2000)	Ref.[c]	d [pc]	ed [pc]	Ref.[d e]
J14155+046		GJ 1182	M5.0 V	PMSU	14:15:32.54	+04:39:31.2	2MASS	13.9	0.7	vAl95
J14157+594	..F	LP 097-674	M2.0 V	Lep13	14:15:42.49	+59:27:30.3	2MASS	26.5	0.5	Cor16
J14159+362	..F	G 165-058	M3.5 V	Lep13	14:15:56.37	+36:16:36.8	2MASS	17.1	0.6	Cor16
J14161+233	..F	NLTT 36793	M1.0 V	Lep13	14:16:11.39	+23:23:29.8	2MASS	31.3	0.4	Cor16
J14170+105	..F	LP 499-059	M1.5 V	PMSU	14:17:04.88	+10:35:35.9	2MASS	22.1	0.4	Cor16
J14170+317	B..	LP 325-015 AB	M4.0 V+	PMSU	14:17:02.95	+31:42:47.2	2MASS	16.7	0.6	Dit14
J14171+088	S.f	2MASS J14170731+0851363	M4.5 V+	AF15	14:17:07.31	+08:51:36.3	2MASS	12.3	0.6	Cor16
J14173+454		RX J1417.3+4525	M5.0 V	Gig10	14:17:22.10	+45:25:46.1	2MASS	19.01	0.45	aHIP2
J14174+454	..F	BD+46 1951	M0.0 V	Lep13	14:17:24.38	+45:26:40.1	2MASS	19.01	0.45	HIP2
J14175+025	..F	RX J1417.5+0233	M3.0 V	AF15	14:17:30.21	+02:33:43.6	2MASS	23.8	0.7	Cor16
J14177+214	..F	LP 381-094	M1.0 V	Lep13	14:17:47.85	+21:26:01.9	2MASS	38.02	4.41	HIP2
J14179-005	..F	G 064-063	M2.5 V	PMSU	14:17:59.05	-00:31:29.5	2MASS	25.1	0.6	Cor16
J14189+386	..F	LP 220-078	M1.0 V	Lep13	14:18:59.15	+38:38:26.7	2MASS	36.74	3.56	HIP2
J14191-073	..F	Wolf 534	M3.0 V	PMSU	14:19:11.07	-07:18:11.3	2MASS	19.3	1.6	vAl95
J14194+029	..F	NLTT 36959	M5.0 V	AF15	14:19:29.58	+02:54:36.5	2MASS	28.6	4.2	Dit14
J14200+390	..F	StKM 1- 1145	M2.5 V	PMSU	14:20:04.69	+39:03:01.5	2MASS	20.2	0.5	Cor16
J14201-096	..f	Ross 848	M3.5 V	PMSU	14:20:07.39	-09:37:12.7	2MASS	10.98	1.81	vAl95
J14210+275	B.F	G 166-021	M2.5 V+	PMSU	14:21:03.49	+27:35:32.8	2MASS	23.8	0.5	Cor16
J14212-011	..F	LP 620-003	M3.5 V	PMSU	14:21:15.13	-01:07:19.9	2MASS	13.4	0.4	Ried10
J14215-079	..F	2MASS J14213406-0755165	M4.0 V	AF15	14:21:34.06	-07:55:16.6	2MASS	17.8	0.7	Cor16
J14219+376	..F	LP 270-068	M1.5 V	Lep13	14:21:55.07	+37:39:50.8	2MASS	31.8	0.5	Cor16
J14227+164	..F	NLTT 37131	M5.0 V	AF15	14:22:43.41	+16:24:46.4	2MASS	24.2	2.5	Dit14
J14231-222	.mF	LP 857-029	M4.0 V	PMSU	14:23:07.85	-22:17:08.3	2MASS	27.6	1.1	Cor16
J14249+088	..F	LP 500-019	M2.5 V	PMSU	14:24:55.99	+08:53:15.6	2MASS	14.3	1.0	HIP2
J14251+518		θ Boo B	M2.5 V	AF15	14:25:11.61	+51:49:53.5	2MASS	14.53	0.03	aHIP2
J14255-118	..F	2MASS J14253413-1148515	M4.0 V	AF15	14:25:34.13	-11:48:51.5	2MASS	17.0	0.7	Cor16
J14257+236E		BD+24 2733B	M0.5 V	PMSU	14:25:46.67	+23:37:13.3	2MASS	16.36	0.38	aHIP2
J14257+236W		BD+24 2733A	M0.0 V	PMSU	14:25:43.49	+23:37:01.1	2MASS	16.36	0.38	HIP2
J14259+142	..F	StKM 1-1155	M0.0 V	Lep13	14:25:55.94	+14:12:10.2	2MASS	28.2	0.3	Cor16
J14269+241	..F	LSPM J1426+2408	M1.0 V	Lep13	14:26:58.82	+24:08:56.9	2MASS	34.2	0.4	Cor16
J14279-003N	..F	GJ 1183B	M4.5 V	PMSU	14:27:56.40	-00:22:19.1	2MASS	13.7	0.6	Cor16
J14279-003S	..F	GJ 1183A	M4.5 V	PMSU	14:27:56.07	-00:22:31.1	2MASS	13.4	0.6	Cor16
J14280+139	..F	LP 500-035	M7.5 V	Lep09	14:28:04.19	+13:56:13.7	2MASS	12.08	0.6	Lep09

Table B.2: Names, spectral types, distances and astrometric parameters of Carmencita stars (continued).

Karmn	Flags[a]	Name	SpT	Ref.[b]	α (J2000)	δ (J2000)	Ref.[c]	d [pc]	ed [pc]	Ref.[d e]
J14282+053	..F	LP 560-026	M3.5 V	Lep13	14:28:17.58	+05:18:45.9	2MASS	17.0	0.6	Cor16
J14283+053	..f	LP 560-027	M3.0 V	Lep13	14:28:21.52	+05:19:01.4	2MASS	18.5	0.5	Cor16
J14294+155		Ross 130	M2.0 V	PMSU	14:29:29.72	+15:31:57.9	2MASS	14.0	0.4	HIP2
J14299+295	..F	G 166-033	M4.0 V	PMSU	14:29:59.56	+29:34:02.9	2MASS	27.2	1.4	Dit14
J14306+597	..F	LP 098-079	M6.5 V	Jen09	14:30:37.88	+59:43:24.9	2MASS	9.6	0.1	vAl95
J14307-086		BD-07 3856	M0.5 V	Gra03	14:30:47.79	-08:38:46.6	2MASS	16.99	0.42	HIP2
J14310-122		Wolf 1478	M3.5 V	PMSU	14:31:01.20	-12:17:45.2	2MASS	10.8	0.5	HIP2
J14312+754	..F	2MASS J14311348+7526423	M4.0 V	AF15	14:31:13.49	+75:26:42.4	2MASS	14.5	0.6	Dit14
J14320+738	..f	G 255-055	M2.0 V	Lep13	14:32:02.73	+73:49:25.3	2MASS	19.1	0.4	Cor16
J14321+081	..f	LP 560-035	M6.0 V	New14	14:32:08.50	+08:11:31.3	2MASS	9.2	0.6	Cor16
J14321+160	..f	LP 440-038	M4.0 V	PMSU	14:32:10.79	+16:00:49.5	2MASS	16.5	0.6	Cor16
J14322+496	..F	LP 174-355	M3.5 V	PMSU	14:32:14.54	+49:39:05.8	2MASS	17.2	0.5	Dit14
J14331+610	B.f	G 224-013	M2.5 V+	Lep13	14:33:06.38	+61:00:44.5	2MASS	16.8	0.4	Cor16
J14342-125		HN Lib	M4.0 V	PMSU	14:34:16.83	-12:31:10.7	2MASS	6.06	0.08	HIP2
J14366+143	..F	StKM 1-1170	M1.0 V	Lep13	14:36:38.91	+14:21:52.2	2MASS	30.7	0.4	Cor16
J14368+583	S.f	LP 098-132	M2.5 V+	PMSU	14:36:53.02	+58:20:55.0	2MASS	16.1	0.4	Cor16
J14371+756	..F	LSPM J1437+7536N	M2.0 V	Lep13	14:37:09.23	+75:36:57.2	2MASS	24.1	0.5	Cor16
J14376+677	..F	G 239-022	M1.5 V	Lep13	14:37:39.99	+67:45:31.6	2MASS	30.9	0.5	Cor16
J14388+422	..F	GPM219.718548+42.229288	M1.5 V	Lep13	14:38:51.87	+42:13:44.5	2MASS	29.2	0.5	Cor16
J14415+064	..F	LP 560-066	M1.5 V	Lep13	14:41:33.02	+06:27:46.4	2MASS	27.78	3.64	HIP2
J14423+660	B..	G 239-025	M2.0 V+	Lep13	14:42:21.65	+66:03:20.8	2MASS	10.73	0.15	HIP2
J14438+667	..F	NLTT 38291	M1.0 V	Lep13	14:43:51.32	+66:44:32.7	2MASS	34.6	0.4	Cor16
J14469+170	..F	Ross 994	M1.5 V	Lep13	14:46:59.88	+17:05:09.1	2MASS	30.75	3.98	HIP2
J14472+570	..F	RX J1447.2+5701	M4.0 V	AF15	14:47:13.54	+57:01:55.1	2MASS	22.0	0.9	Cor16
J14485+101	..F	G 066-027	M3.5 V	AF15	14:48:33.16	+10:06:57.4	2MASS	21.9	0.7	Cor16
J14501+323	..F	LP 326-034	M3.5 V	AF15	14:50:11.12	+32:18:17.3	2MASS	18.8	0.6	Cor16
J14511+311	V..	LP 326-038	M4.0 V	Lep13	14:51:10.44	+31:06:40.7	2MASS	12.5	0.5	Dit14
J14524+123		G 066-037	M2.0 V	PMSU	14:52:28.54	+12:23:33.0	2MASS	17.6	0.3	Cor16
J14525+001	..F	G 066-036	M2.0 V	PMSU	14:52:32.17	+00:10:07.9	2MASS	28.4	0.6	Cor16
J14538+235	B..	Ross 52	M3.5 V+	PMSU	14:53:51.44	+23:33:20.8	2MASS	10.2	0.5	HIP2
J14544+161	B..	CE Boo A	M1.0 V:	AF15	14:54:29.23	+16:06:04.0	2MASS	9.6	0.2	HIP2
J14544+355		Ross 1041	M3.5 V	PMSU	14:54:27.91	+35:32:57.0	2MASS	18.7	3.8	vAl95
J14548+099	..F	Ross 1028b	M1.0 V	PMSU	14:54:53.47	+09:56:36.4	2MASS	24.52	1.49	HIP2

Table B.2: Names, spectral types, distances and astrometric parameters of Carmencita stars (continued).

Karmn	Flags[a]	Name	SpT	Ref.[b]	α (J2000)	δ (J2000)	Ref.[c]	d [pc]	ed [pc]	Ref.[d e]
J14549+411	..F	LP 222-015	M4.5 V	PMSU	14:54:54.97	+41:08:48.1	2MASS	79.4	12.0	Dit14
J14557+072	..F	G 066-042	M0.5 V	Lep13	14:55:47.99	+07:17:51.6	2MASS	34.66	3.45	HIP2
J14564+168	..F	G 136-035	M1.5 V	Lep13	14:56:28.09	+16:48:34.3	2MASS	31.5	0.5	Cor16
J14574-214	Bm.	KX Lib BC	M1.0 V+	PMSU	14:57:27.88	-21:24:52.7	2MASS	5.84	0.03	aHIP2
J14575+313	B.f	Ross 53 AB	M2.0 V+	Jen09	14:57:32.28	+31:23:44.6	2MASS	38.82	6.51	HIP2
J14578+566	..F	GJ 1187	M5.5 V	PMSU	14:57:53.75	+56:39:24.2	2MASS	9.9	0.5	Dit14
J15009+454	B..	BD+45 2247	M0.5 V+	Lep13	15:00:55.57	+45:25:34.3	2MASS	11.79	0.15	HIP2
J15011+071	..f	Ross 1030a	M3.5 V	PMSU	15:01:10.74	+07:09:47.7	2MASS	15.2	0.5	Cor16
J15011+354	..F	Ross 1042	M1.5 V	PMSU	15:01:11.76	+35:27:15.2	2MASS	27.6	0.4	Cor16
J15013+055		G 015-002	M3.0 V	PMSU	15:01:20.11	+05:32:55.4	2MASS	15.4	0.4	Cor16
J15018+550	..F	LP 135-097	M3.5 V	PMSU	15:05:49.51	+55:04:43.1	2MASS	19.6	0.7	Cor16
J15030+704	..F	LP 041-431	M3.0 V	Lep13	15:03:02.44	+70:26:07.5	2MASS	19.8	0.6	Cor16
J15043+294	..F	GJ 575.1	M2.5 V	PMSU	15:04:22.25	+29:28:42.6	2MASS	21.9	6.8	vAl95
J15043+603	..f	Ross 1051	M1.0 V	PMSU	15:04:18.56	+60:23:04.4	2MASS	17.85	0.42	HIP2
J15049-211	.mF	LP 801-053	M4.5 V	PMSU	15:04:58.35	-21:07:00.3	2MASS	20.1	0.9	Cor16
J15060+453	..F	HAT 147-00476	M1.5 V	Lep13	15:06:02.84	+45:21:52.3	2MASS	32.1	0.5	Cor16
J15073+249	..f	BD+25 2874	M0.0 V	Lep13	15:07:23.62	+24:56:07.6	2MASS	16.7	1.0	vAl95
J15079+762	..f	LSPM J1507+7613	M4.5 V	AF15	15:07:57.24	+76:13:59.0	2MASS	28.8	0.5	aHIP2
J15081+623	B.f	LSPM J1508+6221	M4.0 V+	AF15	15:08:11.93	+62:21:53.6	2MASS	16.6	0.6	Cor16
J15095+031		Ross 1047	M3.0 V	PMSU	15:09:35.59	+03:10:00.8	2MASS	14.4	0.5	HIP2
J15100+193	..f	G 136-072	M4.0 V	PMSU	15:10:04.81	+19:21:28.7	2MASS	17.0	0.8	Dit14
J15118-102	..F	G 151-034	M4.5 V	PMSU	15:11:50.66	-10:14:17.8	2MASS	14.8	0.7	vAl95
J15119+179	..F	LP 442-017	M3.5 V	PMSU	15:11:56.02	+17:57:17.5	2MASS	23.5	1.7	vAl95
J15126+457	B..	G 179-020	M4.0 V+	PMSU	15:12:38.18	+45:43:46.4	2MASS	18.5	1.2	Dit14
J15147+645	..F	G 224-057	M3.5 V	AF15	15:14:46.81	+64:33:43.9	2MASS	17.5	0.3	Dit14
J15151+333	..F	LP 272-063	M2.0 V	AF15	15:15:07.06	+33:18:03.3	2MASS	31.2	0.6	Cor16
J15156+638	..F	2MASS J15153756+6349528	M1.5 V	Lep13	15:15:37.56	+63:49:52.8	2MASS	32.0	0.5	Cor16
J15166+391	..F	LP 222-065	M6.5 V	Met15	15:16:40.73	+39:10:48.7	2MASS	15.6	0.7	Dit14
J15188+292	..F	StKM 1-1229	M1.0 V	Lep13	15:18:49.85	+29:15:07.4	2MASS	30.0	0.4	Cor16
J15191-127	B..	LP 742-061	M4.0 V+	PMSU	15:19:11.82	-12:45:06.2	2MASS	21.12	1.64	Wein16
J15193+678	..F	LP 068-073	M3.0 V	PMSU	15:19:18.70	+67:51:17.1	2MASS	27.3	0.8	Cor16
J15194-077		HO Lib	M3.0 V	PMSU	15:19:26.89	-07:43:20.1	2MASS	6.2	0.1	HIP2
J15197+046	..F	2MASS J15194584+0439344	M4.0 V	AF15	15:19:45.85	+04:39:34.5	2MASS	18.6	0.7	Cor16

Table B.2: Names, spectral types, distances and astrometric parameters of Carmencita stars (continued).

Karmn	Flags[a]	Name	SpT	Ref.[b]	α (J2000)	δ (J2000)	Ref.[c]	d [pc]	ed [pc]	Ref.[d e]
J15210+309	..F	2MASS J15210067+3057012	M2.5 V	Lep13	15:21:00.68	+30:57:01.2	2MASS	24.2	0.6	Cor16
J15214+042	..F	TYC 344-504-1	M1.5 V	Lep13	15:21:25.30	+04:14:49.3	2MASS	26.1	0.4	Cor16
J15218+209		OT Ser	M1.5 V	PMSU	15:21:52.92	+20:58:39.5	2MASS	11.41	0.23	HIP2
J15219+185	..F	LP 442-037	M1.5 V	Lep13	15:21:56.79	+18:35:51.9	2MASS	33.72	3.97	HIP2
J15238+174	..f	Ross 508	M4.5 V	PMSU	15:23:51.13	+17:27:57.0	2MASS	11.7	0.4	vAl95
J15238+561	..F	StKM 1-1240	M1.0 V	Lep13	15:23:53.86	+56:09:32.0	2MASS	32.5	0.4	Cor16
J15238+584	..F	G 224-065	M4.0 V	AF15	15:23:51.44	+58:28:06.4	2MASS	21.9	0.9	Cor16
J15273+415	..F	TYC 3055-1525-1	M1.5 V	Lep13	15:27:19.22	+41:30:10.6	2MASS	23.9	0.4	Cor16
J15276+408	..F	G 179-029	M1.0 V	Lep13	15:27:39.05	+40:51:57.3	2MASS	32.52	2.44	HIP2
J15280+257	..F	GJ 587.1	M0.0 V	PMSU	15:28:01.31	+25:47:23.9	2MASS	24.55	1.54	HIP2
J15290+467	B.F	RX J1529.0+4646 AB	M4.5 V+	AF15	15:29:02.97	+46:46:24.0	2MASS	18.0	0.8	Cor16
J15297+428	B.F	G 179-033	M4.5 V+	PMSU	15:29:43.93	+42:52:49.9	2MASS	19.5	0.8	Dit14
J15305+094	..f	NLTT 40406	M5.5 V	AF15	15:30:30.33	+09:26:01.4	2MASS	8.1	0.3	Dit14
J15319+288	S.F	G 167-047	M4.5 V+	PMSU	15:31:54.27	+28:51:09.6	2MASS	22.9	1.2	Dit14
J15336+462	..F	LP 176-055	M3.5 V	PMSU	15:33:39.34	+46:15:02.7	2MASS	21.8	1.0	Dit14
J15339+379	B.F	GJ 588.1	M0.5 V+	Lep13	15:33:54.83	+37:54:49.8	2MASS	31.34	1.95	HIP2
J15340+513	..F	LP 135-414	M4.5 V	AF15	15:34:03.87	+51:22:02.4	2MASS	14.9	0.4	Dit14
J15345+142	..F	Ross 512	M4.0 V	PMSU	15:34:30.54	+14:16:18.2	2MASS	20.6	1.4	vAl95
J15349-143	..F	2MASSUCD 11346	M7.0 V	Schm07	15:34:57.04	-14:18:48.7	2MASS	10.96	0.08	Wein16
J15353+177N	..F	Ross 513B	M4.5 V	PMSU	15:35:20.40	+17:43:04.6	2MASS	14.6	0.6	Dit14
J15353+177S	..F	Ross 513A	M2.5 V	PMSU	15:35:20.59	+17:42:47.1	2MASS	14.2	0.4	vAl95
J15357+221	..f	LP 384-018	M3.5 V	PMSU	15:35:46.10	+22:09:03.7	2MASS	18.6	1.2	vAl95
J15368+375	..F	BK CrB	M0.0 V	Lep13	15:36:50.38	+37:34:49.6	2MASS	57.8	5.91	HIP2
J15369-141	.m.	Ross 802	M4.0 V	PMSU	15:36:58.68	-14:08:00.6	2MASS	13.3	0.7	vAl95
J15386+371	..F	G 179-042	M3.5 V	AF15	15:38:37.08	+37:07:24.7	2MASS	29.4	1.0	Weis87
J15400+434N	B..	vB 24 A	M3.0 V	PMSU	15:40:03.53	+43:29:39.7	2MASS	13.5	0.9	vAl95
J15400+434S	B..	vB 24 B	M3.5 V	PMSU	15:40:03.74	+43:29:35.5	2MASS	13.5	0.9	avAl95
J15412+759		UU UMi	M3.0 V	PMSU	15:41:16.43	+75:59:34.8	2MASS	13.3	0.4	HIP2
J15416+184	..F	StKM 1-1264	M1.5 V	Lep13	15:41:37.26	+18:28:08.3	2MASS	53.08	1.1	aHIP2
J15421-194	Sm.	GJ 595 AB	M3.0 V+	PMSU	15:42:06.78	-19:28:16.7	2MASS	10.43	0.61	HIP2
J15474+451	S.f	LP 177-102 AB	M4.0 V+	AF15	15:47:27.44	+45:07:51.2	2MASS	15.0	0.6	Cor16
J15474-108		LP 743-031	M2.0 V	PMSU	15:47:24.64	-10:53:47.1	2MASS	15.1	0.7	HIP2
J15476+226	..F	LSPM J1547+2241	M4.5 V	AF15	15:47:40.71	+22:41:16.5	2MASS	25.1	1.8	Dit14

Table B.2: Names, spectral types, distances and astrometric parameters of Carmencita stars (continued).

Karmn	Flags[a]	Name	SpT	Ref.[b]	α (J2000)	δ (J2000)	Ref.[c]	d [pc]	ed [pc]	Ref.[d e]
J15480+043	..F	RX J1548.0+0421	M2.5 V	AF15	15:48:02.80	+04:21:39.3	2MASS	25.3	0.6	Cor16
J15488+305	..F	2MASS J15484846+3030388	M3.0 V	Lep13	15:48:48.47	+30:30:38.9	2MASS	20.6	0.6	Cor16
J15493+250	..F	G 168-013	M2.0 V	Lep13	15:49:20.40	+25:03:42.3	2MASS	26.9	0.5	Cor16
J15496+348	B..	LP 274-008	M4.0 V+	PMSU	15:49:38.33	+34:48:55.5	2MASS	16.98	1.09	vAl95
J15496+510	..F	G 202-016	M2.0 V	PMSU	15:49:36.26	+51:02:57.3	2MASS	19.1	1.1	HIP2
J15499+796	..f	LP 022-420	M5.0 V	AF15	15:49:55.18	+79:39:51.7	2MASS	12.4	0.8	Dit14
J15501+009	..F	Wolf 587	M2.5 V	PMSU	15:50:11.21	+00:57:32.6	2MASS	21.2	0.5	Cor16
J15512+306	..F	TYC 2572-633-1	M1.5 V	Lep13	15:51:14.86	+30:40:42.2	2MASS	31.7	0.5	Cor16
J15513+295	..F	G 168-014	M3.5 V	PMSU	15:51:21.79	+29:31:06.3	2MASS	15.6	0.8	Dit14
J15531+347N	..f	Ross 806	M2.5 V	PMSU	15:53:06.36	+34:45:13.7	2MASS	19.3	1.4	vAl95
J15531+347S	..F	LP 274-021	M3.5 V	PMSU	15:53:06.64	+34:44:47.4	2MASS	19.3	1.4	avAl95
J15538+641	..F	NLTT 41533	M0.5 V	Lep13	15:53:48.66	+64:09:33.4	2MASS	37.27	2.6	HIP2
J15555+352	B.F	G 180-011 AB	M4.5 V+	PMSU	15:55:31.78	+35:12:02.9	2MASS	28.3	3.0	Dit14
J15557+686	..F	RX J1555.7+6840	M2.5 V	Lep13	15:55:47.25	+68:40:13.9	2MASS	20.4	0.5	Cor16
J15569+376	..F	RX J1556.9+3738	M2.5 V	AF15	15:56:58.24	+37:38:13.8	2MASS	29.8	0.7	Cor16
J15578+090	..f	LSPM J1557+0901	M4.0 V	AF15	15:57:48.27	+09:01:09.9	2MASS	16.5	0.6	Cor16
J15581+494	..F	V1022 Her	M1.0 V	Lep13	15:58:10.28	+49:27:08.4	2MASS	31.5	0.4	Cor16
J15583+354	..f	G 180-018	M3.5 V	PMSU	15:58:18.83	+35:24:23.7	2MASS	15.3	0.5	Cor16
J15587+346	..F	StM 258	M3.5 V	Lep13	15:58:45.68	+34:48:54.9	2MASS	16.1	0.5	Cor16
J15597+440	..F	RX J1559.7+4403	M2.0 V	Lep13	15:59:47.29	+44:03:59.5	2MASS	22.6	0.4	Cor16
J15598-082		BD-07 4156	M1.0 V	PMSU	15:59:53.37	-08:15:11.4	2MASS	13.9	0.36	HIP2
J16008+403	..F	G 180-021	M3.0 V	PMSU	16:00:50.83	+40:19:44.1	2MASS	23.2	0.6	Cor16
J16017+301	..f	G 168-024	M3.0 V	PMSU	16:01:43.60	+30:10:50.2	2MASS	18.4	1.8	Dit14
J16017+304	..F	LP 329-019	M4.5 V	PMSU	16:01:44.53	+30:27:40.8	2MASS	27.4	3.5	Dit14
J16018+304	..F	LP 329-020	M2.5 V	PMSU	16:01:52.63	+30:27:34.7	2MASS	35.6	4.9	Dit14
J16028+205		GJ 609	M4.0 V	PMSU	16:02:50.98	+20:35:21.8	2MASS	10.0	0.3	vAl95
J16033+175	..F	2MASS J16032066+1735546	M2.0 V	Lep13	16:03:20.66	+17:35:54.6	2MASS	26.1	0.5	Cor16
J16043-062	..F	LP 684-017	M4.5 V	PMSU	16:04:19.99	-06:16:45.4	2MASS	16.6	1.2	GJ91
J16046+263	..F	BPM 91242	M0.5 V	Lep13	16:04:36.97	+26:20:43.1	2MASS	27.6	0.3	Cor16
J16048+391	..F	G 180-027	M4.0 V	AF15	16:04:50.93	+39:09:36.0	2MASS	14.52	0.07	aHIP2
J16054+769	..F	G 256-030	M2.5 V	PMSU	16:05:28.21	+76:54:57.2	2MASS	20.8	0.5	Cor16
J16062+290	..F	LP 329-030	M2.0 V	Lep13	16:06:13.64	+29:01:55.4	2MASS	42.6	2.7	Dit14
J16066+083	B.F	GJ 611.3 AB	M0.5 V+	PMSU	16:06:41.18	+08:23:18.2	2MASS	35.5	9.31	HIP2

Table B.2: Names, spectral types, distances and astrometric parameters of Carmencita stars (continued).

Karmn	Flags[a]	Name	SpT	Ref.[b]	α (J2000)	δ (J2000)	Ref.[c]	d [pc]	ed [pc]	Ref.[d e]
J16074+059	..F	G 016-030	M3.5 V	PMSU	16:07:28.20	+05:57:59.4	2MASS	25.3	1.0	Dit14
J16082-104	..F	G 153-027	M4.5 V	PMSU	16:08:14.98	-10:26:13.4	2MASS	21.2	1.2	vAl95
J16090+529	..f	MCC 759	M0.0 V	PMSU	16:09:03.09	+52:56:37.9	2MASS	16.93	0.3	HIP2
J16092+093		G 137-084	M3.0 V	Lep13	16:09:16.25	+09:21:07.7	2MASS	13.1	0.4	Cor16
J16120+033	..f	TYC 371-1053-1	M2.0 V	Lep13	16:12:04.65	+03:18:20.8	2MASS	19.0	0.4	Cor16
J16139+337	B.F	σ CrB Cab	M2.5 V+	AF15	16:13:56.31	+33:46:24.4	2MASS	21.1	0.5	aHIP2
J16144-028	..F	LP 624-054	M6.0 V	PBB06	16:14:25.20	-02:51:00.9	2MASS	16.0	1.1	Cor16
J16145+191	..F	GJ 1200	M3.5 V	PMSU	16:14:32.85	+19:06:10.2	2MASS	16.5	0.6	Dit14
J16147+048	..F	G 017-007	M3.5 V	PMSU	16:14:43.79	+04:52:08.5	2MASS	32.2	3.3	Dit14
J16155+244	..F	LP 385-058	M1.0 V	PMSU	16:15:32.18	+24:27:46.7	2MASS	30.3	0.4	Cor16
J16167+672N		EW Dra	M3.0 V	PMSU	16:16:45.37	+67:15:22.4	2MASS	10.7	0.1	aHIP2
J16167+672S		HD 147379	M0.0 V	AF15	16:16:42.80	+67:14:19.7	2MASS	10.7	0.1	HIP2
J16170+552	B..	CR Dra AB	M1.0 V+	PMSU	16:17:05.37	+55:16:09.4	2MASS	20.53	0.45	HIP2
J16180+062	..F	EXO 161538+0624.2	M3.0 V	Lep13	16:18:04.93	+06:17:11.0	2MASS	20.5	0.6	Cor16
J16204-042	..F	LP 685-051	M0.0 V	PMSU	16:20:24.77	-04:16:02.3	2MASS	33.42	3.0	HIP2
J16220+228	..F	BPS BS 16542-0001	M1.5 V	Lep13	16:22:01.19	+22:50:21.7	2MASS	30.7	0.5	Cor16
J16241+483	B..	GJ 623 AB	M2.5 V+	PMSU	16:24:09.13	+48:21:11.3	2MASS	8.1	0.1	HIP2
J16247+229	..F	BPM 91545	M1.0 V	Lep13	16:24:43.87	+22:54:20.9	2MASS	22.7	0.3	Cor16
J16254+543		GJ 625	M1.5 V	AF15	16:25:24.59	+54:18:14.9	2MASS	6.52	0.04	HIP2
J16255+260	S..	LTT 14889	M3.0 V+	PMSU	16:25:32.35	+26:01:37.9	2MASS	15.9	0.5	Cor16
J16255+323	..F	LP 330-013	M2.0 V	Lep13	16:25:32.80	+32:18:31.3	2MASS	26.7	0.5	Cor16
J16259+834	..F	TYC 4647-2406-1	M1.5 V	Lep13	16:25:58.33	+83:24:24.2	2MASS	27.2	0.4	Cor16
J16268-173	Bmf	LP 805-010	M4.5 V+	PMSU	16:26:48.16	-17:23:33.6	2MASS	15.0	0.7	Cor16
J16280+155	B.F	G 138-033	M2.5 V+	PMSU	16:28:02.06	+15:33:57.6	2MASS	29.3	0.7	Cor16
J16302-146	Bm.	LP 745-051	M3.0 V+	PMSU	16:30:13.14	-14:39:49.5	2MASS	22.4	2.7	HIP2
J16303-126		V2306 Oph	M3.5 V	PMSU	16:30:18.09	-12:39:43.4	2MASS	4.29	0.03	HIP2
J16313+408		G 180-060	M5.0 V	PMSU	16:31:18.79	+40:51:51.6	2MASS	12.0	0.4	Dit14
J16315+175	..F	GJ 1202	M3.5 V	PMSU	16:31:35.08	+17:33:49.5	2MASS	15.5	0.7	Dit14
J16327+126		GJ 1203	M3.0 V	PMSU	16:32:45.25	+12:36:46.0	2MASS	16.8	1.0	HIP2
J16328+098	..F	G 138-040	M3.5 V	PMSU	16:32:52.85	+09:50:26.0	2MASS	13.8	0.4	Dit14
J16342+543	..F	LP 137-037	M1.0 V	Lep13	16:34:13.72	+54:23:39.8	2MASS	31.4	0.4	Cor16
J16343+571	B..	CM Dra Aab	M4.5 V+	PMSU	16:34:20.41	+57:09:43.9	2MASS	14.7	0.9	HD80
J16354+350	B..	LP 275-068	M4.0 V+	PMSU	16:35:27.41	+35:00:57.7	2MASS	16.2	0.7	Dit14

Table B.2: Names, spectral types, distances and astrometric parameters of Carmencita stars (continued).

Karmn	Flags[a]	Name	SpT	Ref.[b]	α (J2000)	δ (J2000)	Ref.[c]	d [pc]	ed [pc]	Ref.[d e]
J16360+088	..F	G 138-043	M4.0 V	PMSU	16:36:05.63	+08:48:49.2	2MASS	15.34	0.99	vAl95
J16395+505	..F	G 202-068	M1.0 V	Lep13	16:39:30.21	+50:34:04.2	2MASS	21.07	0.87	HIP2
J16401+007	..f	LP 625-034	M4.0 V	PMSU	16:40:06.00	+00:42:18.8	2MASS	11.2	0.09	Wein16
J16403+676	..F	LP 069-457	M5.5 V	PMSU	16:40:20.68	+67:36:04.7	2MASS	13.5	0.5	Dit14
J16408+363	..f	Ross 812	M2.0 V	PMSU	16:40:48.92	+36:18:59.6	2MASS	19.2	0.8	HIP2
J16420+192	..F	2MASS J16420074+1916104	M2.5 V	Lep13	16:42:00.75	+19:16:10.5	2MASS	21.4	0.5	Cor16
J16462+164		LP 446-006	M2.5 V	PMSU	16:46:13.72	+16:28:40.7	2MASS	16.1	0.8	HIP2
J16465+345	..F	LP 276-022	M6.0 V	AF15	16:46:31.55	+34:34:55.5	2MASS	11.9	0.1	GC09
J16487+106	B..	LSPM J1648+1038	M2.5 V+	Lep13	16:48:46.58	+10:38:51.7	2MASS	14.3	0.3	Cor16
J16487-157	.mf	LP 806-008	M1.5 Vk:	Gra06	16:48:45.97	-15:44:19.9	2MASS	18.23	0.72	HIP2
J16508-048	..F	[RHG95] 2653	M3.5 V	PMSU	16:50:53.83	-04:50:34.9	2MASS	21.8	0.7	Cor16
J16509+224	..f	G 169-029	M4.5 V	PMSU	16:50:57.95	+22:27:05.8	2MASS	10.0	0.3	Dit14
J16528+630	..F	GSC 04194-01561	M4.5 V	AF15	16:52:49.48	+63:04:39.0	2MASS	12.8	0.6	Dit14
J16529+400	..F	G 203-033	M3.5 V	PMSU	16:52:55.00	+40:05:08.3	2MASS	21.0	0.7	Cor16
J16542+119	..F	Ross 644	M0.0 V	Lep13	16:54:12.02	+11:54:52.9	2MASS	19.47	0.82	Lep13
J16554-083N		GJ 643	M3.5 V	PMSU	16:55:25.27	-08:19:20.8	2MASS	6.2	0.2	aHIP2
J16554-083S	S..	V1054 Oph ABab	M3.0 V+	PMSU	16:55:28.81	-08:20:10.3	2MASS	6.2	0.2	HIP2
J16555-083		vB 8	M7.0 V	AF15	16:55:35.29	-08:23:40.1	2MASS	6.48	0.02	Wein16
J16570-043		LP 686-027	M3.5 V	PMSU	16:57:05.71	-04:20:56.0	2MASS	9.6	1.2	vAl95
J16573+124	..F	LP 506-037	M4.0 V	PMSU	16:57:22.95	+13:28:09.3	2MASS	32.4	1.9	Dit14
J16573+271	..F	2MASS J16572235+2708304	M2.0 V	Fri13	16:57:22.35	+27:08:30.5	2MASS	33.4	0.6	Cor16
J16574+777	..F	G 259-005	M2.5 V	PMSU	16:57:28.79	+77:43:03.6	2MASS	24.4	0.6	Cor16
J16577+132	B.f	GJ 647	M0.0 V+	Lep13	16:57:46.09	+13:17:29.6	2MASS	40.8	3.78	HIP2
J16578+473		BD+47 2415B	M1.5 V	Lep13	16:57:53.58	+47:22:01.6	2MASS	18.3	0.2	aHIP2
J16581+257		BD+25 3173	M1.0 V	PMSU	16:58:08.85	+25:44:39.2	2MASS	10.34	0.15	HIP2
J16584+139	B..	G 139-003	M4.0 V+	PMSU	16:58:25.31	+13:58:10.7	2MASS	17.8	0.7	Dit14
J16587+688	..F	LP 043-338	M1.5 V	Lep13	16:58:43.75	+68:53:52.7	2MASS	28.6	0.4	Cor16
J16591+209	B..	RX J1659.1+2058	M3.5 V+	Lep13	16:59:09.63	+20:58:16.0	2MASS	13.0	0.4	Cor16
J17003+253	..F	LP 587-031	M2.5 V	PMSU	17:00:20.34	+25:21:02.8	2MASS	29.7	0.7	Cor16
J17006+063	..F	G 139-004	M1.0 V	Lep13	17:00:38.67	+06:18:47.1	2MASS	29.5	0.4	Cor16
J17010+082	..F	G 139-005	M3.5 V	PMSU	17:01:02.11	+08:12:26.4	2MASS	17.7	0.5	Dit14
J17027-060	..F	BD-05 4394	M0.0 V	PMSU	17:02:49.59	-06:04:06.4	2MASS	18.93	0.71	HIP2
J17033+514		G 203-042	M4.5 V	PMSU	17:03:23.85	+51:24:21.9	2MASS	9.5	0.2	vAl95

Table B.2: Names, spectral types, distances and astrometric parameters of Carmencita stars (continued).

Karmn	Flags[a]	Name	SpT	Ref.[b]	α (J2000)	δ (J2000)	Ref.[c]	d [pc]	ed [pc]	Ref.[d e]
J17038+321	B..	LP 331-057	M2.0 V+	Dae07	17:03:52.83	+32:11:45.6	2MASS	17.0	0.3	Cor16
J17043+169	..F	G 170-012	M2.5 V	PMSU	17:04:22.34	+16:55:55.2	2MASS	17.2	0.9	vAl95
J17052-050		Wolf 636	M1.5 V	AF15	17:05:13.84	-05:05:38.6	2MASS	10.7	0.1	aHIP2
J17058+260	..F	LP 387-037	M1.5 V	Lep13	17:05:52.59	+26:05:32.3	2MASS	30.5	0.5	Cor16
J17071+215		Ross 863	M3.0 V	PMSU	17:07:07.52	+21:33:14.4	2MASS	13.4	0.5	HIP2
J17076+073	B..	GJ 1210 AB	M5.0 V+	PMSU	17:07:40.84	+07:22:06.6	2MASS	12.2	0.3	Dit14
J17082+516	..F	G 203-044	M1.0 V	Lep13	17:08:12.52	+51:38:04.4	2MASS	32.5	0.4	Cor16
J17095+436	S..	G 203-047 AB	M3.5 V+	PMSU	17:09:31.53	+43:40:53.2	2MASS	7.4	0.1	HIP2
J17098+119	..F	G 139-017	M4.0 V	PMSU	17:09:52.75	+11:55:34.1	2MASS	19.2	0.7	Cor16
J17104+279	..F	StM 336	M2.5 V	Lep13	17:10:25.46	+27:58:40.0	2MASS	24.5	0.6	Cor16
J17115+384		Wolf 654	M3.5 V	PMSU	17:11:34.72	+38:26:34.1	2MASS	12.0	0.3	HIP2
J17118-018	B..	LP 627-009	M3.0 V+	PMSU	17:11:52.34	-01:51:05.7	2MASS	10.2	1.2	HIP2
J17121+456	B..	HD 155876 AB	M3.5 V+	PMSU	17:12:07.80	+45:39:58.8	2MASS	6.0	0.2	HIP2
J17136-084	S..	V2367 Oph	M3.5 V+	PMSU	17:13:40.48	-08:25:14.4	2MASS	18.7	1.7	HIP2
J17146+269	..F	G 170-028	M2.0 V	PMSU	17:14:40.24	+26:55:41.8	2MASS	36.9	4.9	vAl95
J17153+049	..F	GJ 1214	M4.5 V	PMSU	17:15:18.94	+04:57:49.7	2MASS	14.65	0.09	Wein16
J17158+190	B.f	BD+19 3268	M0.5 V+	PMSU	17:15:50.10	+19:00:00.1	2MASS	17.1	0.2	Cor16
J17160+110	..f	BD+11 3149	M1.0 V	PMSU	17:16:00.63	+11:03:27.4	2MASS	17.79	0.72	HIP2
J17166+080		GJ 2128	M2.0 V	PMSU	17:16:40.97	+08:03:30.2	2MASS	14.9	0.6	HIP2
J17177+116	B.F	GJ 1215	M5.0 V+	PMSU	17:17:44.08	+11:40:11.8	2MASS	12.7	0.5	vAl95
J17177-118	..F	LTT 6883	M3.0 V	PMSU	17:17:45.32	-11:48:54.2	2MASS	19.3	0.5	Cor16
J17183+181	B.F	LP 447-038	M3.0 V+	PMSU	17:18:22.44	+18:08:56.5	2MASS	21.5	0.6	Cor16
J17183-017	B.F	MCC 791	M0.0 V+	PMSU	17:18:21.73	-01:46:53.6	2MASS	19.28	0.93	HIP2
J17198+265	J..	V639 Her	M4.5 V	AF15	17:19:52.98	+26:30:02.6	2MASS	11.6	0.5	aHIP2
J17198+417		GJ 671	M2.5 V	PMSU	17:19:52.67	+41:42:51.1	2MASS	12.4	0.2	HIP2
J17199+265	V..	V647 Her	M3.5 V	AF15	17:19:54.22	+26:30:03.0	2MASS	11.6	0.5	HIP2
J17207+492	..F	G 203-063	M4.0 V	PMSU	17:20:46.22	+49:15:22.2	2MASS	16.3	0.8	Dit14
J17219+214	..F	G 170-036	M4.0 V	PMSU	17:21:54.65	+21:25:46.8	2MASS	13.4	0.4	Dit14
J17225+055	..F	2MASS J17223390+0531153	M2.5 V	Lep13	17:22:33.91	+05:31:15.3	2MASS	24.2	0.6	Cor16
J17242-043	..F	LP 687-031	M2.5 V	PMSU	17:24:16.95	-04:21:52.1	2MASS	19.7	0.5	Cor16
J17276+144	..F	GJ 1219	M3.5 V	PMSU	17:27:40.07	+14:29:02.8	2MASS	19.96	1.04	vAl95
J17285+374	..F	Wolf 750	M3.0 V	PMSU	17:28:30.39	+37:27:07.4	2MASS	25.1	0.7	Cor16
J17303+055		BD+05 3409	M0.0 V	PMSU	17:30:22.73	+05:32:54.7	2MASS	9.98	0.11	HIP2

Table B.2: Names, spectral types, distances and astrometric parameters of Carmencita stars (continued).

Karmn	Flags[a]	Name	SpT	Ref.[b]	α (J2000)	δ (J2000)	Ref.[c]	d [pc]	ed [pc]	Ref.[d e]
J17312+820	..F	GJ 1220	M4.0 V	PMSU	17:31:17.25	+82:05:19.8	2MASS	14.1	0.7	vAl95
J17316+047	..F	Wolf 755	M1.5 V	Lep13	17:31:38.16	+01:47:49.7	2MASS	26.5	0.4	Cor16
J17321+504	..F	LP 180-017	M2.5 V	PMSU	17:32:07.83	+50:24:51.0	2MASS	28.1	2.8	vAl95
J17328+543	..F	G 226-064	M2.0 V	Lep13	17:32:53.56	+54:20:12.3	2MASS	27.5	0.5	Cor16
J17338+169		1RXS J173353.5+165515	M5.5 V	Lep13	17:33:53.15	+16:55:12.9	2MASS	11.7	0.4	Dit14
J17340+446	B.f	2MASS J17340562+4447082	M3.5 V+	Lep13	17:34:05.62	+44:47:08.2	2MASS	15.6	0.5	Cor16
J17355+616		BD+61 1678C	M0.5 V	PMSU	17:35:34.46	+61:40:54.0	2MASS	14.19	0.07	aHIP2
J17364+683	B..	BD+68 946 AB	M3.0 V+	AF15	17:36:25.94	+68:20:22.0	2MASS	4.53	0.02	HIP2
J17376+220	..F	G 170-054	M4.0 V	PMSU	17:37:36.48	+22:05:51.0	2MASS	18.6	0.7	Dit14
J17378+185		BD+18 3421	M1.0 V	PMSU	17:37:53.3	+18:35:29.5	2MASS	8.09	0.1	HIP2
J17386+612	..F	[RHG95] 2805	M4.0 V	PMSU	17:38:40.92	+61:13:59.3	2MASS	33.12	2.19	aHIP2
J17388+080	..F	G 139-050	M2.5 V	PMSU	17:38:51.25	+08:01:35.3	2MASS	21.5	0.5	Cor16
J17395+277N	B.F	LTT 15242	M3.0 V+	PMSU	17:39:32.23	+27:46:36.7	2MASS	24.97	1.53	aHIP2
J17395+277S	..F	LP 332-045	M0.5 V	PMSU	17:39:30.70	+27:45:43.8	2MASS	24.97	1.53	HIP2
J17419+407	..F	G 204-025	M1.5 V	Lep13	17:41:57.30	+40:44:40.9	2MASS	36.87	4.3	HIP2
J17421-088	..F	Wolf 1471	M3.0 V	PMSU	17:42:10.79	-08:48:59.9	2MASS	23.1	1.7	vAl95
J17425-166	VmF	GJ 690.1	M2.5 V	PMSU	17:42:32.29	-16:38:23.6	2MASS	19.4	2.0	vAl95
J17430+057	B..	G 140-009 AB	M1.0 V+	PMSU	17:43:00.82	+05:47:21.6	2MASS	19.96	0.99	HIP2
J17431+854	..F	G 259-020	M2.0 V	Lep13	17:43:09.37	+85:26:29.6	2MASS	25.1	0.5	Cor16
J17432-185	.mF	Ross 133	M1.5 V	PMSU	17:43:17.55	-18:31:17.9	2MASS	24.51	7.15	vAl95
J17439+433	B..	GJ 694	M2.5 V+	PMSU	17:43:55.95	+43:22:44.1	2MASS	9.5	0.1	HIP2
J17455+468	B.F	BD+46 2361	M0.0 V+	PMSU	17:45:33.54	+46:51:19.4	2MASS	21.49	0.53	HIP2
J17460+246	..F	LP 389-032	M3.5 V	Klu13	17:46:04.66	+24:39:05.0	2MASS	14.5	0.5	vAl95
J17464+277	B..	mu Her BC	M3.5 V+	AF15	17:46:25.08	+27:43:01.4	2MASS	8.31	0.01	aHIP2
J17464-087	S..	Wolf 1473	M3.5 V+	Bid85	17:46:29.35	-08:42:36.2	2MASS	12.2	0.4	Cor16
J17469+228	..F	StKM 1-1528	M1.0 V	Lep13	17:46:55.96	+22:48:00.1	2MASS	30.7	0.4	Cor16
J17502+237	..F	LP 389-021	M3.5 V	PMSU	17:50:15.13	+23:45:51.1	2MASS	22.32	2.04	vAl95
J17515+147	..F	G 183-006	M3.5 V	PMSU	17:51:30.79	+14:45:30.7	2MASS	26.9	0.9	Dit14
J17521+647	..F	G 227-020	M0.5 V	Lep13	17:52:11.85	+64:46:08.7	2MASS	30.25	1.29	HIP2
J17530+169	B.f	G 183-010	M3.0 V+	PMSU	17:53:00.63	+16:55:02.9	2MASS	18.3	0.5	Cor16
J17542+073		GJ 1222	M4.0 V	PMSU	17:54:17.10	+07:22:44.7	2MASS	15.0	0.4	Dit14
J17547+128	..F	LSPM J1754+1251	M2.0 V	Lep13	17:54:43.32	+12:51:20.6	2MASS	25.1	0.5	Cor16
J17570+157	B..	LP 449-006 AB	M3.0 V+	PMSU	17:57:03.56	+15:46:43.2	2MASS	15.4	0.4	Cor16

Table B.2: Names, spectral types, distances and astrometric parameters of Carmencita stars (continued).

Karmn	Flags[a]	Name	SpT	Ref.[b]	α (J2000)	δ (J2000)	Ref.[c]	d [pc]	ed [pc]	Ref.[d e]
J17572+707	..F	LP 044-162	M7.5 V	Schm07	17:57:15.40	+70:42:01.2	2MASS	19.08	0.4	Lep09
J17578+046		Barnards Star	M3.5 V	AF15	17:57:48.49	+04:41:40.5	2MASS	1.824	0.005	HIP2
J17578+465		G 204-039	M2.5 V	AF15	17:57:50.96	+46:35:18.2	2MASS	14.1	0.4	HIP2
J17589+807	..F	LP 024-152	M3.5 V	Lep13	17:58:56.74	+80:42:43.6	2MASS	21.5	1.2	Dit14
J18010+508	..F	Wolf 1403	M1.5 V	Lep13	18:01:05.58	+50:49:36.9	2MASS	31.0	0.5	Cor16
J18022+642		LP 071-082	M5.0 V	AF15	18:02:16.60	+64:15:44.6	2MASS	8.5	0.3	Dit14
J18027+375	..f	GJ 1223	M5.0 V	PMSU	18:02:46.25	+37:31:04.9	2MASS	12.0	0.6	vAl95
J18031+179	..F	G 183-019	M1.0 V	Lep13	18:03:06.36	+17:54:22.6	2MASS	30.6	0.4	Cor16
J18037+247	..F	Ross 820	M0.0 V	Lep13	18:03:47.73	+25:45:20.3	2MASS	26.6	0.3	Cor16
J18042+359	B.F	BD+35 3145	M0.5 V+	PMSU	18:04:17.59	+35:57:25.9	2MASS	21.16	0.76	HIP2
J18051-030		HD 165222	M1.0 V	PMSU	18:05:07.56	-03:01:52.4	2MASS	7.76	0.09	HIP2
J18063+728	..F	NLTT 46021	M0.0 V	Lep13	18:06:18.09	+72:49:16.3	2MASS	33.0	0.3	Cor16
J18074+184	..F	Wolf 806	M1.0 V	Lep13	18:07:28.27	+18:27:55.5	2MASS	30.3	0.4	Cor16
J18075-159	.m.	GJ 1224	M4.5 V	PMSU	18:07:32.93	-15:57:46.5	2MASS	8.1	0.05	Wein16
J18096+318	..F	LP 334-011	M1.0 V	Lep13	18:09:40.71	+31:52:12.4	2MASS	21.46	1.48	HIP2
J18103+512	..F	Wolf 1412	M2.0 V	Lep13	18:10:23.27	+51:15:52.6	2MASS	28.3	0.5	Cor16
J18109+220	..F	StKM 1-1582	M0.0 V	Lep13	18:10:56.20	+22:01:31.7	2MASS	32.2	0.3	Cor16
J18116+061	..F	NLTT 46076	M3.0 V	Fri13	18:11:36.38	+06:06:27.0	2MASS	23.7	0.7	Cor16
J18131+260		LP 390-016	M4.0 V	AF15	18:13:06.57	+26:01:51.9	2MASS	17.7	0.6	Dit14
J18134+054	..F	LP 569-015 A	M1.5 V	Lep13	18:13:28.18	+05:26:58.4	2MASS	24.7	0.4	Cor16
J18135+055	..F	NLTT 46124	M4.0 V	AF15	18:13:33.16	+05:32:11.9	2MASS	20.0	0.8	Cor16
J18157+189	..F	BD+18 3609	M0.0 V	PMSU	18:15:43.60	+18:56:19.9	2MASS	22.72	1.25	HIP2
J18160+139	..F	BD+13 3578	M0.0 V	Lep13	18:16:02.24	+13:54:48.1	2MASS	18.18	0.55	HIP2
J18163+015	..f	GJ 708.3	M3.0 V	PMSU	18:16:18.20	+01:31:27.8	2MASS	16.64	1.99	vAl95
J18165+048	..f	G 140-051	M5.0 V	New14	18:16:31.54	+04:52:45.6	2MASS	13.0	0.2	Dit14
J18165+455	..f	BD+45 2688	M0.5 V	PMSU	18:16:31.09	+45:33:27.6	2MASS	16.95	0.3	HIP2
J18174+483		TYC 3529-1437-1	M2.0 V	Ria06	18:17:25.14	+48:22:02.4	2MASS	16.1	0.3	Cor16
J18180+387E		G 204-058	M3.0 V	PMSU	18:18:04.28	+38:46:34.2	2MASS	10.7	0.4	Dit14
J18180+387W	..f	G 204-057	M4.0 V	PMSU	18:18:03.46	+38:46:36.0	2MASS	10.4	0.5	Dit14
J18189+661		LP 071-165	M4.5 V	PMSU	18:18:57.26	+66:11:33.2	2MASS	7.2	0.1	Dit14
J18193-057	..F	LP 689-001	M2.0 V	PMSU	18:19:21.26	-05:46:26.9	2MASS	24.2	6.2	vAl95
J18195+420	..F	HAT 153-01130	M1.5 V	Lep13	18:19:34.57	+42:01:37.6	2MASS	29.1	0.4	Cor16
J18209-010	B..	GJ 1226	M3.5 V+	PMSU	18:20:57.21	-01:02:57.4	2MASS	29.3	3.4	Jao05

Table B.2: Names, spectral types, distances and astrometric parameters of Carmencita stars (continued).

Karmn	Flags[a]	Name	SpT	Ref.[b]	α (J2000)	δ (J2000)	Ref.[c]	d [pc]	ed [pc]	Ref.[d e]
J18221+063		Ross 136	M4.0 V	PMSU	18:22:06.71	+06:20:37.7	2MASS	13.4	0.4	Dit14
J18224+620		GJ 1227	M4.0 V	AF15	18:22:27.19	+62:03:02.5	2MASS	8.23	0.15	vAl95
J18227+379	..F	G 205-019	M1.0 V	Lep13	18:22:43.47	+37:57:48.3	2MASS	36.7	3.35	HIP2
J18234+281	B..	Ross 708	M3.5 V+	PMSU	18:23:28.35	+28:10:04.1	2MASS	13.3	0.4	Dit14
J18240+016	..f	G 021-013	M2.0 V	PMSU	18:24:05.18	+01:41:16.1	2MASS	20.5	0.4	Cor16
J18248+282	..F	Ross 710	M1.5 V	Lep13	18:24:52.54	+28:17:21.8	2MASS	34.73	4.92	HIP2
J18250+246	..F	HD 336196	M0.0 V	PMSU	18:25:04.79	+24:38:04.4	2MASS	21.85	0.92	HIP2
J18255+383	..F	G 205-020	M0.0 V	PMSU	18:25:31.94	+38:21:13.7	2MASS	24.78	0.99	HIP2
J18264+113	V.F	G 141-010	M3.5 V	PMSU	18:26:24.59	+11:20:57.5	2MASS	16.9	0.6	Cor16
J18292+638	..F	TYC 4222-2195-1	M1.5 V	Lep13	18:29:12.87	+63:51:10.8	2MASS	28.2	0.4	Cor16
J18296+338	..F	2MASS J18294012+3350130	M3.0 V	Fri13	18:29:40.12	+33:50:13.0	2MASS	30.9	0.9	Cor16
J18312+068	..f	LP 570-092	M1.0 V	Lep13	18:31:16.06	+06:50:09.7	2MASS	18.5	0.2	Cor16
J18319+406		G 205-028	M3.5 V	PMSU	18:31:58.40	+40:41:10.4	2MASS	11.4	0.4	Cor16
J18346+401		LP 229-017	M3.5 V	PMSU	18:34:36.64	+40:07:26.7	2MASS	7.2	2.1	Rei02
J18352+243	..F	G 184-013	M2.5 V	Lep13	18:35:13.55	+24:18:44.5	2MASS	20.4	0.5	Cor16
J18352+414	..F	G 205-029	M1.5 V	PMSU	18:35:17.79	+41:29:14.9	2MASS	17.54	3.14	vAl95
J18353+457		BD+45 2743	M0.5 V	AF15	18:35:18.33	+45:44:37.9	2MASS	15.55	0.23	HIP2
J18354+457	..F	GJ 720 B (vB 9)	M2.5 V	AF15	18:35:27.23	+45:45:40.3	2MASS	13.1	0.5	Dit14
J18356+329		LSR J1835+3259	M8.5 V	Schm07	18:35:37.90	+32:59:54.6	2MASS	5.34	0.1	Dit14
J18358+800	..F	LP 025-002	M3.5 V	PMSU	18:35:51.82	+80:05:39.5	2MASS	14.9	0.5	Dit14
J18362+567	..F	G 227-039	M0.0 V	Lep13	18:36:12.68	+56:44:44.4	2MASS	31.0	0.3	Cor16
J18363+136		Ross 149	M4.0 V	PMSU	18:36:19.23	+13:36:26.2	2MASS	10.5	0.2	Dit14
J18387+047	..F	LP 570-022	M0.5 V	Lep13	18:38:47.83	+04:46:03.1	2MASS	28.5	0.3	Cor16
J18387-144	Bm.	GJ 2138	M2.5 V+	PMSU	18:38:44.75	-14:29:25.0	2MASS	12.9	0.5	HIP2
J18394+690	..F	RX J1839.4+6903	M2.0 V	Lep13	18:39:25.68	+69:03:03.6	2MASS	22.9	0.4	Cor16
J18395+298	..F	LP 335-012	M6.5 V	Rei03	18:39:33.08	+29:52:16.4	2MASS	11.7	0.1	GC09
J18395+301	..F	LP 335-013	M0.0 V	Lep13	18:39:32.13	+30:09:55.2	2MASS	26.35	1.1	HIP2
J18399+334	..F	G 206-037	M3.5 V	PMSU	18:39:59.91	+33:24:53.8	2MASS	20.5	1.1	Dit14
J18400+726	..F	LP 044-334	M6.5 V	AF15	18:40:02.38	+72:40:54.0	2MASS	16.86	0.63	Lep09
J18402-104	..F	Ross 719	M0.0 V	PMSU	18:40:17.84	-10:27:55.0	2MASS	32.8	8.49	HIP2
J18405+595	..F	G 227-043	M2.0 V	Lep13	18:40:35.45	+59:30:49.5	2MASS	25.6	0.5	Cor16
J18409+315	..F	BD+31 3330B	M1.0 V	AF15	18:40:55.19	+31:31:52.1	2MASS	23.54	0.62	aHIP2
J18409-133	.m.	BD-13 5069	M1.0 V	PMSU	18:40:57.33	-13:22:45.6	2MASS	16.35	0.55	HIP2

Table B.2: Names, spectral types, distances and astrometric parameters of Carmencita stars (continued).

Karmn	Flags[a]	Name	SpT	Ref.[b]	α (J2000)	δ (J2000)	Ref.[c]	d [pc]	ed [pc]	Ref.[d e]
J18411+247N	B..	GJ 1230 B	M5.0 V	PMSU	18:41:09.82	+24:47:19.5	2MASS	10.0	0.2	aDit14
J18411+247S	S..	GJ 1230 Aab	M4.5 V+	PMSU	18:41:09.78	+24:47:14.4	2MASS	10.0	0.2	Dit14
J18416+397	..f	G 205-035	M4.0 V	PMSU	18:41:37.42	+39:42:12.3	2MASS	11.5	0.2	Dit14
J18419+318		Ross 145	M3.0 V	PMSU	18:41:59.09	+31:49:49.8	2MASS	11.4	0.3	HIP2
J18427+139	V..	V816 Her	M4.0 V	PMSU	18:42:44.99	+13:54:16.8	2MASS	10.91	0.1	Wein16
J18427+596N	J..	HD 173739	M3.0 V	AF15	18:42:46.66	+59:37:49.9	2MASS	3.57	0.03	HIP2
J18427+596S	J..	HD 173740	M3.5 V	AF15	18:42:46.88	+59:37:37.4	2MASS	3.57	0.03	aHIP2
J18432+253	..F	TYC 2112-920-1	M1.0 V	Lep13	18:43:14.46	+25:22:46.5	2MASS	32.1	0.4	Cor16
J18433+406	..F	V492 Lyr	M8.0 V	Schm07	18:43:22.14	+40:40:21.1	2MASS	14.1	0.2	vAl95
J18451+063	..f	TYC 460-624-1	M1.0 V	Lep13	18:45:10.27	+06:20:15.8	2MASS	19.2	0.2	Cor16
J18453+188	..f	G 184-024	M4.0 V	AF15	18:45:22.94	+18:51:58.5	2MASS	12.8	0.2	Dit14
J18480-145	.mF	G 155-042	M2.5 V	PMSU	18:48:01.29	-14:34:50.8	2MASS	18.5	0.4	Cor16
J18482+076		G 141-036	M5.0 V	AF15	18:48:17.52	+07:41:21.0	2MASS	7.17	0.15	Dit14
J18487+615	..F	LSPM J1848+6135	M2.0 V	Lep13	18:48:46.69	+61:35:07.5	2MASS	27.9	0.5	Cor16
J18499+186	..F	G 184-031	M4.5 V	AF15	18:49:54.49	+18:40:29.5	2MASS	13.9	0.6	Cor16
J18500+030	..F	Ross 142	M0.5 V	PMSU	18:50:00.83	+03:05:17.4	2MASS	21.24	0.96	HIP2
J18507+479	..f	G 205-038	M3.5 V	PMSU	18:50:45.21	+47:58:19.5	2MASS	15.2	0.5	Cor16
J18515+027	..F	BD+02 3698	M0.5 V	Lep13	18:51:35.78	+02:46:23.9	2MASS	30.0	0.3	Cor16
J18516+244	..F	G 184-036	M3.0 V	PMSU	18:51:40.84	+24:27:32.2	2MASS	20.3	0.6	Cor16
J18518+165	..f	HD 229793	M0.0 V	PMSU	18:51:51.18	+16:34:59.9	2MASS	15.48	0.39	HIP2
J18519+130	..F	2MASS J18515965+1300034	M2.0 V	Lep13	18:51:59.66	+13:00:03.4	2MASS	21.0	0.4	Cor16
J18534+028	..F	G 141-046	M2.5 V	Lep13	18:53:25.37	+02:50:49.0	2MASS	22.8	0.5	Cor16
J18548+008	..F	BD+00 4050	M0.0 V	Lep13	18:54:53.21	+00:51:47.0	2MASS	23.9	0.2	Cor16
J18548+109	B..	V1436 Aql B	M3.5 V	PMSU	18:54:53.81	+10:58:43.5	2MASS	19.2	4.1	aJen63
J18554+084	S..	V1285 Aql AB	M3.0 V+	PMSU	18:55:27.41	+08:24:09.0	2MASS	11.8	0.2	HIP2
J18563+544	..F	G 229-019	M2.0 V	PMSU	18:56:18.22	+54:29:51.0	2MASS	46.5	3.5	aHIP2
J18564+463	..F	G 205-047	M4.0 V	PMSU	18:56:26.29	+46:22:53.2	2MASS	15.3	0.5	Dit14
J18571+075	..F	LP 571-080	M2.0 V	PMSU	18:57:10.54	+07:34:17.1	2MASS	20.8	0.4	Cor16
J18576+535	B.f	LP 141-012	M3.5 V+	Lep13	18:57:37.94	+53:31:14.1	2MASS	16.8	0.6	Cor16
J18580+059		BD+05 3993	M0.5 V	PMSU	18:58:00.14	+05:54:29.7	2MASS	10.91	0.18	HIP2
J18596+079	..F	BD+07 3922	M0.0 V	PMSU	18:59:38.60	+07:59:14.0	2MASS	25.97	1.55	HIP2
J19025+704	..F	LP 045-128	M2.5 V	PMSU	19:02:30.88	+70:25:50.2	2MASS	24.2	0.6	Cor16
J19032+034	..f	G 141-057	M3.0 V	Lep13	19:03:13.61	+03:24:02.8	2MASS	18.0	0.5	Cor16

Table B.2: Names, spectral types, distances and astrometric parameters of Carmencita stars (continued).

Karmn	Flags[a]	Name	SpT	Ref.[b]	α (J2000)	δ (J2000)	Ref.[c]	d [pc]	ed [pc]	Ref.[d e]
J19032+639	B..	StKM 1-1676	M3.5 V+	Lep13	19:03:17.29	+63:59:34.1	2MASS	10.0	0.3	Cor16
J19032-135	.mF	LP 751-001	M4.0 V	PMSU	19:03:16.64	-13:34:05.1	2MASS	19.08	1.38	vAl95
J19041+211	..F	1RXS J190405.9+2110	M2.0 V	Lep13	19:04:06.12	+21:10:31.6	2MASS	25.3	0.5	Cor16
J19044+590	V..	LSPM J1907+5905	M3.0 V	Lep13	19:07:24.83	+59:05:09.5	2MASS	16.3	0.5	Cor16
J19045+240	..F	TYC 2122-1204-1	M2.0 V	Lep13	19:04:31.42	+24:01:54.5	2MASS	25.7	0.5	Cor16
J19070+208		Ross 730	M2.0 V	AF15	19:07:05.56	+20:53:16.8	2MASS	8.51	0.16	HIP2
J19072+208		HD 349726	M2.0 V	PMSU	19:07:13.20	+20:52:37.3	2MASS	8.51	0.16	aHIP2
J19077+325	B..	GJ 747 AB	M3.0 V+	PMSU	19:07:42.83	+32:32:39.7	2MASS	8.2	0.2	vAl95
J19082+265	..F	G 207-018	M4.5 V	PMSU	19:08:15.77	+26:35:05.5	2MASS	17.3	1.0	vAl95
J19084+322		G 207-019	M3.0 V	PMSU	19:08:29.96	+32:16:52.0	2MASS	12.7	0.4	Cor16
J19093+382	B.F	StKM 1-1680	M1.0 V+	PMSU	19:09:19.19	+39:12:03.7	2MASS	22.2	0.3	Cor16
J19093-147	.mF	Ross 727	M2.5 V	PMSU	19:09:19.89	-14:44:55.2	2MASS	21.4	4.8	vAl95
J19095+391	..F	TYC 3120-1055-1	M2.0 V	Lep13	19:09:31.71	+39:10:51.5	2MASS	26.4	0.5	Cor16
J19098+176		GJ 1232	M4.5 V	PMSU	19:09:50.98	+17:40:07.4	2MASS	10.3	0.3	Dit14
J19106+015	..F	G 022-017	M1.5 V	Lep13	19:10:38.55	+01:32:10.5	2MASS	37.6	3.7	Dit14
J19116+050	..F	TYC 471-1564-1	M1.0 V	Lep13	19:11:47.79	+05:00:36.0	2MASS	27.2	0.4	Cor16
J19122+028	B..	Wolf 1062 AB	M3.5 V+	PMSU	19:12:14.55	+02:53:11.2	2MASS	10.2	0.3	HIP2
J19124+355	..F	G 207-022	M2.5 V	PMSU	19:12:29.38	+35:33:52.6	2MASS	17.2	0.8	vAl95
J19146+193N	V..	Ross 733	M3.5 V	PMSU	19:14:39.26	+19:19:02.6	2MASS	19.08	1.07	HIP2
J19146+193S	..F	Ross 734	M3.5 V	PMSU	19:14:39.32	+19:18:21.9	2MASS	19.08	1.07	aHIP2
J19169+051N		V1428 Aql	M2.5 V	AF15	19:16:55.26	+05:10:08.6	2MASS	5.87	0.03	HIP2
J19169+051S		V1298 Aql (vB 10)	M8.0 V	AF15	19:16:57.62	+05:09:02.2	2MASS	5.95	0.02	Wein16
J19185+580	..F	LSPM J1918+5803	M1.0 V	Lep13	19:18:30.37	+58:03:13.9	2MASS	35.3	0.5	Cor16
J19205-076	B..	GJ 754.1B	M2.5 V	PMSU	19:20:33.46	-07:39:43.6	2MASS	10.9	0.5	aHIP2
J19215+425	B.f	LSPM J1921+4230	M2.0 V+	Lep13	19:21:32.10	+42:30:52.1	2MASS	23.9	0.5	Cor16
J19216+208		GJ 1235	M4.5 V	PMSU	19:21:38.68	+20:52:02.8	2MASS	10.3	0.2	Dit14
J19218+286	..F	V2078 Cyg	M1.5 V	PMSU	19:21:51.34	+28:39:57.9	2MASS	22.42	1.72	HIP2
J19220+070	V.f	GJ 1236	M3.0 V	PMSU	19:22:02.07	+07:02:31.0	2MASS	10.54	0.15	Wein16
J19228+307	..F	GSC 02654-01527	M0.0 V	Lep13	19:22:48.71	+30:45:12.1	2MASS	24.7	0.2	Cor16
J19234+666	..F	NLTT 47788	M1.0 V	Lep13	19:23:25.06	+66:39:52.6	2MASS	33.5	0.4	Cor16
J19237+797	..F	2MASS J19234595+7944372	M1.5 V	Lep13	19:23:45.96	+79:44:37.2	2MASS	29.4	0.5	Cor16
J19242+755	..F	GJ 1238	M5.5 V	PMSU	19:24:16.34	+75:33:12.1	2MASS	11.1	0.6	vAl95
J19242+797	..F	TYC 4592-101-1	M1.0 V	Lep13	19:24:15.17	+79:43:36.7	2MASS	30.6	0.4	Cor16

Table B.2: Names, spectral types, distances and astrometric parameters of Carmencita stars (continued).

Karmn	Flags[a]	Name	SpT	Ref.[b]	α (J2000)	δ (J2000)	Ref.[c]	d [pc]	ed [pc]	Ref.[d e]
J19251+283		Ross 164	M3.0 V	PMSU	19:25:08.46	+28:21:13.2	2MASS	16.2	0.5	Cor16
J19255+096	..f	LSPM J1925+0938	M8.0 V	New14	19:25:30.89	+09:38:23.5	2MASS	14.4	0.6	Dit14
J19260+244	..F	G 185-023	M4.5 V	AF15	19:26:01.61	+24:26:17.0	2MASS	18.0	0.4	Dit14
J19268+167	..F	LTT 15678	M3.0 V	PMSU	19:26:49.37	+16:43:01.9	2MASS	21.0	0.6	Cor16
J19284+289	..F	TYC 2137-1575-1	M0.0 V	Lep13	19:28:25.52	+28:54:10.3	2MASS	26.6	0.3	Cor16
J19289+066	..F	2MASS J19285563+0638259	M1.5 V	Lep13	19:28:55.63	+06:38:25.9	2MASS	31.8	0.5	Cor16
J19312+361	S.F	G 125-015	M4.5 V+	AF15	19:31:12.56	+36:07:30.1	2MASS	15.2	0.7	Dit14
J19326+005	..F	GJ 761.2	M0.0 V	Lep13	19:32:37.91	+00:34:39.0	2MASS	22.5	0.87	HIP2
J19336+395	..F	Ross 1063	M1.5 V	PMSU	19:33:39.41	+39:31:37.3	2MASS	21.4	0.3	Cor16
J19346+045		BD+04 4157	M0.0 V	Kir91	19:34:39.82	+04:34:57.2	2MASS	14.43	0.32	HIP2
J19349+532	..F	Wolf 1108	M2.5 V	PMSU	19:34:54.97	+53:15:22.9	2MASS	13.9	1.4	vAl95
J19351+084N	..F	GJ 4114 B	M2.5 V	PMSU	19:35:06.37	+08:27:44.4	2MASS	15.77	1.14	aHIP2
J19351+084S	B..	GJ 4114 Aab	M0.0 V+	PMSU	19:35:06.29	+08:27:38.9	2MASS	15.77	1.14	HIP2
J19354+377	S..	RX J1935.4+3746	M3.5 V+	Lep13	19:35:29.23	+37:46:08.2	2MASS	9.1	0.3	Cor16
J19358+413	..F	BD+40 3796	M0.0 V	Lep13	19:35:51.44	+41:19:07.9	2MASS	21.6	0.2	Cor16
J19395+718	..F	BD+71 8595	M0.0 V	PMSU	19:39:32.89	+71:52:19.2	2MASS	22.25	0.64	HIP2
J19419+031	..F	GJ 1242	M2.0 V	PMSU	19:41:54.22	+03:09:16.3	2MASS	23.2	1.4	vAl95
J19420-210	S..	LP 869-019	M4.0 V+	Sch05	19:42:00.66	-21:04:05.2	2MASS	18.63	0.22	Wein16
J19422-207	..f	2MASS J19421282-2045477	M5.1 V	Shk09	19:42:12.82	-20:45:47.8	2MASS	15.78	0.27	Ried14
J19457+271	B..	Ross 165 AB	M4.0 V+	PMSU	19:45:45.49	+27:07:31.8	2MASS	11.8	0.3	Dit14
J19457+323	..f	LP 337-003	M1.0 V	PMSU	19:45:49.69	+32:23:13.2	2MASS	11.49	0.99	HIP2
J19463+320	J..	BD+31 3767A	M0.5 V	PMSU	19:46:23.86	+32:01:02.1	2MASS	13.61	0.33	HIP2
J19464+320	J..	BD+31 3767B	M2.5 V	Kir91	19:46:24.15	+32:00:58.6	2MASS	13.61	0.33	aHIP2
J19468-019	..f	2MASS J19465050-0157397	M3.0 V	Rei07	19:46:50.51	-01:57:39.7	2MASS	16.8	0.5	Cor16
J19470+352	..F	LSPM J1947+3516	M2.0 V	Lep13	19:47:03.46	+35:16:57.5	2MASS	26.3	0.5	Cor16
J19486+359	..F	G 125-034	M3.5 V	Lep13	19:48:40.81	+35:55:17.8	2MASS	14.4	0.5	Dit14
J19500+325	B.f	LP 338-002	M2.5 V+	PMSU	19:50:02.53	+32:35:01.3	2MASS	17.01	0.98	vAl95
J19502+317	..F	LP 338-004	M2.5 V	PMSU	19:50:15.93	+31:46:59.9	2MASS	26.7	0.6	Cor16
J19510+104	..F	*o* Aql B	M3.5 V	PMSU	19:51:00.68	+10:24:40.1	2MASS	19.19	0.11	aHIP2
J19511+464		G 208-042	M4.0 V	PMSU	19:51:09.31	+46:28:59.9	2MASS	11.9	0.3	vAl95
J19512+622	..F	G 260-035	M2.0 V	Lep13	19:51:12.06	+62:17:11.8	2MASS	21.0	0.4	Cor16
J19535+341	..F	LP 282-007	M1.5 V	PMSU	19:53:32.71	+34:08:28.2	2MASS	23.6	0.4	Cor16
J19539+444E	J..	GJ 1245 C	M5.5 V	AF15	19:53:55.09	+44:24:55.0	2MASS	4.4	0.1	Dit14

Table B.2: Names, spectral types, distances and astrometric parameters of Carmencita stars (continued).

Karmn	Flags[a]	Name	SpT	Ref.[b]	α (J2000)	δ (J2000)	Ref.[c]	d [pc]	ed [pc]	Ref.[d e]
J19539+444W	B..	V1581 Cyg AB	M5.5 V+	AF15	19:53:54.43	+44:24:54.2	2MASS	4.56	0.03	HD80
J19540+325	..F	G 125-043	M2.0 V	PMSU	19:54:02.64	+32:33:52.8	2MASS	27.7	0.5	Cor16
J19546+202	..F	TYC 1624-397-1	M0.0 V	Lep13	19:54:37.56	+20:13:06.5	2MASS	27.2	0.3	Cor16
J19558+512	..F	Wolf 1122	M1.0 V	PMSU	19:55:52.85	+51:16:22.0	2MASS	24.74	1.47	HIP2
J19564+591	..F	BD+58 2015B	M3.5 V	AF15	19:56:24.90	+59:09:21.7	2MASS	31.67	1.82	aHIP2
J19565+591	..F	BD+58 2015A	M0.0 V	AF15	19:56:34.01	+59:09:42.1	2MASS	31.67	1.82	HIP2
J19573-125	..F	HD 188807 B	M5.0 V	PMSU	19:57:23.81	-12:33:49.9	2MASS	18.7	0.4	aHIP2
J19582+020	..F	LP 634-002	M2.5 V	PMSU	19:58:15.72	+02:02:15.2	2MASS	15.8	0.9	vAl95
J19582+650	..f	G 260-038	M3.5 V	Lep13	19:58:16.51	+65:02:18.4	2MASS	21.2	0.8	Dit14
J20005+593	B.F	2MASS J20003177+5921289	M4.1 V+	Shk09	20:00:31.78	+59:21:29.0	2MASS	18.6	0.7	Cor16
J20011+002	..f	NLTT 48567	M2.0 V	Lep13	20:01:06.15	+00:16:15.5	2MASS	18.8	0.4	Cor16
J20034+298	..F	HD 190360 B	M4.5 V	AF15	20:03:26.52	+29:52:00.1	2MASS	14.0	0.3	Dit14
J20037+644	..F	TYC 4240-978-1	M0.0 V	Lep13	20:03:47.81	+64:25:47.1	2MASS	29.8	0.3	Cor16
J20038+059	..F	GJ 1248	M1.5 V	PMSU	20:03:50.98	+05:59:44.0	2MASS	13.6	0.4	Dit14
J20039-081	..f	LP 694-016	M4.0 V	PMSU	20:03:58.92	-08:07:47.3	2MASS	15.7	0.6	Cor16
J20050+544	S.F	V1513 Cyg	M1.0 V+*	Lep13	20:05:02.28	+54:26:03.8	2MASS	15.83	0.96	HIP2
J20057+529	..F	Wolf 1131	M3.5 V	PMSU	20:05:44.25	+52:58:18.1	2MASS	19.7	0.7	Dit14
J20079-015	..F	G 024-005	M3.0 V	PMSU	20:07:57.52	-01:32:27.8	2MASS	27.5	0.8	Cor16
J20082+333	..F	GJ 1250	M4.5 V	PMSU	20:08:17.86	+33:18:12.2	2MASS	21.6	2.5	vAl95
J20093-012		2MASS J20091824-0113377	M5.0 V	AF15	20:09:18.24	-01:13:37.7	2MASS	10.42	0.17	Ried14
J20105+065	S..	LSPM J2010+0632	M3.5 V+	Shk10	20:10:34.45	+06:32:14.0	2MASS	15.6	0.3	Dit14
J20112+161	..F	BD+15 4074B	M4.0 V	AF15	20:11:13.29	+16:11:07.5	2MASS	18.0	0.9	Dit14
J20112+379	..F	LSPM J2011+3757	M1.5 V	Lep13	20:11:12.63	+37:57:50.2	2MASS	26.6	0.4	Cor16
J20129+342	..F	LP 283-004	M1.0 V	Lep13	20:12:54.93	+34:16:39.7	2MASS	24.8	0.3	Cor16
J20132+029	..F	[R78b] 440	M1.0 V	Lep13	20:13:12.83	+02:56:02.1	2MASS	36.48	2.28	Lep13
J20138+133	..F	Ross 754	M1.0 V	Lep13	20:13:51.78	+13:23:19.8	2MASS	26.15	1.83	HIP2
J20139+066	..F	LP 574-001	M3.5 V	PMSU	20:13:58.98	+06:41:16.1	2MASS	22.4	0.9	vAl95
J20151+635	..F	LP 106-240	M0.0 V	Lep13	20:15:09.88	+63:31:12.7	2MASS	31.5	0.3	Cor16
J20165+351	..F	G 210-011	M2.0 V	Lep13	20:16:32.16	+35:10:42.9	2MASS	27.2	0.5	Cor16
J20187+158	..f	LTT 15944	M2.5 V	PMSU	20:18:44.54	+15:50:46.4	2MASS	16.8	0.4	Cor16
J20195+080	..F	LTT 15948	M3.0 V	PMSU	20:19:34.48	+08:00:29.9	2MASS	22.9	0.6	Cor16
J20198+229		LP 395-008	M3.0 V	Lep13	20:19:49.25	+22:56:36.7	2MASS	14.3	0.4	Cor16
J20220+216	..F	TYC 1643-120-1	M2.0 V	Lep13	20:22:01.62	+21:47:21.9	2MASS	25.2	0.5	Cor16

Table B.2: Names, spectral types, distances and astrometric parameters of Carmencita stars (continued).

Karmn	Flags[a]	Name	SpT	Ref.[b]	α (J2000)	δ (J2000)	Ref.[c]	d [pc]	ed [pc]	Ref.[d e]
J20223+322	..F	2MASS J20221862+3217154	M3.5 V	Lep13	20:22:18.62	+32:17:15.4	2MASS	16.1	0.5	Cor16
J20229+106	..F	NLTT 49159	M3.0 V	PB97	20:22:56.19	+10:40:50.6	2MASS	27.3	1.4	Dit14
J20232+671	B.F	NLTT 49224	M5.0 V+	Law08	20:23:17.90	+67:10:09.7	2MASS	20.7	1.2	Dit14
J20260+585		Wolf 1069	M5.0 V	PMSU	20:26:05.29	+58:34:22.5	2MASS	9.3	0.3	vAl95
J20269+275	..F	G 186-027	M2.0 V	PMSU	20:26:56.29	+27:30:57.9	2MASS	25.4	0.5	Cor16
J20287-114	V..	L 755-019	M3.0 V	Ried14	20:28:43.62	-11:28:30.8	2MASS	18.8	0.6	Ried14
J20298+096	B..	HU Del AB	M4.5 V+	PMSU	20:29:48.34	+09:41:20.2	2MASS	7.45	0.21	Dit14
J20301+798	S..	GSC 04593-01344	M3.0 V+	Lep13	20:30:07.11	+79:50:46.8	2MASS	16.5	0.5	Cor16
J20305+654		GJ 793	M2.5 V	PMSU	20:30:32.08	+65:26:58.6	2MASS	7.99	0.07	HIP2
J20314+385	B.f	Ross 188	M4.0 V+	PMSU	20:31:25.61	+38:33:43.2	2MASS	14.5	0.3	Dit14
J20336+617		GJ 1254	M4.0 V	PMSU	20:33:40.31	+61:45:13.6	2MASS	15.9	0.7	vAl95
J20337+233	B.F	G 186-029	M3.0 V+	PMSU	20:33:42.76	+23:22:13.8	2MASS	22.1	0.6	Cor16
J20339+643	..F	G 262-018	M3.5 V	PMSU	20:33:59.85	+64:19:10.0	2MASS	19.5	0.7	Cor16
J20347+033	..F	G 024-020	M2.5 V	PMSU	20:34:43.04	+03:20:50.9	2MASS	26.9	7.9	HIP2
J20349+592	..F	Wolf 1074	M3.5 V	PMSU	20:34:55.31	+59:17:26.9	2MASS	21.6	0.8	Dit14
J20367+388	..F	G 209-038	M3.5 V	PMSU	20:36:46.01	+38:50:33.0	2MASS	19.9	0.7	Cor16
J20373+219	..F	Wolf 1351	M0.5 V	PMSU	20:37:20.81	+21:56:52.5	2MASS	26.4	0.3	Cor16
J20403+616	..F	TYC 4246-488-1	M1.0 V	Lep13	20:40:18.67	+61:41:30.1	2MASS	24.2	0.4	Cor16
J20405+154		GJ 1256	M4.5 V	AF15	20:40:33.64	+15:29:57.2	2MASS	9.54	0.09	Wein16
J20407+199	B.f	GJ 797B	M2.5 V+	AF15	20:40:44.50	+19:54:02.3	2MASS	20.9	0.2	aHIP2
J20409-101	S.F	StKM 1-1806	M1.5 V+	PMSU	20:40:56.39	-10:06:45.3	2MASS	25.9	0.4	Cor16
J20429-189	.mf	BD-19 5899	M1.5 V	PMSU	20:42:57.09	-18:55:04.8	2MASS	17.95	0.77	HIP2
J20433+553	B..	GJ 802 AabB	M5.0 V+	PMSU	20:43:19.21	+55:20:52.1	2MASS	15.7	0.3	Ir08
J20435+240	..f	Wolf 1360	M2.5 V	Lep13	20:43:34.53	+24:07:40.8	2MASS	17.4	0.4	Cor16
J20436+642	..F	G 262-026	M0.0 V	Lep13	20:43:41.35	+64:16:54.1	2MASS	21.13	0.74	HIP2
J20436-001	..F	LP 635-046	M0.0 V	PMSU	20:43:41.29	-00:10:41.9	2MASS	27.5	2.38	HIP2
J20443+197	B.f	HD 352860	M0.0 V+	PMSU	20:44:21.96	+19:45:00.6	2MASS	21.08	0.94	HIP2
J20445+089N	S.f	LP 576-039	M3.5 V+	PMSU	20:44:30.45	+08:54:25.3	2MASS	14.7	0.5	Cor16
J20445+089S	..F	LP 576-040	M1.5 V	PMSU	20:44:30.73	+08:54:10.7	2MASS	21.6	0.3	Cor16
J20450+444		BD+44 3567	M1.5 V	PMSU	20:45:04.03	+44:29:56.2	2MASS	12.31	0.26	HIP2
J20488+197	B.f	G 144-039	M4.0 V+	PMSU	20:48:52.46	+19:43:05.0	2MASS	33.56	2.03	vAl95
J20496-003	..F	Wolf 882	M3.5 V	PMSU	20:49:39.51	-00:21:03.1	2MASS	20.8	5.2	Daw05
J20519+691	B.F	G 262-029	M1.0 V+	PMSU	20:51:59.91	+69:10:07.2	2MASS	32.8	11.8	vAl95

Table B.2: Names, spectral types, distances and astrometric parameters of Carmencita stars (continued).

Karmn	Flags[a]	Name	SpT	Ref.[b]	α (J2000)	δ (J2000)	Ref.[c]	d [pc]	ed [pc]	Ref.[d e]
J20525-169	.m.	LP 816-060	M4.0 V	Gra06	20:52:33.04	-16:58:29.0	2MASS	5.7	0.2	HIP2
J20532-023	B.F	LP 636-019	M2.9 V+	Shk09	20:53:14.65	-02:21:21.9	2MASS	37.9	2.2	Shk12
J20533+621		BD+61 2068	M0.5 V	PMSU	20:53:19.78	+62:09:15.8	2MASS	7.05	0.03	HIP2
J20535+106	..F	G 025-008	M4.0 V	PMSU	20:53:33.04	+10:37:02.0	2MASS	13.9	0.5	vAl95
J20549+675	..F	LP 074-035	M2.0 V	Lep13	20:54:54.47	+67:35:08.1	2MASS	25.3	0.5	Cor16
J20556-140N	.m.	GJ 810 A	M4.0 V	PMSU	20:55:37.72	-14:02:07.8	2MASS	12.66	0.25	Wein16
J20556-140S	.mf	GJ 810 B	M5.0 V	PMSU	20:55:37.07	-14:03:54.6	2MASS	12.65	0.11	Wein16
J20567-104		Wolf 896	M2.5 V	PMSU	20:56:46.59	-10:26:53.4	2MASS	15.3	0.7	HIP2
J20568-048	S..	FR Aqr	M4.0 V+	PMSU	20:56:48.46	-04:50:49.0	2MASS	17.7	1.2	HIP2
J20574+223	..F	Wolf 3273	M2.0 V	PMSU	20:57:25.38	+22:21:45.7	2MASS	14.3	0.5	Dit14
J20586+342	..F	LP 285-005	M0.0 V	PMSU	20:58:41.92	+34:16:27.2	2MASS	24.1	1.3	HIP2
J21000+400	S..	V1396 Cyg AB	M1.5 V+	PMSU	21:00:05.29	+40:04:13.6	2MASS	15.29	0.43	HIP2
J21001+495	..F	G 212-014	M2.0 V	Lep13	21:00:08.92	+49:35:17.2	2MASS	23.0	0.4	Cor16
J21012+332	B..	LP 340-547	M3.0 V+	PMSU	21:01:16.10	+33:14:32.8	2MASS	16.2	0.5	Cor16
J21013+332	B.F	LP 340-548	M3.5 V+	PMSU	21:01:20.62	+33:14:28.0	2MASS	17.1	0.6	Cor16
J21014+207	B.F	G 144-050	M3.5 V+	PMSU	21:01:24.81	+20:43:37.8	2MASS	22.7	0.6	Dit14
J21019-063		Wolf 906	M2.5 V	AF15	21:01:58.66	-06:19:07.1	2MASS	14.4	0.6	HIP2
J21027+349	..F	G 211-009	M4.5 V	AF15	21:02:46.06	+34:54:36.0	2MASS	29.7	1.7	Dit14
J21044+455	..F	TYC 3588-5589-1	M2.0 V	Lep13	21:04:28.68	+45:35:43.1	2MASS	28.3	0.5	Cor16
J21048-169	.mF	Ross 769	M1.0 V	PMSU	21:04:53.41	-16:57:31.1	2MASS	19.17	1.07	HIP2
J21055+061	..f	2MASS J21053205+0609155	M3.0 V	Lep13	21:05:32.06	+06:09:15.6	2MASS	18.2	0.5	Cor16
J21057+502	..F	2MASS J21054537+5015435	M3.5 V	AF15	21:05:45.38	+50:15:43.6	2MASS	22.6	0.7	Cor16
J21059+044	..F	LP 576-034	M2.5 V	PMSU	21:05:56.38	+04:25:40.7	2MASS	24.98	2.29	HIP2
J21074+468	..F	2MASS J21072810+4651537	M2.0 V	AF15	21:07:28.10	+46:51:53.8	2MASS	35.5	0.7	Cor16
J21076-130	.mf	1RXS J120736.5-130500	M3.0 V	Ria06	21:07:36.78	-13:04:58.2	2MASS	18.6	0.5	Cor16
J21087-044N	..F	[RHG95] 3306	M3.0 V	PMSU	21:08:44.80	-04:25:18.2	2MASS	27.1	1.1	aHIP2
J21087-044S	B.f	BD-05 5480A	M1.0 V+	Mon01	21:08:45.47	-04:25:36.7	2MASS	27.1	1.1	HIP2
J21092-133	.mf	Wolf 918	M1.0 V	PMSU	21:09:17.41	-13:18:08.0	2MASS	12.17	0.32	HIP2
J21100-193	.mf	BPS CS 22898-0065	M2.0 V	Ria06	21:10:05.36	-19:19:57.4	2MASS	18.8	0.4	Cor16
J21109+294	B.f	Ross 824 AB	M1.5 V+	PMSU	21:10:54.75	+29:25:23.2	2MASS	32.26	2.73	HIP2
J21123+359	..F	LP 285-009	M1.5 V	Lep13	21:12:22.40	+35:55:23.3	2MASS	25.4	0.4	Cor16
J21127-073	..F	2MASS J21124559-0719558	M3.5 V	AF15	21:12:45.60	-07:19:55.8	2MASS	26.6	0.9	Cor16
J21137+087	..F	LSPM J2113+0846N	M2.0 V	Lep13	21:13:44.59	+08:46:10.3	2MASS	21.4	0.4	Cor16

Table B.2: Names, spectral types, distances and astrometric parameters of Carmencita stars (continued).

Karmn	Flags[a]	Name	SpT	Ref.[b]	α (J2000)	δ (J2000)	Ref.[c]	d [pc]	ed [pc]	Ref.[d e]
J21138+180	..F	Ross 772	M3.0 V	Lep13	21:13:52.46	+18:05:59.6	2MASS	20.7	0.6	Cor16
J21145+508	..F	LSPM J2114+5052	M2.5 V	Lep13	21:14:32.22	+50:52:31.4	2MASS	19.2	0.4	Cor16
J21147+380	B.F	τ Cyg B	M2.5 V+	PMSU	21:14:46.86	+38:01:13.7	2MASS	20.34	0.16	aHIP2
J21152+257		LP 397-041	M3.0 V	PMSU	21:15:12.59	+25:47:45.4	2MASS	15.9	0.4	Cor16
J21160+298E	B..	Ross 776	M3.5 V+	PMSU	21:16:05.77	+29:51:51.1	2MASS	20.1	0.7	aCor16
J21160+298W	..F	Ross 826	M3.5 V	PMSU	21:16:03.79	+29:51:46.0	2MASS	20.1	0.7	Cor16
J21164+025		LSPM J2116+0234	M3.0 V	Lep13	21:16:27.29	+02:34:51.5	2MASS	14.7	0.4	Cor16
J21173+208N	B..	Ross 773 A	M3.5 V	PMSU	21:17:22.64	+20:53:58.5	2MASS	21.9	6.0	vAl95
J21173+208S	B..	Ross 773 B	M3.0 V	PMSU	21:17:22.73	+20:53:54.8	2MASS	21.9	6.0	avAl95
J21173+640	..F	G 262-038	M5.0 V	Law08	21:17:21.96	+64:02:39.2	2MASS	30.8	1.8	Dit14
J21176-089N	B.F	StKM 1-1876	M2.5 V+	PMSU	21:17:36.14	-08:54:11.3	2MASS	19.3	0.4	Cor16
J21176-089S	..F	GJ 4188B	M3.0 V	PMSU	21:17:39.63	-08:54:49.2	2MASS	26.6	0.7	Cor16
J21185+302	..F	GSC 02703-00706	M1.5 V	Lep13	21:18:33.75	+30:14:34.7	2MASS	27.2	0.4	Cor16
J21221+229		GSC 02187-00512	M1.0 V	Lep13	21:22:06.27	+22:55:53.1	2MASS	17.1	0.2	Cor16
J21243+085	..F	G 093-006	M3.5 V	PMSU	21:24:19.27	+08:30:06.4	2MASS	38.6	2.8	Dit14
J21245+400	..F	LSR J2124+4003	M5.5 V	AF15	21:24:32.34	+40:03:59.9	2MASS	14.99	0.3	GC09
J21267+037	..F	GJ 828.1	M0.0 V	Lep13	21:26:42.46	+03:44:13.7	2MASS	27.08	1.67	HIP2
J21272-068	..F	Wolf 920	M0.5 V	PMSU	21:27:16.85	-06:50:39.1	2MASS	16.34	0.64	HIP2
J21275+340	..F	V2160 Cyg	M1.0 V	PMSU	21:27:32.99	+34:01:28.9	2MASS	27.9	2.4	HIP2
J21277+072	..F	Ross 778	M1.0 V	PMSU	21:27:46.43	+07:17:55.9	2MASS	24.6	3.6	vAl95
J21280+179	..F	LP 457-038	M1.5 V	Lep13	21:28:05.48	+17:54:00.3	2MASS	30.8	0.5	Cor16
J21283-223	.mF	LP 873-049	M2.5 V	PMSU	21:28:18.31	-22:18:32.0	2MASS	19.6	0.5	Cor16
J21296+176	S..	Ross 775	M3.5 V+	PMSU	21:29:36.71	+17:38:35.4	2MASS	6.7	0.1	HIP2
J21313-097	B..	BB Cap AB	M4.5 V+	PMSU	21:31:18.59	-09:47:26.3	2MASS	8.3	0.4	HIP2
J21323+245	B..	LP 397-034	M3.5 V+	PMSU	21:32:21.98	+24:33:41.9	2MASS	22.0	0.7	Dit14
J21338+017N	..F	LP 638-066	M4.0 V	PMSU	21:33:49.14	+01:47:01.3	2MASS	14.6	1.2	avAl95
J21338+017S	..F	NLTT 51554	M4.0 V	PMSU	21:33:49.13	+01:46:56.1	2MASS	14.6	1.2	vAl95
J21338-068	..F	Wolf 923	M4.0 V	PMSU	21:33:48.90	-06:51:10.0	2MASS	18.7	0.7	Cor16
J21348+515		Wolf 926	M3.0 V	PMSU	21:34:50.36	+51:32:13.8	2MASS	17.9	0.8	HIP2
J21366+394	B..	V2168 Cyg AB	M0.0 V+	PMSU	21:36:38.53	+39:27:20.6	2MASS	20.93	1.1	HIP2
J21369+561	..F	Ross 215	M1.5 V	Lep13	21:36:58.83	+56:07:04.6	2MASS	27.9	0.4	Cor16
J21374-059	B.f	2MASS J21372900-0555082	M3.0 V+	Rei07	21:37:29.00	-05:55:08.3	2MASS	19.0	0.5	Cor16
J21376+016	B..	GSC 00543-00620	M4.5 V+	AF15	21:37:40.19	+01:37:13.7	2MASS	10.7	0.5	Cor16

Table B.2: Names, spectral types, distances and astrometric parameters of Carmencita stars (continued).

Karmn	Flags[a]	Name	SpT	Ref.[b]	α (J2000)	δ (J2000)	Ref.[c]	d [pc]	ed [pc]	Ref.[d e]
J21378+530	..F	Ross 199	M0.0 V	PMSU	21:37:50.23	+53:04:49.1	2MASS	31.47	1.37	HIP2
J21380+277	B..	BD+27 4120 AabC	M0.0 V+	PMSU	21:38:00.37	+27:43:25.5	2MASS	13.32	0.33	HIP2
J21399+276	B.f	LP 342-008 AB	M1.5 V+	PMSU	21:39:54.33	+27:36:43.9	2MASS	24.43	1.82	HIP2
J21402+370	..F	LP 286-001	M0.5 V	Lep13	21:40:12.78	+37:03:28.5	2MASS	27.1	7.2	vAl95
J21419+276	..F	G 188-019	M3.5 V	PMSU	21:41:58.43	+27:41:15.1	2MASS	21.7	0.7	Dit14
J21421-121	..F	Ross 206	M3.0 V	PMSU	21:42:07.46	-12:09:47.8	2MASS	35.0	3.2	vAl95
J21441+170N	..F	G 126-030	M4.5 V	PMSU	21:44:07.95	+17:04:37.2	2MASS	14.3	0.6	Dit14
J21441+170S	..F	G 126-031	M4.0 V	PMSU	21:44:09.01	+17:03:34.9	2MASS	15.3	0.6	Dit14
J21442+066	S..	G 093-033	M3.0 V+	PMSU	21:44:12.98	+06:38:29.2	2MASS	20.8	1.5	HIP2
J21449+442	B.f	BD+43 4035	M1.5 V+	Lep13	21:44:54.00	+44:17:09.6	2MASS	26.46	1.74	HIP2
J21450+198	..F	LP 458-033	M1.5 V	Lep13	21:45:04.93	+19:53:35.5	2MASS	33.59	4.68	HIP2
J21450-057	..F	Wolf 937	M3.0 V	PMSU	21:45:00.79	-05:47:12.8	2MASS	29.8	17.7	vAl95
J21454-059	..F	Wolf 939	M3.5 V	PMSU	21:45:24.91	-05:54:05.5	2MASS	23.2	0.8	Cor16
J21463+382		LSPM J2146+3813	M4.0 V	Lep13	21:46:22.06	+38:13:04.8	2MASS	6.7	0.1	Dit14
J21466+668		G 264-012	M4.0 V	AF15	21:46:40.22	+66:48:10.6	2MASS	13.66	0.58	Dit14
J21466-001		Wolf 940	M4.0 V	PMSU	21:46:40.40	-00:10:23.4	2MASS	12.0	0.6	vAl95
J21469+466	..f	Wolf 944	M4.0 V	PMSU	21:46:56.26	+46:38:06.2	2MASS	15.0	0.6	Dit14
J21472-047	..F	2MASS J21471744-0444406	M4.5 V	AF15	21:47:17.44	-04:44:40.6	2MASS	14.2	0.6	Cor16
J21478+502	..F	Wolf 945	M3.5 V	PMSU	21:47:52.52	+50:14:48.0	2MASS	21.1	0.8	Dit14
J21479+058	..F	Ross 779	M1.5 V	PMSU	21:47:57.24	+05:49:21.3	2MASS	27.0	0.4	Cor16
J21481+014	..F	LP 638-040	M3.5 V	PMSU	21:48:10.23	+01:26:42.5	2MASS	28.5	1.5	Dit14
J21482+279	..F	G 188-026	M2.0 V	PMSU	21:48:15.30	+27:55:43.6	2MASS	18.4	1.7	vAl95
J21512+128	..F	G 018-001	M4.0 V	PMSU	21:51:17.41	+12:50:30.3	2MASS	26.2	2.5	vAl95
J21518+136	B.F	LP 518-058	M4.5 V+	PMSU	21:51:48.32	+13:36:15.5	2MASS	16.0	0.5	Dit14
J21521+056	B..	StKM 1-1950	M3.0 V+	PMSU	21:52:10.40	+05:37:35.7	2MASS	30.5	5.2	HIP2
J21521+274	..F	G 188-028	M4.0 V	PMSU	21:52:11.79	+27:25:00.1	2MASS	23.5	0.9	Dit14
J21539+417	..F	GJ 839	M0.0 V	PMSU	21:53:59.02	+41:46:44.3	2MASS	23.22	0.87	HIP2
J21566+197	..F	Ross 263	M3.5 V	PMSU	21:56:37.94	+19:46:14.5	2MASS	17.0	0.6	Cor16
J21569-019	..F	LP 639-001	M5.0 V	PMSU	21:56:55.14	-01:54:10.1	2MASS	13.4	0.6	vAl95
J21574+081	..f	Wolf 953	M1.5 V	PMSU	21:57:26.24	+08:08:13.9	2MASS	20.49	0.89	HIP2
J21584+755	..F	GJ 842.2	M0.5 V	PMSU	21:58:24.51	+75:35:20.6	2MASS	20.77	0.47	HIP2
J21585+612	..F	LSPM J2158+6117	M6.0 V	Lep03	21:58:34.58	+61:17:06.0	2MASS	16.7	0.7	Dit14
J21593+418	..F	G 215-030	M3.0 V	PMSU	21:59:21.92	+41:51:32.7	2MASS	20.8	0.6	Cor16

Table B.2: Names, spectral types, distances and astrometric parameters of Carmencita stars (continued).

Karmn	Flags[a]	Name	SpT	Ref.[b]	α (J2000)	δ (J2000)	Ref.[c]	d [pc]	ed [pc]	Ref.[d e]
J22012+283		V374 Peg	M4.0 V	PMSU	22:01:13.11	+28:18:24.9	2MASS	8.9	0.2	HIP2
J22012+323	V.F	TYC 2723-908-1	M1.5 V	Lep13	22:01:13.95	+32:23:12.8	2MASS	29.7	0.5	Cor16
J22018+164	B..	Ross 265	M2.0 V+	PMSU	22:01:49.02	+16:28:02.7	2MASS	16.2	0.6	HIP2
J22020-194	.m.	LP 819-017	M3.5 V	PMSU	22:02:00.70	-19:28:59.3	2MASS	12.5	1.0	vAl95
J22021+014		BD+00 4810	M0.5 V	AF15	22:02:10.26	+01:24:00.6	2MASS	10.24	0.16	HIP2
J22033+674	..F	G 264-017	M3.5 V	PMSU	22:03:21.29	+67:29:59.7	2MASS	17.6	0.6	Dit14
J22035+036	B.F	2MASS J22033338+0340235	M4.0 V+	AF15	22:03:33.38	+03:40:23.6	2MASS	20.4	0.8	Cor16
J22051+051	..F	Wolf 983	M4.0 V	PMSU	22:05:06.83	+05:08:12.0	2MASS	18.4	0.7	Cor16
J22057+656		G 264-018 A	M3.5 V	PMSU	22:05:45.36	+65:38:55.5	2MASS	13.5	0.4	Cor16
J22058-119	..f	BD-12 6174	M0.0 V	PMSU	22:05:51.31	-11:54:50.7	2MASS	22.22	1.32	HIP2
J22060+393	..F	G 189-001	M3.0 V	PMSU	22:06:00.68	+39:18:02.7	2MASS	20.2	0.6	Cor16
J22063+173	..F	Ross 268	M3.5 V	Lep13	22:06:22.59	+17:22:20.6	2MASS	17.2	0.6	Dit14
J22067+034	..F	Wolf 990	M4.0 V	PMSU	22:06:46.38	+03:25:03.7	2MASS	17.5	0.7	Cor16
J22088+117	..F	2MASS J22085034+1144131	M4.5 V	AF15	22:08:50.35	+11:44:13.2	2MASS	17.7	0.8	Cor16
J22095+118	..F	LP 519-038	M3.0 V	AF15	22:09:31.68	+11:52:53.7	2MASS	31.8	0.9	Cor16
J22096-046		BD-05 5715	M3.5 V	PMSU	22:09:40.30	-04:38:26.8	2MASS	9.1	0.2	HIP2
J22097+410	..f	G 214-012	M3.5 V	PMSU	22:09:43.01	+41:02:05.3	2MASS	22.5	1.7	vAl95
J22107+079	B.f	Wolf 1003	M0.5 V+	Lep13	22:10:44.73	+07:54:33.1	2MASS	38.02	5.65	HIP2
J22112+410	..F	G 214-014	M0.0 V	Lep13	22:11:16.98	+41:00:54.6	2MASS	22.74	1.14	HIP2
J22112-025	..F	G 027-017	M2.0 V	PMSU	22:11:13.47	-02:32:36.9	2MASS	24.6	0.5	Cor16
J22114+409	..f	1RXS J221124.3+410000	M5.5 V	AF15	22:11:24.17	+40:59:58.7	2MASS	10.1	0.6	Cor16
J22115+184		Ross 271	M2.0 V	PMSU	22:11:30.08	+18:25:34.1	2MASS	11.6	0.2	HIP2
J22117-207	.mF	WT 2221 A	M3.5 V	PMSU	22:11:42.09	-20:44:18.1	2MASS	24.0	0.8	Cor16
J22125+085		Wolf 1014	M3.0 V	PMSU	22:12:35.96	+08:33:11.1	2MASS	14.96	0.99	HIP2
J22129+550	..F	LF 4 +54 152	M0.0 V	Lep13	22:12:56.80	+55:04:49.9	2MASS	27.9	0.3	Cor16
J22134-147	.mF	Wolf 1556	M3.5 V	PMSU	22:13:28.84	-14:44:53.9	2MASS	21.6	0.7	Cor16
J22135+259	..F	LP 399-165	M3.5 V	PMSU	22:13:35.67	+25:58:10.9	2MASS	18.5	0.6	Dit14
J22137-176	.m.	LP 819-052	M4.5 V	PMSU	22:13:42.78	-17:41:08.2	2MASS	10.39	0.05	Wein16
J22138+052	B.F	Wolf 1019	M1.5 V+	PMSU	22:13:53.33	+05:16:35.7	2MASS	26.55	2.47	HIP2
J22142+255	B.F	2MASS J22141765+2534066	M4.3 V+	Shk09	22:14:17.66	+25:34:06.6	2MASS	32.9	1.6	Dit14
J22154+662	..f	G 264-022	M3.5 V	PMSU	22:15:26.16	+66:13:27.8	2MASS	15.7	0.5	Cor16
J22160+546	..F	G 232-062	M4.0 V	AF15	22:16:02.59	+54:39:59.5	2MASS	19.7	1.2	Dit14
J22163+709	..F	LP 48-567	M2.0 V	PMSU	22:16:20.28	+70:56:39.5	2MASS	22.1	1.1	vAl95

Table B.2: Names, spectral types, distances and astrometric parameters of Carmencita stars (continued).

Karmn	Flags[a]	Name	SpT	Ref.[b]	α (J2000)	δ (J2000)	Ref.[c]	d [pc]	ed [pc]	Ref.[d e]
J22173-088N	B.f	FG Aqr A	M4.0 V+	PMSU	22:17:19.00	-08:48:12.2	2MASS	10.4	0.6	HD80
J22173-088S	B..	Wolf 1561 BC	M5.0 V+	PMSU	22:17:18.71	-08:48:18.7	2MASS	10.0	0.3	vAl95
J22176+565	..F	2MASS J22173704+5633100	M1.5 V	Lep13	22:17:37.05	+56:33:10.0	2MASS	32.0	0.5	Cor16
J22202+067	..F	Wolf 1034	M2.5 V	AF15	22:20:13.27	+06:43:32.1	2MASS	31.0	0.7	Cor16
J22212+377	..F	LSPM J2221+3744	M1.5 V	Lep13	22:21:12.91	+37:44:49.8	2MASS	29.7	0.5	Cor16
J22228+280	..F	G 127-022	M4.0 V	PMSU	22:22:50.80	+28:01:47.6	2MASS	26.5	1.1	Dit14
J22231-176	.m.	LP 820-012	M4.5 V	PMSU	22:23:06.97	-17:36:25.0	2MASS	7.27	0.03	Wein16
J22234+324	B..	Wolf 1225 AB	M3.0 V+	AF15	22:23:29.05	+32:27:33.4	2MASS	14.97	0.92	Dit14
J22249+520	..F	G 232-069	M4.5 V	PMSU	22:24:55.94	+52:00:19.1	2MASS	16.0	0.9	vAl95
J22250+356	..F	1RXS J222501.1+354008	M2.0 V	Lep13	22:25:01.74	+35:40:07.9	2MASS	22.9	0.4	Cor16
J22252+594		G 232-070	M4.0 V	PMSU	22:25:17.06	+59:24:49.6	2MASS	18.3	0.7	Dit14
J22262+030	..F	Wolf 1201	M3.5 V	PMSU	22:26:15.76	+03:00:18.2	2MASS	21.0	0.8	Dit14
J22264+583	..F	2MASS J22262498+5823051	M3.0 V	AF15	22:26:24.98	+58:23:05.1	2MASS	26.0	0.7	Cor16
J22270+068	..F	G 018-049	M3.5 V	PMSU	22:27:02.80	+06:49:32.4	2MASS	13.8	0.3	Dit14
J22279+576	B..	HD 239960 + DO Cep	M3.0 V+	PMSU	22:27:59.58	+57:41:45.3	2MASS	4.0	0.1	vAl95
J22287+189	..F	LP 460-060	M0.0 V	PMSU	22:28:45.91	+18:55:54.5	2MASS	22.02	0.84	HIP2
J22289-134	.mF	LP 760-003	M6.5 V	PMSU	22:28:54.40	-13:25:17.9	2MASS	10.89	0.08	Wein16
J22290+016	..F	LP 640-074	M0.5 V	Lep13	22:29:05.87	+01:39:48.1	2MASS	21.32	0.9	HIP2
J22298+414		G 215-050	M4.0 V	PMSU	22:29:48.86	+41:28:48.0	2MASS	13.8	0.5	vAl95
J22300+488	B.F	1RXS J223004.8+485127	M4.5 V+	AF15	22:30:04.19	+48:51:34.7	2MASS	14.9	0.7	Cor16
J22330+093		BD+08 4887	M1.0 V	PMSU	22:33:02.25	+09:22:41.1	2MASS	12.71	0.43	HIP2
J22333-096	B..	StKM 1-2018 AB	M3.0 V+	PMSU	22:33:22.65	-09:36:53.8	2MASS	16.9	0.5	Cor16
J22347+040	..F	LP 580-033	M2.5 V	PMSU	22:34:46.20	+04:02:37.7	2MASS	24.2	0.6	Cor16
J22348-010	..F	LP 640-043	M4.5 V	PMSU	22:34:53.64	-01:04:58.2	2MASS	23.5	2.0	vAl95
J22353+746	..F	G 242-003	M0.0 V	Lep13	22:35:19.68	+74:41:18.9	2MASS	37.15	1.88	HIP2
J22361-008	B.f	HD 214100	M0.0 V+	PMSU	22:36:09.67	-00:50:29.8	2MASS	17.12	0.52	HIP2
J22373+299	..F	LP 344-027	M1.5 V	Lep13	22:37:23.04	+29:59:09.4	2MASS	31.5	0.5	Cor16
J22374+395	Bm.	BD+38 4818	M0.0 V+	Lep13	22:37:29.87	+39:22:51.9	2MASS	19.54	0.62	HIP2
J22385-152	Bm.	EZ Aqr	M5.5 V+	PMSU	22:38:33.73	-15:17:57.3	2MASS	3.45	0.05	vAl95
J22387+252	..F	G 127-042	M3.5 V	AF15	22:38:44.26	+25:13:30.5	2MASS	25.1	0.8	Cor16
J22387-206N	Sm.	FL Aqr	M3.5 V+	PMSU	22:38:45.31	-20:36:51.9	2MASS	8.7	0.1	aHIP2
J22387-206S	Sm.	FK Aqr	M1.5 V+	PMSU	22:38:45.60	-20:37:16.1	2MASS	8.7	0.1	HIP2
J22406+445	..F	G 216-011	M3.5 V	PMSU	22:40:41.79	+44:35:47.5	2MASS	30.6	1.6	Dit14

Table B.2: Names, spectral types, distances and astrometric parameters of Carmencita stars (continued).

Karmn	Flags[a]	Name	SpT	Ref.[b]	α (J2000)	δ (J2000)	Ref.[c]	d [pc]	ed [pc]	Ref.[d e]
J22415+188	..F	BD+18 5029	M0.0 V	PMSU	22:41:35.02	+18:49:27.7	2MASS	36.4	3.0	HIP2
J22415+260	V.F	2MASS J22413577+2602128	M3.5 V	AF15	22:41:35.78	+26:02:12.9	2MASS	17.9	0.6	Cor16
J22426+176	..f	GJ 1271	M2.5 V	PMSU	22:42:38.72	+17:40:09.1	2MASS	21.04	1.24	HIP2
J22433+221	..F	G 127-050	M4.5 V	PMSU	22:43:23.13	+22:08:17.9	2MASS	19.1	1.1	Dit14
J22437+192	..F	RX J2243.7+1916	M3.0 V	AF15	22:43:43.78	+19:16:54.5	2MASS	23.5	0.7	Cor16
J22440+405	..F	LDS 1064B	M1.0 V	Lep13	22:44:04.61	+40:30:00.4	2MASS	24.3	0.3	Cor16
J22441+405	..F	LDS 1064A	M1.0 V	Lep13	22:44:06.26	+40:30:00.3	2MASS	24.7	0.3	Cor16
J22457+016	..F	LP 641-004	M1.0 V	Lep13	22:45:46.29	+01:41:23.0	2MASS	26.62	2.89	HIP2
J22464-066	..F	LP 701-007	M5.0 V	PMSU	22:46:26.33	-06:39:25.9	2MASS	18.8	1.6	vAl95
J22468+443		EV Lac	M3.5 V	PMSU	22:46:49.81	+44:20:03.1	2MASS	5.12	0.05	HIP2
J22476+184	..F	LP 461-011	M2.5 V	AF15	22:47:38.84	+18:26:36.5	2MASS	25.8	0.6	Cor16
J22479+318	..F	LP 344-044	M3.0 V	PMSU	22:47:54.04	+31:52:15.4	2MASS	21.9	0.6	Cor16
J22489+183	..F	2MASS J22485459+1819592	M4.5 V	AF15	22:48:54.59	+18:19:59.3	2MASS	18.2	0.8	Cor16
J22503-070		BD-07 5871	M0.5 V	Gra03	22:50:19.43	-07:05:24.5	2MASS	14.13	0.37	HIP2
J22506+348	..F	GJ 1274	M1.5 V	PMSU	22:50:37.62	+34:51:21.3	2MASS	17.52	0.82	HIP2
J22507+286	..F	LP 344-047	M3.0 V	PMSU	22:50:45.49	+28:36:08.5	2MASS	19.2	0.5	Cor16
J22509+499	..F	2MASS J22505505+4959132	M4.0 V	AF15	22:50:55.05	+49:59:13.2	2MASS	20.9	0.8	Cor16
J22518+317		GT Peg	M3.0 V	PMSU	22:51:53.49	+31:45:15.3	2MASS	14.5	0.6	HIP2
J22524+099	B.F	σ Peg B	M3.0 V+	AF15	22:52:29.77	+09:54:04.3	2MASS	22.6	1.3	Dit14
J22526+750	..f	NLTT 55174	M4.5 V	AF15	22:52:39.64	+75:04:19.0	2MASS	12.8	0.5	Dit14
J22532-142	.m.	IL Aqr	M4.0 V	PMSU	22:53:16.72	-14:15:48.9	2MASS	4.69	0.03	HIP2
J22543+609	..F	Ross 226	M3.5 V	PMSU	22:54:21.71	+60:59:44.0	2MASS	15.2	1.4	vAl95
J22547-054	..F	G 156-063	M4.0 V	PMSU	22:54:46.46	-05:28:26.5	2MASS	25.06	0.58	Wein16
J22559+057	..F	LP 581-036	M1.0 V	PMSU	22:55:56.83	+05:45:17.9	2MASS	24.46	1.27	HIP2
J22559+178		StKM 1-2065	M1.0 V	PMSU	22:55:59.85	+17:48:39.9	2MASS	16.5	0.2	Cor16
J22565+165		HD 216899	M1.5 V	PMSU	22:56:34.97	+16:33:13.0	2MASS	6.84	0.05	HIP2
J22576+373	..F	G 189-053	M3.0 V	Lep13	22:57:40.93	+37:19:23.3	2MASS	20.8	0.6	Cor16
J23028+436	..F	LSPM J2302+4338	M4.0 V	AF15	23:02:52.51	+43:38:15.7	2MASS	12.6	0.3	Dit14
J23036+097	..F	2MASS J23033745+0942585	M3.5 V	AF15	23:03:37.45	+09:42:58.5	2MASS	27.8	0.9	Cor16
J23045+667	..f	BD+65 1846	M0.5 V	Lep13	23:04:30.19	+66:45:51.8	2MASS	20.19	0.33	HIP2
J23051+452	..F	LSPM J2305+4517	M3.5 V	AF15	23:05:08.71	+45:17:31.8	2MASS	25.7	0.8	Dit14
J23051+519	..F	2MASS J23050631+5159133	M3.5 V	AF15	23:05:06.32	+51:59:13.3	2MASS	24.0	0.8	Cor16
J23060+639	..F	MCC 858	M0.0 V	PMSU	23:06:04.83	+63:55:33.9	2MASS	24.5	0.96	HIP2

Table B.2: Names, spectral types, distances and astrometric parameters of Carmencita stars (continued).

Karmn	Flags[a]	Name	SpT	Ref.[b]	α (J2000)	δ (J2000)	Ref.[c]	d [pc]	ed [pc]	Ref.[d e]
J23063+126	S.f	LP 521-079	M0.5 V+	Jan12	23:06:23.78	+12:36:26.9	2MASS	45.33	9.43	HIP2
J23064-050	..F	2MASSUCD 12171	M8.0 V	Schm07	23:06:29.28	-05:02:28.6	2MASS	12.49	0.18	Wein16
J23065+717	..F	LP 048-822	M2.5 V	PMSU	23:06:35.86	+71:43:25.8	2MASS	18.1	0.4	Cor16
J23075+686	..f	G 241-045	M3.5 V	PMSU	23:07:30.04	+68:40:05.1	2MASS	15.3	0.8	vAl95
J23081+033	..F	GJ 889.1	M0.0 V	PMSU	23:08:06.99	+03:19:44.5	2MASS	15.86	0.54	HIP2
J23083-154	.mF	HK Aqr	M0.0 V	PMSU	23:08:19.54	-15:24:35.5	2MASS	22.28	1.14	HIP2
J23088+065	..F	StKM 1-2100	M0.0 V	Lep13	23:08:52.49	+06:33:39.9	2MASS	38.8	3.6	HIP2
J23089+551	..F	G 233-042	M5.0 V	New14	23:09:57.81	+55:06:47.3	2MASS	14.8	0.5	Dit14
J23096-019	B.f	G 028-044	M3.5 V+	PMSU	23:09:39.32	-01:58:23.0	2MASS	15.1	0.5	Cor16
J23107-192	.mF	GJ 1281	M2.5 V	PMSU	23:10:42.16	-19:13:32.8	2MASS	24.3	1.3	Jao05
J23113+085		NLTT 56083	M3.5 V	Lep13	23:11:23.78	+08:31:01.4	2MASS	13.7	0.5	Cor16
J23121-141	.mF	LP 762-003	M3.0 V	PMSU	23:12:11.33	-14:06:10.8	2MASS	21.6	0.6	Cor16
J23142-196N	.mF	BD-20 6558	M0.5 V	PMSU	23:14:16.60	-19:38:39.3	2MASS	19.8	0.8	HIP2
J23142-196S	.mF	BD-20 6558B	M4.0 V	PMSU	23:14:16.43	-19:38:46.2	2MASS	19.8	0.8	aHIP2
J23161+067	..F	G 028-050	M3.0 V	PMSU	23:16:08.47	+06:44:36.1	2MASS	17.9	1.0	Dit14
J23166+196	B.F	GJ 893.4 AB	M0.5 V+	PMSU	23:16:39.71	+19:37:16.9	2MASS	30.74	2.45	HIP2
J23174+196	B.F	G 067-053 AB	M3.5 V+	PMSU	23:17:28.07	+19:36:46.9	2MASS	9.1	0.2	Dit14
J23174+382	S..	G 190-017	M2.5 V+	PMSU	23:17:24.41	+38:12:42.0	2MASS	17.5	1.0	vAl95
J23175+063	..f	G 029-019	M3.0 V	PMSU	23:17:34.55	+06:23:28.3	2MASS	18.9	0.5	Cor16
J23182+462	..F	Ross 244	M0.0 V	PMSU	23:18:17.89	+46:17:21.4	2MASS	24.76	1.22	HIP2
J23182+795	..F	LP 012-069	M3.0 V	AF15	23:18:17.06	+79:34:47.4	2MASS	29.1	0.8	Cor16
J23193+154	..F	StKM 1-2115	M1.0 V	Lep13	23:19:20.95	+15:24:16.0	2MASS	33.9	0.4	Cor16
J23194+790	J..	HD 220140B	M3.5 V	AF15	23:19:24.47	+79:00:03.7	2MASS	19.2	0.2	aHIP2
J23215+568	..F	LSPM J2321+5651	M1.0 V	Lep13	23:21:32.28	+56:51:22.9	2MASS	34.1	0.4	Cor16
J23216+172		LP 462-027	M4.0 V	PMSU	23:21:37.52	+17:17:28.5	2MASS	10.99	0.35	HIP2
J23220+569	..F	G 217-006	M3.0 V	AF15	23:22:00.71	+56:59:19.9	2MASS	26.1	0.7	Cor16
J23228+787	..F	NLTT 56725	M5.0 V	AF15	23:22:53.85	+78:47:38.6	2MASS	14.0	1.2	Dit14
J23229+372	..F	2MASS J23225835+3717143	M2.0 V	Lep13	23:22:58.36	+37:17:14.3	2MASS	25.8	0.5	Cor16
J23234+155	..f	LP 522-065	M2.0 V	Lep13	23:23:24.72	+15:34:17.9	2MASS	20.1	0.4	Cor16
J23245+578		BD+57 2735	M1.0 V	PMSU	23:24:30.49	+57:51:15.3	2MASS	12.96	0.22	HIP2
J23249+506	..f	2MASS J23545647+5036148	M3.0 V	Lep13	23:54:56.47	+50:36:14.5	2MASS	19.1	0.5	Cor16
J23252+009	..F	G 029-030	M1.0 V	Lep13	23:25:16.36	+00:57:51.7	2MASS	35.1	0.5	Cor16
J23256+531	..F	FZ And	M4.5 V	PMSU	23:25:40.17	+53:08:05.6	2MASS	22.2	0.8	Dit14

Table B.2: Names, spectral types, distances and astrometric parameters of Carmencita stars (continued).

Karmn	Flags[a]	Name	SpT	Ref.[b]	α (J2000)	δ (J2000)	Ref.[c]	d [pc]	ed [pc]	Ref.[d e]
J23261+170	B.F	2MASS J23261182+1700082AB	M4.0 V+	AF15	23:26:11.82	+17:00:08.3	2MASS	17.0	0.7	Cor16
J23262+088	..F	GJ 2155	M0.0 V+	Lep13	23:26:12.38	+08:53:37.8	2MASS	23.27	1.07	HIP2
J23262+278	B..	GSC 02245-00754	M3.0 V+	Ria06	23:26:17.07	+27:52:03.4	2MASS	16.3	0.5	Cor16
J23265+121	..F	LP 522-049	M3.0 V	PMSU	23:26:32.39	+12:09:32.8	2MASS	26.1	10.1	vAl95
J23293+414N	V..	G 190-028	M3.5 V	PMSU	23:29:23.46	+41:28:06.9	2MASS	14.9	0.5	vAl95
J23293+414S	B..	G 190-027	M4.0 V+	PMSU	23:29:22.58	+41:27:52.2	2MASS	14.9	0.5	avAl95
J23301-026	..F	2MASS J23301129-0237227	M6.0 V	Rei07	23:30:11.30	-02:37:22.7	2MASS	11.8	0.8	Cor16
J23302-203	Sm.	GJ 1284	M3.0 V+	PMSU	23:30:13.41	-20:23:27.1	2MASS	16.2	0.9	HIP2
J23308+157	B.f	LP 462-052	M1.0 V+	Lep13	23:30:53.74	+15:47:40.9	2MASS	27.2	0.4	Cor16
J23317-027	..F	AF Psc	M4.5 V	Ria06	23:31:44.93	-02:44:39.6	2MASS	29.1	2.6	vAl95
J23318+199E	S..	EQ Peg Aab	M3.5 V+	PMSU	23:31:52.09	+19:56:14.2	2MASS	6.2	0.1	HIP2
J23318+199W	S..	EQ Peg Bab	M4.5 V+	PMSU	23:31:52.45	+19:56:13.8	2MASS	6.2	0.1	aHIP2
J23323+540	..F	G 217-012	M2.0 V	Lep13	23:32:20.19	+54:01:48.3	2MASS	27.3	0.5	Cor16
J23327-167	Bm.	HD 221503 BC	M2.0 V+	PMSU	23:32:46.56	-16:45:08.2	2MASS	15.2	0.4	aHIP2
J23340+001		GJ 899	M2.5 V	PMSU	23:34:03.28	+00:10:45.2	2MASS	13.98	0.64	HIP2
J23350+016	B..	BD+00 5017	M0.0 V+	Lep13	23:35:00.29	+01:36:19.4	2MASS	19.02	0.47	HIP2
J23350+252	..F	Ross 298	M3.0 V	PMSU	23:35:03.86	+25:14:57.3	2MASS	22.4	0.6	Cor16
J23351-023		GJ 1286	M5.5 V	PMSU	23:35:10.50	-02:23:21.4	2MASS	7.21	0.03	Wein16
J23354+300	..F	G 128-082	M3.5 V	PMSU	23:35:24.29	+30:03:45.0	2MASS	27.9	1.0	Dit14
J23357+419	..F	NLTT 16947	M1.0 V	PMSU	23:35:44.45	+41:58:03.8	2MASS	27.01	1.7	HIP2
J23364+554	..F	Ross 303	M1.5 V	PMSU	23:36:25.53	+55:29:43.6	2MASS	24.89	1.47	HIP2
J23376-128	..F	LP 763-003	M6.0 V	Rei03	23:37:38.31	-12:50:27.7	2MASS	17.0	1.2	Cor16
J23381-162	.m.	G 273-093	M2.0 V	PMSU	23:38:08.19	-16:14:10.0	2MASS	16.4	0.3	Cor16
J23386+391	..F	G 171-008	M3.5 V	PMSU	23:38:41.76	+39:09:26.2	2MASS	17.4	0.5	Dit14
J23389+210	..F	G 068-034	M3.5 V	PMSU	23:38:55.69	+21:01:21.8	2MASS	27.1	0.9	Cor16
J23401+606	B.f	G 241-062 AB	M1.0 V+	PMSU	23:40:07.72	+60:41:18.8	2MASS	24.0	0.3	Cor16
J23414+200	B.f	TYC 1727-1708-1	M0.5 V+	Lep13	23:41:29.21	+20:02:33.2	2MASS	30.8	0.3	Cor16
J23419+441		HH And	M5.0 V	AF15	23:41:54.99	+44:10:40.8	2MASS	3.16	0.01	vAl95
J23423+349	..F	2MASS J23422211+3458276	M4.0 V	AF15	23:42:22.11	+34:58:27.7	2MASS	16.7	0.7	Cor16
J23428+308	..F	GJ 1288	M4.5 V	PMSU	23:42:52.74	+30:49:21.9	2MASS	12.6	0.3	Dit14
J23431+365		GJ 1289	M4.0 V	PMSU	23:43:06.29	+36:32:13.2	2MASS	8.1	0.2	vAl95
J23438+325	B..	G 130-006	M3.0 V+	PMSU	23:43:53.10	+32:35:38.8	2MASS	17.6	0.6	vAl95
J23438+610	..F	G 217-018	M3.0 V	AF15	23:43:53.31	+61:02:15.7	2MASS	18.2	0.6	Dit14

Table B.2: Names, spectral types, distances and astrometric parameters of Carmencita stars (continued).

Karmn	Flags[a]	Name	SpT	Ref.[b]	α (J2000)	δ (J2000)	Ref.[c]	d [pc]	ed [pc]	Ref.[d e]
J23439+647	S.F	Ross 676 AB	M0.4 V+	Shk10	23:43:59.45	+64:44:29.1	2MASS	28.44	1.67	HIP2
J23443+216	V.F	GJ 1290	M3.5 V	PMSU	23:44:20.84	+21:36:05.0	2MASS	22.0	1.9	vAl95
J23455-161	Bm.	LP 823-004 AB	M5.0 V+	PMSU	23:45:31.28	-16:10:19.8	2MASS	12.5	0.2	Ried10
J23462+284	..F	2MASS J23461405+2826036	M3.5 V	Lep13	23:46:14.05	+28:26:03.6	2MASS	17.2	0.6	Cor16
J23480+490	..F	Ross 249	M1.0 V	PMSU	23:48:03.12	+49:00:57.3	2MASS	14.8	0.6	Dit14
J23489+098	..F	[R78b] 377	M1.0 V	Lep13	23:48:58.83	+09:51:54.2	2MASS	47.92	10.68	HIP2
J23492+024		BR Psc	M1.0 V	PMSU	23:49:12.56	+02:24:03.8	2MASS	5.98	0.04	HIP2
J23492+100	..F	G 029-069	M4.0 V	PMSU	23:49:15.02	+10:05:38.5	2MASS	17.9	0.7	Cor16
J23496+083	..F	StKM 1-2166	M1.0 V	PMSU	23:49:37.65	+08:21:30.2	2MASS	25.6	0.3	Cor16
J23505-095		LP 763-012	M4.0 V	PMSU	23:50:31.59	-09:33:32.1	2MASS	16.0	0.4	Ried10
J23506+099	B..	NLTT 58143	M3.0 V+	PMSU	23:50:36.20	+09:56:53.8	2MASS	11.4	0.3	Cor16
J23509+384	..F	LP 291-024	M4.0 V	PMSU	23:50:54.03	+38:29:33.4	2MASS	20.9	1.1	Dit14
J23517+069	B.F	G 030-026	M3.0 V+	PMSU	23:51:44.83	+06:58:15.9	2MASS	19.5	0.5	Cor16
J23523-146	.mF	LP 823-008	M4.5 V	PMSU	23:52:23.40	-14:41:24.0	2MASS	22.6	1.0	Cor16
J23535+121	..F	RX J2353.5+1206 2	M2.5 V	Lep13	23:53:35.63	+12:06:16.8	2MASS	41.51	5.25	aHIP2
J23541+516	..F	G 217-023	M3.5 V	PMSU	23:54:10.49	+51:41:09.9	2MASS	17.3	0.7	Dit14
J23544+081	..F	G 030-028	M3.0 V	PMSU	23:54:26.80	+08:09:43.5	2MASS	23.5	0.7	Cor16
J23548+385		RX J2354.8+3831	M4.0 V	Lep13	23:54:51.47	+38:31:36.3	2MASS	15.9	0.7	Dit14
J23554-039	..F	NLTT 58410	M3.5 V	PMSU	23:55:25.92	-03:59:00.0	2MASS	26.2	0.9	Cor16
J23556-061		GJ 912	M2.5 V	PMSU	23:55:39.81	-06:08:32.8	2MASS	18.6	1.0	HIP2
J23560+150	..F	LP 523-078	M2.5 V	AF15	23:56:00.29	+15:01:40.9	2MASS	29.4	0.7	Cor16
J23569+230	..F	G 129-045	M1.5 V	AF15	23:56:54.85	+23:05:08.9	2MASS	25.3	0.4	Cor16
J23573-129E	..f	LP 704-015 A	M3.0 V	PMSU	23:57:20.57	-12:58:48.7	2MASS	17.8	0.5	Cor16
J23573-129W	S..	LP 704-014 Bab	M4.0 V+	PMSU	23:57:19.35	-12:58:40.7	2MASS	15.3	0.6	Cor16
J23577+197	..F	LP 404-006	M3.5 V	PMSU	23:57:45.17	+19:46:11.2	2MASS	18.7	1.0	Dit14
J23577+233	V..	GJ 1292	M3.5 V	PMSU	23:57:44.10	+23:18:17.0	2MASS	13.7	0.5	vAl95
J23578+386	B..	LP 291-034	M3.0 V+	PMSU	23:57:49.90	+38:37:46.9	2MASS	18.2	0.5	Cor16
J23582-174	B.F	LP 764-040	M1.9 V+	Shk09	23:58:13.66	-17:24:33.8	2MASS	21.2	0.4	Cor16
J23585+076		Wolf 1051	M3.0 V	PMSU	23:58:32.64	+07:39:30.4	2MASS	16.8	0.8	HIP2
J23587+467	B..	BD+45 4378 AB	M0.0 V+	PMSU	23:58:43.42	+46:43:45.3	2MASS	17.54	0.68	HIP2
J23590+208	..F	G 129-051	M2.5 V	AF15	23:59:00.42	+20:51:38.8	2MASS	25.5	0.6	Cor16
J23598+477	..F	LP 149-014	M5.0 V	PMSU	23:59:49.41	+47:45:44.8	2MASS	19.3	0.3	vAl95

Notes. [a]See Table 2.2 for the definition.
[b]AF15: Alonso-Floriano et al. (2015a); Bid85: Bidelman (1985); Boc05: Bochanski et al. (2005); Bri98: Briceño et al. (1998); Bri99: Briceño et al. (1999); Bus98: Buscombe et al. (1998); Clo03: Close et al. (2003); CR02: Cruz & Reid (2002); Cru03: Cruz et al. (2003); Cve12: Cvetkovic et al. (2012); Dae07: Daemgen et al. (2007); Dea12: Deacon et al. (2012); Fle88: Fleming et al. (1988); Fri13: Frith et al. (2013); GR97: Gizis & Reid (1997); Gig10: Gigoyan et al. (2010); Gra03: Gray et al. (2003); Gra06: Gray et al. (2006); JA74: Joy & Abt (1974); Jahr08: Jahreiss et al. (2008); Jan12: Janson et al. (2012); Jen09: Jenkins et al. (2009); Kir91: Kirkpatrick et al. (1991); Klu13: Klutsch et al. priv. comm.; Koe10: Koen et al. (2010); Kon10: Konopacky et al. (2010); Law08: Law et al. (2008); Lep03: Lépine et al. (2003); Lep09: Lépine et al. (2009); Lep13: Lépine et al. (2013); Lod05: Lodieu et al. (2005); Met15: Metodieva et al. (2015); Mon01: Montes et al. (2001); New14: Newton et al. (2014); PB97: Pesch & Bidelman (1997); PMSU: (Palomar/Michigan State University survey catalogue of nearby stars) Reid et al. (1995), Hawley et al. (1996), Gizis et al. (2002); PBB06: Phan-Bao & Bessell (2006); Pra06: Pravdo et al. (2006); Raj13: Rajpurohit et al. (2013); Rei03: Reid et al. (2003); Rei04: Reid et al. (2004); Rei07: Reid et al. (2007); Ria06: Riaz et al. (2006); Ried14: Riedel et al. (2014); Sch05: Scholz et al. (2005); Schm07: Schmidt et al. (2007); Shk09: Shkolnik et al. (2009); Shk10: Shkolnik et al. (2010); Ski14: Skiff (2014); Stra09: Strassmeier (2009); Yi14: Yi et al. (2014).
[c]2MASS: Skrutskie et al. (2006).
[d]"a" or "b" preceeding the reference indicates that it comes from the primary or secondary of a binary system.
[e]Cor16: This work; Cru03: Cruz et al. (2003); Daw05: Dawson et al. (2005); Dit14: Dittmann et al. (2014); DL12: Dupuy & Liu (2012); GC09: Gatewood & Coban (2009); GJ91: Gliese & Jahreiss (1991); HD80: Harrington & Dahn (1980); HIP1: Perryman et al. (1997); HIP2: van Leeuwen (2007); Hen06; Henry et al. (2006); Ir08: Ireland et al. (2008); Jao05: Jao et al. (2005); Jen52: Jenkins (1952); Jen63: Jenkins (1963); Jen09: Jenkins et al. (2009); Lep09: Lépine et al. (2009); Lep13: Lépine et al. (2013); Lod05: Lodieu et al. (2005); New14: Newton et al. (2014); PBB06: Phan-Bao & Bessell (2006); Pra06: Pravdo et al. (2006); RB09: Reiners & Basri (2009); Rei02: Reid et al. (2002); Ried10: Riedel et al. (2010); Ried14: Riedel et al. (2014); Shk12: Shkolnik et al. (2012); Sub09; Subasavage et al. (2009); Wein16: Weinberger et al. (2016); Weis87: Weis (1987); vAl95: van Altena et al. (1995).

Table B.3: Proper motions and UVW space velocities of Carmencita stars.

Karmn	$\mu_\alpha \cos\delta$ [mas a^{-1}]	$e\mu_\alpha \cos\delta$ [mas a^{-1}]	μ_δ [mas a^{-1}]	$e\mu_\delta$ [mas a^{-1}]	Ref.[a b]	V_r [km s^{-1}]	Ref.[c]	U [km s^{-1}]	V [km s^{-1}]	W [km s^{-1}]	Ref.[d]
J00012+139N	27.99	4.93	138.84	3.13	HIP2	-4.0	Dy54	-13.9	9.31	17.12	Mon16
J00012+139S	27.99	4.93	138.84	3.13	aHIP2			-13.9	12.1		Lep13
J00026+383	-72.2	4.7	-30.5	4.7	PPMXL						
J00033+046	-25.51	3.22	-86.28	2.16	HIP2			8.5	-6.8		Lep13
J00051+457	870.19	0.91	-150.45	0.85	HIP2	-0.4	Schf15	-38.03	-22.9	-15.73	Mon16
J00056+458	878.72	1.66	-153.9	1.64	aHIP1	-1.3	Schf15	-39.73	-24.99	-16.36	Mon16
J00067-075	-818.4	6.6	-1883.1	6.6	PPMXL	-35.7	Des12	37.97	-39.51	21.74	Mon16
J00077+603	343.2	4.9	-31.7	4.9	PPMXL	1.89	Schf15	-21.2	-9.18	-6.24	Mon16
J00078+676	-39.6	0.5	-100.4	0.3	Cortes			5.1		-8.5	Lep13
J00079+080	-367.0	0.4	-418.6	0.3	Gal15	-51.3	PMSU	63.31	-41.73	21.92	Mon16
J00081+479	-122.1	4.7	3.9	4.7	PPMXL	-29.64	Shk10	18.14	-22.8	8.64	Mon16
J00084+174	-92.98	1.86	-64.25	1.49	HIP2	10.3	PMSU	8.89	7.66	-10.21	Mon16
J00088+208	-53.3	0.4	-251.1	0.5	Cortes	10.44	Schf15	8.0	-0.16	-19.22	Mon16
J00110+052	234.52	4.07	66.96	2.33	HIP2			-48.5	-14.3		Lep13
J00115+591	-904.6	4.9	-1165.7	4.9	PPMXL						
J00118+229	131.0	4.5	-226.2	4.5	PPMXL	-47.24	Ter15	11.55	-48.05	14.58	Mon16
J00119+330	-553.1	5.1	-396.7	5.1	PPMXL						
J00122+304	52.7	5.1	-25.9	5.1	PPMXL						
J00131+703	45.5	1.8	139.5	1.8	PPMXL			-6.2		16.8	Lep13
J00132+693	723.93	6.3	-293.85	7.0	HIP2	10.2	PMSU	-59.73	-17.41	-34.42	Mon16
J00133+275	16.3	4.4	-116.4	4.4	PPMXL						
J00136+806	253.1	2.1	183.7	2.1	PPMXL	-13.2	PMSU	-13.43	-27.65	8.55	Mon16
J00137+806	257.1	0.6	181.4	0.2	Gal15	-17.6	PMSU	-11.57	-31.33	6.95	Mon16
J00154-161	632.2	0.4	-619.5	0.7	Cortes	-18.2	PMSU	-6.17	-23.89	12.75	Mon16
J00156+722	311.7	2.6	175.3	2.6	PPMXL			-36.1		17.6	Lep13
J00158+135	620.0	4.6	326.4	4.6	PPMXL	50.0	New14	-43.62	26.74	-31.4	Mon16
J00159-166	-124.1	0.4	8.5	0.7	Cortes	21.0	Shk12	9.41	10.49	-18.85	Mon16
J00162+198E	718.2	0.7	-767.3	0.4	Gal15	-1.47	Schf15	-23.12	-59.97	-49.74	Mon16
J00162+198W	718.2	0.7	-767.3	0.4	aGal15	24.01	Schf15	-30.1	-42.45	-66.87	Mon16
J00169+051	-88.3	5.2	-621.0	5.2	PPMXL	13.9	PMSU	28.5	-25.53	-38.19	Mon16
J00169+200	235.2	5.1	15.9	5.1	PPMXL	26.0	PMSU	-31.28	5.98	-19.68	Mon16
J00173+291	689.56	2.5	427.58	1.25	HIP2	-33.7	PMSU	-71.33	-42.11	47.3	Mon16

Table B.3: Proper motions and UVW space velocities of Carmencita stars (continued).

Karmn	$\mu_\alpha \cos\delta$ [mas a^{-1}]	$e\mu_\alpha \cos\delta$ [mas a^{-1}]	μ_δ [mas a^{-1}]	$e\mu_\delta$ [mas a^{-1}]	Ref.[a b]	V_r [km s^{-1}]	Ref.[c]	U [km s^{-1}]	V [km s^{-1}]	W [km s^{-1}]	Ref.[d]
J00176-086	304.4	1.6	18.9	1.2	PPMXL	17.5	PMSU	-45.6	-15.57	-21.97	Mon16
J00179+209	-252.7	5.7	-362.0	5.7	PPMXL			63.0		-39.0	Lep13
J00182+102	1.9	0.4	-30.3	0.4	Cortes	-45.4	PMSU	10.38	-28.04	34.25	Mon16
J00183+440	2888.92	0.6	410.1	0.48	HIP2	11.5	PMSU	-49.31	-12.46	-3.37	Mon16
J00184+440	2888.92	0.6	410.1	0.48	aHIP2	6.0	New14	-47.09	-17.19	-1.62	Mon16
J00188+278	389.7	4.5	-110.7	4.5	PPMXL	3.1	PMSU	-21.44	-14.04	-11.33	Mon16
J00201-170	140.61	4.92	-10.42	2.25	HIP2	23.6	PMSU	-12.42	-3.44	-25.13	Mon16
J00204+330	1077.9	5.6	-867.9	5.6	PPMXL	-29.5	PMSU	-27.06	-73.81	-37.61	Mon16
J00207+596	-27.8	1.0	-117.7	0.1	Cortes			3.1		-12.9	Lep13
J00209+176	37.5	1.6	-83.9	1.7	PPMXL			0.9	-10.6		Lep13
J00210+557	382.2	2.7	-235.6	0.2	Cortes						
J00218+382	618.4	5.0	-323.9	5.0	PPMXL	-39.79	Daw05	-26.44	-71.59	-19.02	Mon16
J00219+492	205.1	0.8	-36.0	1.3	Gal15	3.1	PMSU	-22.56	-10.53	-7.97	Mon16
J00234+243	-230.0	0.3	119.0	0.7	Cortes	-2.1	PMSU	12.59	11.91	10.44	Mon16
J00234+771	-841.42	2.44	46.46	2.06	HIP2	-66.3	PMSU	99.65	-18.23	-4.13	Mon16
J00235+771	-837.7	2.5	44.8	2.5	aPPMXL	-60.7	PMSU	96.63	-13.66	-2.91	Mon16
J00240+264	141.6	0.2	-48.7	0.5	Gal15	16.0	West15	-16.46	1.96	-15.07	Mon16
J00244+360	291.7	2.6	32.5	2.7	PPMXL			-44.5		-1.7	Lep13
J00245+300	585.9	5.1	7.4	5.1	PPMXL	11.0	New14	-49.68	-17.43	-10.82	Mon16
J00253+228	-232.0	5.2	-465.0	5.2	PPMXL	-52.2	PMSU	42.66	-44.82	10.93	Mon16
J00268+701	-136.47	1.57	-146.94	1.09	HIP2	-25.6	PMSU	22.39	-14.65	-13.6	Mon16
J00271+496	361.1	4.8	-230.1	4.8	PPMXL	-74.3	PMSU	8.59	-84.67	-8.79	Mon16
J00279+223	412.3	4.8	-177.6	4.8	PPMXL	-15.8	Des12	-15.49	-32.63	-2.29	Mon16
J00286-066	-329.3	5.0	-797.5	5.0	PPMXL	-12.13	Schf15	44.13	-33.5	-4.41	Mon16
J00288+503	422.8	1.1	118.4	0.7	Gal15	-7.1	PMSU	-28.55	-22.32	8.01	Mon16
J00315-058	349.2	5.0	-1046.7	5.0	PPMXL	-9.22	Schf15	18.16	-79.64	-22.48	Mon16
J00322+544	-218.1	4.9	-442.9	4.9	PPMXL	-1.83	Ter15	24.62	5.41	-40.03	Mon16
J00324+672N	1738.21	2.19	-224.11	1.91	HIP2	-4.9	PMSU	-68.54	-45.53	-17.16	Mon16
J00324+672S	1738.21	2.19	-224.11	1.91	aHIP2	-3.4	PMSU	-69.31	-44.25	-17.05	Mon16
J00325+074	105.0	3.1	-63.4	3.0	PPMXL	0.9	PMSU	-3.4	-4.59	-3.02	Mon16
J00328-045	73.6	5.0	-156.6	5.0	PPMXL						
J00333+368	493.6	4.7	119.2	4.7	PPMXL			-46.6		8.6	Lep13
J00341+253	86.7	1.6	-94.8	1.6	PPMXL	-12.4	Shk10	-1.64	-22.94	-5.11	Mon16

Table B.3: Proper motions and UVW space velocities of Carmencita stars (continued).

Karmn	$\mu_\alpha \cos\delta$ [mas a^{-1}]	$e\mu_\alpha \cos\delta$ [mas a^{-1}]	μ_δ [mas a^{-1}]	$e\mu_\delta$ [mas a^{-1}]	Ref.[a b]	V_r [km s^{-1}]	Ref.[c]	U [km s^{-1}]	V [km s^{-1}]	W [km s^{-1}]	Ref.[d]
J00346+711	522.1	4.7	-346.7	4.7	PPMXL	-14.6	PMSU	-36.28	-32.96	-38.52	Mon16
J00357+025	158.0	4.6	-176.8	4.6	PPMXLs						
J00358+526	775.8	4.8	-180.0	4.8	PPMXL	-18.33	Daw05	-39.46	-47.77	-13.85	Mon16
J00359+104	1085.4	1.2	-388.8	0.4	Gal15	35.0	PMSU	-65.94	-41.69	-50.2	Mon16
J00361+455	-248.1	0.1	-145.0	0.3	Gal15	-32.7	PMSU	41.75	-16.67	-3.64	Mon16
J00374+515	-497.5	3.1	-24.9	2.8	PPMXL			64.0		0.4	Lep13
J00380+169	-105.4	4.9	-97.1	4.9	PPMXL						
J00382+523	-74.76	1.24	-136.62	1.24	HIP2	22.1	BE12	-1.88	21.04	-18.67	Mon16
J00385+514	-214.9	0.1	40.6	0.4	Cortes	-0.5	PMSU	13.36	8.29	3.83	Mon16
J00389+306	1549.6	0.7	35.1	0.4	Gal15	-0.6	PMSU	-78.59	-47.48	-2.36	Mon16
J00395+149N	330.0	4.9	32.9	4.9	aPPMXL						
J00395+149S	330.0	4.9	32.9	4.9	PPMXL	4.11	Schf15	-40.83	-18.02	-2.14	Mon16
J00395+605	-156.1	4.7	-290.2	4.7	PPMXL	-45.7	PMSU	43.15	-28.82	-34.47	Mon16
J00409+313	-48.3	0.4	-334.3	0.3	Gal15	21.2	PMSU	2.85	5.81	-34.8	Mon16
J00413+558	312.9	0.3	-65.9	0.3	Gal15	-30.7	PMSU	-12.41	-44.56	-4.73	Mon16
J00427+438	-23.5	0.6	-53.6	0.1	Cortes			2.3		-3.3	Lep13
J00428+355	266.54	2.57	74.44	1.72	HIP2	3.4	PMSU	-28.72	-9.91	4.76	Mon16
J00435+284	-122.6	0.6	-1069.5	0.6	Gal15	-62.6	PMSU	67.41	-83.98	-44.98	Mon16
J00443+091	813.9	0.6	-5.1	0.4	Cortes	8.3	PMSU	-50.31	-26.13	-8.46	Mon16
J00443+126	285.2	1.2	-186.1	1.2	PPMXL	32.75	Schf15	-23.27	-3.09	-35.09	Mon16
J00449-152	315.2	0.5	-591.5	0.7	Cortes	-78.1	PMSU	10.2	-62.82	66.89	Mon16
J00459+337	260.4	5.0	16.4	5.0	PPMXL						
J00463+353	-54.7	3.7	-112.2	3.8	PPMXL			12.3		-12.6	Lep13
J00464+506	415.8	4.8	-213.9	4.8	PPMXL						
J00468+160	-117.6	4.9	-59.5	4.9	PPMXL			10.6	3.3		Lep13
J00484+753	214.8	4.8	-47.5	4.8	PPMXL						
J00487+270	-159.7	0.3	-291.7	0.2	Gal15	-48.8	PMSU	45.14	-39.41	3.87	Mon16
J00489+445	119.2	0.3	-134.6	0.8	Gal15	50.2	PMSU	-33.64	29.77	-29.32	Mon16
J00490+657	119.3	4.9	-65.5	4.9	PPMXL						
J00502+086	64.7	4.8	-35.9	4.8	PPMXL	12.86	Ter15	-7.04	1.69	-12.1	Mon16
J00505+248	195.38	4.57	-39.46	2.52	HIP2	9.2	PMSU	-13.42	-1.87	-7.67	Mon16
J00511+225	43.4	2.1	-125.4	2.1	PPMXL			-0.6	-7.8		Lep13
J00514+583	1567.03	1.99	404.79	1.72	HIP2	-33.1	PMSU	-98.99	-100.08	38.07	Mon16

Table B.3: Proper motions and UVW space velocities of Carmencita stars (continued).

Karmn	$\mu_\alpha \cos\delta$ [mas a^{-1}]	$e\mu_\alpha \cos\delta$ [mas a^{-1}]	μ_δ [mas a^{-1}]	$e\mu_\delta$ [mas a^{-1}]	Ref.[a b]	V_r [km s^{-1}]	Ref.[c]	U [km s^{-1}]	V [km s^{-1}]	W [km s^{-1}]	Ref.[d]
J00515-229	613.33	1.22	-276.64	0.79	aHIP2	30.0	PMSU	-28.18	-39.95	-31.4	Mon16
J00520+205	177.31	2.71	-109.2	2.04	HIP2			-16.6	-23.6		Lep13
J00532+190	-111.2	5.0	-122.4	5.0	PPMXL			15.3	-1.9		Lep13
J00538+459	304.53	1.86	69.64	1.27	HIP2			-33.7		8.9	Lep13
J00540+691	74.1	4.9	-261.0	4.9	PPMXL						
J00548+275	340.0	4.9	7.9	4.9	PPMXL	7.3	Shk12	-35.24	-15.43	-3.01	Mon16
J00566+174	686.5	0.5	-290.8	0.4	Gal15	-26.55	Schf15	-28.15	-61.89	2.91	Mon16
J00570+450	633.3	0.2	-74.3	0.2	Gal15	6.82	Schf15	-37.65	-18.99	-5.83	Mon16
J00577+058	-60.8	1.6	2.7	1.4	PPMXL			5.2	3.6		Lep13
J00580+393	-109.3	0.3	25.9	0.3	Cortes	-1.34	Schf15	6.83	3.96	2.03	Mon16
J01008+669	-257.7	5.0	-55.5	5.0	PPMXL	3.8	PMSU	18.95	17.84	-6.23	Mon16
J01009-044	1237.4	5.1	439.8	5.1	PPMXL	28.75	Schf15	-93.9	-15.88	-11.51	Mon16
J01013+613	352.7	0.4	-804.3	0.2	Gal15	13.3	PMSU	-23.41	-1.09	-41.53	Mon16
J01019+541	-304.1	5.0	-115.6	5.0	PPMXL	-1.6	PMSU	14.2	6.63	-6.3	Mon16
J01025+716	1745.38	1.23	-380.81	1.16	HIP2	0.5	PMSU	-57.43	-35.71	-11.47	Mon16
J01026+623	731.52	1.15	90.43	1.08	HIP2	-5.31	Schf15	-25.42	-23.66	5.81	Mon16
J01032+200	673.45	2.84	45.14	1.72	HIP2	-3.8	PMSU	-42.25	-29.33	7.49	Mon16
J01032+316	217.8	6.2	-7.2	6.2	PPMXL	27.4	PMSU	-47.65	-4.96	-13.43	Mon16
J01032+712	505.3	1.4	-60.0	0.4	Gal15						
J01033+623	731.52	1.15	90.43	1.08	aHIP2	-4.0	New14	-26.11	-22.6	5.89	Mon16
J01036+408	122.86	1.94	-163.46	1.55	HIP2			-10.1		-21.1	Lep13
J01037+408	122.86	1.94	-163.46	1.55	aHIP2	-10.9	Shk12	-4.45	-25.78	-16.55	Mon16
J01041+108	34.2	3.0	-67.9	3.0	PPMXL			1.8	-10.5		Lep13
J01048-181	1288.7	0.5	489.0	1.1	Cortes	10.0	PMSU	-63.02	-14.2	-3.18	Mon16
J01056+284	1917.9	0.4	-189.5	0.2	Gal15	18.1	PMSU	-90.56	-51.16	-12.91	Mon16
J01066+152	-112.0	2.66	-253.44	1.68	HIP2	15.7	PMSU	13.31	-1.73	-30.15	Mon16
J01069+804	202.3	4.7	-26.6	4.7	PPMXL						
J01078+128	275.4	1.0	-24.9	1.0	PPMXL			-31.4	-23.3		Lep13
J01102-118	222.1	0.8	-119.6	0.9	Cortes						
J01114+154	181.9	4.7	-129.9	4.7	PPMXL	3.0	New14	-9.36	-13.65	-8.21	Mon16
J01116+120	-1.7	1.2	-291.1	1.2	PPMXL			16.6	-25.8		Lep13
J01119+049N	374.4	4.9	-534.9	4.9	PPMXL	24.1	PMSU	-13.37	-35.57	-39.48	Mon16
J01119+049S	363.8	4.9	-532.0	4.9	PPMXL	15.5	PMSU	-8.96	-30.25	-28.68	Mon16

Table B.3: Proper motions and UVW space velocities of Carmencita stars (continued).

Karmn	$\mu_\alpha \cos\delta$ [mas a^{-1}]	$e\mu_\alpha \cos\delta$ [mas a^{-1}]	μ_δ [mas a^{-1}]	$e\mu_\delta$ [mas a^{-1}]	Ref.[a b]	V_r [km s^{-1}]	Ref.[c]	U [km s^{-1}]	V [km s^{-1}]	W [km s^{-1}]	Ref.[d]
J01125-169	1208.53	5.57	640.73	3.71	HIP2	37.0	PMSU	-29.72	0.53	-32.57	Mon16
J01133+589	158.5	4.9	-129.5	4.9	PPMXL			-16.0		-13.2	Lep13
J01134-229	153.0	4.9	25.4	4.9	PPMXL	2.5	PMSU	-14.62	-6.96	-0.94	Mon16
J01141+790	55.1	4.7	71.6	4.7	PPMXL						
J01147+253	376.1	2.2	-193.1	2.2	PPMXL			-42.9		-21.0	Lep13
J01158+470	198.6	4.9	-20.1	4.9	PPMXL						
J01161+601	375.6	3.7	-201.4	4.1	PPMXL			-45.8		-23.9	Lep13
J01178+054	85.1	0.7	-629.9	0.8	Cortes	-65.8	PMSU	46.3	-73.93	22.98	Mon16
J01178+286	-343.7	1.9	-269.5	1.9	PPMXL	-85.2	PMSU	89.3	-46.03	14.88	Mon16
J01182-128	173.92	3.5	-679.48	2.15	HIP2	-2.2	PMSU	24.88	-67.83	-13.58	Mon16
J01198+841	-974.8	0.1	459.6	0.1	Gal15	-30.5	PMSU	76.65	7.1	9.95	Mon16
J01214+243	339.56	3.09	8.44	2.43	HIP2			-33.9	-24.3		Lep13
J01221+221	237.0	5.3	-152.7	5.3	PPMXL	-0.7	Mo02	-5.61	-10.01	-3.22	Mon16
J01227+005	-209.7	4.7	-534.0	4.7	PPMXL	-4.0	New14	27.18	-17.84	-13.07	Mon16
J01256+097	198.7	4.9	-403.8	4.9	PPMXL	-14.23	Schf15	7.06	-34.81	-4.48	Mon16
J01317+209	413.7	1.1	-130.5	0.5	Cortes			-54.1	-64.0		Lep13
J01324-219	-589.19	1.86	-887.83	1.24	HIP2	-28.4	PMSU	88.87	-29.27	12.79	Mon16
J01339-176	41.3	5.2	-177.8	5.2	PPMXL	-5.3	RAVE	5.76	-10.76	3.67	Mon16
J01352-072	106.5	5.1	-60.7	5.1	PPMXL	11.7	Shk12	-7.37	-5.45	-11.0	Mon16
J01369-067	173.9	0.3	-99.9	1.7	Cortes	12.2	Shk12	-13.53	-18.62	-11.73	Mon16
J01373+610	-21.9	2.7	-74.1	2.7	PPMXL			1.1		-9.8	Lep13
J01383+572	-188.2	0.7	-347.1	0.3	Gal15	-29.5	PMSU	24.95	-19.91	-17.97	Mon16
J01384+006	512.42	3.35	162.2	1.96	HIP2	0.278	Schf15	-45.4	-18.31	15.9	Mon16
J01390-179	3204.9	1.9	702.4	0.5	Gal15	29.0	Schf15	-42.93	-16.85	-19.36	Mon16
J01395+050	119.1	4.5	136.1	4.5	PPMXL	12.7	PMSU	-21.98	6.83	-0.48	Mon16
J01402+317	456.0	4.8	-1.0	4.8	PPMXL	-19.4	PMSU	-19.16	-36.7	17.22	Mon16
J01431+210	-78.1	5.1	-10.2	5.1	PPMXL	-47.0	Mo02	31.81	-20.4	28.59	Mon16
J01432+278	551.29	1.89	-34.19	1.22	HIP2	-0.7	PMSU	-40.95	-36.31	8.65	Mon16
J01433+043	-418.45	2.19	-763.81	1.43	HIP2	-28.4	PMSU	49.03	-24.75	-2.4	Mon16
J01437-060	45.4	5.3	-25.1	5.3	PPMXL	11.1	RAVE	-5.8	-1.66	-10.1	Mon16
J01449+163	-749.4	5.0	-431.2	5.0	PPMXL	5.0	Schf15	52.88	16.5	-38.33	Mon16
J01453+465	394.15	3.06	215.97	1.84	HIP2	17.85	Shk10	-48.37	-8.09	29.92	Mon16
J01466-086	414.8	5.1	-160.8	5.1	PPMXL	10.6	PMSU	-19.13	-24.44	-7.32	Mon16

Table B.3: Proper motions and UVW space velocities of Carmencita stars (continued).

Karmn	$\mu_\alpha \cos\delta$ [mas a^{-1}]	$e\mu_\alpha \cos\delta$ [mas a^{-1}]	μ_δ [mas a^{-1}]	$e\mu_\delta$ [mas a^{-1}]	Ref.[a b]	V_r [km s^{-1}]	Ref.[c]	U [km s^{-1}]	V [km s^{-1}]	W [km s^{-1}]	Ref.[d]
J01480+212	342.96	4.44	-213.27	3.333	HIP2	-19.1	PMSU	-7.72	-42.57	4.23	Mon16
J01510-061	545.3	0.7	-264.3	0.4	Cortes	5.9	PMSU	-14.95	-24.65	-3.96	Mon16
J01514+213	-9.8	5.1	-350.9	5.1	PPMXL	1.1	PMSU	8.36	-17.07	-22.74	Mon16
J01518+644	211.3	4.7	-167.9	4.7	PPMXL	-18.8	PMSU	-1.18	-24.86	-8.56	Mon16
J01518-108	567.12	2.95	-539.39	2.53	HIP2	1.3	PMSU	-9.94	-60.72	-3.04	Mon16
J01531-210	272.3	2.4	70.0	2.4	PPMXL	10.9	Tor06	-29.35	-13.19	-2.66	Mon16
J01538-149	106.9	2.2	-50.6	2.2	PPMXL	2.0	RAVE	-3.68	-6.46	-1.0	Mon16
J01544+576	-26.8	5.0	-287.0	6.4	PPMXL			-0.1		-28.5	Lep13
J01550+379	227.9	0.1	-474.7	0.6	Gal15						
J01556+028	-295.13	3.79	-287.24	2.64	HIP2			66.4	-4.5		Lep13
J01567+305	219.2	4.6	-12.5	4.6	PPMXL						
J01592+035E	257.59	4.12	24.96	3.68	HIP2	-9.0	New14	-24.86	-23.59	19.13	Mon16
J01592+035W	257.59	4.12	24.96	3.68	aHIP2	-9.0	New14	-24.86	-23.59	19.13	Mon16
J01593+585	321.75	3.57	-195.78	2.9	PPMXL	-29.5	PMSU	4.15	-36.21	-4.46	Mon16
J02000+437	121.0	5.0	-281.2	5.0	PPMXL	-10.0	PMSU	-4.2	-31.37	-26.72	Mon16
J02001+366	52.8	5.0	-257.9	5.0	PPMXL	3.5	PMSU	-3.74	-14.24	-23.58	Mon16
J02002+130	1090.4	0.7	-1765.9	0.9	Gal15	-28.68	Schf15	13.36	-51.03	2.91	Mon16
J02007-103	-372.5	5.4	-367.4	5.4	PPMXL	25.9	PMSU	49.89	-4.28	-49.83	Mon16
J02015+637	-255.6	2.1	-92.9	2.1	PPMXL	-69.9	PMSU	55.41	-44.09	-11.93	Mon16
J02019+735	274.8	0.7	-113.4	0.6	Cortes	40.8	PMSU	-37.44	21.98	6.25	Mon16
J02020+039	-340.75	4.03	-322.76	3.13	PPMXL	-57.1	PMSU	101.55	-17.98	-0.62	Mon16
J02022+103	-687.1	0.2	-286.8	0.1	Gal15	17.0	New14	16.83	15.86	-28.4	Mon16
J02026+105	-50.5	4.4	-43.6	4.9	PPMXL	22.8	Schf15	-10.83	7.65	-18.76	Mon16
J02027+135	459.7	0.3	-92.5	0.3	Gal15	-19.0	New14	-23.11	-47.67	21.17	Mon16
J02028+047	-79.6	5.1	-129.1	5.1	PPMXL			9.3	-3.6		Lep13
J02033-212	-199.3	2.7	-424.6	2.6	PPMXL	0.3	PMSU	57.45	-27.89	-14.98	Mon16
J02044-018	-589.3	0.5	-574.5	0.7	Cortes	-44.0	PMSU	84.93	-12.58	1.08	Mon16
J02050-176	1313.71	1.71	-176.07	1.36	HIP2	23.675	Schf15	-43.86	-42.96	-7.75	Mon16
J02055+056	100.74	4.79	-283.36	3.32	HIP2			-21.2	1.6		Lep13
J02069+451	258.7	1.5	-450.4	1.4	PPMXL	70.32	Daw05	-66.31	16.11	-49.07	Mon16
J02070+496	235.3	0.9	-427.8	0.4	Gal15	18.64	Schf15	-29.4	-11.6	-31.15	Mon16
J02071+642	220.3	4.8	-168.4	4.8	PPMXL	9.2	PMSU	-22.61	-7.01	-7.71	Mon16
J02082+802	478.0	2.5	-289.3	2.6	PPMXL			-80.9		-21.4	Lep13

Table B.3: Proper motions and UVW space velocities of Carmencita stars (continued).

Karmn	$\mu_\alpha \cos\delta$ [mas a^{-1}]	$e\mu_\alpha \cos\delta$ [mas a^{-1}]	μ_δ [mas a^{-1}]	$e\mu_\delta$ [mas a^{-1}]	Ref.[a b]	V_r [km s^{-1}]	Ref.[c]	U [km s^{-1}]	V [km s^{-1}]	W [km s^{-1}]	Ref.[d]
J02088+494	229.8	5.1	-274.1	5.1	PPMXL	-33.0	PMSU	11.37	-38.13	-5.47	Mon16
J02096-143	519.59	2.13	-351.48	1.43	HIP2	17.54	Schf15	-21.42	-56.49	-9.46	Mon16
J02116+185	197.4	5.3	275.2	5.3	PPMXL	-55.32	Schf15	17.0	-17.68	57.47	Mon16
J02123+035	-1760.7	2.39	-1852.91	1.45	HIP2	-2.62	Schf15	103.6	-11.94	-71.0	Mon16
J02129+000	554.0	4.6	29.6	4.8	PPMXL	27.83	Schf15	-33.68	-11.11	-14.44	Mon16
J02133+368	28.2	5.2	46.8	5.2	PPMXL	42.24	Ter15	-31.54	24.94	-13.43	Mon16
J02142-039	508.2	5.4	-153.6	5.4	PPMXL	-15.6	Des12	-10.92	-31.83	20.15	Mon16
J02149+174	347.4	5.0	-468.0	5.0	PPMXL	-3.3	PMSU	-7.53	-52.97	-18.14	Mon16
J02153+074	398.55	3.7	-410.7	2.96	HIP2			-16.1	-80.4		Lep13
J02155+339	160.5	4.7	-374.4	4.7	PPMXL	19.6	PMSU	-20.98	-18.35	-34.05	Mon16
J02158-126	498.3	5.1	217.3	5.1	PPMXL	58.9	PMSU	-64.82	-13.63	-35.12	Mon16
J02164+135	490.4	0.7	-438.9	0.4	Gal15	4.4	PMSU	-10.37	-23.47	-7.98	Mon16
J02171+354	553.6	4.7	-263.0	4.7	PPMXL	-4.0	New14	-14.86	-26.51	-0.52	Mon16
J02185+207	-25.4	0.5	-287.5	0.6	Cortes				-19.0	-25.5	Lep13
J02186+123	154.6	1.0	-103.9	1.0	PPMXL	27.0	Shk12	-24.42	-9.96	-20.61	Mon16
J02190+238	298.0	4.9	-74.9	4.9	PPMXL	7.9	PMSU	-23.81	-19.89	-0.34	Mon16
J02190+353	670.3	1.0	-430.2	1.0	Cortes	-27.88	Schf15	-15.54	-70.72	-0.58	Mon16
J02204+377	332.8	4.8	-67.9	4.8	PPMXL	35.2	PMSU	-51.26	-8.27	-6.98	Mon16
J02207+029	150.2	4.7	-288.0	4.7	PPMXL	35.4	PMSU	-17.8	-20.31	-36.3	Mon16
J02210+368	741.0	4.8	-564.6	4.8	PPMXL	75.8	PMSU	-97.19	-25.22	-49.83	Mon16
J02222+478	215.95	1.06	39.76	0.98	HIP2	-38.61	Schf15	20.06	-32.15	14.46	Mon16
J02230+181	161.6	2.3	-151.7	2.3	PPMXL				-33.5	-8.0	Lep13
J02234+227	92.43	3.05	-113.69	2.36	HIP2	10.4	Schl10	-12.2	-13.64	-13.05	Mon16
J02247+259	-94.3	1.6	-174.9	1.6	PPMXL	-20.3	PMSU	28.4	-15.68	-13.21	Mon16
J02254+246	-96.6	1.6	-0.5	1.6	PPMXL				10.5	-4.4	Lep13
J02256+375	283.7	4.8	-70.1	4.8	PPMXL	6.4	PMSU	-23.92	-18.99	1.8	Mon16
J02272+545	118.9	0.9	-107.2	0.5	Gal15						
J02274+031	-130.6	4.8	-12.4	4.8	PPMXL						
J02277+044	86.42	1.85	240.0	0.96	HIP2	5.99	BE12	-16.84	10.86	8.0	Mon16
J02282+014	285.4	4.7	-125.8	4.7	PPMXL	19.0	PMSU	-25.84	-28.95	-10.19	Mon16
J02283+219	55.2	2.2	-19.2	2.2	PPMXL				-6.6	0.2	Lep13
J02285-200	613.99	1.01	189.1	1.06	aHIP2	22.9	PMSU	-57.24	-27.08	2.24	Mon16
J02287+156	160.2	4.8	-3.0	4.8	PPMXL				-12.6	8.0	Lep13

Table B.3: Proper motions and UVW space velocities of Carmencita stars (continued).

Karmn	$\mu_\alpha \cos\delta$ [mas a^{-1}]	$e\mu_\alpha \cos\delta$ [mas a^{-1}]	μ_δ [mas a^{-1}]	$e\mu_\delta$ [mas a^{-1}]	Ref.[a b]	V_r [km s^{-1}]	Ref.[c]	U [km s^{-1}]	V [km s^{-1}]	W [km s^{-1}]	Ref.[d]
J02289+120	5.13	4.03	81.87	2.33	HIP2	-52.9	PMSU	30.97	-8.01	43.33	Mon16
J02289+226	143.2	1.6	-44.6	1.6	PPMXL				-20.9	5.4	Lep13
J02292+195	149.7	4.7	-222.5	4.7	PPMXL				-29.2	-12.0	Lep13
J02293+884	-131.0	4.3	414.3	4.3	PPMXL	-25.6	PMSU	40.11	-15.5	14.0	Mon16
J02314+573	1113.0	0.5	9.5	0.1	Gal15	3.4	PMSU	-68.0	-62.99	38.33	Mon16
J02330+078	212.88	4.23	-75.89	2.87	HIP2			-18.0	-32.5		Lep13
J02336+249	50.0	0.0	-661.0	3.0	PPMXL	-6.14	Schf15	8.88	-23.38	-18.84	Mon16
J02337+150	435.5	5.2	32.1	5.2	PPMXL	37.1	PMSU	-57.48	-17.45	-3.95	Mon16
J02340+417	287.1	4.6	83.8	4.6	PPMXL	74.4	PMSU	-74.06	29.05	-4.39	Mon16
J02345+566	96.8	5.4	-226.6	5.4	PPMXL				-17.9	-22.1	Lep13
J02353+235	-84.3	4.6	-67.4	4.6	PPMXL	4.7	PMSU	3.84	3.14	-11.4	Mon16
J02358+202	252.38	2.38	-140.57	1.63	HIP2	0.54	Schf15	-8.62	-16.52	-0.33	Mon16
J02362+068	1807.78	0.89	1444.02	0.46	aHIP2	26.59	Schf15	-76.92	0.54	31.5	Mon16
J02364+554	-248.2	0.2	-257.5	0.8	Gal15	-45.9	PMSU	41.95	-24.96	-22.73	Mon16
J02367+226	-42.6	4.5	-374.3	4.5	PPMXL	-0.6	West15	7.71	-14.62	-19.01	Mon16
J02367+320	-331.6	0.7	-70.1	0.6	Gal15	-9.5	PMSU	23.15	8.27	-9.49	Mon16
J02392+074	479.7	0.3	-137.8	0.2	Gal15	34.3	PMSU	-46.63	-33.49	-13.68	Mon16
J02412-045	351.6	5.5	-63.4	5.5	PPMXL						
J02419+435	-48.4	2.1	-22.6	2.2	PPMXL				2.5	-5.2	Lep13
J02424+182	220.96	6.11	112.55	3.52	HIP2				-10.1	25.1	Lep13
J02438-088	616.01	4.3	-753.49	3.88	HIP2	-10.0	PMSU	11.47	-126.19	9.71	Mon16
J02441+492	334.66	0.17	-89.99	0.17	aHIP2	27.7	PMSU	-32.98	3.45	-1.44	Mon16
J02442+255	863.9	1.95	-364.16	1.49	HIP2	27.0	New14	-37.54	-17.94	-10.58	Mon16
J02443+109E	68.43	3.14	-37.36	2.44	aHIP2						
J02443+109W	68.43	3.14	-37.36	2.44	HIP2				-11.4	1.1	Lep13
J02455+449	279.6	4.6	-163.8	4.6	PPMXL	46.1	PMSU	-48.1	9.91	-12.24	Mon16
J02456+449	411.43	2.1	-127.07	2.32	HIP2	46.1	PMSU	-65.12	-9.51	-3.67	Mon16
J02462-049	1688.2	1.5	-1881.8	1.8	Cortes	44.0	PMSU	-27.97	-198.99	-36.4	Mon16
J02465+164	-828.4	5.3	-573.6	5.3	PPMXL	-14.6	PMSU	57.48	6.15	-41.65	Mon16
J02502+628	210.1	0.3	-208.1	0.6	Cortes						
J02518+062	464.4	4.9	-124.4	4.9	PPMXL	65.1	PMSU	-72.02	-39.0	-29.69	Mon16
J02518+294	-92.5	5.0	-161.9	5.0	PPMXL	-12.9	PMSU	18.09	-9.63	-12.21	Mon16
J02519+224	108.7	4.6	-109.4	4.6	PPMXL						

Table B.3: Proper motions and UVW space velocities of Carmencita stars (continued).

Karmn	$\mu_\alpha \cos\delta$ [mas a^{-1}]	$e\mu_\alpha \cos\delta$ [mas a^{-1}]	μ_δ [mas a^{-1}]	$e\mu_\delta$ [mas a^{-1}]	Ref.[a b]	V_r [km s^{-1}]	Ref.[c]	U [km s^{-1}]	V [km s^{-1}]	W [km s^{-1}]	Ref.[d]
J02524+269	15.42	3.24	-233.16	2.12	HIP2	-8.7	PMSU	9.98	-24.28	-18.01	Mon16
J02530+168	3437.3	4.7	-3813.5	4.7	PPMXL	68.55	Schf15	-69.69	-71.48	-58.87	Mon16
J02534+174	1.9	0.5	-262.0	0.3	Gal15	-32.35	Schf15	30.27	-24.31	4.72	Mon16
J02555+268	264.78	1.17	-193.1	0.76	aHIP2	37.6	PMSU	-39.63	-8.33	-19.6	Mon16
J02560-006	258.3	5.1	69.6	5.1	PPMXL	37.0	Boc05	-39.47	-8.65	-15.69	Mon16
J02562+239	75.5	4.7	168.5	4.7	PPMXL						
J02565+554E	713.28	0.7	-445.0	4.0	Cortes	70.5	PMSU	-110.35	-22.81	-10.7	Mon16
J02565+554W	701.15	0.1	-424.9	0.0	Cortes	39.2	PMSU	-85.08	-41.2	-7.67	Mon16
J02575+107	1750.4	0.5	-416.2	0.4	Gal15	-96.0	New14	-13.28	-156.15	117.29	Mon16
J02581-128	277.5	5.2	544.5	5.2	PPMXL	100.6	Schf15	-77.78	-2.04	-70.61	Mon16
J02591+366	595.0	5.0	-279.9	5.0	PPMXL	21.1	PMSU	-48.15	-39.76	-2.44	Mon16
J02592+317	40.9	0.5	186.4	0.4	Gal15	-6.4	PMSU	1.35	6.58	20.16	Mon16
J02597+389	230.8	5.1	-91.4	5.1	PPMXL	29.8	West15	-42.32	-12.11	-4.54	Mon16
J03018-165N	-343.6	2.2	-291.3	2.3	PPMXL	7.9	PMSU	13.34	-0.69	-16.94	Mon16
J03018-165S	-343.6	2.2	-291.3	2.3	PPMXL	7.9	PMSU	13.34	-0.69	-16.94	Mon16
J03026-181	401.12	4.33	161.84	3.91	HIP2	19.91	Schf15	-40.82	-18.07	3.97	Mon16
J03033-080	121.6	5.2	-40.1	5.2	PPMXL						
J03036-128	231.9	5.2	-113.6	5.2	aPPMXL	17.1	PMSU	-16.65	-31.02	-4.43	Mon16
J03037-128	231.9	5.2	-113.6	5.2	PPMXL	10.0	PMSU	-12.36	-28.33	0.9	Mon16
J03040-203	496.4	4.7	-487.5	4.7	PPMXL	28.39	Schf15	-8.59	-62.68	-11.11	Mon16
J03047+617	720.57	0.6	-695.55	0.61	PPMXL	-0.9	PMSU	-74.73	-82.27	-29.13	Mon16
J03075-039	-266.12	6.79	-388.35	5.08	HIP2	-51.1	PMSU	124.39	-27.26	-35.78	Mon16
J03077+249	228.1	5.0	-126.5	5.0	PPMXL						
J03090+100	280.1	0.4	-589.3	0.4	Gal15	-30.6	PMSU	26.21	-39.21	8.45	Mon16
J03095+457	-429.55	1.87	-386.04	1.66	HIP2	-27.0	PMSU	35.59	-8.12	-35.61	Mon16
J03102+059	-130.7	5.67	-549.76	4.59	HIP2	-5.86	Schf15	28.12	-26.22	-24.61	Mon16
J03104+584	102.7	4.7	-203.0	4.7	PPMXL	19.1	PMSU	-29.96	-6.04	-15.15	Mon16
J03109+737	1821.0	4.8	-1073.1	4.8	PPMXL	27.0	PMSU	-106.21	-62.12	8.47	Mon16
J03110-046	2.6	0.6	-300.2	0.5	Cortes						
J03112+011	110.3	4.6	-21.5	4.6	PPMXL	3.0	Boc05	-5.81	-6.6	1.27	Mon16
J03118+196	212.8	1.6	-226.9	1.6	PPMXL	9.53	Lat02	-15.41	-33.42	-10.33	Mon16
J03119+615	-3.21	2.47	115.42	1.98	HIP2	-8.3	Mon01	14.85	2.87	18.29	Mon16
J03133+047	-176.6	6.5	458.0	6.8	PPMXL	28.3	Schf15	-24.63	20.38	-13.46	Mon16

Table B.3: Proper motions and UVW space velocities of Carmencita stars (continued).

Karmn	$\mu_\alpha \cos\delta$ [mas a^{-1}]	$e\mu_\alpha \cos\delta$ [mas a^{-1}]	μ_δ [mas a^{-1}]	$e\mu_\delta$ [mas a^{-1}]	Ref.[a b]	V_r [km s^{-1}]	Ref.[c]	U [km s^{-1}]	V [km s^{-1}]	W [km s^{-1}]	Ref.[d]
J03136+653	-94.8	0.4	167.6	0.4	Gal15				17.1	12.9	Lep13
J03142+286	310.8	4.1	-751.3	4.1	PPMXL	32.3	PMSU	-32.93	-30.82	-37.48	Mon16
J03145+594	182.3	4.7	-163.6	4.7	PPMXL				-14.3	-3.3	Lep13
J03147+114	62.2	0.8	-44.8	0.4	Cortes	26.34	Ter15	-23.29	-8.05	-15.29	Mon16
J03147+485	130.3	4.2	-353.8	4.2	PPMXL	19.2	PMSU	-28.96	-14.24	-24.34	Mon16
J03162+581N	428.87	3.64	-323.65	2.98	aHIP2	-117.9	PMSU	68.76	-102.46	-4.42	Mon16
J03162+581S	428.87	3.64	-323.65	2.98	HIP2	-117.9	PMSU	68.76	-102.46	-4.42	Mon16
J03167+389	-85.1	5.1	23.4	5.1	PPMXL						
J03172+453	-266.2	0.5	-87.3	0.4	Gal15	-1.5	PMSU	12.32	10.57	-18.33	Mon16
J03177+252	784.13	3.09	-365.36	2.77	HIP2	-13.8	PMSU	-25.47	-83.09	21.98	Mon16
J03181+382	444.95	2.82	-570.94	2.03	HIP2	-40.6	PMSU	13.78	-68.12	-5.96	Mon16
J03181+426	201.6	5.2	-149.8	5.2	PPMXL	10.4	West15	-21.48	-17.3	-3.84	Mon16
J03185+103	148.43	5.63	-81.59	4.77	HIP2				-38.1	7.7	Lep13
J03186+326	209.12	4.23	-99.01	3.24	HIP2	-0.2	PMSU	-13.15	-25.34	4.49	Mon16
J03187+606	457.0	4.8	-388.2	4.8	PPMXL	27.7	PMSU	-68.21	-37.59	-8.97	Mon16
J03194+619	220.8	4.8	-194.6	4.8	PPMXL	17.5	Schf15	-38.59	-17.58	-4.83	Mon16
J03207+397	123.6	3.1	-124.1	3.1	PPMXL				-16.3	-1.1	Lep13
J03213+799	409.92	1.33	284.75	1.7	HIP2	-47.6	PMSU	26.1	-49.9	13.86	Mon16
J03217-066	320.4	2.4	-48.3	2.5	PPMXL	26.57	Schf15	-28.15	-22.84	-7.59	Mon16
J03220+029	336.1	0.4	-748.7	0.5	Gal15	64.6	PMSU	-36.44	-52.1	-56.42	Mon16
J03224+271	220.89	3.29	-64.0	2.49	HIP2	8.1	PMSU	-23.18	-26.58	7.93	Mon16
J03230+420	275.1	4.6	-694.8	4.6	PPMXL	-14.7	PMSU	-3.58	-49.46	-26.78	Mon16
J03233+116	-247.5	1.8	-143.7	1.7	PPMXL	6.2	Schf15	10.11	5.79	-22.78	Mon16
J03236+056	79.8	5.1	-71.7	5.1	PPMXL	30.27	Ter15	-23.83	-7.56	-19.22	Mon16
J03241+237	225.26	4.54	-131.38	3.7	HIP2	18.5	PMSU	-24.35	-17.31	-5.49	Mon16
J03242+237	225.26	4.54	-131.38	3.7	aHIP2	19.6	Schf15	-25.28	-17.02	-5.98	Mon16
J03247+447	-106.2	4.8	-29.8	4.8	PPMXL				5.5	-9.5	Lep13
J03257+058	-178.0	5.1	-168.3	5.1	PPMXL	-3.4	PMSU	18.02	-0.87	-16.07	Mon16
J03263+171	83.2	4.9	-71.5	4.9	PPMXL	26.76	Schf15	-24.52	-5.68	-14.1	Mon16
J03267+192	4.7	0.6	-161.0	0.1	Gal15	-31.8	PMSU	29.67	-17.37	6.62	Mon16
J03272+273	-99.43	4.32	-58.16	3.38	HIP2				4.0	-13.8	Lep13
J03275+222	-39.0	6.3	-53.0	6.3	PPMXL						
J03284+352	98.6	4.0	-122.2	4.0	PPXML				-21.3	-5.2	Lep13

Table B.3: Proper motions and UVW space velocities of Carmencita stars (continued).

Karmn	$\mu_\alpha \cos\delta$ [mas a^{-1}]	$e\mu_\alpha \cos\delta$ [mas a^{-1}]	μ_δ [mas a^{-1}]	$e\mu_\delta$ [mas a^{-1}]	Ref.[a b]	V_r [km s^{-1}]	Ref.[c]	U [km s^{-1}]	V [km s^{-1}]	W [km s^{-1}]	Ref.[d]
J03286-156	190.6	5.7	37.9	5.7	PPMXL	-40.8	PMSU	8.4	-2.22	46.55	Mon16
J03288+264	217.3	4.6	-131.2	4.6	PPMXL	1.0	New14	-7.44	-16.4	1.64	Mon16
J03303+346	35.8	5.4	-41.6	5.4	PPMXL	5.2	Schf15	-6.5	-3.5	-2.82	Mon16
J03308+542	160.0	5.1	-9.0	5.1	PPMXL	2.0	New14	-5.31	-3.89	3.77	Mon16
J03309+706	367.4	4.7	-485.4	4.7	PPMXL	21.15	Des13	-60.86	-26.72	-14.42	Mon16
J03317+143	45.68	6.55	-668.88	6.47	HIP2	-32.06	Schf15	45.05	-61.01	-23.93	Mon16
J03325+287	51.5	5.6	-72.1	5.6	PPMXL	7.4	Mo02	-7.75	-3.19	-4.27	Mon16
J03332+462	68.5	1.0	-176.8	0.8	Gal15	-4.6	BE12	-7.02	-25.85	-16.1	Mon16
J03340+585	299.4	1.9	-174.1	1.9	PPMXL				-39.1	4.6	Lep13
J03346-048	408.0	5.6	-325.4	5.6	PPMXL	9.5	PMSU	-8.8	-71.86	8.2	Mon16
J03361+313	117.6	5.2	-136.3	5.2	PPMXL	15.0	New14	-16.29	-5.18	-6.91	Mon16
J03366+034	116.5	5.0	-123.0	5.0	PPMXL	28.0	Schf15	-21.55	-11.47	-17.43	Mon16
J03372+691	159.0	4.7	-117.8	4.7	PPMXL	7.7	PMSU	-28.67	-19.53	1.65	Mon16
J03375+178N	173.1	4.5	-27.7	4.5	PPMXL	35.0	PMSU	-38.95	-10.92	-6.97	Mon16
J03375+178S	173.1	4.5	-27.7	4.5	aPPMXL	39.6	PMSU	-40.57	-5.98	-11.89	Mon16
J03394+249	111.7	4.7	195.4	4.7	PPMXL	38.3	PMSU	-40.58	15.24	2.78	Mon16
J03396+254E	235.0	4.7	-580.4	4.7	PPMXL	11.0	PMSU	-13.76	-54.45	-31.05	Mon16
J03396+254W	235.0	4.7	-580.4	4.7	aPPMXL	11.0	PMSU	-13.76	-54.46	-31.04	Mon16
J03397+334	-108.0	2.8	23.6	0.8	Cortes	-31.0	PMSU	37.74	7.17	-0.34	Mon16
J03416+552	96.17	2.49	-117.69	2.26	HIP2	-3.2	Zuck11	-11.28	-22.14	-6.03	Mon16
J03430+459	-211.4	0.4	-33.3	0.4	Cortes	-25.07	Schf15	32.05	2.09	-14.82	Mon16
J03433-095	400.5	5.1	302.5	5.1	PPMXL	38.1	PMSU	-62.33	-12.82	8.28	Mon16
J03437+166	157.51	3.07	-318.95	3.13	HIP2	22.5	PMSU	-18.67	-24.09	-19.22	Mon16
J03438+166	157.7	2.41	-317.9	2.45	HIP2	34.54	Schf15	-29.04	-24.17	-25.56	Mon16
J03445+349	197.34	2.51	-160.7	1.91	HIP2	8.0	BE12	-18.33	-25.63	-2.08	Mon16
J03454+729	205.4	2.6	-439.6	2.7	PPMXL			-41.0		-24.2	Lep13
J03455+703	133.7	4.7	14.5	4.7	PPMXL				-14.1	16.7	Lep13
J03459+147	97.1	0.8	-263.3	0.8	PPMXL				-37.0	-14.7	Lep13
J03463+262	385.2	2.68	-200.78	2.12	HIP2	35.94	Schf15	-42.5	-19.07	-6.66	Mon16
J03467+821	86.4	0.3	-74.8	1.2	Cortes			-16.2		0.1	Lep13
J03467-112	549.6	5.1	105.8	5.1	PPMXL	78.4	PMSU	-86.5	-52.52	-12.9	Mon16
J03473+086	461.0	0.4	-650.6	0.2	Gal15	10.5	PMSU	-6.45	-47.18	-10.18	Mon16
J03473-019	185.53	3.77	-273.48	3.95	HIP2	17.54	Schf15	-8.52	-27.1	-11.8	Mon16

Table B.3: Proper motions and UVW space velocities of Carmencita stars (continued).

Karmn	$\mu_\alpha \cos\delta$ [mas a^{-1}]	$e\mu_\alpha \cos\delta$ [mas a^{-1}]	μ_δ [mas a^{-1}]	$e\mu_\delta$ [mas a^{-1}]	Ref.[a b]	V_r [km s^{-1}]	Ref.[c]	U [km s^{-1}]	V [km s^{-1}]	W [km s^{-1}]	Ref.[d]
J03479+027	-388.03	3.39	-429.46	2.37	HIP2	13.9	PMSU	17.72	-6.35	-44.46	Mon16
J03480+686	127.18	1.6	240.72	2.76	aHIP2	9.4	PMSU	-0.76	6.61	23.34	Mon16
J03486+735	396.8	1.9	-272.2	1.8	PPMXL	-9.5	PMSU	-19.48	-33.56	1.1	Mon16
J03505+634	-5.01	2.25	-237.6	2.49	HIP2	-3.3	PMSU	-16.93	-19.77	-33.46	Mon16
J03507-060	-448.9	5.6	-1368.8	5.6	PPMXL	-9.05	Schf15	49.62	-30.08	-30.38	Mon16
J03510+142	64.5	4.8	-77.5	4.8	PPMXL	36.28	Ter15	-31.69	-4.11	-18.5	Mon16
J03510-008	17.7	3.9	-474.2	3.9	PPMXL	-11.9	Des12	24.01	-22.52	-5.6	Mon16
J03519+397	32.12	1.41	-52.11	1.18	aHIP2				-7.7	-6.0	Lep13
J03526+170	436.7	4.6	-651.6	4.6	PPMXL	43.6	West15	-39.54	-31.3	-26.18	Mon16
J03531+625	26.9	1.7	-266.2	1.7	PPMXL	-119.8	Schf15	86.42	-80.68	-24.62	Mon16
J03543-146	-59.9	0.7	81.5	0.9	Gal15	9.9	Des12	-8.34	3.85	-8.17	Mon16
J03544-091	-100.5	1.1	113.7	1.2	Cortes	-16.7	PMSU	8.8	18.46	9.08	Mon16
J03548+163	137.5	0.3	-28.9	0.4	Gal15						
J03565+319	123.4	5.2	-71.0	5.2	PPMXL						
J03567+039	312.41	3.53	-391.51	3.31	HIP2	-28.9	PMSU	-8.34	-68.63	-12.64	Mon16
J03574-011	-186.0	1.38	-142.85	1.55	aHIP2	13.2	PMSU	0.52	-0.83	-21.68	Mon16
J03586+520	364.0	4.8	-213.5	4.8	PPMXL				-60.8	13.5	Lep13
J03588+125	251.2	0.7	-310.2	0.7	Cortes	38.76	Schf15	-34.27	-51.2	-21.29	Mon16
J03598+260	729.6	4.4	-258.4	4.4	PPMXL	53.54	Schf15	-77.28	-60.76	14.16	Mon16
J04011+513	367.0	0.3	-806.8	0.6	Gal15	-35.2	PMSU	-11.0	-91.82	-38.29	Mon16
J04056+057	33.0	4.9	-38.5	4.9	PPMXL	28.0	PMSU	-23.2	-6.06	-14.96	Mon16
J04059+712E	166.4	5.1	-375.0	4.7	PPMXL						
J04059+712W	166.4	5.1	-375.0	4.7	PPMXL						
J04061-055	32.6	6.9	-145.1	6.9	PPMXL						
J04077+142	177.0	1.9	-157.8	1.9	aPPMXL						
J04079+142	-177.0	1.9	-157.8	1.9	aPPMXL						
J04081+743	668.7	4.6	-596.6	4.6	PPMXL						
J04083+691	270.6	4.7	-80.6	4.7	PPMXL						
J04086+336	523.58	4.11	125.35	3.46	HIP2	40.8	PMSU	-49.73	-4.47	18.72	Mon16
J04093+057	221.9	4.9	-126.1	4.9	PPMXL	43.3	West15	-39.37	-27.49	-14.44	Mon16
J04108-128	-144.4	1.4	-386.4	1.0	Cortes						
J04112+495	121.9	4.8	-469.8	4.8	PPMXL	40.7	PMSU	-55.73	-20.83	-29.06	Mon16
J04122+647	491.7	0.0	-431.4	0.0	Gal15	27.2	PMSU	-43.3	-12.73	6.29	Mon16

Table B.3: Proper motions and UVW space velocities of Carmencita stars (continued).

Karmn	$\mu_\alpha \cos\delta$ [mas a^{-1}]	$e\mu_\alpha \cos\delta$ [mas a^{-1}]	μ_δ [mas a^{-1}]	$e\mu_\delta$ [mas a^{-1}]	Ref.[a b]	V_r [km s^{-1}]	Ref.[c]	U [km s^{-1}]	V [km s^{-1}]	W [km s^{-1}]	Ref.[d]
J04123+162	149.5	0.7	-32.3	0.3	Gal15						
J04129+526	-318.4	0.6	-816.2	0.7	Gal15	-26.3	PMSU	10.95	-32.28	-57.07	Mon16
J04131+505	-400.0	4.6	-194.8	4.6	PPMXL	-70.7	PMSU	69.24	-20.88	-35.7	Mon16
J04137+476	-111.1	5.1	-129.0	5.1	PPMXL				-0.7	-19.7	Lep13
J04139+829	88.67	1.21	-251.87	1.47	HIP2	5.5	PMSU	-39.66	-16.98	-13.77	Mon16
J04148+277	234.2	5.0	-119.1	5.1	PPMXL	37.2	Schf15	-40.42	-10.86	-4.42	Mon16
J04153-076	-2240.12	0.23	-3420.27	0.2	aHIP2	-43.26	Schf15	97.03	-11.92		
-40.38	Mon16										
J04166-125	-75.6	1.7	225.7	1.7	PPMXL	30.8	PMSU	-33.4	10.06	-17.69	Mon16
J04173+088	129.2	5.0	-377.0	5.0	PPMXL	16.0	Schf15	-7.64	-27.19	-15.5	Mon16
J04177+410	66.3	4.8	-212.4	4.8	PPMXL						
J04188+013	-1.77	5.59	-58.74	4.06	HIP2				-5.7	-3.9	Lep13
J04191+097	36.6	4.9	129.8	4.9	PPMXL						
J04191-074	-165.6	6.9	-69.2	6.9	PPMXL						
J04198+425	536.0	4.6	-1453.1	4.6	PPMXL	18.0	New14	-39.3	-59.73	-33.99	Mon16
J04199+364	210.3	3.4	-454.2	3.4	PPMXL	39.2	Daw05	-48.63	-37.17	-24.14	Mon16
J04205+815	-117.9	4.6	-75.1	4.6	PPMXL						
J04206+272	5.5	0.3	-26.4	0.5	Cortes						
J04207+152	159.7	0.6	-75.8	0.9	Gal15						
J04218+213	120.9	4.9	-217.7	4.9	PPMXL	23.7	PMSU	-22.6	-19.01	-12.3	Mon16
J04219+751	551.7	4.7	-493.2	4.7	PPMXL	31.6	PMSU	-68.89	-29.96	16.66	Mon16
J04221+192	-97.6	0.4	-35.8	0.6	Cortes	-48.7	PMSU	49.43	0.96	7.54	Mon16
J04224+036	133.9	0.4	6.4	0.4	Cortes	39.39	Schf15	-38.85	-15.94	-7.92	Mon16
J04224+740	44.5	0.1	-326.0	0.6	Cortes				-21.6	-25.8	Lep13
J04225+105	244.8	5.1	28.9	5.1	PPMXL	37.02	Schf15	-43.34	-18.27	6.28	Mon16
J04225+390	581.3	0.4	-606.9	0.2	Gal15	30.5	PMSU	-52.2	-61.24	-4.78	Mon16
J04227+205	106.8	0.4	-42.0	0.4	Gal15						
J04229+259	33.6	4.5	-249.6	4.5	PPMXL						
J04234+495	-25.4	0.3	-211.9	0.6	Cortes				-9.6	-14.3	Lep13
J04234+809	-120.3	6.0	393.9	6.2	PPMXL						
J04238+092	102.4	0.3	-1.2	0.3	Gal15						
J04238+149	119.8	0.5	-24.9	0.5	Gal15						
J04247-067	147.0	0.3	5.7	0.1	Cortes	13.5	Shk10	-14.49	-11.88	1.69	Mon16

Table B.3: Proper motions and UVW space velocities of Carmencita stars (continued).

Karmn	$\mu_\alpha \cos\delta$ [mas a^{-1}]	$e\mu_\alpha \cos\delta$ [mas a^{-1}]	μ_δ [mas a^{-1}]	$e\mu_\delta$ [mas a^{-1}]	Ref.[a b]	V_r [km s^{-1}]	Ref.[c]	U [km s^{-1}]	V [km s^{-1}]	W [km s^{-1}]	Ref.[d]
J04248+324	215.5	3.4	-126.6	3.3	PPMXL	-40.1	PMSU	29.64	-37.5	16.71	Mon16
J04251+515	81.4	4.8	-97.9	4.8	PPMXL				-16.8	-0.1	Lep13
J04252+080N	140.4	4.9	2.3	4.9	PPMXL	37.4	Schf15	-38.65	-15.26	-3.84	Mon16
J04252+080S	140.4	4.9	2.3	4.9	PPMXL	33.0	PMSU	-34.74	-14.78	-1.87	Mon16
J04252+172	107.4	0.6	-29.8	0.5	Gal15						
J04274+203	-80.5	2.2	-4.8	2.2	PPMXL				8.5	-12.2	Lep13
J04276+595	117.6	0.4	-194.3	0.3	Cortes	0.5	PMSU	-13.75	-19.31	-5.02	Mon16
J04278+117	317.8	5.1	-503.2	5.1	PPMXL	54.8	PMSU	-42.43	-73.43	-28.72	Mon16
J04284+176	108.2	5.1	-45.9	5.1	PPMXL				-10.1	7.1	Lep13
J04290+219	-65.7	1.14	174.33	1.03	HIP2	-35.49	BE12	33.33	6.84	14.25	Mon16
J04293+142	248.6	5.2	155.4	5.2	PPMXL	11.6	PMSU	-19.74	-3.17	17.12	Mon16
J04294+262	2.1	0.6	-26.8	0.3	Cortes						
J04302+708	-117.0	4.7	26.3	4.7	PPMXL				10.9	-8.9	Lep13
J04304+398	269.8	4.8	-566.8	4.8	PPMXL	27.4	PMSU	-34.15	-20.01	-12.14	Mon16
J04308-088	3.5	0.3	-164.7	0.5	Cortes						
J04310+367	-54.8	0.7	-21.6	0.4	Cortes						
J04311+589	1274.0	0.2	-2032.0	1.8	Gal15	29.5	Schf15	-59.3	-37.06	-7.96	Mon16
J04312+422	-16.2	0.3	-121.2	0.2	Cortes				-7.7	-7.7	Lep13
J04313+241	5.8	0.6	-23.6	0.6	Cortes						
J04326+098	105.9	5.2	-11.6	5.2	PPMXL				-6.8	7.2	Lep13
J04329+001E	-165.7	0.4	-84.3	0.6	Cortes						
J04329+001N	-169.4	0.3	-80.1	0.4	Cortes						
J04329+001S	-165.9	0.3	-83.4	0.9	Cortes						
J04333+239	94.3	4.5	-54.4	4.5	PPMXL				-9.9	4.0	Lep13
J04335+207	452.7	5.1	-324.9	5.1	PPMXL	-2.0	New14	-2.7	-34.64	9.36	Mon16
J04347-004	-81.8	0.3	-229.1	1.0	Cortes						
J04350+086	87.2	3.0	-3.9	3.0	PPMXL				-7.9	9.9	Lep13
J04352-161	162.3	1.7	307.7	0.7	Cortes	48.5	Des12	-45.11	-16.12	-18.84	Mon16
J04366+112	544.8	5.2	329.9	5.2	PPMXL	60.6	PMSU	-84.11	-14.94	44.56	Mon16
J04369+593	129.19	3.97	-131.12	4.36	HIP2				-21.2	3.7	Lep13
J04369-162	71.8	5.9	-34.4	5.9	PPMXL	15.7	Malo14a	-10.0	-12.8	-5.65	Mon16
J04373+193	90.7	0.2	-31.9	0.3	Gal15						
J04376+528	305.54	0.87	-475.51	0.66	HIP2	34.29	BE12	-42.85	-8.34	-1.98	Mon16

Table B.3: Proper motions and UVW space velocities of Carmencita stars (continued).

Karmn	$\mu_\alpha \cos\delta$ [mas a^{-1}]	$e\mu_\alpha \cos\delta$ [mas a^{-1}]	μ_δ [mas a^{-1}]	$e\mu_\delta$ [mas a^{-1}]	Ref.[a b]	V_r [km s^{-1}]	Ref.[c]	U [km s^{-1}]	V [km s^{-1}]	W [km s^{-1}]	Ref.[d]
J04376-024	44.22	0.34	-64.39	0.27	aHIP2	17.6	PMSU	-11.26	-15.27	-8.3	Mon16
J04376-110	-225.75	1.94	-192.57	1.88	HIP2	-6.98	Schf15	14.56	3.06	-8.44	Mon16
J04382+282	386.9	5.0	-94.5	5.0	PPMXL	36.0	New14	-40.27	-12.95	5.33	Mon16
J04386-115	-263.1	5.0	-238.4	5.0	PPMXL						
J04388+217	183.6	0.9	-209.0	0.7	Gal15						
J04393+335	15.3	0.2	-47.4	0.2	Gal15	34.43	Ter15	-33.98	2.35	-7.27	Mon16
J04395+162	-82.0	0.6	-793.1	0.5	Gal15	-33.0	New14	42.14	-30.44	-17.12	Mon16
J04398+251	-99.8	4.6	-49.2	4.6	PPMXL						
J04403-055	330.5	0.7	131.6	0.4	Cortes	31.1	Des12	-31.75	-15.02	-2.31	Mon16
J04404-091	-108.0	2.2	-110.2	2.2	PPMXL	-3.3	PMSU	11.24	0.25	-9.57	Mon16
J04407+022	170.6	1.6	49.4	1.6	PPMXL	44.3	PMSU	-43.89	-16.01	-6.65	Mon16
J04413+327	259.9	0.4	-144.7	0.6	Cortes						
J04414+132	99.0	1.4	-18.3	1.4	PPMXL				-11.7	9.8	Lep13
J04422+577	-79.04	2.13	-532.61	2.01	HIP2				-39.6	-56.8	Lep13
J04423+207	296.1	5.1	42.3	5.1	PPMXL				-18.1	25.8	Lep13
J04425+204	91.7	0.3	-37.2	0.5	Gal15	41.4	Mo02	-41.57	-9.34	-6.21	Mon16
J04429+095	-66.5	5.2	-38.1	5.2	PPMXL				5.4	-12.0	Lep13
J04429+189	656.85	3.81	-1116.2	2.49	HIP2	26.1	Schf15	-22.7	-56.64	-14.78	Mon16
J04429+214	32.9	5.0	115.3	5.0	PPMXL	3.542	Schf15	-4.65	3.78	3.87	Mon16
J04433+296	0.5	0.6	-23.3	0.5	Cortes						
J04444+278	96.4	1.9	-422.2	1.9	PPMXL	-15.0	PMSU	13.83	-37.57	-14.43	Mon16
J04458-144	-29.7	5.6	142.5	5.6	PPMXL						
J04468-112	-150.5	5.0	-58.1	5.0	PPMXL	14.9	Shk12	-4.7	-1.47	-20.06	Mon16
J04471+021	-196.1	1.9	-7.9	1.9	PPMXL	11.0	PMSU	-2.76	13.69	-26.94	Mon16
J04472+206	83.9	5.1	-95.6	5.1	PPMXL	27.3	Ter15	-26.49	-6.28	-6.94	Mon16
J04480+170	86.2	2.4	-30.3	2.4	PPMXL				-10.9	6.9	Lep13
J04488+100	-70.9	3.1	-78.8	3.1	PPMXL	21.97	Ter15	-17.48	-4.27	-14.43	Mon16
J04494+484	175.3	4.6	-180.7	4.6	PPMXL	25.2	Shk12	-32.77	-13.88	2.94	Mon16
J04499+236	23.9	6.6	-156.6	6.6	PPMXL	0.5	Schf15	0.82	-16.57	-9.12	Mon16
J04499+711	180.3	4.7	-38.7	4.7	PPMXL						
J04502+459	189.0	4.8	-238.8	4.8	PPMXL	24.2	PMSU	-37.02	-30.52	-0.64	Mon16
J04504+199	39.9	2.1	-140.6	2.1	PPMXL				-17.6	-7.5	Lep13
J04508+221	631.4	6.2	-433.5	6.2	PPMXL	55.2	PMSU	-57.93	-41.05	0.02	Mon16

Table B.3: Proper motions and UVW space velocities of Carmencita stars (continued).

Karmn	$\mu_\alpha \cos\delta$ [mas a^{-1}]	$e\mu_\alpha \cos\delta$ [mas a^{-1}]	μ_δ [mas a^{-1}]	$e\mu_\delta$ [mas a^{-1}]	Ref.[a b]	V_r [km s^{-1}]	Ref.[c]	U [km s^{-1}]	V [km s^{-1}]	W [km s^{-1}]	Ref.[d]
J04508+261	571.5	0.5	-247.0	0.3	Gal15	62.1	PMSU	-73.6	-62.78	23.85	Mon16
J04520+064	142.98	4.06	-309.39	2.38	HIP2	-1.1	PMSU	6.24	-18.75	-2.21	Mon16
J04524-168	120.8	2.9	-212.4	2.9	PPMXL	26.72	Schf15	-8.27	-29.0	-12.68	Mon16
J04525+407	1164.6	0.2	-1091.3	0.1	Gal15	95.0	New14	-117.8	-65.56	9.06	Mon16
J04536+623	269.0	4.6	-239.5	4.6	PPMXL						
J04538+158	50.8	0.4	-171.5	0.6	Cortes						
J04538-177	408.07	2.49	-642.82	2.06	HIP2	-31.6	PMSU	43.0	-21.26	24.6	Mon16
J04544+650	54.1	0.5	-103.1	0.5	Cortes	2.17	Schf15	-16.41	-18.24	-3.41	Mon16
J04559+046	136.12	0.63	-183.19	0.32	aHIP2	61.4	PMSU	-46.45	-50.85	-21.31	Mon16
J04560+432	374.2	4.6	-162.7	4.6	PPMXL						
J04587+509	503.72	2.89	-336.78	2.08	HIP2	23.0	PMSU	-40.36	-40.01	19.31	Mon16
J04588+498	112.25	1.6	-115.46	1.29	PPMXL	-34.5	Schf15	27.22	-24.54	-1.36	Mon16
J04595+017	34.6	2.34	-94.27	1.44	HIP2	19.66	Schf15	-12.6	-16.71	-10.01	Mon16
J05012+248	229.0	2.5	-392.2	2.6	PPMXL	30.3	Schf15	-30.89	-61.13	-12.32	Mon16
J05013+226	-63.6	0.3	-354.4	0.4	Gal15	30.6	West15	-26.61	-15.84	-22.72	Mon16
J05018+037	130.2	1.9	-134.3	1.9	PPMXL	24.3	PMSU	-17.65	-26.17	-4.97	Mon16
J05019+011	35.4	1.2	-91.0	1.2	Gal15	18.54	Schf15	-14.1	-10.33	-8.2	Mon16
J05019+099	28.4	0.2	-130.5	0.3	Cortes	18.8	PMSU	-13.0	-17.37	-11.45	Mon16
J05019-069	-550.8	0.4	-533.3	0.6	Cortes	42.3	Schf15	-23.22	-18.01	-36.28	Mon16
J05024-212	-143.42	1.1	-221.81	1.18	HIP2	-29.2	PMSU	26.11	14.46	8.8	Mon16
J05030+213	103.4	1.6	-138.9	1.7	aPPMXL	51.3	West15	-49.83	-23.32	-10.52	Mon16
J05032+213	103.4	1.6	-138.9	1.7	PPMXL						
J05033-173	-226.51	2.14	-447.19	1.97	HIP2	18.3	PMSU	3.22	-15.79	-23.52	Mon16
J05034+531	1302.97	2.37	-1538.36	1.7	HIP2	65.5	Schf15	-112.18	-91.71	15.42	Mon16
J05042+110	-63.2	4.9	192.6	4.9	PPMXL	-2.0	New14	-0.55	9.6	3.09	Mon16
J05050+442	92.8	4.7	-29.3	4.7	PPMXL	9.01	Schf15	-10.0	-2.27	3.91	Mon16
J05051-120	-220.2	5.5	-145.7	5.5	PPMXL	31.4	PMSU	-9.86	-11.22	-39.0	Mon16
J05060+043	399.3	2.9	112.0	2.7	PPMXL	76.6	PMSU	-81.76	-37.98	18.24	Mon16
J05062+046	38.2	0.5	-90.1	0.2	Gal15	27.5	Schf15	-22.64	-13.08	-10.67	Mon16
J05068-215E	48.1	3.2	-22.7	3.4	PPMXL	31.7	PMSU	-18.82	-21.98	-13.87	Mon16
J05068-215W	48.1	3.2	-22.7	3.4	aPPMXL	31.7	PMSU	-18.89	-21.7	-14.09	Mon16
J05072+375	-105.5	5.0	-8.0	5.0	PPMXL						
J05076+275	60.9	1.8	-87.2	1.8	PPMXL				-15.8	-0.3	Lep13

Table B.3: Proper motions and UVW space velocities of Carmencita stars (continued).

Karmn	$\mu_\alpha \cos\delta$ [mas a^{-1}]	$e\mu_\alpha \cos\delta$ [mas a^{-1}]	μ_δ [mas a^{-1}]	$e\mu_\delta$ [mas a^{-1}]	Ref.[a b]	V_r [km s^{-1}]	Ref.[c]	U [km s^{-1}]	V [km s^{-1}]	W [km s^{-1}]	Ref.[d]
J05078+179	78.0	0.3	-287.3	0.7	Gal15	31.4	PMSU	-27.65	-20.03	-13.33	Mon16
J05083+756	200.8	4.6	-121.6	4.6	PPMXL						
J05084-210	36.5	4.9	-15.3	4.9	PPMXL	23.5	BJ14	-14.47	-15.23	-10.8	Mon16
J05085-181	502.99	1.32	-1399.76	1.52	HIP2	33.9	PMSU	19.16	-68.77	-18.78	Mon16
J05091+154	139.6	4.8	-627.5	4.8	PPMXL	-25.55	Schf15	42.7	-79.74	-25.74	Mon16
J05103+095	55.68	4.28	-354.28	2.72	HIP2				-39.9	-17.2	Lep13
J05103+272	-391.0	5.7	-207.7	5.7	PPMXL						
J05103+488	172.9	0.3	-392.7	0.6	Cortes	17.6	PMSU	-31.38	-31.81	-7.2	Mon16
J05106+297	110.3	5.4	-65.3	5.0	PPMXL				19.1	-15.7	Lep13
J05109+186	-232.9	4.7	-640.4	4.7	PPMXL	-21.9	PMSU	33.49	-30.25	-40.03	Mon16
J05111+158	56.4	5.9	-25.4	5.9	PPMXL				-9.1	8.4	Lep13
J05114+101	-39.32	4.5	-215.07	2.84	HIP2				-36.9	-35.0	Lep13
J05127+196	278.73	3.15	242.33	1.69	HIP2	-20.2	PMSU	15.41	3.46	24.95	Mon16
J05151-073	260.37	4.1	-432.15	2.69	HIP2	25.0	PMSU	3.99	-58.72	-6.61	Mon16
J05152+236	36.7	4.6	-71.5	4.6	PPMXL						
J05155+591	114.5	4.0	-1008.9	4.0	PPMXL						
J05173+321	82.2	5.1	-304.5	5.1	PPMXL						
J05173+458	75.25	0.54	-426.89	0.28	aHIP2	31.9	PMSU	-38.47	-13.65	-8.83	Mon16
J05173+721	-34.8	2.5	-111.7	2.5	PPMXL				-6.3	-12.4	Lep13
J05187+464	34.8	4.5	-111.2	4.5	PPMXL	9.9	Schf15	-12.56	-6.08	-2.1	Mon16
J05195+649	7.7	4.8	147.5	4.8	PPMXL	-45.48	Schf15	43.64	-16.72	-5.46	Mon16
J05206+587N	149.5	0.7	-502.7	0.3	Gal15	18.1	PMSU	-45.73	-41.19	-12.63	Mon16
J05206+587S	151.4	0.7	-501.7	0.7	Gal15	3.7	PMSU	-32.0	-45.75	-14.78	Mon16
J05211+557	117.5	5.2	-282.2	5.2	PPMXL	111.2	PMSU	-114.07	16.91	14.42	Mon16
J05223+305	74.7	5.0	-87.0	5.0	PPMXL						
J05226+795	81.8	1.9	-60.4	1.9	PPMXL			-7.2		5.5	Lep13
J05228+202	36.4	1.8	19.0	0.6	Cortes				0.9	4.5	Lep13
J05243-160	20.5	5.2	-36.7	5.2	PPMXL	17.5	Malo14a	-11.17	-11.33	-7.56	Mon16
J05256-091	39.9	0.1	-190.2	0.1	Cortes	26.3	Shk12	-13.2	-22.46	-13.13	Mon16
J05280+096	-190.3	5.77	-759.45	3.33	HIP2	60.72	Schf15	-43.64	-40.34	-41.98	Mon16
J05282+029	-400.5	5.1	-1157.5	5.1	bPPMXL	132.0	New14	-70.04	-104.2	-118.15	Mon16
J05289+125	80.2	1.04	-218.45	0.52	aHIP2	58.4	PMSU	-48.32	-41.38	-18.14	Mon16
J05294+155E	-82.19	2.63	-128.03	1.3	HIP2	4.2	PMSU	-1.24	-5.58	-11.83	Mon16

Table B.3: Proper motions and UVW space velocities of Carmencita stars (continued).

Karmn	$\mu_\alpha \cos\delta$ [mas a^{-1}]	$e\mu_\alpha \cos\delta$ [mas a^{-1}]	μ_δ [mas a^{-1}]	$e\mu_\delta$ [mas a^{-1}]	Ref.[a b]	V_r [km s^{-1}]	Ref.[c]	U [km s^{-1}]	V [km s^{-1}]	W [km s^{-1}]	Ref.[d]
J05294+155W	-82.19	2.63	-128.03	1.3	aHIP2	4.2	PMSU	-1.21	-5.62	-11.92	Mon16
J05298+320	-217.2	0.7	-675.0	0.0	Gal15	-10.44	Schf15	8.14	-44.08	-53.8	Mon16
J05298-034	-311.5	2.7	-474.4	2.7	PPMXL	21.67	Schf15	4.5	-23.48	-46.26	Mon16
J05306+152	-123.7	4.6	-134.7	4.6	PPMXL				-2.5	-19.8	Lep13
J05314-036	761.86	1.37	-2093.6	0.76	HIP2	7.8	PMSU	22.61	-54.99	-9.97	Mon16
J05320-030	6.7	2.2	-50.4	2.2	PPMXL	23.84	Ell14	-18.06	-13.26	-9.1	Mon16
J05322+098	-178.35	4.28	-219.16	1.69	HIP2	47.6	PMSU	-39.99	-16.61	-26.16	Mon16
J05328+338	-253.0	5.4	-426.7	5.4	PPMXL						
J05333+448	57.9	4.8	-365.2	4.8	PPMXL	23.19	Schf15	-29.73	-17.67	-8.07	Mon16
J05337+019	-239.06	4.53	-156.72	1.65	HIP2	65.88	Schf15	-52.43	-22.92	-39.14	Mon16
J05339-023	7.8	0.4	-58.3	0.4	Cortes	20.9	BJ14	-15.39	-12.52	-8.13	Mon16
J05341+475	-58.4	1.2	37.1	1.3	Cortes				6.4	-3.6	Lep13
J05341+512	-51.71	2.36	-222.83	1.25	HIP2	-65.6	PMSU	50.73	-39.68	-30.37	Mon16
J05342+103N	-82.3	0.1	-347.6	0.5	Gal15	-17.0	New14	25.44	-14.97	-16.31	Mon16
J05342+103S	-99.8	0.2	-441.5	2.0	Gal15	-15.0	New14	22.95	-14.43	-15.26	Mon16
J05348+138	-116.2	2.0	-395.2	2.0	PPMXL	32.0	New14	-24.55	-21.64	-23.22	Mon16
J05360-076	108.1	5.3	471.2	5.3	PPMXL	28.9	PMSU	-38.44	0.19	5.32	Mon16
J05365+113	-5.94	1.12	-56.71	0.71	HIP2	21.92	Schf15	-19.95	-7.48	-5.97	Mon16
J05366+112	-5.94	1.12	-56.71	0.71	aHIP2	22.4	Schf15	-20.41	-7.61	-6.05	Mon16
J05394+406	642.8	0.5	-831.4	0.5	Gal15						
J05394+747	7.0	0.2	-146.2	0.3	Gal15						
J05402+126	-16.7	0.9	-261.0	0.9	PPMXL	104.8	PMSU	-92.45	-46.39	-33.45	Mon16
J05404+248	103.2	0.5	-383.0	0.2	Gal15	21.0	New14	-19.68	-19.74	-6.81	Mon16
J05415+534	6.8	0.1	-517.7	0.6	Gal15	11.1	PMSU	-22.62	-19.38	-12.01	Mon16
J05419+153	79.4	1.4	-44.1	1.2	PPMXL	27.5	PMSU	-25.79	-13.23	0.82	Mon16
J05421+124	2000.53	2.93	-1569.63	1.75	HIP2	105.74	Schf15	-89.85	-89.32	8.25	Mon16
J05422-054	-152.1	5.5	957.7	5.5	PPMXL	51.7	PMSU	-75.34	21.27	1.19	Mon16
J05425+154	-77.6	4.4	-73.4	4.4	PPMXL						
J05455-119	41.5	7.0	74.8	7.0	PPMXL						
J05456+729	81.5	0.7	114.3	0.3	Cortes						
J05458+729	81.5	0.7	112.3	0.5	Cortes						
J05466+441	-562.9	4.8	-359.0	4.8	PPMXL	32.1	PMSU	-40.56	6.72	-61.3	Mon16
J05468+665	93.7	2.4	84.1	2.4	PPMXL				1.0	16.5	Lep13

Table B.3: Proper motions and UVW space velocities of Carmencita stars (continued).

Karmn	$\mu_\alpha \cos\delta$ [mas a^{-1}]	$e\mu_\alpha \cos\delta$ [mas a^{-1}]	μ_δ [mas a^{-1}]	$e\mu_\delta$ [mas a^{-1}]	Ref.[a b]	V_r [km s^{-1}]	Ref.[c]	U [km s^{-1}]	V [km s^{-1}]	W [km s^{-1}]	Ref.[d]
J05471-052	530.2	5.5	-550.3	5.5	PPMXL	-64.5	PMSU	78.52	-22.34	35.89	Mon16
J05472-000	-75.4	1.4	-70.1	1.4	PPMXL	-23.0	PMSU	24.28	7.94	-6.32	Mon16
J05484+077	57.8	0.2	-258.2	0.6	Gal15	15.2	PMSU	-4.96	-27.89	-10.12	Mon16
J05511+122	72.9	0.8	-47.4	0.5	Cortes						
J05530+047	259.6	2.6	-296.2	2.6	PPMXL				-54.2	13.2	Lep13
J05530+251	86.3	4.4	-170.9	4.4	PPMXL				-17.2	-1.1	Lep13
J05532+242	152.6	4.4	-609.3	4.4	PPMXL	24.6	Schf15	-19.52	-57.27	-16.76	Mon16
J05547+109	-140.5	4.6	-75.6	4.6	PPMXL	14.2	Shk12	-11.8	-3.19	-16.36	Mon16
J05558+406	-55.4	5.8	-296.9	5.8	PPMXL				-10.4	-14.9	Lep13
J05566-103	-30.2	0.3	126.8	0.3	Cortes	23.42	Schf15	-25.1	-4.77	-4.53	Mon16
J05587+259	91.0	4.4	20.7	4.4	PPMXL				-3.3	15.4	Lep13
J05588+213	178.5	0.3	-437.2	0.2	Gal15						
J05596+585	10.96	1.73	-253.28	1.19	HIP2	-13.7	PMSU	3.92	-18.39	-9.92	Mon16
J05599+585	10.96	1.73	-253.28	1.19	aHIP2	1.0	New14	-8.84	-12.43	-5.72	Mon16
J06000+027	310.0	2.7	-42.0	2.7	PPMXL	30.8	Schf15	-26.69	-17.19	0.75	Mon16
J06007+681	414.1	4.6	-1101.2	4.6	aPPMXL	27.43	Schf15	-85.09	-77.64	7.06	Mon16
J06008+681	414.1	4.6	-1101.2	4.6	PPMXL	29.5	PMSU	-86.7	-76.54	7.82	Mon16
J06011+595	-110.2	0.0	-912.5	0.2	Gal15	1.5	Schf15	-18.01	-22.23	-15.86	Mon16
J06017+130	-135.8	2.7	-51.9	2.7	PPMXL				3.3	-16.9	Lep13
J06023-203	-40.4	0.2	530.3	3.4	Cortes	12.9	PMSU	-45.54	19.57	10.09	Mon16
J06024+498	64.6	0.9	-851.4	0.1	Gal15	15.0	New14	-27.14	-28.17	-10.56	Mon16
J06024+663	345.1	4.5	-481.2	4.5	PPMXL	-25.67	Schf15	-1.58	-54.63	1.73	Mon16
J06025+371	130.1	2.3	-57.6	2.3	PPMXL				-14.9	11.6	Lep13
J06034+478	-54.0	4.8	-567.7	4.8	PPMXL	35.1	PMSU	-53.62	-40.59	-25.34	Mon16
J06035+155	-63.7	0.8	-37.0	0.8	PPMXL				0.0	-11.6	Lep13
J06035+168	-94.2	5.1	-21.5	5.1	PPMXL						
J06039+261	335.9	0.3	-541.3	0.1	Gal15	68.2	PMSU	-60.56	-98.23	6.48	Mon16
J06054+608	288.8	5.0	-787.2	5.0	PPMXL	117.0	New14	-125.15	1.15	33.49	Mon16
J06066+465	-75.9	4.7	-4.1	4.7	PPMXL						
J06071+335	85.5	3.3	-416.3	3.3	PPMXL	6.5	PMSU	-9.42	-46.97	-13.55	Mon16
J06075+472	38.3	0.7	-186.6	0.3	Gal15	34.6	West15	-38.5	-10.32	2.61	Mon16
J06097+001	149.0	1.8	-117.6	1.8	PPMXL				-23.3	10.9	Lep13
J06102+225	34.8	0.4	-140.3	0.3	Cortes	9.58	Schf15	-7.52	-15.55	-3.53	Mon16

Table B.3: Proper motions and UVW space velocities of Carmencita stars (continued).

Karmn	$\mu_\alpha \cos\delta$ [mas a^{-1}]	$e\mu_\alpha \cos\delta$ [mas a^{-1}]	μ_δ [mas a^{-1}]	$e\mu_\delta$ [mas a^{-1}]	Ref.[a b]	V_r [km s^{-1}]	Ref.[c]	U [km s^{-1}]	V [km s^{-1}]	W [km s^{-1}]	Ref.[d]
J06103+225	40.5	0.7	-157.5	0.5	Cortes						
J06103+722	-50.1	4.5	-154.7	4.5	PPMXL						
J06103+821	-50.62	1.15	-1336.14	1.16	HIP2	5.2	PMSU	-50.68	-29.04	-12.83	Mon16
J06105+024	-38.7	1.9	-50.8	1.9	PPMXL				-3.3	-8.5	Lep13
J06105-218	-137.09	0.5	-713.66	0.81	HIP2	9.4	PMSU	8.79	-15.02	-13.33	Mon16
J06107+259	158.2	4.1	-563.5	4.1	PPMXL	81.1	PMSU	-73.96	-89.81	-14.25	Mon16
J06109+103	62.96	6.28	-932.06	4.47	HIP2	70.0	PMSU	-50.24	-63.82	-25.17	Mon16
J06140+516	-379.2	5.0	-107.6	5.0	PPMXL	65.9	PMSU	-66.3	25.36	-8.87	Mon16
J06145+025	-145.3	0.1	-472.9	0.2	Gal15						
J06151-164	79.9	0.8	-374.7	0.9	Cortes						
J06171+051	-187.72	0.37	170.69	0.28	aHIP2	13.4	PMSU	-20.57	14.76	-9.1	Mon16
J06171+751	-41.0	1.9	67.6	1.9	PPMXL	56.6	Schf15	-35.35	39.29	21.36	Mon16
J06171+838	-53.3	4.6	-196.4	4.6	PPMXL			-11.5		-6.3	Lep13
J06185+250	2.5	4.6	-325.5	4.6	PPMXL						
J06193-066	-39.3	0.6	-625.8	0.3	Gal15	-29.6	PMSU	48.77	-11.84	-16.32	Mon16
J06194+139	105.6	1.6	-44.2	1.6	PPMXL				-10.2	8.6	Lep13
J06212+442	153.3	0.4	-249.9	0.9	Cortes	-19.4	PMSU	13.43	-37.46	-0.61	Mon16
J06216+163	242.4	1.0	-151.8	1.0	PPMXL				-29.5	17.3	Lep13
J06217+163	238.2	1.2	-149.1	1.2	PPMXL						
J06218-227	-633.79	1.86	274.33	2.21	HIP2	23.9	PMSU	-50.31	32.31	-60.79	Mon16
J06223+334	-49.6	5.1	-107.4	5.5	PPMXL	30.75	Ter15	-32.59	-11.08	-8.97	Mon16
J06236-096	-61.4	6.2	22.1	6.2	PPMXL						
J06237+020	34.3	1.9	-72.4	1.9	PPMXL				-7.4	-0.4	Lep13
J06238+456	-28.8	4.6	-285.8	4.6	PPMXL	49.5	West15	-54.39	-11.55	0.25	Mon16
J06246+234	544.4	0.2	-509.5	0.1	Gal15	-11.92	Schf15	16.98	-25.57	8.79	Mon16
J06258+561	108.8	0.6	-499.6	0.4	Gal15	17.1	PMSU	-36.92	-43.04	-2.05	Mon16
J06262+238	-10.8	2.2	-137.6	2.2	PPMXL				-17.2	-11.2	Lep13
J06277+093	-123.5	5.0	-145.1	5.0	PPMXL	42.5	Schf15	-36.63	-22.07	-17.7	Mon16
J06293-028	705.28	2.66	-611.92	2.4	HIP2	23.2	PMSU	-10.77	-27.16	4.33	Mon16
J06298-027	159.7	5.5	-207.2	5.5	PPMXL	129.31	Ter15	-96.38	-88.5	-9.62	Mon16
J06306+456	-100.9	4.5	87.7	4.5	PPMXL				22.7	-10.2	Lep13
J06307+397	100.0	4.9	87.4	4.9	PPMXL	-19.26	Schf15	23.96	4.05	15.63	Mon16
J06310+500	-108.8	0.1	-169.7	0.5	Cortes	-16.1	PMSU	6.3	-15.05	-22.01	Mon16

Table B.3: Proper motions and UVW space velocities of Carmencita stars (continued).

Karmn	$\mu_\alpha \cos\delta$ [mas a^{-1}]	$e\mu_\alpha \cos\delta$ [mas a^{-1}]	μ_δ [mas a^{-1}]	$e\mu_\delta$ [mas a^{-1}]	Ref.[a b]	V_r [km s^{-1}]	Ref.[c]	U [km s^{-1}]	V [km s^{-1}]	W [km s^{-1}]	Ref.[d]
J06318+414	-5.4	0.7	-211.9	0.2	Gal15	2.0	New14	-4.27	-9.65	-4.13	Mon16
J06322+378	-112.6	1.9	-132.6	1.9	PPMXL				-8.4	-18.6	Lep13
J06323-097	-11.1	5.5	-57.0	5.5	PPMXL						
J06325+641	256.8	4.7	-493.4	4.7	PPMXL	30.18	Schf15	-47.81	-36.85	21.25	Mon16
J06345+315	28.8	4.8	-195.5	4.8	PPMXL				-15.7	-4.5	Lep13
J06354-040	-108.8	0.3	80.1	0.2	Cortes	49.7	Schf15	-43.15	-24.21	-7.02	Mon16
J06361+116	-205.8	0.4	-850.4	0.1	Gal15	88.5	PMSU	-63.81	-85.62	-46.66	Mon16
J06361+201	87.8	5.1	-227.1	5.1	PPMXL						
J06371+175	-767.47	2.52	336.3	1.82	HIP2	-58.14	Schf15	45.68	43.9	-29.43	Mon16
J06396-210	-154.2	5.1	103.2	5.1	PPMXL	-7.51	Schf15	-1.31	12.0	-3.62	Mon16
J06400+285	25.3	2.3	-239.9	2.3	PPMXL	-23.29	Schf15	23.7	-19.54	-11.75	Mon16
J06401-164	87.0	6.1	304.1	6.1	PPMXL						
J06414+157	31.0	4.7	-316.3	4.7	PPMXL	90.1	PMSU	-78.28	-52.79	-2.4	Mon16
J06421+035	38.1	2.6	-257.3	2.7	PPMXL	82.48	Schf15	-63.69	-55.33	-6.72	Mon16
J06422+035	38.1	2.6	-257.3	2.7	aPPMXL	82.99	Schf15	-64.34	-55.21	-6.57	Mon16
J06435+166	-215.8	5.5	39.7	5.5	PPMXL						
J06438+511	91.0	5.1	-881.7	5.1	PPMXL	6.7	PMSU	-32.84	-72.42	-15.18	Mon16
J06447+718	-119.94	1.32	-551.6	2.12	HIP2	57.6	PMSU	-81.79	-5.88	3.93	Mon16
J06461+325	-452.64	1.41	99.28	0.81	aHIP2	-46.1	PMSU	32.55	35.82	-55.72	Mon16
J06467+159	-97.7	1.1	-26.4	1.1	PPMXL				1.7	-10.8	Lep13
J06474+054	46.0	0.6	-301.7	0.1	Gal15						
J06486+532	140.4	0.6	-324.7	0.3	Cortes				-52.0	8.2	Lep13
J06489+211	-32.8	4.4	-66.4	4.4	PPMXL						
J06490+371	202.3	5.7	-1587.9	5.7	PPMXL	4.5	PMSU	-13.51	-97.1	-24.4	Mon16
J06509-091	-98.3	5.4	-569.9	5.4	PPMXL	-0.84	Ter15	33.08	-32.77	-34.33	Mon16
J06523-051	-544.14	0.44	-3.32	0.34	aHIP2	-10.4	PMSU	2.66	14.81	-19.66	Mon16
J06524+182	121.9	0.9	122.9	0.3	Gal15	12.13	Schf15	-11.04	0.9	13.11	Mon16
J06540+608	495.89	2.24	-989.85	1.71	HIP2	-40.9	PMSU	15.9	-66.57	-5.02	Mon16
J06548+332	-723.99	1.84	-398.4	1.21	HIP2	22.52	Schf15	-27.27	-3.7	-15.14	Mon16
J06564+121	40.5	0.9	-93.3	0.9	PPMXL				-9.8	-0.4	Lep13
J06564+400	114.95	1.31	-436.22	0.89	aHIP2	46.0	PMSU	-48.58	-49.42	9.02	Mon16
J06564+759	56.1	0.3	-339.3	0.4	Gal15				-46.5	0.7	Lep13
J06565+440	182.3	4.8	-684.6	4.8	PPMXL	4.81	Schf15	-15.66	-70.21	-3.77	Mon16

Table B.3: Proper motions and UVW space velocities of Carmencita stars (continued).

Karmn	$\mu_\alpha \cos\delta$ [mas a^{-1}]	$e\mu_\alpha \cos\delta$ [mas a^{-1}]	μ_δ [mas a^{-1}]	$e\mu_\delta$ [mas a^{-1}]	Ref.[a b]	V_r [km s^{-1}]	Ref.[c]	U [km s^{-1}]	V [km s^{-1}]	W [km s^{-1}]	Ref.[d]
J06574+740	-89.3	4.6	-30.8	4.6	PPMXL	3.02	Schf15	-5.06	2.39	-4.14	Mon16
J06579+623	318.9	4.9	-512.5	4.9	PPMXL	10.0	New14	-17.65	-25.49	14.24	Mon16
J06582+511	152.2	1.0	-327.0	1.0	Cortes				-58.4	10.1	Lep13
J06594+193	896.8	0.8	-891.2	0.1	Gal15	-30.6	PMSU	44.04	-32.85	10.13	Mon16
J06594+195	-181.9	4.7	-214.2	4.7	PPMXL				-10.7	-21.7	Lep13
J06596+057	-27.2	5.5	-73.4	5.5	PPMXL				-6.0	-7.5	Lep13
J07001-190	155.0	5.4	-74.7	5.4	PPMXL						
J07009-023	-48.7	5.3	50.8	5.3	PPMXL						
J07012+008	1.5	5.2	-116.2	5.2	PPMXL				-10.9	-3.7	Lep13
J07033+346	-62.5	4.9	134.4	4.9	PPMXL	2.45	Schf15	-2.89	9.5	0.16	Mon16
J07034+767	17.3	5.0	-232.5	5.0	PPMXL				-17.4	0.5	Lep13
J07039+527	675.6	4.7	-922.9	4.7	PPMXL	17.6	PMSU	-21.53	-42.21	23.52	Mon16
J07042-105	-123.73	3.68	-814.92	2.87	HIP2	-5.6	PMSU	39.97	-31.87	-36.42	Mon16
J07044+682	345.5	1.56	53.77	2.04	HIP2	-49.81	Schf15	47.0	-29.7	0.12	Mon16
J07047+249	-176.1	2.4	-275.6	2.4	PPMXL	-3.5	PMSU	0.36	-20.1	-29.66	Mon16
J07051-101	123.7	5.4	77.5	5.4	PPMXL						
J07052+084	51.3	1.2	-428.1	1.5	Cortes				-50.6	-16.7	Lep13
J07076+486	-35.6	4.7	-309.8	4.7	PPMXL	-50.4	PMSU	40.33	-23.31	-25.0	Mon16
J07078+672	-290.39	1.03	-45.62	1.52	HIP2	-10.7	PMSU	-1.44	0.2	-26.72	Mon16
J07081-228	-407.9	2.9	-227.6	2.9	PPMXL	19.63	Schf15	-6.88	-13.06	-43.38	Mon16
J07086+307	174.2	2.3	107.1	2.3	PPMXL	1.7	PMSU	6.28	5.73	28.57	Mon16
J07095+698	-174.7	4.7	-275.2	4.7	PPMXL	38.4	PMSU	-52.34	1.9	-2.35	Mon16
J07100+385	-437.44	5.21	-947.44	2.85	HIP2	32.7	PMSU	-38.54	-21.66	-9.28	Mon16
J07102+376	-230.9	0.4	-265.5	0.8	Gal15	-14.0	PMSU	1.44	-19.55	-37.43	Mon16
J07105-087	-81.8	6.1	96.9	6.1	PPMXL						
J07111+434	350.2	5.0	-572.8	5.0	PPMXL	-43.0	New14	39.22	-44.03	-6.67	Mon16
J07119+773	11.8	1.9	-106.6	1.8	PPMXL				-7.1	0.6	Lep13
J07121+522	-138.76	2.81	-261.58	2.03	HIP2	-1.3	PMSU	-16.12	-24.83	-23.36	Mon16
J07129+357	58.0	4.8	-5.2	4.8	PPMXL				-2.5	6.5	Lep13
J07140+507	-125.8	3.5	-262.3	3.5	PPMXL				-30.7	-25.1	Lep13
J07163+271	-37.4	3.04	-195.77	2.22	HIP2	-10.3	PMSU	9.65	-7.85	-8.94	Mon16
J07163+331	-103.52	4.8	-439.4	4.8	PPMXL	7.0	New14	-10.19	-27.48	-14.37	Mon16
J07172-050	420.2	6.0	-396.4	6.0	PPMXL	21.25	Ter15	12.34	-45.91	16.07	Mon16

Table B.3: Proper motions and UVW space velocities of Carmencita stars (continued).

Karmn	$\mu_\alpha \cos\delta$ [mas a^{-1}]	$e\mu_\alpha \cos\delta$ [mas a^{-1}]	μ_δ [mas a^{-1}]	$e\mu_\delta$ [mas a^{-1}]	Ref.[a b]	V_r [km s^{-1}]	Ref.[c]	U [km s^{-1}]	V [km s^{-1}]	W [km s^{-1}]	Ref.[d]
J07174+195	-323.1	0.5	-267.9	0.1	Gal15	12.6	PMSU	-17.69	-17.64	-36.25	Mon16
J07181+392	-213.3	2.85	-113.92	1.9	HIP2	10.0	Schf15	-15.39	-2.57	-11.51	Mon16
J07182+137	-34.4	0.2	-32.2	0.7	Cortes						
J07195+328	422.1	1.5	-346.6	1.2	PPMXL	-69.78	Schf15	77.99	-36.16	0.31	Mon16
J07199+840	-38.3	1.9	-85.4	1.9	PPMXL			-6.9		-2.5	Lep13
J07212+005	97.0	2.3	-19.7	2.3	PPMXL				-6.6	11.9	Lep13
J07227+306	-423.4	0.1	-603.9	0.3	Gal15	28.1	PMSU	-42.71	-53.08	-54.9	Mon16
J07232+460	-118.04	2.02	-237.83	1.57	HIP2	-36.4	PMSU	25.07	-19.34	-27.37	Mon16
J07274+052	572.51	1.5	-3693.51	0.96	HIP2	18.26	Schf15	15.97	-65.74	-17.02	Mon16
J07274+220	-266.6	3.15	-144.4	2.05	HIP2	22.5	PMSU	-27.75	-11.12	-19.64	Mon16
J07282-187	-1.1	0.5	653.8	0.6	Cortes	75.47	Schf15	-71.11	-41.72	16.78	Mon16
J07287-032	437.8	0.4	-783.3	0.7	Cortes	4.6	PMSU	30.36	-42.82	1.79	Mon16
J07295+359	-31.2	2.3	-101.7	2.3	PPMXL				-11.1	-7.2	Lep13
J07307+481	-204.0	4.4	-1272.6	4.4	PPMXL	-62.1	PMSU	33.14	-69.99	-49.58	Mon16
J07310+460	-16.6	5.1	-97.5	5.1	PPMXL	23.48	Ter15	-24.01	-6.54	6.51	Mon16
J07319+362N	-273.6	0.6	-255.1	0.6	Gal15	-1.37	Schf15	-5.81	-9.37	-17.98	Mon16
J07319+362S	-259.9	0.6	-222.7	0.8	Gal15	2.3	PMSU	-8.74	-8.0	-15.35	Mon16
J07319+392	145.4	4.8	-253.9	4.8	PPMXL	16.1	PMSU	-11.86	-30.39	13.33	Mon16
J07320+173E	-219.59	4.34	-182.9	2.67	aHIP2	22.5	PMSU	-26.9	-23.69	-34.43	Mon16
J07320+173W	-219.59	4.34	-182.9	2.67	HIP2	21.9	PMSU	-26.37	-23.48	-34.6	Mon16
J07320+686	174.59	1.14	-117.63	1.71	HIP2	-11.6	PMSU	8.95	-23.06	12.37	Mon16
J07325+248	-208.5	2.4	85.6	2.3	PPMXL				20.8	-22.6	Lep13
J07342+009	-54.7	4.8	-590.0	4.8	PPMXL	-7.2	PMSU	23.36	-25.62	-23.06	Mon16
J07344+629	-495.43	2.12	-105.88	2.27	HIP2	-47.6	PMSU	23.86	-16.22	-46.82	Mon16
J07346+223	168.44	3.55	-99.67	2.16	HIP2	-0.5	PMSU	10.93	-17.35	13.97	Mon16
J07346+318	-191.45	2.95	-145.19	2.95	aHIP2	10.6	PMSU	-15.38	-7.64	-11.54	Mon16
J07349+147	-76.7	1.2	-107.3	1.2	PPMXL	31.4	Schf15	-27.56	-15.72	3.8	Mon16
J07353+548	-120.2	2.86	16.98	2.3	HIP2	-10.8	PMSU	6.53	0.11	-11.33	Mon16
J07354+482	105.7	1.0	-189.9	1.0	Cortes				-32.8	12.2	Lep13
J07359+785	-142.6	4.5	-200.2	4.5	PPMXL						
J07361-031	69.9	0.71	-278.33	0.31	aHIP2	-16.42	Schf15	24.03	-4.0	-7.02	Mon16
J07364+070	222.2	0.7	-303.3	0.2	Gal15	20.0	New14	-8.09	-22.81	7.16	Mon16
J07365-006	-21.2	6.0	88.3	6.4	PPMXL						

Table B.3: Proper motions and UVW space velocities of Carmencita stars (continued).

Karmn	$\mu_\alpha \cos\delta$ [mas a^{-1}]	$e\mu_\alpha \cos\delta$ [mas a^{-1}]	μ_δ [mas a^{-1}]	$e\mu_\delta$ [mas a^{-1}]	Ref.[a b]	V_r [km s^{-1}]	Ref.[c]	U [km s^{-1}]	V [km s^{-1}]	W [km s^{-1}]	Ref.[d]
J07366+440	-103.4	5.0	-333.0	5.0	PPMXL	35.27	Schf15	-45.24	-34.98	-5.03	Mon16
J07383+344	8.44	4.31	111.03	2.91	PPMXL	15.0	Wil53	-12.5	14.43	11.76	Mon16
J07384+240	-173.9	0.6	-107.1	0.4	Cortes	14.0	New14	-17.23	-7.81	-9.98	Mon16
J07386-212	450.28	3.5	-477.71	2.72	HIP2	-28.9	Schf15	42.61	6.89	7.79	Mon16
J07393+021	-147.83	1.6	-246.05	0.77	HIP2	19.64	Schf15	-11.98	-21.93	-12.67	Mon16
J07395+334	-156.16	3.6	-177.35	2.75	HIP2	-8.0	PMSU	-4.37	-21.12	-34.56	Mon16
J07403-174	1143.2	1.4	-531.6	1.5	Cortes	-30.8	PMSU	54.67	-0.03	30.29	Mon16
J07418+050	-273.3	4.7	-79.2	4.7	PPMXL	23.3	PMSU	-28.07	-12.0	-24.99	Mon16
J07421+500	215.1	4.4	34.8	4.4	PPMXL				-0.8	17.7	Lep13
J07431+181	-51.73	2.94	-472.67	1.86	HIP2	29.7	PMSU	-13.93	-70.82	-22.33	Mon16
J07446+035	-349.1	1.3	-446.7	0.9	Cortes	26.26	Schf15	-19.48	-22.41	-8.01	Mon16
J07467+574	-33.3	0.7	-238.0	0.8	Gal15	-1.86	Schf15	-8.63	-21.14	-5.26	Mon16
J07470+760	150.7	4.7	-387.4	4.7	PPMXL						
J07472+503	91.6	5.6	94.1	5.6	PPMXL	-14.84	Schf15	16.91	1.67	-1.42	Mon16
J07482+203	1451.48	3.07	-989.9	2.28	HIP2	53.5	PMSU	11.87	-104.89	82.77	Mon16
J07493+849	-151.5	0.2	-352.7	0.2	Gal15	25.0	PMSU	-45.1	-3.17	5.26	Mon16
J07497-033	-139.4	5.5	-50.8	5.5	PPMXL	9.75	Ter15	-9.88	-6.76	-9.47	Mon16
J07518+055	448.3	0.4	-413.6	0.2	Gal15	51.3	PMSU	-12.23	-60.94	29.69	Mon16
J07519-000	248.8	4.6	-742.6	4.6	PPMXL	36.0	PMSU	-7.1	-47.99	3.15	Mon16
J07523+162	176.9	0.2	-355.2	0.6	Gal15	-7.0	West15	21.0	-28.38	-0.76	Mon16
J07525+063	26.2	0.3	-214.9	0.3	Gal15	31.2	PMSU	-11.85	-40.58	-0.3	Mon16
J07545+085	-224.3	5.1	17.5	5.1	PPMXL						
J07545-096	-93.3	6.0	-12.1	6.0	PPMXL						
J07558+833	-295.0	4.3	-600.9	4.3	PPMXL	6.3	Schf15	-35.64	-17.11	-4.98	Mon16
J07581+072	-325.8	4.0	-33.5	4.0	PPMXL	-2.0	New14	-6.62	3.42	-17.36	Mon16
J07582+413	211.27	5.41	-691.29	4.16	HIP2	-21.96	Schf15	19.81	-28.76	-8.47	Mon16
J07583+496	318.4	4.7	-742.0	4.7	PPMXL	-26.87	Schf15	20.73	-55.51	-0.89	Mon16
J07585+155N	-87.9	4.6	-112.9	4.6	PPMXL	18.0	PMSU	-16.54	-18.02	-8.57	Mon16
J07585+155S	-87.9	4.6	-112.9	4.6	aPPMXL	10.3	PMSU	-9.84	-12.98	-8.71	Mon16
J07590+153	-182.3	0.3	-64.4	0.6	Gal15	23.0	PMSU	-28.91	-12.12	-16.34	Mon16
J07591+173	-87.2	0.7	-38.8	0.4	Cortes						
J08005+258	118.9	1.8	-43.8	1.7	PPMXL	16.07	Schf15	-8.04	-10.05	15.25	Mon16
J08017+237	-106.6	1.1	-117.5	1.1	PPMXL	9.08	Schf15	-10.64	-9.88	-6.56	Mon16

Table B.3: Proper motions and UVW space velocities of Carmencita stars (continued).

Karmn	$\mu_\alpha \cos\delta$ [mas a^{-1}]	$e\mu_\alpha \cos\delta$ [mas a^{-1}]	μ_δ [mas a^{-1}]	$e\mu_\delta$ [mas a^{-1}]	Ref.[a b]	V_r [km s^{-1}]	Ref.[c]	U [km s^{-1}]	V [km s^{-1}]	W [km s^{-1}]	Ref.[d]
J08023+033	-402.9	0.3	-379.9	0.6	Cortes	6.3	PMSU	-8.6	-31.1	-62.24	Mon16
J08025-130	157.7	5.9	-254.4	5.9	PPMXL						
J08031+203	-108.6	4.3	-62.0	4.3	PPMXL	35.5	Shk12	-33.86	-15.24	4.24	Mon16
J08033+528	362.42	3.68	-676.32	2.82	HIP2	22.1	Daw05	-19.97	-102.23	51.65	Mon16
J08066+558	145.45	2.97	-84.3	2.81	HIP2	-36.35	Schf15	35.76	-24.76	-2.3	Mon16
J08068+367	-149.9	0.9	-384.1	0.7	Cortes	6.4	PMSU	-14.5	-34.78	-16.55	Mon16
J08069+422	-225.9	4.9	-278.9	4.9	PPMXL	36.7	West15	-44.85	-19.98	-1.88	Mon16
J08082+211	-298.51	1.88	-352.69	1.46	aHIP2	83.2	PMSU	-76.27	-48.73	7.68	Mon16
J08083+585	-174.9	5.0	-64.5	5.0	PPMXL	42.6	PMSU	-43.59	10.33	9.77	Mon16
J08089+328	-42.9	1.6	-193.3	1.6	PPMXL	19.4	PMSU	-18.39	-20.3	1.84	Mon16
J08095+219	-318.6	4.41	-64.99	3.42	HIP2	19.0	PMSU	-31.95	-6.36	-21.91	Mon16
J08103+095	-81.9	3.5	-34.3	3.5	PPMXL				-1.2	-7.5	Lep13
J08105-138	-249.81	0.23	57.76	0.25	aHIP2	32.915	Schf15	-36.4	-18.18	-13.01	Mon16
J08108+039	105.2	0.3	-338.4	0.1	Gal15	37.0	New14	-7.42	-49.92	6.54	Mon16
J08117+531	-283.9	4.8	-183.2	4.8	PPMXL						
J08119+087	1130.9	0.4	-5129.7	0.1	Cortes	13.0	New14	70.37	-151.32	-31.49	Mon16
J08126-215	12.5	0.2	-694.3	0.8	Gal15	17.2	PMSU	5.76	-23.97	-8.09	Mon16
J08158+346	-101.8	3.4	-189.4	3.4	PPMXL	90.95		-84.2	-41.92	25.86	Mon16
J08161+013	-374.45	1.97	60.1	1.33	HIP2	62.09	Schf15	-53.55	-34.43	8.36	Mon16
J08175+209	-372.3	0.5	-226.0	1.1	Cortes				-16.6	-47.4	Lep13
J08178+311	-81.0	3.2	222.3	3.2	PPMXL	41.7	PMSU	-40.9	16.81	19.67	Mon16
J08202+055	-389.4	6.0	-38.9	5.6	PPMXL				1.9	-5.6	Lep13
J08258+690	-689.9	4.5	-1259.2	4.5	PPMXL	-1.0	New14	-50.63	-54.61	-19.24	Mon16
J08282+201	-265.7	0.4	-635.3	0.2	Gal15	128.7	PMSU	-102.52	-103.89	21.54	Mon16
J08283+350	-1035.41	8.89	-329.06	4.48	HIP2	32.2	PMSU	-81.08	-21.54	-65.37	Mon16
J08283+553	-36.2	4.8	-103.0	4.8	PPMXL						
J08286+660	26.1	4.5	95.4	4.5	PPMXL	-5.5	Schf15	7.95	3.89	-2.59	Mon16
J08293+039	-94.2	2.6	-73.9	2.6	PPMXL	22.69	Schf15	-17.27	-16.98	1.32	Mon16
J08298+267	-1110.2	1.2	-613.0	0.1	Gal15	8.0	PMSU	-15.94	-9.73	-13.56	Mon16
J08313-060	-462.84	2.63	-56.13	2.58	HIP2	73.3	Schf15	-73.72	-51.4	-26.21	Mon16
J08313-104	-592.9	5.5	-322.1	5.5	PPMXL	23.3	PMSU	-30.02	-32.62	-65.76	Mon16
J08314-060	-462.84	2.63	-56.13	2.58	aHIP2	74.75	Schf15	-74.59	-52.48	-25.71	Mon16
J08315+730	604.5	4.5	272.1	4.5	PPMXL				9.7	24.6	Lep13

Table B.3: Proper motions and UVW space velocities of Carmencita stars (continued).

Karmn	$\mu_\alpha \cos\delta$ [mas a^{-1}]	$e\mu_\alpha \cos\delta$ [mas a^{-1}]	μ_δ [mas a^{-1}]	$e\mu_\delta$ [mas a^{-1}]	Ref.[a b]	V_r [km s^{-1}]	Ref.[c]	U [km s^{-1}]	V [km s^{-1}]	W [km s^{-1}]	Ref.[d]
J08316+193N	-232.8	0.7	-121.6	1.4	Cortes	-18.6	PMSU	8.91	2.4	-21.26	Mon16
J08316+193S	-226.7	0.8	-143.6	1.2	Cortes	4.4	Del99a	-8.54	-7.2	-9.69	Mon16
J08317+057	-45.9	5.5	26.8	5.5	PPMXL				-13.2	-13.2	Lep13
J08321+844	351.1	4.3	248.5	4.3	PPMXL	-4.9	PMSU	38.77	10.9	18.0	Mon16
J08325+451	-144.6	4.7	-61.6	4.7	PPMXL				-4.5	-14.2	Lep13
J08334+185	-64.7	0.4	-654.0	0.2	Gal15	21.1	PMSU	-4.42	-63.41	-13.1	Mon16
J08344-011	225.1	0.3	-423.8	0.7	Cortes	60.28	Schf15	-16.39	-62.05	21.72	Mon16
J08353+141	-132.3	6.4	-79.4	5.2	PPMXL	12.0	New14	-14.96	-11.79	-9.18	Mon16
J08358+680	-840.8	2.4	-558.0	2.4	PPMXL	17.0	PMSU	-56.39	-17.31	-24.84	Mon16
J08364+264	-251.8	6.1	211.7	6.1	PPMXL				-2.3	-22.1	Lep13
J08364+672	-1064.12	0.64	66.38	0.93	HIP2	8.4	Daw05	-45.33	14.68	-51.49	Mon16
J08371+151	-121.54	3.69	-894.53	3.14	HIP2	83.54	Schf15	-44.68	-107.37	6.1	Mon16
J08375+035	67.3	0.1	-174.0	0.1	Gal15	1.32	Schf15	9.18	-13.12	-1.27	Mon16
J08387+516	-95.4	4.9	-113.4	4.9	PPMXL				-12.2	-9.2	Lep13
J08398+089	-230.3	4.8	191.2	4.5	PPMXL	11.5	PMSU	-43.34	24.24	-12.67	Mon16
J08402+314	192.4	4.4	119.4	4.4	PPMXL	98.38	Ter15	-72.37	-11.69	66.68	Mon16
J08404+184	-816.4	1.0	-453.6	0.4	Gal15	69.8	PMSU	-77.62	-49.91	-15.19	Mon16
J08410+676	-680.0	4.7	-342.0	4.7	PPMXL	33.0	PMSU	-83.59	-12.6	-32.74	Mon16
J08413+594	-259.5	5.0	-1281.8	5.0	PPMXL	8.0	New14	-29.4	-49.45	2.71	Mon16
J08427+095	214.59	3.05	-633.35	1.91	HIP2	24.01	Schf15	10.11	-53.16	6.37	Mon16
J08428+095	214.59	3.05	-633.35	1.91	aHIP2	21.12	Schf15	12.15	-51.64	4.98	Mon16
J08443-104	299.3	5.8	-515.2	5.8	PPMXL	-34.4	PMSU	76.72	-14.1	-15.69	Mon16
J08447+182	-236.0	6.1	-454.5	6.1	PPMXL	77.64	Ter15	-60.38	-75.8	5.61	Mon16
J08449-066	-58.3	5.3	-126.4	5.3	PPMXL						
J08517+181	-893.23	5.29	-56.79	3.17	HIP2	-1.2	PMSU	-47.11	0.52	-61.94	Mon16
J08526+283	-485.8	0.97	-234.05	0.68	aHIP2	12.5	PMSU	-24.41	-13.68	-14.91	Mon16
J08531-202	37.4	6.8	-110.8	6.8	PPMXL						
J08536-034	-502.7	5.2	-205.6	5.2	PPMXL	6.7	Burg15	-12.66	-9.61	-17.15	Mon16
J08537+149	-25.6	0.8	-79.6	0.9	PPMXL				-9.8	-6.3	Lep13
J08540-131	338.0	5.5	-547.7	5.5	PPMXL	-17.3	PMSU	41.96	-6.45	-8.38	Mon16
J08551+015	44.83	1.69	-1044.6	1.05	HIP2	-4.13	Schf15	51.04	-72.48	-42.19	Mon16
J08555+664	35.9	4.5	-90.2	4.5	PPMXL				-8.6	6.2	Lep13
J08563+126	-44.8	4.9	-253.5	4.9	PPMXL	-17.0	New14	15.78	-7.71	-18.14	Mon16

Table B.3: Proper motions and UVW space velocities of Carmencita stars (continued).

Karmn	$\mu_\alpha \cos\delta$ [mas a^{-1}]	$e\mu_\alpha \cos\delta$ [mas a^{-1}]	μ_δ [mas a^{-1}]	$e\mu_\delta$ [mas a^{-1}]	Ref.[a b]	V_r [km s^{-1}]	Ref.[c]	U [km s^{-1}]	V [km s^{-1}]	W [km s^{-1}]	Ref.[d]
J08570+116	-37.2	2.97	-315.32	1.94	HIP2	-6.9	PMSU	11.73	-18.43	-15.02	Mon16
J08572+194	121.4	0.5	-153.5	0.5	Cortes						
J08582+197	-852.5	1.0	-62.0	1.1	Gal15	13.0	New14	-23.86	-5.47	-10.17	Mon16
J08589+084	376.4	0.6	-321.8	1.0	Gal15	-25.3	PMSU	28.37	4.69	-8.25	Mon16
J08595+537	-289.2	4.6	-197.6	4.6	PPMXL	11.7	Schf15	-26.95	-12.44	-8.43	Mon16
J08599+729	964.9	0.2	-20.2	1.0	Gal15	-29.5	PMSU	58.94	-18.62	30.35	Mon16
J09003+218	-513.6	1.0	-582.2	0.6	Gal15						
J09005+465	-474.4	0.5	-526.3	0.7	Gal15	1.78	Schf15	-18.12	-23.7	-14.8	Mon16
J09008+052E	-256.52	8.85	-202.63	3.75	HIP2	-37.68	Schf15	15.15	6.97	-46.87	Mon16
J09008+052W	-256.52	8.85	-202.63	3.75	bHIP2	-38.16	Schf15	15.45	7.26	-47.11	Mon16
J09011+019	-375.5	0.8	-81.5	0.2	Gal15	61.7	PMSU	-49.23	-42.48	11.1	Mon16
J09023+084	616.47	3.81	-200.97	2.68	HIP2	39.5	Schf15	19.9	-38.75	57.05	Mon16
J09023+177	-134.1	0.5	-47.5	0.9	Cortes						
J09028+680	194.9	4.6	339.1	4.6	PPMXL	-8.5	PMSU	19.12	12.49	-2.32	Mon16
J09033+056	-50.2	5.2	-381.6	5.2	PPMXL	-26.0	New14	25.74	-8.05	-28.3	Mon16
J09037+520	240.8	0.3	-220.0	0.4	Cortes				-21.9	20.4	Lep13
J09038+129	-14.9	1.1	-212.2	1.1	PPMXL				-26.1	-10.2	Lep13
J09040-159	-111.6	0.7	-32.0	0.1	Cortes						
J09050+028	-317.9	2.0	41.7	2.0	PPMXL	31.4	PMSU	-42.61	-15.63	-6.68	Mon16
J09057+186	48.9	0.3	-389.9	0.9	Cortes				-45.4	-8.8	Lep13
J09062+128	-287.2	0.4	-290.5	0.5	Gal15	49.1	PMSU	-40.74	-46.97	-0.32	Mon16
J09070-221	-305.8	5.4	-409.7	5.4	PPMXL	6.4	PMSU	2.36	-18.2	-31.75	Mon16
J09087+665	203.2	4.5	-152.8	4.5	PPMXL	-14.2	PMSU	20.72	-23.7	15.44	Mon16
J09091+227	-81.2	4.2	-71.8	4.2	PPMXL						
J09093+401	-555.0	5.0	-582.2	5.0	PPMXL	31.1	PMSU	-61.07	-60.83	-22.6	Mon16
J09095+328	-335.28	2.36	-628.67	1.02	HIP2	0.0	PMSU	-15.5	-59.92	-30.5	Mon16
J09096+067	72.8	5.5	-32.2	5.5	PPMXL	-9.8	PMSU	13.07	2.56	-0.81	Mon16
J09099+004	342.9	4.5	-365.1	4.5	PPMXL			68.4		15.5	Lep13
J09115+126	175.3	1.3	-329.4	1.4	PPMXL						
J09115+466	-351.57	2.41	-41.4	1.43	HIP2	87.2	PMSU	-91.84	2.74	29.73	Mon16
J09120+279	-195.0	1.8	-421.6	2.4	PPMXL	36.4	PMSU	-33.73	-62.63	-3.51	Mon16
J09133+688	-163.0	4.9	-237.1	4.9	PPMXL	13.86	Schf15	-21.58	-7.7	5.64	Mon16
J09140+196	-149.6	0.7	-143.0	0.5	Cortes	12.63	Schf15	-13.34	-14.92	-2.93	Mon16

Table B.3: Proper motions and UVW space velocities of Carmencita stars (continued).

Karmn	$\mu_\alpha \cos\delta$ [mas a^{-1}]	$e\mu_\alpha \cos\delta$ [mas a^{-1}]	μ_δ [mas a^{-1}]	$e\mu_\delta$ [mas a^{-1}]	Ref.[a b]	V_r [km s^{-1}]	Ref.[c]	U [km s^{-1}]	V [km s^{-1}]	W [km s^{-1}]	Ref.[d]
J09143+526	-1535.72	6.94	-576.59	4.53	HIP2	11.14	BE12	-39.27	-13.75	-20.83	Mon16
J09144+526	-1535.72	6.94	-576.59	4.53	aHIP2	13.17	Mald10	-40.72	-13.36	-19.45	Mon16
J09156-105	-396.2	5.2	-186.0	5.2	PPMXL						
J09160+293	-133.7	0.5	-529.2	0.6	Gal15				-68.1	-22.9	Lep13
J09161+018	51.3	0.7	-101.8	1.3	Cortes	-12.29	Schf15	11.84	3.08	-7.12	Mon16
J09163-186	-314.6	3.3	148.0	3.4	PPMXL	14.742	Schf15	-27.31	-7.87	-4.54	Mon16
J09165+841	-511.2	0.8	420.4	0.6	Gal15	-87.8	PMSU	27.91	-22.01	-114.39	Mon16
J09168+248	-70.9	4.2	-123.3	4.2	PPMXL						
J09177+462	-132.6	0.4	-15.6	0.6	Cortes	-7.0	Schf15	-2.31	-1.94	-12.2	Mon16
J09177+584	17.0	4.7	-1169.8	4.7	PPMXL	-92.0	PMSU	47.36	-108.96	-42.05	Mon16
J09187+267	-194.0	2.4	-353.8	2.4	PPMXL	33.7	PMSU	-30.4	-46.68	1.28	Mon16
J09193+385N	-249.3	0.5	-3.5	0.2	Cortes	21.0	PMSU	-28.75	-1.84	0.72	Mon16
J09193+385S	-243.8	0.5	8.2	0.1	Cortes	21.0	PMSU	-28.5	-0.91	1.05	Mon16
J09193+620	-287.25	2.25	-383.82	1.29	HIP2	53.9	PMSU	-84.26	-41.49	17.99	Mon16
J09200+308	-80.8	3.3	-35.7	3.4	PPMXL			-7.0	-4.1		Lep13
J09201+037	-125.8	1.9	72.2	0.9	Cortes						
J09209+033	310.6	4.2	-1135.9	4.2	PPMXL	13.6	PMSU	57.29	-86.31	-15.34	Mon16
J09213+731	-914.4	4.5	-342.5	4.5	PPMXL	94.8	PMSU	-98.83	32.65	29.0	Mon16
J09218+435	-294.1	4.6	-115.5	4.6	PPMXL	-13.6	PMSU	-11.77	-13.11	-30.35	Mon16
J09218-023	174.5	0.4	7.3	0.6	Cortes	-58.02	Schf15	39.45	41.19	-19.0	Mon16
J09228+467	-204.9	1.3	-115.5	1.0	Cortes			-25.1	-18.1		Lep13
J09231+223	-127.74	2.98	-177.33	1.08	aHIP2	0.8	Schf15	-8.35	-29.54	-21.27	Mon16
J09238+001	-212.0	3.07	-227.56	2.0	HIP2	25.9	PMSU	-18.5	-40.03	-18.19	Mon16
J09248+306	-104.2	4.9	-165.6	4.9	PPMXL						
J09256+634	-318.6	4.7	-274.8	4.7	PPMXL	30.37	Schf15	-46.02	-12.53	7.32	Mon16
J09275+506	-225.17	2.96	-145.86	1.41	HIP2	28.8	PMSU	-46.09	-18.77	0.02	Mon16
J09288-073	-168.04	3.81	-713.14	2.42	HIP2	8.43	Schf15	16.85	-42.99	-33.48	Mon16
J09289-073	-168.04	3.81	-713.14	2.42	aHIP2	16.1	PMSU	13.59	-48.77	-29.63	Mon16
J09291+259	-1046.4	4.1	-268.2	4.1	PPMXL						
J09300+396	120.7	1.2	-164.9	0.4	Cortes	2.1	PMSU	7.51	-14.55	9.26	Mon16
J09302+265	-149.8	0.7	-133.5	0.4	Gal15	39.9	West15	-34.95	-25.58	14.7	Mon16
J09307+003	-571.9	4.49	-553.76	2.85	HIP2	46.45	Schf15	-29.59	-51.13	-2.91	Mon16
J09308+024	-25.4	0.6	64.2	0.7	Cortes						

Table B.3: Proper motions and UVW space velocities of Carmencita stars (continued).

Karmn	$\mu_\alpha \cos\delta$ [mas a^{-1}]	$e\mu_\alpha \cos\delta$ [mas a^{-1}]	μ_δ [mas a^{-1}]	$e\mu_\delta$ [mas a^{-1}]	Ref.[a b]	V_r [km s^{-1}]	Ref.[c]	U [km s^{-1}]	V [km s^{-1}]	W [km s^{-1}]	Ref.[d]
J09313-134	692.52	4.19	104.68	4.41	HIP2	5.2	PMSU	19.18	0.42	27.59	Mon16
J09315+202	27.1	0.3	-804.0	0.4	Gal15	-17.1	PMSU	34.56	-65.28	-27.77	Mon16
J09319+363	-208.96	2.01	-524.16	1.06	HIP2	19.77	Schf15	-19.8	-36.96	4.14	Mon16
J09328+269	-142.7	0.7	-242.4	0.5	Cortes	3.3	PMSU	-6.41	-20.51	-8.31	Mon16
J09352+612	115.8	2.0	41.5	2.0	PPMXL	-40.0	PMSU	35.81	-8.55	-20.3	Mon16
J09360-061	-682.4	0.3	-353.8	1.1	Cortes	70.0	PMSU	-68.17	-86.9	-41.78	Mon16
J09360-216	136.67	1.53	-989.13	1.41	HIP2	-37.7	PMSU	40.35	14.93	-37.32	Mon16
J09362+375	-103.9	0.5	-86.4	0.6	Gal15	-44.4	Malo14a	17.05	-14.01	-45.79	Mon16
J09370+405	-175.3	0.5	-77.7	0.4	Gal15	29.4	PMSU	-31.07	-8.72	11.42	Mon16
J09394+146	-164.0	0.7	-83.4	0.6	Cortes						
J09394+317	-190.72	3.67	-206.97	2.02	HIP2			-12.5	-26.2		Lep13
J09410+220	471.7	0.6	-494.0	0.7	Gal15	41.0	New14	4.92	-39.15	42.61	Mon16
J09411+132	-665.12	2.19	-141.27	1.38	HIP2	11.14	Schf15	-29.96	-14.87	-17.96	Mon16
J09423+559	-710.9	4.7	-509.5	4.7	PPMXL	15.9	Schf15	-57.84	-40.9	-16.15	Mon16
J09425+700	-668.54	1.53	-268.64	1.47	HIP2	-1.0	PMSU	-32.66	-17.59	-19.6	Mon16
J09425-192	-474.79	3.16	-212.0	2.44	HIP2	44.3	Schf15	-28.7	-49.29	-14.38	Mon16
J09428+700	-668.54	1.53	-268.64	1.47	aHIP2	22.7	PMSU	-47.06	-6.31	-4.51	Mon16
J09430+237	-161.7	0.5	-211.2	0.6	Gal15			-11.8	-37.0		Lep13
J09439+269	-585.54	4.55	-97.24	2.69	HIP2	34.9	Schf15	-49.32	-18.48	0.02	Mon16
J09447-182	-1604.3	5.1	-168.2	5.1	PPMXL	7.9	PMSU	-59.98	-19.09	-56.0	Mon16
J09449-123	-330.4	0.8	35.5	0.2	Cortes	19.8	Schf15	-23.44	-16.55	-2.26	Mon16
J09461-044	-550.8	5.1	166.9	5.1	PPMXL	39.6	PMSU	-63.29	-22.44	-2.67	Mon16
J09468+760	87.27	1.27	-997.6	1.26	HIP2	-28.23	Schf15	-2.01	-78.02	25.05	Mon16
J09473+263	-212.42	2.4	-351.6	1.65	HIP2			-1.8	-55.2		Lep13
J09475+129	-88.3	1.4	226.3	1.4	PPMXL	50.63	Schf15	-41.4	-5.75	36.92	Mon16
J09488+156	-34.8	0.5	226.4	0.4	Cortes	-0.8	Shk12	-11.68	23.1	3.91	Mon16
J09506-138	152.0	5.3	-99.0	5.3	PPMXL						
J09511-123	1140.3	2.22	-1457.94	1.31	HIP2	62.31	Schf15	91.13	-97.34	23.96	Mon16
J09526-156	-127.2	5.5	-125.5	5.5	PPMXL	-14.2	RAVE	1.34	3.76	-22.01	Mon16
J09527+554	288.6	4.4	-197.8	4.4	PPMXL			35.6	-25.0		Lep13
J09531-036	-101.43	2.63	-460.5	1.65	HIP2	17.6	PMSU	5.17	-37.83	-11.52	Mon16
J09535+507	-530.84	3.01	18.99	2.23	HIP2			-51.0	-5.6		Lep13
J09539+209	-347.7	0.7	387.3	0.4	Gal15	6.7	PMSU	-21.34	12.2	-1.28	Mon16

Table B.3: Proper motions and UVW space velocities of Carmencita stars (continued).

Karmn	$\mu_\alpha \cos\delta$ [mas a^{-1}]	$e\mu_\alpha \cos\delta$ [mas a^{-1}]	μ_δ [mas a^{-1}]	$e\mu_\delta$ [mas a^{-1}]	Ref.[a b]	V_r [km s^{-1}]	Ref.[c]	U [km s^{-1}]	V [km s^{-1}]	W [km s^{-1}]	Ref.[d]
J09557+353	-44.3	0.5	-311.0	0.6	Gal15	-16.6	PMSU	11.57	-27.38	-15.63	Mon16
J09561+627	-304.27	0.8	-582.81	0.83	HIP2	15.1	Schf15	-25.1	-23.31	11.75	Mon16
J09564+226	-464.3	0.3	-253.8	0.6	Gal15	41.9	PMSU	-49.45	-40.31	2.21	Mon16
J09579+118	-419.0	0.8	-157.6	0.4	Cortes	17.2	PMSU	-38.41	-30.06	-22.12	Mon16
J09587+555	-40.0	0.5	-242.4	0.6	Gal15			-6.1	-37.2		Lep13
J09589+059	-179.5	5.0	-71.2	5.0	PPMXL	19.0	West15	-15.98	-16.54	3.65	Mon16
J09593+438E	-101.7	0.3	-218.7	0.2	aGal15	16.6	PMSU	-17.64	-26.38	8.89	Mon16
J09593+438W	-101.7	0.3	-218.7	0.2	Gal15	-7.0	New14	-3.07	-27.52	-9.64	Mon16
J09597+472	74.2	0.8	-273.3	0.5	Cortes	-24.6	PMSU	22.33	-28.88	-9.89	Mon16
J09597+721	-31.0	4.7	91.5	4.7	PPMXL						
J10004+272	-15.27	1.96	118.91	1.38	HIP2			-7.2	18.1		Lep13
J10007+323	-1006.4	3.04	-664.43	2.16	HIP2	46.9	Giz02	-110.67	-107.47	-42.68	Mon16
J10020+697	-40.3	4.5	-273.3	4.5	PPMXL						
J10023+480	-637.87	1.3	-1472.52	0.86	HIP2	-10.06	Schf15	-25.62	-111.34	-15.62	Mon16
J10027+149	144.6	0.3	-233.6	0.1	Gal15	12.5	PMSU	6.09	-16.83	10.87	Mon16
J10028+484	-330.6	4.7	-273.9	4.7	PPMXL	-5.0	New14	-16.65	-25.59	-15.31	Mon16
J10035+059	-565.2	0.6	-168.0	0.4	Gal15	32.6	PMSU	-49.32	-39.44	-15.21	Mon16
J10040+187	-154.85	2.6	-225.24	1.21	HIP2			-8.9	-45.6		Lep13
J10043+503	-140.0	2.3	-194.8	2.3	PPMXL	0.3	Schf15	-8.34	-16.06	-2.82	Mon16
J10067+417	-270.61	3.19	-414.53	2.13	HIP2	-20.0	PMSU	-4.39	-44.55	-27.32	Mon16
J10068-127	-107.6	5.3	2.1	5.3	PPMXL						
J10069+126	-325.1	0.4	-38.2	0.6	Cortes			-34.2	-11.2		Lep13
J10079+692	-907.6	4.5	23.2	4.5	PPMXL	0.1	PMSU	-60.73	-10.56	-45.42	Mon16
J10087+027	-79.2	0.4	-450.9	0.4	Cortes	29.79	Schf15	0.75	-48.08	1.2	Mon16
J10094+512	-449.4	4.9	-829.6	4.9	PPMXL	46.43	Schf15	-49.24	-47.03	32.52	Mon16
J10094+544	68.1	4.6	-137.8	4.6	PPMXL			7.5	-15.8		Lep13
J10117+353	130.0	5.1	-255.0	5.1	PPMXL	-23.3	PMSU	25.96	-16.86	-12.45	Mon16
J10120-026	526.16	3.07	-605.63	2.33	HIP2	28.8	PMSU	32.94	-39.48	19.32	Mon16
J10122-037	-151.09	1.4	-244.31	1.17	HIP2	7.46	Schf15	-2.27	-12.53	-2.9	Mon16
J10125+570	-347.4	4.5	-535.2	4.5	PPMXL			-18.9	-34.3		Lep13
J10130+233	164.9	5.0	-240.0	5.0	PPMXL	-8.8	Ter15	23.27	-15.33	-1.82	Mon16
J10133+467	-248.3	5.2	-82.3	5.2	PPMXL	-26.0	PMSU	-0.85	-13.1	-31.3	Mon16
J10143+210	-144.06	1.9	-154.79	1.1	HIP2	5.8	BE12	-9.98	-20.43	-7.21	Mon16

Table B.3: Proper motions and UVW space velocities of Carmencita stars (continued).

Karmn	$\mu_\alpha \cos\delta$ [mas a^{-1}]	$e\mu_\alpha \cos\delta$ [mas a^{-1}]	μ_δ [mas a^{-1}]	$e\mu_\delta$ [mas a^{-1}]	Ref.[a b]	V_r [km s^{-1}]	Ref.[c]	U [km s^{-1}]	V [km s^{-1}]	W [km s^{-1}]	Ref.[d]
J10148+213	-192.4	5.0	-223.9	5.0	PPMXL						
J10151+314	-58.8	5.3	-207.4	5.3	PPMXL	-1.4	PMSU	0.89	-16.67	-4.26	Mon16
J10155-164	-196.0	6.2	-76.0	6.2	PPMXL						
J10158+174	288.7	0.3	2.8	0.7	Cortes	24.21	Schf15	5.63	-5.31	31.06	Mon16
J10167-119	-419.8	2.48	-602.45	1.98	HIP2	-10.519	Schf15	1.47	-20.06	-44.13	Mon16
J10182-204	-392.2	4.9	114.0	4.9	PPMXL						
J10185-117	-340.5	5.6	-250.9	5.6	PPMXL	-0.44	Schf15	-9.62	-14.5	-23.29	Mon16
J10196+198	-520.3	0.3	-24.5	0.3	Gal15	12.1	PMSU	-15.26	-7.02	3.15	Mon16
J10200+289	-466.2	2.8	-203.7	2.7	PPMXL						
J10206+492	-373.3	5.2	-133.1	5.2	PPMXL	30.1	PMSU	-58.59	-23.79	0.13	Mon16
J10238+438	170.5	4.8	-2.1	4.8	PPMXL						
J10240+366	-22.8	4.9	-153.1	4.9	PPMXL						
J10243+119	-25.4	1.2	180.9	1.2	PPMXL	-4.96	Schf15	-9.93	21.15	1.13	Mon16
J10251-102	-690.28	1.75	120.59	1.21	HIP2	21.21	Schf15	-41.41	-20.02	-4.16	Mon16
J10255+263	-317.4	0.6	-501.2	0.3	Cortes	57.2	PMSU	-36.98	-59.11	30.26	Mon16
J10260+504E	-384.3	4.8	-544.1	4.8	bPPMXL	61.6	PMSU	-57.23	-39.1	44.83	Mon16
J10260+504W	-384.3	4.8	-544.1	4.8	PPMXL	28.96	Schf15	-37.56	-41.93	18.74	Mon16
J10273+799	-101.5	2.0	-71.9	2.0	PPMXL			-12.9		-0.9	Lep13
J10278+028	-489.4	0.9	-93.8	0.3	Cortes						
J10284+482	600.3	4.8	-154.1	4.8	PPMXL	-20.6	PMSU	62.3	-4.67	17.69	Mon16
J10286+322	-468.6	5.2	175.3	5.2	PPMXL	34.3	PMSU	-68.62	3.44	0.37	Mon16
J10289+008	-603.75	1.9	-728.94	2.04	HIP2	8.28	Schf15	-7.47	-28.11	-15.42	Mon16
J10303+328	-402.4	0.5	-387.9	0.5	Gal15	54.3	PMSU	-45.5	-42.95	30.74	Mon16
J10315+570	-65.81	1.06	171.91	0.78	aHIP2	-6.0	New14	-1.72	10.59	-12.84	Mon16
J10320+033	37.7	0.6	-8.6	1.0	Cortes			4.4	0.1		Lep13
J10345+463	-418.9	5.1	-97.5	5.1	PPMXL	-21.2	PMSU	-21.1	-20.93	-36.0	Mon16
J10350-094	225.6	2.8	-186.7	2.6	PPMXL	14.5	Schf15	17.64	-15.32	9.89	Mon16
J10354+694	-1657.8	4.4	-644.5	4.4	PPMXL	-62.6	Schf15	-55.52	-88.73	-73.15	Mon16
J10359+288	-114.4	0.6	-79.6	0.4	Gal15						
J10360+051	-654.3	0.3	130.9	0.3	Gal15	21.307	Schf15	-48.16	-15.27	-2.25	Mon16
J10364+415	234.5	0.6	-241.4	0.1	Gal15			26.8	-15.8		Lep13
J10367+153	72.7	1.0	-38.7	0.9	PPMXL	-12.7	Shk12	8.56	4.25	-9.3	Mon16
J10368+509	245.6	4.8	-194.0	4.8	PPMXL	-12.0	West15	27.85	-14.18	6.92	Mon16

Table B.3: Proper motions and UVW space velocities of Carmencita stars (continued).

Karmn	$\mu_\alpha \cos\delta$ [mas a^{-1}]	$e\mu_\alpha \cos\delta$ [mas a^{-1}]	μ_δ [mas a^{-1}]	$e\mu_\delta$ [mas a^{-1}]	Ref.[a b]	V_r [km s^{-1}]	Ref.[c]	U [km s^{-1}]	V [km s^{-1}]	W [km s^{-1}]	Ref.[d]
J10379+127	-236.1	1.2	24.8	1.2	PPMXL	16.81	Schf15	-24.21	-10.52	4.35	Mon16
J10384+485	-196.0	4.8	-85.5	4.8	PPMXL	31.2	PMSU	-35.68	-11.56	16.81	Mon16
J10385+354	-440.3	0.9	264.2	0.9	Cortes	48.28	Ter15	-67.13	11.48	18.85	Mon16
J10389+250	-175.6	1.2	-74.5	1.1	Cortes	76.45	Ter15	-49.39	-33.61	54.05	Mon16
J10396-069	-714.67	3.33	-109.03	2.45	HIP2	3.46	Schf15	-42.95	-21.87	-29.11	Mon16
J10403+015	-44.5	2.7	-49.4	2.7	PPMXL			-2.6	-7.5		Lep13
J10416+376	-1469.3	5.3	-356.9	5.3	PPMXL	-5.0	New14	-53.81	-34.87	-36.93	Mon16
J10430-092	-1918.6	1.4	336.4	1.9	Cortes						
J10443+124	-271.0	1.7	4.2	1.7	PPMXL						
J10448+324	-215.1	4.5	-10.8	4.5	PPMXL	17.7	PMSU	-41.12	-14.41	-2.92	Mon16
J10453+385	-34.68	1.48	148.08	1.02	HIP2	-4.8	Eva79	-1.95	8.88	-6.41	Mon16
J10456-191	-1868.0	2.29	-600.41	1.82	aHIP2	40.5	PMSU	-121.84	-108.91	-98.02	Mon16
J10460+096	-119.9	4.7	-261.9	4.7	PPMXL	24.2	PMSU	-5.95	-37.13	5.75	Mon16
J10472+404	-294.8	3.9	-37.5	3.9	PPMXL						
J10474+025	170.7	0.8	36.3	1.4	Cortes			17.2	10.8		Lep13
J10482-113	580.9	0.8	-1532.4	0.7	Cortes	-0.2	PMSU	27.92	-16.83	-14.26	Mon16
J10485+191	235.0	0.5	-108.4	0.2	Gal15	-7.9	PMSU	32.93	-1.67	4.0	Mon16
J10497+355	-646.5	4.5	-1020.3	4.5	PPMXL	54.0	New14	-37.01	-56.34	38.17	Mon16
J10504+331	63.4	4.5	-626.1	4.5	PPMXL	-60.1	Schf15	52.04	-57.15	-48.01	Mon16
J10506+517	-189.37	1.83	30.37	1.43	aHIP2	26.7	PMSU	-29.71	3.33	13.04	Mon16
J10508+068	-874.5	0.9	-812.6	0.9	Gal15	-0.72	Schf15	-12.09	-29.37	-23.11	Mon16
J10513+361	-198.2	4.5	-56.8	4.5	PPMXL	31.0	PMSU	-37.46	-18.27	14.86	Mon16
J10520+005	-409.8	0.9	8.6	0.4	Gal15	16.0	New14	-29.26	-17.51	-0.63	Mon16
J10520+139	-1130.3	0.6	198.9	0.4	Gal15	22.94	Schf15	-75.12	-18.66	-9.49	Mon16
J10522+059	-699.4	4.1	-58.3	4.1	PPMXL	12.4	PMSU	-34.38	-19.88	-8.1	Mon16
J10546-073	-164.4	1.1	-383.9	0.5	Cortes	27.5	Schf15	-0.11	-38.61	1.22	Mon16
J10555-093	-269.3	5.3	452.4	5.3	PPMXL	24.2	PMSU	-43.18	1.41	29.56	Mon16
J10563+042	47.0	4.2	-95.5	4.2	PPMXL						
J10564+070	-3721.9	0.5	-2803.0	0.6	Cortes	19.07	Schf15	-26.45	-48.24	-13.93	Mon16
J10576+695	-629.68	1.3	56.66	1.34	HIP2	-4.5	PMSU	-55.97	-17.34	-35.55	Mon16
J10584-107	-189.5	4.5	-76.0	4.5	PPMXL						
J11000+228	-427.01	1.75	-281.82	1.08	HIP2	-21.6	PMSU	-0.7	-6.71	-26.11	Mon16
J11003+728	-154.3	4.4	-390.9	4.4	PPMXL			-23.8	-58.4		Lep13

Table B.3: Proper motions and UVW space velocities of Carmencita stars (continued).

Karmn	$\mu_\alpha \cos\delta$ [mas a^{-1}]	$e\mu_\alpha \cos\delta$ [mas a^{-1}]	μ_δ [mas a^{-1}]	$e\mu_\delta$ [mas a^{-1}]	Ref.[a b]	V_r [km s^{-1}]	Ref.[c]	U [km s^{-1}]	V [km s^{-1}]	W [km s^{-1}]	Ref.[d]
J11008+120	123.7	4.7	-119.5	4.7	PPMXL	-21.9	PMSU	20.58	3.25	-17.35	Mon16
J11013+030	1070.6	4.2	-396.0	4.2	PPMXL	-9.0	New14	74.7	6.21	10.91	Mon16
J11014+568	-195.0	0.4	-13.4	0.6	Cortes			-28.4	-12.2		Lep13
J11023+165E	-12.2	2.3	-164.2	2.3	PPMXL	20.7	PMSU	5.25	-36.44	10.58	Mon16
J11023+165W	-17.9	2.3	-170.7	2.3	PPMXL	0.6	PMSU	10.75	-30.81	-7.99	Mon16
J11026+219	142.3	1.16	-51.69	0.65	HIP2	-14.19	Schf15	12.66	3.6	-9.97	Mon16
J11030+037	110.4	4.2	-218.2	4.2	PPMXL						
J11031+152	-417.4	1.2	-95.4	4.4	PPMXL	27.85	Ter15	-33.11	-27.17	9.51	Mon16
J11031+366	-194.9	4.6	27.3	4.56	PPMXL	-9.0	New14	-16.22	-3.69	-17.49	Mon16
J11033+359	-580.27	0.62	-4765.85	0.64	HIP2	-85.07	Schf15	46.31	-53.68	-74.64	Mon16
J11036+136	-192.1	1.6	76.9	1.7	PPMXL	-18.1	Shk12	-10.92	7.7	-20.51	Mon16
J11042+400	-197.54	1.74	-55.43	1.68	HIP2	37.5	PMSU	-37.44	-14.53	24.17	Mon16
J11054+435	-4410.43	0.78	942.93	0.7	HIP2	69.4	Schf15	-123.51	-5.29	16.9	Mon16
J11055+435	-4410.43	0.78	942.93	0.7	aHIP2	68.9	PMSU	-123.29	-5.35	16.47	Mon16
J11055+450	157.15	2.29	-219.35	1.73	HIP2	-16.0	PMSU	35.31	-25.44	3.16	Mon16
J11057+102	620.51	4.12	-699.5	3.2	HIP2	-57.0	Schf15	92.29	-11.05	-46.44	Mon16
J11075+437	-121.7	4.8	-5.0	4.8	PPMXL	9.59	Schf15	-20.15	-5.8	1.45	Mon16
J11081-052	-58.9	2.7	-431.4	2.7	PPMXL	23.463	Schf15	11.04	-41.18	-2.78	Mon16
J11108+479	-299.2	4.5	-524.3	4.5	PPMXL	13.0	PMSU	-21.66	-63.9	15.97	Mon16
J11110+304	591.8	0.99	-197.6	0.8	aHIP2	-15.89	Schf15	38.41	2.47	-1.97	Mon16
J11113+434	-653.0	6.0	-450.6	1.1	Gal15	-9.7	PMSU	-31.68	-52.11	-20.37	Mon16
J11118+335	-174.6	4.5	118.0	4.5	PPMXL	-3.0	New14	-11.15	3.62	-7.49	Mon16
J11126+189	-21.2	1.7	8.0	0.4	Cortes	30.95	Schf15	-10.15	-9.32	27.76	Mon16
J11131+002	-413.9	1.3	-194.0	1.1	PPMXL	55.6	PMSU	-38.83	-65.92	16.13	Mon16
J11151+734	-403.8	1.1	111.7	1.2	PPMXL	2.0	PMSU	-25.61	-2.55	-13.93	Mon16
J11152+194	183.6	0.6	-483.5	0.5	Gal15	24.048	Schf15	22.44	-36.61	21.25	Mon16
J11152-181	136.9	5.7	-735.8	5.7	PPMXL	-21.3	PMSU	63.78	-29.61	-74.29	Mon16
J11154+410	78.6	5.1	-233.0	5.1	PPMXL	30.19	Ter15	-1.03	-13.98	33.56	Mon16
J11159+553	-171.7	2.2	-97.4	2.2	PPMXL	66.5	PMSU	-47.85	0.28	52.86	Mon16
J11195+466	304.7	4.4	-611.5	4.4	PPMXL						
J11200+658	-2946.85	0.96	184.03	0.8	HIP2	47.0	New14	-131.85	-16.35	-12.08	Mon16
J11201-104	-205.9	2.1	18.8	2.2	PPMXL	11.0	RAVE	-14.73	-12.31	3.3	Mon16
J11214-204	177.15	1.2	-115.74	0.87	aHIP2	8.5	PMSU	13.83	-6.4	3.8	Mon16

Table B.3: Proper motions and UVW space velocities of Carmencita stars (continued).

Karmn	$\mu_\alpha \cos\delta$ [mas a^{-1}]	$e\mu_\alpha \cos\delta$ [mas a^{-1}]	μ_δ [mas a^{-1}]	$e\mu_\delta$ [mas a^{-1}]	Ref.[a b]	V_r [km s^{-1}]	Ref.[c]	U [km s^{-1}]	V [km s^{-1}]	W [km s^{-1}]	Ref.[d]
J11216+061	-762.1	0.9	-1591.9	0.8	Gal15	58.4	PMSU	-0.75	-163.07	-22.72	Mon16
J11231+258	-1009.1	4.8	-327.5	4.8	PPMXL	-1.3	PMSU	-52.5	-46.62	-26.22	Mon16
J11233+448	-330.6	4.5	-137.8	4.5	PPMXL	14.9	PMSU	-37.01	-28.79	4.19	Mon16
J11237+085	-1003.9	2.95	194.69	1.82	HIP2	50.2	PMSU	-105.5	-42.66	17.08	Mon16
J11238+106	159.7	1.6	-65.9	1.6	PPMXL			19.2	0.4		Lep13
J11239-183	-619.1	5.8	-40.7	5.8	PPMXL	0.3	PMSU	-55.9	-26.68	-24.93	Mon16
J11240+381	123.8	4.9	-13.8	4.9	PPMXL	-14.0	RB09	14.63	2.4	-9.38	Mon16
J11247+675	312.5	0.3	-237.7	0.5	Gal15			44.6	-10.8		Lep13
J11249+024	-232.4	2.7	145.9	2.7	PPMXL			-45.4	6.7		Lep13
J11254+782	-641.2	4.6	-201.5	4.6	PPMXL	12.5	PMSU	-54.47	-24.95	2.08	Mon16
J11266+379	-142.5	3.6	-56.1	3.4	PPMXL	26.78	Ter15	-21.14	-10.95	20.9	Mon16
J11276+039	-85.2	1.67	11.27	1.88	HIP2	-19.7	PMSU	-8.3	6.88	-19.89	Mon16
J11289+101	-756.8	3.9	563.3	3.9	PPMXL	36.78	Schf15	-74.11	-1.21	28.1	Mon16
J11306-080	-356.47	3.19	264.16	3.44	HIP2						
J11307+549	34.7	2.3	105.9	2.2	PPMXL			0.8	19.1		Lep13
J11311-149	399.0	5.5	-1370.6	5.5	PPMXL	-9.6	PMSU	54.83	-28.56	-49.42	Mon16
J11315+022	-607.2	0.5	-509.6	0.5	Gal15			-38.9	-84.2		
J11317+226	-582.86	1.71	30.9	1.21	HIP2	-13.0	PMSU	-36.28	-11.82	-25.41	Mon16
J11351-056	-297.7	0.3	-950.2	1.0	Cortes	37.1	PMSU	20.3	-99.45	-30.0	Mon16
J11355+389	-709.0	0.8	-220.7	0.3	Gal15	-10.6	PMSU	-42.46	-41.2	-24.13	Mon16
J11376+587	-316.5	3.1	-275.6	3.1	PPMXL	-10.7	PMSU	-20.24	-45.25	-3.72	Mon16
J11404+770	-548.8	2.6	5.1	2.7	PPMXL			-48.8	-22.0		Lep13
J11417+427	-578.87	1.96	-89.22	1.31	HIP2	-9.49	Schf15	-21.81	-17.7	-15.84	Mon16
J11420+147	-271.5	0.3	227.5	0.6	Gal15	10.7	PMSU	-33.51	4.52	8.07	Mon16
J11421+267	896.07	2.89	-813.54	1.77	HIP2	9.4	Schf15	51.99	-19.11	19.43	Mon16
J11433+253	-224.3	0.9	-27.5	0.4	Gal15	-5.4	PMSU	-26.46	-16.57	-14.16	Mon16
J11451+183	-292.8	0.8	-289.5	0.5	Cortes						
J11467-140	714.66	3.02	-787.86	1.78	HIP2	20.29	Schf15	96.7	-30.48	-17.1	Mon16
J11470+700	-341.6	4.4	-45.4	4.4	PPMXL	11.5	PMSU	-28.26	-7.89	3.95	Mon16
J11474+667	-121.6	0.5	4.4	0.3	Cortes						
J11476+002	-316.2	4.5	-94.9	4.5	PPMXL	6.4	Schf15	-21.74	-22.45	-5.85	Mon16
J11476+786	743.61	1.87	481.4	1.51	HIP2	-111.8	Schf15	68.15	-54.66	-73.3	Mon16
J11477+008	605.26	2.32	-1219.28	1.97	HIP2	-30.86	Schf15	17.79	5.02	-32.87	Mon16

Table B.3: Proper motions and UVW space velocities of Carmencita stars (continued).

Karmn	$\mu_\alpha \cos\delta$ [mas a^{-1}]	$e\mu_\alpha \cos\delta$ [mas a^{-1}]	μ_δ [mas a^{-1}]	$e\mu_\delta$ [mas a^{-1}]	Ref.[a b]	V_r [km s^{-1}]	Ref.[c]	U [km s^{-1}]	V [km s^{-1}]	W [km s^{-1}]	Ref.[d]
J11483-112	-737.7	5.6	-39.9	5.6	PPMXL	49.2	PMSU	-58.12	-65.86	16.43	Mon16
J11485+076	133.8	4.8	-177.3	4.8	PPMXL	8.0	West15	24.42	-14.01	3.9	Mon16
J11496+220	-124.6	1.3	-41.0	1.3	PPMXL			-15.5	-15.8		Lep13
J11509+483	-1542.4	4.9	-960.6	4.9	PPMXL	-36.09	Schf15	-27.32	-66.18	-34.14	Mon16
J11511+352	-272.08	1.11	254.07	0.76	HIP2	-0.02	Schf15	-13.88	4.64	-3.86	Mon16
J11519+075	-126.1	5.6	110.4	5.6	PPMXL			-6.6	-11.3		Lep13
J11521+039	-320.0	5.5	46.2	5.5	PPMXL	30.53	Schf15	-15.88	-19.14	24.35	Mon16
J11529+244	-321.1	4.2	77.3	4.2	PPMXL	22.2	PMSU	-31.58	-9.44	15.66	Mon16
J11532-073	-173.75	3.88	-510.25	2.87	HIP2	26.667	Schf15	10.88	-54.94	-9.07	Mon16
J11533+430	186.2	0.7	-44.5	0.3	Cortes			23.3	4.7		Lep13
J11538+069	296.5	1.1	-894.8	0.8	Gal15	9.9	PMSU	46.4	-43.88	-7.52	Mon16
J11541+098	85.6	0.7	-805.2	0.6	Gal15	2.09	Schf15	25.26	-35.0	-10.36	Mon16
J11549-021	98.8	4.5	49.8	4.5	PPMXL	15.91	Schf15	8.83	1.68	19.31	Mon16
J11551+009	-740.98	2.74	33.79	1.23	HIP2	22.6	PMSU	-82.12	-47.99	1.55	Mon16
J11557-189	526.8	4.9	-313.7	4.9	PPMXL	22.3	PMSU	82.28	-8.35	0.6	Mon16
J11557-227	-373.8	5.2	-197.3	5.2	PPMXL	-13.1	RB09	-13.52	-3.02	-18.9	Mon16
J11575+118	-683.93	2.66	238.97	1.92	HIP2	-21.2	PMSU	-80.65	-4.53	-28.84	Mon16
J11582+425	126.5	4.7	-373.8	4.7	PPMXL	2.0	PMSU	22.47	-24.55	12.65	Mon16
J11585+595	-734.31	4.74	-8.37	2.41	HIP2			-121.9	-62.9		Lep13
J11589+426	-327.0	0.4	68.7	0.4	Gal15	11.4	PMSU	-43.61	-9.21	0.04	Mon16
J12006-138	-504.1	0.0	-26.0	0.5	Cortes	-16.6	Schf15	-36.14	-7.8	-21.17	Mon16
J12016-122	-51.5	3.0	-231.9	3.2	PPMXL	-39.7	Schf15	-1.13	10.81	-43.34	Mon16
J12023+285	-791.5	4.9	-34.2	4.9	PPMXL	10.0	New14	-66.42	-37.73	-4.48	Mon16
J12054+695	-461.2	4.7	-57.6	4.7	PPMXL	5.5	Schf15	-29.04	-14.38	1.01	Mon16
J12057+784	-200.9	0.3	14.9	0.9	Cortes			-18.9		-5.2	Lep13
J12063-132	71.5	5.4	-59.1	5.4	PPMXL	-8.1	RAVE	4.94	4.92	-7.89	Mon16
J12088+303	91.3	5.0	-26.1	5.0	PPMXL						
J12093+210	-102.1	4.5	-123.4	4.5	PPMXL						
J12100-150	-60.5	5.0	-705.0	5.0	PPMXL	80.37	Schf15	33.1	-79.69	29.26	Mon16
J12104-131	-102.1	4.5	-123.4	4.5	PPMXL						
J12109+410	7.95	1.16	231.79	1.49	HIP2	62.1	PMSU	-24.67	29.46	54.26	Mon16
J12111-199	-214.44	2.04	-183.72	1.35	HIP2	-15.5	PMSU	-10.49	-1.11	-20.33	Mon16
J12112-199	-214.44	2.04	-183.72	1.35	aHIP2	-8.97	Schf15	-8.82	-5.67	-15.97	Mon16

Table B.3: Proper motions and UVW space velocities of Carmencita stars (continued).

Karmn	$\mu_\alpha \cos\delta$ [mas a^{-1}]	$e\mu_\alpha \cos\delta$ [mas a^{-1}]	μ_δ [mas a^{-1}]	$e\mu_\delta$ [mas a^{-1}]	Ref.[a b]	V_r [km s^{-1}]	Ref.[c]	U [km s^{-1}]	V [km s^{-1}]	W [km s^{-1}]	Ref.[d]
J12121+488	199.2	4.9	-311.3	4.9	PPMXL	7.9	PMSU	36.53	-20.25	25.95	Mon16
J12122+714	-370.1	0.3	170.0	0.3	Cortes			-31.6	-3.9		Lep13
J12123+544N	231.48	1.3	89.86	1.26	aHIP2	-18.61	Schf15	18.63	7.17	-16.79	Mon16
J12123+544S	231.48	1.3	89.86	1.26	HIP2	-17.53	Schf15	18.26	7.53	-15.83	Mon16
J12124+121	-66.2	1.5	8.0	1.5	PPMXL						
J12124+396	162.97	2.24	-162.53	3.11	HIP2	13.4	PMSU	27.68	-7.9	21.41	Mon16
J12133+166	-504.66	4.62	-459.12	1.96	HIP2	-14.9	PMSU	-27.58	-80.1	-35.62	Mon16
J12142+006	-956.8	5.0	-278.4	5.0	PPMXL	-13.0	New14	-24.97	-16.58	-20.37	Mon16
J12144+245	8.4	2.3	-367.7	2.4	PPMXL	-23.9	PMSU	24.72	-35.33	-25.65	Mon16
J12151+487	-243.43	1.52	-33.18	1.44	HIP2	0.3	PMSU	-23.43	-16.9	-2.34	Mon16
J12154+391	-344.8	2.2	47.8	0.9	Cortes	8.3	PMSU	-42.53	-14.67	0.73	Mon16
J12156+526	102.9	0.5	-1.2	0.4	Gal15	-14.2	Schf15	9.58	-1.71	-11.88	Mon16
J12162+508	-73.8	4.9	34.0	4.9	PPMXL						
J12168+029	-647.0	5.1	272.2	5.1	PPMXL	9.7	PMSU	-73.79	-14.95	11.44	Mon16
J12168+248	-5.1	4.5	50.0	4.5	PPMXL			-2.8	8.2		Lep13
J12169+311	-124.0	5.0	-42.0	5.0	PPMXL	-28.6	PMSU	-6.84	-12.0	-30.03	Mon16
J12189+111	-1278.5	0.8	201.9	0.5	Gal15	6.2	Schf15	-36.68	-15.72	2.71	Mon16
J12191+318	-313.9	0.7	9.2	0.5	Gal15			-17.4	-8.3		Lep13
J12194+283	-650.54	2.38	76.75	1.36	HIP2	7.0	PMSU	-73.07	-30.21	-2.92	Mon16
J12198+527	-169.94	1.9	-121.5	1.79	HIP2	-4.9	UH96	-11.61	-25.61	-0.29	Mon16
J12199+364	138.41	3.83	-138.92	3.56	HIP2	-15.01	Wh07	25.62	-7.59	-10.55	Mon16
J12204+005	86.0	1.8	-14.3	1.9	PPMXL	-1.5	PMSU	5.82	2.97	-1.04	Mon16
J12214+306E	-193.6	0.2	-242.3	0.3	Gal15						
J12214+306W	-199.6	0.5	-270.6	0.1	Gal15	4.4	Mo02	-4.16	-29.13	3.7	Mon16
J12217+682	-378.6	4.6	210.8	4.6	PPMXL	4.9	Mo02	-38.0	-1.01	-12.94	Mon16
J12223+251	-692.78	2.72	-200.19	1.75	HIP2	29.2	PMSU	-73.06	-75.39	16.87	Mon16
J12225+123	-143.66	2.11	-30.52	1.53	HIP2	1.0	Eva79	-16.49	-14.65	-1.4	Mon16
J12228-040	-252.3	0.4	-67.9	0.3	Cortes						
J12230+640	-668.12	2.0	372.37	2.14	HIP2	8.9	Schf15	-64.34	-0.74	-18.49	Mon16
J12235+279	-138.51	2.87	118.54	2.09	HIP2			-29.1	5.9		Lep13
J12235+671	235.19	3.25	-122.94	4.08	HIP2	7.1	PMSU	12.05	5.49	11.76	Mon16
J12238+125	39.77	2.08	-167.25	1.43	HIP2	1.9	PMSU	11.88	-12.31	-1.96	Mon16
J12248-182	1095.66	2.14	-2308.56	1.38	HIP2	51.08	Schf15	94.14	-65.74	-28.06	Mon16

Table B.3: Proper motions and UVW space velocities of Carmencita stars (continued).

Karmn	$\mu_\alpha \cos\delta$ [mas a^{-1}]	$e\mu_\alpha \cos\delta$ [mas a^{-1}]	μ_δ [mas a^{-1}]	$e\mu_\delta$ [mas a^{-1}]	Ref.[a b]	V_r [km s^{-1}]	Ref.[c]	U [km s^{-1}]	V [km s^{-1}]	W [km s^{-1}]	Ref.[d]
J12269+270	93.52	1.35	-249.31	0.71	aHIP2	-2.13	Des13	23.77	-19.26	-1.22	Mon16
J12274+374	-230.02	3.91	106.27	3.64	HIP2	-16.81	Wh07	-27.13	-4.67	-21.29	Mon16
J12277-032	-299.6	5.0	-41.1	5.0	PPMXL	3.44	Schf15	-17.2	-15.11	-0.67	Mon16
J12288-106N	-282.3	0.2	4.3	0.2	Cortes	34.4	PMSU	-9.11	-29.54	25.44	Mon16
J12288-106S	-282.3	0.2	4.3	0.2	aCortes	34.4	PMSU	-9.34	-29.67	25.42	Mon16
J12289+084	-632.02	4.28	-257.34	2.2	HIP2	-10.0	PMSU	-26.82	-29.64	-18.05	Mon16
J12290+417	-195.9	5.6	-217.1	5.6	PPMXL	-3.8	PMSU	-4.23	-21.94	-0.87	Mon16
J12292+535	-1221.3	4.7	100.1	4.7	PPMXL	-66.4	PMSU	-110.58	-86.61	-77.07	Mon16
J12294+229	-169.8	5.0	-16.6	5.0	PPMXL	-25.9	PMSU	-14.9	-8.74	-27.54	Mon16
J12299-054E	-610.5	0.9	-308.8	0.3	Gal15	-10.0	PMSU	-39.66	-46.8	-29.8	Mon16
J12299-054W	-575.8	0.4	-313.8	0.2	Cortes	-10.0	PMSU	-36.82	-45.9	-29.99	Mon16
J12312+086	-635.05	1.49	-522.1	0.82	HIP2	18.89	Schf15	-16.36	-53.84	4.03	Mon16
J12323+315	-420.7	0.2	228.8	0.7	Gal15	9.1	PMSU	-67.29	-2.23	2.27	Mon16
J12324+203	38.4	0.6	23.2	0.6	Cortes	-8.3	PMSU	2.57	5.94	-7.54	Mon16
J12327+682	-101.0	1.9	-181.5	1.8	PPMXL			-3.6	-27.2		Lep13
J12332+090	-1756.9	5.1	211.8	5.1	PPMXL	1.0	New14	-33.51	-15.5	-0.26	Mon16
J12349+322	28.0	4.6	78.2	4.6	PPMXL						
J12350+098	-448.12	3.04	-319.37	1.87	HIP2	33.58	Schf15	-15.72	-52.03	21.26	Mon16
J12363-043	-489.4	5.2	-132.3	5.2	PPMXL	27.1	PMSU	-37.17	-55.17	11.15	Mon16
J12364+352	-351.6	4.6	-117.4	4.6	PPMXL	13.0	New14	-14.47	-13.93	12.63	Mon16
J12368-019	-161.2	5.0	72.3	5.0	PPMXL						
J12373-208	-43.1	0.2	-428.6	0.7	Cortes	9.266	Schf15	11.91	-23.56	-15.55	Mon16
J12387-043	-756.6	5.2	-194.9	5.2	PPMXL	12.6	PMSU	-48.69	-55.74	-2.23	Mon16
J12388+116	-1157.37	3.06	-247.06	1.68	HIP2	-4.28	Schf15	-59.03	-53.9	-12.47	Mon16
J12390+470	389.71	4.02	-121.33	3.1	HIP2	-12.5	PMSU	42.98	7.54	-5.55	Mon16
J12397+255	-179.9	4.9	-152.2	4.9	PPMXL	0.3	West15	-9.51	-29.06	-1.33	Mon16
J12416+482	216.0	0.4	-155.0	0.7	Gal15	-16.0	PMSU	36.28	-5.89	-6.79	Mon16
J12417+567	114.5	4.8	2.4	4.8	PPMXL	-8.7	Shk12	12.53	2.98	-7.24	Mon16
J12428+418	-550.0	0.3	39.6	0.5	Cortes	-4.4	Schf15	-23.73	-13.85	-5.68	Mon16
J12436+251	-378.4	0.3	-42.6	0.2	Gal15	3.4	PMSU	-32.8	-26.19	1.96	Mon16
J12440-111	-483.7	5.8	-155.3	5.8	PPMXL						
J12470+466	-761.21	1.72	-297.39	1.66	HIP2	22.3	PMSU	-53.19	-57.88	29.55	Mon16
J12471-035	-509.4	0.4	-12.0	0.3	Cortes	-18.3	Schf15	-42.8	-17.23	-17.04	Mon16

Table B.3: Proper motions and UVW space velocities of Carmencita stars (continued).

Karmn	$\mu_\alpha \cos\delta$ [mas a^{-1}]	$e\mu_\alpha \cos\delta$ [mas a^{-1}]	μ_δ [mas a^{-1}]	$e\mu_\delta$ [mas a^{-1}]	Ref.[a b]	V_r [km s^{-1}]	Ref.[c]	U [km s^{-1}]	V [km s^{-1}]	W [km s^{-1}]	Ref.[d]
J12479+097	-1006.76	2.63	-460.19	1.79	HIP2	19.5	Schf15	-21.41	-41.31	12.59	Mon16
J12481+472	195.5	4.8	-553.9	4.8	PPMXL	-3.5	PMSU	49.58	-37.94	18.01	Mon16
J12485+495	110.9	4.9	-16.4	4.9	PPMXL	-6.43	Schf15	8.69	1.35	-5.4	Mon16
J12490+661	-434.99	1.73	-105.61	1.73	HIP2	22.4	PMSU	-23.33	-2.93	20.43	Mon16
J12495+094	-437.4	0.7	34.6	0.5	Gal15	10.5	PMSU	-44.44	-27.65	10.88	Mon16
J12505+269	-185.6	4.4	-172.6	4.4	PPMXL	32.9	PMSU	-8.07	-31.83	32.74	Mon16
J12508-213	440.9	4.0	-334.9	4.0	PPMXL						
J12513+221	-177.9	5.1	54.7	5.1	PPMXL	25.0	PMSU	-17.73	-7.23	25.41	Mon16
J12576+352E	-264.16	2.95	-176.16	2.26	HIP2	-7.8	PMSU	-10.75	-27.6	-4.87	Mon16
J12576+352W	-264.16	2.95	-176.16	2.26	aHIP2	-11.0	Schf15	-10.57	-28.02	-8.04	Mon16
J12583+405	224.06	4.14	-135.89	4.02	HIP2			53.8	1.4		Lep13
J12594+077	-680.4	4.3	2.0	4.3	PPMXL	5.5	PMSU	-54.38	-38.44	7.31	Mon16
J13000-056	-345.6	0.4	43.1	0.4	Gal15	-4.71	Schf15	-27.52	-11.72	-1.0	Mon16
J13005+056	-942.2	4.3	225.4	4.3	PPMXL	-26.3	Schf15	-41.55	-6.38	-19.88	Mon16
J13007+123	-616.31	1.51	-13.59	1.0	HIP2	-43.4	PMSU	-35.34	-11.37	-40.89	Mon16
J13019+335	-462.2	3.2	-163.0	3.1	PPMXL			-45.0	-61.0		Lep13
J13027+415	-542.1	4.5	-185.4	4.5	PPMXL						
J13047+559	-165.74	2.0	32.92	1.92	HIP2			-23.9	-11.1		Lep13
J13054+371	-303.75	4.95	-205.8	2.89	HIP2	18.1	PMSU	-16.59	-36.42	23.9	Mon16
J13068+308	173.8	5.0	-475.0	5.0	PPMXL	1.0	New14	35.72	-24.93	2.72	Mon16
J13084+169	-102.48	3.02	-39.55	2.16	HIP2	-52.6	PMSU	-15.57	-5.16	-51.68	Mon16
J13088+163	-517.3	4.4	-169.1	4.4	PPMXL	-0.8	PMSU	-43.6	-56.95	-0.36	Mon16
J13089+490	-102.5	2.3	60.3	2.4	PPMXL	20.4	PMSU	-16.29	5.47	17.17	Mon16
J13095+289	-348.6	5.0	-197.8	5.0	PPMXL	-3.0	New14	-10.26	-21.6	-1.17	Mon16
J13102+477	-634.1	5.2	-612.4	5.2	PPMXL	-10.0	New14	-9.42	-54.42	6.84	Mon16
J13113+285	-410.9	5.0	-448.0	5.0	PPMXL	-11.8	PMSU	-8.35	-62.36	-7.45	Mon16
J13118+253	-463.3	0.2	-174.2	0.8	Cortes	-32.2	PMSU	-29.73	-40.56	-29.05	Mon16
J13130+201	-620.0	4.3	144.1	4.3	PPMXL	-39.9	PMSU	-51.32	-16.75	-34.01	Mon16
J13140+038	-734.0	0.0	11.0	0.0	PPMXL	-2.1	PMSU	-56.43	-38.11	4.47	Mon16
J13142+792	-245.3	2.6	-158.6	2.6	PPMXL			-18.9		21.7	Lep13
J13143+133	-247.4	1.2	-185.2	1.1	Gal15	-16.5	West15	-11.17	-20.27	-17.69	Mon16
J13165+278	-745.6	5.1	227.9	5.1	PPMXL	-2.0	New14	-54.52	-18.58	3.2	Mon16
J13167-123	-289.2	5.4	-52.1	5.4	PPMXL						

Table B.3: Proper motions and UVW space velocities of Carmencita stars (continued).

Karmn	$\mu_\alpha \cos\delta$ [mas a^{-1}]	$e\mu_\alpha \cos\delta$ [mas a^{-1}]	μ_δ [mas a^{-1}]	$e\mu_\delta$ [mas a^{-1}]	Ref.[a b]	V_r [km s^{-1}]	Ref.[c]	U [km s^{-1}]	V [km s^{-1}]	W [km s^{-1}]	Ref.[d]
J13168+170	620.7	1.4	-257.8	1.3	aPPMXL	-11.9	PMSU	31.8	9.11	-17.27	Mon16
J13168+231	266.3	0.8	-95.8	0.4	Cortes	-20.2	PMSU	29.06	9.02	-23.91	Mon16
J13179+362	-71.98	1.74	-336.95	1.7	HIP2	38.9	PMSU	14.12	-24.25	44.34	Mon16
J13180+022	-367.1	0.7	-60.5	0.5	Gal15	4.8	Schf15	-24.99	-27.43	5.56	Mon16
J13182+733	73.9	0.3	-110.3	0.6	Cortes						
J13195+351E	387.77	1.49	-777.74	1.18	aHIP2	12.0	PMSU	48.84	-22.33	15.76	Mon16
J13195+351W	387.77	1.49	-777.74	1.18	HIP2	-16.89	Schf15	48.64	-27.34	-12.69	Mon16
J13196+333	-298.54	1.41	-143.74	1.03	HIP2	-12.05	Schf15	-12.7	-25.12	-8.07	Mon16
J13197+477	152.9	1.5	-17.4	1.4	PPMXL	15.5	PMSU	4.83	9.22	13.89	Mon16
J13209+342	486.24	1.81	-295.92	1.33	HIP2	-35.7	Schf15	42.37	-1.95	-36.73	Mon16
J13215+035	75.9	4.7	171.7	4.7	PPMXL			-1.6	34.0		Lep13
J13215+037	-518.5	4.7	-45.8	4.7	PPMXL	2.7	PMSU	-52.56	-47.19	8.24	Mon16
J13229+244	-633.3	0.6	-868.6	0.6	Gal15	-19.58	Schf15	-2.03	-70.41	-17.21	Mon16
J13235+292	-471.17	0.99	248.0	0.81	HIP2	-39.13	BE12	-49.88	-11.11	-34.3	Mon16
J13239+694	50.7	1.8	-170.9	1.8	PPMXL			21.9	-10.7		Lep13
J13247-050	77.3	5.4	-304.7	5.4	PPMXL						
J13251-114	-111.0	2.5	222.7	2.4	PPMXL						
J13254+377	-200.62	2.08	63.8	1.75	HIP2			-30.2	-10.6		Lep13
J13260+275	-3.3	4.4	69.0	4.4	PPMXL						
J13282+300	-186.01	1.71	-185.07	1.18	HIP2			-8.1	-62.2		Lep13
J13283-023E	152.8	3.09	-486.54	1.98	aHIP2	-41.13	Schf15	6.52	-4.31	-52.52	Mon16
J13283-023W	152.8	3.09	-486.54	1.98	HIP2	-39.61	Schf15	7.12	-4.79	-51.21	Mon16
J13293+114	324.4	0.4	-1193.6	0.2	Gal15	27.93	Schf15	76.53	-60.1	-1.57	Mon16
J13294-143	103.5	5.4	-41.0	5.4	PPMXL	-1.8	Shk12	7.42	3.86	-4.95	Mon16
J13299+102	1128.32	0.89	-1073.47	0.52	HIP2	14.29	Schf15	57.55	-8.16	-3.9	Mon16
J13300-087	-1106.3	4.1	-475.97	2.52	aHIP2	-46.9	PMSU	-76.51	-63.48	-46.73	Mon16
J13305+191	-506.3	4.2	-1289.1	4.2	PPMXL	-60.9	PMSU	11.85	-90.25	-66.97	Mon16
J13317+292	-235.4	1.7	-137.8	1.7	PPMXL	-7.0	New14	-9.26	-22.24	-3.42	Mon16
J13318+233	-276.2	2.1	48.7	2.1	PPMXL	4.0	PMSU	-26.9	-14.18	9.17	Mon16
J13319+311	-131.97	2.92	15.9	1.72	HIP2	-13.1	PMSU	-18.27	-12.08	-9.93	Mon16
J13326+309	-199.1	4.3	-81.2	4.3	PPMXL	-10.0	New14	-11.13	-19.31	-6.3	Mon16
J13327+168	283.3	2.7	-236.8	2.7	PPMXL	-5.1	PMSU	20.51	-0.8	-10.32	Mon16
J13335+704	-139.9	4.7	29.7	4.7	PPMXL						

Table B.3: Proper motions and UVW space velocities of Carmencita stars (continued).

Karmn	$\mu_\alpha \cos\delta$ [mas a^{-1}]	$e\mu_\alpha \cos\delta$ [mas a^{-1}]	μ_δ [mas a^{-1}]	$e\mu_\delta$ [mas a^{-1}]	Ref.[a b]	V_r [km s^{-1}]	Ref.[c]	U [km s^{-1}]	V [km s^{-1}]	W [km s^{-1}]	Ref.[d]
J13343+046	154.03	1.28	-123.98	1.06	HIP2	14.49	Schf15	23.77	-3.27	5.78	Mon16
J13348+201	51.7	4.9	-185.7	4.9	PPMXL	27.3	PMSU	22.75	-13.16	23.06	Mon16
J13348+745	-436.1	1.1	-19.2	1.09	aHIP2	21.1	PMSU	-44.4	-16.91	23.92	Mon16
J13358+146	-22.7	0.8	-275.2	0.5	Cortes			14.2	-22.7		Lep13
J13369+229	103.9	4.3	-169.8	4.3	PPMXL	-10.1	PMSU	19.29	-8.7	-13.58	Mon16
J13376+481	-239.17	1.72	-137.17	1.81	aHIP2	-8.4	PMSU	-8.62	-26.06	0.79	Mon16
J13378+481	-239.17	1.52	-137.17	1.81	HIP2	-26.7	PMSU	-8.04	-35.45	-15.14	Mon16
J13386+258	-589.5	0.7	58.0	0.4	Gal15	-31.35	Schf15	-48.53	-30.62	-21.15	Mon16
J13386-115	144.1	5.5	-88.7	5.5	PPMXL						
J13388-022	-302.9	0.2	-78.0	0.7	Cortes	-31.6	PMSU	-35.65	-17.77	-25.02	Mon16
J13394+461	-41.9	1.21	390.07	1.43	HIP2	-36.1	PMSU	-15.1	2.47	-40.68	Mon16
J13401+437	-1078.2	4.3	299.5	4.3	PPMXL	-28.7	Schf15	-79.81	-44.66	-17.52	Mon16
J13413-091	-46.5	6.3	56.2	6.3	PPMXL	-6.8	Ter15	-11.77	4.05	0.67	Mon16
J13414+489	108.1	5.0	-166.4	5.0	PPMXL			17.1	-3.6		Lep13
J13415+148	-274.7	4.9	42.8	4.9	PPMXL	-23.8	PMSU	-44.01	-20.02	-12.89	Mon16
J13417+582	72.4	4.5	-60.9	4.5	PPMXL	-10.6	Schf15	8.82	-4.77	-7.75	Mon16
J13421-160	-503.6	5.2	-20.9	5.2	PPMXL	-50.1	PMSU	-52.81	0.66	-29.8	Mon16
J13427+332	-110.07	2.57	-709.17	1.96	HIP2	4.0	New14	16.65	-26.04	7.84	Mon16
J13430+090	-339.7	0.1	-112.1	0.4	Gal15	-35.2	PMSU	-32.78	-26.14	-29.33	Mon16
J13434+111	73.1	0.9	-128.8	0.9	PPMXL			19.1	-8.2		Lep13
J13444+516	-758.5	5.1	-3.6	5.1	PPMXL	17.0	PMSU	-68.03	-46.82	33.21	Mon16
J13445+249	-243.5	1.5	-90.5	1.5	PPMXL			-19.3	-34.7		Lep13
J13450+176	450.69	0.95	-1831.32	0.65	HIP2	18.9	BE12	97.21	-75.03	-7.83	Mon16
J13455+609	-39.09	1.21	51.3	1.23	HIP2			-8.8	0.7		Lep13
J13457+148	1778.45	0.86	-1456.44	0.78	HIP2	15.51	Schf15	60.66	-1.79	-2.83	Mon16
J13458-179	-314.67	5.01	-554.44	4.37	HIP2	4.82	Schf15	-0.08	-28.67	-12.31	Mon16
J13477+214	75.29	2.22	-83.13	1.83	HIP2			14.3	-2.4		Lep13
J13481-137	-691.4	0.4	-511.6	0.5	Cortes						
J13482+236	-1479.1	4.3	118.3	4.3	PPMXL	-75.3	PMSU	-84.29	-53.52	-54.28	Mon16
J13485+563	-356.7	3.3	70.8	3.3	PPMXL			-40.7	-23.5		Lep13
J13488+041	-3.8	4.3	-182.5	4.3	PPMXL	-3.4	PMSU	4.9	-9.17	-7.94	Mon16
J13490+026	150.6	1.9	-315.6	1.9	PPMXL	7.1	PMSU	27.31	-14.38	-8.33	Mon16
J13503-216	-32.9	0.4	-379.1	0.3	Cortes						

Table B.3: Proper motions and UVW space velocities of Carmencita stars (continued).

Karmn	$\mu_\alpha \cos\delta$ [mas a^{-1}]	$e\mu_\alpha \cos\delta$ [mas a^{-1}]	μ_δ [mas a^{-1}]	$e\mu_\delta$ [mas a^{-1}]	Ref.[a b]	V_r [km s^{-1}]	Ref.[c]	U [km s^{-1}]	V [km s^{-1}]	W [km s^{-1}]	Ref.[d]
J13507-216	-32.3	0.4	-378.9	0.3	Cortes	12.2	PMSU	15.08	-29.53	-17.99	Mon16
J13508+367	-462.3	0.8	102.3	0.2	Gal15	-2.0	New14	-31.1	-16.47	4.83	Mon16
J13518+127	98.1	1.4	-12.8	1.1	PPMXL			10.2	7.1		Lep13
J13526+144	54.3	0.3	-289.4	1.3	Cortes	2.69	Schf15	18.73	-16.44	-4.17	Mon16
J13528+656	-553.67	2.1	-158.52	2.3	HIP2	-29.7	PMSU	-32.36	-71.73	5.64	Mon16
J13528+668	-472.2	4.9	-562.2	4.9	PPMXL	-6.4	PMSU	1.3	-42.67	25.71	Mon16
J13529+536	77.4	2.2	-206.8	2.2	PPMXL			28.9	-11.3		Lep13
J13534+129	-152.71	1.63	-646.34	1.11	HIP2	-19.9	PMSU	18.84	-58.44	-31.25	Mon16
J13536+776	-222.6	4.6	-17.2	4.6	PPMXL	-7.5	Schf15	-6.05	-13.41	-0.97	Mon16
J13537+521	5.8	0.4	-134.4	0.6	Cortes						
J13537+788	-254.48	1.29	116.34	1.35	HIP2	-19.0	PMSU	-21.61	-26.53	-14.71	Mon16
J13582+125	-326.8	4.9	712.5	4.9	PPMXL	-10.46	Schf15	-38.67	19.01	4.66	Mon16
J13582-120	-335.9	4.9	41.2	4.9	PPMXL						
J13583-132	-346.5	0.9	-61.0	0.1	Cortes						
J13587-000	-368.4	5.1	-404.3	5.1	PPMXL	-32.2	PMSU	-25.12	-62.65	-39.09	Mon16
J13591-198	-559.1	0.5	-185.2	0.4	Gal15	-34.6	PMSU	-39.46	-8.47	-21.75	Mon16
J14010-026	-823.47	1.4	598.19	1.2	HIP2	-25.99	Schf15	-54.8	2.32	3.0	Mon16
J14019+154	96.94	3.6	-18.26	2.45	HIP2	-25.5	PMSU	1.91	6.05	-27.89	Mon16
J14019+432	-72.7	4.9	-38.6	4.9	PPMXL						
J14023+136	96.42	1.7	-139.94	1.22	HIP2	-2.6	PMSU	13.35	-4.38	-8.07	Mon16
J14024-210	490.3	5.0	-386.8	5.0	PPMXL	75.7	PMSU	89.46	-28.1	10.11	Mon16
J14025+463N	581.8	0.4	-45.8	1.0	Cortes	-24.6	PMSU	24.49	8.23	-30.25	Mon16
J14025+463S	575.4	0.5	-47.3	0.8	Cortes	-24.6	PMSU	24.3	7.96	-30.13	Mon16
J14039+242	-57.1	4.3	151.4	4.3	PPMXL			-17.9	10.1		Lep13
J14041+207	-127.64	1.78	-16.97	1.41	aHIP2			-9.4	-13.1		Lep13
J14062+693	-83.6	4.8	-181.1	4.8	PPMXL	-24.56	Schf15	11.7	-27.19	-5.73	Mon16
J14082+805	212.41	1.11	-542.85	1.43	HIP2	7.0	Schf15	34.71	2.68	31.99	Mon16
J14083+758	-401.7	2.5	367.9	2.6	PPMXL	-27.3	PMSU	-50.94	-33.27	-34.32	Mon16
J14121-005	-721.6	5.2	241.9	5.2	PPMXL	-46.9	PMSU	-98.2	-25.03	0.46	Mon16
J14130-120	-619.7	5.6	-381.3	5.6	PPMXL	51.7	PMSU	15.11	-54.03	34.79	Mon16
J14142-153	-207.86	7.24	-172.84	4.49	aHIP2	-21.6	PMSU	-26.45	-28.17	-21.7	Mon16
J14144+234	-183.9	4.3	-456.6	4.3	PPMXL	-40.2	PMSU	6.27	-54.63	-36.06	Mon16
J14152+450	-686.7	0.6	-224.9	0.5	Gal15	14.51	Schf15	-23.91	-39.39	34.71	Mon16

Table B.3: Proper motions and UVW space velocities of Carmencita stars (continued).

Karmn	$\mu_\alpha \cos\delta$ [mas a^{-1}]	$e\mu_\alpha \cos\delta$ [mas a^{-1}]	μ_δ [mas a^{-1}]	$e\mu_\delta$ [mas a^{-1}]	Ref.[a b]	V_r [km s^{-1}]	Ref.[c]	U [km s^{-1}]	V [km s^{-1}]	W [km s^{-1}]	Ref.[d]
J14153+153	135.5	1.1	-128.9	1.3	PPMXL			22.3	-0.7		Lep13
J14155+046	-750.7	0.3	-772.4	0.1	Gal15	0.0	New14	-7.61	-70.46	-3.9	Mon16
J14157+594	-184.1	4.9	-80.1	4.9	PPMXL			-10.2	-24.9		Lep13
J14159+362	9.6	4.6	298.3	4.6	PPMXL			-21.1	23.4		Lep13
J14161+233	-100.8	2.1	-172.1	2.1	PPMXL			6.2	-30.3		Lep13
J14170+105	-281.5	2.1	-105.6	2.1	PPMXL	6.7	PMSU	-11.08	-27.61	12.33	Mon16
J14170+317	-582.7	4.6	-147.4	4.6	PPMXL	-24.2	PMSU	-28.68	-44.43	-7.32	Mon16
J14171+088	-139.4	4.8	17.9	4.8	PPMXL						
J14173+454	43.3	0.3	-21.1	0.6	Cortes	3.96	Schf15	4.2	2.98	2.83	Mon16
J14174+454	42.7	0.3	-19.7	0.3	Cortes	3.37	Schf15	4.05	2.78	2.28	Mon16
J14175+025	-31.9	4.9	-63.1	4.9	PPMXL						
J14177+214	-71.59	3.19	-172.62	2.36	HIP2			12.1	-31.8		Lep13
J14179-005	-279.0	5.0	-271.6	5.0	PPMXL	23.5	PMSU	5.4	-49.36	15.26	Mon16
J14189+386	-701.36	1.86	-235.44	2.02	HIP2			-54.7	-107.1		Lep13
J14191-073	-1120.4	5.4	-749.3	5.1	PPMXL	75.6	PMSU	3.25	-134.39	53.4	Mon16
J14194+029	-199.6	5.2	-146.5	5.2	PPMXL	0.0	New14	-8.4	-32.49	0.81	Mon16
J14200+390	-26.8	0.3	64.7	0.6	Gal15	3.5	PMSU	-5.8	3.76	3.08	Mon16
J14201-096	-621.4	5.6	-842.9	5.6	PPMXL	42.5	PMSU	21.14	-63.73	16.39	Mon16
J14210+275	-283.8	4.5	93.2	4.5	PPMXL	-2.7	PMSU	-29.71	-13.67	8.56	Mon16
J14212-011	176.3	5.0	-614.2	5.0	PPMXL	-11.3	PMSU	19.76	-19.95	-31.41	Mon16
J14215-079	-97.0	0.5	-87.5	0.6	Cortes						
J14219+376	366.1	4.3	-302.2	4.3	PPMXL			72.7	6.3		Lep13
J14227+164	-188.9	4.9	39.3	4.9	PPMXL	-20.9	West15	-25.73	-12.23	-10.73	Mon16
J14231-222	-273.1	5.2	-464.4	5.2	PPMXL	-37.7	PMSU	-36.05	-46.38	-54.21	Mon16
J14249+088	546.54	4.84	158.13	4.59	HIP2	-5.0	New14	16.45	32.34	-13.99	Mon16
J14251+518	-235.4	0.14	-399.07	0.13	aHIP2	-10.1	Schf15	9.8	-31.25	6.92	Mon16
J14255-118	-296.5	5.7	-5.8	5.7	PPMXL						
J14257+236E	792.44	1.4	-1113.72	1.05	aHIP2	8.3	Schf15	101.62	-22.22	-22.02	Mon16
J14257+236W	792.44	1.4	-1113.72	1.05	HIP2	9.26	Schf15	101.93	-22.06	-21.12	Mon16
J14259+142	-46.5	0.3	-23.4	0.3	Cortes			-3.7	-8.9		Lep13
J14269+241	-161.9	2.6	-1.6	2.6	PPMXL			-17.4	-17.2		Lep13
J14279-003N	-364.6	1.8	58.3	2.0	Cortes	41.3	PMSU	6.08	-18.08	43.78	Mon16
J14279-003S	-362.8	1.5	30.9	2.2	Cortes	17.5	PMSU	-6.24	-15.88	23.45	Mon16

Table B.3: Proper motions and UVW space velocities of Carmencita stars (continued).

Karmn	$\mu_\alpha \cos\delta$ [mas a^{-1}]	$e\mu_\alpha \cos\delta$ [mas a^{-1}]	μ_δ [mas a^{-1}]	$e\mu_\delta$ [mas a^{-1}]	Ref.[a b]	V_r [km s^{-1}]	Ref.[c]	U [km s^{-1}]	V [km s^{-1}]	W [km s^{-1}]	Ref.[d]
J14280+139	-360.2	3.7	-491.1	3.7	PPMXL	-29.7	West15	-9.6	-36.4	-26.1	Mon16
J14282+053	-353.2	5.2	-66.9	5.2	aPPMXL			-18.3	-24.5		Lep13
J14283+053	-353.2	5.2	-66.9	5.2	PPMXL	-10.69	Schf15	-23.01	-24.05	0.0	Mon16
J14294+155	-1053.12	1.9	1299.5	1.54	HIP2	7.32	Schf15	-96.54	19.83	51.6	Mon16
J14299+295	-232.0	4.6	-471.1	4.6	PPMXL	-7.0	PMSU	21.24	-64.5	4.76	Mon16
J14306+597	-803.8	4.8	161.9	4.8	PPMXL	-7.0	New14	-28.65	-24.48	4.6	Mon16
J14307-086	-1269.36	1.69	-241.31	1.05	HIP2	-24.2	BE12	-75.19	-75.32	9.44	Mon16
J14310-122	-404.4	4.54	-398.21	2.81	HIP2	-1.78	Schf15	-7.66	-27.42	-6.06	Mon16
J14312+754	-201.2	4.7	-33.5	4.7	PPMXL	5.9	West15	-9.41	-5.65	10.53	Mon16
J14320+738	-188.8	2.0	-115.1	2.0	PPMXL	-11.38	Schf15	-0.52	-22.31	5.67	Mon16
J14321+081	-481.2	2.0	9.1	0.4	Cortes	-18.0	New14	-23.07	-13.31	-7.44	Mon16
J14321+160	177.8	6.5	-118.3	6.5	PPMXL	-1.0	New14	14.46	2.07	-8.17	Mon16
J14322+496	-583.2	4.8	-109.3	4.8	PPMXL	-25.6	PMSU	-24.55	-48.9	-1.38	Mon16
J14331+610	194.5	2.2	-44.2	2.2	PPMXL	-21.39	Schf15	15.72	-4.28	-21.08	Mon16
J14342-125	-354.45	3.29	595.35	2.52	HIP2	-1.44	Schf15	-13.48	5.78	13.53	Mon16
J14366+143	59.2	1.2	23.8	1.2	PPMXL			1.1	11.1		Lep13
J14368+583	613.1	4.7	-698.8	4.7	PPMXL	-42.3	PMSU	74.8	-19.41	-29.17	Mon16
J14371+756	164.7	0.4	-149.5	0.4	Cortes			27.1		2.4	Lep13
J14376+677	-217.3	5.1	177.7	5.1	PPMXL			-37.0	-8.1		Lep13
J14388+422	-134.8	4.3	-22.9	4.3	PPMXL			-9.6	-14.0		Lep13
J14415+064	-278.21	3.37	-339.78	3.76	HIP2			1.9	-57.6		Lep13
J14423+660	-301.43	1.32	-36.08	1.58	HIP2	30.1	PMSU	-14.1	8.69	29.5	Mon16
J14438+667	-225.1	5.1	109.9	5.1	PPMXL			-36.1	-15.4		Lep13
J14469+170	-541.76	3.67	-88.83	3.31	HIP2			-40.2	-61.6		Lep13
J14472+570	75.9	4.7	-32.6	4.7	PPMXL	-5.899	Schf15	7.93	0.18	-6.79	Mon16
J14485+101	-341.1	4.9	-117.8	4.9	PPMXL						
J14501+323	11.7	5.3	-182.6	5.3	PPMXL						
J14511+311	-343.5	0.4	-181.6	0.6	Gal15			-5.6	-26.3		Lep13
J14524+123	-61.5	0.5	-229.3	0.5	Cortes	5.241	Schf15	11.29	-17.04	1.39	Mon16
J14525+001	91.5	5.3	-321.0	5.3	PPMXL	52.6	PMSU	61.82	-26.98	15.36	Mon16
J14538+235	-677.89	6.54	107.1	5.41	HIP2	-15.7	PMSU	-29.35	-22.0	1.55	Mon16
J14544+161	276.0	1.89	-121.69	1.52	HIP2	-9.0	New14	6.68	2.85	-14.72	Mon16
J14544+355	146.1	5.2	-846.7	5.2	PPMXL	-40.02	Schf15	55.62	-54.98	-35.88	Mon16

Table B.3: Proper motions and UVW space velocities of Carmencita stars (continued).

Karmn	$\mu_\alpha \cos\delta$ [mas a^{-1}]	$e\mu_\alpha \cos\delta$ [mas a^{-1}]	μ_δ [mas a^{-1}]	$e\mu_\delta$ [mas a^{-1}]	Ref.[a b]	V_r [km s^{-1}]	Ref.[c]	U [km s^{-1}]	V [km s^{-1}]	W [km s^{-1}]	Ref.[d]
J14548+099	-313.83	2.11	-399.67	2.56	HIP2	13.9	PMSU	13.3	-57.65	13.47	Mon16
J14549+411	-238.7	4.9	133.5	4.9	PPMXL	-1.5	PMSU	-93.13	-30.34	31.71	Mon16
J14557+072	-171.36	3.4	-246.22	2.79	HIP2			5.9	-49.2		Lep13
J14564+168	47.7	4.9	-316.3	5.2	PPMXL	22.56	Ter15	45.74	-25.76	5.89	Mon16
J14574-214	1037.06	1.05	-1725.87	0.72	aHIP2	33.2	PMSU	52.96	-23.8	-28.95	Mon16
J14575+313	-692.59	4.68	-1156.56	5.93	HIP2	8.1	BE12	87.78	-222.07	67.75	Mon16
J14578+566	278.4	4.8	-647.3	4.8	PPMXL	5.0	New14	32.01	-1.83	9.51	Mon16
J15009+454	240.63	1.15	370.16	1.15	HIP2	-18.6	PMSU	-11.17	10.77	-26.72	Mon16
J15011+071	-497.5	0.8	-92.1	0.4	Gal15	-19.13	Schf15	-28.26	-29.94	-0.61	Mon16
J15011+354	150.2	5.1	-277.1	5.1	PPMXL	7.4	PMSU	41.36	-6.65	-0.57	Mon16
J15013+055	82.9	0.3	-444.5	0.4	Gal15	-6.46	Schf15	17.24	-20.47	-20.38	Mon16
J15018+550	-445.8	5.1	149.7	5.1	PPMXL	-40.5	PMSU	-34.27	-45.76	-16.75	Mon16
J15030+704	-241.7	5.0	379.3	5.0	PPMXL			-47.4		-10.1	Lep13
J15043+294	241.8	5.2	-171.8	5.2	PPMXL	-22.3	PMSU	19.94	-2.88	-32.25	Mon16
J15043+603	-656.02	1.42	178.61	1.52	HIP2	-26.52	Schf15	-41.41	-47.94	0.42	Mon16
J15049-211	-657.5	5.2	-202.5	5.2	PPMXL	-39.3	PMSU	-62.67	-43.61	-3.48	Mon16
J15060+453	107.3	4.8	26.3	4.8	PPMXL			7.6	16.2		Lep13
J15073+249	-839.8	2.4	499.2	2.4	PPMXL	-68.9	Schf15	-93.74	-38.06	-22.23	Mon16
J15079+762	-130.2	0.1	162.6	0.2	Gal15						
J15081+623	-139.3	5.0	190.3	5.0	PPMXL	-15.96	Schf15	-16.59	-12.43	-13.01	Mon16
J15095+031	-603.68	3.85	484.19	2.56	HIP2	-32.49	Schf15	-61.1	-3.84	9.9	Mon16
J15100+193	5.4	4.7	-449.2	4.7	PPMXL	14.72	Schf15	32.04	-21.72	5.38	Mon16
J15118-102	-984.1	5.5	-225.2	5.5	PPMXL	31.6	PMSU	-7.94	-61.73	46.28	Mon16
J15119+179	-420.3	4.7	-559.6	4.7	PPMXL	-16.6	PMSU	8.05	-79.25	-2.91	Mon16
J15126+457	-391.8	4.7	358.3	4.7	PPMXL	-11.06	Schf15	-46.17	-12.43	2.11	Mon16
J15147+645	-418.5	5.1	393.7	5.1	PPMXL						
J15151+333	-92.5	8.9	-351.5	3.8	PPMXL						
J15156+638	38.3	5.1	-113.5	5.1	PPMXL			18.0	-0.7		Lep13
J15166+391	-209.5	5.0	-60.1	5.0	PPMXL	-6.9	West15	-6.2	-16.16	2.78	Mon16
J15188+292	-64.6	2.3	-53.6	2.3	PPMXL			1.0	-11.5		Lep13
J15191-127	-726.5	5.4	-185.3	5.4	PPMXL	1.1	PMSU	-31.21	-62.1	28.39	Mon16
J15193+678	-476.2	5.1	397.4	5.1	PPMXL	-11.5	PMSU	-72.89	-35.53	0.01	Mon16
J15194-077	-1228.3	0.4	-99.9	0.4	Cortes	-9.28	Schf15	-24.75	-25.44	11.76	Mon16

Table B.3: Proper motions and UVW space velocities of Carmencita stars (continued).

Karmn	$\mu_\alpha \cos\delta$ [mas a^{-1}]	$e\mu_\alpha \cos\delta$ [mas a^{-1}]	μ_δ [mas a^{-1}]	$e\mu_\delta$ [mas a^{-1}]	Ref.[a b]	V_r [km s^{-1}]	Ref.[c]	U [km s^{-1}]	V [km s^{-1}]	W [km s^{-1}]	Ref.[d]
J15197+046	23.2	5.2	97.6	5.2	PPMXL						
J15210+309	-99.5	5.0	-20.4	5.0	PPMXL			-3.3	-7.0		Lep13
J15214+042	86.7	0.4	38.0	0.2	Cortes			5.0	11.9		Lep13
J15218+209	78.6	1.49	130.41	2.06	HIP2	6.67	Schf15	0.47	9.63	4.39	Mon16
J15219+185	33.34	3.94	-213.01	3.64	HIP2			26.1	-20.4		Lep13
J15238+174	-399.7	4.5	-1261.2	4.5	PPMXL	47.1	PMSU	61.2	-51.74	34.36	Mon16
J15238+561	70.9	3.0	-33.9	3.0	PPMXL			10.8	5.5		Lep13
J15238+584	-182.0	4.7	299.7	4.7	PPMXL	-0.04	Ter15	-36.37	-1.33	-0.81	Mon16
J15273+415	-113.9	0.6	-43.7	1.1	Cortes						
J15276+408	-115.0	2.22	279.53	2.35	HIP2			-44.7	11.2		Lep13
J15280+257	91.42	2.35	-56.89	2.77	HIP2	4.6	PMSU	12.25	4.42	-2.94	Mon16
J15290+467	-118.3	4.8	-21.9	4.8	PPMXL						
J15297+428	423.7	4.9	-617.9	4.9	PPMXL	35.2	PMSU	74.74	15.91	13.99	Mon16
J15305+094	-185.4	4.9	182.8	4.8	PPMXL	4.0	New14	-5.1	1.09	9.42	Mon16
J15319+288	-545.7	4.6	34.1	4.6	PPMXL	-48.0	New14	-50.93	-56.64	-4.94	Mon16
J15336+462	-7.1	0.4	200.3	0.4	Gal15	-7.7	PMSU	-19.47	4.78	-9.3	Mon16
J15339+379	-0.21	1.77	-80.42	1.92	HIP2	26.6	PMSU	17.45	6.94	22.31	Mon16
J15340+513	-192.8	4.9	274.1	4.8	PPMXL						
J15345+142	-671.3	4.6	-145.7	4.6	PPMXL	-4.6	PMSU	-24.54	-54.58	30.65	Mon16
J15349-143	-158.8	8.2	-267.0	7.8	PPMXL	-75.5	RB09	-62.85	-6.64	-44.35	Mon16
J15353+177N	-1213.0	4.6	-168.2	4.6	aPPMXL	-19.1	PMSU	-42.18	-69.14	31.44	Mon16
J15353+177S	-1213.0	4.6	-168.2	4.6	PPMXL	-42.0	New14	-54.03	-74.08	12.34	Mon16
J15357+221	-707.3	5.3	-129.4	5.3	PPMXL	-60.13	Schf15	-51.16	-69.6	-13.16	Mon16
J15368+375	-273.99	1.65	-90.62	1.72	HIP2			-14.8	-63.2		Lep13
J15369-141	-450.7	5.4	-621.1	5.4	PPMXL	2.12	Schf15	-0.17	-48.08	-5.84	Mon16
J15386+371	-297.8	4.4	203.7	4.4	PPMXL						
J15400+434N	1168.9	1.7	-300.0	4.0	Gal15	-141.2	PMSU	21.21	-40.88	-154.21	Mon16
J15400+434S	1211.7	0.5	-378.8	0.2	Gal15	-104.5	PMSU	34.48	-20.49	-126.14	Mon16
J15412+759	776.36	2.17	-758.27	2.52	HIP2	-41.5	Schf15	74.44	-3.37	-29.18	Mon16
J15416+184	-73.22	0.33	56.29	0.32	aHIP2			-10.0	-1.9		Lep13
J15421-194	-1966.4	1.9	-1010.2	0.7	Cortes	78.6	PMSU	34.95	-113.83	62.82	Mon16
J15474+451	-247.6	5.0	191.6	5.0	PPMXL						
J15474-108	-332.19	2.9	-352.83	2.62	HIP2	7.4	Schf15	4.31	-34.94	4.35	Mon16

Table B.3: Proper motions and UVW space velocities of Carmencita stars (continued).

Karmn	$\mu_\alpha \cos\delta$ [mas a^{-1}]	$e\mu_\alpha \cos\delta$ [mas a^{-1}]	μ_δ [mas a^{-1}]	$e\mu_\delta$ [mas a^{-1}]	Ref.[a b]	V_r [km s^{-1}]	Ref.[c]	U [km s^{-1}]	V [km s^{-1}]	W [km s^{-1}]	Ref.[d]
J15476+226	-180.9	5.0	-29.5	5.0	PPMXL	-20.0	New14	-17.0	-24.08	-2.61	Mon16
J15480+043	-20.1	5.0	-52.9	5.0	PPMXL						
J15488+305	102.2	2.4	-16.8	2.4	PPMXL			5.3	6.3		Lep13
J15493+250	-42.4	5.0	380.8	5.0	PPMXL			-40.6	28.9		Lep13
J15496+348	-657.8	4.4	693.3	4.4	PPMXL	-70.48	Schf15	-93.84	-40.31	-21.31	Mon16
J15496+510	-377.89	3.8	291.01	3.79	HIP2	-75.1	PMSU	-46.1	-61.05	-40.67	Mon16
J15499+796	-212.1	4.7	128.1	4.7	PPMXL						
J15501+009	182.7	0.2	-49.0	0.4	Gal15	0.0	PMSU	10.2	8.37	-13.68	Mon16
J15512+306	-181.1	1.5	-10.6	1.5	PPMXL			-10.7	-19.6		Lep13
J15513+295	-228.7	4.4	-445.5	4.4	PPMXL	38.5	PMSU	35.84	-12.68	37.53	Mon16
J15531+347N	269.6	6.2	-504.3	6.2	PPMXL	23.5	PMSU	57.24	3.23	1.68	Mon16
J15531+347S	269.6	6.2	-504.3	6.2	aPPMXL	36.9	PMSU	62.04	10.24	12.04	Mon16
J15538+641	-144.9	1.97	178.7	2.02	HIP2			-39.2		4.2	Lep13
J15555+352	-231.7	4.3	156.2	4.3	PPMXL	-18.0	New14	-36.63	-18.62	6.43	Mon16
J15557+686	-54.2	5.1	123.9	5.1	PPMXL			-18.1		-4.3	Lep13
J15569+376	-84.6	4.7	31.0	4.7	PPMXL						
J15578+090	141.5	4.6	-152.8	4.6	PPMXL	-20.31	Schf15	-2.54	-6.38	-25.11	Mon16
J15581+494	60.3	1.7	-170.9	1.7	PPMXL			27.7	-3.0		Lep13
J15583+354	-140.6	0.3	319.7	0.4	Gal15	9.54	Schf15	-20.27	10.85	14.29	Mon16
J15587+346	67.1	4.3	-60.9	4.3	PPMXL			5.6	0.6		Lep13
J15597+440	-72.4	4.9	-17.3	4.9	PPMXL	-15.8	Malo14a	-4.95	-15.63	-6.66	Mon16
J15598-082	204.67	1.91	-23.62	1.88	HIP2	-17.54	Schf15	-9.0	7.08	-19.0	Mon16
J16008+403	-282.5	5.3	-300.6	5.3	PPMXL	-45.3	PMSU	4.06	-62.76	-12.44	Mon16
J16017+301	-322.6	0.3	147.1	0.6	Gal15	8.24	Schf15	-17.63	-6.79	25.84	Mon16
J16017+304	-142.7	4.6	128.1	4.6	aPPMXL	-8.0	PMSU	-24.14	-6.54	7.66	Mon16
J16018+304	-142.7	4.6	128.1	4.6	PPMXL	-23.7	PMSU	-37.12	-15.19	0.02	Mon16
J16028+205	-938.4	0.3	-1223.0	0.3	Gal15	6.44	Schf15	29.12	-63.84	21.42	Mon16
J16033+175	-45.0	4.7	25.5	4.7	PPMXL			-5.5	-0.9		Lep13
J16043-062	-68.7	5.3	-862.7	5.3	PPMXL	33.8	PMSU	53.12	-52.73	-13.35	Mon16
J16046+263	-97.9	1.8	84.9	1.8	PPMXL	-14.69	Ter15	-20.77	-8.46	-0.64	Mon16
J16048+391	-571.08	0.29	52.34	0.29	aHIP2	-56.0	PMSU	-35.07	-56.71	-15.74	Mon16
J16054+769	-332.9	4.7	73.3	4.7	PPMXL	-27.9	PMSU	-10.39	-42.36	2.36	Mon16
J16062+290	-165.8	1.7	366.4	1.7	PPMXL	-56.25	Ter15	-97.98	-6.96	-10.55	Mon16

Table B.3: Proper motions and UVW space velocities of Carmencita stars (continued).

Karmn	$\mu_\alpha \cos\delta$ [mas a^{-1}]	$e\mu_\alpha \cos\delta$ [mas a^{-1}]	μ_δ [mas a^{-1}]	$e\mu_\delta$ [mas a^{-1}]	Ref.[a b]	V_r [km s^{-1}]	Ref.[c]	U [km s^{-1}]	V [km s^{-1}]	W [km s^{-1}]	Ref.[d]
J16066+083	-503.0	1.7	82.5	0.8	Cortes	-27.1	PMSU	-58.65	-51.91	44.25	Mon16
J16074+059	-297.0	4.8	-226.9	4.8	PPMXL	-91.0	PMSU	-65.08	-64.24	-43.91	Mon16
J16082-104	-370.7	6.0	-1307.7	6.0	PPMXL	6.1	PMSU	35.43	-124.27	-44.69	Mon16
J16090+529	204.24	1.3	60.48	1.29	HIP2	-19.18	Schf15	-0.47	-1.21	-25.66	Mon16
J16092+093	-289.8	5.2	230.8	5.2	PPMXL	-44.98	Schf15	-47.05	-14.17	-11.73	Mon16
J16120+033	28.2	2.6	-61.3	2.7	PPMXL	9.13	Schf15	10.87	-0.47	1.37	Mon16
J16139+337	-263.39	0.93	-92.67	1.31	aHIP2	-16.3	PMSU	-7.64	-30.89	5.74	Mon16
J16144-028	-8.4	0.2	381.1	1.3	Cortes	12.8	Des12	-2.4	23.22	21.32	Mon16
J16145+191	-1971.6	0.4	360.1	0.4	Gal15	-34.0	New14	-93.09	-94.57	90.12	Mon16
J16147+048	-416.8	5.0	72.3	5.0	PPMXL	-75.5	PMSU	-85.21	-50.98	3.16	Mon16
J16155+244	-57.9	2.4	250.2	2.4	PPMXL	-66.7	PMSU	-66.36	-15.27	-34.24	Mon16
J16167+672N	-498.28	0.99	86.05	1.04	aHIP2	-18.43	Schf15	-9.99	-29.64	4.38	Mon16
J16167+672S	-498.28	0.99	86.05	1.04	HIP2	-18.92	Schf15	-9.93	-30.01	4.06	Mon16
J16170+552	85.34	1.18	-438.47	1.23	HIP2	-23.5	PMSU	41.42	-23.25	-13.63	Mon16
J16180+062	71.7	4.8	49.9	4.8	PPMXL				7.5	-2.1	Lep13
J16204-042	-415.27	1.94	-21.88	1.73	HIP2	-98.3	PMSU	-102.92	-58.14	-5.51	Mon16
J16220+228	-52.6	1.6	71.6	1.6	PPMXL			-9.1	-0.3		Lep13
J16241+483	1146.26	1.21	-451.86	1.11	HIP2	-27.0	Del98	24.66	3.12	-48.47	Mon16
J16247+229	-152.2	1.6	-98.1	1.6	PPMXL			3.3	-18.0		Lep13
J16254+543	432.29	1.14	-170.2	1.08	HIP2	-13.19	Schf15	7.86	-2.58	-17.65	Mon16
J16255+260	-198.9	0.6	-4.8	0.1	Cortes	-25.9	PMSU	-17.84	-23.04	-6.83	Mon16
J16255+323	81.4	6.8	129.0	6.4	PPMXL			-10.8	15.0		Lep13
J16259+834	84.0	1.9	-60.9	1.9	PPMXL			10.6		-4.6	Lep13
J16268-173	-330.5	5.5	-411.7	5.5	PPMXL	-54.1	PMSU	-50.99	-36.46	-20.18	Mon16
J16280+155	-14.2	5.7	-308.6	5.7	PPMXL	19.6	PMSU	41.94	-21.58	0.83	Mon16
J16302-146	-502.76	6.54	-198.7	4.44	HIP2	-101.4	PMSU	-103.31	-52.53	-12.03	Mon16
J16303-126	-94.81	2.3	-1183.43	1.74	HIP2	-21.26	Schf15	-12.99	-21.06	-20.56	Mon16
J16313+408	-148.3	4.8	310.3	4.8	PPMXL	-23.627	Schf15	-25.73	-13.48	-9.84	Mon16
J16315+175	-327.4	4.6	-806.7	4.6	PPMXL	7.0	New14	40.02	-50.12	5.27	Mon16
J16327+126	-765.52	2.99	-143.85	3.08	HIP2	-32.91	Schf15	-32.41	-58.56	21.26	Mon16
J16328+098	225.5	4.9	157.4	4.9	PPMXL	-5.3	PMSU	-6.25	14.5	-10.12	Mon16
J16342+543	-247.7	0.7	538.7	0.6	Gal15			-98.9		17.0	Lep13
J16343+571	-1117.4	0.2	1181.2	0.7	Gal15	-164.3	PMSU	-107.51	-155.23	-64.65	Mon16

Table B.3: Proper motions and UVW space velocities of Carmencita stars (continued).

Karmn	$\mu_\alpha \cos\delta$ [mas a^{-1}]	$e\mu_\alpha \cos\delta$ [mas a^{-1}]	μ_δ [mas a^{-1}]	$e\mu_\delta$ [mas a^{-1}]	Ref.[a b]	V_r [km s^{-1}]	Ref.[c]	U [km s^{-1}]	V [km s^{-1}]	W [km s^{-1}]	Ref.[d]
J16354+350	133.8	4.8	-144.6	4.8	PPMXL	-2.61	Schf15	11.37	-0.53	-10.3	Mon16
J16360+088	-517.4	4.8	-156.1	4.8	PPMXL	-6.0	PMSU	-7.46	-33.42	20.2	Mon16
J16395+505	321.45	1.9	-404.84	1.74	HIP2			46.4		-20.5	Lep13
J16401+007	169.4	0.7	-157.6	0.1	Gal15	10.0	New14	14.69	1.9	-5.61	Mon16
J16403+676	-266.2	5.2	359.1	5.2	PPMXL	-15.0	New14	-24.36	-21.05	-2.57	Mon16
J16408+363	-138.6	1.68	179.18	2.46	HIP2	-81.0	PMSU	-49.19	-52.6	-42.41	Mon16
J16420+192	-25.0	4.4	72.4	4.4	PPMXL				2.9	2.9	Lep13
J16462+164	-345.4	3.0	-467.6	2.5	HIP2	18.38	Schf15	31.6	-30.36	19.65	Mon16
J16465+345	-382.7	5.0	-389.5	5.0	PPMXL						
J16487+106	-172.9	1.7	-43.5	1.7	PPMXL				-12.2	9.1	Lep13
J16487-157	-9.48	2.45	-221.0	1.72	HIP2	-78.1	Schf15	-69.7	-20.29	-34.57	Mon16
J16508-048	-750.5	5.5	-241.4	5.5	PPMXL	0.6	PMSU	-5.28	-65.86	47.66	Mon16
J16509+224	30.3	4.8	397.1	4.8	PPMXL	-43.39	Schf15	-40.32	-11.67	-21.85	Mon16
J16528+630	142.3	4.9	147.6	4.9	PPMXL	-21.0	New14	-6.08	-10.72	-21.07	Mon16
J16529+400	-56.5	0.3	-227.0	0.2	Gal15	11.2	PMSU	23.46	-4.36	9.93	Mon16
J16542+119	-545.29	1.53	316.68	1.36	HIP2	-62.3	PMSU	-74.57	-37.64	17.05	Mon16
J16554-083N	-825.84	6.68	-873.53	3.53	aHIP2	15.2	PMSU	18.41	-31.86	11.19	Mon16
J16554-083S	-825.84	6.68	-873.53	3.53	HIP2	14.2	PMSU	17.5	-32.04	10.83	Mon16
J16555-083	-825.84	6.68	-873.53	3.53	aHIP2	16.1	PMSU	19.43	-33.27	11.75	Mon16
J16570-043	472.6	5.4	-376.3	5.4	PPMXL	-4.3	Schf15	7.28	-1.33	-26.82	Mon16
J16573+124	159.2	4.6	-157.9	4.6	PPMXL	35.5	PMSU	46.26	14.98	-9.04	Mon16
J16573+271	-40.7	4.5	42.0	4.5	PPMXL						
J16574+777	195.5	4.8	156.5	4.8	PPMXL	-14.4	PMSU	-8.69	-0.29	-31.16	Mon16
J16577+132	46.09	1.93	71.09	1.49	PPMXL	-22.5	PMSU	-23.81	4.02	-13.85	Mon16
J16578+473	-147.62	0.58	270.8	0.68	aHIP2	-6.38	Tok02	-26.24	-5.64	6.0	Mon16
J16581+257	-114.07	0.95	-506.26	1.33	HIP2	3.87	Schf15	21.21	-14.53	0.98	Mon16
J16584+139	-401.3	0.4	20.4	0.6	Cortes	1.6	PMSU	-6.08	-18.25	27.96	Mon16
J16587+688	-529.4	4.9	205.8	4.9	PPMXL			-41.1		51.2	Lep13
J16591+209	-28.9	0.9	116.3	0.3	Cortes	7.45	Schf15	-1.08	7.25	7.51	Mon16
J17003+253	-136.1	4.9	131.3	4.9	PPMXL	29.5	PMSU	-1.4	16.24	36.24	Mon16
J17006+063	-11.2	2.7	-307.6	2.7	PPMXL				-34.6	-15.7	Lep13
J17010+082	-249.9	5.1	-177.4	5.1	PPMXL	7.7	PMSU	11.42	-19.61	14.34	Mon16
J17027-060	-128.49	2.56	-82.48	1.33	HIP2	-9.8	PMSU	-7.87	-14.76	1.97	Mon16

Table B.3: Proper motions and UVW space velocities of Carmencita stars (continued).

Karmn	$\mu_\alpha \cos\delta$ [mas a^{-1}]	$e\mu_\alpha \cos\delta$ [mas a^{-1}]	μ_δ [mas a^{-1}]	$e\mu_\delta$ [mas a^{-1}]	Ref.[a b]	V_r [km s^{-1}]	Ref.[c]	U [km s^{-1}]	V [km s^{-1}]	W [km s^{-1}]	Ref.[d]
J17033+514	121.2	4.8	610.4	4.8	PPMXL	37.36	Schf15	-19.98	38.39	17.54	Mon16
J17038+321	176.6	4.6	95.1	4.3	PPMXL	-5.5	Shk12	-6.98	8.29	-13.19	Mon16
J17043+169	133.1	0.3	-1134.1	0.5	Gal15	38.6	PMSU	94.04	-31.33	-18.24	Mon16
J17052-050	-917.08	1.14	-1137.93	0.67	aHIP2	34.67	Schf15	47.51	-63.2	21.11	Mon16
J17058+260	-30.9	0.3	-284.7	0.6	Cortes			33.3		-5.7	Lep13
J17071+215	-464.9	2.73	-27.56	2.86	HIP2	-51.1	Schf15	-34.9	-47.45	-4.04	Mon16
J17076+073	-493.5	4.7	-375.2	4.7	PPMXL	31.0	New14	33.31	-18.94	27.89	Mon16
J17082+516	106.7	0.5	361.4	0.7	Gal15			-66.4		-17.9	Lep13
J17095+436	334.58	2.1	-282.08	2.28	HIP2	-45.0	PMSU	-2.11	-30.15	-36.71	Mon16
J17098+119	-357.2	4.8	-99.6	4.8	PPMXL	-22.6	PMSU	-15.37	-35.55	12.24	Mon16
J17104+279	18.9	4.4	-86.7	4.4	PPMXL			7.9		-4.0	Lep13
J17115+384	211.59	1.71	-46.23	2.08	HIP2	-44.31	Schf15	-12.74	-26.14	-35.63	Mon16
J17118-018	-444.1	0.3	-270.7	0.2	Cortes	-2.1	PMSU	1.36	-22.93	10.46	Mon16
J17121+456	249.8	1.6	-1572.6	1.6	PPMXL	-29.8	PMSU	36.01	-31.47	-25.54	Mon16
J17136-084	-424.37	6.11	-410.3	3.4	HIP2	5.5	PMSU	13.32	-49.01	13.75	Mon16
J17146+269	-295.0	2.3	152.3	2.3	PPMXL	-27.7	PMSU	-43.38	-33.6	33.6	Mon16
J17153+049	578.4	4.4	-746.2	4.4	PPMXL	44.1	PMSU	69.77	3.71	-36.9	Mon16
J17158+190	-132.0	1.3	14.5	1.3	PPMXL	-20.78	Schf15	-15.86	-17.17	-1.09	Mon16
J17160+110	-136.21	2.3	-347.84	1.93	HIP2	-45.34	Schf15	-16.89	-47.86	-21.74	Mon16
J17166+080	-278.96	2.64	-64.83	1.91	HIP2	-30.23	Schf15	-23.36	-27.84	1.59	Mon16
J17177+116	-345.5	4.7	-416.9	4.7	PPMXL	-47.2	PMSU	-21.44	-51.56	-13.13	Mon16
J17177-118	-17.6	0.6	-295.9	0.6	Gal15	50.5	PMSU	55.78	-13.21	0.04	Mon16
J17183+181	-10.9	0.2	-231.0	0.4	Gal15	10.0	PMSU	23.83	-9.15	-1.95	Mon16
J17183-017	88.9	0.6	-111.3	1.1	Cortes	-17.2	PMSU	-9.71	-8.69	-17.19	Mon16
J17198+265	-226.4	0.8	345.9	0.4	Gal15	-35.14	Schf15	-36.6	-20.08	-3.0	Mon16
J17198+417	285.4	1.65	-825.23	2.17	HIP2	-19.74	Schf15	40.78	-21.22	-30.18	Mon16
J17199+265	-213.2	1.1	350.7	0.5	Gal15	-35.59	Schf15	-37.0	-19.82	-3.76	Mon16
J17207+492	532.0	5.2	-1177.9	5.2	PPMXL	-21.0	PMSU	88.4	-13.56	-49.15	Mon16
J17219+214	-165.8	0.3	255.9	0.5	Gal15	-22.6	PMSU	-27.76	-10.4	2.66	Mon16
J17225+055	-105.7	4.4	-17.1	4.4	PPMXL				-6.9	7.8	Lep13
J17242-043	-243.4	2.1	-125.9	1.7	Cortes	79.3	PMSU	74.86	2.43	36.51	Mon16
J17276+144	-1113.7	0.2	-340.6	0.1	Gal15	20.2	PMSU	29.53	-67.43	84.45	Mon16
J17285+374	22.9	0.6	-195.9	0.9	Gal15	10.2	PMSU	25.57	0.62	-0.86	Mon16

Table B.3: Proper motions and UVW space velocities of Carmencita stars (continued).

Karmn	$\mu_\alpha \cos\delta$ [mas a^{-1}]	$e\mu_\alpha \cos\delta$ [mas a^{-1}]	μ_δ [mas a^{-1}]	$e\mu_\delta$ [mas a^{-1}]	Ref.[a b]	V_r [km s^{-1}]	Ref.[c]	U [km s^{-1}]	V [km s^{-1}]	W [km s^{-1}]	Ref.[d]
J17303+055	29.13	1.01	-248.15	0.63	HIP2	-12.06	Schf15	-3.19	-12.95	-10.36	Mon16
J17312+820	-296.4	4.5	488.4	4.5	PPMXL	56.3	PMSU	-51.71	24.86	36.54	Mon16
J17316+047	-183.2	5.1	-100.1	5.1	PPMXL				-22.9	12.7	Lep13
J17321+504	-2.1	0.1	-528.9	0.3	Gal15	-0.1	PMSU	69.12	-13.05	-3.9	Mon16
J17328+543	-264.3	0.6	425.5	0.5	Cortes			-59.8		32.1	Lep13
J17338+169	-108.6	4.8	-133.1	4.8	PPMXL	-24.0	Schf15	-11.66	-21.78	-7.5	Mon16
J17340+446	-109.6	4.9	13.9	4.9	PPMXL	-8.9	Schf15	-3.83	-11.24	2.21	Mon16
J17355+616	277.02	0.36	-524.88	0.46	aHIP2	-15.26	Schf15	36.16	-3.22	-22.55	Mon16
J17364+683	-320.57	1.14	-1269.33	1.39	HIP2	-14.8	PMSU	28.66	-13.7	0.63	Mon16
J17376+220	30.4	4.7	-311.7	4.7	PPMXL	8.0	PMSU	26.47	-8.34	-7.5	Mon16
J17378+185	934.1	0.7	967.42	0.8	Cortes	-9.82	Schf15	-32.93	34.73	-21.58	Mon16
J17386+612	-23.3	2.03	47.71	2.2	aHIP2	-9.4	PMSU	-7.56	-9.82	-2.1	Mon16
J17388+080	-86.4	0.7	-218.3	0.3	Gal15	24.6	PMSU	32.8	-7.67	6.58	Mon16
J17395+277N	18.54	1.94	-200.74	2.56	aHIP2	18.73	Schf15	30.19	3.01	0.13	Mon16
J17395+277S	18.54	1.94	-200.74	2.56	HIP2	35.5	PMSU	39.39	14.76	7.77	Mon16
J17419+407	-182.95	3.03	205.94	4.21	HIP2			-33.3		33.4	Lep13
J17421-088	-849.2	5.3	-483.5	5.3	PPMXL	-57.0	PMSU	-36.52	-107.68	42.07	Mon16
J17425-166	-97.7	0.8	-688.2	0.2	Cortes	-37.6	PMSU	-23.36	-63.97	-29.37	Mon16
J17430+057	225.31	2.0	-60.42	1.25	HIP2	0.5	PMSU	3.88	7.43	-20.42	Mon16
J17431+854	-101.4	2.2	-270.4	2.2	PPMXL			31.0		18.8	Lep13
J17432-185	-153.8	0.5	-555.4	0.2	Cortes	66.8	PMSU	77.2	-53.48	-11.2	Mon16
J17439+433	10.0	1.37	-603.33	1.31	HIP2	-14.59	Schf15	21.46	-18.7	-11.88	Mon16
J17455+468	-21.9	0.7	19.6	0.2	Cortes	-2.5	PMSU	-2.55	-2.81	0.9	Mon16
J17460+246	-373.4	4.5	499.8	4.5	PPMXL	-80.0	New14	-75.09	-50.99	-0.85	Mon16
J17464+277	-291.66	0.12	-749.6	0.15	aHIP2	-14.1	PMSU	16.95	-29.88	-4.78	Mon16
J17464-087	-37.6	5.3	-424.6	5.3	PPMXL	2.16	Ter15	10.52	-20.16	-9.75	Mon16
J17469+228	3.2	1.9	91.6	1.9	PPMXL			-11.1		3.9	Lep13
J17502+237	-339.4	4.6	451.4	4.6	PPMXL	-63.4	PMSU	-75.76	-37.56	20.97	Mon16
J17515+147	-205.6	5.2	102.2	5.2	PPMXL	-22.0	PMSU	-24.31	-18.63	20.07	Mon16
J17521+647	-2.02	1.77	-347.25	1.61	HIP2			49.6		0.7	Lep13
J17530+169	-257.8	4.6	-222.0	4.4	PPMXL	-0.42	Schf15	14.16	-22.97	11.97	Mon16
J17542+073	-592.0	1.5	-291.0	2.0	Gal15	-28.28	Schf15	-9.12	-50.28	19.72	Mon16
J17547+128	-79.1	1.3	-133.6	1.4	PPMXL				-15.6	1.1	Lep13

Table B.3: Proper motions and UVW space velocities of Carmencita stars (continued).

Karmn	$\mu_\alpha \cos\delta$ [mas a^{-1}]	$e\mu_\alpha \cos\delta$ [mas a^{-1}]	μ_δ [mas a^{-1}]	$e\mu_\delta$ [mas a^{-1}]	Ref.[a b]	V_r [km s^{-1}]	Ref.[c]	U [km s^{-1}]	V [km s^{-1}]	W [km s^{-1}]	Ref.[d]
J17570+157	-175.6	1.0	-238.6	1.0	PPMXL	-42.0	New14	-16.99	-43.1	-9.23	Mon16
J17572+707	4.9	3.9	330.5	3.9	PPMXL	-15.3	Des12	-26.89	-17.79	-9.4	Mon16
J17578+046	-798.58	1.72	10328.12	1.22	HIP2	-110.25	Schf15	-140.79	4.73	18.26	Mon16
J17578+465	-16.57	2.24	580.06	1.75	HIP2	-31.56	Schf15	-45.32	-19.72	-7.63	Mon16
J17589+807	-249.6	4.7	623.6	4.7	PPMXL			-53.9		12.6	Lep13
J18010+508	163.7	4.4	127.6	4.4	PPMXL			-22.7		-28.6	Lep13
J18022+642	198.5	4.7	-384.0	4.7	PPMXL	-1.2	Schf15	14.98	4.12	-7.97	Mon16
J18027+375	180.1	4.6	-1139.2	4.6	PPMXL	5.0	New14	60.63	-11.54	-22.82	Mon16
J18031+179	-300.1	0.5	-184.5	0.8	Cortes				-38.9	31.2	Lep13
J18037+247	-42.9	1.7	-227.4	1.7	PPMXL			25.1		-4.9	Lep13
J18042+359	80.47	1.47	-262.7	1.69	HIP2	-5.6	PMSU	20.88	-9.5	-16.27	Mon16
J18051-030	570.26	1.28	-333.47	1.05	HIP2	39.6	PMSU	39.3	17.17	-17.88	Mon16
J18063+728	12.2	0.5	234.9	0.7	Gal15			-39.5		-3.2	Lep13
J18074+184	-221.3	0.7	-84.6	0.6	Cortes			12.7		26.5	Lep13
J18075-159	-621.7	1.0	-343.4	0.2	Cortes	-4.2	PMSU	0.89	-23.58	14.31	Mon16
J18096+318	51.0	2.0	196.3	2.0	PPMXL			-18.0		1.5	Lep13
J18103+512	52.6	4.7	161.2	4.7	PPMXL			-24.6		-4.5	Lep13
J18109+220	-46.0	0.8	-16.8	0.3	Cortes			3.9		3.4	Lep13
J18116+061	104.8	4.6	42.9	4.6	PPMXL	-16.37	Ter15	-17.24	-0.06	-11.51	Mon16
J18131+260	217.5	0.1	-36.7	0.2	Gal15	-9.0	New14	-4.51	0.34	-20.08	Mon16
J18134+054	-69.2	2.8	-226.2	2.8	PPMXL				-24.1	-5.6	Lep13
J18135+055	-72.4	0.4	-228.2	0.5	Cortes	15.0	New14	25.23	-10.16	-0.64	Mon16
J18157+189	-36.82	1.68	-428.96	1.75	HIP2	70.0	PMSU	81.06	21.28	5.14	Mon16
J18160+139	100.33	1.58	-502.99	1.17	HIP2	29.69	Daw05	49.94	-3.34	-18.16	Mon16
J18163+015	-415.0	0.1	-635.0	0.3	Gal15	-30.48	Schf15	3.17	-67.06	1.63	Mon16
J18165+048	-163.6	0.6	385.1	0.7	Gal15	-51.0	New14	-53.97	-15.54	10.54	Mon16
J18165+455	-12.76	1.13	338.35	1.06	HIP2	-38.29	Schf15	-35.95	-28.82	-9.13	Mon16
J18174+483	-44.7	0.4	48.4	0.3	Cortes						
J18180+387E	-348.1	0.0	-1038.5	0.7	Gal15	0.23	Schf15	50.72	-22.65	1.17	Mon16
J18180+387W	-365.5	0.0	-1016.6	0.0	Gal15	-0.84	Schf15	48.01	-23.0	1.78	Mon16
J18189+661	429.2	0.2	-452.3	0.2	Gal15	4.84	Schf15	12.94	13.11	-11.71	Mon16
J18193-057	385.3	2.0	-399.8	1.0	Cortes	24.4	PMSU	34.61	-6.28	-58.44	Mon16
J18195+420	-59.8	5.2	-12.4	5.2	PPMXL			2.4		6.7	Lep13

Table B.3: Proper motions and UVW space velocities of Carmencita stars (continued).

Karmn	$\mu_\alpha \cos\delta$ [mas a^{-1}]	$e\mu_\alpha \cos\delta$ [mas a^{-1}]	μ_δ [mas a^{-1}]	$e\mu_\delta$ [mas a^{-1}]	Ref.[a b]	V_r [km s^{-1}]	Ref.[c]	U [km s^{-1}]	V [km s^{-1}]	W [km s^{-1}]	Ref.[d]
J18209-010	-518.2	5.2	-974.6	5.2	PPMXL	-47.0	PMSU	31.96	-157.1	-3.67	Mon16
J18221+063	-1194.8	0.4	104.3	0.2	Gal15	-43.77	Schf15	-28.54	-54.46	62.77	Mon16
J18224+620	-954.3	4.7	-1237.2	4.7	PPMXL	-18.0	New14	53.4	-28.67	19.14	Mon16
J18227+379	9.85	2.3	-395.54	2.21	HIP2			62.6		-21.6	Lep13
J18234+281	-76.5	4.7	-181.7	4.7	PPMXL	-21.9	Schf15	-1.42	-24.27	-6.56	Mon16
J18240+016	146.1	0.4	-234.3	0.3	Cortes	-75.58	Schf15	-54.6	-49.35	-31.87	Mon16
J18248+282	-181.41	3.2	40.16	3.75	HIP2			1.0		27.6	Lep13
J18250+246	-40.65	1.14	-448.02	1.62	HIP2	-11.7	HIP2	30.91	-32.7	-16.85	Mon16
J18255+383	-77.08	1.92	-744.0	2.19	HIP2	30.0	PMSU	92.55	-2.64	-6.95	Mon16
J18264+113	-10.8	0.5	-263.3	1.2	Gal15	-16.6	PMSU	1.28	-24.32	-11.33	Mon16
J18292+638	204.3	0.6	5.0	0.3	Cortes			-6.9		-24.6	Lep13
J18296+338	-73.6	4.3	16.9	4.3	PPMXL						
J18312+068	140.6	1.9	-111.0	1.9	PPMXL	13.64	Schf15	14.37	6.75	-13.45	Mon16
J18319+406	-98.2	0.6	413.1	0.2	Gal15	-19.25	Schf15	-26.18	-13.84	4.5	Mon16
J18346+401	58.0	2.2	-204.0	2.2	PPMXL	53.3	PMSU	24.28	45.78	14.43	Mon16
J18352+243	-113.2	0.3	-275.0	4.0	Cortes			26.8		-0.3	Lep13
J18352+414	381.6	2.2	-30.0	2.2	PPMXL	-77.8	PMSU	-28.53	-55.75	-56.07	Mon16
J18353+457	452.45	1.06	364.7	1.04	HIP2	-24.7	PMSU	-37.99	-4.0	-31.41	Mon16
J18354+457	452.45	1.06	364.7	1.04	aHIP2	-29.0	New14	-34.05	-10.73	-29.48	Mon16
J18356+329	-71.3	1.1	-773.8	1.2	Gal15	8.4	Des12	21.21	-0.47	-2.72	Mon16
J18358+800	121.3	0.8	209.6	0.3	Gal15	9.8	PMSU	-18.55	6.04	-2.82	Mon16
J18362+567	22.7	3.6	-409.9	3.9	PPMXL			66.3		-17.1	Lep13
J18363+136	170.4	0.4	289.0	0.2	Gal15	-45.18	Schf15	-43.63	-18.42	-8.78	Mon16
J18387+047	-169.6	1.8	-90.3	1.8	PPMXL				-19.0	16.0	Lep13
J18387-144	114.61	3.37	-569.52	2.4	HIP2	-44.1	PMSU	-34.22	-40.87	-19.1	Mon16
J18394+690	0.6	0.3	202.2	0.6	Cortes			-32.3		0.9	Lep13
J18395+298	83.6	3.7	-223.9	3.7	PPMXL						
J18395+301	-91.0	1.24	-171.8	1.43	HIP2	-30.34	Wh07	5.53	-37.99	-6.02	Mon16
J18399+334	24.6	4.5	282.8	4.5	PPMXL	-37.2	PMSU	-40.97	-21.38	-3.06	Mon16
J18400+726	-30.2	4.0	190.2	4.0	PPMXL						
J18402-104	-117.4	0.3	-529.8	0.1	Cortes	-66.9	PMSU	-31.58	-101.24	-18.66	Mon16
J18405+595	160.9	4.5	261.1	4.5	PPMXL			-38.6		-11.0	Lep13
J18409+315	86.87	0.85	-837.41	1.16	aHIP2	44.75	Daw05	99.13	7.66	-30.71	Mon16

Table B.3: Proper motions and UVW space velocities of Carmencita stars (continued).

Karmn	$\mu_\alpha \cos\delta$ [mas a^{-1}]	$e\mu_\alpha \cos\delta$ [mas a^{-1}]	μ_δ [mas a^{-1}]	$e\mu_\delta$ [mas a^{-1}]	Ref.[a b]	V_r [km s^{-1}]	Ref.[c]	U [km s^{-1}]	V [km s^{-1}]	W [km s^{-1}]	Ref.[d]
J18409-133	-89.77	2.27	-667.83	1.72	HIP2	-43.2	PMSU	-24.91	-61.36	-14.42	Mon16
J18411+247N	462.7	0.6	42.0	0.5	Gal15	-9.0	New14	-11.31	2.72	-20.76	Mon16
J18411+247S	502.0	0.2	65.9	0.7	Gal15	-9.0	New14	-12.6	3.99	-21.96	Mon16
J18416+397	-258.4	5.1	-178.7	5.1	PPMXL	-19.1	PMSU	5.32	-24.89	3.22	Mon16
J18419+318	-302.08	2.04	8.55	2.74	HIP2	4.7	PMSU	5.27	-2.49	15.96	Mon16
J18427+139	-40.5	4.6	360.1	4.6	PPMXL	-34.61	Schf15	-36.56	-13.68	5.03	Mon16
J18427+596N	-1332.03	2.23	1807.48	2.75	HIP2	-1.3	PMSU	-25.01	-12.67	25.68	Mon16
J18427+596S	-1332.03	2.23	1807.48	2.75	aHIP2	1.0	Del98	-24.98	-10.57	26.62	Mon16
J18432+253	38.1	1.7	-210.4	1.7	PPMXL			27.0		-19.8	Lep13
J18433+406	-120.0	4.1	587.2	4.1	PPMXL	-19.3	Des12	-40.65	-11.69	13.71	Mon16
J18451+063	-39.9	2.0	-78.6	2.0	PPMXL	-24.27	Schf15	-14.18	-21.19	-1.8	Mon16
J18453+188	-140.7	4.5	-261.2	4.5	PPMXL	16.92	Schf15	24.41	0.77	3.75	Mon16
J18480-145	-241.3	3.2	-238.4	0.7	Cortes	-34.3	PMSU	-21.82	-37.62	13.03	Mon16
J18482+076	366.7	0.5	231.1	0.6	Gal15	-33.9	Schf15	-33.71	-11.36	-10.03	Mon16
J18487+615	162.3	4.7	-72.6	4.7	PPMXL			3.0		-22.2	Lep13
J18499+186	-107.2	0.4	-283.8	0.2	Gal15	30.0	New14	34.57	9.83	2.79	Mon16
J18500+030	-179.66	2.3	-407.45	1.79	HIP2	-14.2	PMSU	14.52	-44.63	-3.0	Mon16
J18507+479	255.1	4.9	-113.6	4.9	PPMXL	-78.51	Schf15	-12.69	-65.81	-45.57	Mon16
J18515+027	-178.0	1.9	-275.6	1.9	PPMXL				-40.5	5.1	Lep13
J18516+244	-344.2	0.3	-22.4	0.4	Gal15	-75.7	PMSU	-32.71	-74.54	14.36	Mon16
J18518+165	-226.31	1.28	-481.31	1.4	HIP2	-14.8	Schf15	19.12	-37.01	-2.57	Mon16
J18519+130	14.3	0.9	-149.9	1.2	PPMXL				-8.8	-7.8	Lep13
J18534+028	280.3	0.3	16.9	0.7	Cortes				16.7	-27.7	Lep13
J18548+008	-72.0	1.4	-125.4	1.5	PPMXL				-14.9	0.9	Lep13
J18548+109	15.1	2.5	124.1	1.6	Cortes	-25.1	PMSU	-25.79	-9.49	2.01	Mon16
J18554+084	91.71	1.93	-69.59	1.38	HIP2	-22.8	PMSU	-16.23	-15.55	-7.5	Mon16
J18563+544	37.64	1.72	-343.54	1.57	aHIP2	-30.6	PMSU	67.72	-24.17	-39.62	Mon16
J18564+463	66.9	4.9	311.1	4.9	PPMXL	1.3	PMSU	-22.15	5.61	3.51	Mon16
J18571+075	-130.7	2.1	-139.0	2.1	PPMXL	-12.6	PMSU	1.94	-22.05	4.75	Mon16
J18576+535	248.5	0.3	-50.4	0.4	Cortes			-3.0		-31.7	Lep13
J18580+059	-196.11	1.68	-1222.54	1.43	HIP2	10.35	Schf15	46.65	-40.59	-19.6	Mon16
J18596+079	366.74	2.35	-179.98	1.84	HIP2	-82.1	PMSU	-61.32	-52.09	-52.87	Mon16
J19025+704	5.8	0.8	213.2	0.4	Gal15	-47.9	PMSU	-14.62	-49.31	-15.76	Mon16

Table B.3: Proper motions and UVW space velocities of Carmencita stars (continued).

Karmn	$\mu_\alpha \cos\delta$ [mas a^{-1}]	$e\mu_\alpha \cos\delta$ [mas a^{-1}]	μ_δ [mas a^{-1}]	$e\mu_\delta$ [mas a^{-1}]	Ref.[a b]	V_r [km s^{-1}]	Ref.[c]	U [km s^{-1}]	V [km s^{-1}]	W [km s^{-1}]	Ref.[d]
J19032+034	-182.7	0.7	-94.0	0.8	Cortes	-5.51	Schf15	4.42	-14.57	10.29	Mon16
J19032+639	63.1	1.9	111.4	1.9	PPMXL	-0.2	PMSU	-5.89	-0.07	-1.46	Mon16
J19032-135	-484.2	0.3	-485.8	0.2	Cortes	63.9	PMSU	83.42	-29.46	10.23	Mon16
J19041+211	105.1	4.6	57.4	4.6	PPMXL			-10.9		-7.5	Lep13
J19044+590	79.2	4.8	165.6	4.8	PPMXL			-16.2		-1.1	Lep13
J19045+240	-146.7	2.1	4.3	2.1	PPMXL			4.8		16.7	Lep13
J19070+208	-480.71	1.53	-346.11	2.44	HIP2	32.35	Schf15	35.52	12.2	14.39	Mon16
J19072+208	-480.71	1.53	-346.11	2.44	aHIP2	32.34	Schf15	35.52	12.2	14.37	Mon16
J19077+325	1207.6	0.1	1089.5	0.3	Gal15	-43.0	New14	-68.87	-8.12	-32.21	Mon16
J19082+265	-197.1	0.3	-499.1	0.2	Gal15	-2.5	PMSU	36.41	-24.53	-3.9	Mon16
J19084+322	-225.2	0.9	-231.9	0.4	Gal15	-2.23	Schf15	15.05	-11.15	5.74	Mon16
J19093+382	-112.0	3.0	-180.4	3.0	HIP2	-32.0	PMSU	10.13	-37.41	-4.58	Mon16
J19093-147	175.0	3.1	-471.7	3.1	PPMXL	-2.7	PMSU	4.42	-36.49	-35.51	Mon16
J19095+391	-112.0	3.0	-180.4	3.0	PPMXL			29.4		3.2	Lep13
J19098+176	-641.9	0.6	-428.7	0.5	Gal15	-14.17	Schf15	15.75	-32.79	17.26	Mon16
J19106+015	-163.4	0.6	-198.2	0.6	Cortes	61.6	PMSU	76.52	0.95	5.82	Mon16
J19116+050	95.9	2.2	79.7	2.2	PPMXL				13.9	-7.3	Lep13
J19122+028	1788.23	2.89	-519.72	2.39	PPMXL	-41.4	PMSU	-47.38	-14.7	-85.8	Mon16
J19124+355	233.0	5.2	-135.5	5.2	PPMXL	-80.7	PMSU	-27.24	-69.62	-37.5	Mon16
J19146+193N	-617.45	2.46	433.25	2.77	HIP2	-86.0	Schf15	-61.85	-66.37	61.81	Mon16
J19146+193S	-617.45	2.46	433.25	2.77	aHIP2	-51.0	New14	-40.7	-38.57	64.12	Mon16
J19169+051N	-578.78	1.07	-1331.95	0.74	HIP2	35.8	Schf15	53.22	-7.59	-4.97	Mon16
J19169+051S	-578.78	1.07	-1331.95	0.74	aHIP2	29.0	New14	48.4	-12.43	-4.63	Mon16
J19185+580	53.2	4.8	162.3	4.8	PPMXL			-33.0		1.1	Lep13
J19205-076	-60.87	4.03	-162.15	2.64	aHIP2	24.9	PMSU	25.61	4.19	-5.18	Mon16
J19215+425	43.2	0.2	150.8	0.7	Cortes			-17.9		6.1	Lep13
J19216+208	-962.3	0.3	-1462.3	0.3	Gal15	5.95	Schf15	72.76	-44.46	8.37	Mon16
J19218+286	867.45	2.35	262.36	3.28	HIP2	-23.9	PMSU	-66.63	17.81	-71.36	Mon16
J19220+070	-745.5	0.9	-425.0	1.1	Gal15	24.24	Schf15	43.37	-9.23	21.44	Mon16
J19228+307	-64.6	1.7	96.7	1.6	PPMXL			-7.4		13.6	Lep13
J19234+666	-188.5	5.0	88.8	5.0	PPMXL			-3.3		31.0	Lep13
J19237+797	95.6	2.0	36.2	2.0	PPMXL			-9.8		-9.5	Lep13
J19242+755	367.1	4.7	590.7	4.7	PPMXL	-20.1	PMSU	-29.32	-23.74	-17.89	Mon16

Table B.3: Proper motions and UVW space velocities of Carmencita stars (continued).

Karmn	$\mu_\alpha \cos\delta$ [mas a^{-1}]	$e\mu_\alpha \cos\delta$ [mas a^{-1}]	μ_δ [mas a^{-1}]	$e\mu_\delta$ [mas a^{-1}]	Ref.[a b]	V_r [km s^{-1}]	Ref.[c]	U [km s^{-1}]	V [km s^{-1}]	W [km s^{-1}]	Ref.[d]
J19242+797	82.9	1.9	31.9	1.9	PPMXL			-3.3		31.0	Lep13
J19251+283	207.5	4.7	365.5	4.7	PPMXL	-40.61	Schf15	-47.44	-20.33	-5.16	Mon16
J19255+096	83.7	5.1	-252.1	5.1	PPMXL	-21.0	New14	-6.34	-24.19	-12.02	Mon16
J19260+244	180.8	4.7	90.8	4.7	PPMXL	-35.0	New14	-29.93	-21.84	-12.27	Mon16
J19268+167	34.7	0.6	-207.0	2.0	Gal15	-41.4	PMSU	-12.66	-42.72	-12.85	Mon16
J19284+289	5.3	0.4	-37.9	0.2	Cortes			5.2		-2.4	Lep13
J19289+066	63.3	0.4	-92.5	0.3	Cortes				-5.1	-12.0	Lep13
J19312+361	-126.7	0.5	104.6	0.4	Gal15	-21.0	Cab10	-10.18	-20.16	8.42	Mon16
J19326+005	221.15	1.6	23.85	0.97	HIP2	-70.7	PMSU	-65.45	-34.71	-8.57	Mon16
J19336+395	218.8	4.2	-423.3	3.8	PPMXL	-10.4	PMSU	25.46	-11.87	-40.69	Mon16
J19346+045	526.69	1.96	311.18	1.11	HIP2	-58.2	Schf15	-68.91	-13.92	-13.98	Mon16
J19349+532	301.1	0.3	484.2	0.7	Gal15	-48.8	PMSU	-40.86	-42.72	-17.28	Mon16
J19351+084N	-64.11	5.98	-55.31	4.15	aHIP2	-15.2	PMSU	-6.22	-14.78	3.73	Mon16
J19351+084S	-64.11	5.98	-55.31	4.15	HIP2	-15.2	PMSU	-6.22	-14.78	3.74	Mon16
J19354+377	-136.7	2.4	-99.2	2.4	PPMXL	-33.3	Shk12	-4.52	-33.75	-1.66	Mon16
J19358+413	-285.9	1.6	-67.7	1.5	PPMXL			19.7		23.9	Lep13
J19395+718	-191.33	1.5	-444.77	1.31	HIP2	-49.8	PMSU	60.76	-33.74	-16.07	Mon16
J19419+031	-275.0	0.5	-470.2	0.5	Gal15	-17.3	PMSU	27.27	-55.85	5.09	Mon16
J19420-210	67.6	0.3	-244.8	0.6	Cortes	-7.6	Schf15	-5.47	-20.64	-10.24	Mon16
J19422-207	-12.5	4.8	-134.0	4.8	PPMXL	-1.7	Ried11	0.71	-9.95	-2.18	Mon16
J19457+271	-20.8	0.5	-1222.9	0.6	Gal15	-3.0	New14	52.24	-29.15	-33.34	Mon16
J19457+323	384.25	5.76	191.71	8.06	HIP2	-14.8	PMSU	-23.31	-5.41	-13.91	Mon16
J19463+320	461.97	1.23	-386.5	1.84	HIP2	-4.2	Schf15	5.49	-4.25	-38.47	Mon16
J19464+320	461.97	1.23	-386.5	1.84	aHIP2	-4.56	Schf15	5.36	-4.58	-38.49	Mon16
J19468-019	125.3	4.4	-15.0	4.4	PPMXL						
J19470+352	-114.4	3.8	-121.0	3.8	PPMXL			18.6		5.9	Lep13
J19486+359	46.6	4.8	-285.4	4.8	PPMXL	14.6	Ter15	19.55	9.81	-11.15	Mon16
J19500+325	419.9	0.4	239.0	0.2	Gal15	-39.5	PMSU	-45.59	-23.07	-21.62	Mon16
J19502+317	131.7	0.4	345.5	0.3	Gal15	-7.0	PMSU	-45.46	10.83	7.47	Mon16
J19510+104	242.28	0.27	-136.48	0.23	aHIP2	11.0	PMSU	4.67	5.58	-26.61	Mon16
J19511+464	183.9	4.5	273.0	4.5	PPMXL	-19.8	Schf15	-21.44	-15.89	-4.95	Mon16
J19512+622	-158.2	1.8	245.5	1.8	PPMXL			-16.7		26.5	Lep13
J19535+341	22.4	3.7	226.8	3.7	PPMXL	-29.2	PMSU	-31.9	-20.05	9.1	Mon16

Table B.3: Proper motions and UVW space velocities of Carmencita stars (continued).

Karmn	$\mu_\alpha \cos\delta$ [mas a^{-1}]	$e\mu_\alpha \cos\delta$ [mas a^{-1}]	μ_δ [mas a^{-1}]	$e\mu_\delta$ [mas a^{-1}]	Ref.[a b]	V_r [km s^{-1}]	Ref.[c]	U [km s^{-1}]	V [km s^{-1}]	W [km s^{-1}]	Ref.[d]
J19539+444E	426.5	2.6	-470.7	0.2	Cortes	73.2	PMSU	18.34	72.07	-1.64	Mon16
J19539+444W	427.8	2.4	-463.8	2.1	Cortes	3.0	New14	4.94	4.01	-12.43	Mon16
J19540+325	153.0	0.8	158.3	0.4	Gal15	-44.5	PMSU	-42.33	-30.87	-8.46	Mon16
J19546+202	-37.9	1.3	-64.5	1.3	PPMXL			9.4		-0.2	Lep13
J19558+512	467.9	2.48	346.35	2.39	HIP2	-27.0	PMSU	-63.78	-15.39	-32.94	Mon16
J19564+591	-433.59	1.91	-101.61	2.25	aHIP2	16.6	PMSU	43.58	4.38	53.17	Mon16
J19565+591	-433.59	1.91	-101.61	2.25	HIP2	5.3	PMSU	44.03	-6.48	50.17	Mon16
J19573-125	-95.85	1.69	-512.2	1.38	aHIP2	0.0	PMSU	18.23	-41.13	-10.46	Mon16
J19582+020	-340.8	0.4	-818.0	0.2	Gal15	2.4	PMSU	45.16	-48.15	-7.29	Mon16
J19582+650	-73.5	4.9	368.0	4.9	PPMXL	-51.5	Schf15	-21.91	-59.63	6.26	Mon16
J20005+593	101.0	0.3	78.1	1.0	Cortes	-5.2	Shk12	-10.1	-4.33	-5.74	Mon16
J20011+002	54.2	0.5	-215.9	0.9	Gal15	-32.52	Schf15	-16.54	-34.05	-4.31	Mon16
J20034+298	683.94	0.34	-524.7	0.27	aHIP2	-30.1	PMSU	-6.93	-30.42	-56.61	Mon16
J20037+644	-26.0	1.6	-116.7	1.6	PPMXL			18.3		-4.9	Lep13
J20038+059	-504.8	0.4	-810.2	0.3	Gal15	36.4	PMSU	69.47	-15.83	-5.94	Mon16
J20039-081	-501.5	5.0	-251.4	5.0	PPMXL	-14.173	Schf15	14.52	-30.2	28.66	Mon16
J20050+544	-1163.29	4.56	-899.98	4.16	HIP2	78.73	Daw05	104.02	65.9	56.71	Mon16
J20057+529	197.1	0.2	193.9	0.5	Gal15	-26.2	PMSU	-26.07	-23.25	-11.52	Mon16
J20079-015	348.1	6.1	-217.8	5.7	PPMXL	7.1	PMSU	-4.78	-8.97	-53.03	Mon16
J20082+333	346.0	4.9	369.9	4.9	PPMXL	-34.6	PMSU	-59.55	-15.86	-9.44	Mon16
J20093-012	-52.1	0.9	-379.9	0.8	Gal15						
J20105+065	38.3	0.3	-208.4	1.0	Gal15	-52.15	Shk10	-26.52	-47.46	3.02	Mon16
J20112+161	-414.75	0.5	398.26	0.56	aHIP2	-72.5	PMSU	-43.35	-47.64	59.29	Mon16
J20112+379	148.4	3.1	-123.9	3.1	PPMXL			3.8		-23.7	Lep13
J20129+342	-390.0	2.2	-134.2	2.2	PPMXL			44.6		35.4	Lep13
J20132+029	104.8	1.96	19.24	1.67	aHIP2			-11.2		-12.8	Lep13
J20138+133	422.36	2.51	21.01	2.67	HIP2			-29.3		-42.4	Lep13
J20139+066	-259.9	0.4	-595.4	0.5	Gal15	8.4	PMSU	55.44	-40.66	-10.13	Mon16
J20151+635	307.9	3.9	229.5	3.9	PPMXL			-56.9		-23.1	Lep13
J20165+351	-108.7	5.0	-347.2	5.0	PPMXL			45.3		-16.5	Lep13
J20187+158	207.0	4.6	-64.3	4.6	PPMXL	-13.17	Schf15	-12.56	-11.13	-13.78	Mon16
J20195+080	115.4	4.9	-182.9	4.9	PPMXL	-104.4	PMSU	-59.2	-88.81	7.66	Mon16
J20198+229	76.8	1.2	106.0	1.2	PPMXL	-22.1	Schf15	-17.72	-15.71	2.55	Mon16

Table B.3: Proper motions and UVW space velocities of Carmencita stars (continued).

Karmn	$\mu_\alpha \cos\delta$ [mas a^{-1}]	$e\mu_\alpha \cos\delta$ [mas a^{-1}]	μ_δ [mas a^{-1}]	$e\mu_\delta$ [mas a^{-1}]	Ref.[a b]	V_r [km s^{-1}]	Ref.[c]	U [km s^{-1}]	V [km s^{-1}]	W [km s^{-1}]	Ref.[d]
J20220+216	3.5	1.5	-136.1	1.5	PPMXL			12.9		-11.0	Lep13
J20223+322	149.2	4.7	-17.2	4.7	PPMXL			-7.5		-13.3	Lep13
J20229+106	-382.6	4.9	-403.6	4.9	PPMXL						
J20232+671	231.1	4.7	182.8	4.7	PPMXL						
J20260+585	260.7	0.5	537.8	0.8	Gal15	-60.21	Schf15	-22.16	-61.26	-8.72	Mon16
J20269+275	-7.1	4.7	286.4	4.7	PPMXL	-59.8	PMSU	-46.96	-42.87	26.89	Mon16
J20287-114	166.4	5.2	-93.3	5.2	PPMXL	-25.61	Schf15	-24.73	-17.9	-3.61	Mon16
J20298+096	674.0	4.9	118.1	4.9	PPMXL	-26.0	New14	-30.93	-14.51	-9.63	Mon16
J20301+798	99.5	2.0	37.9	2.0	PPMXL				-5.6	-2.51	Lep13
J20305+654	443.01	0.92	283.32	1.14	HIP2	10.23	Schf15	-19.96	8.69	-5.23	Mon16
J20314+385	201.4	4.6	718.1	4.6	PPMXL	-19.0	New14	-50.89	-8.25	18.19	Mon16
J20336+617	541.0	4.8	914.7	4.8	PPMXL	-21.03	Schf15	-76.67	-31.29	0.83	Mon16
J20337+233	306.5	5.2	92.1	5.2	PPMXL	13.6	PMSU	-20.08	19.87	-22.61	Mon16
J20339+643	-425.5	0.4	-133.2	0.5	Gal15	-20.4	PMSU	36.02	-20.56	19.87	Mon16
J20347+033	290.6	0.3	-476.1	0.6	Cortes	-71.2	PMSU	-34.21	-88.69	-33.04	Mon16
J20349+592	-238.8	0.7	-44.3	0.4	Gal15	-95.8	PMSU	26.25	-95.42	-1.55	Mon16
J20367+388	165.0	4.6	-152.0	4.6	PPMXL	6.4	PMSU	3.19	5.42	-21.2	Mon16
J20373+219	-46.1	2.2	-295.7	2.2	PPMXL	-18.5	PMSU	21.26	-33.57	-12.89	Mon16
J20403+616	-36.9	3.1	-102.9	3.1	PPMXL			11.5		-3.5	Lep13
J20405+154	1320.4	5.6	657.4	5.6	PPMXL	-59.68	Schf15	-83.66	-28.19	-14.74	Mon16
J20407+199	118.14	0.3	312.63	0.26	aHIP2	-34.88	Schf15	-42.82	-14.6	16.32	Mon16
J20409-101	-71.9	2.9	139.9	3.0	PPMXL	-23.0	PMSU	-17.18	1.93	24.56	Mon16
J20429-189	597.94	2.44	-860.12	1.85	HIP2	5.7	Schf15	-8.2	-60.91	-64.81	Mon16
J20433+553	857.0	4.8	1716.3	4.8	PPMXL	-74.7	PMSU	-136.7	-83.68	16.55	Mon16
J20435+240	146.5	4.9	-43.5	4.9	PPMXL	-16.2	Schf15	-10.94	-15.18	-8.43	Mon16
J20436+642	311.25	1.35	-99.46	1.61	HIP2			-11.2		-30.2	Lep13
J20436-001	362.34	2.98	256.85	2.49	HIP2	-67.9	PMSU	-87.59	-15.69	6.65	Mon16
J20443+197	-14.44	1.59	-599.57	1.35	HIP2	-4.2	PMSU	39.0	-32.54	-32.09	Mon16
J20445+089N	200.7	2.2	96.9	2.1	aPPMXL	-26.3	PMSU	-26.68	-14.79	1.61	Mon16
J20445+089S	200.7	2.2	96.9	2.1	PPMXL	-37.5	PMSU	-38.58	-20.84	1.98	Mon16
J20450+444	432.91	1.58	272.81	1.46	HIP2	-24.91	Schf15	-30.59	-21.69	-10.31	Mon16
J20488+197	-167.5	4.9	-203.2	4.9	PPMXL	15.67	Schf15	44.54	-3.6	-1.99	Mon16
J20496-003	312.1	4.6	-193.7	4.6	PPMXL	-48.9	PMSU	-40.07	-44.48	-10.88	Mon16

Table B.3: Proper motions and UVW space velocities of Carmencita stars (continued).

Karmn	$\mu_\alpha \cos\delta$ [mas a^{-1}]	$e\mu_\alpha \cos\delta$ [mas a^{-1}]	μ_δ [mas a^{-1}]	$e\mu_\delta$ [mas a^{-1}]	Ref.[a b]	V_r [km s^{-1}]	Ref.[c]	U [km s^{-1}]	V [km s^{-1}]	W [km s^{-1}]	Ref.[d]
J20519+691	206.6	0.0	36.9	0.6	Gal15	-41.0	PMSU	-14.86	-38.45	-32.36	Mon16
J20525-169	-307.74	3.86	34.79	4.26	HIP2	16.41	Schf15	16.76	7.2	-2.55	Mon16
J20532-023	189.1	0.1	16.6	0.9	Cortes	-39.9	Shk12	-47.71	-21.04	-6.03	Mon16
J20533+621	1.56	0.57	-774.55	0.68	HIP2	-17.09	Schf15	22.04	-10.44	-19.17	Mon16
J20535+106	-490.8	4.8	-448.7	4.8	PPMXL	-17.0	New14	29.55	-33.24	15.2	Mon16
J20549+675	160.1	4.6	119.9	4.6	PPMXL			-25.3		-6.7	Lep13
J20556-140N	1423.9	5.5	-462.7	5.5	PPMXL	-141.92	Schf15	-144.14	-86.12	4.54	Mon16
J20556-140S	1423.9	5.5	-462.7	5.5	aPPMXL	-136.1	PMSU	-140.12	-83.36	1.39	Mon16
J20567-104	-32.57	4.04	-1118.99	2.78	HIP2	35.41	Schf15	55.08	-51.18	-46.83	Mon16
J20568-048	787.86	4.78	-222.36	2.65	HIP2	-34.2	PMSU	-56.22	-32.47	-40.9	Mon16
J20574+223	775.47	2.47	-210.18	1.81	HIP2	-27.0	New14	-34.28	-28.26	-41.5	Mon16
J20586+342	291.81	1.64	-144.2	2.11	HIP2	12.1	PMSU	-7.25	9.0	-37.36	Mon16
J21000+400	616.3	1.47	-249.0	1.7	HIP2	-28.7	PMSU	-19.7	-29.44	-43.48	Mon16
J21001+495	186.4	0.2	217.2	0.4	Gal15			-43.5		1.9	Lep13
J21012+332	319.8	4.7	-126.8	4.7	PPMXL	-39.01	Schf15	-17.61	-39.41	-18.87	Mon16
J21013+332	319.8	4.7	-126.8	4.7	aPPMXL	-25.0	New14	-15.1	-26.0	-22.33	Mon16
J21014+207	-386.2	4.8	-397.6	4.8	PPMXL	-24.5	PMSU	46.52	-42.81	12.71	Mon16
J21019-063	-227.71	3.59	-445.1	1.55	HIP2	-15.53	Schf15	13.3	-34.21	7.67	Mon16
J21027+349	235.3	4.6	-253.7	4.6	PPMXL						
J21044+455	171.7	0.7	-39.6	0.3	Cortes			-17.9		-26.5	Lep13
J21048-169	-918.58	3.68	-2038.13	2.5	HIP2	-1.4	PMSU	110.07	-170.55	8.55	Mon16
J21055+061	24.8	0.3	47.4	1.5	Cortes	-12.21	Schf15	-9.85	-6.26	5.85	Mon16
J21057+502	85.4	1.1	29.1	0.8	Cortes	-13.32	Schf15	-8.28	-13.25	-5.17	Mon16
J21059+044	134.64	4.18	-170.66	1.9	HIP2	-78.3	PMSU	-40.99	-70.13	13.95	Mon16
J21074+468	15.2	4.7	97.9	4.7	PPMXL						
J21076-130	54.2	5.5	-90.0	5.5	PPMXL	3.6	Malo14a	1.86	-5.18	-8.27	Mon16
J21087-044N	-77.56	2.42	33.89	0.87	aHIP2	27.6	PMSU	21.1	20.07	-5.65	Mon16
J21087-044S	-77.56	2.42	33.89	0.87	HIP2	14.1	PMSU	13.15	11.9	1.58	Mon16
J21092-133	713.18	2.82	-1994.64	0.95	HIP2	-56.7	PMSU	-25.13	-127.87	-34.18	Mon16
J21100-193	93.0	3.9	-87.4	3.9	PPMXL	-5.7	Moo13	-7.37	-9.32	-4.53	Mon16
J21109+294	-226.61	1.82	-294.84	1.47	HIP2	-10.8	PMSU	52.22	-24.94	-1.51	Mon16
J21123+359	176.2	2.0	90.6	2.0	PPMXL			-25.5		-7.5	Lep13
J21127-073	101.3	5.2	-28.6	5.2	PPMXL	-10.85	Schf15	-13.8	-9.13	-4.5	Mon16

Table B.3: Proper motions and UVW space velocities of Carmencita stars (continued).

Karmn	$\mu_\alpha \cos\delta$ [mas a^{-1}]	$e\mu_\alpha \cos\delta$ [mas a^{-1}]	μ_δ [mas a^{-1}]	$e\mu_\delta$ [mas a^{-1}]	Ref.[a b]	V_r [km s^{-1}]	Ref.[c]	U [km s^{-1}]	V [km s^{-1}]	W [km s^{-1}]	Ref.[d]
J21137+087	155.8	0.3	-88.0	0.3	Gal15			-6.0		-15.4	Lep13
J21138+180	443.5	4.9	-50.5	4.9	PPMXL	-36.37	Ter15	-40.06	-34.15	-21.67	Mon16
J21145+508	219.0	0.4	0.9	0.5	Cortes			-12.8		-13.1	Lep13
J21147+380	196.99	0.3	410.28	0.3	aHIP2	-25.5	PMSU	-44.43	-18.16	16.51	Mon16
J21152+257	131.8	0.5	-271.0	0.3	Gal15	-15.89	Schf15	2.46	-22.6	-15.87	Mon16
J21160+298E	200.2	4.8	33.5	4.8	PPMXL	-5.0	New14	-16.55	-3.96	-10.47	Mon16
J21160+298W	200.2	4.8	33.5	4.8	aPPMXL	-10.3	PMSU	-17.71	-8.98	-9.26	Mon16
J21164+025	246.0	0.3	-39.6	0.4	Cortes	-22.1	Schf15	-21.76	-17.62	-2.46	Mon16
J21173+208N	315.4	5.0	290.8	5.6	PPMXL	-36.0	New14	-53.72	-18.55	7.07	Mon16
J21173+208S	315.4	5.0	290.8	5.6	PPMXL	-36.0	New14	-53.72	-18.55	7.07	Mon16
J21173+640	332.5	4.9	-24.4	4.9	PPMXL	7.0	New14	-32.89	6.95	-35.9	Mon16
J21176-089N	-76.4	5.7	-25.7	5.7	PPMXL	8.8	PMSU	11.06	2.9	-1.1	Mon16
J21176-089S	-76.4	5.7	-25.7	5.7	aPPMXL	35.3	PMSU	29.03	16.53	-15.29	Mon16
J21185+302	57.0	1.7	-21.0	1.7	PPMXL	-22.14	Schf15	-7.93	-22.02	-1.92	Mon16
J21221+229	110.0	4.6	122.6	4.8	PPMXL	5.54	Schf15	-11.16	9.01	-1.79	Mon16
J21243+085	-181.0	4.8	-171.2	4.8	PPMXL	-21.5	PMSU	31.76	-35.38	16.74	Mon16
J21245+400	545.4	4.9	441.0	4.9	PPMXL						
J21267+037	-38.1	2.94	-49.06	2.34	HIP2	-2.9	PMSU	5.41	-6.27	1.83	Mon16
J21272-068	23.27	3.3	-403.82	2.03	HIP2	16.9	PMSU	21.19	-16.12	-23.63	Mon16
J21275+340	-275.59	1.65	-183.74	2.15	HIP2	-70.6	PMSU	32.87	-72.71	23.17	Mon16
J21277+072	-222.8	4.8	-649.6	4.8	PPMXL	-12.3	PMSU	54.58	-57.82	-15.58	Mon16
J21280+179	75.7	4.9	150.6	4.9	PPMXL			-24.5		6.5	Lep13
J21283-223	-208.2	0.3	-266.2	0.9	Cortes	24.8	PMSU	36.3	-14.22	-9.02	Mon16
J21296+176	1007.13	2.75	377.27	1.13	HIP2	-25.1	PMSU	-38.54	-17.05	-4.6	Mon16
J21313-097	1191.3	1.8	-62.0	1.0	Cortes	-57.5	PMSU	-65.37	-34.93	4.02	Mon16
J21323+245	215.5	0.7	-30.1	0.7	Cortes	2.05	Schf15	-13.94	-0.72	-18.01	Mon16
J21338+017N	-40.7	0.2	-689.0	1.1	Gal15	-27.0	PMSU	13.4	-52.93	-5.44	Mon16
J21338+017S	-15.3	0.2	-767.7	1.3	Gal15	-27.0	PMSU	14.82	-57.0	-9.21	Mon16
J21338-068	121.4	0.3	-499.1	0.5	Cortes	-43.4	PMSU	-12.18	-61.64	3.07	Mon16
J21348+515	456.93	2.32	309.46	2.57	HIP2	-14.03	Schf15	-44.99	-17.94	-6.61	Mon16
J21366+394	-205.88	2.01	-156.57	1.84	HIP2	-15.7	PMSU	24.7	-16.44	4.96	Mon16
J21369+561	-6.5	5.1	149.6	5.1	PPMXL			-15.2		18.8	Lep13
J21374-059	13.6	5.4	151.7	5.4	PPMXL						

Table B.3: Proper motions and UVW space velocities of Carmencita stars (continued).

Karmn	$\mu_\alpha \cos\delta$ [mas a^{-1}]	$e\mu_\alpha \cos\delta$ [mas a^{-1}]	μ_δ [mas a^{-1}]	$e\mu_\delta$ [mas a^{-1}]	Ref.[a b]	V_r [km s^{-1}]	Ref.[c]	U [km s^{-1}]	V [km s^{-1}]	W [km s^{-1}]	Ref.[d]
J21376+016	79.3	0.3	-60.2	0.2	Gal15	-0.9	Schf15	-1.87	-3.14	-3.6	Mon16
J21378+530	312.22	1.44	52.64	1.51	HIP2	-57.0	PMSU	-33.59	-60.77	-25.69	Mon16
J21380+277	471.53	1.69	-75.12	1.38	HIP2	-18.0	PMSU	-22.39	-20.7	-17.42	Mon16
J21399+276	281.48	2.72	-231.09	2.26	HIP2	6.7	PMSU	-6.0	-5.92	-41.86	Mon16
J21402+370	-399.5	4.7	-293.4	4.7	PPMXL	-29.2	Daw05	61.16	-31.81	12.45	Mon16
J21419+276	-302.4	4.7	-61.2	4.7	PPMXL	23.1	PMSU	31.37	21.96	8.63	Mon16
J21421-121	109.2	0.4	-678.8	1.0	Cortes	-19.8	PMSU	18.29	-109.1	-34.17	Mon16
J21441+170N	244.2	0.4	2.3	0.6	Cortes	12.8	PMSU	-9.0	9.41	-16.39	Mon16
J21441+170S	252.6	0.1	-2.2	0.8	Cortes	3.3	PMSU	-12.81	1.01	-13.47	Mon16
J21442+066	-328.07	4.01	-166.73	2.03	HIP2	26.9	PMSU	43.48	11.98	-2.47	Mon16
J21449+442	-138.73	2.38	-654.99	2.61	HIP2			67.2		-50.3	Lep13
J21450+198	-18.25	3.91	-249.49	4.73	HIP2			24.1		-21.2	Lep13
J21450-057	-176.3	5.4	-437.7	5.4	PPMXL	11.8	PMSU	51.61	-40.84	-15.85	Mon16
J21454-059	-146.9	5.4	-342.5	5.4	PPMXL	-45.3	PMSU	6.67	-55.14	25.44	Mon16
J21463+382	168.2	4.7	-125.3	4.7	PPMXL	-83.13	Schf15	-5.01	-82.6	10.36	Mon16
J21466+668	390.5	4.9	204.5	4.9	PPMXL	-9.54	Schf15	-24.41	-15.66	-8.05	Mon16
J21466-001	767.8	5.1	-503.7	5.1	PPMXL	20.4	PMSU	-10.48	-12.47	-53.66	Mon16
J21469+466	277.6	0.3	-2.7	0.5	Gal15	-6.23	Schf15	-14.55	-8.19	-12.24	Mon16
J21472-047	255.2	0.2	4.6	0.5	Cortes	-31.68	Schf15	-28.12	-20.29	9.82	Mon16
J21478+502	695.1	4.8	426.1	4.8	PPMXL	-3.3	PMSU	-79.95	-11.64	-11.55	Mon16
J21479+058	326.2	2.3	-322.1	2.1	PPMXL	-28.4	PMSU	-20.94	-52.93	-31.77	Mon16
J21481+014	219.4	0.3	-34.3	0.4	Gal15	30.0	PMSU	-7.81	13.78	-39.36	Mon16
J21482+279	-179.6	1.4	-685.8	0.8	Gal15	11.0	PMSU	51.21	-9.21	-35.17	Mon16
J21512+128	663.4	5.0	125.0	5.5	PPMXL	-81.0	PMSU	-96.44	-65.48	-1.35	Mon16
J21518+136	173.4	5.0	-118.2	5.0	PPMXL	-14.3	PMSU	-9.19	-18.25	-6.34	Mon16
J21521+056	119.17	7.95	-150.29	4.89	HIP2	-20.5	PMSU	-9.43	-31.61	-10.05	Mon16
J21521+274	280.3	4.5	-757.3	4.5	PPMXL	-130.0	New14	9.33	-154.39	-32.69	Mon16
J21539+417	384.09	1.28	-357.27	1.29	HIP2	-50.4	PMSU	-6.92	-59.55	-47.75	Mon16
J21566+197	-106.1	4.6	-490.1	4.6	PPMXL	-81.0	PMSU	12.7	-88.14	16.26	Mon16
J21569-019	1280.2	5.1	615.9	5.1	PPMXL	-45.8	PMSU	-100.74	-9.18	-2.76	Mon16
J21574+081	380.42	2.34	101.76	2.08	PPMXL	-26.58	Schf15	-42.74	-18.4	-2.0	Mon16
J21584+755	231.85	1.24	21.91	1.26	HIP2	-18.03	Schf15	-12.24	-19.98	-17.38	Mon16
J21585+612	803.3	0.8	111.1	0.4	Gal15						

Table B.3: Proper motions and UVW space velocities of Carmencita stars (continued).

Karmn	$\mu_\alpha \cos\delta$ [mas a^{-1}]	$e\mu_\alpha \cos\delta$ [mas a^{-1}]	μ_δ [mas a^{-1}]	$e\mu_\delta$ [mas a^{-1}]	Ref.[a b]	V_r [km s^{-1}]	Ref.[c]	U [km s^{-1}]	V [km s^{-1}]	W [km s^{-1}]	Ref.[d]
J21593+418	108.3	4.9	-401.1	4.9	PPMXL	-26.9	PMSU	17.07	-32.73	-32.24	Mon16
J22012+283	374.05	2.74	37.45	3.27	HIP2	-2.0	Schf15	-13.58	-3.53	-7.65	Mon16
J22012+323	116.6	3.7	60.1	2.3	Cortes			-19.3		-3.9	Lep13
J22018+164	391.82	2.08	156.08	2.21	HIP2	-23.8	PMSU	-36.02	-17.79	1.34	Mon16
J22020-194	927.7	5.3	79.79	5.3	PPMXL	-23.25	Schf15	-56.96	-11.99	-14.02	Mon16
J22021+014	-454.53	1.86	-279.09	0.97	HIP2	18.18	Schf15	30.78	5.41	-4.93	Mon16
J22033+674	532.2	4.8	-299.6	4.8	PPMXL	-82.6	PMSU	3.28	-76.23	-59.98	Mon16
J22035+036	1.1	4.7	-120.0	4.7	PPMXL						
J22051+051	458.3	4.7	140.5	4.7	PPMXL	-13.7	PMSU	-42.46	-7.44	-8.79	Mon16
J22057+656	-336.9	0.4	223.1	0.4	Gal15	-46.56	Schf15	22.88	-44.78	17.53	Mon16
J22058-119	-265.45	2.75	-174.46	1.57	HIP2	16.88	Schf15	37.27	-3.48	-1.83	Mon16
J22060+393	69.4	1.9	-458.3	1.3	Cortes	-1.0	PMSU	21.42	-9.4	-37.73	Mon16
J22063+173	368.3	1.1	80.6	1.1	PPMXL			-34.3		-15.1	Lep13
J22067+034	468.3	4.8	-324.4	4.8	PPMXL	-36.2	PMSU	-29.48	-50.1	-12.86	Mon16
J22088+117	90.5	5.0	-50.9	5.0	PPMXL	-8.9	Schf15	-5.98	-10.77	-1.84	Mon16
J22095+118	163.5	5.0	-125.0	5.0	PPMXL						
J22096-046	1130.27	2.56	-19.27	1.33	HIP2	-15.57	Schf15	-44.74	-17.78	-17.39	Mon16
J22097+410	419.8	4.9	240.0	4.9	PPMXL	-90.91	Schf15	-46.63	-92.55	13.59	Mon16
J22107+079	248.1	4.11	24.21	2.69	HIP2	-7.0	Dy54	-40.11	-9.87	-19.02	Mon16
J22112+410	-209.23	1.49	233.23	1.63	HIP2			3.1		32.5	Lep13
J22112-025	425.8	4.7	-92.1	4.7	PPMXL	-32.7	PMSU	-46.94	-36.67	-10.09	Mon16
J22114+409	-89.6	4.9	68.0	4.9	PPMXL	-16.64	Schf15	2.4	-15.03	8.61	Mon16
J22115+184	329.12	1.27	178.2	1.23	HIP2	-51.45	Schf15	-29.29	-41.65	21.87	Mon16
J22117-207	142.0	6.7	-71.3	6.7	PPMXL	-10.0	PMSU	-15.27	-13.64	-2.73	Mon16
J22125+085	112.89	4.89	-664.43	3.5	HIP2	8.63	Schf15	20.86	-25.26	-35.85	Mon16
J22129+550	-106.0	2.0	34.6	2.0	PPMXL			9.3		12.8	Lep13
J22134-147	-297.9	5.2	-270.5	5.2	HIP2	-31.0	PMSU	21.03	-32.48	34.08	Mon16
J22135+259	154.3	0.5	-144.2	0.8	Gal15	-28.5	PMSU	-6.23	-33.08	-4.73	Mon16
J22137-176	859.4	5.2	-311.8	5.2	PPMXL	-24.073	Schf15	-39.99	-30.64	-8.29	Mon16
J22138+052	183.17	3.68	-38.13	2.23	HIP2	10.7	PMSU	-12.96	0.19	-22.38	Mon16
J22142+255	159.6	4.6	-51.8	4.6	PPMXL	-19.9	Shk12	-17.31	-25.56	-11.3	Mon16
J22154+662	4.9	0.2	206.1	0.4	Cortes	-0.29	Schf15	-7.91	-4.7	12.28	Mon16
J22160+546	207.9	0.3	67.0	0.8	Gal15	5.0	PMSU	-20.17	0.78	-5.8	Mon16

Table B.3: Proper motions and UVW space velocities of Carmencita stars (continued).

Karmn	$\mu_\alpha \cos\delta$ [mas a^{-1}]	$e\mu_\alpha \cos\delta$ [mas a^{-1}]	μ_δ [mas a^{-1}]	$e\mu_\delta$ [mas a^{-1}]	Ref.[a b]	V_r [km s^{-1}]	Ref.[c]	U [km s^{-1}]	V [km s^{-1}]	W [km s^{-1}]	Ref.[d]
J22163+709	862.4	3.4	-41.3	3.5	PPMXL	-11.7	PMSU	-67.02	-25.78	-56.23	Mon16
J22173-088N	-439.3	2.1	-226.1	3.2	Cortes	34.7	PMSU	36.18	12.64	-18.12	Mon16
J22173-088S	-449.0	0.5	-237.6	0.5	Cortes	34.7	PMSU	35.93	12.47	-18.37	Mon16
J22176+565	98.8	4.8	76.8	4.8	PPMXL			-20.4		2.8	Lep13
J22202+067	280.2	5.0	282.9	5.0	PPMXL						
J22212+377	144.8	4.9	44.6	4.9	PPMXL			-23.2		-5.3	Lep13
J22228+280	402.7	0.5	-78.3	0.5	Cortes	-43.3	PMSU	-37.76	-53.19	-16.59	Mon16
J22231-176	305.3	5.1	-723.0	5.1	PPMXL	-2.39	Schf15	-0.5	-25.55	-9.18	Mon16
J22234+324	252.8	4.1	-208.0	3.0	Cortes	-21.0	New14	-6.23	-27.58	-13.46	Mon16
J22249+520	227.5	4.9	439.4	4.9	PPMXL	10.6	PMSU	-34.1	5.51	18.1	Mon16
J22250+356	-50.1	3.4	-154.8	3.5	PPMXL			14.3		-9.1	Lep13
J22252+594	117.8	4.8	-314.9	4.8	PPMXL	3.77	Schf15	4.4	5.96	-28.46	Mon16
J22262+030	-494.7	0.6	-454.4	0.2	Gal15	15.5	PMSU	67.31	-11.46	-7.09	Mon16
J22264+583	-131.5	5.0	70.9	5.0	PPMXL						
J22270+068	169.4	5.0	-33.7	5.0	PPMXL	5.7	PMSU	-6.66	0.23	-10.76	Mon16
J22279+576	-865.47	2.16	-461.53	2.03	HIP2	-29.0	PMSU	25.31	-23.34	1.09	Mon16
J22287+189	166.77	1.45	-128.11	1.44	HIP2	-59.3	PMSU	-13.86	-60.12	13.84	Mon16
J22289-134	-322.2	5.1	-1041.6	5.1	PPMXL	-7.4	PMSU	32.57	-46.5	-0.21	Mon16
J22290+016	43.96	2.17	-195.16	1.53	HIP2			6.0	-15.5		Lep13
J22298+414	1190.8	4.8	449.2	4.8	PPMXL	1.77	Schf15	-80.85	-11.29	-16.44	Mon16
J22300+488	-78.0	5.0	68.7	5.0	PPMXL	-3.0	Schf15	2.52	-1.61	7.35	Mon16
J22330+093	537.64	2.57	139.45	2.04	HIP2	-4.7	PMSU	-32.22	-5.58	-8.54	Mon16
J22333-096	144.4	5.1	6.7	5.1	PPMXL	-4.4	Shk12	-11.39	-4.38	-2.14	Mon16
J22347+040	-97.4	5.1	129.5	5.1	PPMXL	1.1	PMSU	2.12	13.78	12.34	Mon16
J22348-010	1102.5	4.6	217.6	4.6	PPMXL	-12.9	PMSU	-117.56	-18.34	-41.01	Mon16
J22353+746	255.33	1.57	79.02	1.4	HIP2			-43.2		-10.7	Lep13
J22361-008	48.8	2.01	-628.16	1.46	HIP2	-15.8	PMSU	16.92	-49.12	-12.86	Mon16
J22373+299	199.5	4.9	-229.2	4.9	PPMXL			-6.8		-39.9	Lep13
J22374+395	18.63	1.71	-342.34	1.31	HIP2	-53.4	BE12	21.39	-57.13	-11.77	Mon16
J22385-152	2307.5	0.9	2293.6	0.5	Gal15	-37.4	PMSU	-60.51	8.97	22.09	Mon16
J22387+252	295.0	0.4	5.1	0.4	Gal15						
J22387-206N	448.87	1.33	-79.69	1.01	aHIP2	-7.0	PMSU	-17.16	-9.77	-3.55	Mon16
J22387-206S	448.87	1.33	-79.69	1.01	HIP2	-28.5	PMSU	-25.89	-16.54	14.89	Mon16

Table B.3: Proper motions and UVW space velocities of Carmencita stars (continued).

Karmn	$\mu_\alpha \cos\delta$ [mas a^{-1}]	$e\mu_\alpha \cos\delta$ [mas a^{-1}]	μ_δ [mas a^{-1}]	$e\mu_\delta$ [mas a^{-1}]	Ref.[a b]	V_r [km s^{-1}]	Ref.[c]	U [km s^{-1}]	V [km s^{-1}]	W [km s^{-1}]	Ref.[d]
J22406+445	481.7	0.6	-38.8	0.4	Cortes	33.5	PMSU	-61.35	14.17	-45.51	Mon16
J22415+188	235.62	2.12	54.4	2.03	HIP2	-52.5	PMSU	-43.03	-48.72	16.49	Mon16
J22415+260	-24.5	4.9	58.1	4.9	PPMXL						
J22426+176	1105.72	2.46	515.57	2.41	HIP2	-12.83	Schf15	-121.33	-11.63	-10.77	Mon16
J22433+221	390.0	5.0	1.3	5.0	PPMXL	-24.5	PMSU	-30.69	-29.86	-3.66	Mon16
J22437+192	-6.1	6.4	51.6	6.4	PPMXL						
J22440+405	-71.9	1.6	-117.9	1.6	PPMXL			14.6		-7.8	Lep13
J22441+405	-73.1	1.6	-126.0	1.6	PPMXL			14.8		-7.7	Lep13
J22457+016	199.19	4.36	-49.49	3.61	HIP2			-18.7	-11.0		Lep13
J22464-066	691.5	5.0	-543.1	5.0	PPMXL	36.1	PMSU	-20.1	-37.02	-75.3	Mon16
J22468+443	-705.36	1.12	-460.72	1.33	HIP2	0.57	Schf15	20.0	3.9	-1.85	Mon16
J22476+184	385.8	5.1	195.4	5.1	PPMXL						
J22479+318	460.2	4.9	173.1	4.9	PPMXL	1.2	PMSU	-50.03	-6.18	-8.11	Mon16
J22489+183	-24.7	5.1	-132.8	5.1	PPMXL						
J22503-070	-106.5	3.16	104.55	1.62	HIP2	-6.03	BE12	1.27	4.62	10.64	Mon16
J22506+348	840.63	2.18	317.29	1.83	HIP2	-4.9	PMSU	-72.43	-16.83	-8.0	Mon16
J22507+286	193.7	0.6	-55.9	0.7	Cortes	-7.2	PMSU	-11.97	-13.15	-8.5	Mon16
J22509+499	106.4	6.1	-12.0	6.1	PPMXL	-17.7	Schf15	-4.2	-19.95	-3.18	Mon16
J22518+317	523.75	2.39	-51.73	2.1	HIP2	8.6	PMSU	-29.5	-3.45	-22.37	Mon16
J22524+099	521.04	0.24	42.65	0.24	aHIP2	-11.0	PMSU	-51.15	-20.8	-14.47	Mon16
J22526+750	101.2	4.6	-104.9	4.6	PPMXL	-20.2	West15	5.2	-16.97	-13.09	Mon16
J22532-142	959.84	3.36	-675.33	1.68	HIP2	-3.3	PMSU	-12.91	-20.47	-10.29	Mon16
J22543+609	-707.4	5.0	-131.1	5.0	PPMXL	-21.4	PMSU	54.36	-4.03	13.2	Mon16
J22547-054	615.0	5.0	334.9	5.0	PPMXL	-12.2	PMSU	-83.7	4.39	-6.61	Mon16
J22559+057	356.76	2.34	-269.79	1.75	HIP2	-1.0	PMSU	-19.84	-34.09	-33.68	Mon16
J22559+178	29.2	1.6	-111.6	1.6	PPMXL	-32.2	Schf15	1.57	-30.96	12.55	Mon16
J22565+165	-1034.34	0.97	-284.09	1.06	HIP2	-81.7	PMSU	30.15	-59.33	58.78	Mon16
J22576+373	545.4	4.9	-362.0	4.9	PPMXL			67.0		-6.8	Lep13
J23028+436	-138.0	0.4	-4.9	0.2	Cortes	1.0	New14	7.01	3.45	2.83	Mon16
J23036+097	88.4	4.7	42.8	4.7	PPMXL						
J23045+667	303.36	0.94	-79.96	0.9	HIP2	20.4	PMSU	-30.26	11.49	-16.44	Mon16
J23051+452	165.9	5.0	65.9	5.0	PPMXL	-3.0	New14	-20.32	-8.32	-0.22	Mon16
J23051+519	79.6	4.9	-96.2	4.9	PPMXL						

Table B.3: Proper motions and UVW space velocities of Carmencita stars (continued).

Karmn	$\mu_\alpha \cos\delta$ [mas a^{-1}]	$e\mu_\alpha \cos\delta$ [mas a^{-1}]	μ_δ [mas a^{-1}]	$e\mu_\delta$ [mas a^{-1}]	Ref.[a b]	V_r [km s^{-1}]	Ref.[c]	U [km s^{-1}]	V [km s^{-1}]	W [km s^{-1}]	Ref.[d]
J23060+639	171.46	1.59	-58.55	1.57	HIP2	-22.8	Schf15	-6.4	-26.14	-15.44	Mon16
J23063+126	319.96	5.9	-64.32	3.89	HIP2	-3.53	Shk10	-52.46	-32.78	-33.23	Mon16
J23064-050	878.5	2.5	-496.7	1.3	Cortes	-56.3	RB09	-41.8	-68.99	15.27	Mon16
J23065+717	1255.4	0.5	435.0	0.4	Gal15	-30.8	PMSU	-91.11	-73.75	-14.33	Mon16
J23075+686	1136.6	4.6	50.5	4.6	PPMXL	18.7	PMSU	-79.73	-10.48	-26.31	Mon16
J23081+033	491.92	2.35	255.74	1.92	HIP2	-42.8	PMSU	-46.27	-24.94	28.4	Mon16
J23083-154	104.58	2.76	-23.03	2.19	HIP2	-11.67	Schf15	-11.59	-9.92	5.6	Mon16
J23088+065	100.9	2.89	-45.21	2.61	HIP2	-6.8	Tor06	-12.47	-16.14	-6.61	Mon16
J23089+551	329.9	5.0	38.1	5.0	PPMXL	-54.0	New14	-3.81	-58.66	-1.73	Mon16
J23096-019	273.0	0.9	-381.4	1.3	Cortes	-11.7	PMSU	-5.61	-33.78	-9.58	Mon16
J23107-192	43.4	6.0	-1435.9	6.0	PPMXL	-18.4	PMSU	58.77	-155.28	-12.49	Mon16
J23113+085	-320.5	5.8	-316.2	5.8	PPMXL	-10.57	Schf15	27.63	-13.73	3.84	Mon16
J23121-141	-187.5	0.7	-702.6	0.7	Cortes	39.5	PMSU	57.68	-40.96	-45.82	Mon16
J23142-196N	442.94	2.45	59.06	2.22	HIP2	5.8	PMSU	-36.75	-7.42	-19.67	Mon16
J23142-196S	442.94	2.45	59.06	2.22	aHIP2	5.8	PMSU	-36.75	-7.42	-19.67	Mon16
J23161+067	176.1	5.9	-253.5	5.9	PPMXL	29.7	PMSU	-0.73	-0.23	-39.59	Mon16
J23166+196	-178.86	2.52	-178.41	2.08	HIP2	9.0	New14	34.91	2.72	-14.49	Mon16
J23174+196	361.1	0.6	-101.8	0.2	Gal15	0.0	New14	-11.37	-7.64	-8.62	Mon16
J23174+382	-194.1	0.8	-423.1	0.5	Gal15	14.9	PMSU	26.46	10.83	-29.93	Mon16
J23175+063	176.3	0.3	-256.4	0.2	Gal15	26.03	Schf15	-1.04	-4.23	-37.89	Mon16
J23182+462	330.15	1.25	135.65	1.67	HIP2	-9.5	PMSU	-37.55	-20.64	3.03	Mon16
J23182+795	505.4	4.7	-107.4	4.7	PPMXL						
J23193+154	59.9	4.7	-144.9	4.7	PPMXL			2.2		-19.7	Lep13
J23194+790	201.6	0.5	71.6	0.4	Gal15	-16.5	Schf15	-9.67	-23.0	-5.38	Mon16
J23215+568	-32.3	4.9	-186.9	4.9	PPMXL			13.4		-28.9	Lep13
J23216+172	-534.13	3.29	-1382.74	2.1	HIP2	-6.43	Schf15	59.82	-34.32	-35.34	Mon16
J23220+569	389.0	0.4	84.5	0.4	Cortes	-26.32	Ter15	-36.05	-42.38	-4.74	Mon16
J23228+787	201.6	0.5	71.6	0.4	Gal15						
J23229+372	63.8	4.8	-61.0	4.8	PPMXL	16.21	Ter15	-7.17	9.84	-15.2	Mon16
J23234+155	3.0	1.0	-468.0	1.0	PPMXL	-44.34	Schf15	23.69	-58.25	0.26	Mon16
J23245+578	-63.62	1.47	-280.37	1.32	HIP2	-30.3	PMSU	20.13	-25.45	-13.32	Mon16
J23249+506	50.9	0.3	5.8	0.4	Cortes			-4.2		0.5	Lep13
J23252+009	420.9	5.0	-496.6	5.0	PPMXL			-22.4	-88.5		Lep13

Table B.3: Proper motions and UVW space velocities of Carmencita stars (continued).

Karmn	$\mu_\alpha \cos\delta$ [mas a^{-1}]	$e\mu_\alpha \cos\delta$ [mas a^{-1}]	μ_δ [mas a^{-1}]	$e\mu_\delta$ [mas a^{-1}]	Ref.[a b]	V_r [km s^{-1}]	Ref.[c]	U [km s^{-1}]	V [km s^{-1}]	W [km s^{-1}]	Ref.[d]
J23256+531	1012.9	0.7	326.9	0.4	Gal15	-32.8	PMSU	-93.82	-69.41	1.87	Mon16
J23261+170	132.7	4.7	-68.1	4.7	PPMXL						
J23262+088	519.44	2.13	213.24	2.1	HIP2	-44.0	PMSU	-61.41	-34.88	28.02	Mon16
J23262+278	-47.4	0.3	-38.1	0.4	Cortes						
J23265+121	692.6	0.5	263.0	0.6	Cortes	-19.1	PMSU	-90.04	-24.93	6.24	Mon16
J23293+414N	412.9	1.0	-40.8	0.4	Gal15	-14.7	Schf15	-20.27	-24.82	-6.93	Mon16
J23293+414S	401.4	0.4	-47.5	0.7	Gal15	-8.8	PMSU	-20.99	-19.26	-9.0	Mon16
J23301-026	101.7	4.6	-77.3	4.6	PPMXL						
J23302-203	311.76	3.18	-207.38	2.96	HIP2	-43.4	PMSU	-23.72	-34.2	31.28	Mon16
J23308+157	-163.6	1.6	-108.8	1.4	PPMXL			24.5		-1.7	Lep13
J23317-027	95.1	4.7	-73.3	4.7	PPMXL	-5.0	Malo14a	-6.98	-15.35	-3.89	Mon16
J23318+199E	554.64	1.4	-60.43	1.08	HIP2	27.8	PMSU	-16.62	14.19	-23.75	Mon16
J23318+199W	554.64	1.4	-60.43	1.08	aHIP2	27.8	PMSU	-16.62	14.19	-23.75	Mon16
J23323+540	211.9	4.8	-6.4	4.8	PPMXL			-25.0		-8.2	Lep13
J23327-167	342.97	2.55	-218.93	4.02	aHIP2	-13.8	PMSU	-17.08	-27.43	2.41	Mon16
J23340+001	-994.63	3.51	-937.22	2.79	HIP2	-5.0	Schf15	87.46	-23.55	-4.86	Mon16
J23350+016	341.31	1.73	25.5	1.02	HIP2	-11.68	Tok15	-28.33	-16.82	1.81	Mon16
J23350+252	31.4	4.7	174.4	5.1	PPMXL	-29.3	PMSU	-6.36	-16.68	29.9	Mon16
J23351-023	776.9	0.6	-845.3	0.9	Gal15	-41.9	PMSU	-11.81	-53.81	16.14	Mon16
J23354+300	-188.6	4.8	-273.9	4.8	PPMXL	8.1	PMSU	36.0	2.88	-26.38	Mon16
J23357+419	700.81	1.65	149.82	1.57	HIP2	-31.0	PMSU	-76.68	-59.15	1.36	Mon16
J23364+554	492.23	2.2	-92.56	2.16	HIP2	-39.3	PMSU	-32.59	-58.69	-23.03	Mon16
J23376-128	204.6	0.5	-322.0	0.4	Cortes						
J23381-162	-281.1	3.7	-82.8	3.4	PPMXL	20.67	Schf15	25.42	9.36	-14.58	Mon16
J23386+391	-244.8	4.9	-510.1	4.9	PPMXL	15.2	PMSU	29.82	11.27	-37.32	Mon16
J23389+210	276.7	0.4	185.6	0.4	Gal15	-9.3	PMSU	-40.69	-9.18	13.36	Mon16
J23401+606	89.6	2.1	-270.1	2.1	PPMXL	3.7	PMSU	-2.6	2.27	-32.4	Mon16
J23414+200	-184.0	1.9	-132.8	2.0	PPMXL			35.2		-7.4	Lep13
J23419+441	103.5	4.7	-1591.2	4.7	PPMXL	-75.2	Des12	31.74	-72.23	-0.4	Mon16
J23423+349	72.8	4.8	-134.3	4.8	PPMXL						
J23428+308	-341.9	4.8	-299.2	4.8	PPMXL	-8.0	New14	27.3	-5.02	-5.46	Mon16
J23431+365	947.7	0.4	-149.2	0.2	Gal15	2.0	New14	-30.15	-14.73	-15.34	Mon16
J23438+325	-219.0	1.9	-57.8	1.8	PPMXL	-14.0	PMSU	21.54	-6.02	7.27	Mon16

Table B.3: Proper motions and UVW space velocities of Carmencita stars (continued).

Karmn	$\mu_\alpha \cos\delta$ [mas a^{-1}]	$e\mu_\alpha \cos\delta$ [mas a^{-1}]	μ_δ [mas a^{-1}]	$e\mu_\delta$ [mas a^{-1}]	Ref.[a b]	V_r [km s^{-1}]	Ref.[c]	U [km s^{-1}]	V [km s^{-1}]	W [km s^{-1}]	Ref.[d]
J23438+610	-617.7	0.4	-496.5	0.4	Gal15						
J23439+647	541.53	2.0	91.27	1.83	HIP2	28.9	PMSU	-79.07	-5.8	-5.56	Mon16
J23443+216	456.0	4.9	80.9	4.9	PPMXL	-8.9	PMSU	-43.88	-22.05	-0.43	Mon16
J23455-161	-396.5	5.0	-560.8	5.0	PPMXL	-25.5	PMSU	32.55	-26.43	23.42	Mon16
J23462+284	78.9	4.7	66.7	4.7	PPMXL	15.82	Ter15	-11.62	12.42	-5.66	Mon16
J23480+490	624.7	2.3	69.68	2.15	HIP2	18.0	New14	-46.56	-1.6	-9.94	Mon16
J23489+098	157.44	4.68	-49.41	2.83	HIP2			-25.6	-22.6		Lep13
J23492+024	996.96	1.93	-967.88	0.69	HIP2	-71.226	Schf15	-9.06	-70.63	39.42	Mon16
J23492+100	30.2	4.7	-382.1	4.7	PPMXL	26.1	PMSU	10.55	-5.36	-39.99	Mon16
J23496+083	121.8	3.0	-68.7	3.0	PPMXL	-10.1	PMSU	-8.1	-18.01	-0.4	Mon16
J23505-095	635.9	4.9	-422.0	4.9	PPMXL	-21.85	Schf15	-28.18	-55.07	-0.95	Mon16
J23506+099	633.8	4.1	248.2	3.9	PPMXL	-5.0	New14	-35.8	-9.01	3.85	Mon16
J23509+384	-86.3	4.7	-206.9	4.7	PPMXL	-8.7	PMSU	17.74	-9.35	-12.91	Mon16
J23517+069	-44.8	4.8	-291.9	4.8	PPMXL	13.6	PMSU	15.39	-8.45	-24.94	Mon16
J23523-146	416.7	4.8	-257.6	4.8	PPMXL	17.6	PMSU	-24.24	-37.29	-32.96	Mon16
J23535+121	45.55	3.2	-111.52	1.85	aHIP2			2.9	-17.4		Lep13
J23541+516	256.6	4.7	84.8	4.7	PPMXL	-27.9	PMSU	-9.16	-33.72	6.97	Mon16
J23544+081	-273.6	0.7	-49.5	0.5	Cortes	-20.8	PMSU	31.39	-3.09	19.93	Mon16
J23548+385	-136.3	4.7	-91.5	4.7	PPMXL	5.74	Schf15	9.55	7.52	-6.18	Mon16
J23554-039	524.2	5.3	2.1	5.3	PPMXL	30.1	PMSU	-57.17	-14.57	-40.8	Mon16
J23556-061	-493.74	3.95	-387.51	1.64	HIP2	17.79	Schf15	54.88	-0.79	-19.14	Mon16
J23560+150	-123.9	4.5	-177.5	4.5	PPMXL						
J23569+230	-77.4	5.3	-267.2	5.3	PPMXL	-18.46	Ter15	26.07	-25.57	-10.98	Mon16
J23573-129E	200.5	0.8	18.3	0.4	Cortes	20.5	PMSU	-14.2	0.4	-22.52	Mon16
J23573-129W	200.8	0.8	20.4	0.8	Cortes	12.3	PMSU	-12.64	-1.23	-14.29	Mon16
J23577+197	127.0	4.9	-484.7	4.9	PPMXL	18.7	PMSU	5.18	-14.42	-45.69	Mon16
J23577+233	1013.5	4.6	-1048.8	4.6	PPMXL	-35.79	Schf15	-20.13	-89.21	-43.46	Mon16
J23578+386	-137.6	1.0	-144.9	0.5	Cortes	-5.0	New14	16.43	-2.46	-6.8	Mon16
J23582-174	221.0	0.4	14.3	0.3	Cortes	-8.7	Shk12	-20.95	-10.74	4.08	Mon16
J23585+076	79.75	3.02	-311.83	1.79	HIP2	-7.72	Schf15	7.07	-24.12	-9.22	Mon16
J23587+467	668.39	1.51	-7.98	1.47	HIP2	14.4	PMSU	-53.93	-11.93	-15.67	Mon16
J23590+208	264.1	4.9	-111.9	4.9	PPMXL						
J23598+477	867.6	0.9	-199.4	1.2	Gal15	-47.0	PMSU	-45.58	-79.38	-21.54	Mon16

Notes. [a] The "a" or "b" letter preceeding the reference indicates that the value was taken from the A or B component of the multiple system.
[b] Cortes: this work; Gal5: Gallardo (2015); HIP2: van Leeuwen (2007); PPMXL: Roeser et al. (2010).
[c] BJ14: Binks & Jeffries (2014); Boc05: Bochanski et al. (2005); BE12: de Bruijne & Eilers (2012); Burg15: Burgasser et al. (2015); Cab10: Caballero et al. (2010); Daw05: Dawson et al. (2005); Del98: Delfosse et al. (1998); Del99a: Delfosse et al. (1999a); Des12: Deshpande et al. (2012); Dy54: Dyer (1954); Ell14: Elliott et al. (2014); Eva79: Evans (1979); Lat02: Latham et al. (2002); Mald10: Maldonado et al. (2010); Malo14a: Malo et al. (2014a); Mo02: Mochnacki et al. (2002); Mon01: Montes et al. (2001); Moo13: Moór et al. (2013); New14: Newton et al. (2014); PMSU: (Palomar/Michigan State University survey catalogue of nearby stars) Reid et al. (1995), Hawley et al. (1996), Gizis et al. (2002); RB09: Reiners & Basri (2009); Ried11: Riedel et al. (2011); RAVE: Siebert et al. (2011); Schf15: Schöfer (2015); Schl10: Schlieder et al. (2010); Shk10: Shkolnik et al. (2010); Shk12: Shkolnik et al. (2012); Ter15: Terrien et al. (2015); Tok02: Tokovinin et al. (2002); Tokovinin et al. (2015); Tor06: Torres et al. (2006); UH96: Upgren & Harlow (1996); West15: West et al. (2015); Wh07: White et al. (2007); Wil53: Wilson (1953); Zuck11: Zuckerman et al. (2011).
[d] Lep13: Lépine et al. (2013); Mon16: Montes priv. comm.

Table B.4: Activity indicators, stellar kinematic associations and poputation of Carmencita stars.

Karmn	Activity[a]							
	pEW(Hα)	X-rays	$v \sin i$	P	SKG[b]	Ref.[c]	Population[d]	Ref.[e]
J00012+139S		×						
J00012+139N		×					D	Mon16
J00026+383		×						
J00033+046		×						
J00051+457					HS	Mon16	YD	Mon16
J00056+458		×			HS	Mon16	YD	Mon16
J00067-075							D	Mon16
J00077+603	×	×	×		IC	Mon16	YD	Mon16
J00078+676	×							
J00079+080							D	Mon16
J00081+479	×	×		×			D	Mon16
J00084+174					UMa	Mon16	D	Mon16
J00088+208	×	×	×		UMa	Mon16	D	Mon16
J00110+052								
J00115+591	×							
J00118+229		×					D	Mon16
J00119+330								
J00122+304	×	×						
J00131+703								
J00132+693							D	Mon16
J00133+275	×							
J00136+806			×				YD	Mon16
J00137+806	×	×					D	Mon16
J00154-161		×					YD	Mon16
J00156+722								
J00158+135							D	Mon16
J00159-166		×					D	Mon16
J00162+198W	×	×		×			TD	Mon16
J00162+198E							TD-D	Mon16
J00169+051							D	Mon16
J00169+200	×	×	×	×			D	Mon16
J00173+291							TD	Mon16
J00176-086		×					YD	Mon16
J00179+209								
J00182+102							D	Mon16
J00183+440		×					D	Mon16
J00184+440		×			HS	Mon16	YD	Mon16
J00188+278	×			×	IC	Mon16	YD	Mon16
J00201-170							YD	Mon16
J00204+330			×				TD-D	Mon16
J00207+596								
J00209+176								
J00210+557								
J00218+382							D	Mon16
J00219+492	×	×		×	IC	Mon16	YD	Mon16
J00234+243							D	Mon16

Table B.4: Activity indicators, stellar kinematic associations and poputation of Carmencita stars (continued).

Karmn	Activity[a]				SKG[b]	Ref.[c]	Population	Ref.[d]
	pEW(Hα)	X-rays	$v \sin i$	P				
J00234+771							D	Mon16
J00235+771							D	Mon16
J00240+264	×			×			D	Mon16
J00244+360								
J00245+300	×	×	×	×	HS	Mon16	D	Mon16
J00253+228							D	Mon16
J00268+701							D	Mon16
J00271+496							TD-D	Mon16
J00279+223		×	×				D	Mon16
J00286-066							D	Mon16
J00288+503	×	×		×			YD	Mon16
J00315-058							TD-D	Mon16
J00322+544							D	Mon16
J00324+672N		×	×				D	Mon16
J00324+672S			×				D	Mon16
J00325+074	×	×	×		bPic	Schl12b	YD	Mon16
J00328-045	×							
J00333+368								
J00341+253	×	×	×	×	ABDor?	Schl10	YD	Mon16
J00346+711							D	Mon16
J00357+025								
J00358+526							D	Mon16
J00359+104							TD-D	Mon16
J00361+455							D	Mon16
J00374+515		×		×				
J00380+169								
J00382+523							D	Mon16
J00385+514					UMa	Mon16	D	Mon16
J00389+306		×					D	Mon16
J00395+149S		×			HS	Mon16	YD	Mon16
J00395+149N	×							
J00395+605							D	Mon16
J00409+313							D	Mon16
J00413+558							D	Mon16
J00427+438		×						
J00428+355	×	×	×	×			YD	Mon16
J00435+284							TD	Mon16
J00443+126							D	Mon16
J00443+091							D	Mon16
J00449-152							TD	Mon16
J00459+337		×						
J00463+353	×							
J00464+506								
J00468+160								
J00484+753	×							
J00487+270							D	Mon16
J00489+445	×	×	×	×	ABDor?	Schl12b	D	Mon16
J00490+657								

Table B.4: Activity indicators, stellar kinematic associations and poputation of Carmencita stars (continued).

	Activity[a]							
Karmn	pEW(Hα)	X-rays	$v \sin i$	P	SKG[b]	Ref.[c]	Population	Ref.[d]
J00502+086	×	×					D	Mon16
J00505+248	×	×	×	×	Arg	Malo14a	YD	Mon16
J00511+225								
J00514+583							TD	Mon16
J00515-229	×						D	Mon16
J00520+205								
J00532+190								
J00538+459								
J00540+691								
J00548+275	×	×			HS	Mon16	YD	Mon16
J00566+174							D	Mon16
J00570+450					HS	Mon16	YD	Mon16
J00577+058								
J00580+393	×	×			UMa	Mon16	D	Mon16
J01008+669							D	Mon16
J01009-044							D	Mon16
J01013+613		×	×				D	Mon16
J01019+541	×				UMa	Mon16	D	Mon16
J01025+716		×					D	Mon16
J01026+623		×					YD	Mon16
J01032+316							D	Mon16
J01032+200		×					YD	Mon16
J01032+712								
J01033+623	×	×		×			YD	Mon16
J01036+408	×	×		×	ABDor?	Schl12b		
J01037+408	×	×			ABdor?	Schl12b	YD	Mon16
J01041+108								
J01048-181							D	Mon16
J01056+284			×				D	Mon16
J01066+152			×				D	Mon16
J01069+804	×	×						
J01078+128								
J01102-118								
J01114+154	×	×	×		bPic	Ried14	YD	Mon16
J01116+120								
J01119+049N							D	Mon16
J01119+049S							YD	Mon16
J01125-169	×	×					D	Mon16
J01133+589	×	×		×	ABDor?	Schl12b		
J01134-229	×	×			Cas	Mon16	YD	Mon16
J01141+790								
J01147+253								
J01158+470		×						
J01161+601								
J01178+286							TD-D	Mon16
J01178+054							TD	Mon16
J01182-128							D	Mon16
J01198+841							D	Mon16

Table B.4: Activity indicators, stellar kinematic associations and poputation of Carmencita stars (continued).

	Activity[a]							
Karmn	pEW(Hα)	X-rays	$v \sin i$	P	SKG[b]	Ref.[c]	Population	Ref.[d]
J01214+243								
J01221+221	×	×	×		Cas	Mon16	YD	Mon16
J01227+005							D	Mon16
J01256+097							D	Mon16
J01324-219							D	Mon16
J01317+209								
J01339-176		×					YD	Mon16
J01352-072	×	×			bPic	Malo13	YD	Mon16
J01369-067	×	×			bPic?	AF15b	YD	Mon16
J01373+610								
J01383+572			×				D	Mon16
J01384+006							D	Mon16
J01390-179	×	×	×		HS	Mon16	YD	Mon16
J01395+050			×				D	Mon16
J01402+317							D	Mon16
J01431+210	×	×	×				D	Mon16
J01432+278							D	Mon16
J01433+043		×					D	Mon16
J01437-060		×					YD	Mon16
J01449+163							D	Mon16
J01453+465	×	×		×			D	Mon16
J01466-086					LA	Mon16	YD	Mon16
J01480+212							D	Mon16
J01510-061	×	×			LA	Mon16	YD	Mon16
J01514+213							D	Mon16
J01518-108							D	Mon16
J01518+644			×				D	Mon16
J01531-210		×		×			YD	Mon16
J01538-149	×	×			bPic	Malo14a	YD	Mon16
J01544+576		×						
J01550+379								
J01556+028								
J01567+305	×	×						
J01592+035E	×	×					D	Mon16
J01592+035W	×						D	Mon16
J01593+585	×	×	×				D	Mon16
J02000+437							D	Mon16
J02001+366							YD	Mon16
J02002+130	×	×					D	Mon16
J02007-103	×	×					D	Mon16
J02015+637							D	Mon16
J02019+735	×	×					D	Mon16
J02020+039							D	Mon16
J02022+103	×		×				D	Mon16
J02026+105	×	×	×				D	Mon16
J02027+135	×	×	×	×			D	Mon16
J02028+047	×	×						
J02033-212							D	Mon16

Table B.4: Activity indicators, stellar kinematic associations and poputation of Carmencita stars (continued).

	Activity[a]							
Karmn	pEW(Hα)	X-rays	$v \sin i$	P	SKG[b]	Ref.[c]	Population	Ref.[d]
J02044-018							D	Mon16
J02050-176		×					D	Mon16
J02055+056								
J02069+451							D	Mon16
J02070+496		×					D	Mon16
J02071+642	×	×					YD	Mon16
J02082+802								
J02088+494	×	×	×				D	Mon16
J02096-143							D	Mon16
J02116+185							TD	Mon16
J02123+035							TD	Mon16
J02129+000	×	×		×	HS	Mon16	YD	Mon16
J02133+368	×	×					D	Mon16
J02142-039	×		×				D	Mon16
J02149+174		×					D	Mon16
J02153+074								
J02155+339	×	×					D	Mon16
J02158-126							D	Mon16
J02164+135	×	×	×		LA	Mon16	YD	Mon16
J02171+354	×		×	×	LA	Mon16	YD	Mon16
J02185+207								
J02186+123	×	×					YD	Mon16
J02190+238	×	×	×				YD	Mon16
J02190+353							D	Mon16
J02204+377							D	Mon16
J02207+029	×		×	×			D	Mon16
J02210+368							TD-D	Mon16
J02222+478		×					D	Mon16
J02230+181								
J02234+227		×	×		bPic	Malo13	YD	Mon16
J02247+259							D	Mon16
J02254+246								
J02256+375	×	×		×			YD	Mon16
J02272+545		×						
J02274+031	×							
J02277+044							D	Mon16
J02282+014							YD	Mon16
J02283+219								
J02285-200							D	Mon16
J02287+156								
J02289+120							TD-D	Mon16
J02289+226								
J02292+195	×	×						
J02293+884							D	Mon16
J02314+573							TD	Mon16
J02330+078								
J02336+249	×	×					D	Mon16
J02337+150							D	Mon16

Table B.4: Activity indicators, stellar kinematic associations and poputation of Carmencita stars (continued).

Karmn	Activity[a]				SKG[b]	Ref.[c]	Population	Ref.[d]
	pEW(Hα)	X-rays	$v \sin i$	P				
J02340+417							D	Mon16
J02345+566								
J02353+235	×	×					D	Mon16
J02358+202		×			LA	Mon16	YD	Mon16
J02362+068							D	Mon16
J02364+554							D	Mon16
J02367+226	×	×		×			YD	Mon16
J02367+320		×					D	Mon16
J02392+074	×	×					D	Mon16
J02412-045	×	×						
J02419+435								
J02424+182								
J02438-088							TD	Mon16
J02441+492		×					D	Mon16
J02442+255		×			HS	Mon16	YD	Mon16
J02443+109W	×	×		×				
J02443+109E								
J02455+449	×						D	Mon16
J02456+449							D	Mon16
J02462-049							H	Mon16
J02465+164			×				D	Mon16
J02502+628								
J02518+294	×	×					D	Mon16
J02518+062							D	Mon16
J02519+224	×	×						
J02524+269			×				D	Mon16
J02530+168							TD	Mon16
J02534+174							D	Mon16
J02555+268			×				D	Mon16
J02560-006							D	Mon16
J02562+239	×							
J02565+554W			×				D	Mon16
J02565+554E			×				D	Mon16
J02575+107							H	Mon16
J02581-128							TD	Mon16
J02591+366							D	Mon16
J02592+317							D	Mon16
J02597+389	×			×	HS	Mon16	YD	Mon16
J03018-165N		×	×		UMa	Mon16	D	Mon16
J03018-165S	×	×			UMa	Mon16	D	Mon16
J03026-181					HS	Mon16	YD	Mon16
J03033-080	×	×						
J03036-128							D	Mon16
J03037-128					LA	Mon16	YD	Mon16
J03040-203							D	Mon16
J03047+617							TD	Mon16
J03075-039							TD	Mon16
J03077+249				×				

Table B.4: Activity indicators, stellar kinematic associations and poputation of Carmencita stars (continued).

	Activity[a]							
Karmn	pEW(Hα)	X-rays	$v \sin i$	P	SKG[b]	Ref.[c]	Population	Ref.[d]
J03090+100			×				D	Mon16
J03095+457		×					D	Mon16
J03102+059							D	Mon16
J03104+584		×	×				YD	Mon16
J03109+737							TD	Mon16
J03110-046								
J03112+011		×					YD	Mon16
J03118+196							D	Mon16
J03119+615		×					D	Mon16
J03133+047							D	Mon16
J03136+653								
J03142+286							D	Mon16
J03145+594								
J03147+485							YD	Mon16
J03147+114	×	×					YD	Mon16
J03162+581S							TD	Mon16
J03162+581N							TD	Mon16
J03167+389								
J03172+453		×			UMa	Mon16	D	Mon16
J03177+252							TD	Mon16
J03181+426					LA	Mon16	YD	Mon16
J03181+382							D	Mon16
J03185+103								
J03186+326			×		LA	Mon16	YD	Mon16
J03187+606							D	Mon16
J03194+619	×	×	×		HS	Mon16	YD	Mon16
J03207+397								
J03213+799			×				D	Mon16
J03217-066		×					YD	Mon16
J03220+029							TD	Mon16
J03224+271				×			YD	Mon16
J03230+420							D	Mon16
J03233+116	×	×			UMa	Mon16	D	Mon16
J03236+056	×	×					YD	Mon16
J03241+237		×	×		IC	Mon16	YD	Mon16
J03242+237				×	IC	Mon16	YD	Mon16
J03247+447								
J03257+058	×	×			UMa	Mon16	D	Mon16
J03263+171							YD	Mon16
J03267+192	×		×	×			D	Mon16
J03272+273		×		×				
J03275+222	×							
J03284+352				×				
J03286-156	×	×					TD-D	Mon16
J03288+264	×	×		×	LA	Mon16	YD	Mon16
J03303+346	×	×	×				YD	Mon16
J03308+542		×					YD	Mon16
J03309+706							D	Mon16

Table B.4: Activity indicators, stellar kinematic associations and poputation of Carmencita stars (continued).

Karmn	Activity[a]				SKG[b]	Ref.[c]	Population	Ref.[d]
	pEW(Hα)	X-rays	$v \sin i$	P				
J03317+143							D	Mon16
J03325+287	×	×	×		bPic	Malo14a	YD	Mon16
J03332+462	×	×			AB Dor	Zuck11	YD	Mon16
J03340+585								
J03346-048							D	Mon16
J03361+313	×	×		×	Cas	Mon16	YD	Mon16
J03366+034	×	×	×	×	IC	Mon16	YD	Mon16
J03372+691	×	×		×			YD	Mon16
J03375+178N	×	×		×	HS	Mon16	YD	Mon16
J03375+178S	×	×		×			D	Mon16
J03394+249		×	×				D	Mon16
J03396+254E							D	Mon16
J03396+254W							D	Mon16
J03397+334	×	×					D	Mon16
J03416+552	×	×			Col	Zuck11	YD	Mon16
J03430+459							D	Mon16
J03433-095		×					D	Mon16
J03437+166					LA	Mon16	YD	Mon16
J03438+166							YD	Mon16
J03445+349				×	LA	Mon16	YD	Mon16
J03454+729								
J03455+703								
J03459+147								
J03463+262		×			HS	Mon16	YD	Mon16
J03467+821								
J03467-112							D	Mon16
J03473+086							D	Mon16
J03473-019	×	×	×	×	AB Dor	Zuck04	YD	Mon16
J03479+027							D	Mon16
J03480+686		×					D	Mon16
J03486+735							D	Mon16
J03505+634							D	Mon16
J03507-060							D	Mon16
J03510-008	×		×				D	Mon16
J03510+142	×	×					D	Mon16
J03519+397		×						
J03526+170	×	×					D	Mon16
J03531+625							TD	Mon16
J03543-146			×				D	Mon16
J03544-091		×					D	Mon16
J03548+163	×	×						
J03565+319	×	×		×				
J03567+039			×				D	Mon16
J03574-011	×	×	×				D	Mon16
J03586+520								
J03588+125							D	Mon16
J03598+260							TD-D	Mon16
J04011+513							TD	Mon16

Table B.4: Activity indicators, stellar kinematic associations and poputation of Carmencita stars (continued).

	Activity[a]							
Karmn	pEW(Hα)	X-rays	$v \sin i$	P	SKG[b]	Ref.[c]	Population	Ref.[d]
J04056+057	×	×		×			YD	Mon16
J04059+712W		×						
J04059+712E		×						
J04061-055								
J04077+142								
J04079+142								
J04081+743								
J04083+691	×							
J04086+336							D	Mon16
J04093+057				×			YD	Mon16
J04108-128								
J04112+495							D	Mon16
J04122+647	×	×			HS	Mon16	YD	Mon16
J04123+162	×	×			HSc	Ste95		
J04129+526							TD-D	Mon16
J04131+505							D	Mon16
J04137+476								
J04139+829					HS	Mon16	YD	Mon16
J04148+277	×	×		×	HS	Mon16	YD	Mon16
J04153-076	×	×			bPic	AF15b	TD-D	Mon16
J04166-125							D	Mon16
J04173+088	×	×	×	×	LA	Mon16	YD	Mon16
J04177+410	×	×			ABDor?	Schl12b		
J04188+013								
J04191-074								
J04191+097								
J04198+425							D	Mon16
J04199+364							D	Mon16
J04205+815								
J04206+272	×	×			Tau	Re10		
J04207+152	×	×						
J04218+213					IC	Mon16	YD	Mon16
J04219+751							D	Mon16
J04221+192	×	×					D	Mon16
J04224+036	×	×	×		HS	Mon16	YD	Mon16
J04224+740								
J04225+105					HS	Mon16	YD	Mon16
J04225+390							D	Mon16
J04227+205	×							
J04229+259								
J04234+495								
J04234+809	×	×						
J04238+149	×	×			HSc	Ste95		
J04238+092	×	×						
J04247-067	×						YD	Mon16
J04248+324							D	Mon16
J04251+515								
J04252+172	×	×						

Table B.4: Activity indicators, stellar kinematic associations and poputation of Carmencita stars (continued).

	Activity[a]							
Karmn	pEW(Hα)	X-rays	$v \sin i$	P	SKG[b]	Ref.[c]	Population	Ref.[d]
J04252+080S	×	×			HS	Mon16	YD	Mon16
J04252+080N		×	×		HS	Mon16	YD	Mon16
J04274+203								
J04276+595	×	×			LA	Mon16	YD	Mon16
J04278+117							TD-D	Mon16
J04284+176	×	×						
J04290+219		×					D	Mon16
J04293+142							D	Mon16
J04294+262					Tau	Re10		
J04302+708								
J04304+398	×	×		×	HS	Mon16	YD	Mon16
J04308-088	×							
J04310+367	×	×		×				
J04311+589		×					D	Mon16
J04312+422	×	×						
J04313+241	×		×		Tau	Re10		
J04326+098		×						
J04329+001N		×						
J04329+001S		×						
J04329+001E		×						
J04333+239	×	×	×					
J04335+207	×	×		×			D	Mon16
J04347-004	×							
J04350+086		×		×				
J04352-161	×		×				YD	Mon16
J04366+112							TD	Mon16
J04369-162		×			LA	Mon16	YD	Mon16
J04369+593								
J04373+193	×	×						
J04376-024	×	×	×	×	bPic	Malo13	YD	Mon16
J04376+528		×			HS	Mon16	D	Mon16
J04376-110					UMa	Mon16	D	Mon16
J04382+282	×	×	×	×	HS	Mon16	YD	Mon16
J04386-115								
J04388+217		×						
J04393+335	×	×		×			D	Mon16
J04395+162	×			×			D	Mon16
J04398+251								
J04403-055	×	×	×		HS	Mon16	YD	Mon16
J04404-091					UMa	Mon16	D	Mon16
J04407+022		×			HS	Mon16	YD	Mon16
J04413+327		×		×				
J04414+132								
J04422+577								
J04423+207								
J04425+204	×	×	×		HS	Mon16	D	Mon16
J04429+095								
J04429+189		×					D	Mon16

Table B.4: Activity indicators, stellar kinematic associations and poputation of Carmencita stars (continued).

	Activity[a]							
Karmn	pEW(Hα)	X-rays	$v \sin i$	P	SKG[b]	Ref.[c]	Population	Ref.[d]
J04429+214							D	Mon16
J04433+296					Tau	BG6		
J04444+278							D	Mon16
J04458-144								
J04468-112	×	×					YD	Mon16
J04471+021							D	Mon16
J04472+206	×	×					YD	Mon16
J04480+170		×						
J04488+100	×	×					YD	Mon16
J04494+484	×	×		×	HS	Mon16	YD	Mon16
J04499+711								
J04499+236	×	×	×				YD	Mon16
J04502+459							YD	Mon16
J04504+199								
J04508+261							TD-D	Mon16
J04508+221							D	Mon16
J04520+064							D	Mon16
J04524-168	×	×	×		AB Dor	Tor08	YD	Mon16
J04525+407							TD	Mon16
J04536+623								
J04538-177							D	Mon16
J04538+158								
J04544+650	×	×			LA	Mon16	YD	Mon16
J04559+046	×	×					D	Mon16
J04560+432								
J04587+509			×				D	Mon16
J04588+498		×					D	Mon16
J04595+017	×	×	×	×	bPic	Malo13	YD	Mon16
J05012+248		×					D	Mon16
J05013+226	×	×					YD	Mon16
J05018+037		×			LA	Mon16	YD	Mon16
J05019+011	×	×	×		bPic	Schl12b	YD	Mon16
J05019-069	×	×					D	Mon16
J05019+099	×	×		×	bPic	Ried14	YD	Mon16
J05024-212		×					D	Mon16
J05030+213	×			×			D	Mon16
J05032+213		×						
J05033-173							YD	Mon16
J05034+531							TD	Mon16
J05042+110	×	×		×			D	Mon16
J05050+442							YD	Mon16
J05051-120	×	×					D	Mon16
J05060+043							D	Mon16
J05062+046	×	×	×	×	bPic	Schl12b	YD	Mon16
J05068-215E	×	×	×	×	bPic	Ried14	YD	Mon16
J05068-215W	×				bPic	Ried14	YD	Mon16
J05072+375	×	×						
J05076+275								

Table B.4: Activity indicators, stellar kinematic associations and poputation of Carmencita stars (continued).

Karmn	Activity[a]				SKG[b]	Ref.[c]	Population	Ref.[d]
	pEW(Hα)	X-rays	$v \sin i$	P				
J05078+179		×					YD	Mon16
J05083+756								
J05084-210	×	×			bPic	Malo14a	YD	Mon16
J05085-181		×					D	Mon16
J05091+154	×	×	×				TD	Mon16
J05103+095								
J05103+272		×						
J05103+488							D	Mon16
J05106+297								
J05109+186							D	Mon16
J05111+158		×						
J05114+101								
J05127+196							D	Mon16
J05151-073							D	Mon16
J05152+236	×							
J05155+591								
J05173+321	×	×						
J05173+721								
J05173+458		×			HS	Mon16	YD	Mon16
J05187+464	×				Cas	Mon16	YD	Mon16
J05195+649	×	×	×				D	Mon16
J05206+587S							D	Mon16
J05206+587N							D	Mon16
J05211+557							TD-D	Mon16
J05223+305								
J05226+795								
J05228+202		×						
J05243-160	×	×			bPic	Malo14a	YD	Mon16
J05256-091	×	×			AB Dor	Malo14a	YD	Mon16
J05280+096							D	Mon16
J05282+029							TD	Mon16
J05289+125	×	×					D	Mon16
J05294+155W							YD	Mon16
J05294+155E							YD	Mon16
J05298-034		×					D	Mon16
J05298+320							TD-D	Mon16
J05306+152								
J05314-036		×					D	Mon16
J05320-030	×	×	×		bPic	Malo13	YD	Mon16
J05322+098	×	×	×	×	Cas	Cab10	YD	Mon16
J05328+338								
J05333+448	×	×	×		HS	Mon16	YD	Mon16
J05337+019	×	×	×	×			D	Mon16
J05339-023	×	×			bPic	Malo14a	YD	Mon16
J05341+512		×					D	Mon16
J05341+475	×	×		×				
J05342+103S		×					D	Mon16
J05342+103N		×	×				D	Mon16

Table B.4: Activity indicators, stellar kinematic associations and poputation of Carmencita stars (continued).

	Activity[a]							
Karmn	pEW(Hα)	X-rays	$v \sin i$	P	SKG[b]	Ref.[c]	Population	Ref.[d]
J05348+138		×					YD	Mon16
J05360-076			×				D	Mon16
J05365+113		×	×	×			YD	Mon16
J05366+112	×						YD	Mon16
J05394+406								
J05394+747								
J05402+126	×	×		×			TD-D	Mon16
J05404+248	×	×			LA	Mon16	YD	Mon16
J05415+534		×			IC	Mon16	YD	Mon16
J05419+153		×					YD	Mon16
J05421+124		×					TD	Mon16
J05422-054			×				D	Mon16
J05425+154	×	×						
J05455-119								
J05456+729								
J05458+729								
J05466+441							TD-D	Mon16
J05468+665								
J05471-052			×				TD-D	Mon16
J05472-000		×		×			D	Mon16
J05484+077					LA	Mon16	YD	Mon16
J05511+122								
J05530+251								
J05530+047								
J05532+242							D	Mon16
J05547+109	×	×			Cas	Mon16	YD	Mon16
J05558+406								
J05566-103	×	×	×				YD	Mon16
J05587+259								
J05588+213	×							
J05596+585							YD	Mon16
J05599+585	×	×		×	ABDor?	Schl12b	YD	Mon16
J06000+027	×	×	×	×			YD	Mon16
J06007+681							TD	Mon16
J06008+681							TD	Mon16
J06011+595					LA	Mon16	YD	Mon16
J06017+130		×						
J06023-203							D	Mon16
J06024+663							D	Mon16
J06024+498			×				YD	Mon16
J06025+371								
J06034+478							D	Mon16
J06035+168	×	×						
J06035+155		×						
J06039+261							TD	Mon16
J06054+608	×	×					TD	Mon16
J06066+465								
J06071+335							D	Mon16

Table B.4: Activity indicators, stellar kinematic associations and poputation of Carmencita stars (continued).

	Activity[a]							
Karmn	pEW(Hα)	X-rays	$v \sin i$	P	SKG[b]	Ref.[c]	Population	Ref.[d]
J06075+472	×	×		×	HS	Mon16	YD	Mon16
J06097+001								
J06102+225	×		×		LA	Mon16	YD	Mon16
J06103+722								
J06103+821		×					D	Mon16
J06103+225		×						
J06105+024								
J06105-218		×					YD	Mon16
J06107+259							TD	Mon16
J06109+103							D	Mon16
J06140+516							D	Mon16
J06145+025								
J06151-164								
J06171+838		×						
J06171+051							D	Mon16
J06171+751	×	×	×	×			D	Mon16
J06185+250								
J06193-066							D	Mon16
J06194+139								
J06212+442	×	×					D	Mon16
J06216+163								
J06217+163								
J06218-227				×			TD	Mon16
J06223+334					HS	Mon16	YD	Mon16
J06236-096	×	×						
J06237+020		×						
J06238+456	×			×			D	Mon16
J06246+234							D	Mon16
J06258+561							D	Mon16
J06262+238		×						
J06277+093					HS	Mon16	YD	Mon16
J06293-028	×	×	×		LA	Mon16	YD	Mon16
J06298-027	×	×					TD	Mon16
J06306+456								
J06307+397							D	Mon16
J06310+500	×	×					YD	Mon16
J06318+414	×	×	×		Cas	Mon16	YD	Mon16
J06322+378				×				
J06323-097	×							
J06325+641							D	Mon16
J06345+315								
J06354-040	×	×	×		HS	Mon16	YD	Mon16
J06361+116			×				TD	Mon16
J06361+201								
J06371+175		×					D	Mon16
J06396-210		×					D	Mon16
J06400+285							D	Mon16
J06401-164								

Table B.4: Activity indicators, stellar kinematic associations and poputation of Carmencita stars (continued).

	Activity[a]							
Karmn	pEW(Hα)	X-rays	$v \sin i$	P	SKG[b]	Ref.[c]	Population	Ref.[d]
J06414+157							D	Mon16
J06421+035							D	Mon16
J06422+035							D	Mon16
J06435+166								
J06438+511		×					D	Mon16
J06447+718		×					D	Mon16
J06461+325							TD	Mon16
J06467+159		×		×				
J06474+054								
J06486+532								
J06489+211	×	×						
J06490+371							TD	Mon16
J06509-091							D	Mon16
J06523-051		×					D	Mon16
J06524+182							D	Mon16
J06564+759								
J06540+608							D	Mon16
J06548+332		×					YD	Mon16
J06564+121								
J06564+400							D	Mon16
J06565+440							D	Mon16
J06574+740	×	×	×				D	Mon16
J06579+623	×	×					YD	Mon16
J06582+511								
J06594+193	×						D	Mon16
J06594+195								
J06596+057	×	×			bPic	Schl12b		
J07001-190	×	×						
J07009-023								
J07012+008								
J07033+346	×						D	Mon16
J07034+767								
J07039+527			×				D	Mon16
J07042-105		×					D	Mon16
J07044+682							D	Mon16
J07047+249							YD	Mon16
J07051-101	×	×						
J07052+084								
J07076+486							D	Mon16
J07078+672							D	Mon16
J07081-228							D	Mon16
J07086+307							D	Mon16
J07095+698							D	Mon16
J07100+385	×	×	×	×	HS	Mon16	YD	Mon16
J07102+376							D	Mon16
J07105-087	×	×						
J07111+434	×						D	Mon16
J07119+773								

Table B.4: Activity indicators, stellar kinematic associations and poputation of Carmencita stars (continued).

Karmn	Activity[a]				SKG[b]	Ref.[c]	Population	Ref.[d]
	pEW(Hα)	X-rays	$v \sin i$	P				
J07121+522					LA	Mon16	YD	Mon16
J07129+357		×						
J07140+507		×						
J07163+331	×	×			LA	Mon16	YD	Mon16
J07163+271		×					YD	Mon16
J07172-050	×	×					D	Mon16
J07174+195							D	Mon16
J07181+392					Cas	Mon16	YD	Mon16
J07182+137								
J07195+328							D	Mon16
J07199+840								
J07227+306							TD	Mon16
J07232+460		×					D	Mon16
J07274+052		×					D	Mon16
J07274+220							YD	Mon16
J07282-187							D	Mon16
J07287-032							D	Mon16
J07295+359	×	×	×		bPic	Schl12b		
J07307+481							TD	Mon16
J07310+460	×	×		×			YD	Mon16
J07212+005		×						
J07319+392							YD	Mon16
J07319+362N	×	×			Cas	Cab10	YD	Mon16
J07319+362S	×	×	×		Cas	Mon16	YD	Mon16
J07320+686							D	Mon16
J07320+173E							D	Mon16
J07320+173W				×			D	Mon16
J07325+248								
J07342+009							D	Mon16
J07344+629							D	Mon16
J07346+318	×	×		×	Cas	Mon16	YD	Mon16
J07346+223				×			D	Mon16
J07349+147	×		×				YD	Mon16
J07353+548					UMa	Mon16	D	Mon16
J07354+482								
J07359+785								
J07361-031		×		×	UMa	Mon16	D	Mon16
J07364+070	×		×				YD	Mon16
J07365-006	×							
J07366+440							D	Mon16
J07383+344							D	Mon16
J07384+240	×	×		×	Cas	Mon16	YD	Mon16
J07386-212							D	Mon16
J07393+021					LA	Mon16	YD	Mon16
J07395+334							D	Mon16
J07403-174		×					D	Mon16
J07418+050							YD	Mon16
J07421+500		×						

Table B.4: Activity indicators, stellar kinematic associations and poputation of Carmencita stars (continued).

	Activity[a]							
Karmn	pEW(Hα)	X-rays	$v \sin i$	P	SKG[b]	Ref.[c]	Population	Ref.[d]
J07431+181							D	Mon16
J07446+035	×	×	×	×	bPic	AF15b	YD	Mon16
J07467+574	×	×	×		LA	Mon16	YD	Mon16
J07470+760								
J07472+503	×	×	×		UMa	Mon16	D	Mon16
J07482+203							TD	Mon16
J07493+849							D	Mon16
J07497-033	×				Cas	Mon16	YD	Mon16
J07518+055							TD-D	Mon16
J07519-000		×					D	Mon16
J07523+162	×		×	×			D	Mon16
J07525+063							D	Mon16
J07545-096	×							
J07545+085		×	×					
J07558+833	×	×	×	×	HS	Mon16	YD	Mon16
J07581+072	×	×		×			D	Mon16
J07582+413							D	Mon16
J07583+496							D	Mon16
J07585+155S	×				LA	Mon16	YD	Mon16
J07585+155N	×				LA	Mon16	YD	Mon16
J07590+153							YD	Mon16
J07591+173	×	×						
J08005+258							D	Mon16
J08017+237					Cas	Mon16	YD	Mon16
J08023+033							TD-D	Mon16
J08025-130								
J08031+203	×	×			HS	Mon16	YD	Mon16
J08033+528							TD	Mon16
J08066+558							D	Mon16
J08068+367							D	Mon16
J08069+422	×			×	HS	Mon16	YD	Mon16
J08082+211	×	×	×				D	Mon16
J08083+585							D	Mon16
J08089+328	×	×		×	LA	Mon16	YD	Mon16
J08095+219							YD	Mon16
J08103+095								
J08105-138					HS	Mon16	YD	Mon16
J08108+039							D	Mon16
J08117+531								
J08119+087							TD	Mon16
J08126-215	×	×					D	Mon16
J08158+346							TD-D	Mon16
J08161+013							D	Mon16
J08175+209								
J08178+311				×			D	Mon16
J08202+055								
J08258+690							D	Mon16
J08282+201							TD	Mon16

Table B.4: Activity indicators, stellar kinematic associations and poputation of Carmencita stars (continued).

Karmn	Activity[a]				SKG[b]	Ref.[c]	Population	Ref.[d]
	pEW(Hα)	X-rays	$v \sin i$	P				
J08283+553								
J08283+350							TD	Mon16
J08286+660	×	×	×		UMa	Mon16	D	Mon16
J08293+039					LA	Mon16	YD	Mon16
J08298+267	×		×		Cas	Mon16	YD	Mon16
J08313-060							D	Mon16
J08313-104		×					TD	Mon16
J08314-060							D	Mon16
J08315+730								
J08316+193N	×		×		UMa	Mon16	D	Mon16
J08316+193S	×	×		×	Cas	Mon16	YD	Mon16
J08317+057	×	×			ABDor?	Schl12b		
J08321+844							D	Mon16
J08325+451								
J08334+185							D	Mon16
J08344-011							D	Mon16
J08353+141	×				LA	Mon16	YD	Mon16
J08358+680		×					D	Mon16
J08364+672							D	Mon16
J08364+264								
J08371+151							TD	Mon16
J08375+035							YD	Mon16
J08387+516								
J08398+089							D	Mon16
J08402+314							TD	Mon16
J08404+184		×					D	Mon16
J08410+676							D	Mon16
J08413+594			×				D	Mon16
J08427+095							D	Mon16
J08428+095							D	Mon16
J08443-104							D	Mon16
J08447+182							TD-D	Mon16
J08449-066								
J08517+181		×					TD-D	Mon16
J08526+283					IC	Mon16	YD	Mon16
J08531-202								
J08536-034	×	×	×		Cas	Mon16	YD	Mon16
J08537+149								
J08540-131							D	Mon16
J08551+015							TD	Mon16
J08555+664								
J08563+126		×		×	UMa	Mon16	YD	Mon16
J08570+116			×				D	Mon16
J08572+194								
J08582+197	×	×	×				YD	Mon16
J08589+084	×	×					D	Mon16
J08595+537	×	×	×		IC	Mon16	YD	Mon16
J08599+729		×					D	Mon16

Table B.4: Activity indicators, stellar kinematic associations and poputation of Carmencita stars (continued).

	Activity[a]							
Karmn	pEW(Hα)	X-rays	$v \sin i$	P	SKG[b]	Ref.[c]	Population	Ref.[d]
J09003+218	×	×	×					
J09005+465	×	×			LA	Mon16	YD	Mon16
J09008+052W							D	Mon16
J09008+052E							D	Mon16
J09011+019							D	Mon16
J09023+084							TD	Mon16
J09023+177								
J09028+680			×				D	Mon16
J09033+056	×						D	Mon16
J09037+520								
J09038+129								
J09040-159	×	×						
J09050+028					HS	Mon16	YD	Mon16
J09057+186								
J09062+128							D	Mon16
J09070-221							D	Mon16
J09087+665							D	Mon16
J09091+227								
J09093+401							D	Mon16
J09095+328							D	Mon16
J09096+067	×	×			UMa	Mon16	D	Mon16
J09099+004								
J09115+466			×				D	Mon16
J09115+126								
J09120+279							D	Mon16
J09133+688		×			ABDor?	Schl12b	YD	Mon16
J09140+196					LA	Mon16	YD	Mon16
J09143+526		×			LA?	Tet11	YD	Mon16
J09144+526		×			LA?	Tet11	YD	Mon16
J09156-105	×	×						
J09160+293								
J09161+018	×	×	×		UMa	Mon16	D	Mon16
J09163-186		×					YD	Mon16
J09165+841							TD	Mon16
J09168+248					ABDor?	Schl12b		
J09177+462	×	×	×	×			YD	Mon16
J09177+584							TD	Mon16
J09187+267							D	Mon16
J09193+385S	×	×					D	Mon16
J09193+385N	×	×					D	Mon16
J09193+620	×	×		×	LA?	Tet11	D	Mon16
J09200+308		×						
J09201+037	×	×						
J09209+033							TD	Mon16
J09213+731							TD	Mon16
J09218-023							D	Mon16
J09218+435	×	×		×			D	Mon16
J09228+467		×		×				

Table B.4: Activity indicators, stellar kinematic associations and poputation of Carmencita stars (continued).

Karmn	Activity[a]				SKG[b]	Ref.[c]	Population	Ref.[d]
	pEW(Hα)	X-rays	$v \sin i$	P				
J09231+223			×		LA	Mon16	YD	Mon16
J09238+001							D	Mon16
J09248+306	×	×			ABDor?	Schl12b		
J09256+634	×		×		HS	Mon16	D	Mon16
J09275+506		×			HS	Mon16	YD	Mon16
J09288-073							D	Mon16
J09289-073							D	Mon16
J09291+259								
J09300+396							YD	Mon16
J09302+265	×	×		×			YD	Mon16
J09307+003							D	Mon16
J09308+024	×	×						
J09313-134		×					D	Mon16
J09315+202							D	Mon16
J09319+363							D	Mon16
J09328+269	×				LA	Mon16	YD	Mon16
J09352+612		×					D	Mon16
J09360-216							D	Mon16
J09360-061							TD	Mon16
J09362+375	×	×	×		bPic	Schl12b	D	Mon16
J09370+405							YD	Mon16
J09394+317								
J09394+146	×	×						
J09410+220							TD-D	Mon16
J09411+132		×					YD	Mon16
J09423+559							D	Mon16
J09425+700		×	×				YD	Mon16
J09425-192							D	Mon16
J09428+700	×	×					D	Mon16
J09430+237								
J09439+269					HS	Mon16	D	Mon16
J09447-182							TD-D	Mon16
J09449-123	×	×	×		Arg	Malo13	YD	Mon16
J09461-044							D	Mon16
J09468+760							TD	Mon16
J09473+263								
J09475+129							D	Mon16
J09488+156	×	×					D	Mon16
J09506-138								
J09511-123							TD	Mon16
J09526-156							D	Mon16
J09527+554								
J09531-036			×				D	Mon16
J09535+507								
J09539+209	×	×	×				D	Mon16
J09557+353	×	×					D	Mon16
J09561+627		×					YD	Mon16
J09564+226							D	Mon16

Table B.4: Activity indicators, stellar kinematic associations and poputation of Carmencita stars (continued).

	Activity[a]							
Karmn	pEW(Hα)	X-rays	$v \sin i$	P	SKG[b]	Ref.[c]	Population	Ref.[d]
J09579+118							YD	Mon16
J09587+555								
J09589+059	×	×		×	LA	Mon16	YD	Mon16
J09593+438W	×			×			D	Mon16
J09593+438E	×						YD	Mon16
J09597+721								
J09597+472							D	Mon16
J10004+272								
J10007+323							TD	Mon16
J10020+697	×	×						
J10023+480							TD	Mon16
J10027+149							YD	Mon16
J10028+484	×	×	×	×	LA	Mon16	YD	Mon16
J10035+059							D	Mon16
J10040+187								
J10043+503	×	×	×	×	ABDor?	Schl12b	YD	Mon16
J10067+417							D	Mon16
J10068-127	×							
J10069+126								
J10079+692							D	Mon16
J10087+027							D	Mon16
J10094+544								
J10094+512							TD-D	Mon16
J10117+353							D	Mon16
J10120-026			×				D	Mon16
J10122-037		×		×			YD	Mon16
J10125+570								
J10130+233							D	Mon16
J10133+467	×						D	Mon16
J10143+210	×	×	×	×	bPic*	Malo13	YD	Mon16
J10148+213	×	×						
J10151+314							YD	Mon16
J10155-164	×							
J10158+174							D	Mon16
J10167-119							D	Mon16
J10182-204	×	×						
J10185-117					LA	Mon16	YD	Mon16
J10196+198	×	×	×	×	Cas	Cab10	YD	Mon16
J10200+289								
J10206+492							D	Mon16
J10238+438	×							
J10240+366	×			×				
J10243+119							D	Mon16
J10251-102		×			HS	Mon16	YD	Mon16
J10255+263							TD-D	Mon16
J10260+504W							D	Mon16
J10260+504E							TD	Mon16
J10273+799								

Table B.4: Activity indicators, stellar kinematic associations and poputation of Carmencita stars (continued).

Karmn	Activity[a]				SKG[b]	Ref.[c]	Population	Ref.[d]
	pEW(Hα)	X-rays	$v \sin i$	P				
J10278+028								
J10284+482							D	Mon16
J10286+322		×					D	Mon16
J10289+008		×			AB Dor	Zuck11	YD	Mon16
J10303+328							D	Mon16
J10315+570	×						D	Mon16
J10320+033								
J10345+463							D	Mon16
J10350-094							D	Mon16
J10354+694							TD	Mon16
J10359+288	×	×			bPic	Schl12b		
J10360+051	×	×			HS	Mon16	YD	Mon16
J10364+415		×						
J10367+153	×	×			UMa	Mon16	D	Mon16
J10368+509	×	×		×			D	Mon16
J10379+127							YD	Mon16
J10384+485	×	×	×	×			D	Mon16
J10385+354							D	Mon16
J10389+250							TD	Mon16
J10396-069							YD	Mon16
J10403+015								
J10416+376			×				D	Mon16
J10430-092	×							
J10443+124								
J10448+324					HS	Mon16	YD	Mon16
J10453+385		×					D	Mon16
J10456-191							TD	Mon16
J10460+096							D	Mon16
J10472+404								
J10474+025								
J10482-113	×	×					D	Mon16
J10485+191							D	Mon16
J10497+355			×				TD	Mon16
J10504+331		×					TD	Mon16
J10506+517	×						D	Mon16
J10508+068					Her-Lyr	LS06	YD	Mon16
J10513+361	×	×		×	HS	Mon16	YD	Mon16
J10520+005	×	×		×			YD	Mon16
J10520+139							D	Mon16
J10522+059	×	×	×		HS	Mon16	YD	Mon16
J10546-073							D	Mon16
J10555-093							D	Mon16
J10563+042								
J10564+070	×	×					D	Mon16
J10576+695							D	Mon16
J10584-107	×	×						
J11000+228		×					YD	Mon16
J11003+728								

Table B.4: Activity indicators, stellar kinematic associations and poputation of Carmencita stars (continued).

	Activity[a]							
Karmn	pEW(Hα)	X-rays	$v \sin i$	P	SKG[b]	Ref.[c]	Population	Ref.[d]
J11008+120	×				UMa	Mon16	D	Mon16
J11013+030							D	Mon16
J11014+568								
J11023+165W							D	Mon16
J11023+165E							D	Mon16
J11026+219		×	×		UMa	Mon16	D	Mon16
J11030+037								
J11031+152	×	×					YD	Mon16
J11031+366	×	×		×			YD	Mon16
J11033+359		×					TD	Mon16
J11036+136	×	×					D	Mon16
J11042+400				×			D	Mon16
J11054+435		×					TD-D	Mon16
J11055+435	×	×	×				TD-D	Mon16
J11055+450		×					D	Mon16
J11057+102	×						TD	Mon16
J11075+437	×			×			YD	Mon16
J11081-052							D	Mon16
J11108+479							D	Mon16
J11110+304		×					D	Mon16
J11113+434							D	Mon16
J11118+335	×	×		×			D	Mon16
J11126+189							D	Mon16
J11131+002							D	Mon16
J11151+734							YD	Mon16
J11152+194							D	Mon16
J11152-181							TD	Mon16
J11154+410							D	Mon16
J11159+553	×	×					TD	Mon16
J11195+466								
J11200+658		×					TD-D	Mon16
J11201-104	×	×					YD	Mon16
J11214-204	×				UMa	Mon16	YD	Mon16
J11216+061							TD	Mon16
J11231+258							D	Mon16
J11233+448							YD	Mon16
J11237+085							TD-D	Mon16
J11238+106		×						
J11239-183							D	Mon16
J11240+381	×	×		×	UMa	Mon16	D	Mon16
J11247+675								
J11249+024								
J11254+782		×					D	Mon16
J11266+379				×			D	Mon16
J11276+039							D	Mon16
J11289+101							D	Mon16
J11306-080								
J11307+549								

Table B.4: Activity indicators, stellar kinematic associations and poputation of Carmencita stars (continued).

Karmn	Activity[a]				SKG[b]	Ref.[c]	Population	Ref.[d]
	pEW(Hα)	X-rays	$v \sin i$	P				
J11311-149							TD-D	Mon16
J11315+022								
J11317+226							YD	Mon16
J11351-056							TD	Mon16
J11355+389							D	Mon16
J11376+587							D	Mon16
J11404+770								
J11417+427					IC	Mon16	YD	Mon16
J11420+147							D	Mon16
J11421+267		×		×			D	Mon16
J11433+253	×				IC	Mon16	YD	Mon16
J11451+183								
J11467-140							D	Mon16
J11470+700	×	×		×			YD	Mon16
J11474+667	×	×						
J11476+002	×	×		×	LA	Mon16	YD	Mon16
J11476+786		×					TD	Mon16
J11477+008		×			TW Hya	Rei02	D	Mon16
J11483-112							TD-D	Mon16
J11485+076	×			×			D	Mon16
J11496+220								
J11509+483							TD-D	Mon16
J11511+352		×					D	Mon16
J11519+075	×	×		×	bPic?	Schl12b		
J11521+039							D	Mon16
J11529+244							D	Mon16
J11532-073							D	Mon16
J11533+430								
J11538+069							D	Mon16
J11541+098							D	Mon16
J11549-021							D	Mon16
J11551+009							D	Mon16
J11557-227							YD	Mon16
J11557-189							D	Mon16
J11575+118							D	Mon16
J11582+425							D	Mon16
J11585+595								
J11589+426					HS	Mon16	D	Mon16
J12006-138							YD	Mon16
J12016-122							D	Mon16
J12023+285	×	×					D	Mon16
J12054+695							YD	Mon16
J12057+784		×						
J12063-132		×					D	Mon16
J12088+303		×						
J12093+210								
J12100-150							TD	Mon16
J12104-131	×	×						

Table B.4: Activity indicators, stellar kinematic associations and poputation of Carmencita stars (continued).

	Activity[a]							
Karmn	pEW(Hα)	X-rays	$v \sin i$	P	SKG[b]	Ref.[c]	Population	Ref.[d]
J12109+410							TD	Mon16
J12111-199							YD	Mon16
J12112-199					Cas	Mon16	YD	Mon16
J12121+488		×					D	Mon16
J12122+714								
J12123+544S					UMa	Mon16	D	Mon16
J12123+544N					UMa	Mon16	D	Mon16
J12124+121								
J12124+396		×					D	Mon16
J12133+166							TD	Mon16
J12142+006	×	×	×	×			YD	Mon16
J12144+245							D	Mon16
J12151+487					IC	Mon16	YD	Mon16
J12154+391					HS	Mon16	YD	Mon16
J12156+526	×	×	×		UMa	Mon16	YD	Mon16
J12162+508	×	×						
J12168+029							D	Mon16
J12168+248		×						
J12169+311	×	×					D	Mon16
J12189+111	×	×	×	×	HS	Mon16	YD	Mon16
J12191+318								
J12194+283		×					D	Mon16
J12198+527		×			ABDor?	Schl12b	YD	Mon16
J12204+005					UMa	Mon16	D	Mon16
J12214+306E			×					
J12214+306W			×				D	Mon16
J12217+682							D	Mon16
J12223+251							TD	Mon16
J12225+123					LA	Mon16	YD	Mon16
J12228-040	×	×						
J12230+640							D	Mon16
J12235+671							D	Mon16
J12235+279								
J12238+125	×						YD	Mon16
J12248-182							TD	Mon16
J12269+270		×					D	Mon16
J12274+374			×				YD	Mon16
J12277-032					LA	Mon16	YD	Mon16
J12288-106N		×					D	Mon16
J12288-106S		×					D	Mon16
J12289+084							YD	Mon16
J12290+417	×	×		×	TucHor?	Shk12	YD	Mon16
J12292+535							TD	Mon16
J12294+229	×	×					YD	Mon16
J12299-054W							D	Mon16
J12299-054E							D	Mon16
J12199+364			×				D	Mon16
J12312+086							D	Mon16

Table B.4: Activity indicators, stellar kinematic associations and poputation of Carmencita stars (continued).

Karmn	Activity[a]						Population	Ref.[d]
	pEW(Hα)	X-rays	$v \sin i$	P	SKG[b]	Ref.[c]		
J12323+315							D	Mon16
J12324+203	×	×					D	Mon16
J12327+682	×							
J12332+090	×				HS	Mon16	YD	Mon16
J12349+322								
J12350+098		×					D	Mon16
J12363-043							D	Mon16
J12364+352	×						YD	Mon16
J12368-019								
J12373-208							D	Mon16
J12387-043							D	Mon16
J12388+116		×					D	Mon16
J12390+470	×	×					D	Mon16
J12397+255	×	×		×	LA	Mon16	YD	Mon16
J12416+482							D	Mon16
J12417+567	×	×			UMa	Mon16	D	Mon16
J12428+418	×	×			IC	Mon16	YD	Mon16
J12436+251							YD	Mon16
J12440-111	×							
J12470+466							TD-D	Mon16
J12471-035					HS	Mon16	YD	Mon16
J12479+097							D	Mon16
J12481+472							D	Mon16
J12485+495	×	×	×		UMa	Mon16	D	Mon16
J12490+661		×	×				D	Mon16
J12495+094	×						YD	Mon16
J12505+269							D	Mon16
J12508-213								
J12513+221							D	Mon16
J12576+352W	×		×		ABDor?	Schl12b	YD	Mon16
J12576+352E	×	×	×	×	LA	Mon16	YD	Mon16
J12583+405								
J12594+077							D	Mon16
J13000-056							YD	Mon16
J13005+056	×	×	×	×			D	Mon16
J13007+123	×	×	×	×			D	Mon16
J13019+335								
J13027+415								
J13047+559								
J13054+371							D	Mon16
J13068+308							D	Mon16
J13084+169							D	Mon16
J13088+163							D	Mon16
J13089+490							D	Mon16
J13095+289	×	×		×	LA	Mon16	YD	Mon16
J13102+477	×	×	×	×			D	Mon16
J13113+285							D	Mon16
J13118+253							D	Mon16

Table B.4: Activity indicators, stellar kinematic associations and poputation of Carmencita stars (continued).

	Activity[a]							
Karmn	pEW(Hα)	X-rays	$v \sin i$	P	SKG[b]	Ref.[c]	Population	Ref.[d]
J13130+201							D	Mon16
J13140+038							D	Mon16
J13142+792								
J13143+133	×		×		ABDor?	Schl12	YD	Mon16
J13165+278							D	Mon16
J13167-123								
J13168+170		×					D	Mon16
J13168+231							D	Mon16
J13179+362							TD-D	Mon16
J13180+022							YD	Mon16
J13182+733								
J13195+351W		×					D	Mon16
J13195+351E							D	Mon16
J13196+333		×			LA	Mon16	YD	Mon16
J13197+477							D	Mon16
J13209+342		×					D	Mon16
J13215+035								
J13215+037							D	Mon16
J13229+244							D	Mon16
J13235+292							D	Mon16
J13239+694		×						
J13247-050	×							
J13251-114	×							
J13254+377		×						
J13260+275	×	×						
J13282+300		×						
J13283-023W							D	Mon16
J13283-023E							D	Mon16
J13293+114							TD-D	Mon16
J13294-143	×	×			UMa	Mon16	D	Mon16
J13299+102		×					D	Mon16
J13300-087							TD	Mon16
J13305+191							TD	Mon16
J13317+292	×	×	×	×	LA	Mon16	YD	Mon16
J13318+233							YD	Mon16
J13319+311					IC	Mon16	YD	Mon16
J13326+309	×	×	×		LA	Mon16	YD	Mon16
J13327+168		×			UMa	Mon16	D	Mon16
J13335+704								
J13343+046							D	Mon16
J13348+201							D	Mon16
J13348+745							D	Mon16
J13358+146								
J13369+229							D	Mon16
J13376+481	×	×		×	LA	Mon16	YD	Mon16
J13378+481		×					D	Mon16
J13386+258							YD	Mon16
J13386-115	×							

Table B.4: Activity indicators, stellar kinematic associations and poputation of Carmencita stars (continued).

Karmn	Activity[a]						Population	Ref.[d]
	pEW(Hα)	X-rays	$v \sin i$	P	SKG[b]	Ref.[c]		
J13388-022							YD	Mon16
J13394+461							D	Mon16
J13401+437							D	Mon16
J13413-091							D	Mon16
J13414+489								
J13415+148					HS	Mon16	YD	Mon16
J13417+582	×	×	×		UMa	Mon16	YD	Mon16
J13421-160	×	×					D	Mon16
J13427+332			×				D	Mon16
J13430+090							YD	Mon16
J13434+111								
J13444+516							TD-D	Mon16
J13445+249								
J13450+176							TD	Mon16
J13455+609								
J13457+148		×					D	Mon16
J13458-179							D	Mon16
J13477+214		×						
J13481-137								
J13482+236							TD	Mon16
J13485+563								
J13488+041	×	×					YD	Mon16
J13490+026							D	Mon16
J13503-216								
J13507-216							D	Mon16
J13508+367					HS	Mon16	YD	Mon16
J13518+127	×	×						
J13526+144		×					D	Mon16
J13528+656							D	Mon16
J13528+668							D	Mon16
J13529+536								
J13534+129							D	Mon16
J13536+776	×	×	×	×	LA	Mon16	YD	Mon16
J13537+521		×						
J13537+788							YD	Mon16
J13582+125							D	Mon16
J13582-120								
J13583-132	×							
J13587-000							TD-D	Mon16
J13591-198	×	×					D	Mon16
J14010-026							D	Mon16
J14019+154							D	Mon16
J14019+432								
J14023+136		×	×		UMa	Mon16	YD	Mon16
J14024-210							D	Mon16
J14025+463S		×					D	Mon16
J14025+463N		×					D	Mon16
J14039+242								

Table B.4: Activity indicators, stellar kinematic associations and poputation of Carmencita stars (continued).

	Activity[a]							
Karmn	pEW(Hα)	X-rays	$v \sin i$	P	SKG[b]	Ref.[c]	Population	Ref.[d]
J14041+207		×						
J14062+693							D	Mon16
J14082+805							D	Mon16
J14083+758							D	Mon16
J14121-005							D	Mon16
J14130-120	×	×					TD-D	Mon16
J14142-153	×						YD	Mon16
J14144+234							D	Mon16
J14152+450							D	Mon16
J14153+153								
J14155+046			×				D	Mon16
J14157+594								
J14159+362		×						
J14161+233		×						
J14170+317	×	×					D	Mon16
J14170+105		×					YD	Mon16
J14171+088								
J14173+454	×	×	×				D	Mon16
J14174+454							D	Mon16
J14175+025	×	×						
J14177+214								
J14179-005							D	Mon16
J14189+386								
J14191-073							TD	Mon16
J14194+029	×	×		×			D	Mon16
J14200+390	×	×		×			D	Mon16
J14201-096			×				D	Mon16
J14210+275							YD	Mon16
J14212-011							D	Mon16
J14215-079								
J14219+376								
J14227+164	×			×	IC	Mon16	YD	Mon16
J14231-222							TD-D	Mon16
J14249+088							D	Mon16
J14251+518							D	Mon16
J14255-118	×							
J14257+236W							D	Mon16
J14257+236E		×					D	Mon16
J14259+142	×	×		×	bPic	Schl12b		
J14269+241								
J14279-003S	×	×					D	Mon16
J14279-003N	×						D	Mon16
J14280+139	×						D	Mon16
J14282+053								
J14283+053							YD	Mon16
J14294+155							TD	Mon16
J14299+295							D	Mon16
J14306+597	×		×				YD	Mon16

Table B.4: Activity indicators, stellar kinematic associations and poputation of Carmencita stars (continued).

Karmn	Activity[a]				SKG[b]	Ref.[c]	Population	Ref.[d]
	pEW(Hα)	X-rays	$v \sin i$	P				
J14307-086							TD	Mon16
J14310-122					LA	Mon16	YD	Mon16
J14312+754	×	×		×			YD	Mon16
J14320+738							YD	Mon16
J14321+081					IC	Mon16	YD	Mon16
J14321+160	×	×			UMa	Mon16	D	Mon16
J14322+496							D	Mon16
J14331+610			×		UMa	Mon16	YD	Mon16
J14342-125							D	Mon16
J14366+143								
J14368+583	×	×					D	Mon16
J14371+756								
J14376+677		×						
J14388+422								
J14415+064								
J14423+660		×					D	Mon16
J14438+667								
J14469+170								
J14472+570	×	×	×		UMa	Mon16	D	Mon16
J14485+101								
J14501+323								
J14511+311	×	×						
J14524+123							D	Mon16
J14525+001							D	Mon16
J14538+235			×				YD	Mon16
J14544+355							TD-D	Mon16
J14544+161	×	×		×	UMa	Mon16	D	Mon16
J14548+099							D	Mon16
J14549+411	×	×		×			TD-D	Mon16
J14557+072								
J14564+168							D	Mon16
J14574-214		×					D	Mon16
J14575+313							H	Mon16
J14578+566	×		×				D	Mon16
J15009+454		×					D	Mon16
J15011+071			×				YD	Mon16
J15011+354							D	Mon16
J15013+055							D	Mon16
J15030+704	×							
J15043+603							D	Mon16
J15043+294							D	Mon16
J15049-211							D	Mon16
J15018+550							D	Mon16
J15060+453								
J15073+249							D	Mon16
J15079+762	×							
J15081+623					LA	Mon16	YD	Mon16
J15095+031							D	Mon16

Table B.4: Activity indicators, stellar kinematic associations and poputation of Carmencita stars (continued).

	Activity[a]							
Karmn	pEW(Hα)	X-rays	$v \sin i$	P	SKG[b]	Ref.[c]	Population	Ref.[d]
J15100+193							D	Mon16
J15118-102							TD	Mon16
J15119+179							TD-D	Mon16
J15126+457	×	×	×		HS	Mon16	D	Mon16
J15147+645								
J15151+333			×					
J15156+638								
J15166+391	×			×	LA	Mon16	YD	Mon16
J15188+292		×						
J15191-127							TD-D	Mon16
J15193+678							D	Mon16
J15194-077							YD	Mon16
J15197+046	×							
J15210+309								
J15214+042								
J15218+209	×	×	×	×	LA?	Tet11	D	Mon16
J15219+185								
J15238+174							TD	Mon16
J15238+584	×	×					D	Mon16
J15238+561	×	×						
J15273+415								
J15276+408								
J15280+257					UMa	Mon16	D	Mon16
J15290+467	×	×						
J15297+428							D	Mon16
J15305+094	×						D	Mon16
J15319+288	×						D	Mon16
J15336+462							D	Mon16
J15339+379							D	Mon16
J15340+513	×							
J15345+142							D	Mon16
J15349-143							D	Mon16
J15353+177N							TD	Mon16
J15353+177S							TD-D	Mon16
J15357+221							D	Mon16
J15368+375		×		×				
J15369-141							D	Mon16
J15386+371								
J15400+434N							TD	Mon16
J15400+434S							TD	Mon16
J15412+759							D	Mon16
J15416+184	×	×						
J15421-194							TD	Mon16
J15474-108							D	Mon16
J15474+451	×	×		×				
J15476+226	×	×			LA	Mon16	YD	Mon16
J15480+043	×	×		×				
J15488+305								

Table B.4: Activity indicators, stellar kinematic associations and poputation of Carmencita stars (continued).

Karmn	Activity[a]				SKG[b]	Ref.[c]	Population	Ref.[d]
	pEW(Hα)	X-rays	$v \sin i$	P				
J15493+250								
J15496+510							TD-D	Mon16
J15496+348	×	×					D	Mon16
J15499+796	×	×						
J15501+009					UMa	Mon16	D	Mon16
J15512+306								
J15513+295							D	Mon16
J15531+347N							D	Mon16
J15531+347S							D	Mon16
J15538+641								
J15555+352	×	×	×	×	Arg	Malo14a	YD	Mon16
J15557+686	×	×						
J15569+376	×	×		×				
J15578+090							YD	Mon16
J15581+494	×	×						
J15583+354							D	Mon16
J15587+346								
J15597+440	×	×			LA	Mon16	YD	Mon16
J15598-082		×					D	Mon16
J16008+403							D	Mon16
J16017+301							D	Mon16
J16017+304	×						YD	Mon16
J16018+304					HS	Mon16	YD	Mon16
J16028+205							TD-D	Mon16
J16033+175								
J16043-062							D	Mon16
J16046+263							YD	Mon16
J16048+391	×						D	Mon16
J16054+769							D	Mon16
J16062+290							D	Mon16
J16066+083		×					TD	Mon16
J16074+059							TD	Mon16
J16082-104							TD	Mon16
J16090+529		×					YD	Mon16
J16092+093					HS	Mon16	YD	Mon16
J16120+033		×			UMa	Mon16	D	Mon16
J16139+337		×					D	Mon16
J16144-028	×		×				D	Mon16
J16145+191							TD	Mon16
J16147+048							D	Mon16
J16155+244							D	Mon16
J16167+672S		×					YD	Mon16
J16167+672N		×					YD	Mon16
J16170+552	×	×	×				D	Mon16
J16180+062	×	×						
J16204-042							TD-D	Mon16
J16220+228	×	×		×				
J16241+483							D	Mon16

Table B.4: Activity indicators, stellar kinematic associations and poputation of Carmencita stars (continued).

Karmn	Activity[a]				SKG[b]	Ref.[c]	Population	Ref.[d]
	pEW(Hα)	X-rays	$v \sin i$	P				
J16247+229								
J16254+543		×			UMa	Mon16	YD	Mon16
J16255+260		×			LA	Mon16	YD	Mon16
J16255+323								
J16259+834								
J16268-173	×	×					D	Mon16
J16280+155							D	Mon16
J16302-146							TD-D	Mon16
J16303-126		×			LA	Mon16	YD	Mon16
J16313+408	×		×	×	IC	Mon16	YD	Mon16
J16315+175							D	Mon16
J16327+126							D	Mon16
J16328+098							D	Mon16
J16342+543								
J16343+571	×	×	×	×			TD	Mon16
J16354+350	×	×	×	×	UMa	Mon16	D	Mon16
J16360+088	×	×		×			D	Mon16
J16395+505								
J16401+007	×	×		×	UMa	Mon16	D	Mon16
J16403+676	×	×		×			YD	Mon16
J16408+363		×	×	×			D	Mon16
J16420+192								
J16462+164							D	Mon16
J16465+345	×							
J16487-157		×					D	Mon16
J16487+106								
J16508-048							TD	Mon16
J16509+224	×	×	×				YD	Mon16
J16528+630							YD	Mon16
J16529+400							D	Mon16
J16542+119							D	Mon16
J16554-083N							D	Mon16
J16554-083S	×	×			LA?	Tet11	D	Mon16
J16555-083	×	×	×				D	Mon16
J16570-043	×	×	×	×			YD	Mon16
J16573+271		×						
J16573+124		×					D	Mon16
J16574+777							D	Mon16
J16577+132							D	Mon16
J16578+473		×					YD	Mon16
J16581+257		×					D	Mon16
J16584+139	×						D	Mon16
J16587+688								
J16591+209	×	×	×	×			D	Mon16
J17003+253							D	Mon16
J17006+063								
J17010+082							D	Mon16
J17027-060					LA	Mon16	YD	Mon16

Table B.4: Activity indicators, stellar kinematic associations and poputation of Carmencita stars (continued).

Karmn	Activity[a]				SKG[b]	Ref.[c]	Population	Ref.[d]
	pEW(Hα)	X-rays	$v \sin i$	P				
J17033+514							D	Mon16
J17038+321	×	×		×			D	Mon16
J17043+169							D	Mon16
J17052-050		×					TD-D	Mon16
J17058+260								
J17071+215							D	Mon16
J17076+073							D	Mon16
J17082+516								
J17095+436			×				D	Mon16
J17098+119							D	Mon16
J17104+279								
J17115+384							D	Mon16
J17118-018							D	Mon16
J17121+456		×	×				D	Mon16
J17136-084							D	Mon16
J17146+269							D	Mon16
J17153+049				×			D	Mon16
J17158+190			×		LA	Mon16	YD	Mon16
J17160+110							D	Mon16
J17166+080							YD	Mon16
J17177+116							D	Mon16
J17177-118							D	Mon16
J17183-017		×			Cas	Mon16	YD	Mon16
J17183+181		×	×				D	Mon16
J17198+417							D	Mon16
J17198+265	×	×	×	×	HS	Mon16	YD	Mon16
J17199+265	×	×		×	HS	Mon16	YD	Mon16
J17207+492							TD	Mon16
J17219+214							YD	Mon16
J17225+055								
J17242-043							TD-D	Mon16
J17276+144							TD	Mon16
J17285+374		×					D	Mon16
J17303+055							YD	Mon16
J17312+820							TD-D	Mon16
J17316+047								
J17321+504							D	Mon16
J17328+543								
J17338+169	×	×	×	×	LA	Mon16	YD	Mon16
J17340+446		×					YD	Mon16
J17355+616		×					D	Mon16
J17364+683		×					D	Mon16
J17376+220							D	Mon16
J17378+185							D	Mon16
J17386+612	×				Cas	Mon16	YD	Mon16
J17388+080							D	Mon16
J17395+277S							D	Mon16
J17395+277N							D	Mon16

Table B.4: Activity indicators, stellar kinematic associations and poputation of Carmencita stars (continued).

Karmn	Activity[a]						Population	Ref.[d]
	pEW(Hα)	X-rays	$v \sin i$	P	SKG[b]	Ref.[c]		
J17419+407								
J17421-088							TD	Mon16
J17425-166							D	Mon16
J17430+057		×					D	Mon16
J17431+854								
J17432-185							D	Mon16
J17439+433		×					D	Mon16
J17455+468		×					YD	Mon16
J17460+246							D	Mon16
J17464+277							D	Mon16
J17464-087		×					D	Mon16
J17469+228		×						
J17502+237			×				D	Mon16
J17515+147							D	Mon16
J17521+647								
J17530+169							D	Mon16
J17542+073							D	Mon16
J17547+128								
J17570+157							D	Mon16
J17572+707			×		IC	Mon16	YD	Mon16
J17578+046		×					TD	Mon16
J17578+465		×			HS	Mon16	YD	Mon16
J17589+807								
J18010+508								
J18022+642	×	×	×		UMa	Mon16	D	Mon16
J18027+375			×				D	Mon16
J18031+179		×						
J18037+247								
J18042+359			×	×			D	Mon16
J18051-030		×					D	Mon16
J18063+728		×						
J18074+184								
J18075-159	×	×					D	Mon16
J18096+318		×						
J18103+512								
J18109+220								
J18116+061							D	Mon16
J18131+260	×	×		×			D	Mon16
J18134+054								
J18135+055							D	Mon16
J18157+189							D	Mon16
J18160+139							D	Mon16
J18163+015							D	Mon16
J18165+455							YD	Mon16
J18165+048							D	Mon16
J18174+483		×						
J18180+387W							D	Mon16
J18180+387E							D	Mon16

Table B.4: Activity indicators, stellar kinematic associations and poputation of Carmencita stars (continued).

Karmn	Activity[a]						Population	Ref.[d]
	pEW(Hα)	X-rays	$v \sin i$	P	SKG[b]	Ref.[c]		
J18189+661	×	×	×				D	Mon16
J18193-057							TD-D	Mon16
J18195+420				×				
J18209-010							TD	Mon16
J18221+063							TD	Mon16
J18224+620							D	Mon16
J18227+379								
J18234+281					LA	Mon16	YD	Mon16
J18240+016							D	Mon16
J18248+282								
J18250+246			×				D	Mon16
J18255+383							D	Mon16
J18264+113							D	Mon16
J18292+638								
J18296+338								
J18312+068					UMa	Mon16	D	Mon16
J18319+406		×					YD	Mon16
J18346+401		×					D	Mon16
J18352+243								
J18352+414							TD	Mon16
J18353+457		×					D	Mon16
J18354+457			×				YD	Mon16
J18356+329		×	×		UMa	Mon16	D	Mon16
J18358+800	×	×					D	Mon16
J18362+567								
J18363+136	×	×			HS	Mon16	YD	Mon16
J18387-144							D	Mon16
J18387+047								
J18394+690	×	×						
J18395+301			×				D	Mon16
J18395+298								
J18399+334					HS	Mon16	YD	Mon16
J18400+726	×							
J18402-104							TD	Mon16
J18405+595								
J18409+315							TD-D	Mon16
J18409-133							D	Mon16
J18411+247S	×	×	×				D	Mon16
J18411+247N	×		×				D	Mon16
J18416+397	×	×					D	Mon16
J18419+318							D	Mon16
J18427+139	×	×		×	HS	Mon16	YD	Mon16
J18427+596N							D	Mon16
J18427+596S		×					D	Mon16
J18432+253								
J18433+406	×		×		HS	Mon16	YD	Mon16
J18451+063		×		×	Car	Ell14	YD	Mon16
J18453+188	×		×	×			D	Mon16

Table B.4: Activity indicators, stellar kinematic associations and poputation of Carmencita stars (continued).

	Activity[a]							
Karmn	pEW(Hα)	X-rays	$v \sin i$	P	SKG[b]	Ref.[c]	Population	Ref.[d]
J18480-145							D	Mon16
J18482+076	×	×			HS	Mon16	YD	Mon16
J18487+615								
J18499+186	×						D	Mon16
J18500+030							D	Mon16
J18507+479							TD-D	Mon16
J18515+027								
J18516+244							TD-D	Mon16
J18518+165							D	Mon16
J18519+130	×	×			ABDor?	Schl12b		
J18534+028								
J18548+008		×			Cas	Cab10		
J18548+109							YD	Mon16
J18554+084	×	×	×		LA	Mon16	YD	Mon16
J18563+544							D	Mon16
J18564+463							D	Mon16
J18571+075							D	Mon16
J18576+535								
J18580+059		×					D	Mon16
J18596+079			×				TD	Mon16
J19025+704							D	Mon16
J19032+034							YD	Mon16
J19032-135							D	Mon16
J19032+639	×	×					D	Mon16
J19041+211		×						
J19045+240								
J19070+208							D	Mon16
J19072+208							D	Mon16
J19044+590								
J19077+325		×					D	Mon16
J19082+265							D	Mon16
J19084+322							D	Mon16
J19093+382							D	Mon16
J19093-147							D	Mon16
J19095+391								
J19098+176							D	Mon16
J19106+015							D	Mon16
J19116+050		×						
J19122+028			×				TD	Mon16
J19124+355							TD-D	Mon16
J19146+193N	×	×	×	×			TD	Mon16
J19146+193S							TD	Mon16
J19169+051N		×			LA?	Tet11	D	Mon16
J19169+051S	×	×	×				D	Mon16
J19185+580								
J19205-076							D	Mon16
J19215+425		×		×				
J19216+208							D	Mon16

Table B.4: Activity indicators, stellar kinematic associations and poputation of Carmencita stars (continued).

Karmn	Activity[a]				SKG[b]	Ref.[c]	Population	Ref.[d]
	pEW(Hα)	X-rays	$v \sin i$	P				
J19218+286							TD	Mon16
J19220+070							D	Mon16
J19228+307								
J19234+666								
J19237+797								
J19242+797								
J19242+755							YD	Mon16
J19251+283					HS	Mon16	YD	Mon16
J19255+096	×				LA	Mon16	YD	Mon16
J19260+244	×	×		×			YD	Mon16
J19268+167	×	×					D	Mon16
J19284+289								
J19289+066								
J19312+361	×	×		×			YD	Mon16
J19326+005							D	Mon16
J19336+395							D	Mon16
J19346+045							D	Mon16
J19349+532							D	Mon16
J19351+084S			×				YD	Mon16
J19351+084N							YD	Mon16
J19354+377	×	×	×				D	Mon16
J19358+413				×				
J19395+718			×				D	Mon16
J19419+031							D	Mon16
J19420-210	×	×			LA	Mon16	YD	Mon16
J19422-207	×	×					YD	Mon16
J19457+271							D	Mon16
J19457+323			×				YD	Mon16
J19463+320							D	Mon16
J19464+320							D	Mon16
J19468-019								
J19470+352								
J19486+359					UMa	Mon16	D	Mon16
J19500+325							YD	Mon16
J19502+317		×					D	Mon16
J19510+104		×					D	Mon16
J19511+464	×	×	×	×	IC	Mon16	YD	Mon16
J19512+622								
J19535+341					HS	Mon16	YD	Mon16
J19539+444W	×	×	×	×			D	Mon16
J19539+444E	×		×				TD	Mon16
J19540+325							YD	Mon16
J19546+202								
J19558+512							D	Mon16
J19564+591							TD	Mon16
J19565+591							TD	Mon16
J19573-125							D	Mon16
J19582+020							D	Mon16

Table B.4: Activity indicators, stellar kinematic associations and poputation of Carmencita stars (continued).

	Activity[a]							
Karmn	pEW(Hα)	X-rays	$v \sin i$	P	SKG[b]	Ref.[c]	Population	Ref.[d]
J19582+650							D	Mon16
J20005+593		×			Cas	Mon16	YD	Mon16
J20011+002							D	Mon16
J20034+298	×	×					D	Mon16
J20037+644		×						
J20038+059							D	Mon16
J20039-081							D	Mon16
J20050+544	×	×	×				H	Mace13
J20057+529							YD	Mon16
J20079-015							D	Mon16
J20082+333	×	×	×				D	Mon16
J20093-012	×	×						
J20105+065	×	×		×			D	Mon16
J20112+379								
J20112+161	×						TD	Mon16
J20129+342		×						
J20132+029		×						
J20138+133								
J20139+066							D	Mon16
J20151+635								
J20165+351								
J20187+158		×			LA	Mon16	YD	Mon16
J20195+080							TD	Mon16
J20198+229	×	×	×		LA	Mon16	YD	Mon16
J20220+216		×						
J20223+322								
J20229+106								
J20232+671		×						
J20260+585							D	Mon16
J20269+275							D	Mon16
J20287-114	×	×	×		IC	Mon16	YD	Mon16
J20298+096	×	×	×	×	HS	Mon16	YD	Mon16
J20301+798	×	×						
J20305+654		×					D	Mon16
J20314+385							D	Mon16
J20336+617							D	Mon16
J20337+233							D	Mon16
J20339+643							D	Mon16
J20347+033							TD	Mon16
J20349+592							TD	Mon16
J20367+388							D	Mon16
J20373+219	×			×			D	Mon16
J20403+616								
J20405+154							D	Mon16
J20407+199							D	Mon16
J20409-101							D	Mon16
J20429-189							TD	Mon16
J20433+553	×	×	×				TD	Mon16

Table B.4: Activity indicators, stellar kinematic associations and poputation of Carmencita stars (continued).

Karmn	Activity[a]				SKG[b]	Ref.[c]	Population	Ref.[d]
	pEW(Hα)	X-rays	$v \sin i$	P				
J20435+240	×	×	×	×	LA	Mon16	YD	Mon16
J20436-001							D	Mon16
J20436+642								
J20443+197							D	Mon16
J20445+089N							YD	Mon16
J20445+089S					HS	Mon16	YD	Mon16
J20450+444					HS	Mon16	YD	Mon16
J20488+197							D	Mon16
J20496-003							D	Mon16
J20519+691			×				D	Mon16
J20525-169					UMa	Mon16	D	Mon16
J20532-023		×			HS	Mon16	YD	Mon16
J20533+621		×					D	Mon16
J20535+106							D	Mon16
J20549+675								
J20556-140S							TD	Mon16
J20556-140N							TD	Mon16
J20567-104							TD-D	Mon16
J20568-048	×	×					D	Mon16
J20574+223			×				D	Mon16
J20586+342			×				D	Mon16
J21000+400	×		×				D	Mon16
J21001+495								
J21012+332	×	×		×			D	Mon16
J21013+332		×			LA	Mon16	YD	Mon16
J21014+207							D	Mon16
J21019-063		×					D	Mon16
J21027+349	×	×						
J21044+455								
J21048-169							TD	Mon16
J21055+061							YD	Mon16
J21057+502					LA	Mon16	YD	Mon16
J21059+044							TD-D	Mon16
J21074+468								
J21076-130	×	×			bPic	Malo13	YD	Mon16
J21087-044N	×						D	Mon16
J21087-044S		×					D	Mon16
J21092-133		×					TD	Mon16
J21100-193	×				bPic	Malo14a	YD	Mon16
J21109+294							D	Mon16
J21123+359								
J21127-073					Cas	Mon16	YD	Mon16
J21137+087								
J21138+180							D	Mon16
J21145+508								
J21147+380		×					D	Mon16
J21152+257							D	Mon16
J21160+298W	×	×			Cas	Mon16	YD	Mon16

Table B.4: Activity indicators, stellar kinematic associations and poputation of Carmencita stars (continued).

	Activity[a]							
Karmn	pEW(Hα)	X-rays	$v \sin i$	P	SKG[b]	Ref.[c]	Population	Ref.[d]
J21160+298E	×	×			Cas	Mon16	YD	Mon16
J21164+025					IC	Mon16	YD	Mon16
J21173+640	×	×		×			D	Mon16
J21173+208N							D	Mon16
J21173+208S							D	Mon16
J21176-089N	×	×			UMa	Mon16	D	Mon16
J21176-089S		×					D	Mon16
J21185+302	×	×	×		bPic?	Schl12b	YD	Mon16
J21221+229							D	Mon16
J21243+085							D	Mon16
J21245+400	×							
J21267+037							YD	Mon16
J21272-068							D	Mon16
J21275+340							TD	Mon16
J21277+072							D	Mon16
J21280+179								
J21283-223							D	Mon16
J21296+176			×		HS	Mon16	YD	Mon16
J21313-097		×					D	Mon16
J21323+245	×	×		×			D	Mon16
J21338-068	×						D	Mon16
J21338+017S							D	Mon16
J21338+017N							D	Mon16
J21348+515					HS	Mon16	YD	Mon16
J21366+394		×					D	Mon16
J21369+561								
J21374-059								
J21376+016	×	×	×	×	bPic?	Schl12b	YD	Mon16
J21378+530							D	Mon16
J21380+277		×	×				YD	Mon16
J21399+276							D	Mon16
J21402+370							D	Mon16
J21419+276							D	Mon16
J21421-121		×					TD	Mon16
J21441+170N		×					D	Mon16
J21441+170S							D	Mon16
J21442+066		×					D	Mon16
J21449+442								
J21450-057							D	Mon16
J21450+198								
J21454-059							D	Mon16
J21463+382							TD	Mon16
J21466+668					IC	Mon16	YD	Mon16
J21466-001			×				D	Mon16
J21469+466					Cas	Mon16	YD	Mon16
J21472-047							YD	Mon16
J21478+502							D	Mon16
J21479+058							D	Mon16

Table B.4: Activity indicators, stellar kinematic associations and poputation of Carmencita stars (continued).

Karmn	Activity[a]				SKG[b]	Ref.[c]	Population	Ref.[d]
	pEW(Hα)	X-rays	$v \sin i$	P				
J21481+014							D	Mon16
J21482+279							D	Mon16
J21512+128							TD-D	Mon16
J21518+136					LA	Mon16	YD	Mon16
J21521+056	×	×					D	Mon16
J21521+274							TD	Mon16
J21539+417			×				TD-D	Mon16
J21566+197							TD	Mon16
J21569-019							D	Mon16
J21574+081		×			HS	Mon16	YD	Mon16
J21584+755					LA	Mon16	YD	Mon16
J21585+612								
J21593+418							D	Mon16
J22012+283	×	×	×	×	Cas	Mon16	YD	Mon16
J22012+323								
J22018+164		×			HS	Mon16	YD	Mon16
J22020-194							D	Mon16
J22021+014		×					D	Mon16
J22033+674							TD	Mon16
J22035+036	×							
J22051+051					HS	Mon16	D	Mon16
J22057+656							D	Mon16
J22058-119					Cas	Cab10	D	Mon16
J22060+393							D	Mon16
J22063+173								
J22067+034							D	Mon16
J22088+117	×		×				YD	Mon16
J22095+118								
J22096-046					HS	Mon16	YD	Mon16
J22097+410							TD	Mon16
J22107+079							YD	Mon16
J22112-025							D	Mon16
J22112+410								
J22114+409	×	×					YD	Mon16
J22115+184							D	Mon16
J22117-207	×	×			LA	Mon16	YD	Mon16
J22125+085							D	Mon16
J22129+550		×						
J22134-147							D	Mon16
J22135+259	×	×					D	Mon16
J22137-176		×					YD	Mon16
J22138+052							D	Mon16
J22142+255		×			LA	Mon16	YD	Mon16
J22154+662		×					YD	Mon16
J22160+546	×				Cas	Cab10	D	Mon16
J22163+709							TD-D	Mon16
J22173-088S	×						D	Mon16
J22173-088N	×						D	Mon16

Table B.4: Activity indicators, stellar kinematic associations and poputation of Carmencita stars (continued).

	Activity[a]							
Karmn	pEW(Hα)	X-rays	$v \sin i$	P	SKG[b]	Ref.[c]	Population	Ref.[d]
J22176+565								
J22202+067								
J22212+377								
J22228+280							D	Mon16
J22231-176	×	×					D	Mon16
J22234+324	×	×	×	×	AB Dor	Zuck04	YD	Mon16
J22249+520			×				D	Mon16
J22250+356		×		×				
J22252+594							D	Mon16
J22262+030							D	Mon16
J22264+583								
J22270+068							D	Mon16
J22279+576		×	×				D	Mon16
J22287+189			×				D	Mon16
J22289-134	×		×				D	Mon16
J22290+016								
J22298+414							D	Mon16
J22300+488	×	×	×	×			YD	Mon16
J22330+093							YD	Mon16
J22333-096	×	×			Arg	Malo14a	YD	Mon16
J22347+040							D	Mon16
J22348-010							TD-D	Mon16
J22353+746		×						
J22361-008							D	Mon16
J22373+299								
J22374+395		×					D	Mon16
J22385-152	×	×					D	Mon16
J22387+252								
J22387-206N	×	×	×	×	IC	Mon16	YD	Mon16
J22387-206S	×	×	×	×			YD	Mon16
J22406+445							D	Mon16
J22415+188		×					D	Mon16
J22415+260	×	×						
J22426+176							D	Mon16
J22433+221	×			×			YD	Mon16
J22437+192	×							
J22440+405								
J22441+405								
J22457+016								
J22464-066							TD	Mon16
J22468+443	×	×	×		UMa	Mon16	D	Mon16
J22476+184								
J22479+318							D	Mon16
J22489+183	×							
J22503-070							D	Mon16
J22506+348							D	Mon16
J22507+286					LA	Mon16	YD	Mon16
J22509+499	×	×	×		LA	Mon16	YD	Mon16

Table B.4: Activity indicators, stellar kinematic associations and poputation of Carmencita stars (continued).

Karmn	Activity[a]				SKG[b]	Ref.[c]	Population	Ref.[d]
	pEW(Hα)	X-rays	$v \sin i$	P				
J22518+317	×	×	×	×	IC?	Laf07	YD	Mon16
J22524+099							D	Mon16
J22526+750	×						YD	Mon16
J22532-142		×			LA	Mon16	YD	Mon16
J22543+609		×					D	Mon16
J22547-054							D	Mon16
J22559+057		×	×				D	Mon16
J22559+178							D	Mon16
J22565+165		×					TD	Mon16
J22576+373								
J23028+436	×	×		×	UMa	Mon16	D	Mon16
J23036+097								
J23045+667		×					D	Mon16
J23051+519								
J23051+452	×	×		×			YD	Mon16
J23060+639	×	×	×	×	AB Dor	Zuck04	YD	Mon16
J23063+126	×	×		×			D	Mon16
J23064-050	×		×				TD-D	Mon16
J23065+717							TD	Mon16
J23075+686							D	Mon16
J23081+033							D	Mon16
J23083-154	×	×	×	×	Cas	Cab10	YD	Mon16
J23088+065		×	×		LA	Mon16	YD	Mon16
J23096-019							D	Mon16
J23089+551							D	Mon16
J23107-192							TD	Mon16
J23113+085							D	Mon16
J23121-141							TD-D	Mon16
J23142-196S							YD	Mon16
J23142-196N							YD	Mon16
J23161+067							D	Mon16
J23166+196							D	Mon16
J23174+382							D	Mon16
J23174+196	×	×			Cas	Mon16	YD	Mon16
J23175+063							D	Mon16
J23182+795								
J23182+462				×	HS	Mon16	YD	Mon16
J23193+154								
J23194+790	×	×	×		LA	Mon16	YD	Mon16
J23215+568								
J23216+172							D	Mon16
J23220+569							D	Mon16
J23228+787	×	×						
J23229+372							D	Mon16
J23234+155							D	Mon16
J23245+578		×					D	Mon16
J23252+009								
J23256+531	×	×		×			TD	Mon16

Table B.4: Activity indicators, stellar kinematic associations and poputation of Carmencita stars (continued).

	Activity[a]							
Karmn	$pEW(\mathrm{H}\alpha)$	X-rays	$v \sin i$	P	SKG[b]	Ref.[c]	Population	Ref.[d]
J23261+170	×	×						
J23262+088							D	Mon16
J23262+278	×	×						
J23265+121							D	Mon16
J23293+414S	×		×		LA	Mon16	YD	Mon16
J23293+414N	×	×	×		LA	Mon16	YD	Mon16
J23301-026					bPic?	AF15b		
J23302-203	×	×					D	Mon16
J23308+157								
J23317-027		×			bPic?	Malo13	YD	Mon16
J23318+199E	×		×		Cas	Cab10	D	Mon16
J23318+199W	×		×	×	Cas	Cab10	D	Mon16
J23323+540								
J23327-167	×	×	×		LA	Mon16	YD	Mon16
J23340+001		×					D	Mon16
J23350+016		×	×				YD	Mon16
J23350+252							D	Mon16
J23351-023			×				D	Mon16
J23354+300							D	Mon16
J23357+419							D	Mon16
J23364+554				×			D	Mon16
J23376-128								
J23381-162							D	Mon16
J23386+391							D	Mon16
J23389+210	×	×					D	Mon16
J23401+606							D	Mon16
J23414+200								
J23419+441	×	×					TD-D	Mon16
J23423+349								
J23428+308	×						D	Mon16
J23431+365		×					YD	Mon16
J23438+325							D	Mon16
J23438+610								
J23439+647	×	×					D	Mon16
J23443+216	×	×			HS	Mon16	YD	Mon16
J23455-161	×	×		×			D	Mon16
J23462+284							D	Mon16
J23480+490							D	Mon16
J23489+098								
J23492+024		×					TD	Mon16
J23492+100	×	×					D	Mon16
J23496+083					LA	Mon16	YD	Mon16
J23505-095							D	Mon16
J23506+099					HS	Mon16	YD	Mon16
J23509+384							D	Mon16
J23517+069							YD	Mon16
J23523-146							D	Mon16
J23535+121	×	×						

Table B.4: Activity indicators, stellar kinematic associations and poputation of Carmencita stars (continued).

Karmn	Activity[a]				SKG[b]	Ref.[c]	Population	Ref.[d]
	$pEW(\mathrm{H}\alpha)$	X-rays	$v \sin i$	P				
J23541+516							D	Mon16
J23544+081							D	Mon16
J23548+385	×	×	×	×	UMa	Mon16	D	Mon16
J23249+506								
J23554-039							D	Mon16
J23556-061							D	Mon16
J23560+150								
J23569+230							D	Mon16
J23573-129W	×	×	×		Cas	Mon16	YD	Mon16
J23573-129E	×	×					D	Mon16
J23577+233			×				TD	Mon16
J23577+197							D	Mon16
J23578+386	×	×			UMa	Mon16	YD	Mon16
J23582-174	×	×					YD	Mon16
J23585+076							D	Mon16
J23587+467							D	Mon16
J23590+208								
J23598+477			×				TD-D	Mon16

Notes. [a]For each category, activity means: $pEW(H\alpha) < -0.75$ Å, $v \sin i > 4.0\,\mathrm{km\,s^{-1}}$, $P < 50$ d, and X-ray emission. [b]AB Dor: AB Doradus; Arg: Argus; Car: Carina; Cas: Castor; Col: Columba; HS: Hyades; HSc: Hyades cluster; Her-Lyr: Hercules-Lyra; IC: IC2391; LA: Local Association; TucHor: Tucana-Horologium; UMa: Ursa Major; bPic: β Pictoris; Tau: Taurus; TW Hya: TW hydrae. [c]AF15b: Alonso-Floriano et al. (2015b); BG06: Bertout & Genova (2006); Cab10: Caballero et al. (2010); Ell14: Elliott et al. (2014); LS06: López-Santiago et al. (2006); Laf07: Lafrenière et al. (2007); Malo13: Malo et al. (2013); Malo14a: Malo et al. (2014a); Mon16: Montes priv. comm.; Re10: Rebull et al. (2010); Rei02: Reid et al. (2002); Ried14: Riedel et al. (2014); Schl10: Schlieder et al. (2010); Schl12a: Schlieder et al. (2012a); Schl12b: Schlieder et al. (2012b); Shk12: Shkolnik et al. (2012); Ste95: Stern et al. (1995); Tet11: Tetzlaff et al. (2011); Tor06: Torres et al. (2006); Tor08: Torres et al. (2008); Zuck04: Zuckerman et al. (2004); Zuck11: Zuckerman et al. (2011). [d]YD: Young disc; D: Thin disc; TD-D: Transition Thin/Thick disc; TD: Thick disc; H: Halo. [e]Mace13: Mace et al. 2013 ; Mon16: Montes priv. comm.

Table B.5: Colour indices for M0.0 V to M6.5 V stars from Holgado (2014).

SpT	$NUV - u'$ [mag]	$u' - g'$ [mag]	$g' - r'$ [mag]	$r' - i'$ [mag]	$i' - J$ [mag]	$J - H$ [mag]	$H - K_s$ [mag]	$K_s - W1$ [mag]	$W1 - W2$ [mag]	$W2 - W3$ [mag]	$W3 - W4$ [mag]
M0.0 V	2.89 ± 0.09	...	1.38 ± 0.10	0.92 ± 0.16	1.63 ± 0.10	0.65 ± 0.04	0.18 ± 0.03	0.11 ± 0.05	0.14 ± 0.10	-0.10 ± 0.07	0.07 ± 0.04
M0.5 V	3.02 ± 0.49	4.40 ± 1.20	1.37 ± 0.21	0.92 ± 0.14	1.63 ± 0.14	0.62 ± 0.05	0.23 ± 0.03	0.09 ± 0.02	0.16 ± 0.06	-0.08 ± 0.08	0.07 ± 0.07
M1.0 v	3.48 ± 0.77	4.14 ± 0.51	1.31 ± 0.09	0.93 ± 0.10	1.72 ± 0.08	0.61 ± 0.04	0.22 ± 0.02	0.11 ± 0.05	0.13 ± 0.09	-0.02 ± 0.07	0.10 ± 0.06
M1.5 V	3.87 ± 1.31	4.21 ± 0.59	1.34 ± 0.12	1.03 ± 0.07	1.80 ± 0.10	0.60 ± 0.06	0.24 ± 0.04	0.11 ± 0.04	0.17 ± 0.13	-0.03 ± 0.10	0.10 ± 0.03
M2.0 V	4.35 ± 1.39	3.60 ± 0.38	1.33 ± 0.07	1.06 ± 0.15	1.88 ± 0.14	0.59 ± 0.04	0.24 ± 0.03	0.14 ± 0.03	0.15 ± 0.06	0.00 ± 0.07	0.13 ± 0.05
M2.5 V	5.27 ± 0.47	3.32 ± 0.44	1.36 ± 0.12	1.15 ± 0.10	1.89 ± 0.12	0.60 ± 0.03	0.24 ± 0.03	0.15 ± 0.03	0.13 ± 0.08	0.03 ± 0.06	0.11 ± 0.08
M3.0 V	5.38 ± 0.94	3.11 ± 0.20	1.33 ± 0.06	1.28 ± 0.07	1.96 ± 0.10	0.59 ± 0.04	0.26 ± 0.03	0.15 ± 0.03	0.15 ± 0.08	0.05 ± 0.07	0.12 ± 0.05
M3.5 V	4.92 ± 1.45	3.13 ± 0.38	1.32 ± 0.05	1.39 ± 0.14	2.10 ± 0.11	0.56 ± 0.05	0.27 ± 0.03	0.16 ± 0.03	0.20 ± 0.13	0.11 ± 0.09	0.11 ± 0.07
M4.0 V	4.18 ± 1.53	2.79 ± 0.29	1.33 ± 0.08	1.51 ± 0.09	2.19 ± 0.09	0.57 ± 0.04	0.27 ± 0.03	0.17 ± 0.03	0.17 ± 0.05	0.04 ± 0.10	0.13 ± 0.10
M4.5 V	2.34 ± 0.98	2.55 ± 0.15	1.42 ± 0.08	1.72 ± 0.12	2.33 ± 0.11	0.56 ± 0.05	0.29 ± 0.03	0.21 ± 0.04	0.20 ± 0.06	0.07 ± 0.14	0.14 ± 0.06
M5.0 V	3.54 ± 1.33	2.42 ± 0.26	1.43 ± 0.15	1.90 ± 0.15	2.57 ± 0.11	0.59 ± 0.04	0.32 ± 0.03	0.22 ± 0.02	0.19 ± 0.03	0.04 ± 0.17	0.12 ± 0.11
M5.5 V	2.16	2.29 ± 0.88	1.45 ± 0.04	2.08 ± 0.07	2.67 ± 0.05	0.60 ± 0.05	0.32 ± 0.03	0.23 ± 0.02	0.18 ± 0.02	0.17 ± 0.03	0.19 ± 0.11
M6.0 V	2.97	1.98	1.50	2.44	2.23	0.60	0.40	0.28	0.32	0.00	0.17
M6.5 V	...	...	...	...	3.25	0.60 ± 0.01	0.36 ± 0.03	0.22 ± 0.01	0.21 ± 0.00	0.21 ± 0.02	0.09 ± 0.22

SpT	$FUV - NUV$ [mag]	$r' - J$ [mag]	$r' - K_s$ [mag]	$W1 - W3$ [mag]	$W2 - W4$ [mag]
M0.0 V	3.19 ± 0.24	2.49 ± 0.25	3.32 ± 0.26	0.04 ± 0.05	-0.03 ± 0.09
M0.5 V	2.88 ± 0.30	2.48 ± 0.09	3.32 ± 0.11	0.09 ± 0.04	0.02 ± 0.08
M1.0 v	2.58 ± 0.55	2.63 ± 0.12	3.47 ± 0.13	0.12 ± 0.05	0.08 ± 0.08
M1.5 V	2.54 ± 0.46	2.79 ± 0.11	3.62 ± 0.12	0.14 ± 0.06	0.06 ± 0.11
M2.0 V	2.18 ± 0.48	2.93 ± 0.09	3.77 ± 0.10	0.16 ± 0.04	0.13 ± 0.10
M2.5 V	2.16 ± 0.28	3.05 ± 0.14	3.90 ± 0.13	0.16 ± 0.03	0.15 ± 0.10
M3.0 V	1.37 ± 0.61	3.25 ± 0.10	4.10 ± 0.11	0.20 ± 0.03	0.17 ± 0.08
M3.5 V	1.32 ± 0.29	3.49 ± 0.12	4.33 ± 0.12	0.24 ± 0.04	0.16 ± 0.13
M4.0 V	1.51 ± 0.33	3.71 ± 0.13	4.56 ± 0.16	0.27 ± 0.04	0.22 ± 0.11
M4.5 V	1.09 ± 0.34	4.04 ± 0.18	4.90 ± 0.20	0.30 ± 0.04	0.24 ± 0.09

M5.0 V	0.97 ± 0.31	4.47 ± 0.21	5.38 ± 0.24	0.33 ± 0.03	0.26 ± 0.11
M5.5 V	1.17	4.90 ± 0.28	5.82 ± 0.27	0.36 ± 0.03	0.37 ± 0.03

C

Long tables of Chapter 4

This appendix includes the tables referenced in Chapter 4.

- Table C.1 contains the 490 Carmencita M dwarfs observed with the lucky imager FastCam at the Telescopio Carlos Sánchez at the Observatorio del Teide. It contains the Karmn and common names, J2000.0 coordinates, 2MASS J magnitude, spectral type, distance, epoch of observation, the number of frames taken and the exposure times. This table corresponds to Table A.1 in the article.
- Table C.2 lists the observed ADS standard stars during the programme for calibration purposes. It contains the ADS name of the star, the ρ and θ literature values, and our measured values for each observed night. This table corresponds to Table A.2 in the article.
- Table C.3 displays the ρ and θ measured values from our FastCam images of all the confirmed visual (i.e., not bound) stars. This table corresponds to Table A.3 in the article.
- Table C.4 contains the astrometric parameters (ρ, θ) and magnitude differences (ΔI) of the 80 detected companions to our Carmencita stars in every observed night. For previously known pairs, it shows the Washington Double Star catalogue (WDS) name and discoverer code. When it was available, it is also included the multiplicity flag from version 1.2 of the Guide Star Catalogue. This table corresponds to Table A.4 in the article.
- Table C.5 contains the individual I magnitudes, literature and inferred spectral types, and derived masses for the components of the detected systems in our FastCam images. For all the M dwarf systems, we computed the orbital periods. This table corresponds to Table A.5 in the article.
- Table C.6 lists all the known companions to our observed Carmencita stars separated by more than 5 arcsec. It includes the WDS discoverer code, the Karmn or common name of the stars in the system and the angular separation between components. Notes to some systems are added. This table corresponds to Table A.6 in the article.

Table C.1: Log of observed stars.

No.	Karmn	Name	α (J2000)	δ (J2000)	J [mag]	SpT	Ref.[a]	d [pc]	Ref.[b]	Observation date	N × $t_{\rm exp}$ [s]
1	J00067-075	GJ 1002	00:06:43.26	–07:32:14.7	8.323	M5.5 V	PMSU	4.82	Wein16	23 Oct 2011	10 × 50
2	J00088+208	LP 404–033	00:08:53.92	+20:50:25.2	8.870	M4.5 V	PMSU	14.8	Dit14	24 Oct 2011	10 × 50
3	J00154-161	GJ 1005 AB	00:15:27.99	–16:08:00.9	7.215	M4.0 V	PMSU	6.0	HT98	10 Jul 2012	10 × 50
4	J00158+135	GJ 12	00:15:49.20	+13:33:21.9	8.619	M3.0 V	PMSU	10.0	Dit14	16 Sep 2012	10 × 50
5	J00169+051	GJ 1007	00:16:56.29	+05:07:26.1	9.398	M4.5 V	PMSU	17.57	vAl95	25 Oct 2011	10 × 50
6	J00169+200	G 131–047	00:16:56.78	+20:03:55.1	9.681	M3.5 V	PMSU	24.5	This work	14 Jan 2013	10 × 50
										17 Nov 2015	10 × 50
7	J00182+102	GJ 16	00:18:16.59	+10:12:10.1	7.564	M1.5 V	PMSU	16.34	HIP2	17 Nov 2015	10 × 50
8	J00183+440	GX And	00:18:22.57	+44:01:22.2	5.252	M1.0 V	AF15	3.59	HIP2	23 Oct 2011	10 × 35
9	J00184+440	GQ And	00:18:25.50	+44:01:37.6	6.789	M3.5 V	PMSU	3.6	Dit14	23 Oct 2011	10 × 35
										17 Sep 2012	10 × 50
										13 Jan 2013	10 × 50
10	J00188+278	LP 292–066	00:18:53.53	+27:48:50.0	9.535	M4.0 V	PMSU	14.5	Dit14	25 Oct 2011	10 × 50
11	J00234+243	GJ 1011	00:23:28.03	+24:18:24.4	9.753	M4.0 V	PMSU	16.39	vAl95	25 Oct 2011	10 × 50
12	J00245+300	G 130–068	00:24:34.78	+30:02:29.5	9.776	M4.5 V	PMSU	18.94	vAl95	24 Oct 2011	10 × 50
13	J00253+228	LP 349–018	00:25:20.64	+22:53:12.1	9.716	M4.0 V	PMSU	14.2	Dit14	24 Oct 2011	10 × 50
14	J00271+496	G 217–051	00:27:06.74	+49:41:53.1	9.733	M4.5 V	PMSU	20.9	Dit14	25 Oct 2011	10 × 50
15	J00286-066	GJ 1012	00:28:39.48	–06:39:48.1	8.038	M4.0 V	PMSU	13.26	Rei02	25 Oct 2011	10 × 50
16	J00315-058	GJ 1013	00:31:35.39	–05:52:11.6	8.762	M3.5 V	PMSU	16.1	vAl95	16 Sep 2012	10 × 50
17	J00385+514	G 172–015	00:38:33.88	+51:27:58.0	8.892	M2.5 V	PMSU	15.6	vAl95	14 Jan 2013	10 × 50
18	J00389+306	Wolf 1056	00:38:58.79	+30:36:58.4	7.453	M2.5 V	AF15	12.5	vAl95	16 Sep 2012	10 × 50
19	J00409+313	G 069–011	00:40:56.23	+31:22:56.5	9.491	M4.0 V	PMSU	17.7	Dit14	24 Oct 2011	10 × 50
20	J00413+558	GJ 1015 A	00:41:20.78	+55:50:04.5	9.839	M4.0 V	PMSU	23.04	vAl95	25 Oct 2011	10 × 50
21	J00443+126	G 032–044	00:44:19.34	+12:37:02.7	8.868	M3.5 V	PMSU	16.5	This work	16 Sep 2012	10 × 50
22	J00443+091	NLTT 2413	00:44:20.70	+09:07:34.6	9.501	M4.5 V	PMSU	14.6	This work	25 Oct 2011	10 × 50
23	J00566+174	GJ 1024	00:56:38.42	+17:27:34.7	9.285	M4.0 V	PMSU	17.73	vAl95	25 Oct 2011	10 × 50
24	J00570+450	G 172-030	00:57:02.61	+45:05:09.9	8.101	M3.0 V	Lep13	13.8	This work	17 Nov 2015	10 × 50
25	J01009-044	GJ 1025	01:00:56.44	–04:26:56.1	9.042	M4.0 V	AF15	14.7	This work	16 Sep 2012	10 × 50
26	J01026+623	BD+61 195	01:02:38.96	+62:20:42.2	6.230	M1.5 V	AF15	9.96	HIP2	17 Sep 2012	10 × 50
										13 Jan 2013	10 × 50
27	J01033+623	V388 Cas	01:03:19.72	+62:21:55.7	8.611	M5.0 V	AF15	9.96	aHIP2	23 Oct 2011	10 × 50
28	J01056+284	GJ 1029	01:05:37.32	+28:29:34.0	9.486	M5.0 V	PMSU	11.3	Dit14	25 Oct 2011	10 × 50
29	J01066+152	GJ 1030	01:06:41.52	+15:16:22.9	8.005	M2.0 V	PMSU	22.1	HIP2	17 Sep 2012	10 × 50

Table C.1: Log of observed stars (continued).

No.	Karmn	Name	α (J2000)	δ (J2000)	J [mag]	SpT	Ref.[a]	d [pc]	Ref.[b]	Observation date	N $\times$ $t_{\rm exp}$ [s]
30	J01119+049N	G 070–043	01:11:55.63	+04:55:04.9	8.804	M3.0 V	PMSU	15.9	vAl95	24 Oct 2011	10 × 50
31	J01119+049S	G 070–044	01:11:57.99	+04:54:12.0	9.641	M3.5 V	PMSU	15.9	avAl95	24 Oct 2011	10 × 50
32	J01182-128	GJ 56.1	01:18:15.99	–12:53:58.1	8.356	M2.0 V	PMSU	22.1	HIP2	17 Sep 2012	10 × 50
33	J01221+221	G 034-023	01:22:10.28	+22:09:03.2	8.412	M4.5 V	Lep13	10.2	This work	17 Nov 2015	10 × 50
34	J01384+006	G 071–024	01:38:29.98	+00:39:05.9	8.189	M2.0 V	PMSU	20.2	HIP2	17 Sep 2012	10 × 50
35	J01402+317	G 072–023	01:40:16.49	+31:47:30.7	9.437	M4.0 V	PMSU	18.7	Dit14	25 Oct 2011	10 × 50
36	J01433+043	GJ 70	01:43:20.15	+04:19:17.2	7.370	M2.0 V	PMSU	11.4	HIP2	17 Sep 2012	10 × 50
37	J01449+163	Wolf 1530	01:44:58.52	+16:20:39.7	9.584	M4.0 V	PMSU	16.39	vAl95	24 Oct 2011	10 × 50
38	J01453+465	G 173-018	01:45:18.20	+46:32:07.8	8.058	M2.0 V	Lep13	25.63	HIP2	17 Nov 2015	10 × 50
39	J01510-061	NLTT 6192	01:51:04.05	–06:07:04.8	9.413	M4.5 V	PMSU	9.92	Hen06	25 Oct 2011	10 × 50
40	J01518-108	Ross 555	01:51:48.65	–10:48:12.0	8.375	M2.0 V	PMSU	16.6	HIP2	17 Sep 2012	10 × 50
41	J01518+644	G 244–037	01:51:51.08	+64:26:06.1	7.838	M2.5 V	PMSU	14.7	This work	17 Sep 2012	10 × 50
42	J01593+585	V596 Cas	01:59:23.50	+58:31:16.2	7.790	M4.0 V	PMSU	12.25	HIP2	23 Oct 2011	10 × 50
										17 Sep 2012	10 × 50
										13 Jan 2013	10 × 50
43	J02022+103	LP 469–067	02:02:16.21	+10:20:13.7	9.842	M5.5 V	AF15	9.19	Wein16	25 Oct 2011	10 × 50
44	J02044-018	G 159–034	02:04:27.55	–01:52:56.1	9.585	M4.0 V	PMSU	18.8	This work	25 Oct 2011	10 × 50
45	J02070+496	G 173-037	02:07:03.83	+49:38:44.1	8.366	M3.5 V	Lep13	17.4	Dit14	17 Nov 2015	10 × 50
46	J02088+494	G 173–039	02:08:53.60	+49:26:56.6	8.423	M3.5 V	PMSU	13.4	This work	17 Sep 2012	10 × 50
47	J02096-143	LP 709–040	02:09:36.09	–14:21:32.1	8.122	M2.5 V	PMSU	19.7	HIP2	14 Jan 2013	10 × 50
48	J02129+000	G 159–046	02:12:54.58	+00:00:16.8	9.055	M4.0 V	PMSU	10.0	Dit14	23 Oct 2011	10 × 50
49	J02149+174	GJ 1045	02:14:59.79	+17:25:09.0	9.966	M4.0 V	PMSU	20.41	vAl95	24 Oct 2011	10 × 50
50	J02155+339	G 074–011	02:15:34.38	+33:57:41.8	9.320	M3.5 V	PMSU	20.3	This work	14 Jan 2013	10 × 50
51	J02158-126	LP 709–062	02:15:48.83	–12:40:27.7	9.051	M3.5 V	PMSU	17.9	This work	17 Sep 2012	10 × 50
52	J02164+135	LP 469–206	02:16:29.78	+13:35:13.7	9.871	M5.5 V	PMSU	8.496	vAl95	24 Oct 2011	10 × 50
53	J02171+354	LP 245–010	02:17:09.93	+35:26:33.0	9.983	M5.0 V	PMSU	10.37	vAl95	25 Oct 2011	10 × 50
54	J02190+238	LTT 10787	02:19:02.29	+23:52:55.1	9.777	M4.0 V	PMSU	20.6	Dit14	25 Oct 2011	10 × 50
55	J02190+353	Ross 19	02:19:03.06	+35:21:18.2	8.662	M3.5 V	PMSU	17.7	vAl95	17 Sep 2012	10 × 50
56	J02256+375	G 074–025	02:25:38.42	+37:32:34.0	9.712	M4.0 V	PMSU	21.6	Dit14	25 Oct 2011	10 × 50
57	J02358+202	BD+19 381	02:35:53.28	+20:13:11.9	7.208	M2.0 V	PMSU	13.6	HIP2	17 Sep 2012	10 × 50
58	J02362+068	BX Cet	02:36:15.36	+06:52:19.1	7.333	M4.0 V	AF15	7.18	aHIP2	23 Oct 2011	10 × 50
59	J02392+074	G 076–019	02:39:17.35	+07:28:17.0	9.881	M4.0 V	PMSU	20.3	Dit14	25 Oct 2011	10 × 50
60	J02442+255	VX Ari	02:44:15.38	+25:31:25.0	6.752	M3.0 V	PMSU	7.51	HIP2	24 Oct 2011	10 × 50
61	J02518+294	LP 298–042	02:51:49.73	+29:29:13.2	9.518	M4.0 V	PMSU	22.7	Dit14	24 Oct 2011	10 × 50

Table C.1: Log of observed stars (continued).

No.	Karmn	Name	α (J2000)	δ (J2000)	J [mag]	SpT	Ref.[a]	d [pc]	Ref.[b]	Observation date	N $\times$ $t_{\rm exp}$ [s]
										17 Nov 2015	20 × 50
										07 Jan 2016	20 × 50
62	J02519+224	RBS 365	02:51:54.09	+22:27:30.0	8.919	M4.0 V	Ria06	13.9	This work	17 Nov 2015	10 × 50
63	J02530+168	Teegarden's Star	02:53:00.85	+16:52:53.3	8.394	M7.0 V	AF15	3.84	Wein16	23 Oct 2011	10 × 50
64	J02555+268	HD 18143 C	02:55:35.73	+26:52:20.9	9.561	M4.0 V	AF15	23.49	aHIP2	25 Oct 2011	10 × 50
65	J02565+554W	Ross 364	02:56:34.35	+55:26:14.5	7.425	M1.0 V	PMSU	19.5	vAl95	17 Sep 2012	10 × 50
66	J02565+554E	Ross 365	02:56:35.07	+55:26:30.2	8.006	M3.0 V	PMSU	19.5	avAl95	17 Sep 2012	10 × 50
										13 Jan 2013	10 × 50
67	J02575+107	Ross 791	02:57:31.04	+10:47:24.6	9.162	M3.0 V	PMSU	20.0	vAl95	14 Jan 2013	10 × 50
68	J02591+366	Ross 331	02:59:10.60	+36:36:40.3	9.064	M3.5 V	PMSU	18.87	Daw05	14 Jan 2013	10 × 50
69	J03047+617	G 246–022	03:04:43.35	+61:44:09.7	8.877	M3.0 V	AF15	24.2	aHIP2	17 Sep 2012	10 × 50
70	J03102+059	EK Cet	03:10:15.47	+05:54:31.1	8.363	M2.0 V	PMSU	16.9	HIP2	17 Sep 2012	10 × 50
71	J03133+047	CD Cet	03:13:23.00	+04:46:29.4	8.775	M5.0 V	PMSU	8.62	Wein16	23 Oct 2011	10 × 50
72	J03181+382	HD 275122	03:18:07.42	+38:15:08.2	7.023	M1.5 V	PMSU	15.53	HIP2	09 Dec 2014	10 × 50
73	J03233+116	G 005–032	03:23:22.41	+11:41:13.4	8.386	M2.5 V	PMSU	18.3	vAl95	17 Sep 2012	10 × 50
74	J03242+237	GJ 140C	03:24:12.81	+23:46:19.3	8.276	M2.0 V	PMSU	19.49	aHIP2	13 Jan 2013	10 × 50
75	J03288+264	LP 356–106	03:28:49.58	+26:29:12.2	9.288	M3.0 V	PMSU	15.0	Dit14	14 Jan 2013	10 × 50
76	J03317+143	GJ 143.3	03:31:47.12	+14:19:19.4	8.695	M2.0 V	PMSU	22.9	HIP2	14 Jan 2013	10 × 50
77	J03346-048	LP 653–008	03:34:39.59	–04:50:32.9	8.829	M3.5 V	PMSU	29.2	Ried10	13 Jan 2013	10 × 50
78	J03366+034	[R78b] 233	03:36:40.84	+03:29:19.5	9.295	M4.5 V	PMSU	13.3	This work	23 Oct 2011	10 × 50
79	J03394+249	KP Tau	03:39:29.72	+24:58:02.9	8.813	M3.0 V	PMSU	19.2	Dit14	24 Oct 2011	10 × 50
80	J03396+254E	Wolf 204	03:39:36.21	+25:28:20.3	8.747	M3.0 V	PMSU	21.3	bvAl95	24 Oct 2011	10 × 50
81	J03396+254W	Wolf 205	03:39:40.51	+25:28:47.7	9.079	M3.5 V	PMSU	21.3	vAl95	14 Jan 2013	10 × 50
82	J03437+166	BD+16 502B	03:43:45.22	+16:40:02.7	7.533	M1.0 V	PMSU	16.69	HIP2	09 Dec 2014	10 × 50
83	J03438+166	BD+16 502A	03:43:52.53	+16:40:19.9	7.406	M0.0 V	Lep13	17.71	HIP2	09 Dec 2014	10 × 50
84	J03463+262	HD 23453	03:46:20.12	+26:12:56.0	6.689	M0.0 V	PMSU	14.75	HIP2	09 Dec 2014	10 × 50
85	J03473+086	LTT 11262	03:47:20.91	+08:41:46.4	9.849	M4.5 V	PMSU	14.39	vAl95	23 Oct 2011	10 × 50
86	J03507-060	GJ 1065	03:50:44.32	–06:05:40.0	8.570	M3.5 V	PMSU	9.5	vAl95	13 Jan 2013	10 × 50
87	J03526+170	Wolf 227	03:52:41.69	+17:01:05.7	8.933	M4.5 V	PMSU	9.8	Dit14	24 Oct 2011	10 × 50
88	J03531+625	Ross 567	03:53:10.42	+62:34:08.2	7.782	M3.0 V	Lep13	11.9	This work	09 Dec 2014	10 × 50
89	J03574-011	BD–01 565B	03:57:28.92	–01:09:23.2	7.773	M2.5 V	AF15	15.5	aHIP2	13 Jan 2013	10 × 50
90	J03598+260	Ross 873	03:59:53.55	+26:05:24.1	8.714	M3.0 V	PMSU	22.8	vAl95	13 Jan 2013	10 × 50
91	J04122+647	G 247–015	04:12:16.93	+64:43:56.1	9.156	M4.0 V	PMSU	11.79	vAl95	13 Jan 2013	10 × 50
92	J04148+277	HG 8-1	04:14:53.49	+27:45:28.4	8.763	M3.5 V	Lep13	15.7	This work	17 Nov 2015	10 × 50

Table C.1: Log of observed stars (continued).

No.	Karmn	Name	α (J2000)	δ (J2000)	J [mag]	SpT	Ref.[a]	d [pc]	Ref.[b]	Observation date	N $\times$ $t_{\rm exp}$ [s]
93	J04153-076	o^{02} Eri C	04:15:21.73	–07:39:17.4	6.747	M4.5 V	AF15	4.98	aHIP2	25 Oct 2011	10 × 50
94	J04173+088	LTT 11392	04:17:18.52	+08:49:22.1	9.030	M4.5 V	PMSU	14.8	Dit14	23 Oct 2011	10 × 50
95	J04218+213	G 008–029	04:21:50.06	+21:19:43.4	9.080	M3.5 V	PMSU	18.2	This work	13 Jan 2013	10 × 50
96	J04225+105	LSPM J0422+1031	04:22:31.99	+10:31:18.8	8.471	M3.5 V	Lep13	25.4	Dit14	02 Mar 2014	10 × 50
97	J04248+324	G 039–011	04:24:49.19	+32:26:58.4	8.818	M2.0 V	PMSU	26.0	This work	14 Jan 2013	10 × 50
98	J04252+080S	HG 7–206	04:25:15.07	+08:02:55.9	8.908	M2.5 V	PMSU	28.5	This work	14 Jan 2013	10 × 50
99	J04278+117	NLTT 13316	04:27:53.52	+11:46:54.8	9.699	M4.0 V	PMSU	25.1	Dit14	25 Oct 2011	10 × 50
100	J04290+219	BD+21 652	04:29:00.14	+21:55:21.5	5.674	M0.5 V	Gra06	11.39	HIP2	17 Nov 2015	10 × 50
101	J04293+142	LTT 11438	04:29:18.47	+14:13:59.5	9.350	M4.0 V	PMSU	16.9	This work	23 Oct 2011	10 × 50
102	J04304+398	V546 Per	04:30:25.27	+39:51:00.1	9.113	M4.5 V	PMSU	10.43	vAl95	24 Oct 2011	10 × 50
103	J04311+589	STN 2051 A	04:31:11.48	+58:58:37.6	6.622	M4.0 V	PMSU	5.62	HD80	25 Oct 2011	10 × 50
104	J04335+207	G 008–041	04:33:33.93	+20:44:46.2	9.769	M4.0 V	PMSU	13.6	Dit14	23 Oct 2011	10 × 50
105	J04352-161	LP 775–031	04:35:16.13	–16:06:57.5	10.406	M7.0 V	Cru03	10.46	Wein16	01 Mar 2014	10 × 50
106	J04376-110	BD–11 916	04:37:41.88	–11:02:19.8	6.943	M1.5 V	PMSU	11.1	HIP2	02 Mar 2014	10 × 50
107	J04376+528	BD+52 857	04:37:40.92	+52:53:37.2	5.866	M0.0 V	Gra03	10.11	HIP2	17 Nov 2015	10 × 50
108	J04429+189	HD 285968	04:42:55.81	+18:57:28.5	6.462	M2.0 V	PMSU	9.3	HIP2	31 Jan 2012	10 × 50
109	J04429+214	2M J04425586+2128230	04:42:55.86	+21:28:23.0	7.958	M3.5 V	Lep13	10.8	This work	02 Mar 2014	10 × 50
110	J04488+100	1RXS J044847.6+100302	04:48:47.39	+10:03:02.6	8.127	M3.0 V	Lep13	15.2	This work	02 Mar 2014	10 × 50
111	J04508+221	GJ 1072	04:50:50.83	+22:07:22.5	9.896	M5.0 V	PMSU	12.3	Dit14	23 Oct 2011	10 × 50
112	J04520+064	Wolf 1539	04:52:05.73	+06:28:35.6	7.814	M3.5 V	PMSU	12.29	HIP2	25 Oct 2011	10 × 50
113	J04525+407	GJ 1073	04:52:34.48	+40:42:25.5	9.071	M4.0 V	PMSU	12.7	Dit14	24 Oct 2011	10 × 50
114	J04538-177	GJ 180	04:53:49.95	–17:46:23.5	7.413	M2.0 V	PMSU	12.1	HIP2	14 Jan 2013	10 × 50
115	J04588+498	BD+49 1280	04:58:50.58	+49:50:57.3	6.925	M0.0 V	PMSU	16.31	HIP2	01 Mar 2014	10 × 50
116	J04595+017	V1005 Ori	04:59:34.83	+01:47:00.7	7.117	M0.0 V	PMSU	25.88	HIP2	28 Feb 2014	10 × 50
										01 Mar 2014	10 × 50
117	J05019+099	LP 476–207 AB	05:01:58.81	+09:58:58.8	7.212	M4.0 V	PMSU	24.88	Ried14	28 Feb 2014	10 × 50
118	J05012+248	Ross 794	05:01:15.51	+24:52:24.5	8.084	M2.0 V	PMSU	29.1	vAl95	31 Jan 2012	10 × 50
119	J05032+213	HD 285190 A	05:03:16.08	+21:23:56.4	7.451	M1.5 V	AF15	27.4	vAl95	23 Oct 2011	10 × 50
										31 Jan 2012	10 × 50
120	J05033-173	LP 779–046	05:03:20.10	–17:22:24.5	7.819	M3.0 V	PMSU	9.2	HIP2	14 Jan 2013	10 × 50
121	J05034+531	BD+52 911	05:03:24.02	+53:07:41.2	7.001	M0.5 V	PMSU	13.62	HIP2	01 Mar 2014	10 × 50
										17 Nov 2015	20 × 50
122	J05042+110	G 097–015	05:04:14.76	+11:03:23.8	9.144	M4.0 V	PMSU	10.3	Dit14	23 Oct 2011	10 × 50
123	J05068-215E	BD–21 1074A	05:06:49.92	–21:35:09.2	7.046	M1.5 V	PMSU	19.79	Ried14	25 Oct 2011	10 × 50

Table C.1: Log of observed stars (continued).

No.	Karmn	Name	α (J2000)	δ (J2000)	J [mag]	SpT	Ref.[a]	d [pc]	Ref.[b]	Observation date	N × $t_{\rm exp}$ [s]
										17 Sep 2012	10 × 50
										14 Jan 2013	10 × 50
124	J05068-215W	BD–21 1074BC	05:06:49.47	–21:35:03.8	7.003	M3.5 V	PMSU	18.3	Ried14	25 Oct 2011	10 × 50
										17 Sep 2012	10 × 50
										14 Jan 2013	10 × 50
125	J05078+179	G 085–041	05:07:49.24	+17:58:58.4	8.023	M3.0 V	PMSU	23.1	This work	13 Jan 2013	10 × 50
										02 Mar 2014	10 × 50
126	J05085-181	GJ 190 AB	05:08:35.01	–18:10:17.9	6.175	M3.5 V	PMSU	9.3	HIP2	14 Jan 2013	10 × 50
127	J05091+154	Ross 388	05:09:09.97	+15:27:32.5	8.770	M3.0 V	PMSU	29.7	vAl95	13 Jan 2013	10 × 50
128	J05103+488	G 096–021 AB	05:10:22.08	+48:50:32.7	7.827	M2.5 V	PMSU	...	...	13 Jan 2013	10 × 50
										15 Apr 2015	10 × 35
129	J05106+297	G 086–028	05:10:39.56	+29:46:47.9	8.600	M3.0 V	Lep13	17.4	This work	01 Mar 2014	10 × 50
130	J05127+196	GJ 192	05:12:42.23	+19:39:56.6	7.299	M2.0 V	PMSU	12.3	HIP2	31 Jan 2012	10 × 50
131	J05289+125	HD 35956 B	05:28:56.50	+12:31:53.9	9.649	M4.0 V	AF15	28.17	aHIP2	23 Oct 2011	10 × 50
132	J05298-034	Wolf 1450	05:29:52.05	–03:26:29.6	8.276	M2.5 V	PMSU	17.6	vAl95	31 Jan 2012	10 × 50
133	J05298+320	Ross 406	05:29:52.69	+32:04:52.5	8.649	M3.0 V	PMSU	20.6	Dit14	13 Jan 2013	10 × 50
134	J05314-036	HD 36395	05:31:27.35	–03:40:35.7	4.999	M1.5 V	AF15	5.66	HIP2	25 Oct 2011	10 × 50
135	J05339-023	RX J0534.0–0221	05:33:59.81	–02:21:32.5	8.564	M3.0 V	Ria06	17.1	This work	28 Feb 2014	10 × 50
136	J05333+448	GJ 1081	05:33:19.13	+44:48:58.8	8.197	M3.5 V	PMSU	15.34	vAl95	24 Oct 2011	20 × 50
										25 Mar 2012	10 × 50
										26 Mar 2012	10 × 50
										17 Sep 2012	10 × 50
										13 Jan 2013	10 × 50
										28 Feb 2014	10 × 50
137	J05342+103S	Ross 45 B	05:34:15.08	+10:19:09.2	9.186	M4.5 V	AF15	18.0	This work	13 Jan 2013	10 × 50
138	J05342+103N	Ross 45 A	05:34:15.14	+10:19:14.2	8.561	M3.0 V	AF15	17.1	This work	13 Jan 2013	10 × 50
139	J05348+138	Ross 46	05:34:52.12	+13:52:47.2	7.781	M3.5 V	PMSU	12.4	vAl95	13 Jan 2013	10 × 50
140	J05360-076	Wolf 1457	05:36:00.08	–07:38:58.1	8.464	M4.0 V	PMSU	11.2	This work	25 Oct 2011	10 × 50
141	J05365+113	V2689 Ori	05:36:30.99	+11:19:40.2	6.126	M0.0 V	Lep13	11.24	HIP2	02 Mar 2014	10 × 50
142	J05366+112	2M J05363846+1117487	05:36:38.47	+11:17:48.8	8.266	M4.0 V	Lep13	11.24	aHIP2	01 Mar 2014	10 × 50
143	J05421+124	V1352 Ori	05:42:08.98	+12:29:25.3	7.124	M4.0 V	AF15	5.83	Wein16	23 Oct 2011	3 × 50
										31 Jan 2012	10 × 50
144	J05466+441	Wolf 237	05:46:38.45	+44:07:19.8	8.459	M4.0 V	PMSU	21.0	Dit14	24 Oct 2011	10 × 50
										01 Mar 2014	10 × 50

Table C.1: Log of observed stars (continued).

No.	Karmn	Name	α (J2000)	δ (J2000)	J [mag]	SpT	Ref.[a]	d [pc]	Ref.[b]	Observation date	N $\times$ $t_{\rm exp}$ [s]
145	J05484+077	LTT 17868	05:48:24.08	+07:45:38.8	9.784	M4.0 V	PMSU	20.6	This work	23 Oct 2011	10 × 50
146	J05530+251	LSPM J0553+2507	05:53:01.80	+25:07:44.0	8.552	M3.0 V	Lep13	17.0	This work	01 Mar 2014	10 × 50
147	J05532+242	Ross 59	05:53:14.04	+24:15:32.9	7.485	M1.5 V	PMSU	19.4	vAl95	01 Mar 2014	10 × 50
148	J05599+585	G 192–012	05:59:55.69	+58:34:15.6	9.028	M4.0 V	PMSU	13.53	aHIP2	25 Oct 2011	10 × 50
149	J06000+027	G 099–049	06:00:03.51	+02:42:23.6	6.905	M4.0 V	PMSU	5.22	Wein16	23 Oct 2011	10 × 50
										26 Mar 2012	10 × 50
										09 Dec 2014	10 × 50
150	J06024+498	G 192–015	06:02:29.18	+49:51:56.2	9.350	M5.0 V	AF15	9.3	Jen09	24 Oct 2011	10 × 50
151	J06054+608	LP 086–173	06:05:29.36	+60:49:23.2	9.096	M4.5 V	AF15	14.0	Dit14	15 Apr 2015	10 × 35
152	J06105-218	HD 42581 A	06:10:34.62	–21:51:52.2	5.104	M0.5 V	PMSU	5.75	HIP2	14 Jan 2013	10 × 50
153	J06140+516	G 192–022	06:14:02.40	+51:40:08.1	8.860	M3.5 V	PMSU	14.9	Dit14	13 Jan 2013	10 × 50
154	J06212+442	G 101–035	06:21:13.00	+44:14:30.7	8.724	M2.0 V	PMSU	24.7	This work	14 Jan 2013	10 × 50
										17 Nov 2015	20 × 50
155	J06277+093	Ross 603	06:27:43.97	+09:23:54.1	8.269	M2.0 V	Lep13	22.6	This work	17 Nov 2015	10 × 50
156	J06318+414	LP 205–044	06:31:50.74	+41:29:45.9	9.680	M5.0 V	PMSU	11.1	Jen09	24 Oct 2011	10 × 50
157	J06345+315	G 103-041	06:34:33.44	+31:30:08.4	8.705	M3.5 V	Lep13	15.3	This work	17 Nov 2015	10 × 50
158	J06361+116	NLTT 16724	06:36:06.39	+11:37:03.2	9.794	M4.5 V	PMSU	18.28	Jen09	23 Oct 2011	10 × 50
										26 Mar 2012	10 × 50
										17 Sep 2012	10 × 50
159	J06400+285	LP 307–008	06:40:05.50	+28:35:14.3	8.270	M2.0 V	PMSU	24.1	This work	31 Jan 2012	10 × 50
										17 Sep 2012	10 × 50
										13 Jan 2013	10 × 50
										28 Feb 2014	10 × 50
										15 Apr 2015	10 × 50
160	J06414+157	Wolf 289	06:41:28.18	+15:45:48.2	9.570	M4.0 V	PMSU	18.7	This work	23 Oct 2011	10 × 50
161	J06421+035	G 108–021	06:42:11.18	+03:34:52.7	8.166	M3.5 V	PMSU	15.39	Wein16	23 Oct 2011	10 × 50
162	J06422+035	G 108–022	06:42:13.34	+03:35:31.1	9.112	M4.0 V	PMSU	15.04	Wein16	23 Oct 2011	10 × 50
163	J06490+371	GJ 1092	06:49:05.42	+37:06:53.4	9.561	M4.0 V	PMSU	13.3	vAl95	24 Oct 2011	10 × 50
164	J06523-051	BD–05 1844Bab	06:52:18.04	–05:11:24.1	6.579	M2.0 V	Klu13	8.71	aHIP2	31 Jan 2012	10 × 50
165	J06524+182	LP 421–007	06:52:24.30	+18:17:04.7	9.052	M4.0 V	PMSU	14.7	This work	31 Jan 2012	10 × 50
166	J06548+332	Wolf 294	06:54:49.03	+33:16:05.9	6.104	M3.0 V	AF15	5.59	HIP2	24 Oct 2011	10 × 50
										26 Mar 2012	10 × 50
167	J06594+193	GJ 1093	06:59:28.69	+19:20:57.7	9.160	M5.0 V	PMSU	7.8	vAl95	23 Oct 2011	10 × 50
168	J07033+346	LP 255–011	07:03:23.17	+34:41:51.0	8.773	M4.0 V	PMSU	13.7	Dit14	24 Oct 2011	10 × 50

Table C.1: Log of observed stars (continued).

No.	Karmn	Name	α (J2000)	δ (J2000)	J [mag]	SpT	Ref.[a]	d [pc]	Ref.[b]	Observation date	N × $t_{\rm exp}$ [s]
169	J07076+486	G 107–048	07:07:37.76	+48:41:13.8	9.106	M3.5 V	PMSU	10.8	Dit14	14 Jan 2013	10 × 50
170	J07163+331	GJ 1096	07:16:18.02	+33:09:10.4	9.763	M4.0 V	PMSU	14.9	vAl95	24 Oct 2011	10 × 50
171	J07195+328	BD+33 1505	07:19:31.27	+32:49:48.3	7.184	M0.0 V	AF15	12.39	HIP2	09 Dec 2014	10 × 50
172	J07227+306	G 087-036	07:22:42.03	+30:40:12.0	9.506	M3.5 V	PMSU	23.7	vAl95	27 Mar 2012	10 × 50
173	J07274+052	Luyten's Star	07:27:24.50	+05:13:32.9	5.714	M3.5 V	AF15	3.8	HIP2	24 Oct 2011	10 × 50
174	J07307+481	GJ 275.2 A	07:30:42.80	+48:12:00.0	9.141	M4.0 V	PMSU	11.1	vAl95	25 Oct 2011	10 × 50
										15 Apr 2015	10 × 35
175	J07319+392	G 111–009	07:31:56.52	+39:13:38.5	9.164	M3.0 V	AF15	22.6	This work	14 Jan 2013	10 × 50
176	J07319+362N	BL Lyn	07:31:57.35	+36:13:47.8	7.571	M3.5 V	PMSU	11.87	aHIP2	23 Oct 2011	10 × 50
177	J07342+009	GJ 1099	07:34:17.58	+00:59:09.3	8.261	M2.5 V	PMSU	14.6	vAl95	31 Jan 2012	10 × 50
178	J07349+147	TYC 777–141–1	07:34:56.33	+14:45:54.5	7.287	M3.0 V	Lep13	9.1	This work	02 Mar 2014	10 × 50
										14 Apr 2015	10 × 50
										17 Nov 2015	20 × 50
179	J07361-031	BD–02 2198	07:36:07.08	–03:06:38.5	6.791	M1.0 V	AF15	14.2	aHIP2	02 Mar 2014	10 × 50
180	J07386-212	LP 763–001	07:38:40.89	–21:13:27.6	7.848	M3.0 V	PMSU	10.6	HIP2	27 Mar 2012	10 × 50
181	J07395+334	G 090–016	07:39:35.81	+33:27:45.8	8.420	M2.0 V	PMSU	35.66	HIP2	31 Jan 2012	10 × 50
182	J07403-174	LP 783–002	07:40:19.22	–17:24:45.0	10.155	M6.0 V	PMSU	9.1	aSub09	27 Mar 2012	10 × 50
183	J07418+050	G 050–001	07:41:52.82	+05:02:24.3	8.910	M2.5 V	PMSU	28.5	This work	14 Jan 2013	10 × 50
184	J07446+035	YZ CMi	07:44:40.18	+03:33:09.0	6.581	M4.5 V	PMSU	5.96	HIP2	23 Oct 2011	10 × 50
185	J07472+503	2M J07471385+5020386	07:47:13.85	+50:20:38.5	8.855	M4.0 V	Lep13	13.5	This work	09 Dec 2014	10 × 50
186	J07518+055	G 050–006	07:51:51.38	+05:32:57.3	9.966	M4.5 V	PMSU	15.9	vAl95	31 Jan 2012	10 × 50
187	J07581+072	G 050–012	07:58:09.10	+07:17:01.5	9.272	M4.0 V	PMSU	12.1	Dit14	31 Jan 2012	10 × 50
188	J07582+413	GJ 1105	07:58:12.70	+41:18:13.5	7.734	M3.5 V	PMSU	8.3	Dit14	27 Mar 2012	10 × 50
189	J07583+496	LP 163–047	07:58:22.73	+49:39:53.4	8.706	M3.5 V	Lep13	13.8	Dit14	01 Mar 2014	10 × 50
190	J08005+258	TYC 1930–667–1	08:00:34.71	+25:53:33.5	8.204	M2.0 V	Lep13	19.6	This work	09 Dec 2014	10 × 50
191	J08017+237	TYC 1926–794–1	08:01:43.57	+23:42:27.1	7.670	M1.5 V	Lep13	17.4	This work	15 Apr 2015	10 × 50
192	J08066+558	LP 123–075	08:06:36.46	+55:53:38.4	8.050	M2.0 V	PMSU	30.1	HIP2	31 Jan 2012	10 × 50
										13 Jan 2013	10 × 50
										28 Feb 2014	10 × 50
										15 Apr 2015	10 × 35
193	J08068+367	G 090–044	08:06:48.42	+36:45:39.0	8.976	M3.0 V	PMSU	20.7	This work	27 Mar 2012	10 × 50
194	J08082+211	BD+21 1764B	08:08:13.59	+21:06:09.4	7.336	M3.0 V	AF15	16.64	aHIP2	31 Jan 2012	20 × 50
										17 Nov 2015	10 × 50
195	J08083+585	LP 089–101	08:08:18.19	+58:31:09.6	8.804	M3.0 V	PMSU	19.1	This work	27 Mar 2012	10 × 50

Table C.1: Log of observed stars (continued).

No.	Karmn	Name	α (J2000)	δ (J2000)	J [mag]	SpT	Ref.[a]	d [pc]	Ref.[b]	Observation date	N $\times$ $t_{\rm exp}$ [s]
196	J08105-138	18 Pup B	08:10:34.29	–13:48:51.4	8.276	M2.5 V	AF15	22.4	aHIP2	27 Mar 2012	10 × 50
										14 Jan 2013	10 × 50
197	J08108+039	G 050–021	08:10:53.63	+03:58:33.6	9.238	M3.5 V	PMSU	20.8	Dit14	14 Jan 2013	10 × 50
198	J08119+087	Ross 619	08:11:57.58	+08:46:22.1	8.424	M4.5 V	PMSU	6.80	Wein16	15 Apr 2015	10 × 35
199	J08126-215	GJ 300 AB	08:12:40.88	–21:33:05.7	7.601	M4.0 V	PMSU	5.9	vAl95	27 Mar 2012	10 × 50
200	J08161+013	GJ 2066	08:16:07.98	+01:18:09.2	6.625	M2.0 V	AF15	9.1	HIP2	31 Jan 2012	10 × 50
201	J08293+039	2M J08292191+0355092	08:29:21.92	+03:55:09.3	7.932	M2.5 V	Lep13	15.0	This work	01 Mar 2014	10 × 50
202	J08371+151	NLTT 19893	08:37:07.99	+15:07:47.6	8.122	M2.5 V	PMSU	18.96	HIP2	31 Jan 2012	10 × 50
										02 Mar 2014	10 × 50
203	J08413+594	LP 090–018	08:41:20.13	+59:29:50.6	9.615	M5.5 V	PMSU	9.2	Dit14	26 Mar 2012	10 × 50
204	J08428+095	BD+10 1857C	08:42:52.23	+09:33:11.2	8.122	M2.5 V	PMSU	15.43	aHIP2	31 Jan 2012	10 × 50
										13 Jan 2013	10 × 50
205	J08595+537	G 194–047	08:59:35.93	+53:43:50.5	9.014	M3.5 V	AF15	17.2	Dit14	01 Mar 2014	30 × 50
										14 Apr 2015	10 × 50
206	J09003+218	LP 368–128	09:00:23.59	+21:50:05.4	9.436	M6.5 V	AF15	5.0	This work	27 Mar 2012	10 × 50
207	J09005+465	GJ 1119	09:00:32.54	+46:35:11.8	8.604	M4.5 V	PMSU	9.9	Dit14	31 Jan 2012	10 × 50
208	J09008+052W	Ross 686	09:00:48.53	+05:14:41.3	8.605	M3.0 V	PMSU	20.96	HIP2	31 Jan 2012	10 × 50
209	J09011+019	Ross 625	09:01:10.49	+01:56:35.0	7.932	M3.0 V	PMSU	16.2	This work	25 Mar 2012	20 × 50
										13 Jan 2013	10 × 50
										14 Apr 2015	10 × 50
										17 Nov 2015	10 × 50
210	J09023+084	NLTT 20817	09:02:19.88	+08:28:06.4	8.145	M2.5 V	PMSU	19.5	HIP2	27 Mar 2012	10 × 50
										02 Mar 2014	10 × 50
211	J09120+279	G 047–028	09:12:02.72	+27:54:24.2	8.430	M3.0 V	PMSU	27.8	vAl95	25 Mar 2012	10 × 50
212	J09140+196	LP 427–016	09:14:03.21	+19:40:06.0	8.424	M3.0 V	Lep13	16.1	This work	01 Mar 2014	10 × 50
213	J09143+526	HD 79210	09:14:22.98	+52:41:12.5	4.889	M0.0 V	AF15	5.81	HIP2	26 Mar 2012	10 × 50
214	J09144+526	HD 79211	09:14:24.86	+52:41:11.8	4.779	M0.0 V	AF15	5.81	aHIP2	26 Mar 2012	10 × 50
										02 Mar 2014	10 × 50
215	J09161+018	RX J0916.1+0153	09:16:10.19	+01:53:08.8	8.770	M4.0 V	Lep13	13.0	This work	22 May 2014	12 × 50
216	J09163-186	LP 787–052	09:16:20.66	–18:37:32.9	7.351	M1.5 V	PMSU	15.0	This work	02 Mar 2014	10 × 50
217	J09177+462	RX J0917.7+4612	09:17:44.73	+46:12:24.7	8.126	M2.5 V	Lep13	19.8	This work	22 May 2014	10 × 50
218	J09187+267	G 047–033 A	09:18:46.24	+26:45:11.4	8.296	M1.5 V	PMSU	23.2	This work	14 Jan 2013	10 × 50
219	J09288-073	Ross 439	09:28:53.34	–07:22:14.8	8.446	M2.5 V	PMSU	16.24	HIP2	30 Jan 2012	10 × 50
220	J09300+396	LP 211-012	09:30:01.67	+39:37:24.0	8.467	M2.5 V	PMSU	19.2	This work	30 Jan 2012	10 × 50

Table C.1: Log of observed stars (continued).

No.	Karmn	Name	α (J2000)	δ (J2000)	J [mag]	SpT	Ref.[a]	d [pc]	Ref.[b]	Observation date	N × $t_{\rm exp}$ [s]
221	J09307+003	GJ 1125	09:30:44.58	+00:19:21.4	7.697	M3.5 V	PMSU	9.7	HIP2	25 Mar 2012	10 × 50
222	J09319+363	BD+36 1970	09:31:56.33	+36:19:12.9	7.121	M0.0 V	PMSU	13.91	HIP2	01 Mar 2014	10 × 50
										14 Apr 2015	10 × 50
										09 Jun 2015	10 × 50
223	J09360-216	GJ 357	09:36:01.61	–21:39:37.1	7.337	M2.5 V	PMSU	9.02	HIP2	14 Jan 2013	10 × 50
224	J09425-192	LP 788–024	09:42:35.73	–19:14:04.6	8.298	M2.5 V	PMSU	15.7	HIP2	14 Jan 2013	10 × 50
225	J09430+237	LP 370–035	09:43:01.33	+23:49:22.2	8.994	M1.0 V	Lep13	35.5	This work	22 May 2014	10 × 50
226	J09447-182	GJ 1129	09:44:47.31	–18:12:48.9	8.122	M4.0 V	PMSU	10.97	Wein16	14 Jan 2013	10 × 50
227	J09449-123	G 161–071	09:44:54.22	–12:20:54.4	8.496	M5.0 V	AF15	13.26	Wein16	01 Mar 2014	10 × 50
228	J09475+129	LP 488–037	09:47:34.81	+12:56:39.1	9.267	M4.0 V	PMSU	20.3	Dit14	26 Mar 2012	10 × 50
229	J09506-138	LP 728–070	09:50:40.54	-13:48:38.6	8.579	M4.0 V	Sch05	11.9	This work	09 Dec 2014	10 × 50
										17 Nov 2015	15 × 50
230	J09511-123	BD–11 2741	09:51:09.64	-12:19:47.8	6.988	M0.5 V	PMSU	13.7	HIP2	09 Dec 2014	10 × 50
231	J09539+209	NLTT 22870	09:53:55.23	+20:56:46.0	9.208	M4.5 V	PMSU	9.2	Hen06	30 Jan 2012	10 × 50
										13 Jan 2013	10 × 50
232	J09557+353	G 116–065	09:55:43.61	+35:21:42.2	8.850	M3.0 V	PMSU	19.5	This work	25 Mar 2012	10 × 50
										13 Jan 2013	10 × 50
233	J09564+226	NLTT 22978	09:56:27.00	+22:39:01.5	9.621	M4.0 V	PMSU	19.2	This work	14 Jan 2013	10 × 50
234	J10028+484	G 195–055	10:02:49.36	+48:27:33.4	9.963	M5.5 V	AF15	16.6	Dit14	26 Mar 2012	15 × 50
										14 Apr 2015	10 × 50
235	J10035+059	NLTT 23292	10:03:33.37	+05:57:48.1	9.290	M3.5 V	PMSU	20.0	This work	27 Mar 2012	10 × 50
236	J10043+503	G 196–003 A	10:04:21.49	+50:23:13.6	8.081	M2.5 V	Lep13	16.1	This work	02 Mar 2014	10 × 50
237	J10087+027	LP 549–023	10:08:44.61	+02:43:56.8	8.590	M3.0 V	Lep13	17.3	This work	01 Mar 2014	10 × 50
238	J10094+512	LP 127–132	10:09:29.97	+51:17:19.8	9.299	M4.0 V	PMSU	13.3	vAl95	26 Mar 2012	10 × 50
239	J10125+570	LP 092–048	10:12:34.81	+57:03:49.6	7.759	M3.5 V	Lep13	9.9	This work	02 Mar 2014	10 × 50
240	J10151+314	G 118–043	10:15:06.91	+31:25:11.0	9.326	M4.0 V	PMSU	20.4	This work	25 Mar 2012	10 × 50
										13 Jan 2013	10 × 50
										28 Feb 2014	10 × 50
										14 Apr 2015	10 × 50
241	J10158+174	LSPM J1015+1729	10:15:53.90	+17:29:27.2	8.696	M3.5 V	Lep13	15.2	This work	22 May 2014	10 × 50
242	J10167-119	GJ 386	10:16:46.00	–11:57:41.3	7.323	M3.0 V	PMSU	13.6	HIP2	26 Mar 2012	10 × 50
243	J10185-117	LP 729–054	10:18:35.17	–11:42:59.9	9.007	M4.0 V	Sch05	14.4	This work	22 May 2014	10 × 50
244	J10196+198	**BD+20 2465**	10:19:36.35	+19:52:12.2	5.449	M3.0 V	AF15	4.89	vAl95	30 Jan 2012	11 × 40
										17 Nov 2015	11 × 40

Table C.1: Log of observed stars (continued).

No.	Karmn	Name	α (J2000)	δ (J2000)	J [mag]	SpT	Ref.[a]	d [pc]	Ref.[b]	Observation date	N $\times$ $t_{\rm exp}$ [s]
245	J10243+119	StKM 1–852	10:24:20.17	+11:57:20.7	8.847	M2.0 V	PMSU	26.4	This work	30 Jan 2012	10 × 50
246	J10255+263	G 054–026	10:25:30.35	+26:23:18.5	9.030	M3.5 V	PMSU	17.8	This work	27 Mar 2012	10 × 50
247	J10260+504W	LP 127–371	10:26:02.66	+50:27:09.1	9.268	M4.0 V	PMSU	16.3	This work	25 Mar 2012	10 × 50
										02 Mar 2014	10 × 50
248	J10260+504E	LP 127–372	10:26:03.32	+50:27:22.0	9.404	M4.0 V	PMSU	17.3	This work	25 Mar 2012	10 × 50
249	J10284+482	G 146–035	10:28:27.81	+48:14:20.0	9.055	M3.5 V	PMSU	20.96	vAl95	27 Mar 2012	10 × 50
250	J10345+463	LP 167–064	10:34:30.21	+46:18:09.0	9.195	M3.0 V	PMSU	20.4	Dit14	27 Mar 2012	10 × 50
251	J10350-094	LP 670–017	10:35:01.11	–09:24:38.5	8.276	M3.0 V	Sch05	15.0	This work	02 Mar 2014	10 × 50
252	J10379+127	LP 490–042	10:37:55.28	+12:46:36.9	8.730	M3.0 V	Lep13	20.4	This work	01 Mar 2014	10 × 50
										17 Nov 2015	10 × 50
253	J10384+485	LP 167–071	10:38:29.81	+48:31:44.9	9.495	M3.0 V	PMSU	26.3	This work	27 Mar 2012	10 × 50
										14 Apr 2015	10 × 50
254	J10396-069	GJ 399	10:39:40.61	–06:55:25.6	7.664	M2.5 V	PMSU	16.4	HIP2	26 Mar 2012	10 × 50
255	J10416+376	GJ 1134	10:41:38.10	+37:36:39.8	8.493	M4.5 V	PMSU	10.3	vAl95	25 Mar 2012	10 × 50
256	J10448+324	LP 316–604 A	10:44:52.70	+32:24:41.2	9.494	M3.0 V	PMSU	39.1	Dit14	14 Jan 2013	10 × 50
										15 Apr 2015	10 × 50
257	J10504+331	G 119–037	10:50:26.00	+33:06:05.2	8.899	M4.0 V	PMSU	22.9	vAl95	25 Mar 2012	10 × 50
258	J10513+361	LP 263–035	10:51:20.60	+36:07:25.6	9.422	M3.0 V	PMSU	32.3	Dit14	14 Jan 2013	10 × 50
259	J10522+059	NLTT 25568	10:52:14.23	+05:55:09.9	9.834	M5.0 V	PMSU	11.6	Dit14	26 Mar 2012	10 × 50
260	J10546-073	LP 671–008	10:54:41.98	–07:18:32.7	8.877	M4.0 V	AF15	16.8	This work	02 Mar 2014	10 × 50
										14 Apr 2015	10 × 50
261	J10584-107	LP 731–076	10:58:28.00	–10:46:30.5	9.512	M5.0 V	AF15	11.7	This work	22 May 2014	10 × 50
262	J11031+366	LP 263–064	11:03:10.00	+36:39:08.5	9.464	M3.5 V	PMSU	24.0	Dit14	14 Jan 2013	10 × 50
263	J11033+359	HD 95735	11:03:20.24	+35:58:11.8	4.203	M1.5 V	AF15	2.547	HIP2	30 Jan 2012	11 × 35
264	J11036+136	LP 491–051	11:03:21.25	+13:37:57.1	8.759	M4.0 V	Lep13	16.8	Dit14	01 Mar 2014	10 × 50
265	J11055+435	WX UMa	11:05:31.33	+43:31:17.1	8.742	M5.5 V	AF15	4.85	aHIP2	26 Mar 2012	10 × 50
266	J11152+194	G 056–026	11:15:12.40	+19:27:12.4	8.919	M3.5 V	PMSU	16.9	This work	26 Mar 2012	10 × 50
267	J11289+101	Wolf 398	11:28:56.24	+10:10:39.5	8.478	M3.5 V	PMSU	15.7	vAl95	25 Mar 2012	10 × 50
268	J11355+389	G 122–034	11:35:31.98	+38:55:37.3	9.034	M3.5 V	PMSU	23.0	This work	26 Mar 2012	10 × 50
										10 Jul 2012	11 × 50
										11 Jul 2012	10 × 50
										13 Jan 2013	10 × 50
										28 Feb 2014	10 × 50
										14 Apr 2015	10 × 50

Table C.1: Log of observed stars (continued).

No.	Karmn	Name	α (J2000)	δ (J2000)	J [mag]	SpT	Ref.[a]	d [pc]	Ref.[b]	Observation date	N × $t_{\rm exp}$ [s]
269	J11376+587	Ross 112	11:37:38.99	+58:42:42.8	8.978	M3.5 V	PMSU	24.3	This work	14 Jan 2013	10 × 50
270	J11420+147	Ross 115	11:42:01.77	+14:46:35.7	8.859	M3.0 V	PMSU	19.6	This work	27 Mar 2012	10 × 50
271	J11467-140	GJ 443	11:46:42.82	–14:00:50.5	7.965	M3.0 V	PMSU	19.99	HIP2	14 Jan 2013	10 × 50
272	J11476+002	LP 613–049 A	11:47:40.74	+00:15:20.2	8.991	M4.0 V	PMSU	19.9	Dit14	31 Jan 2012	10 × 50
273	J11483-112	LP 733–024	11:48:19.43	–11:17:14.4	9.028	M3.0 V	PMSU	21.2	This work	14 Jan 2013	10 × 50
274	J11509+483	GJ 1151	11:50:57.88	+48:22:39.6	8.488	M4.5 V	PMSU	8.2	vAl95	26 Mar 2012	10 × 50
275	J11521+039	StM 162	11:52:09.82	+03:57:23.3	8.382	M4.0 V	Lep13	13.1	This work	01 Mar 2014	10 × 50
										14 Apr 2015	10 × 50
276	J11532-073	GJ 452	11:53:16.09	–07:22:27.3	8.303	M2.5 V	PMSU	19.6	HIP2	25 Mar 2012	10 × 50
277	J11575+118	Ross 122	11:57:32.78	+11:49:39.8	8.429	M2.0 V	PMSU	24.2	HIP2	30 Jan 2012	10 × 50
										14 Apr 2015	10 × 50
278	J12006-138	LP 734–011 A	12:00:36.91	–13:49:36.4	8.852	M3.5 V	PMSU	16.4	This work	31 Jan 2012	10 × 50
										13 Jan 2013	10 × 50
279	J12016-122	LTT 4484	12:01:40.80	–12:13:53.7	8.685	M3.0 V	PMSU	18.1	This work	27 Mar 2012	16 × 50
										13 Jan 2013	10 × 50
										15 Apr 2015	10 × 50
280	J12100-150	LP 734–032	12:10:05.60	–15:04:15.7	7.768	M3.5 V	PMSU	12.8	Ried10	14 Jan 2013	10 × 50
										01 Mar 2014	10 × 50
281	J12112-199	LP 794–031	12:11:16.98	–19:58:21.4	8.596	M3.5 V	PMSU	12.6	aHIP2	14 Jan 2013	10 × 50
282	J12123+544S	HD 238090	12:12:20.85	+54:29:08.7	6.875	M0.0 V	PMSU	15.52	HIP2	26 Mar 2012	10 × 50
283	J12123+544N	BD+55 1519B	12:12:21.12	+54:29:23.2	9.171	M3.0 V	PMSU	15.52	HIP2	26 Mar 2012	10 × 50
284	J12142+006	GJ 1154 A	12:14:16.54	+00:37:26.3	8.456	M5.0 V	PMSU	7.16	Wein16	27 Mar 2012	14 × 50
285	J12156+526	StKM 2–809	12:15:39.37	+52:39:08.9	8.588	M4.0 V	Lep13	11.9	This work	02 Mar 2014	10 × 50
286	J12162+508	RX J1216.2+5053	12:16:15.06	+50:53:37.7	9.291	M4.0 V	AF15	19.9	This work	01 Mar 2014	13 × 50
										22 May 2014	10 × 50
										14 Apr 2015	10 × 50
287	J12189+111	GL Vir	12:18:59.40	+11:07:33.9	8.525	M5.0 V	PMSU	6.44	Wein16	30 Jan 2012	10 × 50
288	J12191+318	LP 320–626	12:19:06.00	+31:50:43.3	8.289	M4.0 V	Lep13	14.7	This work	28 Feb 2014	10 × 50
289	J12248-182	Ross 695	12:24:52.43	–18:14:30.3	7.734	M2.0 V	PMSU	8.8	HIP2	14 Jan 2013	10 × 50
290	J12277-032	LP 615–149	12:27:44.72	–03:15:00.6	8.763	M3.5 V	Sch05	17.1	This work	01 Mar 2014	10 × 50
291	J12290+417	G 123–035	12:29:02.90	+41:43:49.7	8.786	M3.5 V	PMSU	15.9	This work	26 Mar 2012	10 × 50
										14 Apr 2015	10 × 50
292	J12332+090	FL Vir AB	12:33:17.38	+09:01:15.8	6.995	M5.0 V	PMSU	4.4	Jen52	31 Jan 2012	18 × 50
										25 Mar 2012	20 × 50

Table C.1: Log of observed stars (continued).

No.	Karmn	Name	α (J2000)	δ (J2000)	J [mag]	SpT	Ref.[a]	d [pc]	Ref.[b]	Observation date	N $\times$ $t_{\rm exp}$ [s]
										26 Mar 2012	10 × 50
										27 Mar 2012	10 × 50
										10 Jul 2012	10 × 50
										11 Jul 2012	10 × 50
										14 Jan 2013	10 × 50
										28 Feb 2014	20 × 50
293	J12364+352	G 123–045	12:36:28.70	+35:12:00.8	9.113	M4.5 V	AF15	11.3	Dit14	02 Mar 2014	10 × 50
294	J12373-208	LP 795–038	12:37:21.57	–20:52:34.9	8.972	M4.0 V	Sch05	14.2	This work	28 Feb 2014	10 × 50
295	J12428+418	G 123–055	12:42:49.96	+41:53:46.9	8.118	M4.0 V	Lep13	10.6	vAl95	28 Feb 2014	10 × 50
296	J12470+466	Ross 991	12:47:01.02	+46:37:33.4	8.104	M2.5 V	AF15	20.9	HIP2	30 Jan 2012	10 × 50
297	J12471-035	LP 616–013	12:47:09.77	–03:34:17.7	8.767	M3.0 V	PMSU	18.8	This work	25 Mar 2012	10 × 50
298	J12485+495	RX J1248.5+4933	12:48:34.49	+49:33:54.1	8.684	M3.5 V	Lep13	15.1	This work	01 Mar 2014	16 × 50
										22 May 2014	10 × 50
299	J13000-056	Ross 972	13:00:03.98	–05:37:47.7	8.655	M3.0 V	PMSU	17.8	This work	27 Mar 2012	10 × 50
300	J13130+201	GJ 1168	13:13:04.79	+20:11:26.5	8.867	M3.5 V	PMSU	16.5	This work	26 Mar 2012	10 × 50
301	J13140+038	G 062-018	13:14:05.83	+03:53:58.7	9.490	M3.0 V	PMSU	19.6	Dit14	27 Mar 2012	10 × 50
302	J13165+278	GJ 1169	13:16:32.84	+27:52:29.8	9.267	M3.5 V	PMSU	15.6	Dit14	26 Mar 2012	10 × 50
303	J13168+170	HD 115404 B	13:16:51.56	+17:01:00.1	6.532	M0.5 V	AF15	11.1	aHIP2	28 Feb 2014	10 × 50
										15 Apr 2015	10 × 50
304	J13180+022	G 062–028	13:18:01.81	+02:14:01.1	8.787	M3.5 V	PMSU	21.1	Dit14	25 Mar 2012	10 × 50
										13 Jan 2013	10 × 50
										28 Feb 2014	10 × 50
										14 Apr 2015	10 × 50
305	J13300-087	Wolf 485 B	13:30:02.85	–08:42:25.2	9.599	M4.0 V	PMSU	17.4	aHIP2	27 Mar 2012	10 × 50
306	J13317+292	DG CVn AB	13:31:46.62	+29:16:36.7	7.561	M4.0 V	PMSU	18.02	Ried14	10 Jul 2012	11 × 50
										12 Jul 2012	10 × 50
										14 Apr 2015	10 × 50
307	J13318+233	G 150–007	13:31:50.57	+23:23:20.3	8.608	M2.0 V	PMSU	23.6	This work	26 Mar 2012	10 × 50
308	J13343+046	BD+05 2767	13:34:21.50	+04:40:02.6	7.213	M0.0 V	Lep13	21.32	HIP2	01 Mar 2014	10 × 50
309	J13369+229	Ross 1021	13:36:55.22	+22:58:01.1	8.979	M2.5 V	PMSU	24.3	This work	26 Mar 2012	10 × 50
310	J13386+258	Ross 1022	13:38:37.05	+25:49:49.6	8.751	M3.0 V	PMSU	18.7	This work	01 Mar 2014	10 × 50
311	J13388-022	Ross 488	13:38:53.45	–02:15:47.1	8.595	M2.0 V	PMSU	23.5	This work	27 Mar 2012	10 × 50
312	J13417+582	StM 187	13:41:46.31	+58:15:19.8	8.733	M3.5 V	Lep13	19.9	This work	02 Mar 2014	10 × 50
										14 Apr 2015	10 × 50

Table C.1: Log of observed stars (continued).

No.	Karmn	Name	α (J2000)	δ (J2000)	J [mag]	SpT	Ref.[a]	d [pc]	Ref.[b]	Observation date	N $\times$ $t_{\rm exp}$ [s]
313	J13430+090	G 063–050	13:43:01.27	+09:04:23.6	9.093	M3.0 V	PMSU	21.8	This work	26 Mar 2012	10 × 50
314	J13450+176	BD+18 2776	13:45:05.03	+17:47:10.5	6.997	M1.0 V	Koe10	13.6	HIP2	28 Feb 2014	10 × 50
315	J13458-179	LP 798–034	13:45:50.75	–17:58:04.8	7.745	M3.5 V	PMSU	10.2	HIP2	27 Mar 2012	10 × 50
316	J13481-137	LP 739–014	13:48:07.22	–13:44:32.1	10.413	M4.5 V	Dea12	22.3	This work	27 Mar 2012	10 × 50
317	J13503-216	LP 798–041	13:50:23.77	–21:37:19.3	9.458	M3.5 V	AF15	21.6	This work	27 Mar 2012	10 × 50
318	J13507-216	LP 798–044	13:50:44.00	–21:41:26.4	8.871	M3.0 V	PMSU	19.7	This work	27 Mar 2012	10 × 50
319	J13508+367	Ross 1019	13:50:51.82	+36:44:16.9	9.299	M3.5 V	PMSU	15.8	Dit14	26 Mar 2012	10 × 50
320	J13526+144	G 150–046	13:52:36.20	+14:25:20.9	8.013	M2.0 V	PMSU	19.4	This work	30 Jan 2012	10 × 50
										13 Jan 2013	10 × 50
										15 Apr 2015	10 × 50
321	J13582+125	Ross 837	13:58:13.93	+12:34:43.8	8.269	M3.0 V	PMSU	11.32	vAl95	26 Mar 2012	10 × 50
322	J13591-198	LP 799–007	13:59:10.46	–19:50:03.5	8.334	M4.0 V	PMSU	10.77	Ried14	27 Mar 2012	10 × 50
323	J14152+450	Ross 992	14:15:17.07	+45:00:53.6	8.014	M3.0 V	PMSU	16.3	vAl95	26 Mar 2012	10 × 50
324	J14155+046	GJ 1182	14:15:32.54	+04:39:31.2	9.433	M5.0 V	PMSU	13.9	vAl95	25 Mar 2012	10 × 50
325	J14157+594	LP 097–674	14:15:42.49	+59:27:30.3	8.850	M2.0 V	Lep13	26.4	This work	02 Mar 2014	10 × 50
										22 May 2014	10 × 50
										15 Apr 2015	10 × 50
326	J14171+088	2M J14170731+0851363	14:17:07.31	+08:51:36.3	9.109	M4.5 V	AF15	17.4	This work	01 Mar 2014	10 × 50
327	J14173+454	RX J1417.3+4525	14:17:22.10	+45:25:46.1	9.467	M5.0 V	Gig10	19.01	aHIP2	28 Feb 2014	10 × 50
328	J14200+390	StKM 1–1145	14:20:04.69	+39:03:01.5	8.572	M2.5 V	PMSU	20.2	This work	26 Mar 2012	10 × 50
329	J14210+275	G 166–021	14:21:03.49	+27:35:32.8	8.928	M2.5 V	PMSU	25.1	This work	26 Mar 2012	10 × 50
										14 Apr 2015	10 × 50
330	J14212-011	LP 620–003	14:21:15.13	–01:07:19.9	8.948	M3.5 V	PMSU	13.4	Ried10	25 Mar 2012	10 × 50
331	J14249+088	LP 500–019	14:24:55.99	+08:53:15.6	8.420	M2.5 V	PMSU	14.3	HIP2	30 Jan 2012	10 × 50
										31 Jan 2012	10 × 50
332	J14251+518	θ Boo B	14:25:11.60	+51:49:53.6	7.883	M2.5 V	AF15	14.53	aHIP2	31 Jan 2012	10 × 50
333	J14257+236W	BD+24 2733A	14:25:43.49	+23:37:01.1	6.769	M0.0 V	PMSU	16.36	HIP2	28 Feb 2014	10 × 50
334	J14257+236E	BD+24 2733B	14:25:46.67	+23:37:13.3	6.889	M0.5 V	PMSU	16.36	aHIP2	28 Feb 2014	10 × 50
335	J14279-003S	GJ 1183A	14:27:56.07	–00:22:31.1	9.305	M4.5 V	PMSU	13.4	This work	25 Mar 2012	10 × 50
336	J14279-003N	GJ 1183B	14:27:56.40	–00:22:19.1	9.345	M4.5 V	PMSU	13.6	This work	25 Mar 2012	10 × 50
337	J14283+053	LP 560–027	14:28:21.52	+05:19:01.4	8.721	M3.0 V	Lep13	18.4	This work	01 Mar 2014	10 × 50
338	J14294+155	Ross 130	14:29:29.72	+15:31:57.9	7.229	M2.0 V	PMSU	14.0	HIP2	30 Jan 2012	10 × 50
339	J14310-122	Wolf 1478	14:31:01.20	–12:17:45.2	7.803	M3.5 V	PMSU	10.8	HIP2	25 Mar 2012	10 × 50
340	J14321+081	LP 560–035	14:32:08.50	+08:11:31.3	10.108	M6.0 V	New14	9.1	This work	22 May 2014	10 × 50

Table C.1: Log of observed stars (continued).

No.	Karmn	Name	α (J2000)	δ (J2000)	J [mag]	SpT	Ref.[a]	d [pc]	Ref.[b]	Observation date	N $\times$ $t_{\rm exp}$ [s]
341	J14322+496	LP 174–355	14:32:14.54	+49:39:05.8	9.277	M3.5 V	PMSU	17.2	Dit14	26 Mar 2012	10 × 50
342	J14331+610	G 224–013	14:33:06.38	+61:00:44.5	8.171	M2.5 V	Lep13	18.3	This work	01 Mar 2014	10 × 50
										14 Apr 2015	10 × 50
343	J14342-125	HN Lib	14:34:16.83	–12:31:10.7	6.838	M4.0 V	PMSU	6.06	HIP2	30 Jan 2012	6 × 50
344	J14368+583	LP 098–132	14:36:53.02	+58:20:55.0	8.079	M2.5 V	PMSU	19.4	This work	31 Jan 2012	10 × 50
345	J15011+071	Ross 1030a	15:01:10.74	+07:09:47.7	8.682	M3.5 V	PMSU	15.1	This work	25 Mar 2012	10 × 50
										14 Apr 2015	10 × 50
346	J15013+055	G 015–002	15:01:20.11	+05:32:55.4	8.326	M3.0 V	PMSU	15.3	This work	26 Mar 2012	10 × 50
347	J15043+603	Ross 1051	15:04:18.56	+60:23:04.4	7.701	M1.0 V	PMSU	17.85	HIP2	01 Mar 2014	10 × 50
348	J15018+550	LP 135–097	15:05:49.51	+55:04:43.1	9.239	M3.5 V	PMSU	19.6	This work	26 Mar 2012	10 × 50
349	J15073+249	BD+25 2874	15:07:23.62	+24:56:07.6	7.296	M0.0 V	Lep13	16.7	vAl95	02 Mar 2014	10 × 50
350	J15081+623	LSPM J1508+6221	15:08:11.93	+62:21:53.6	9.296	M4.0 V	AF15	19.9	This work	01 Mar 2014	10 × 50
										22 May 2014	10 × 50
										15 Apr 2015	10 × 50
351	J15095+031	Ross 1047	15:09:35.59	+03:10:00.8	7.720	M3.0 V	PMSU	14.4	HIP2	26 Mar 2012	10 × 50
352	J15100+193	G 136–072	15:10:04.81	+19:21:28.7	9.056	M4.0 V	PMSU	17.0	Dit14	25 Mar 2012	10 × 50
										15 Apr 2015	10 × 50
353	J15126+457	G 179–020	15:12:38.18	+45:43:46.4	8.977	M4.0 V	PMSU	18.5	Dit14	26 Mar 2012	10 × 50
										15 Apr 2015	10 × 50
354	J15191-127	LP 742–061	15:19:11.82	–12:45:06.2	8.507	M4.0 V	PMSU	21.12	Wein16	27 Mar 2012	10 × 50
355	J15214+042	TYC 344–504–1	15:21:25.30	+04:14:49.3	8.553	M1.5 V	Lep13	26.1	This work	02 Mar 2014	10 × 50
356	J15305+094	NLTT 40406	15:30:30.33	+09:26:01.4	9.569	M5.5 V	AF15	8.1	Dit14	22 May 2014	10 × 50
357	J15357+221	LP 384–018	15:35:46.10	+22:09:03.7	8.681	M3.5 V	PMSU	18.6	vAl95	25 Mar 2012	10 × 50
358	J15369-141	Ross 802	15:36:58.68	–14:08:00.6	8.432	M4.0 V	PMSU	13.3	vAl95	28 Feb 2014	10 × 50
359	J15400+434N	vB 24 A	15:40:03.53	+43:29:39.7	8.312	M3.0 V	PMSU	13.5	vAl95	01 Mar 2014	10 × 50
										22 May 2014	10 × 50
360	J15474-108	LP 743–031	15:47:24.64	–10:53:47.1	7.582	M2.0 V	PMSU	15.1	HIP2	26 Mar 2012	10 × 50
										15 Apr 2015	10 × 50
361	J15496+348	LP 274–008	15:49:38.33	+34:48:55.5	8.728	M4.0 V	PMSU	16.98	vAl95	27 Mar 2012	10 × 50
										10 Jul 2012	10 × 50
										11 Jul 2012	10 × 50
										28 Feb 2014	10 × 50
362	J15531+347S	LP 274–021	15:53:06.64	+34:44:47.4	8.994	M3.5 V	PMSU	19.3	avAl95	25 Mar 2012	10 × 50
363	J15578+090	LSPM J1557+0901	15:57:48.27	+09:01:09.9	9.282	M4.0 V	AF15	16.4	This work	02 Mar 2014	10 × 50

Table C.1: Log of observed stars (continued).

No.	Karmn	Name	α (J2000)	δ (J2000)	J [mag]	SpT	Ref.[a]	d [pc]	Ref.[b]	Observation date	N $\times$ $t_{\rm exp}$ [s]
364	J15598-082	BD-07 4156	15:59:53.37	–08:15:11.4	7.185	M1.0 V	PMSU	13.9	HIP2	01 Mar 2014	10 × 50
365	J16017+301	G 168–024	16:01:43.60	+30:10:50.2	8.666	M3.0 V	PMSU	18.4	Dit14	27 Mar 2012	20 × 50
366	J16092+093	G 137–084	16:09:16.25	+09:21:07.7	7.969	M3.0 V	Lep13	13.0	This work	22 May 2014	10 × 50
367	J16120+033	TYC 371–1053–1	16:12:04.65	+03:18:20.8	8.127	M2.0 V	Lep13	18.9	This work	01 Mar 2014	10 × 50
368	J16145+191	GJ 1200	16:14:32.85	+19:06:10.2	8.990	M3.5 V	PMSU	16.5	Dit14	27 Mar 2012	10 × 50
369	J16241+483	GJ 623 AB	16:24:09.32	+48:21:10.5	6.638	M2.5 V	PMSU	8.1	HIP2	10 Jul 2012	10 × 50
										12 Jul 2012	10 × 50
370	J16255+260	LTT 14889	16:25:32.35	+26:01:37.9	8.403	M3.0 V	PMSU	18.9	This work	25 Mar 2012	30 × 50
										15 Apr 2015	10 × 50
371	J16313+408	G 180–060	16:31:18.79	+40:51:51.6	9.461	M5.0 V	PMSU	12.0	Dit14	27 Mar 2012	10 × 50
372	J16315+175	GJ 1202	16:31:35.08	+17:33:49.5	8.926	M3.5 V	PMSU	15.5	Dit14	27 Mar 2012	10 × 50
373	J16327+126	GJ 1203	16:32:45.25	+12:36:46.0	8.429	M3.0 V	PMSU	16.8	HIP2	25 Mar 2012	10 × 50
										22 May 2014	10 × 50
										09 Jun 2015	10 × 50
374	J16328+098	G 138–040	16:32:52.85	+09:50:26.0	8.988	M3.5 V	PMSU	13.8	Dit14	27 Mar 2012	10 × 50
										10 Jul 2012	10 × 50
										11 Jul 2012	10 × 50
										17 Sep 2012	10 × 50
										28 Feb 2014	10 × 50
										15 Apr 2015	10 × 50
375	J16354+350	LP 275–068	16:35:27.41	+35:00:57.7	8.615	M4.0 V	PMSU	16.2	Dit14	11 Jul 2012	10 × 50
376	J16360+088	G 138–043	16:36:05.63	+08:48:49.2	9.419	M4.0 V	PMSU	15.34	vAl95	25 Mar 2012	10 × 50
377	J16401+007	LP 625–034	16:40:06.00	+00:42:18.8	9.116	M4.0 V	PMSU	11.20	Wein16	11 Jul 2012	10 × 50
378	J16462+164	LP 446–006	16:46:13.72	+16:28:40.7	7.951	M2.5 V	PMSU	16.1	HIP2	25 Mar 2012	10 × 50
										10 Jul 2012	10 × 50
										11 Jul 2012	10 × 50
										17 Sep 2012	10 × 50
										28 Feb 2014	10 × 50
										15 Apr 2015	10 × 50
379	J16487+106	LSPM J1648+1038	16:48:46.58	+10:38:51.7	7.820	M2.5 V	Lep13	17.1	This work	01 Mar 2014	10 × 50
										22 May 2014	10 × 50
										14 Apr 2015	10 × 50
380	J16509+224	G 169–029	16:50:57.95	+22:27:05.8	9.136	M4.5 V	PMSU	10.0	Dit14	11 Jul 2012	10 × 50
381	J16528+630	GSC 04194–01561	16:52:49.48	+63:04:39.0	9.592	M5.0 V	New14	12.1	This work	22 May 2014	10 × 50

Table C.1: Log of observed stars (continued).

No.	Karmn	Name	α (J2000)	δ (J2000)	J [mag]	SpT	Ref.[a]	d [pc]	Ref.[b]	Observation date	N $\times$ $t_{\rm exp}$ [s]
382	J16554-083N	GJ 643	16:55:25.27	–08:19:20.8	7.555	M3.5 V	PMSU	6.2	aHIP2	26 Mar 2012	10 × 50
383	J16554-083S	GJ 644 ABab	16:55:28.81	–08:20:10.3	5.270	M3.0 V	PMSU	6.2	HIP2	26 Mar 2012	10 × 50
384	J16555-083	vB 8	16:55:35.29	–08:23:40.1	9.776	M7.0 V	AF15	6.48	Wein16	26 Mar 2012	10 × 50
385	J16578+473	BD+47 2415B	16:57:53.58	+47:22:01.6	6.874	M1.5 V	Lep13	18.3	aHIP2	22 May 2014	10 × 50
386	J17010+082	G 139–005	17:01:02.11	+08:12:26.4	9.437	M3.5 V	PMSU	17.7	Dit14	10 Jul 2012	10 × 50
387	J17033+514	G 203–042	17:03:23.85	+51:24:21.9	8.768	M4.5 V	PMSU	9.5	vAl95	11 Jul 2012	10 × 50
388	J17115+384	Wolf 654	17:11:34.72	+38:26:34.1	7.630	M3.5 V	PMSU	12.0	HIP2	25 Mar 2012	10 × 50
389	J17177+116	GJ 1215	17:17:44.08	+11:40:11.8	9.817	M5.0 V	PMSU	12.7	vAl95	11 Jul 2012	10 × 50
390	J17177-118	LTT 6883	17:17:45.32	–11:48:54.2	8.818	M3.0 V	PMSU	19.2	This work	26 Mar 2012	10 × 50
391	J17219+214	G 170–036	17:21:54.65	+21:25:46.8	9.344	M4.0 V	PMSU	13.4	Dit14	25 Mar 2012	10 × 50
392	J17321+504	LP 180–017	17:32:07.83	+50:24:51.0	9.008	M2.5 V	PMSU	28.1	vAl95	27 Mar 2012	10 × 50
393	J17338+169	1RXS J173353.5+165515	17:33:53.15	+16:55:12.9	8.895	M5.5 V	Lep13	11.7	Dit14	01 Mar 2014	10 × 50
394	J17340+446	2M J17340562+4447082	17:34:05.62	+44:47:08.2	8.742	M3.5 V	Lep13	20.2	This work	22 May 2014	10 × 50
										14 Apr 2015	10 × 50
395	J17425-166	GJ 690.1	17:42:32.29	–16:38:23.6	9.441	M2.5 V	PMSU	19.4	vAl95	27 Mar 2012	10 × 50
396	J17460+246	LP 389–032	17:46:04.66	+24:39:05.0	8.814	M3.5 V	Klu13	14.5	vAl95	11 Jul 2012	10 × 50
397	J17530+169	G 183–010	17:53:00.63	+16:55:02.9	8.699	M3.0 V	PMSU	19.8	This work	26 Mar 2012	10 × 50
										10 Jul 2012	10 × 50
										12 Jul 2012	10 × 50
										16 Sep 2012	10 × 50
										15 Apr 2015	10 × 50
398	J17542+073	GJ 1222	17:54:17.10	+07:22:44.7	8.772	M4.0 V	PMSU	15.0	Dit14	25 Mar 2012	10 × 50
399	J17578+046	Barnard's Star	17:57:48.49	+04:41:40.5	5.244	M3.5 V	AF15	1.824	HIP2	11 Jul 2012	10 × 50
400	J17578+465	G 204–039	17:57:50.96	+46:35:18.2	7.847	M2.5 V	AF15	14.1	HIP2	11 Jul 2012	10 × 50
401	J18010+508	Wolf 1403	18:01:05.58	+50:49:36.9	8.927	M1.5 V	Lep13	31.0	This work	22 May 2014	11 × 50
402	J18027+375	GJ 1223	18:02:46.25	+37:31:04.9	9.720	M5.0 V	PMSU	12.0	vAl95	12 Jul 2012	10 × 50
403	J18075-159	GJ 1224	18:07:32.93	–15:57:46.5	8.639	M4.5 V	PMSU	8.10	Wein16	10 Jul 2012	10 × 50
404	J18165+048	G 140–051	18:16:31.54	+04:52:45.6	9.798	M5.0 V	New14	13.3	This work	22 May 2014	10 × 50
405	J18180+387W	G 204–057	18:18:03.46	+38:46:36.0	9.197	M4.0 V	PMSU	10.4	Dit14	11 Jul 2012	10 × 50
406	J18180+387E	G 204-058	18:18:04.28	+38:46:34.2	8.040	M3.0 V	PMSU	10.7	Dit14	11 Jul 2012	10 × 50
407	J18224+620	GJ 1227	18:22:27.19	+62:03:02.5	8.640	M4.0 V	AF15	8.23	vAl95	12 Jul 2012	10 × 50
408	J18240+016	G 021–013	18:24:05.18	+01:41:16.1	8.297	M2.0 V	PMSU	20.5	This work	11 Jul 2012	10 × 50
409	J18264+113	G 141–010	18:26:24.59	+11:20:57.5	8.918	M3.5 V	PMSU	16.9	This work	10 Jul 2012	10 × 50
410	J18312+068	LP 570–092	18:31:16.06	+06:50:09.7	7.579	M1.0 V	Lep13	18.5	This work	22 May 2014	10 × 50

Table C.1: Log of observed stars (continued).

No.	Karmn	Name	α (J2000)	δ (J2000)	J [mag]	SpT	Ref.[a]	d [pc]	Ref.[b]	Observation date	N $\times$ $t_{\rm exp}$ [s]
411	J18319+406	G 205–028	18:31:58.40	+40:41:10.4	8.065	M3.5 V	PMSU	11.4	This work	12 Jul 2012	10 × 50
412	J18354+457	GJ 720 B (vB 9)	18:35:27.23	+45:45:40.3	8.886	M2.5 V	AF15	13.1	Dit14	12 Jul 2012	10 × 50
413	J18387-144	GJ 2138	18:38:44.75	–14:29:25.0	7.661	M2.5 V	PMSU	12.9	HIP2	10 Jul 2012	10 × 50
414	J18411+247S	GJ 1230 Aab	18:41:09.78	+24:47:14.4	7.528	M4.5 V	PMSU	10.2	This work	12 Jul 2012	10 × 50
415	J18411+247N	GJ 1230 B	18:41:09.82	+24:47:19.5	8.860	M5.0 V	PMSU	10.2	This work	12 Jul 2012	10 × 50
416	J18427+139	V816 Her	18:42:44.99	+13:54:16.8	8.361	M4.0 V	PMSU	10.91	Wein16	11 Jul 2012	10 × 50
										17 Sep 2012	10 × 50
417	J18427+596N	HD 173739	18:42:46.66	+59:37:49.9	5.189	M3.0 V	AF15	3.57	HIP2	12 Jul 2012	10 × 50
418	J18427+596S	HD 173740	18:42:46.88	+59:37:37.4	5.721	M3.5 V	AF15	3.57	aHIP2	12 Jul 2012	10 × 50
419	J18451+063	TYC 460–624–1	18:45:10.27	+06:20:15.8	7.656	M1.0 V	Lep13	19.2	This work	22 May 2014	10 × 50
420	J18453+188	G 184–024	18:45:22.94	+18:51:58.5	9.273	M4.0 V	AF15	16.3	This work	01 Mar 2014	10 × 50
421	J18480-145	G 155–042	18:48:01.29	–14:34:50.8	8.375	M2.5 V	PMSU	18.4	This work	10 Jul 2012	10 × 50
422	J18482+076	G 141–036	18:48:17.52	+07:41:21.0	8.853	M5.0 V	AF15	7.2	Dit14	22 May 2014	10 × 50
423	J18507+479	G 205–038	18:50:45.21	+47:58:19.5	8.686	M3.5 V	PMSU	15.2	This work	12 Jul 2012	10 × 50
424	J18516+244	G 184–036	18:51:40.84	+24:27:32.2	8.925	M3.0 V	PMSU	20.2	This work	12 Jul 2012	10 × 50
425	J18548+109	V1436 Aql B	18:54:53.81	+10:58:43.5	7.139	M3.5 V	PMSU	19.2	aJen63	22 May 2014	10 × 50
426	J18571+075	LP 571–080	18:57:10.54	+07:34:17.1	8.331	M2.0 V	PMSU	20.8	This work	11 Jul 2012	10 × 50
427	J19032+034	G 141–057	19:03:13.61	+03:24:02.8	8.665	M3.0 V	Lep13	17.9	This work	15 Apr 2015	10 × 50
428	J19084+322	G 207–019	19:08:29.96	+32:16:52.0	7.905	M3.0 V	PMSU	12.6	This work	11 Jul 2012	10 × 50
429	J19098+176	GJ 1232	19:09:50.98	+17:40:07.4	8.819	M4.5 V	PMSU	10.3	Dit14	10 Jul 2012	10 × 50
430	J19122+028	Wolf 1062 AB	19:12:14.55	+02:53:11.2	7.087	M3.5 V	PMSU	10.2	HIP2	10 Jul 2012	10 × 50
431	J19124+355	G 207–022	19:12:29.38	+35:33:52.6	8.399	M2.5 V	PMSU	17.2	vAl95	12 Jul 2012	10 × 50
432	J19220+070	GJ 1236	19:22:02.07	+07:02:31.0	8.524	M3.0 V	PMSU	10.54	Wein16	15 apr 2015	10 × 50
433	J19354+377	RX J1935.4+3746	19:35:29.23	+37:46:08.2	7.562	M3.5 V	Lep13	9.2	This work	15 Apr 2015	10 × 50
434	J19463+320	BD+31 3767A	19:46:23.86	+32:01:02.1	6.883	M0.5 V	PMSU	13.61	HIP2	11 Jul 2012	10 × 50
										17 Sep 2012	10 × 50
										15 Apr 2015	10 × 50
435	J19464+320	BD+31 3767B	19:46:24.15	+32:00:58.6	7.323	M2.5 V	Kir91	13.61	aHIP2	11 Jul 2012	10 × 50
										17 Sep 2012	10 × 50
										15 Apr 2015	10 × 50
436	J19511+464	G 208–042	19:51:09.31	+46:28:59.9	8.586	M4.0 V	PMSU	11.9	vAl95	12 Jul 2012	10 × 50
437	J19539+444W	V1581 Cyg AB	19:53:54.43	+44:24:54.2	7.791	M5.5 V	AF15	4.6	HD80	12 Jul 2012	10 × 50
										17 Sep 2012	10 × 50
438	J19539+444E	GJ 1245 C	19:53:55.09	+44:24:55.0	8.275	M5.5 V	AF15	4.4	Dit14	12 Jul 2012	10 × 50

Table C.1: Log of observed stars (continued).

No.	Karmn	Name	α (J2000)	δ (J2000)	J [mag]	SpT	Ref.[a]	d [pc]	Ref.[b]	Observation date	N $\times$ $t_{\rm exp}$ [s]
										17 Sep 2012	10 × 50
439	J19582+020	LP 634–002	19:58:15.72	+02:02:15.2	8.371	M2.5 V	PMSU	15.8	vAl95	12 Jul 2012	10 × 50
440	J20039-081	LP 694–016	20:03:58.92	–08:07:47.3	9.184	M4.0 V	PMSU	15.7	This work	12 Jul 2012	10 × 50
441	J20187+158	LTT 15944	20:18:44.54	+15:50:46.4	8.174	M2.5 V	PMSU	16.8	This work	11 Jul 2012	10 × 50
442	J20298+096	HU Del AB	20:29:48.34	+09:41:20.2	8.228	M4.5 V	PMSU	8.86	Ben00	10 Jul 2012	10 × 50
443	J20336+617	GJ 1254	20:33:40.31	+61:45:13.6	8.287	M4.0 V	PMSU	15.9	vAl95	12 Jul 2012	10 × 50
444	J20347+033	G 024–020	20:34:43.04	+03:20:50.9	8.446	M2.5 V	PMSU	26.9	HIP2	12 Jul 2012	10 × 50
445	J20367+388	G 209–038	20:36:46.01	+38:50:33.0	9.270	M3.5 V	PMSU	19.8	This work	11 Jul 2012	10 × 50
446	J20407+199	GJ 797 B	20:40:44.50	+19:54:02.3	8.160	M2.5 V	AF15	20.9	aHIP2	12 Jul 2012	10 × 50
										17 Sep 2012	10 × 50
										14 Apr 2015	10 × 50
447	J20433+553	GJ 802 AabB	20:43:19.21	+55:20:52.1	9.563	M5.0 V	PMSU	15.7	Ire08	10 Jul 2012	10 × 50
448	J20445+089N	LP 576–039	20:44:30.45	+08:54:25.3	8.607	M3.5 V	PMSU	22.2	This work	12 Jul 2012	10 × 50
449	J20445+089S	LP 576–040	20:44:30.73	+08:54:10.7	8.136	M1.5 V	PMSU	22.2	This work	12 Jul 2012	10 × 50
										17 Sep 2012	10 × 50
450	J20488+197	G 144–039	20:48:52.46	+19:43:05.0	9.236	M4.0 V	PMSU	33.56	vAl95	11 Jul 2012	10 × 50
										17 Sep 2012	10 × 50
451	J20535+106	G 025–008	20:53:33.04	+10:37:02.0	9.348	M4.0 V	PMSU	13.9	vAl95	12 Jul 2012	10 × 50
452	J20556-140N	GJ 810 A	20:55:37.72	–14:02:07.8	8.117	M4.0 V	PMSU	12.66	Wein16	12 Jul 2012	10 × 50
453	J21012+332	LP 340–547	21:01:16.10	+33:14:32.8	8.439	M3.0 V	PMSU	18.2	This work	11 Jul 2012	10 × 50
										17 Sep 2012	10 × 50
										14 Apr 2015	10 × 50
										15 Apr 2015	10 × 50
454	J21013+332	LP 340–548	21:01:20.62	+33:14:28.0	8.936	M3.5 V	PMSU	18.2	This work	11 Jul 2012	10 × 50
455	J21152+257	LP 397–041	21:15:12.59	+25:47:45.4	8.403	M3.0 V	PMSU	15.9	This work	12 Jul 2012	10 × 50
456	J21160+298E	Ross 776	21:16:05.77	+29:51:51.1	8.448	M3.5 V	PMSU	20.1	This work	12 Jul 2012	10 × 50
457	J21313-097	BB Cap AB	21:31:18.61	–09:47:26.5	7.316	M4.5 V	PMSU	8.3	HIP2	10 Jul 2012	10 × 50
458	J21323+245	LP 397–034	21:32:21.98	+24:33:41.9	8.476	M3.5 V	PMSU	22.0	Dit14	11 Jul 2012	10 × 50
										17 Sep 2012	10 × 50
459	J21512+128	G 018–001	21:51:17.41	+12:50:30.3	9.349	M4.0 V	PMSU	26.2	vAl95	11 Jul 2012	10 × 50
460	J21518+136	LP 518–058	21:51:48.32	+13:36:15.5	9.311	M4.5 V	PMSU	16.0	Dit14	11 Jul 2012	10 × 50
										17 Sep 2012	10 × 50
										29 Jul 2015	10 × 50
461	J21593+418	G 215–030	21:59:21.92	+41:51:32.7	8.982	M3.0 V	PMSU	20.8	This work	16 Sep 2012	10 × 50

Table C.1: Log of observed stars (continued).

No.	Karmn	Name	α (J2000)	δ (J2000)	J [mag]	SpT	Ref.[a]	d [pc]	Ref.[b]	Observation date	N × $t_{\rm exp}$ [s]
462	J22012+283	V374 Peg	22:01:13.11	+28:18:24.9	7.635	M4.0 V	PMSU	8.9	HIP2	11 Jul 2012	10 × 50
463	J22060+393	G 189–001	22:06:00.68	+39:18:02.7	8.912	M3.0 V	PMSU	20.1	This work	16 Sep 2012	10 × 50
464	J22097+410	G 214–012	22:09:43.01	+41:02:05.3	8.755	M3.5 V	PMSU	22.5	vAl95	11 Jul 2012	10 × 50
465	J22252+594	G 232–070	22:25:17.06	+59:24:49.6	8.745	M4.0 V	PMSU	12.8	This work	16 Sep 2012	10 × 50
466	J22279+576	HD 239960 + DO Cep	22:27:59.58	+57:41:45.3	5.575	M3.0 V	PMSU	4.0	vAl95	23 Oct 2011	3 × 35
467	J22298+414	G 215–050	22:29:48.86	+41:28:48.0	8.849	M4.0 V	PMSU	13.8	vAl95	11 Jul 2012	10 × 50
468	J22426+176	GJ 1271	22:42:38.72	+17:40:09.1	8.062	M2.5 V	PMSU	20.3	HIP2	16 Sep 2012	10 × 50
469	J22507+286	LP 344–047	22:50:45.49	+28:36:08.5	8.810	M3.0 V	PMSU	19.2	This work	16 Sep 2012	10 × 50
470	J23096-019	G 028–044	23:09:39.32	–01:58:23.0	8.671	M3.5 V	PMSU	20.2	This work	16 Sep 2012	10 × 50
										14 Jan 2013	10 × 50
471	J23174+382	G 190–017	23:17:24.41	+38:12:42.0	7.761	M2.5 V	PMSU	17.5	vAl95	11 Jul 2012	10 × 50
472	J23174+196	G 067–053 AB	23:17:28.07	+19:36:46.9	8.020	M3.5 V	PMSU	9.1	Dit14	10 Jul 2012	10 × 50
473	J23216+172	LP 462–027	23:21:37.52	+17:17:28.5	7.391	M4.0 V	PMSU	10.99	HIP2	16 Sep 2012	10 × 50
474	J23265+121	LP 522–049	23:26:32.39	+12:09:32.8	8.962	M3.0 V	PMSU	38.3	vAl95	16 Sep 2012	10 × 50
475	J23293+414S	G 190–027	23:29:22.58	+41:27:52.2	8.017	M4.0 V	PMSU	14.9	avAl95	11 Jul 2012	10 × 50
										29 Jul 2015	10 × 50
476	J23293+414N	G 190–028	23:29:23.46	+41:28:06.9	7.925	M3.5 V	PMSU	14.9	vAl95	11 Jul 2012	10 × 50
										29 Jul 2015	10 × 50
477	J23318+199E	EQ Peg Aab	23:31:52.09	+19:56:14.2	6.162	M3.5 V	PMSU	6.2	HIP2	23 Oct 2011	69 × 150
										25 Oct 2011	60 × 150
478	J23318+199W	EQ Peg Bab	23:31:52.48	+19:56:13.8	7.101	M4.5 V	PMSU	6.2	aHIP2	23 Oct 2011	69 × 150
										25 Oct 2011	60 × 150
479	J23351-023	GJ 1286	23:35:10.50	–02:23:21.4	9.148	M5.5 V	PMSU	7.21	Wein16	16 Sep 2012	10 × 50
480	J23381-162	G 273–093	23:38:08.19	–16:14:10.0	7.813	M2.0 V	PMSU	16.4	This work	16 Sep 2012	10 × 50
481	J23428+308	GJ 1288	23:42:52.74	+30:49:21.9	9.637	M4.5 V	PMSU	12.6	Dit14	16 Sep 2012	10 × 50
482	J23431+365	GJ 1289	23:43:06.29	+36:32:13.2	8.110	M4.0 V	PMSU	8.1	vAl95	11 Jul 2012	10 × 50
483	J23455-161	LP 823–004 AB	23:45:31.28	–16:10:19.8	9.206	M5.0 V	PMSU	12.5	Ried10	10 Jul 2012	10 × 50
484	J23492+024	BR Psc	23:49:12.56	+02:24:03.8	5.827	M1.0 V	PMSU	5.98	HIP2	16 Sep 2012	10 × 50
485	J23492+100	G 029–069	23:49:15.02	+10:05:38.5	9.459	M4.0 V	PMSU	17.8	This work	16 Sep 2012	10 × 50
486	J23505-095	LP 763–012	23:50:31.59	–09:33:32.1	8.943	M4.0 V	PMSU	16.0	Ried10	16 Sep 2012	10 × 50
487	J23517+069	G 030–026	23:51:44.83	+06:58:15.9	8.841	M3.0 V	PMSU	21.0	This work	16 Sep 2012	10 × 50
										14 Jan 2013	10 × 50
										29 Jul 2015	10 × 50
488	J23573-129W	LP 704–014 Bab	23:57:19.35	–12:58:40.7	9.128	M4.0 V	PMSU	15.6	This work	14 Jan 2013	10 × 50

Table C.1: Log of observed stars (continued).

No.	Karmn	Name	α (J2000)	δ (J2000)	J [mag]	SpT	Ref.[a]	d [pc]	Ref.[b]	Observation date	N $\times$ $t_{\rm exp}$ [s]
489	J23573-129E	LP 704–015 A	23:57:20.57	–12:58:48.7	8.636	M3.0 V	PMSU	17.7	This work	14 Jan 2013	10 $\times$ 50
490	J23577+233	GJ 1292	23:57:44.10	+23:18:17.0	7.800	M3.5 V	PMSU	13.7	vAl95	11 Jul 2012	10 $\times$ 50

Notes. [a] AF15: Alonso-Floriano et al. 2015a; Cru03: Cruz et al. 2003; Dea12: Deacon et al. 2012; Gig10: Gigoyan et al. 2010; Gra03: Gray et al. 2003; Gra06: Gray et al. 2006; Klutsch et al. priv. comm.; Koe10: Koen et al. 2010; Lep13: Lépine et al. 2013; Mon01: Montes et al. 2001; New14: Newton et al. 2014; PMSU: (Palomar/Michigan State University survey catalogue of nearby stars) Reid et al. 1995., Hawley et al. 1996, Gizis et al. 2002; Ria06: Riaz et al. 2006; Sch05: Scholz et al. 2005; Sim15: Simon-Díaz et al. 2015; ZS04: Zuckerman & Song 2014. [b] Ben00: Benedict et al. 2000; Cru03: Cruz et al. 2003; Daw05: Dawson et al. 2005; Dit14: Dittmann et al. 2014; GC09: Gatewood & Coban 2009; HD80: Harrington & Dahn 1980; Hen06: Henry et al. 2006; HT98: Hershey & Taff 1998; HIP2: van Leeuwen 2007; Ire08: Ireland et al. 2008; Jen52: Jenkins 1952; Jen63: Jenkins 1963; Jen09: Jenkins et al. 2009; Lep13: Lépine et al. 2013; New14: Newton et al. 2014; PMSU: (Palomar/Michigan State University survey catalogue of nearby stars) Reid et al. 1995., Hawley et al. 1996, Gizis et al. 2002; Rei02: Reid et al. 2002; Ried10: Ria06: Riaz et al. 2006; Reidel et al. 2010; Ried14: Riedel et al. 2014; Sub09: Subasavage et al. 2009; vAl95: van Altena et al. 1995; Wein16: Weinberger et al. 2016. An "a" or "b" preceding the reference indicates that no measure for this component was found but we used instead the measure of the A or B companion, respectively.

Table C.2: ADS standard stars.

ADS	Literature		Epoch	Ref.[a]	This work		Epoch
	ρ [arcsec]	θ [deg]			ρ [arcsec]	θ [deg]	
2999	3.55	222.2	J2011.662	Mas12	3.634 ± 0.016	222.56 ± 0.22	J2012.078
					3.621 ± 0.010	222.43 ± 0.16	J2012.081
					3.611 ± 0.010	222.19 ± 0.17	J2013.034
3297	2.93	276.8	J2011.064	Mas12	3.073 ± 0.012	276.98 ± 0.23	J2012.078
					3.070 ± 0.009	276.92 ± 0.18	J2012.081
					3.067 ± 0.013	277.05 ± 0.17	J2012.229
					3.069 ± 0.008	277.03 ± 0.16	J2012.231
					3.073 ± 0.010	276.74 ± 0.16	J2013.034
3853	3.041	74.2	J2008.867	Har11	3.072 ± 0.012	74.80 ± 0.30	J2012.078
					3.085 ± 0.013	74.85 ± 0.13	J2012.081
					3.070 ± 0.009	74.92 ± 0.15	J2012.231
					3.079 ± 0.023	74.66 ± 0.12	J2013.034
4241 (A–B)[b]	0.2526 ± 0.0010	80.1 ± 0.4	J2013.710	Sim15	0.243 ± 0.008	85.89 ± 2.46	J2012.234
4241 (AB–C)	11.24	239.2	J2013.168	Schl13	11.439 ± 0.071	238.25 ± 0.24	J2012.234
7878	3.743 ± 0.021	161.7 ± 0.3	J2008.036	Pru09	3.768 ± 0.011	161.81 ± 0.13	J2012.234
					3.769 ± 0.010	161.74 ± 0.18	J2014.936
8105	3.678 ± 0.035	96.8 ± 0.3	J2010.392	Pru12	3.665 ± 0.012	97.64 ± 0.13	J2012.234
					3.673 ± 0.012	97.54 ± 0.15	J2014.936
8220	3.495	208.14	J2013.314	Ben14	3.506 ± 0.009	207.84 ± 0.14	J2012.234
					3.510 ± 0.010	207.91 ± 0.18	J2014.936
9168	2.199 ± 0.013	254.9 ± 0.3	J2011.491	Sca13	2.200 ± 0.006	255.52 ± 0.19	J2012.231
					2.203 ± 0.008	255.19 ± 0.16	J2012.527
					2.209 ± 0.011	255.31 ± 0.13	J2013.034
					2.197 ± 0.011	255.42 ± 0.25	J2013.036
					2.182 ± 0.008	255.62 ± 0.20	J2014.159
					2.188 ± 0.010	255.52 ± 0.23	J2014.162
9312	3.029 ± 0.016	37.6 ± 0.3	J2011.496	Sca13	3.049 ± 0.010	37.95 ± 0.19	J2012.229
					3.046 ± 0.007	37.88 ± 0.19	J2012.231
					3.052 ± 0.011	37.81 ± 0.13	J2012.234
					3.048 ± 0.010	37.96 ± 0.19	J2012.527
					3.047 ± 0.009	37.83 ± 0.18	J2013.036
					3.042 ± 0.012	37.54 ± 0.18	J2014.159
					3.052 ± 0.016	37.55 ± 0.19	J2014.162
					3.035 ± 0.018	37.57 ± 0.14	J2014.164
9461	4.130 ± 0.015	276.95 ± 0.16	J2008.608	Des11	4.111 ± 0.012	277.05 ± 0.16	J2012.229
					4.118 ± 0.017	277.01 ± 0.16	J2012.231
					4.104 ± 0.013	276.76 ± 0.16	J2012.527
					4.092 ± 0.014	276.76 ± 0.14	J2013.036
					4.084 ± 0.012	276.95 ± 0.16	J2014.159
					4.094 ± 0.012	277.10 ± 0.22	J2014.162
					4.094 ± 0.012	277.06 ± 0.13	J2014.164
14708	2.48	28.6	J2010.693	Thor11	2.453 ± 0.015	28.15 ± 0.16	J2011.812
					2.454 ± 0.014	28.45 ± 0.13	J2012.708
					2.460 ± 0.014	28.57 ± 0.16	J2012.710
					2.451 ± 0.011	28.06 ± 0.12	J2014.386

Table C.2: ADS standard stars (continued).

ADS	Literature		Epoch	Ref.[a]	This work		Epoch
	ρ [arcsec]	θ [deg]			ρ [arcsec]	θ [deg]	
14733	2.601 ± 0.021	123.9 ± 0.4	J2011.876	Sca13	2.662 ± 0.012	125.11 ± 0.13	J2011.812
					2.631 ± 0.013	125.19 ± 0.16	J2012.708
					2.647 ± 0.015	125.54 ± 0.16	J2012.710
					2.638 ± 0.012	125.60 ± 0.14	J2014.386
14878	6.85	113.9	J2012.595	Mas13	6.897 ± 0.012	113.60 ± 0.12	J2011.807
					6.842 ± 0.015	113.57 ± 0.14	J2012.708
					6.864 ± 0.013	113.98 ± 0.13	J2012.710
					6.842 ± 0.012	113.96 ± 0.13	J2014.386
15935	3.593	224.19	J1990.809	Ha4	3.899 ± 0.014	225.11 ± 0.16	J2011.807
					3.906 ± 0.011	225.29 ± 0.14	J2012.710
16389	3.893 ± 0.019	13.9 ± 0.3	J2009.957	Sca11	3.970 ± 0.012	13.85 ± 0.15	J2011.810
					3.999 ± 0.011	14.20 ± 0.17	J2012.522
					3.973 ± 0.011	14.55 ± 0.18	J2012.524
					3.983 ± 0.013	14.47 ± 0.16	J2012.527
					3.982 ± 0.013	14.45 ± 0.14	J2012.708
16496	2.664 ± 0.027	164.9 ± 0.5	J2011.860	Sca13	2.702 ± 0.010	165.07 ± 0.20	J2012.522
					2.681 ± 0.012	165.59 ± 0.13	J2012.708
16982	2.590 ± 0.028	210.8 ± 0.7	J2011.874	Sca13	2.626 ± 0.015	211.37 ± 0.14	J2011.810
					2.625 ± 0.014	211.81 ± 0.13	J2012.708
					2.637 ± 0.014	211.96 ± 0.13	J2012.710
17140	3.094 ± 0.030	325.4 ± 0.5	J2011.874	Sca13	3.197 ± 0.012	325.81 ± 0.18	J2012.522
					3.155 ± 0.007	326.24 ± 0.14	J2012.524
					3.149 ± 0.015	326.08 ± 0.12	J2012.708

Notes. [a]Ben14: Benavides 2014; Des11: Desidera et al.2011; Har11: Hartkopf et al. 2011; Mas12: Mason et al. 2012; Mas13: Mason et al. 2013; Sca11: Scardia et al. 2011 ; Sca13: Scardia et al. 2013; Schl13: Schlimmer 2013; Sim15: Simon–Díaz et al. 2015; Thor11: Thorel et al. 2011. [b]$\Delta I = 0.35$ mag for A-B and $\Delta I = 5.39$ mag for AB-C (this work).

Table C.3: List of observed stars with confirmed visual (unbound) companions.

Karmn	No.	ρ [arcsec]	θ [deg]	Observation date
J00234+243	#1	2.4	257	J2011.812
J00413+558	#1	13.1	129	J2011.812
J01033+623	#1	10.6	13	J2011.807
J01593+585	#1	7.5	7	J2011.807
	#1	7.8	5	J2013.034
	#2	4.2	93	J2013.034
J02565+554W	#1	7.6	241	J2012.710
	#1	7.7	242	J2013.034
J03102+059	#1	10.6	174	J2012.710
J05106+297	#1	3.1	308	J2014.162
J06000+027	#1	7.8	313	J2011.807
	#1	7.9	315	J2012.231
	#1	8.5	311	J2014.936
J06361+116	#1	8.7	114	J2011.807
	#1	8.7	112	J2012.231
J06422+035	#1	8.2	34	J2011.807
J06490+371	#1	12.6	302	J2011.810
J07033+346	#1	9.3	357	J2011.810
J07227+306	#1	9.0	29	J2012.234
J07518+055	#1	9.7	340	J2012.081
J07581+072	#1	11.1	260	J2012.081
	#2	11.8	315	J2012.081
J08105-138	#1	9.6	55	J2012.234
	#1	9.74	55	J2013.036
J08126-215	#1	12.7	329	J2012.234
J08428+095	#1	6.2	145	J2012.081
	#1	5.62	144	J2013.034
J11289+101	#1	14.0	217	J2012.229
J11420+147	#1	6.4	93	J2012.234
J13165+278	#1	6.2	1	J2012.231
J16462+164	#1	12.8	35	J2012.229
	#1	13.0	36	J2012.524
	#1	13.2	35	J2012.710
	#1	14.6	36	J2015.284
J16509+224	#1	9.1	318	J2012.524
J17177-118	#1	5.3	149	J2012.231
J17321+504	#1	12.5	23	J2012.234
J17425-166	#1	8.9	123	J2012.234
	#2	3.2	276	J2012.234
J17460+246	#1	6.4	357	J2012.524
J17530+169	#1	8.9	31	J2012.522
	#1	8.9	31	J2012.527
	#1	9.0	31	J2012.708
J18240+016	#1	7.0	216	J2012.524
J18264+113	#1	4.2	10	J2012.522
J18387-144	#1	4.8	261	J2012.522

Table C.3: List of observed stars with confirmed visual (unbound) companions (continued).

Karmn	No.	ρ [arcsec]	θ [deg]	Observation date
	#2	9.6	300	J2012.522
	#3	7.3	61	J2012.522
J18427+139	#1	3.6	178	J2012.524
	#1	3.7	177	J2012.710
J18480-145	#1	7.6	234	J2012.522
J19098+176	#1	6.7	326	J2012.522
J19124+355	#1	12.4	125	J2012.527
J19220+070	#1	4.7	73	J2015.284
J19463+320	#1	11.8	186	J2012.524
	#1	11.7	186	J2012.710
	#1	11.0	194	J2015.284
	#2	8.5	25	J2012.524
	#2	8.7	27	J2012.710
	#3	8.8	117	J2012.524
	#3	9.0	117	J2012.710
J19539+444W	#1	14.9	116	J2012.527
	#1	14.9	112	J2012.710
J20298+096	#1	9.2	201	J2012.522
J20347+033	#1	10.5	300	J2012.527
J21013+332	#1	10.1	63	J2012.524
J21518+136	#1	11.4	124	J2012.524
J22252+594	#1	11.8	34	J2012.708
J23577+233	#1	4.6	76	J2012.524

Table C.4: Astrometric properties of the physically and likely bound binaries in the sample.

Karmn	WDS	ρ [arcsec]	θ [deg]	ΔI [mag]	Epoch	GSC 1.2[a]
Physically bound systems						
J00154-161	00155-1608 HEI299	0.275 ± 0.013	204.96 ± 3.10	0.58 ± 0.08	J2012.522	F
J00413+558	00415+5550 GIC13	10.833 ± 0.047	68.25 ± 0.28	2.92 ± 0.13	J2011.812	F
J02518+294	New	0.626 ± 0.008	249.44 ± 1.29	0.53 ± 0.10	J2011.810	F
		0.798 ± 0.011	247.05 ± 0.11	0.50 ± 0.07	J2015.875	
		0.803 ± 0.015	246.30 ± 1.54	...	J2016.015	
J02565+554W	02565+5526 LDS5401	16.664 ± 0.051	21.15 ± 0.17	0.97 ± 0.04	J2012.710	F
J02591+366[b]	New	1.949 ± 0.010	4.35 ± 0.28	3.10 ± 0.13	J2013.036	F
		1.900 ± 0.054	358.58 ± 0.83	...	J2016.094	
J03574-011	03575-0110 BU543	10.972 ± 0.027	14.61 ± 0.16	2.29 ± 0.01	J2013.034	F
J04153-076	04153-0739 STF518	8.598 ± 0.030	152.13 ± 0.14	1.62 ± 0.04	J2011.812	...
J04311+589	04312+5858 STI2051	9.885 ± 0.039	59.64 ± 0.23	3.64 ± 0.05	J2011.812	...
J05019+099	05020+0959 HDS654	1.354 ± 0.012	148.90 ± 0.34	0.67 ± 0.15	J2014.159	F
J05034+531	Ward-Duong et al. 2015	5.600 ± 0.021	279.58 ± 0.19	5.83 ± 0.07	J2014.162	F
		5.614 ± 0.006	279.27 ± 0.14	5.53 ± 0.15	J2015.875	
J05068-215E(A)	05069-2135 DON93	8.499 ± 0.053	307.94 ± 0.33	0.81 ± 0.04	J2011.812	T
		8.459 ± 0.024	308.08 ± 0.17	0.82 ± 0.03	J2012.710	
		8.462 ± 0.019	308.04 ± 0.17	0.69 ± 0.02	J2013.036	
J05068-215W(BC)	05069-2135 DON93	0.767 ± 0.004	128.97 ± 1.58	0.51 ± 0.07	J2011.812	T
		0.803 ± 0.029	126.86 ± 1.52	0.61 ± 0.04	J2012.710	
		0.811 ± 0.010	125.54 ± 0.60	0.64 ± 0.02	J2013.036	
J05078+179	New	0.540 ± 0.003	286.30 ± 0.66	1.94 ± 0.02	J2013.034	T
		0.348 ± 0.010	288.28 ± 1.34	1.99 ± 0.05	J2014.164	
		Unresolved	...	...	J2015.284	
J05103+488	05104+4850 HEI321	1.993 ± 0.051	113.00 ± 0.87	0.90 ± 0.02	J2013.034	F
		1.989 ± 0.009	112.78 ± 0.17	0.50 ± 0.10	J2015.284	
J05333+448[c]	05333+449 BH76	0.205 ± 0.008	38.55 ± 2.80	0.24 ± 0.05	J2011.810	T
		0.192 ± 0.011	36.47 ± 0.19	...	J2012.229	
		0.183 ± 0.004	35.75 ± 1.18	0.22 ± 0.04	J2012.231	
		0.164 ± 0.066	33.95 ± 5.65	...	J2012.710	
		0.144 ± 0.060	35.24 ± 5.29	...	J2013.034	
		0.140 ± 0.070	34.13 ± 5.10	...	J2014.159	
J05342+103N	05342+1019 LDS6189	5.061 ± 0.012	188.72 ± 0.14	1.02 ± 0.03	J2013.034	F
J05466+441	New	3.729 ± 0.016	222.80 ± 0.20	5.71 ± 0.04	J2011.810	F
		3.712 ± 0.022	222.70 ± 0.41	6.21 ± 0.08	J2014.162	
J06212+442	Ansdell et al. 2015	1.222 ± 0.060	204.6 ± 3.69	...	J2013.036	F
		1.319 ± 0.019	203.67 ± 0.22	2.85 ± 0.13	J2015.875	
J06400+285	New	0.258 ± 0.004	80.35 ± 1.76	...	J2012.081	F
		0.251 ± 0.001	87.30 ± 0.18	0.30 ± 0.06	J2012.710	
		0.269 ± 0.003	91.35 ± 1.65	0.23 ± 0.05	J2013.034	
		Unresolved	...	...	J2014.159	
		Unresolved	...	...	J2015.284	
J07395+334	07397+3328 LDS3755	13.675 ± 0.066	48.97 ± 0.32	4.81 ± 0.08	J2012.081	F
J08066+558	New	0.274 ± 0.004	257.27 ± 1.23	0.53 ± 0.11	J2012.081	T
		0.248 ± 0.004	253.75 ± 0.88	0.55 ± 0.08	J2013.034	
		0.202 ± 0.011	245.61 ± 3.40	0.54 ± 0.03	J2014.159	

Table C.4: Astrometric properties of the physically and likely bound binaries in the sample (continued).

Karmn	WDS	ρ [arcsec]	θ [deg]	ΔI [mag]	Epoch	GSC 1.2
		0.174 ± 0.060	236.52 ± 8.48	...	J2015.284	
J08082+211[d]	08082+2106 COU91	10.617 ± 0.030	144.74 ± 0.18	1.03 ± 0.03	J2012.081	F
		10.633 ± 0.095	144.10 ± 1.52	0.88 ± 0.01	J2015.875	
	New	0.329 ± 0.020	74.26 ± 0.74	2.31 ± 0.05	J2012.081	...
		0.580 ± 0.045	36.48 ± 1.57	3.22 ±0.05	J2015.875	
J08105-138	08107-1348 JOD4	0.927 ± 0.006	283.74 ± 0.34	1.80 ± 0.05	J2012.234	T
		0.913 ± 0.009	283.11 ± 0.87	1.77 ± 0.05	J2013.036	
J08595+537	New	0.229 ± 0.011	219.10 ± 4.19	0.29 ± 0.06	J2014.162	F
		0.301 ± 0.012	223.00 ± 1.49	0.26 ± 0.05	J2015.281	
J09011+019	New	2.954 ± 0.014	154.77 ± 0.17	4.68 ± 0.06	J2012.229	F
		2.994 ± 0.016	155.08 ± 0.23	4.58 ± 0.07	J2013.034	
		3.096 ± 0.065	156.22 ± 0.40	4.40 ± 0.14	J2015.875	
J10151+314	New	1.799 ± 0.005	306.58 ± 0.20	0.69 ± 0.05	J2012.229	F
		1.806 ± 0.007	306.43 ± 0.26	0.69 ± 0.09	J2013.034	
		1.822 ± 0.012	306.41 ± 0.58	0.57 ± 0.10	J2014.159	
		1.815 ± 0.010	306.40 ± 0.23	0.66 ± 0.08	J2015.281	
J10196+198	10200+1950 BAG32	0.195 ± 0.061	23.81 ± 3.68	2.00 ± 0.2	J2012.078	T
J10260+504W	10261+5029 LDS1241	14.413 ± 0.038	25.83 ± 0.18	0.24 ± 0.04	J2012.229	T
		14.410 ± 0.045	25.58 ± 0.25	0.24 ± 0.09	J2014.164	
J10379+127	New	0.848 ± 0.010	333.88 ± 1.08	0.47 ± 0.09	J2014.162	F
		0.792 ± 0.013	336.27 ± 0.94	0.49 ± 0.10	J2015.281	
		0.806 ± 0.020	336.05 ± 0.83	0.58 ± 0.11	J2015.875	
J10448+324	New	1.292 ± 0.025	157.62 ± 0.81	0.55 ± 0.11	J2013.036	T
		1.267 ± 0.014	159.63 ± 0.57	0.47 ± 0.08	J2015.284	
J10546-073	New	0.793 ± 0.028	60.71 ± 1.66	0.41 ± 0.08	J2014.164	F
		0.813 ± 0.039	64.75 ± 2.66	0.45 ± 0.09	J2015.281	
J11355+389	New	0.244 ± 0.020	50.84 ± 1.90	0.51 ± 0.10	J2012.231	F
		0.219 ± 0.005	46.41 ± 2.14	0.63 ± 0.12	J2012.524	
		0.278 ± 0.004	55.49 ± 2.22	0.64 ± 0.12	J2013.034	
		0.281 ± 0.007	61.37 ± 1.43	0.44 ± 0.08	J2014.159	
		0.339 ± 0.017	65.67 ± 1.96	0.55 ± 0.10	J2015.281	
J11521+039	New	0.224 ± 0.014	29.25 ± 3.75	0.51 ± 0.11	J2014.162	F
		0.337 ± 0.008	26.06 ± 2.08	0.46 ± 0.10	J2015.281	
J12006-138	12007-1348 LDS4166	6.839 ± 0.021	234.14 ± 0.17	2.44 ± 0.03	J2012.081	F
		6.836 ± 0.023	234.05 ± 0.16	2.40 ± 0.03	J2013.034	
J12016-122	New	6.123 ± 0.013	24.42 ± 0.13	5.05 ± 0.13	J2012.234	T
		6.134 ± 0.012	24.41 ± 0.19	5.13 ± 0.19	J2013.034	
		6.109 ± 0.018	24.58 ± 0.16	5.14 ± 0.17	J2015.284	
J12123+544S	12123+5429 VYS5	14.677 ± 0.044	9.91 ± 0.15	2.86 ± 0.04	J2012.231	F
J12162+508	New	1.884 ± 0.014	188.92 ± 0.84	0.48 ± 0.07	J2014.162	F
		...	...	...	J2014.386	
		1.828 ± 0.010	190.85 ± 0.33	0.42 ± 0.08	J2015.281	
J12277-032	New	1.496 ± 0.018	15.84 ± 0.45	1.67 ± 0.04	J2014.162	T
		1.459 ± 0.007	15.73 ± 0.50	1.75 ± 0.06	J2015.281	
J12332+090	12335+0901 REU1	0.398 ± 0.005	173.37 ± 0.76	0.55 ± 0.11	J2012.081	...
		0.447 ± 0.003	170.25 ± 0.46	0.46 ± 0.09	J2012.299	
		0.445 ± 0.003	170.043 ± 0.49	0.41 ± 0.07	J2012.231	
		0.446 ± 0.004	169.92 ± 0.75	0.40 ± 0.08	J2012.234	

Table C.4: Astrometric properties of the physically and likely bound binaries in the sample (continued).

Karmn	WDS	ρ [arcsec]	θ [deg]	ΔI [mag]	Epoch	GSC 1.2
		0.529 ± 0.003	163.46 ± 0.35	0.44 ± 0.04	J2012.522	
		0.531 ± 0.005	164.74 ± 0.64	0.52 ± 0.10	J2012.524	
		0.667 ± 0.007	159.16 ± 0.31	0.55 ± 0.06	J2013.036	
		0.921 ± 0.011	151.76 ± 0.37	0.46 ± 0.08	J2014.159	
J13168+170	13169+1701 BU800	7.658 ± 0.024	104.89 ± 0.18	2.11 ± 0.02	J2014.159	F
		7.659 ± 0.024	104.50 ± 0.18	2.04 ± 0.01	J2015.284	
J13180+022	New	0.637 ± 0.007	213.25 ± 0.51	0.78 ± 0.15	J2012.229	T
		0.646 ± 0.012	217.48 ± 0.69	0.45 ± 0.08	J2013.034	
		0.592 ± 0.004	222.91 ± 0.37	0.55 ± 0.10	J2014.159	
		0.530 ± 0.055	225.78 ± 2.51	0.53 ± 0.10	J2015.281	
J13317+292	13318+2917 BEU17	0.193 ± 0.066	79.42 ± 11.91	1.5 ± 0.2	J2012.522	F
		0.190 ± 0.095	85.41 ± 3.58	...	J2012.527	
		Unresolved	...	...	J2015.281	
J13417+582	13418+5815 JNN94	0.675 ± 0.020	251.26 ± 1.42	0.38 ± 0.08	J2014.164	F
		0.699 ± 0.022	251.33 ± 0.56	...	J2015.281	
J13526+144	13526+1425 JOD7	1.252 ± 0.008	356.75 ± 0.30	1.52 ± 0.03	J2012.078	T
		1.231 ± 0.015	357.72 ± 0.34	1.64 ± 0.04	J2013.034	
		1.197 ± 0.016	359.55 ± 0.79	1.69 ± 0.04	J2015.284	
J14157+594	14157+5928 LDS2707	5.014 ± 0.054	231.04 ± 0.59	0.46 ± 0.07	J2014.164	F
		5.021 ± 0.075	230.87 ± 0.54	0.46 ± 0.09	J2014.386	
		5.064 ± 0.020	230.90 ± 0.19	0.76 ± 0.03	J2015.284	
J14210+275	New	0.626 ± 0.008	82.25 ± 0.93	1.82 ± 0.04	J2012.231	F
		0.683 ± 0.009	84.96 ± 0.39	1.73 ± 0.05	J2015.281	
J14279-003S	14279-0032 GIC20	13.032 ± 0.007	21.96 ± 0.28	0.19 ± 0.03	J2012.229	F
J14331+610	New	0.899 ± 0.020	255.34 ± 1.15	0.65 ± 0.13	J2014.162	F
		0.944 ± 0.005	252.63 ± 0.27	0.58 ± 0.11	J2015.281	
J15081+623	New	0.983 ± 0.022	61.15 ± 1.62	0.50 ± 0.10	J2014.162	T
		0.947 ± 0.032	68.06 ± 3.30	0.40 ± 0.08	J2014.386	
		0.884 ± 0.024	67.63 ± 0.37	0.42 ± 0.10	J2015.284	
J15126+457	15126+4544 MCT8	0.527 ± 0.080	216.82 ± 2.36	0.37 ± 0.08	J2012.231	F
		0.481 ± 0.021	219.63 ± 1.32	0.36 ± 0.08	J2015.284	
J15191-127[e]	New	0.305 ± 0.064	246.58 ± 2.22	3.4 ± 0.15	J2012.234	...
J15400+434N	15400+4330 VBS25	4.529 ± 0.028	154.66 ± 0.21	1.47 ± 0.01	J2014.162	...
		4.525 ± 0.016	154.78 ± 0.12	1.59 ± 0.07	J2014.386	
J15496+348[f]	15496+3449 BWL41	0.211 ± 0.002	89.25 ± 0.42	3.00 ± 0.10	J2012.234	...
		Unresolved	...	...	J2012.522	
		0.226 ± 0.003	91.31 ± 1.54	...	J2012.524	
		0.208 ± 0.013	98.68 ± 1.40	...	J2012.708	
		Unresolved	...	...	J2014.159	
J16487+106	New	0.212 ± 0.010	20.25 ± 1.62	0.39 ± 0.08	J2014.162	F
		Unresolved	...	...	J2014.386	
		0.235 ± 0.012	31.97 ± 2.08	0.30 ± 0.06	J2015.281	
J16554-083S	16555-0820 KUI75	0.206 ± 0.004	216.03 ± 1.02	0.43 ± 0.09	J2012.231	...
J16578+473	16579+4722 A1874	5.082 ± 0.020	62.27 ± 0.25	2.48 ± 0.02	J2014.386	F
J17340+446	New	0.544 ± 0.018	143.11 ± 2.15	0.54 ± 0.11	J2014.386	T
		0.596 ± 0.009	144.97 ± 0.71	0.47 ± 0.09	J2015.281	
J17530+169	New	0.896 ± 0.006	123.69 ± 0.49	0.60 ± 0.06	J2012.231	T
		0.887 ± 0.003	122.86 ± 0.24	0.66 ± 0.09	J2012.522	

Table C.4: Astrometric properties of the physically and likely bound binaries in the sample (continued).

Karmn	WDS	ρ [arcsec]	θ [deg]	ΔI [mag]	Epoch	GSC 1.2
		0.893 ± 0.004	122.56 ± 0.21	0.61 ± 0.12	J2012.527	
		0.871 ± 0.010	122.20 ± 0.41	0.69 ± 0.11	J2012.708	
		0.823 ± 0.016	114.50 ± 1.37	0.68 ± 0.13	J2015.284	
J18180+387E	18180+3846 GIC151	9.940 ± 0.031	277.79 ± 0.13	1.50 ± 0.03	J2012.524	...
J18264+113	18264+1121 NI38	8.141 ± 0.030	196.27 ± 0.33	5.89 ± 0.09	J2012.522	F
J18411+247N	18411+2247 LDS6330	4.828 ± 0.015	5.67 ± 0.15	2.25 ± 0.02	J2012.527	F
J18427+596N	18428+5938 STF2398	11.712 ± 0.034	178.19 ± 0.17	0.88 ± 0.03	J2012.527	...
J18548+109	18550+1058 VYS8	3.854 ± 0.017	44.30 ± 0.24	2.33 ± 0.08	J2014.386	F
J19463+320	19464+3201 KAM3	5.603 ± 0.040	134.79 ± 0.43	0.81 ± 0.01	J2012.524	F
		5.576 ± 0.016	134.66 ± 0.15	0.79 ± 0.02	J2012.710	
		5.675 ± 0.017	134.85 ± 0.19	0.74 ± 0.01	J2015.284	
J19539+444E	19539+4425 GIC59	6.461 ± 0.024	70.41 ± 0.16	0.30 ± 0.05	J2012.527	F
		6.454 ± 0.027	70.28 ± 0.20	0.65 ± 0.07	J2012.710	
	19539+4425 MCY3	0.642 ± 0.016	352.19 ± 1.49	2.11 ± 0.02	J2012.527	
		0.615 ± 0.048	349.91 ± 1.67	2.58 ± 0.13	J2012.710	
J20407+199	20408+19656 RAO23	0.166 ± 0.081	227.02 ± 6.45	1.4 ± 0.2	J2012.527	F
		0.290 ± 0.080	245.37 ± 3.69	2.1 ± 0.3	J2015.281	
J20445+089S	20446+0854 LDS1046	15.075 ± 0.064	344.47 ± 0.14	1.06 ± 0.04	J2012.527	F
		15.173 ± 0.049	344.42 ± 0.14	0.97 ± 0.03	J2012.710	
J20488+197	20488+1943 JNN286	0.191 ± 0.006	132.95 ± 1.68	0.33 ± 0.09	J2012.524	F
		0.184 ± 0.011	134.71 ± 1.71	0.31 ± 0.06	J2012.710	
J21012+332	New	0.246 ± 0.022	7.38 ± 1.70	1.61 ± 0.09	J2012.524	F
		0.232 ± 0.016	6.31 ± 2.67	1.75 ± 0.10	J2012.710	
		Unresolved	...	...	J2015.281	
		Unresolved	...	...	J2015.284	
J21323+245	21324+2434 MCT12	1.426 ± 0.005	243.98 ± 0.14	0.75 ± 0.15	J2012.524	T
		1.438 ± 0.006	243.66 ± 0.27	0.72 ± 0.10	J2012.710	
J21518+136	New	0.701 ± 0.010	116.96 ± 1.25	1.50 ± 0.03	J2012.524	F
		0.686 ± 0.022	118.08 ± 1.40	1.40 ± 0.05	J2012.710	
		0.674 ± 0.011	130.80 ± 1.04	...	J2015.572	
J22279+576	22280+5742 KR60	1.649 ± 0.010	359.82 ± 0.16	1.21 ± 0.03	J2011.807	T
J23096-019[g]	New	1.715 ± 0.006	19.37 ± 0.23	1.80 ± 0.04	J2012.708	T
		1.672 ± 0.019	19.82 ± 0.37	1.84 ± 0.09	J2013.036	
J23293+414S(Bab)	23294+4128 BWL59	0.257 ± 0.027	209.09 ± 2.31	0.73 ± 0.09	J2012.524	F
		Unresolved	...	...	J2015.572	
J23293+414N(AB)	23294+4128 GIC193	17.670 ± 0.069	213.92 ± 0.18	0.38 ± 0.01	J2012.524	F
		17.676 ±0.024	214.40 ±0.15	0.38 ± 0.01	J2015.572	
J23318+199E	23317+1956 WIR1	5.412 ± 0.019	81.14 ± 0.14	1.67 ± 0.02	J2011.807	F
		5.411 ± 0.018	81.07 ± 0.14	1.66 ± 0.01	J2011.812	
J23455-161[h]	23455-1610 MTG5	∼0.50	∼15	...	J2012.522	...
J23517+069	New	2.178 ± 0.015	102.48 ± 0.40	0.47 ± 0.09	J2012.708	F
		2.165 ± 0.013	102.51 ± 0.35	0.55 ± 0.11	J2013.036	
		2.181 ± 0.013	103.23 ± 0.13	...	J2015.572	
Likely bound systems						
J00169+200	New	1.076 ± 0.023	288.33 ± 0.54	0.70 ± 0.12	J2013.036	F
J01221+221	New	0.271 ± 0.014	175.04 ± 2.00	0.86 ± 0.17	J2015.875	F
J04352-161	New	7.887 ± 0.043	131.61 ± 0.56	4.60 ± 0.38	J2014.162	

Table C.4: Astrometric properties of the physically and likely bound binaries in the sample (continued).

Karmn	WDS	ρ [arcsec]	θ [deg]	ΔI [mag]	Epoch	GSC 1.2
J06277+093	New	1.103 ± 0.090	221.11 ± 1.26	1.16 ± 0.04	J2015.875	F
J07349+147	New	1.008 ± 0.019	297.13 ± 0.64	0.77 ± 0.04	J2014.164	T
		0.988 ± 0.014	293.70 ± 0.32	0.74 ± 0.03	J2015.281	
		0.995 ± 0.010	292.83 ± 0.21	0.78 ± 0.08	J2015.281	
J10028+484[i]	New	0.208 ± 0.014	336.81 ± 3.05	0.31 ± 0.06	J2012.231	F

Notes. [a]Guide Star Catalog multiplicity flag. "F" is False, "T" is true, and "..." indicates no data. [b]ρ and θ measures in the second epoch correspond to observations with the CARMENES acquisition and guiding camera, which were carried out only for confirming physical association.. [c]Similar periods between Behall & Harrington 1976 and this work suggest that we are resolving the same pair. [d]The B component is a double lined spectroscopic binary with a period shorter than 215.0 d (Shkolnik et al. 2010) and is not the third component resolved here. [e]We considered that this resolved binary is the spectroscopic binary identified by Bonfils et al. 2013, according to the radial-velocity amplitude and period estimation of the pair. Nevertheless, we can not affirm whether the system is double or triple. [f]Close visual binary in Bowler et al. 2015 in one epoch. Our multi-epoch images confirm physical binding. [g]It is also a spectroscopic binary. [h]Faint pair for which we could not measure ρ and θ with precision. The companion, also detected by Tokovinin et al. 2015, seems to be physically related and consistent over time with the companion identified by Montagnier et al. 2006 at 0.068 arcsec. [i]Also observed and identified as single in Law et al. 2008, probably due to the crossing of the companion behind the primary at the observing epoch, in agreement with the 13 a period estimated in this work.

Table C.5: Derived parameters for confirmed physical pairs.

Karmn[a]	Component	ΔI [mag]	I_1 [mag]	I_2 [mag]	SpT	SpT_1	SpT_2	$\mathcal{M}_1$ [$M_\odot$]	$\mathcal{M}_2$ [$M_\odot$]	P^b [a]
J00154-161	A, B	0.58 ± 0.08	9.24	9.82	M4.0 V	m4.0	m5.0	0.17 ± 0.08	0.15 ± 0.07	3.7
J00413+558	A, B	2.92 ± 0.13	11.36	...	...	M4.0	DC	0.22 ± 0.10	...	...
J02518+294	A, B	0.52 ± 0.10	11.56	12.08	M4.0 V	m4.0	m5.0	0.20± 0.09	0.15 ± 0.08	130
J02565+554W	A, B	0.97 ± 0.04	8.56	9.53	...	M1.0	m2.5	0.50 ± 0.16	0.35 ± 0.13	6400
J02591+366	A, B	3.10 ± 0.13	10.50	13.60	M3.5 V	m3.5	m6.0	0.24 ± 0.13	0.10 ± 0.07	380
J03574-011	A, B	2.29 ± 0.01	...	9.10	...	K4	M2.5	...	0.34 ± 0.12	...
J04153-076	AB, C	1.62 ± 0.04	...	8.39	...	K0.5+DA	M4.5	...	**0.33 ± 0.05**	...
J04311+589	A, B	3.64 ± 0.05	8.14	...	...	M4.0	DC	0.23 ± 0.10	...	...
J05019+099	Aab, B	0.67 ± 0.15	9.20	9.87	M4.0 V	...	...	...	0.33 ±0.05	200
J05019+099	Aa, Ab	...	9.95	9.95	...	...	...	0.31 ±0.05	0.31 ±0.05	
J05034+531	A, B	5.68 ± 0.07	8.04	13.72	M0.5 V	m1.0	m7.0	0.45 ± 0.16	0.09 ± 0.05	910
J05068-215E	A, BC	0.77 ± 0.08	8.19	8.96	...	M1.5	...	0.62 ± 0.05	...	1600
J05068-215W	B, C	0.59 ± 0.08	8.67	9.26	M3.5	...	...	0.49 ± 0.05	0.35 ± 0.05	62
J05078+179	Aab, B	1.96 ± 0.05	9.51	11.47	M3.0 V	m2.0	m4.0	...	0.23 ± 0.08	...
J05078+179	Aa, Ab	...	10.26	10.26	m2.0	m2.5	m2.5	0.33 ± 0.05	0.33 ± 0.05	50
J05103+488	A, B	0.70 ± 0.06	9.62	10.32	M2.5 V	...	...	0.45 ± 0.05	0.31 ± 0.05	...
J05333+448	A, B	0.23 ± 0.05	10.31	10.54	M3.5 V	m3.5	m3.5	0.23 ± 0.10	0.22 ± 0.09	8.3
J05342+103N	A, Bab	1.02 ± 0.03	9.88	10.90	...	M3.0	m4.0	...	0.30 ± 0.10	990
J05342+103N	Ba, Bb	...	11.65	11.65	M4.5	m4.5	m4.5	0.18 ± 0.08	0.18 ± 0.08	...
J05466+441	Aab, B	5.76 ± 0.09	9.98	15.74	...	M4.0	m8.0	...	0.07 ± 0.03	920
J05466+441	Aa, Ab	...	10.73	10.73	M4	m3.5	m3.5	0.25 ± 0.09	0.25 ± 0.09	...
J06212+442	A, B	2.85 ± 0.13	9.99	12.84	M2.0 V	m2.0	m5.0	0.38 ± 0.11	0.16 ± 0.06	250
J06400+285	A, B	0.24 ± 0.10	10.09	10.33	M2.0 V	m2.5	m2.5	0.36 ± 0.15	0.33 ± 0.14	20
J07395+334	A, B	4.81 ± 0.08	9.62	14.43	...	M2.0	m6.5	0.54 ± 0.19	0.12 ± 0.07	13000
J08066+558	A, B	0.54 ± 0.07	9.76	10.30	M2.0 V	m2.0	m2.5	0.45 ± 0.16	0.37 ± 0.14	26
J08082+211	Bab, C	2.76 ± 0.07	8.78	11.54	M3.0 V	m2.5	m5.0	...	0.17 ± 0.09	33
J08082+211	Ba, Bb	...	9.53	9.53	m2.5	m3.0	m3.0	0.32± 0.10	0.32 ± 0.10	...
J08105-138	B, C	1.78 ± 0.05	9.80	11.58	M2.5 V	m2.5	m4.5	0.36 ± 0.13	0.20 ± 0.09	130
J08595+537	A, B	0.28 ± 0.06	11.11	11.39	M3.5 V	m3.5	m3.5	0.20 ± 0.09	0.18 ± 0.08	19
J09011+019	Aab, B	4.55 ± 0.17	9.27	13.82	M3.0 V	m3.0	m6.5	...	0.09 ± 0.04	460
J09011+019	Aa, Ab	...	10.02	10.02	m3.0 V	m3.5	m3.5	0.26 ± 0.10	0.26 ± 0.10	...
J10151+314	A, B	0.65 ± 0.10	11.32	11.97	M4.0 V	m4.0	m4.5	0.22 ± 0.11	0.18 ± 0.10	360
J10196+198	A, B	2.00 ± 0.20	6.93	8.93	M3.0 V	m3.0	m5.0	0.32 ± 0.12	0.18 ± 0.11	1.5

Table C.5: continued.

Karmn[a]	Component	ΔI [mag]	I_1 [mag]	I_2 [mag]	SpT	SpT_1	SpT_2	$\mathcal{M}_1$ [$M_\odot$]	$\mathcal{M}_2$ [$M_\odot$]	P^b [a]
J10260+504W	A, B	0.24 ± 0.06	10.79	11.03	...	M4.0	m4.5	0.21 ± 0.09	0.20 ± 0.08	5600
J10379+127	A, B	0.51 ± 0.12	10.73	11.24	M3.0 V	m3.5	m4.0	0.26 ± 0.10	0.22 ± 0.09	**100**
J10448+324	Aa, Ab	0.51 ± 0.11	11.07	11.58	M3.0 V	m2.5	m3.5	0.35 ± 0.13	0.32 ± 0.12	440
J10546-073	A, B	0.43 ± 0.09	11.08	11.51	M4.0 V	m4.0	m4.5	0.21 ± 0.09	0.19 ± 0.08	80
J11355+389	A, B	0.55 ± 0.13	11.02	11.57	M3.5 V	m3.5	m4.0	0.26 ± 0.10	0.22 ± 0.09	31
J11521+039	A, B	0.48 ± 0.11	10.44	10.92	M4.0 V	m4.0	m4.5	0.22 ± 0.09	0.19 ± 0.08	15
J12006-138	A, B	2.42 ± 0.04	10.32	12.74	...	M3.5	m5.5	0.24 ± 0.13	0.12 ± 0.08	2000
J12016-122	A, B	5.11 ± 0.10	10.00	15.11	...	M3.0	m8.0	0.29 ± 0.12	0.07 ± 0.05	2000
J12123+544S	A, B	2.86 ± 0.04	7.90	10.76	...	M0.0	m4.0	0.52 ± 0.17	0.20 ± 0.09	4100
J12162+508	A, B	0.45 ± 0.11	11.36	11.81	M4.0 V	m4.0	m5.0	0.21 ± 0.11	0.19 ± 0.09	360
J12277-032	A, B	1.71 ± 0.08	10.44	12.15	M3.5 V	m3.5	m5.0	0.25 ± 0.11	0.16 ± 0.08	200
J12332+090	A, B	0.47 ± 0.10	9.36	9.83	M5.0 V	m5.0	m5.5	0.14 ± 0.07	0.12 ± 0.07	16
J13168+170	A, B	2.08 ± 0.05	...	7.562	...	K2	M0.5	...	0.46 ± 0.16	...
J13180+022	A, B	0.58 ± 0.18	10.76	11.34	M3.5 V	m3.5	m4.5	0.25 ± 0.11	0.21 ± 0.09	73
J13317+292	A,B	1.5 ± 0.2	9.23	10.73	M4.0 V	...	...	0.39 ± 0.05	0.17 ± 0.05	8.6
J13417+582	A, B	0.38 ± 0.08	10.78	11.16	M3.5 V	m3.5	m4.0	0.23 ± 0.09	0.21 ± 0.08	78
J13526+144	A, B	1.62 ± 0.09	9.42	11.04	M2.0 V	m2.0	m4.0	0.38 ± 0.17	0.23 ± 0.11	150
J14157+594	A, B	0.56 ± 0.18	10.04	10.60	...	M2.0	m3.0	0.38 ± 0.17	0.31 ± 0.14	1900
J14210+275	A, B	1.77 ± 0.08	10.45	12.22	M2.5 V	m2.5	m4.5	0.33 ± 0.13	0.20 ± 0.09	97
J14279-003S	A, B	0.19 ± 0.03	10.82	11.01	...	M4.5	m5.0	0.18 ± 0.07	0.17 ± 0.07	3900
J14331+610	A, B	0.62 ± 0.13	9.99	10.61	M2.5 V	m3.0	m3.5	0.31 ± 0.12	0.25 ± 0.11	96
J15081+623	A, B	0.44 ± 0.11	11.37	11.81	M4.0 V	m4.0	m4.5	0.21 ± 0.10	0.19 ± 0.09	140
J15126+457	A, B	0.36 ± 0.08	11.20	11.56	M4.0 V	m4.5	m5.0	0.20 ± 0.09	0.18 ± 0.09	43
J15191-127	A, B	3.40 ± 0.15	10.03	13.43	M4.0 V	m3.0	m5.5	0.33 ± 0.06	0.13 ± 0.05	13
J15400+434N	A, B	1.53 ± 0.09	9.63	11.16	...	M3.0	m4.5	0.26 ± 0.10	0.17 ± 0.08	730
J15496+348	A,B	3.00 ± 0.10	10.30	13.30	M4.0 V	m3.5	m7.0	0.26 ± 0.11	0.11 ± 0.09	12
J16487+106	A, B	0.34 ± 0.09	9.60	9.94	M2.5 V	m2.5	m3.0	0.33 ± 0.14	0.30 ± 0.12	10
J16554-083S	A, Bab	0.43 ± 0.09	7.15	7.58	M3.0 V	m3.0	m3.0	0.34 ± 0.13	...	1.4
J16554-083S	Ba, Bb	...	8.33	8.33	m3.0 V	m3.5	m3.5	0.23 ± 0.13	0.23 ± 0.13	...
J16578+473	A, B	2.48 ± 0.02	...	8.01	...	K0.0 V	M1.5	...	0.57 ± 0.18	...
J17340+446	A, B	0.50 ± 0.11	10.74	11.24	M3.5 V	m3.5	m4.0	0.26 ± 0.12	0.22 ± 0.11	60
J17530+169	A, B	0.65 ± 0.11	10.64	11.29	M3.0 V	m3.5	m4.0	0.26 ± 0.14	0.21 ± 0.12	110
J18180+387E	A, B	1.50 ± 0.03	9.36	10.86	...	M3.0	m4.5	0.24 ± 0.10	0.16 ± 0.07	1700
J18264+113	A, B	5.89 ± 0.09	10.39	16.28	...	M3.5	WD	0.25 ± 0.08	...	...

Table C.5: continued.

Karmn[a]	Component	ΔI [mag]	I_1 [mag]	I_2 [mag]	SpT	SpT_1	SpT_2	$\mathcal{M}_1$ [$M_\odot$]	$\mathcal{M}_2$ [$M_\odot$]	P^b [a]
J18411+247S	Aab, B	2.25 ± 0.02	9.18	11.43	...	M3.5	m5.5	...	0.14 ± 0.07	460
J18411+247S	Aa, Ab	...	9.92	9.92	M3.5	m4.0	m4.0	0.21 ± 0.08	0.21 ± 0.08	...
J18427+596N	A, B	0.88 ± 0.03	6.51	7.39	...	M3.0	m4.0	0.28 ± 0.10	0.22 ± 0.09	380
J18548+109	A, B	2.33 ± 0.08	8.29	10.62	...	M0.0	m3.0	0.56 ± 0.12	0.26 ± 0.11	700
J19463+320	A, B	0.78 ± 0.04	7.91	8.69	...	M0.5	m2.0	0.47 ± 0.15	0.36 ± 0.12	750
J19539+444W	A, B	2.34 ± 0.34	9.94	12.28	M5.5 V	m5.5	m8.0	0.12 ± 0.07	0.07 ± 0.05	11
J19539+444E	AB, C	0.48 ± 0.25	...	9.83	M5.5 V	...	M5.5	...	0.14 ± 0.06	260
J20407+199	B, C	1.4 ± 0.2	9.75	11.15	M2.5	m2.5	m4.0	0.36 ± 0.10	0.23 ± 0.09	8.4
J20445+089S	A, Bab	1.02 ± 0.07	9.28	10.30	...	M1.5	m3.0	0.44 ± 0.15	...	6400
J20445+089N	Ba, Bb	...	11.05	11.05	m3.0 V	m3.5	m3.5	0.25 ± 0.10	0.25 ± 0.10	...
J20488+197	A, B	0.32 ± 0.08	11.48	11.80	M4.0 V	m4.5	m5.0	0.27 ± 0.12	0.25 ± 0.11	22
J21012+332	Aa, Ab	1.68 ± 0.14	9.77	11.45	M3.0 V	m2.5	m4.5	0.33 ± 0.14	0.18 ± 0.10	13
J21323+245	A, B	0.74 ± 0.13	10.39	11.13	M3.5 V	m3.5	m4.5	0.29 ± 0.12	0.23 ± 0.11	250
J21518+136	A, B	1.45 ± 0.08	11.08	12.53	M4.5 V	m4.0	m5.5	0.19 ± 0.08	0.13 ± 0.07	66
J22279+576	A, B	1.21 ± 0.03	7.35	8.56	M3.0 V	m3.5	m5.0	0.23 ± 0.10	0.16 ± 0.09	27
J23096-019	Aab, B	1.82 ± 0.08	10.33	12.15	M3.5 V	m3.5	m5.0	...	0.17 ± 0.08	260
J23096-019	Aa, Ab	...	11.08	11.08	m3.0 V	m3.5	m3.5	0.23 ± 0.12	0.23 ± 0.12	...
J23293+441N	A, Bab	0.38 ± 0.02	9.39	9.77	M3.5 V	...	...	0.32 ± 0.05	...	4500
J23293+414S	Ba, Bb	0.73 ± 0.09	9.54	10.27	M4.0 V	...	...	0.34 ± 0.05	0.24 ± 0.05	10
J23318+199E	Aab, B	1.66 ± 0.02	7.63	9.29	...	M3.5	m5.0	...	...	230
J23318+199E	Aa, Ab	...	8.38	8.38	M3.5	m3.5	m3.5	0.23 ± 0.11	0.23 ± 0.11	...
J23318+199E	Ba, Bb	...	10.04	10.04	M4.5	m5.0	m5.0	0.14 ± 0.09	0.14 ± 0.09	...
J23517+069	A, B	0.51 ± 0.11	10.84	11.35	M3.0 V	m3.5	m4.0	0.26 ± 0.13	0.22 ± 0.12	450
J00169+200	A, B	0.70 ± 0.12	11.67	12.37	M3.5 V	m4.0	m4.5	0.23 ± 0.14	0.19 ± 0.09	210
J01221+221	A, B	0.86 ± 0.17	10.46	11.32	M4.5 V	...	...	0.18 ± 0.05	0.15 ± 0.05	8.0
J04352-161	Aab, B	4.60 ± 0.38	12.88	17.48	M7.0 V	...	...	...	¡0.07	1600[c]
J04352-161	Aa, Ab	...	13.63	13.63	M7.0 V	m7.0	m7.0	0.08 ± 0.04	0.08± 0.04	
J06277+093	A, B	1.16 ± 0.04	9.78	10.94	M2.0 V	m2.0	m3.5	0.38 ± 0.12	0.26 ± 0.11	160
J07349+147	A, B	0.76 ± 0.04	9.19	9.95	M3.0 V	m3.5	m4.5	0.25 ± 0.11	0.20 ± 0.09	40
J10028+484	A, B	0.31 ± 0.06	12.61	12.92	M5.5 V	...	...	0.15 ± 0.08	0.12 ± 0.08	12

Notes. [a]Karmn stars in italics are associated to young stellar populations (see Table 3 in the article). [b]The periods given are a lower limit, as we equal our maximum separation measured to the semimajor axis. [c]The B component of the system is too faint to estimate its mass with our M_I-mass relation and the period was calculated using the stellar mass limit ($0.07\,M_\odot$). Hence, the period of this system should be considered as a lower approximation.

Table C.6: Known binaries at $\rho > 5$ arcsec.

WDS	Primary		Secondary		ρ	Notes
	Name	SpT	Name	SpT	[arcsec]	
GRB34	J00183+440	M1.0 V	J00184+440	M3.5 V	34.8	[a]
GIC13	J00413+558	M4.0 V	EGGR 245	DC	10.8	
WNO51	J01026+623	M1.5 V	J01033+623	M5.0 V	293.1	
GIC20	J01119+049N	M3.0 V	J01119+049S	M3.5 V	63.6	
GIC27	J01518+644	M2.5 V	GJ3118 B	DAs	13.4	
PLW32	HD 16160 AB	K3 V + M7.0 V	J02362+068	M4.0 V	164.0	
LDS883	HD 18143 AB	G5 V + K7 V	J02555+268	M4.0 V	44.0	
LDS5401	J02565+554W	M1.0 V	J02565+554E	M3.0 V	16.7	
KUI11	HD 18757	G4 V	J03047+617	M3.0 V	263.2	
LDS884	GJ 140	M0.0 V+	J03242+237	M2.0 V	99.5	[b]
LDS9158	J03396+254E	M3.0 V	J03396+254W	M3.5 V	64.4	
GIC44	J03438+166	M0.0 V	J03437+166	M1.0 V	106.50	[c]
BU543	BD–01 564	K4 V	J03574–011	M2.5 V	11.0	[d]
STF518	o^{02} Eri A	K0.5 V	J04153–076	M4.5 V	77.9	[e]
STF518	o^{02} Eri B	DA	J04153–076	M4.5 V	8.6	[e]
LDS3584	J04252+080S	M2.5 V+	HG 7–207	M4.0 V	73.4	[f]
STI205	J04311+589	M4.0 V	EGGR 180	DC	10.0	[g]
LDS6160	J05032+213	M1.5 V+	HD 285190 BC	M5.0 V + M5.5 V	167.0	[h]
WDK1	J05034+531	M0.5 V	...	m7.0	5.6	[i]
DON93	J05068–215E	M1.5 V	J05068–215W	m3.0 V + m4.0 V	8.5	[j]
LDS6186	HD 35956	G0 V+	J05289+125	M4.0 V	99.4	[k]
LDS6189	J05342+103N	M3.0 V	J05342+103S	M4.5 V	5.1	
TOK255	J05365+113	M0.0 V	J05366+112	M 4.0 V	156.5	
GIC61	EG Cam	M0.5 V	J05599+585	M4.0 V	161.2	
NAJ1	J06105–218	M0.5 V	GJ229 B	T7	6.8	
GIC65	J06421+035	M2.0 V	J06422+035	M4.0 V	49.7	
WNO17	HD 50281	K3 V	J06523–051	M3.5 V+	58.3	[l]
GIC75	J07307+481	M4.0+	EGGR 52	DC9+DC9	103.4	
LDS6206	VV Lyn AB	M2.5 V+	J07319+362N	M3.5 V	38.20	
Pov09	V869 Mon + GJ 282 B	K2 V + K5 V	J07361–031	M1.0 V	3892.0	
LDS3755	J07395+334	M2.0 V	LP 256–044	M6:	13.7	
LUY5693	EGGR5 54 A	DAZ6	J07403–174	M6.0 V	21.0	[m]
COU91	BD 21+1764A	K7 V	J08082+211	M3.0 + m3.0 + m5.0	10.7	[n]
LDS204	GJ 9255 A	F6.5 V	J08105–138	M2.0 V + M5.5 V	97.6	
LUY6218	BD+10 1857 AB	M0.0 V+	J08428+095	M2.5 V	114.4	
OSV2	J09008+052W	M3.0 V	Ross 687	M3.5 V	29.40	
STF1321	J09143+526	M0.0 V+	J09144+526	M0.0 V	17.20	[o]
LDS6226	J09187+267	M1.5 V	LP 313–038	M5.0 V	76.3	
GIC87	J09288–073	M2.5 V	GJ 347 B	M4.5	35.9	

Table C.6: continued.

WDS	Primary		Secondary		ρ	Notes
	Name	SpT	Name	SpT	[arcsec]	
LDS3917	J09430+237	M1.0 V	LP 370–034	M7.0 V	131.20	
REB1	J10043+503	M2.5 V	G 196–003 B	L2	16.0	
LDS3977	J10185–117	M4.0 V	LP 729–055	M5.0 V	15.8	
LDS1241	J10260+504W	M4.0 V	J10260+504E	M4.0 V	14.4	
LDS3999	J10345+465	M3.0 V	NLTT 24709	M4.5 V	46.5	
LDS1258	J10448+324	M2.0 V + M4.0 V	LP 316–605 B	M4.5 V	35.1	
VBS18	BD+44 2051A	M1.0 V	J11055+435	M5.5 V	31.4	
LDS5207	J11476+002	M4.0 V	LP 613–050 B	M5.5 V	24.8	
LDS4166	J12006–138	M3.5 V	LP 734–010 B	M4.5	6.8	
LDS390	LTT 4562	M3.0 V	J12112–199	M3.5 V	85.3	
VYS5	J12123+544S	M0.0 V	J12123+544N	M3.0 V	14.7	
(Haw96)	J12142+006	M5.0 V+	...	...	5.0	[p]
BU800	HD 115404	K2 V	J13168+170	M0.5 V	7.5	
LDS448	BD–07 3632	DA5.0	J13300–087	M4.0 V	503.0	
DEA1	J13481–137	M4.5 V	LHS 2803B	T5.5	67.6	
LDS461	J13507–216	M3.0 V	J13503–216	M3.5 V	374.90	
VVO12	BD+46 1951	M0.0 V	J14173+454	M5.0 V	59.2	
STT580	θ Boo A	F7 V	J14251+518	M2.5 V	69.5	
BUI442	J14257+236W	M0.0 V	J14257+236E	M0.5 V	45.4	[q]
GIC120	J14279–003S	M4.5 V	J14279–003N	M4.5 V	13.0	
LDS961	J14283+053	M3.0 V	LP 560–026	M3.5 V	60.2	
LDS6309	Ross 806	M2.5 V	J15531+347S	M3.5 V	26.50	
LDS573	J16554–083S	M3.0 V + M4.0V	J16554–083N	M3.5 V	72.2	[r]
LDS573	J16554–083S	M3.0 V + M4.0V	J16555–083	M7.0 V	230.8	[r]
A184	V1090 Her	K0 V	J16578+473	M1.5 V	5.08	[e]
STFA32	V1089 Her	K0 V	J16578+473	M1.5 V	111.60	[e]
LDS593	J17177–118	M3.0 V	2MASS J17174454–1148261	m4.0	30.1	[s]
BDK9	J17578+465	M2.5 V	G 204–039 B	T6.5	197.0	
GIC151	J18180+387E	M3.0 V	J18180+387W	M4.0 V	9.9	
NI38	J18264+113	M3.5 V	2MASS J18262449+1120498	"WD"	8.1	
LDS6329	BD+45 2743	M0.5 V	J18354+457	M2.5 V	112.2	
STF2398	J18427+596N	M3.0 V	J18427+596B	M3.5V	11.7	
KAM3	J19463+320	M0.5 V	J19464+320	M2.5 V	5.7	[t]
GIC159	J19539+444W	M4.5 V + M8.0 V	J19539+444E	M5.5 V	6.4	
LDS1045	GJ 797 A	G5 V	J20407+199	M2.5 V+	125.1	[u]
LDS1046	J20445+089S	M1.5 V	J20445+089N	M3.5 V+	15.2	[v]
LDS6418	J20556–140N	M4.0 V	GJ 810 B	M5.0 V	107.1	
LDS1049	J21012+332	m2.5 V + m4.5 V	J21013+332	M2.0 V + M5.0 V	56.9	
LDS1053	21160+298E	M3.5 V+	21160+298W	M3.5 V	26.1	[w]
GIC193	J23293+414N	M3.5 V	J2393+414S	M4.0 V	17.7	[x]
WIR1	J23318+199E	M3.5 V+	J23318+199W	M4.5 V+	5.3	[y]
LDS830	J23573–129E	M3.0 V	J23573–129W	M4.0 V+	19.6	[z]

Notes. [a]C is background (GRB34). [b]AB is separated by 2.5 arcsec (WOR4). [c]"B-G" are background (LMP3). [d]Simbad indicates that J03574–011 is a spectroscopic binary but we did not find any reference. [e]Triple system. [f]Primary is SB2 (Llamas 2014). [g]Primary is an astrometric binary separated by 0.07 arcseconds (Strand 1977). [h]The primary is a SB2 (Schöfer 2015). [i]It was also observed with the CAMELOT low resolution imager at the Observatorio del Teide (Tenerife) in September 2015 with the *BVIgri* filters in order to obtain more photometric information but we could not avoid the saturation of the primary. [j]BC is separated by 0.8 arcsec. [k]Primary is a SB (Simbad). [l]Background source at 9.62 arcsec (TNN6).[m]WDS VBS41 at 4 arcsec and 208 deg was not detected in this work nor in Davison et al. 2015. It could be an unrelated companion. The WDS "AC" designation refers to the pair in the table. [n]Hierarchical quadruple. [o]Primary is a SB1 (Schöfer 2015). Two other WDS entries under the same discoverer code (STF1321) are not physically bound components. [p]SB2 (Bonfils et al. 2013). Hawley et al. (1996) listed in Table 1.(b) a companion at 5.0 arcsec 1.2 mag fainter in V. 2MASS resolved a source 6.5 mag fainter in the J band at 5.9 arcsec and 179 deg (quality flag: AUU). Neither Law et al. (2008) nor Dieterich et al. (2012 – with NICMOS onboard *Hubble*) detected it. We believe that Hawley et al. (1996) made reference to the background star 2MASS J12141817+0037297. [q]Other WDS entries under BU 1442 and STG 6 are unrelated sources. [r]Quintuple system. [s]Simbad mixes up the true primary GJ 3999 ("L 845-016"), the true secondary 2MASS J17174454–1148261, and the background star GJ 4000 B ("L 845-015", see Table C.3). We preserve the current (wrong) nomenclature. [t]C is background (HEL3). [u]Other WDS entries under RAO 23 are unrelated sources. [v]Secondary is SB1 (Schöfer 2015). [w]AB is separated by 0.05 arcsec (BWL56). [x]Bab is separated by 0.26 arcsec (BWL59). AC is background (BWL59). [y]A and B are SB1 (Delfosse et al. 1999). Other WDS entries under LMP 24 are unrelated sources. [z]Secondary is SB2 (Schöfer 2015).

D

Long tables and figures of Chapter 5

This appendix includes the tables and Figures referenced Chapter 5.

- Table D.1 contains the list of the 34 M dwarfs for which a common proper motion companion candidate was found. There are included the Karmn name, distances, proper motions, youth label (i.e. population or stellar kinematic association) and references. See the text for the explanation of the stars in italics J11008+120 and J10155-164.
- Table D.2 lists the 38 common proper motion companions analyzed in Section 5.2.4. I adopted the name of the star in the proper motion catalogue. The table includes 2MASS coordinates, and proper motions from the literature or obtained in this work. A flag of companionship indicates whether the star is likely a true companion or a background star with similar proper motion. See the text for the explanation of the stars in italics J11008+120 and J10155-164.
- Figures D.1–D.14 display the proper motion and M_J vs. $J - K_s$ diagrams of the Carmencita M dwarfs and their common proper motion likely or doubtful but probable companions listed in Table 5.2. Also the two previously known systems listed in the table are included.
- Figures D.15–D.33 show the proper motion and M_J vs. $J - K_s$ diagrams for the Carmencita M dwarfs and the rejected common proper motion candidates.

Table D.1: Parameters of the M Carmencita stars with potential common proper motion companions.

Karmn	d [pc]	Ref.[a]	μ_α [mas a^{-1}]	eμ_α [mas a^{-1}]	μ_δ [mas a^{-1}]	eμ_δ [mas a^{-1}]	Ref.[b]	Youth[c]	Ref.[d]
J00240+264	22.1	Dit14	141.6	0.2	-48.7	0.5	Gal15	D	Mon16
J01041+108	34.4	Cor16	34.2	3.0	-67.9	3.0	PPMXL		
J02026+105	8.8	Cor16	-50.5	4.4	-43.6	4.9	PPMXL	D	Mon16
J03167+389	18.9	Cor16	-85.1	5.1	23.4	5.1	PPMXL		
J03288+264	15.0	Dit14	217.3	4.6	-131.2	4.6	PPMXL	LA	Mon16
J03303+346	22.9	Cor16	35.8	5.4	-41.6	5.4	PPMXL	YD	Mon16
J04056+057	16.1	Cor16	33.0	4.9	-38.5	4.9	PPMXL	YD	Mon16
J05243-160	10.0	Cor16	20.5	5.2	-36.7	5.2	PPMXL	bPic	Malo14a
J05320-030	16.9	Cor16	6.7	2.2	-50.4	2.2	PPMXL	bPic	Malo13
J05456+729	25.2	Cor16	81.5	0.7	114.3	0.3	Cortes		
J05458+729	28.8	Cor16	81.5	0.7	112.3	0.5	Cortes		
J07182+137	20.8	Cor16	-34.4	0.2	-32.2	0.7	Cortes		
J07310+460	22.4	Cor16	-16.6	5.1	-97.5	5.1	PPMXL	YD	Mon16
J07497-033	16.7	Cor16	-139.4	5.5	-50.8	5.5	PPMXL	Cas	Mon16
J07545-096	24.2	Cor16	-93.3	6.0	-12.1	6.0	PPMXL		
J09040-159	26.5	Cor16	-111.6	0.7	-32.0	0.1	Cortes		
J10155-164	17.1	Cor16	-438.9	0.4	+185.8	0.5	Cortes		
J10403+015	32.4	Cor16	-44.5	2.7	-49.4	2.7	PPMXL		
J11008+120	19.6	Dit14	128.2	0.6	-120.5	0.8	Cortes	UMa	Mon16
J11238+106	22.3	Cor16	159.72	1.6	-65.9	1.6	PPMXL		
J11307+549	33.2	Cor16	34.7	2.3	105.9	2.2	PPMXL		
J12162+508	16.5	Cor16	-73.8	4.9	34.0	4.9	PPMXL		
J13417+582	15.5	Cor16	72.4	4.5	-60.9	4.5	PPMXL	UMa	Mon16
J14175+025	23.8	Cor16	-31.9	4.9	-63.1	4.9	PPMXL		
J14259+142	28.2	Cor16	-46.5	0.3	-23.4	0.3	Cortes	bPic	Schl12b
J15480+043	25.3	Cor16	-20.1	5.0	-52.9	5.0	PPMXL		
J16120+033	19.0	Cor16	28.2	2.6	-61.3	2.7	PPMXL	UMa	Mon16
J17338+169	11.7	Dit14	-108.6	4.8	-133.1	4.8	PPMXL	LA	Mon16
J18135+055	20.0	Cor16	-72.4	0.4	-228.2	0.5	Cortes	D	Mon16
J18174+483	16.1	Cor16	-44.7	0.4	48.4	0.3	Cortes		
J21267+037	27.08	HIP2	-38.1	2.94	-49.1	2.34	HIP2	YD	Mon16
J21376+016	10.7	Cor16	79.3	0.3	-60.2	0.2	Gal15	bPic?	Schl12b
J21463+382	6.7	Dit14	168.2	4.7	-125.3	4.7	PPMXL	TD	Mon16
J23317-027	29.1	vAl95	95.1	4.7	-73.3	4.7	PPMXL	bPic?	Malo13

Notes. [a]Cor16: Cortés-Contreras et al. 2016; Dit14: Dittmann et al. 2014; Gal15: Gallardo 2015; HIP2: van Leeuwen 2007; vAl95: van Altena et al. 1995. [b]Cortes: This work; HIP2: van Leeuwen 2007; PPMXL: Roeser et al. 2010. [c]bPic: β Pictoris; Cas: Castor; LA: Local Association; UMa: Ursa Major; YD: Young Disc; D: Thin disc; TD: Thick disc. [d]Malo13: Malo et al. 2013; Malo14a: Malo et al. 2014a; Mon16: Montes priv. comm.; Schl12b: Schlieder et al. 2012b.

Table D.2: Candidate companions to Carmencita M dwarfs.

Karmn	Candidate name	α (J2000.0)	δ (J2000.0)	μ_α [mas a^{-1}]	eμ_α [mas a^{-1}]	μ_δ [mas a^{-1}]	eμ_δ [mas a^{-1}]	Ref.[a]
J00240+264	PPMXL 2163158045175199340	00:24:24.57	+26:29:26.7	147.6	0.2	-46.4	1.1	Cortes
J01041+108	PPMXL 2047217074249143658	01:04:15.86	+10:50:17.2	40.1	0.7	-53.7	1.4	Cortes
J02026+105	PPMXL 2102333982850420201	02:02:36.36	+10:32:14.9	-32.0	0.34	-42.7	0.4	Cortes
	PPMXL 2102330425525959009	02:01:38.53	+10:37:16.2	-35.6	0.24	-43.6	0.2	Cortes
J03167+389	PPMXL 394449348926562027	03:16:55.88	+38:57:49.8	-86.3	0.2	25.8	0.4	Cortes
J03288+264	PPMXL 3041372475460023448	03:28:03.73	+26:31:51.9	185.0	4.6	-126.8	4.6	PPMXL
J03303+346	PPMXL 3071422664308970376	03:30:16.81	+34:39:50.6	32.0	0.1	-40.5	0.2	Cortes
	PPMXL 3071421786149345561	03:30:48.35	+34:38:04.4	35.5	0.4	-32.7	0.1	Cortes
J04056+057	PPMXL 2908977255675800728	04:05:53.09	+05:37:11.9	37.9	0.3	-19.3	0.6	Cortes
J05243-160	PPMXL 2552838223399433365	05:24:52.07	-16:17:19.2	26.2	0.6	-42.0	1.2	Cortes
J05320-030	PPMXL 2591858631666979215	05:32:05.96	-03:01:15.9	7.9	0.5	-53.4	0.6	Cortes
J05456+729	PPMXL 498625384126281078	05:45:49.74	+72:54:07.2	82.3	0.5	112.4	0.5	Cortes
J05458+729	PPMXL 498625259746845583	05:45:38.80	+72:55:12.7	82.7	0.5	114.1	0.3	Cortes
J07182+137	PPMXL 3226017874533491871	07:18:16.50	+13:36:03.3	-29.6	0.2	-29.3	1.0	Cortes
J07310+460	PPMXL 998368542027956669	07:31:09.05	+45:56:57.3	-17.5	0.8	-97.6	0.3	Cortes
	PPMXL 1004326060565163279	07:31:38.84	+46:00:19.7	-13.4	0.3	-77.11	0.5	Cortes
	PPMXL 1004373792460974930	07:31:38.49	+45:57:17.4	-12.5	0.2	-101.0	0.5	Cortes
J07497-033	PPMXL 2856105300336770891	07:49:50.88	-03:17:19.5	-160.2	0.6	-51.9	0.2	Cortes
J07545-096	PPMXL 2847318747985584270	07:54:37.33	-09:43:18.5	-46.9	1.0	-11.7	0.8	Cortes
J09040-159	PPMXL 3606018957268756502	09:04:20.70	-15:54:51.2	-108.7	0.9	-29.6	0.6	PPMXL
J10155-164	*PPMXL 3684574399141311521*	*10:16:08.65*	*-16:32:51.5*	*-156.7*	*4.0*	*-98.1*	*4.0*	*PPMXL*
J10403+015	PPMXL 4111995391072861394	10:40:13.28	+01:34:56.2	-37.9	1.1	-43.6	0.6	Cortes
J11008+120	HIP 53859	11:01:05.69	+12:02:46.7	145.2	0.4	-98.8	0.4	UrHip
J11238+106	HIP 55642	11:23:55.46	+10:31:45.9	151.4	0.53	-78.6	0.5	UrHip
J11307+549	PPMXL 1021315941850983881	11:30:42.58	+54:56:55.4	32.2	3.6	91.1	3.6	PPMXL
J12162+508	PPMXL 854563106897995198	12:16:15.34	+50:47:14.4	-75.0	0.2	17.06	0.5	Cortes
J13417+582	PPMXL 799317777967965521	13:41:40.52	+58:09:30.8	49.7	0.2	-79.3	0.3	Cortes
J14175+025	PPMXL 4401106107294582340	14:17:29.51	+02:34:53.8	-29.6	0.4	-45.2	0.7	Cortes
J14259+142	PPMXL 4439781685804388360	14:26:12.61	+14:10:28.1	-58.2	0.4	-25.1	0.3	Cortes
J15480+043	PPMXL 5210004709267384143	15:47:54.91	+04:18:03.8	-18.7	0.7	-56.7	0.4	Cortes
J16120+033	APOP 53884+0000138	16:12:05.04	+03:18:53.3	23.0	0.3	-49.0	0.3	Cortes
J17338+169	PPMXL 5319498649352790063	17:33:14.02	+16:59:50.0	-108.9	3.7	-110.7	3.7	PPMXL
J18135+055	PPMXL 5479566472157363638	18:13:28.18	+05:26:58.4	-69.2	2.8	-226.2	2.8	PPMXL

Table D.2: Proper motions and UVW space velocities of Carmencita stars (continued).

Karmn	Candidate name	α (J2000.0)	δ (J2000.0)	μ_α [mas a^{-1}]	eμ_α [mas a^{-1}]	μ_δ [mas a^{-1}]	eμ_δ [mas a^{-1}]	Ref.[a]
J18174+483	PPMXL 191371594233401412	18:17:27.65	+48:20:42.6	-38.8	0.7	66.6	0.3	Cortes
J21267+037	PPMXL 1737490464551960203	21:26:36.69	+03:47:10.6	-35.7	2.2	-42.8	1.2	Cortes
J21376+016	PPMXL 1748251883493747406	21:37:43.33	+01:41:24.4	94.9	0.8	-41.8	0.7	Cortes
J21463+382	PPMXL 1938510747653241525	21:46:08.72	+37:54:48.9	169.5	3.7	-149.0	3.7	PPMXL
J23317-027	PPMXL 1435944420390491774	23:31:28.62	-02:42:20.2	65.1	0.9	-50.6	5.2	Cortes

Notes. [a]Cortes: This work; PPMXL: Roeser et al. 2010; UrHip: Frouard et al. 2015.

Proper motion and colour-magnitude diagrams of the likely and dubbious pairs.

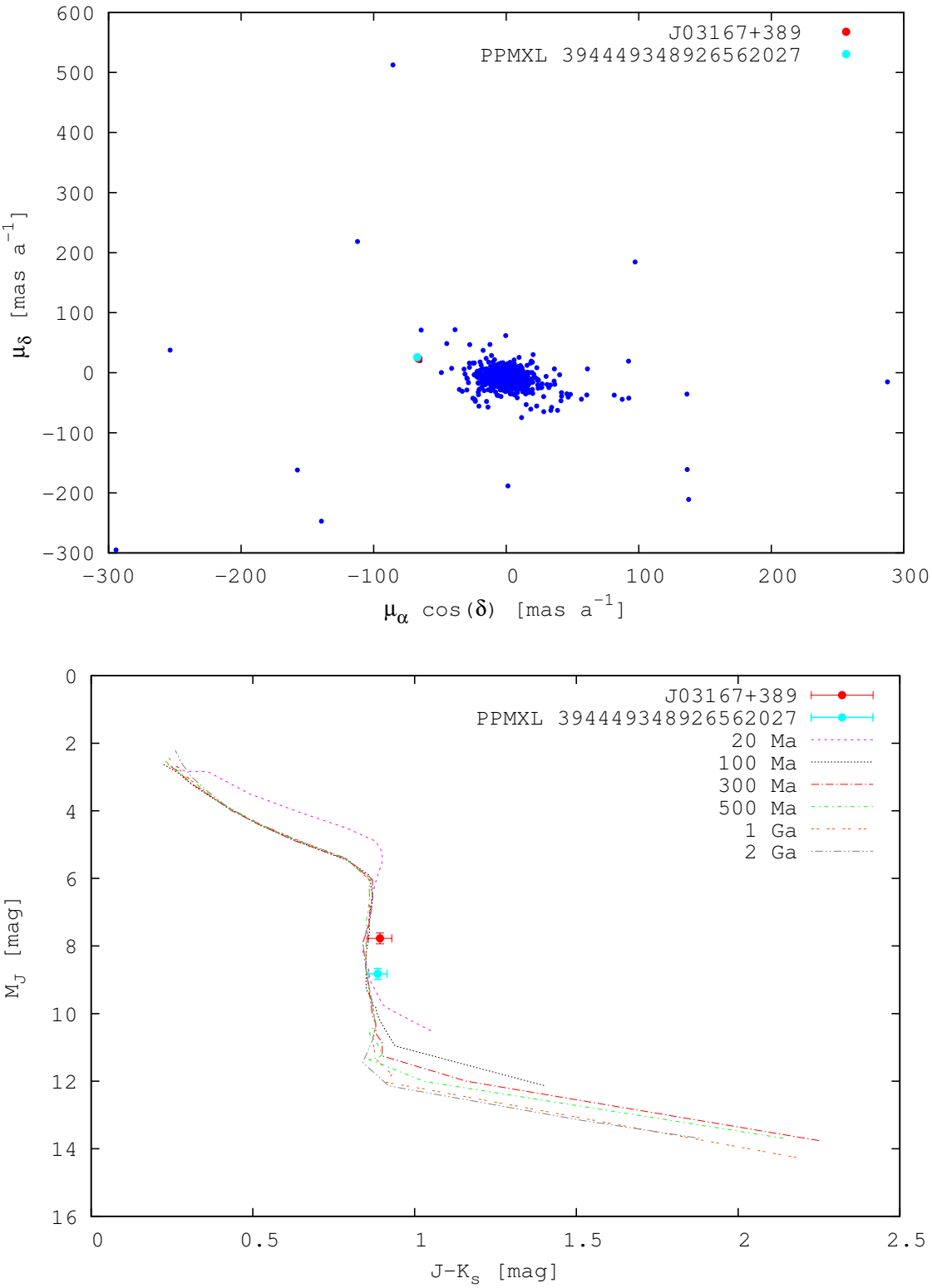

FIGURE D.1— Proper motion and colour-magnitude diagrams for the Carmencita targets and their common proper motion likely and dubious candidates.

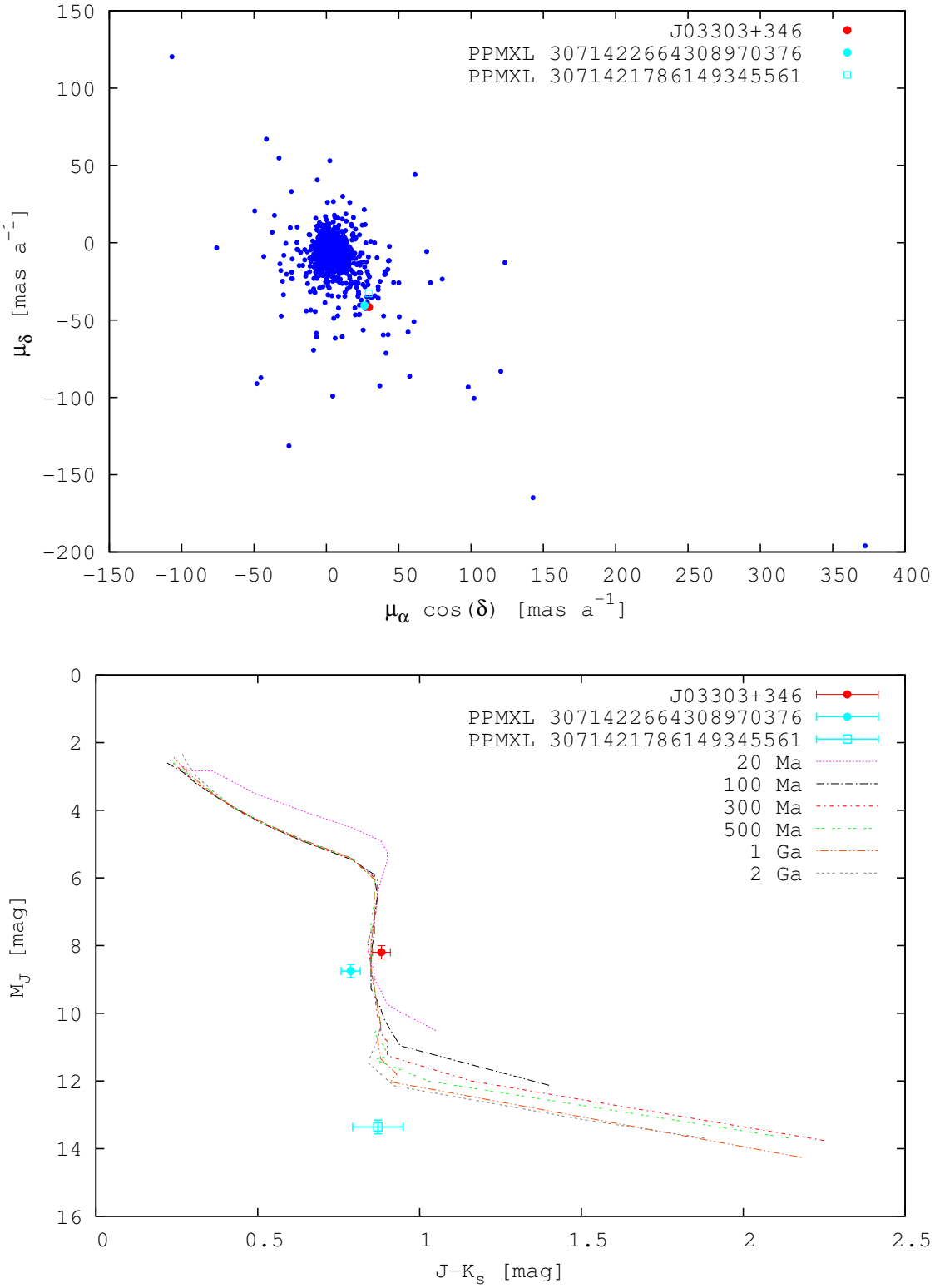

FIGURE D.2— Proper motion and colour-magnitude diagrams for the Carmencita targets and their common proper motion likely and dubious candidates (cont.)

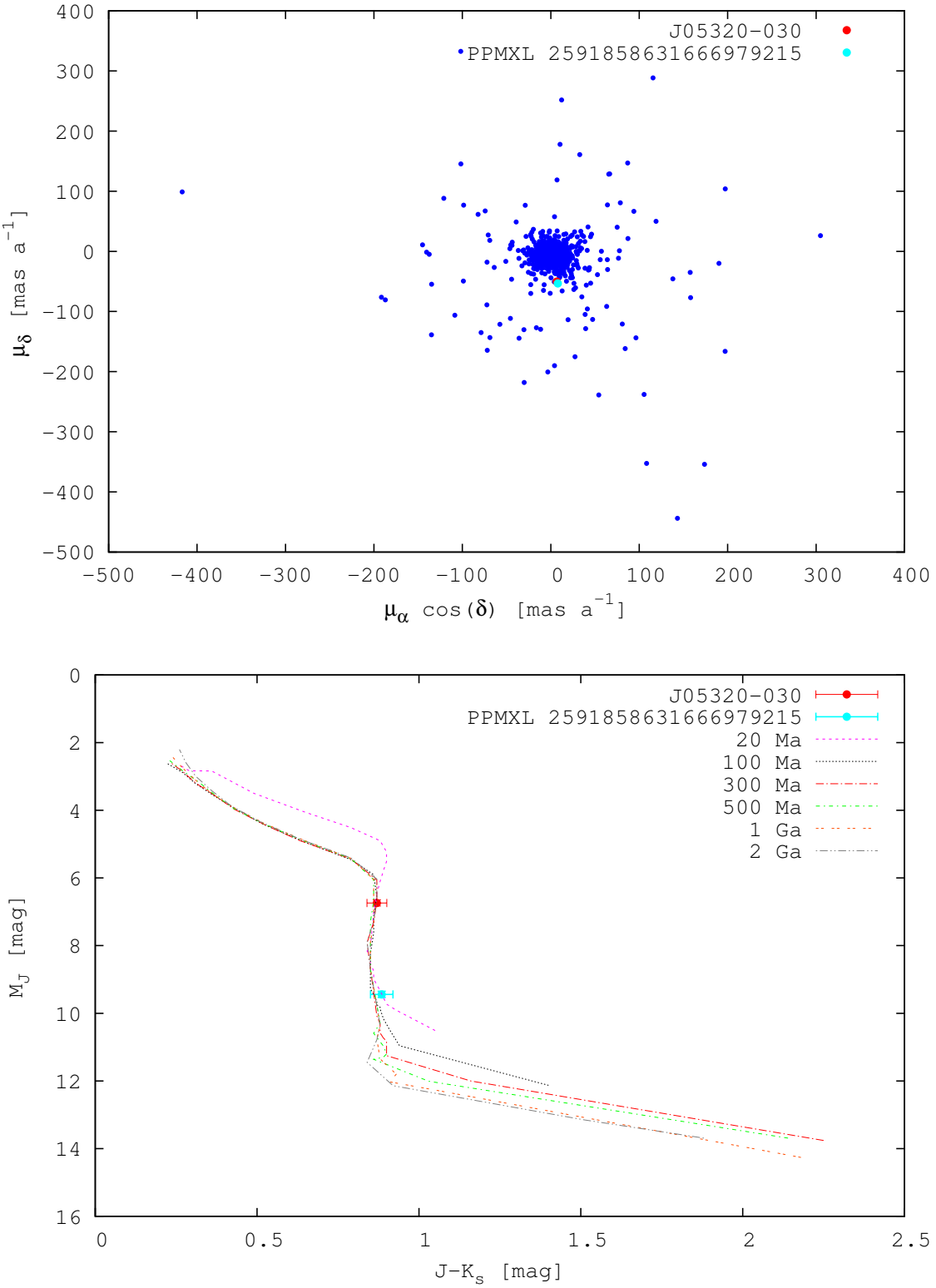

FIGURE D.3— Proper motion and colour-magnitude diagrams for the Carmencita targets and their common proper motion likely and dubious candidates (cont.)

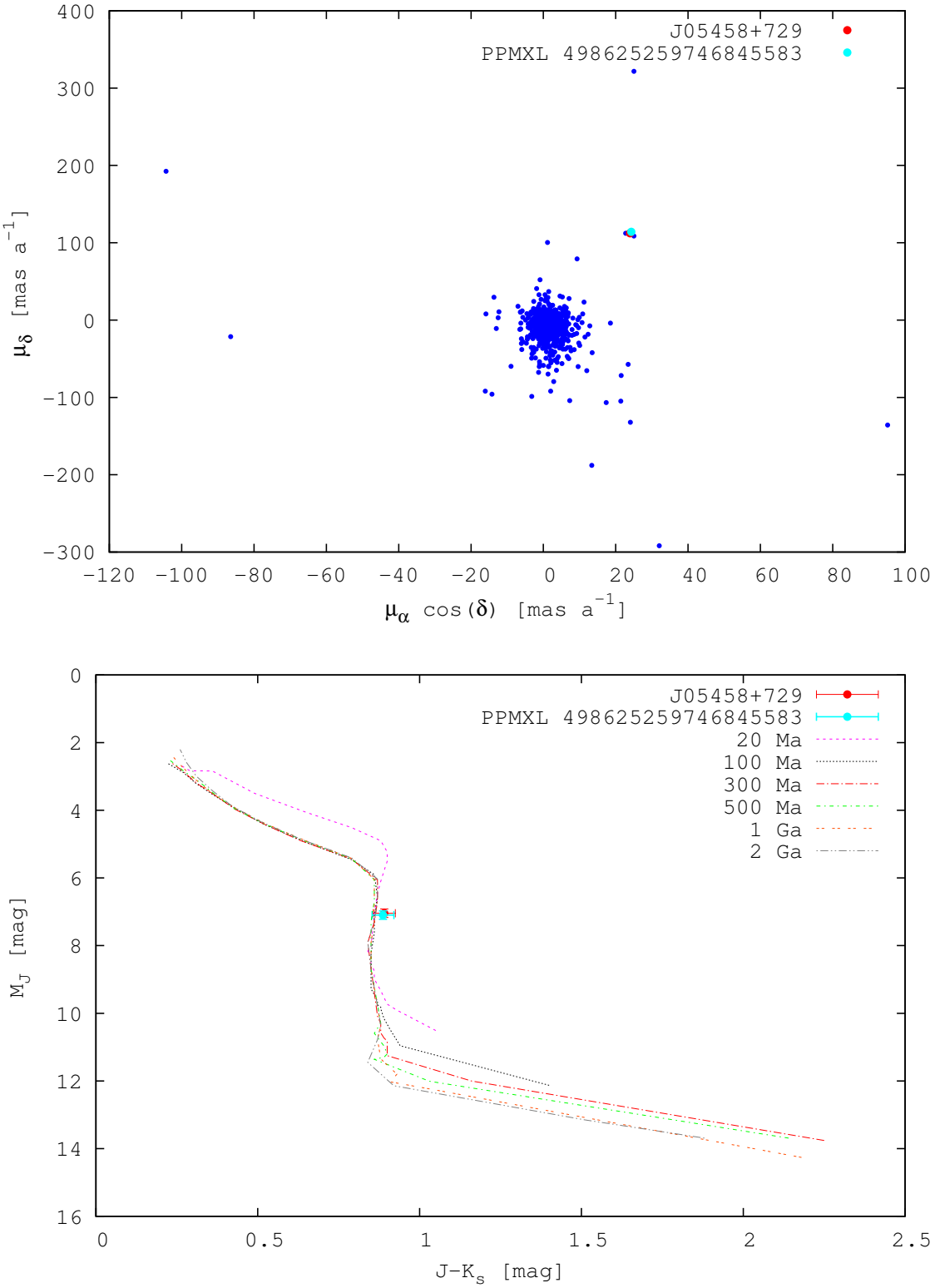

FIGURE D.4— Proper motion and colour-magnitude diagrams for the Carmencita targets and their common proper motion likely and dubious candidates (cont.)

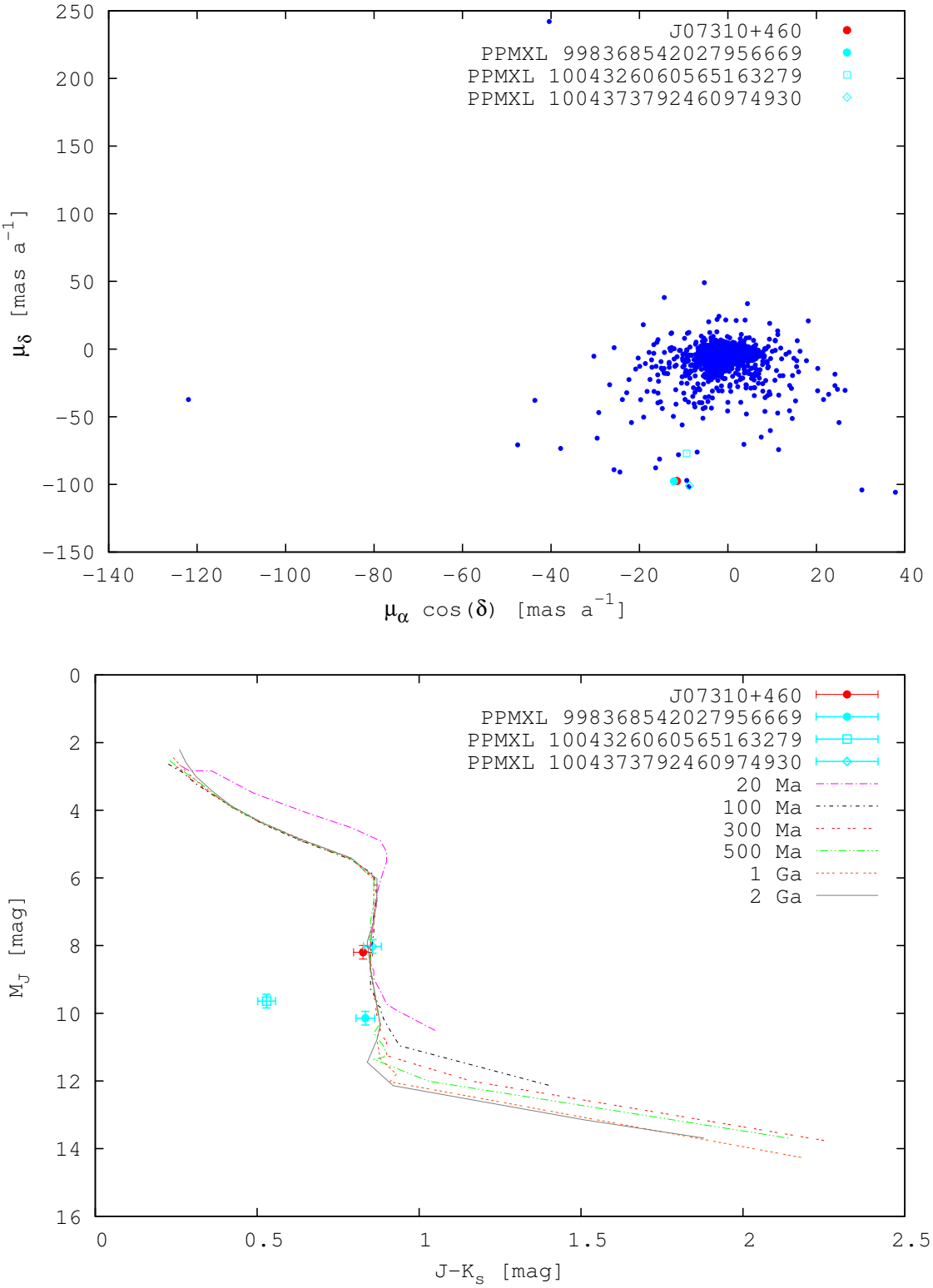

FIGURE D.5— Proper motion and colour-magnitude diagrams for the Carmencita targets and their common proper motion likely and dubious candidates (cont.)

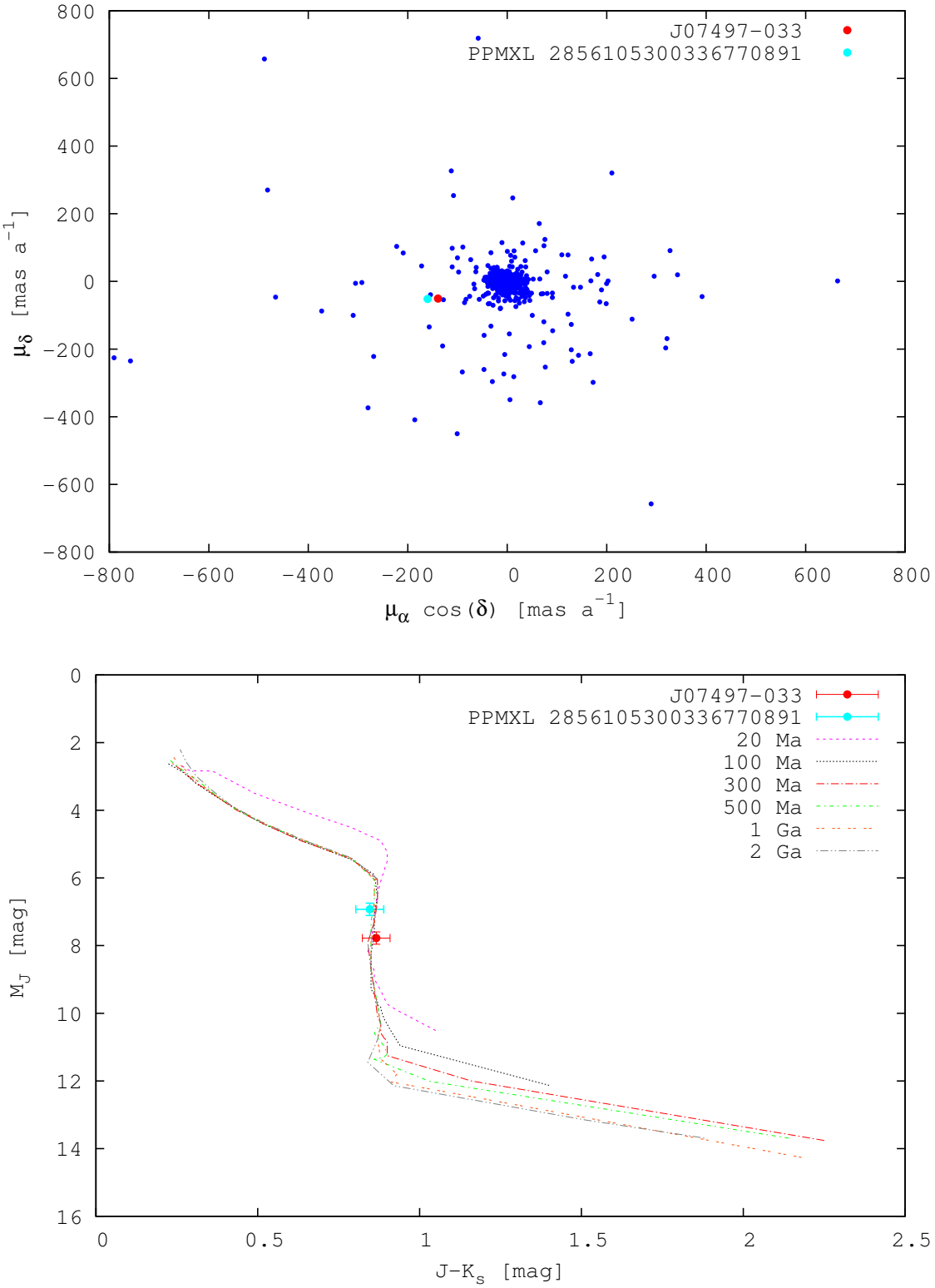

FIGURE D.6— Proper motion and colour-magnitude diagrams for the Carmencita targets and their common proper motion likely and dubious candidates (cont.)

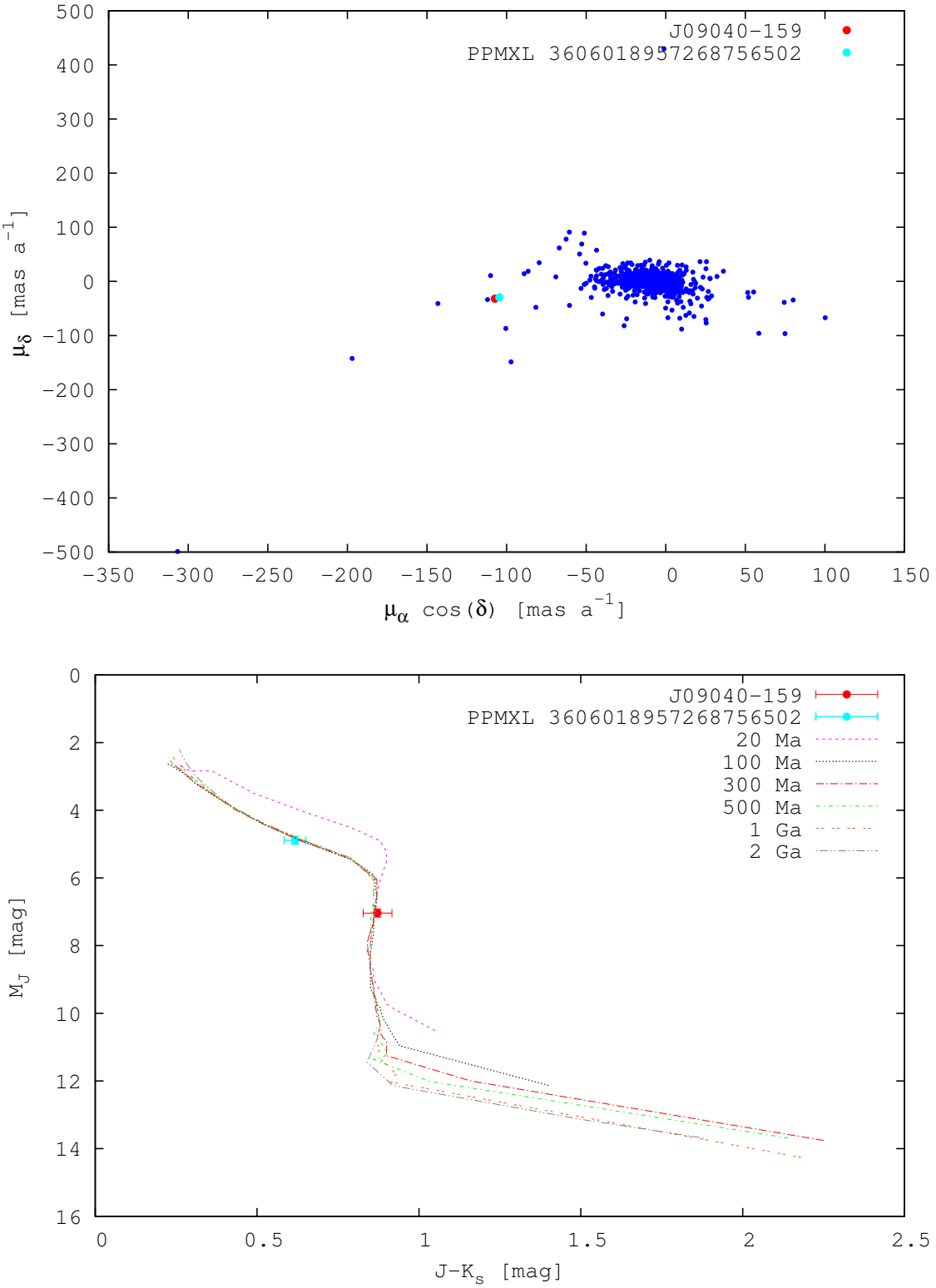

FIGURE D.7— Proper motion and colour-magnitude diagrams for the Carmencita targets and their common proper motion likely and dubious candidates (cont.)

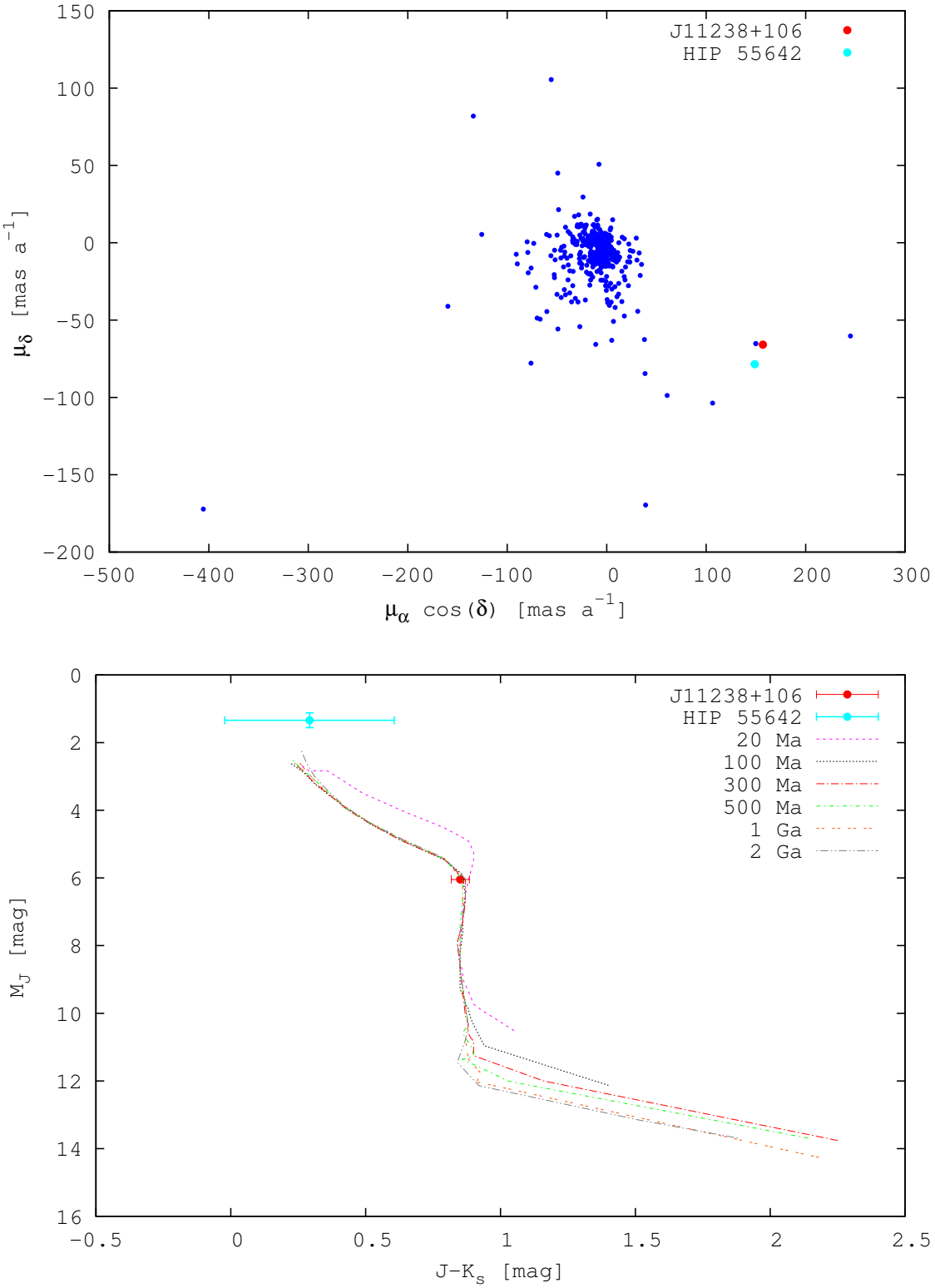

FIGURE D.8— Proper motion and colour-magnitude diagrams for the Carmencita targets and their common proper motion likely and dubious candidates (cont.)

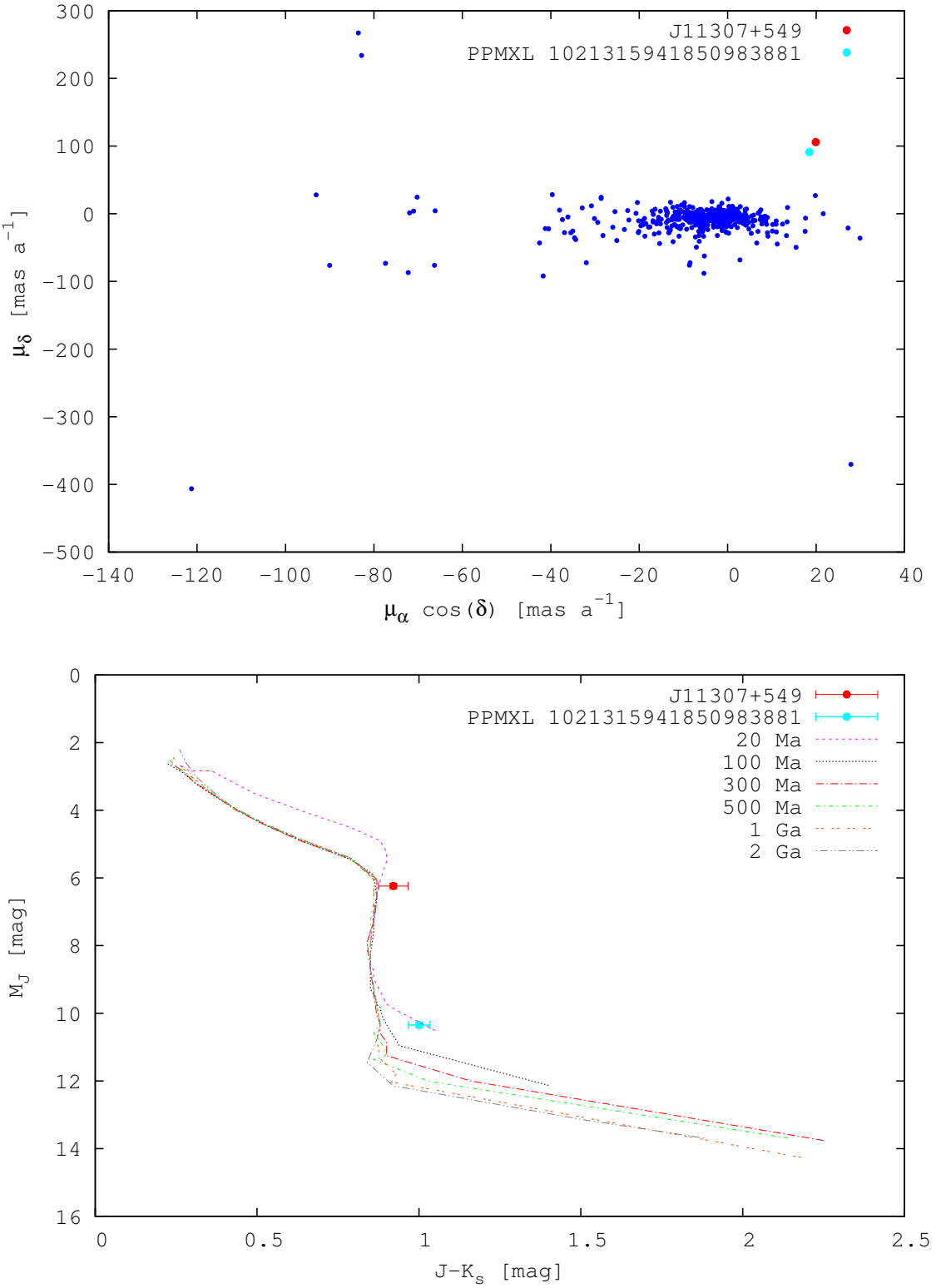

FIGURE D.9— Proper motion and colour-magnitude diagrams for the Carmencita targets and their common proper motion likely and dubious candidates (cont.)

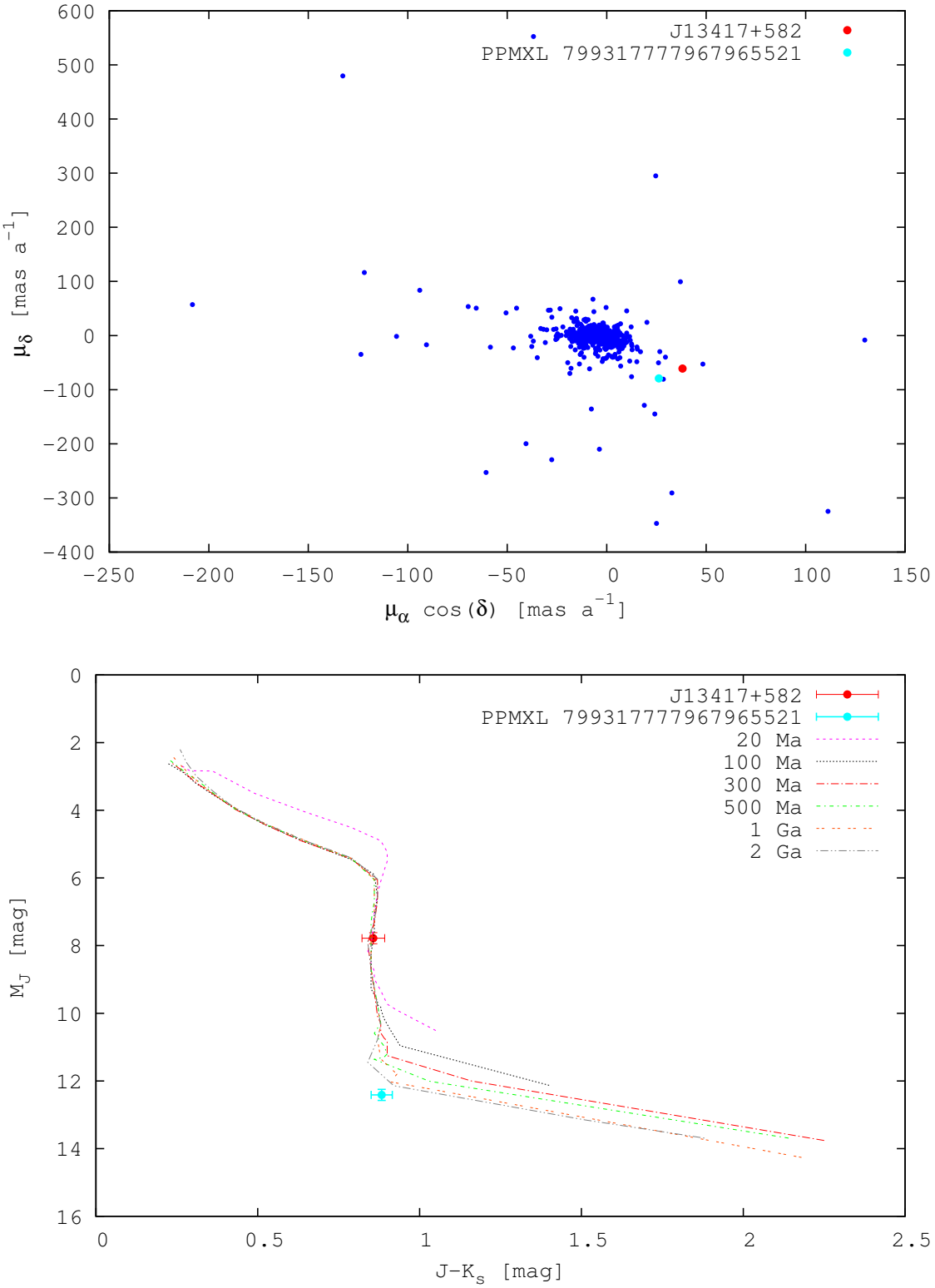

FIGURE D.10— Proper motion and colour-magnitude diagrams for the Carmencita targets and their common proper motion likely and dubious candidates (cont.)

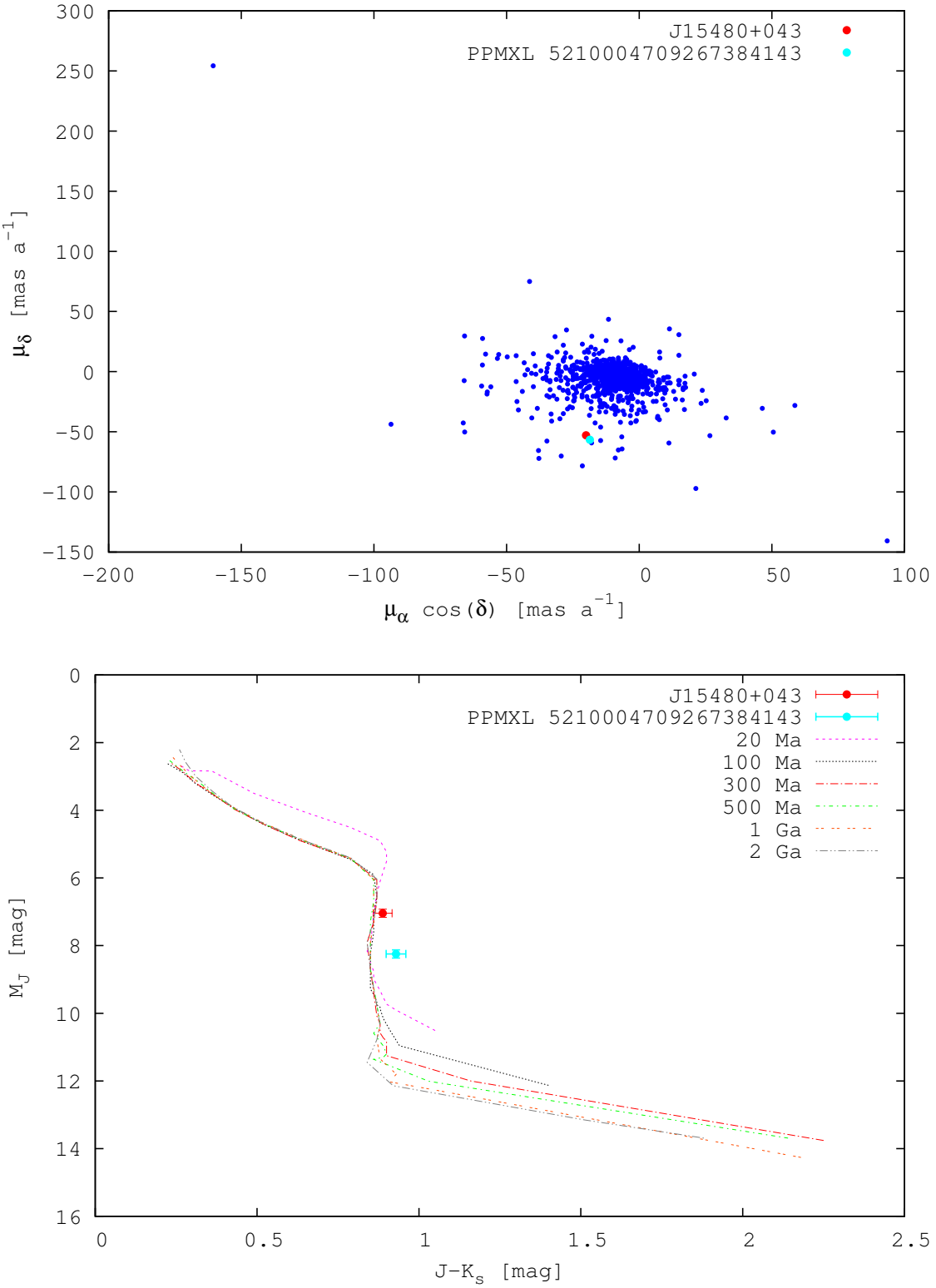

FIGURE D.11— Proper motion and colour-magnitude diagrams for the Carmencita targets and their common proper motion likely and dubious candidates (cont.)

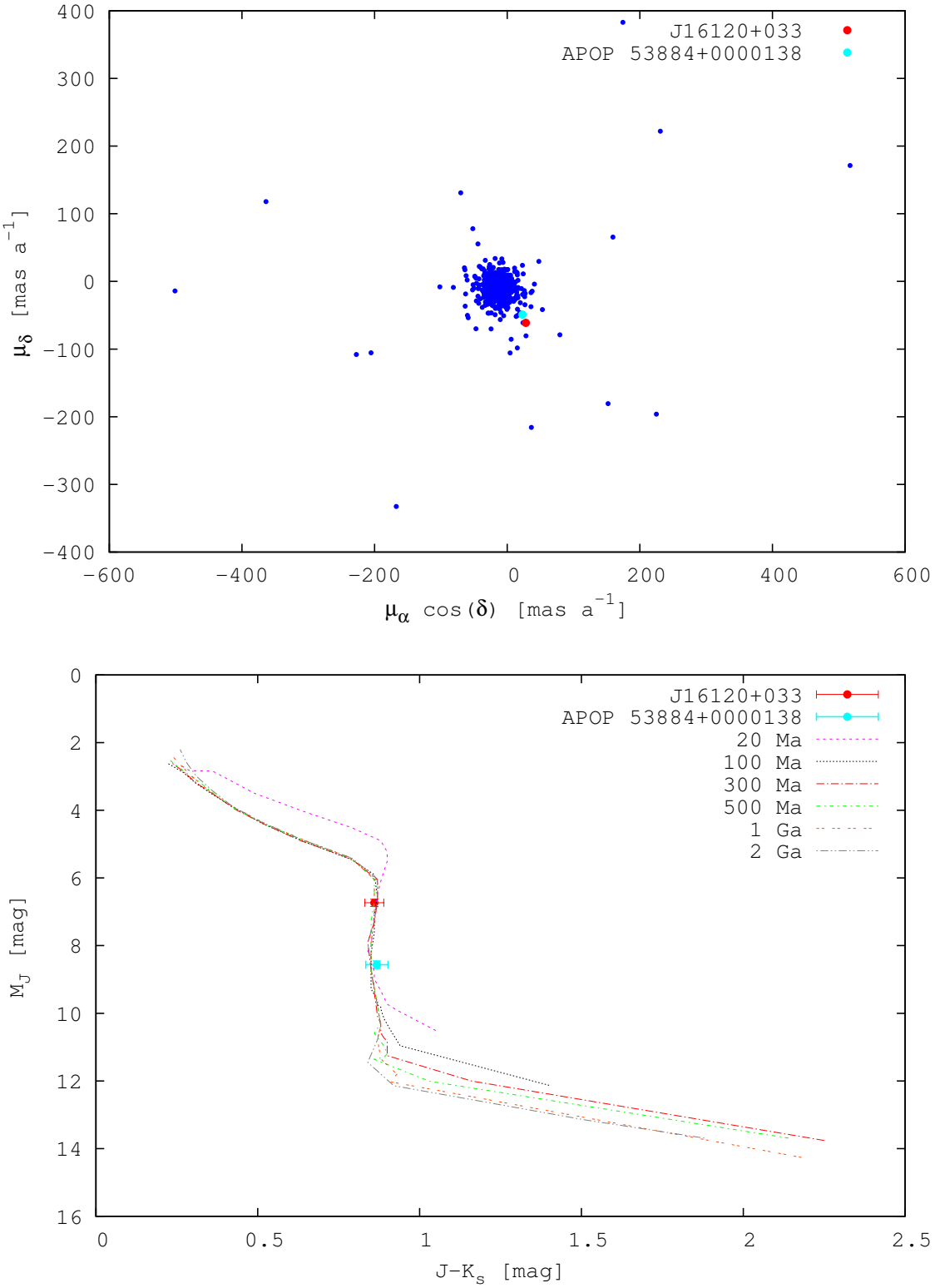

FIGURE D.12— Proper motion and colour-magnitude diagrams for the Carmencita targets and their common proper motion likely and dubious candidates (cont.)

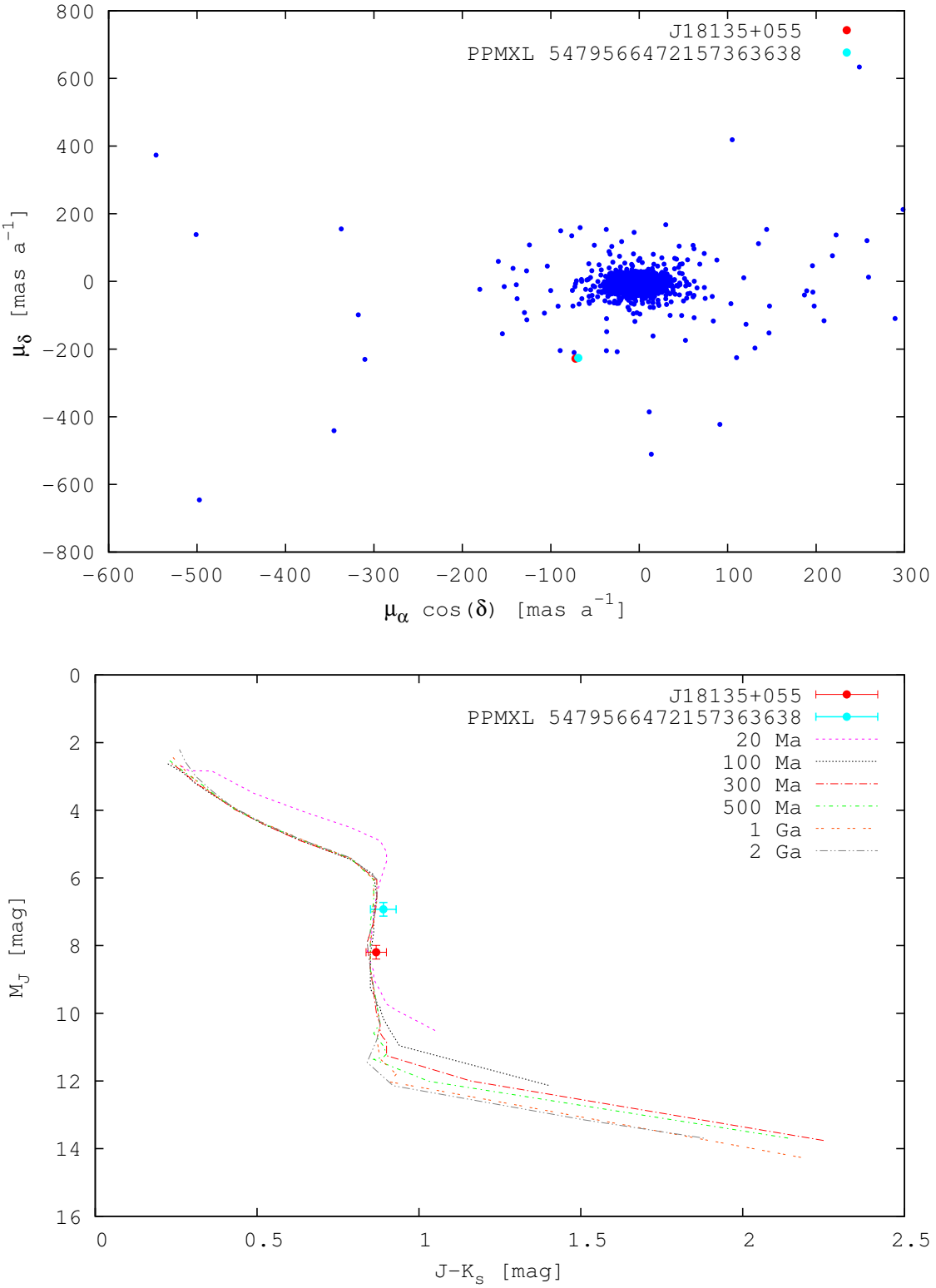

FIGURE D.13— Proper motion and colour-magnitude diagrams for the Carmencita targets and their common proper motion likely and dubious candidates (cont.)

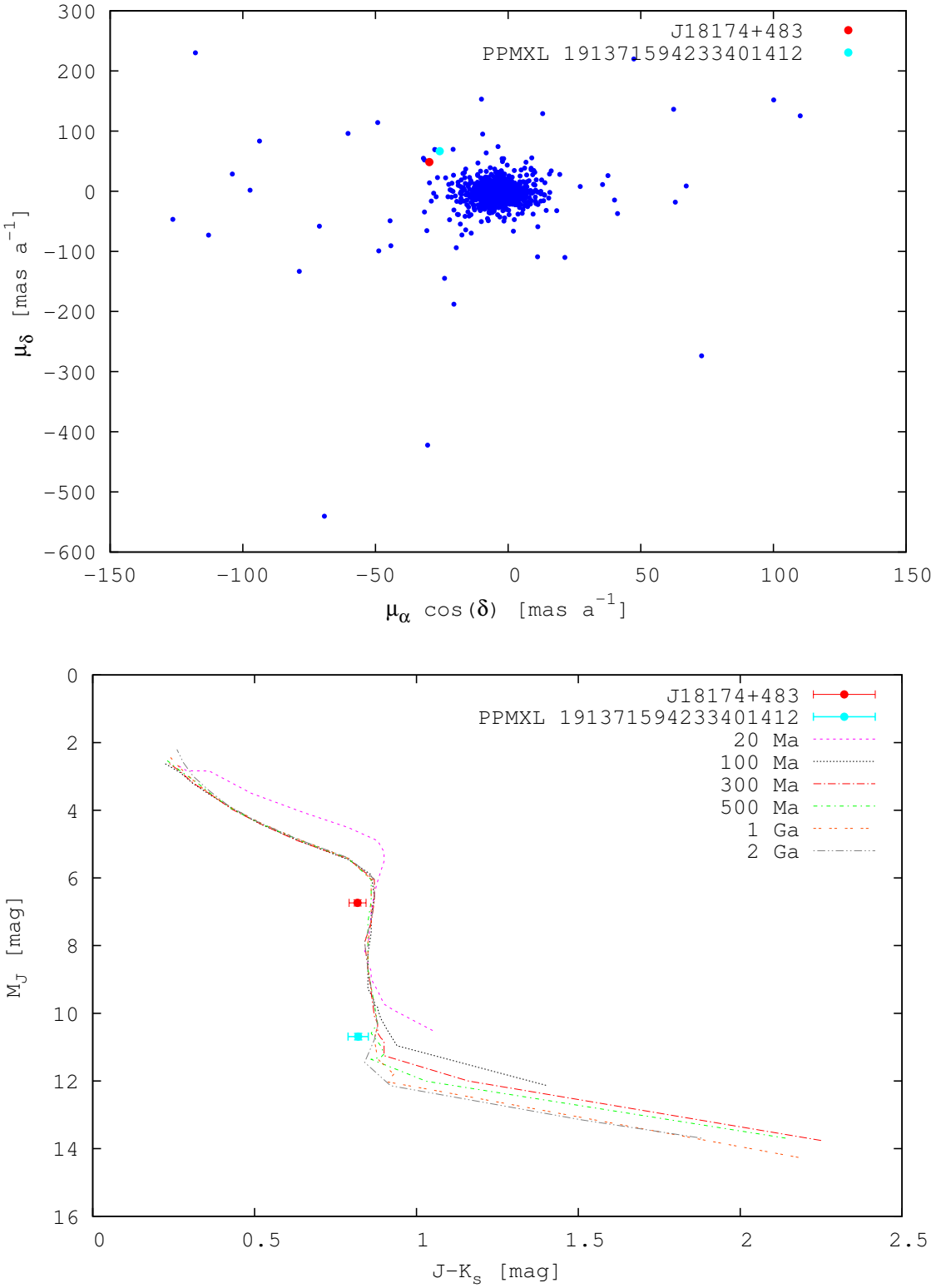

FIGURE D.14— Proper motion and colour-magnitude diagrams for the Carmencita targets and their common proper motion likely and dubious candidates (cont.)

Proper motion and colour-magnitude diagrams of the rejected candidates.

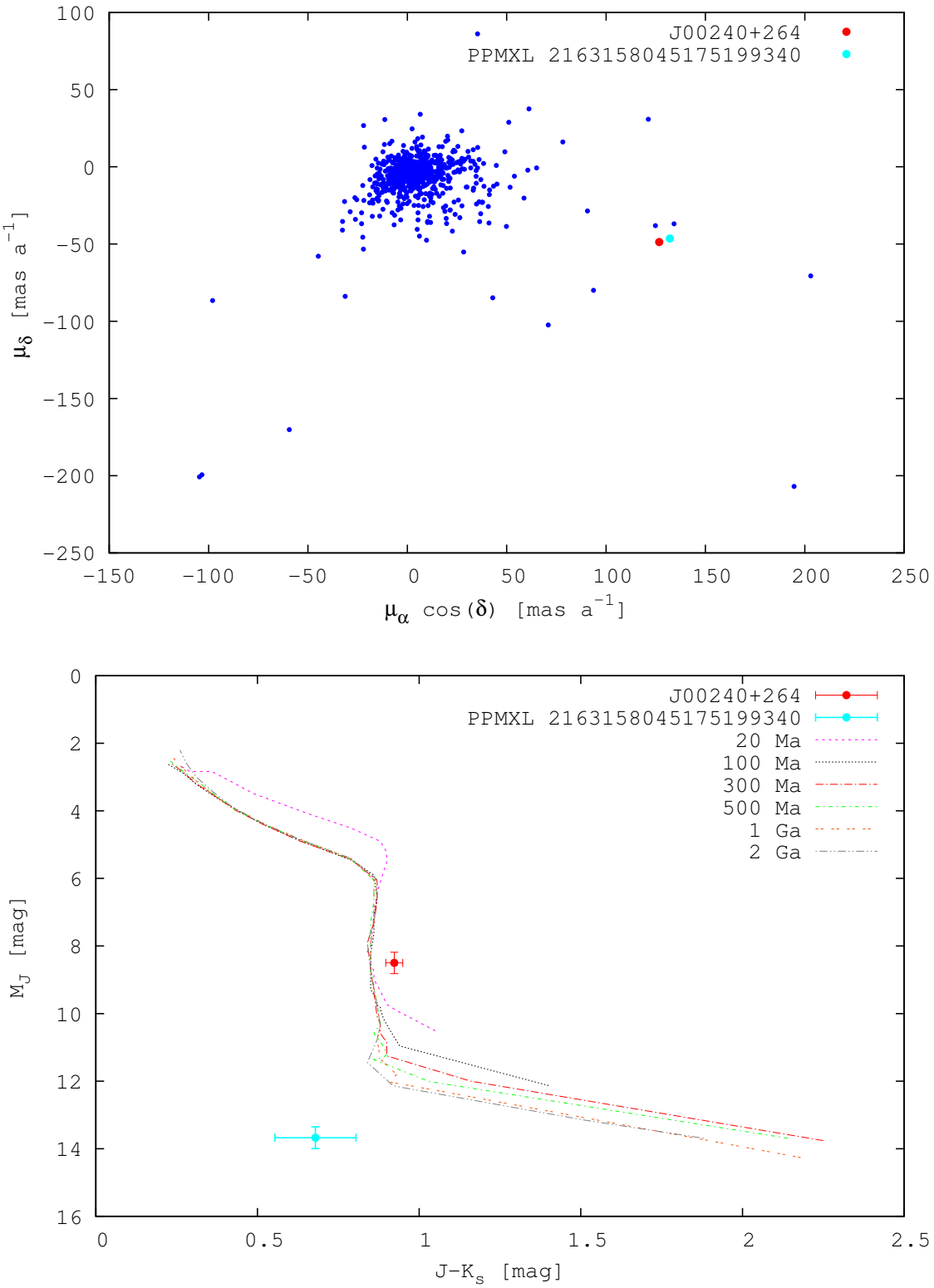

FIGURE D.15— Proper motion and colour-magnitude diagrams for the Carmencita targets and their rejected common proper motion candidates.

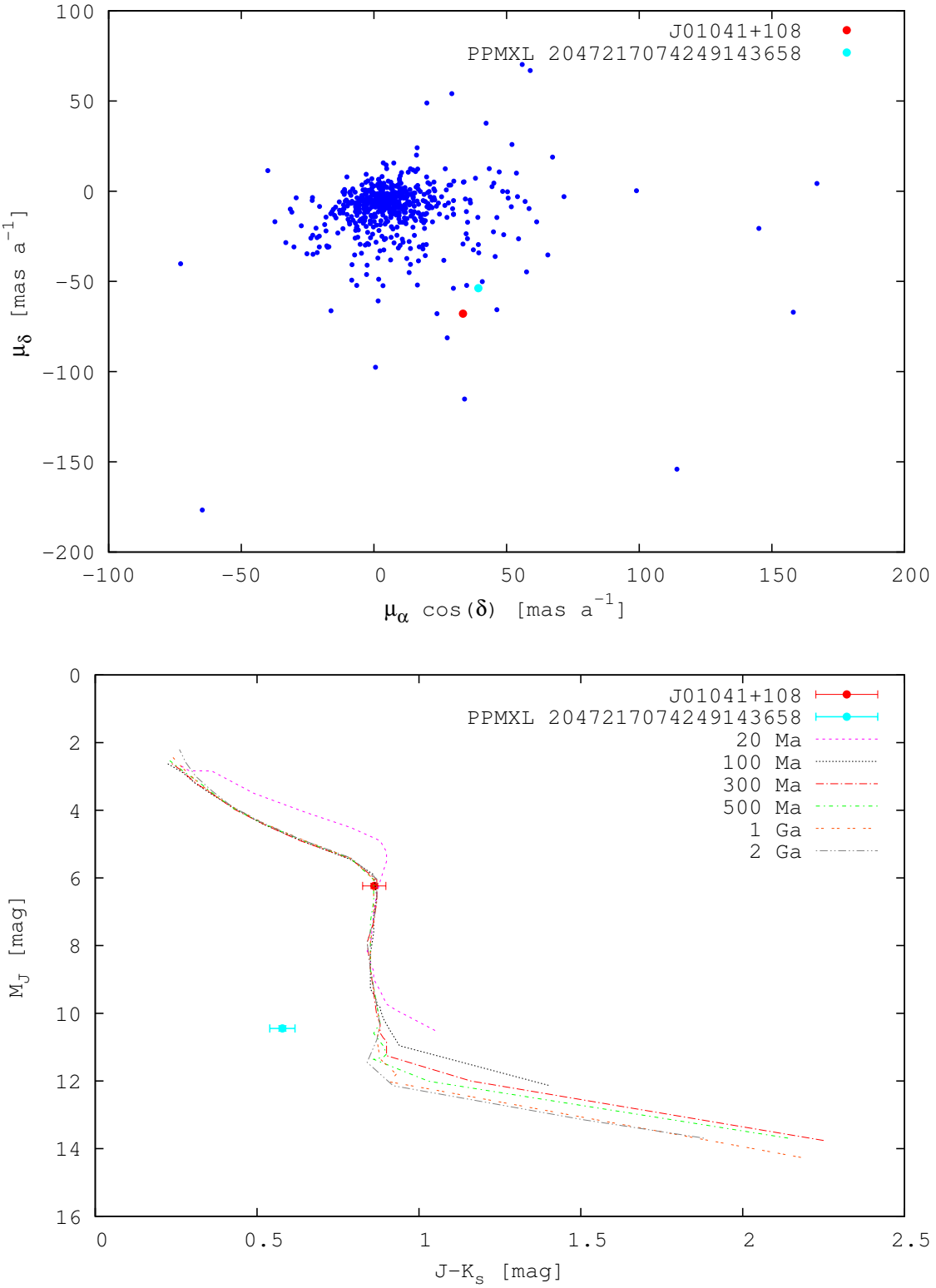

FIGURE D.16— Proper motion and colour-magnitude diagrams for the Carmencita targets and their rejected common proper motion candidates (cont.)

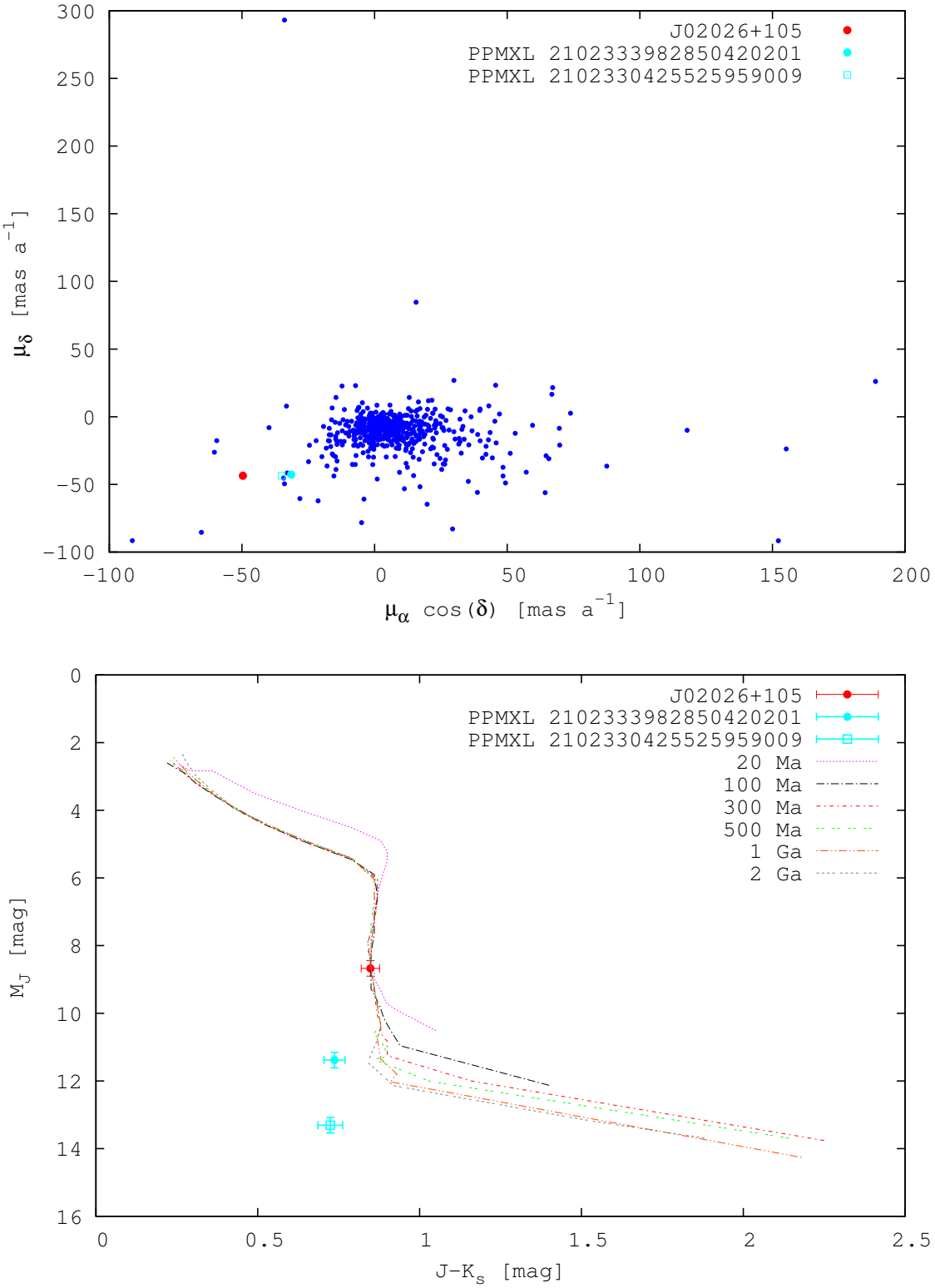

FIGURE D.17— Proper motion and colour-magnitude diagrams for the Carmencita targets and their rejected common proper motion candidates (cont.)

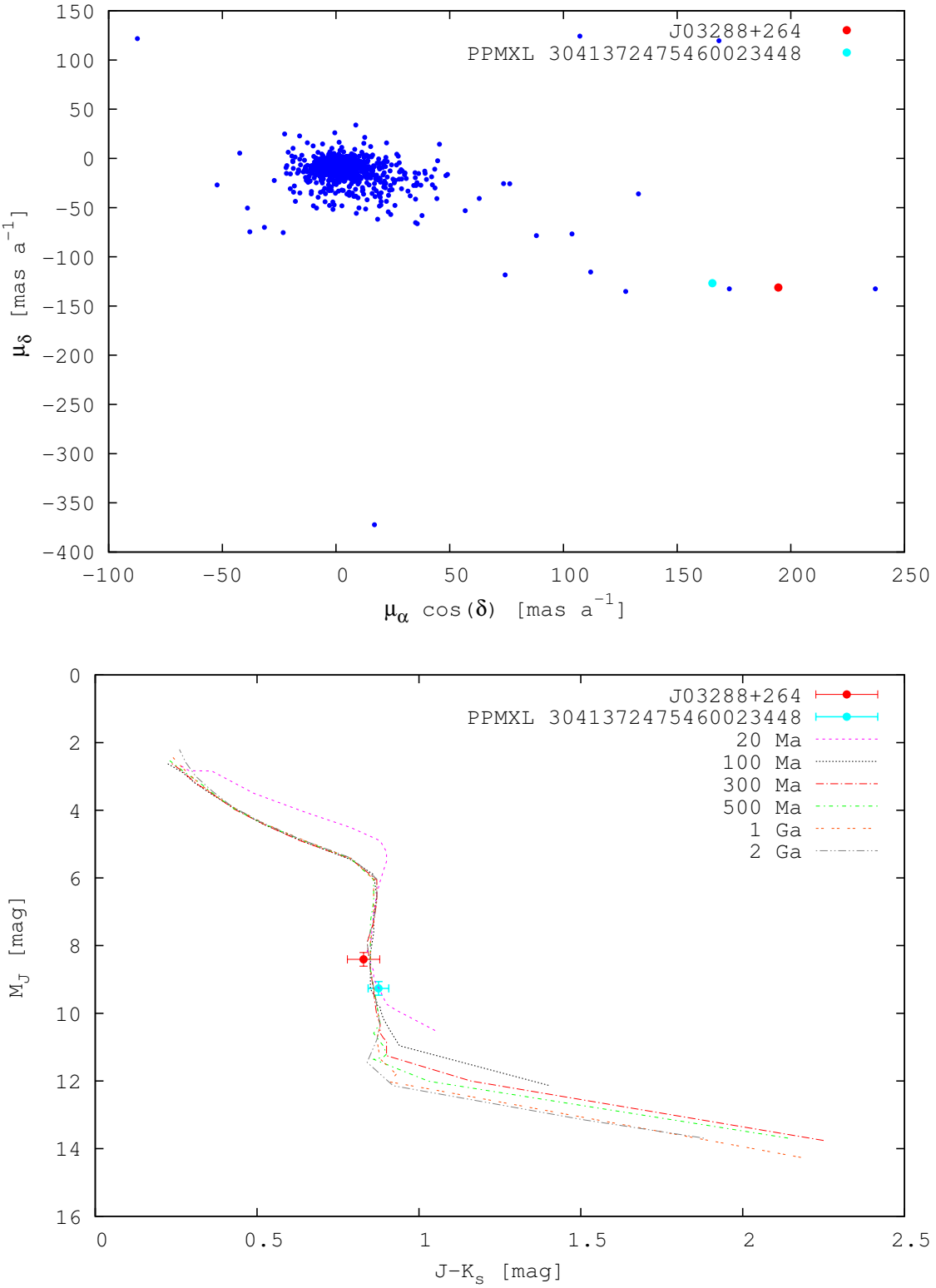

FIGURE D.18— Proper motion and colour-magnitude diagrams for the Carmencita targets and their rejected common proper motion candidates (cont.)

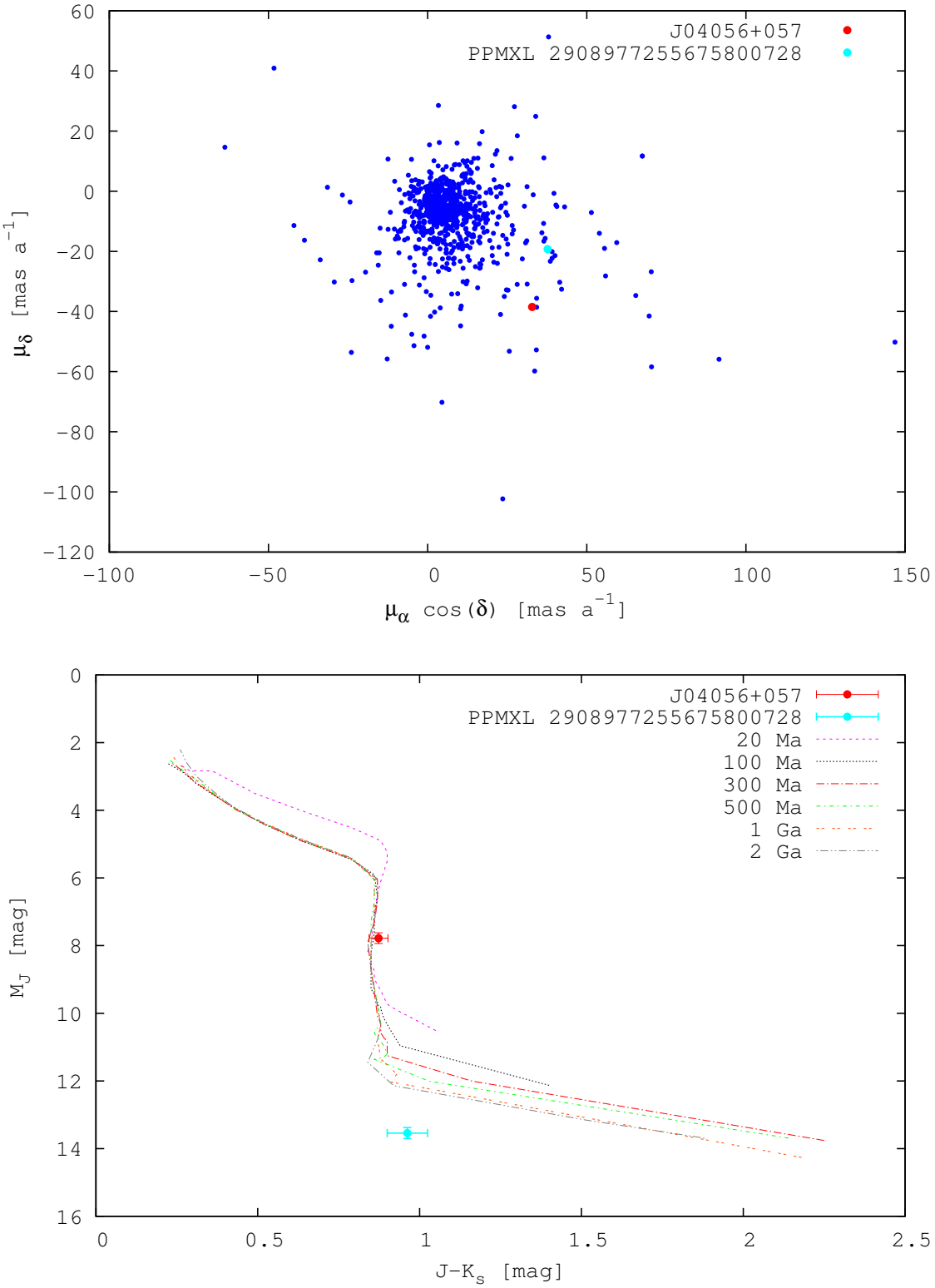

FIGURE D.19— Proper motion and colour-magnitude diagrams for the Carmencita targets and their rejected common proper motion candidates (cont.)

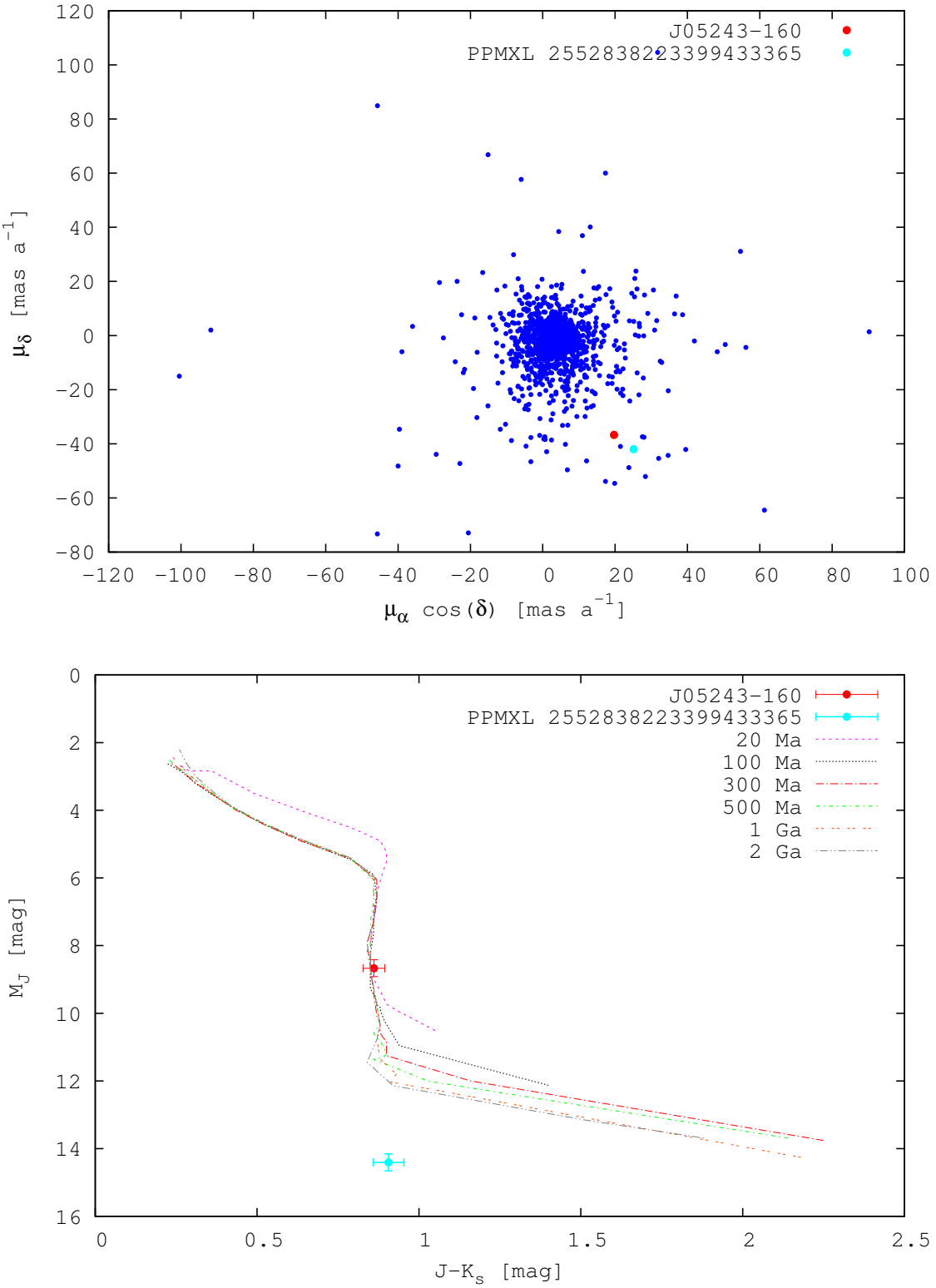

FIGURE D.20— Proper motion and colour-magnitude diagrams for the Carmencita targets and their rejected common proper motion candidates (cont.)

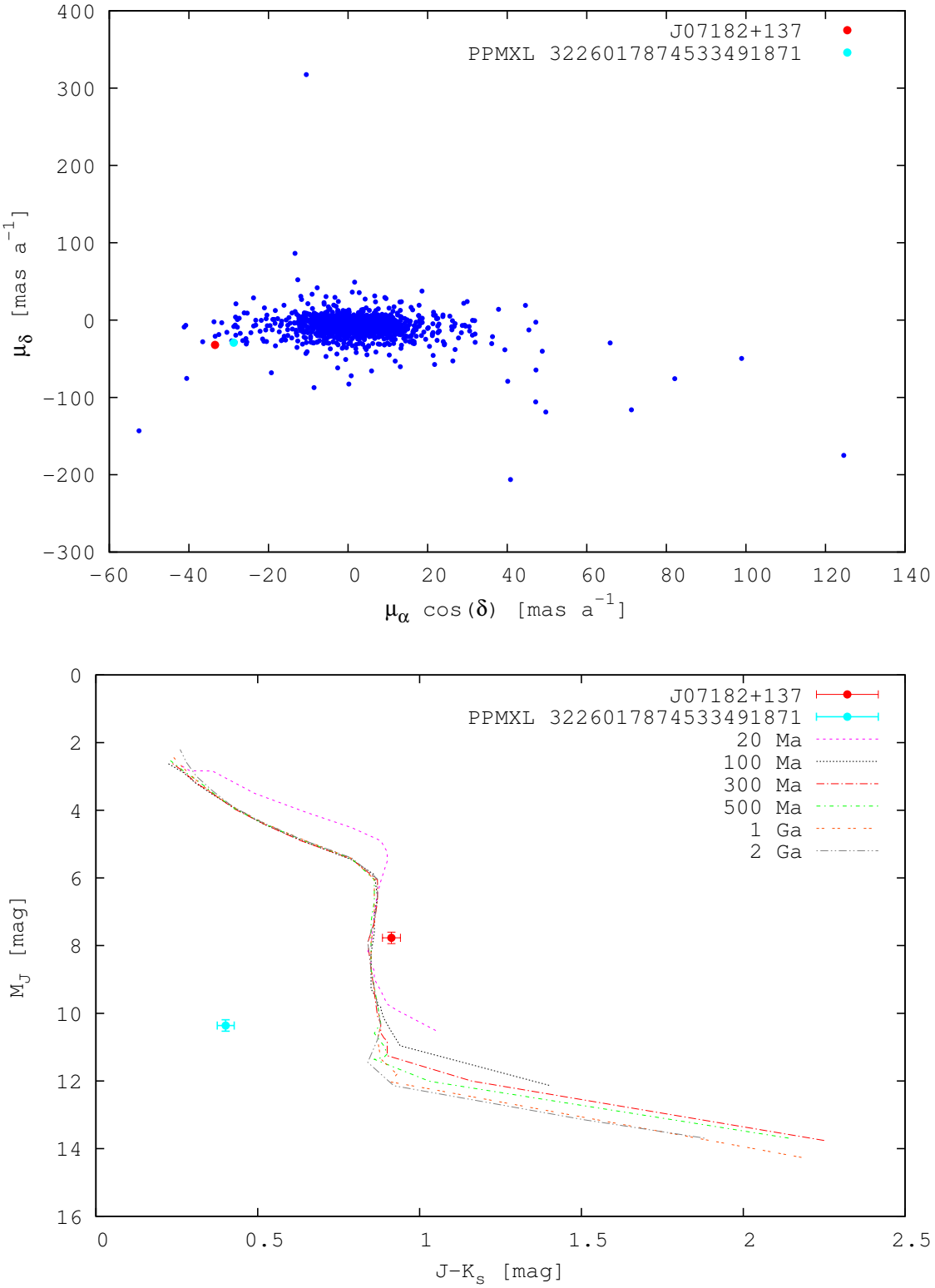

FIGURE D.21— Proper motion and colour-magnitude diagrams for the Carmencita targets and their rejected common proper motion candidates (cont.)

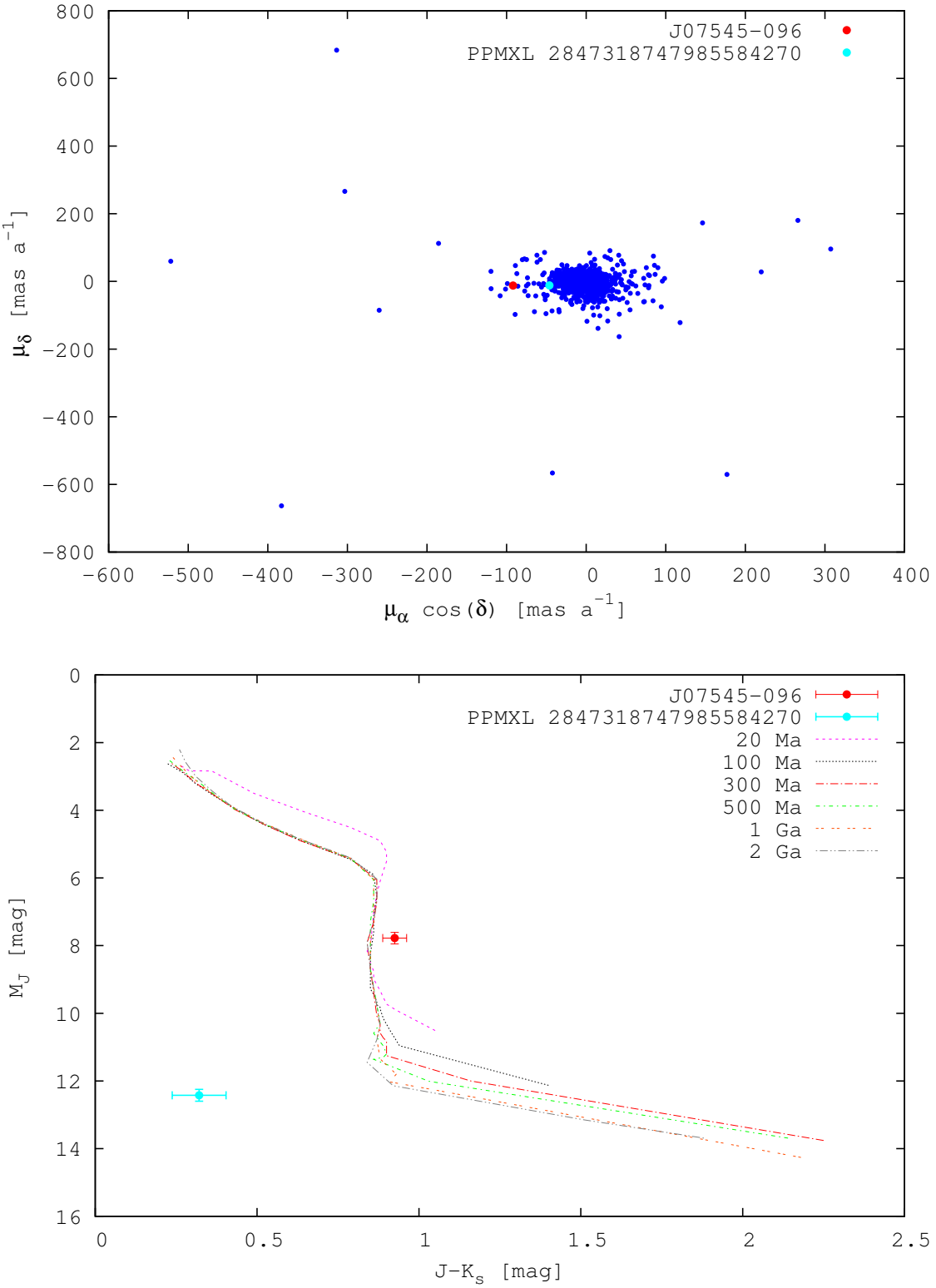

FIGURE D.22— Proper motion and colour-magnitude diagrams for the Carmencita targets and their rejected common proper motion candidates (cont.)

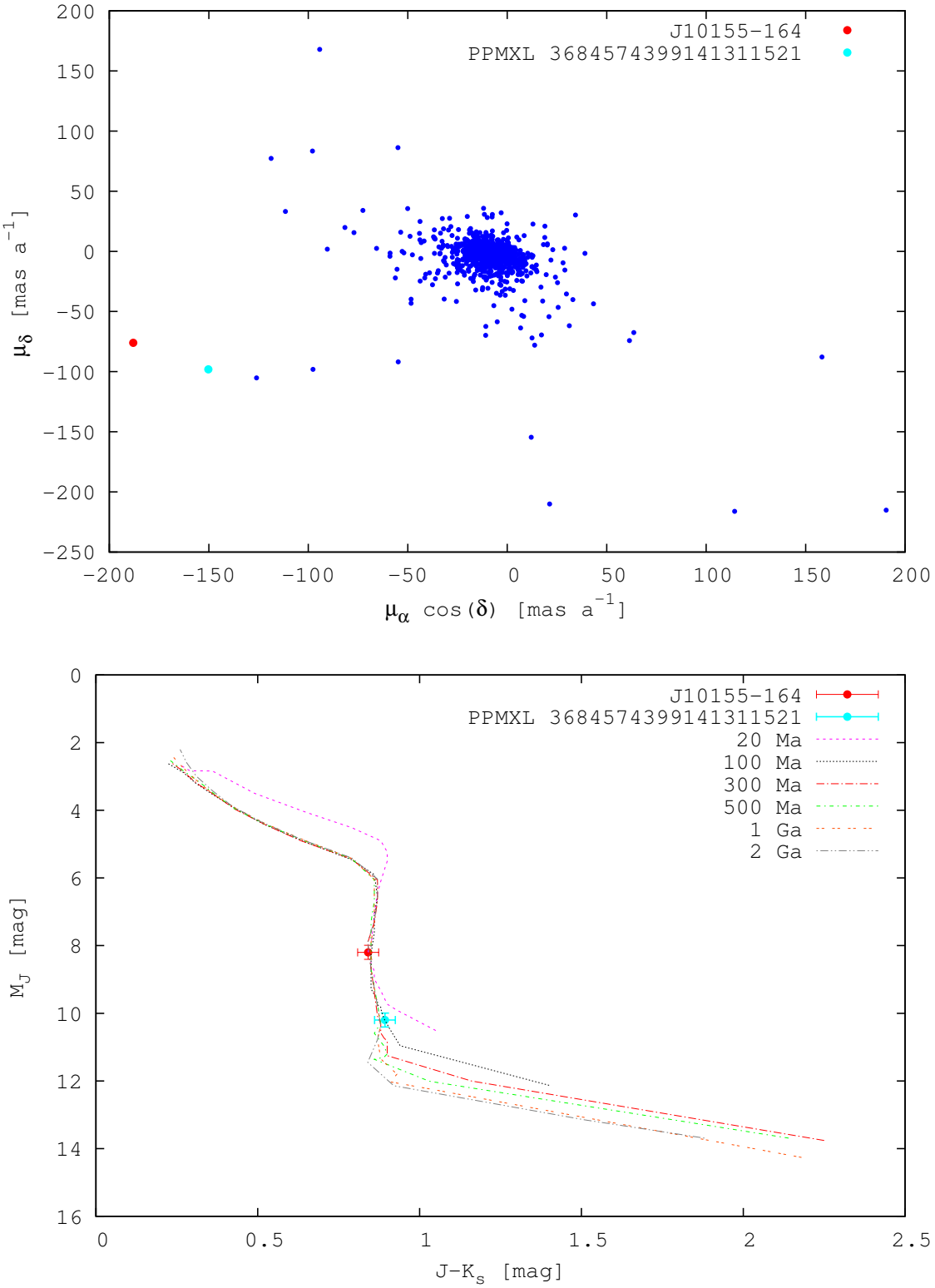

FIGURE D.23— Proper motion and colour-magnitude diagrams for the Carmencita targets and their rejected common proper motion candidates (cont.)

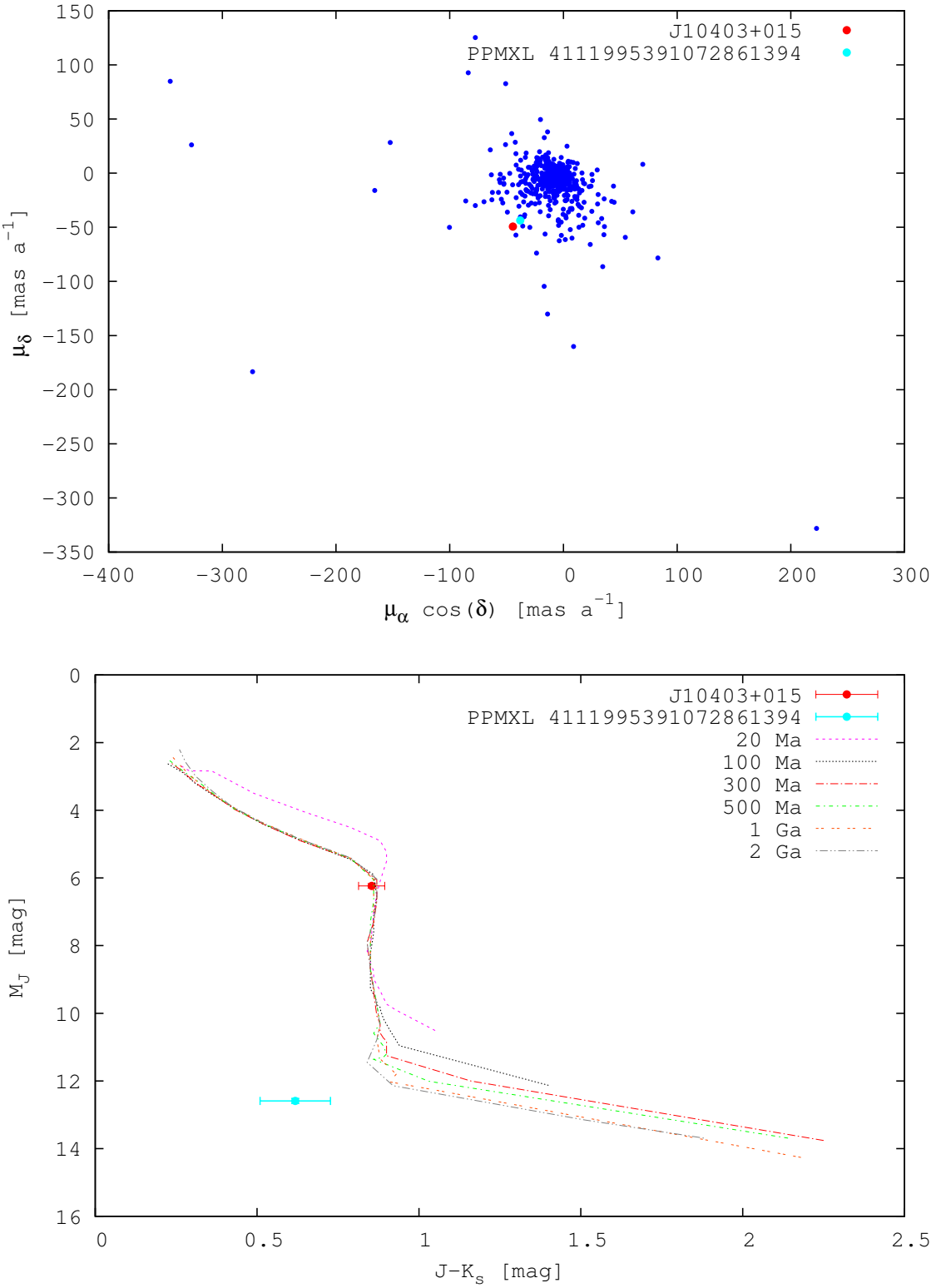

FIGURE D.24— Proper motion and colour-magnitude diagrams for the Carmencita targets and their rejected common proper motion candidates (cont.)

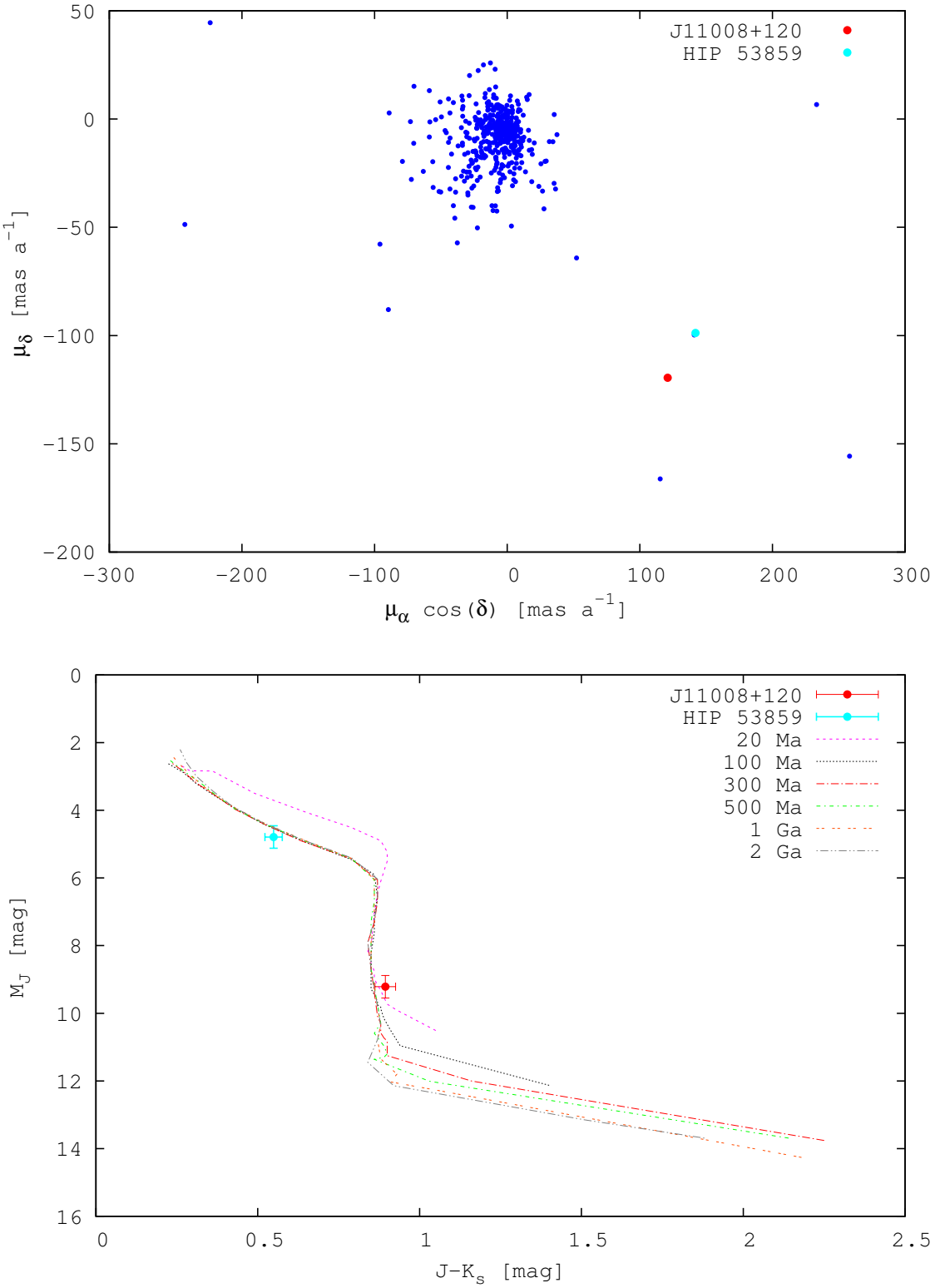

FIGURE D.25— Proper motion and colour-magnitude diagrams for the Carmencita targets and their rejected common proper motion candidates (cont.)

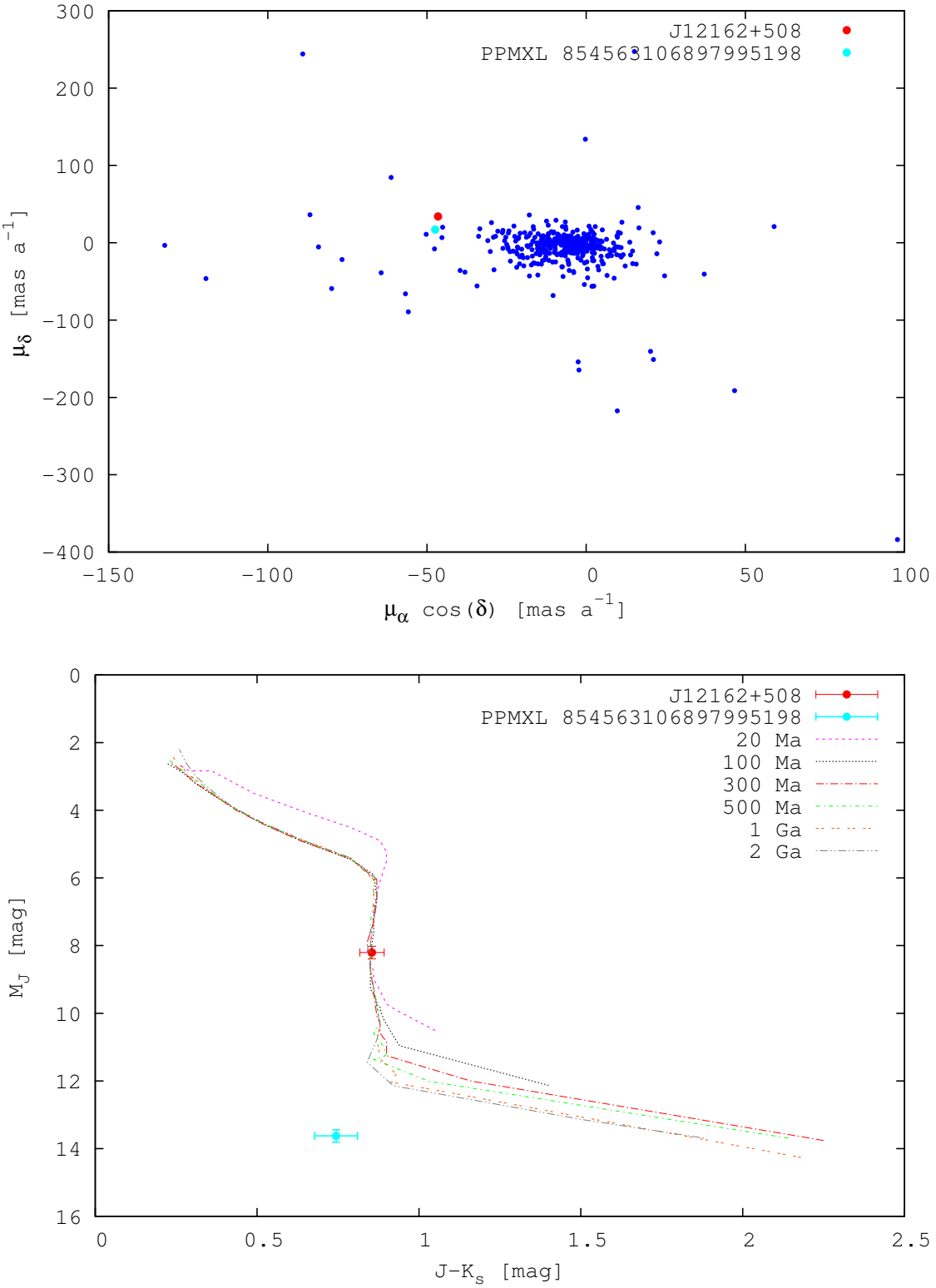

FIGURE D.26— Proper motion and colour-magnitude diagrams for the Carmencita targets and their rejected common proper motion candidates (cont.)

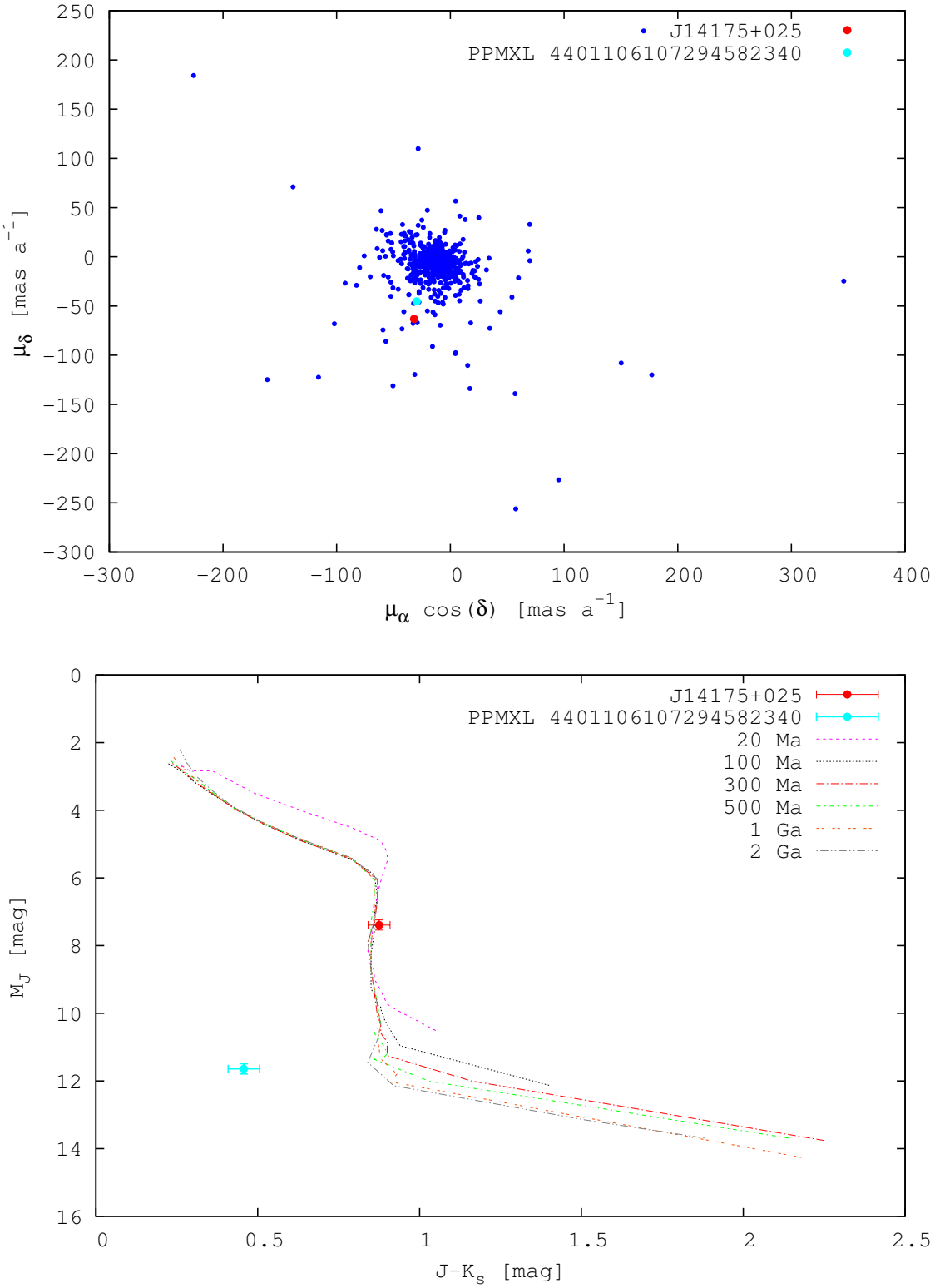

FIGURE D.27— Proper motion and colour-magnitude diagrams for the Carmencita targets and their rejected common proper motion candidates (cont.)

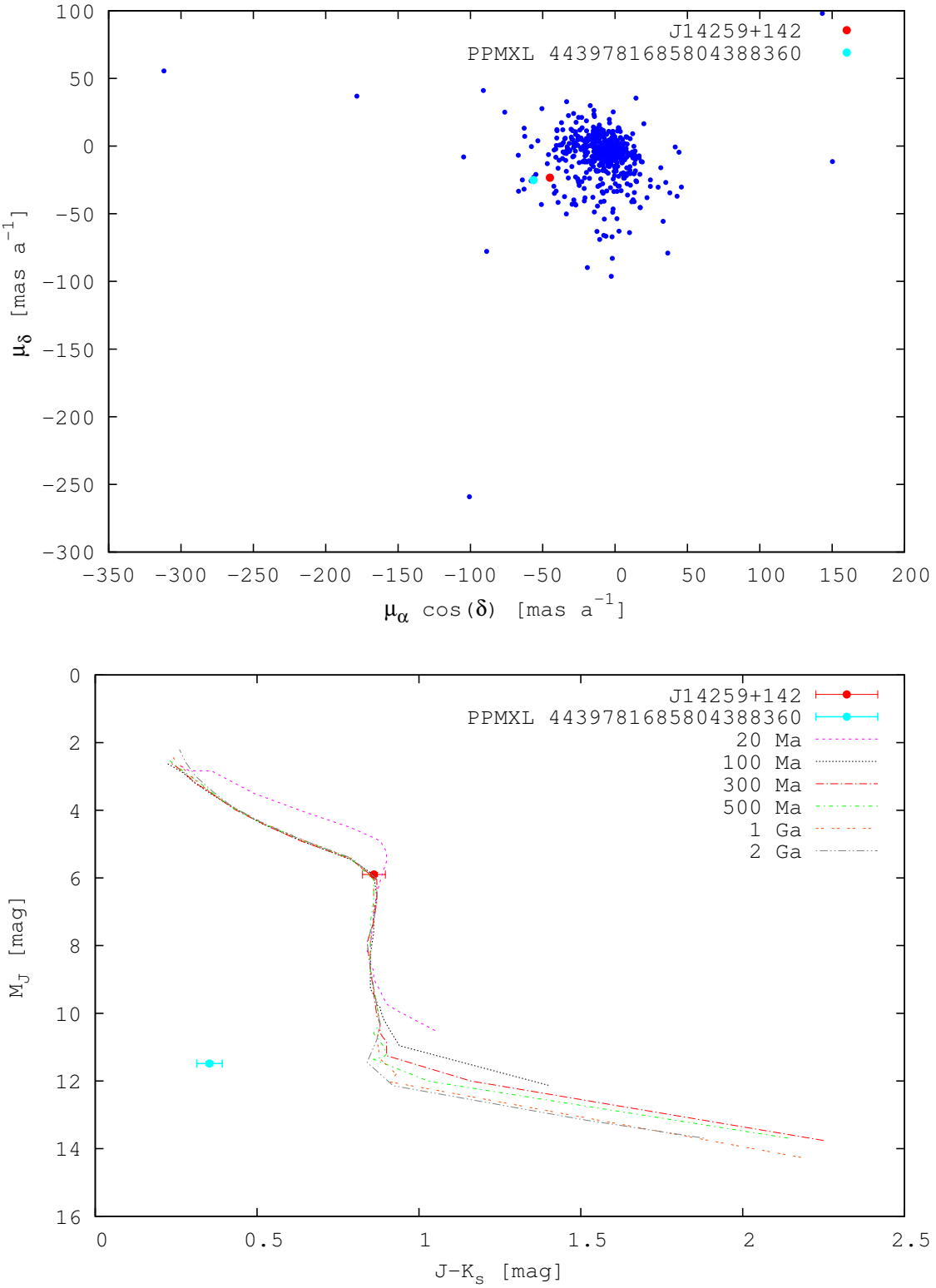

FIGURE D.28— Proper motion and colour-magnitude diagrams for the Carmencita targets and their rejected common proper motion candidates (cont.)

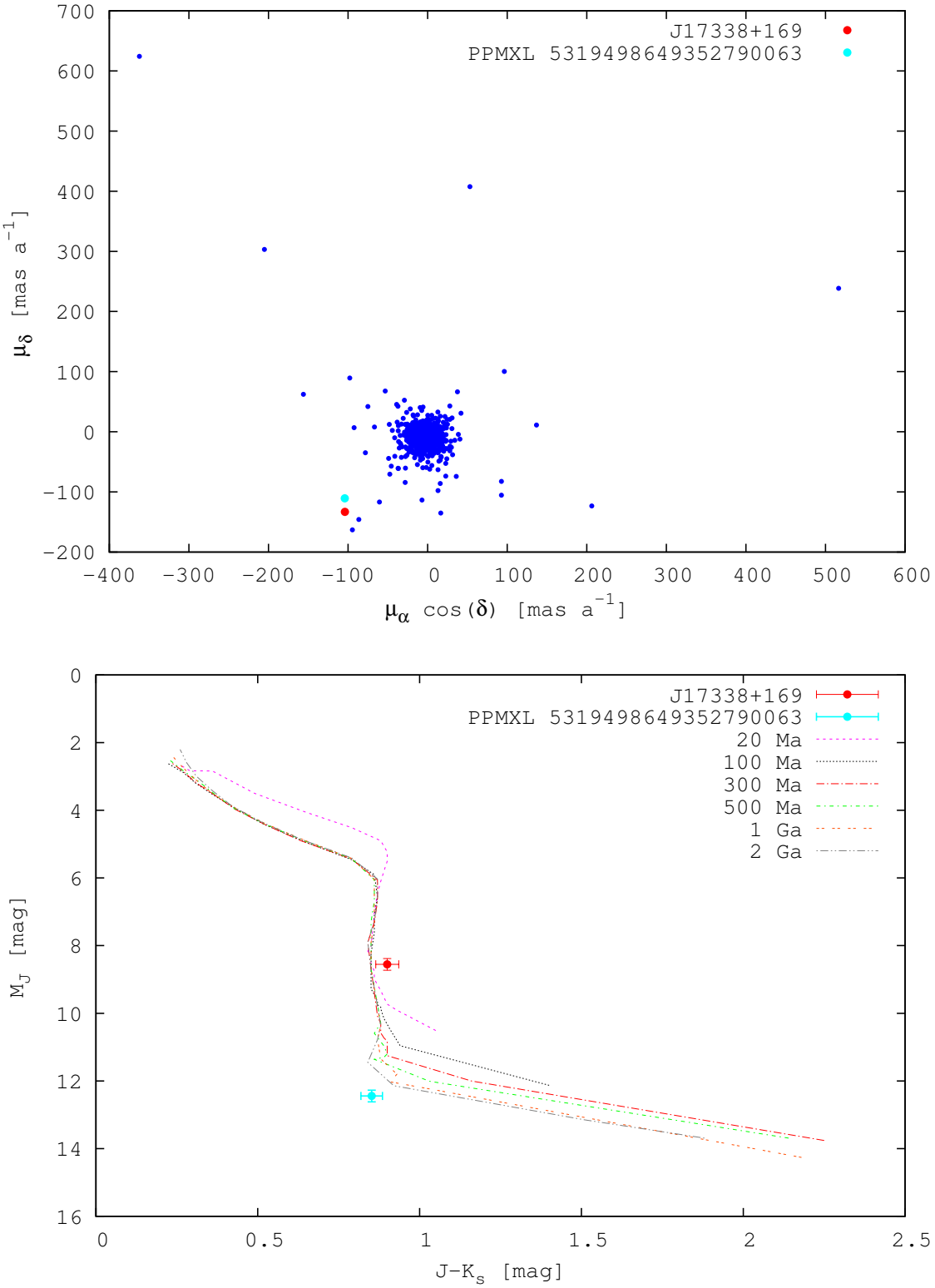

FIGURE D.29— Proper motion and colour-magnitude diagrams for the Carmencita targets and their rejected common proper motion candidates (cont.)

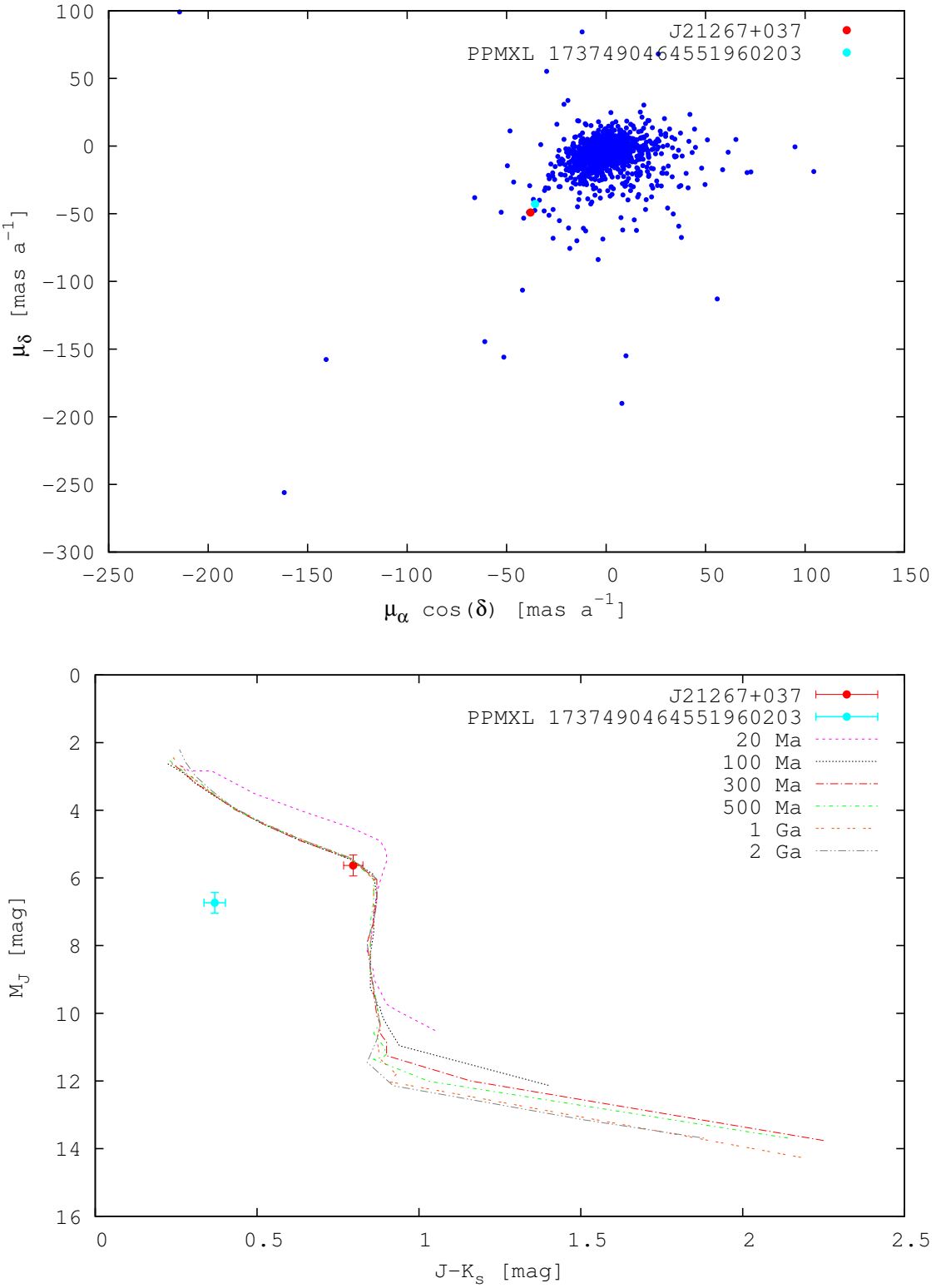

FIGURE D.30— Proper motion and colour-magnitude diagrams for the Carmencita targets and their rejected common proper motion candidates (cont.)

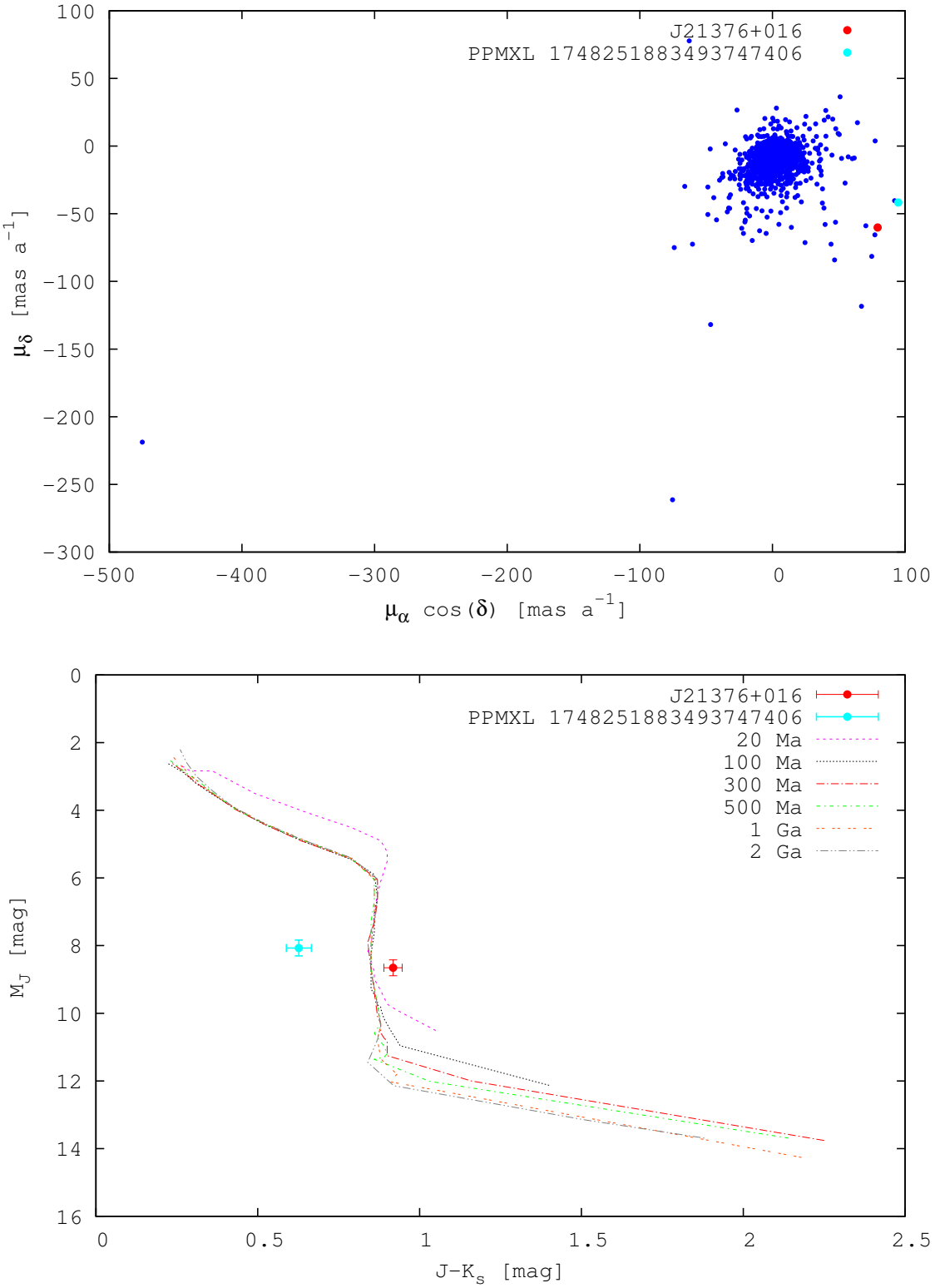

FIGURE D.31— Proper motion and colour-magnitude diagrams for the Carmencita targets and their rejected common proper motion candidates (cont.)

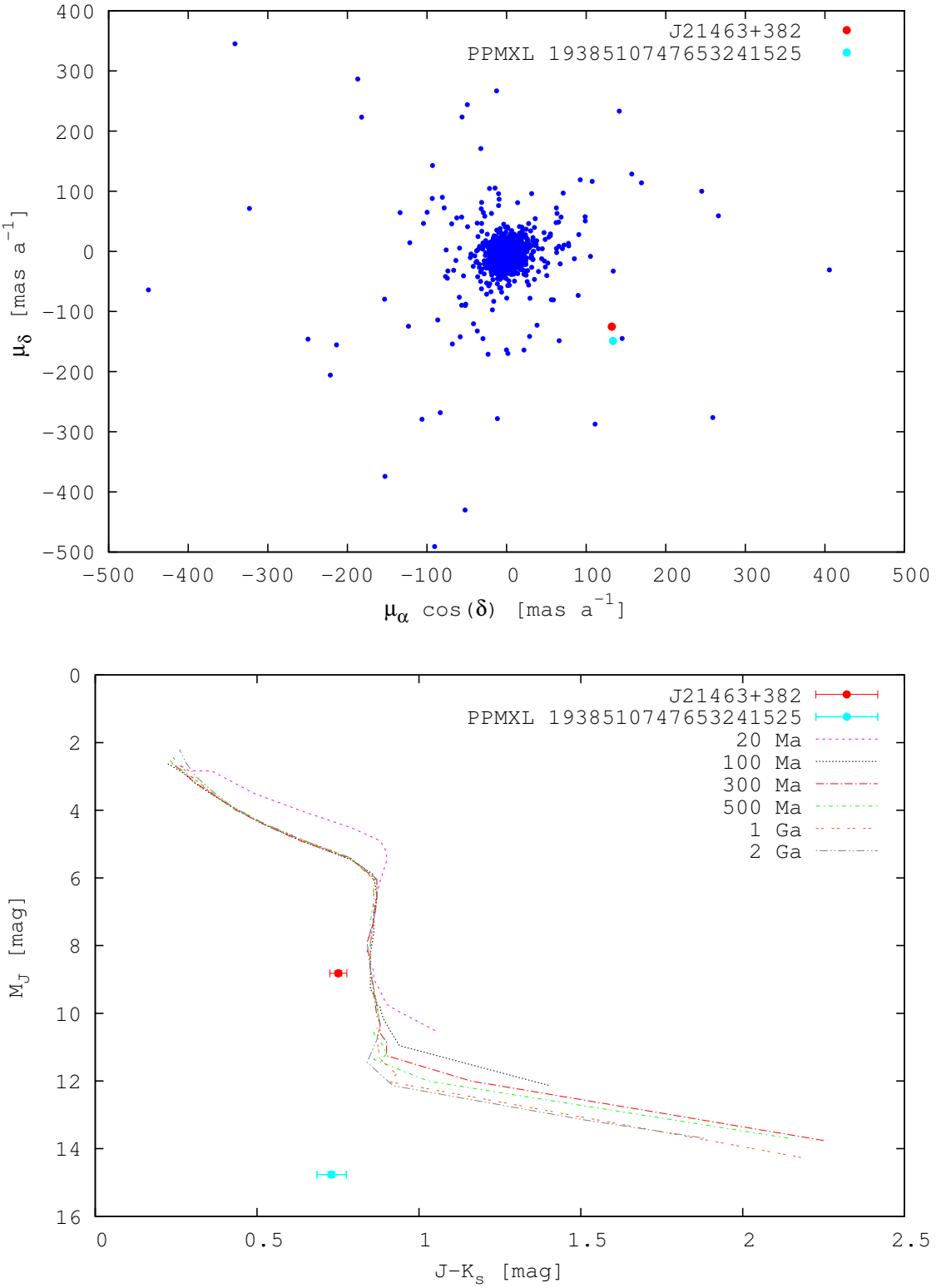

FIGURE D.32— Proper motion and colour-magnitude diagrams for the Carmencita targets and their rejected common proper motion candidates (cont.)

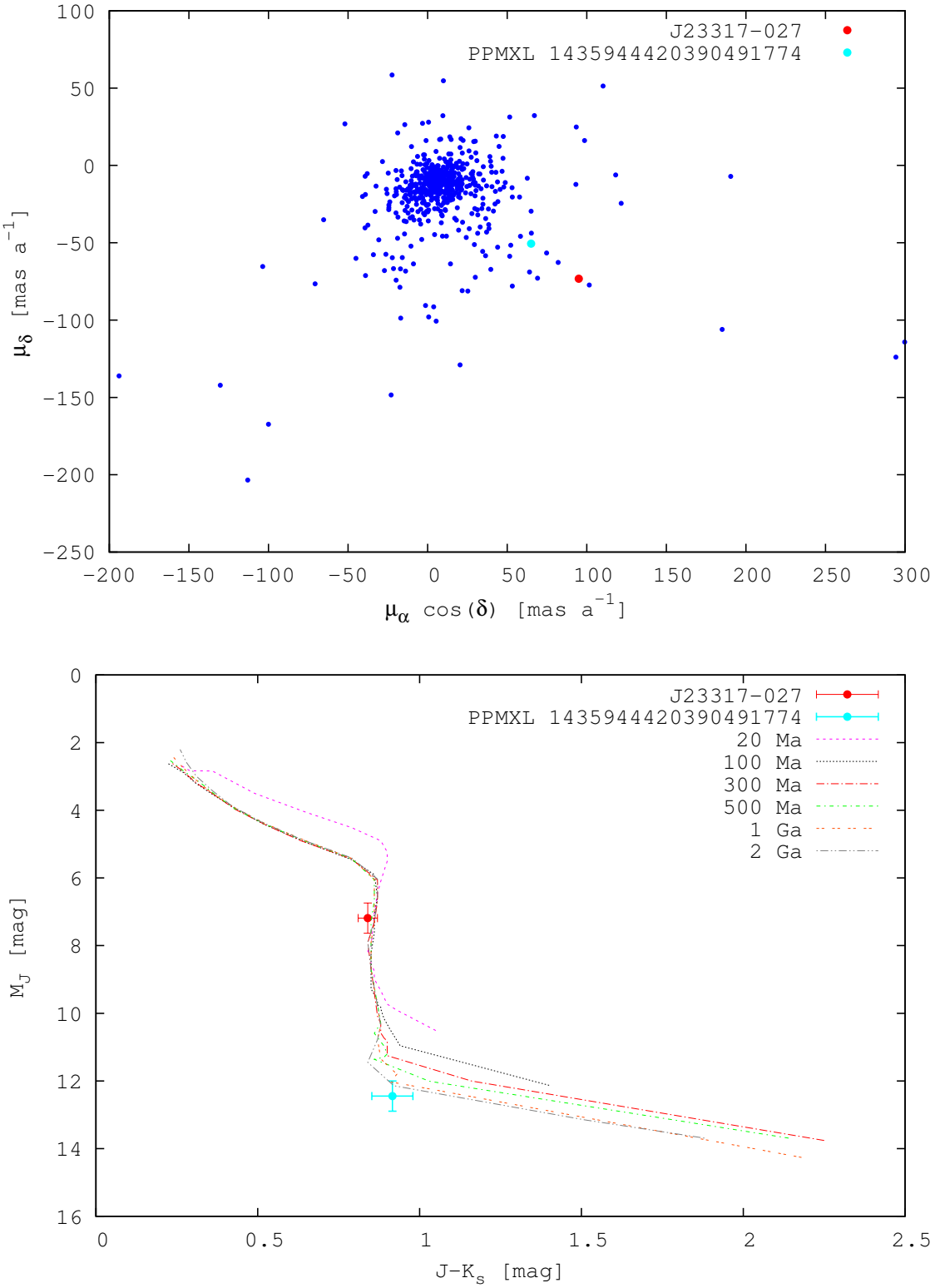

FIGURE D.33— Proper motion and colour-magnitude diagrams for the Carmencita targets and their rejected common proper motion candidates (cont.)